

Exxon Valdez Oil Spill
Restoration Project Annual Report

SEA97: Sound Ecosystem Assessment (SEA) -
An Integrated Science Plan for the Restoration
of Injured Species in Prince William Sound, Alaska

Restoration Project 97320
Annual Report

This annual report has been prepared for peer review as part of the *Exxon Valdez* Oil Spill Trustee Council restoration program for the purpose of assessing project progress. Peer review comments have not been addressed in this annual report.

Robert T. Cooney

Institute of Marine Science
University of Alaska Fairbanks
Fairbanks, Alaska 99775-7220

for:

Alaska Department of Fish and Game
Habitat and Restoration Division
333 Raspberry Road
Anchorage, Alaska 99518

April 1998

SEA97: Sound Ecosystem Assessment (SEA) -
An Integrated Science Plan for the Restoration
of Injured Species in Prince William Sound, Alaska

Restoration Project 97320
Annual Report

Study History: The Sound Ecosystem Assessment (SEA) program was initiated in April 1994, as an integrated, interdisciplinary, multi-project study of processes influencing the recovery of damaged pink salmon and herring populations in Prince William Sound. Annual reports of progress toward stated SEA goals have been submitted as a SEA annual report series (1994-96). The latest report in this series was submitted in April 1997, under the title SEA96: Sound Ecosystem Assessment (SEA): An Integrated Science Plan for the Restoration of Injured Species in Prince William Sound. That report contained 13 chapters contributed by the principal investigators and the SEA lead scientist. The FY 97 annual report, submitted as this document, reports progress by SEA investigators during year 4 of the planned 5-year study. Results from the last fully-funded year of SEA (FY 98) will be reported as part of the program's final report to be submitted in April, 1999.

Abstract: The FY97 SEA program entered a period of increased emphasis on data analysis and interpretation, and on model development and validation. Several new insights were obtained concerning the dynamics of the region relative to the production of pink salmon and herring. These included: 1) mapping of fine-scale currents with lagrangian drifters demonstrated unexpectedly complex patterns in upper-layer flow fields with trajectories tracing small and meso-scale eddies inside and outside Prince William Sound; 2) partial affirmation that macrozooplankton-forced shifts in food-web structure favors the survival of juveniles fishes; 3) the identification of a chlorophyll front located about 30 km north of Hinchinbrook Entrance partitioning the biology into northern and southern sectors; 4) further evidence, using stable isotopes, of plankton intrusions from the Gulf of Alaska with Lake/River implications; 5) confirmation of juvenile herring rearing areas, forage resources, and distributions relative to other dominant near-shore fishes like pollock; and 6) a realization that pre-winter whole body energy levels rather than the oceanographic characteristics in winter rearing areas probably determine juvenile herring overwintering survival. Modeling activities includedssssss fresh-water refinements to the ocean state simulation, additions to the NPZ model, and the addition of observed zooplankton fields to test cases of the nekton model.

Key Words: Biophysical models, circulation, ecosystem modeling, marine acoustics, marine food webs, numerical models, nutrients, oceanography, Pacific herring, phytoplankton, pink salmon, Prince William Sound, somatic energy, stable isotopes, zooplankton.

Project Data: (will be addressed in the final report)

Citation:

Cooney, R.T. 1998. SEA97: Sound Ecosystem Assessment (SEA) - An integrated science plan for the restoration of injured species in Prince William Sound, Alaska, *Exxon Valdez* Oil Spill Restoration Project Annual Report (Restoration Project 97320), Alaska Department of Fish and Game, Habitat and Restoration Division, Anchorage, Alaska.

Table of Contents

Study History/Abstract/Key Words/Project Data/Citation	i
Preface.....	iv
A SEA 1997 Synthesis.....	Chapter 1
Juvenile Salmon Predation.....	Chapter 2
Phytoplankton and Nutrients.....	Chapter 3
The Role of Zooplankton	Chapter 4
Biophysical Modeling and Remote Sensing	Chapter 5
Stable Isotopes as Food -Web Tracers	Chapter 6
Information Systems and Model Development	Chapter 7
Observational Physical Oceanography	Chapter 8
Plankton and Nekton Acoustics	Chapter 9
Juvenile Herring Growth and Habitats; Traditional Ecological Knowledge	Chapter 10
Fish Energetics.....	Chapter 11
Synthesis and Integration.....	Chapter 12

Preface

Each of the individual SEA annual reports compiled here as separate chapters has been written as a stand-alone document. Bundling the reports under a single cover with an added synthesis chapter is done at the request of the EVOS Chief Scientist to provide the Trustee Council and its member agencies easy access to all results from work performed in 1997, and with an expanded executive summary of the research. SEA continues to be a work in progress, with FY 98 the last fully funded year. The program is scheduled for close-out in FY 99 and will provide the sponsors of the research with a single, integrated Final Report, and a synthesis volume of summary papers detailing progress toward the resolution of key hypotheses and processes defining the pink salmon and herring portions of the Prince William Sound ecosystem.

SEA was designed in the fall of 1993 to test a series of ideas about possible mechanisms restraining the recovery of pink salmon and herring populations damaged by the oil spill of 1989. Refinements to these conjectures continue to focus the research:

a. The survival of juvenile pink salmon and post-larval Pacific herring rearing in Prince William Sound is determined primarily by predation losses to marine birds, mammals and other fishes.

b. Predation losses are related in part to the energetic condition and size of juvenile Pacific herring and pink salmon. Condition and size are determined by growth rates which vary between regions of the Sound, and from year to year as a function of food and water temperature.

c. For juvenile Pacific herring, the somatic energy content of individuals at the beginning of the winter fast is a critical overwintering survival determinant. Young-of-the-year herring particularly, and older juveniles in general with low levels of somatic energy prior to winter, are at risk to starvation.

d. Predation losses are modified by the species composition of predator communities and their numbers and distributions in juvenile rearing areas. Predation losses are also governed by the amounts, kinds and time/space distributions of alternative prey for predators that also feed on juvenile pink salmon and Pacific herring. Macrozooplankton serves as alternative prey during some seasons and years.

e. Macrozooplankton populations are established by local reproduction driven by phytoplankton productivity and modified by circulation processes that both flush the region and seed the Sound from adjacent shelf and open ocean populations.

SEA investigators met in September, 1997, in Valdez to review the program's overall status and to develop structure for a synthesis volume intended for the journal, Fisheries Oceanography. This planning activity created provisional titles and authorship for ten manuscripts describing the events leading up to and defining SEA, the major findings - both observed and modeled - and implications for the long-term management of herring and salmon stocks.

Chapter 1

A SEA 1997 Synthesis

Chapter 1

A SEA 1997 Synthesis

A Sound Ecosystem Assessment (SEA) Synthesis with Emphasis on Results Reported for the FY 97 Funding Year

Robert T. Cooney
Institute of Marine Science
University of Alaska Fairbanks
Fairbanks, Alaska 99775-7220

Introduction

After four years of intensive field and laboratory study, the SEA program has now begun the process of applying the results of individual project elements to broad questions concerning ecosystem-level suppression of the recovery of injured pink salmon and herring populations following the oil spill in 1989. SEA's approach has been to embed studies of juvenile pink salmon and herring in a matrix of supporting investigations, including the physical environment, forage resources, and the principal predators and competitors of the juveniles, to define critical ecological dependencies influencing survival during early life history. These relationships were sought so that mechanisms of survival could be simulated numerically for predictive and experimental purposes. The disciplines of oceanography, fisheries science, and applied mathematics were linked to the tools of quantitative marine acoustics, remote sensing, stable isotope analyses, and fish energetics to interrogate the natural system of Prince William Sound on time and space scales believed to be important. The program is now entering the final phase of its planned activities - a period of integration and synthesis. The assembly of project results into a coherent picture of variables influencing levels of pink salmon and herring production is expected to be an extraordinarily complex and demanding exercise. To make the problem even more difficult, declining levels of overall support for SEA are forcing many investigators to search elsewhere for funding. This distraction is inevitable but unfortunate as it comes at a very critical time for the overall program.

Ocean State and Plankton Dynamics

Additional refinements were made to the SEA ocean-state model of circulation and hydrography in FY 97. The most important of these refinements included the addition of freshwater input as an external forcing factor for the circulation and a modifier of the hydrography (temperature, salinity and density structure). The region receives substantial amounts of precipitation seasonally as rainfall and snow, and there is little question that this freshwater plays an important seasonal role in driving upper layer circulation. As a first approximation, freshwater in the model was distributed uniformly across the surface of the region. Further refinements (presently underway) will include a line-source input responsive to the size of individual watersheds. This change will provide important spatial differentiation missing in the present simulation. Problems

of local winds (another principal forcing factor) and their application to the model were also addressed. By the spring or summer of 1998, the circulation model is expected to be sufficiently tuned to allow the first of several experiments relative to questions about the seeding, flushing and retention of zooplankton and ichthyoplankton populations in the Sound under varying oceanographic conditions. These experiments are among several designed to help resolve the lake/river conjecture and its implications for pink salmon and herring production.

One of the most unexpected results of SEA oceanographic work in FY 97 arose from releases of satellite-tracked ARGOS drifters at various locations in Prince William Sound. Releases were made in May, July and August. Although the sample size was small (5), the methodology provided startling insight into the complexity of upper-layer transport processes present during the late spring and summer of 1996 and 97. The trajectories of drifting buoys released in the Sound in May revealed complex fields of eddies and current reversals both inside and outside the Sound. In one case, a drifter circled Montague Island against what was considered to be the prevailing flow and traveled east entering and then leaving the gyre near Kayak Island. These observations have important implications for the exchange of zooplankton between the Sound and adjacent shelf, and for larval herring drifting seaward from natal beaches in mid to late May each year. Additional satellite tracked drifter releases are planned for 1998.

The SEA view of seasonal interactions between the Gulf of Alaska water (deep and shallow) and Prince William Sound continues to expand as more observations are processed. The objective interpretation of this data set is tricky since interannual variability has been substantial during the SEA sampling years. During the summer season of relaxed downwelling (or weak upwelling), flows are generally out of the Sound at Hinchinbrook Entrance above 150 m, and inward below that depth. However, strong easterly winds associated with occasional summer storms can inject surface water in the Ekman layer (upper 50-70 m) as short-term northward bursts against the general surface outflow. As the fall/winter period progresses, increasing stronger easterly wind forcing and perhaps other factors initiate a period of inflow in the upper-layers and outflow at depth in the Entrance. By late winter, most transport is into the Sound at all depths at Hinchinbrook. Unfortunately, the lack of simultaneous measurements (another mooring) in Montague Strait precludes an assessment of flow-through and water balance relative to these two entrances. Shipboard measurements of transport (corrected for tides) indicate the notion of a continual outflow at all or some depths in Montague Strait is probably wrong. Also, the drifter experiments demonstrate that under some conditions, water in the near-surface layer can move into rather than leave the Sound at Montague Strait.

SEA is finding that the annual response of plant and animal plankton communities to seasonality in light levels and upper layer mixing regimes is complex but predictable (within limits) from evaluations of spring-time surface stability. The general timing of the phytoplankton bloom seems clearly established by light, but additionally modified by mixing. In almost all years, phytoplankton stocks peak in mid to late April. Modeling studies forced by meteorological time series report two general scenarios for Prince William Sound: 1) relatively warm, quiescent springs leading to short, intense blooms poorly coupled to the pelagic food web; and 2) cool, windy springs during which the plant bloom is extended in time and much more energy is captured by zooplankton. The actual production processes are probably much more complex. The early plant bloom is composed primarily of diatoms, sometimes but not always dominated

by *Skeletonema* spp. As dissolved inorganic nutrients are diminished, the diatom community is replaced by small flagellates. Sometime later (May/June) a modest secondary diatom bloom can appear briefly. Primary production, estimated from changes in total nutrient concentration, suggests rather substantial interannual variability. Plant production in 1997 was apparently less than 50% of that estimated for 1995 and 1996. If correct, these estimates suggest that bottom-up driven production can vary by at least a factor of two between years.

Zooplankton populations exhibit extreme seasonality in Prince William Sound. A late winter and early spring hiatus in standing stock is followed by a period of production resulting in increases of an order of magnitude or more as plankters couple to accelerating plant production. An early bloom of large calanoids peaks predictably in May with implications for the survival of juvenile pink salmon. Stocks of smaller copepods and other holo- and meroplankters combine to produce seasonal highs in June and July; pteropods and larvaceans become important at this time. Upper layer zooplankton stocks begin to decline in September, and larvae and ctenophores become important constituents. Later, with further seasonal diminishment, euphausiids and amphipods contribute in greater proportion. Upper-layer stocks are again low in December, a time when juvenile herring are overwintering in bays and fjords. The composition of offshore and nearshore zooplankton stocks differs throughout the year. Less than half of the dominant species found over deepwater are also ranked high in bays and fjords.

Not only is the zooplankton biomass elevated in the spring, but some taxa exhibit layering or swarming behaviors in the upper layers. These behaviors provide exceptional patch-dependent feeding opportunities for not only juvenile pink salmon and herring, but for other consumers as well. Adult walleye pollock frequent these rich layers to recharge their depleted, post-spawning energy reserves. Copepods and euphausiids are most commonly associated with these layers. New results from studies of pink salmon fry predators indicate that shifts by juvenile and adult pollock and herring toward or away from zooplankton as a dominant forage resource influence amounts of juvenile fishes in their diets.

The so-called Lake/River relationship between wind forcing and stocks of zooplankton measured at the AFK hatchery continues to defy interpretation. Since the program began in the spring of 1994, the statistical correlation has diminished from an r^2 value of 0.80 to less than 0.60. Also, the relationship predicted a strong "lake condition" (much higher than average zooplankton) for April and May, 1997, that did not occur. A reassessment of this relationship is presently underway and will be reported in 1998. An alteration in this correlation might be one signal of a major environmental perturbation or regime shift with unknown consequences for pink salmon and herring survival. Results from stable isotope analyses (carbon and nitrogen) strongly suggest that under certain yet-to-be-described conditions, more or less carbon finds its way to herring and other fishes in the Sound from the Gulf of Alaska rather than being locally produced. This observation also supports results from 1996 that demonstrated an apparent intrusion of outside stocks into the southern Sound. At that time, the outside and south-Sound waters were dominated (tagged) by euphausiids, while other locations were composed primarily of large calanoids. We interpret these patterns to mean that exchanges of water and biota with the bordering shelf can occur, and may influence interannual and seasonal patterns in zooplankton measured at certain locations in the region. These intrusions may also help to feed herbivores in the Sound in some years but not others.

Pink Salmon Recruitment Dynamics

The pink salmon recruitment program has focused on the idea that losses to predation by juveniles rearing in Prince William Sound each spring and summer set limits on the size of the returning adult population one year later. Juvenile survival rates were further thought to reflect growth conditions for the youngest, smallest fishes. For years when the growth rate is high (food and temperature optimal), the young fish would be expected to spend a much shorter time in the smallest, most vulnerable size categories. Conversely, when growth rates were low (food and temperature not optimal), juveniles would remain at the smallest, most vulnerable sizes for a much longer period and losses would be substantially higher. Death by starvation was not considered important, and questions of disease and pollution were studied by others.

SEA further speculated that not only were zooplankton necessary to promote the growth of the juveniles each year, but they might also represent important alternative prey for fish, birds and mammals that could also be targeting juvenile fishes. In years when springtime zooplankton stocks are large, consumers in the system conceivably derive more energy from plankton, reducing their demand for small fish. During years and seasons of low zooplankton abundance, consumers might be more likely to supplement their diets by eating more juvenile fish. Under these hypothesized conditions, zooplankton serves to modulate the degree of predation on small fishes by other consumers and could become a predictor of juvenile survival each year.

The data needed to test these ideas has been acquired since 1994. In 1997, a manuscript was submitted as the first effort to bring closure to this important issue (see Chapter 2 - Salmon Predation, this report). For a time-series where adult survivals were available from coded-wire tagged juveniles (hatchery releases), the duration of the spring-time copepod bloom, juvenile growth rate, body weight at release, and numbers of juveniles released were all variables predicting levels of adult success a year later. These results confirmed that alternative prey for fry predators is an important factor in the survival equation but by no means the only important variable.

Our first observations of predation on juvenile salmon by fishes implicated adult pollock feeding in the offshore waters adjacent to shallow fry nursery areas. As additional samples have been acquired, it has become more apparent that juvenile pollock, juvenile cod and tomcod, dolly varden trout, and herring are important predators as well. The latter regularly invade the shallow fry rearing areas increasing their chances of contacting fry schools. Further it has been shown that herring and juvenile pollock consume large quantities of zooplankton, but will switch to small fish when plankton resources decline. *Neocalanus* spp., a large calanoid copepod that swarms in near-surface layers during late April, May and early June is apparently responsible for providing much of the alternative zooplankton prey for these fishes. Observations in 1997 indicated that predation losses to fry populations were probably lower than estimated for the previous year apparently associated with fewer numbers of predators found in near-shore areas.

SEA's most recent numerical simulations of mechanisms reducing fry survival have focused on historical time-dependent survival patterns of coded-wire tagged fry released by PWSAC hatcheries. The total marine survival for each tag group has been reported by year and hatchery. These patterns of marine survival represent outcomes of natural experiments each year. If the

patterns are established by losses occurring mostly during early marine residence, SEA reasoned that this observed survival variability should be reproducible by model results based on field measurements of fry density, fry predators, and alternative prey for fry predators. This powerful approach to testing some of SEA's fundamental assertions was initiated in 1997.

The initial results from these simulations indicate that: 1) the time-series of observed survival versus pen release date have features that can be reproduced in the model by the early onset of high predation modified by the development of a zooplankton bloom; and 2) additional predation sheltering is apparently afforded by predator-swamping as serial releases increase the numbers of fry in near-shore nursery areas. Though preliminary, these model outcomes are in surprising agreement with the statistical approach discussed above, providing some of the first evidence that patterns of total marine survival within and between years are established by local events occurring during the early marine residence and not in deep-ocean feeding areas.

Pacific Herring Recruitment Dynamics

Fundamental aspects of the early life-history of Pacific herring are being described by field and laboratory studies of this important commercial and ecological species in Prince William Sound. Unlike pink salmon, juveniles and adult herring rear in, and inhabit the region during all months of the year. It is now understood that juveniles require sheltered, near-shore embayments during their first two years of life. Here they apparently draw energy from a mixture of open Sound and edge-zone forage resources. All herring store energy during the summer and fall in preparation for a presumed period of winter fasting when forage stocks are low.

SEA studies of juvenile herring have focused on population dynamics (age, length/weight, growth), on age-related population distributions, on forage resources, and on whole body energy concentrations and stable isotope signatures. The intent of this research has been to describe the general age composition of populations in the Sound, their distributions and environmental dependencies (food and habitat), and critical aspects of the life history that might provide clues to year-class success and patterns in long-term production histories. One of the major organizing ideas for this work has been the notion that juvenile overwintering survivals might establish subsequent levels of recruitment to adult populations in the Sound. Prolonged periods of fasting or accelerated metabolism (warmer winter temperatures) would be expected to place greater demands on energy reserves, with possibly higher mortalities than during cooler winters.

Following a period of broad-scale survey work to establish the general aspects of herring distributions in the Sound, the program selected 4 locations in the region for intensive seasonal study. Samples of the juveniles, their forage resources, and potential predators and competitors were obtained in Simpson Bay, Ziakof Bay, Eaglek Bay and Whale Bay. Field work included determining the distribution (acoustics; nets; aircraft observations) and abundance of juveniles rearing in each of the regions, measurements of their food resources, and assessments of their whole-body energy concentration and stable isotope ratios (carbon and nitrogen). These samples have been used to document the conditions leading to different levels of pre-winter condition, and measurements of the effects of the fast each winter. Starvation experiments with juvenile herring in the laboratory have established whole body energy levels below which survival is problematic.

SEA studies have determined that the Prince William Sound herring population is composed of three size modes (young of the year, 1-2 year old juveniles and sexually mature adults) and that these cohorts are contagiously distributed within the region. Juveniles are apparently restricted to embayments during their first two years, while adults move into shallow water to spawn (April), but immediately migrate away to offshore feeding areas after depositing their demersal eggs.

We are finding that the pre-winter whole body energy content of juveniles varies within schools and between locations - evidence that juvenile herring energy profiles are related to differences in food availability and physical conditions regulating growth (oceanography) at each of the study sites. Seasonal variations in temperature, salinity, and circulation are characteristic of the near-shore regime of Prince William Sound and are apparently related to the size and depth of embayments, tidal mixing and to sources and amounts of freshwater input. Differences in these characteristics between the four core study embayments will be used to evaluate how the physical environment fosters the growth, condition and subsequent survivals of juveniles each year.

An existing Wisconsin-type bioenergetics model for juvenile Baltic herring was used to estimate the consequences of deviations from winter mean temperatures on the fasting basal metabolism of juvenile Pacific herring. This model predicts a relative change of 5% of basal demand per degree change in temperature. Thus a 2 degree C change in average winter temperature would cause a decrease/increase of approximately 10% in the duration of the fast. Based on this result, and information on winter mean temperature variations, we now believe that climate effects on the length of the fast are probably not as important as the pre-fasting condition of the juveniles in the fall. Fortunately, the winter of 1997/98 was unusually warm (up by 2 C) which should allow an evaluation of the predicted shortening of the fast (about 10%) on the condition and survival of juveniles sampled in March, 1998. If the critical period of energy use is roughly 100 days (December through early March), and the model predictions are correct, the fast was reduced to 90 days over the winter of 1997/98. Juveniles were collected in March, 1998 to document their condition indices after the warmer than average conditions. Those results will be reported next year.

Finally, measures of the ratios of the stable isotopes of carbon have been used to infer the sources of food energy available to herring preparing for the winter fast. SEA has evidence that in 1995, a greater proportion of the energy in food was derived from zooplankton with Gulf of Alaska origins. This result suggests that certain, as-yet-to-be-described oceanographic conditions, provide linkages between Gulf-derived forage stocks and juvenile herring rearing in the Sound. Occasionally, the Gulf will feed inshore fishes.

The SEA herring study has also contributed to our overall understanding about the habitat requirements and distributions of juvenile pollock (the second most abundant species in SEA near-shore fish collections). Juvenile pollock are also a species of the edge-zone habitat, but occur deeper in the water than juvenile herring. There is some indication that their distributions may overlap in the surface waters at night. SEA intends to describe the ecological role of pollock in Prince William Sound as part of its synthesis activities.

Summary

Taken in aggregate, and in light of previous results reported by SEA, our findings in 1997 add substantially to the growing understanding of how Prince William Sound functions to promote or constrain the production of pink salmon and herring each year. We have been able to locate and describe critical rearing environments for the juvenile stages, and have simulated some of the processes defining mechanisms of mortality. It is unfortunate that we have not experienced a "lake" year in the region, since without that condition (high zooplankton abundance across the Sound) we are unable to confirm the strong production responses predicted by the models for this special case. Because the lake/river relationship has diminished over the SEA years despite the fact that the independent variable (upwelling index) has remained within the same range as prior to 1994, it seems likely that a fundamental change affecting April/May zooplankton stocks may have occurred even before SEA was initiated. This possibility is being sought in the published work of others studying the Gulf of Alaska prior to start up of SEA and progress will be reported in our close-out documentation. The ramifications for such a change will be investigated with the SEA models.

The users and managers of pink salmon and herring populations in Prince William Sound continue to have high expectations for results from this large program. To promote an exchange of information, SEA continues to work closely with Alaska Department of Fish and Game personnel, and to inform the public about its work each year. These briefings have been well attended, and many have asked about the possibility for extending the investigation into the future. The February supplement volume to the journal *Ecological Applications* titled Ecosystem Management for Sustainable Marine Fisheries hosts several papers by respected marine ecologists that point to the importance of understanding ecosystem-level control of fisheries production (Mooney, 1998; Fogarty, et al., 1998; Hoffman and Powell, 1998; Steele, 1998; Done and Reichelt, 1998) as a principal means for conserving stocks and sustaining productivity in the face of global change. It seems likely that enough will eventually be known about Prince William Sound so that ecosystem management of some commercial stocks can be implemented as an experimental high-latitude test case.

References

- Done, T. J. and R. E. Reichelt. 1998. Integrated coastal zone and fisheries ecosystem management: generic goals and performance indices. *Ecol. Applications*, 8 (1): S110-S118.
- Fogarty, M. J. 1988. Large-scale disturbance and the structure of marine systems: fishery impacts on Georges Bank. *Ecol. Applications*, 8 (1): S6-S22.
- Hofmann, E. T. and T. M. Powell. 1998. Environmental variability effects on marine fisheries: four case histories. *Ecol. Applications*, 8 (1): S23-S32.
- Mooney, H.A. 1998. Ecosystem management for sustained marine fisheries. *Ecol. Applications*, 8 (1): S1
- Steele, J. H. 1998. Regime shifts in marine ecosystems. *Ecol. Applications*, 8 (1): S33-S36.

Chapter 2

Juvenile Salmon Predation

Exxon Valdez Oil Spill
Restoration Project Annual Report

Sound Ecosystem Assessment: Juvenile Salmon Predation

Restoration Project 97320E
Annual Report

This annual report has been prepared for peer review as part of the *Exxon Valdez* Oil spill Trustee Council Restoration program for the purpose of assessing project progress. Peer review comments have not been addressed in this annual report.

Mark Willette
Mark Clapsadl
Penny Saddler
Margaret Powell

Alaska Department of Fish and Game
401 Railroad Avenue
Cordova, Alaska 99574

April 15, 1998

Study History: This project was initiated under Restoration project 94320E. An annual report was issued in 1994 by Willette, M., E. Debevec, Jay Johnson under the title Sound Ecosystem Assessment: Salmon Predation. The project effort was continued under Restoration Projects 95320E and 96320E. The final year of field sampling for this project in FY97 is the subject of this annual report. A final report will be prepared for project 320E in FY99.

Abstract: This project is a component of the Sound Ecosystem Assessment (SEA) program. SEA is a multi-disciplinary effort designed to acquire an ecosystem-level understanding of the marine and freshwater processes that interact to constrain levels of pink salmon and herring production in Prince William Sound (PWS). This project collected data needed to test several hypotheses related to predator-prey interactions affecting the mortality of pink salmon (*Oncorhynchus gorbuscha*) in PWS. Our efforts in 1997 focused on estimation of predator abundance, as well as predator behavior and feeding rates in nearshore habitats. Otolith marked juvenile salmon were also recovered to estimate stock composition and test for differences in size and growth of wild and hatchery salmon fry. Predation on juvenile salmon in nearshore habitats appeared to be lower in 1997 compared to 1996. Mean catch per net set at four sites sampled during both years in western PWS was lower for gadids, herring, and dolly varden trout during 1997 compared with 1996. The percent of the diet comprised of juvenile salmon was also lower for all taxonomic groups of potential predators in 1997 compared with 1996. As in previous years, dolly varden trout, Pacific cod and tomcod appeared to be relatively important predators on juvenile salmon in 1997. Further analyses will be conducted over the next year to evaluate the possible causes for these changes. In 1997, the relative abundance of nearshore benthic fish and herring was greater in eastern than western PWS. The proportion of wild- and hatchery-origin juvenile pink salmon emigrating from PWS was estimated from seine sampling and recovery of otolith thermal marks in the southwest passages in late June, 1997. Thirty-two percent of the pink salmon recovered originated from wildstock streams and the remainder from PWS hatcheries. Pink salmon originating from the Armin F. Koernig hatchery comprised the greatest proportion (33%) and those from the Solomon Gulch hatchery the smallest proportion (7%) of the fish sampled. Estimated energy contents indicated that fish originating from the Solomon Gulch hatchery were in the poorest condition. In 1997, sonic tagging methods were used to study the feeding behavior of age 3+ pollock. Two fish were successfully tagged and tracked for three to four days each. Both fish generally remained in the upper 50 m of the water column throughout the period of tracking. Estimated swimming speeds ranged from 0.04 to 0.11 m sec⁻¹. The fish did not exhibit diel vertical migrations or movements inshore at night. Results from field studies conducted since 1994 will be used to construct the SEA pink salmon recruitment model and conduct tests of the SEA predator/prey hypotheses.

Key Words: *Exxon Valdez*, pink salmon, *Oncorhynchus gorbuscha*, Pacific herring, *Clupea pallasii*, walleye pollock, *Theragra chalcogramma*, Pacific tomcod, *Microgadus proximus*, mortality, predation, food habits.

Citation: Willette, M., M. Clapsadl, P. Saddler, M. Powell. 1998. Sound ecosystem assessment: salmon and herring integration. Exxon Valdez oil spill restoration project annual report (Restoration project 97320E), Alaska Department of Fish and Game, Cordova, Alaska.

Table of Contents

	<u>Page</u>
List of Tables.....	4
List of Figures.....	5
Executive Summary.....	6
Introduction.....	8
Objectives.....	9
Methods.....	9
Results.....	12
Discussion.....	14
Conclusions.....	16
Acknowledgements.....	16
Literature Cited.....	17
Appendix I.....	28

List of Tables

	<u>Page</u>
Table 1: Dates and sites where sampling was conducted in nearshore habitats in Prince William Sound during May-June, 1996-1997. See figure 1 for locations of sampling areas.	20
Table 2: Mean catch per net set for various fish taxonomic groups in nearshore habitats in Prince William Sound during May and June, 1996-1997.	21
Table 3: Mean percent of diet comprised of juvenile salmon for several fish taxonomic groups during three time periods in northwest Prince William Sound during 1996 and 1997. Benthic fishes include various species of sculpin and greenlings. Statistical test for changes in the mean diet percentage comprised of juvenile salmon among time periods. All specimens included in the analysis.	22

List of Figures

	<u>Page</u>
Figure 1:	23
Figure 2:	24
Figure 3:	25
Figure 4:	26
Figure 5:	27

Figure 1: Study sites sampled in Prince William Sound during May-June, 1996-1997.

Figure 2: Mean catch per net set for five taxonomic groups of potential predators on juvenile pink salmon in eastern (solid squares) and western Prince (solid circles) William Sound during May-June 1997. Results from analysis of variance tests for a difference in catch per net set between eastern and western Prince William Sound are indicated.

Figure 3: Mean catch per net set for three taxonomic groups of potential predators on juvenile pink salmon in western Prince William Sound during May-June 1996 (solid squares) and 1997 (open circles). Results from analysis of variance tests for a difference in catch per net set between years are indicated above each group.

Figure 4: (a) Total zooplankton biomass and abundance (no./m³) of (b) large calanoid copepods, (c) small calanoid copepods, and (c) other zooplankters in offshore habitats in Prince William Sound, May-June 1997.

Figure 5: Origins of juvenile pink salmon sampled during late June in southwest Prince William Sound based on recovery of otolith thermal marks. Estimated energy content (derived from moisture content) of wild- and hatchery-origin juvenile pink salmon during 1996 and 1997. Results from analysis of variance tests for a differences in estimated mean energy content between hatcheries within years are indicated. The following codes are used: Armin F. Koernig Hatchery (AFK), Cannery Creek Hatchery (CC), Solomon Gulch Hatchery (VFDA), Wally H. Noerenberg Hatchery (WHN).

Executive Summary

This project is a component of the Sound Ecosystem Assessment (SEA) program. SEA is a multi-disciplinary effort designed to acquire an ecosystem-level understanding of the marine and freshwater processes that interact to constrain levels of pink salmon and herring production in Prince William Sound (PWS). This project collected data needed to test several hypotheses related to predator-prey interactions affecting the mortality of pink salmon (*Oncorhynchus gorbuscha*) in PWS. These hypotheses include the following: (1) predation on juvenile salmon and other age-0 fish is inversely related to the abundance of large calanoid copepods, (2) predation risk is related to the daily foraging times of juvenile salmon, and (3) predation on wild salmon fry is greater when wild fry are mixed with larger hatchery-reared fish. This project was designed to achieve the following objectives: (1) estimate the juvenile salmon consumption rate of fish predators in PWS, (2) estimate the species/size composition of fish predators, and (3) conduct preliminary tests of predator/prey hypotheses. This project also provided logistical support (personnel and equipment) to the SEA herring program.

Our efforts in 1997 focused on estimation of predator abundance, as well as predator behavior and feeding rates in nearshore habitats. Studies were conducted at eight nearshore sites during each of three date periods in PWS during May and June. Four of these sites were located in areas dominated by wild salmon in eastern PWS and four in areas dominated by hatchery salmon in western PWS. Each nearshore study site consisted of an approximately 3000 m long segment of shoreline. Potential predators on juvenile salmon were sampled using variable-mesh gillnets. Sampling was conducted at two stations every 3 hours throughout a 12-hour period spanning the night. Otolith marked juvenile salmon were also recovered at each site to estimate stock composition and test for differences in size and growth of wild and hatchery salmon fry. Laboratory analyses of these samples is still ongoing.

In general, predation on juvenile salmon in nearshore habitats appeared to be lower in 1997 compared to 1996. Mean catch per net set at four sites sampled during both years in western PWS was lower for gadids, herring, and dolly varden trout during 1997 compared with 1996. The percent of the diet comprised of juvenile salmon was also lower for all taxonomic groups of potential predators in 1997 compared with 1996. As in previous years, dolly varden trout, Pacific cod and tomcod appeared to be relatively important predators on juvenile salmon in 1997. But unlike previous years, age 1-2 pollock apparently consumed only small amounts of juvenile salmon. Further analyses will be conducted over the next year to evaluate the possible causes for these changes. In 1997, the relative abundance of nearshore benthic fish and herring was greater in eastern than western PWS. The relative abundance of adult salmon and dolly varden trout increased from May to June in both areas sampled. For tomcod, the proportion of the diet comprised of juvenile salmon was significantly greater in western than eastern PWS, but there was no difference in the proportion of the diet comprised of salmon between these two areas for the other taxonomic groups.

The proportion of wild- and hatchery-origin juvenile pink salmon emigrating from PWS was estimated from seine sampling and recovery of otolith thermal marks in the southwest passages in late June, 1997. Thirty-two percent of the pink salmon recovered originated from wildstock streams and the

remainder from PWS hatcheries. Pink salmon originating from the Armin F. Koernig hatchery comprised the greatest proportion (33%) and those from the Solomon Gulch hatchery the smallest proportion (7%) of the fish sampled. Estimated energy contents indicated that fish originating from the Solomon Gulch hatchery were in the poorest condition.

In 1997, sonic tagging methods were used to study the diel feeding behavior of age 3+ pollock. Two fish were successfully tagged and tracked for three to four days each. Both fish generally remained in the upper 50 m of the water column throughout the period of tracking. Estimated swimming speeds ranged from 0.04 to 0.11 m sec⁻¹. The fish did not exhibit diel vertical migrations or movements inshore at night. Results from field studies conducted since 1994 will be used to construct the SEA pink salmon recruitment model and conduct tests of the SEA predator/prey hypotheses.

Introduction:

This project is a component of the Sound Ecosystem Assessment (SEA) program. SEA is a multi-disciplinary effort to acquire an ecosystem-level understanding of the marine and freshwater processes that interact to constrain levels of pink salmon and herring production in Prince William Sound (PWS). Pink salmon runs to PWS failed in 1992 and 1993, and herring biomass dropped sharply in 1993. These run failures have drastically affected the economy of the PWS region which is largely based on the salmon and herring resources. In 1992, pink salmon returns were low in Kodiak, Lower Cook Inlet, and PWS, but pink salmon returns in 1993 were low only in PWS. Low returns of hatchery-produced salmon in both years indicates that the failures were likely caused by processes occurring during the juvenile lifestage. Damage assessment studies on juvenile pink salmon in PWS have demonstrated that growth during the juvenile lifestage is related to survival to adult (Willette et al. 1994). Growth rates of juvenile salmon were estimated in 1991 and 1992 after the fish were released from hatcheries. Juvenile growth and ocean temperatures were low in PWS during the early marine period in 1991. However, in 1992 juvenile growth and ocean temperatures were near average; although, zooplankton abundance was very low. The growth of juvenile fishes is believed to be related to survival, because slow-growing individuals are vulnerable to predators for a longer time (Parker 1971; Healey 1982; West and Larkin 1987). The growth and mortality rates of juvenile salmon released into PWS in 1992 suggests that a change in predation rate may have contributed to the observed run failures.

During phase I of SEA, pink salmon research focused on identification of the principal species preying on pink salmon and the processes affecting rates of predation. Phase I results indicate that predation by pelagic pollock (age 3+) and seabirds may account for only 15-25% of probable losses of juvenile salmon (Willette et al. 1995b). However, results from an experimental release of large juvenile pink salmon from Wally H. Noerenberg Hatchery suggests that high mortality likely occurred among an early release of small juvenile pink salmon during May, 1994 (Willette et al. 1995a). Age 3+ pollock and squid were the most abundant species in net catches during May, 1994 (Willette et al. 1994b). The following three hypotheses have been developed from our phase I results: (1) predation by age 3+ pollock in offshore habitats was underestimated in 1994, (2) age 3+ pollock that target juvenile salmon in nearshore habitats account for the majority of the predation losses and these predators were not sampled adequately in 1994, (3) other nearshore fish predators not sampled in 1994 account for the majority of the predation losses, and (4) high condition of the late release group resulted in differential mortality between early and late releases after early June.

Several factors may have resulted in underestimation of juvenile salmon consumption by pelagic age 3+ pollock. Pollock biomass may have been underestimated due to vessel avoidance, occurrence of pollock in the surface layer (0-5m) that was not surveyed, and occurrence of pollock below 125 m depth that was not surveyed. These questions are being addressed by project (97320N). In addition, pollock food consumption may have been underestimated if the fish are glut feeding in the surface layer then migrating to depth to rest. This project conducted sonic

tagging studies in FY97 to evaluate the migratory behavior of age 3+ pollock. Sonic telemetry has been used successfully to investigate the daily activity and movement patterns of juvenile Atlantic cod (Clark and Green 1990). During summer, these fish migrated between a warm surface layer to feed at night and a deep cold layer to rest during the day. Much of our effort in FY97 focused on sampling predators in nearshore habitats that may not have been adequately sampled in previous years. This involved sampling with variable mesh gillnets to obtain samples for stomach contents analysis and estimate the species\size composition of potential predators on juvenile salmon.

This project also collected samples to evaluate whether condition-dependent predation may lead to differential mortality of juveniles rearing in nearshore habitats. If condition-dependent predation occurs the presence of large numbers of enhanced salmon may adversely affect wild salmon during the early marine period. An inverse relationship between whole body energy content and fry density at three sites sampled in 1995 suggests that growth may be density-dependent (Paul and Willette 1996). All juvenile pink salmon released from PWS hatcheries will be otolith thermal marked in FY97 providing an essential tool for these investigations. Seine sampling of juveniles emigrating from PWS was also initiated in FY97. It is anticipated that this effort will provide estimates of the proportions of wild- and hatchery-origin juveniles as well as the relative abundance of juveniles emigrating from the Sound (Karpenko 1998). This data will be used to validate the SEA pink salmon recruitment model.

Objectives:

1. Refine estimates of juvenile salmon consumption by pelagic pollock.
2. Estimate the species/size and diet composition of potential predators on juvenile salmon in nearshore habitats.
3. Evaluate condition-dependent predation among wild and hatchery salmon, and estimate the proportions of wild- and hatchery-origin juvenile salmon emigrating from PWS.
4. Use field data to evaluate SEA predator-prey hypotheses.

Methods:

Objective 1:

A sonic tagging study was conducted to examine the diel behavior of pelagic age 3+ pollock during the spring bloom period. Two pollock were tagged and tracked continuously for a total of eight days in June 1997. Fish were collected using a small-mesh purse seine (250 m x 30 m, 1.5 cm stretch mesh web) deployed from a commercial seine vessel. Fish were placed in a 30-gal. container and anesthetized with MS-222. A Vemco™ V16 depth sensitive sonic tag was attached

to the fish between the second and third dorsal fin segment using Kevlar line and suture needles. Each fish was held until recovered (less than 3 minutes) prior to release. A global positioning system (GPS) was used to determine position. Tracking of position and depth of the fish commenced immediately upon release, using the Vemco™ V60 directional receiver operated from a 7 m vessel. Depth and position readings were recorded at least every 15 minutes and whenever any detectable rapid movements occurred. CTD casts were made frequently to determine the temperature gradient in the water column occupied by the tagged fish.

The swimming speed of each fish was estimated from movements of the fish relative to measured current velocities. A drogue and a GPS were employed to calculate current velocity. The drogue, which was connected by a thin Kevlar line to a small lighted buoy, was periodically placed in the water column at the approximate depth of the tagged fish. Initial positions of both the drogue and the fish were simultaneously recorded. After a period of at least 30 minutes, the positions of both the fish and the drogue were again recorded as well as elapsed time. These data were used to calculate the vector of the current at the depth of the tagged fish and the vector of the fish. These vectors were used to calculate the swimming speed of the fish.

Objective 2:

Investigations of predator/prey coupling in the nearshore zone were continued in FY97. Eight sites were sampled during three 9-day sampling trips in May and June (Figure 1, Table 1). Acoustic and net sampling were conducted every three hours from approximately 9 pm to 9 am each day. Project 97320N conducted acoustic surveys utilizing side-looking (420kHz) and downlooking echosounders (120kHz). Acoustic data was collected on one alongshore transect on each three hour cycle to estimate the abundance of predators and juvenile salmon in the nearshore zone. Acoustic data was also collected along five transects perpendicular to shore to relate nearshore and offshore predator abundances. A purse seine vessel sampled fish in the upper 20 m of the water column in nearshore areas with bottom depths greater than 20 m. The seine vessel deployed a small-mesh purse seine (250 m x 30 m, 1.5 cm stretch mesh web) holding a hook with the seine open in the direction of the prevailing current for 20 minutes. In nearshore areas shallower than 20 m, variable mesh sinking and floating gill nets (150 m, 1.5 cm to 10 cm stretch mesh) were used to sample fish predators. These gear were deployed from an approximately 6 m aluminum skiff. Each gill net was attached to the beach and set perpendicular to shore. A hotel boat provided room and board for field sampling crews. All sample processing was conducted on board the hotel boat by a single processing crew.

Processing of fish samples from each net set occurred in two stages following procedures outlined by Livingston (1989) and Dwyer et al. (1987). If less than 300 fish were captured, all fish in the catch were enumerated by species. If a large number of fish were caught, species composition was estimated from a random sample of 300 individuals. Fish greater than 150 mm FL were processed differently than those less than 150 mm FL. Fish less than 150 mm FL were identified to the lowest possible taxonomic level. A sample of 30 individuals from each species was preserved in 10% buffered formaldehyde for later analysis of stomach contents under project 97163 (Forage

Fish Influence on Recovery of Injured Species). The purpose of these studies is to examine diet overlap among forage fish.

For large fish (greater than 150 mm FL), a randomly selected sample (n=60) from each net set and each species was taken. The stomach was excised, placed in a cloth bag, and preserved in 10% buffered formaldehyde for later analysis of stomach contents. Fish showing evidence of regurgitation were not included in the sample. Fork length was measured to the nearest millimeter. Weight was measured to the nearest gram when conditions permitted. Sex and sexual maturity was recorded. Later in the laboratory, total stomach contents wet weight was measured to the nearest .01 gram. Invertebrate prey in the gut were generally identified to the family level. Fish in the gut were identified to the lowest possible taxonomic level, enumerated, and measured to the nearest millimeter. The proportion of total stomach contents in each taxonomic group was visually estimated. Stomach fullness was expressed as a proportion of fish body weight. In cases where distinct size classes occurred within species, stomach contents analysis was conducted for each size class as described above. Size related shifts in diet toward piscivory have been noted in several species of gadoid fishes, including Pacific cod (*Gadus macrocephalus*) (Livingston 1989), walleye pollock (*Theragra chalcogramma*) (Dwyer et al. 1987), Atlantic cod (*Gadus morhua*) (Daan 1973), Pacific whiting (*Merluccius productus*) (Livingston 1983), and silver hake (*Merluccius bilinearis*) (Langton 1982).

An analysis of variance was conducted to test for differences in the natural-logarithm transformed mean catch per net set of potential predators on juvenile salmon by date period (5/13-5/21, 5/26-6/3, and 6/10-6/18) as well as between the four sites in western and eastern PWS, respectively. An analysis of variance was also conducted to test for differences in the natural-logarithm transformed mean catch per net set of potential predators between 1996 and 1997. Only four sites in western PWS which were sampled in both years using the same gear type were included in the analysis.

An analysis of variance was conducted to test for differences in the mean percent of predator diets comprised of juvenile salmon among three date periods in May and June. Data were arcsin square root transformed prior to conducting the test (Zar 1984). Several species of nearshore benthic fish (*Hemilepidotus hemilepidotus*, *Myxocephalus verrucosus*, *Hexagrammos decagrammus*, *Hexagrammos octogrammus*, *Blepsias bilobus*) were pooled in the analysis. All specimens were included in the analysis to examine changes in diet for the population within each taxonomic group as a whole.

Objective 3:

At each site, two samples (n=20) of juvenile salmon were obtained with a small mesh purse seine (10 m x 40 m, 2 mm mesh) deployed from an approximately 4 m skiff every three hours. All samples were frozen as soon as possible after collection. At each site, CTD and zooplankton samples (20m vertical tow, 243 um mesh) were also collected in association with each fry sample to evaluate environmental conditions. In the laboratory, the otolith was extracted from each

juvenile pink salmon, length was measured to the nearest millimeter, wet weight to the nearest .01 g and stomach contents weight to the nearest milligram. The proportion of total stomach contents weight in three taxonomic groups (large calanoid copepod (>2.5 mm), small calanoid copepod (<2.5 mm), and 'other' prey) was visually estimated. Otolith thermal marks were used to determine the wild or hatchery-origin of the fish. Zooplankton samples were subsampled with a stimpel pipette and zooplankton enumerated into the following groups: large calanoid copepod (>2.5 mm), small calanoid copepod (<2.5 mm), and 'other' zooplankters.

The proportion of wild- and hatchery-origin juvenile pink salmon emigrating from PWS was estimated from seine sampling at seven sites in the southwest passages of PWS during late June. A purse seine vessel sampled fish in the upper 20 m of the water column in nearshore areas with bottom depths greater than 20 m. The seine vessel deployed a small-mesh purse seine (250 m x 30 m, 1.5 cm stretch mesh web) holding a hook with the seine open in the direction of the prevailing current for 20 minutes. A sample (n=100) of juvenile salmon was taken from each net set and immediately frozen for later laboratory analysis. In the laboratory, the otolith was extracted from each juvenile pink salmon, length was measured to the nearest millimeter, headless stomachless wet weight to the nearest 0.01 mg and stomach contents weight to the nearest 0.01 mg. Each headless stomachless fish was dried to a constant weight at 80° C and then weighed to the nearest 0.01 mg. Energy content was estimated from moisture content using data provided by Parker and Vanstone (1966).

Objective 4:

See appendix I.

Results:

Objective 1:

The first fish was tagged at Unakwik Inlet at 0230 on May 31, 1997 and was tracked until 0225 on June 4, 1997. After release the fish immediately swam to a depth of 14 m and remained within a few meters of this depth for several hours. After this time any changes in depth were generally gradual. The fish ranged from 3 to 19 m in depth over the 4-day tracking period, averaging 8.67 m (sd = 3.05 m). The fish covered 14.5 km of horizontal distance over the tracking period but never moved more than 3.5 km from the original point of capture. The fish generally remained within the thermocline at temperatures ranging from 6-10 °C, in waters where the bottom depth exceeded 100 m. The results from two drogue-swimming speed trials indicated that the tagged fish was actively swimming at 0.08 and 0.09 m s⁻¹. No diel patterns of vertical migration or movements inshore at night were observed.

A second fish was tagged at Sheep Bay on June 12, 1997 at 0100 and was tracked until 0030 on June 16, 1997. After release the fish swam to a depth of about 35 m and then quickly moved to a

depth of 13 m. The fish then began a gradual descent reaching about 68 m at 2300 hrs on June 16. By 0030 on June 17, the fish had ascended to around 45 m in 60 m of water. It remained approximately at this depth throughout June 17. On June 18 the fish made two rapid descents and ascents in 60 and 70 m of water. Both of these descents took the fish very near to the bottom, and both ascents took the fish back to around 50 m depth. On the last full day of tracking the fish made multiple descents and ascents that were 5-10 m in magnitude. The mean depth of the fish for the duration of the tracking period was 43.6 m (sd = 11.41 m) with a range from 13 to 72 m. It was generally below the thermocline in water approximately 5 °C. No diel patterns of vertical migration or movements inshore at night were observed.

The horizontal movements of the fish tagged at Sheep Bay were similar to those of the fish tracked at Unakwik Inlet. Both fish remained within 5 km of the release point and moved a total of less than 20 km. Multiple drogue-swimming speed trials indicated that swimming speeds averaged 0.067 m s⁻¹ (sd = 0.028 m s⁻¹) with a range from 0.040 to 0.110 m s⁻¹. No trends between proximity to shore and time of day were observed and no trends between pollock position and temperature were observed.

Objective 2:

Nearshore benthic fishes (rockfish, sculpins, greenlings, etc.), gadids (Pacific cod, tomcod, and black cod) and herring were the most abundant taxonomic groups in nearshore gill net catches in 1997 (Table 2). The relative abundances of nearshore benthic fishes, gadids and herring were significantly greater ($P < 0.01$) in eastern than western PWS in 1997 (Figure 2). In addition, the relative abundance of gadids increased from May to June in eastern PWS but not in western PWS (Figure 2). The relative abundance of adult salmon and dolly varden trout increased significantly ($P < 0.01$) from May to June in both areas sampled. Comparison of relative abundances of fishes between 1996 and 1997 at four western PWS sites indicated significantly greater ($P < 0.01$) abundances of gadids, herring and dolly varden trout in 1996 (Figure 3).

Approximately 3,400 stomach samples from potential predators on juvenile salmon were examined in 1997. The mean proportion of the diet comprised of juvenile salmon was substantially lower in 1997 than in 1996 for all taxonomic groups of potential predators (Table 3). The mean proportion of tomcod diets comprised of juvenile salmon decreased significantly ($P = 0.001$) from May to June, 1997 (Table 3). The mean proportion of benthic fishes diets comprised of juvenile salmon was greatest during late May, 1997 (Table 3). For the other taxonomic groups included in the analysis, there were no significant differences in the mean proportion of the diet comprised of juvenile salmon between the three date periods (Table 3). For tomcod, the mean proportion of the diet comprised of juvenile salmon was significantly greater ($P < 0.01$) in western (13.5 %) than eastern PWS (1.3 %) but there was no difference ($P > 0.05$) in the proportion of the diet comprised of salmon between these two areas for the other taxonomic groups.

Objective 3:

Laboratory analyses of juvenile pink salmon samples collected at each nearshore study sites in 1997 are ongoing. Therefore, a complete dataset from 1997 is not currently available for evaluation of condition-dependent predation on juvenile salmon. In 1997, total zooplankton biomass in the passages adjacent to each study site peaked in mid-May and thereafter ranged from approximately 0.1-0.3 g m⁻³ (Figure 4a). The abundance of large calanoid copepods ranged from 0-100 m⁻³ and did not exhibit a clear seasonal decline (Figure 4b). The abundance of small copepods and 'other' zooplankters exhibited a peak in mid-May followed by a general decline (Figures 4c and 4d).

Thirty-two percent of the juvenile pink salmon sampled in the southwest passages of PWS during late June, 1997 originated from wildstock streams and the remainder from PWS hatcheries. Pink salmon originating from the Armin F. Koernig hatchery comprised the greatest proportion (33%) and those from the Solomon Gulch hatchery the smallest proportion (7%) of the fish sampled (Figure 5). Estimated energy content (derived from moisture content) ranged from approximately 4.6-5.0 KJ g⁻¹ (Figure 5). Estimated energy content was generally greater in 1996 than in 1997, and the fish originating from the Solomon Gulch hatchery appeared to be in the poorest condition during both years (Figure 5).

Objective 4:

See appendix I.

Discussion:

Sampling with fixed gear in nearshore habitats revealed an assemblage of fish species that may be important predators on juvenile salmon. The species composition of this assemblage was generally similar between 1996 and 1997 (Table 2). Fixed gear sampling in 1997 consisted of sinking and floating variable-mesh gillnets deployed from the shore in nearshore habitats. These gear appeared to be very efficient for capturing potential predators in shallow nearshore habitats.

In general, predation on juvenile salmon in nearshore habitats appeared to be lower in 1997 compared with 1996. Mean catch per net set at four sites sampled during both years in western PWS was lower for gadids, herring, and dolly varden trout during 1997 compared with 1996 (Figure 3). The percent of the diet comprised of juvenile salmon was also lower for all taxonomic groups of potential predators in 1997 compared with 1996 (Table 3). The cause of these changes is unclear at this time.

As in previous years, dolly varden trout (*Salvelinus malma*), age 1-2 Pacific cod (*Gadus macrocephalus*) and Pacific tomcod (*Microgadus proximus*) appeared to be relatively important

predators on juvenile salmon (Willette et al. 1995b, 1996b, 1997). However, unlike previous years age 1-2 pollock apparently only consumed small amounts of juvenile salmon (Table 3). Bakshtanskiy (1964) concluded that juvenile pollack (*Pollachius virens*) and cod (*Melanogrammus morhua morhua*) were important predators on juvenile pink and chum salmon in the White Sea. He observed that juvenile pink and chum salmon were at times driven from nearshore nursery habitats by large schools of juvenile pollack and cod. Consumption of juvenile salmon by nearshore benthic fish and herring appeared to increase in early June, 1996, but this pattern was not apparent in 1997 (Table 3). Bakshtanskiy (1964, 1965) concluded that predation by herring largely determined survival of juvenile pink and chum salmon in the Barents Sea and White Sea. Predation by herring and pollock on juvenile salmon has also been observed in Alaska (Thorsteinson 1962, Armstrong and Winslow 1968).

Mean catch per net set of herring and age 1-2 pollock tended to increase from May to June in 1996 (Willette et al. 1997). A similar seasonal increase in net catches was observed for all gadids in eastern PWS in 1997, but no seasonal increase in relative abundance was observed for herring or gadids in western PWS in 1997 (Figure 2). Rogers et al. (1986) noted a substantial seasonal increase in fish species diversity and density in PWS. In winter, fish distributions shifted further offshore and deeper in the water column (Rogers et al. 1986). Seasonal migrations of fish into deeper water in winter and shallow water in summer are well known (Trout 1957, Alverson 1960, Jean 1964, Heeseen 1983). These seasonal shifts in distribution may be related to temperature, light or food abundance (Laevastu and Hela 1970). Seasonal changes in the vertical distribution and activity patterns of cod have been related to seasonal stratification of the water column (Clark and Green 1990).

Sonic tagging studies of age 3+ pollock behavior suggest that this technique may be used effectively on this species. These studies were initiated to determine whether age 3+ pollock were glut feeding on large calanoid copepods in the surface layer or on juvenile salmon in nearshore habitats and then descending to depth for gastric evacuation. The results from our limited studies in 1997 indicated that adult pollock were not vertically migrating or moving inshore at night. The fish generally remained in the surface layer near the bottom of the thermocline. However, acoustic data collected by project 97320N and our net catch data indicated relatively low abundances of adult pollock in the surface layer during May-June 1997. Results from previous years indicated that adult pollock only remained in the surface layer when the abundance of macrozooplankton was relatively high during May and early June (Willette et al. 1995b, 1996b, 1997). In 1997, adult pollock were in relatively low abundance in the surface layer suggesting that macrozooplankton may not have been present at sufficient densities for profitable feeding. The first fish was not tagged until June 12, because of low pollock abundances and the resulting difficulties catching fish for the study. Therefore, the results from the present study may not be representative of the feeding and migratory behavior exhibited by adult pollock feeding on macrozooplankton during the peak of the bloom.

Conclusions:

1. Predation on juvenile salmon appeared to be lower in 1997 compared with 1996.
2. Dolly varden trout, Pacific cod, and tomcod appeared to be relatively important predators on juvenile salmon in nearshore habitats in 1997.
3. Catches of juvenile pink salmon emigrating from PWS appeared to be dominated by hatchery-origin fish. Estimated energy content indicated that fish originating from the Solomon Gulch hatchery were in the poorest condition.
4. Sonic tagging of age 3+ pollock appears to be an effective method for studying the behavior of these fish. The fish tagged in 1997 did not exhibit diel vertical migrations or movements inshore at night.

Acknowledgements:

We would like to thank the staff of the Alaska Department of Fish and Game, Prince William Sound Science Center, and University of Alaska Fairbanks who endured difficult field conditions to obtain the samples needed for this study. The staff of the Prince William Sound Aquaculture Corporation was always very helpful when we needed logistical support in the western sound. This project would not have been possible without the charter vessel captains and crew who provided their equipment, assistance, and expertise.

Literature Cited:

- Alverson, D.L. 1960. A study of annual and seasonal bathymetric catch patterns for commercially important groundfishes of the Pacific Northwest coast of North America. Bull. Pacific Mar. Fish. Comm. Portland. 4, 66p.
- Armstrong, R.H. and P.C. Winslow. 1968. An incidence of walleye pollock feeding on young salmon. Trans. Amer. Fish. Soc. 97(2): 202-203.
- Bakshanskiy, E.L. 1964. Effect of predators on the young of *Oncorhynchus gorbusha* and *Oncorhynchus keta* in the White and Barents Seas. Voprosy Ikhtiologii 4(1): 136-141.
- Bakshanskiy, E.L. 1965. The impact of the environmental factors on survival of the far eastern young salmon during the acclimatization of the latter in the northwest part of the USSR. ICNAF Spec. Publ. 6: 477-479.
- Clark, D.S. and J.M. Green. 1990. Activity and movement patterns of juvenile Atlantic cod, *Gadus morhua*, in Conception Bay, Newfoundland, as determined by sonic telemetry. Can. J. Zool. 68: 1434-1442.
- Cooney, R.T. 1995. The role of zooplankton in the Prince William Sound Ecosystem. In Sound Ecosystem Assessment 1994 Final Report to the *Exxon Valdez* Oil Spill Trustee Council, 13p.
- Crowder, L.B. 1985. Optimal foraging and feeding mode shifts in fishes. Environ. Biol. Fish. 12(1): 57-62.
- Daan, N. 1973. A quantitative analysis of the food intake of North Sea cod, *Gadus morhua*. Neth. J. Sea Res. 6: 479-517.
- Dwyer, D.A., K.M. Bailey, P.A. Livingston. 1987. Feeding habits and daily ration of walleye pollock (*Theragra chalcogramma*) in the eastern Bering Sea, with special reference to cannibalism. Can. J. Fish. Aquat. Sci. 44: 1972-1984.
- Healey, M.C. 1982. Timing and relative intensity of size-selective mortality of juvenile chum salmon during early sea life. Can. J. Fish. Aquat. Sci. 39: 952-957.
- Heessen, H.J.L. 1983. Distribution and abundance of young cod and whiting in the southeastern North Sea in the period 1980-1982. Int. Coun. Expl. Sea., C.M. 1983/G: 30.
- Jean, Y. 1964. Seasonal distribution of cod (*Gadus morhua* L.) along the Canadian Atlantic coast in relation to water temperature. J. Fish. Res. Board Can. 21: 429-460.

- Karpenko, V.I. 1998. Ocean mortality of northeast Kamchatka pink salmon and influencing factors. N. Pac. Anadr. Fish Comm. Gull. No. 1: 251-261.
- Laevastu, T. and I. Hela. 1970. Fisheries Oceanography. Fishing News Ltd., London, 238p.
- Langton, R.W. 1982. Diet overlap between Atlantic cod, *Gadus morhua*, silver hake, *Merluccius bilinearis*, and fifteen other northwest Atlantic finfish. Fish. Bull. 80: 745-759.
- Livingston, P.A. 1983. Food habits of Pacific whiting, *Merluccius productus*, off the west coast of North America, 1967 and 1980. Fish. Bull. 81: 629-636.
- Livingston, P.A. 1989. Interannual trends in Pacific Cod, *Gadus macrocephalus*, predation on three commercially important crab species in the eastern Bering Sea. Fish. bull. 87: 807-827.
- Parker, R.R. and W.E. Vanstone. 1966. Changes in chemical composition of central British Columbia pink salmon during early sea life. J. Fish. Res. Bd. Canada 23(9): 1353-1383.
- Parker, R.R. 1971. Size-selective predation among juvenile salmonid fishes in a British Columbia inlet. J. Fish. Res. Board Can. 28: 1503-1510.
- Paul, A.J. and T.M. Willette. 1996. Geographical variation in somatic energy content of migrating pink salmon fry from Prince William Sound: a tool to measure nutritional status. In Proceedings of the Wakefield Forage Fish Symposium, Alaska Sea Grant Program, in press.
- Rogers, D.E., B.J. Rogers and R.J. Rosenthal. 1986. The nearshore fish. pp. 399-416 In D.W. Hood and S.T. Zimmerman (eds.), The Gulf of Alaska: physical environment and biological resources. NOAA, Anchorage, Alaska.
- Thorsteinson, F.V. 1962. Herring predation on pink salmon fry in a southeastern Alaska estuary. Trans. Am. Fish. Soc. 91(3): 321-323.
- Trout, G.C. 1957. The bear Island cod: migrations and movements. Fish. Invest. London. Ser. 2(21): 51p.
- West, C.J. and P.A. Larkin. 1987. Evidence of size-selective mortality of juvenile sockeye salmon (*Oncorhynchus nerka*) in Babine Lake, British Columbia. Can. J. Fish. Aquat. Sci. 44: 712-721.
- Willette, T.M., G. Carpenter, P. Shields, S. Carlson. 1994. Early marine salmon injury assessment in Prince William Sound. Exxon Valdez Natural Resource Damage Assessment Program, Final Report, Alaska Department of Fish and Game, 64p.

- Willette, T.M., G. Carpenter, E. Debevec. 1995a. Sound ecosystem assessment: salmon growth and mortality. *Exxon Valdez* Oil Spill Restoration Project Annual Report (Restoration Project 94320A), Alaska Department of Fish and Game, Anchorage, Alaska.
- Willette, T.M., E. Debevec. J. Johnson. 1995b. Sound ecosystem assessment: salmon predation. *Exxon Valdez* Oil Spill Restoration Project Annual Report (Restoration Project 94320E), Alaska Department of Fish and Game, Anchorage, Alaska.
- Willette, T.M., G. Carpenter, P. Saddler, M. Powell. 1996a. Sound ecosystem assessment: salmon growth and mortality. *Exxon Valdez* Oil Spill Restoration Project Annual Report (Restoration Project 95320A), Alaska Department of Fish and Game, Anchorage, Alaska.
- Willette, T.M., E. Debevec. J. Johnson. 1996b. Sound ecosystem assessment: salmon predation. *Exxon Valdez* Oil Spill Restoration Project Annual Report (Restoration Project 95320E), Alaska Department of Fish and Game, Anchorage, Alaska.
- Willette, T.M., M. Clapsadl, P. Saddler, M. Powell. 1997. Sound ecosystem assessment: salmon predation. *Exxon Valdez* Oil Spill Restoration Project Annual Report (Restoration Project 96320E), Alaska Department of Fish and Game, Anchorage, Alaska.
- Yoshida, H. 1994. Food and feeding habits of pelagic walleye pollock in the central Bering Sea in summer, 1976-1980. *Sci. Rep. Hokkaido Fish. Exp. Stn.* 45: 1-35.
- Zar, J.H. 1984. *Biostatistical Analysis*. Prentice-Hall, Englewood Cliffs, New Jersey.

Table 1: Dates and sites where sampling was conducted in nearshore habitats in Prince William Sound during May-June 1996-1997. See figure 1 for locations of sampling areas.

Year	Area	Dates Sampled
1996	501	May 3, May 6, June 5
	502	May 4, May 7, May 24, June 1
	525	May 5, May 8, May 19, May 23, June 2, June 8
	504	May 25, June 6
	506	May 20, June 7
	586	May 21, June 3
	587	May 22, June 4
1997	502	May 19, June 1
	505	June 16
	525	May 20, June 2, June 17
	585	May 15, May 28, June 12
	586	May 17, May 30, June 14
	587	May 18, May 31, June 15
	588	May 13, May 26, June 10
	589	May 14, May 27, June 11
	590	May 16, May 29, June 13

Table 2: Mean catch per net set for various fish taxonomic groups in nearshore habitats in Prince William Sound during May and June, 1996-1997 .

Species	1996			1997		
	n	Mean	SE	n	Mean	SE
Sculpins, gunnels, etc.	86	1.6	0.11	107	0.5	0.98
Pacific cod, tomcod	122	3.4	0.35	142	1.9	4.51
Flatfish	8	1.0	0.00	40	0.2	0.60
Greenlings	155	2.6	0.17	187	1.0	1.29
Rockfish	149	6.3	0.83	212	3.7	6.58
Herring	130	87.8	36.90	113	111.5	1256.52
Pollock	63	5.7	1.44	63	0.7	2.89
Adult Salmon	30	2.5	0.58	24	0.1	0.71
Sandlance, capelin	1	1.0	-	0	0	0
Dolly Varden	48	4.2	0.76	49	0.4	2.04
Squid	15	1.6	0.36	13	0.1	0.25

Table 3: Mean percent of diet comprised of juvenile salmon for several fish taxonomic groups during three time periods in northwest Prince William Sound during 1996 and 1997. Benthic fishes include various species of sculpin and greenlings. Statistical test for changes in the mean diet percentage comprised of juvenile salmon among time periods. All specimens included in the analysis.

Date	Pacific Herring	Pacific Cod	Pacific Tomcod	Pollock (age 1-2)	Pollock (age 3+)	Dolly Varden	Benthic Fishes
<u>1996</u>							
5/3 - 5/9	.19	14.68	25.00	20.33	1.21	-	.39
5/19-5/26	.60	15.16	25.54	11.56	1.61	65.69	0
6/1 - 6/9	8.31	24.12	14.52	9.42	1.50	28.59	5.70
P-value	0.043	0.634	0.638	0.556	0.937	0.027	0.057
<u>1997</u>							
5/13 - 5/21	0.00	0.00	15.75	0.27	0.00	0.00	0.06
5/26- 6/3	1.01	10.29	6.51	0.00	0.00	25.67	1.35
6/10 - 6/18	0.00	0.00	0.00	0.00	0.00	26.63	0.57
P-value	0.156	0.425	0.001	0.750	1.000	0.373	0.024

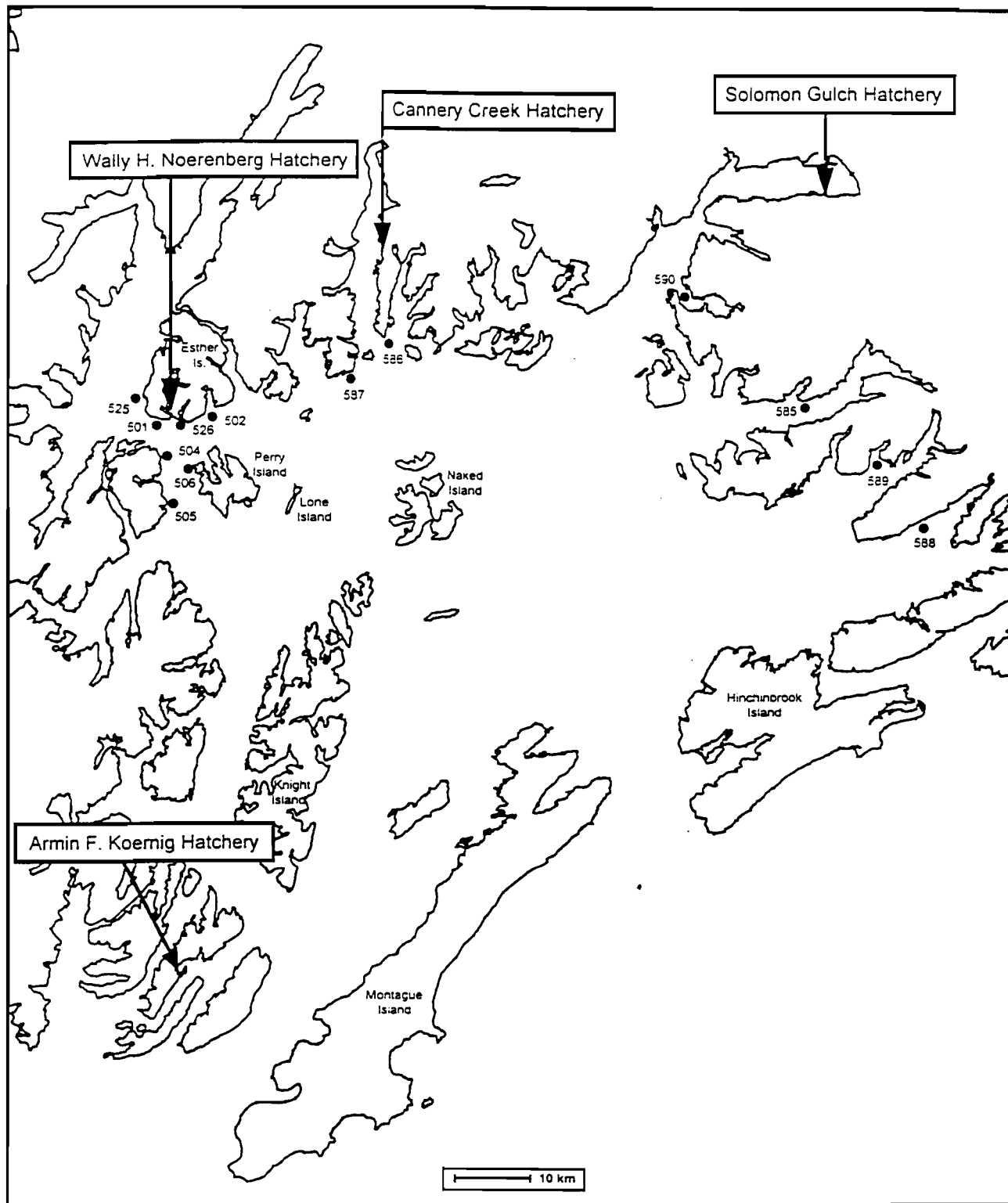


Figure 1: Study sites sampled in Prince William Sound during May-June, 1996-1997.

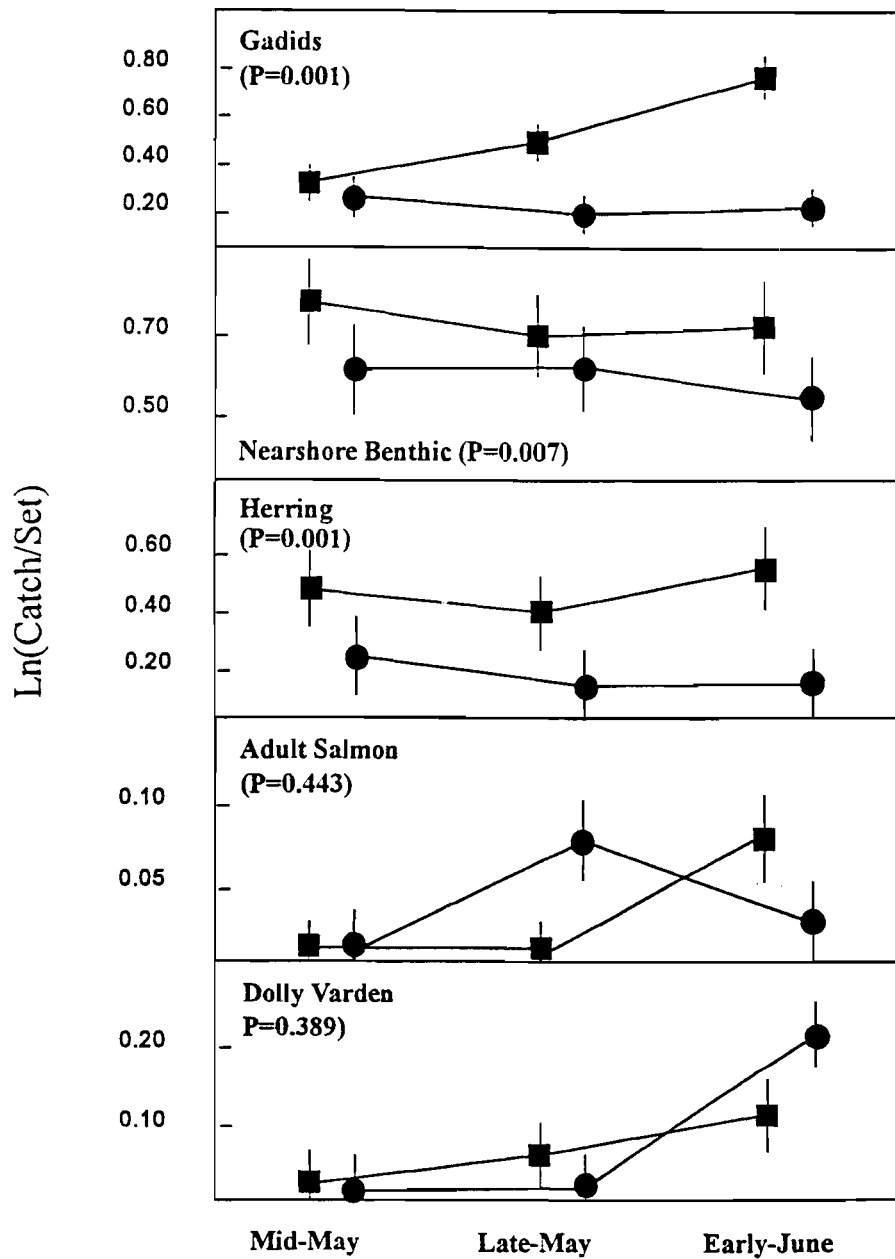


Figure 2: Mean catch per net set for five taxonomic groups of potential predators on juvenile pink salmon in eastern (solid squares) and western Prince (solid circles) William Sound during May-June 1997. Results from analysis of variance tests for a difference in mean catch per net set between eastern and western Prince William Sound are indicated.

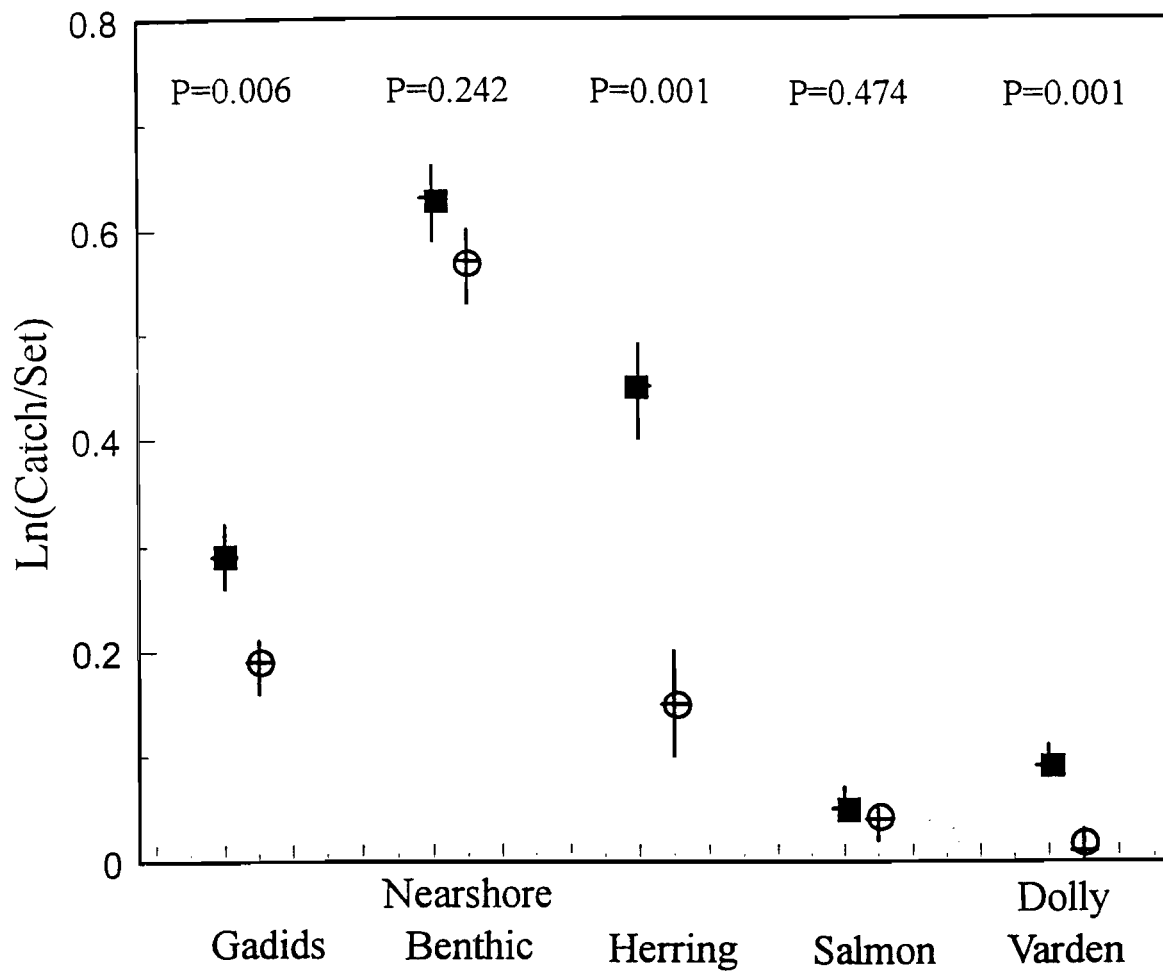


Figure 3: Mean catch per net set for three taxonomic groups of potential predators on juvenile pink salmon in western Prince William Sound during May-June 1996 (solid squares) and 1997 (open circles). Results from analysis of variance tests for a difference in mean catch per net set between years are indicated above each group.

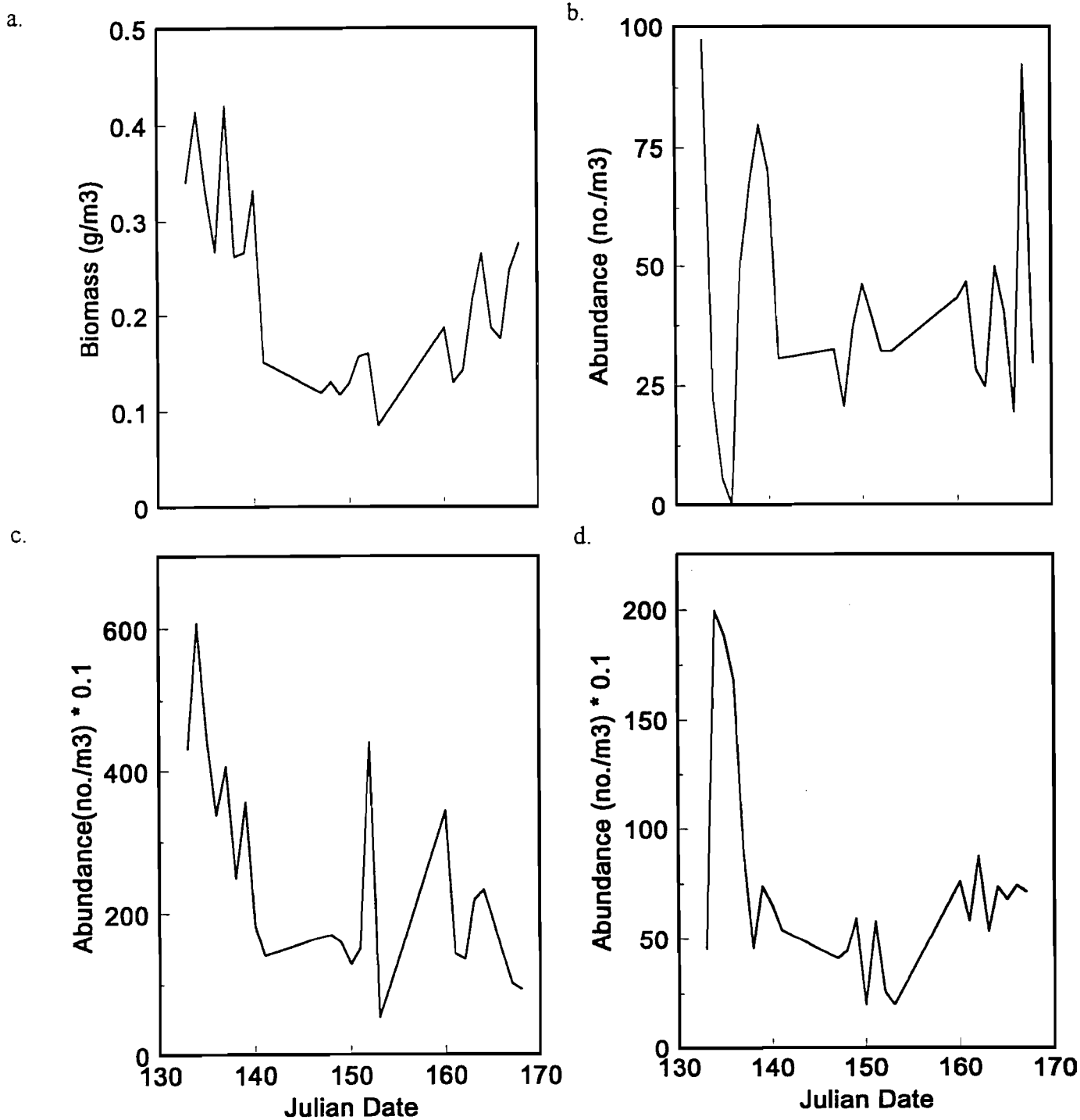


Figure 4: (a) Total zooplankton biomass and abundance (no./m3) of (b) large calanoid copepods, (c) small calanoid copepods, and (c) other zooplankters in offshore habitats in Prince William Sound, May-June 1997.

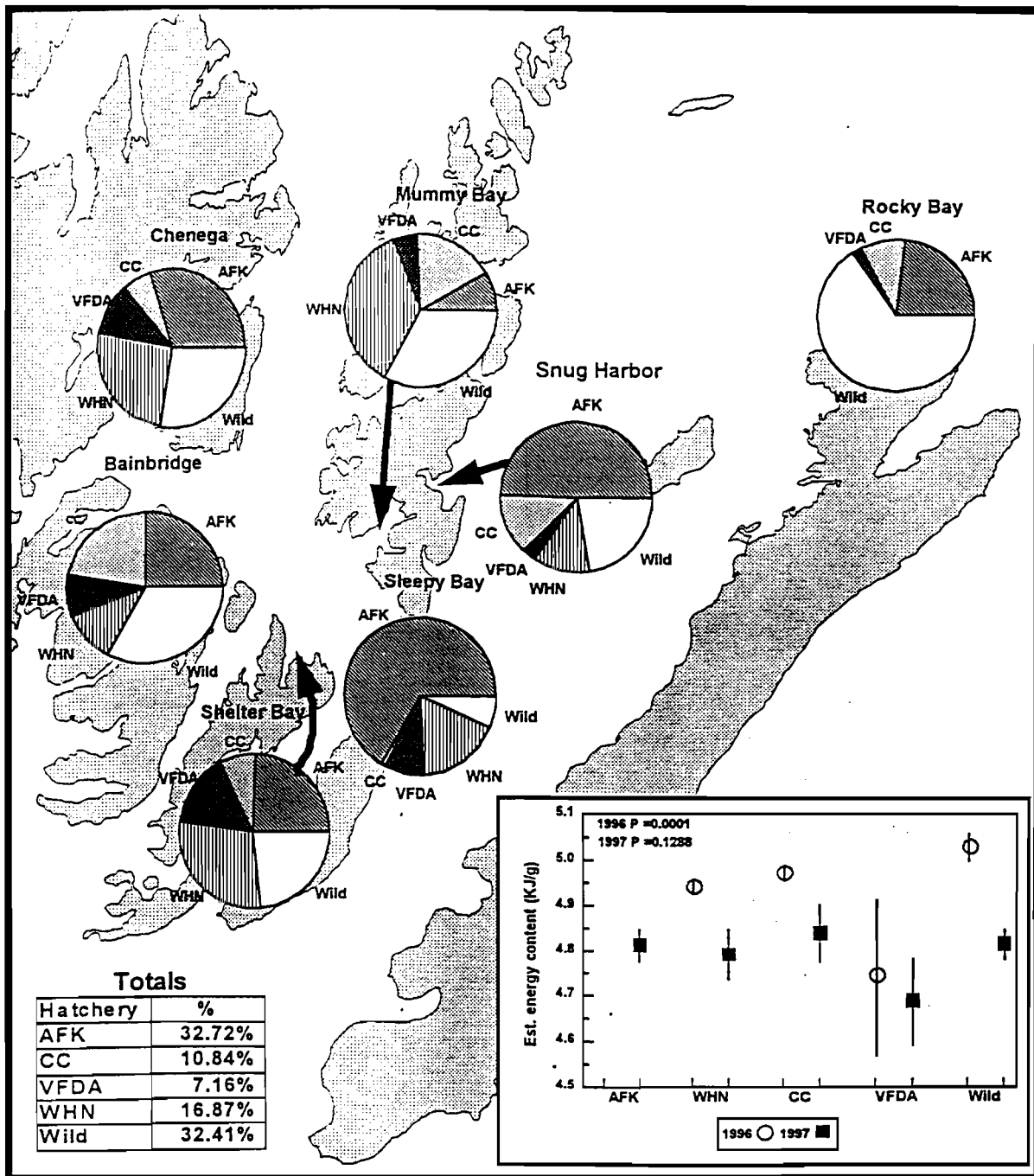


Figure 5: Origins of juvenile pink salmon sampled during late June in southwest Prince William Sound based on recovery of otolith thermal marks. Estimated energy content (derived from moisture content) of wild- and hatchery-origin juvenile pink salmon during 1996 and 1997. Results from analysis of variance tests for a differences in estimated mean energy content between hatcheries within years are indicated. The following codes are used: Armin F. Koernig Hatchery (AFK), Cannery Creek Hatchery (CC), Solomon Gulch Hatchery (VFDA), Wally H. Noerenberg Hatchery (WHN).

**An evaluation of some factors affecting piscivory among pelagic fish
during the spring bloom in a subarctic embayment**

T.M. Willette¹, R.T. Cooney², K. Hyer¹

FOR SUBMISSION TO THE CANADIAN JOURNAL OF FISHERIES AND AQUATIC SCIENCES

¹ Alaska Department of Fish and Game, Commercial Fisheries Management and Development, P.O. Box 669, Cordova, Alaska 99574.

² School of Fisheries and Ocean Sciences, University of Alaska Fairbanks, Fairbanks, Alaska 99775.

November 1997

Abstract

Factors affecting piscivory among herring (*Clupea pallasii*) and walleye pollock (*Theragra chalcogramma*) during the spring bloom in Prince William Sound, Alaska were examined using field data. Analyses of predator stomach contents indicated that predation by herring and pollock on larval and juvenile fishes was reduced during the spring bloom of large calanoid copepods, principally *Neocalanus spp.* Functional response models developed for herring and adult pollock feeding on large calanoid copepods (>2.5 mm) indicated that each predator began to switch to alternative prey when copepod biomass declined below 0.2 g m⁻³ and 1.0 g m⁻³, respectively. The parameters of the functional response models for herring and adult pollock were consistent with particulate and filter feeding modes, respectively. Large calanoid copepod biomass was negatively correlated with the proportion of the diet comprised of fish for herring (P=0.083) and immature pollock (P=0.150), but not for adult pollock (P=0.564). Juvenile gadids and salmonids (*Oncorhynchus spp.*) less than 50-70 mm in length were the most common fish prey taken by herring and immature pollock; whereas, squid (<150 mm) were the most common fish prey taken by adult pollock. Thus, mortality among juvenile gadids and salmonids is likely affected by the timing of the seasonal decline of the *Neocalanus spp.* bloom relative to the prey fishes' growth rate. Analyses of seven years of data from hatchery-reared coded-wire tagged pink salmon (*O. gorbuscha*) support conclusions drawn from stomach content analyses. Mortality of pink salmon was negatively correlated with the duration of the copepod bloom during the juvenile lifestage (P=0.013), as well as juvenile growth rate (P<0.001), juvenile body weight at release (P<0.001), and the number of juveniles released (P<0.001). The duration of the spring bloom of *Neocalanus spp.* appeared to be more abbreviated in years when the water column (0-100 m) was more highly stratified. Thus, bottom-up processes affecting secondary production and juvenile growth rate appear to also modify top-down processes involving predator switching behavior and thus mortality of juvenile fishes.

Introduction

Trophic interactions during the spring bloom period are critical to the successful reproduction of many fish species that release larvae at this time. Mortality during these early lifestages is typically very high and may determine recruitment to adult populations (Hjort 1914). Year-class success may be determined by the match or mismatch between the release of larvae and the production of their food (Cushing 1967). This concept is based on the notion that recruitment success is driven by production from lower trophic levels (bottom up). However, these processes may be modified by interactions with animals at higher trophic levels (top down). The spring bloom is also an important period in the seasonal energy cycle for the later lifestages of subarctic fishes (Smith and Paul 1986, Paul et al. 1993). Movements of these larger animals into the surface layer during this season leads to an overlap in distributions of larvae or juveniles with potential predators. Feeding mode shifts toward piscivory among these larger individuals may modify the mortality rates of larval or juvenile lifestages predicted by bottom up processes.

This paper examines some processes affecting feeding mode shifts toward piscivory among the later lifestages of Pacific herring (*Clupea pallasii*) and walleye pollock (*Theragra chalcogramma*) during the spring bloom period in coastal waters of the northern Gulf of Alaska. These species are relatively abundant pelagic fishes in this region (Rogers et al. 1986). The early life stages of herring, pollock, pink salmon (*Oncorhynchus gorbuscha*), chum salmon (*O. keta*), capelin (*Mallotus villosus*), Pacific sandlance (*Ammodytes hexapterus*) and others enter the coastal ocean as larvae or juveniles during spring (Rogers et al. 1986). Older lifestages of herring and pollock are also distributed in the surface layers at this time feeding heavily on calanoid copepods (Okada 1986, Rogers et al. 1986, Coyle and Paul 1992). The copepods *Neocalanus plumchrus* and *N. flemingeri* (Miller 1988) comprise the majority of the zooplankton biomass in the region during the spring bloom (Cooney 1986). *N. plumchrus* and *N. flemingeri* reproduce at depth in late winter. Their progeny migrate to the surface layer to graze during the phytoplankton bloom for a brief period in late April and early May (Fulton 1973, Cooney 1986, Miller and Clemons 1988). During this period, these large copepods build a substantial high-energy lipid reserve which is

utilized during the subsequent winter for egg development (Cooney 1986). The relatively high energy content of these copepods (Platt et al. 1969) makes them an attractive food source for many fishes. Large calanoid copepods comprise a major part of the diet of herring and pollock during this season (Okada 1986, Dwyer et al. 1987, Coyle and Paul 1992, Yoshida 1994), but both species are also piscivorous (Thorsteinson 1962, Bakshtansky 1965, Armstrong and Winslow 1968, Dwyer et al. 1987).

Particulate and filter feeding are two common foraging strategies employed by fish. Most optimal foraging models (based on particulate feeding behavior) predict prey selection from the relative profitabilities of potential prey (Charnov 1976, Mittelbach 1981, Osenberg and Mittelbach 1989) which are a function of the energy content of prey and the time (energy) required to capture and ingest prey. Shifts between particulate and filter feeding modes are likely related to the relative profitability of each feeding strategy, which is largely determined by prey size and density (Crowder 1985). Two types of filter feeding have been observed among fish. Ram filtering involves continuous swimming with the mouth agape and opercles flared. Pump filtering (or gulping) involves a series of nondirected suction while the fish is stationary (Gerking 1994). Pump filtering appears to be a relatively rare behavior (Gibson and Ezzi 1992). It likely involves sighting of prey patches, and it tends to be employed at lower prey densities than those required for ram filtering (Gibson and Ezzi 1992, Gerking 1994). Durbin (1979) postulated that particulate feeders consume relatively large prey (prey-predator size ratio 0.5 to 5%); whereas, filter feeders consumer smaller prey (prey-predator size ratio 0.01 to 0.7%). Piscivory is a special case of particulate feeding. Prey-predator size ratios typically range from 20 to 30% for piscivores but ratios as high as 50% sometimes occur at ontogenetic transitions to piscivory (Popova 1978, Juanes 1994). Herring exhibit particulate and filter feeding modes which appear to be determined by prey density and light level (Gibson and Ezzi 1985, 1992). Adult pollock in the Bering Sea consume macrozooplankton greater than 4 mm in length; although, based on gill raker spacing they have the ability to feed on prey greater than 2 mm (Yoshida 1994). These prey sizes are near the threshold for filter feeding suggested by Durbin (1979). Adult pollock are also known to prey heavily on juvenile pollock when conditions lead to an overlap in their distributions (Dwyer et al. 1987). Walline (1983)

concluded that predation on juvenile pollock likely determined year-class strength rather than the match or mismatch of pollock larvae with their food.

In the analysis that follows, we will first present data indicating seasonal changes in ocean conditions, calanoid copepod biomass, the relative abundance of herring and pollock, and the relative abundance and size of various juvenile fishes in Prince William Sound (PWS), Alaska. An analysis of the functional responses of herring, immature pollock and adult pollock feeding on large calanoid copepods will be conducted to determine the biomass of large calanoid copepods at which these predators begin to feed on alternative prey. This analysis will also examine the probable feeding modes employed by herring and pollock feeding on large calanoid copepods, because this may affect the timing of shifts to other strategies such as piscivory. We will then examine whether piscivory in these predators is a function of prey-predator size ratio, the relative abundance of prey fish, or the biomass of large calanoid copepods. Finally, we will evaluate the effect of size-selective predation and copepod biomass on the mortality of juvenile coded-wire tagged pink salmon released from four hatcheries in PWS.

Methods

Prince William Sound is an approximately 8500 km² basin surrounded by numerous deepwater fjords and islands. Herring, pollock and their prey were sampled in the passages of western PWS in 1994, 1995, and 1996. Seven areas were sampled from late April through mid-July in 1994 (Table 1, Figure 1). In 1995 and 1996, several sites in northwest PWS were sampled from early May through mid-June (Table 1, Figure 1). Sampling was conducted from approximately 6 pm to 6 am each day. The sampling area\dates indicated in Table 1 were generally used as sample units in the following analyses.

Adult pollock (>30 cm) were collected in deepwater passages with a mid-water wing trawl (40 m x 28 m) equipped with a net sounder. The net was towed at about 1.5 m sec⁻¹ for approximately 30 minutes in the 0-60 m layer of the water column. At least two zooplankton samples were taken at stations located near the center of the passages to estimate the mean density of large calanoid copepods available to adult pollock at each location. Zooplankton samples in the passages were collected with a 0.5 m diameter ring net (335 μ m mesh) towed vertically from 50 m depth to the surface. Herring and immature pollock (<30 cm) and various juvenile fishes were collected with small-mesh purse seines (250 m x 20 m, 1.5 cm stretch mesh). Seines were set in an approximate semi-circle with the net open in the direction of the prevailing current for approximately 20 minutes (Hartt (1980)). Seine sampling was conducted within 1 km of the shore up to the 20 m isobath. Samples of herring and immature pollock were also obtained with variable-mesh gill nets set out from the shore at two locations within each study site. At least four zooplankton samples were taken at stations located near the 20 m isobath to estimate the mean density of large calanoid copepods available to herring and immature pollock in nearshore habitats. These samples were collected with a 0.5 m ring net (243 μ m mesh) towed vertically from 20 m depth to the surface. At each study site, temperature and salinity was measured to a depth of 100 m with a conductivity-temperature-depth profiler (CTD).

Over 15,000 specimens were analyzed to determine the diet composition of herring and pollock during the spring bloom period from 1994 through 1996 (Table 2). At least thirty specimens from each fish species were randomly selected from each net set for length-weight measurements and analysis of stomach contents. Fork length was measured to the nearest millimeter and wet weight to the nearest gram. Stomachs were excised and preserved in formalin for later analysis. In the laboratory, total stomach contents wet weight was measured to the nearest 0.01g, and the proportion of total stomach contents weight in several taxonomic groups (large calanoid copepod, small calanoid copepod, euphausiid, amphipod, etc.) was visually estimated. Fish found in the stomachs were measured to the nearest millimeter. The weighted mean proportion of the diet comprised of various prey taxa was estimated for herring, immature pollock and adult pollock within each sample unit. The catch of each respective predator in each net set was used as the weighing variable.

Over 300 samples were analyzed to estimate the species composition and biomass of zooplankton available to herring and pollock. In the field, zooplankton samples were preserved in formalin. In the laboratory, zooplankters collected with the 335-um mesh net were identified to the lowest possible taxonomic level and enumerated using standard subsampling techniques (Coyle et al. 1990). Zooplankters collected with the 243 um mesh net were enumerated into three taxonomic groups (large calanoid copepods (>2.5 mm), small calanoid copepods (<2.5 mm), and 'other' zooplankton) using standard subsampling techniques. Zooplankton biomass was calculated as the product of abundance and the mean individual wet weight for each taxonomic group (Coyle et al. 1990).

Changes in the relative abundance of herring, immature pollock, adult pollock and various juvenile fishes was examined through analyses of net catch data. Mean catch per hour in mid-water trawls was used as a measure of relative abundance of adult pollock in the surface layer of the passages within each sample unit. Mean catch per net set in small-mesh purse seines and variable-mesh gillnets was used as a measure of relative abundance of herring and immature pollock, respectively within each sample unit. Catch data were natural logarithm transformed prior to calculating the mean catch for each of the sample units indicated in Table 1.

Functional responses of herring, immature pollock and adult pollock

The functional responses of herring, immature pollock and adult pollock feeding on large calanoid copepods were evaluated using non-linear regression analyses of field data. Type II and III functional response curves were fit to field estimates of total daily consumption of large calanoid copepods in relation to measured copepod densities. The type II functional response rises at a decelerating rate to an asymptote and generally applies to particulate feeders (Hassel 1978), i.e.

$$I = \frac{\gamma p U}{1 + \gamma p U h} \quad 1$$

where I is the daily food consumption (g day^{-1}), γ is the cross-sectional area of the reactive field (m^2), p is the prey density (g m^{-3}), U is the swimming speed (m day^{-1}) and h is the prey handling time (day g^{-1}). The type III functional response is a sigmoid. It often best describes situations where alternative prey are available, and the predator switches from feeding on one prey type to another (Lawton et al. 1974, Akre and Johnson 1979), i.e.

$$I = \frac{\gamma p^2 U}{1 + \gamma p^2 U h} \quad 2$$

Because our analysis utilizes field estimates of daily food consumption, swimming speed represents the total distance traversed while feeding throughout the entire day, and handling time includes the time required to capture and ingest prey as well as any time during which the fish is not searching for prey due to satiation or low light level.

Daily consumption of large calanoid copepods (I) was estimated from

$$I = 24 \bar{S} \alpha \quad 3$$

where \bar{S} is the mean wet weight of large calanoid copepods in the stomach over a twenty-four hour period and α is the gastric evacuation rate (Eggers 1977). In the present study, the daily consumption of copepods was estimated using diet data for the period from 6 pm to 6 am. This was done because data was available from this time period for each of our sample units. Analysis of variance was conducted to test for a difference in the mean wet weight of large calanoid copepods in the stomachs of herring, immature pollock and adult pollock between the 6 pm to 6 am period and the full 24 hour day using data from sixteen diel studies conducted in 1995. Results indicated that the mean weight of copepods in the stomachs was not significantly different ($P > 0.350$) between this 12 hour period and the full 24 hour day for any of these three predators. Temperature-specific gastric evacuation rates were

estimated for herring using an equation for juvenile menhaden provided by Peters and Kjelson (1975), i.e. $\alpha = -0.0132 + 0.0316 \log T - 0.0403 (\log T)^2$, where T is temperature ($^{\circ}\text{C}$). Data provided by Smith et al. (1989) were used to estimate a relationship between temperature and gastric evacuation rate for adult pollock ($\alpha = -0.0235 e^{1.68T}$) and immature pollock ($\alpha = -0.0217 e^{1.68T}$). Mean 0-15 m ocean temperatures were used to estimate gastric evacuation rates of herring and immature pollock which were sampled in this layer. Mean 0-50 m temperatures were used to estimate gastric evacuation rates of adult pollock which were sampled in this layer.

Two values were used for γ to evaluate whether the fish were likely particulate or filter feeding. For particulate feeders, γ is the cross-sectional area of the reactive field, i.e. πd_r^2 , where d_r is the reactive distance (Ware 1972). Reactive distance is a function of fish size (Ware 1978) and prey size (Ware 1972). Data provided by Ware (1972) were used to estimate a regression equation relating reactive distance to fish length and prey length, i.e.,

$$d_r = 0.29L_f^{1.1} + 3.3L_p \quad 4$$

($R^2=0.960$, $P=0.005$) where d_r is the reactive distance (cm), L_f is total fish length (cm) and L_p is prey length (mm).

For ram filter feeders, γ is simply the cross-sectional area of the mouth gape, because individual prey are not sighted and attacked.

Ware's (1978) analysis of the bioenergetics of foraging pelagic fishes was used to determine an appropriate range of swimming speeds for evaluation of functional response models. Ware (1978) found that the optimal foraging speed of pelagic fishes likely ranged between 1 and 3 L sec^{-1} . Three body lengths per second is likely an appropriate upper range for swimming speeds of foraging pelagic fishes. Brett and Glass (1973) found that maximum sustained swimming speeds of sockeye salmon (>150 mm) range between 3 and 4.5 L sec^{-1} depending on temperature. In the present study, swimming speeds were varied between 1 and 3 L sec^{-1} . However, we also

evaluated a swimming speed of 15 km day^{-1} (0.3 L sec^{-1}) which was estimated for adult pollock schools feeding in the Bering Sea (Radchenko and Sobolevskiy 1993).

Densities of large calanoid copepods in layers found within the upper 50 m of the water column were estimated in 1996 using a MOCNESS sampler. Samples were collected from eight discrete layers (0-5 m, 5-10 m, 10-15 m, 15-20 m, 20-25 m, 25-30 m, 30-40 m, 40-50 m) at 24 stations in PWS. The weighted mean biomass of large calanoid copepods across all layers within the upper 50 m was regressed against the biomass of large calanoid copepods for samples collected within high density layers. Samples having a copepod biomass greater than the mean for the upper 50 m as a whole were considered to have come from high density layers. The results from this analysis indicated that probable mean biomass of large calanoid copepods in layers was about 2.25 times the biomass estimated from 0-50 m vertical net tows ($R^2 = 0.451$, $P < 0.001$). The probable mean copepod biomass in layers was used in the evaluation of functional responses of adult pollock, because adult pollock were likely feeding in these high density layers. For herring and immature pollock feeding nearshore, we assumed that 0-20 m vertical net tows adequately estimated the mean biomass of copepods available in these relatively shallow habitats which are likely vertically mixed by tidal currents (Simpson and Hunter 1974).

Non-linear regression analysis was used to fit type II and III functional response models to field estimates of daily consumption of large calanoid copepods in relation to copepod density. Each analysis was conducted for an average size herring ($\bar{L} = 195 \text{ mm}$), immature pollock ($\bar{L} = 195$) or adult pollock ($\bar{L} = 501$). The mean length for each predator was used to estimate the cross-sectional area of the mouth gape, swimming speed and reactive distance for an average individual fish. The cross-sectional area of the mouth gape was estimated for an average-size herring and pollock using measurements from samples obtained during this study. The analysis of functional response models was conducted in two stages. In the first stage, non-linear regression analyses were conducted using several possible combinations of the values of γ and U as constants to estimate handling time (h). Studentized deleted

residuals were calculated to identify and exclude outliers in the data at this stage (Neter et al. 1989). The combinations of γ and U that resulted in the smallest mean square error were considered to provide the best fit of the functional response model to the data. In the second stage, the handling times (h) estimated from the two 'best fit' models obtained in the first stage were used as constants to estimate U using the two values of γ associated with ram filter and particulate feeding. The value of γ that resulted in the best fit of the data was considered to indicate the probable feeding mode of the predator.

Piscivory in herring, immature and adult pollock

The mean percent of the diet comprised of fish was estimated for herring, immature pollock and adult pollock for several prey taxonomic groups (herring, gadids, salmonids, capelin, sandlance, squid, 'other fish', unidentified fish). Diet proportions were weighted by the catch of each respective predator in each net set. The ratio of the length of prey fish to predator length was calculated for herring, immature pollock and adult pollock as predators with all prey species pooled and by prey taxonomic group. Analyses of variance were conducted to test for a difference in the prey-predator length ratio (arcsin square root transformed) among predator species and among prey species. Mean catch per net set in purse seines and mean length was also estimated for each of the prey fish taxonomic groups consumed by herring and pollock.

Multiple regression analyses were conducted to test the hypothesis that piscivory in herring and pollock is reduced when the biomass of large calanoid copepods is high. The percent of the diet comprised of fish (arcsin square root transformed) was the dependent variable in the analysis and the relative abundance of prey fish and the mean biomass of large calanoid copepods were the independent variables. The mean catch per net set of juvenile fish in purse seines was used as a measure of the relative abundance of prey fish (Hartt 1980). Catch data were natural

logarithm transformed prior to calculating the mean catch for each of the sample units indicated in Table 1. The mean biomass of large calanoid copepods in nearshore habitats was used as an independent variable in the analyses for herring and immature pollock. For adult pollock, the mean biomass of large calanoid copepods in offshore habitats was used as an independent variable.

Effect of size-selective predation and copepod biomass on mortality of juvenile salmonids

The effect of copepod biomass and size-selective predation on mortality of juvenile salmonids was evaluated using estimates of survival from fry release to adult for 147 coded-wire tag groups of pink salmon released from the Armin F. Koernig, Wally H. Noerenberg, Cannery Creek and Solomon Gulch hatcheries from 1989 through 1995 (Figure 1). An analysis of covariance was conducted to test the following null hypothesis: mortality of juvenile pink salmon is not related to the duration of the bloom of large calanoid copepods from ocean entry to the time the fish reach 60 mm in length, or the body weight of juveniles at release, or juvenile growth rate, or number of juveniles released at each hatchery each day.

Instantaneous natural mortality from ocean entry to adult return was the dependent variable in this analysis of covariance while mean body weight at release, mean juvenile growth rate, mean zooplankton settled volume and number of juveniles in each tag group were the independent variables. The survival of pink salmon in each tag group from ocean entry to adult was estimated from recovery of tagged adults at the hatcheries as well as in gill net and purse seine fisheries in PWS. A tag group was comprised of one or more net pens of juveniles released from the same hatchery on the same day. The methods used to estimate survival are described by Peltz and Miller (1990) and Geiger (1990). Instantaneous natural mortality was estimated on a daily basis assuming a total of 470 days at sea. Mean body weight at release was estimated from three samples collected from each net pen immediately prior to the release of each tag group. The three samples were composited and a random subsample of approximately

100 individuals was weighed to the nearest 0.01 g. The mean growth rate of juveniles belonging to each tag group was estimated from an equation developed from an analysis of covariance involving juvenile growth as the dependent variable and number of juveniles in each tag group as well as environmental data as independent variables. The methods used in this analysis will be described later in detail. Mean zooplankton settled volume weighted by the number of days elapsed between each measurement was estimated for the 30 days immediately following release of each tag group. This was done because sampling of tagged juveniles indicated that 98.5% of these fish did not reach 60 mm in length within 30 days after release. A threshold zooplankton volume was set at 2.0 ml m^{-3} , i.e. zooplankton volumes greater than 2.0 ml m^{-3} were set equal to 2.0 ml m^{-3} . This was done because analyses of predator stomach contents indicated that consumption of fish was greater when the biomass of large calanoid copepods declined below about 0.2 g m^{-3} (Figure 13). Also, data provided by Willette et al. (1994) as well as data obtained in the present study indicated that this threshold biomass corresponded to a settled volume equal to about 2.0 ml m^{-3} , and that total zooplankton biomass in May was correlated ($R^2=0.658$) with the biomass of large calanoid copepods. A class variable was established based upon the value of the mean zooplankton settled volume that divided the data into three groups with roughly equal numbers of observations. The mean zooplankton settled volume (ml m^{-3}) for the low, moderate, and high classes was 1.3 ($n=50$), 1.9 ($n=56$), and 2.0 ($n=48$), respectively. The data used to estimate zooplankton settled volume was obtained from samples collected twice each week (late April-early June) using a 0.5 m ring net (243 μm mesh) towed vertically from 20 m depth to the surface in the passages adjacent to each hatchery. Generally, one to three samples were composited to obtain sufficient material to estimate the settled volume of zooplankton in the samples collected each day. Tag groups with mean body weights at release greater than 0.35 g were not included in the analysis. This was done because groups comprised of larger fish (up to 1.3 g) were relatively rare (<9% of the data), and they occurred more frequently in association with moderate and high zooplankton volumes. Each of the continuous independent variables in the analysis was natural logarithm transformed. A stepwise analysis of covariance procedure was used to develop the most parsimonious model of mortality, and the least-squares mean mortality was estimated for the low, moderate and high zooplankton classes.

As previously indicated, mean growth rate was estimated from an analysis of covariance function of growth data on juvenile release and environmental data. Growth rate estimates were available for 2,637 individual coded-wire tagged juvenile pink salmon collected during May and early June in PWS (1989-1994). The methods used to recover tagged juveniles and estimate growth are described by Willette (1996). Mean growth was estimated for 108 groups of juveniles which exhibited a common release site, release date and recapture date. Mean zooplankton settled volume and ocean temperature weighted by the number of days between each measurement was estimated from the date of release of each tag group to the date of recapture. The ocean temperature data was obtained from measurements taken at 1 m depth when each zooplankton sample was collected. These environmental variables (natural logarithm transformed) were used as independent variables in the analysis. A class variable was established based upon the number of juvenile pink salmon released each day from each hatchery that divided the data into two groups with approximately equal numbers of observations. Groups with less than and greater than 20 million juveniles were designated as small and large releases, respectively. A stepwise analysis of covariance procedure was used to develop the most parsimonious model of juvenile growth.

Results

Ocean conditions in May 1994 were characterized by relatively frequent storms (Figure 2), weak surface layer stratification (Figure 3), cooler surface layer temperatures (Figure 3), and a prolonged bloom of large calanoid copepods (Figure 4). In May 1995, storms were again frequent in the area (Figure 2), but the water column was more strongly stratified (Figure 3), and surface temperatures were warmer than in 1994 (Figure 3). The bloom of large calanoid copepods in May 1995 was also more abbreviated than in 1994 (Figure 4). In May 1996, storms were less frequent (Figure 2), the water column was again strongly stratified (Figure 3), surface layer temperatures

were relatively warm (Figure 3), and the bloom of large calanoid copepods was very abbreviated (Figure 4). In each of the three years of this study, the surface layer became strongly stratified in June and the bloom of large calanoid copepods declined. *Neocalanus* spp. comprised the majority of the biomass of large calanoid copepods during the spring bloom in both 1994 and 1995 (Figure 4).

Herring and pollock were the most abundant pelagic fishes during each of the three years of this study; although, adult salmonids (*Oncorhynchus* spp.) and squid (mostly *Berryteuthis* spp.) were commonly encountered (Table 3).

The mean catch of herring in purse seines tended to increase from May through June in each of the three years of the study (Figure 5). In 1994, total catch of immature pollock in all gear types increased in late July. A similar increase in mean catch per set of immature pollock in variable-mesh gillnets was seen in June 1996 but not in 1995 (Figure 5). Mean catch per hour of tow of adult pollock in the upper 50 m of the water column declined from June through July in 1994 (Figure 5). However, in 1995 adult pollock catches declined in mid May but increased again in early June. In 1996, adult pollock catches were lower than in the previous two years and no seasonal changes in abundance were evident (Figure 5).

Large calanoid copepods tended to dominate herring diets during the calanoid copepod bloom in early May (Figures 4 and 6). In 1995 and 1996, herring continued to feed predominately on large calanoid copepods several weeks after copepod densities declined. In all three years of the study, herring eventually switched to feeding on other prey by mid-June. In 1994, herring switched to feeding primarily on euphausiids and amphipods; in 1995 to euphausiids, amphipods, pteropods and fish; and in 1996 to euphausiids, amphipods and fish (Figure 6). Large calanoid copepods also dominated the diets of immature pollock in May 1995 (Figure 7). However, in 1994 and 1996 diets of immature pollock were more varied. In 1994, immature pollock fed primarily on euphausiids and amphipods, although few samples were obtained during May. In both 1995 and 1996, immature pollock tended to feed more heavily on fish during June. Adult pollock diets were dominated by large calanoid copepods during May, 1994-1995 (Figure 8). After the seasonal decline in copepod density, adult pollock switched to feeding primarily on

euphausiids, amphipods and fish in 1994 and 1996; whereas, pteropods comprised the majority of adult pollock diets after the bloom in 1995. Large copepods did not dominate adult pollock diets during the bloom in May 1996.

Functional responses of herring, immature pollock and adult pollock

The functional response for herring feeding on large calanoid copepods was best described by a type III model (Table 4). The Studentized deleted residuals identified two outliers in the data that were excluded from the analysis of functional responses of herring. The value of γ consistent with a particulate feeding mode provided the best fit of the herring data at all values of U used with the type III model (Appendix I, Table 1). When a value for γ consistent with a ram filter feeding mode was used, handling time estimates were negative in four of the six parameter combinations used in the analysis (Appendix I, Table 1). The best fit functional response model for herring resulted in a swimming speed estimate of 10.0 km day^{-1} (Table 4) and a daily food consumption of 0.8 g day^{-1} at the asymptote (Figure 9). Herring began to feed on alternative prey as the mean biomass of large calanoid copepods in the upper 20 m of the water column declined below about 0.2 g m^{-3} (Figure 9). The functional response for immature pollock feeding on large calanoid copepods was not adequately described by the type II or III models regardless of the values of the parameters used (Table 4 and Appendix I, Table 2). The response function for immature pollock did not reach an asymptote within the range of the data used in the analysis (Figure 9). The functional response for adult pollock feeding on large calanoid copepods was best described by a type III model (Table 4 and Appendix I, Table 3). A value of γ consistent with a ram filter feeding mode provided the best fit of the adult pollock data at all values of U used in the analysis. The best fit functional response model for adult pollock resulted in a swimming speed estimate of 16.7 km day^{-1} and a daily food consumption of 7.0 g day^{-1} at the

asymptote (Figure 9). Adult pollock began to feed on alternative prey as the mean biomass of large calanoid copepods in high density layers declined below about 1.0 g m^{-3} (Figure 9).

Piscivory in herring, immature pollock and adult pollock

Immature pollock generally exhibited a greater degree of piscivory than either herring or adult pollock. The overall mean percent of the diet comprised of fish ranged from 13.9 to 26.2 for immature pollock, 4.2-11.4 for herring, and 6.7-17.1 for adult pollock (Table 5). Juvenile gadids (mostly age-0 pollock) and salmonids (mostly pink and chum salmon) were the most commonly encountered fish in the diets of herring and immature pollock, but squid was the most important fish species in the diets of adult pollock (Table 5). Herring and immature pollock generally consumed fish less than 50-70 mm in length; whereas, adult pollock generally consumed fish less than 150 mm (Figure 10). Mean lengths of fish prey consumed by immature and adult pollock did not differ substantially, but adult pollock occasionally consumed larger fish that were not taken by immature pollock. Mean prey-predator length ratios differed significantly between herring, immature pollock and adult pollock ($P < 0.001$). Herring generally consumed fish ranging from 5-25% of their length, immature pollock 5-35%, and adult pollock 3-40% (Figure 10). Mean prey-predator length ratios also differed significantly ($P < 0.001$) among prey species (Table 6). The smaller prey fish consumed by adult pollock were generally juvenile gadids, juvenile salmonids and 'other fish'; whereas, the larger prey were herring, capelin, sandlance and squid (Table 6).

In 1994, the mean catch per net set of juvenile fishes ($< 150 \text{ mm}$) increased considerably from May through June (Figure 11). In 1995 and 1996, juvenile fish catches were much higher in May than in 1994. Juvenile fish catches increased in June of 1996, but no appreciable increase in catches was observed from May to June in 1995. In 1994, juvenile fish catches were dominated by gadids and salmonids; whereas, in 1995 and 1996 salmonids and capelin were most numerous (Table 7). Squid were more abundant in 1996 than in the previous two years. Mean lengths of

the fish species consumed by herring and pollock did not appear to differ substantially from year to year (Figure 12). Juvenile gadids grew from about 40 to 60 mm from late May to July; whereas, juvenile salmonids were somewhat larger throughout this period. Mean lengths of herring and capelin increased slightly from May through July (Figure 12).

Sequential sums of squares (Type I) and partial sums of squares (Type III) indicated that the proportion of herring diets comprised of fish was marginally significantly related to the biomass of large calanoid copepods but the relative abundance of prey fish was not related to consumption of fish (Table 8). For immature pollock, the relative abundance of prey fish was significantly related ($P=0.044$) to the proportion of the diet comprised of fish. Sequential sums of squares indicated that the biomass of large copepods was significantly related to consumption of fish by immature pollock, but partial sums of squares indicated that this variable was only marginally significant in the model (Table 8). Neither independent variable was significantly related to the proportion of adult pollock diets comprised of fish (Table 8). The variance inflation factor was calculated to assess whether multicollinearity may have affected estimation of the regression coefficients and their statistical significance (Neter et al. 1989). The variance inflation factors were 1.07 for herring, 1.17 for immature pollock, and 1.11 for adult pollock. Graphical evaluation of the original data indicated that the proportion of the diet comprised of fish tended to be greater for all three predators when the biomass of large copepods was less than about 0.2 g m^{-3} (Figure 13).

Effect of size-selective predation and copepod biomass on mortality of juvenile salmonids

Analysis of covariance indicated that the growth rate of coded-wire tagged juvenile pink salmon was positively correlated to mean ocean temperature ($P<0.001$) and mean zooplankton settled volume ($P=0.002$) during the period from juvenile release to recapture (Table 9). The intercepts and slopes of the relationship between growth

and zooplankton settled volume were also significantly different between small and large release groups from each hatchery (Table 9, Figure 14). The variance inflation factor for this analysis was 4.60.

Analysis of covariance further indicated that the instantaneous natural mortality of pink salmon was significantly correlated to zooplankton settled volume, mean juvenile growth rate, mean body weight of juveniles at release and number of juveniles released ($R^2=0.350$, $P<0.001$). Mortality was significantly greater when zooplankton settled volume during the initial 30 days of marine residence was relatively low (Tables 10 and 11). Mortality was also greater when mean growth rate, mean body weight at release, or the number of juveniles released was relatively low (Table 10). The variance inflation factor for this analysis was 6.54.

Discussion

The environmental conditions observed during the three years of this study provide for a useful comparison of the effect of physical conditions on secondary production in the PWS ecosystem. The duration of the bloom of large calanoid copepods in May appeared to be associated with the degree of stratification of the surface layer. In 1994, the surface layer was weakly stratified, and the bloom of large copepods extended to the end of May. In May 1995 and 1996, the surface layer was more highly stratified, and the bloom of large copepods was more abbreviated (Figures 3-4). These associations are likely related to the frequency of storms with winds sufficiently strong to breakdown surface stratification, resupply nutrients to the surface mixed layer, and thus prolong the phytoplankton bloom (Iverson et al. 1974, Walsh et al. 1978, Sambrotto and Goering 1983, Sambrotto 1985, Ziemann et al. 1991). In years when storms are more frequent and the phytoplankton bloom is prolonged, the mean (April-June) abundance and growth of *Neocalanus plumchrus* is greater (Smith and Vidal 1982, Sambrotto and Goering 1983). The frequency of wind events was similar during May in 1994 and 1995 (Figure 2), yet the surface layer remained more highly stratified in 1995 (Figure 3). This indicates that the effect of intense storms on primary and secondary

production at this time of year is likely modified by other physical processes that affect development of surface stratification during the spring bloom period. The stronger surface layer stratification observed in May 1995 and 1996 was associated with higher salinities and lower temperatures below 50 m depth compared to 1994 (Figure 3). The strength of surface stratification during this season is largely determined by the vertical salinity gradient because seawater density is primarily a function of salinity at low temperatures (Royer 1979). In years when the 0-100 m salinity is relatively high at the onset of the spring bloom, the seasonal decrease in surface salinity due to increased freshwater discharge (Xiong and Royer 1984) results in a greater vertical salinity (density) gradient compared to years when the 0-100 m salinity is relatively low at the onset of the spring bloom. Higher wind speeds are required to breakdown the stronger surface stratification that occurs under these conditions. Thus, in 1995 although wind speeds were relatively high, the surface stratification was not broken down and the spring bloom of large calanoid copepods was relatively abbreviated.

Large scale oceanographic processes occurring the previous winter may determine the 0-100 m temperature-salinity conditions present at the onset of the spring bloom period. Lower ocean temperatures and sea levels in the northeast Pacific are associated with a weaker winter Aleutian low (Emery and Hamilton 1985). Higher salinities in this region are associated with reduced freshwater discharge (Xiong and Royer 1984), and lower sea levels are associated with reduced precipitation and dynamic height of the upper layers of the ocean (Royer 1979). Thus, a weak (strong) Aleutian low during the previous winter may result in relatively high (low) 0-100 m salinities and low (high) 0-100 m temperatures at the onset of the spring bloom. Niebauer et al. (1994) concluded that 200% of the volume of PWS was flushed during winter (October-April), and that flushing of the surface layer (0-100 m) was most rapid during winter. Thus, large-scale oceanographic processes in the Gulf of Alaska may be expected to affect conditions in the surface layer of PWS during winter.

Herring and pollock were the most commonly encountered and abundant species in surface layer net catches during each of the three years of this study (Table 3). These two species have been found to dominate the pelagic fish community in other areas of the northern Gulf of Alaska (Rogers et al. 1986). In the present study, the relative abundance of herring, immature pollock, and various species of juvenile fishes tended to increase from May through June (Figures 5 and 11). A similar seasonal increase in the abundance of nearshore fishes has been observed in other areas of the North Pacific (Miller et al. 1976, Moulton 1977, Cross et al. 1978, Rosenthal 1983).

Size-related shifts in amounts of copepods and fish consumed by pollock have been reported in other areas but were not consistently observed in the present study. Dwyer et al. (1987) found that the proportion of the diet comprised of copepods declined from about 75-100 % in small pollock (< 30 cm) to less than 50% among large pollock (>30 cm) during spring and summer in the Bering Sea. In the present study, a similar pattern was observed in 1995 but not in 1996 (Figures 7-8). In other regions, the proportion of pollock diets comprised of age-0 pollock (Dwyer et al. 1987) and fish (Clausen 1983) have been found to increase with pollock size. However, in the present study, the overall mean proportion of the diet comprised of juvenile gadids and all fish combined was greater for immature pollock than for adult pollock in two out of three years (Table 5). In the present study, pteropods also dominated the diet of adult pollock in June 1995 (Figure 8), but in previous studies pteropods have been absent from or comprised only a minor portion of pollock diets (Clausen 1983, Dwyer et al. 1987, Maeda 1986, Okada 1986, Gorbatenko and Dolganova 1989, Yoshida 1994).

Determining the appropriate functional response model for specific predator-prey interactions has often proved difficult. Most often prey density is manipulated under controlled laboratory conditions and feeding rates of predators are estimated (Ware 1972, Ranta and Nuutinen 1985, Gulbrandsen 1991, Winkler and Orellana 1992). This approach can minimize ambiguities caused by predator satiation, prey patchiness, and variable light level and swimming speeds that can complicate interpretation of results from field studies. However, results from laboratory experiments may be difficult to extrapolate to nature, because many laboratory studies do not adequately account

for variables known to affect prey encounter rates and selection (MacKenzie et al. 1990). This may be especially true for relatively large predators such as adult pollock. In the present study, least-squares non-linear regression analysis was used to estimate the functional responses of herring and pollock feeding on large calanoid copepods using field data. Visual examination of the relation between predator consumption and prey density has commonly been employed to determine functional responses of fish predators using field data (Peterman and Gatto 1978, Ruggerone and Rogers 1984, Fresh and Schroder 1987), but this approach has often proved difficult due to the highly variable predation rates observed in nature. Non-linear regression analysis provides a more quantitative procedure for determining the underlying functional response when using field data.

We recognize that herring and pollock probably feed in high density patches or layers of copepods, because relatively mobile predators often aggregate in areas where relatively immobile invertebrate prey occur at high densities (Goss-Custard 1970, Krebs et al. 1974, Smith and Sweatman 1974, Zach and Falls 1976a, 1976b, Cowie 1977, Cook and Hubbard 1977, Waage 1979). Our analysis is based on the assumption that relatively large-scale seasonal changes in mean surface layer copepod densities are correlated with densities in patches exploited by herring and pollock. An analysis of plankton patchiness off California provides some insight into the validity of this assumption. Studies employing a Longhurst plankton recorder (Longhurst et al. 1966) indicated that the ratio of copepod densities in patches varied horizontally by a mean factor of 2.6 above background densities, and the patch-to-background density ratio did not differ significantly among 11 tow lines (Wiebe 1970). Owen's (1989) results were similar, i.e. the median prey density within a patch was approximately 2 times the density that would be obtained with an integrative sampler. However, the validity of this assumption to our analysis may not be critical, because our method of estimating daily consumption of copepods integrates amounts taken from many patches by many individuals over a 12 hour period.

A sigmoid type III functional response model provided the best fit of the data for both herring and adult pollock. This function typically fits a predator's response to the principal prey when alternative prey are available and prey

switching occurs (Lawton et al. 1974, Akre and Johnson 1979). In a system involving two prey types (A and B), Murdoch (1969) defined switching as $A/B \text{ in the diet} = c(A/B \text{ available})$, i.e. for prey type A, fewer prey than expected are taken at a low density and more prey than expected are taken at a high density. Switching behavior is often associated with predator preferences for particular prey resulting in differential rejection of encountered prey (Holling 1965, Murdoch 1969, Oaten and Murdoch 1975). In vertebrate predators, prey preferences and switching behavior may result from learning (Holling 1965, Krebs 1973, Murdoch and Oaten 1975, Curio 1976). Predators may learn the shape (Jacobs 1965), visibility (Mellors 1975, Zaret and Kerfoot 1975), or movement patterns (Zaret 1980, Wright and O'Brien 1982) of a particular prey type. Prey capture success rate may also increase as predators learn successful techniques for capturing prey, thus increasing the profitability associated with preferred prey (Vinyard 1982). Hassell (1978) indicated that the shape of the type III response model may arise from an underlying relationship between attack rate and prey density. Such a relationship may result from predator preferences, but a relationship between prey density and swimming speed (Ware 1978) affecting encounter rate ($\gamma \cdot U$) may also result in a type III functional response. Several authors have also indicated that predators capable of concentrating their search efforts in high density prey patches may exhibit type III functional responses if different prey types dominate different patches (Hassell and May 1974, Murdoch et al. 1975, Murdoch and Oaten 1975). In the present study, numerous alternative prey types were available at varying (unknown) densities, so application of Murdoch's (1969) test for switching behavior is not possible and the mechanisms underlying our type III response models are unknown. We will use the term 'switching' in this paper to describe cases when the dominant prey type in the diet changes abruptly.

Our analysis indicated that herring may begin to switch to alternative prey as the mean biomass of large calanoid copepods in the upper 20 m of the water column declines below about 0.2 g m^{-3} . Similarly, adult pollock may begin to switch to alternative prey as the mean biomass of large calanoid copepods in high density layers declines below about 1.0 g m^{-3} . There was considerable variability about the functional response near this threshold as each

predator began to switch to alternative prey. This variability may result from the presence of different alternative prey at varying densities at each location or individual or group variation in prey preferences. In an experiment conducted by Olmsted et al. (1979), one group of mimic shiners (*Notropis volucellus*) developed a strong preference for a particular prey type and another group a weak preference. When an alternative prey was offered, the strong preference group did not switch to the alternative prey even when it was presented at a much higher density than the preferred prey. Olmsted et al. (1979) also found a high degree of individual variability in prey preferences. A high degree of individual variation in prey preferences has also been documented from field studies of fishes (Bryan and Larkin 1972, Ehlinger 1990). In the present study, the percent of herring and immature pollock diets comprised of large calanoid copepods remained relatively high in late May 1995 (Figures 6-7), well after copepod densities in the surface layer had declined (Figure 4). This may be an indication of a preference for large calanoid copepods among herring and immature pollock for a period of time after the bloom.

The parameters of our best fit functional response model for herring were consistent with a particulate feeding mode. Values for γ (0.0791 m^2) and U (10.0 km day^{-1}) consistent with particulate feeding provided the best fit to the data. An identical fit could be obtained with values for γ and U of 0.0001 m^2 (consistent with ram filter feeding) and 7900 km day^{-1} (469 L sec^{-1}), respectively. However, burst swimming speeds of fish typically range between $10\text{-}20 \text{ L sec}^{-1}$ (Brett and Groves 1979), so the swimming speed required to obtain a similar fit of our herring data using a value of γ consistent with ram filter feeding is not physiologically possible. Filter feeding is energetically more profitable than particulate feeding for herring (13-20 cm) feeding on *Calanus finmarchicus* (2.8 mm) at prey densities exceeding about $13,000 \text{ ind. m}^{-3}$ (Gibson and Ezzi 1992). In the present study, densities of large calanoid copepods were only 80 ind. m^{-3} at the asymptote of our functional response model for herring. It is likely that herring were feeding in high density patches of copepods, but it seems unlikely that copepod densities in patches were high enough for profitable filter feeding by herring. Copepod densities have been found to vary horizontally by a factor of 7.0 off British Columbia (Parsons and LeBrasseur 1973) and 2.5-6.0 off California

(Huntley et al. 1995), but densities more than two orders of magnitude greater than densities measured in the present study would be required for profitable filter feeding by herring.

The parameters of our best fit functional response model for adult pollock were consistent with a ram filter feeding mode with limitation of daily food consumption by gastric evacuation. As previously indicated, our handling time estimate includes time spent capturing and ingesting prey, as well as, any time spent not searching for prey due to satiation or low light level. Our functional response model for adult pollock reached an asymptote at a mean surface layer prey density of 1.0 g m^{-3} (385 ind. m^{-3}), and the daily food consumption at the asymptote was about 7.0 g day^{-1} ($0.8\% \text{ BW day}^{-1}$) or 0.08 mg sec^{-1} . If we assume continuous feeding throughout the day and no limitation due to gastric evacuation rate, an adult pollock swimming at 0.2 m sec^{-1} , filter feeding on copepods at a density of 1.0 g m^{-3} should consume prey at a rate of about 0.4 mg sec^{-1} . This rate is about 5 times greater than the daily food consumption at the asymptote of our functional response model indicating some portion of the day is likely spent not feeding due to satiation or low light level. If adult pollock are filter feeding, low light level will likely not limit the time spent feeding, indicating that gastric evacuation rate may limit daily food consumption. Our best fit of the functional response model for adult pollock was obtained with values for γ and U of 0.0022 m^2 (consistent with ram filter feeding) and 16.7 km day^{-1} (0.4 L sec^{-1}), respectively. This swimming speed estimate is very similar to that estimated from field measurements (15 km day^{-1}) for foraging schools of adult pollock in the Bering Sea (Radchenko and Sobolevskiy 1993). However, an identical fit of the functional response for adult pollock could be obtained with values for γ and U of 0.2778 m^2 (consistent with particulate feeding) and 0.13 km day^{-1} ($3.0 \times 10^{-6} \text{ L sec}^{-1}$), respectively. Further direct measurements of swimming speeds of individual adult pollock foraging on large calanoid copepods are needed to resolve this question. Feeding mode is likely determined by the relative profitability of each strategy (Crowder 1985) which is a function of fish size, prey size, and prey density (Durbin 1979, Gerking 1994). Studies involving herring and alewives and Pacific mackerel have shown that ram filter feeding generally occurs at prey densities greater than $10,000 \text{ ind. m}^{-3}$ (Janssen 1976, Gibson and Ezzi 1985,

1992). In the present study, the mean copepod density in layers was about 385 ind. m³ at the asymptote of our best fit functional response model for adult pollock. Thus, laboratory studies suggest that copepod densities more than an order of magnitude greater would be required for profitable filter feeding by adult pollock. However, no laboratory data is available regarding the densities required for fish the size of adult pollock to profitably filter feed on prey the size of large calanoid copepods. The prey-predator size ratio estimated in the present study for adult pollock feeding on large calanoid copepods is about 0.5%. This ratio is at the lower end of the range for particulate feeding and the upper end of the range for filter feeding as estimated by Durbin (1979). Yoshida (1994) predicted from gill raker spacings that adult pollock would likely consume prey greater than 2 mm, but zooplankton greater than 4 mm were generally taken. Yoshida (1994) suggested that sight was involved in selecting larger prey. However, retention probabilities calculated from gill raker spacing have been found to underestimate the size of prey actually retained by a factor of two (Wright et al. 1983). Further studies focused on plankton densities actually utilized by foraging adult pollock, swimming speeds while foraging, and the relationship between prey size, predator size and gill raker spacing (Lammens 1985) will help determine the feeding mode utilized by adult pollock feeding on large calanoid copepods.

In the present study, mean prey-predator length ratios estimated for herring and adult pollock were below the range for mean prey-predator length ratios (20-30%) typically observed among piscivorous fish. The mean prey-predator length ratio for adult pollock was 8.4%, minimum and modal prey lengths were similar for both immature and adult pollock, but adult pollock consumed prey up to 15 cm which were not taken by immature pollock (Figure 10). In a review of piscivory in freshwater systems, Popova (1978) showed that maximum prey size increases as predaceous fish grow whereas minimum prey size remains constant. Thus, mean prey-predator length ratios tend to stabilize around 10% for larger predators. The results from the present study are generally consistent with Popova's (1978) conclusions suggesting that similar generalizations may apply in marine systems. Mean prey-predator length ratios were smallest for juvenile gadids and salmonids as prey (Table 6). This was likely due simply to the smaller lengths of these prey fish in the environment (Figure 12) rather than any difference in escape response

between these species and the others. The relationship between burst swimming speeds of potential prey and optimal foraging speeds of predaceous fish may largely determine mean prey-predator length ratios. Burst swimming speeds typically range from 10-20 L sec⁻¹ (Brett and Groves 1979, Puckett and Dill 1984); whereas, optimal foraging speeds range from 1-3 L sec⁻¹ (Ware 1978). Thus, a mean prey-predator length ratio of 10% roughly equalizes the burst swimming speed of potential prey and the optimal foraging speeds of predators. Thus, generally a predator may prey on fish up to 10% of its length and still maximize its production (Ware 1978).

Multiple regression analysis indicated that herring and immature pollock tend to switch from large calanoid copepods to fish after the decline of the copepod bloom, but adult pollock do not switch to fish after the bloom. Much of the variance in copepod biomass and relative abundances of prey fish was associated with a seasonal decrease (increase) of each variable, respectively (Figures 4 and 11), suggesting that multicollinearity may have affected our results. But, the variance inflation factors for these analyses were substantially less than the threshold above which multicollinearity is generally considered to adversely affect parameter estimates (Neter et al. 1989). Our regression results indicate that consumption of fish by herring and immature pollock was associated copepod biomass, but consumption of fish by adult pollock was not (Table 8). Herring, immature pollock and adult pollock diets were generally dominated by large calanoid copepods during the bloom in May (Figures 6-8). Consumption of alternative prey including fish by these predators was generally reduced at this time. After the copepod bloom, herring and immature pollock tended to consume more fish (Table 8), but other alternative prey were also taken (Figures 6-7). Consumption of fish by immature pollock was also associated with the relative abundance of prey fish, but this was not the case for the other two predators (Table 8). Immature pollock also exhibited the greatest degree of piscivory overall (Table 5) suggesting a preference for fish as prey. Juvenile gadids and salmonids were the most commonly encountered fish in the diets of herring and immature pollock (Table 5). Thus, as herring and immature pollock switch to feeding on fish after the copepod bloom, mortality among juvenile gadids and salmonids will likely increase.

Coded-wire tag data allowed us to further examine whether mortality among juvenile pink salmon was related to copepod biomass. The analysis was structured to enable examination of the simultaneous effects of zooplankton density on juvenile growth rate and predator switching behavior. The results from this analysis support the hypothesis that a prolonged spring bloom of large calanoid copepods generally results in reduced mortality among juvenile pelagic fishes (Tables 10 and 11). This result is also generally consistent with our results from analyses of predator stomach contents (Table 8, Figure 13) suggesting that predator switching behavior is the cause. The range of juvenile body weights (0.20-0.35 g) in our data corresponds roughly to lengths ranging from 30-36 mm. The apparent decrease in mortality with size among juvenile pink salmon over this relatively narrow size range indicates that predation is highly size-selective. Sizes of prey fish in stomachs of herring and adult pollock are generally consistent with this conclusion, but sizes of prey fish in immature pollock stomachs are not (Figure 10). Size-selective predation by other fish species/sizes not included in this analysis may have also caused the observed relationship. Differences in mortality over similar narrow size ranges have been observed among juvenile sockeye (West and Larkin 1987) and chum salmon (Healey 1982).

In the present study, mortality of hatchery-reared pink salmon during the marine lifestage appeared to be depensatory. Several studies have documented density-dependent mortality during the marine lifestage of salmonids without identifying the processes causing the observed relationships (Peterman 1980, Kaeriyama 1983, Elmen et al. 1990). In the present study, we also cannot conclusively determine the processes causing the observed depensation. Our estimates of natural mortality of pink salmon include effects over a 470 day period during which these fishes range throughout the Gulf of Alaska (Heard 1991). However, saturation of predator populations feeding on juvenile pink salmon is a possible cause of the observed relationship. Data presented by Dobrynina et al. (1989) indicates that several marine fish species feeding on juvenile pink salmon emigrating from the Utka River were likely operating near the lower end of their functional response curves. But, the densities of juveniles in this natural setting were likely much lower than those resulting from large-scale releases of hatchery-reared fish.

Further study is needed to determine whether predator saturation is the cause of the apparent compensatory mortality among juvenile pink salmon released from hatcheries in PWS.

Our results also indicate that growth of juvenile pink salmon is reduced when zooplankton densities are low and juvenile salmonid densities are high (Figure 14). This suggests that competition for food among juvenile pink salmon is likely under these conditions. Walters et al. (1978) concluded that competition for food among juvenile salmonids is unlikely in the coastal ocean; whereas, Bailey et al. (1975) estimated that enhancement programs may lead to food limitation among juvenile salmonids in nearshore habitats. Walters and Juanes (1993) suggest that consumption per time spent feeding and foraging times should be density dependent when juveniles occupy restricted feeding habitats to avoid predation. This is likely the case with juvenile pink salmon which often occupy nearshore habitats before reaching a length of about 60 mm (Heard 1991).

The results from these analyses indicate that mortality among juvenile gadids and salmonids is likely affected by the timing of the seasonal decline of the *Neocalanus* spp. bloom relative to the prey fishes' growth rate. Mortality among other larval or relatively small juvenile fishes (e.g. sandlance, capelin, herring etc.) that occur in pelagic habitats during the spring bloom period is also likely affected by these processes. Juvenile gadids and salmonids are growing rapidly at this time of year (Figure 12). Individuals that reach a length exceeding 50-70 mm are probably less vulnerable to predation by herring and immature pollock (Figure 10). Predation by herring and immature pollock may be relatively high in early June in some years (Figures 6 and 7), because copepod densities have generally declined by that time (Figure 4), yet a substantial portion of the juvenile gadid and salmonid population is still vulnerable to predation due to their small size (range approximately 40-65 mm, Figure 12). These results are consistent with Healey (1982) who concluded that mortality was probably high and strongly size selective among juvenile chum salmon over the length range 45-55 mm corresponding to the size of emigration from nearshore habitats. In the present study, the relative abundance of herring and immature pollock also increased in nearshore habitats during early June in some years (Figure 5). This may indicate a numerical response

to the presence of juvenile salmonids (Holling 1959, Beddington et al. 1976, Hassel et al. 1976) after the decline of the copepod bloom.

Our analysis indicates that bottom-up processes affecting the duration of the spring copepod bloom also modify top-down processes involving the timing of feeding mode shifts toward piscivory among the later lifestages of herring and pollock. As previously indicated, the bloom of *Neocalanus spp.* may be prolonged during May when the surface layer is weakly stratified and cooler. At the present time, we are only beginning to understand how these conditions may affect predation on juvenile fishes. Lower temperatures will likely slow the growth of juvenile fishes (Brett and Groves 1979), yet a prolonged *Neocalanus spp.* bloom may accelerate juvenile growth and shelter juveniles from predation for a longer time. The converse may be true when the surface layer is more strongly stratified and warmer. Further study is needed to define the relationship between growth rates of juvenile fishes, the timing of the seasonal decline of the *Neocalanus spp.* bloom and mortality of juvenile fishes.

Acknowledgements

We would like to thank the numerous staff of the Alaska Department of Fish and Game and University of Alaska Fairbanks as well as our charter vessel operators who endured very long work hours and difficult conditions to obtain the samples used in this study. M. Powell, S. Karpovich, A. Dibiccari, R. Dunbar, N. Spear and P. Saddler conducted stomach content analyses and processed zooplankton samples. P. Saddler also designed and maintained the databases used in the project. The Prince William Sound Science Center kindly provided laboratory space for sample processing, and the Prince William Sound Aquaculture Corporation provided the zooplankton settled volume, ocean temperature and juvenile release data used in this analysis. Wind speed data was provided by D.L. Eslinger and physical oceanographic data was provided by S.L. Vaughan. This project was funded by the Exxon Valdez Oil Spill Trustee Council through the Sound Ecosystem Assessment project. However, the findings presented by the authors are their own and do not represent the position of the Trustee Council.

List of Tables

- Table 1: Dates and areas where sampling was conducted in western Prince William Sound, 1994-1996. See figure 1 for locations of sampling areas.
- Table 2: Number of specimens processed for stomach contents analysis in western Prince William Sound, 1994-1996.
- Table 3: Geometric mean catch per net set for immature and adult fishes (>150 mm length) in purse seines in western Prince William Sound, 1994-1996. Catch per hour of tow in mid-water trawls used for pollock.
- Table 4: Summary of 'best fit' non-linear regression models for type II and III functional responses for herring, immature pollock and adult pollock feeding on large calanoid copepods. The best fit model for each species is indicated with an asterisk, and the standard error of the estimated swimming speed (U) is indicated in parentheses.
- Table 5: Mean percent of the diet for various prey fish consumed by herring, immature pollock and adult pollock in western Prince William Sound, 1994-1996. The standard error of the mean is indicated in parentheses.
- Table 6: Mean length and prey-predator length ratios for various prey fish in the diets of herring, immature pollock, and adult pollock. Data from 1994-1996 combined.

List of Tables (con't)

- Table 7: Geometric mean catch per net set for juvenile fishes (<150 mm length) in purse seines in western Prince William Sound, 1994-1996.
- Table 8: Parameters estimated from a multiple regression analysis with the proportion of herring and pollock diets comprised of fish as the dependent variable and the relative abundance of prey fish and the biomass of large calanoid copepods as independent variables.
- Table 9: Parameters estimated from an analysis of covariance relating the growth rate of coded-wire tagged juvenile pink salmon to mean zooplankton settled volume, mean ocean temperature, and number of juveniles released from each hatchery each day.
- Table 10: Parameters estimated from an analysis of covariance relating the instantaneous natural mortality of coded-wire tagged pink salmon to zooplankton settled volume, mean juvenile growth rate, mean body weight at release, and number of juveniles released from each hatchery each day.
- Table 11: Least-squares means estimated from an analysis of covariance relating the instantaneous natural mortality of coded-wire tagged pink salmon to zooplankton settled volume, mean juvenile growth rate, mean body weight at release, and number of juveniles released from each hatchery each day. P-values for pairwise comparisons of the means are indicated.

Table 1: Dates and areas where sampling was conducted in western Prince William Sound, 1994-1996.

See figure 1 for locations of sampling areas.

Year	Area	Dates Sampled
1994	60	April 27, May 7, May 22, June 5, July 8
	61	May 9, May 23, June 9, July 10
	62	May 12, May 26, June 8, July 18
	63	June 7, June 22, July 9
	64	June 21, July 13
	65	June 28, July 14
	66	May 13, June 23, July 12
1995	501	May 3, May 11, May 30
	502	May 17, June 5
	504	June 9
	505	June 11
	506	May 5, May 15, June 8
	509	June 13
	525	May 8, May 13, June 3
	526	May 9

Table 1: continued.

Year	Area	Dates Sampled
1996	501	May 3, May 6, June 5
	502	May 4, May 7, May 24, June 1
	525	May 5, May 8, May 19, May 23, June 2, June 8
	504	May 25, June 6
	506	May 20, June 7
	586	May 21, June 3
	587	May 22, June 4

Table 2: Number of specimens processed for stomach contents analysis in western Prince William Sound,
1994-1996.

Year	Herring	Immature Pollock	Adult Pollock
1994	1,594	280	2,232
1995	3,486	745	3,111
1996	2,659	398	901

Table 3: Geometric mean catch per net set for immature and adult fishes (>150 mm length) in purse seines in western Prince William Sound, 1994-1996. Catch per hour of tow in mid-water trawls is used for pollock.

Year	Taxonomic	% Frequency	Geometric Mean
	Group	Occurrence	Catch/Set
1994	Herring	43.6	5.4
	Pollock	66.8	18.3
	Salmonids	27.7	1.8
	Capelin	0.2	1.0
	Sandlance	0.2	1.0
	Squid	3.0	1.1
	Other Fish	10.7	1.1
1995	Herring	36.9	10.5
	Pollock	81.8	33.5
	Salmonids	18.6	1.6
	Capelin	1.3	1.0
	Sandlance	0.6	1.0
	Squid	4.0	1.1
	Other Fish	21.1	1.4

Table 3: continued.

Year	Taxonomic	% Frequency	Geometric Mean
	Group	Occurrence	Catch/Set
1996	Herring	33.0	3.1
	Pollock	80.9	13.6
	Salmonids	16.0	1.5
	Capelin	3.2	1.2
	Sandlance	0	0
	Squid	22.3	4.7
	Other Fish	16.0	1.1

Table 4: Summary of 'best fit' non-linear regression models for type II and III functional responses for herring, immature pollock and adult pollock feeding on large calanoid copepods. The best fit model for each species is indicated with an asterisk, and the standard error of the estimated swimming speed (U) is indicated in parentheses.

Predator Type		γ (m ²)	Estimated		MS	MS
			U (km day ⁻¹)	H (day g ⁻¹)	Regression	Error
Herring	II	0.0001	43.0 (7.3)	.167	7.86	0.16
		0.0791	0.6 (0.5)	1.930	7.91	0.16
	III	0.0001	17.2 (2.0)	-1.913	2.99	0.33
		0.0791	10.0 (5.3)	1.247	9.40	0.10 *
Immature	II	0.0003	16.7 (3.7)	.304	5.27	0.14
Pollock		0.0791	0.3 (0.4)	2.813	3.29	0.22
	III	0.0003	61.3 (18.4)	.319	4.59	0.16
		0.0791	4.5 (5.6)	2.151	3.96	0.19
Adult	II	0.0022	8.1 (3.8)	.248	208.02	5.52
Pollock		0.2788	0.1 (0.2)	.524	156.47	6.96
	III	0.0022	16.7 (5.0)	.142	243.46	4.54 *
		0.2788	0.4 (0.5)	.438	185.24	6.16

Table 5: Mean percent of the diet for various prey fish consumed by herring, immature pollock and adult pollock in western Prince William Sound, 1994-1996. The standard error of the mean is indicated in parentheses.

Year	Prey	Herring	Immature Pollock	Adult Pollock
1994	Herring	0.12 (0.37)	0.01 (0.70)	0.91 (0.36)
	Gadids	0.39 (0.98)	3.42 (1.83)	2.16 (0.93)
	Salmonids	0.04 (0.23)	0.03 (0.43)	0.94 (0.22)
	Capelin	0	0	0
	Sandlance	0.11 (0.09)	0	0.16 (0.09)
	Squid	0	0	4.90 (0.93)
	Other Fish	0.14 (0.77)	0.22 (1.44)	2.22 (0.73)
	Uni. Fish	3.64 (1.53)	10.75 (2.86)	5.76 (1.45)
	All Fish	4.44 (2.14)	14.43 (4.01)	17.06 (2.04)
1995	Herring	0	0	0.11 (0.04)
	Gadids	1.13 (0.73)	2.03 (1.01)	0.30 (0.72)
	Salmonids	0.09 (0.66)	4.08 (0.91)	0.13 (0.65)
	Capelin	0	0	0
	Sandlance	0	0	0
	Squid	0.01 (0.44)	0	3.81 (0.44)
	Other Fish	0.31 (0.22)	0.67 (0.31)	0.14 (0.22)
	Uni. Fish	9.85 (1.49)	7.17 (2.06)	2.16 (1.46)
	All Fish	11.39 (1.91)	13.90 (2.64)	6.69 (1.88)

Table 5: continued.

Year	Prey	Herring	Immature Pollock	Adult Pollock
1996	Herring	0	0	1.69 (0.72)
	Gadids	0.05 (0.03)	0	0.01 (0.03)
	Salmonids	3.18 (1.81)	10.32 (2.43)	1.10 (1.84)
	Capelin	0	0	0.73 (0.45)
	Sandlance	0	7.23 (1.90)	0
	Squid	0	0	7.67 (1.39)
	Uni. Fish	0.35 (0.33)	1.38 (0.44)	0.27 (0.33)
	Other Fish	0.59 (1.40)	7.33 (1.87)	4.60 (1.42)
	Total Fish	4.18 (2.86)	26.25 (3.83)	16.02 (2.90)

Table 6: Mean length and prey-predator length ratios for various prey fish in the diets of herring, immature pollock, and adult pollock. Data from 1994-1996 combined.

Prey Species	<u>Herring</u>		<u>Immature Pollock</u>		<u>Adult Pollock</u>	
	Length	Ratio	Length	Ratio	Length	Ratio
Herring	-	-	-	-	115.5	20.9
Gadids	28.0	14.1	34.3	20.3	22.7	5.0
Salmonids	40.3	18.9	40.5	19.5	39.1	8.1
Capelin	-	-	-	-	92.5	19.1
Sandlance	-	-	57.4	22.9	98.8	17.6
Squid	-	-	-	-	68.9	13.1
Other Fish	19.3	10.4	24.5	12.5	47.9	8.6
Uni. Fish	21.7	11.4	23.7	9.6	42.2	8.2

Table 7: Geometric mean catch per net set for juvenile fishes (<150 mm length) in purse seines in western Prince William Sound, 1994-1996.

Year	Taxonomic	% Frequency	Geometric Mean
	Group	Occurrence	Catch/Set
1994	Herring	12.5	1.7
	Gadids	33.2	54.6
	Salmonids	30.0	5.4
	Capelin	3.7	1.2
	Sandlance	1.6	1.0
	Squid	0.7	1.0
	Other Fish	18.2	1.6
1995	Herring	15.5	1.6
	Gadids	5.5	1.3
	Salmonids	23.2	3.7
	Capelin	18.2	2.1
	Sandlance	2.7	1.0
	Squid	6.5	1.6
	Other Fish	28.4	3.1

Table 7: continued.

Year	Taxonomic	% Frequency	Geometric Mean
	Group	Occurrence	Catch/Set
1996	Herring	4.9	1.1
	Gadids	6.5	1.5
	Salmonids	32.4	27.5
	Capelin	20.0	2.4
	Sandlance	0	0
	Squid	13.0	3.5
	Other Fish	23.2	2.4

Table 8: Parameters estimated from a multiple regression analysis with the proportion of herring and pollock diets comprised of fish as the dependent variable and the relative abundance of prey fish and the biomass of large calanoid copepods as independent variables.

Fish Species	Independent Variable	Regression Parameter	Standard Error	Type I Test P-value	Type III Test P-value
Herring	Copepod biomass	-0.620	0.346	0.126	0.083
	Prey fish abundance	-0.028	0.026	0.298	0.298
Immature	Copepod biomass	-1.145	0.771	0.020	0.150
Pollock	Prey fish abundance	0.117	0.055	0.044	0.044
Adult Pollock	Copepod biomass	-0.194	0.332	0.646	0.564
	Prey fish abundance	0.005	0.019	0.748	0.709

Table 9: Parameters estimated from an analysis of covariance relating the growth rate of coded-wire tagged juvenile pink salmon to mean zooplankton settled volume, mean ocean temperature, and number of juveniles released from each hatchery each day.

Parameter	Estimate	Standard	Type III Test
		Error	P-value
Intercept	-5.762	1.468	<0.001
Mean zooplankton volume	3.201	0.445	<0.001
Mean ocean temperature	2.421	0.780	0.002
Number juveniles released: low	4.850	0.676	<0.001
high	0.000	-	-
Zooplankton x release number: low	-2.729	0.480	<0.001
high	0.000	-	-

Table 10: Parameters estimated from an analysis of covariance relating the instantaneous natural mortality of coded-wire tagged pink salmon to zooplankton settled volume, mean juvenile growth rate, mean body weight at release, and number of juveniles released from each hatchery each day.

Parameter		Estimate	Standard Error	Type III Test P-value
Intercept		0.0774	0.0123	<0.001
Zooplankton volume:	low	0.0014	0.0006	0.013
	moderate	0.0002	0.0005	-
	high	0.0000	-	-
Mean juvenile growth rate		-0.0112	0.0024	<0.001
Body weight at release		-0.2419	0.0455	<0.001
Number juveniles released		-0.0077	0.0020	<0.001
Growth x release weight:		0.0391	0.0085	<0.001
Number released x release weight		0.0264	0.0075	<0.001

Table 11: Least-squares means estimated from an analysis of covariance relating the instantaneous natural mortality of coded-wire tagged pink salmon to zooplankton settled volume, mean juvenile growth rate, mean body weight at release, and number of juveniles released from each hatchery each day. P-values for pairwise comparisons of the means are indicated.

Zooplankton Volume	Least Squares	Standard	<u>Pairwise Comparisons</u>		
	Mean	Error	Low	Mod.	High
low	0.0097	0.0003	-	0.008	0.013
moderate	0.0085	0.0003	-	-	0.644
high	0.0083	0.0004	-	-	-

References

- Akre, B.G. and D.M. Johnson. 1979. Switching and sigmoid functional response curves by damselfly naiads with alternative prey available. *J. Anim. Ecol.* 48: 703-720.
- Armstrong, R.H. and P.C. Winslow. 1968. An incidence of walleye pollock feeding on salmon young. *Trans. Amer. Fish Soc.* 97(2): 202-203.
- Bailey, J.E., B.L. Wing and C.R. Mattson. 1975. Zooplankton abundance and feeding habits of fry of pink salmon, *Oncorhynchus gorbuscha*, and chum salmon *Oncorhynchus keta*, in Traitors Cove, Alaska, with speculations on the carrying capacity of the area. *Fish. Bull.* 73(4): 846-861.
- Bakshantansky, E.L. 1965. The impact of the environmental factors on survival of the far eastern young salmon during the acclimatization of the latter in the northwest part of the USSR. ICNAF Environmental Symposium, Spec. Publ. no. 6, pp. 477-479.
- Beddington, J.R., M.P. Hassell, and J.H. Lawton. 1976. The components of arthropod predation II: The predator rate of increase. *J. Anim. Ecol.* 45: 165-186.
- Brett, J.R. 1964. The respiratory metabolism and swimming performance of young sockeye salmon. *J. Fish. Res. Board Can.* 21: 1183-1226.
- Brett, J.R. and N.R. Glass. 1973. Metabolic rates and critical swimming speeds of sockeye salmon (*Oncorhynchus nerka*) in relation to size and temperature. *J. Fish. Res. Board Can.* 30: 379-387.

- Brett, J.R. and T.D.D. Groves. 1979. Physiological energetics. Pages 279-352. In W.S. Hoar, D.J. Randall, and J.R. Brett (eds.), Fish Physiology. Vol VIII. Academic Press, New York, NY.
- Bryan, J.E. and P.A. Larkin. 1972. Food specialization by individual trout. J. Fish. Res. Board Can. 29: 1615-1624.
- Charnov, E. 1976. Optimal foraging: Attach strategy of a mantid. Amer. Naturalist 110: 141-151.
- Clausen, D.M. 1983. Food of walleye pollock, *Theragra chalcogramma*, in an embayment of southeastern Alaska. Fish. Bull. 81(3): 637-642.
- Cook, R.M. and S.F. Hubbard. 1977. Adaptive search strategies in insect parasites. J. Anim. Ecol. 46: 115-125.
- Cooney, R.T. 1986. Zooplankton. Pages 285-304. In D.W. Hood and S.T. Zimmerman. (eds.) The Gulf of Alaska, physical environment and biological resources. U.S. Dept. of Commerce, Minerals Management Service, Anchorage, Alaska.
- Cowie, R.J. 1977. Optimal foraging in great tits. Nature 268: 137-139.
- Coyle, K.O., A.J. Paul, D.A. Ziemann. 1990. Copepod populations during the spring bloom in an Alaskan subarctic embayment. J. Plankton Research 12(4): 759-797.
- Coyle, K.O. and A.J. Paul. 1992. Interannual differences in prey taken by capelin, herring, and red salmon relative to zooplankton abundance during the spring bloom in a southeast Alaska embayment. Fish. Oceanogr. 1(4): 294-305.

- Cross, J.N., K.L. Fresh, B.S. Miller, C.A. Simenstad, S.N. Steinfort, J.C. Fegley. 1978. Nearshore fish and macroinvertebrate assemblages along the Strait of Juan De Fuca including food habits of the common nearshore fish. NOAA Technical Memorandum ERL MESA-32, 188p.
- Crowder, L.B. 1985. Optimal foraging and feeding mode shifts in fishes. *Environ. Biol. Fish.* 12(1): 57-62.
- Curio, E. 1976. The Ethology of Predation. Springer-Verlag, New York.
- Cushing, D.H. 1967. The grouping of herring populations. *J. Mar. Biol. Ass., U.K., N.S.*, 47: 193-208.
- Dobrynina, M.V., S.A. Gorshkov and N.M. Kinas. 1989. Effect of density of juvenile pink salmon, *Oncorhynchus gorbuscha*, on their vulnerability to predators in the Utka River (Kamchatka). *J. Ichthy.* 29(1): 148-155.
- Durbin, A.G. 1979. Food selection by plankton feeding fishes. Pages 203-218 *In* R.H. Stroud and M. Clapper (eds.), Predator-prey systems in fisheries management. Sport Fishing Inst., Washington, D.C.
- Dwyer, D.A., K.M. Bailey, P.A. Livingston. 1987. Feeding habits and daily ration of walleye pollock (*Theragra chalcogramma*) in the eastern Bering Sea, with special reference to cannibalism. *Can. J. Fish. Aquat. Sci.* 44: 1972-1984.
- Eggers, D.M. 1977. Factors in interpreting data obtained by diel sampling of fish stomachs. *J. Fish. Res. Board Can.* 34: 290-294.

Ehlinger, T.J. 1990. Habitat choice and phenotype-limited feeding efficiency in blue gill: individual differences and trophic polymorphism. *Ecology* 71: 886-896.

Elmen, J.M., R.R. Reisenbichler and A.M. McGie. 1990. Density-dependence at sea for coho salmon (*Oncorhynchus kisutch*). *Can. J. Fish. Aquat. Sci.* 47(9): 1765.

Emery, W.J. and K. Hamilton. 1985. Atmospheric forcing of interannual variability in the northeast Pacific Ocean: connections with El Nino. *J. Geophys. Res* 90(C1): 857-868.

Fresh, K.L. and S.L. Schroder. 1987. Influence of the abundance, size, and yolk reserves of juvenile chum salmon (*Oncorhynchus keta*) on predation by freshwater fishes in a small coastal stream. *Can. J. Fish. Aquat. Sci.* 44: 236-242.

Fulton, J.D. 1973. Some aspects of the life history of *Calanus plumchrus* in the Strait of Georgia. *J. Fish. Res. Board. Can.* 30: 811-815.

Gerking, S.D. 1994. Feeding ecology of fish. Academic Press, New York, NY.

Gibson, R.N. and I.A. Ezzi. 1985. Effect of particle concentration on filter and particulate feeding in the herring, *Clupea harengus*. *Mar. Biol.* 88(2): 109-116.

Gibson, R.N. and I.A. Ezzi. 1992. The relative profitability of particulate- and filter- feeding in the herring, *Clupea harengus*. *J. Fish. Biol.* 40: 577-590.

- Gorbatenko, K.M. and N.T. Dolganova. 1989. Feeding of sexually mature walleye pollock, *Theragra chalcogramma*, and utilization of the food resources in the Okhotsk Sea during autumn. *Voprosy Ikhtiologii* 2: 249-256.
- Goss-Custard, J.D. 1970. The responses of redshank (*Tringa totanus* (L.)) to spatial variation in the density of their prey. *J. Anim. Ecol.* 39: 91-113.
- Gulbrandsen, J. 1991. Functional response of Atlantic halibut larvae related to prey density and distribution. *Aquaculture* 94: 89-98.
- Hartt, A.C. 1980. Juvenile salmonids in the oceanic ecosystem - the critical first summer. Pages 25-58. *In* W.J. McNeil and D.C. Himsworth (eds.), *Salmonid ecosystems of the North Pacific*. Oregon State University Press.
- Hassell, M.P. and R.M. May. 1974. Aggregation of predators and insect parasites and its effect on stability. *J. Anim. Ecol.* 45: 135-164.
- Hassell, M.P., J.H. Lawton, and J.R. Beddington. 1976. The components of arthropod predation I: The prey death-rate. *J. Anim. Ecol.* 45: 135-164.
- Hassel, M.P. 1978. *The dynamics of arthropod predator-prey systems*. Princeton Univ. Press, Princeton, NJ.
- Healey, M.C. 1982. Timing and relative intensity of size-selective mortality of juvenile chum salmon (*Oncorhynchus keta*) during early sea life. *Can. J. Fish. Aquat. Sci.* 39: 952-957.

Heard, W.R. 1991. Life history of pink salmon (*Oncorhynchus gorbushca*). Pages 119-230. In C. Groot and L. Margolis (eds.), Pacific salmon life histories. University of British Columbia Press, Vancouver, British Columbia.

Hjort, J. 1914. Fluctuations in the great fisheries of northern Europe viewed in the light of biological research. Rapp. P.-v. Reun. Cons. int. Explor. Mer, 20: 1-228.

Holling, C.S. 1959. The components of predation as revealed by a study of small mammal predation of the European pine sawfly. Can. Entomol. 91: 293-320.

Holling, C.S. 1965. The functional response of predators to prey density and its role in mimicry and population regulation. Mem. Entomol. Soc. Can. 45: 1-60.

Huntley, M.E., M. Zhou, and W. Nordhausen. 1995. Mesoscale distribution of zooplankton in the California current in late spring, observed by optical plankton counter. J. Mar. Res. 53: 647-674.

Geiger, H.J. 1990. Pilot studies in tagging Prince William Sound hatchery pink salmon with coded-wire tags. Fishery Research Bulletin No. 90-02, Alaska Dept. of Fish and Game, Div. Commercial Fisheries, P.O. Box 3-2000, Juneau, Alaska 99802-2000

Iverson, R.L., H.C. Curl, Jr., H.B. O'Connors, Jr., D. Kirk. and K. Zakar. 1974. Summer phytoplankton blooms in Auke Bay, Alaska, driven by wind mixing of the water column. Limnol. Oceanogr. 19: 271-278.

Jacobs, J. 1965. Significance of morphology and physiology of *Daphnia* for its survival in predator-prey experiments. Naturwissenschaften 52: 141.

Janseen, J. 1976. Feeding modes and prey size selection in the alewife (*Alosa pseudoharengus*). J. Fish. Res. Board Can. 33: 1972-1975.

Juanes, F. 1994. What determines prey size selection in piscivorous fishes ? Pages 79-100. In D.J. Stouder, K.L. Fresh, R.J. Feller (eds.) Theory and application of fish feeding ecology. Univ. of South Carolina Press, Columbia, South Carolina.

Kaeriyama, M. 1989. Aspects of salmon ranching in Japan. Physiol. Ecol. Japan, Spec. Vol 1: 625-638.

Krebs, J.R. 1973. Behavioral aspects of predation. Pages 73-111. In P.P.G. Bateson and P.H. Klopfer (eds), Perspectives in Ethology. Plenum Press, New York.

Krebs, J.R., J.C. Ryan, and E.L. Krebs. 1974. Hunting by expectation or optimal foraging? A study of patch use by chickadees. Anim. Behav. 22: 953-964.

Lammens, E.H.R.R. 1985. A test for planktivorous filter feeding by bream, *Abramis brama*. Environ. Biol. Fishes 13: 289-296.

Lawton, J.H., J.R. Beddington, R. Bonser. 1974. Switching in invertebrate predators. Pages 141-158. In M.B. Usher and M.H. Williamson (eds.), Ecological stability, Chapman and Hall, Great Britain.

Longhurst, A.R., A.D. Reith, R.E. Bower, and D.L.R. Seibert. 1966. A new system for the collection of multiple serial plankton samples. Deep-Sea Res. 13: 213-222.

- MacKenzie, B.R., W.C. Leggett, and R.H. Peters. 1990. Estimating larval fish ingestion rates: can laboratory derived values be reliably extrapolated to the wild ? Mar. Ecol. Prog. Ser. 67: 209-225.
- Madison, D.M., R.M. Horrall, A.B. Stasko, and A.D. Hasler. 1972. Migratory movements of adult sockeye salmon (*Oncorhynchus nerka*) in coastal British Columbia as revealed by ultrasonic tracking. J. Fish. Res. Board Can. 29: 1025-1033.
- Maeda, T. 1986. Life cycle and behavior of adult pollock (*Theragra chalcogramma*) in waters adjacent of Funka Bay, Hokkaido Island. INPFC Bulletin 45, 39-65.
- Mellors, W.K. 1975. Selective predation of ephippial *Daphnia* and the resistance of ephippial eggs to digestion. Ecology 56: 974.
- Miller, B.S., C.A. Simenstad and L.L. Moulton. 1976. Puget Sound Baseline Program: Nearshore fish survey. Annual Report to Washington State Dept. of Ecology. FRI-UW-7604, 196p.
- Miller, C.B. 1988. *Neocalanus flemingeri* new species of the Calanidae copepoda Calanoida from the subarctic Pacific Ocean with a comparative redescription of the *Neocalanus plumchrus*, Marukawa 1921. Prog. Oceanogr. 20(4): 223-274.
- Miller, C.B. and M.J. Clemons. 1988. Revised life history analysis for large grazing copepods in the subarctic Pacific Ocean. Prog. Oceanogr. 20(4): 293-313.
- Mittelbach, G.G. 1981. Foraging efficiency and body size: a study of optimal diet and habitat use by bluegills. Ecology 62: 1370-1386.

- Moulton, L.L. 1977. An ecological analysis of fishes inhabiting the rocky nearshore regions of northern Puget Sound, Washington. Ph.D. Thesis, University of Washington, Seattle, 144p.
- Murdoch, W.W. 1969. Switching in general predators: experiments on predator specificity and stability of prey populations. *Ecol. Monogr.* 39: 335-354.
- Murdoch, W.W., S.L. Avery, M.E.B. Smyth. 1975. Switching in predatory fish. *Ecology* 56: 1094-1105.
- Neter, J., W. Wasserman, M.H. Kutner. 1989. Applied linear regression models. Irwin, Boston, Massachusetts.
- Niebauer, H.J., T.C. Royer, and T.J. Weingartner. 1994. Circulation in Prince William Sound, Alaska. *J. Geophys. Res.* 99(C7): 14,113-14,126.
- Oaten, A. and W.W. Murdoch. 1975. Switching, functional response, and stability in predator-prey systems. *Amer. Natur.* 109: 299-318.
- Okada, K. 1986. Biological characteristics and abundance of pelagic pollock in the Aleutian Basin. *INPFC Bulletin* 45, 150-176.
- Olmsted, L.R., S. Krater, G.E. Williams, and R.G. Jaeger. 1979. Foraging tactics of the mimic shiner in a two-prey system. *Copeia* 3: 437-441.
- Osenberg, C.W. and G.G. Mittelbach. 1989. Effects of body size on the predator-prey interaction between pumpkinseed sunfish and gastropods. *Ecol. Monographs* 59: 405-432.

Owen, R.W. 1989. Microscale and finescale variations of small plankton in coastal and pelagic environments. J. Mar. Res. 47: 197-240.

Peltz, L. and J. Miller. 1990. Performance of half-length coded wire tags in a pink salmon hatchery marking program. Amer. Fish. Soc. Symposium 7: 244-252.

Peterman, R.M. 1980. Testing for density-dependent marine survival in Pacific salmonids. Pages 1-24. In W.J. McNeil and D.C. Himsworth (eds.), Salmonid Ecosystems of the North Pacific. Oregon State University Press, Corvallis, Oregon.

Parsons, T.R. and R.J. LeBrasseur. 1973. The availability of food to different trophic levels in the marine food chain. Pages 325-343. In J.H. Steele (ed.), Marine Food Chains, Oliver & Boyd, Edinburgh.

Paul, A.J., J.M. Paul, and R.L. Smith. 1993. The seasonal changes in somatic energy content of Gulf of Alaska yellowfin sole, *Pleuronectes asper*. J. Fish Biol. 43: 131-138.

Peterman, R.M. and M. Gatto. 1978. Estimation of functional responses of predators on juvenile salmon. J. Fish. Res. Board. Can. 35(6): 797-808.

Peters, D.S. and M.A. Kjelson. 1975. Consumption and utilization of food by various post-larval and juvenile fishes of North Carolina estuaries. Pages 448-472. In L.E. Cronin (ed), Estuarine Research, Academic Press, New York.

Platt, T., V.M. Brawn, B. Irwin. 1969. Caloric and carbon equivalents of zooplankton biomass. J. Fish. Res. Bd. Can. 20: 2345-2349.

Popova, O.A. 1978. The role of predaceous fish in ecosystems. Pages 215-249. In S.D. Gerking (ed.), Ecology of Freshwater Fish Production. John Wiley & Sons, New York.

Puckett, K.J. and L.M. Dill. 1984. Cost of sustained and burst swimming to juvenile coho salmon (*Oncorhynchus kisutch*). Can. J. Fish. Aquat. Sci. 41: 1546-1551.

Radchenko, V.I. and Y.I. Sobolevskiy. 1993. Seasonal spatial distribution dynamics of walleye pollock, *Theragra chalcogramma*, in the Bering Sea. J. Ichthyology 33(2): 63-75.

Ranta, E. and V. Nuutinen. 1985. Foraging by the smooth newt (*Triturus vulgaris*) on zooplankton: functional responses and diet choice. J. Anim. Ecol. 54: 275-293.

Rogers, D.E., B.J. Rogers and R.J. Rosenthal. 1986. The nearshore fishes. Pages 399-416. In D.W. Hood and S.T. Zimmerman (eds.), The Gulf of Alaska: physical environment and biological resources. U.S. Department of Commerce, Minerals Management Service, Anchorage, Alaska.

Rosenthal, R.J. 1983. Shallow water fish assemblages in the northeastern Gulf of Alaska: habitat evaluation, species composition, abundance, spatial distribution and trophic interaction. Research Unit 542. Environ. Assess. Alaskan Cont. Shelf, Final Rep. Principal Investigators 17 (Biological Studies):451-540.

Royer, T.C. 1979. On the effect of precipitation and runoff on coastal circulation in the Gulf of Alaska. J. Phys. Ocn. 9: 555-563.

Ruggerone, G.T. and D.E. Rogers. 1984. Arctic char predation on sockeye salmon smolts at Little Togiak River, Alaska. Fish. Bull. 82: 401-410.

Sambrotto, R.N. 1985. The dependence of phytoplankton nutrient utilization on physical processes in the eastern Bering Sea area. Pages 268-280. In W.S. Wooster and D.L. Fluharty (eds.), El Nino North: Nino effects in the eastern subarctic Pacific Ocean. Washington Sea Grant Program. University of Washington, Seattle.

Sambrotto, R.N. and J.J. Goering. 1983. Interannual variability of phytoplankton and zooplankton production on the southeast Bering Sea shelf. Pages 161-177. In W.S. Wooster (ed.), From year to year: interannual variability of the environment and fisheries of the Gulf of Alaska and the eastern Bering Sea. University of Washington, Seattle.

Simpson, J.H. and J.R. Hunter. 1974. Fronts in the Irish Sea. Nature 250: 404-406.

Smith, J.N.M., and H.P.A. Sweatman. 1974. Food searching behavior of titmice in patchy environments. Ecology 55: 1216-1232.

Smith, R.L. and A.J. Paul. 1986. A theoretical energy budget for juvenile walleye pollock in Alaskan waters. Int. N. Pac. Fish. Comm. Bull. 47: 79-85.

Smith, R.L., J.M. Paul, and A.J. Paul. 1989. Gastric evacuation in Walleye pollock, *Theragra chalcogramma*. Can. J. Fish. Aquat. Sci. 46: 489-493.

- Smith, S.L. and J. Vidal. 1982. Seasonal distribution and abundance of zooplankton and micronekton in the southeast Bering Sea. PROBES Annual Prog. Rept., vol. 1, Inst. Mar. Sci., Univ. Alaska, Fairbanks.
- Stasko, A.B., R.M. Horrall, A.D. Hasler, and D. Stasko. 1973. Coastal movements of mature Fraser River pink salmon (*Oncorhynchus gorbuscha*) as revealed by ultrasonic tracking. J. Fish. Res. Board. Can. 30: 1309-1316.
- Sverdrup, H.U. 1953. On conditions of the vernal blooming of phytoplankton. J. Cons. Explor. Mer 18: 287-295.
- Thorsteinson, F.V. 1962. Herring predation on pink salmon fry in a southeastern Alaska estuary. Trans. Amer. Fish Soc. 91(3): 321-323.
- Trexler, J.C., C.E. McCulloch, J. Travis. 1988. How can the functional response best be determined ? Oecologia 76: 206-214.
- Vinyard, G.L. 1982. Variable kinematics of Sacramento perch (*Archoplites interruptus*) capturing evasive and nonevasive prey. Can. J. Fish. Aquat. Sci. 39: 208.
- Waage, J.K. 1979. Foraging for patchily-distributed hosts by the parasitoid, *Nemeritis canescens* (Grav.). J. Anim. Ecol. 48: 353-371.
- Walline, P.D. 1983. Growth of larval and juvenile walleye pollock related to year-class strength. Ph.D. thesis, University of Washington, Seattle, WA. 144p.

- Walsh, J.J., T.E. Whitledge, F.W. Barvonik, C.D. Wirick and S.O. Howe. 1978. Wind events and food chain dynamics within the New York Bight. *Limnol. Oceanogr.* 23(4): 659-683.
- Walters, C.J., R. Hilborn, R.M. Peterman and M.J. Staley. 1978. Model for examining early ocean limitation of Pacific salmon production. *J. Fish Res. Board Can.* 35: 1303-1315.
- Walters, C.J. and F. Juanes. 1993. Recruitment limitation as a consequence of natural selection for use of restricted feeding habitats and predation risk taking by juvenile fishes. *Can. J. Fish. Aquat. Sci.* 50: 2058-2070.
- Ware, D.M. 1972. Predation by rainbow trout (*Salmo gairdneri*): the influence of hunger, prey density, and prey size. *J. Fish. Res. Board Can.* 29: 1193-1201.
- Ware, D.M. 1978. Bioenergetics of pelagic fish: theoretical change in swimming speed and ration with body size. *J. Fish. Res. Board Can.* 35: 220-228.
- West, C.J. and P.A. Larkin. 1987. Evidence for size-selective mortality of juvenile sockeye salmon (*Oncorhynchus nerka*) in Babine Lake, British Columbia. *Can. J. Fish. Aquat. Sci.* 44: 712-721.
- Winkler, H. and C.P. Orellana. 1992. Functional responses of five cyprinid species to planktonic prey. *Environ. Biol. Fish.* 33: 53-62.
- Wiebe, P.H. 1970. Small-scale spatial distribution in oceanic zooplankton. *Limnol. Oceanogr.* 15: 205-217.

- Willette, T.M., G. Carpenter, P. Shields, and S.R. Carlson. 1994. Early marine salmon injury assessment in Prince William Sound, *Exxon Valdez* Oil Spill State/Federal Natural Resource Damage Assessment Final Report (Fish/Shellfish Study Number 4A), Alaska Dept. Fish and Game, Commercial Fisheries Management and Development Division, Cordova, Alaska.
- Willette, T.M. 1996. Impacts of the *Exxon Valdez* Oil Spill on the migration, growth, and survival of juvenile pink salmon in Prince William Sound. Amer. Fish. Soc. Symposium 18: 533-550.
- Wright, D.I. and W.J. O'Brien. 1982. Differential location of *Chaoborus* larvae and *Daphnia* by fish: the importance of motion and visible size. Amer. Midl. Nat. 108: 68.
- Wright, D.I., W.J. O'Brien and C. Luecke. 1983. A new estimate of zooplankton retention by gill rakers and its ecological significance. Trans. Am. Fish. Soc. 112: 638-646.
- Xiong, Q. and T.C. Royer. 1984. Coastal temperature and salinity in the northern Gulf of Alaska, 1970-1983. J. Geophys. Res. 89(C5): 8061-8068.
- Yoshida, H. 1994. Food and feeding habits of pelagic walleye pollock in the central Bering Sea in summer, 1976-1980. Sci. Rep. Hokkaido Fish. Exp. Stn. 45: 1-35.
- Zach, R., and J.B. Falls. 1976a. Ovenbird (Aves:Parulidae) hunting behavior in a patchy environment: an experimental study. Can. J. Zool. 54: 1863-1879.
- Zach, R., and J.B. Falls. 1976b. Do ovenbirds (Aves:Parulidae) hunt by expectation? Can. J. Zool. 54: 1894-1903.

Zaret, T.M. 1980. The effect of prey motion on planktivore choice. Pages 594-603. *In* W.C. Kerfoot (ed.) *Evolution and Ecology of Zooplankton Communities*, University Press of New England, Hanover.

Zaret, T.M. and W.C. Kerfoot. 1975. Fish predation on *Bosmina longirostris*: body-size selection versus visibility selection. *Ecology* 56: 232.

Ziemann, D.A., L.D. Conquest, M. Olaizola, P.K. Bienfang. 1991. Interannual variability in the spring phytoplankton bloom in Auke Bay, Alaska. *Mar. Biol.* 109: 321-334.

Appendix I: Summary of results of non-linear regression analysis of type II and III functional response models for herring, immature pollock and adult pollock feeding on large calanoid copepods using all possible parameter values.

Table 1: Summary of non-linear regression models for type II and III functional responses of herring feeding on large calanoid copepods. 'Best fit' type II and III models are indicated with an asterisk.

Type	γ (m ²)	U (km day ⁻¹)	Estimated H (day g ⁻¹)	MS Regression	MS Error
II	0.0001	16.8	-0.469	6.14	0.22
	0.0791	16.8	1.906	7.11	0.25
	0.0001	33.7	0.167	7.60	0.17 *
	0.0791	33.7	1.930	7.06	0.19 *
	0.0001	50.5	0.400	7.12	0.19
	0.0791	50.5	1.940	7.04	0.19
III	0.0001	16.8	-1.913	2.98	0.33 *
	0.0791	16.8	1.247	9.30	0.11 *
	0.0001	33.7	-0.515	3.65	0.31
	0.0791	33.7	1.359	8.92	0.12
	0.0001	50.5	-0.061	4.16	0.29
	0.0791	50.5	1.433	8.63	0.13

Table 2: Summary of non-linear regression models for type II and III functional responses of immature pollock feeding on large calanoid copepods. 'Best fit' type II and III models are indicated with an asterisk.

Type	γ (m ²)	U (m day ⁻¹)	Estimated	MS	MS
			H (day g ⁻¹)	Regression	Error
II	0.0003	16.8	0.304	5.27	0.14 *
	0.0791	16.8	2.679	2.81	0.24 *
	0.0003	33.7	0.726	4.99	0.15
	0.0791	33.7	2.770	2.79	0.24
	0.0003	50.5	0.978	4.64	0.16
	0.0791	50.5	2.808	2.78	0.24
III	0.0003	16.8	-0.355	3.66	0.20
	0.0791	16.8	1.304	3.88	0.19
	0.0003	33.7	0.137	4.26	0.18
	0.0791	33.7	1.567	3.55	0.21
	0.0003	50.5	0.319	4.53	0.17 *
	0.0791	50.5	1.719	3.38	0.21 *

Table 3: Summary of non-linear regression models for type II and III functional responses of adult pollock feeding on large calanoid copepods. 'Best fit' type II and III models are indicated with an asterisk.

Type	γ (m ²)	U (km day ⁻¹)	Estimated H (day g ⁻¹)	MS Regression	MS Error
II	0.0022	15.0	0.248	196.18	5.85 *
	0.2778	15.0	0.524	131.85	7.64 *
	0.0022	43.3	0.367	164.12	6.74
	0.2778	43.3	0.529	131.04	7.66
	0.0022	86.7	0.423	151.01	7.11
	0.2778	86.7	0.531	130.82	7.67
	0.0022	130.0	0.449	145.47	7.26
	0.2778	130.0	0.531	130.75	7.67
III	0.0022	15.0	0.142	242.91	4.55 *
	0.2778	15.0	0.438	152.64	7.06 *
	0.0022	43.3	0.217	229.88	4.92
	0.2778	43.3	0.468	144.27	7.29
	0.0022	86.7	0.268	209.98	5.47
	0.2778	86.7	0.486	139.63	7.42
	0.0022	130.0	0.296	198.46	5.79
	0.2778	130.0	0.496	137.35	7.49

List of Figures

- Figure 1: Location of study areas in western Prince William Sound in (a) 1994 and (b) 1995 and 1996.
- Figure 2: Smoothed sea level wind speed (2-day running mean) in central Prince William Sound during May-July (a) 1994, (b) 1995, and (c) 1996. The dashed line shown for 1995 indicates wind speeds at Middleton Island (see Figure 1 for location).
- Figure 3: Time series of ocean temperatures (left panel), salinity (center panel), and sigma-t (right panel) in western Prince William Sound during May-July (a) 1994, (b) 1995 and (c) 1996.
- Figure 4: Biomass of large calanoid copepods (dashed line) and *Neocalanus spp.* (solid line) in the upper 50 m of the water column in western Prince William Sound during (a) 1994 and (b) 1995. Biomass of large calanoid copepods in the upper 20 m of the water column in nearshore habitats of western Prince William Sound during (c) 1995 and (d) 1996.
- Figure 5: Mean catch per net set for herring in purse seines (left panel), immature pollock in variable-mesh gillnets (center panel), and adult pollock in mid-water trawls (right panel) in western Prince William Sound during May-July (a) 1994, (b) 1995 and (c) 1996. Catches of immature pollock in all gear types are indicated for 1994. Vertical bars indicate the standard error of the mean.

List of Figures (con't)

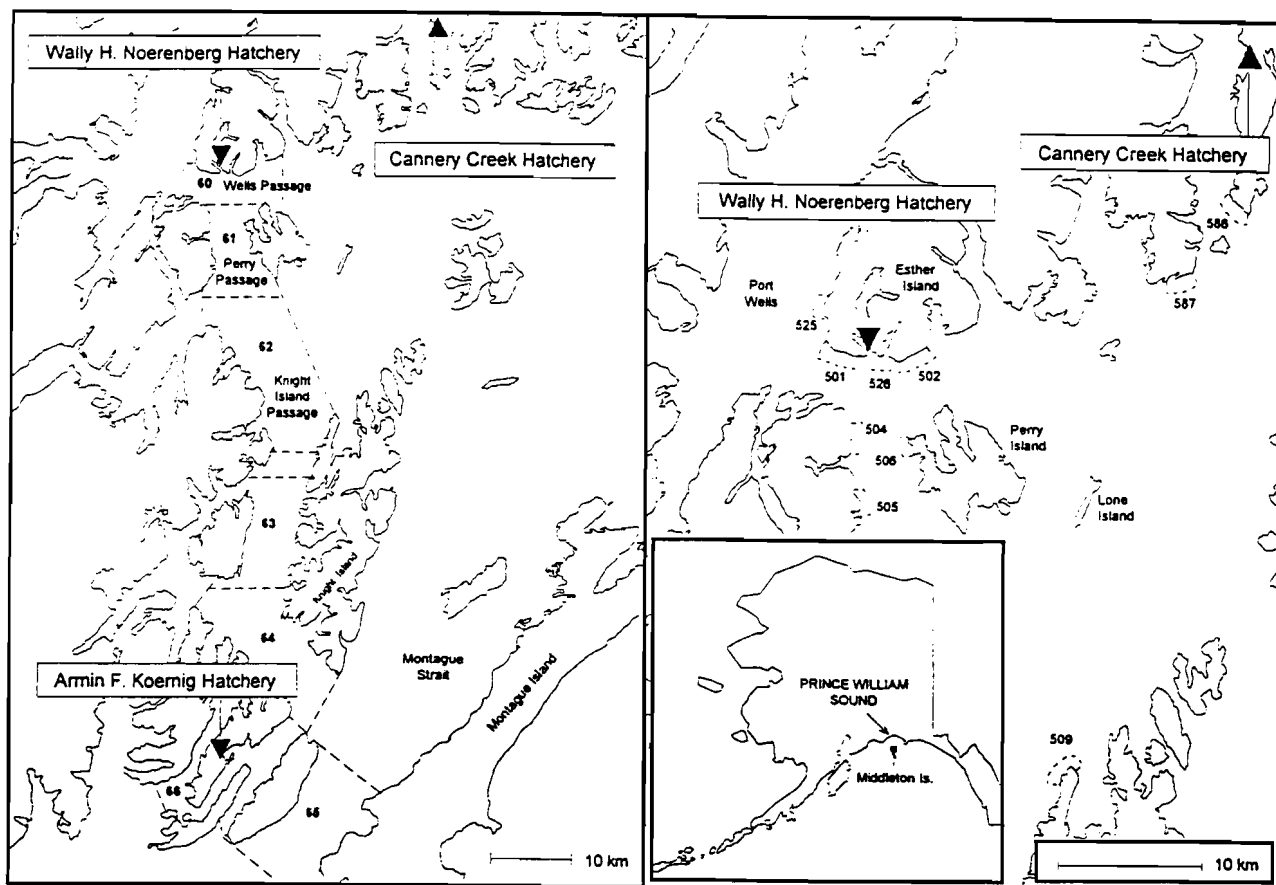
- Figure 6: Mean percent of herring diets comprised of large copepods, pteropods, euphausiids\amphipods and fish in western Prince William Sound, (a) 1994, (b) 1995 and (c) 1996. Vertical bars indicate the standard error of the mean.
- Figure 7: Mean percent of immature pollock diets comprised of large copepods, pteropods, euphausiids\amphipods and fish in western Prince William Sound, (a) 1994, (b) 1995 and (c) 1996. Vertical bars indicate the standard error of the mean.
- Figure 8: Mean percent of adult pollock diets comprised of large copepods, pteropods, euphausiids\amphipods and fish in western Prince William Sound, (a) 1994, (b) 1995 and (c) 1996. Vertical bars indicate the standard error of the mean.
- Figure 9: 'Best fit' functional response models for (a) herring, (b) immature pollock and (c) adult pollock feeding on large calanoid copepods.
- Figure 10: (a) Length frequency and mean length of fish found in stomachs of herring (left panel), immature pollock (center panel), and adult pollock (right panel), (b) length frequency and mean length of herring (left panel) immature pollock (center panel), and adult pollock (right panel), and (c) frequency distribution of prey-predator length ratio and mean ratio for herring (left panel), immature pollock (center panel), and adult pollock (right panel). Data from 1994-1996.

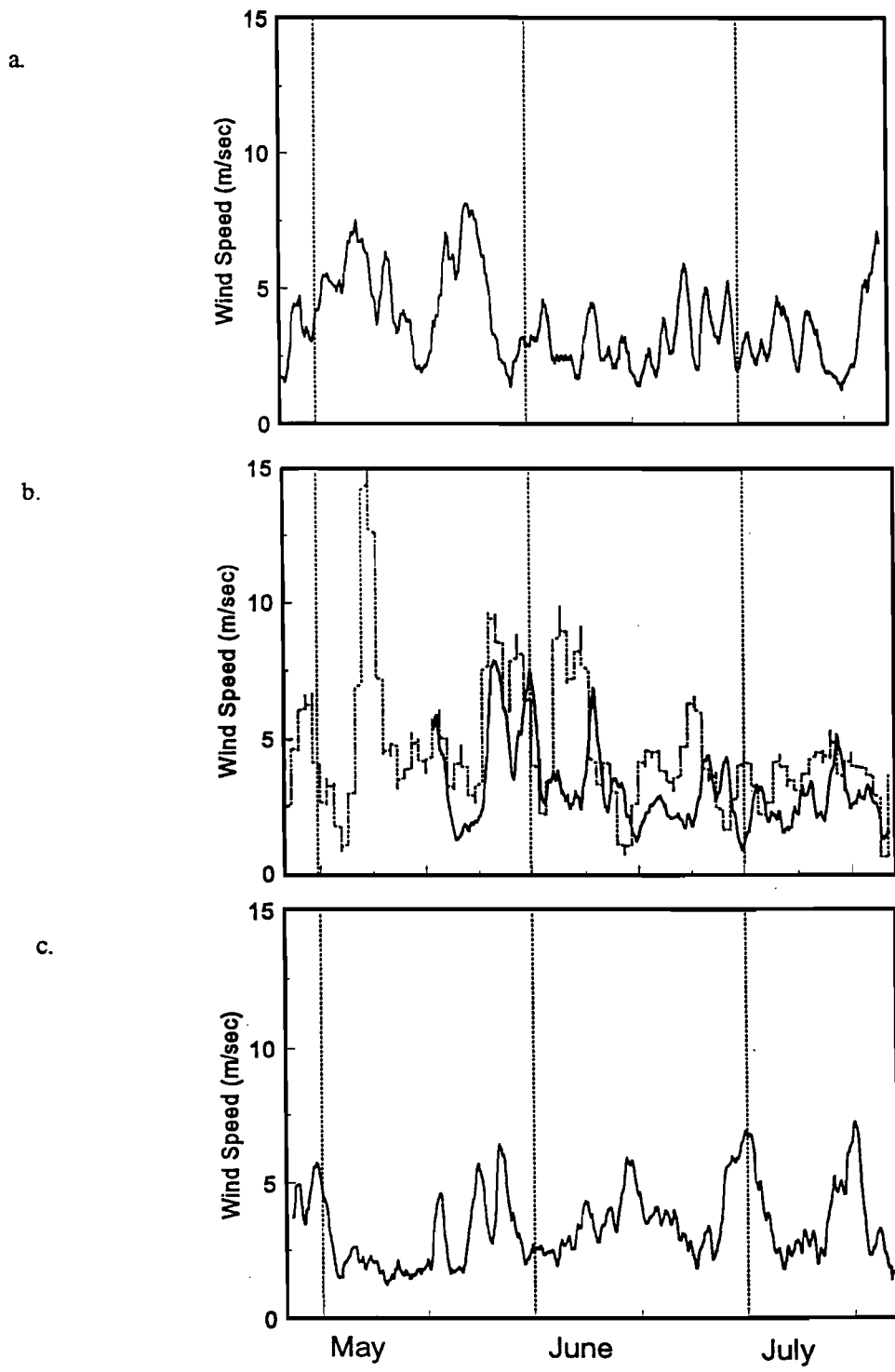
List of Figures (con't)

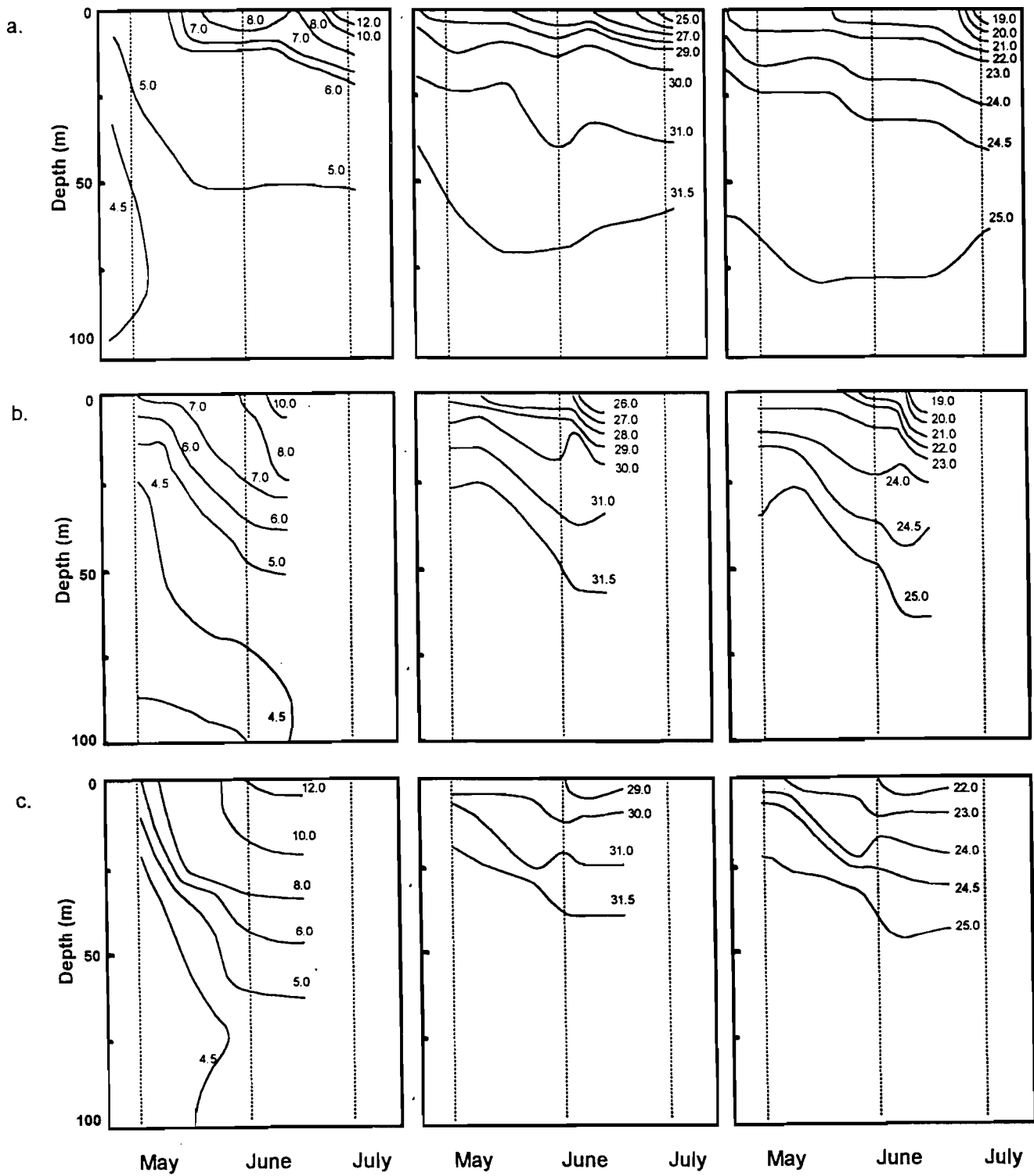
- Figure 11: Mean catch per net set for all fishes (<150 mm) in purse seines in western Prince William Sound (a) 1994, (b) 1995 and (c) 1996. Vertical bars indicate the standard error of the mean.
- Figure 12: Mean lengths of juvenile gadids, juvenile pink and chum salmon, herring, capelin, sandlance, and squid in nearshore habitats of western Prince William Sound in 1994 (solid squares), 1995 (open circles) and 1996.
- Figure 13: Relationship between the biomass of large calanoid copepods and percent of the diet comprised of fish for (a) herring, (b) immature pollock and (c) adult pollock (left panel). And, relationship between the relative abundance of prey fish and percent of the diet comprised of fish for (a) herring, (b) immature pollock and (c) adult pollock (right panel).
- Figure 14: Relationship between zooplankton density and growth rate of coded-wire tagged juvenile pink salmon for tag groups (a) less than and (b) greater than 20 million upon ocean entry.

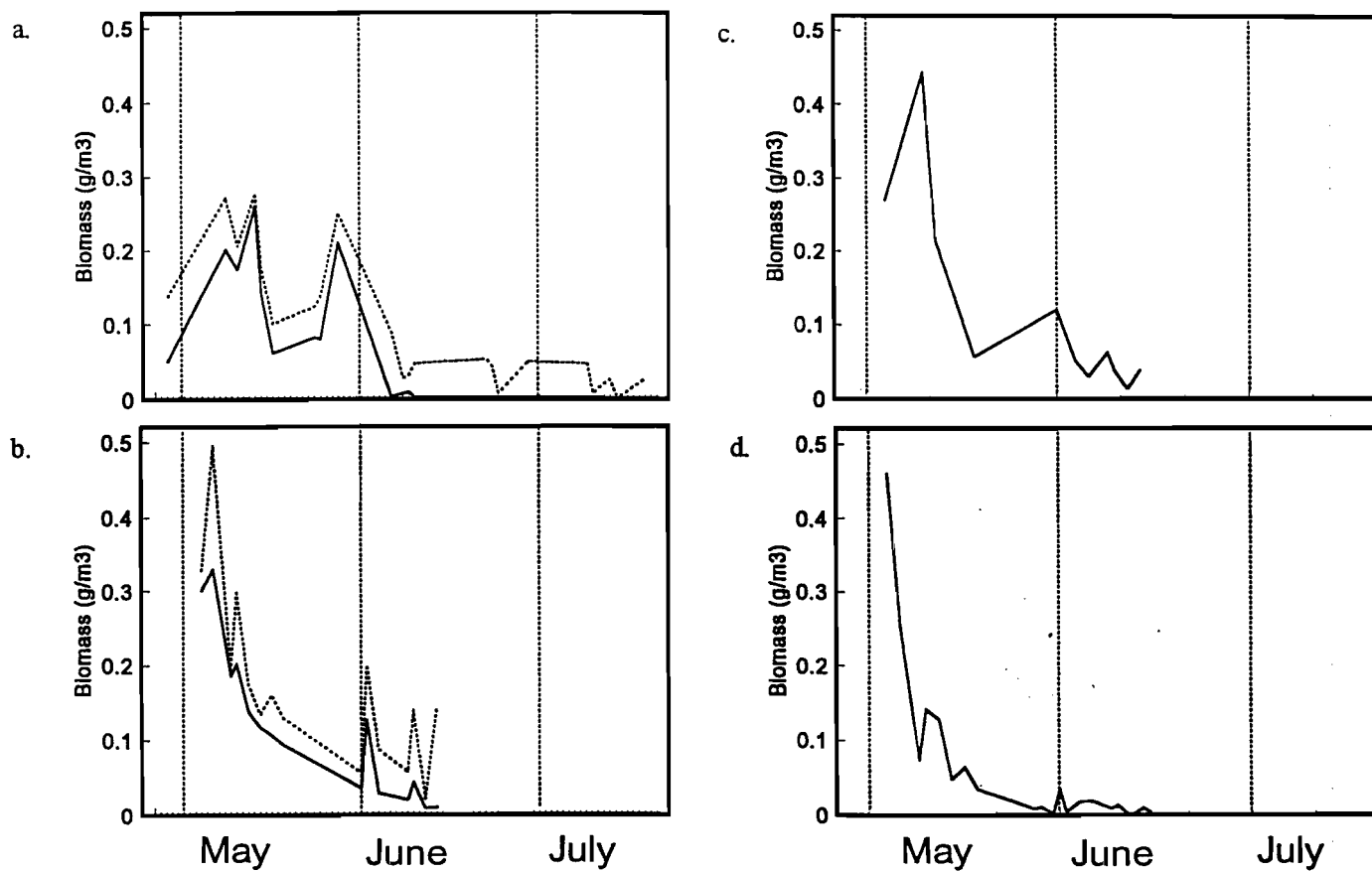
a.

b.









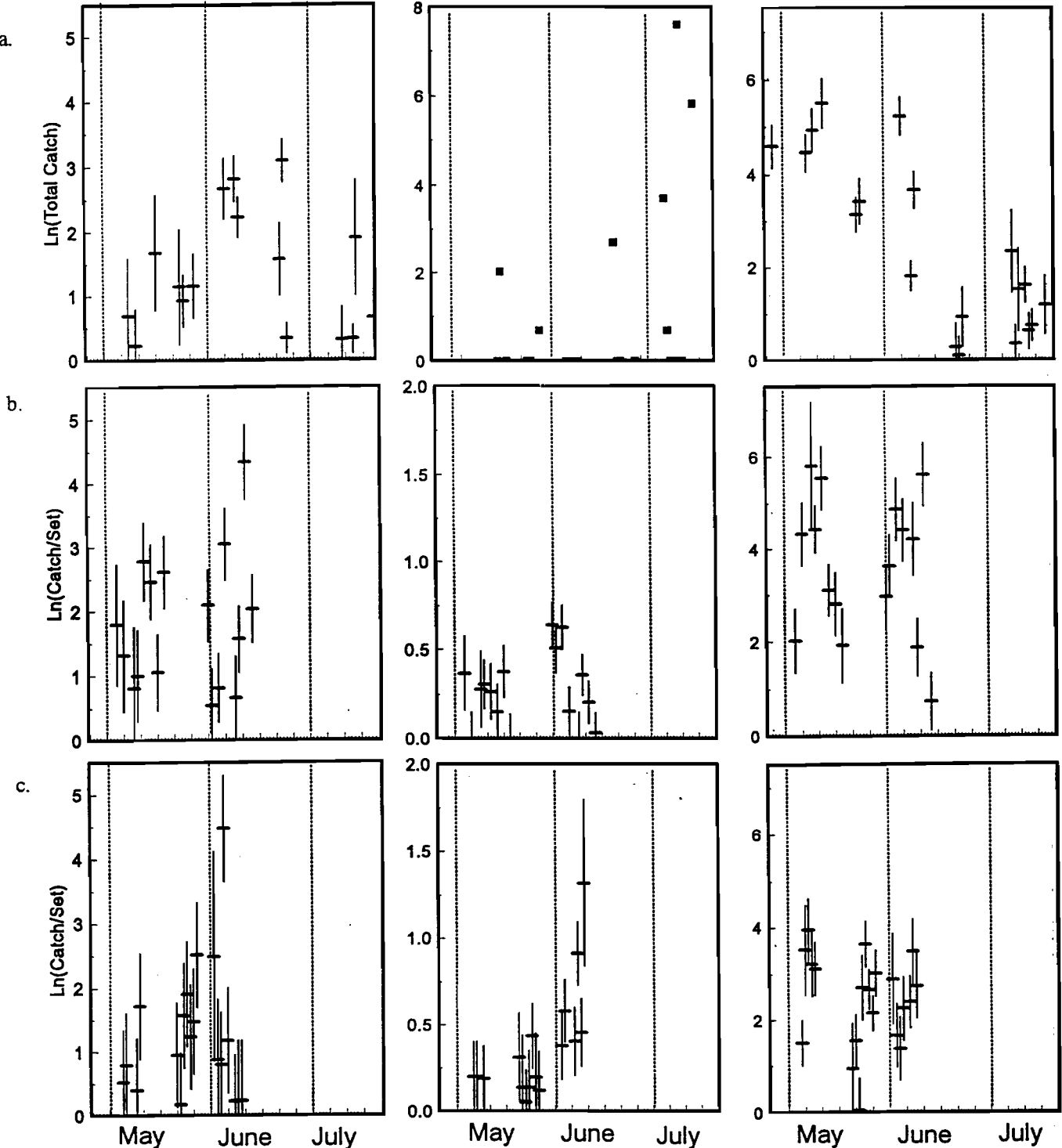
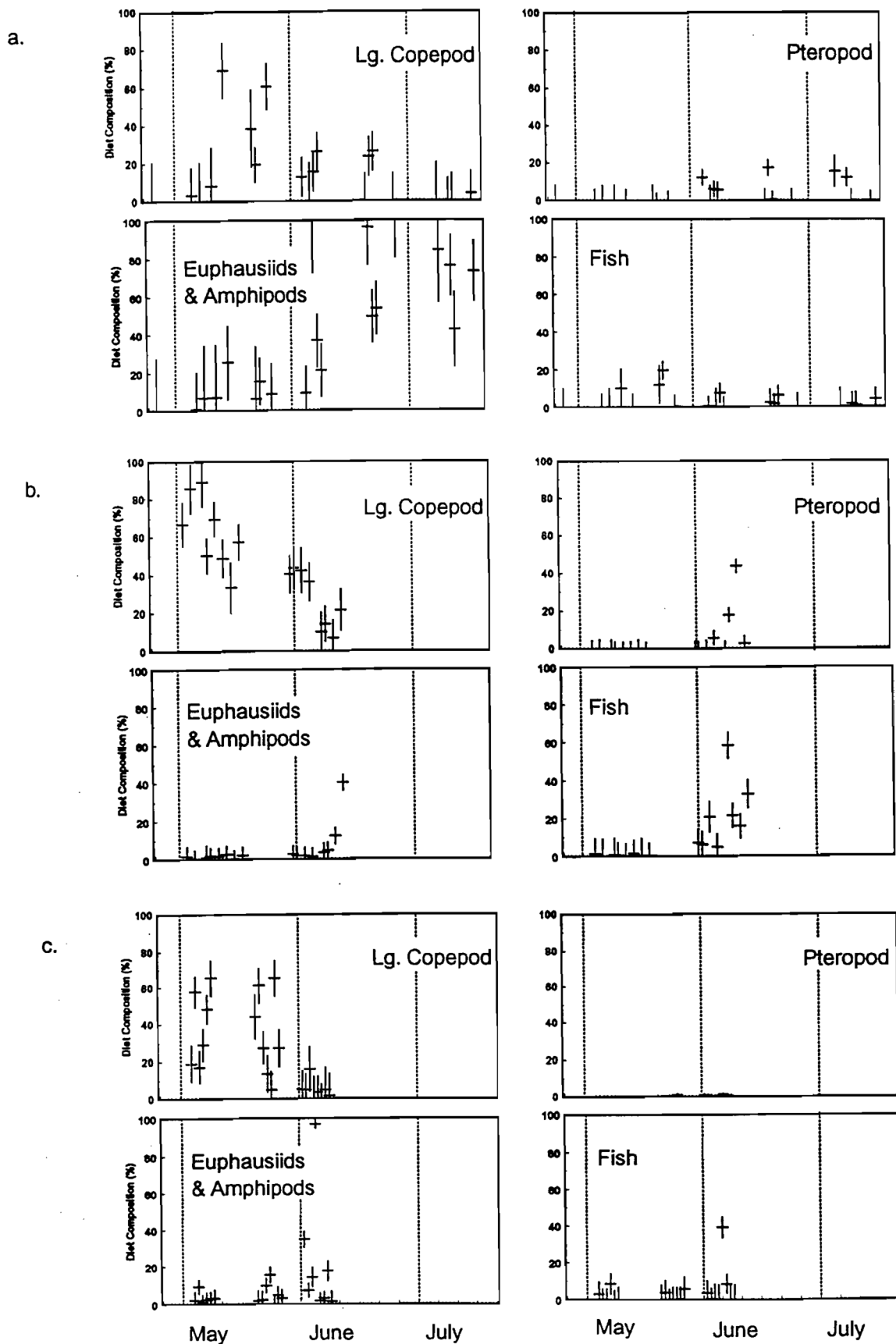
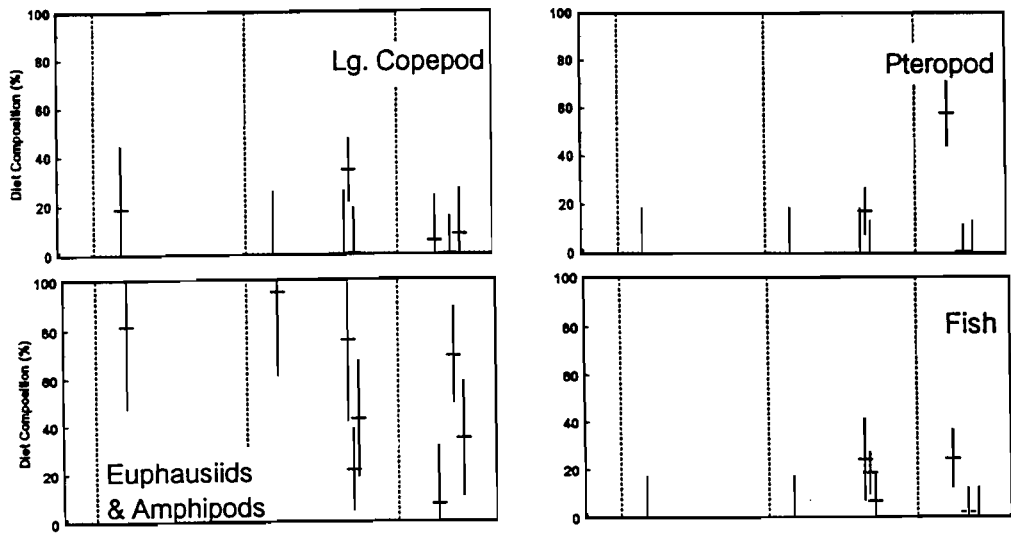


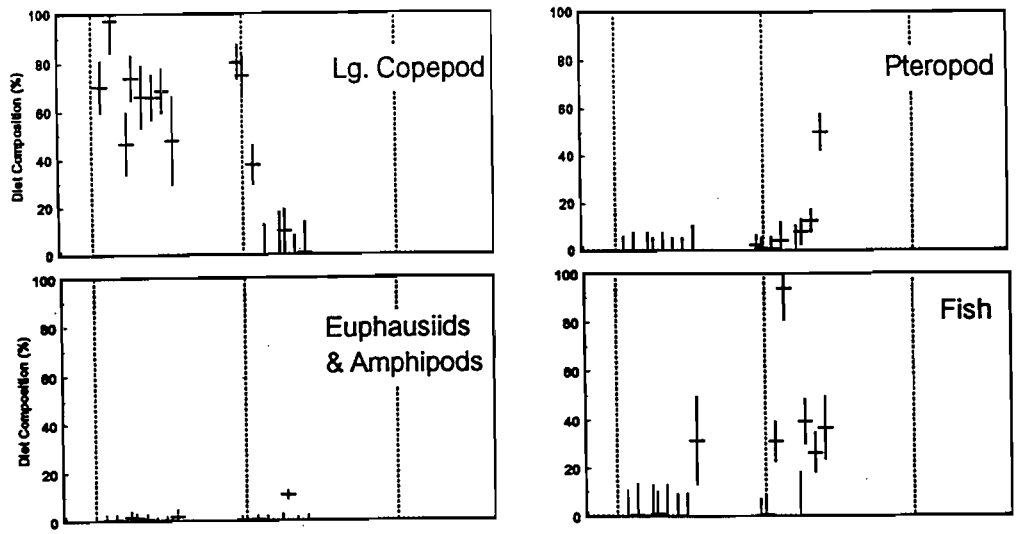
Figure 5



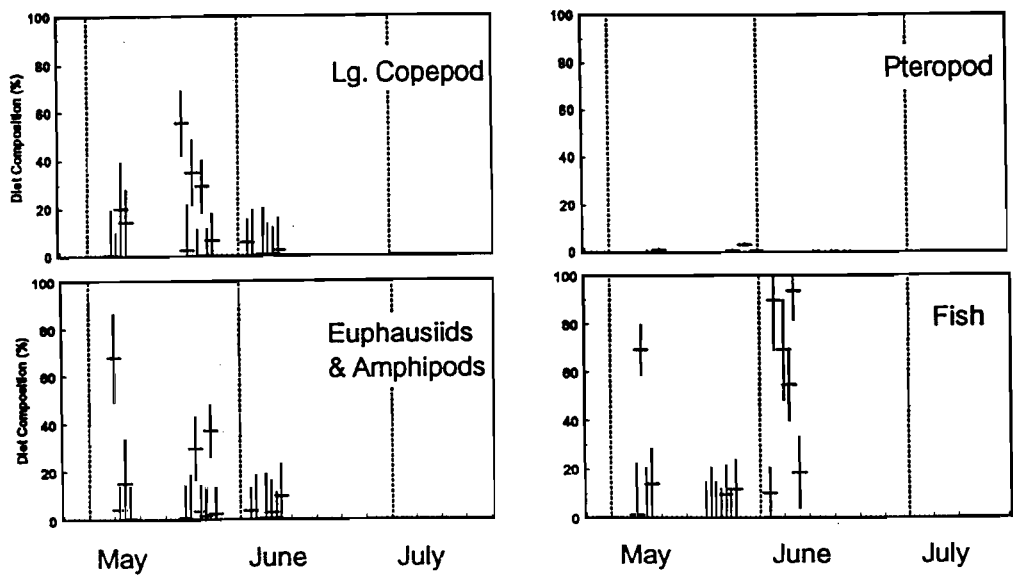
a.

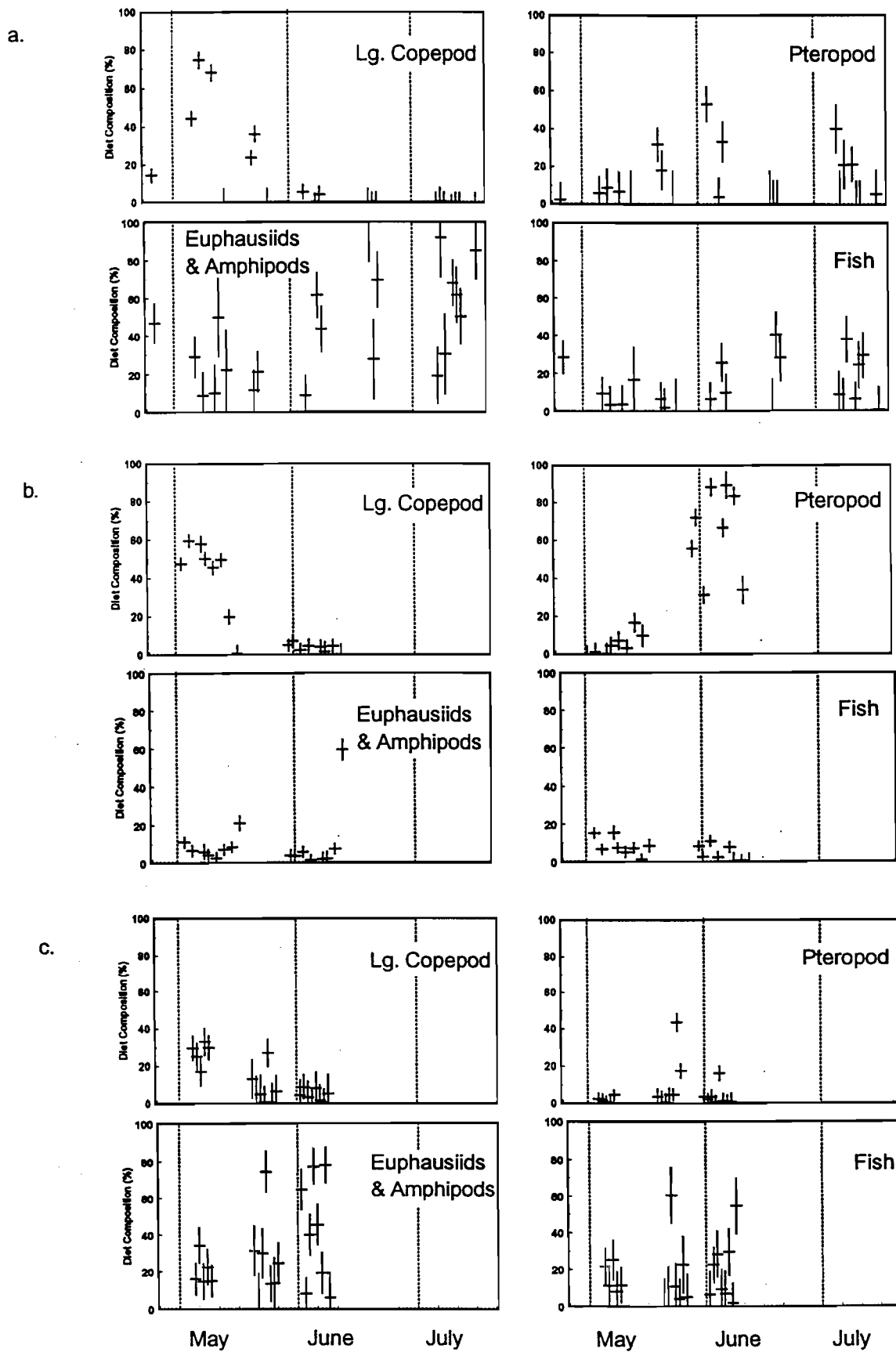


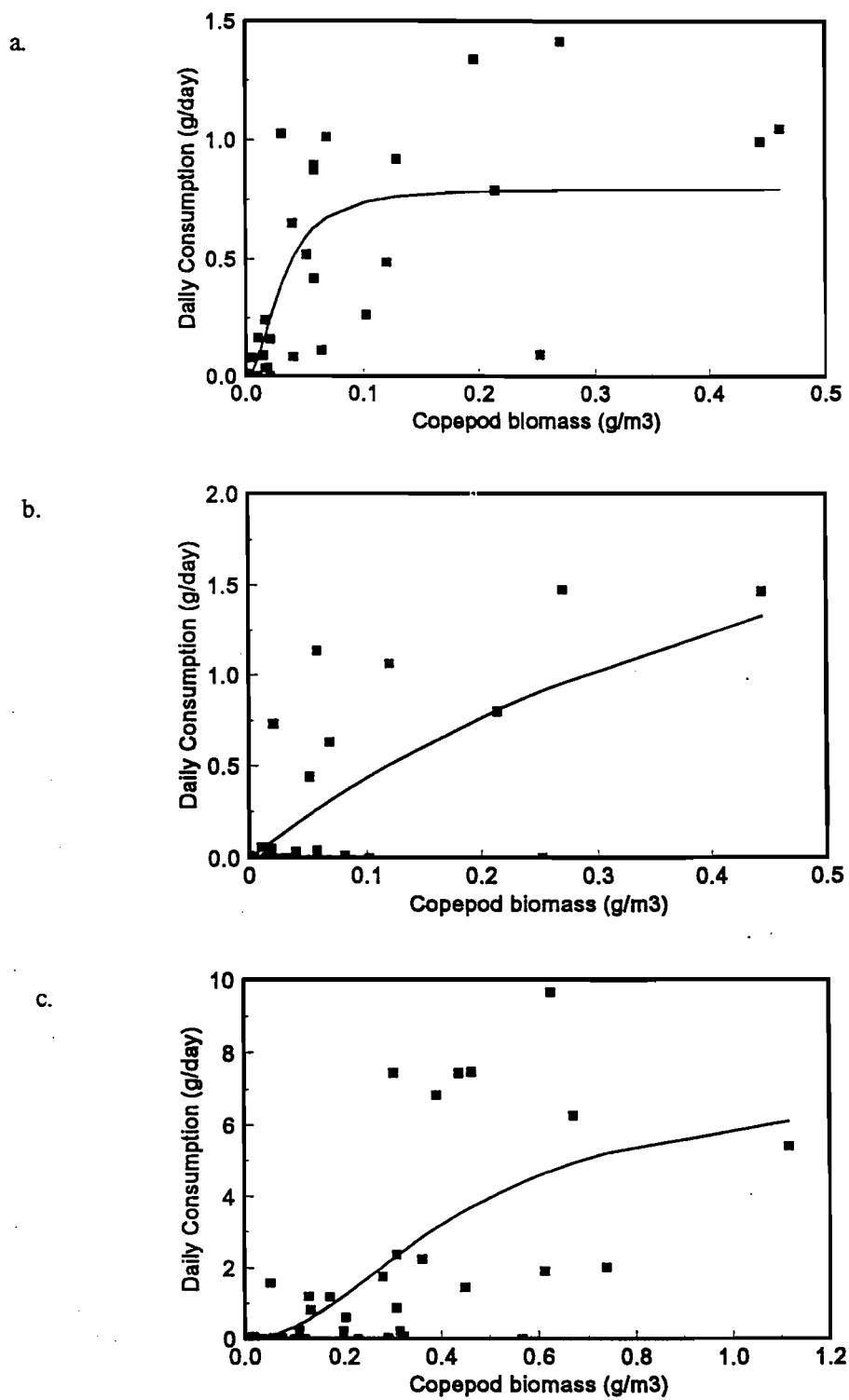
b.

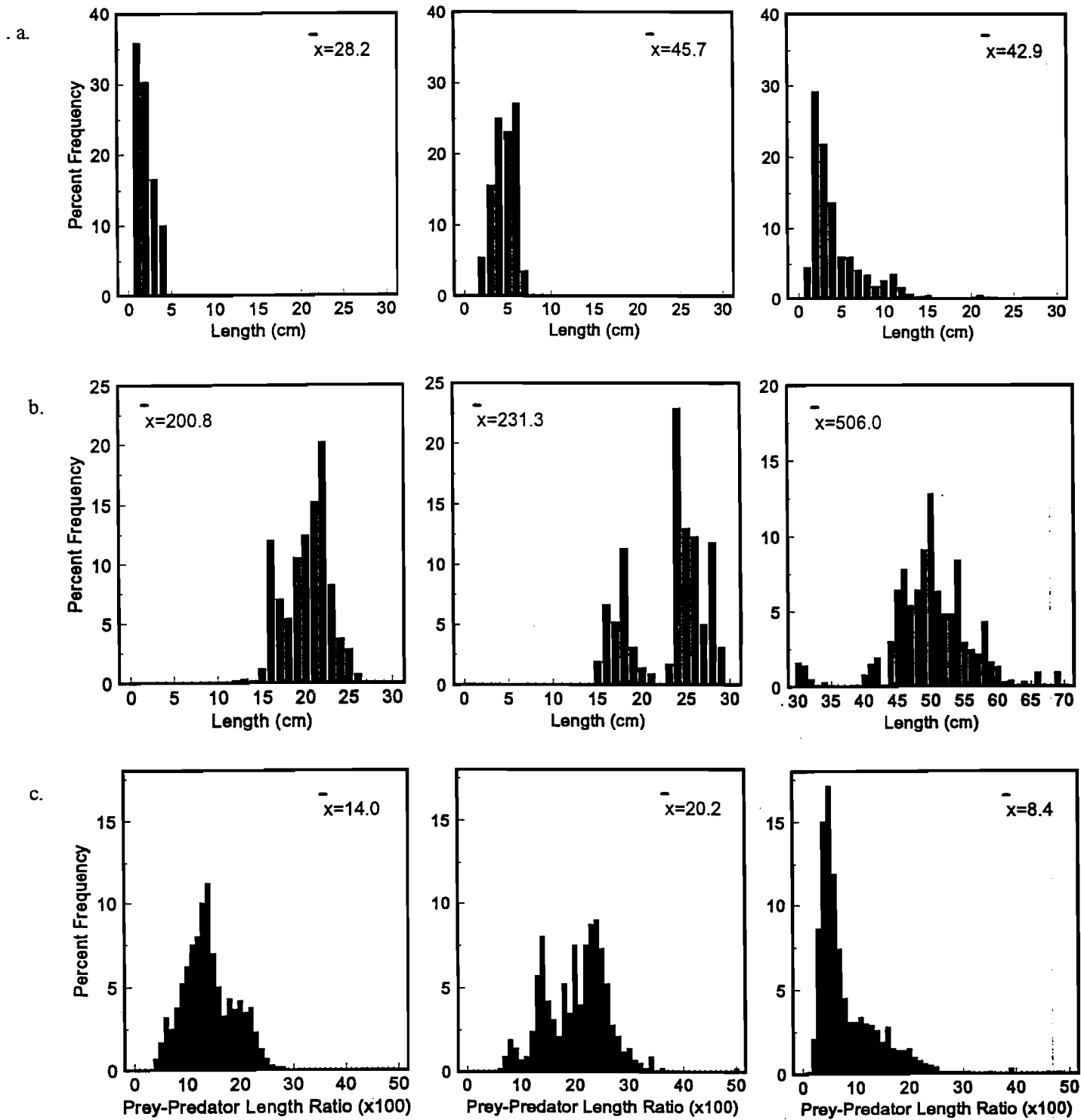


c.

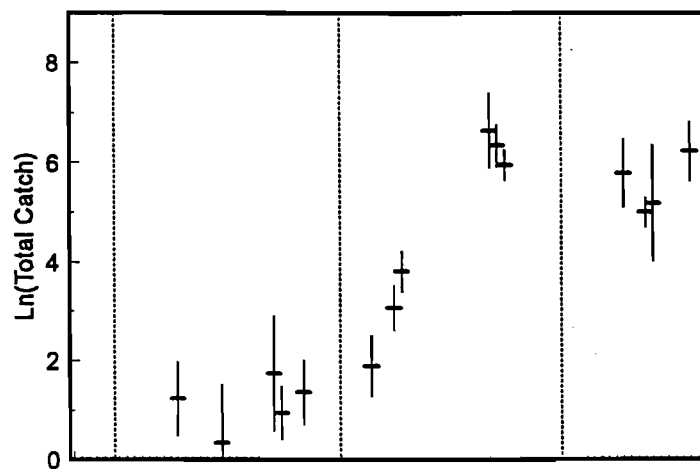




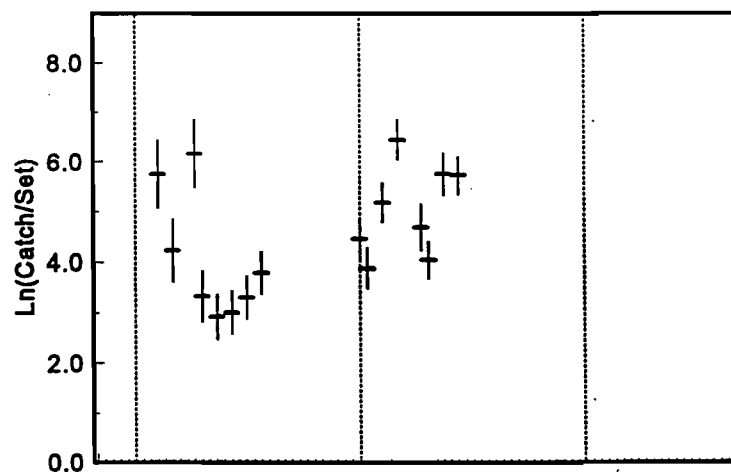




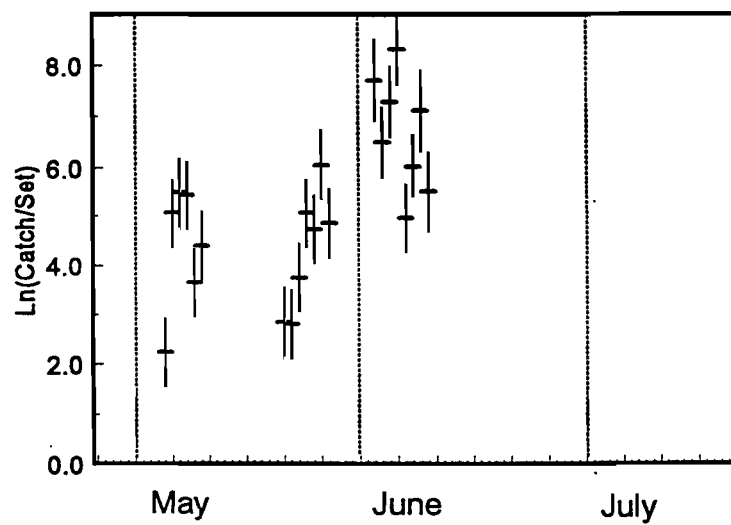
a.

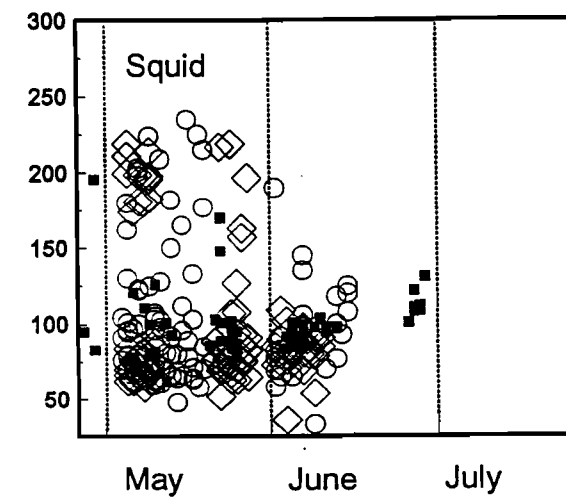
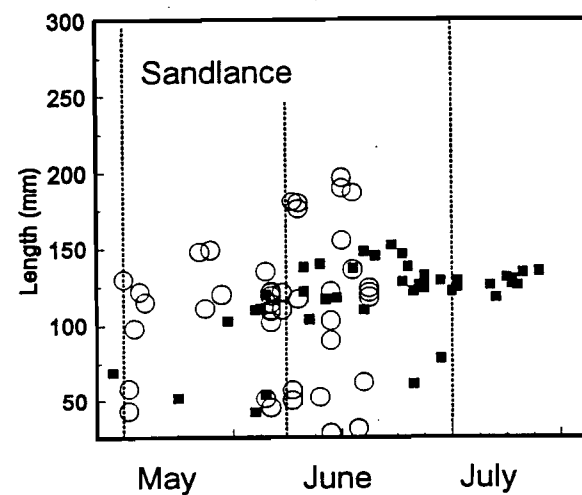
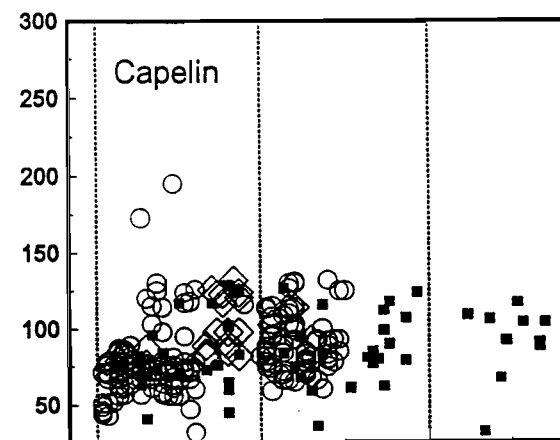
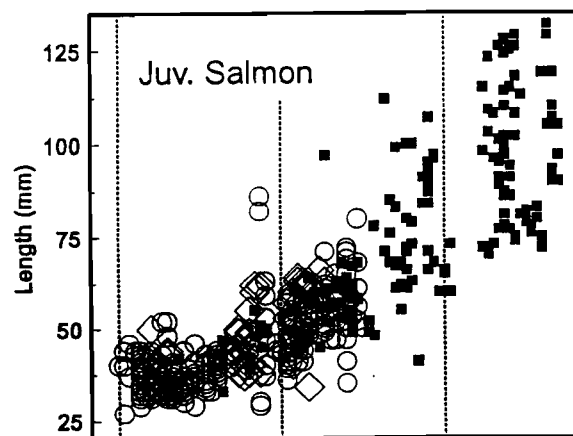
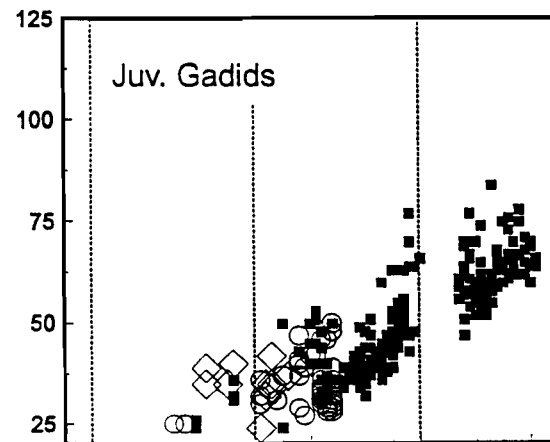
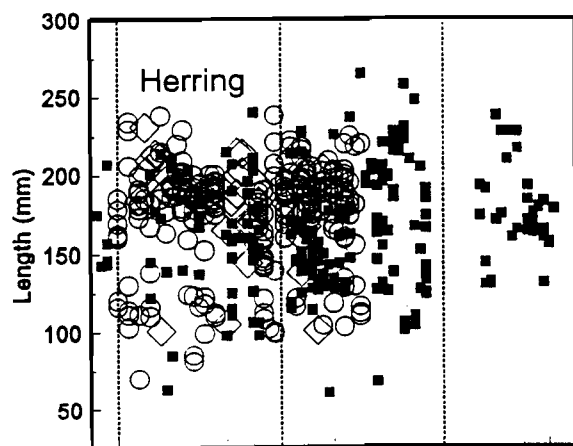


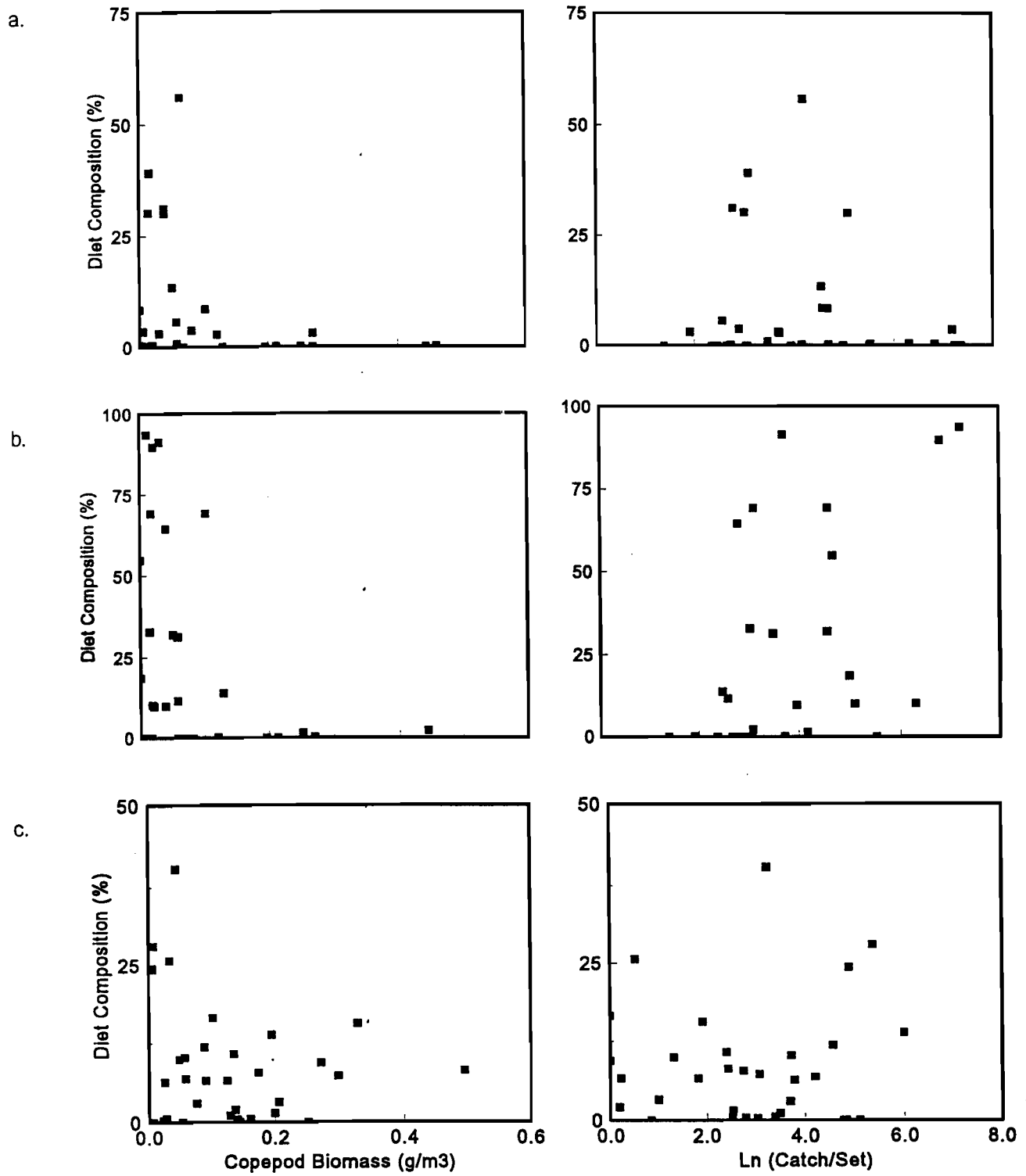
b.



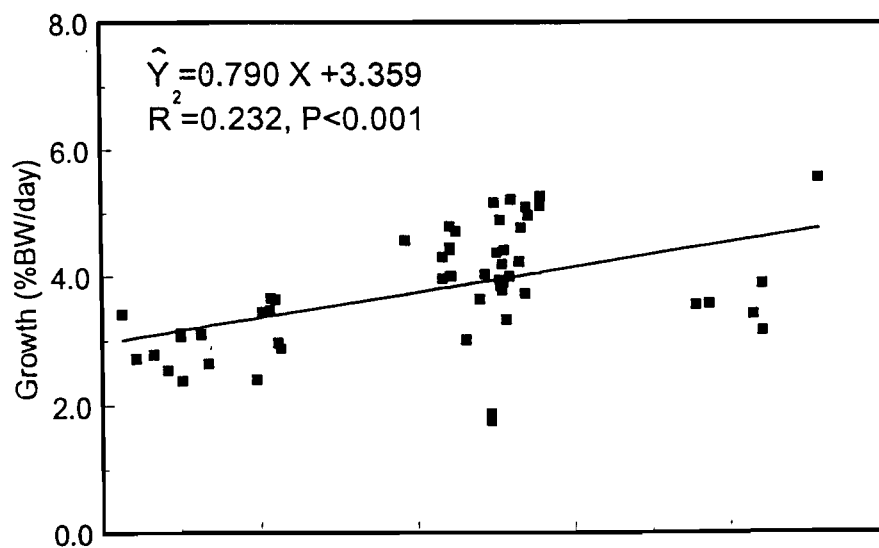
c.



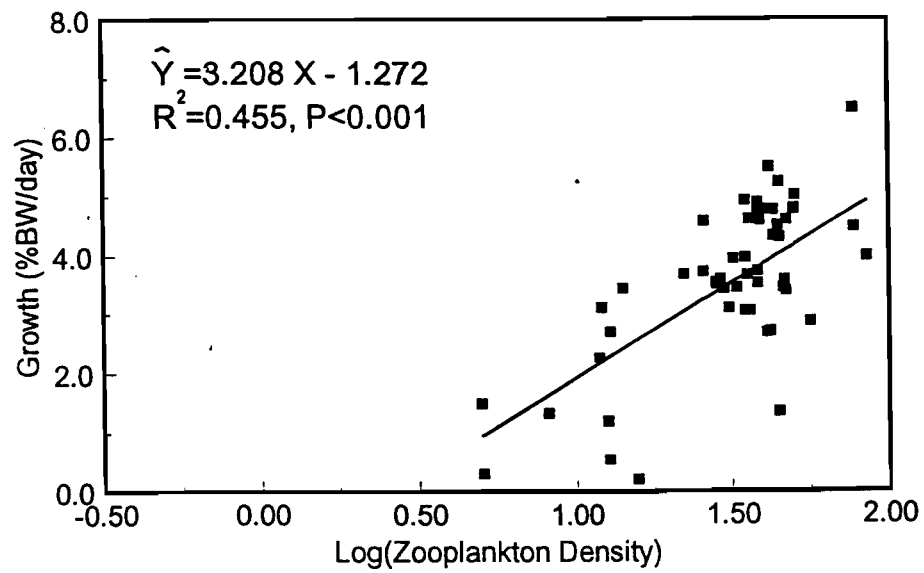




a.



b.



Chapter 3

Phytoplankton and Nutrients

Exxon Valdez Oil Spill
Restoration Project Annual Report

Sound Ecosystem Analysis: Phytoplankton and Nutrients
Restoration Project 97320G

This annual report has been prepared for peer review as part of the Exxon Valdez Oil Spill Trustee Council restoration program for the purpose of assessing project progress. Peer review comments have not been addressed in this annual report.

C. Peter McRoy
Alison Ward
E. Paul Simpson
Katy Tamburello
Jill Cameron
Sue McCullough
Patrick Cassidy

Institute of Marine Science
University of Alaska Fairbanks
Fairbanks AK 99775

April 1998

Sound Ecosystem Analysis: Phytoplankton and Nutrients

Restoration Project 97320G Annual Report

Study History: The project was initiated as Restoration Project 94320G. A "Draft Final Report" was produced as an annual report in 1995, 1996 and 1997 under the title "SOUND ECOSYSTEM ANALYSIS: Phytoplankton and Nutrients" and continues under the present grant number. Papers were presented at the AAAS Arctic Science Conference, AGU/ASLO Ocean Sciences meeting and The Oceanography Society meeting.

Abstract: In 1997 we collected 636 water samples for analysis which were from cruise BE705 (5-12 May 97) and daily collections (April through June) from a location (same place as 1995 and 1996) in Elrington Passage near AFK Hatchery. Measurements included chlorophyll, nutrients, particulate carbon and nitrogen, species composition, CTD, and dissolved oxygen from 6 depths in the upper water column. This is the third consecutive year for a spring cruise to study the spatial distributions of phytoplankton and nutrients. The data indicate the presence of a re-occurring front located about 30 km inside Hinchinbrook entrance that partitions biological processes into inner and outer regions. The front is an upwelling zone with moderate sustained phytoplankton biomass (chlorophyll).

This is also the third data set for a daily time series in Elrington Passage for phytoplankton and nutrients that fully includes the spring bloom. Here the spring phytoplankton increase is strongly influenced by light and mixing. The decline of phytoplankton biomass is a result of nutrient depletion and grazing. The spring phytoplankton cycle begins with a bloom dominated by diatoms, particularly *Skeletonema costatum*, followed by a low biomass of flagellates and succeeded by another low biomass of diatoms. The timing of the spring increase in phytoplankton, as measured by chlorophyll, based on the data collected here and historical work back to 1971, is remarkably similar with the peak occurring on or about 28 April. The only exceptions to this were in 1993 and 1977. This fact indicates that solar angle, rather than mixing, determines the initiation of the bloom in most years. Estimated primary productivity in 1997 was 46% lower than 1996 and 36% lower than 1995. Overall, the data indicate a robust, healthy foundation for the pelagic ecosystem in Prince William Sound. A detailed analysis of the phytoplankton community for 1995 and 1996 is included as an attachment.

Key Words: Exxon Valdez, phytoplankton, nutrients, primary productivity, algae

Citation: McRoy, C.P., A. Ward, E.P. Simpson, J. Cameron, K. Tamburello, S. McCullough and P. Cassidy. 1998. Sound Ecosystem Analysis: Phytoplankton and Nutrients, *Exxon Valdez* Oil Spill Restoration Project Annual Report (Restoration Project 97320G), Institute of Marine Science, University of Alaska, Fairbanks, Alaska

Table of Contents

LIST OF TABLES	4
LIST OF FIGURES	4
INTRODUCTION	5
OBJECTIVES.....	6
METHODS	6
PHYTOPLANKTON BIOMASS, SPATIAL AND TEMPORAL PATTERNS:	6
PHYTOPLANKTON PRIMARY PRODUCTION	6
PHYTOPLANKTON COMMUNITY COMPOSITION:	6
NUTRIENT FIELDS:	7
PERSONNEL.....	7
RESULTS	7
SAMPLE COLLECTION	7
TIME SERIES MEASUREMENTS	8
PRIMARY PRODUCTION.....	8
SPATIAL MEASUREMENTS:.....	9
DISCUSSION	9
CONCLUSIONS.....	10
PAPERS PRESENTED	11
LITERATURE CITED.....	11

List of Tables

- Table 1. Summary of data collection, including number of samples collected, and sampling days for 1995, 1996 and 1997 at AFK Station SB2.
- Table 2. Summary of sample collection for 1995, 1996 and 1997 from oceanographic cruises.
- Table 3. Interannual comparison of features that provide evidence supporting a bottom-up hypothesis.

List of Figures

- Figure 1. SEA 1997 station locations for phytoplankton and nutrient sample collection.
- Figure 2. Integrated Chlorophyll a (upper 50 m) for the spring time series in Elrington Passage in 1995, 1996 and 1997.
- Figure 3. Comparison of timing of phytoplankton spring bloom for all known studies of Prince William Sound. Data from the Apprise Project time series in Auke Bay in Southeast Alaska for 1985-89 are also included. The vertical bars indicate the day of the peak of the biomass; the average for all studies is day 118 (dashed line).
- Figure 4. Time series of integrated (upper 50 m) nitrate+nitrite content of the water column in 1995, 1996 and 1997 with estimated primary production rate.
- Figure 5. Transects from Hinchinbrook Entrance to the central region of Prince William Sound showing the 30 km front in chlorophyll (mg m^{-3}) in spring of 1995, 1996 and 1997.
- Figure 6. Variability of the location of the chlorophyll maximum by month for the years studied.

INTRODUCTION:

The project seeks to determine the driving force of ecosystem variability from a bottom-up perspective. In this component our hypothesis is that the timing, quantity and species composition of the plant community, that is, the phytoplankton, is a major determinant of variability in upper trophic levels, a bottom-up scenario of ecosystem forcing.

The Sound Ecosystem Assessment program (SEA) aims to understand and predict restoration of populations of pink salmon and herring in Prince William Sound. Fundamental to this goal is the understanding of controls of ecosystem processes that nourish the food web at its primary level. Restoration of marine populations that have been damaged by human activity is usually limited to a few options that focus on controlling loss rate processes, i.e. harvest level, predator control, etc., or minor habitat modification. Pink salmon and herring offer a spectrum of strategies since a large portion of salmon are protected in hatcheries in their early life and herring are completely wild subject to the variance of nature. What then is the role of the annual cycle of primary production in the success of these upper trophic level species? Does the magnitude of the phytoplankton production determine the strength of a year class? Is the phytoplankton species composition an important determinant of the grazing zooplankton community? Does any of this matter or is there always enough food at the right time of the year so that predator populations are determined by the uppermost consumer on the food web? All are questions that are being examined in this study.

One central SEA hypothesis concerns the impact of circulation and physical conditions on the restoration of fish stocks (the Lake-River Hypothesis). This proposes that the circulation of Prince William Sound alternates irregularly between years of strong through-flow, river-like conditions, and relatively stagnant, lake-like conditions. The consequence is a high biomass of large zooplankton (copepods) in 'lake' years that are the major food for target fish (salmon, herring) and their predators (termed 'middle-out' food web control by Cooney and associates). In alternate 'river' years, the large zooplankton are sparse and predation on the target fish species predominates (top-down control).

While middle-out or top-down are principal hypotheses being tested by SEA research, the possibility of bottom-up control, where the production of upper trophic level species is modulated by variations in light- and nutrient-driven phytoplankton production. In this hypothesis, the production and/or composition of the zooplankton community is determined by variations in phytoplankton primary production and by the species composition of the phytoplankton community. For example, a phytoplankton community dominated by large diatoms can support a high biomass of large oceanic copepods, whereas a phytoplankton population dominated by smaller flagellates results in a reduced number of larger copepods, or in a shift to a zooplankton community dominated by smaller neritic copepod species. Variations in the timing of phytoplankton populations have been previously suggested to be a control of ecosystem events in Prince William Sound (McRoy 1988). A further complication in the interrelationship is that the large zooplankton are one year old when they become major prey for fishes (Cooney, personal communication) so their abundance must be determined by the events of the previous year and their specific biomass by the production cycle of the present year.

In this component, we provide the nutrient and phytoplankton data that are essential to evaluate the influence of phytoplankton dynamics on the food web and to test the bottom-up hypothesis. We will characterize the interannual spatial and temporal variation in nutrient and phytoplankton fields. We will evaluate the role of phytoplankton production in zooplankton

recruitment and growth (especially for *Neocalanus* and *Pseudocalanus*). In a general sense we will provide an answer to the question “Is it food?”.

A central tenet of the Lake/River Hypothesis is the variable advection of Gulf of Alaska waters into Prince William Sound. This advection affects not only zooplankton populations, but also the Prince William Sound phytoplankton populations and production. Strong advection may confound the effects of in situ primary production in the Sound. To test the hypotheses further, we use satellite-derived sea-surface temperatures to examine the movement of Gulf of Alaska surface waters into Prince William Sound.

OBJECTIVES:

This study is designed to investigate the distribution, amount, and type of phytoplankton growth and the major inorganic nutrient fields associated with the growth processes. Our hypothesis is that variations in the phytoplankton production and populations are transferred to the zooplankton and that such variations are a function of oceanographic conditions that control the supply of inorganic nutrients and light. The objectives for 1997 were:

1. Analysis of phytoplankton community ecology in Prince William Sound.
2. Determination of basin-wide patterns of temperature, salinity nutrients and chlorophyll from ship-board observations.
3. Determination of temporal patterns of temperature, salinity, nutrients and chlorophyll in western Prince William Sound from a station near AFK Hatchery.
4. Determination of the linking between phytoplankton and upper trophic levels.

METHODS:

Phytoplankton Biomass, Spatial and Temporal Patterns

Phytoplankton biomass is measured using the standard chlorophyll techniques (Parsons et al., 1984) on a Turner Designs Fluorometer. Samples were collected at specific 309 time/space locations on cruises and at a shore-based station. Data allow mapping the areal pattern and description of the water column profile.

Phytoplankton Primary Production

The biomass pattern provides a picture of what is present, but it does not provide information on the phytoplankton dynamics. We can estimate production using dissolved oxygen and nutrient data. Productivity data are also available in our historical database (McRoy, unpublished data; Goering et al. 1973b). Methods used involved uptake of ^{14}C by phytoplankton in containers under neutral density filters (Strickland and Parsons, 1972; Parsons et al., 1984).

Phytoplankton Community Composition

The composition of the phytoplankton community can be as important as the total primary production in determining zooplankton species and abundance. We collected 50 ml aliquots from water samples and preserved them in Lugol's solution for species identification. Identifications and cell counts were done using an inverted microscopy method (Sournia 1978). On low (20x) magnification, all visible cells in two transects are counted. On high (40x) magnification, fields are counted until a total of 300 cells is reached. For cell volume calculations and calculation of carbon content, cells identified to genus were grouped according

to the maximum cell dimension. At least 20 cells of each species for size class were measured. The procedure is labor intensive and only a portion of the samples collected can be counted.

Nutrient Fields

Phytoplankton require the major inorganic nutrients (nitrogen, phosphorus and silica) for growth. General oceanographic circulation and land run-off supply nutrients. Since phytoplankton also require light, the problem is understanding how the nutrients are supplied to the illuminated zone of the sea. We routinely collected water samples for quantitative nutrient analysis. In the field, water samples were collected with Niskin Bottles at standard depths over the upper 100 m (deeper if necessary). A small aliquot (250 ml) was filtered and frozen for later chemical analysis. Chemical determination of the quantity of dissolved nitrogen (as nitrate, nitrite and ammonium), phosphate and silicate were measured using prescribed Continuous Flow Analysis methods with an Alpkem Auto-Analyzer in our laboratory in Fairbanks.

Personnel

The following people have contributed to sample and data collection and analysis:

P. Simpson	Graduate Student
A. Ward	Graduate Student
K. Tamburello	Graduate Student
J. Cameron	Senior Technician
S. McCullough	Field Technician
P. Cassidy	Field Technician

RESULTS:

Samples were collected to document the time series of events in the annual phytoplankton/nutrient cycle as well as to examine spatial variations in Prince William Sound. These data are collected in conjunction with other SEA projects and are supplied to the SEA data base after appropriate analysis and verification.

Sample Collection

We collected water samples for analysis from two types of platforms in Prince William Sound. In 1997 a single cruise on board chartered vessel in May permitted regional sampling from the standard SEA ocean stations. The second sample site is a station in Elrington Passage (60°01'N, 148°00'W) near the AFK Hatchery on Evans Island in the southwestern corner of the sound. We used this shore facility to collect daily samples from mid-April until late June. The station was visited daily by skiff and all samples were collected from a 5 liter Niskin bottle lowered repeatedly to each sample depth with a hand winch. These data provide temporal continuity to the ship-board sampling.

The field season began in April and ended in June. In 1997 we collected 636 samples from 1 cruise and a time series station. An decrease of 42% over 1996 (Tables 1 and 2). The chartered vessel provided areal coverage of the Sound for oceanographic and biological parameters (Figure 1). The time series began on 01 April 97 and ended on 15 June 97.

The Phytoplankton-Nutrient Component database includes dissolved nutrients (nitrate+nitrite, ammonia, phosphate, and silicate), dissolved oxygen, CTD (salinity, temperature, depth), chlorophyll a, and particulate carbon (PC) and nitrogen (PN) from all sampling

Oceanography Cruise - May 1997

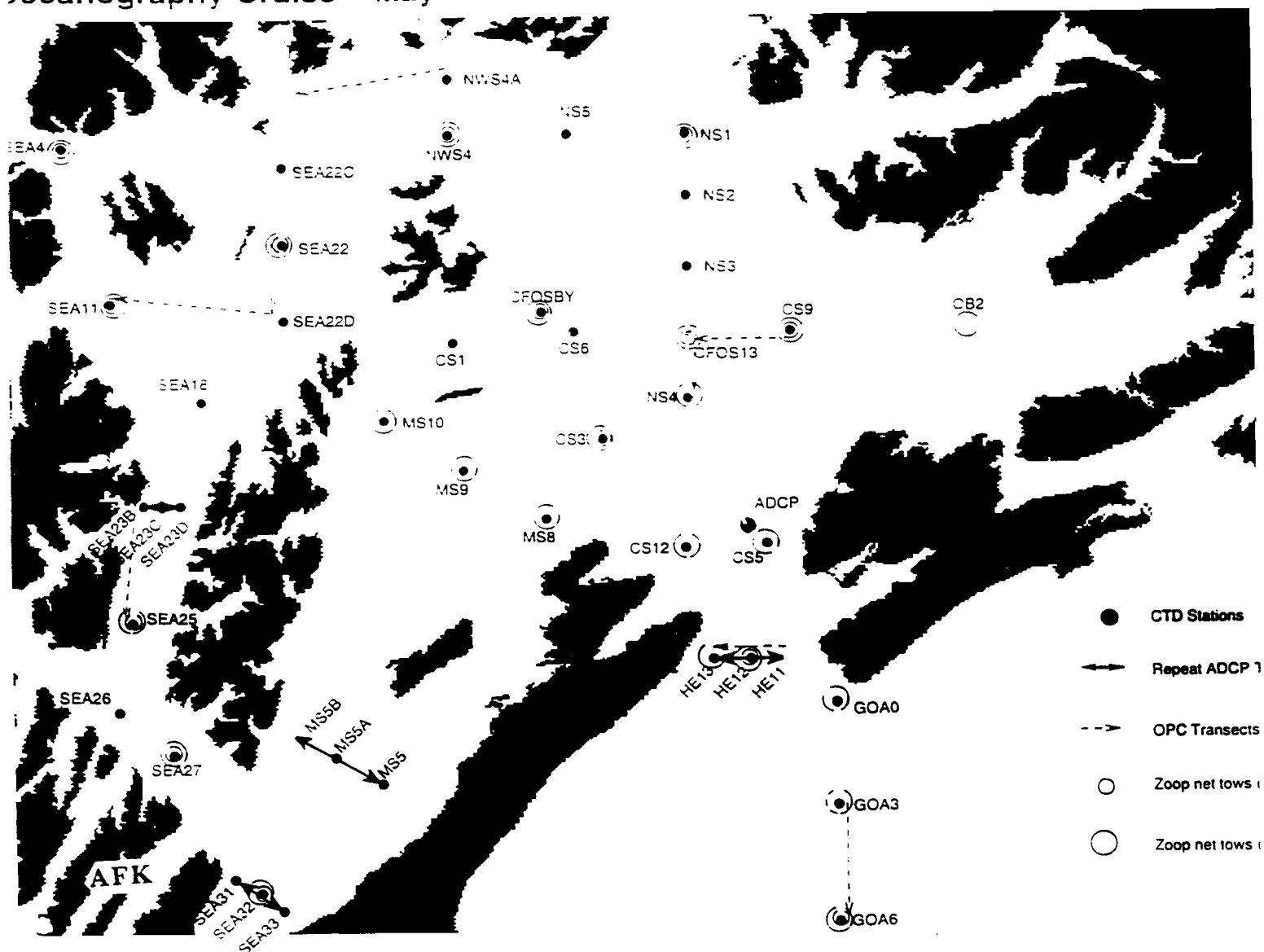


Figure 1. SEA 1997 station locations for phytoplankton and nutrient sample collection.

platforms. In addition selected representative samples for phytoplankton identification and enumeration were processed.

Phytoplankton Time Series Measurements in Prince William Sound

The temporal pattern of the spring phytoplankton increase was similar in all 3 years (Figure 2). In 1997 the bloom began on day 93 and terminated by day 137. Chlorophyll levels in 1997 were only about half those reached in 1995 and 1996 but the duration of the bloom was about 10 days longer in 1997.

The peak biomass, as measured by chlorophyll concentration, in 1997 occurred on day 107 which was very close to the peak in 1996. The 1995 peak occurred on day 117 which is close to the mean for all phytoplankton time series measurements for the Sound (Figure 3). The mean from all current and historical measurements is day 118 (28 April). This is also the mean date for peak occurrence for 1985-89 in Auke Bay in Southeast Alaska (Ziemann et al. 1990). With 2 exceptions there is a remarkable coincidence of peak chlorophyll around day 118 for 11 years from 1971 to present. The exceptions are 1995 (data source: CFOS buoy) when the peak occurred about 2 weeks earlier on day 95 and 1977 (data source: Alexander and Chapman 1980) when the bloom maximum occurred around day 165. The first exception is a result of unusually calm spring conditions as supported by the ancillary hydrographic data collected by the buoy instrumentation. The data from 1980 are for Port Valdez and can not be readily explained but it may simply be a plotting error on the figure.

The cluster of peak biomass values around day 118 (28 April) in 11 of the 13 years for which there are data is an indication of the forces that control phytoplankton production. A coincidence of dates suggests that in most years sun angle is a primary physical mechanism controlling production and that this even dominates over mixing processes, or the lack thereof, as seen in 1995.

A detailed analysis of the 1995 and 1996 phytoplankton data written by Alison Ward as a thesis for the degree of Master of Science at the University of Alaska Fairbanks is included with this report as Attachment A. The 1997 data set is in the process of analysis.

Primary Production

As stated in the methods section, direct measurements of primary production were not made during this study but the growth rate of the phytoplankton during the spring bloom can be determined from the time course of nitrate+nitrite depletion (Figure 4) and by invoking the Redfield ratio of 6.6 for Carbon to Nitrogen. The results are overall primary production rates of 2.33, 2.75 and 1.49 gCm⁻² d⁻¹ for 1995, 1996 and 1997 respectively, a nearly two-fold difference between the highest and lowest value. These rates fall well within the values for the spring bloom measured by Goering et al (1973a and 1973b) in Port Valdez and Valdez Arm using direct ¹⁴C uptake. The total production can be twice these values if the *f* ratio is less than 0.5 as would be expected for the region.

Spatial Measurements:

Biological data collected during the single cruise in May 1997 further illustrates the high temporal variability of Prince William Sound. Nitrate throughout the central sound was more depleted in May 1997 and chlorophyll concentrations were an order of magnitude higher than in

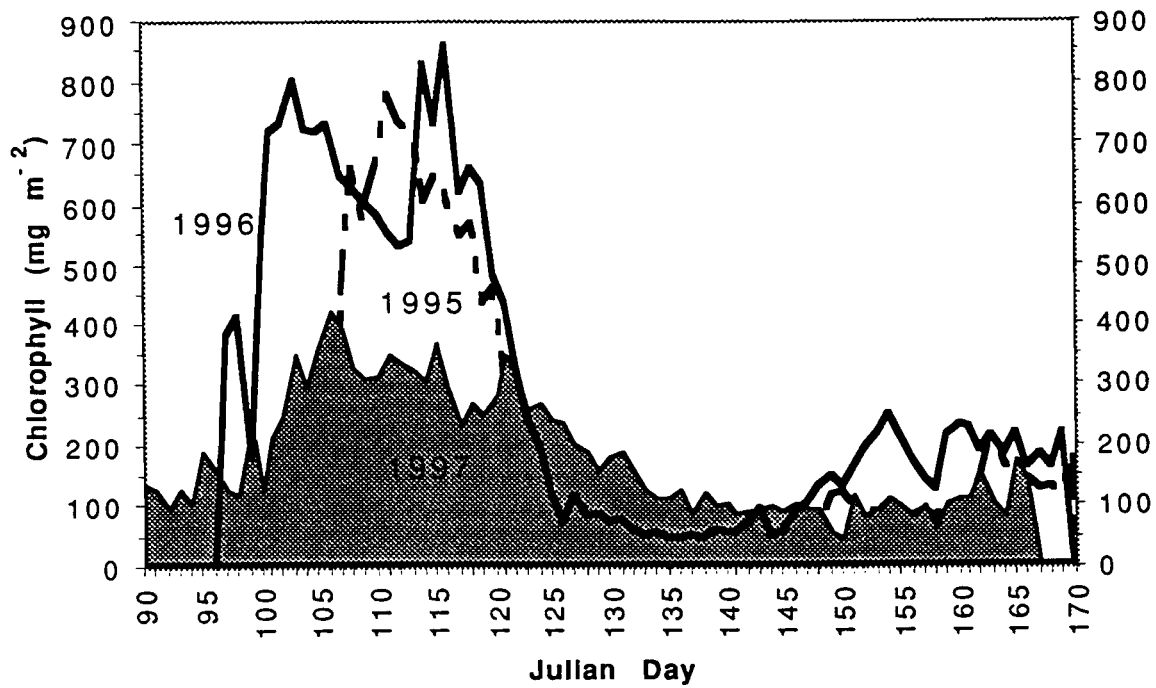


Figure 2. Integrated Chlorophyll a (upper 50 m) for the spring time series in Elrington Passage in 1995, 1996 and 1997.

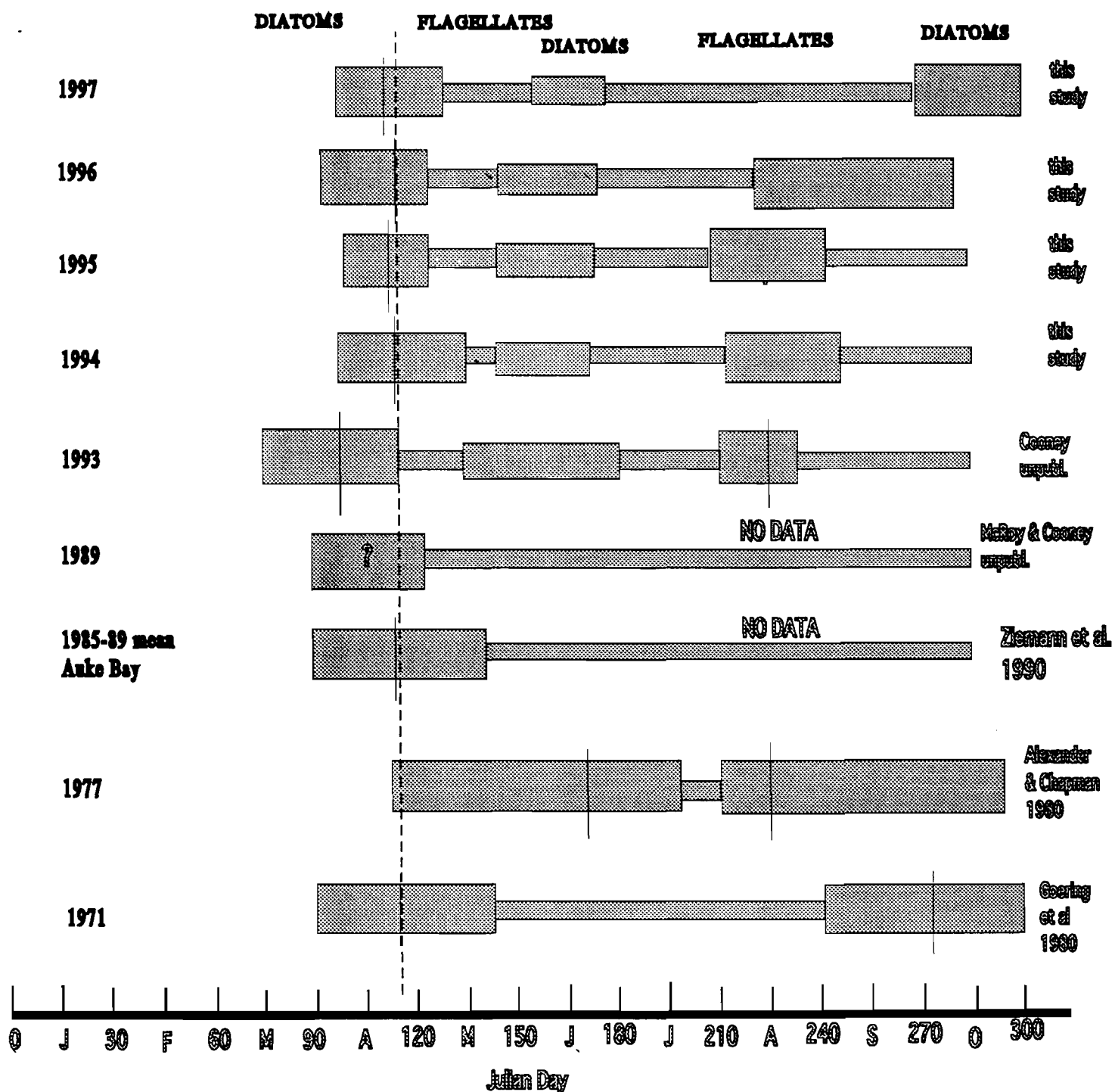


Figure 3. Comparison of timing of phytoplankton spring bloom for all known studies of Prince William Sound. Data from the Apprise Project time series in Auke Bay in Southeast Alaska for 1985-89 are also included. The vertical bars indicate the day of the peak biomass; the average for all studies is day 118 (dashed line).

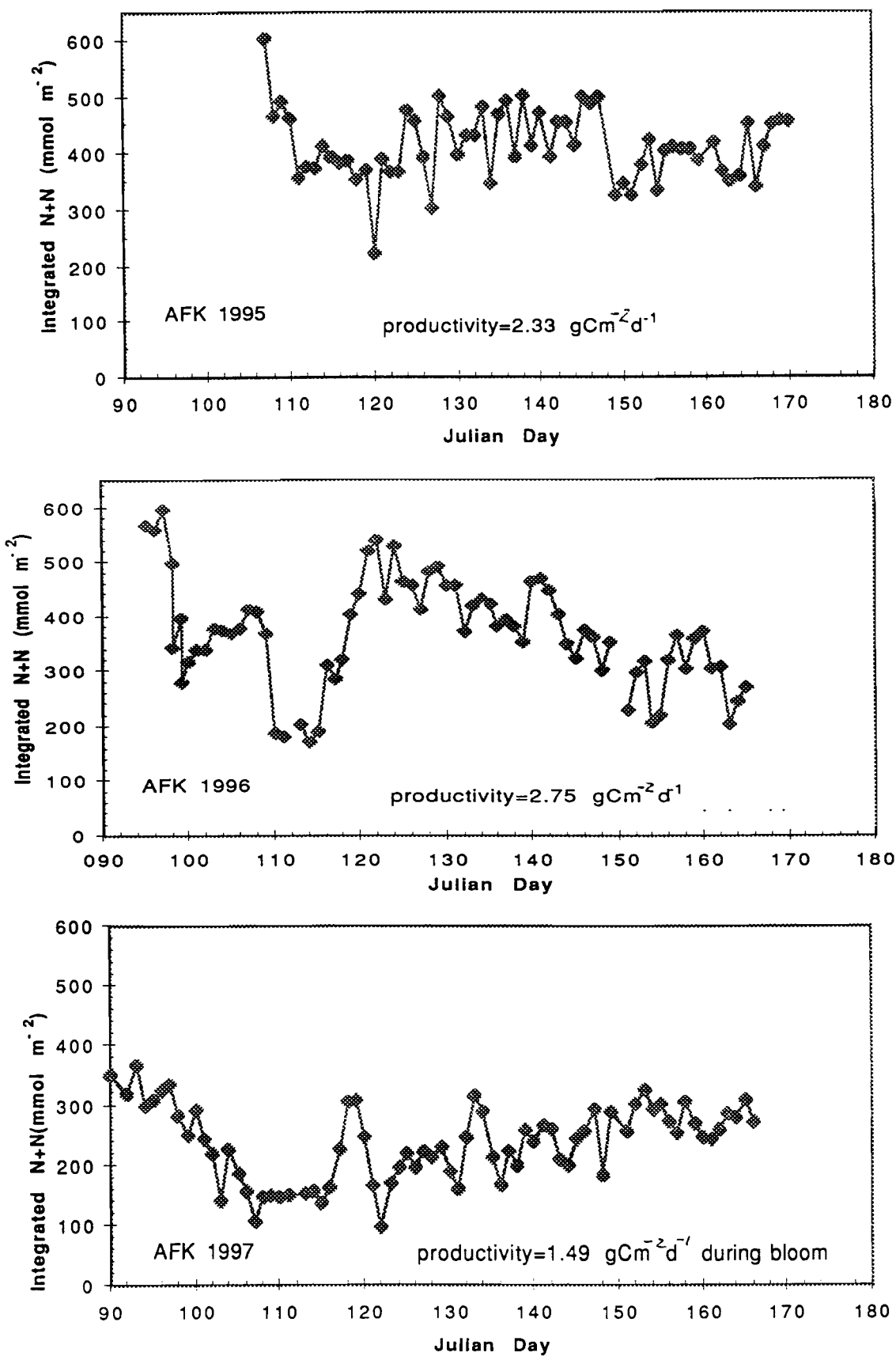


Figure 4. Time series of integrated (upper 50 m) nitrate+nitrite content of the water column in 1995, 1996, and 1997 with estimated primary production rate.

May of previous years. Despite such high variability, several apparent fronts and upwelling zones consistently appear every year. The central sound in spring is characterized by a front centered 30 km north of Hinchinbrook Entrance (Figure 5). North of this front the phytoplankton bloom early and fast, depleting the surface nutrients and disappearing within a few weeks. South of this front the phytoplankton bloom begins later and lasts longer than in the north, possibly a result of higher vertical mixing rates in this region. This front disappears in the summer to be replaced by an upwelling zone which supplies deep nutrients that supports a moderate phytoplankton community at that location.

Montague Strait is characterized by 2 sets of fronts, one in the south associated with Knight Island Passage and one in the north where Montague Strait enters the central sound. Chlorophyll concentrations within Montague Strait vary from year to year much like they do in the central sound, and the location of the peak chlorophyll concentration changes from month to month, but the location of the peak chlorophyll concentrations each month has been the same every year (Figure 6). These consistent patterns in the face of the recognized high temporal variability within Prince William Sound implies a similar pattern in the physical environment. The consistent spatial pattern of chlorophyll peaks implies consistent large scale circulation patterns within the sound, while variability in chlorophyll concentrations, nutrient depletion and bloom timing imply variability in smaller time scale events such as wind driven mixing. Under conditions such as these it may be sufficient to use the density structure and circulation pattern of a "typical" year and annual wind records to adequately model the biology of lower trophic levels in Prince William Sound. However, such a tactic may result in dramatic errors in years with atypical circulation patterns such as we might expect as a result of El Niño.

Discussion

The general pattern of the time course of phytoplankton biomass is a rapid spring increase followed by an equally sharp decline after about 3 weeks. The increase begins in early April and the decline occurs in early of May. The high biomass of the spring bloom, consisting of a dominant diatom flora, is followed by a short period of very low biomass characterized by a flagellate community. A small increase of biomass and diatoms can again occur for a few weeks in June. While our field work did not include daily sampling beyond mid June, past research in Prince William Sound and other coastal embayments around the Gulf of Alaska have documented fall increases in phytoplankton (Goering et al 1973b). A large flagellate population is often observed in August (Alexander and Chapman 1980) and the CFOS buoy recorded such chlorophyll increases in 1993, 1994, 1995, and 1996. In addition the CFOS buoy indicated an fall (October) phytoplankton increase in 1997. The later phytoplankton increase was most likely a diatom community (Goering et al. 1973b).

The pattern of the phytoplankton cycle indicates the classic response of increasing light and stratification in spring followed by nutrient limitation. This pattern has been reported for previous studies of Prince William Sound (Goering et al., 1973a, 1973b). The time series data indicate that nutrient limitation is a significant factor in terminating the bloom. The nutrient-nutrient plot of silicate vs. nitrate shows that the diatoms are able to utilize silicate below the threshold level required for growth (Paasche 1980). The condition must also be a powerful force in species succession. The end of the bloom period is also influenced by zooplankton grazing since the increase in zooplankton directly follows the decrease in phytoplankton. It is likely that both nutrient limitation and grazing lead to the decrease in phytoplankton biomass. These forces

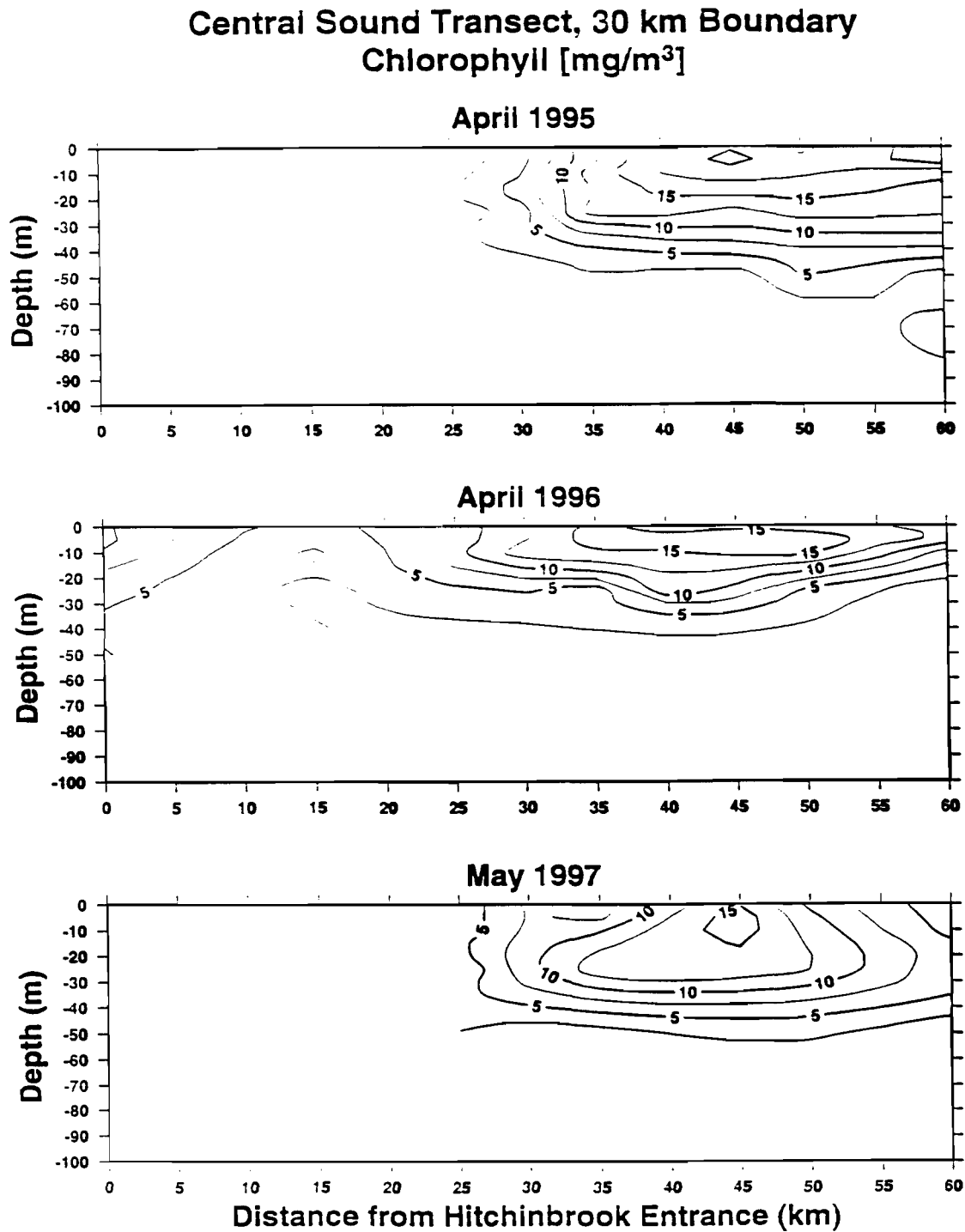
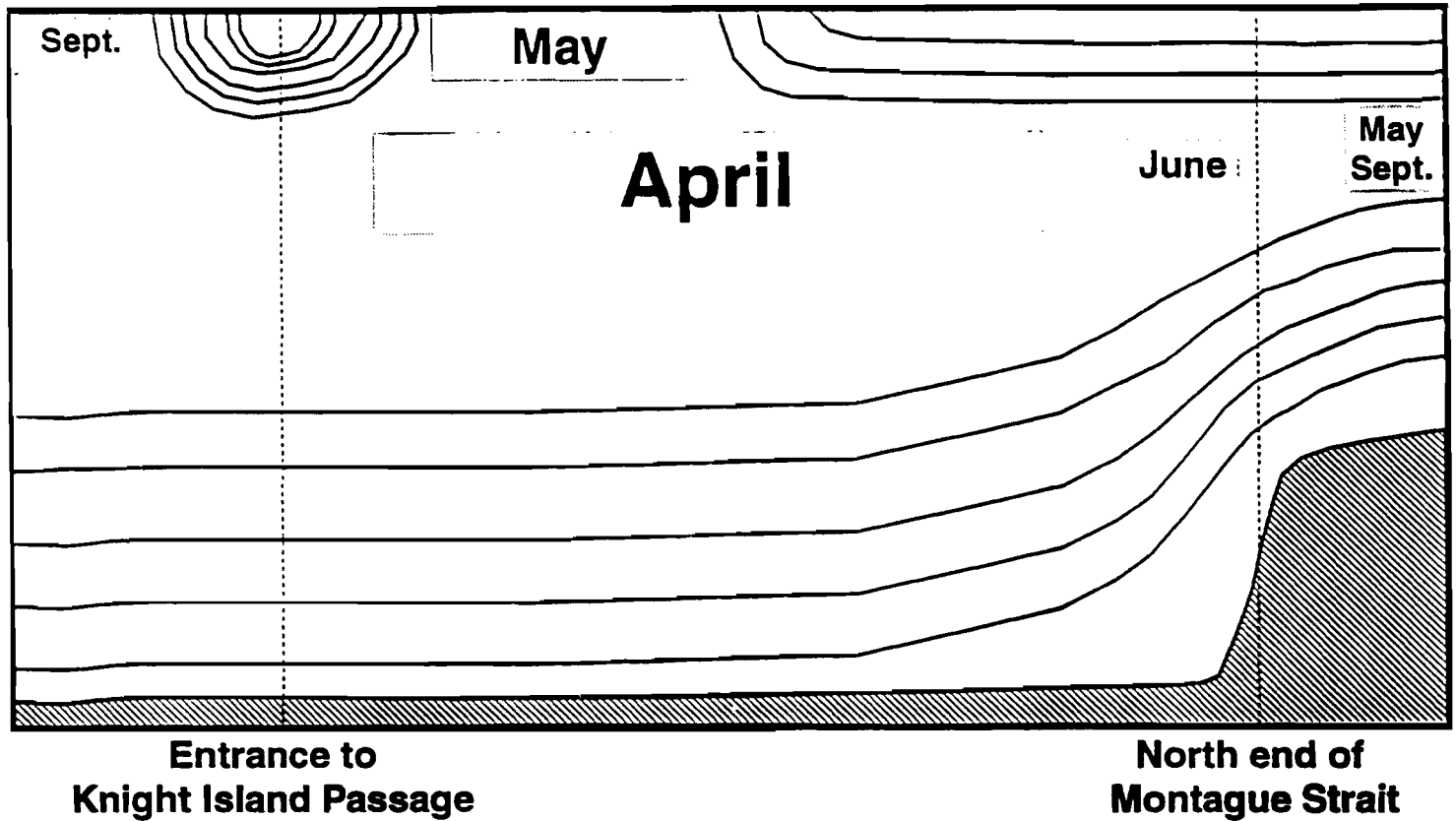


Figure 5. Transects from Hinchinbrook Entrance to the central region of Prince William Sound showing the 30 km front in chlorophyll (mg m^{-3}) in spring of 1995, 1996 and 1997.

Location of chlorophyll maximum in Montague Strait each month.



Contours represent salinity.

May includes 3 years data, other months represent 2 years data

Figure 6. Variability of the location of the chlorophyll maximum by month for the years studied.

can also have a major impact on the composition of the phytoplankton community. Horner et al. (1973) report a detailed list of phytoplankton species for Port Valdez that can also be used for comparison

Alexander and Chapman (1980) report that the phytoplankton community consisted of 97% diatoms in April but by July it was 95 % microflagellates. We found that the diatom abundance in April 1995 and 1996 was over 55%, with remainder consisting of flagellates. The presence of abundant flagellates is indicative of a mechanism for channeling dissolved organic matter (DOM) that is excreted by phytoplankton through a microbial loop. Such a mechanism retains energy in the food web that might otherwise be lost through excreted DOM. The process is relatively inefficient since at least 3 trophic levels are probably involved (Azam et al. 1983).

The diatoms present in April and May are expected to be prime food for the large zooplankton, and hence a major energy source for upper trophic level species. On the other hand the picoplankton are a poor food source for these zooplankton but contribute to a microbial food web that can eventually provide energy to the larger consumers.

Do phytoplankton drive the food web? We have compiled a table of features of the Prince William sound ecosystem for the three years of the study to quantitatively and qualitatively compare the basis of the food web with production of upper trophic level target species (Table 3). In all features compared there appears to be a direct relationship between the quantity and quality of primary production and the production of pink salmon and herring. This finding though somewhat preliminary will certainly warrant discussion and further documentation during the synthesis of the SEA Project. It is at least positive evidence that the food ecosystem is driven by bottom up processes.

Conclusions:

1. A well-defined spring bloom of phytoplankton occurs in Prince William Sound. The timing of the bloom depends on light but the lack of mixing in a given year can predominate. The average peak of the phytoplankton biomass for all studies of Prince William Sound is day 118 (28 April).
2. Phytoplankton bloom community consists of at least 55% diatoms in 1995, 1996, and 1997, followed by a post-bloom period of 3 weeks consisting of more than 80% flagellates. A resurgence of diatoms occurred after the post-bloom period but attained only 33% of their former abundance.
3. Primary production was highest ($2.75 \text{ gCm}^{-2} \text{ d}^{-1}$) in 1996 and lowest ($1.49 \text{ gCm}^{-2} \text{ d}^{-1}$) in 1997. Productivity was ultimately silica limited.
4. A physical front located about 30 km inside Hitchinbrook Entrance is an upwelling feature and separates the central sound into biological regions that have different timings of biological events.
5. Evidence is accumulating that during the years studied there is a direct relationship between nutrient supply, primary production and upper trophic level production.

Papers Presented

McRoy, C.P. R.T. Cooney, A. Ward, E.P. Simpson, D.L. Eslinger, T.C. Kline, S.L. Vaughan and J. Wang. 1997. The architecture of the Prince William Sound ecosystem: nutrients, phytoplankton and zooplankton interactions. American Society of Limnology & Oceanography, Annual Meeting, Santa Fe, NM, February 1997.

Ward, A. and C. P. McRoy. 1997. The spring phytoplankton bloom in Prince William Sound, Alaska. The Oceanography Society meeting, Seattle WA, April 1997.

Vaughan, S.L. and C. P. McRoy. 1997. Relating phytoplankton abundance to upper layer water mass variability in Prince William Sound, Alaska. The Oceanography Society meeting, Seattle WA, April 1997.

Simpson, E.P. and C.P. McRoy. 1997. The architecture of the Prince William Sound ecosystem: I. Variability of chlorophyll and nutrient fields. Arctic Division, AAAS Meeting, Valdez AK, September 1997.

Literature Cited

Alexander, V. and T. Chapman. 1980. Phytotoxicity. pp. 125-142, in J.M. Colonell, ed., Port Valdez, Alaska: Environmental Studies 1976-1979. Institute of marine Science, University of Alaska, Fairbanks.

Azam, F., T. Fenchel, J.G. Field, J.S. Gray, L.A. Meyer-Reil, and F. Thingstad. 1983. The ecological role of water-column microbes in the sea. *Marine Ecology Prog. Ser.* 10:257-263.

Goering, J.J., C.J. Patton, and W.E. Shiels. 1973a. Nutrient cycles. Pp. 225-248, in D.W. Hood, W.E. Shiels and E.J. Kelley. Environmental studies of Port Valdez. Institute of Marine Science, University of Alaska, Fairbanks.

Goering, J.J., W.E. Shiels, and C.J. Patton. 1973b. Primary production. Pp. 225-248, in D.W. Hood, W.E. Shiels and E.J. Kelley. Environmental studies of Port Valdez. Institute of Marine Science, University of Alaska, Fairbanks.

Horner, R.A. L.S. Dick and W.E. Shiels. 1973a. Nutrient cycles. Pp. 283-294, in D.W. Hood, W.E. Shiels and E.J. Kelley. Environmental studies of Port Valdez. Institute of Marine Science, University of Alaska, Fairbanks.

McRoy, C.P. 1988. Natural and anthropogenic disturbances at the ecosystem level. Pp. 329-334, in D.G. Shaw and M.J. Hameedi, eds., Environmental Studies in Port Valdez, Alaska, Lecture Notes on Coastal and Estuarine Studies Vol. 24. Springer-Verlag. Berlin.

- Paasche, E. 1980. Silicon. Pp. 259-284 in I. Morris (ed.), *The Physiological Ecology of Phytoplankton*. Univ. California.
- Parsons, T.R., Y. Maita, and C.M. Lalli. 1984. *A Manual of Chemical and Biological Methods of Seawater Analysis*, Pergamon Press, New York.
- Sournia, A. 1978. *Phytoplankton manual*, UNESCO, Paris, 337 pp.
- Strickland, J.D.H. and T.R. Parsons. 1972. *A Practical Handbook of Seawater Analysis*. Bulletin 167, Fisheries Research Board of Canada, Ottawa, 310 pp.
- Ziemann, D.A., L.D. Conquest, K.W. Fulton-Bennett and P.K. Bienfang. 1990. Interannual variability in the Auke Bay phytoplankton. Pp. 129-170 in D.A. Ziemann and K.W. Fulton-Bennet [eds.], *APPRISE: Interannual variability and fisheries recruitment*. The Oceanic Institute, Hawaii.

Table 1. Summary of data collection, including number of samples collected, and sampling days for 1995, 1996 and 1997 at AFK Station SB2.

Data Collection	1995	1996	1997	Totals all years
Sampling Dates (Julian)	107 - 170	97 - 169	91-166	91-170
Sampling Depths	0, 5, 10, 25, 50, 75	0, 5, 10, 25, 50, 75	0, 5, 10, 25, 50, 75	0, 5, 10, 25, 50, 75
No. Sampling Days	64	73	73	210
CTD Casts	63	73	73	210
Secchi Depth Measurements	63	73	73	210
Chlorophyll <i>a</i> Concentration Measurements	372	437	435	1244
Size Fractionation Measurements	0	68	219	287
Nitrate + Nitrite Concentration Measurements	372	438	435	1245
Silicate Concentration Measurements	369	438	435	1242
Phosphate Concentration Measurements	372	438	435	1245
Species Composition and Abundance Measurements	73	80	110	263
Autotrophic Carbon Biomass Measurements	68	80	110	258

Table 2. Summary of sample collection for 1995, 1996 and 1997 from oceanographic cruises.

Data Collection	1995	1996	1997	Totals all years
No. Cruises	5	3	1	9
No. Stations	153	112	29	294
Chlorophyll <i>a</i> Concentration Measurements	918	672	174	1764
Size Fractionation Samples	329	0	0	329
Nitrate + Nitrite Concentration Measurements	918	672	174	1764
Silicate Concentration Measurements	918	672	174	1764
Phosphate Concentration Measurements	918	672	174	1764
Species Composition and Abundance Samples	760	672	174	1764

Table 3. Interannual comparison of features that provide evidence supporting a bottom-up hypothesis.

FEATURE	1995	1996	1997
Initial N+N Content of Water Column (mmole m ⁻²)	604	597	368
Silicate / N+N Ratio	1.55	1.55	3.00
Maximum Phytoplankton Biomass (mg Chl <i>a</i> m ⁻²)	723	863	423
Year Day of Maximum Biomass	113	116	106
Dominant Diatom Species	<i>Thalassiosira sp.</i> <i>Skeletonema sp.</i> <i>Chaetoceros sp.</i>	<i>Skeletonema sp.</i>	<i>Thalassiosira sp.</i>
Carbon / Chlorophyll Ratio	12 +/- 3	22 +/-6	(30) preliminary
Estimated Primary Production During Bloom (g C m ⁻² d ⁻¹)	2.33	2.75	1.49
Zooplankton, maximum settled volume (ml) (R.T. Cooney data)	5.61	6.21	4.97
Wild Pink Returns (ln total) (M. Willette data)	14.987	15.316	should be low
Herring Growth, fork length of 0 class (mm) in Oct., Zaikof Bay (K. Stokesbury data)	78.19+/-14.77	93.49+/-8.49	75.94+/-7.54

ATTACHMENT A

A TEMPORAL STUDY OF THE PHYTOPLANKTON SPRING BLOOM IN
PRINCE WILLIAM SOUND, ALASKA

A
THESIS

Presented to the Faculty
of the University of Alaska Fairbanks
in Partial Fulfillment of the Requirements
for the Degree of

MASTERS OF SCIENCE

By
Alison Emmett Ward, B.A.

Fairbanks, Alaska

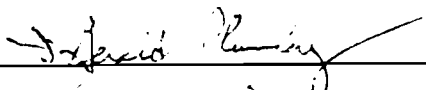
August 1997

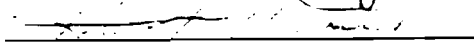
A TEMPORAL STUDY OF THE PHYTOPLANKTON SPRING BLOOM IN
PRINCE WILLIAM SOUND, ALASKA

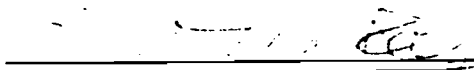
By

Alison Emmett Ward

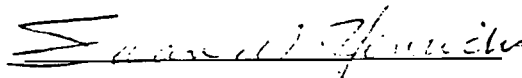
RECOMMENDED:







Advisory Committee Chair




Department Head

APPROVED:



Dean School of Fisheries and Ocean Sciences



Dean of the Graduate School



Date

ABSTRACT

The phytoplankton bloom in southwest Prince William Sound, Alaska began in early April, declined by May and had a small recovery in June 1995 and 1996. Phytoplankton bloom was nutrient-limited in April and phytoplankton biomass was controlled by zooplankton grazing in May. The bloom consisted of 80 % microplankton; the post bloom was predominantly flagellates, followed by a small diatom recovery. A seasonal succession in the diatom community occurred from *Skeletonema costatum*, *Thalassiosira* spp. and *Chaetoceros* spp. in April to *Rhizosolenia fragilissima* in June. There was little vertical variation in species composition. More than twice as much organic carbon due to phytoplankton was present in 1996 as in 1995. In 1995, *Thalassiosira* spp. was 73-80 % of diatom carbon and in 1996 *Skeletonema costatum* made up 58-78 %. The timing of the bloom, cell abundance and patterns of succession resembled other marine environments of similar latitude.

TABLE OF CONTENTS

ABSTRACT.....	III
LIST OF FIGURES	VI
LIST OF TABLES.....	VIII
ACKNOWLEDGMENTS	IX
INTRODUCTION	1
METHODS	4
1. SAMPLING DATES AND STUDY SITE	4
2. SAMPLE COLLECTION.....	6
2.1 Field Procedures.....	6
2.2 Nutrients.....	7
2.3 Phytoplankton Community Measurements.....	7
2.3.1 Chlorophyll a.....	7
2.3.2 Size fractionation	7
2.3.3 Species identification and enumeration	8
2.3.4 Carbon biomass.....	9
RESULTS	11
1. HYDROGRAPHY.....	11
2. NUTRIENT TIME SERIES.....	16
3. PHYTOPLANKTON COMMUNITY.....	18
3.1 Chlorophyll Time Series	18
3.2 Size Structure	23
3.3 Species Composition.....	25
3.3.1 Species descriptions	25
3.3.2 Distribution and abundance	27
3.3.2.1 Total diatoms and flagellates	27
3.3.2.2 Diatom species and genera.....	31
3.3.3 Integrated abundance	34
3.4 Carbon Content	38
3.4.1 Carbon biomass by time and depth.....	38
3.4.2 Integrated carbon.....	43
3.5 Community Interactions.....	47
3.5.1 Physics, nutrients and chlorophyll relationships.....	47
3.5.2 Chlorophyll and carbon relationships	49
DISCUSSION	53
1. TEMPORAL PATTERN OF THE PHYTOPLANKTON BLOOM	53
2. TEMPORAL AND VERTICAL PATTERNS OF SUCCESSION.....	55
2.1 Phytoplankton Biomass.....	55
2.2 Species Succession.....	60
3. RELATIONSHIP TO UPPER TROPHIC LEVELS.....	66
3.1 Food Availability	66
4. FUTURE RESEARCH.....	67

CONCLUSIONS.....	69
REFERENCES.....	70
APPENDIX 1.....	75
APPENDIX 2.....	80
APPENDIX 3.....	85

LIST OF FIGURES

	Page
Figure 1. Prince William Sound showing the location of the sampling site between Evans Island and Elrington Island.	5
Figure 2. Vertical profiles of temperature, salinity and sigma-t for the upper 75 m of the water column in spring 1995 and 1996.	13
Figure 3. Monthly mean precipitation from rain and melted snow collected at AFK Hatchery from March-September 1995 and 1996.	14
Figure 4. Vertical profiles of N+N, silicate, and phosphate concentrations for the upper 75 m of the water column in 1995 and 1996.	17
Figure 5. Vertical profiles of chlorophyll <i>a</i> for the upper 75 m of the water column in spring 1995 and 1996.	19
Figure 6. Chlorophyll <i>a</i> integrated over the upper 50 m of the water column (A) and Secchi depth (B) from spring 1995 and 1996.	21
Figure 7. Chlorophyll <i>a</i> time series divided into size fractions (<5 μm , $\geq 5 < 20 \mu\text{m}$, $\geq 20 < 100 \mu\text{m}$ and $\geq 100 \mu\text{m}$) from the chlorophyll maximum during 1996; chlorophyll <i>a</i> by size fraction (A) and % chlorophyll contributed by each size fraction (B).	24
Figure 8. Abundance of major diatoms and flagellates from five depths in the upper 50 m from spring 1995.	28
Figure 9. Abundance of major diatoms and flagellates from five depths in the upper 50 m from spring 1996.	29
Figure 10. Diatom species composition (% total diatoms) from five depths in the upper 50 m from spring 1995.	32
Figure 11. Diatom species composition (% total diatoms) from five depths in the upper 50 m from spring 1996.	33

Figure 12. Diatom and flagellate abundance integrated over the upper 50 m from spring 1995 and 1996.	36
Figure 13. Diatom species composition (% total diatoms integrated over 50 m) from spring 1995 and 1996.	37
Figure 14. Estimated carbon for major diatoms and flagellates from five depths in the upper 50 m from spring 1995.	40
Figure 15. Estimated carbon for major diatoms and flagellates from five depths in the upper 50 m from spring 1996.	41
Figure 16. Estimated carbon for diatoms and flagellates integrated over the upper 50 m from spring 1995 and 1996.	44
Figure 17. Estimated carbon (% total diatom carbon integrated over 50 m) of major diatoms from spring 1995 and 1996.	45
Figure 18. Chlorophyll <i>a</i> vs. nutrient concentration from spring 1995 and 1996.	48
Figure 19. Estimated autotrophic carbon vs. chlorophyll <i>a</i> for the upper 50 m from spring 1995 and 1996.	52
Figure 20. Depth-integrated chlorophyll <i>a</i> and zooplankton settled volume from spring 1995 and 1996.	58

LIST OF TABLES

	Page
Table 1. Summary of data collection, sampling days and periods of the phytoplankton cycle from spring 1995 and 1996 in Elrington Passage, Prince William Sound.	12
Table 2. Species list of diatom and flagellate taxa and their size ranges in the upper 50 m from spring 1995 and 1996.	26
Table 3. Cell shape, volume equations, measurements, cell volume and cell carbon 39 estimates for major phytoplankton taxa.	39
Table 4. Mean, range, standard deviation and number of observations of chlorophyll <i>a</i> in the upper 50 m from spring 1995 and 1996.	50
Table 5. Mean, range, standard deviation and number of observations of estimated carbon/chlorophyll <i>a</i> in the upper 50 m from spring 1995 and 1996.	50
Table 6. Comparison of the timing of the spring bloom and chlorophyll concentrations at other regions in Prince William Sound and northern regions.	54
Table 7. Number of days having < 50 % cloud cover, median cloud cover during each period, and number of days observed from April-June 1995 and 1996 at AFK Hatchery.	62

ACKNOWLEDGMENTS

I acknowledge the chair of my advisory committee, Dr. C. Peter McRoy, for giving me the opportunity to complete this research under full funding and for his support along the way. I also thank him for the numerous research opportunities and the encouragement to attend local and national oceanographic conferences to learn and present my findings. I appreciate the guidance, encouragement and references provided by my committee members, Dr. Gerry Plumley and Dr. R. Ted Cooney, who always dropped everything to help with my current dilemma. I am very grateful for the instructional assistance in phytoplankton identification and sampling strategies provided by Dr. Freda Reid, UCSD, and Dr. Rita Horner, UW. I express gratitude to the Prince William Sound Aquaculture Corporation and the staff of AFK Hatchery for providing field laboratories, meteorological data, unlimited access to skiffs and the gas shed, and accommodations. I thank the staff of the Prince William Sound Science Center for the use of their CTD. I am particularly grateful to the following individuals who made this study possible. Beth Bergeron and Jill Cameron processed the water samples for nutrient analysis. Paul Simpson analyzed the CTD and nutrient data. Deena Clayton, Sue McCullough, Erik Suring and Loren Tuttle participated in the field research and were always enthusiastic workers under any conditions. I am indebted to my friends, Ted Maksym, Ryan Woodard and Liz Chilton and my parents, Patricia Burns Ward and James E. Ward, for their guidance and encouragement throughout my graduate career.

This work was supported by a grant from the *Exxon Valdez* Oil Spill Trustee Council as part of the Sound Ecosystem Assessment Project.

INTRODUCTION

On 28 March 1989, the *Exxon Valdez* oil tanker spilled 11 million gallons of crude oil into the estuarine waters of Prince William Sound (PWS), Alaska. This event precipitated the question of how such a widespread pollutant would affect the long-term health of Prince William Sound. In order to address this question from a broad perspective, the Sound Ecosystem Assessment (SEA) Project was initiated in the spring of 1994. SEA originated as an interdisciplinary, multifaceted study designed to evaluate Prince William Sound from an ecosystem perspective to determine the factors that constrain the restoration of commercially important fish stocks (especially pink salmon and herring) in the region of the spill (Cooney 1996). The Phytoplankton and Nutrient Component SEA, of which this study is an integral part, was designed to assess the health of the sound temporally and spatially from the base of the food-chain. It provides four years of supporting field data to modeling components and establishes a database of biological and chemical information for future reference. The data presented here are the results of a collaborative effort of a group of marine scientists and technicians led by Dr. C. Peter McRoy at the Institute of Marine Science, University of Alaska, Fairbanks.

This thesis, one sub-set of the Phytoplankton and Nutrient Component of SEA, is an analysis of the seasonal and interannual dynamics of the phytoplankton community in 1995 and 1996. This study involved collecting and analyzing a series of daily observations on the phytoplankton and nutrients in the springs of two consecutive years. I proposed that an assessment of the phytoplankton community in the sound would be a basis for inferences about on the transfer of energy to higher trophic levels, i.e. a test of the bottom-up driven ecosystem hypothesis. I planned to accomplish this by means of a temporal understanding of the phytoplankton biomass, species composition, size structure and limiting nutrient availability. From these results I asked questions such as: is

phytoplankton standing stock controlled from the bottom-up? What is the species succession during the bloom? Does succession vary temporally and how does standing stock translate into organic carbon? How pronounced is interannual variability in the phytoplankton dynamics and how could this affect upper trophic levels?

Few phytoplankton community studies had been conducted in Prince William Sound before or after the oil spill. In Port Valdez and Valdez Arm, a fjord in northeast Prince William Sound used heavily by oil tanker traffic and vulnerable to crude oil pollution, four phytoplankton studies were conducted in the late 1960s and 1970s. Alexander and Nauman (1969), in September 1969, found low cell abundance, low chlorophyll *a* concentration and a phytoplankton community dominated by dinoflagellates, primarily *Ceratium* spp. In Galena Bay off Valdez Arm, AK during 1971-1972, Goering et al. (1973) used chlorophyll *a* analysis and net phytoplankton tows to investigate a spring diatom bloom, dominated by *Biddulphis aurita* and *Chaetoceros debilis*. This bloom began in March and declined by May due to nutrient depletion. Horner et al. (1973) studied Port Valdez from 1971-1972 and reported a spring diatom bloom dominated by *Thalassiosira* spp., *Chaetoceros* spp, and *Skeletonema costatum*, followed by a succession to a lower abundance of small flagellates and dinoflagellates in late summer, fall and winter. A classic spring diatom bloom beginning in late March followed by microflagellate dominance by July was also found by Alexander and Chapman (1980) in Port Valdez from 1976-1978.

Since 1978, studies of phytoplankton species composition in Alaskan waters have been conducted in geographically close regions like the Bering Sea (Goering and Iverson 1978; Goering and Iverson 1982; Kocur 1982), Auke Bay in Southeast Alaska (Ziemann et al. 1990; Ziemann et al. 1991), and Boca de Quadra, Southeast Alaska (VTN Consolidated, Inc. 1980), but not within Prince William Sound.

This study was based in Elrington Passage, a major channel connecting the sound with the Gulf of Alaska, in southwest Prince William Sound. Elrington Passage was one of the heavily oiled regions in 1989 (Galt et al. 1991). At this location I carried out and analyzed a daily series of phytoplankton observations never before conducted in this region. This level of detail is unprecedented for any type of study of Prince William Sound. This study augments the concurrent biological (McRoy and Eslinger 1995; McRoy et al. 1996 and 1997; Eslinger 1997) research, begun in September 1994, targeting the regional distribution of phytoplankton within Prince William Sound.

METHODS

The data sets are a contribution to the SEA project and will be subjected to several analyses in addition to this thesis. I chose to study the phytoplankton bloom through a detailed analysis of the species composition at a location in southwest Prince William Sound in conjunction with supporting physical and chemical oceanographic data obtained during the SEA study. The following methods describe the collection of phytoplankton and chlorophyll *a* samples, and analyses of water samples for species composition, autotrophic biomass, and nutrient concentrations; also included are methods for measuring water transparency, temperature and salinity.

1. Sampling Dates and Study Site

Oceanographic data were collected daily from 17 April to 19 June, 1995 (Julian days 107-170) and from 6 April to 17 June, 1996 (Julian days 97-169) at a station in Prince William Sound, Alaska (Figure 1). Prince William Sound is located on the coast of South-central Alaska and lies adjacent to the Gulf of Alaska in the Pacific Ocean. The station was located in southwest Prince William Sound in Elrington Passage between Bettie Island and Elrington Island (60° 02.4'N, 148° 00.6'W). The sampling station was in the middle of the passage and had a bottom depth of 140 m. During sampling, sea conditions varied from flat calm (glassy) to rough depending on the wind speed and direction.

The circulation of Prince William Sound is complicated and influenced by fresh water input and the Alaska Coastal Current in the Gulf of Alaska (Muench and Schmidt 1975; Niebauer et al. 1994). Prince William Sound is diluted by freshwater input from precipitation and glacial and snow melt, making it a cold-water estuarine region with a

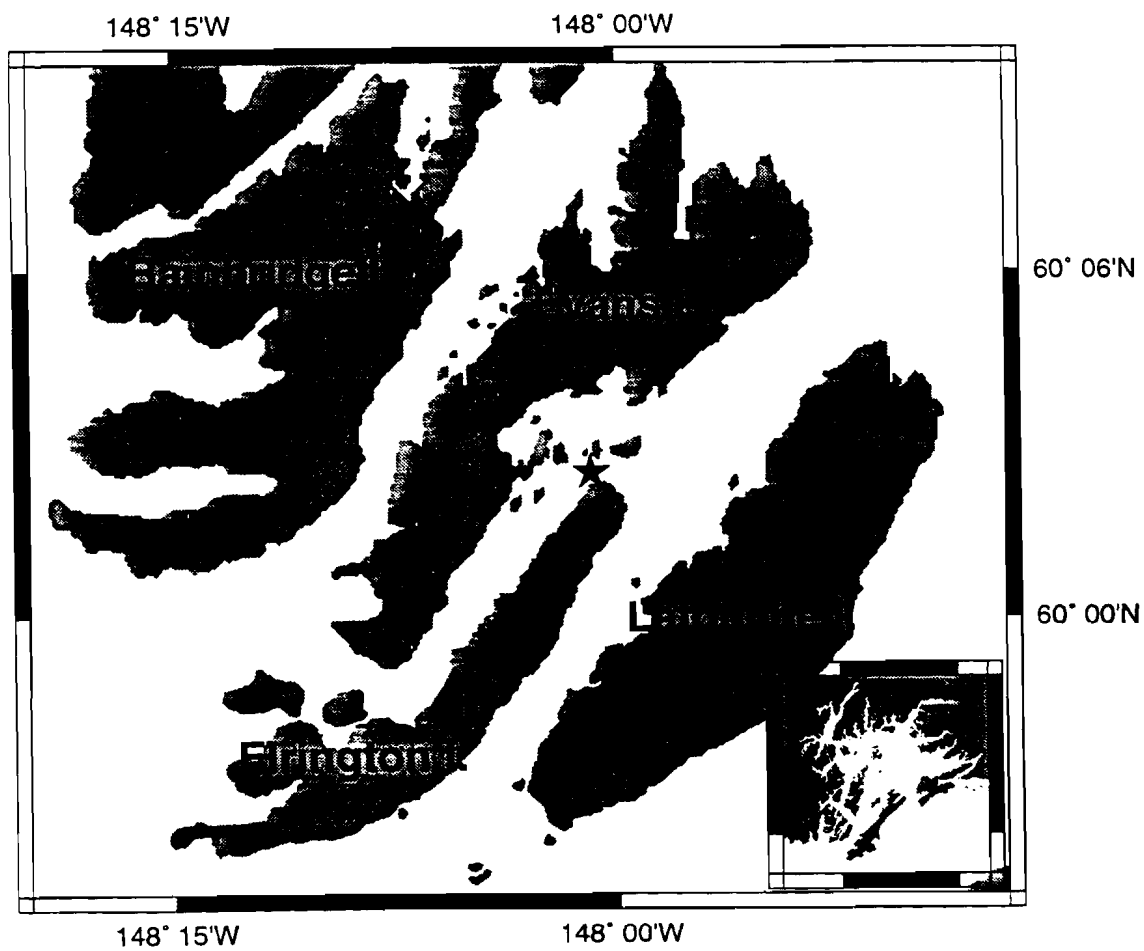


Figure 1. Prince William Sound showing the location of the sampling site (star) between Evans Island and Elrington Island.

fluctuating pattern of circulation (Niebauer et al. 1994). In general, geostrophic flows enter through Hinchinbrook Entrance and exit the sound through Montague Strait in the southwest, or flow back out Hinchinbrook Entrance, depending on fresh water input, winds and tides (Niebauer et al. 1994; Vaughan et al. 1997). An upwelling cyclonic gyre exists in the central sound in summer and fall (Muench and Schmidt 1975; Vaughan et al. 1997). The current flow in southwest Prince William Sound and Elrington Passage, the region of detailed biological studies, varies directionally and seasonally. Currents flow southwest into the Gulf of Alaska in April, northeast into Latouche Passage in May and southwest again into the Gulf of Alaska by October (Niebauer et al. 1994). Prince William Sound is also influenced by strong tidal currents that drive vertical mixing in shallow water (Muench and Schmidt 1975).

2. Sample Collection

Water samples for biological and chemical analyses and CTD (conductivity, temperature and depth) measurements were collected daily in Elrington Passage from April to June from a small skiff. Water samples were processed at the Armin F. Koernig Hatchery (AFK), a pink salmon hatchery operated by Prince William Sound Aquaculture Corporation, in Port San Juan immediately following collection.

2.1. Field Procedures

We collected hydrographic data (temperature, salinity and transparency), biological samples (chlorophyll and phytoplankton) and water samples for nutrient analysis during the hours of 0800-1000 using a 5 L Niskin bottle and SeaCat Sea-Bird Electronics, Inc. CTD (Model 19-03) attached to a hand-operated winch. One CTD cast was lowered to 80 m each sampling day. Data were collected from the downcast and filtered and processed to 1 m averages. Additional bottle casts were deployed to collect water at 0, 5, 10, 25, 50 and 75 m. Approximately 4 L of water from each depth were

collected and stored in dark plastic bottles until processing. After water collection, a Secchi disk was lowered to depth of disappearance as an estimate of water transparency.

2.2 Nutrients

Water samples for chemical analysis were processed within one hour of collection. A sample of 100 mL was filtered through Gelman A/E glass fiber filters, stored in acid-washed plastic bottles and frozen. Later at the University of Alaska Fairbanks, samples were analyzed for nitrate+nitrite (N+N), silicate, and phosphate using CFA techniques on an Alpkem 305 auto analyzer within 3-6 months after collection.

2.3 Phytoplankton Community Measurements

2.3.1 Chlorophyll *a*

Water samples for chlorophyll *a* analysis were processed at the AFK laboratory after collection. Chlorophyll *a* was measured by filtering 250-1,000 mL (depending on standing stock) of seawater through Gelman 25 mm glass fiber filters, extracting the chlorophyll in 10 mL of 90 % acetone and measuring the fluorescence of the supernatant after 10 minutes of centrifugation. Fluorescence was measured with a Turner Designs fluorometer, calibrated with spinach before each field season using a Hitachi spectrophotometer (Model 100-40) (Strickland and Parsons 1977; Parsons et al. 1984).

2.3.2 Size fractionation

Water was filtered through three mesh sizes to collect the cells in different size ranges and determine the percentage of chlorophyll *a* contributed by each size fraction. The filter mesh sizes were chosen to roughly determine what proportion of the bloom was composed of picoplankton (0.2-3.0 μm), nanoplankton 2-20 μm (Tomas 1993), microplankton (>20 μm) and chains of cells (>100 μm). Filtration sizes were secondarily based on the availability of the smallest Nitex netting (5 μm).

Size fractionation of phytoplankton was done only on water from the depth of the chlorophyll maximum after determination of chlorophyll *a* content at the 6 depths. Techniques were based on the methods of Ray et al. 1989. After thoroughly mixing 2 L of water, a 500 mL sub-sample was removed and processed for chlorophyll *a* without pre-filtration. The remaining 1500 mL were filtered through 100 μm Nitex netting. A 500 mL portion of this water was immediately removed and set aside for the 100 μm fraction. The remaining liter was filtered through 20 μm Nitex netting and 500 mL set aside for the <20 μm portion. The last 500 mL were filtered through 5 μm Nitex netting and set aside for the <5 μm portion (Ray et al. 1989). Chlorophyll concentrations in four categories (≥ 100 μm , 100-20 μm , 20-5 μm , and <5 μm) were calculated following fluorescence measurements.

2.3.3 Species identification and enumeration

Phytoplankton identification and enumeration were conducted on samples from the spring bloom and two post-bloom periods at 5 depths (0, 5, 10, 25 and 50 m) for 1995 and 1996 using an inverted microscope technique (Utermohl 1931). Although samples were collected daily, only a subset of these collections were analyzed, based on the chlorophyll *a* time series, to represent the seasonal succession. For 1995, samples were analyzed on Julian days 108 to 119, 131, 133, 135, 162, 164 and 166. In 1996, days 102 to 120 (even days only), as well as 136, 138, 140, 159, 161 and 163, were analyzed. The first series of days covers the primary bloom, from pre-bloom until the chlorophyll biomass distinctly falls. The second series was selected from the time of minimum chlorophyll *a*. The third subset was selected from mid-June, when the chlorophyll biomass increased slightly.

In the field, 50 mL of sea-water were preserved with 1 mL of Lugol's solution and stored in the dark until analysis. In the laboratory at UAF, a subsample of 25-50 mL of water was settled in the dark at room temperature in a settling chamber according to

Utermohl (1931) for a minimum of 24 hours. Water was slowly poured down the side of the cylinder to prevent convection currents. Using a Zeiss Telaval 31 Inverted Microscope, live cells (at the time of preservation) $\geq 15 \mu\text{m}$ were counted and identified within a rectangular field using 200 x magnification on two transacts (one horizontal, one vertical) across the diameter of the settling chamber. All cells within a chain were counted separately. If at least 300 cells were not enumerated, additional transacts were counted. In addition, cells $< 15 \mu\text{m}$ were counted at 400 x magnification across the same horizontal transact until a minimum of 300 cells were totaled. Cells $\leq 2 \mu\text{m}$, the size limit for accurate identification using a light microscope, were not identified or counted. These enumeration techniques are based on the compilation of several published phytoplankton sampling approaches (Utermohl 1931; Lund et al. 1958; Venrick 1978; Sandgren and Robinson 1984). This technique enabled me to achieve $95 \pm 10 \%$ confidence for samples in April and June (Lund et al. 1958). In May, when cell abundance was extremely low, additional transacts were enumerated until at least 100 cells on 200 x magnification were enumerated. For these samples the error increased to $\pm 20 \%$ (Lund et al. 1958). All fields viewed were counted and recorded for abundance calculations. Diatoms were identified to the lowest possible taxon (usually genus) while nano-plankton ($2\text{-}20 \mu\text{m}$) were identified to genus or class. Phytoplankton identification was based on comparison with several taxonomic guides (Gemeinhardt 1930; Schiller 1933; Cupp 1943; Hustedt 1959; Brunel 1962; Vinyard 1979; Yamaji 1986; Tomas 1993; Tomas 1996)

2.3.4 Carbon biomass

Phytoplankton with the greatest numerical abundance were measured for biomass determination using cell dimension techniques (Kovals and Larrance 1966).

Phytoplankton that could only be identified to genus were placed in size categories. For each dominant species or size category, length and width were measured to the nearest 1

μm. Average dimensions were calculated from the measurements of 20 cells and used for volume calculations. Cell depth measurements (Table 3) were estimated from equations specific for each cell type (F. Reid, personnel communication). Cell volume was calculated by using the geometric shapes and volume equations from Kovalá and Larrance (1966). Cell carbon was estimated from cell volume calculations using separate equations for diatoms and other non-diatom phytoplankton (Strathmann 1967).

RESULTS

The following results are a compilation and analysis of data sets that describe the phytoplankton spring bloom on a daily basis for two years from one location in southwest Prince William Sound (Table 1). Additional information on the physical and chemical oceanography that influence the biology are also presented. In 1995, Julian days 148 and 160 were not sampled due to rough weather conditions. In 1996, no days were missed but on day 99 at 25 m, the chlorophyll *a* sample was lost. In 1996, not enough water was collected for size fractionation analysis on days 97, 98, 123, 126, and 137.

The spring chlorophyll time series in both years exhibits three distinct events; a bloom of high biomass, followed by a period of very low biomass, and then a period of increase. This pattern allowed the data to be separated into three periods to study phytoplankton succession: (1) spring bloom, the period of highest chlorophyll, (2) post-bloom, the period of lowest chlorophyll following the spring bloom, and (3) the recovery, when chlorophyll biomass increased again from the lowest levels.

1. Hydrography

The waters were cold and isothermal throughout the water column during the bloom in 1995 and 1996 (Figure 2). In 1995, from April through early May temperatures remained between 4-5 °C. Surface warming was not apparent until day 121.

Stratification was weak and occurred earlier in 1995, around day 115, due to freshening at the surface from precipitation (Figure 3). In 1995, the salinity averaged 31.2 at 5 m and density profiles mirrored salinity. Density remained between 24.2-25.2 sigma-t. In 1996, temperatures were the same as 1995 and mixing extended down to 80 m prior to day 110. Fresh water input was lower in 1996 (Figure 3) and salinity averaged 31.6 at

Table 1. Summary of data collection, sampling days and periods of the phytoplankton cycle from spring 1995 and 1996 in Elrington Passage, Prince William Sound.

Data Collection	1995	1996
Sampling Period (Julian days)	107-170	97-169
Spring Bloom Period (Julian days)	107-123	97-126
Post Bloom Period (Julian days)	124-145	127-145
Recovery Period (Julian days)	146-170	146-169
Sampling Depths (m)	0, 5, 10, 25, 50, 75	0, 5, 10, 25, 50, 75
Total Sampling Days	64	73
CTD Casts	63	73
Secchi Depth Measurements	63	73
Chlorophyll <i>a</i> Measurements	372	437
Size fractionation Measurements	0	68
N+N Measurements	372	438
Silicate Measurements	369	438
Phosphate Measurements	372	438
Species Composition/Abundance Measurements	73	80
Autotrophic Biomass Measurements	68	80

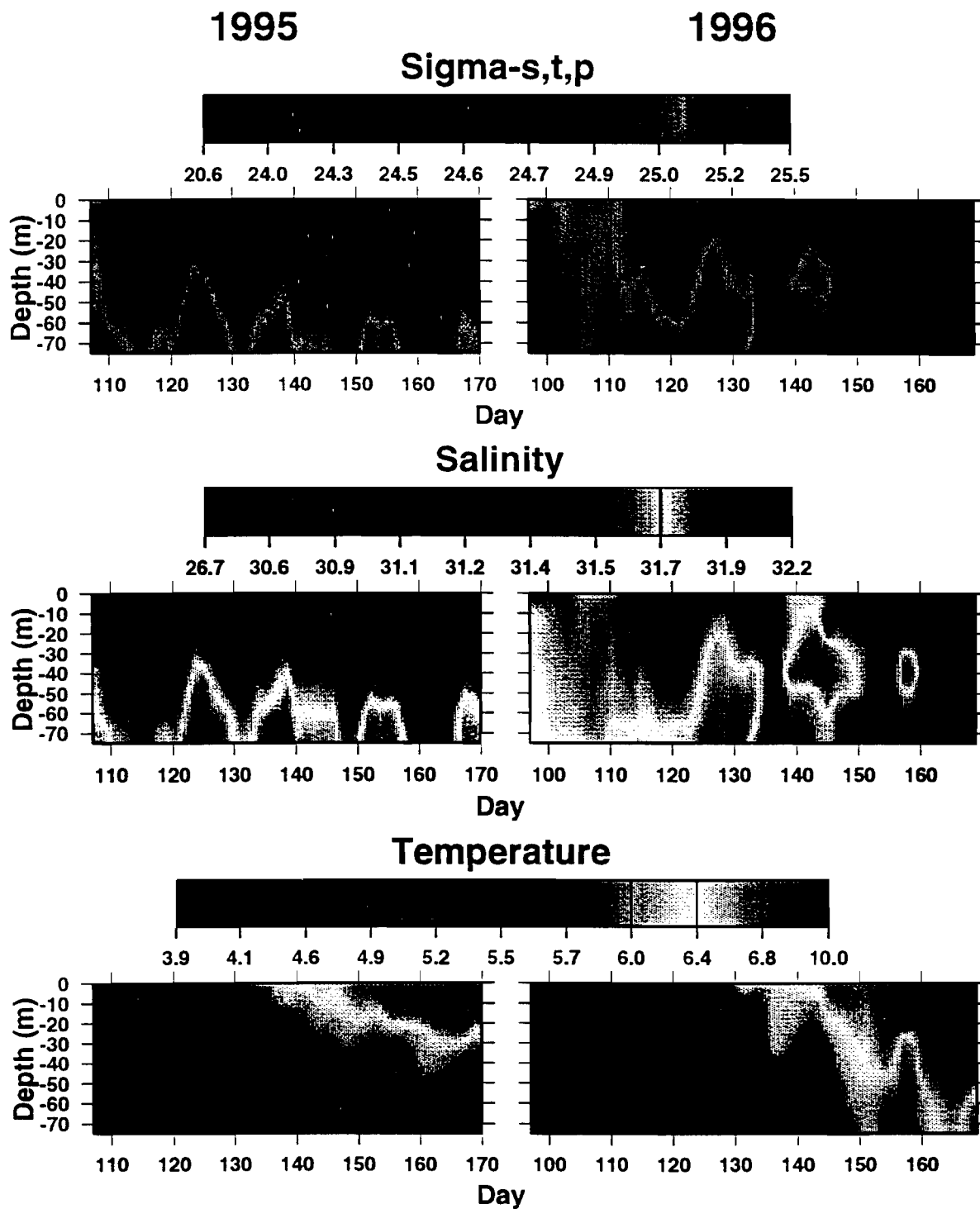


Figure 2. Vertical profiles of temperature (°C), salinity and sigma-t for the upper 75 m of the water column in spring 1995 and 1996.

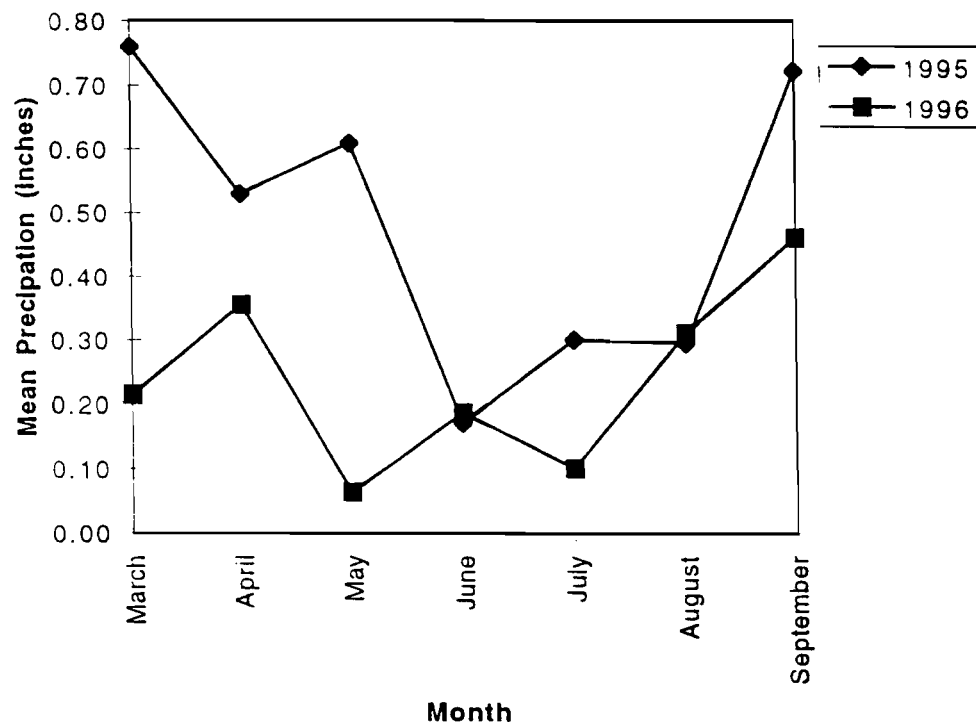


Figure 3. Monthly mean precipitation from rain and melted snow collected at AFK Hatchery from March-September 1995 and 1996 (unpublished data).

5 m. After day 111, stratification was weak in April and the density of the water remained between 24.8-25.2.

During the post-bloom, stronger stratification was achieved as solar heating and fresh water runoff increased in both years (Figure 2). In 1995, the surface waters warmed to 6.8°C by day 143. A strong pycnocline was formed in the upper water column due to heavy fresh water input. Surface salinity fell to 29 after day 130. In 1996, intense solar input increased water temperatures to 7 °C by day 144. Salinity ranged from 31.2-31.8 in the upper 75 m during the post-bloom. Salinity and density remained higher in 1996 than 1995, probably due to reduced precipitation (Figure 3) and increased evaporation. In 1996, deep mixing to 75 m (days 135-139) occurred during this period. A salty intrusion (31.7-31.9 psu) was detected on day 140 between 20 and 60 m and lasted for several days.

Following day 145, surface waters gained their greatest stability and temperature in both years. In 1995, surface temperature reached a maximum of 9°C as the surface salinity dropped to 26.7 psu. Strong stratification and a pycnocline formation caused by both heating and fresh water remained throughout the month of June. In 1996, surface temperature rose to 10°C by day 163 and warm waters penetrated to 75 m. Freshening occurred in the surface waters after day 150, probably due to snow and glacial melt, but the minimum salinity in June reached only 30. Solar radiation warmed the surface waters but only had a small effect on stability. In June the water column was less stable in 1996 than 1995 and stratification in the upper 25 m was interspersed with deep mixing events on days 153 and 162. Another high salinity intrusion (31.7-31.9) at mid depths was seen on day 158 and lasted two days.

Throughout the year increases in salinity and density every 15 days corresponded to the spring tides. This was especially pronounced in the 1995 salinity and density series (Figure 2). In both 1995 and 1996, the spring tides ranged between -2 and 13 ft. The maximum spring tides occurred around days 120, 135, 150 and 165. These days had between 31.7-31.9 salinity and 25-25.2 sigma-t below 30 m. In 1996, tidal influences were less apparent in the salinity and density data but slight increases in both were observed. Maximum spring tides occurred around days 110, 125, 140 and 155. Slight increases in density and salinity corresponded to spring tides.

2. Nutrient Time Series

In 1995 and 1996, nutrient concentrations were high preceding the spring bloom then decreased in surface waters as production increased (Figure 4). In 1995, concentrations of all nutrients were highest around day 107 and a nutricline was apparent throughout the bloom. In the upper 75 m, concentrations of N+N, silicate and phosphate ranged from 10-15, 15-25, and 1-2 μM , respectively. As the bloom progressed, nutrients were depleted in the surface waters but remained high below 50 m. By day 120 concentrations of N+N, silicate and phosphate in the upper 10 m had dropped to levels of 1.5-2.5, 3-4.5 and 0.3-0.8 μM , respectively. Following day 120, all nutrient concentrations remained low but detectable in the surface waters. In 1996, a similar pattern emerged, but concentrations of all nutrients were lower throughout the bloom, especially at depth. On day 97, N+N, silicate and phosphate in the upper 75 m ranged from 10-11.5, 16-17 and 1.2-1.5 μM , respectively. As the month of April passed, all the nutrient concentrations were reduced at the surface especially around days 104 and 117. No nutrients were completely assimilated by plankton but ratios of N+N:silicate were very low. Nutrients were replenished by mixing events around days 109-111.

During the post-bloom of both years nutrients were replenished from depth. Low nutrient concentrations did not exist below 25 m. In 1995, all nutrient concentrations

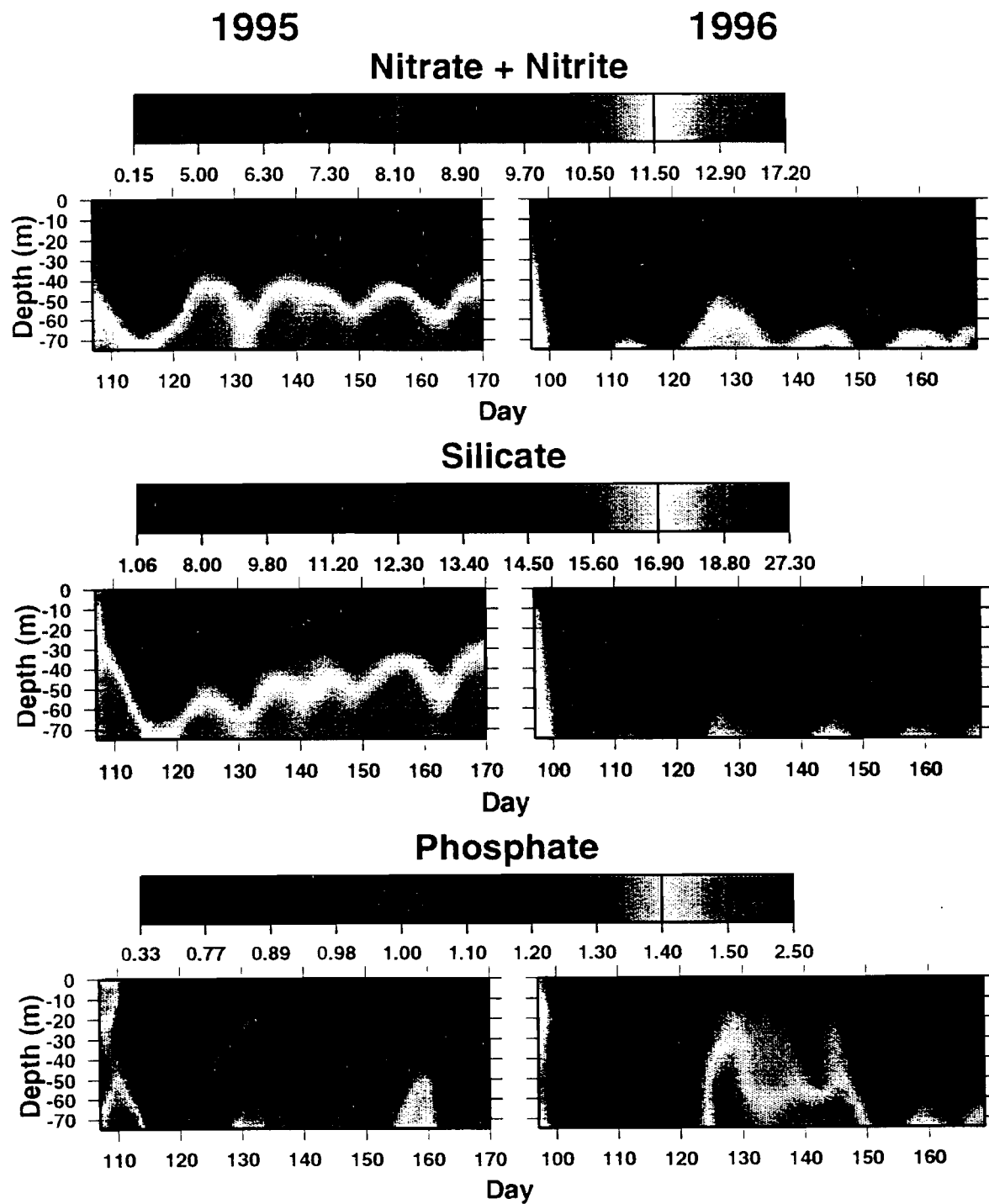


Figure 4. Vertical profiles of N+N (μM), silicate (μM), and phosphate (μM) concentrations for the upper 75 m of the water column in 1995 and 1996.

were high. Only around days 138-143 did all the nutrients show a slight decline in the upper 10 m. Nutrients remained highest below 50 m, with maximum N+N, silicate and phosphate concentrations of 16, 25 and 2 μM , respectively. In 1996, all nutrients were also replenished in the upper layers. Only two times in the post-bloom, around days 131 and 141 had decreased concentrations. Maximum values, at depth and at the surface, were lower in 1996. Below 50 m maximum N+N, silicate and phosphate concentrations reached 14, 17 and 2.4 μM , respectively. Higher concentrations of phosphate existed below 10 m in 1996.

During the recovery period, nutrients in the surface waters decreased again, but concentrations below 25 m remained high. In 1995, all nutrient concentrations remained low in surface waters and high below 25 m. The highest N+N concentrations during the recovery appeared in June at 75 m. In 1996, all surface nutrients were reduced in the upper 25 m throughout the recovery period. Concentrations were highest below 25 m but considerably lower than in 1995.

Similar to the salinity and density, the nutrients increased at depth in response to mixing from spring tides. This was most apparent in the silicate and N+N data (Figure 4). In 1995, nutrients increased at depth after days 120, 135, 150 and 165, when spring tides occurred. In 1996, silicate and N+N increased below 50 m after days 110, 125, 140 and 155, the maxima of the spring tidal cycle.

3. Phytoplankton Community

3.1 Chlorophyll Time Series

During the spring bloom chlorophyll extended below 50 m, and the highest concentrations of chlorophyll were present at this time during both 1995 and 1996 (Figure 5). In 1995, the chlorophyll levels were between 2 and 19 mg/m^3 in the upper 25 m and between 1 and 13 mg/m^3 below 25 m. The peak concentration occurred as a short

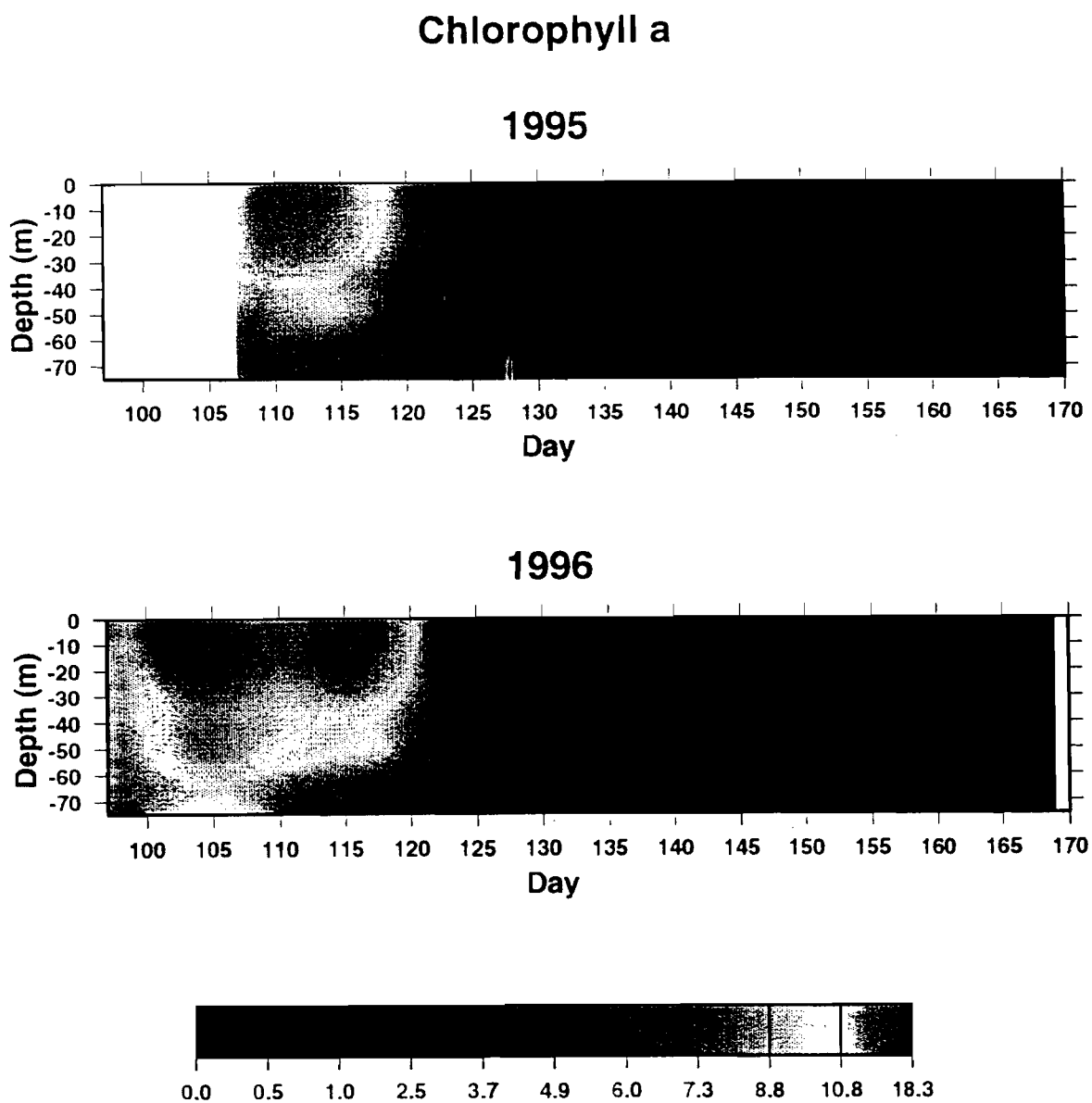


Figure 5. Vertical profiles of chlorophyll *a* (mg/m^3) for the upper 75 m of the water column in spring 1995 and 1996.

pulse between days 111-114 in the upper 25 m. In 1996 chlorophyll levels were higher, variations with depth were less, and the length of the bloom increased. High levels of chlorophyll were present between days 97 and 121. In the upper 25 m, chlorophyll ranged from 2-20 mg/m³; at 50 m and below the range was 0.5-16 mg/m³. There were two distinct periods of high concentration between days 100 and 104 and 114 and 116; both periods had high levels of chlorophyll below 25 m.

During the post-bloom, chlorophyll concentration was uniformly low throughout the water column in both years. In 1995, chlorophyll ranged from 0.15-4 mg/m³ in the water column. Low concentrations (< 4 mg/m³) occurred in the upper 10 m on days 125-127 and 138; chlorophyll levels below 50 m were ≤ 2 mg/m³. In 1996, chlorophyll ranged from 0.2-3.2 mg/m³. Highest relative concentrations were in the upper 25 m.

Following day 145 in both years, chlorophyll increased above 25 m (Figure 5). In 1995, chlorophyll recovered to 7 mg/m³ as stratification strengthened. Concentrations between 0.5-7 mg/m³ remained until day 170 in the upper 50 m. Small transitory increases in chlorophyll occurred in 1996 above 25 m. Chlorophyll increased to highs around 5 mg/m³ on days 153-154, 160-163, 165 and 169. Levels remained low below 25 m except on day 154 where 6.3 mg/m³ was measured at 50 m.

Depth-integrated chlorophyll was highest during the spring bloom in 1995 and 1996 (Figure 6A). In 1995, the spring bloom had already begun on day 107 (17 Apr), reached its highest integrated chlorophyll concentrations on day 110 and decreased to low levels by day 123. Chlorophyll ranged from 157-780 mg/m² and averaged 541 mg/m². In 1996, the bloom appeared between days 97-126, with two peaks in biomass occurring at different times throughout the bloom. On day 103 (12 Apr), integrated chlorophyll reached 804 mg/m² and on day 116 (25 Apr) it peaked at 863 mg/m². Chlorophyll ranged from 72-863 mg/m² and averaged 545 mg/m². The concentrations are similar to those in 1995.

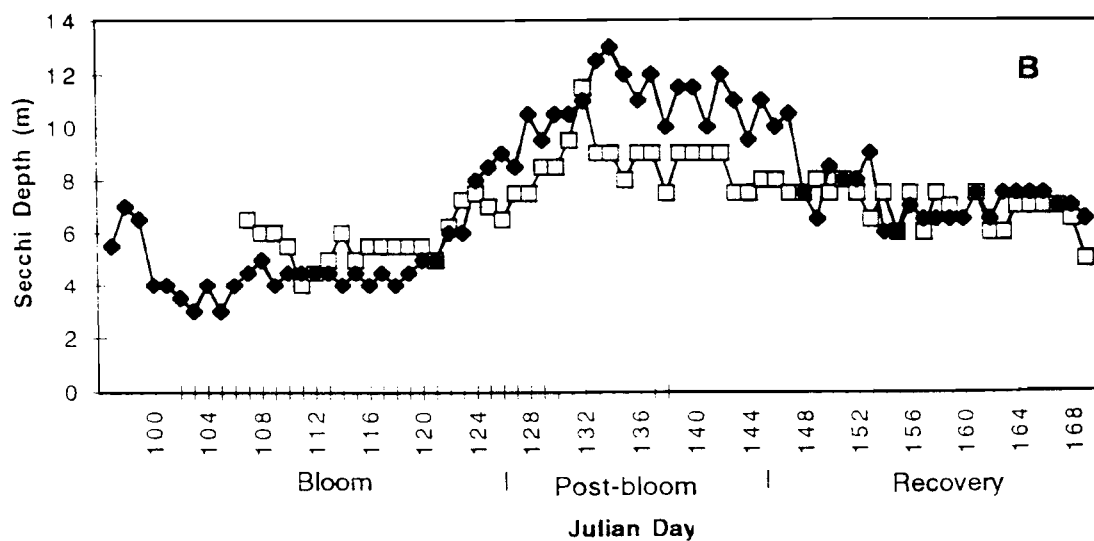
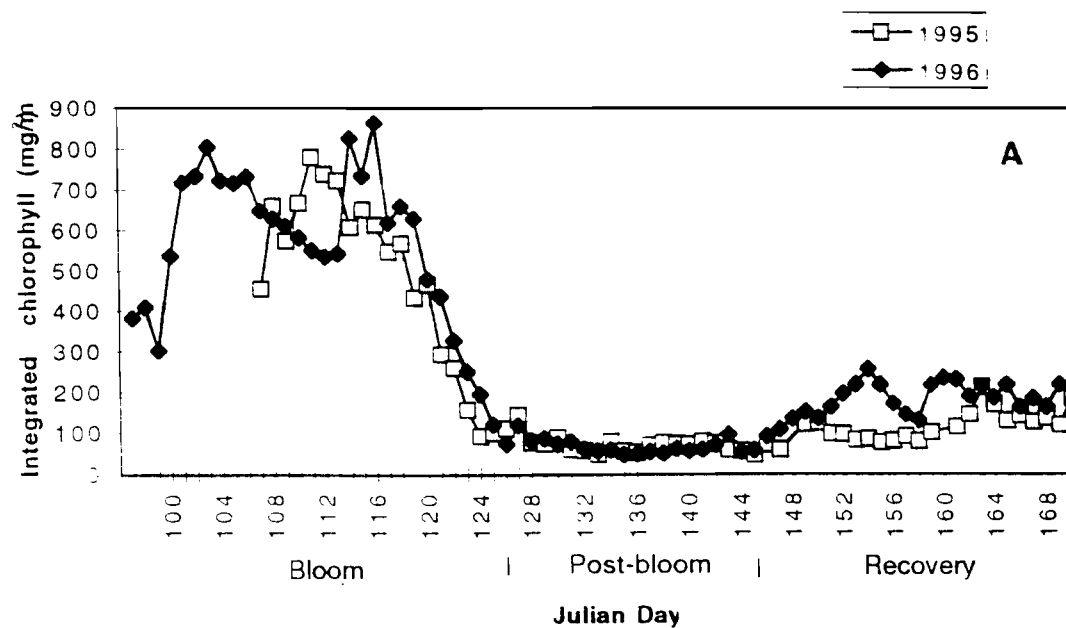


Figure 6. Chlorophyll *a* integrated over the upper 50 m of the water column (A) and Secchi depth (m) (B) from spring 1995 and 1996.

During the post-bloom period in both years, integrated chlorophyll levels were low (Figure 6A). In 1995, concentrations ranged from 47-144 mg/m² and the mean was 75 mg/m². In 1996, concentrations were approximately the same as in the previous year, ranging between 46-118 mg/m² with a mean concentration of 66 mg/m². Daily chlorophyll levels fluctuated only slightly during this period.

A slight increase in the integrated chlorophyll concentration occurred after day 145 in both years (Figure 6A). Chlorophyll concentrations increased to a maximum of 213 mg/m² by day 163 in 1995. Levels remained higher than during the post-bloom period until the last day of sample collection. In 1996, chlorophyll concentrations increased to higher levels. Chlorophyll stayed higher than post-bloom concentrations, ranging between 91-254 mg/m². Concentrations were at least 30 % higher in 1996 than 1995 during the first 10 days of June.

Secchi depths showed reduced water transparency in April and June when chlorophyll was high and increased transparency in May when chlorophyll was low (Figure 6B). During the spring bloom Secchi depths ranged from 4-6.5 m in 1995 and 3-9 m in 1996. During the post-bloom depths ranged from 6.5-11.5 m in 1995 and from 8.5-13 m in 1996. During the recovery period Secchi depths increased slightly both years ranging from 5-8 m in 1995 and 6.5-9 m in 1996. The depths in 1995 were slightly greater during periods of higher chlorophyll. In 1996 during the post-bloom the depths were greater for the same quantity of chlorophyll. This probably was a result of measurement error. The depth of disappearance of the Secchi depth is difficult to determine under rough weather conditions. Overcast skies, heavy rain and rough waters made visibility poor and measurements less accurate in 1995. In 1996, calm waters, clear skies and greater light intensity enabled the disk to be seen at deeper depths.

3.2 Size Structure

The phytoplankton community was partitioned into size fractions in 1996 to assess the biomass contributed by picoplankton, nanoplankton and microplankton (Figures 7A and 7B). In this year, the maximum chlorophyll *a* content over the study period ranged from 1.1-19.4 mg/m³. The sample depth for size fractionation was chosen from the highest daily chlorophyll value, and ranged from 0-75 m with a median of 5 m for the study period.

During the spring bloom the phytoplankton community was dominated by microplankton (cells >20 µm). The mean chlorophyll concentrations for each size fraction were 3.9 mg/m³ for microplankton ≥100 µm, 7.0 mg/m³ for microplankton <100 µm and 1.5 mg/m³ for nanoplankton (5-20 µm). Over the bloom, at least 85 % of the chlorophyll was contributed by cells greater than 5 µm, with the largest portion (80 %) from microplankton.

During the post-bloom the lowest levels of chlorophyll occurred and picoplankton dominated the community. The total chlorophyll biomass ranged from 1.1-6.1 mg/m³. In the post-bloom, a shift in the community structure from microplankton and nanoplankton to picoplankton occurred. Up to day 138, microplankton and nanoplankton accounted for greater than 60 % of the chlorophyll but picoplankton accounted for 20-100 % of the total chlorophyll during the post-bloom. From days 138 to 145, greater than 60 % of the chlorophyll was contributed by picoplankton.

As the season progressed the phytoplankton community structure shifted from picoplankton back to microplankton with increased chlorophyll *a* (Figure 7). In this recovery period, chlorophyll concentrations were about 30 % of previous bloom levels. Nanoplankton consisted of 0-31 % of the chlorophyll and picoplankton dominated with greater than 50 % until day 154. Following day 154, microplankton increased and

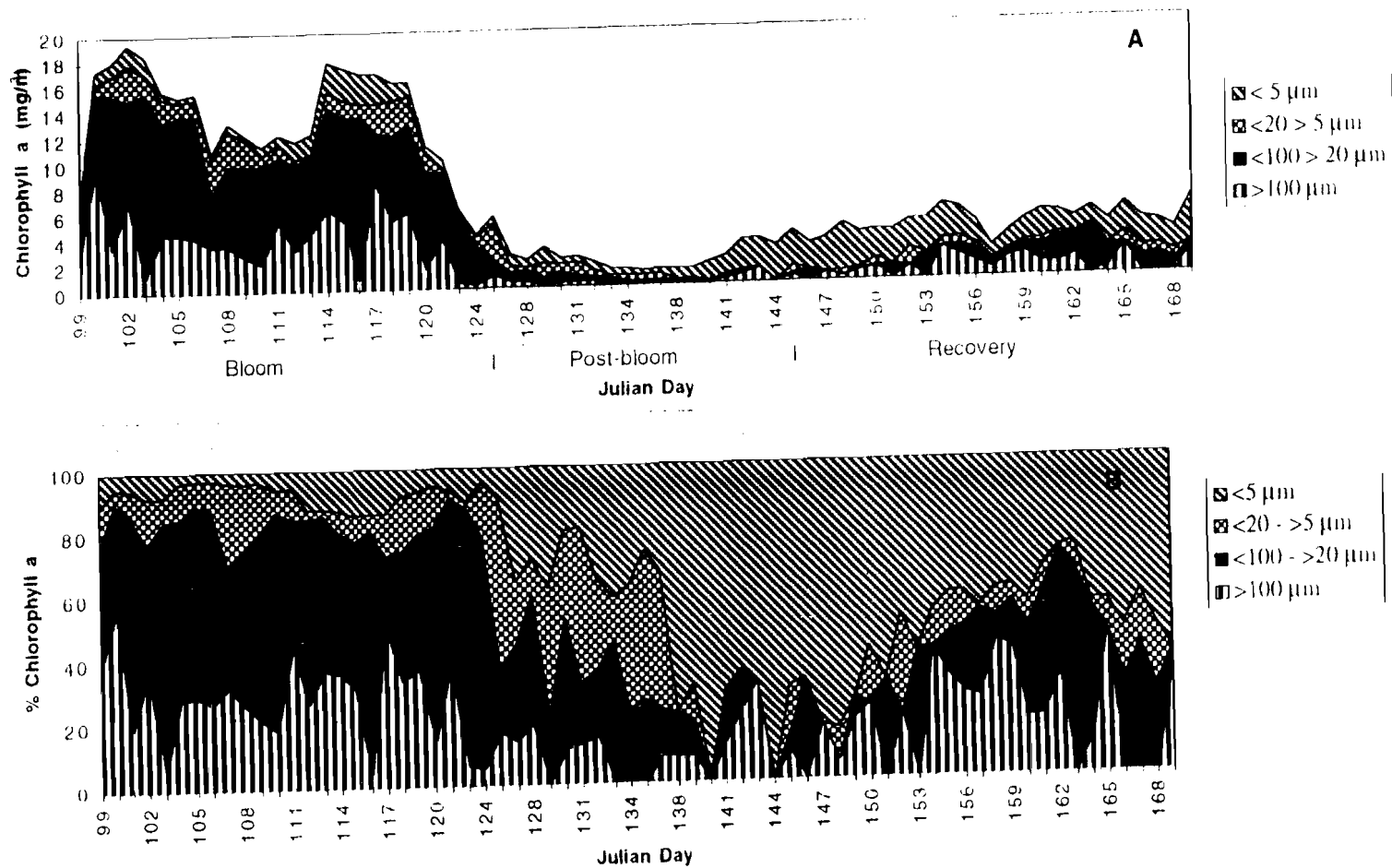


Figure 7. Chlorophyll *a* time series divided into size fractions (<5 µm, >5<20 µm, >20<100 µm and >100 µm) from the chlorophyll maximum during 1996; chlorophyll *a* by size fraction (A) and % of chlorophyll contributed by each size fraction (B).

regained over 50 % of the chlorophyll. Large algae $>100\text{ }\mu\text{m}$ reappeared and contributed as much as 45 % of the chlorophyll by day 165.

A delay occurred in the succession to picoplankton after chlorophyll levels declined in early May (Figure 7). The chlorophyll concentrations decreased to 6.2 mg/m^3 on day 122 and fell to a low of 1.1 mg/m^3 by day 135, but the shift to picoplankton lagged the decline by approximately 12 days. Plankton $\geq 100\text{ }\mu\text{m}$ disappeared around day 133 while microplankton $< 100\text{ }\mu\text{m}$ comprised at least 20 % of the biomass until day 136.

3.3 Species Composition

3.3.1 Species descriptions

The phytoplankton community in both years was composed of a few species of chain forming diatoms and single-celled flagellates (Table 2). A detailed list of phytoplankton and their abundance per day and depth sampled for 1995 and 1996 is given in Appendices 1 and 2. Due to orientation on the settling plate, weak silicification, poor preservation, lack of distinguishing features and/or the limitations of inverted light microscopy, many of the cells could only be identified to genus. The flagellates, single celled flagellated eukaryotic nano- and picoplankton, were from two algal divisions, Chromophyta and Chlorophyta. The most abundant were spherical cells $<10\text{ }\mu\text{m}$ that closely resembled *Phaeocystis* spp., but no colonies were seen. These cells were identified only as flagellates and placed into size categories because verification was not possible without higher magnification. A few flagellates from the class Dinophyceae, including *Ceratium* spp., were encountered but their abundance was very low in comparison with other phytoplankton.

The major constituents of the diatom community in 1995 and 1996 were *Skeletonema costatum*, *Thalassiosira* spp., *Chaetoceros* spp., *Pseudo-nitzschia* spp., *Leptocylindrus* spp. and *Rhizosolenia fragilissima*. *Skeletonema costatum* is a small diatom that is united in chains by external silica structures. The chains vary in length

Table 2. Species list of diatom and flagellate taxa and their size ranges in the upper 50 m from spring 1995 and 1996

<u>Diatoms</u>	<u>Size Range</u> (LxW) μm	<u>Flagellates</u>	<u>Size Range</u> (LxW) μm
<i>Asterionella glacialis</i>	10x5-20x5	<i>Ceratium furca</i>	80x75
<i>Biddulphia</i> sp.	15x15	<i>Ceratium</i> spp.	20x12-90x90
<i>Chaetoceros</i> spp.	2.5x2.5-40x30	<i>Dinophysis</i> spp.	50x45
<i>Chaetoceros deciprens</i>	25x15-25x20	<i>Distephanus speculum</i>	20x20-25x25
<i>Cocconeis</i> sp.	40x20	<i>Ebria tripartita</i>	15x15-30x30
<i>Coscinodiscus</i> sp.	135-190	<i>Oxytoxum</i> spp.	20x10-40x15
<i>Eucampia</i> spp.	30x25-55x25	<i>Peridinium</i> spp.	20x15-65x50
<i>Fragilariopsis</i> sp.	10x2-15x2.5		
<i>Grammatophora</i> sp.	40x2.5-35x20	Unidentified flagellate	5-17.5
<i>Leptocylindrus danicus</i>	20x10-85x10	Unidentified silicoflagellate	no data
<i>Leptocylindrus minimus</i>	20x2.5-35x2	Unidentified dinoflagellate	15x10-60x20
<i>Leptocylindrus</i> spp.	35x5-40x7		
<i>Licmophora glacialis</i>			
<i>Navicula</i> spp.	20x5-80x5		
<i>Pseudo-nitzschia</i> spp.	30x2-65x2		
<i>Rhizosolenia fragilissima</i>	15x5-35x5		
<i>Rhizosolenia stolterforthii</i>	45x8-60x10		
<i>Rhizosolenia</i> spp.	25x14-500x15		
<i>Skeletonema costatum</i>	7.5x5-17.5x5		
<i>Stephanopyxis nipponica</i>	30x20-60x20		
<i>Thalassiosira</i> spp.	10x7-55x15		
<i>Thalassionema nitzschioides</i>	25x5-45x5		
Unidentified centric diatom	10x15-45x35		
Unidentified pennate diatom	20x5-45x7		
Unidentified diatom	15x10-130x15		

from a few cells to more than 10. *Thalassiosira* spp. are larger centric diatoms with a width of 10 μm to 55 μm . Like *Skeletonema*, they also form long chains connected by organic threads (Tomas 1996). Since this species frequently appears in girdle view and is difficult to identify in this orientation, cells were placed in three size categories (<25, 25-44, \geq 45) for identification purposes. *Chaetoceros* spp. are diverse centric chain-forming diatoms varying in length from 2.5 μm to 40 μm and often having long, coarse setae. Due to their great diversity only one species, *C. decipiens*, could be identified to species level with high precision. All others were placed into size categories. *Pseudo-nitzschia* spp. are narrow elongate pennate diatoms that are multi-celled chains or solitary. Their length is as great as 30 times their width (2 μm) and they have the smallest cell volume of any phytoplankton in this study. *Leptocylindrus minimus* and *Leptocylindrus danicus* are cylindrical chain forming diatoms that appear like adjacent rectangles in girdle view. The two species were differentiated based on diameter and appearance. *L. danicus* is larger, averaging 11.5 μm in width, often appearing singly or in chains of two or three cells. *L. minimus* is smaller, having an average width of 2.5 μm , and more cells per chain. *Rhizosolenia fragilissima*, also known as *Dacryliosolen fragilissimus* (Tomas 1996), is a cylindrical centric diatom that averaged 22 x 5 μm (l x w) and formed chains by uniting the valve surfaces of two cells. They often appeared in chains of only a few cells.

3.3.2 Distribution and abundance

3.3.2.1 Total diatoms and flagellates

In both 1995 and 1996 during the spring bloom diatoms and flagellates were present at all depths (Figures 8 and 9). Cell numbers remained high throughout the bloom and started to decline by the end of the bloom at all depths. The highest

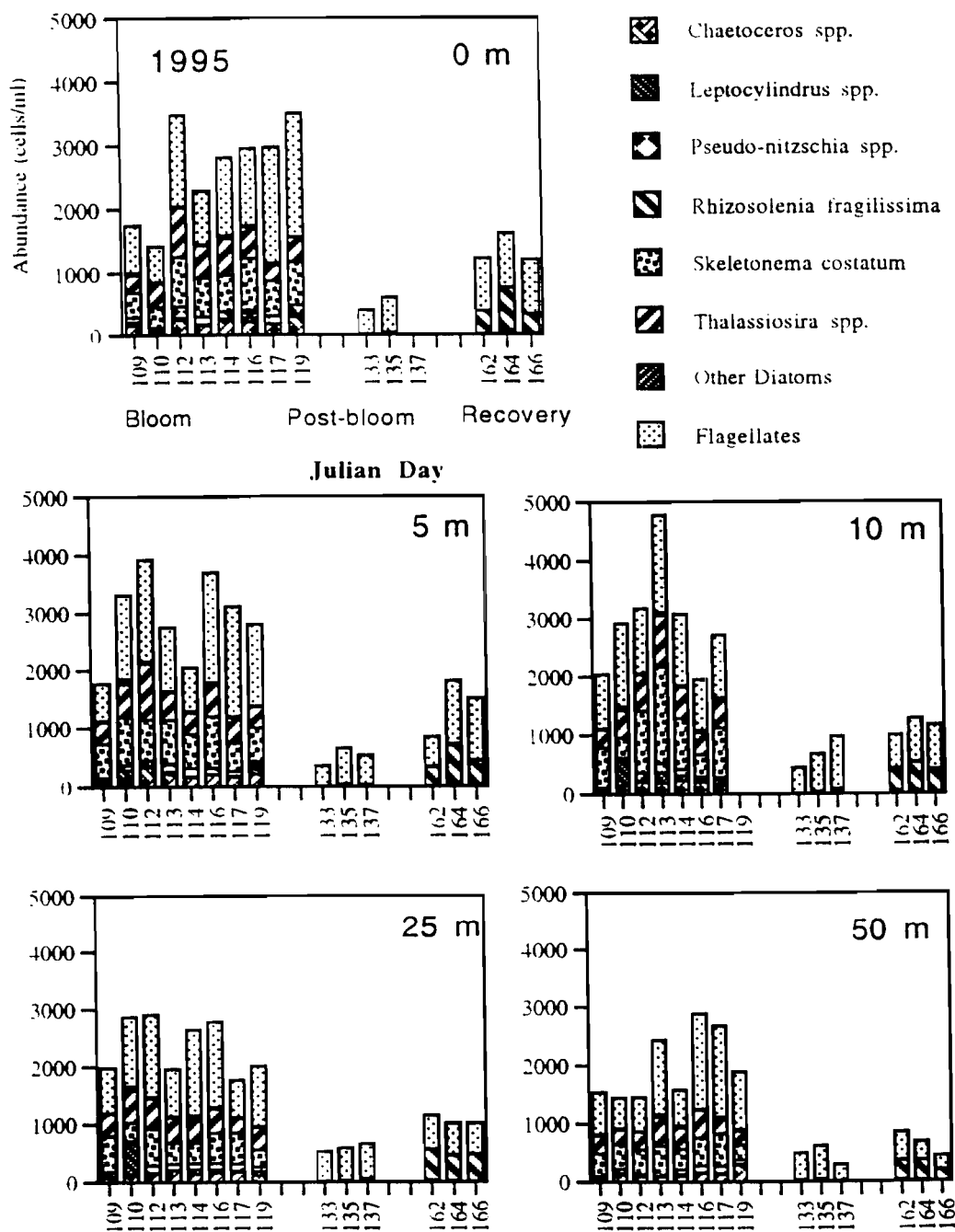


Figure 8. Abundance of major diatoms and flagellates from five depths in the upper 50 m from spring 1995.

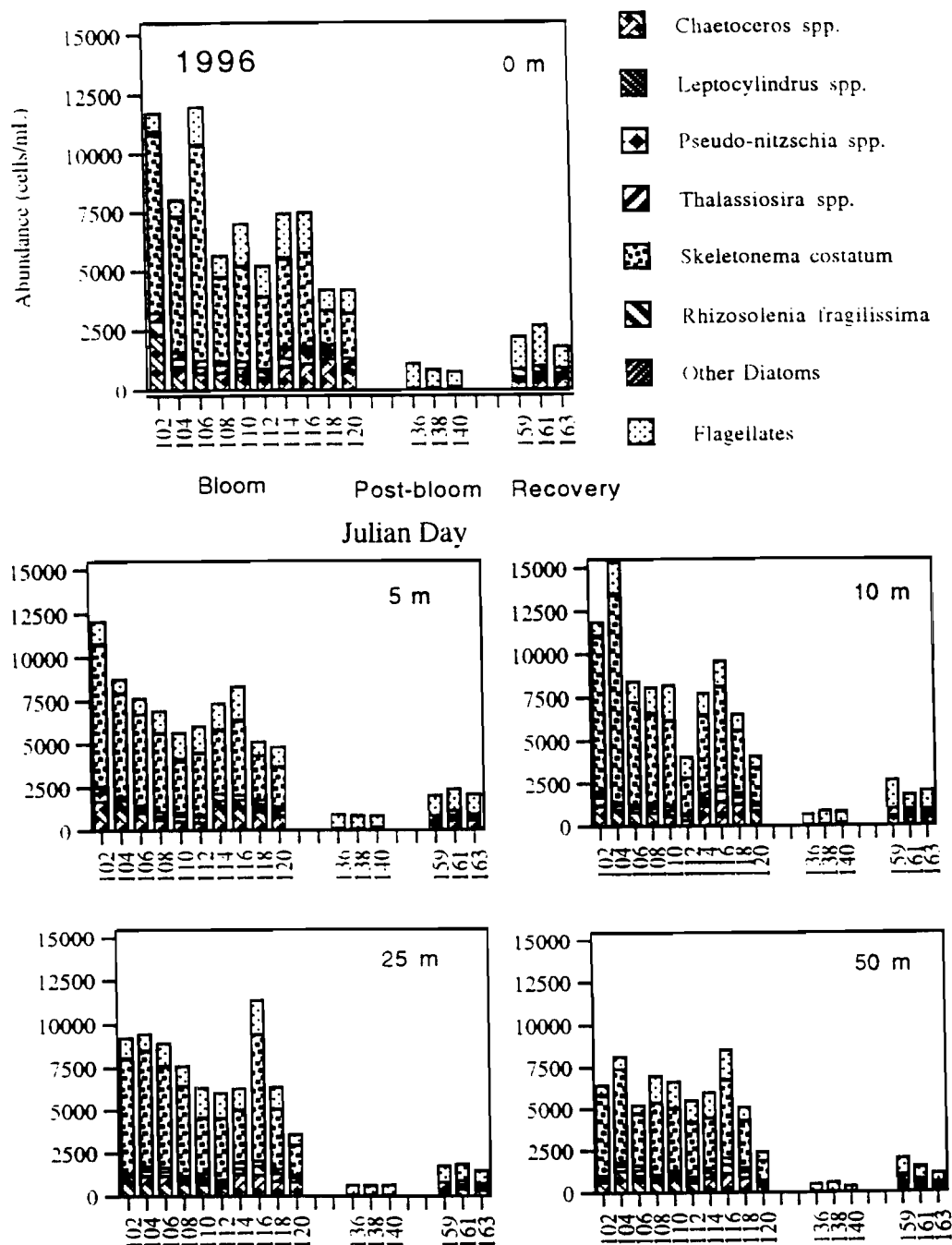


Figure 9. Abundance of major diatoms and flagellates from five depths in the upper 50 m from spring 1996.

abundance of cells was within the upper 10 m and the lowest abundance was at 50 m. In 1995, diatom abundance ranged from 813-3,110 cells/mL within the top 50 m. Flagellates appeared in high abundance and ranged from 525 cells/mL at 50 m to 1,900 cells/mL at the surface. Flagellates were the most numerous phytoplankton constituting as much as 61 % of the total abundance, and a mean of 45 % of the total for all depths. In 1996, diatom abundance was approximately three times as great as 1995. Diatom abundance ranged from 1,872-13,500 cells/mL in the upper 50 m. However, flagellate abundance remained about the same in 1996 as in 1995. Flagellates peaked at 2,021 cells/mL on day 110 at 10 m. During the bloom their lowest abundance of 481 cells/mL occurred at 50 m on day 106. At this time, they accounted for ≤ 25 % of the total phytoplankton abundance. In both years, dinoflagellates (Dinophyceae) and silicoflagellates, mainly *Distephanus speculum*, were less than 1 % of total cell abundance.

During the post-bloom and recovery periods flagellates were more abundant than diatoms at all depths and abundance was low (Figures 8 and 9). In 1995, flagellates composed greater than 90 % of the phytoplankton abundance and ranged from 283-880 cells/mL throughout the upper 50 m during periods of low chlorophyll. Abundance increased slightly (250-1,088 cells/mL) during the recovery period and flagellates composed about 60 % of the community. In 1996, more than 80 % of the post-bloom phytoplankton was composed of flagellates. At this time the lowest flagellate abundance at 50 m was 300 cells/mL and the highest abundance (1,014 cells/mL) was at the surface. Day to day variations at all depths were slight. In June of 1996, abundance increased but flagellates composed an average of 53 % of the phytoplankton over 50 m. Flagellate abundance over the upper 50 m ranged from 494-1,689 cells/mL.

3.3.2.2 Diatom species and genera

In both years, centric diatoms were the most common phytoplankton during the bloom at all depths, but interannual differences in abundance were large. In 1995 and 1996, *Chaetoceros* spp., *Skeletonema costatum*, *Thalassiosira* spp., and *Leptocylinndrus* spp. were most abundant throughout the upper 50 m (Figures 8 and 9). Species composition remained the same with depth but diatom abundance decreased with depth below 10 m. In 1995, total diatom abundance ranged from a low of 813 cells/mL at 50 m on day 109 to a maximum of 3,110 cells/mL at 10 m on day 113. *Skeletonema costatum* and *Thalassiosira* spp. averaged over 37 % and 30 %, respectively, of the total diatom abundance during the bloom at all depths (Figure 10). *Chaetoceros* spp. was always present at all depths and constituted between 5-31 % of the total diatoms. *Leptocylinndrus* spp. appeared inconsistently, composing only a small portion of the bloom. In 1996, the same species and genera reappeared but the smaller diatoms tripled in abundance while the larger species declined (Figure 9). *Skeletonema costatum* represented greater than 72 % of the total diatom abundance throughout the water column ranging from 1,150-12,072 cells/mL (Figure 11). *Chaetoceros* spp. increased at all depths and reached a maximum of 2,311 cells/mL at the surface on day 102. In this year the abundance of *Thalassiosira* spp. and *Leptocylinndrus* spp. was lower than in 1995. These genera composed < 9 % and < 2 % , respectively, of the diatom population. For both years, other diatoms, in order of abundance, that were ≤ 5 % of the total diatom numbers were *Fragilariopsis* spp. , *Asterionella glacialis*, *Navicula* spp., *Eucampia* spp., *Stephanopyxis nipponica* and *Rhizosolenia stolterforthii* (Appendices 1 and 2).

During the post-bloom, diatom abundance was lower in both 1995 and 1996 (Figures 8 and 9). In 1995, less than 100 cells/mL existed at all depths in mid May. Only small variations in cell abundance occurred with depth. The small diatoms, *Pseudo* -

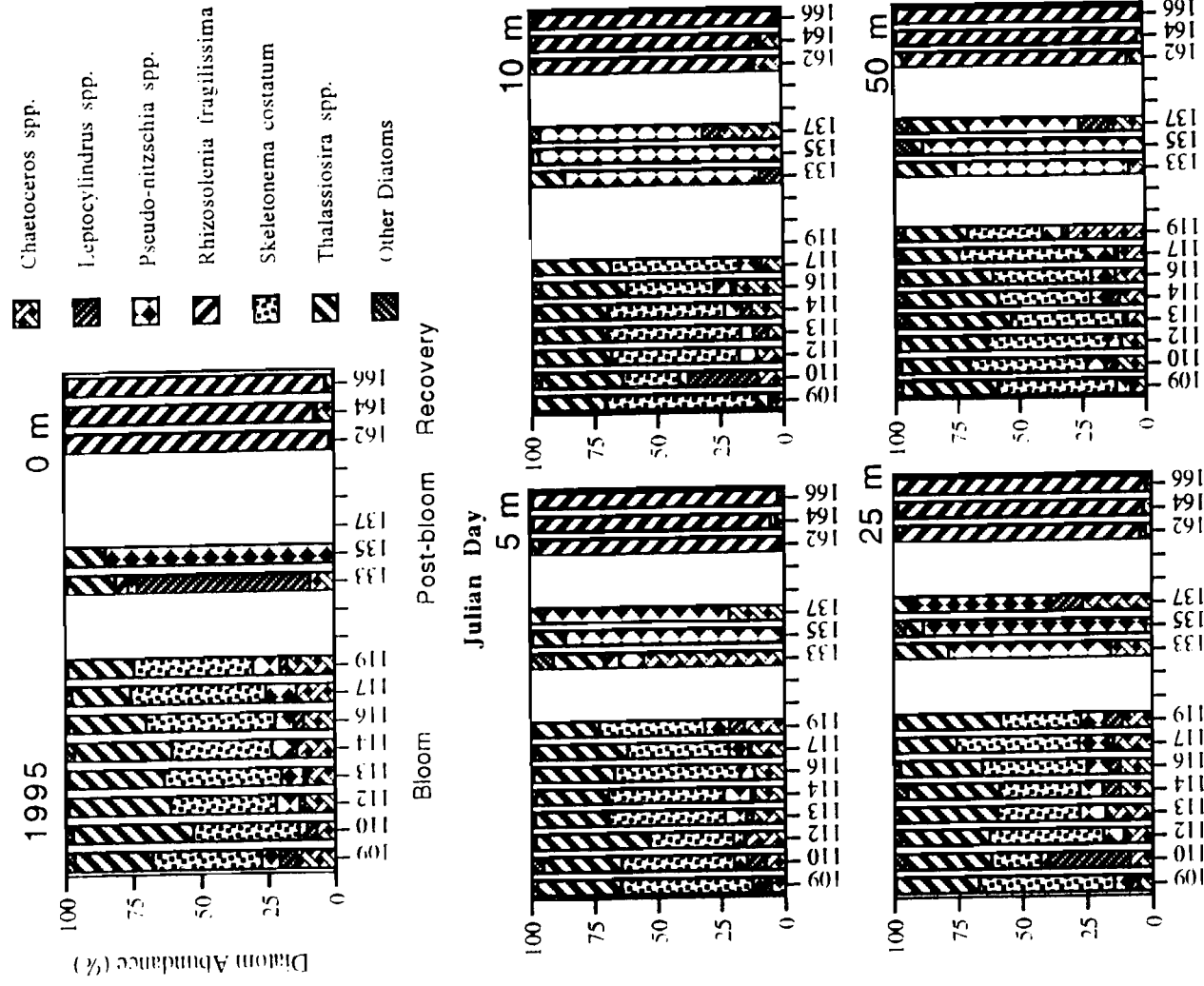


Figure 10. Diatom species composition (% total diatoms) from five depths in the upper 50 m from spring 1995.

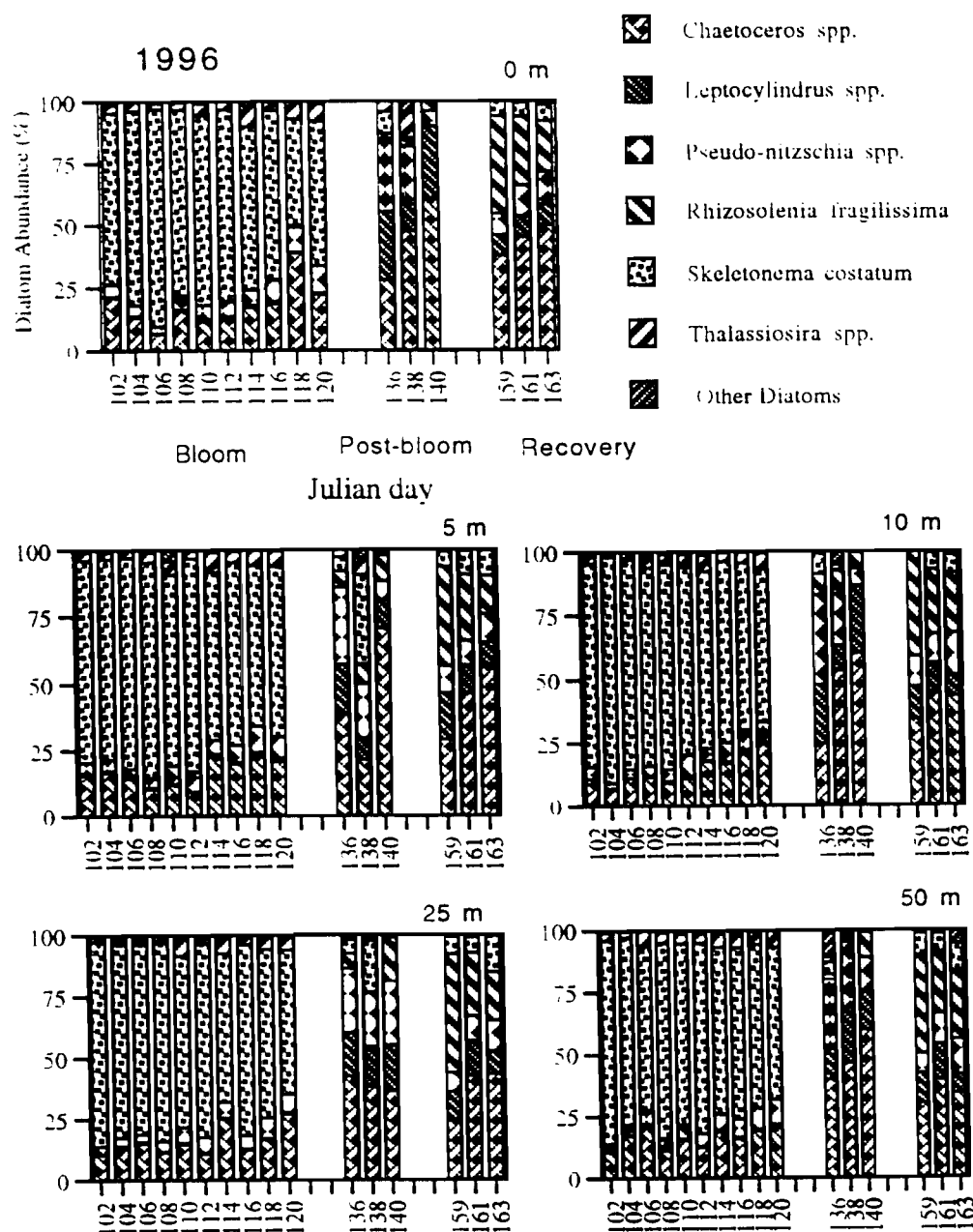


Figure 11. Diatom species composition (% total diatoms) from five depths in the upper 50 m from spring 1996.

nitzschia spp. and *Chaetoceros* spp., dominated the community and the proportion of *Thalassiosira* spp. decreased (Figure 10). In the 1996 post-bloom period, less than 150 cells/mL were observed and lowest abundance was at 50 m. *Chaetoceros* spp. numerically dominated at all depths. *Pseudo-nitzschia* spp. and *Leptocylindrus* spp., present during the bloom in low abundance, were still present accounting for as much as 35 % of the diatom abundance (Figure 11). *Skeletonema costatum* abundance declined and was zero at several depths around day 138. *Rhizosolenia fragilissima*, not present during the bloom, first appeared in low abundance at this time in 1996 but not 1995.

In June, the diatom abundance recovered slightly and a shift in species composition occurred (Figures 8 and 9). In 1995, total diatom abundance increased to about 30 % of the bloom abundance. This phytoplankton community was composed almost entirely of *Rhizosolenia fragilissima* at all depths (Figure 10). *Chaetoceros* spp. was the second most abundant diatom with <10 % of the abundance. *Skeletonema costatum* was absent at this time. In June of 1996, diatoms resurged during the post-bloom period with abundances ranging from 560 cells/mL at 50 m to 1,088 cells/mL at 5 m (Figure 9). *Rhizosolenia fragilissima* returned in 1996, constituting 25-48 % of the diatom community, and was co-dominant with *Chaetoceros* spp. (Figure 11). *Pseudo-nitzschia* spp. and *Leptocylindrus* spp. were the third most abundant diatoms. *Skeletonema costatum* was present but averaged only 6 % of the abundance in the upper 50 m.

3.3.3 Integrated abundance

Abundances of phytoplankton were integrated with depth to calculate what potential food was available to herbivores in the upper water column during the spring bloom. Values were integrated for the upper 50 m because the majority of phytoplankton existed in this region.

The spring bloom in the upper 50 m was composed of the same flagellates and diatom species each year, but 1996 had a greater abundance of diatoms (Figures 12 and 13). In 1995, flagellates were approximately 50 % of the integrated phytoplankton abundance with a mean abundance of 5.6×10^{10} (cells/m²) during April. Diatoms composed the remainder of the phytoplankton. Total cell abundance fluctuated only slightly from day to day. Of the diatoms in 1995, *Skeletonema costatum* had the highest abundance, ranging from 28-52 % of the total diatom abundance. It averaged 2.8×10^{10} (cells/m²). *Thalassiosira* spp. was the second most abundant, averaging 33 % of the integrated abundance. *Chaetoceros* spp., *Leptocylindrus* spp. and *Pseudo-nitzschia* spp. composed between 6-13 %, 0.5-22 % and 4-9 %, respectively, of total diatom abundance. In 1996, diatom abundance increased by two- to three-fold, while flagellates remained about the same, and total cell abundance varied greatly throughout the bloom. *Skeletonema costatum* dominated the diatom component with a mean of 2.3×10^{11} (cells/m²) over the 10 sampling days in April, constituting > 60 % of the diatom abundance. *Chaetoceros* spp. had a higher percentage of the abundance (11-24 %) in 1996 than 1995 and greater than four times as many cells. *Thalassiosira* spp. composed only 4.2 % of abundance with a mean of 1.2×10^{10} (cells/m²). This was 45 % lower than the 1995 spring bloom abundance. *Pseudo-nitzschia* spp. increased but remained between 4-9 % in 1996.

During the post-bloom, a low abundance of flagellates dominated and interannual differences were small (Figures 12 and 13). Flagellate abundance ranged from 2.3 - 3.1×10^{10} (cells/m²) for both years. They constituted over 92 % of the total abundance. In 1995, of the few diatoms remaining, *Pseudo-nitzschia* spp. was dominant. *Chaetoceros* spp., and *Thalassiosira* spp. were also present in small numbers. In 1996, *Chaetoceros* spp. was dominant and *Pseudo-nitzschia* spp. and *Leptocylindrus* spp. made up the majority of the remaining 55 % of the diatom community.

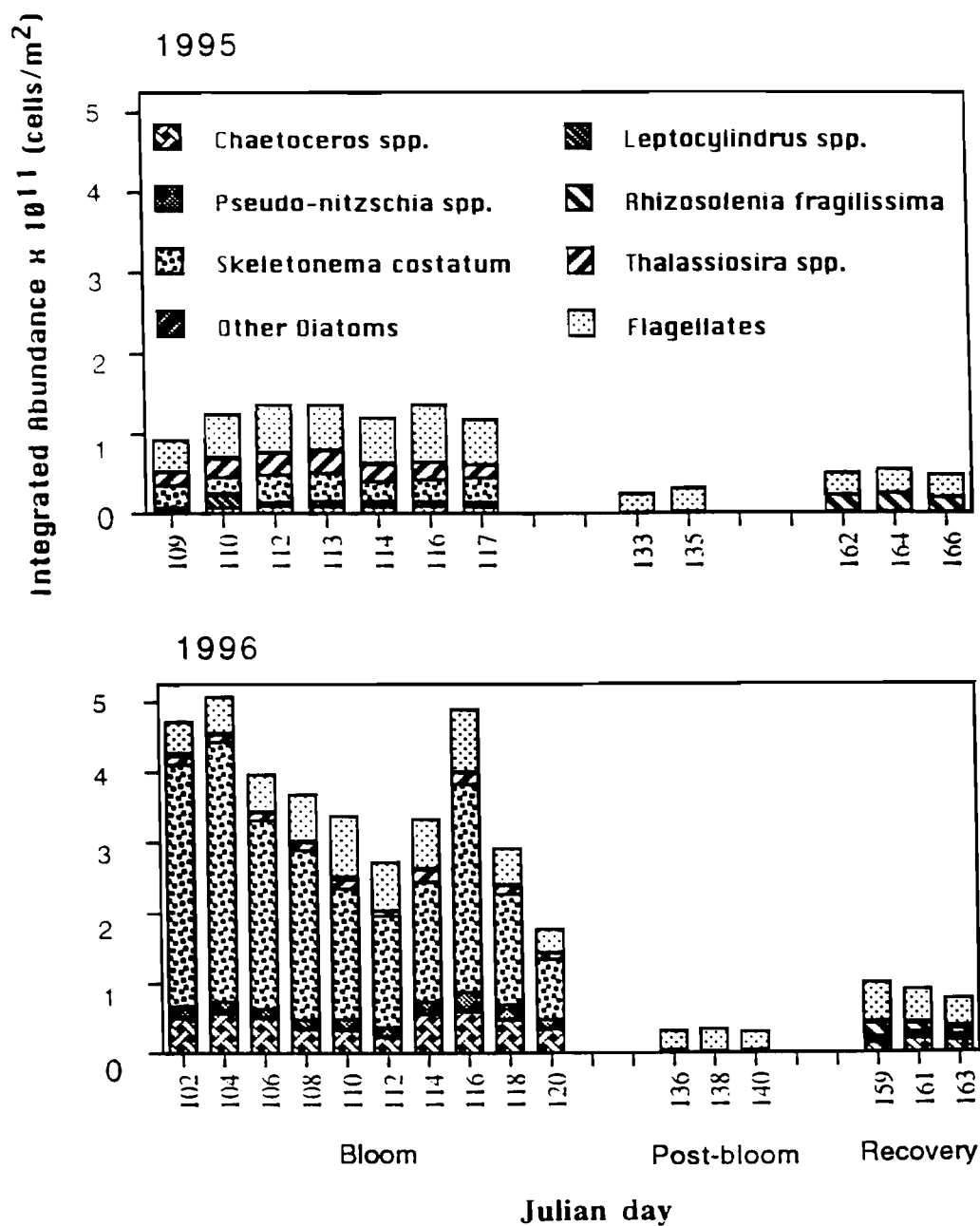


Figure 12. Diatom and flagellate abundance integrated over the upper 50 m from spring 1995 and 1996.

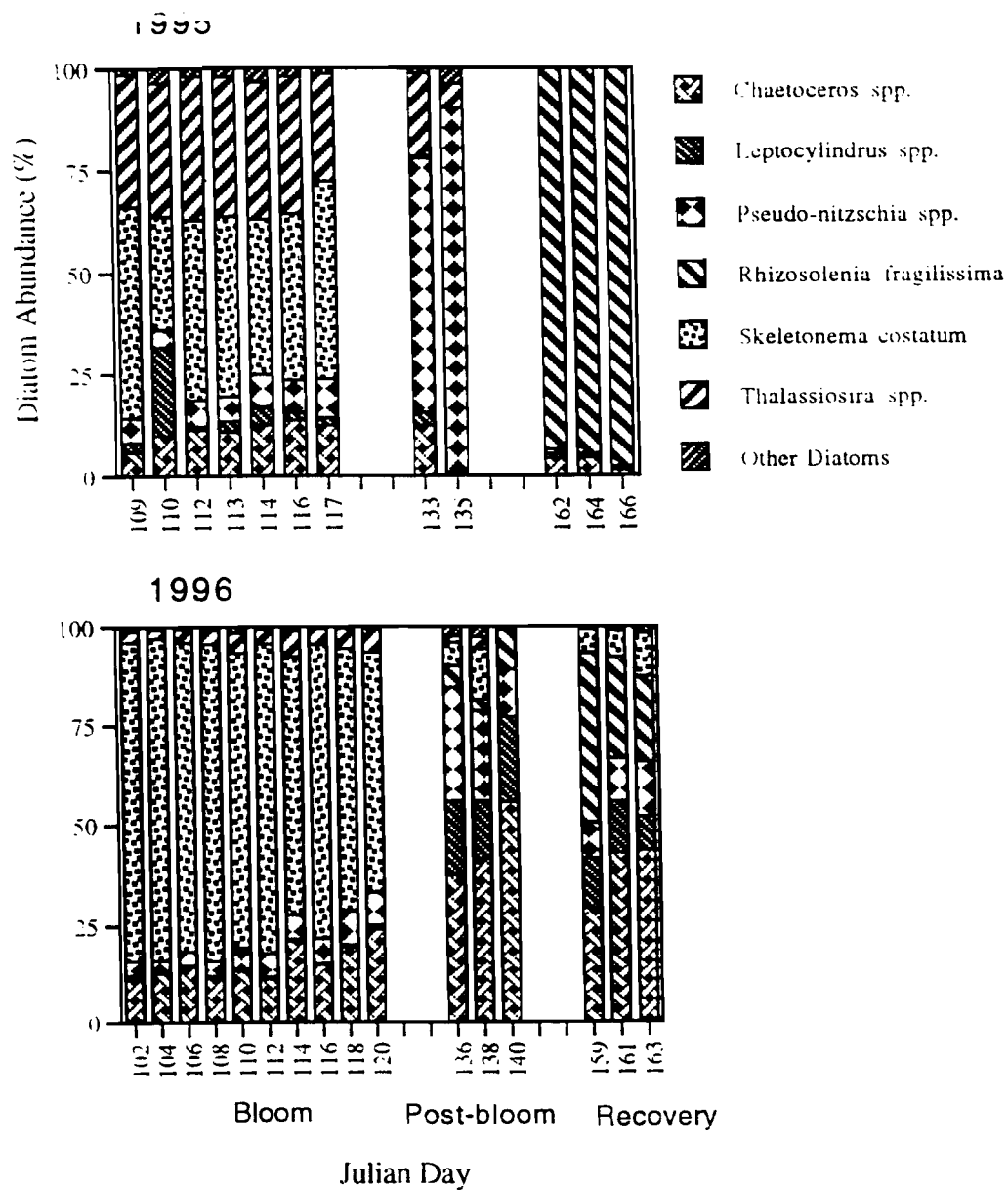


Figure 13. Diatom species composition (% total diatoms integrated over 50 m) from spring 1995 and 1996.

During the recovery period of both years diatom abundance increased, flagellates remained a large constituent, and a succession in the diatom community occurred (Figures 12 and 13). In 1995, flagellate abundance equaled post-bloom levels. Diatoms increased and a previously unseen species, *Rhizosolenia fragilissima*, was the major constituent with > 93 % of the abundance and a mean of 2.1×10^{10} (cells/m²). In 1996, diatoms and flagellates also increased but the diatom community had greater diversity. *Rhizosolenia fragilissima* averaged only 30 % of the abundance. The other major diatoms were *Chaetoceros* spp. (38.5 %), *Leptocylindrus* spp. (17 %), *Pseudo-nitzschia* spp. (11 %) and *Skeletonema costatum* (7.8 %).

3.4 Carbon Content

Carbon biomass was calculated from cell volume to get a perspective on the phytoplankton standing stock in terms of available organic carbon (Table 3). Abundance studies alone can misrepresent the available plant resources in terms of trophic interactions and energy transfer. There is the potential to overemphasize large numbers of small cells that, due to their small cell volume and equivalent small carbon biomass, contribute minimally to the available pool of energy. In this study only the most abundant species or genera were converted into carbon. Carbon biomass was calculated only for the dominant species of diatoms and flagellates, determined from the abundance measurements. Carbon estimates were calculated from cell volume and converted into mg carbon/m³. The same dominant phytoplankton were present in 1995 and 1996.

3.4.1 Carbon biomass by time and depth

Estimated carbon biomass was highest during the spring bloom, had approximately the same proportion of diatoms and flagellates throughout the water column, and had great interannual variability compared to later in the season (Figures 14 and 15). In both years, species composition remained the same with depth but biomass

Table 3. Cell shape, volume equations, measurements, cell volumes and cell carbon estimates for major phytoplankton taxa.

Phytoplankton taxa	Cell Shape	Volume Equation	Mean Diameter (µm) A	Mean Height (µm) (B or C)	Thickness Equation	Thickness (µm) (B or C)	Cell Volume (µm ³)	Carbon (pg/cell)
<i>Chaetoceros</i> <25 µm	flattened cylinder	$V = BC(A \cdot B + \pi/4(B))$	4.60	9.90	$B = 2/3A$	3.08	120.21	14.28
<i>Chaetoceros</i> 25-44 µm	flattened cylinder	$V = BC(A \cdot B + \pi/4(B))$	10.25	25.25	$B = 2/3A$	6.83	1514.90	97.44
<i>Chaetoceros</i> deciprens	flattened cylinder	$V = BC(A \cdot B + \pi/4(B))$	24.65	19.90	$B = 2/3A$	13.27	5576.71	261.67
<i>Fragilariopsis</i> spp. <25 µm	rectangular box	$V = BC(A \cdot B + \pi/4(B))$	14.25	2.43	$B = 2C$	4.86	112.80	13.60
<i>Leptocylindrus damicus</i>	rectangular box	$V = ABC$	47.35	11.50	$C = 1/2B$	5.75	3131.02	168.94
<i>Leptocylindrus minimus</i>	rectangular box	$V = ABC$	26.75	2.75	$C = 1/2B$	1.38	101.15	12.52
<i>Pseudo-nitzschia</i> 25-44 µm	ellipsoid	$V = \pi/6 (ABC)$	33.90	2.15	$C = 1/2B$	1.07	41.36	6.36
<i>Pseudo-nitzschia</i> ≥45 µm	ellipsoid	$V = \pi/6 (ABC)$	52.30	2.50	$C = 1/2B$	1.25	85.60	11.04
<i>Rhizosolenia fragilissima</i>	right circular cylinder	$V = \pi/4 (A \cdot B)$	22.40	5.00			1970.41	118.93
<i>Skeletonema costatum</i>	right circular cylinder	$V = \pi/4 (A \cdot B)$	12.88	4.15			540.72	44.63
<i>Thalassiosira</i> <25 µm	right circular cylinder	$V = \pi/4 (A \cdot B)$	18.88	10.35			2897.57	159.30
<i>Thalassiosira</i> 25-44 µm	right circular cylinder	$V = \pi/4 (A \cdot B)$	29.25	10.50			7055.55	312.74
<i>Thalassiosira</i> ≥45 µm	right circular cylinder	$V = \pi/4 (A \cdot B)$	48.83	14.90			27902.92	886.75
Unidentified flagellates <10 µm sphere		$V = \pi/6 (A^3)$	5.75				99.54	18.63
Unidentified flagellates ≥ 10 µm sphere		$V = \pi/6 (A^3)$	13.44				1269.70	168.97

Note: Mean diameter and height were calculated from measurements of 20 cells.

Shapes and equations were modified versions from the work of Koval and Larrance (1966).

Carbon was calculated from two equations (Strathmann, 1967) :

Diatoms : $\log C = -0.422 + 0.758 (\log V)$

Other phytoplankton: $\log C = -0.460 + 0.866 (\log V)$

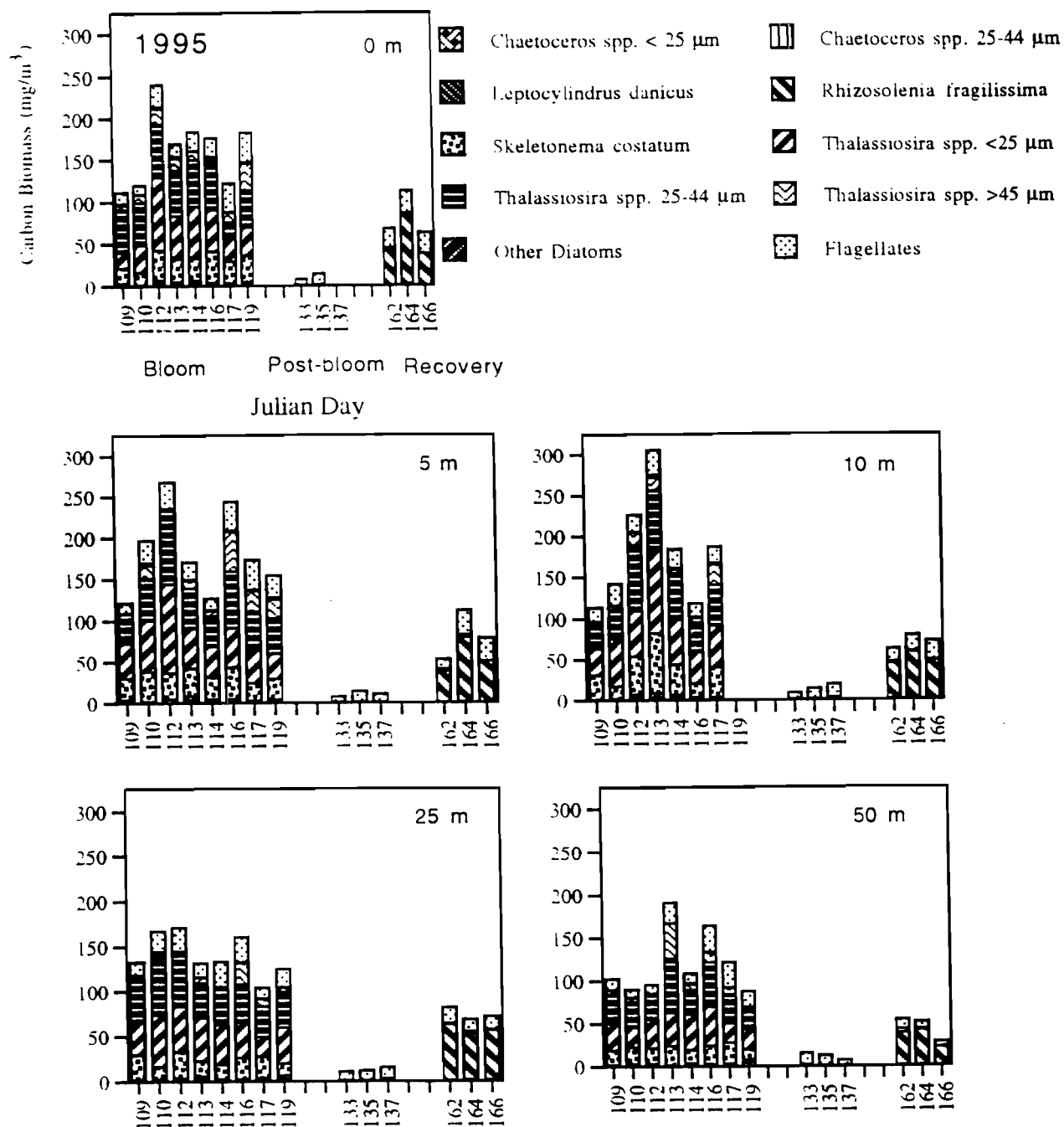


Figure 14. Estimated carbon for major diatoms and flagellates from five depths in the upper 50 m from spring 1995.

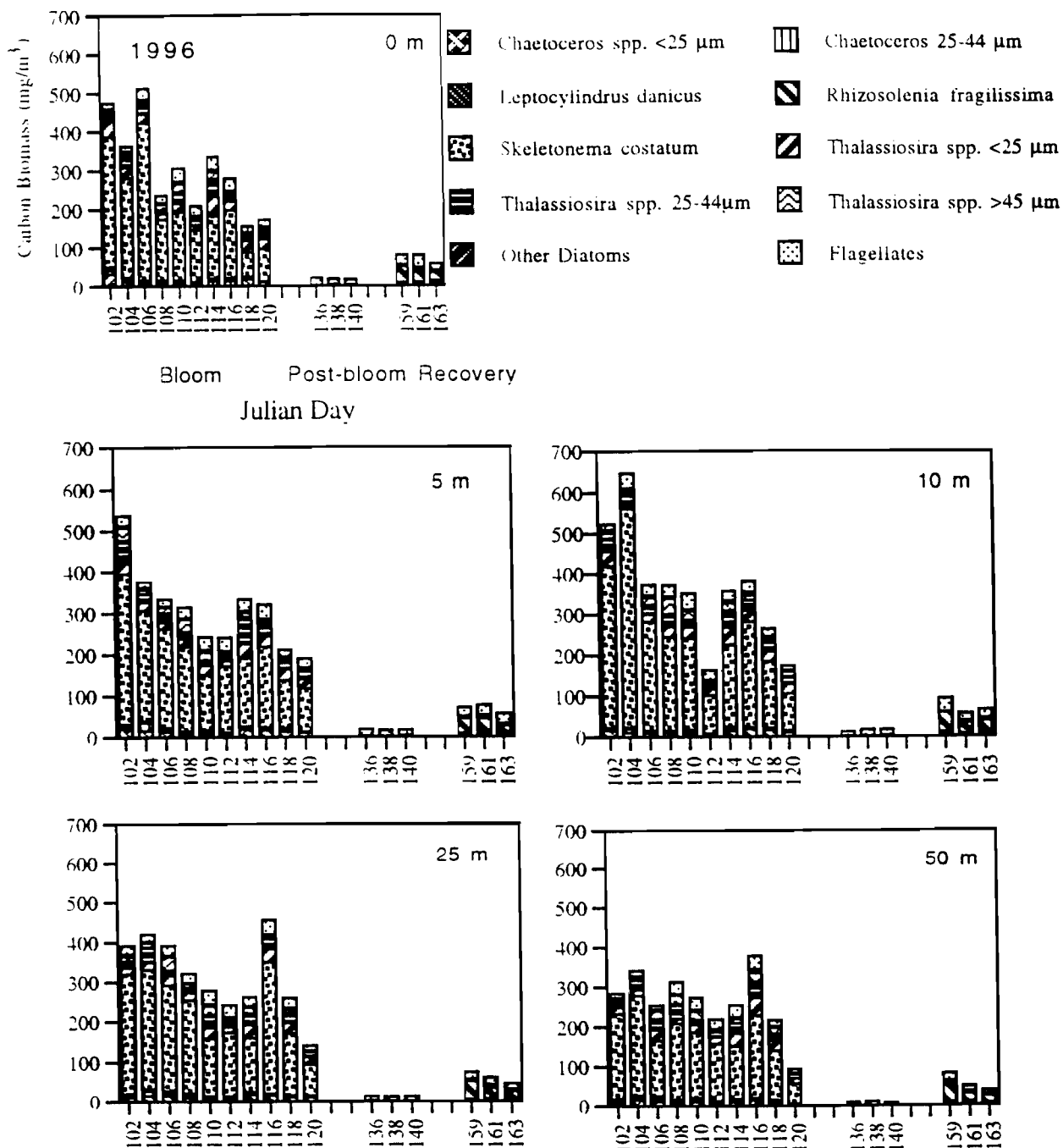


Figure 15. Estimated carbon for major diatoms and flagellates from five depths in the upper 50 m from spring 1996.

decreased below 10 m. In 1995, total autotrophic carbon ranged from 88 mg/m³ at 50 m to 306 mg/m³ at 10 m. At all depths the major constituent of the carbon was *Thalassiosira* spp. from the smallest (<25 µm) and middle (25-44 µm) size classes. *Skeletonema costatum* was the second dominant diatom and averaged 17-23 % of the total diatom carbon biomass over all depths. Flagellate carbon was present in small amounts at all depths throughout the bloom in 1995, with a mean ranging from 18 mg/m³ at 50 m to 25 mg/m³ at 10 m. In 1996, the same species constituted the bulk of the carbon at all depths, but *Skeletonema costatum* biomass increased and *Thalassiosira* spp. decreased. The total autotrophic carbon increased from 94 mg/m³ on day 120 at 50 m to 647 mg/m³ at 10 m on day 104. In 1996, the contribution by all three size classes of *Thalassiosira* spp. approximately equaled the contribution of *Skeletonema costatum* from the previous year. In contrast, in 1996, *Skeletonema costatum* averaged 68-73 % of the total diatom carbon over the upper 50 m. Chaetoceros spp. <25 µm had a greater biomass in 1996 but only accounted for < 7 % of the total diatom carbon. Flagellate carbon was present at all depths in the same proportions as 1995; the mean ranged from 21-24 mg/m³.

In the post-bloom of each year, carbon was low throughout the water column when flagellates composed the majority of the biomass (Figures 14 and 15). In 1995, flagellate carbon ranged from 6-16 mg/m³ and showed no decrease with depth except on day 137. Diatom carbon constituted < 15 % of the total. Small *Thalassiosira* spp. were the main constituent of this biomass. In 1996, flagellate carbon ranged from 6-19 mg/m³. Diatom carbon was < 23 % of total carbon and was composed of a small proportion of several genera (see Section 3.4.2).

In the recovery period, diatom carbon increased at all depths and a late season bloomer, *Rhizosolenia fragilissima*, composed the majority of the biomass (Figures 14 and 15). Flagellate biomass remained unchanged throughout this period. In 1995, total

carbon recovered to reach highs of 112 mg/m^3 at both the surface and 5 m on day 164. About 75 % of this carbon originated from diatoms other than *Skeletonema costatum*. At all depths, >94 % of the total mean carbon was from *Rhizosolenia fragilissima*. Flagellate carbon decreased with depth and averaged $< 25 \text{ mg/m}^3$ during June. In 1996, total carbon ranged from $38\text{--}93 \text{ mg/m}^3$, but the biomass did not have a two-fold difference from 1995, as seen in the bloom period. On a daily basis, total biomass was often lower in 1996 than 1995 during this period. *Rhizosolenia fragilissima* accounted for 60-70 % of the diatom carbon throughout the 50 m layer. The other major contributors to the diatom carbon biomass were *Chaetoceros* spp., *Leptocylindrus danicus* and *Skeletonema costatum*. Flagellate carbon increased from low levels in the post-bloom period and remained below 33 mg/m^3 .

3.4.2 Integrated carbon

The phytoplankton, in terms of carbon potentially available to zooplankton in the upper water column, were integrated for the upper 50 m (Figure 16). During the bloom integrated carbon throughout the water column was highest in both years, but the 1996 values were two to three times those of 1995. Each year the same genera were responsible for this biomass but there were differences in dominance between years. In 1995, total carbon varied $< 30 \%$ between days 109-117. On day 113 (23 Apr) the highest carbon occurred ($9,400 \text{ mgC/m}^2$). The mean was $7,600 \text{ mgC/m}^2$. During the bloom, diatoms were 84-88 % of the total carbon. *Thalassiosira* spp., from three size classes, made up 73-80 % of the diatom carbon (Figure 17). *Skeletonema costatum* had the second largest biomass, comprising 14-24 % of the diatom biomass. *Chaetoceros* spp. and *Leptocylindrus* spp. composed less than 2 % and 3.8 %, respectively, of the carbon. *Pseudo-nitzschia* spp., due to small cell volume ($41 \text{ } \mu\text{m}^3$), constituted only 0.30-0.82 % of the diatom carbon. Flagellates averaged only 7.5 % of the total carbon during the bloom. In 1996, the mean carbon biomass ($15,500 \text{ mgC/m}^2$) was approximately twice

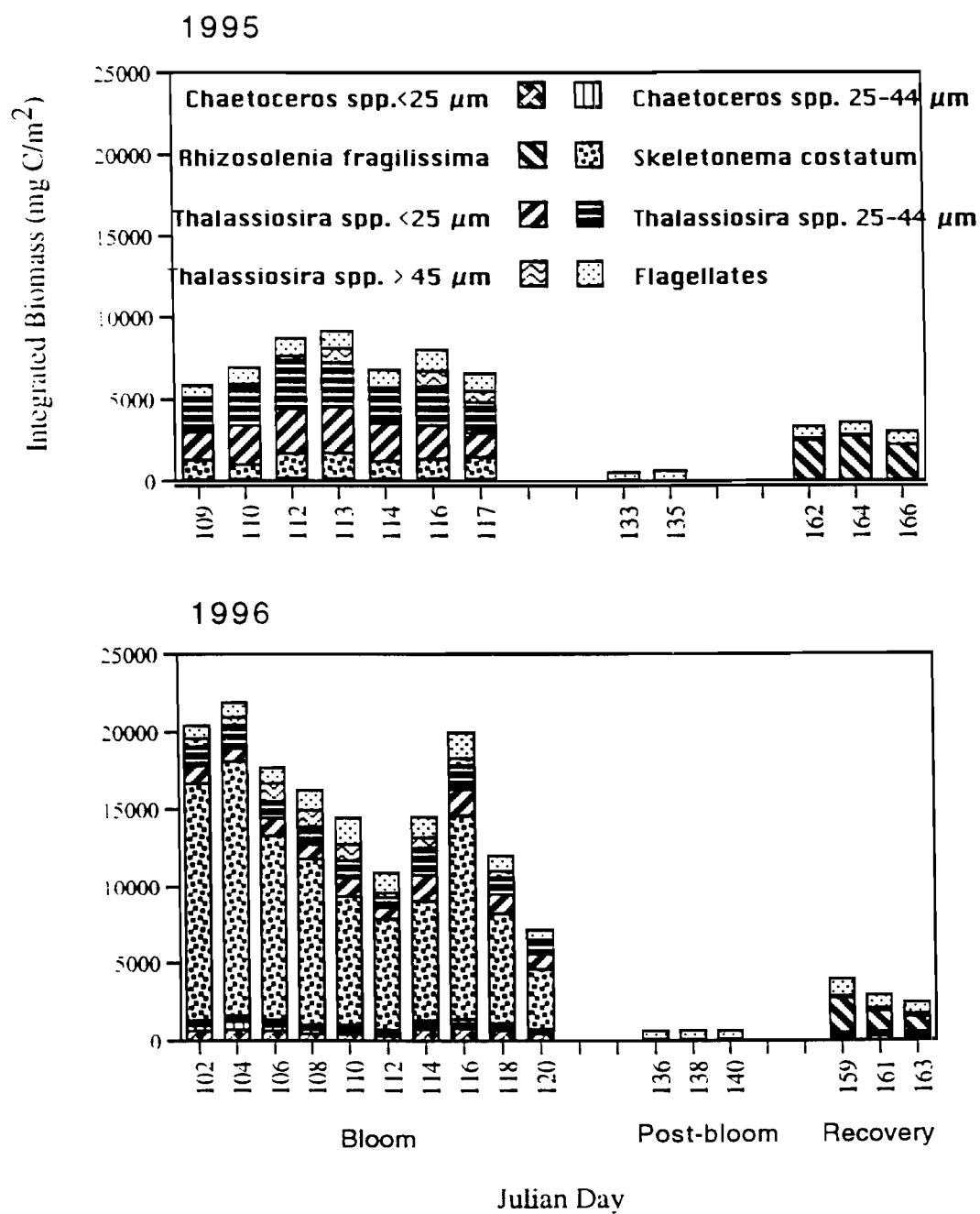


Figure 16. Estimated carbon for diatoms and flagellates integrated over the upper 50 m from spring 1995 and 1996.

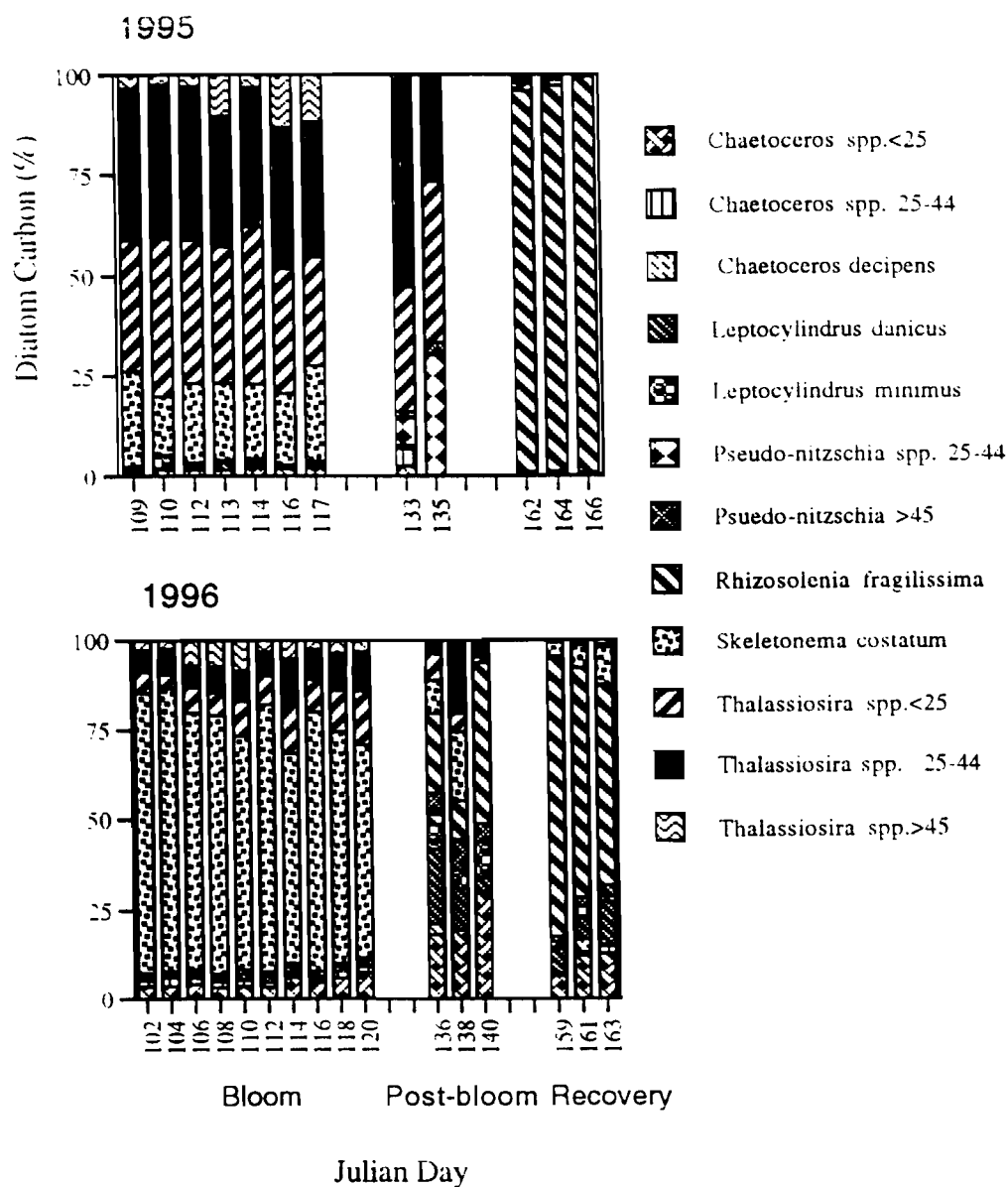


Figure 17. Estimated carbon (% total diatom carbon integrated over 50 m) of major diatoms from spring 1995 and 1996.

as large as 1995 and the peak biomass was 22,000 mgC/m². Diatoms were 88-96 % of the total autotrophic biomass. *Skeletonema costatum*, not *Thalassiosira* spp., was the primary constituent in 1996; it contributed 58-78 % of diatom carbon, while *Thalassiosira* spp., on average, constituted only 22 %. *Chaetoceros* spp., dominated by the small cells < 25 µm, had less than 9 % of the diatom carbon. *Pseudo-nitzschia* spp. constituted only 0.8-2 % of the diatom carbon. Flagellates averaged 13.8 % of the total autotrophic carbon during the bloom.

During the post-bloom, carbon fell to its lowest levels. Flagellate carbon dominated and only a few taxa contributed to the small amount of diatom carbon (Figure 16). In 1995, the mean biomass was 600 mgC/m². Diatom carbon consisted of < 8 % of the total. This biomass was almost all from *Thalassiosira* spp. (66-84 %), *Pseudo-nitzschia* spp. (7-30 %) and *Chaetoceros* spp. (0-7 %). *Rhizosolenia fragilissima* did not appear at this time in 1995. In 1996, the mean post-bloom phytoplankton biomass, 700 mgC/m², was slightly higher than 1995. Again most of the carbon originated from flagellates and < 18 % was from diatoms. *Chaetoceros* spp. (<25µm), *Leptocylindrus* spp., *Rhizosolenia fragilissima*, *Skeletonema costatum* and *Thalassiosira* spp., in nearly equal proportions, were the main constituents. *Pseudo-nitzschia* made up <9 % of the diatom biomass.

During the recovery period the diatom carbon increased and a shift in the community composition occurred (Figure 17). Diatoms recovered and composed greater than 50 % of the biomass. In contrast to the spring bloom period, the recovery period in 1995 had a greater biomass than 1996. In 1995, the mean total biomass was 3,300 mgC/m² and daily fluctuations were small (Figure 16). A shift in species composition from *Thalassiosira* spp. and *Skeletonema costatum* to *Rhizosolenia fragilissima* occurred late in the bloom. *Rhizosolenia fragilissima* averaged 96.5 %, of the diatom carbon; on day 164, it reached 2,700 mgC/m². *Thalassiosira* spp., *Chaetoceros* spp. and

Leptocylindrus danicus amounted to less than 140 mgC/m² during the recovery.

Skeletonema costatum was not present at this time in 1995. In 1996, the mean total, 3,100 mgC/m², was lower than 1995 and was only composed of 70 % diatoms.

Rhizosolenia fragilissima, after first appearing in the post-bloom, averaged 66 % of the diatom carbon in the recovery period. The remaining carbon was comprised primarily of *Chaetoceros* spp., *Leptocylindrus* spp., *Skeletonema costatum*, *Pseudo-nitzschia* spp., *Thalassiosira* spp. and *Fragilariopsis* spp.

3.5 Community Interactions

3.5.1 Physics, nutrients and chlorophyll relationships

Daily inorganic nutrient concentrations were compared with chlorophyll *a* concentrations and physical data to determine how the phytoplankton interacted within the marine environment of southwest Prince William Sound (Figure 18). Chlorophyll *a* concentrations from all days and depths were compared with corresponding nutrient concentrations for 1995 and 1996. Scatter diagrams show negative or no correlation between chlorophyll concentrations and nutrients in both years. In 1995, chlorophyll *a* vs N+N and silicate had a weak negative correlation. Chlorophyll *a* vs phosphate showed no relationship ($r=0.03$). In 1996, stronger negative relationships between all nutrients and chlorophyll existed.

During the spring bloom when chlorophyll profiles were compared to nutrient profiles similarities were apparent (Figures 4 and 5). In 1995, high patches of chlorophyll, for example around day 111, corresponded to low nutrient patches ranging from 5-7 μ M of N+N and 8-12 μ M of silicate in the upper 10 m. Nutrient decline was most evident above 50 m and fell to between 0.15-3 μ M N+N and 1-5 μ M silicate at 5 m and above after days 121-126. In 1996, N+N, silicate and phosphate concentrations decreased at the same time and depth as chlorophyll increased. Nutrients remained high

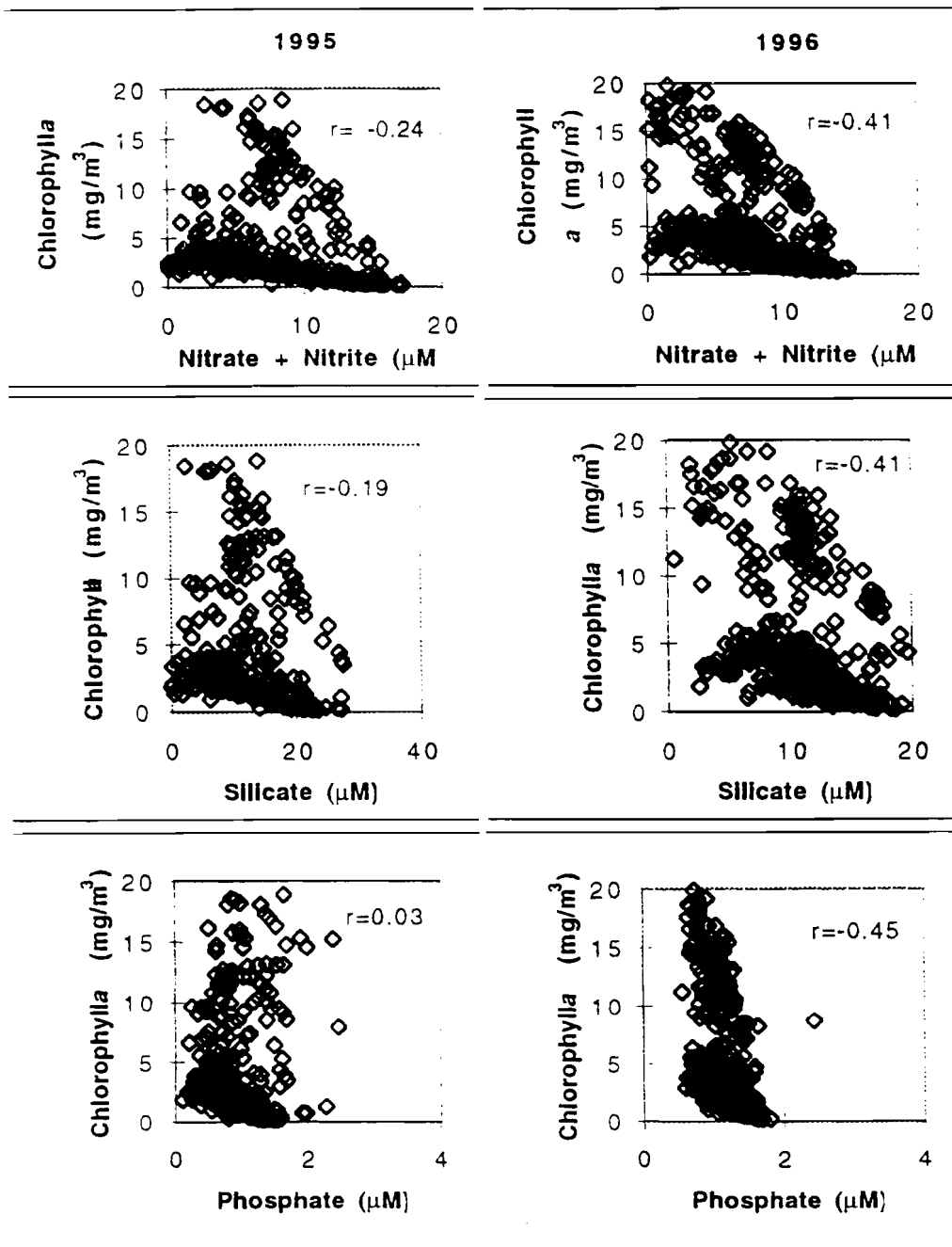


Figure 18. Chlorophyll *a* (mg/m³) vs. nutrient (μM) concentration from spring 1995 and 1996.

throughout the upper 75 m until day 100. As chlorophyll increased to 15-20 mg/m³ in the upper 25 m after day 101, nutrient concentrations decreased to close to zero at the surface. After day 104, chlorophyll levels remained between 10-15 mg/m³ and N+N, silicate and phosphate remained between 5-9 µM, 8-15 µM and 1-1.25 µM, respectively, throughout most of the water column. As the chlorophyll biomass increased again around day 114, nutrients decreased showing highest values only below 50 m.

During the post-bloom and recovery periods, thermal stratification started to occur and chlorophyll decreased. A negative correlation existed between temperature and chlorophyll ($r = -0.494$ in 1995 and $r = -0.565$ in 1996). After day 128 in 1995 and 1996, chlorophyll declined to its lowest levels and was vertically uniform throughout the post-bloom. Nutrients remained low in surface waters but increased with depth as standing stock diminished. In 1995, accompanied by strong stratification, chlorophyll rebounded in the upper 25 m during the recovery period to values between 1-7 mg/m³. At the same time, nutrient concentrations fell again to near depletion in the upper 5 m. In 1996, chlorophyll increased between 2-7 mg/m³ in the upper few meters after day 146 of the recovery. As in 1995, the phytoplankton biomass rebounded as N+N, silicate and phosphate levels (µM) were reduced to 0.15-3, 1-10 and 0.5-1 µM, respectively, in the upper 10 m.

3.5.2 Chlorophyll and carbon relationships

Carbon to chlorophyll ratios and chlorophyll per cell were calculated to assess physiological condition of the phytoplankton community (Table 4 and 5). High carbon/chlorophyll ratios (e.g. 60) and low chlorophyll/cell ratios (e.g. 0.1 pg/cell) often indicate nutrient limitation (Darley 1982). Carbon was not estimated for phytoplankton < 2 µm and numerically minor constituents.

Table 4. Mean, range, standard deviation and number of observations of chlorophyll *a* (pg/cell) in the upper 50 m from spring 1995 and 1996.

Period	<u>1995</u>				<u>1996</u>			
	Mean	Range	SD	n	Mean	Range	SD	n
Bloom	5.3	2.6-10.3	1.7	39	2.0	1.0-3.5	0.5	50
Post-bloom	2.6	1.1-3.1	0.5	14	1.6	0.9-2.2	0.3	15
Recovery	3.0	2.7-3.8	0.4	15	2.4	1.5-3.5	0.6	15

Table 5. Mean, range, standard deviation and number of observations of estimated carbon/chlorophyll *a* (mg/mg) in the upper 50 m from spring 1995 and 1996.

Period	<u>1995</u>				<u>1996</u>			
	Mean	Range	SD	n	Mean	Range	SD	n
Bloom	12	8-20	3	39	22	11-43	6	50
Post-bloom	15	6-20	3	14	14	10-20	3	15
Recovery	21	16-27	3	15	15	9-22	4	15

Relationships between calculated autotrophic and chlorophyll *a* of the same day and depth showed strong associations (Figure 19). Diatom carbon in 1995 and 1996 was positively correlated with chlorophyll concentrations ($r = 0.86$ in 1995, $r = 0.91$ in 1996). Flagellate carbon was not as significantly correlated with chlorophyll. The regression of carbon vs. chlorophyll *a* is statistically significant ($p = <0.0001$). A least squares regression of total phytoplankton carbon on chlorophyll *a* concentration can explain 75 % in 1995 and 83 % in 1996 of the variability in phytoplankton carbon. The slopes of the least squares line differ between years and show interannual variability between phytoplankton carbon and chlorophyll concentration, a reflection of species abundance and composition.

Carbon to chlorophyll ratios and chlorophyll per cell ratios had interannual variability (Tables 4 and 5). In 1995, chlorophyll *a* ranged from 1.1 to 10.3 pg/cell throughout the season. Highest chlorophyll/cell ratios occurred in the first few days of the spring bloom and lowest occurred during the post-bloom. Carbon/chlorophyll ranged from 6-27 throughout the sampling season in 1995. Ratios were low in the bloom and post-bloom periods and increased to between 16 and 27 during the recovery. In 1996, mean chlorophyll/cell ratios were lower. Ratios ranged from 0.9-3.5 pg/cell throughout all periods. Cell ratios remained approximately the same between the bloom and recovery. Lowest chlorophyll/cell ratios occurred during the post-bloom. In contrast to chlorophyll/cell ratios, carbon/chlorophyll ratios were higher in 1996. They ranged from 9-43 throughout the study period. The highest ratios occurred at the beginning of the bloom at all depths. Lower ratios, between 10 and 22, occurred in the post bloom and recovery periods.

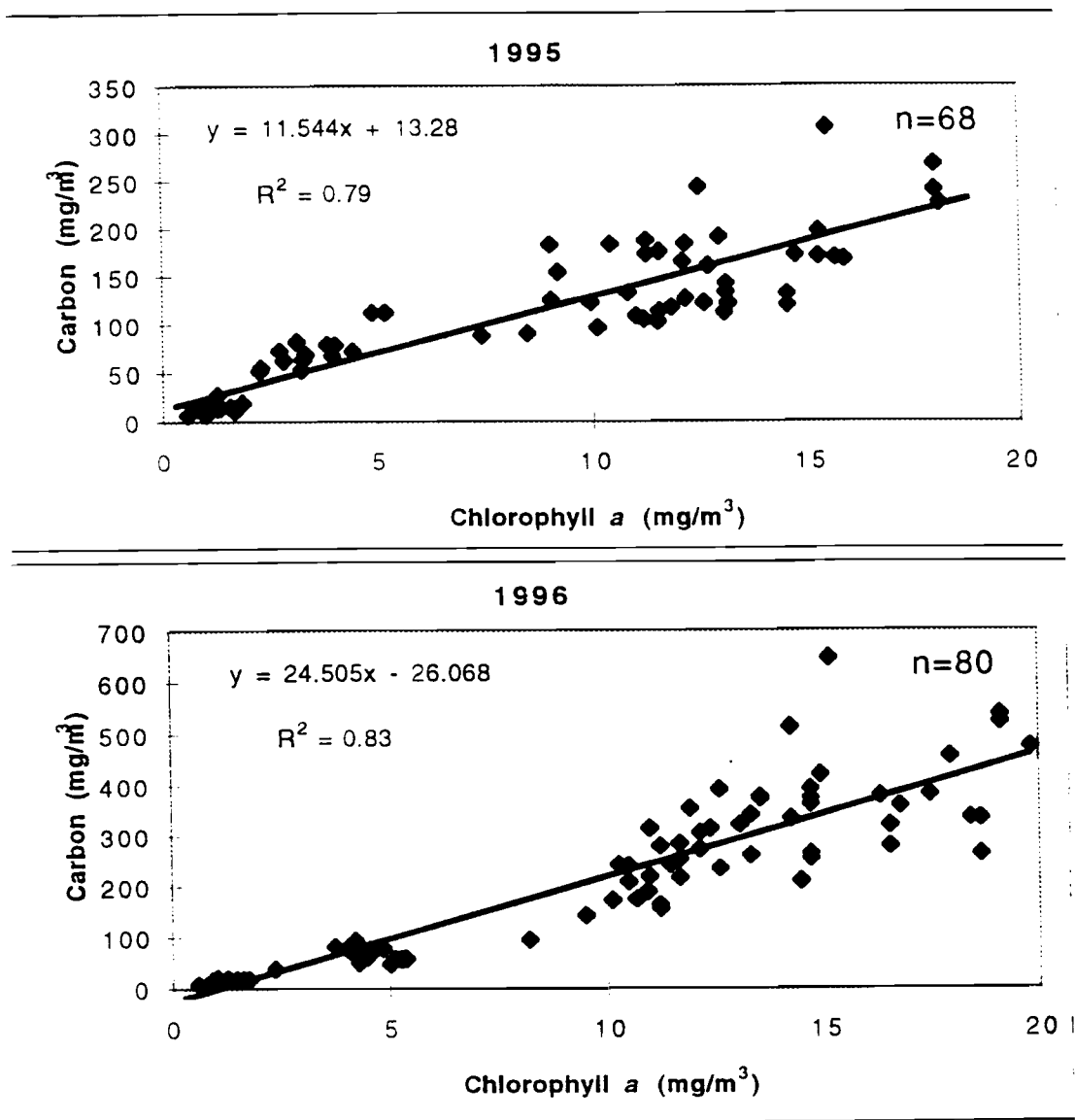


Figure 19. Estimated autotrophic carbon (mg/m^3) vs. chlorophyll a (mg/m^3) for the upper 50 m from spring 1995 and 1996.

DISCUSSION

1. Temporal Pattern of the Phytoplankton Bloom

In high latitudes, the timing of the spring bloom is due to a combination of atmospheric and oceanic events. It is believed that the timing of the bloom is a function of warming air temperatures, reduced wind stress, decreased deep mixing events, increased solar radiation, intensity and duration, and stratification of the water column (Lalli and Parsons 1993). The physical oceanographic conditions that can affect the timing of the bloom in Prince William Sound were originally described by Sverdrup (1953) for the Norwegian Sea. He theorized that in the spring in high latitudes, as solar heating increased and mixing decreased, the mixed layer depth rose above the critical depth and net photosynthesis exceeded net respiration throughout the water column, enabling the phytoplankton to bloom in nutrient-rich waters. In Prince William Sound, these physical events are coupled with local hydrography to initiate the bloom within a short window of time. Local features such as the narrow, shallow basin of Elrington Passage, high precipitation rates, the tidal cycle and terrestrial run-off can also affect the timing.

The timing of the spring bloom in southwest Prince William Sound reported here is similar to that found during other studies of Prince William Sound (Goering et al. 1973; McRoy et al. 1996; Eslinger 1997) and northern subarctic marine waters (VTN Consolidated, Inc. 1980; Goering and Iverson 1982; Ziemann et al. 1991) (Table 6). In 1995 and 1996, the phytoplankton bloom started in early to mid April, had peaked by late April and declined to low levels by the first week of May. A slight, secondary recovery of the bloom occurred in June. In accordance with this study, monthly research cruises in Prince William Sound in 1995 and 1996 recorded highest chlorophyll concentrations in

Table 6. Comparison of the timing of the spring bloom and chlorophyll concentrations at other regions in Prince William Sound and northern regions.

Location	Latitude (°N)	Timing of peak bloom (Julian day)	Max. chlor. conc. (mg/m ³)	Study period	Reference
Southwest PWS	60	107-123	2-19	Apr-June 1995	present study
Southwest PWS	60	97-126	2-20	Apr-June 1996	present study
Port Valdez, AK	61	75-135	0-10	May 1971 - Apr 1972	Goering et al. 1973
Central PWS	60.5	95-115	nd	Mar-July 1993	McRoy et al. 1996
Central PWS	60.5	95-130	nd	Mar-July 1994	McRoy et al. 1996
Central PWS	60.5	95-125	nd	Mar-July 1996	Eslinger 1997
Auke Bay, AK	58	90-120	1->50	Mar-June 1985-1989	Ziemann et al. 1991
Auke Bay, AK	58	91-120	nd	Mar-June 1968	Schell 1971
Boca de Quadra, AK	55	86-89	1-53	Mar-July 1980	VTN Consolidated Inc. 1980
Bering Sea	57	118-132	nd	Mar-June 1981	Goering & Iverson 1982
Bering Sea ice edge	58	116-133	0-35	Apr-May 1988	Niebauer et al. 1995
Gulf of Alaska Station P	50	122-244	0.20-0.50	Jan-Dec 1959-1970	Sambrotto & Lorenzen 1986

April (McRoy et al. 1996; McRoy et al. 1997). The C-LAB (Communications-Linked Automated Buoy), a moored buoy equipped with a fluorometer, stationed in the central region of Prince William Sound east of Naked Island, was deployed in 1991 to collect continuous biological and physical oceanographic data. The fluorescence data from C-LAB support these results: highest chlorophyll occurred between days 95-125 for years 1993, 1994 and 1996 (McRoy et al. 1996; Eslinger 1997). Following a nadir in chlorophyll, an increase occurred after day 150 in agreement with these field site measurements.

In Port Valdez, a fjord in northern Prince William Sound Goering et al. (1973) found high levels of productivity and chlorophyll in mid-April followed by low levels in May, 1971. In southeastern Alaska in Auke Bay, the spring bloom lasted from early April to the first week of May (Ziemann et al. 1991). In the southern Bering Sea, the peak of the spring bloom lags the peak biomass in Prince William Sound by approximately three weeks (Goering and Iverson 1982), but blooms in the marginal ice zone begin as early as the last week of April due to salinity-driven stratification and high nutrients (Niebauer et al. 1995). In the Gulf of Alaska, at the Coastal Ocean Weather Station P, chlorophyll *a* concentration remains low ($< 0.50 \text{ mg/m}^3$) throughout the year but primary productivity peaks in early July (Sambrotto and Lorenzen 1986).

2. Temporal and Vertical Patterns of Succession

2.1 Phytoplankton Biomass

The magnitude of the spring bloom is a function of nutrient content and supply and stratification within the marine environment. In 1995, fresh water dilution lowered the salinity, decreased density at the surface and increased stratification. Under such conditions, phytoplankton were maintained in the euphotic zone and biomass increased as a distinct peak that declined as nutrients were depleted. Nitrate+nitrite concentrations

decreased to $< 2 \mu\text{M}$ in the upper surface waters after day 121. Half-saturation constants for nitrate in neritic diatoms range from 0.4-5.1 μM (Valiela 1984). Therefore, diatom growth was limited by low concentrations of nitrate+nitrite in the surface waters at the end of the spring bloom.

In 1995, due to our late arrival in the field (day 107), it is likely that we missed the early portion of the bloom. However, looking at the magnitude of the bloom by day 111, the limited nutrient supply, and comparing the timing with the 1994 and 1996 chlorophyll data from the C-LAB (McRoy et al. 1996; Eslinger 1997), I maintain that we arrived in time to measure the majority of the biomass.

In 1996, the phytoplankton chlorophyll biomass pattern was slightly different. The magnitude was slightly greater and the bloom duration of the bloom was longer than 1995. The salinity of the water column was greater and freshwater dilution was less. Consequently, stabilization of the water column was reduced. Therefore, weak stratification events (around days 105 and 120) promoting increases in phytoplankton stocks were interspersed with mixing events, allowing the nutrient supply to be replenished from depth and lengthening the bloom period. Around day 118, chlorophyll concentrations reached maximum levels and nitrate+nitrite concentrations were reduced to $< 2 \mu\text{M}$ in the upper 10 m. Again the phytoplankton growth was likely controlled from the bottom up by nitrate+nitrite concentrations as in 1995. Similar chlorophyll levels, nutrient concentrations and higher-salinities were also detected throughout Prince William Sound in April 1996 (McRoy et al. 1997; Vaughan et al. 1997).

In both years, silicate concentrations were low in surface waters in April which may also have affected the length of the diatom bloom. Ratios of Nitrate+nitrite:silicate were around 5:10 instead of the modified Redfield ratio of 16:50 (nitrate:silicate) (Broecker and Peng 1982) for optimal nutrient conditions. Also concentrations of silicate in the upper surface waters were lower than nutrient half saturation constants for some

diatoms ($k_s=0.5-5.0 \mu\text{M}$) (Lalli and Parsons 1993). As a result, Prince William Sound may be silicate-limited even though small amounts of the nutrient are usually present at all times. This hypothesis is also supported by weak silicification of diatoms and formation of resting spores, most frequently by *Chaetoceros diadema*, found throughout the study.

In 1995 and 1996, chlorophyll remained very low throughout the month of May while inorganic nutrients were present, suggesting other controls on the phytoplankton community. During the time of lowest chlorophyll (days 124-149), nitrate+nitrite, silicate and phosphate were available in the water column (Figure 4). This suggests that nutrients had been replenished by tidal and wind mixing but chlorophyll biomass remained low, possibly due to grazing control from zooplankton. In addition, ammonia concentrations, not examined in this study, probably increased due to zooplankton excretion and other forms of regeneration. The ammonia would preferentially be removed by phytoplankton, reducing the uptake of nitrate+nitrite and leaving higher concentrations of the “new” nitrogen in the water column.

I speculate that copepods of the genus *Neocalanus*, whose life cycle includes ontogenetic migrations (Fulton 1973; Miller and Clemons 1988), found to be present at this station (Cooney and Coyle 1996), graze heavily during the post-bloom accumulating lipids and keeping phytoplankton standing stocks, but not productivity, at minimal levels. Zooplankton data from the same site showed high settled volumes during the post-bloom but low volumes during the bloom (Figure 20). The zooplankton included the *Neocalanus* copepods (Cooney and Coyle 1996). There exists a negative correlation in 1995 ($r = -0.83$) and 1996 ($r = -0.51$) between zooplankton settled volume and integrated chlorophyll *a* in the bloom and post-bloom periods. This suggests grazing control by zooplankton.

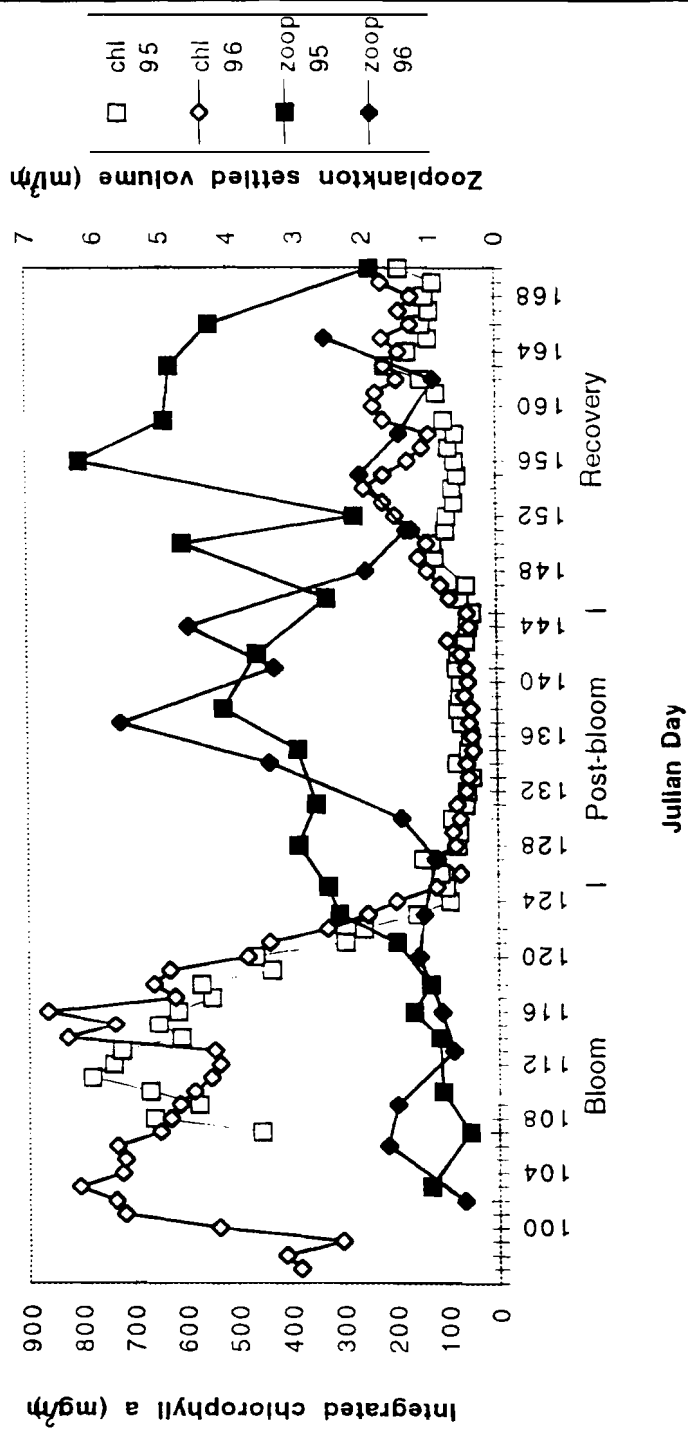


Figure 20. Depth-integrated chlorophyll *a* and zooplankton settled volume (Eslinger 1997) from spring 1995 and 1996.

Another piece of evidence that supports top-down control during the post-bloom period is the 12 day lag in the change of the phytoplankton community size structure as chlorophyll *a* was diminished (Figure 7B). Larger cells persisted until around day 136, suggesting grazing control on microalgae rather than nutrient driven succession in the early days of the decline. *Neocalanus* spp. are known to graze on *Thalassiosira weissflogii*, a centric diatom with a similar diameter to the species found in this study, in the subarctic Pacific Ocean (Frost et al. 1983) and therefore probably fed on the major constituents in Prince William Sound. In both years, chlorophyll reappears after day 146 due to the release of top-down control as the large copepods, *Neocalanus plumchrus* and *Neocalanus flemingeri*, descend to depth in late May (Cooney and Coyle 1996).

The phytoplankton increased after day 146 but remained a fraction of the April biomass. This pattern was a result of a combination of reduced grazing, increased water stability and decreased nutrient concentrations. Large copepods were now mostly absent from surface waters. However, other zooplankton, especially the small copepod *Pseudocalanus* spp., which can feed at low prey density on the same sizes of diatoms as *Neocalanus* (Frost et al. 1983; Valiela 1984), still were present in high biomass (Cooney and Coyle 1996), cropping a smaller proportion of the phytoplankton stocks. By June, the waters were stratified and the nutrient-rich deeper layers were restricted from mixing into surface waters. Nutrient concentrations in the photic zone were lower than in early April and were rapidly depleted by primary producers. These effects restricted the growth of the algae in early summer.

Vertical distribution of chlorophyll fluctuated throughout the season but displayed little interannual variability. During the bloom in both years, the highest chlorophyll concentration was in the upper 25 m. However, substantial concentrations (up to 15 mg/m³) of chlorophyll were measured at 75 m. The chlorophyll concentrations extended into deep layers because vertical mixing occurred in April and the stability of the water

column was weak. This was especially apparent in 1996 when strong stratification did not develop until after the bloom had subsided in May. Cells can survive below the 1 % light depth as long as they spend a portion of the day conducting sufficient photosynthesis to exceed losses from respiration within the photic zone (Round 1981). Thus, phytoplankton sampled below the compensation depth likely survived because they were continuously mixed in and out of the euphotic zone during the bloom period. During May, all depths had low chlorophyll levels. By June, due to solar heating and freshwater additions, the waters stratified and mixing below 25 m was restricted. At this time, the majority of the phytoplankton was confined to the upper 25 m.

2.2 Species Succession

In northern temperate waters the seasonal succession of phytoplankton is well documented (Valiela 1984). During periods of high nutrients, the spring bloom is composed of chain-forming diatoms, with high chlorophyll per cell, followed by flagellate dominance plus sparse numbers of diatoms tolerant of low nutrient conditions. In Prince William Sound, the size fractionation studies were the first to confirm this succession. The succession sequence was from high amounts of microplankton during the bloom to low picoplankton biomass, followed by a slight recovery of the microplankton, nanoplankton and picoplankton biomass. The fractionation results were in agreement with results from Boca de Quadra in southeast Alaska, where the researchers found a shift from netplankton ($> 5 \mu\text{m}$) dominance in March to ultraplankton ($< 5 \mu\text{m}$) by May and July (VTN Consolidated, Inc. 1980).

During the spring bloom, the same species returned annually. There was substantial interannual variability in abundance and carbon biomass, but not chlorophyll. In both years *Thalassiosira* spp., *Skeletonema costatum*, and *Chaetoceros* spp. were major constituents but different species dominated each year and interannual abundance and carbon biomass varied among species. In 1995, *Skeletonema costatum* dominated the

abundance but *Thalassiosira* spp. dominated the carbon biomass. This was due to the larger cell volume of *Thalassiosira*. These diatoms have 4-50 times the volume of the smaller *Skeletonema* cells (Table 3). In contrast to total carbon biomass, the chlorophyll concentration was similar between years, so the chlorophyll per cell was higher in 1995. This may be attributed to different factors. *Thalassiosira* spp. was more abundant in 1995 than 1996. *Thalassiosira* spp. have large cell volumes and therefore, under optimal conditions, potentially should have greater amounts of chlorophyll per cell than smaller diatoms. *Thalassiosira fluviatilis* and *T. allenii*, two species < 35 µm in diameter, contained 1.37-6.63 pg chlorophyll/cell (Perry et al. 1981) and 30-58 pg chlorophyll/cell (Redalje and Laws 1983), respectively, under different light and nutrient conditions. *Skeletonema costatum*, under the same high light conditions as *T. fluviatilis*, has 0.58 pg chlorophyll/cell (Perry et al. 1981). Consequently, 1996 had approximately the same amount of chlorophyll because *Thalassiosira* spp. was less abundant than in 1995, and *Skeletonema costatum*, with low amounts of chlorophyll/cell, occurred in highest abundance.

In 1996, *Skeletonema costatum* dominated both abundance and biomass. *Thalassiosira* spp. and *Chaetoceros* spp. were insignificant in comparison. There were at least two to three times the cell abundance and carbon in 1996 than in 1995, but chlorophyll levels were only slightly higher. There is not a fixed relationship between total chlorophyll and total carbon (Darley 1982). Chlorophyll may have been approximately the same because the predominant species only has one to two chloroplasts per cell (Tomas 1996), a small volume, and a low amount of chlorophyll per cell (Perry et al. 1981; Darley 1982). This hypothesis is also supported by the carbon to chlorophyll ratio. From laboratory studies, *Skeletonema costatum* is known to have a carbon to chlorophyll ratio of 26 if not nutrient limited (Darley 1977). In 1996, in Prince

William Sound, when most of the carbon was derived from *Skeletonema costatum* the carbon to chlorophyll ratio averaged 22 throughout the bloom above 50 m (Table 5).

A second factor that may have contributed to the chlorophyll levels was the response by phytoplankton to different amounts of light each year. High light intensity inhibits photosynthesis and the production of plant pigments (Darley 1982; Valiela 1984). Cells grown in high light intensity have less chlorophyll/cell (Darley 1982). Results from cloud cover data collected daily at the AFK Hatchery revealed that 1996 had a slightly greater number of days with < 50 % cloud cover during the bloom than did 1995 (Table 7). The interannual difference in cloud cover was greater during the post-bloom and recovery periods. The higher frequency of partly cloudy days may have inhibited the production of chlorophyll in algal cells due to greater light intensity at the surface.

Table 7. Number of days having < 50 % cloud cover, median cloud cover during each period, and number of days observed from April-June 1995 and 1996 at AFK Hatchery (unpublished data).

Period	<u>1995</u>			<u>1996</u>		
	< 50 % cloud cover	Median cloud cover (%)	n	< 50 % cloud cover	Median cloud cover (%)	n
Bloom	11	100	27	13	90	29
Post-bloom	4	100	21	10	17.5	18
Recovery	4	50	25	8	95	25

The response to light and species composition could have caused the differences in the chlorophyll/cell in Prince William Sound. The findings in the current study are in agreement with results from in Auke Bay, Alaska by Ziemann et al. (1991) who found

depth-integrated chlorophyll levels lower than peak depth-integrated chlorophyll levels when the abundance of *Skeletonema costatum* reached a maximum of approximately 11,000 cells/mL. They reasoned that this was due to the small size of the species and narrow depth distribution. However this explanation is unconvincing and I hypothesize that the low chlorophyll values were due to the low amounts of chlorophyll/cell in *Skeletonema costatum*.

As the spring bloom progressed, the pattern of phytoplankton succession from flagellate dominance to a mixed different diatom and flagellate community occurred each year from May to June. In May, almost all of the carbon was of flagellate origin in the periods of lowest chlorophyll. As alluded to previously, grazers appeared to harvest the large diatoms as fast as cells replicated. The flagellates and smaller diatoms, like the long narrow *Pseudo-nitzschia* spp., were all that remained in the water.

Most of the flagellates were $< 5 \mu\text{m}$ and may have been an unsuitable size of food for large copepods. *Phaeocystis* sp., a possible major constituent of the flagellate community, has been found unsuitable as food for *Calanus* sp. and *Pseudocalanus* sp. copepods (Bautista et al. 1992). By June, the large *Neocalanus* copepods had left the surface waters (Cooney and Coyle 1996) and large cells again appeared in the water. At this time, *Rhizosolenia fragilissima*, a diatom species not seen in April, became the primary constituent in terms of carbon biomass in both years due to its large cell volume. In 1995, it contributed almost all of the diatom biomass but in 1996 a few previous community constituents, e.g. *Chaetoceros* spp. and *Skeletonema costatum*, persisted in the warmer temperatures and low nutrient conditions and occurred in low numbers.

The major diatom species present in April and June were those adapted to surviving in high latitude coastal waters (Valiela 1984). The dominant diatom genera and species in both years at the peak of the bloom were *Skeletonema costatum*, *Thalassiosira* spp., *Chaetoceros* spp., and *Pseudo-nitzschia* spp. All are characteristically found in the

early stages of the bloom when nutrients concentrations are high. These diatoms are species that can bloom after sedimentation and resuspension and survive in turbid waters (Round 1981). Their dominance of the community is probably a result of rapid uptake of nutrients, high nutrient affinity, cold temperature tolerances and rapid growth.

Skeletonema costatum is found worldwide (Round 1981). It can survive in a broad range of light and temperature conditions, absorb organic material as a nutrient source and, in contrast with other colonial cells, decrease its sinking rate by forming long chains. From laboratory studies, *Skeletonema costatum* was found to have a lower half saturation constant for silicate than *Thalassiosira pseudonana* and *T. decipiens* (Paasche 1973). This may have enabled it to survive longer in low silicate conditions. These adaptations of *Skeletonema costatum* could have given it a competitive edge over *Thalassiosira* spp., especially in 1996 when silicate concentrations were lower and water column stratification was weaker. *Thalassiosira* spp. has a greater diameter and is likewise denser than *Skeletonema costatum*, so it is more likely to sink out of the photic zone as stratification increases and viscosity decreases due to warming. This factor may also have contributed to its lower abundance in 1996.

In June as the microplankton returned, around day 160, there was a shift in succession to *Rhizosolenia fragilissima* in both years. This genus is typically found in late stages of blooms (Round 1981; Valiela 1984). It has the ability to survive under low nutrient conditions in stratified waters (Valiela 1984) and it has been found to have endosymbiotic relationships with nitrogen fixing cyanobacteria in oceanic waters (Paerl 1995). These adaptations could enable *Rhizosolenia fragilissima* to outcomplete *Skeletonema costatum* when environmental conditions were less favorable.

The phytoplankton abundance, carbon biomass and species composition did not change substantially over the upper 50 m. During the bloom, when substantial chlorophyll concentrations extended down to 75 m, large numbers of phytoplankton were

also found at depths below the euphotic zone. At this time, the same species in similar proportions were located at all depths. Only 50 m had lower abundance of algae. These features of the distribution can be attributed to vertical mixing. Sinking of cells is probably a minor factor because the settling of cells from nutrient-rich surface waters is insignificant compared to the turbulent mixing. Even in June when the surface waters were fairly well-stratified (especially in 1995) minor mixing events, due to tidal currents and geostrophic flows presumably submerged live cells as deep as 50 m.

The species composition and abundance of the phytoplankton community in Prince William Sound discussed here are similar to those in Alaska coastal and oceanic regions (Horner et al. 1973; Iverson et al. 1974; VTN Consolidated, Inc. 1980; Kocur 1982; Ziemann et al. 1991). In Valdez Narrows, Horner et al. (1973) found the abundant species in late April to be *Thalassiosira* spp., *Chaetoceros* spp. and *Phaeocystis pouchetii* at the surface. It is possible, based on the similarity in appearance, that what they have identified as *P. pouchetii* may be the same as a flagellate that I could not clearly identify and therefore have labeled "unidentified flagellate". No colonial *Phaeocystis* was observed in either year in Prince William Sound. *Skeletonema costatum* did not appear until November in Valdez Narrows but did appear in April at other Port Valdez study sites (Horner et al. 1973). These results support my findings, except for a greater abundance and earlier appearance of *Skeletonema costatum* in the southwest Prince William Sound study site. However, Horner et al. (1973) only sampled one day at one depth in late April, and the bloom was probably already in decline.

In Auke Bay, Alaska, a time series of diatom species composition from 2 m was collected from 1985-1989 (Ziemann et al. 1991). Like Prince William Sound, the same species returned annually in different proportions to compose the bloom. Two periods during spring and early summer (one around day 100 and the second around day 160) showed peak abundance of different diatoms. Cell abundance ranged from 0-12,000

cells/mL with *Skeletonema costatum* being the major constituent of the phytoplankton after the peak of the bloom. The timing, not the abundance, contrasts with this study. In Prince William Sound, *Skeletonema costatum* occurs in highest abundance during the height of the bloom. In Auke Bay, *Thalassiosira aestivalis* was the dominant plankton during the primary spring bloom (Ziemann et al. 1991). Similar to 1996 in Prince William Sound, Auke Bay in 1987 was a year with high abundance of *Skeletonema costatum* (approximately 11,000 cells/mL) in the spring. This demonstrates how one small chain-forming diatom species can dominate the cell counts in some years but not others. My findings show a succession to *Rhizosolenia fragilissima* in early June. This was not seen in either the Auke Bay (Ziemann et al. 1991) or the Port Valdez studies (Horner et al. 1973).

3. Relationship to Upper Trophic Levels

3.1 Food Availability

When determining food availability for trophic transfer it is necessary to consider organic carbon and species composition in the waters and not just chlorophyll concentrations or cell abundance. In both years, the highest amounts of diatom carbon available to herbivores were present in April. This phytoplankton bloom may have triggered some over-wintering, deep water zooplankton to migrate to upper waters to feed in late April (Cooney and Coyle 1996). Due to the slow reproductive rates of zooplankton in comparison to algae, the phytoplankton escaped predation early in the season. In 1995 and 1996, most of the carbon originated as chain forming diatoms, *Thalassiosira* spp. and *Skeletonema costatum*. These genera are known to be heavily grazed upon by zooplankton (Round 1981; Valiela 1984; Nejstgaard et al. 1995). However, in 1996 there was a two- to three-fold increase in carbon biomass during the bloom. Since zooplankton are known to increase fecundity and therefore increase density in response to food density (Valiela 1984), 1996 should have been a more fruitful year for

secondary producers. Consequently, since copepods including, *Neocalanus* spp. and *Pseudo-calanus* spp., are known to be a major prey for pollock (Cooney and Coyle 1996), salmon (Willette et al. 1995) and Pacific herring (Foy et al. 1997) in Prince William Sound and schools of these forage fish are found in high densities in southwest Prince William Sound (Willette et al. 1995; Stokesbury et al. 1997), 1996 might have been a better year for fisheries recruitment.

The *Exxon Valdez* oil spill occurred March 24, 1989 during the onset of the phytoplankton bloom. Since crude oil affects light transparency and cell respiration (Round 1981) phytoplankton growth may have been hampered or some phytoplankton may have died rapidly from pollutant effects. Data collected two weeks after the spill in Prince William Sound, showed higher concentrations of chlorophyll *a* in the southeast than the southwest (McRoy and Eslinger 1995), where the oil had drifted covering the western region (Galt et al. 1991). These chlorophyll concentrations were lower than levels in either 1995 or 1996, possibly due to oil pollution. In 1989 in southwest Prince William Sound, lower levels of organic carbon biomass would have limited zooplankton production. This loss would have transferred to the 1989 year class of pink salmon, herring and pollock reducing larval survival and recruitment.

4. Future Research

To better understand the phytoplankton and nutrient dynamics of Prince William Sound additional research needs to be conducted. Two to three additional years of data need to be collected to document interannual variability. The addition of a fluorometer attached to the CTD would give more information about the vertical distribution of phytoplankton biomass. A time series of productivity data and ammonium concentrations would help elucidate the controls on the phytoplankton community. The deployment of a sediment trap could determine how much primary productivity is lost to

the benthos due to sinking. Lengthening the study period to include late summer and fall would allow for determination of any fall bloom and the major constituents of that bloom

Additional species composition work needs to be conducted. I would suggest sampling more days from only one depth in the upper 10 m throughout the spring, summer and fall to document changes in species succession. Epi-fluorescence techniques could be applied to determine the abundance and carbon biomass of bacteria, mixotrophs, and heterotrophic phytoplankton. A study of the micro-zooplankton (ciliate) abundance would be beneficial in understanding the grazing controls on the phytoplankton community throughout the year.

CONCLUSIONS

- The bloom began in early April, declined by May and exhibited a small recovery in June.
- The phytoplankton biomass was likely nutrient controlled from the bottom up in April, followed by top-down grazing control in May.
- The bloom consisted of 80 % microplankton: the post bloom was predominantly picoplankton followed by a small diatom recovery.
- High levels of phytoplankton biomass and abundance extended down to 50 m with little variation in species composition.
- A seasonal succession of the diatom community occurred from *Skeletonema costatum*, *Thalassiosira* spp. and *Chaetoceros* spp. in April to *Rhizosolenia fragilissima* in June.
- In 1995, *Thalassiosira* spp. contributed 73-80 % of the diatom carbon, and in 1996 *Skeletonema costatum* made up 58-78 % of the carbon during the bloom.
- Flagellate carbon was the main constituent in the post-bloom of both years while *Rhizosolenia fragilissima* composed the majority of the carbon biomass during the recovery.
- More than twice as much organic carbon was present in 1996 than 1995.
- 1996 had a greater biomass of organic carbon and therefore a potentially greater food supply for zooplankton.
- The timing of the bloom and the temporal and vertical patterns of the phytoplankton succession in southwest Prince William Sound in 1995 and 1996 resembled other marine environments of similar latitude.

REFERENCES

- Alexander, V., and T. Chapman. 1980. Phytotoxicity, p. 127-142. *In* J. M. Colonell [ed.], Port Valdez, Alaska: Environmental studies 1976-1979. Institute of Marine Science, Univ. of Alaska Fairbanks.
- Alexander, V., and R. M. Nauman. 1969. Phytoplankton observations, p. 133-166. *In* D. W. Hood [ed.], Baseline data survey for Valdez pipeline terminal environmental data study. Institute of Marine Science, Univ. of Alaska Fairbanks.
- Bautista, B., R. P. Harris, P. R. G. Tranter, and D. Harbour. 1992. In situ copepod feeding and grazing rates during a spring bloom dominated by *Phaeocystis* sp. in the English Channel. *J. Plankton Res.* **14**: 691-703.
- Booth, B. C., J. Lewin, and J. R. Postel. 1993. Temporal variation in the structure of autotrophic and heterotrophic communities in the subarctic Pacific. *Prog. Oceanog.* **32**: 57-99.
- Broecker, W. S., and T. H. Peng. 1982. Tracers in the sea. Lamont-Doherty Geological Observatory, Columbia Univ.
- Brunel, J. 1962. Le phytoplancton de la baie des chaleurs. Les Presses De L'Universite de Montreal.
- Cooney, R. T. 1996. Sound Ecosystem Assessment (SEA) - An integrated science plan for the restoration of injured species in Prince William Sound. ADF&G, Anchorage.
- Cooney, R. T., and K. O. Coyle. 1996. The role of zooplankton in the Prince William Sound Ecosystem. *In Exxon Valdez oil spill restoration project annual report* (Restoration Project 95320-H). ADF&G, Anchorage.
- Cupp, E. E. 1943. Marine plankton diatoms of the west coast of North America. *Bull. Scripps Instn. Oceanogr.* **5**(1).
- Darley, W. M. 1977. Biochemical composition, p. 198-223. *In* D. Werner [ed.]. The biology of diatoms. Blackwell Scientific.
- Darley, W. M. 1982. Algal biology: A physiological approach. Blackwell Scientific.
- Eslinger, E.L. 1997. Biophysical modeling and validation through remote sensing. *In Exxon Valdez oil spill annual report* (Restoration Project 96320-R). ADF&G, Anchorage.
- Foy, R. J., B. L. Norcross, and A. Blanchard. 1997. Spatial and temporal differences in the diet of Herring (*Clupea pallasii*) in Prince William Sound, Alaska. *In Exxon Valdez oil spill restoration project annual report* (Restoration Project 96320-T). ADF&G, Anchorage.

- Frost, B. W., M. R. Landry, and R. P. Hassett. 1983. Feeding behavior of large calanoid copepods *Neocalanus cristatus* and *N. plumchrus* from the subarctic Pacific Ocean. *Deep-Sea Res.* 30: 1-13.
- Fulton, J. 1973. Some aspects of the life history of *Calanus plumchrus* in Strait of Georgia. *J. Fish. Res. Board Can.* 30: 811-815.
- Galt, J. A., W. J. Lehr, and D. L. Payton. 1991. Fate and transport of the *Exxon Valdez* oil spill. *Environ. Sci. and Tech.* 25: 202-209.
- Gemeinhardt, K. 1930. Kryptogamenflora von Deutschland, Österreich und der Schweiz. Reprinted in 1971 by Johnson Reprint Corp.
- Goering, J. J., and R. L. Iverson. 1978. Primary production and phytoplankton composition, p. 203-239. *In* PROBES phase 1 progress report. 1977-1978. Institute of Marine Science, Univ. of Alaska, Fairbanks.
- Goering, J. J., and R. L. Iverson. 1982. Primary production and phytoplankton composition in the southeast Bering Sea, p 305-385. *In* PROBES final report. Vol. 1. Institute of Marine Science, Univ. of Alaska Fairbanks.
- Goering, J. J., D. M. Nelson, and J. A. Carter. 1973. Silicic acid uptake by natural populations of marine phytoplankton. *Deep Sea Res.* 20: 777-789.
- Goering, J. J., W.E. Shiels, and C.J. Patton. 1973. Primary production. p. 253-279. *In* D. W. Hood, W. E. Shiels, and E. J. Kelley [eds.], *Environmental studies of Port Valdez*. Institute of Marine Science, Univ. of Alaska Fairbanks.
- Horner, R. A., L. S. Dick, and W. E. Shiels. 1973. Phytoplankton studies, p. 283-294. *In* D. W. Hood, W. E. Shiels, and E. J. Kelley [eds.] *Environmental Studies of Port Valdez*. Institute of Marine Science, Univ. of Alaska Fairbanks.
- Hustedt, F. 1930. Kryptogamenflora von Deutschland, Österreich und der Schweiz. Reprinted in 1971 by Johnson Reprint Corp.
- Hustedt, F. 1959. Kryptogamenflora von Deutschland, Österreich und der Schweiz. Reprinted in 1971 by Johnson Reprint Corp.
- Iverson, R. L., J.H.C. Curl, J. H.B. O'Connors, D. Kirk, and K. Zakar. 1974. Summer phytoplankton blooms in Auke Bay, Alaska, driven by wind mixing of the water column. *Limnol. Oceanogr.* 19: 271-278.
- Kocur, C. 1982. Phytoplankton distribution in southeastern Bering Sea shelf waters during spring. M.S. thesis, Florida State Univ.
- Kovala, P. E., and J. D. Larrance. 1966. Computation of phytoplankton cell numbers, cell volume, cell surface and plasma volume per liter, from microscopical counts. *Dept. Oceanogr., Univ. of Washington.*
- Lalli, C.M. and T.R. Parsons. 1993. *Biological oceanography: an introduction.* Pergamon.

- Lund, J. W. G., C. Kipling, and E. D. L. Cren. 1958. The inverted microscope method of estimating algal numbers and the statistical basis of estimations by counting. *Hydrobiologia*. **11**: 147-170.
- McRoy, C. P., and D. L. Eslinger. 1995. Sound Ecosystem Analysis: phytoplankton and nutrients. *In Exxon Valdez oil spill restoration project annual report (Restoration Project 94320-G)*. ADF&G, Anchorage.
- McRoy, C. P., D. L. Eslinger, A. Ward, E. P. Simpson, D. Clayton, B. Bergeron, and J. Cameron. 1996. Sound Ecosystem Analysis: phytoplankton and nutrients. *In Exxon Valdez oil spill restoration project annual report (Restoration Project 95320-G)*. ADF&G, Anchorage.
- McRoy, C. P., A. Ward, E. P. Simpson, D. Clayton, J. Cameron, S. McCullough and E. Suring. 1997. Sound Ecosystem Analysis: phytoplankton and nutrients. *In Exxon Valdez oil spill restoration project annual report (Restoration Project 96320-G)*. ADF&G, Anchorage.
- Miller, C. B., and M. J. Clemons. 1988. Revised life history analysis for large grazing copepods in the subarctic Pacific Ocean. *Progr.Oceanogr.* **20**: 293-313.
- Muench, R. D., and C. M. Schmidt. 1975. Variations in the hydrographic structure of Prince William Sound. IMS Report R75-1. Institute of Marine Science, Univ. of Alaska Fairbanks.
- Nejstgaard, J.C., U. Bamstedt, E. Bagoien and P.T. Solberg. 1995. Algal constraints on copepod grazing. Growth state, toxicity, cell size, and season as regulating factors. *ICES J. Mar. Sci.* **52**: 347-357
- Niebauer, H. J., V. Alexander, and S. M. Henrichs. 1995. A time-series study of the spring bloom at the Bering Sea ice edge I. Physical processes, chlorophyll and nutrient chemistry. *Cont. Shelf Res.* **15**: 1859-1877.
- Niebauer, H. J., T. C. Royer, and T. J. Weingartner. 1994. Circulation of Prince William Sound, Alaska. *J. Geophys. Res.* **99**: 14,113-14,126.
- Paasche, E. 1973. Silicon and the ecology of marine plankton diatoms. II. Silicate-uptake kinetics in five diatom species. *Mar. Biol.* **19**: 262-269.
- Paerl, H. W. 1995. Clarification of the structural and functional roles of heterocysts and anoxic microzones in the control of pelagic nitrogen fixation. *Limno. Oceanogr.* **40**: 634-637.
- Parsons, T. R., Y. Maita, and C. M. Lalli. 1984. A manual of chemical and biological methods for seawater analysis. Peragmon.
- Perry, M. J., M. C. Talbot, and R. S. Alberte. 1981. Photoadaptation in marine phytoplankton: response of the photosynthetic unit. *Mar. Biol.* **62**: 91-101.

- Ray, R. T., L. W. Haas, and M. E. Sieracki. 1989. Autotrophic picoplankton dynamics in a Chesapeake Bay sub-estuary. *Mar. Ecol. Prog. Ser.* 52: 273-285.
- Redalje, D. G., and E. A. Laws. 1983. The effects of environmental factors on growth and the chemical and biochemical composition of marine diatoms, I. Light and temperature effects. *J. Exper. Biol. Ecol.* 68: 59-79.
- Round, F. E. 1981. *The ecology of algae.* Cambridge University Press.
- Sambrotto, R.N. and C.J. Lorenzen. 1986. Phytoplankton and primary production, p. 249-282. *In*: D.W. Hood and S.T. Zimmerman [eds.], *The Gulf of Alaska physical environment and biological resources.* U.S. Gov. Printing Office, Washington, D.C.
- Sandgren, C. D., and J. V. Robinson. 1984. A stratified sampling approach to compensation for non-random sedimentation of phytoplankton cells in inverted microscope settling chambers. *J. Br. Phycol.* 19: 67-72.
- Schell, D.M. 1971. Uptake and regeneration of dissolved organic nitrogen in southeastern Alaskan marine waters. M.S. thesis, Univ. of Alaska Fairbanks.
- Schiller, J. 1933. *Kryptogamenflora von Deutschland, Osterreich und der Schweiz.* Reprinted in 1971 by Johnson Reprint Corp.
- Stokesbury, K. D. E., E. Brown, R. J. Foy, and B. L. Norcross. 1997. Juvenile herring growth and habitats. *In Exxon Valdez oil spill restoration project annual report (Restoration Project 96320-T).* ADF&G, Anchorage.
- Strathmann, R. R. 1967. Estimating the organic carbon content of phytoplankton from cell volume or plasma volume. *Limno. Oceanogr.* 12: 411-418.
- Strickland, J. D. H., and T. R. Parsons. 1977. *A practical handbook of seawater analysis.* Fish. Res. Bd. Can.
- Sverdrup, H. U. 1953. On conditions for the vernal blooming of phytoplankton. *J. Cons. perm. int. Explor. Mer.* 18: 287-295.
- Tomas, C. R. 1993. *Marine phytoplankton: a guide to naked flagellates and coccolithophorids.* Academic Press.
- Tomas, C. R. 1996. *Identifying marine diatoms and dinoflagellates.* Academic Press.
- Utermohl, H. 1931. Neue wege in der quantitativen erfassung des planktons. *Verh. int. Verein. theor. angew. Limnol.* 5: 567-596.
- Valiela, I. 1984. *Marine ecological processes.* Springer-Verlag.
- Vaughan, S.L., S.M. Gay, L.B. Tuttle, and K.E. Osgood. 1997. Water mass variability and circulation in Prince William Sound. *In Exxon Valdez oil spill restoration project annual report (Restoration Project 96320-M).* ADF&G, Anchorage.

- Venrick, E. L. 1978. Sampling strategies, p. 7-16. *In* A. Sournia [ed.] Phytoplankton manual. UNESCO.
- Vinyard, W. C. 1979. Diatoms of North America. Mad River Press.
- VTN Consolidated, Inc. 1980. Phytoplankton, p.16-50. *In* Boca de Quadra baseline report coastal and marine biology program Quartz Hill molybdenum project Southeast Alaska. Environmental Sciences Division, VTN Consolidated, Inc.
- Willette, M., M. Sturdevant, S. Jewitt, E. Debevec. 1995. Forage fish influence on recovery of injured species: forage fish diet overlap. *In Exxon Valdez oil spill restoration project annual report* (Restoration Project 94163). ADF&G, Anchorage.
- Yamaji, I. 1986. Illustrations of the marine phytoplankton of Japan. Hoikusha Publishing Co.
- Ziemann, D. A., L. D. Conquest, M. Olaizola, and P. K. Bienfang. 1991. Interannual variability in the spring phytoplankton bloom in Auke Bay, Alaska. *Mar. Biol.* **109**: 321-334.
- Ziemann, D. A., L.D. Conquest, K.W. Fulton-Bennett and P.K. Bienfang. 1990. Interannual variability in the Auke Bay phytoplankton p. 129 -170. *In* D.A. Ziemann and K.W. Fulton-Bennett [eds.], APPRISE: Interannual variability and fisheries recruitment. The Oceanic Institute, Hawaii.

APPENDIX 1

0 m Phytoplankton (cells/ml)	Julian Day 1995														
	April									May			June		
	108	109	110	112	113	114	116	117	119	133	135	137	162	164	166
<i>Asterionella glacialis</i>	0	19	21	13	17	40	20	28	7	0	0	-	0	0	0
<i>Biddulphia</i> sp.	0	0	0	0	0	0	0	0	0	0	0	-	0	0	0
<i>Chaetoceros</i> spp.	129	145	60	245	148	227	206	164	280	1	0	-	2	19	10
<i>Cocconeis</i> sp.	0	0	0	0	0	0	0	0	0	0	0	-	0	1	0
<i>Coscinodiscus</i> spp.	0	0	0	0	0	0	0	0	0	0	0	-	0	0	0
<i>Eucampia</i> spp.	0	8	0	0	0	5	3	0	4	0	0	-	0	0	0
<i>Fragilaria</i> sp.	0	0	0	0	0	0	0	0	0	0	0	-	0	0	0
<i>Grammatophora</i> sp.	0	4	0	0	0	0	0	0	0	0	0	-	0	0	0
<i>Leptocylindrus damicus</i>	0	5	0	21	12	15	3	0	8	0	0	-	1	2	0
<i>Leptocylindrus minimus</i>	620	64	31	37	20	23	61	0	35	5	0	-	0	4	0
<i>Laeniophora</i> sp.	0	0	0	0	0	0	0	0	0	0	0	-	0	0	0
<i>Navicula</i> spp.	0	0	0	0	0	0	0	0	0	0	0	-	0	0	1
<i>Pseudo-nitzschia</i> spp.	52	67	24	181	121	127	121	133	156	0	29	-	3	2	1
<i>Rhizosolenia fragilissima</i>	0	0	0	0	0	0	0	0	0	0	0	-	364	686	314
<i>Skeletonema costatum</i>	238	399	335	794	624	582	831	568	616	0	0	-	0	0	0
<i>Stephanopyxis nipponica</i>	0	0	0	3	1	0	0	0	5	0	0	-	0	0	0
<i>Thalassionema nitzschoides</i>	0	0	0	0	0	9	0	3	0	0	0	-	0	0	0
<i>Thalassiosira</i> spp.	593	288	377	169	509	576	501	249	386	1	5	-	2	12	1
Unidentified centric	0	0	0	0	0	0	0	0	0	0	0	-	0	0	3
Unidentified diatoms	31	0	0	0	0	0	0	0	0	0	0	-	0	0	3
Unidentified pennate	0	0	1	10	0	0	0	5	0	0	0	-	0	0	0
<i>Ceratium</i> spp.	0	0	0	0	0	0	0	0	0	0	0	-	0	0	0
<i>Dinophysis</i> spp.	0	0	0	0	0	0	0	0	0	0	0	-	0	1	2
<i>Distaplia speculum</i>	0	0	0	0	0	0	0	0	0	0	0	-	3	4	2
<i>Ebria tripartita</i>	0	0	0	0	0	0	0	0	0	0	0	-	1	2	2
<i>Peridinium</i> spp.	0	0	0	0	0	0	0	0	1	0	0	-	0	1	0
Unidentified dinoflagellates	0	0	0	3	0	5	1	6	17	0	1	-	3	0	0
Unidentified flagellates	2489	756	565	1430	840	1210	1198	1805	1901	385	565	-	832	817	858
Unidentified silicoflagellates	0	0	0	0	0	0	0	0	0	0	0	-	0	0	0

5 m Phytoplankton (cells/mL)	Julian Day														
	April									May			June		
	108	109	110	112	113	114	116	117	119	133	135	137	162	164	166
<i>Asterionella glacialis</i>	0	29	85	17	28	19	18	15	15	0	0	0	0	0	0
<i>Biddulphia</i> sp.	1	0	0	0	0	0	0	0	0	0	0	0	0	0	0
<i>Chaetoceros</i> spp.	593	67	143	337	212	186	216	188	214	7	0	5	3	5	0
<i>Cocconeis</i> sp.	0	0	0	0	0	0	0	0	0	0	0	0	1	0	0
<i>Coscinodiscus</i> sp.	0	0	0	3	0	0	0	0	0	0	0	0	0	0	0
<i>Eucampia</i> spp.	0	0	3	0	0	5	3	1	0	0	0	0	0	0	0
<i>Fragilaropsis</i> sp.	0	0	0	0	0	0	0	0	0	0	0	0	0	0	0
<i>Grammatophora</i> sp.	0	0	0	0	0	0	0	0	4	0	0	0	0	0	0
<i>Leptocylindrus danicus</i>	0	18	1	0	32	15	0	0	4	0	0	0	0	0	1
<i>Leptocylindrus minimus</i>	589	24	138	17	43	17	0	16	82	0	0	0	0	0	9
<i>Leptocylindrus</i> spp.	0	0	0	0	0	0	0	0	0	0	0	0	0	0	0
<i>Liemophora</i> sp.	0	0	0	0	0	0	0	0	0	0	0	0	0	0	0
<i>Navicula</i> spp.	0	0	0	8	0	0	0	0	0	0	0	0	1	0	2
<i>Pseudo-nitzschia</i> spp.	117	56	96	89	133	137	99	88	129	1	29	17	5	14	1
<i>Rhizosolenia fragilissima</i>	0	0	0	0	0	0	0	0	0	1	0	0	321	664	425
<i>Skeletonema costatum</i>	362	583	814	707	752	586	885	481	572	0	0	0	0	0	0
<i>Stephanopyxis nipponica</i>	4	0	0	4	0	5	0	0	0	1	0	0	0	0	0
<i>Thalassionema nitzschioides</i>	0	0	0	0	0	0	0	0	0	0	0	0	0	0	0
<i>Thalassiosira</i> spp.	731	372	569	965	471	364	568	434	356	2	4	1	11	12	1
Unidentified centric	0	0	0	5	0	0	0	0	0	0	0	0	0	0	5
Unidentified diatoms	0	0	0	0	0	0	0	0	0	0	0	0	0	0	0
Unidentified pennate	3	0	4	5	0	0	0	4	0	0	0	0	1	0	0
<i>Ceratium</i> spp.	0	0	0	0	0	0	0	0	0	0	0	0	0	1	1
<i>Dinophysis</i> spp.	0	0	0	0	0	0	0	0	0	0	0	0	0	0	0
<i>Distephanus speculum</i>	0	0	0	0	0	0	0	0	0	0	0	0	3	1	3
<i>Ebria tripartita</i>	0	0	0	0	0	0	0	0	0	0	0	0	1	1	6
<i>Peridinium</i> spp.	0	0	0	0	0	0	4	3	0	0	0	1	0	0	0
Unidentified dinoflagellates	9	0	0	7	0	0	24	15	20	1	2	0	1	0	0
Unidentified flagellates	2231	639	1459	1747	1106	752	1880	1900	1402	340	609	502	491	1087	1049
Unidentified silicoflagellates	10	0	0	17	0	0	0	0	0	0	0	0	0	0	0

10 m Phytoplankton (cells/mL)	Julian Day														
	April									May			June		
	108	109	110	112	113	114	116	117	119	133	135	137	162	164	166
<i>Asterionella glacialis</i>	32	12	36	13	45	25	38	6	-	0	0	0	0	0	0
<i>Biddulphia</i> sp.	0	0	0	0	0	0	0	0	-	0	0	0	0	0	0
<i>Chaetoceros</i> spp.	85	57	159	220	196	238	207	145	-	0	0	23	16	44	5
<i>Cocconeis</i> sp.	0	0	0	0	0	0	0	0	-	0	0	0	0	0	0
<i>Coscinodiscus</i> spp.	0	0	0	0	0	0	0	0	-	0	0	0	0	0	0
<i>Eucampia</i> spp.	3	0	4	4	5	3	0	0	-	0	0	0	0	0	0
<i>Fragilaropsis</i> sp.	0	0	0	0	0	0	0	0	-	0	0	4	0	0	0
<i>Grammatophora</i> sp.	0	3	0	0	0	0	0	0	-	0	0	0	0	0	0
<i>Leptocylindrus danicus</i>	7	0	0	23	34	9	0	0	-	0	0	6	0	2	1
<i>Leptocylindrus minimus</i>	195	11	464	7	183	78	17	28	-	1	0	0	1	5	5
<i>Leptocylindrus</i> spp.	0	0	0	0	0	0	0	0	-	0	0	0	0	0	0
<i>Limnophora</i> sp.	0	0	0	0	0	0	0	0	-	0	0	0	0	0	0
<i>Navicula</i> spp.	0	0	0	0	0	0	0	0	-	0	0	0	0	2	1
<i>Pseudo-nitzschia</i> spp.	115	52	56	139	150	116	73	112	-	11	41	59	6	2	0
<i>Rhizosolenia fragilissima</i>	3	0	0	0	0	0	0	4	-	0	0	0	369	480	400
<i>Skeletonema costatum</i>	449	668	332	1047	1645	856	375	832	-	0	0	0	0	0	0
<i>Stephanopyxis nipponica</i>	0	3	4	4	1	0	0	3	-	0	0	0	0	0	0
<i>Thalassionema nitzschioides</i>	0	0	8	0	0	4	0	0	-	0	0	0	0	0	0
<i>Thalassiosira</i> spp.	389	307	479	621	884	529	369	505	-	2	1	0	11	3	3
Unidentified centric	0	0	0	5	0	0	0	0	-	0	0	0	0	0	8
Unidentified diatoms	0	0	0	0	0	0	0	0	-	0	0	0	0	0	0
Unidentified pennate	0	0	4	3	0	0	4	0	-	0	1	0	1	0	0
<i>Ceratium</i> spp.	0	0	0	0	0	0	0	0	-	0	0	0	0	0	0
<i>Dinophysis</i> spp.	0	0	0	0	0	0	0	0	-	0	0	0	0	0	0
<i>Distephanus speculum</i>	0	0	0	0	0	0	0	0	-	0	0	0	3	3	3
<i>Ebria tripartita</i>	0	0	0	0	0	0	0	0	-	0	0	0	4	3	4
<i>Peridinium</i> spp.	0	0	0	0	0	0	0	0	-	0	0	1	0	1	0
Unidentified dinoflagellates	0	0	7	0	20	0	1	11	-	2	1	0	0	0	0
Unidentified flagellates	1573	933	1422	1119	1645	1234	869	1066	-	432	638	881	557	734	731
Unidentified silicoflagellates	0	0	0	0	0	0	0	0	-	0	0	0	0	0	0

25 m Phytoplankton (cells/mL)	Julian Day															
	April									May			June			
	108	109	110	112	113	114	116	117	119	133	135	137	162	164	166	
<i>Asterionella glacialis</i>	44	5	52	32	17	49	22	12	13	0	0	0	0	0	0	
<i>Biddulphia</i> sp.	0	0	0	0	0	0	0	0	0	0	0	0	0	0	0	
<i>Chaetoceros</i> spp.	51	65	145	156	203	145	160	167	112	2	1	17	13	13	8	
<i>Cocconeis</i> sp.	0	0	0	0	0	0	0	0	0	0	0	0	0	0	0	
<i>Coscinodiscus</i> spp.	1	0	0	0	0	0	0	0	0	0	0	0	0	0	0	
<i>Eucampia</i> spp.	0	0	0	4	0	0	0	0	1	0	0	0	0	0	0	
<i>Fragilaropsis</i> sp.	0	0	0	0	0	0	0	0	0	0	0	0	0	0	0	
<i>Grammatophora</i> sp.	0	0	0	0	0	0	0	0	0	0	1	0	0	0	0	
<i>Leptocylindrus danicus</i>	13	4	0	0	15	0	0	4	22	0	0	8	0	3	3	
<i>Leptocylindrus minimus</i>	87	34	518	7	4	75	48	25	43	0	0	0	10	0	0	
<i>Leptocylindrus</i> spp.	0	0	0	0	0	0	0	0	0	0	0	0	0	0	0	
<i>Licnophora</i> sp.	0	0	0	0	0	0	0	0	0	0	0	0	0	0	0	
<i>Navicula</i> spp.	0	0	0	0	0	0	0	0	1	0	0	0	0	0	0	
<i>Pseudo-nitzschia</i> spp.	79	81	53	117	111	99	115	120	86	8	22	35	3	0	0	
<i>Rhizosolenia fragilissima</i>	0	0	0	1	0	0	0	0	0	0	0	0	528	436	469	
<i>Skeletonema costatum</i>	563	618	316	647	363	356	524	533	297	0	0	0	0	0	0	
<i>Stephanopyxis nipponica</i>	1	3	8	3	0	4	3	0	0	0	1	0	0	0	0	
<i>Thalassionema nitzschioides</i>	0	0	0	0	0	0	0	0	0	0	0	0	0	0	0	
<i>Thalassiosira</i> spp.	556	386	567	512	436	413	412	258	387	3	2	4	8	10	3	
Unidentified centric	0	0	0	0	5	1	0	0	0	0	0	0	0	0	3	
Unidentified diatoms	0	0	0	0	0	0	0	0	0	0	0	0	0	0	0	
Unidentified pennate	0	0	3	0	0	5	6	0	0	0	0	0	1	0	0	
<i>Ceratium</i> spp.	0	0	0	0	0	0	0	0	0	0	0	0	1	1	0	
<i>Dinophysis</i> spp.	0	0	0	0	0	0	0	0	0	0	0	0	0	1	0	
<i>Distaplia speculum</i>	0	0	0	0	0	0	0	0	0	0	0	0	5	1	1	
<i>Ebria tripartita</i>	0	0	0	0	0	0	0	0	0	0	0	0	7	1	1	
<i>Peridinium</i> spp.	0	0	0	0	0	0	0	0	1	0	0	1	0	0	0	
Unidentified dinoflagellates	0	0	19	1	3	7	5	12	0	5	0	0	5	1	0	
Unidentified flagellates	1480	791	1185	1425	820	1485	1477	642	1049	513	562	598	568	551	528	
Unidentified silicoflagellates	0	0	0	0	0	0	0	0	0	0	0	0	0	0	0	

50 m Phytoplankton (cells/mL)	Julian Day														
	April									May			June		
	108	109	110	112	113	114	116	117	119	133	135	137	162	164	166
<i>Asterionella glacialis</i>	26	14	21	15	39	34	15	22	19	0	0	0	0	0	0
<i>Biddulphia</i> sp.	0	0	0	0	0	0	0	0	0	0	0	0	0	0	0
<i>Chaetoceros</i> spp.	128	41	124	87	85	102	151	123	277	2	0	1	17	9	2
<i>Cocconeis</i> sp.	0	0	0	0	0	0	0	0	0	0	0	0	0	0	0
<i>Coscinodiscus</i> sp.	0	0	0	0	0	0	0	0	0	0	0	0	0	0	0
<i>Eucampia</i> spp.	3	0	0	0	0	0	0	0	5	0	0	0	0	0	0
<i>Fragilaria</i> spp.	0	0	0	0	0	0	0	0	0	0	0	0	0	0	0
<i>Grammatophora</i> sp.	0	7	0	0	0	0	0	0	0	0	0	0	0	0	0
<i>Leptocylindrus danicus</i>	0	5	7	8	0	12	0	5	21	0	0	1	0	0	0
<i>Leptocylindrus minimus</i>	8	11	26	3	0	30	0	10	0	0	0	0	1	0	0
<i>Leptocylindrus</i> spp.	0	0	0	0	0	0	0	0	0	0	0	0	0	0	0
<i>Licnophora</i> sp.	0	0	0	0	0	0	0	0	0	0	0	0	0	0	0
<i>Navicula</i> spp.	0	0	0	0	0	0	0	1	0	0	0	0	0	0	1
<i>Pseudo-nitzschia</i> spp.	54	46	66	43	18	78	116	127	71	17	31	4	6	0	1
<i>Rhizosolenia fragilissima</i>	0	0	0	0	0	0	0	0	0	0	0	0	324	349	179
<i>Skeletonema costatum</i>	330	379	424	417	510	352	485	557	267	0	0	0	0	0	0
<i>Stephanopyxis nipponica</i>	0	0	0	0	0	0	0	0	0	0	0	0	0	0	0
<i>Thalassionema nitzschioides</i>	12	0	0	0	0	0	0	3	1	0	0	0	0	0	0
<i>Thalassiosira</i> spp.	266	314	251	305	493	361	466	260	229	6	1	2	13	6	0
Unidentified centric	0	0	0	0	1	1	3	0	0	0	0	0	0	0	3
Unidentified diatoms	0	0	0	0	0	0	0	0	10	0	0	0	0	0	0
Unidentified pennate	3	0	0	0	1	0	0	0	0	0	2	0	1	0	0
<i>Ceratium</i> spp.	0	0	0	0	0	0	0	0	0	0	0	0	1	0	0
<i>Dinophysis</i> spp.	0	0	0	0	0	0	0	0	0	0	0	0	0	0	0
<i>Distephanus speculum</i>	0	0	0	0	0	0	0	0	0	0	0	0	0	1	1
<i>Ebria tripartita</i>	0	0	0	0	0	0	0	0	0	0	0	0	1	1	1
<i>Peridinium</i> spp.	0	0	0	0	0	0	0	0	1	0	0	0	0	1	0
Unidentified dinoflagellates	4	10	1	1	10	0	21	3	18	2	0	0	1	0	0
Unidentified flagellates	682	705	525	576	1269	609	1629	1565	960	466	576	284	475	312	249
Unidentified silicoflagellates	0	0	0	0	0	0	0	0	0	0	0	0	0	0	0

APPENDIX 2

0 m Phytoplankton (cells/mL)	Julian Day 1996															
	April										May			June		
	102	104	106	108	110	112	114	116	118	120	136	138	140	159	161	163
Asterionella glacialis	0	0	13	5	14	0	31	3	0	14	0	3	0	0	0	12
Biddulphia sp.	0	0	0	0	0	0	0	0	0	0	0	0	0	0	0	0
Chaetoceros decipiens	0	0	0	0	10	0	0	5	0	0	0	0	0	0	0	4
Chaetoceros spp.	2311	953	686	735	596	502	955	1063	1300	724	21	39	80	320	440	438
Cocconeis sp.	0	2	0	0	0	0	0	0	0	0	0	0	0	0	0	0
Eucampia spp.	0	4	9	0	3	0	4	6	0	0	0	0	0	1	0	0
Fragilaropsis sp.	168	0	39	4	25	0	52	8	0	22	0	0	0	0	0	0
Grammatophora sp.	0	0	0	0	0	0	0	0	0	0	1	3	5	26	21	36
Leptocylindrus danicus	54	26	13	8	26	23	19	0	0	0	20	6	33	45	61	34
Leptocylindrus minimus	0	19	15	23	0	5	28	49	12	15	0	0	0	0	0	0
Licmophora glacialis	0	0	0	0	0	0	0	0	0	0	0	0	0	0	0	0
Navicula spp.	5	4	4	8	5	4	1	3	0	0	0	1	0	0	0	0
Pseudo-nitzschia spp.	529	321	269	281	306	241	331	498	338	347	24	19	8	71	123	120
Rhizosolenia fragilissima	3	9	2	1	0	1	8	5	25	0	0	3	5	139	270	181
Rhizosolenia stolterorthii	0	0	0	0	0	0	0	0	0	0	0	0	0	0	0	0
Skeletonema costatum	7553	5741	9086	3521	3988	3024	3665	3950	1442	1880	7	0	0	51	58	59
Stephanopyxis nipponica	0	0	2	5	0	0	5	0	0	0	0	0	0	0	0	0
Thalassionema nitzschioides	0	0	0	0	0	0	0	0	0	3	0	0	0	0	0	0
Thalassiosira spp.	351	273	260	146	258	132	476	194	244	231	3	8	0	0	1	3
Unidentified centric	0	0	0	0	0	0	0	0	0	0	0	0	0	0	0	0
Unidentified pennate	0	0	0	0	0	0	0	0	0	0	0	0	0	0	0	0
Ceratium furca	0	0	0	0	0	0	0	0	0	0	0	0	1	1	3	0
Ceratium spp.	0	0	0	0	0	0	1	0	0	0	0	0	0	0	0	0
Distephanus speculum	0	0	2	0	1	0	1	0	0	0	0	0	0	0	9	3
Ebria tripartita	0	0	0	1	0	0	0	0	0	0	1	0	0	0	0	0
Peridinium spp.	0	0	0	0	0	0	0	0	0	0	0	0	0	0	3	0
Unidentified dinoflagellates	0	9	0	0	0	12	12	5	17	9	4	7	2	8	8	5
Unidentified flagellates	729	666	1564	899	1771	1262	1834	1691	816	944	1014	776	632	1349	1688	876

5 m Phytoplankton (cells/mL)	Julian Day															
	April								May				June			
	102	104	106	108	110	112	114	116	118	120	136	138	140	159	161	163
<i>Asterionella glacialis</i>	0	0	0	0	0	4	0	18	0	0	0	1	0	0	0	0
<i>Biddulphia</i> sp.	0	0	0	0	0	5	0	0	0	0	0	0	0	0	0	0
<i>Chaetoceros deciprens</i>	0	0	0	0	0	5	0	5	0	1	0	0	0	0	0	0
<i>Chaetoceros</i> spp.	1653	1321	977	585	478	408	1358	1268	1021	757	37	10	103	234	504	502
<i>Cocconeis</i> sp.	0	0	0	0	0	0	0	0	0	0	0	0	0	0	0	0
<i>Eucampia</i> spp.	0	0	0	0	10	3	1	5	3	6	0	0	0	6	0	0
<i>Fragilariopsis</i> sp.	39	58	13	44	165	6	56	0	0	10	0	0	0	0	0	0
<i>Gammatophora</i> sp.	0	0	0	0	0	0	0	0	0	0	0	0	0	0	0	0
<i>Leptocylindrus danicus</i>	29	26	22	14	19	17	12	0	0	0	3	0	0	28	27	25
<i>Leptocylindrus minimus</i>	0	11	19	12	18	0	5	30	26	45	14	4	15	111	85	45
<i>Liemophora glacialis</i>	0	0	0	0	0	0	0	0	0	0	0	0	0	6	0	0
<i>Navicula</i> spp.	8	4	2	3	3	1	1	0	0	3	0	0	2	0	0	0
<i>Pseudo-nitzschia</i> spp.	502	359	202	209	278	336	311	425	423	303	27	10	10	80	101	94
<i>Rhizosolenia fragilissima</i>	0	0	0	4	4	4	10	19	9	1	6	3	14	300	269	124
<i>Rhizosolenia stolterfortii</i>	0	0	0	0	0	0	0	0	0	0	0	0	0	0	0	0
<i>Skeletonema costatum</i>	8147	5968	5339	4561	2981	3578	3675	4379	2592	2331	5	16	0	43	98	84
<i>Stephanopyxis nipponica</i>	0	0	0	0	0	0	0	0	1	0	0	0	0	0	0	0
<i>Thalassionema nitzschioides</i>	0	0	0	0	0	0	0	1	0	0	0	0	0	1	0	0
<i>Thalassiosira</i> spp.	384	211	189	214	207	130	431	274	248	213	3	3	1	1	5	4
Unidentified centric	5	0	0	0	3	0	0	0	0	0	0	0	0	0	0	0
Unidentified pennate	0	0	0	0	0	0	0	0	0	0	0	1	0	0	0	0
<i>Ceratium furca</i>	0	0	0	0	0	0	0	0	0	0	0	0	0	0	1	0
<i>Ceratium</i> spp.	0	0	0	0	1	1	0	0	0	0	0	0	0	1	1	0
<i>Distephanus speculum</i>	3	0	0	0	1	0	0	0	0	0	0	0	1	1	0	4
<i>Ebria tripartita</i>	3	0	0	0	0	1	0	0	0	0	0	0	0	0	0	0
<i>Peridinium</i> spp.	0	0	2	0	0	0	0	0	0	0	0	0	0	0	0	0
Unidentified dinoflagellates	30	6	0	0	0	0	3	8	5	31	5	3	6	7	3	3
Unidentified flagellates	1228	754	880	1291	1472	1538	1461	1859	795	1104	773	773	646	1149	1256	1140

10 m Phytoplankton (cells/ml.)	Julian Day																
	April										May			June			
	102	104	106	108	110	112	114	116	118	120	136	138	140	159	161	163	
<i>Asterionella glacialis</i>	0	0	0	10	12	5	34	17	5	22	0	1	0	1	5	6	
<i>Biddulphia</i> sp.	0	0	0	0	0	0	0	0	0	0	0	0	0	0	0	0	
<i>Chaetoceros deciprens</i>	0	0	15	0	0	0	14	0	0	0	1	0	0	0	0	0	
<i>Chaetoceros</i> spp.	1172	887	768	746	555	305	1110	1349	1197	821	16	25	98	323	407	399	
<i>Cocconeis</i> sp.	0	0	0	0	0	0	0	0	0	0	0	0	0	0	0	0	
<i>Eucampia</i> spp.	0	0	0	0	0	4	3	3	3	0	0	0	0	1	0	3	
<i>Fragilariaopsis</i> sp.	145	47	0	90	39	13	41	22	4	0	0	2	0	0	0	0	
<i>Grammatophora</i> sp.	0	0	0	0	0	0	0	0	0	0	0	0	0	0	0	0	
<i>Leptocylindrus danicus</i>	8	17	0	18	28	9	18	4	0	0	0	1	1	41	4	41	
<i>Leptocylindrus minutus</i>	5	4	13	3	12	8	9	43	39	28	17	4	43	79	103	34	
<i>Leptophora glacialis</i>	0	0	0	0	0	0	0	0	0	0	0	0	0	0	0	0	
<i>Navicula</i> spp.	8	4	0	5	1	1	3	0	0	0	0	0	0	0	0	0	
<i>Pseudo-nitzschia</i> spp.	504	301	232	270	290	241	318	616	423	271	25	11	11	111	105	152	
<i>Rhizosolenia fragilissima</i>	0	2	0	0	1	3	0	4	9	12	6	4	10	389	234	219	
<i>Rhizosolenia stollerforthii</i>	0	0	4	0	0	0	0	0	0	0	0	0	0	0	0	0	
<i>Skeletonema costatum</i>	8891	12072	5967	5156	4977	2691	4520	5775	3642	2037	6	0	0	0	61	65	
<i>Stephanopyxis nipponica</i>	0	0	0	0	0	0	0	0	0	0	0	0	0	0	0	0	
<i>Thalassionema nitzschoides</i>	0	0	0	0	0	0	5	0	0	0	0	0	0	0	0	3	
<i>Thalassiosira</i> spp.	349	155	213	302	261	147	416	274	247	218	1	1	1	0	0	1	
Unidentified centric	0	4	0	3	0	0	0	0	0	0	0	0	0	0	0	0	
Unidentified pennate	0	6	0	0	0	0	0	0	0	0	0	0	0	0	0	0	
<i>Ceratium furca</i>	0	0	0	0	0	0	0	0	0	0	0	0	0	1	0	0	
<i>Ceratium</i> spp.	0	0	0	0	0	0	1	0	0	0	0	0	0	1	0	0	
<i>Distephanus speculum</i>	3	2	0	0	0	0	3	0	0	0	0	0	0	0	0	5	
<i>Ebria tripartita</i>	0	0	0	0	0	0	0	0	0	0	0	0	0	0	0	1	
<i>Peridinium</i> spp.	0	0	0	0	0	0	0	0	0	0	0	0	0	0	0	0	
Unidentified dinoflagellates	0	9	0	1	3	4	10	13	1	5	1	2	6	10	8	9	
Unidentified flagellates	757	1815	1184	1437	2021	1200	1216	1462	948	633	571	807	626	1671	866	1101	

25 m Phytoplankton (cells/mL)	Julian Day															
	April								May				June			
	102	104	106	108	110	112	114	116	118	120	136	138	140	159	161	163
<i>Asterionella glacialis</i>	13	0	4	19	5	4	23	12	27	15	0	0	0	3	5	0
<i>Biddulphia</i> sp.	0	0	0	0	0	0	0	0	0	0	0	0	0	0	0	0
<i>Chaetoceros deciprens</i>	6	0	4	0	0	0	0	0	0	0	0	0	0	0	14	0
<i>Chaetoceros</i> spp.	838	1154	1139	735	675	487	1263	1172	833	794	41	20	19	194	360	310
<i>Cocconeis</i> sp.	0	0	0	0	0	0	0	0	0	0	0	0	0	0	0	0
<i>Eucampia</i> spp.	1	0	0	0	6	0	0	8	0	0	1	0	0	0	0	1
<i>Fragilariopsis</i> sp.	44	75	41	3	71	12	32	25	8	0	0	0	0	0	0	0
<i>Grammatophora</i> sp.	0	0	0	0	0	0	0	0	0	0	0	0	0	0	0	0
<i>Leptocylindrus danicus</i>	6	28	26	22	15	23	18	3	0	0	4	2	0	19	9	23
<i>Leptocylindrus minimus</i>	6	0	23	0	13	5	5	41	22	27	14	7	10	70	116	44
<i>Leptophora glacialis</i>	0	0	1	0	0	0	0	0	0	0	0	0	0	0	0	0
<i>Navicula</i> spp.	5	3	5	1	3	3	1	0	0	0	0	0	0	0	1	0
<i>Pseudo-nitzschia</i> spp.	280	300	231	266	290	274	318	494	434	214	25	11	13	61	88	89
<i>Rhizosolenia fragilissima</i>	1	3	4	8	1	5	5	4	5	9	6	0	9	382	229	143
<i>Rhizosolenia stoltertorfii</i>	0	0	0	0	1	0	0	0	0	0	0	0	0	0	0	0
<i>Skeletonema costatum</i>	6720	6710	5922	5226	3232	3594	3052	7369	3484	1735	5	11	0	86	55	104
<i>Stephanopyxis nipponica</i>	3	0	0	0	0	0	0	1	1	0	0	0	0	0	0	0
<i>Thalassionema nitzschioides</i>	0	0	0	0	0	0	0	0	6	0	0	0	0	0	0	0
<i>Thalassiosira</i> spp.	167	250	235	173	296	141	311	305	249	164	1	1	1	4	3	3
Unidentified centric	0	0	0	3	0	0	0	0	0	0	0	0	0	0	0	0
Unidentified pennate	0	0	0	0	0	0	1	0	0	0	0	0	0	0	0	0
<i>Ceratium tereza</i>	0	0	0	0	0	0	0	0	0	0	0	0	1	0	0	0
<i>Ceratium</i> spp.	0	0	1	0	0	0	0	0	0	0	0	0	0	0	0	0
<i>Distephanus speculum</i>	0	0	0	0	0	0	0	0	0	0	0	0	0	2	3	1
<i>Ebria tripartita</i>	0	0	0	0	0	0	0	0	0	0	1	0	0	0	0	0
<i>Peridinium</i> spp.	0	0	1	0	0	0	0	0	0	0	0	0	0	0	0	0
Unidentified dinoflagellates	0	0	1	0	5	4	1	9	9	4	1	3	3	7	6	5
Unidentified flagellates	1124	935	1295	1141	1716	1477	1269	1917	1266	611	528	546	515	934	919	718

50 m Phytoplankton (cells/mL)	Julian Day																
	April										May			June			
	102	104	106	108	110	112	114	116	118	120	136	138	140	159	161	163	
<i>Asterionella glacialis</i>	0	0	0	6	9	0	0	5	0	8		6	0	0	1	0	0
<i>Biddulphia</i> sp.	0	0	0	0	0	0	0	0	0	0		0	0	0	0	0	0
<i>Chaetoceros deciprens</i>	0	0	4	0	0	0	0	10	0	0		0	0	0	0	0	0
<i>Chaetoceros</i> spp.	622	1259	973	598	782	533	824	1059	810	383		24	12	14	305	283	191
<i>Cocconeis</i> sp.	0	0	0	0	0	0	0	0	0	0		0	0	0	0	0	0
<i>Eucampia</i> spp.	0	1	3	0	0	5	1	0	3	0		0	0	0	0	0	3
<i>Fragilariopsis</i> sp.	61	13	15	15	67	49	6	30	17	0		0	0	0	13	0	28
<i>Granulatophora</i> sp.	3	0	0	0	0	0	0	0	0	0		0	0	0	0	0	0
<i>Leptocylindrus danicus</i>	18	14	30	13	22	9	32	10	0	0		3	6	4	101	74	31
<i>Leptocylindrus minimus</i>	0	10	0	31	4	13	4	31	32	26		0	0	0	0	0	0
<i>Licmophora glacialis</i>	0	0	0	0	0	0	0	0	0	0		0	0	0	0	0	0
<i>Navicula</i> spp.	1	4	1	4	1	0	0	0	3	0		0	0	0	0	0	0
<i>Pseudo-nitzschia</i> spp.	172	301	287	201	287	208	293	501	371	185		17	7	3	81	89	81
<i>Rhizosolenia fragilissima</i>	0	1	10	1	9	3	6	5	9	1		1	0	2	402	177	155
<i>Rhizosolenia stouterforthii</i>	0	0	0	3	0	0	0	0	0	0		0	0	0	0	0	0
<i>Skeletonema costatum</i>	4810	5619	3122	4271	3708	3250	3010	4664	2816	1149		3	0	0	86	51	60
<i>Stephanopyxis nipponica</i>	0	3	0	0	1	0	3	3	0	0		0	0	0	0	3	0
<i>Thalassionema nitzschioides</i>	0	0	0	15	0	5	0	0	0	0		0	0	0	0	5	0
<i>Thalassiosira</i> spp.	176	182	280	223	187	156	289	436	226	120		1	0	0	1	4	0
Unidentified centric	0	0	0	3	0	0	0	0	0	0		0	0	0	0	0	0
Unidentified pennate	0	0	0	0	0	0	0	0	0	0		0	0	0	0	0	0
<i>Ceratium furca</i>	0	0	0	0	0	0	0	0	0	0		0	0	0	1	0	0
<i>Ceratium</i> spp.	0	0	0	0	0	0	1	0	0	0		0	0	0	0	0	0
<i>Distephanus speculum</i>	0	0	0	0	3	0	0	0	0	0		0	0	0	1	1	4
<i>Ebria tripartita</i>	0	0	0	1	0	0	0	0	0	0		0	0	0	0	0	0
<i>Peridinium</i> spp.	0	0	0	0	0	0	0	0	0	0		0	0	0	0	0	0
Unidentified dinoflagellates	0	0	0	3	0	3	6	6	9	3		1	2	1	8	0	8
Unidentified flagellates	546	702	481	1576	1548	1262	1502	1761	783	501		410	542	301	959	722	494

APPENDIX 3

Abundance Calculations

- 1). The dimensions of the settling chamber were determined using a Mitutoya caliper.

$$\text{Diameter} = 25.5 \text{ mm}$$

$$\text{Radius} = 12.75 \text{ mm}$$

$$\text{Area of the settling chamber} = 510.7 \text{ mm}^2$$

- 2). A rectangular box in the eyepiece of the inverted microscope (field of view) was used when counting phytoplankton cells. Using a micrometer, the dimensions of the field of view were determined to equal 0.44 mm (L) x 0.31 mm (W) on 200 x magnification and 0.220 mm (L) x 0.155 mm (W) on 400 x magnification. The area inside the field of view equaled 0.1364 mm^2 on 200 x and 0.0341 mm^2 on 400 x.

- 3). Area of each transact sampled was determined:

$$200 \text{ x: Total sample area} = (\# \text{ of fields viewed}) * .1364 \text{ mm}^2$$

$$400 \text{ x: Total sample area} = (\# \text{ of fields viewed}) * .0341 \text{ mm}^2$$

- 4). Total abundance for the entire sample was calculated by using the equation:

$$\text{Abundance (cells/mL)} = \frac{(\text{area settling chamber} / \text{total sample area}) * \# \text{ of cells counted}}{\text{settled sample volume (mL)}}$$

Chapter 4

The Role of Zooplankton

Exxon Valdez Oil Spill
Restoration Project Annual Report

Sound Ecosystem Assessment (SEA): The Role of Zooplankton
Restoration Project 97320-H
Annual Report

This annual report has been prepared for peer review as part of the Exxon Valdez Oil Spill Trustee Council restoration program for the purpose of assessing project progress. Peer review comments have not been addressed in this annual report.

Robert T. Cooney
Kenneth Coyle
Institute of Marine Science
University of Alaska Fairbanks
Fairbanks, Alaska 99775-7220

April 1998

Sound Ecosystem Assessment (SEA): The Role of Zooplankton
Restoration Project 97320-H
Annual Report

Study History: Project 320-H was established in FY 94 as a core study in the Sound Ecosystem Assessment (SEA) program. The intent of the work has been to demonstrate the role of macrozooplankton in processes supporting the production of pink salmon and herring in Prince William Sound. Zooplankton serves as food for many fish, bird and marine mammal stocks. SEA is investigating it's importance as forage for juvenile pink salmon and herring, and as alternative prey for consumers that also prey on juvenile pink salmon and herring in seasonally-varying complex food-webs. Previous annual reports of project 320-H appear in the SEA annual report series for 1994, 95, and 96. The project will complete a Final Report of all findings in FY 99. That report will include work completed in FY 98.

Abstract: Support for studies of the role of zooplankton in FY 97 emphasized the analysis of data collected in previous years, while diminishing the field activities. Zooplankton samples were only collected during a May oceanographic cruise, and from the AFK hatchery located on Evans Island. These activities reflect the shift in SEA tasks from field investigations to data analysis in the last two fully funded years. Observations from all locations and years were pooled by month to describe changing patterns in community composition and standing stock information needed to assess important linkages between forage supplies and growth and survival of juvenile pink salmon and herring. A manuscript describing patchiness in upper-layer calanoid populations was prepared and is now in review. This work addresses additional questions about patch-dependent feeding as input to models describing juvenile pink salmon survival as a function of predator prey switching. As part of a cooperative investigation of the target strengths of dominant macrozooplankters, project H is supplying information on the sizes of copepodite stages 4 and 5 *Neocalanus plumchrus* and *N. flemingeri*, juvenile euphausiids and pteropods to Dr. Kirsch (project N). Finally, the relationship between upwelling and south-Sound zooplankton stocks in April and May was updated. The regression has explained less variability over the SEA years than previously. The reasons for this change are being investigated.

Key Words: Zooplankton, macrozooplankton, SEA, *Neocalanus*, modeling

Project Data: Project H data resides in the SEA data base, and also in the Institute of Marine Science, University of Alaska Fairbanks, data base. All samples collected by the project have been processed in the laboratory and placed in these electronic archives.

Citation: Cooney, R.. T. 1998. Sound Ecosystem Assessment (SEA):The Role of Zooplankton, Exxon Valdez Oil Spill restoration project Annual Report (320-H), Institute of Marine Science, University of Alaska Fairbanks, Fairbanks, Alaska, 99775-7220.

Table of Contents

Executive Summary	4
Objectives	4
Methods	4
Results	5
Discussion	7
Conclusions	8
Acknowledgments	8
References	9
Appendix I. (attached); Vertical Patchiness in Populations of Large Calanoida in Coastal Waters of the Northern Gulf of Alaska in Spring - Prepared for the Journal of Plankton Research.	

Executive Summary

Work in 1997 focused on four areas: 1) further descriptions of the layering and swarming behavior of large calanoids developing in the upper 50 m of Prince William Sound and in the adjacent coastal waters; 2) describing seasonal changes (numbers and biomass) in upper-layer zooplankton communities; 3) examining the degree of overlap between zooplankton communities sampled in embayments and from the open Sound; and 4) updating the Lake/River statistical relationship. The results of these investigations are reported here.

Objectives

The following general objectives were approved in the FY 97 DPD:

1. Provide information on the vertical and horizontal distributions of selected zooplankters, their sizes, and descriptions of seasonal changes in the composition of macrozooplankton in the upper 50 m of Prince William Sound.
2. Work collaboratively with SEA modeling projects to provide data on the seasonal, horizontal, and vertical compression of biomass serving as patch-dependent forage opportunities for juvenile pink salmon, herring and other planktivores in Prince William Sound.
3. Assist other projects determine the degree to which the open-Sound zooplankton community influences the growth and survival of juvenile herring rearing in edge-zone nursery areas.

Methods

Field collections of zooplankton follow procedures established in 1995 for the conduct of oceanographic cruises operating under SEA funding. A *Bering Explorer* cruise in May, and a collection from the AFK hatchery on Evan's Island provided the only samples taken in FY 97. Samples were processed in the UAF plankton laboratory and the results posted in IMS and SEA data bases.

Results

Vertical Patchiness. Collections obtained using a MOCNESS sampler in May, 1996 were analyzed to further evaluate the degree to which late stage *Neocalanus*, *Calanus* and *Eucalanus* exhibit tendencies to form distinct layers in Prince William Sound and over the adjacent shelf (Appendix I). There was considerable variability over the region, but the vertical patterns previously reported (SEA96) were reaffirmed. Locations sampled in Knight Island Passage and in the northwestern portion of the Sound consistently exhibited high average layer values of abundance and biomass for a composite of a mixture of stage V *Neocalanus flemingeri* and *N. plumchrus*; 568 individuals m^{-3} , and 1.63 g m^{-3} . The highest value for this composite occurred in

the surface waters at the edge of the continental shelf near Middleton Island (1286 individuals m^{-3} ; 3.64 g m^{-3}), while the lowest densities were encountered in southwestern Montague Strait and in Unakwik Inlet (< 25 individual m^{-3} , and < 0.05 g m^{-3}). Stations in the central and eastern portions of Prince William Sound exhibited numbers and biomasses ranging between these highs and lows.

Seasonal Succession. Seasonal changes in the numbers and biomass of the dominant contributors to macrozooplankton populations in Prince William Sound were determined by averaging all shipboard and hatchery collections across the years 1994, 95, 96 and 97 by month. The top 15 taxonomic categories (number and biomass) were then examined for seasonal changes. There were no samples available for the months of January, August and November.

Numbers and biomass were very low in the cold, well-mixed upper 50 m in February (Table 1). Gastropod larvae (undetermined species) and stage 1 copepodites of the Calanidae (probably *Neocalanus*) were the most numerous taxa at about 10 m^{-3} . Because of their size and number, gastropod larvae and adult female *Metridia pacifica* (copepoda) dominated the biomass. The remainder of top 15 taxa were comprised of species and groups common to other seasons, but occurring in very dilute quantities in winter.

By March, Calanidae stages 1 and 2 were obvious (ranked 1 and 4 by abundance respectively) signaling the beginning of the production cycle for *Neocalanus* in the surface waters (Table 2). The biomass was dominated by the large calanoid *Metridia okhotensis* (adult females) and barnacle nauplii, the latter a member of the meroplankton and a somewhat surprising member of the open water community. *Pseudocalanus* spp. (copepoda) was present in the upper 15 ranked taxa by biomass and abundance. This small copepod will dominate the plankton numerically in the months that follow.

By April, high numbers of euphausiid eggs signal reproduction for several species (genus *Thysanoessa* and *Euphausia*) in Prince William Sound (Table 3). *Pseudocalanus* spp. and bryozoan larvae exhibited numbers in excess of 100 individuals m^{-3} . The biomass in April was dominated by the maturing copepodite stages of *Neocalanus plumchrus* and *N. flemingeri* (4 and 5) as these populations build toward seasonally high biomass in May. *Calanus marshallae* was also contributing to the biomass at this time.

In May, abundance values for some species and composites have exceeded 500 m^{-3} (Table 4). Numbers in the upper 50 m are dominated by *Pseudocalanus* spp. (several late stages), while stage 5 *Neocalanus plumchrus* and *N. flemingeri* dominate the biomass; > 100 mg m^{-3} . Some neritic copepods like *Acartia* spp., are beginning to appear in appreciable numbers as the upper layers freshen and warm.

The community composition has shifted to more neritic species by June (Table 5). *Pseudocalanus* spp. claims seasonal highs, but *Evadne* (Cladocera), *Acartia* spp. and *Oikopleura* (Larvacea) are also ranked in the upper 50 by abundance. Because of its high numbers,

Pseudocalanus also dominates the biomass in June, but the pteropod, *Limicina helicina* is a close second. *Neocalanus* falls precipitously in the rankings, as stage 5 copepodites leave the upper layers for overwintering depths. July is similar to June in the composition of the zooplankton community in the upper 50 m (Table 6). However, seasonally high numbers and biomass are beginning to decline.

In September (August missing) *Pseudocalanus* spp. and *Acartia* spp. continue to be the most abundant zooplankters, but most numbers have fallen below 100 individuals m⁻³ (Table 7). Biomass is led by *Pseudocalanus*, but different taxa like ctenophores and *Sagitta elegans* are prominent contributors. Later in October, *Pseudocalanus* spp. and *Metridia pacifica* rank high in numerical abundance and biomass (Table 8).

December completes the year (November missing) with *Pseudocalanus* again dominating the now greatly diminished numbers; < 25 individuals m⁻³. The medium-sized subtropical copepod *Mesocalanus tenuicornis*, and *Euphausia pacific* and *Metridia* spp. stage V lead the biomass rankings (Table 9). The late fall and early winter community contains more jelly plankton, euphausiids and amphipods than were found in other seasons. Presumably, some of these contributors appear when more of the sampling is conducted after dark (short day-length in December).

Nearshore/Offshore Comparisons. Work conducted by the SEA Herring sub-group (see project T) reports that juveniles rearing in embayments derive a large percentage of their energy from plankters that seem to prefer a shallow, edge-zone habitat. When rankings by biomass are compared between the open water zooplankton community (upper 50 m) with that sampled at the herring study sites (upper 30 m), it is evident that the overlap in highly ranked species is generally less than 50% by site, location in the bay (inner, middle and outer) and season (Table 10). There appears to be no seasonal or within-bay patterns that emerge from this comparison. Overall, Whale Bay exhibited the highest overlap (49 % common species), while Simpson Bay showed the least (37%). A more comprehensive analysis will be needed to explain these differences.

The Lake/River Problem. One of the most puzzling problems that project H has been investigating is the process that manifests as the Lake/River phenomenon. In 1993 when the SEA program was developed, a strong statistical correlation was observed between spring-time zooplankton stocks measured at the AFK hatchery and the April/May upwelling index computed for a location on the shelf just east of Prince William Sound. Spring-time settled volumes tended to be much higher at AFK during years when the upwelling index was most positive, and lower when the index was negative. SEA interpreted this relationship to capture relative rates at which locally reproducing zooplankton stocks were flushed from the region each year by the wind-forced coastal flow. When the onwelling was strongest (most negative upwelling indices), more of the Sound would become involved by the intruding coastal flow (river-like) presumably removing larger amounts of upper layer plankton than when the flushing rates were low (more positive upwelling indices). Under less intense flushing (lake-like) stocks were consistently

higher at the south Sound index station.

Since April, 1994, the r^2 value for the Lake/River relationship has fallen from approximately 0.80 to less than 0.60 (Figure 1). Apparently, the relationship has been compromised by data acquired during the SEA sampling period, 1994-97. While it is not clear what has happened, the regression predicted that 1997 would be a very high (lake-like) zooplankton year. Those numbers failed to materialize. In fact, 1989 was the last time that zooplankton populations were extraordinarily high in the Sound. The lack of a strong zooplankton year has precluded directly evaluating the conditions that cause this to happen. Our synthesis work will involve experimental studies with the SEA biophysical model and I have hopes that we may be able to explain, or partially explain the Lake/River phenomenon using this approach.

Discussion

The subarctic pelagic ecosystem is characterized by intense seasonality and the compression of plankton biomass into short bursts of production and accumulation near the ocean surface. A continuing study of patch-dependent foraging opportunities arising from predictable zooplankton patchiness focuses much of the sea modeling efforts. We are now aware that discrete layers of large calanoids (*Neocalanus*, *Calanus* and *Eucalanus* spp.) develop in the upper 50 m of Prince William Sound each spring as part of the one-year life cycles of these animals. These layers are visited by adult pollock recharging their post-spawning energy reserves, and probably by other consumers in the system as well. Our sampling, and observations by the PWSAC hatchery plankton watch program consistently demonstrate high stocks of *Neocalanus* spp. in the northwestern corner of the Sound. It now seems likely that a large percentage of these stocks arise from local deepwater reproduction beginning in February. The predictability of this forage resource is probably responsible for attracting adult pollock into the northern reaches of Knight Island Passage, and around the Perry Island, Lone Island and Port Wells areas during the spring.

A general seasonal picture of upper-layer zooplankton stocks is emerging as the result of SEA collections. February and March represent times of minimal numbers and biomass. However, even at this time, the "seeds" of the coming zooplankton production cycle are in place. April is a time of euphausiid spawning, with huge numbers of eggs occurring in the upper 50 m. April also sees the beginning of *Pseudocalanus* production, and seasonal highs in the numbers of *Neocalanus*. April is also the time of the phytoplankton bloom (see project G report) marking the end of the overwintering period for juvenile herring. Finally, the wild salmon out-migration from natal stream begins in April, with juveniles schooling in nearshore nursery areas. By May, *Neocalanus* has progressed to stage V and dominates the upper-layer animal plankton biomass. Pteropods and larvaceans appear in May, and *Pseudocalanus* populations expand. By June and July, most of the larger calanoids have left the upper water column for overwintering depths and are replaced by pteropods, larvaceans, cladocerans, and seasonal highs in *Pseudocalanus* and *Acartia*. This is the time that surface waters reach seasonal thermal highs and continue to become diluted by runoff. By September and October, the water column is about as fresh as it will become. Plankton stocks are falling rapidly, but are still dominated numerically by

Pseudocalanus, although a variety of other taxa now contribute. A fall phytoplankton bloom with implications for fall feeding juvenile herring may occur from September - November (see report of project G, T). By December, upper-layer stocks of zooplankton have declined to near-seasonal lows. *Pseudocalanus* and *Mesocalanus* dominate, but abundance falls below 25 individuals m^{-3} and a few mg m^{-3} . The winter hiatus has returned. This is the time that juvenile herring are presumably fasting in their nearshore refuges.

Comparisons between the community composition described by rankings of biomass in inshore and offshore zooplankton stocks indicate the nearshore regions are dominated by different species at all locations and seasons. An overlap in the rankings of less than 50% may be partially accounted for by the presence of the planktonic stages of intertidal and shallow sub-tidal invertebrates in the shallow environments. This possibility is being studied (see project T).

The Lake/River relationship continues unresolved. Since the beginning of SEA the statistical correlation between the strength of the upwelling index computed from observed sea-surface pressure and spring-time stocks of zooplankton at AFK has been going down. The implications of this change remain obscure. However, a recent publication by Hayward (1997) discusses regime shifts in the Pacific ocean and may prove useful in determining whether major changes have occurred in the subarctic environment since the oil spill in 1989. Also, an interesting mechanism explaining differences in salmon production between Alaska and Washington waters has been articulated by Gargett (1997). The mechanism involves different and opposite responses to atmospheric forcing and the deepening of the nutricline in these two regions. Her analysis indicates that when production is stimulated in a region by increased nutrient input (bottom-up forcing), the overall production cycle is favored and salmon production increases. SEA has investigated the latter phenomenon (increased consumer production) and has documented why the survivals of salmon should increase under these conditions.

Conclusions

Project H continues to make progress toward understanding and describing the upper-layer net zooplankton community and its role in Prince William Sound. Work completed in 1997 included a detailed description of season changes and layering phenomena by many of the larger calanoid species and consideration of onshore/offshore distributions. These results provide information about seasonally varying forage resources that many of the other consumers in the system track and utilize. The information is being shared with other components of SEA, particularly the juvenile salmon work (project E) and the numerical modeling (projects R, J and T).

Acknowledgments

The assistance of Dr. Ken Coyle, Chris Stark, David Parker and Elizabeth Stockmar is acknowledged for sample processing and data analyses.

References

- Gargett, A. E. 1997. Physics to fish: interactions between physics and biology on a variety of scales. *Oceanography* 10(3): 128-131.
- Hayward, T. L. 1997. Pacific ocean climate change: atmospheric forcing, ocean circulation and ecosystem response. *Tree* 12(4): 150-154.

Table 1.

ZOOPLANKTON SPECIES COMPOSITION OPEN SOUND STATIONS -February			
ABUNDANCE (No./m3)		BIOMASS (g/m3)	
Gastropod larvae	12.6	Gastropod larvae	0.0022
Calanidae I	9.4	<i>Metridia pacifica</i> AF	0.0014
<i>Pseudocalanus</i> spp. AF	8.3	<i>Pseudocalanus</i> spp. AF	0.0009
<i>Oithona</i> spp. copepodites	4.8	<i>Thysanoessa longipes</i>	0.0005
<i>Pseudocalanus</i> spp. V	4.4	<i>Pseudocalanus</i> spp. V	0.0004
Bivalve larvae	3.6	<i>Calanus marshallae</i> V	0.0003
<i>Oithona similis</i> AF	2.7	Calanidae I	0.0003
<i>Acartia longiremis</i> AF	2.0	<i>Metridia okhotensis</i> AF	0.0003
<i>Metridia pacifica</i> AF	1.7	<i>Metridia</i> spp. V	0.0002
Bryozoan larvae	1.5	Hydromedusae	0.0002
<i>Microcalanus</i> sp.	1.4	<i>Acartia longiremis</i> AF	0.0001
<i>Pseudocalanus</i> spp. IV	1.4	<i>Limacina helicina</i> juv	0.0001
<i>Podon</i> sp.	1.3	Barnacle nauplii	0.0001
<i>Pseudocalanus</i> spp. AM	0.9	<i>Aglantha digitale</i>	0.0001
<i>Limacina helicina</i> juv	0.8	<i>Oikopleura</i> sp.	0.0001

Table 2.

ZOOPLANKTON SPECIES COMPOSITION OPEN SOUND STATIONS -March			
ABUNDANCE (No./m3)		BIOMASS (g/m3)	
Calanidae I	56.1	<i>Metridia okhotensis</i> AF	0.0139
Barnacle nauplii	31.8	Barnacle nauplii	0.0060
Bryzoan larvae	25.1	<i>Calanus marshallae</i> AF	0.0024
Calanidae II	23.0	<i>Pseudocalanus</i> spp. AF	0.0023
<i>Pseudocalanus</i> spp. AF	22.2	Calanidae I	0.0018
Euphausiid eggs	21.7	Calanidae II	0.0016
<i>Pseudocalanus</i> spp. V	11.7	<i>Metridia pacifica</i> AF	0.0013
<i>Mertidia okhotensis</i> AF	7.4	<i>Thysanoessa longipes</i>	0.0012
<i>Oithona similis</i> AF	7.0	<i>Thysanoessa spinifera</i>	0.0012
<i>Oithona</i> spp. copepodites	5.2	<i>Neocalanus</i> spp. III	0.0011
<i>Oithona similis</i> V	4.9	<i>Pseudocalanus</i> spp. V	0.0010
<i>Neocalanus</i> spp. III	4.9	<i>Sagitta elegans</i>	0.0009
<i>Pseudocalanus</i> spp. IV	4.1	<i>Parathemisto libellula</i>	0.0007
<i>Pseudocalanus</i> spp. AM	3.6	<i>Aglantha digitale</i>	0.0006
Euphausiid nauplii	3.4	<i>Thysanoessa inermis</i>	0.0006

Table 3.

ZOOPLANKTON SPECIES COMPOSITION OPEN SOUND STATIONS - April			
ABUNDANCE (No./m3)		BIOMASS (g/m3)	
Euphausiid eggs	232.7	<i>Neocalanus</i> spp. IV	0.0362
<i>Pseudocalanus</i> spp. V	121.9	<i>Neocalanus</i> p/f V	0.0343
<i>Pseudocalanus</i> spp. IV	120.7	<i>Metridia okhotensis</i> AF	0.0303
Bryozoan larvae	102.8	<i>Neocalanus</i> spp. III	0.0161
<i>Pseudocalanus</i> spp. III	100.6	Barnacle nauplii	0.0154
Barnacle nauplii	81.1	<i>Pseudocalanus</i> spp. V	0.0107
<i>Neocalanus</i> spp. III	72.7	<i>Calanus marshallae</i> AF	0.0095
Calanidae II	65.3	<i>Pseudocalanus</i> spp. AF	0.0064
<i>Pseudocalanus</i> spp. AF	62.7	<i>Pseudocalanus</i> spp. IV	0.0064
<i>Oithona similis</i> AF	56.9	<i>Sagitta elegans</i>	0.0057
<i>Pseudocalanus</i> spp. II	45.5	Euphausiid eggs	0.0049
<i>Neocalanus</i> spp. IV	43.7	Calanidae II	0.0046
Euphausiid nauplii	41.5	<i>Pseudocalanus</i> spp. III	0.0035
Calanidae I	35.4	Fish eggs	0.0028
<i>Oithona</i> spp. copepodites	28.7	<i>Metridia pacifica</i> AF	0.0028

Table 4.

ZOOPLANKTON SPECIES COMPOSITION OPEN SOUND STATIONS -May			
ABUNDANCE (No./m3)		BIOMASS (g/m3)	
<i>Pseudocalanus</i> spp. V	537.6	<i>Neocalanus p/f</i> V	0.1305
<i>Pseudocalanus</i> spp. IV	393.6	<i>Pseudocalanus</i> spp. V	0.0745
<i>Pseudocalanus</i> spp. AF	259.3	<i>Pseudocalanus</i> spp. AF	0.0267
<i>Pseudocalanus</i> spp. III	171.9	<i>Neocalanus</i> spp. IV	0.0234
Bryozoan larvae	133.1	<i>Pseudocalanus</i> spp. IV	0.0209
<i>Pseudocalanus</i> spp. AM	123.5	Euphausiid calyptopis	0.0111
<i>Acartia longiremis</i> AM	103.6	<i>Metridia okhotensis</i> AF	0.0097
<i>Acartia</i> spp. V	100.4	<i>Calanus marshallae</i> V	0.0091
<i>Acartia longiremis</i> AF	98.1	<i>Calanus marshallae</i> IV	0.0081
<i>Fritilaria</i> sp.	92.5	<i>Acartia longiremis</i> AF	0.0072
Euphausiid nauplii	85.6	<i>Limacina helicina</i> juv	0.0069
<i>Acartia</i> spp. IV	80.1	<i>Oikopleura</i> sp.	0.0063
<i>Oithona similis</i> AF	73.4	<i>Neocalanus cristatus</i> V	0.0062
Euphausiid eggs	73.2	<i>Calanus marshallae</i> AF	0.0061
Euphausiid calyptopis	67.3	<i>Pseudocalanus</i> spp. III	0.0060

Table 5.

ZOOPLANKTON SPECIES COMPOSITION OPEN SOUND STATIONS -June			
ABUNDANCE (No./m3)		BIOMASS (g/m3)	
<i>Pseudocalanus</i> spp. V	1179.9	<i>Pseudocalanus</i> spp. V	0.1032
<i>Pseudocalanus</i> spp. AF	799.7	<i>Pseudocalanus</i> spp. AF	0.0824
<i>Pseudocalanus</i> spp. IV	683.5	<i>Limacina helicina</i> juv	0.0680
<i>Limacina helicina</i> juv	393.2	<i>Limacina helicina</i>	0.0584
<i>Pseudocalanus</i> spp. III	302.7	<i>Pseudocalanus</i> spp. IV	0.0363
<i>Pseudocalanus</i> spp. AM	292.4	<i>Neocalanus</i> p/f V	0.0219
<i>Evadne</i> sp.	236.3	<i>Calanus marshallae</i> V	0.0215
<i>Acartia longiremis</i> AF	216.3	<i>Sagitta elegans</i>	0.0184
<i>Acartia longiremis</i> AM	185.0	<i>Aglantha digitale</i>	0.0182
<i>Oithona similis</i> AF	150.5	<i>Acartia longiremis</i> AF	0.0160
<i>Acartia</i> spp. V	125.1	<i>Aequorea</i> sp.	0.0141
<i>Oikopleura</i> sp.	71.2	<i>Pseudocalanus</i> spp. AM	0.0135
<i>Acartia</i> spp. IV	66.0	<i>Pseudocalanus</i> spp. III	0.0107
<i>Oithona</i> spp. copepodites	63.1	<i>Metridia</i> spp. V	0.0093
Bivalve larvae	53.6	<i>Oikopleura</i> sp.	0.0092

Table 6.

ZOOPLANKTON SPECIES COMPOSITION OPEN SOUND STATIONS -July			
ABUNDANCE (No./m3)		BIOMASS (g/m3)	
<i>Pseudocalanus</i> spp. AF	837.2	<i>Pseudocalanus</i> spp.AF	0.0862
<i>Pseudocalanus</i> spp. V	523.3	<i>Pseudocalanus</i> spp. V	0.0458
<i>Oithona similis</i> AF	246.8	<i>Limacina helicina</i> juv	0.0360
<i>Pseudocalanus</i> spp. IV	219.1	<i>Limacina helicina</i>	0.0323
<i>Limacina helicina</i> juv	216.3	<i>Oikopleura</i> sp.	0.0270
<i>Pseudocalanus</i> spp. AM	187.1	<i>Pseudocalanus</i> spp. IV	0.0116
<i>Pseudocalanus</i> spp. III	112.1	<i>Phacellophora cantschatica</i>	0.0094
Euphausiid eggs	108.0	<i>Pseudocalanus</i> spp. AM	0.0087
<i>Acartia longiremis</i> AF	104.0	<i>Calanus marshallae</i> V	0.0078
<i>Acartia</i> spp. V	72.0	<i>Acartia longiremis</i> AF	0.0078
<i>Oikopleura</i> sp.	69.6	<i>Eirene indicans</i>	0.0070
<i>Acartia</i> spp. IV	69.2	<i>Sagitta elegans</i>	0.0061
<i>Evadne</i> sp.	65.0	Barnacle nauplii	0.0056
<i>Limacina helicina</i>	52.7	Ctenophora	0.0044
<i>Acartia longiremis</i> AM	52.5	<i>Pseudocalanus</i> spp. III	0.0040

Table 7.

ZOOPLANKTON SPECIES COMPOSITION OPEN SOUND STATIONS -September			
ABUNDANCE (No./m3)		BIOMASS (g/m3)	
<i>Pseudocalanus</i> spp. AF	190.2	<i>Pseudocalanus</i> spp.AF	0.0196
<i>Pseudocalanus</i> spp. V	17.9	Ctenophora	0.0085
<i>Pseudocalanus</i> spp. AM	15.9	<i>Sagitta elegans</i>	0.0085
<i>Acartia longiremis</i> AF	13.8	<i>Metridia</i> spp. V	0.0051
<i>Metridia</i> spp. V	13.3	Siphonophora	0.0029
<i>Oikopleura</i> sp.	12.2	<i>Thysanoessa spinifera</i>	0.0024
<i>Limacina helicina</i> juv	10.2	<i>Melicerium campanula</i>	0.0021
<i>Metridia</i> spp. IV	9.8	<i>Calanus pacificus</i> V	0.0021
<i>Metridia</i> spp. III	8.6	<i>Euchaeta elongata</i> V	0.0019
<i>Acartia longiremis</i> AM	7.9	<i>Calanus marshallae</i> IV	0.0018
<i>Calanus pacificus</i> V	5.1	<i>Eirene indicans</i>	0.0016
<i>Metridia pacifica</i> AF	4.8	<i>Pseudocalanus</i> spp. V	0.0015
<i>Calanus marshallae</i> IV	4.5	<i>Limacina helicina</i> juv	0.0013
Euphausiid eggs	4.3	Euphausiid furcillia	0.0013
<i>Calanus marshallae</i> V	3.9	<i>Lar flavicirratu</i>	0.0013

Table 8.

ZOOPLANKTON SPECIES COMPOSITION OPEN SOUND STATIONS -October			
ABUNDANCE (No./m3)		BIOMASS (g/m3)	
<i>Pseudocalanus</i> spp. AF	121.1	<i>Metridia pacifica</i> AF	0.0229
<i>Metridia pacifica</i> AF	29.1	<i>Pseudocalanus</i> spp. AF	0.0125
<i>Acartia longiremis</i> AF	22.3	<i>Oikopleura</i> sp.	0.0097
<i>Oikopleura</i> sp.	19.1	<i>Metridia</i> spp. V	0.0065
<i>Metridia</i> spp. V	17.1	Ctenophora	0.0058
<i>Pseudocalanus</i> spp. V	11.6	<i>Sagitta elegans</i>	0.0057
<i>Acartia longiremis</i> AM	7.4	<i>Aglantha digitale</i>	0.0026
<i>Metridia</i> spp. IV	6.7	Siphonophora	0.0025
<i>Calanus marshallae</i> III	6.2	<i>Parathemisto pacifica</i>	0.0024
<i>Pseudocalanus</i> spp. AM	5.9	<i>Thysanoessa raschii</i>	0.0022
<i>Metridia</i> spp. III	5.2	<i>Thysanoessa longipes</i>	0.0020
<i>Calanus marshallae</i> IV	4.1	<i>Gaetanus intermedius</i> V	0.0020
<i>Oithona spinirostris</i> AF	3.8	<i>Calanus marshallae</i> III	0.0019
<i>Acartia</i> spp. V	3.0	<i>Calanus marshallae</i> V	0.0018
Calanidae II	2.4	<i>Calanus marshallae</i> IV	0.0017

Table 9.

ZOOPLANKTON SPECIES COMPOSITION OPEN SOUND STATIONS -December			
ABUNDANCE (No./m3)		BIOMASS (g/m3)	
<i>Pseudocalanus</i> spp. AF	24.8	<i>Mesocalanus tenuicornis</i>	0.0118
<i>Mesocalanus tenuicornis</i>	18.1	<i>Euphausia pacifica</i>	0.0094
<i>Metridia</i> spp. V	15.8	<i>Metridia</i> spp. V	0.0060
<i>Metridia</i> spp. IV	11.2	<i>Thysanoessa inermis</i>	0.0046
<i>Pseudocalanus</i> spp. V	5.3	<i>Cyphocaris challengerii</i>	0.0043
<i>Metridia</i> spp. III	5.2	<i>Metridia pacifica</i> AF	0.0035
<i>Aglantha digitale</i>	4.8	<i>Sagitta elegans</i>	0.0031
<i>Metridia pacifica</i> AF	4.4	<i>Pseudocalanus</i> spp. AF	0.0026
<i>Oithona spinirostris</i> AF	2.9	<i>Parathemisto libellula</i>	0.0018
<i>Limacina helicina</i> juv	2.7	<i>Thysanoessa raschii</i>	0.0016
<i>Acartia longiremis</i> AF	2.1	<i>Dimophyes arctica</i>	0.0013
<i>Pseudocalanus</i> spp. IV	1.9	<i>Aglantha digitale</i>	0.0012
<i>Limacina helicina</i>	1.8	<i>Metridia</i> spp. IV	0.0012
Gastropod larvae	1.3	<i>Limacina helicina</i>	0.0011
<i>Sagitta elegans</i>	1.3	<i>Aegina rosea</i>	0.0011

Table 10.

Number of the top 15 ranked open-water zooplankters (biomass) also occurring in the top 15 ranked zooplankters (biomass) from the SEA Herring study bays			
<i>Month</i>	<i>Inner Bay</i>	<i>Middle Bay</i>	<i>Outer Bay</i>
Eaglek Bay (6.0)*			
February	Missing	Missing	Missing
May	5	4	5
July	7	9	7
October	5	7	5
Simpson Bay (5.5)			
February	5	7	6
May	5	5	5
July	7	8	7
October	2	4	Missing
Whale Bay (7.4)			
February	8	9	8
May	Missing	7	7
July	6	8	9
October	8	7	4
Zaikof Bay (6.3)			
February	8	7	5
May	6	5	5
July	7	7	9
October	5	5	7
* = Average of all comparisons within a site			

April/May Zooplankton on April/May UW Index

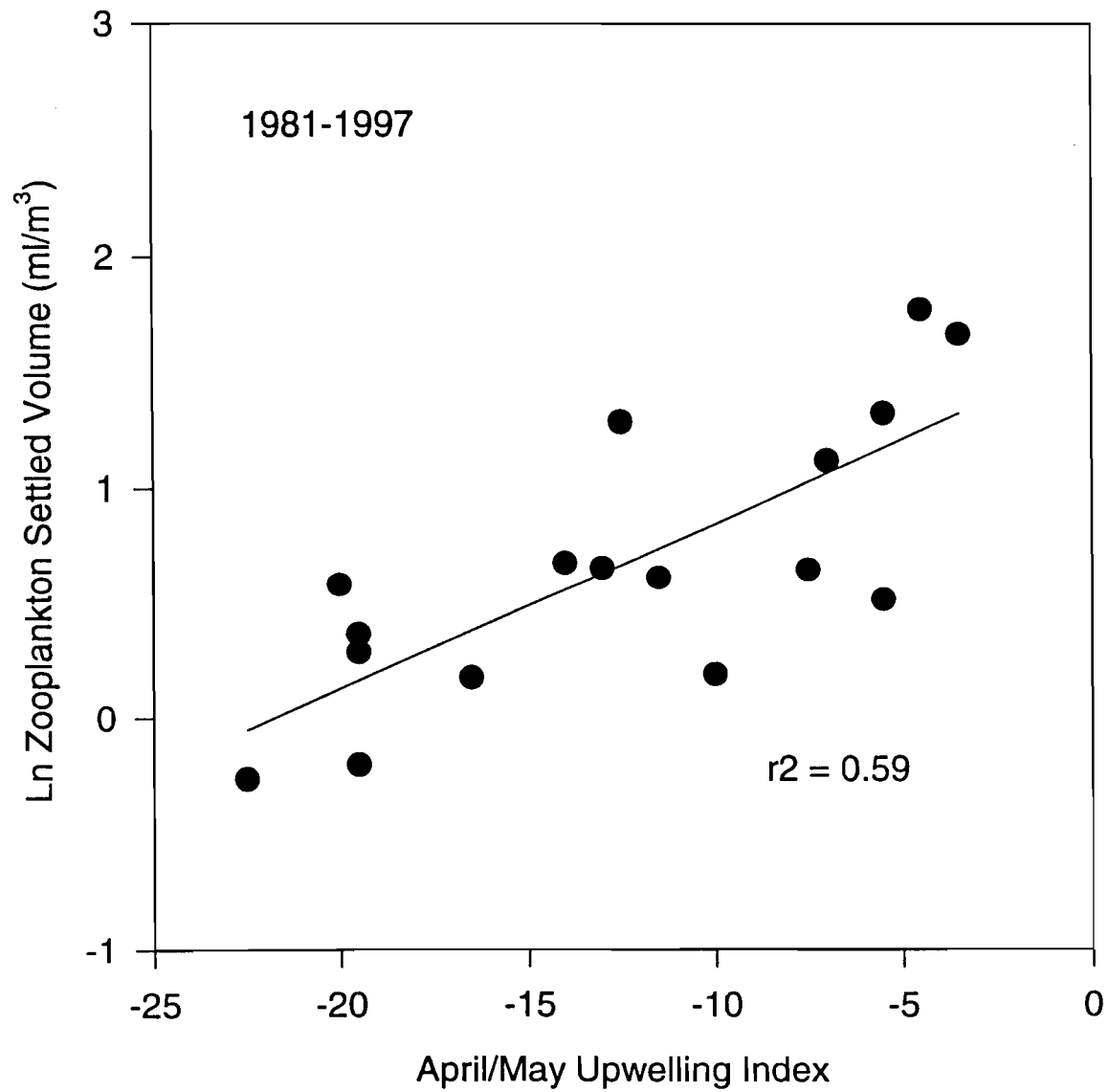


Figure 1. The relationship between zooplankton settled volumes measured at the AFK Hatchery and the upwelling index calculated for a location on the shelf south and east of Prince William Sound, Alaska; 1981-97.

Project 320-H

Appendix 1 (attachment)

Vertical Patchiness in Populations of Large Calanoida in Coastal Waters of
the Northern Gulf of Alaska in Spring

R. Ted Cooney, Kenneth O. Coyle and Elizabeth Stockmar

Institute of Marine Science
University of Alaska Fairbanks
Fairbanks, Alaska 99775

Submitted to the Journal of Plankton Research

April 1998

Vertical Patchiness in Populations of Large Calanoida in Coastal Waters of
the Northern Gulf of Alaska in Spring

R. Ted Cooney, Kenneth O. Coyle and Elizabeth Stockmar

Institute of Marine Science
University of Alaska Fairbanks
Fairbanks, Alaska 99775

Abstract

A suite of large copepods, representing the mid to late copepodite stages of *Neocalanus*, *Eucalanus* and *Calanus* were frequently encountered in distinct strata in the upper 50 m of Prince William Sound and adjacent coastal waters in early May, 1996. *Neocalanus flemingeri* and *N. plumchrus* stage V contributed a large proportion of the numbers and were the largest component of the biomass of zooplankton in these layers. *Neocalanus cristatus*, *Eucalanus bungii*, and *Calanus marshallae* were also present but in lesser proportions. None of these species and stages demonstrated consistent relationships with vertical patterns in either fluorescence or upper-layer mixing. However, there was a tendency for *N. flemingeri* and *N. plumchrus* to occur closer to the surface than *N. cristatus* or *E. bungii* at most locations.

The maximum combined abundance for copepodite stage V of *N. plumchrus* and *N. flemingeri* (similar in size and weight) at the 24 sampling sites averaged 377.1 individuals m⁻³, and ranged from 0.4 to 1286.2 individuals m⁻³. Locations in Knight Island Passage, near Perry Island, south of Esther Island, and at the shelf break near Middleton Island hosted the highest concentrations of these stages. Locations in southwestern Montague Strait and in southern Unakwik Inlet registered the lowest numbers of these large calanoids.

Introduction

Mackas, et al. (1993) described vertical habitat partitioning by large calanoids in the open subarctic Pacific Ocean. Their study demonstrated close correlation between upper-layer seasonal mixing zones and depth preferences for *Neocalanus plumchrus*, *N. flemingeri*, *N. cristatus*, and *Eucalanus bungii* in the spring and summer. Annually developing copepodites of the former two species were consistently found above or in a weak thermocline, while the latter usually occurred in or below the thermal structuring. This vertical separation was interpreted to reflect: 1) different responses to turbulence; and 2) feeding preferences for protozoans in the spring and early summer surface mixed layer by *N. plumchrus* and *N. flemingeri*, and detrital feeding on aggregates settling from the surface zone by *N. cristatus* and *E. bungii*.

Cooney (1986) documented the presence of *Neocalanus plumchrus*, *N. cristatus* and *Eucalanus bungii* over the shelf of the northern Gulf of Alaska south of Prince William Sound. These distributions were attributed to strong on-shelf transport of surface water forced by downwelling favorable winds interacting with source populations in the epipelagic layer of the adjacent deep ocean. Coupled with a growing understanding of coastal flow patterns and the seasonal intrusion of shelf water into Prince William Sound (Neibauer et al., 1994), we now know a mechanism exists to infuse the coastal zone of the northern Gulf of Alaska and Prince William Sound with oceanically-derived copepods each year. This seeding phenomenon has most recently been demonstrated for the waters of Shelikof Strait, a portion of the shelf environment west of Prince William Sound near Kodiak Island (Incze et al., 1997).

Our manuscript describes vertical patchiness in populations of *Neocalanus*, *Eucalanus* and *Calanus* in and near Prince William Sound, Alaska, in May, 1996. The purpose of the work was to investigate the extent to which large calanoids in the Sound and over the adjacent shelf occur in dense, near-surface layers during the time when pink and chum salmon fry emigrate from natal streams into coastal shallows, and when fry predators like juvenile and adult walleye pollock and adult herring are recharging their seasonally depleted energy reserves. Large calanoid copepods comprise a substantial portion of the diet of pollock and herring in the spring (Cooney and Willette, 1997), and it is believed that during years of exceptional copepod biomass, fishes like adult walleye pollock feed primarily on zooplankton and less on alternative forage like

salmon fry and other small fishes. For this mechanism to function energetically, we reasoned that pollock and other planktivores must encounter high-density copepod swarms or layers in the surface waters of the region. Our study in May, 1996, sought evidence for vertical structuring in populations of large calanoids and other zooplankters in Prince William Sound and over the nearby continental shelf.

Methods

The R/V *Alpha Helix* supported our plankton work in and adjacent to Prince William Sound, Alaska, a large coastal fjord-type estuary located at the northern-most reaches of the Gulf of Alaska. The Sound is deep (to 750 m), is bounded to the west, north, and east by the Chugach Mountains, and communicates with the adjacent Gulf of Alaska via the Alaska Coastal Current (ACC) entering through Hinchinbrook Entrance and Montague Strait. Prince William Sound occupies nearly 9000 km² with 3200 km of shoreline (Grant and Higgins, 1910). The adjacent shelf of the northern Gulf of Alaska is a wind-forced downwelling system for approximately 8 months of each year (Neibauer et al., 1994). Stabilization or weak upwelling can occur in the summer months. Deep water is renewed each year during the time of relaxed downwelling, late summer and early fall (Schmidt, 1977).

A MOCNESS sampler was employed at 25 stations inside and outside PWS to collect macrozooplankton in the upper 50 m (Figure 1; station 3 aborted). Sampling was conducted at the peak of the spring zooplankton bloom, early to mid-May, and about two weeks after the maximum in phytoplankton stocks judged by a real-time reporting moored fluorometer in the central region of the Sound. The MOCNESS fished nine, 1-m² Nitex nets of 0.505-mm mesh. Net one (1) was lowered open as a drogue from the surface to a depth below 50 m with the vessel steaming at about 1.5 m sec⁻¹. The remaining nets were then opened and closed during a slow oblique retrieval. Sampling intervals were standardized at 50-40 m, 40-30 m, 30-25 m, 25-20 m, 20-15 m, 15-10 m, 10-5 m, and 5-0 m. Each net filtered at least 100 m³ of water. Collections were carefully rinsed from nets and preserved in 10% seawater formalin. Laboratory processing included identification and enumeration of plankters and the various copepodite stages of the large calanoids. Representative copepodite stages were weighed in size categories

to convert numbers to estimated wet weights (Coyle, et al., 1990). Only copepodite stages II and above were considered in our evaluation of these collections.

A SeaBird 911 CTD and *in situ* fluorometer were lowered at the beginning or end of each MOCNESS station to describe upper-layer hydrography and mixing, and the vertical distribution of phytoplankton. The fluorometer was not calibrated so only relative fluorescence was obtained from each cast. This measurement was believed sufficient to examine the possibility that copepod layers might be strongly associated with vertical patchiness in seasonally declining pelagic plant stocks. Buoyancy frequency was calculated from CTD observations at each location.

Results

Composition of the Near-Surface Net Zooplankton Community

Catches were averaged across all nets and stations to rank taxonomic categories by abundance and biomass (Table 1). The top fifteen categories ranked by average numerical abundance (no. m⁻³) contained 11 representatives of the Copepoda distributed among six species. Copepodite stage V *Neocalanus flemingeri* and *N. plumchrus* ranked first and fifth respectively. For average biomass (mg m⁻³), the Copepoda accounted for 9 of 15 categories; *N. flemingeri* and *N. plumchrus* stage V ranked first and second. Other large calanoid categories ranked in the top 15 by abundance and biomass included a composite of *N. flemingeri* and *N. plumchrus* stage IV, *N. cristatus* stage V, *Eucalanus bungii* stages II, III and IV, *Metridia* spp. stage V, *M. okhotensis* adult female, *Calanus marshallae* stages II, IV and adult female, and *Pseudocalanus* spp., stage V.

Non-copepods ranked in the upper 15 taxa by abundance and biomass, included a composite of euphausiid furcillia and calyptopis stages representing the genera *Euphausia* and *Thysanoessa*, the pteropod *Limacina helicina*, the small medusa, *Aglantha digitale*, the chaetognath *Sagitta elegans*, and zoea of unidentified Pandalidae. In all, 152 taxonomic categories were sorted from the MOCNESS samples in May.

Patterns of Vertical Distribution

Vertical profiles of the large calanoid species *Neocalanus plumchrus*, *N. flemingeri*, *N. cristatus*, *Eucalanus bungii* and *Calanus marshallae* were examined for evidence of layering and association with buoyancy frequency and fluorescence patterns in the upper 50 m at each sampling location. We could only confidently distinguish between *N. flemingeri* and *N. plumchrus* at copepodite stage V, so restrict our accounts of these closely related copepods (Miller, 1988) to that stage. A composite of *N. spp.* stage III and IV was examined separately. For *N. cristatus*, a composite of stages II-V is reported, for *Eucalanus bungii*, all stages were combined, and for *Calanus marshallae*, stages IV through adult were composited to search for patterns in vertical distribution. A distribution was considered "layered" in the upper 50 m when most of the abundance or biomass was restricted to 50% or less of the sampled domain.

Neocalanus plumchrus and *N. flemingeri* stage V copepodites were found in layers at 15 of 23 locations (Table 2). Maximum numbers and biomass (combined stage V; 1286.2 individuals per m³ and 3.63 g per m³) occurred at location 9 near the edge of the continental shelf south of Prince William Sound (Figure 1). While *N. flemingeri* was the dominant of the pair at most locations and depths, *N. plumchrus* was equally abundant in a few collections, particularly those in the upper 25 m and from the more southerly sampling locations (Figure 2). There were no locations where *N. plumchrus* was absent from collections.

The composite of *Neocalanus spp.* (unidentified *N. plumchrus* and *flemingeri*) copepodite stages III-IV were layered at 13 of 23 sampling locations (Table 2). There were only four locations where these stages deviated substantially from the vertical patterns of the older stage V, but copepodite stages III-IV were less abundant than stage V at all but four locations. At no depths or locations did these combined stages exceeded 500 individuals m⁻³ (Figure 3).

Copepodites of *Neocalanus cristatus* exhibited layering behavior at 16 of the 21 locations (Table 2). At all but three locations, levels of abundance were consistently less than 10 m⁻³, or an order of magnitude below densities observed for *N. plumchrus* and *flemingeri*. Where it occurred, *N. cristatus* maximum abundance was generally restricted to water depths below 20 m (Figure 4).

Eucalanus bungii (all copepodites) occurred as layered populations at 16 of 21 locations

(Table 2). Combined densities were less than 10 m^{-3} at all but six locations. *Eucalanus bungii* also occurred most abundantly below the upper 20 m (Figure 5).

Mid to late stage copepodites of *Calanus marshallae* demonstrated diminished layering behavior relative to the other species, exhibiting strata at only 12 of 22 locations (Table 2). Densities of *C. marshallae* did not exceed 100 m^{-3} at any location or depth. This species tended to layer shallower rather than deeper in the upper 50 m (Figure 6).

Spatial Variability in Copepod Layer Densities

Not all locations within Prince William Sound or over the nearby shelf reflected the same densities of large calanoids in near-surface layers. For the dominant species and stage, *Neocalanus flemingeri* and *N. plumchrus* stage V, numbers and biomass were consistently high at locations sampled in Knight Island Passage, near Esther Island, and around Perry and Lone Islands; $569 \text{ individuals m}^{-3}$ and 1.63 g m^{-3} (Table 3). These densities were only exceeded by samples taken at the single shelf edge station near Middleton Island (location 9). In comparison, samples from Unakwik Inlet (location 6), from over the continental shelf (locations 10 and 11) and from the southwestern portions of Montague Strait exhibited the lowest layering numbers and biomass. Locations for the eastern and central portions of Sound fell between these highs and lows. An examination of the hydrographic records from these areas suggested that the water was less stratified in Hinchinbrook Entrance, southern Montague Strait, and over the continental shelf outside the Sound.

Vertical Patchiness in Relation to Patterns in Fluorescence

Profiles of fluorescence in the upper 50 m exhibited subsurface maxima at 20 of 23 locations. At some locations, these maxima were well-defined, narrow regions of the water column; at others the maxima were broad and less-well defined (Figure 7). Stage V *Neocalanus plumchrus* and *N. flemingeri* occurred most abundantly at depths corresponding to the fluorescence maximum at about half the sampling locations (Table 4). At the remainder of the locations, stage V was dispersed above, below, or showed no depth preference relative to fluorescence maxima.

Neocalanus spp. stages III-IV occurred in maximum densities corresponding with fluorescence maxima at 9 of 23 locations (Table 4). At other locations, these same stages were found above, below or demonstrated no relationship to peaks in fluorescence.

Neocalanus cristatus stages III-V were most abundant at subsurface fluorescence maxima at 6 of 21 locations. *Eucalanus bungii* maximum densities corresponded to subsurface fluorescence peaks at 7 of 21 locations, and *Calanus marshallae* stages IV-Adult at only 5 or 22 locations. At other times these species and stages occurred most abundantly above or below maxima, or exhibited no apparent correspondence with fluorescence patterns.

Vertical Patchiness in Relation to Patterns of Upper-Layer Mixing

April and May are typically months of increasing meltwater input to Prince William Sound (Simmons, 1996). Because of the volumes involved, water column stability is established primarily by salinity. During this cruise, there were only 6 locations at which an upper mixed layer was detectable by buoyancy frequency; station 9 at the shelf break is the best example (Figure 8). The remaining surface mixed zones were compressed in the upper 5-m or less. This circumstance eliminated appreciable upper mixed-layer habitats at most sites. Only at station 9 did *Neocalanus plumchrus* and *N. flemingeri* stage V have space to occur abundantly in the upper mixed regime. At the remainder of the sampling sites, most *Neocalanus*, *Calanus* and *Eucalanus* occurred in and below the shallow upper mixed zone.

Discussion

Our survey of near-surface populations of large calanoid copepods in Prince William Sound and the nearby Gulf of Alaska demonstrated that *Neocalanus*, *Calanus* and *Eucalanus* can occur in well-defined strata in the upper 50 m during spring. The numerical dominants in our collections, *Neocalanus flemingeri* and *N. plumchrus* stage V, contributed substantially to the overall upper-layer biomass of macroplankton retained by a 0.505-mm mesh in early May. Fewer numbers of a composite of *N. flemingeri* and *N. plumchrus* copepodite stages III-IV suggest that the seasonal shift in population structure from stage IV to stage V was well underway at the time of our cruise.

Vertical patterns in population structure of *Neocalanus* and *Eucalanus* were similar to those described for open ocean populations (Mackas, et al., 1993). In most cases, *N. flemingeri* and *N. plumchrus* occurred shallower than *N. cristatus* and *E. bungii*. However, unlike the oceanic subarctic ecosystem, these distributions did not appear to be partitioned by surface mixing zones. At the time of our cruise, increasing freshwater input and seasonal surface warming, coupled with exceptionally calm conditions, resulted in pronounced upper layer stability and the absence of a clearly defined surface mixed layer at all but one location. Only at the shelf edge south of Prince William Sound was there a pronounced near-surface mixed layer, and that was only 10-15 m deep. At this location, *N. plumchrus* and *flemingeri* stage V copepodites occurred most abundantly in the surface mixed zone as previously described by others for the open subarctic oceanic environment (Mackas, et al., 1993).

We had predicted that under diminishing phytoplankton production following the peak of the spring bloom, subsurface plant maxima might be responsible for focusing the older developmental stages of *N. flemingeri* and *N. plumchrus* into distinct strata. However, a general lack of coherence between observed fluorescence maxima and copepod distributions indicate this was probably not the case. *N. flemingeri* and *N. plumchrus* stage V occurred above, in and below subsurface plant maxima at roughly similar frequencies. We did not calibrate the *in-situ* fluorometer, so are unable to determine if these large grazers were able to obtain suitable rations in residual plant stocks above or below subsurface maxima. The general lack of convergence around chlorophyll maxima suggests that food was probably non-limiting at most depths in the upper 50 m.

Our observations confirmed the suspicion that near-surface layers or swarms of large copepods are features of the coastal zooplankton communities in the northern Gulf of Alaska in the spring. Because of their densities, these layers probably provide predictable, energetically-optimal forage resources for large pelagic fishes like adult and juvenile pollock and herring, some of which have been found feeding almost exclusively on *Neocalanus* spp. Since the largest, oldest copepodite stages are strictly transient members of the upper layers, these concentrated forage resources are likely only available for a few critical weeks each year. Our observations further demonstrate that the layers of *Calanus*, *Neocalanus* and *Eucalanus* were not

uniform in numbers and biomass within the region. Shallow or constricted areas subjected to high tidal mixing were less likely to host layers than locations over deeper, more stratified water. This observation suggests the ability of these large copepods to swarm in narrow vertical strata can be compromised at some locations by tidal energy or current shears.

Acknowledgments

Our work was supported by a grant from the Exxon Valdez Oil Spill Trustee Council to project 320-H of the Sound Ecosystem Assessment (SEA) program. We thank the crew of the R/V *Alpha Helix*, other SEA personnel and Dr. William Hauser for their assistance on the cruise and in the laboratory in support of our study.

References

- Cooney, R. T. 1986. The seasonal occurrence of *Neocalanus cristatus*, *Neocalanus plumchrus* and *Eucalanus bungii* over the shelf of the northern Gulf of Alaska. *Continental Shelf Res.* 5: 541-553.
- Cooney, R. T. and T. M. Willette. 1997. Factors influencing the marine survival of pink salmon in Prince William Sound, Alaska. NOAA Tech. Memo. NMFS-NWFSC-29, pp. 183-196.
- Coyle, K. O., A. J. Paul and D. A. Ziemann. 1990. Copepod populations in the spring bloom in an Alaskan subarctic embayment. *J. Plank. Res.* 12(4):759-797.
- Damkaer, D. M. 1977. Initial zooplankton investigations in Prince William Sound, Gulf of Alaska and Lower Cook Inlet. Environmental Assessment of the Alaska Continental Shelf, Annual Reports of Principal Investigators for the year ending 1977. 10 (Receptors-fish, littoral and benthos): 137-274.

- Grant, U. S., and D. F. Higgens. 1910. Reconnaissance of the geology and mineral resources of Prince William Sound, Alaska. U.S. Geol. Sur. Bull. 443, 89 pp.
- Fulton, J. D. 1973. Some aspects of the life history of *Calanus plumchrus* in the Strait of Georgia. J. Fish. Res. Bd. Can. 30:811.-815.
- Incze, L. S., D. W. Siefert and J. M. Napp. 1997. Mesozooplankton of Shelikof Strait, Alaska: abundance and community composition. Continental Shelf Res.36:287-305.
- Mackas, D. L., H. Sefton, C. B. Miller and A. Raich. 1993. Vertical Habitat partitioning by large calanoid copepods in the oceanic subarctic Pacific during Spring. Prog. Oceanog. 32: 259-294.
- Miller, C. B. 1988. *Neocalanus flemingeri*, a new species of Calanidae (Copepoda:Calanoida) from the subarctic Pacific Ocean, with a comparative redescription of *Neocalanus plumchrus* (Marukawa) 1921. Prog. Oceanogr. 20:223-274.
- Miller, C. B. 1993. Development of large copepods during spring in the Gulf of Alaska. Prog. Oceanog. 32:295-317.
- Mooers, C. N. K. and J. Wang. (in review). On the development of a three-dimensional circulation model for Prince William Sound, Alaska. Submitted to Continental Shelf Res., December, 1996.
- Neibauer, H. J., T. C. Royer and T. J. Weingartner. 1994. Circulation of Prince William Sound, Alaska. J. Geophy. Res. 99(14):113-126.
- Simmons, H. L. 1996. Estimation of freshwater runoff into Prince William Sound using a digital elevation model. M.S. Thesis, University of Alaska Fairbanks, 156 p.

Table 1. Ranking of macrozooplankton by numerical abundance and biomass

Taxonomic Category	Ranking by Abundance	Ranking by Biomass
<i>Neocalanus flemingeri</i> CV	1	1
Euphausiid furcilia	2	5
<i>Neocalanus</i> spp. CIV	3	3
<i>Pseudocalanus</i> spp. CV	4	
<i>Neocalanus plumchrus</i> CV	5	2
Euphausiid calyptopis	6	14
<i>Eucalanus bungii</i> CIII	7	11
<i>Pseudocalanus</i> spp. AF	8	
<i>Eucalanus bungii</i> CII	9	
<i>Calanus marshallae</i> CIII	10	
<i>Neocalanus</i> spp. CIII	11	
<i>Calanus marshallae</i> CIV	12	12
<i>Limacina helicina</i>	13	9
<i>Aglantha digitale</i>	14	6
<i>Metridia</i> spp. CV	15	
<i>Neocalanus cristatus</i> CV		4
<i>Sagitta elegans</i>		7
<i>Metridia okhotensis</i>		8
<i>Calanus marshallae</i> AF		10
Pandalidae zoea		13
<i>Eucalanus bungii</i> CIV		15

Table 2. The frequency of calanoid layering in the surface waters of Prince William Sound in May

Taxonomic Category	Layered	Not Layered
<i>Neocalanus plumchrus/flemingeri</i> CV	15	8
<i>N. spp.</i> CIII-IV	15	8
<i>N. cristatus</i> Stages CIII-V	16	5
<i>Eucalanus bungii</i> CII-V	16	5
<i>Calanus marshallae</i> CIV-Adult	12	8

Table 3. Maximum numbers and biomass of a composite of *Neocalanus flemingeri* and *N. plumchrus* stage V at locations in Prince William Sound and over the adjacent shelf

Stations and locations	Abundance (No. m ⁻³)	Biomass (g m ⁻³)
Stations 1-8 (excluding Station 6 in Unakwik Inlet) and 19-23 in Knight Island Passage and northwestern Prince William Sound		
Average	567.9	1.629
Station 9 at the shelf break		
	1286.2	3.643
Stations 10 and 11 over the shelf south of Prince William Sound		
Average	95.6	0.286
Stations 13 and 14 in lower Montague Strait		
Average	11.6	0.034
Stations 12, 15-18 and 24-25 in eastern and central Prince William Sound		
Average	183.0	0.531
Station 6 in Unakwik Inlet		
	21.9	0.045

Table 4. Correspondence between the patterns of water column fluorescence and large calanoid depths of maximum abundance		
Taxonomic Category	In Fluorescence Peak	Outside the Fluorescence Peak
<i>Neocalanus plumchrus/flemingeri</i> CV	10	13
<i>N. spp.</i> CIII-IV	7	16
<i>N. cristatus</i> CIII-V	6	15
<i>Eucalanus bungii</i> CII-V	7	14
<i>Calanus marshallae</i> CIV-Adult	6	15

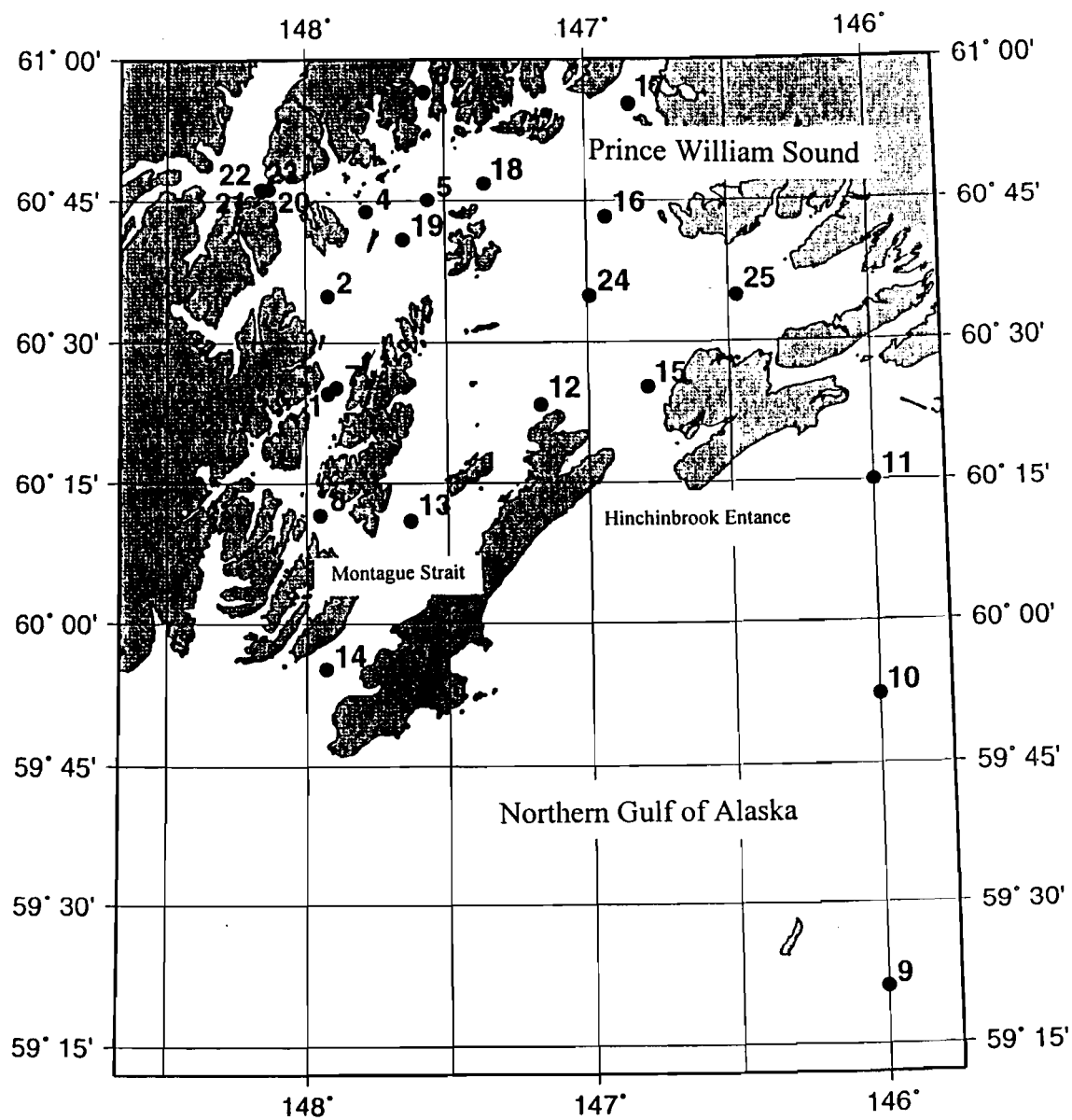


Figure 1. Prince William Sound, Alaska depicting geographic features and the location of MOCNESS stations occupied in May, 1996.

Tow No: 1: *Neocalanus plumchrus*/*flemingeri* V

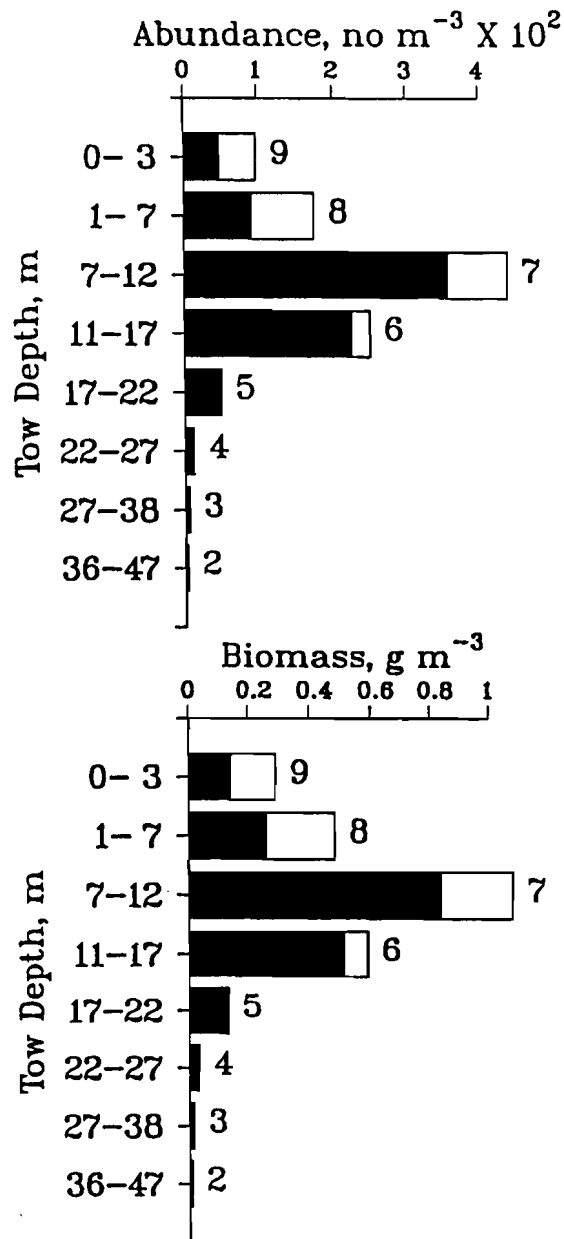


Figure 2. Vertical distributions of *Neocalanus plumchrus* (open) and *N. flemingeri* stage V (closed) demonstrating the former occurs more abundantly in the shallower depths.

Tow No: 1: *Neocalanus* spp. III & IV

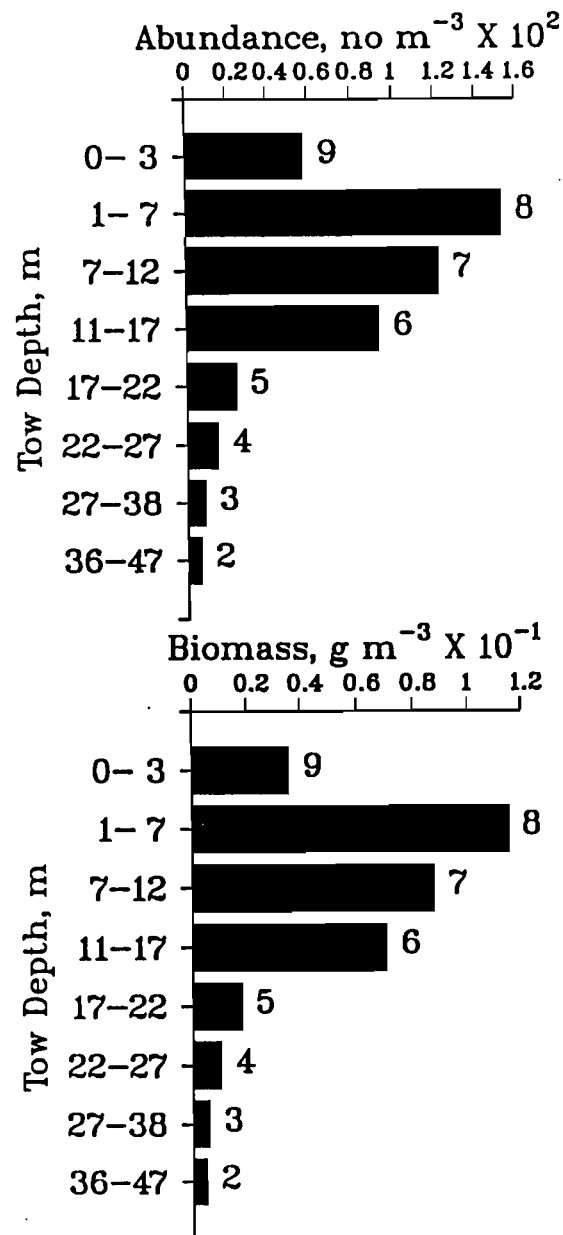


Figure 3. Vertical distributions of a composite of *Neocalanus plumchrus* and *N. flemingeri* stages III and IV.

Tow No: 1: *Neocalanus cristatus* III, IV, V

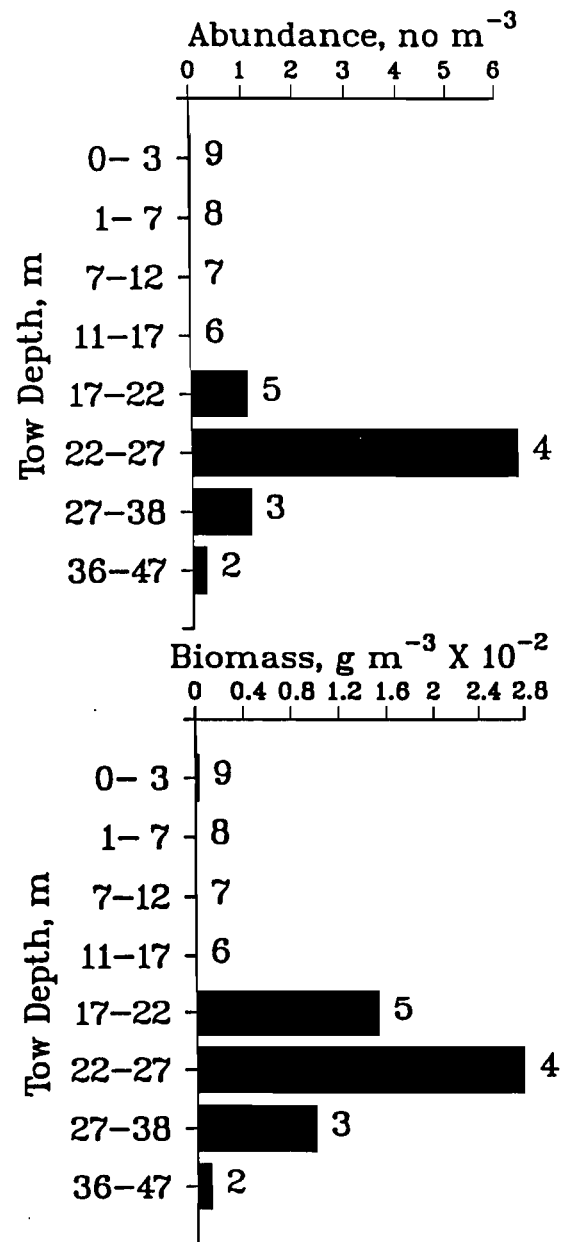


Figure 4. Vertical distributions of *Neocalanus cristatus* stages III-V.

Tow No: 1: *Eucalanus bungii* all stages

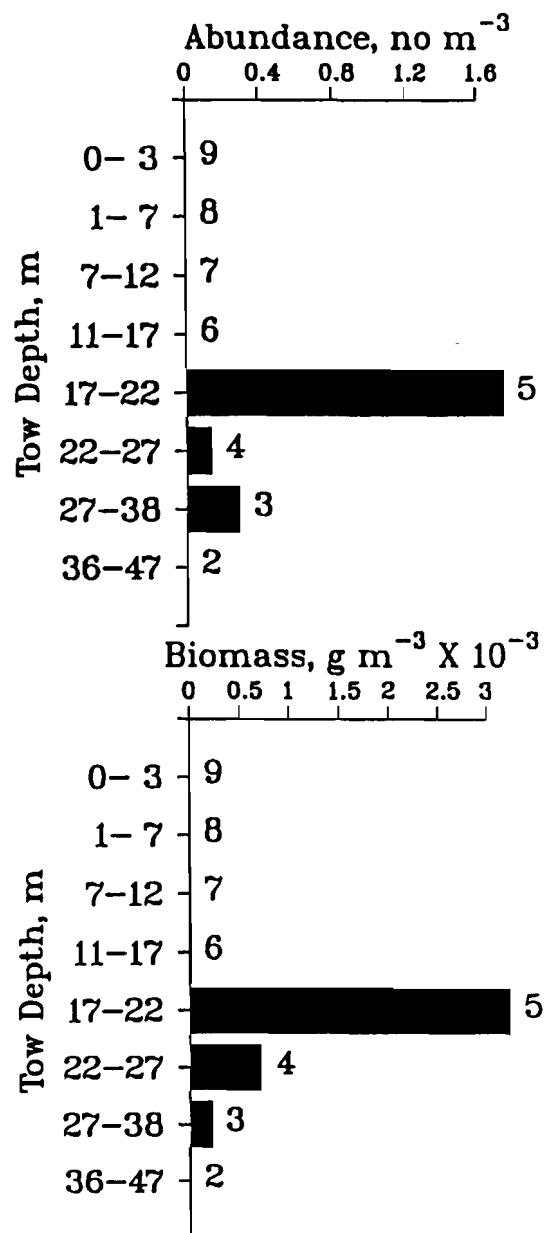


Figure 5. Vertical distributions of all copepodite stages of *Eucalanus bungii*.

Tow No: 2: *Calanus marshallae* adults, IV, V

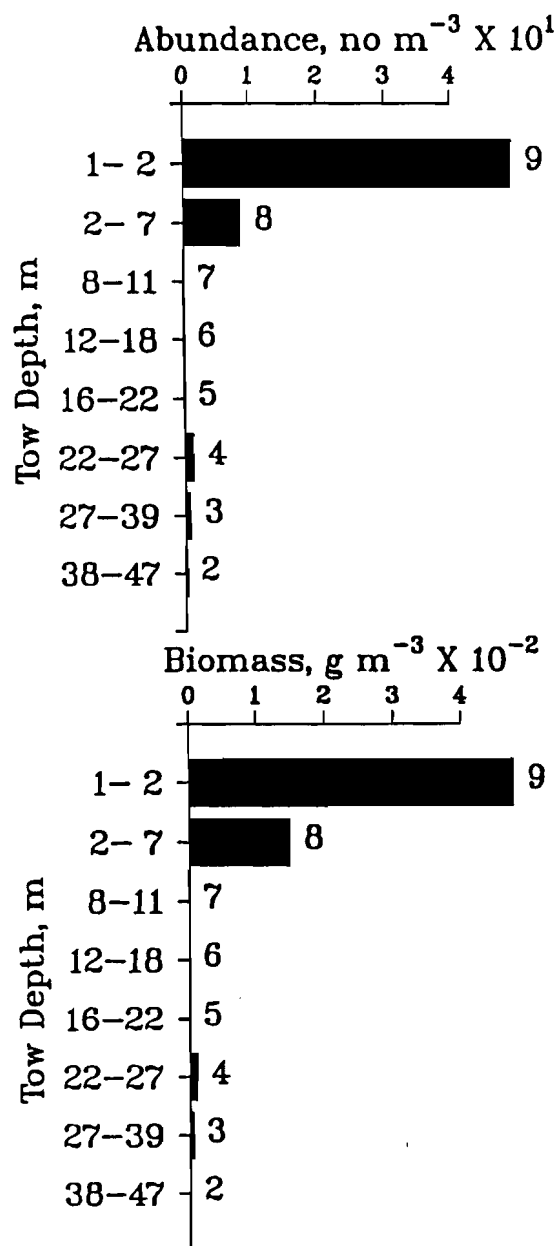


Figure 6. Vertical distribution of a composite of *Calanus marshallae* stages IV-adult.

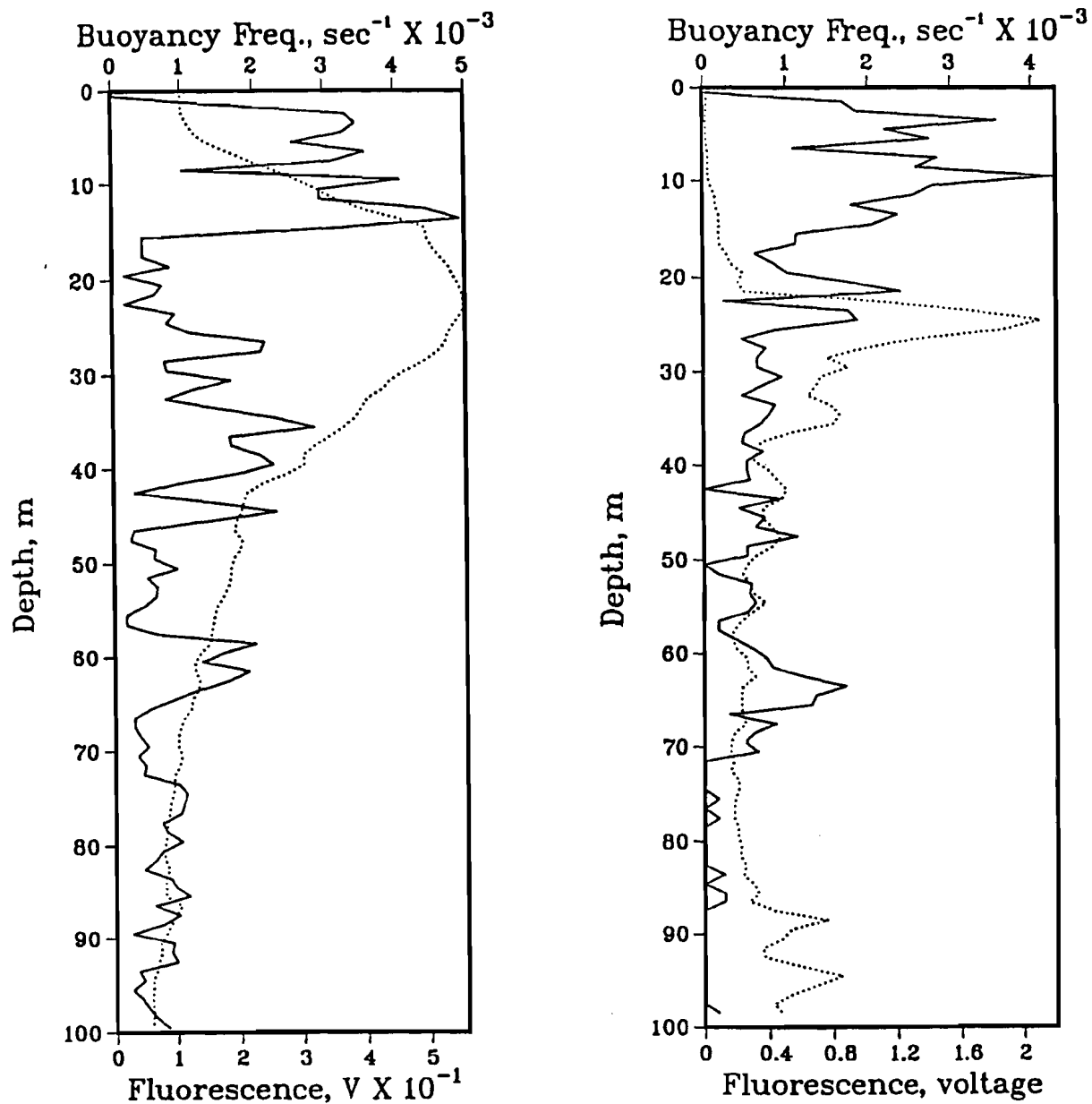


Figure 7. Examples of broad (left) and narrow (right) sub-surface fluorescence maxima (dotted distributions). The solid line depicts the buoyancy frequency at these two locations.

Chapter 5

Biophysical Modeling and Remote Sensing

Exxon Valdez Oil Spill
Restoration Project Annual Report

Biophysical Modeling and Validation Through Remote Sensing

Restoration Project 97320-R
Annual Report

This annual report has been prepared for peer review as part of the *Exxon Valdez* Oil Spill Trustee Council restoration program for the purpose of assessing project progress. Peer review comments have not been addressed in this annual report.

David L. Eslinger

University of Alaska Fairbanks
Institute of Marine Science
Fairbanks, Alaska 99775

April 1998

SEA Trophodynamic Modeling and Validation Through Remote Sensing

Restoration Project 97320-R Annual Report

Study History: This project is the result of an internal reorganization within the Sound Ecosystem Assessment (SEA) program. Some of the work performed under SEA core projects 95320-G and 95320-J in FY94 and FY95 has been done under this project since. We are continuing the trophodynamic modeling of phytoplankton and zooplankton begun in FY95, increasing the detail in the *Pseudocalanus* simulation, and adding modeling of ichthyoplankton, herring larvae in particular. We are evaluating and verifying the model against field data collected using a variety of remote sensing and *in situ* sampling platforms.

Abstract: Previous coupled physical and biological modeling of phytoplankton and zooplankton dynamics in Prince William Sound and the Gulf of Alaska have shown there to be two general types of response to different springtime physical dynamics. Warm, quiescent springs lead to brief intense phytoplankton blooms and relatively low zooplankton biomass, whereas, colder, stormy springs lead to longer phytoplankton blooms and higher zooplankton biomass. However, in FY97, further simulations with the model suggest that it is not simply the winds and temperature during the springtime, that determined what type of planktonic bloom would occur, rather, it is the interaction of springtime weather with the water mass left after the previous winter. A very warm winter produces results similar to a cold, windy spring: a slow phytoplankton bloom and a large zooplankton population. A very cold winter in turn, is similar to a warm spring, producing a brief, short phytoplankton bloom and low populations of zooplankton. These interactions occur because the phytoplankton bloom responds most strongly to the **stratification** of the water column, not to the temperature itself. The stratification process depends on the fluxes of heat, momentum, and salt into the upper water column. In early spring, the heat flux is largely determined by the temperature difference between the air and water. Therefore, a similar bloom occurs if the water is very warm, or the air is very cold. In FY-97, we completed and validated an N-by-one-dimensional model that accurately simulated these dynamics. This model is being expanded into the full three-dimensional domain during FY-98.

Key Words: biophysical modeling, biological oceanography, physical oceanography, phytoplankton, Prince William Sound, spring bloom, zooplankton

Citation: Eslinger, David L, Biophysical Modeling and Validation Through Remote Sensing, *Exxon Valdez Oil Spill Annual Report* (Restoration Project 97320-R), Alaska Department of fish and Game, Anchorage, Alaska.

Table of Contents:

Executive Summary	5
Introduction	6
Objectives	6
Methods	7
Results	8
Discussion	9
Conclusions	10

List of Tables, Figures, and Appendices:

Appendix A	11
Appendix B	19
Figure legends	25
Figure 1	26
Figure 2	27
Figure 3	28
Figure 4	29
Figure 5	30
Figure 6	31
Figure A-1	32
Figure A-2	33
Figure A-3	34
Figure B-1	35

Figure B-2	36
Figure B-3	37

Executive Summary:

As shown in the FY96 annual report, biophysical modeling of phytoplankton and zooplankton, in combination with field data collected as part of 320-G and 320-H, shows that phytoplankton and zooplankton populations in Prince William Sound and the northern Gulf of Alaska are determined by the winds and the differences between air and water temperatures which occur over a relatively short, critical time period in early spring. Although this critical time period may be as short as two weeks, the meteorological conditions occurring during that time will play a dominant role in the dynamics of the phytoplankton and zooplankton populations for the rest of the summer. Changes in the amount of convective mixing, caused by cold air, and of wind mixing, caused by high winds, during the early part of the phytoplankton bloom change the timing and duration of the bloom, the total primary production occurring during the bloom, and the partitioning of that primary production between the upper water column food chain, and the benthic food chain.

In FY97, we made significant expansions of the modeling work previously carried out. The model as described in the FY96 report is being expanded into a fully three-dimensional model. Several steps are necessary to produce a working, accurate 3-D model. We must have a reasonable model of Prince William Sound bathymetry; a set of realistic, spatially-varying wind fields; and a set of realistic currents with which to advect the plankton. The production of the realistic currents depends on the availability of the spatially varying winds. In FY97, we devised a method of using winds, measured at various stations within the PWS region, in conjunction with local knowledge of the effects of topographic steering, to develop a tool with which we can produce spatially varying wind fields. This method and tool are described below. We used the spatially-varying winds and the same model bathymetry as the physical modeling effort is using, to construct a three-dimensional model of plankton dynamics. We examined the effects of bathymetry and varying winds on the plankton populations. There were no results from the physical model available which used the spatially varying wind fields, therefore the plankton model does not include horizontal advection at the present time. The effects shown are due to local processes only. This type of model is commonly referred to as an N-by-one-dimensional model (Nx1D). We found that local effects are significant and that the Nx1D model does a reasonable job in simulating the results of field programs.

In addition to the Nx1D work, we made substantial improvements to the biological dynamics of the model through EVOS-supported graduate research by two students. Ms. Natalia Pintchouk is greatly expanding the *Pseudocalanus* zooplankton model. This work is described in Appendix A. Ms. Sarah Thornton is adding an ichthyoplankton (larval herring) component to the model. This work is described in Appendix B. Both of these students presented their work at the 1998 Ocean Sciences meeting in San Diego, CA, in February 1998. They attracted a good deal of attention for their work and received a great deal of praise. They will be finishing their projects and defending their theses in FY99.

Introduction:

Pacific herring and pink salmon have been identified as non-recovering resources injured by the *Exxon Valdez* oil spill. An ecosystem approach has been recognized by the EVOS Trustee Council as being necessary to reaching an understanding of the underlying processes and variables which may be constraining recovery of these injured resources. The currently proposed work is critical to the ecosystem study being undertaken by the SEA program. The role of the physical environment in controlling phytoplankton, zooplankton, and ichthyoplankton populations, and the role of these populations in the life history of Pacific herring and pink salmon, must be understood for the intelligent, informed planning of successful restoration efforts.

This project directly addresses the SEA pink salmon and Pacific herring restoration objectives. The phytoplankton and zooplankton serve directly as food for both herring and pink salmon at various life stages. Two large calanoid copepod species, *Neocalanus cristatus* and *N. plumchrus*, in particular, are thought to be potentially important as both a dietary item and a refuge from predation for pink salmon. Larval and juvenile herring feed on different stages of calanoid copepods, which reproduce throughout the spring and summer. The reproductive effort of these copepods is dependent on the timing, magnitude, and duration of the phytoplankton primary production in the spring bloom period and throughout the summer. The interactions between the various types of phytoplankton (*e.g.*, diatoms, flagellates) and zooplankton (*e.g.*, oceanic copepods, neritic copepods) varies both between and within years. The timing of the major increase in biomass of phytoplankton or zooplankton, sometimes called the spring phytoplankton or zooplankton bloom, respectively, may be important to the first feeding and subsequent survival of the larval herring and juvenile herring and salmon, *e.g.* Cushing's match-mismatch hypothesis. This project examines these issues through the use of numerical models, remote sensing, and field observations.

Results through FY-96 indicate that physical forcing dominates the dynamics at the lower trophic levels. The physical signal propagates up through the food chain and has relevant consequences months after the physical interaction actually occurred. These effects are highly nonlinear, but can be accurately simulated using the present model.

Objectives:

The major objectives to be achieved over the life of this project as detailed in the FY97 DPD were:

1. To construct a three-dimensional model of the physical/biological processes affecting phytoplankton, zooplankton, and ichthyoplankton dynamics in Prince William Sound.
2. To determine the relative roles of these processes in determining Pacific herring and pink salmon population levels.

3. To determine the spatial and temporal variability, both of the physical environment and of phytoplankton concentrations, using a combination of remote sensing techniques and field observations.

An additional minor objective was:

4. To deploy and maintain an upgraded version of the CLAB buoy, which will provide high temporal resolution time series of wind velocity, air temperature, surface water temperature, and subsurface temperatures at 10 depths. This will be the primary data source for the development of the physical/biological dynamics portion of the model.

These objectives will enable us to test the following hypotheses:

1. That coupling between the physical environment and phytoplankton dynamics can be modeled reliably.
2. That phytoplankton dynamics drive zooplankton dynamics in a predictable manner, which can also be modeled.
3. That the survival of larval herring can be estimated by a combination of modeling of larvae and field work on eggs and 0-class juveniles.
4. That interactions between the physical environment, the zooplankton field, and juvenile pink salmon populations can be predicted using a coupled biological/physical 3-D model.
5. That the spatial variability of the SST and chlorophyll concentrations in Prince William Sound, observed in satellite remote sensing images, can be simulated by a 3-D model of physical and biological dynamics.

Methods:

We are using a combination of coupled biological and physical models and satellite remote sensing data sets to achieve the above objectives. We are continuing the development of a coupled biological-physical model of lower trophic level, i.e. phytoplankton and zooplankton, dynamics for the near-surface layers of Prince William Sound (PWS). We have expanded the one-dimensional, depth-time model developed in FY-95 to include herring larvae. The 1-D model describes the biological and vertical processes that occur through time at a single location. The biological processes contained in the 1-D model are being integrated into a larger three-dimensional model with appropriate vertical resolution. The model is presently working in a Nx1D configuration, where only the local effects at each grid point are simulated. The Nx1D model contains bathymetry effects and spatially varying wind effects. This Nx1D model will become fully three dimensional when it incorporates the vector fields produced by the circulation model being constructed by V. Patrick and C. Mooers as part of 320-J. This will be done in FY98.

Spatially varying wind fields are needed to drive an accurate 3-D model. In conjunction with Vince Patrick, Jennifer Allen, and Stephen Bodner (all part of 97320J), we developed a methodology to use local knowledge from (initially) Cordovan pilots and fishermen to identify portions of the Sound which behaved similarly under different wind conditions. We could then take the measured winds over these areas and apply them to larger portions of the Sound. Again

in collaboration with Jennifer Allen (97320-J) we developed a JAVA-based tool to interactively do this. An example of the regions defined and the resultant wind field can be seen in Figures 1 and 2. Using this definition of the “wind regions” in the model, we ran simulations for 1995 and 1996.

The methodologies for the *Pseudocalanus* and ichthyoplankton models are given in Appendices A and B, respectively.

Our remote sensing work entails reception and processing of National Oceanic and Atmospheric Administration (NOAA) Nimbus series satellite data in Fairbanks, AK. Data from the NOAA Advanced Very High Resolution Radiometer (AVHRR) sensors are processed to produce sea surface temperature (SST) images of both the northern Gulf of Alaska and a more detailed image of Prince William Sound. In late 1997, the long-awaited OrbView-II satellite was launched, carrying the Sea-viewing Wide Field-of-view Sensor (SeaWiFS). Data from this satellite is received and processed at the University of Alaska Fairbanks. The data are available to NASA-authorized SeaWiFS users. We are authorized users and will be using the data to compare with model and field results in the future. Unfortunately, the Japanese ADEOS satellite, carrying another ocean color sensor, was lost due to power problems, and no data have become available to us covering Prince William Sound.

Results:

The results of the simulations using realistic bathymetry and spatially varying winds are shown in Figures 3 - 6. In Figure 3, average euphotic-zone phytoplankton concentrations can be seen to be varying due to local winds. Note the north-south gradient in concentration with highest values in the south, in the area we have been thinking of as the “River”. This north-south gradient is similar to that observed by Peter McRoy’s SEA phytoplankton project in 1995. Not too surprisingly, the model simulates a similar gradient occurring a bit later in zooplankton abundance (Figure 4), similar to that observed by Ted Cooney’s SEA zooplankton project. In contrast, in 1996, phytoplankton are more uniformly distributed, with a smaller east-west gradient (Figure 5), again similar to that observed in the field data. Again, there is a similar gradient in the zooplankton model results. Both of these years were run with identical initial conditions and wind regions. The only differences were the air temperatures and wind velocities over the different regions. These model results show the importance of understanding the spatial gradients in winds, even over the relatively small scale of Prince William Sound.

Detailed results from the one-dimensional modeling work are given in the Results section of Appendices A and B. Briefly, from Appendix A, the *Pseudocalanus* model incorporates 15 different life stages into the model instead of the one stage previously used. This makes a substantial difference in the amount of *Pseudocalanus* biomass that is available as food for larval herring. From Appendix B, we find that food availability plays a large role in the time it takes for larval herring to metamorphose to juveniles. This may have substantial effects on herring recruitment, as the larval stage is thought to be one of particularly high mortality. Therefore, it

appears that the inclusion of the *Pseudocalanus* life-stage details is an important factor if we hope to accurately predict herring recruitment.

We have been processing and archiving AVHRR SST since 1994, and presently have an archive of over 6,000 SST images available to the SEA project. These images are stored on 8 mm tape, CD-ROM, and hard disk. In early FY97, we delivered a subset of these images to the Prince William Sound Science Center (PWSSC) in CD-ROM format, for use by the PWSSC SEA investigators. In FY97, we processed and archived over 1500 SST images.

The measurable tasks which we proposed to perform in FY97 and the progress made are listed below.

- Begin ichthyoplankton model comparison with FY-96 field data. Model DONE, no larval herring field data collect by other groups.
- Recover C-LAB buoy. DONE
- Deploy C-LAB buoy for 1996 field season. DONE
- Collect, process, and analyze AVHRR images for 1997 field season. DONE
- Begin to collect, process and analyze ocean color from SeaWiFS and/or OCTS. Exact date of satellite launches TBD. INCOMPLETE: Satellites not operational in FY97. Presently underway.
- Complete FY-97 field collection efforts. DONE
- 3-D phytoplankton, zooplankton model complete, initial ichthyoplankton component working. 2/3 DONE: 3-D model awaiting vector forcing fields. Other components DONE.
- Complete analysis of AVHRR data from 1994-mid 1997. UNDERWAY, part of ongoing analysis.
- Annual report on FY-97 work. DONE

Discussion:

From the development of the Nx1D model, we can see the dramatic effect that local bathymetry and winds have on phytoplankton and zooplankton populations. Even in the simple simulations shown, with the wind regions constant, there were dramatic differences between the years due to local winds. The spatial patterns seen in the model results agree well with those seen in the field data from the phytoplankton and zooplankton components of SEA. These results underscore the importance of having accurate, spatially varying forcing fields if we are to understand and simulate the Prince William Sound Ecosystem.

Full discussions of the 1-D model results are presented in Appendices A and B.

Conclusions:

The three-dimensional, coupled bio-physical model being developed as part of this project is able to simulate the phytoplankton and zooplankton dynamics in the upper waters of Prince William Sound. In most years, this model requires measurements of only air temperatures and winds to accurately model the timing and magnitude of the phytoplankton and zooplankton blooms. The inclusion of additional life stages in the *Pseudocalanus* component seems justified, given the importance to larval herring survival of the timing and absolute amount of naupliar and younger *Pseudocalanus* copepodites available as food.

Appendix A

Modeling of Life Stage Dynamics of *Pseudocalanus* Spp. In Prince William Sound, Alaska.

Natalia M. Pintchouk and David L. Eslinger

Institute of Marine Science
University of Alaska Fairbanks

ABSTRACT

Springtime zooplankton populations in Prince William Sound, Alaska, are dominated by a number of species of calanoid copepods. These species can be loosely grouped into two categories: large *Neocalanus*-type copepods, which reproduce at depth; and smaller *Pseudocalanus*-type copepods, which reproduce at the surface, after feeding. The *Neocalanus*-type copepods are an important food source for pink salmon, pollock and other fish species in early spring. The *Pseudocalanus*-type copepods are an important food source throughout the spring, summer and fall, for larval and juvenile Pacific herring. Larval herring feed only on the smaller life stages of the *Pseudocalanus*-type copepods. The current study examines the effects of including life-stage information in simulating *Pseudocalanus* biomass.

We have developed a coupled biophysical model of plankton dynamics for Prince William Sound, Alaska. The model includes three potentially limiting nutrients: nitrate, ammonium, and silicon; two phytoplankton “species”: diatoms and flagellates; and three zooplankton “species”: the large *Neocalanus*-type of copepods, smaller *Pseudocalanus*-type copepod, and a euphausiid group. In the current study, we present a comparison of the results of the model using two different formulations for the *Pseudocalanus*-type of copepod. The first formulation combined all life stages in one variable, which simulated total *Pseudocalanus* biomass. For the second formulation, all stages of *Pseudocalanus* development were simulated. This required sixteen different variables, and resulted in a considerably more complicated model. Information on the biomass of different life stages is important in simulating the proportion of the total biomass available as food to Pacific herring.

BACKGROUND

Numerical modeling of phytoplankton, along with field data, shows that phytoplankton populations in Prince William Sound and the Northern Gulf of Alaska are determined by the winds and air temperatures which occur over a relatively short, critical time period in early spring. Changes in the amount of convective mixing, caused by the cold air, and of wind mixing, caused by high winds, change the timing and duration of the bloom. A relatively warm, quiescent

spring produces a relatively short and intense phytoplankton bloom. In colder years the bloom is prolonged due to mixing, which reduces phytoplankton concentrations and increases nutrient concentrations. Because zooplankton reproduce at much slower rates than phytoplankton, a prolonged phytoplankton bloom is beneficial to the zooplankton populations, resulting in higher zooplankton biomass. In other words, zooplankton biomass will be higher in colder years than in warmer years (Eslinger, 1997).

MODEL METHODOLOGY

I. *Pseudocalanus* Life cycle:

Development of *Pseudocalanus* includes next stages: embryo; naupliar stages NI-NVI; copepodites CI-CV and adults (CVI). As for taxonomic status, it was shown that different *Pseudocalanus* species had similar generation times (McLaren et al., 1989; Davis, 1983; Corkett and McLaren, 1978).

1.1 Initial abundance:

The development of *Pseudocalanus* is assumed to be synchronous when the productive season starts with a population of animals that are largely at the same stage of development. In high latitudes synchrony of life cycles lead to synchronous spawning producing a number of cohorts of animals each with distinct characteristics. *Pseudocalanus spp.* in PWS has 1 yr life cycle.

The overwintered G0 generation is assumed to be comprised of CIV, CV copepodites, and adult females. Average abundance of animals in March for open sound stations for a number of years was reported to be 4.1, 11.7 and 22.2 animals per cubic meter respectively (Cooney, personal communication). However, these numbers vary substantially from year to year and from station to station. In the model, initial abundance for each present group was calculated from AFK data and was equal to 33:100:200 animals per cubic meter (CVI, CV, CIV respectively). These numbers were used for both model years 95 and 96, as initial total abundance from AFK hatchery data did not differ much for these years.

1.2 Reproduction: Number of eggs in clutches:

Overwintered adult fertilized females begin reproduce after they feed on spring phytoplankton, so that first clutch is laid around day 70. Minimum, mean and maximum number of eggs per clutch were set to be equal to 3, 16, and 31 respectively (Corkett and McLaren, 1978).

1.3 Embryonic and stage development time; rate of production of sacks, and time between successive clutches.

A female carries a sack until eggs are hatched and the time taken for embryos to develop is controlled by temperature and described by the Belehradec's function $EDT = a \cdot (T - \lambda)^b$, or $\log(EDT) = \log(a) + b \cdot \log(T - \lambda)$, where EDT is embryonic development time in days, T is water temperature in C; $b = -2.05$ is the slope of the line, b is constant and assigned arbitrary; a is an intercept on the y-axis is shown to be related closely to egg size (Corkett and McLaren, 1978); λ

varies with temperature and is called the biological zero since on linear plot it is theoretical temperature at which EDT is infinite.

Parameters of Belehradec's function were calculated for few locations (Corkett and McLaren, 1978). Coyle, Paul and Ziemann (1990) reported that for south central Alaska (Auke bay), the equation for embryonic development was similar to that for the North Sea $EDT = 1845 \cdot (T + 11.45) - 2.05$ and that the above equation predicted a generation time of 64 days at 5C which was similar to their estimate from cohort data. This equation was used in the model. Temperature data (2hrs interpolation) was calculated from Pollard-Thompson mixed layer model

It was estimated that fertilized females can reproduce up to 8-10 times. Corkett, McLaren (1978) summarized results obtained by Thompson (1976; cited by Corkett and, McLaren, 1978) and Paffenhofer, Harris (1976) and assumed that the successive clutches appear at intervals equal to about 1.25 times the duration of embryonic development for the given temperatures. New clutch is laid only if there is enough food for female to get excessive biomass equal at least to the difference between female base weight and minimum egg sack weight.

There is no agreement whether developmental time per stage is a function of temperature only, or if it also depends on food concentration, or if there is a compound effect of these two factors and how big the effect may be. Corkett and McLaren (1978), Huntley, Lopez (1992) assumed that stage development time was a function of temperature only, that micro-patches of food in the sea enabled copepods to graze efficiently and to grow at max rates. Ohman (1985) for Dabob Bay, Washington, and Evans (1981) for the North Sea also reported that food did not seem to influence body size, growth, development and reproduction of *Pseudocalanus*. In case of excess amounts of food, development times for different stages is only a function of temperature and may be approximated from embryonic development time.

Corkett and McLaren (1978) for the populations from Nova Scotia, and Thompson (1976; cited by Corkett and McLaren, 1978) for the populations from the North Sea found that development is roughly isochronal for all copepodids stages and that all copepodide stage has about the same duration as embryonic duration at any temperature. However, stage development time is not isochronal for naupliar stages, and for the North Sea it was estimated that duration of NI, NII, NIII, NIV, NV, and NVI stages was respectively .18, .37, 1.46, .81, .69 and .4 times EDT (Corkett and McLaren, 1978).

In our model, females reproduced 8 times when food was available; females were considered to be reproductive throughout of their life time span. For every cohort entering the pool of reproductive females (sex ratio of molting CV's was set to be 1:1), its ratio to a total number of reproductive females was calculated. Keeping mortality rates stage-specific but constant throughout the reproductive season, it was possible to keep track of the cohort structure of reproductive females and back calculate the proportion of females replenishing the pool of old nonreproductive females. Model shortest time interval between successive clutches was set equal to $1.5 \cdot EDT$ which corresponded to the longest stage duration time. This avoided temporal

overlap between successive broods. The duration of development stages was set as it was reported by Corkett and McLaren (1978).

2. *Pseudocalanus* spp. metabolism:

2.1 Weight estimates

Wet weights (mg) are available only for copepodid and adult stages (Cooney, Coyle, personal communication). Naupliar weights were taken from Hay, Evans (1988), and multiplied by 2.5 because PWS *Pseudocalanus* are, in average, 2.5 times bigger than those of the North Sea.

TABLE 1: *Pseudocalanus* weight, ug dry wt

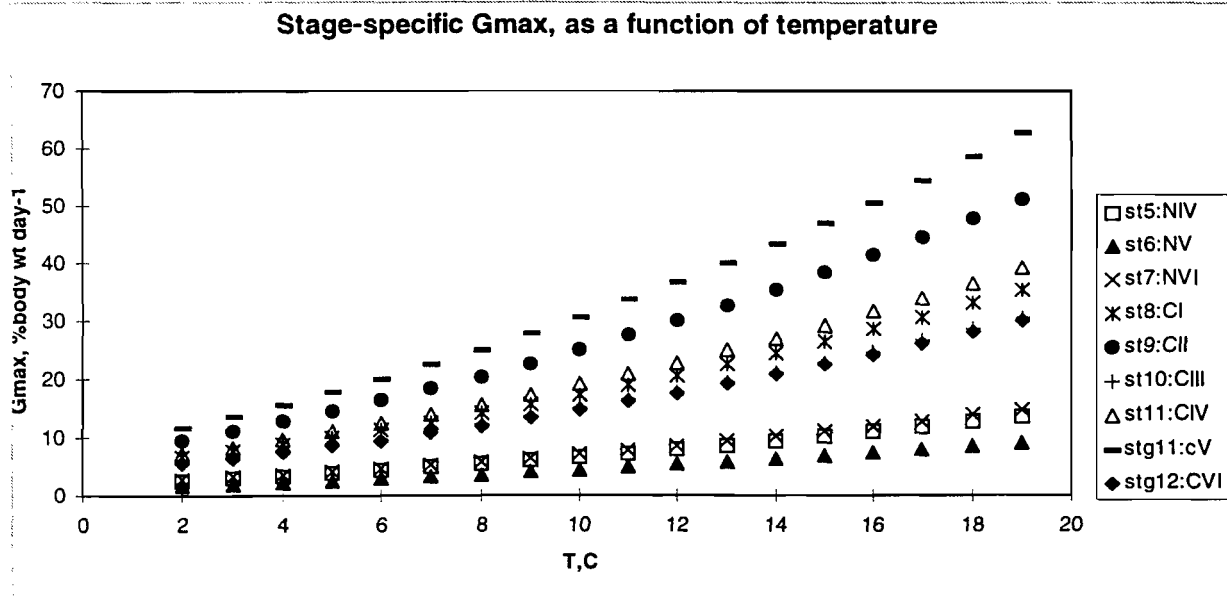
size	Hay,Evans(1988),10C	Vidal(1988), 10C	Cooney and Coyle (1996)
Egg	.304		.760 (2.5*.304 from Hay)
NI	.304		.760 (2.5*.304 from Hay)
NII	.367		.918 (2.5*.367 from Hay)
NIII	.498		1.246 (2.5*.498 from Hay)
NIV	.616		1.540 (2.5*.616 from Hay)
NV	.730		1.826 (2.5*.730 from Hay)
NVI	.809		2.022 (2.5*.809 from Hay)
CI	.551		1.650
CII	1.134	1.5	2.850
CIII	2.128	3.0	5.294
CIV	3.712	5.0	7.950
CV	5.968	7.0	13.126
AF	10.349	10.0	31.350
AM	5.339		9.900

In the model weight for each developmental stage is recalculated at every time step from

biomass estimates and abundance.

2.2 *Pseudocalanus* stage-specific growth rates

A simple growth model was developed to estimate net increase in *Pseudocalanus* biomass. Maximum growth rate for each feeding stage was determined as a difference in maximum weights between the successive stages times reciprocal of stage duration time, and was approximated by the exponential function of temperature. Growth rate for feeding adult female



was defined in a similar way, but upper weight limit was defined as the maximum weight a female can achieve if she carried an egg sack of maximum size (31 eggs). Time to achieve this weight when food is abundant should then be equal to the time between successive clutches, i.e. $1.5 \times \text{EDT}$. Nonreproductive old females and males just maintained balance (growth = ingestion - respiration - egestion) near zero levels, i.e. they did not grow. Food limitation did take place in the system after day 180 (the end of June), and was accounted for in mortality stage-specific pressure.

2.3 *Pseudocalanus* metabolic costs

Nitrogen losses are in the form of ammonia and are modeled by a weight-specific empirical equation developed for boreal zooplankton species by Dagg et al. (1982): $U = 0.072W^{.902}$, $\mu\text{gN}/\text{cop}/\text{day}$. In the model, the ammonia term was added to a nutrient pool.

2.4 Egestion

Conover (1968; cited by Magley, 1990) first found that herbivorous zooplankton assimilated phytoplankton with 60 to 95% efficiency. In the model, assimilation efficiency was set equal to

75% . The egestion term was added to the detritus pool.

2.5 Molting, % of content of body weight:

Vidal (1980) estimated for *C. pacificus* that molting costs were between 2 and .2% of carbon content of body weight. In the model, it was set to 0.5 of *Pseudocalanus* body weight

2.6 Mortality

Most of the available methods for estimating mortality rates for stage-structured zooplankton populations assume that mortality rates are either constant throughout time, uniform across stages, or both. But different stages respond in different ways to changes of temperature, food availability, and their predators remove size selected classes. Ohman and Wood (1996) used a population surface method to get average stage-specific total mortality estimates throughout the reproductive season. In the model, stage-specific mortality estimates followed the general pattern obtained by Ohman and Wood (1996) but varied in magnitude. The potential larval herring feeding pressure was excluded from mortality estimates before larvae herring entered the system (julian day 135).

TABLE 2: Instantaneous stage-specific mortality (d-1) for *Pseudocalanus*, averaged through the reproductive season (from Ohman, Wood, 1996)

Eggs	NI-NVI	CI	CII	CIII	CIV	CV	AF	AM
.0525	.11	.15	.07	.045	.06	.1	.0525	.55

RESULTS AND DISCUSSION

We have developed 1-D coupled biophysical model of plankton dynamics which simulates all life stages of *Pseudocalanus spp.* The model is tuned for 1995 and 1996, the first being a year when copepod biomass was high (including *Pseudocalanus spp.*), and the second, a low year. Good agreement is achieved between two model formulations, without and with *Pseudocalanus* life stages (Figure A-1). Results from modeling stage-specific *Pseudocalanus spp.* dynamics provide information on food availability for Pacific herring over the spring bloom (Figure A-2). It was reported that the earliest life-stages of marine fish have a substantial impact on the population dynamics of *Pseudocalanus spp.* (Bollens S.M., 1988; Hay S.J. et al., 1978). At present, our model stage-specific mortality estimates are similar to those obtained by Ohman and Wood (1996) for *Pseudocalanus* populations from the Dabob Bay, WA. To fit modeled *Pseudocalanus* biomass to the field data, first, potential larvae herring pressure was removed from the system before the day 135, when larvae herring enter the system; and second, stage-specific mortality in 1996 was set to twice that for 1995, causing about a threefold decrease in *Pseudocalanus* biomass (Figure A-1, A-3). At present, the simple growth model is structured to estimate the total *Pseudocalanus* increase in biomass; *Pseudocalanus* grows at maximum rates.

However, food limitation may occur in the system after spring phytoplankton bloom is exhausted (Eslinger, 1997) and we assume that it will be one of the components of stage-specific mortality pressure along with invertebrate and vertebrate predation. Figure A-3 shows that the difference in total *Pseudocalanus* biomass in years 1995 and 1996 is mainly due to the difference in adult female biomass. Food limitation is the likely factor controlling adult female abundance. In year 1995 there is distinct secondary *Pseudocalanus* bloom followed by high summer abundance of adult reproductive females. Food limitation and stage-specific mortality pressure from Prince William Sound field data are not included in the formulations.

REFERENCES

Bollens S.M. 1988. A model of the predatory impact of larval marine fish on the population dynamics of their zooplankton prey. In: J. Plankton res., v.10, n.5, pp. 887-906

Cooney R.T., and K.O. Coyle. 1996. The role of zooplankton in Prince William Sound Ecosystem. In: SEA - An Integrated Science Plan for the Restoration of Injured Species in Prince William Sound, FY 1995 Annual Report; Chapter 5.

Corkett C.J, and McLaren I.A. 1978. The biology of *Pseudocalanus*. In: Russel, F.A. and Yonge, M (eds) Advances in Marine Biology. Academic Press, New-York, V.15, pp.1-231

Coyle K.O., A.J. Paul, and D.A. Ziemann. 1990. Copepod populations during the spring bloom in an Alaskan subarctic embayment. In: J. of plankton Res., V.12, N.4, pp.759-797.

Dagg M. J., J. Vidal, T.E. Whitley, R.L. Iverson and J. J. Goering. The feeding, respiration, and excretion of zooplankton in the Bering Sea during a spring bloom. In: Deep-Sea Res., v.29, n.1a, pp.45-63, 1982.

Davis C.S. 1983. Laboratory rearing of marine calanoid copepods. J. Exp. Mar. Biol. Ecol., 71, pp.119-133

Eslinger D.L. 1997. Biophysical modeling and validation through remote sensing. In: Exxon Valdez Oil Spill Annual Report (Restoration Project 96320-R), Alaska Department of Fish and Game, Anchorage, Alaska.

Evans, F. 1981. An investigation into the relationship of sea temperature and food supply to the size of the planktonic copepod *Temora longicornis* Muller in the North Sea. In: Estuar. coast. Shelf Sci. 13: 145-158.

Hay S.J., Evans G.T, Gamble J.C. 1988. Birth, growth and death rates for enclosed populations of calanoid copepods. In: J. Plankton Res., v.10, pp. 431-454.

Huntley M.E., Lopez M.D.G. 1992. Temperature-dependant production of marine copepods: a

global synthesis. In: Am. Nat., v.140, pp.201-242.

Magley C.W. 1990. A phytoplankton-zooplankton model of the middle and outer shelf domains of the southeast Bering Sea shelf during spring bloom conditions. PhD thesis. The Florida State University. College of Arts and Sciences.

McLaren I.A., Sevigny, J.M., and Corkett, C.J. 1989. Temperature-dependant development in *Pseudocalanus* species. In: Can. J. Zool., v.67, pp.559-564.

Ohman M.D. 1985. Resource-satiated population growth of the copepod *Pseudocalanus* sp. In: Ergeb. Limnol., v.21, pp. 15-32.

Ohman M.D, Wood S.N. 1996. Mortality estimation for planktonic copepods: *Pseudocalanus newmany* in a temperate fjord. In: Limnology and Oceanography, v.41, n.1, pp.126-135.

Paffenhofer, Harris. 1976. Feeding, Growth and Reproduction of the Marine Planktonic Copepod *Pseudocalanus elongatus* Boeck. In: J. Mar.biol. Ass. UK, V.56, pp. 327-344.

Pollard R.T., C.L. Gallegos, and W.G. Harrison. 1973. The deepening of the wind-mixed layer. In: Geophysical Fluid Dynamics, n.4, pp.381-404.

Vidal.1980. Physioecology of zooplankton. 1. Effects of phytoplankton concentration, temperature, and body size on the growth rates of *Calanus pacificus* and *Pseudocalanus* spp. In: J. of Marine Biol., n.56, pp. 111-134

Vidal J. 1980. Physioecology of zooplankton. 2. Effects of phytoplankton concentration, temperature, and body size on the development and molting rate of *Calanus pacificus* and *Pseudocalanus* spp. In: J. of Marine Biol., n.56, pp. 135-146

Appendix B

Effects of Environmental Variability on the Growth of Larval Pacific Herring in Prince William Sound, Alaska

Sarah J Thornton and David L Eslinger

Institute of Marine Science
University of Alaska Fairbanks

Justification

As part of SEA, we have developed a biophysical model of Prince William Sound which accurately simulates lower trophic level dynamics. Here, we present the results of continued modeling work examining the early life history of Pacific herring. Herring dynamics are modeled in conjunction with the biophysical model of phytoplankton and zooplankton dynamics.

Abstract

Growth and survival of larval Pacific herring, *Clupea pallasii*, are simulated for 1993 through 1996 using a larval dynamics model coupled to a biophysical model of plankton dynamics in Prince William Sound, Alaska. The biophysical model, a one-dimensional (z,t), high-resolution plankton model forced by measured meteorological data, closely reproduces the spring phytoplankton bloom and subsequent zooplankton population development in Prince William Sound. The herring model is forced by physical and zooplankton results from the biophysical model and is used to examine the influence of oceanographic processes on the growth and survival of Pacific herring larvae. Small changes in mixed layer temperature and zooplankton concentrations during the larval period lead to substantial differences in the larval stage duration. Larval herring are modeled from hatching through metamorphosis to the juvenile stage. The herring model includes feeding, growth, metabolic costs, starvation and predation components. The model is initialized with hatch date estimates and results are compared with juvenile herring characteristics. We have examined the response of Prince William Sound larval herring to environmental variability and different forcing scenarios. The implications of our results to understanding Pacific herring recruitment variability is discussed.

Introduction and Background

Coupled physical and biological modeling of phytoplankton and zooplankton dynamics in Prince William Sound have shown there to be two general scenarios of springtime dynamics. Warm, quiescent springs lead to brief, intense phytoplankton blooms, whereas colder, stormier springs lead to longer phytoplankton blooms. These two types of phytoplankton blooms produce substantially different zooplankton blooms. The brief, intense blooms occur too quickly for much biomass to be transferred into the upper trophic levels. Therefore, the following zooplankton

bloom is substantially lower. In contrast, the longer duration phytoplankton bloom allows time for the zooplankton to “catch-up” and produce high zooplankton concentrations.

Larval herring feed on certain stages of small calanoid copepods, which reproduce throughout the spring and summer. The reproductive effort of these copepods is dependent on the timing, magnitude, and duration of the phytoplankton primary production in the spring bloom period and throughout the summer. The interactions between the various types of phytoplankton (*e.g.*, diatoms, flagellates) and zooplankton (*e.g.*, oceanic copepods, neritic copepods) varies both between and within years. The timing of the major increase in biomass of phytoplankton or zooplankton, sometimes called the spring phytoplankton or zooplankton bloom, respectively, may be important to the first feeding and subsequent survival of the larval herring. Results through FY96 indicate that physical forcing dominates the dynamics at the lower trophic levels. The physical signal propagates up through the food chain and has relevant consequences months after the physical interaction actually occurred. We have constructed these simple models of larval herring dynamics to examine the possible implications of these lower trophic level differences on herring growth. Are the interannual differences manifested in the growth rates and larval period duration of the herring?

Model Methodology

Herring are modeled from hatch in the planktonic stage through metamorphosis to the juvenile stage. Herring in the Bering Sea, Southeast Alaska, and British Columbia metamorphose at 25 to 30mm in length, regardless of age. Prince William Sound herring hatch in mid-May as yolk-sac larvae and by mid-July are found as juveniles in juvenile nursery areas. As a target for the model, we use a length of 25mm for metamorphosis, and calculate the time for the average fish to reach 25mm. We use 60 days as a reference point at which to judge size-at-age. Larvae hatch as yolk-sac larvae and begin to feed after 48 degree-days have passed.

The models are forced by the biophysical model results of mixed layer temperature and small calanoid copepod biomass. Herring larvae are known to eat smaller calanoid copepods, for example *Pseudocalanus* spp. The biophysical model does not simulate age-structure in the small calanoid (*Pseudocalanus*-type) population. As herring larvae can only eat the smaller stages (eggs and naupliar stages, copepodites for the late larvae) a fraction of the *Pseudocalanus*-type biomass is considered to be available for the larvae to consume. This fraction is set such that in an intermediate year (1995) larvae reach 25mm in 60 days, in agreement with field data. For the purpose of this discussion, 55% of the *Pseudocalanus* biomass is considered to be small enough for the larvae to eat. Annual copepod levels fall into two categories: 1993 and 1996 are low years, 1994 and 1995 are high years. Over the larval period, from hatch in May through the summer, zooplankton biomass shows a gradual decline from peak levels (Figure B1). Mixed layer temperature is relatively similar in all modeled years (1993-1996). Temperatures in the mixed layer range from 5 to 15°C with a gradual warming over the larval period. The warmest year was 1993.

The models include feeding, metabolic costs, and mortality due to predation. Food consumption

is approximately 25% of the fish biomass per day, up to the maximum field-observed zooplankton mortality. Feeding and metabolic rates are a function of temperature. Predation mortality is set at 4% of the fish biomass daily. Feeding occurs only during the day on a 16:10 light:dark cycle.

Depth-integrated model:

The depth-integrated model is a stand-alone, point model which is forced by outputs from the biophysical model. The model simulates larval growth for 1993, 1994, 1995 and 1996. Food concentrations are the average biomass of small calanoid zooplankton if evenly distributed over the top 40m of the water column. Sensitivity analyses are conducted on the depth-integrated model to examine temperature and food effects on growth rates. Sensitivity trial 1 involved modifying the amount of food available to the larvae by $\pm 20\%$. The biophysical model does not include *Pseudocalanus*-type age-structure. The relative proportion of the smaller stages of *Pseudocalanus*-type copepods is unknown at this time, although another modeling effort is working on this problem. The model was run at both higher and lower food availabilities. Sensitivity trial 2 involved modifying the mixed layer temperature by $\pm 2^\circ\text{C}$.

Depth-resolving model:

The depth-resolving model examines the different growth conditions felt by larvae at discrete depths in the water column. It is an enhancement of the biophysical model, and as such, feedback occurs as the larvae consume some of the zooplankton biomass. Larvae are distributed in the upper 50m of the water column, with the same number in each depth-interval. Larvae do not vertically migrate and are not mixed by physical processes, but maintain their position in the water column. Zooplankton are mixed. The model is run for 1995 and 1996 using the same meteorological forcing conditions as the depth-integrated model.

Results

Depth-integrated model results

Using depth-averaged small-sized calanoid biomass, herring growth in all years is similar until the larvae are 40 days old (day 165) (Figure B2). In 1993 and 1996, growth slows due to food limitation after day 165. Table I gives a summary of the growth rate, size-at-age, and larval period duration for each of the test years. Growth rates (% of mass gained per day) vary by a factor of two between the 'high' and 'low' food years and fall within the range of literature values for field and laboratory-reared Pacific and Atlantic herring larvae. The time for the larvae to reach 25 mm ranges from 50 to >100 days. The two food scenarios produce two results. Years with higher food have larger larvae which reach metamorphosis earlier. Years with lower food concentrations have slower growing larvae which reach metamorphosis later. 1995 larvae reach metamorphosis (25mm) almost a month earlier than the 1996 larvae.

Table I: Summary table for 1993 through 1996 specific growth rates (%d⁻¹), size at 60 days (mm) and the time to reach metamorphosis (d).

	1993	1994	1995	1996
Growth rate (%d ⁻¹)	3.3%	6.1%	5.7%	4.5%
Length-at-age60 (mm)	18.2	26.4	25.1	21.4
Larval stage duration (d)	>100	55	60	88

Sensitivity analyses for depth-averaged model

Food availability:

Differences were seen in all measured parameters, including the larval period length and larval growth rates (Table II). Higher food availability increases growth rates and length at 60 days for all four years. In the years in which food was more limiting (1993 and 1996) an increase in food shortened the larval period by up to 6 days. However, in years with higher food abundance (1994 and 1995), the difference in larval stage duration was very small under both higher and lower food availability.

Table II: Summary table for sensitivity trial 1, food availability, showing the larval stage duration (d) under three food levels.

	1993	1994	1995	1996
- 20%	>100	58	64	94
<i>no offset</i>	<i>>100</i>	<i>55</i>	<i>60</i>	<i>88</i>
+ 20%	96	55	58	82

Temperature:

In the second experiment, the model was run at mixed layer temperatures of 2°C higher and lower than actual. Temperature has many effects on Prince William Sound dynamics, affecting food concentrations available to larval fish. In this model, temperature also affects larval herring feeding rates and metabolic rates, following a Q₁₀ relationship. Higher temperatures increase metabolic costs and maximum feeding rates for the larvae. In the poor food years (1993, 1996), the larvae are food-limited and therefore cannot increase the feeding rate. Metabolic rates increase under the higher temperatures, resulting in depressed growth rates and size-at-age. The larval stage duration increases by a few days (Table III). In the higher food years (1994, 1995), there is little or no food limitation, so both feeding and metabolic rates increase. Growth rates and the larval size-at-age are slightly higher due to more feeding. Cooler temperatures decrease the metabolic costs felt by the larvae, but also decrease the maximum feeding rate. In years of

poor food concentrations, the growth rates are slightly enhanced by the cooler temperatures. In years of higher food concentrations, there is a dramatic increase in the larval stage duration (8-10 days) due to a reduction of the non food-limited growth rates by ~1%/d.

Table III: Summary table for sensitivity trial 2, mixed layer temperature, showing the larval stage duration (d) under three temperature regimes.

	1993	1994	1995	1996
- 2°C	99	65	68	85
<i>no offset</i>	<i>>100</i>	<i>55</i>	<i>60</i>	<i>88</i>
+ 2°C	>100	51	56	91

Depth-resolving model results

In the depth-resolving model, small calanoid copepods are concentrated at the depth of the chlorophyll maximum. Larval growth is greatest in the areas of concentrated zooplankton (Figure B3). In 1995, a deep mixed layer results in significant zooplankton biomass down to 40m. Larvae in the top 40m are able to feed and grow. Larval growth continues in the surface 25m after 60 days. In 1996, a shallower mixed layer keeps the zooplankton biomass in the surface 25m. No larval growth occurs below 25m. After 60 days, food becomes limiting at all depths except 15-25m. The position of larvae in the water column has a large effect on the growth rate, size-at-age, and larval stage duration. Herring food is not evenly distributed in the water column; there is vertical structure to the zooplankton community. A further enhancement of the model will be to add herring vertical migration.

Discussion

Subtle changes in spring weather determine summer plankton dynamics in Prince William Sound. Interannual differences exist in the timing, magnitude, and duration of the spring phytoplankton and zooplankton blooms. We have constructed these simple models of larval herring dynamics to examine the possible implications of these lower trophic level differences on herring growth. Are the interannual differences manifested in the growth rates and larval period duration of the herring?

We have constructed simple models of larval herring dynamics representing the fate of the average fish each year. All modeled larvae eat the same proportion of the calanoid population. When herring larvae are small, only the smaller life-stages of the calanoids are small enough for the fish to eat. As the larvae grow, their gape widens and larger stages become available for consumption. The size-structure of the calanoids will also change over the season as reproduction occurs. The current biophysical model does not include this size- or stage-structure for the small calanoid population (see Pintchouck and Eslinger for a version which includes the age-structure). We have scaled the model such that in an intermediate year (1995), the larvae are able to reach metamorphosis in 60 days. As a result, 55% of the calanoids are assumed to be an appropriate

size for the larval herring to eat.

Initial growth rates are similar in 1993 through 1996. All fish are growing at maximum rates, with interannual differences in growth rate controlled by temperature. The zooplankton concentrations are high in the initial days of the larval period. Food limitation occurs later in the larval period, not at first-feeding. As the fish grow, they require more food. In the years with lower food concentrations, the larvae become food limited and their growth slows. In 1993, limitation begins by the time the larvae are 20 days old. In 1996, the higher zooplankton concentrations allow unlimited growth until the larvae are about 30 days old. The larvae continue to feed under these lower food concentrations, but they cannot eat as much, and therefore grow slower. These fish take much longer to reach metamorphosis size. If these growth conditions mimic the true case in Prince William Sound, it can be seen that in years with lower zooplankton concentrations, herring will spend longer in the vulnerable larval stage.

The sensitivity analyses help to clarify the relative effects of temperature and food on larval growth. As expected, when the concentration of food is increased in low-food years, the limitation is eased and growth rates increase. In the high-food years (1994, 1995), decreasing the available biomass of food by 20% does decrease the growth rates. A change of only 20% causes a 3-4 day increase in the larval period, showing that the larvae in 1994 and 1995 were close to food limitation in the base case. When food is not a limiting factor, increasing the temperature can decrease the larval period duration by enhancing growth rates over the increased metabolic costs. If fish are food-limited, however, increasing the temperature can cause drastic decreases in a growth rate due to higher metabolic costs. In 1993, larvae were both food-limited and experiencing the warmest temperatures of the four model years. The 1993 larvae had the lowest growth rates and took over four months to reach 25mm in length. Metamorphosis did not occur in the model until late September.

After metamorphosis to the juvenile stage, the herring are much more motile, actively swimming in pursuit of prey and in avoidance of predators. A larger size range of food particles is available to the fish. The juveniles have only a short time to store energy for the coming winter, when zooplankton have very low standing stocks. There is limited food available to the juvenile herring. The better their condition entering the overwintering period, the greater their chance of surviving the near-fast conditions they experience until the following spring zooplankton bloom. Therefore, the longer the larval period, the harder it is for the juveniles to prepare for the winter. The years examined in this modeling effort show two different summertime zooplankton scenarios. Periodic strong wind mixing events in the spring of 1995 prolonged the phytoplankton bloom resulting in tight pelagic coupling and a high biomass of calanoid copepods. A high copepod biomass developed in 1994 as well. Calm winds in 1996 led to a short, uncoupled phytoplankton bloom and low copepod biomass. The phytoplankton bloom in 1993 was also short and uncoupled. These springtime differences are manifested in the duration of the larval period for Pacific herring. Years with prolonged phytoplankton blooms and high calanoid biomass may lead to earlier larval metamorphosis, allowing more time for the herring to prepare for the overwintering fast.

Figure Legends:

Figure 1. Prince William Sound model domain, with an example of regions influenced by similar winds when the winds are blowing north at Potato Point. In this example, black is land, and the letters correspond to the following locations with measured winds: VZ, Valdez weather station; PP, Potato Point; BI, Bligh Island; MB, Mid-Sound buoy; CB, CLAB buoy; WH, Whittier; AR, Applegate Rocks; and MI, Middleton Island.

Figure 2. Wind pattern produced from using the Java tool, using the pattern shown in Figure 1, for a scenario with strong north winds observed at Potato Point.

Figure 3. Phytoplankton response to spatially varying wind fields in 1995.

Figure 4. Zooplankton response to spatially varying wind fields in 1995.

Figure 5. Phytoplankton response to spatially varying wind fields in 1996.

Figure 6. Zooplankton response to spatially varying wind fields in 1996.

Figure A-1. *Pseudocalanus* total biomass (mg wet weight/m³) comparisons between two model formulations and field data.

Figure A-2. *Pseudocalanus* model total naupliar biomass (mg wet weight/m³).

Figure A-3. Model stage-specific *Pseudocalanus* biomass (mg wet weight/m³).

Figure B-1. Forcing data for the herring depth-integrated model. Top: Total small calanoid biomass in 1993 through 1996. Bottom: Mixed layer temperature. For clarity, only the extreme years are shown (1993 warm, 1995 cool).

Figure B-2. Length (mm) of larval Pacific herring from depth-averaged model for 1993-1996. Dashed lines show 60 days and metamorphosis length (25mm).

Figure B-3. Depth-resolving model results showing larval length after 60 days (solid) and 80 days (dashed) in the surface 50m. Note that lengths are greater in 1995 than in 1996, and that fish grow at deeper depths in 1995.

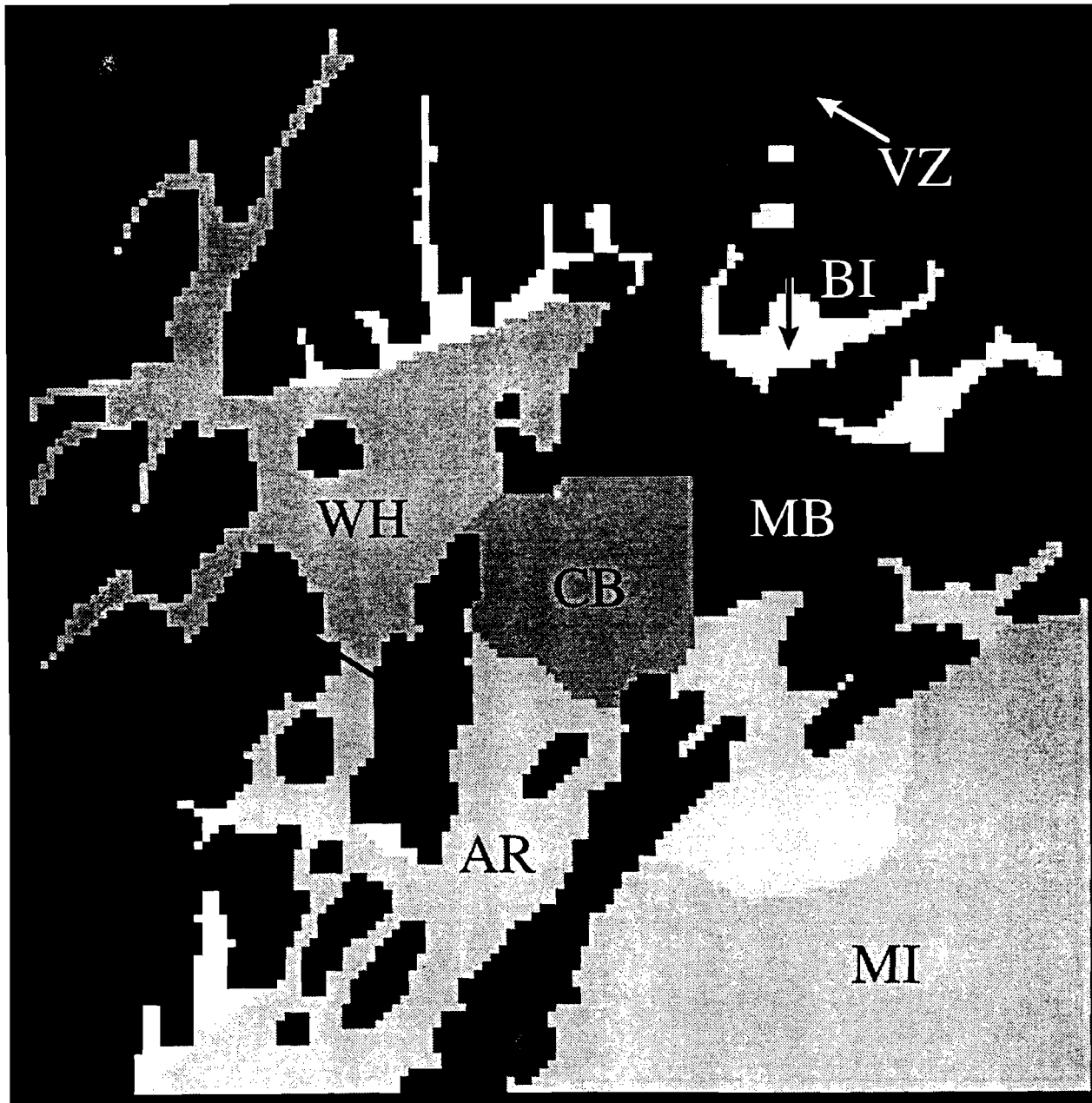


Figure 1: Prince William Sound model domain, with an example of regions influenced by similar winds when the winds are blowing north at Potato Point. In this example, black is land, and the letters correspond to the following locations with measured winds: VZ, Valdez weather station; PP, Potato Point; BI, Bligh Island; MB, Mid-Sound buoy; CB, CLAB buoy; WH, Whittier; AR, Applegate Rocks; and MI, Middleton Island.

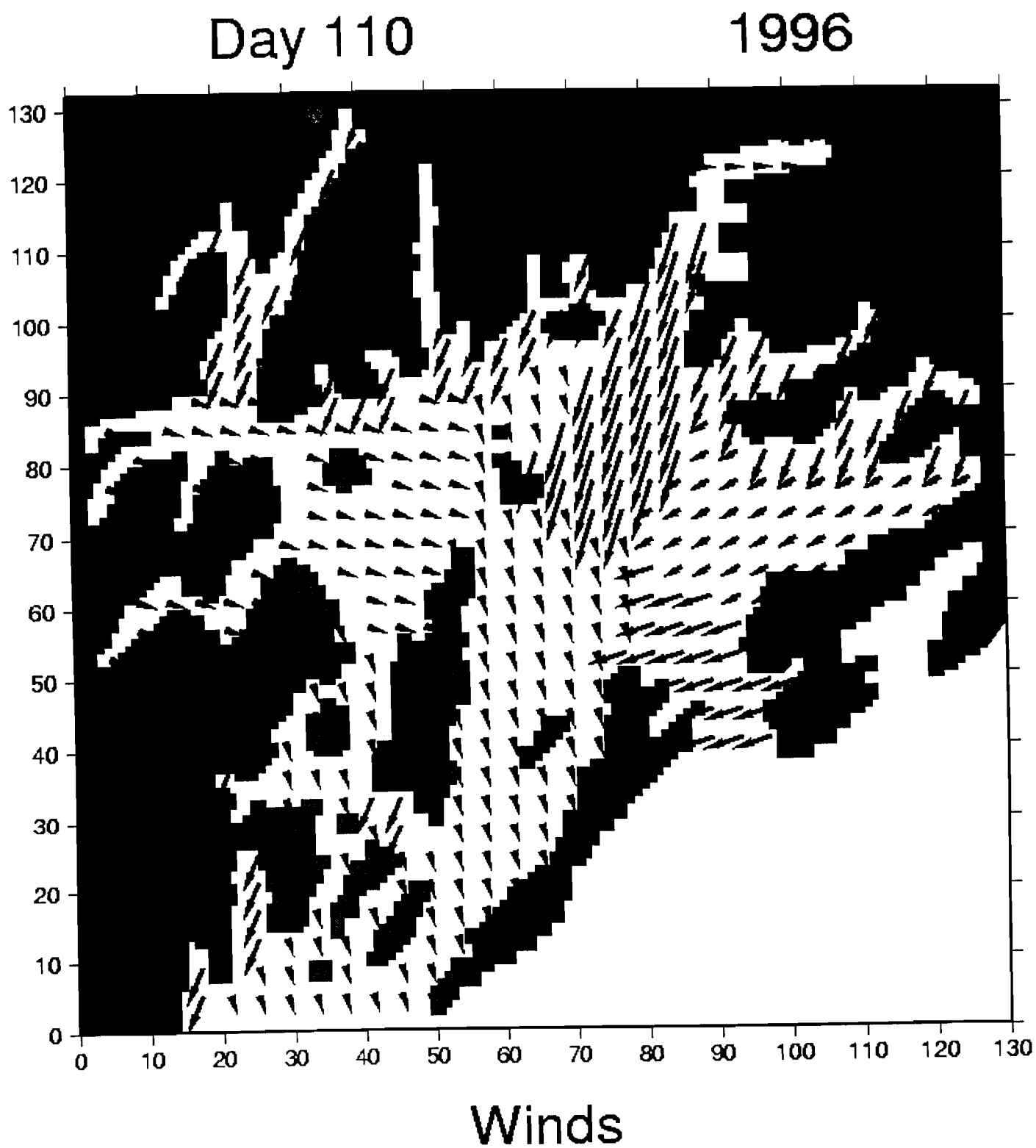


Figure 2:

Day 115

1995

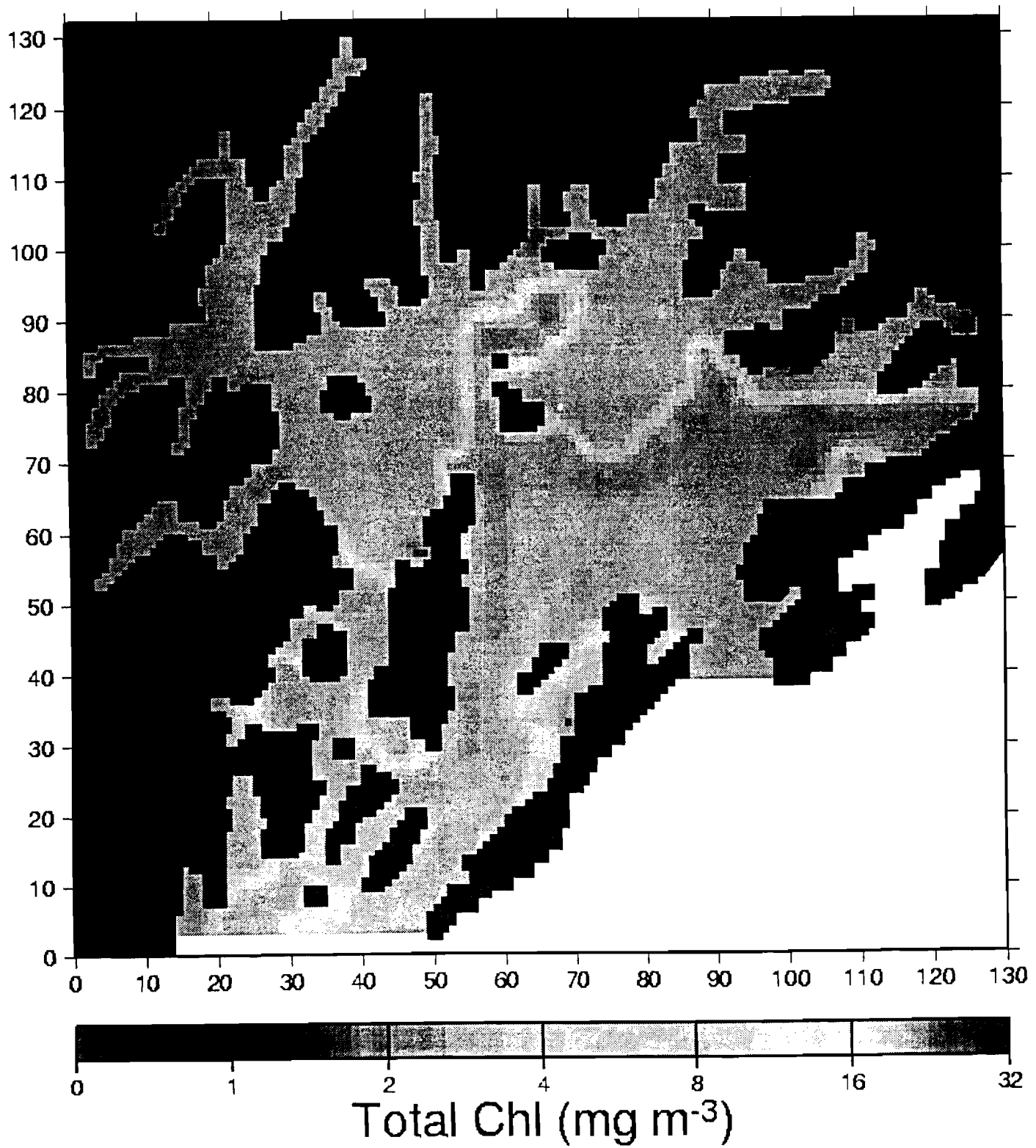


Figure 3:

Day 130

1995

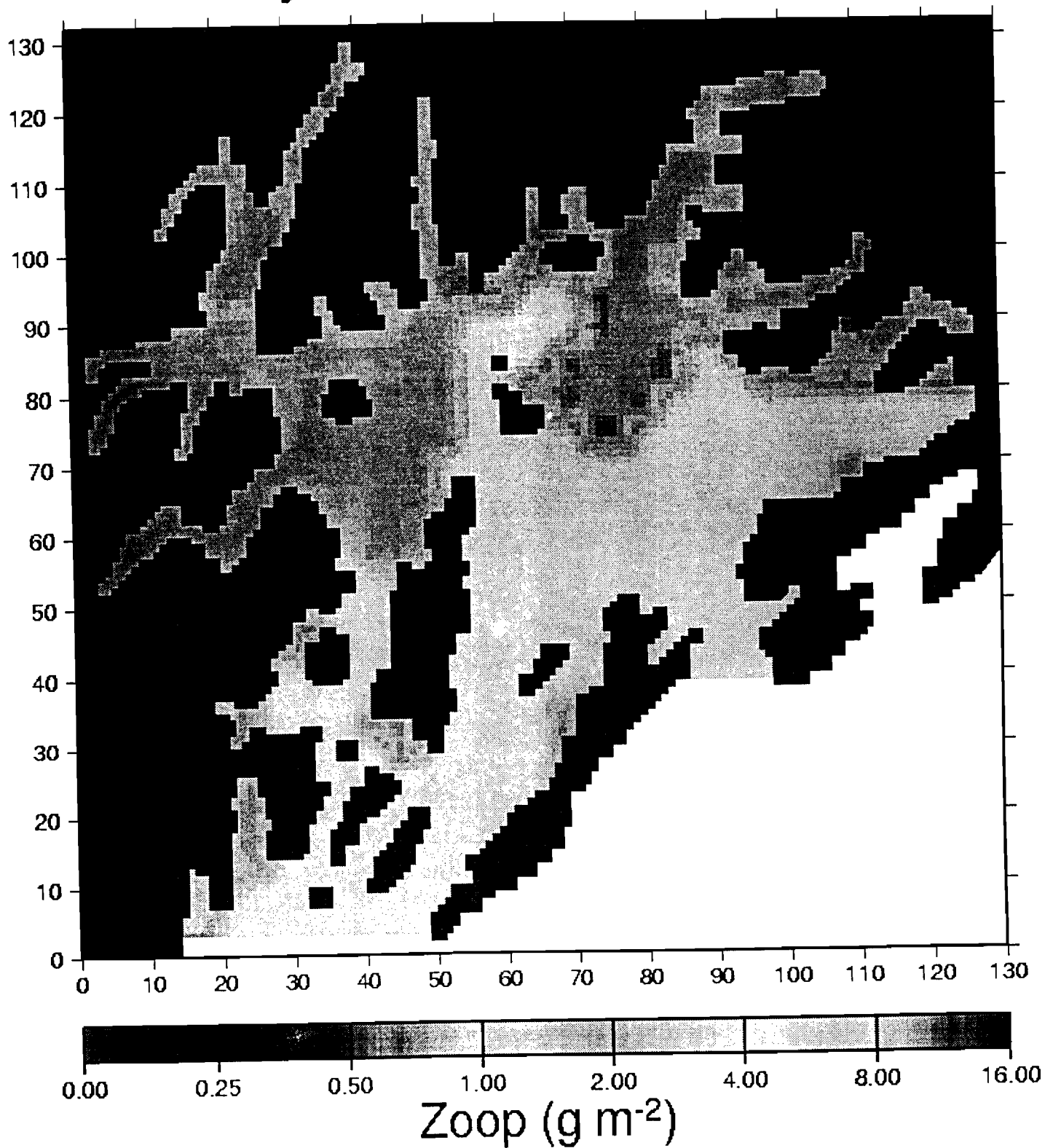


Figure 4

Day 115

1996

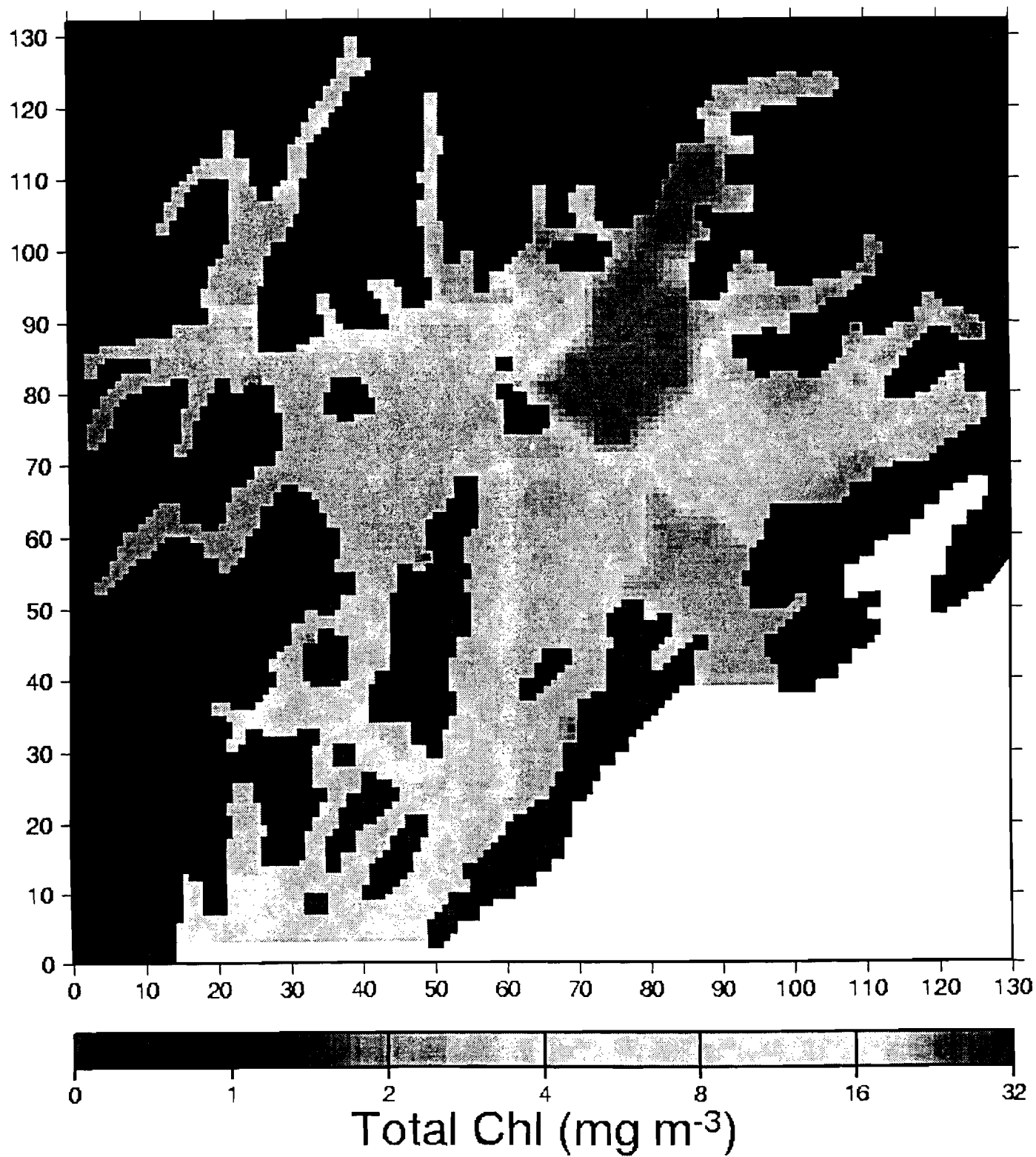


Figure 5

Day 130

1996

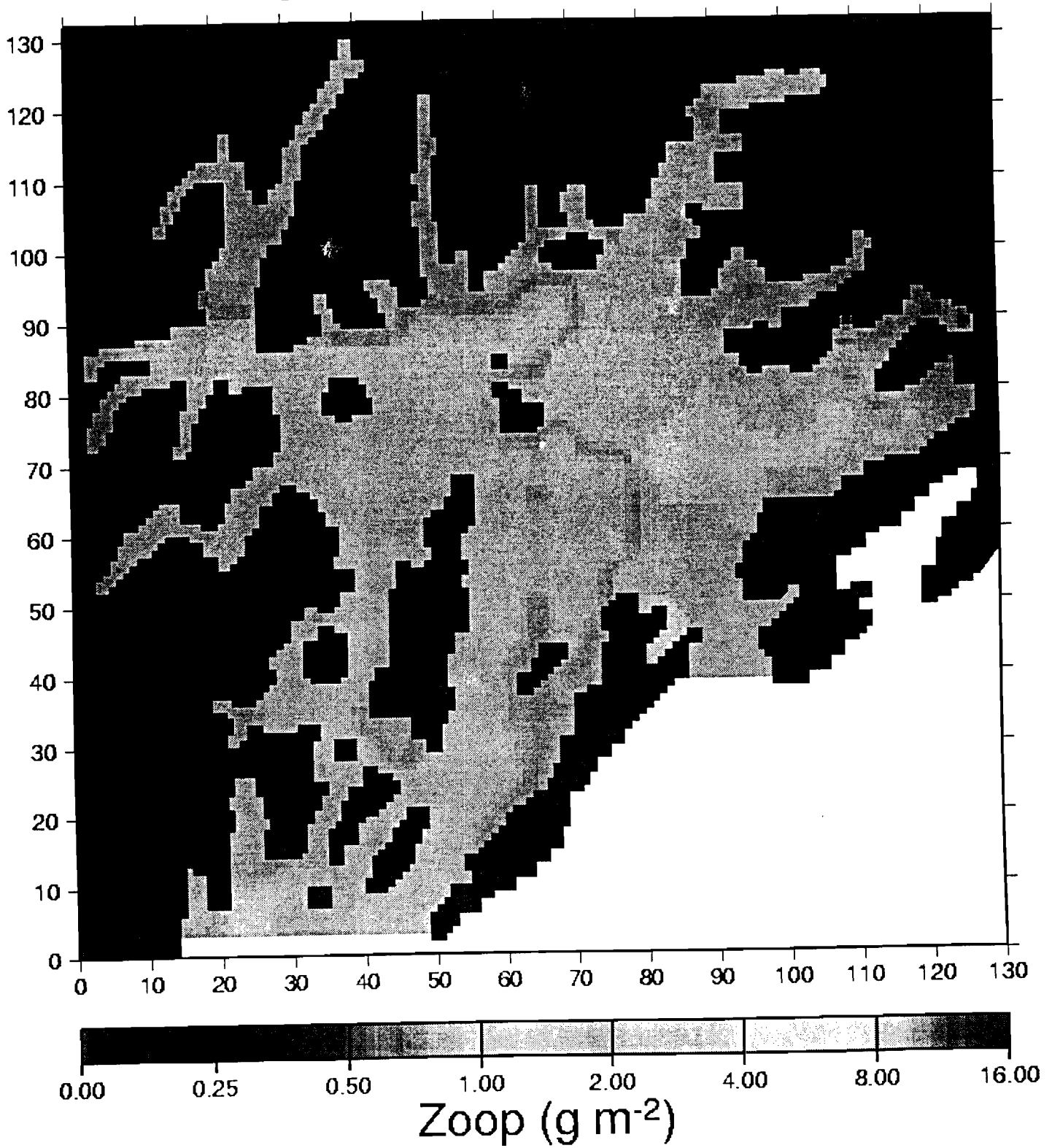


Figure 6

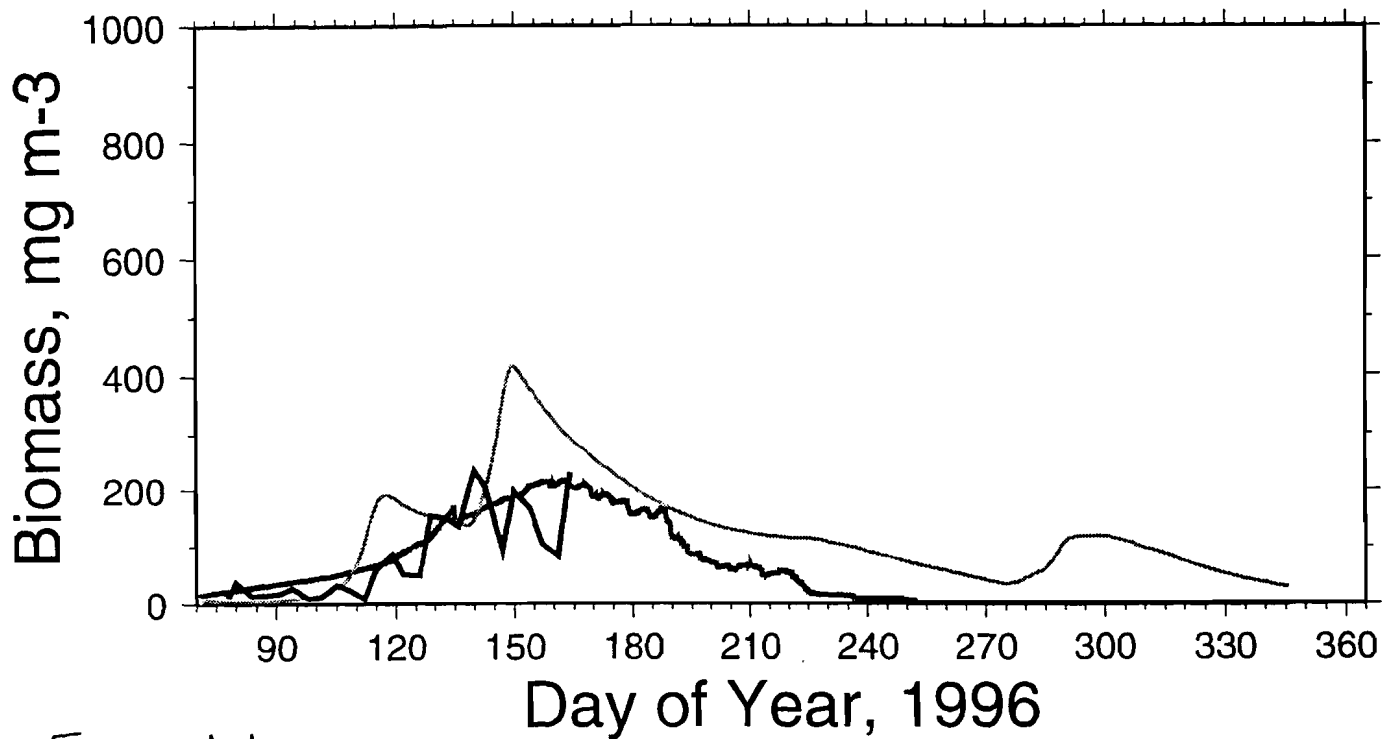
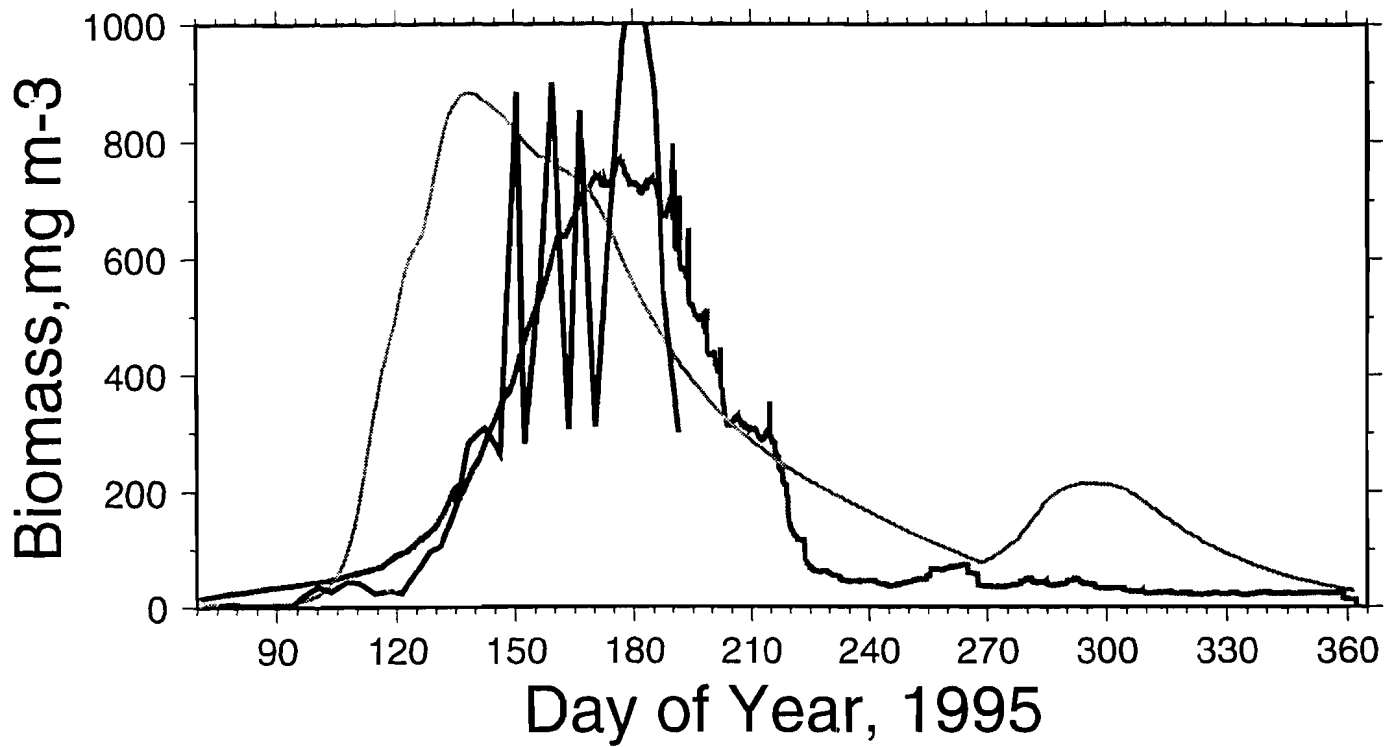


Figure A-1

- Field
- Model, 1st formulation: no life stages
- Model, 2nd formulation: with life stages

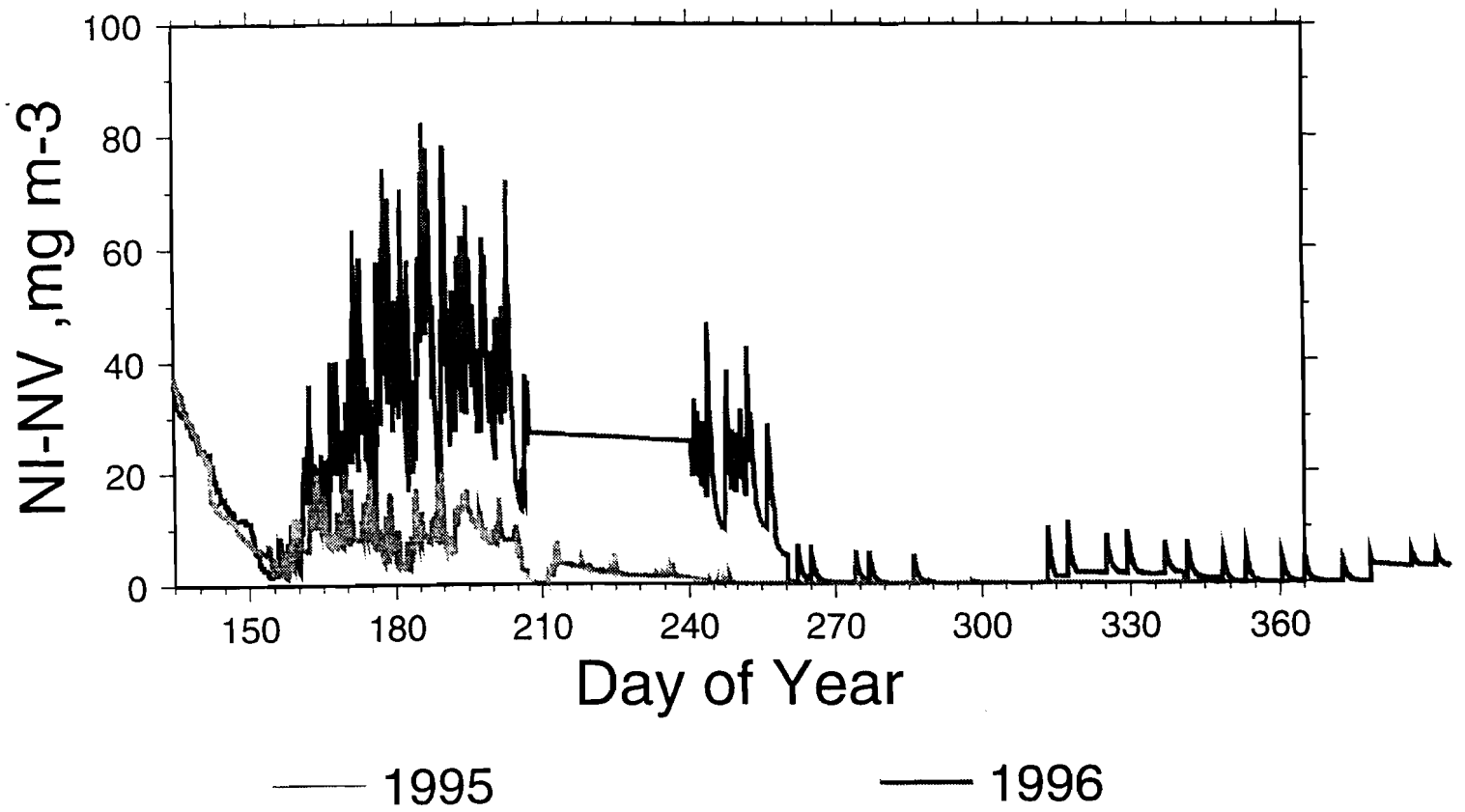
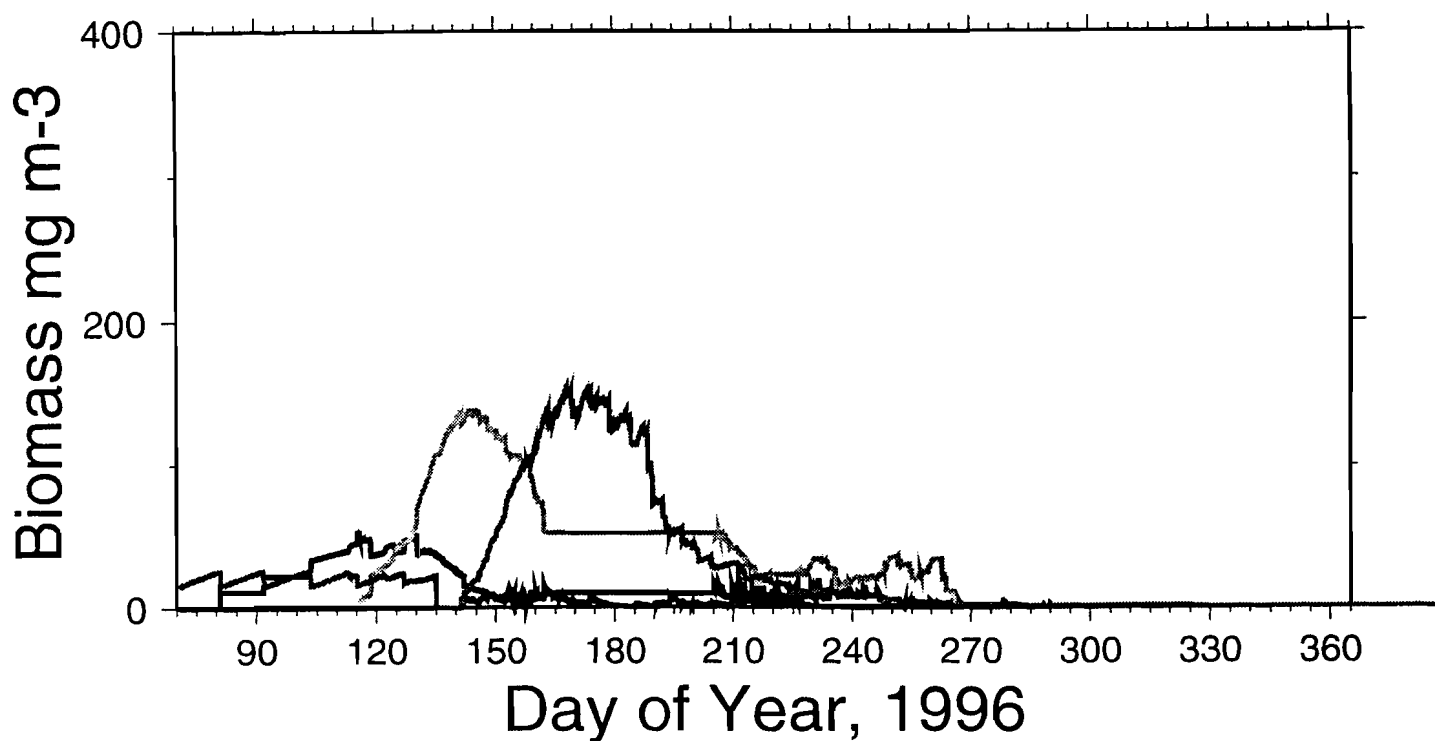
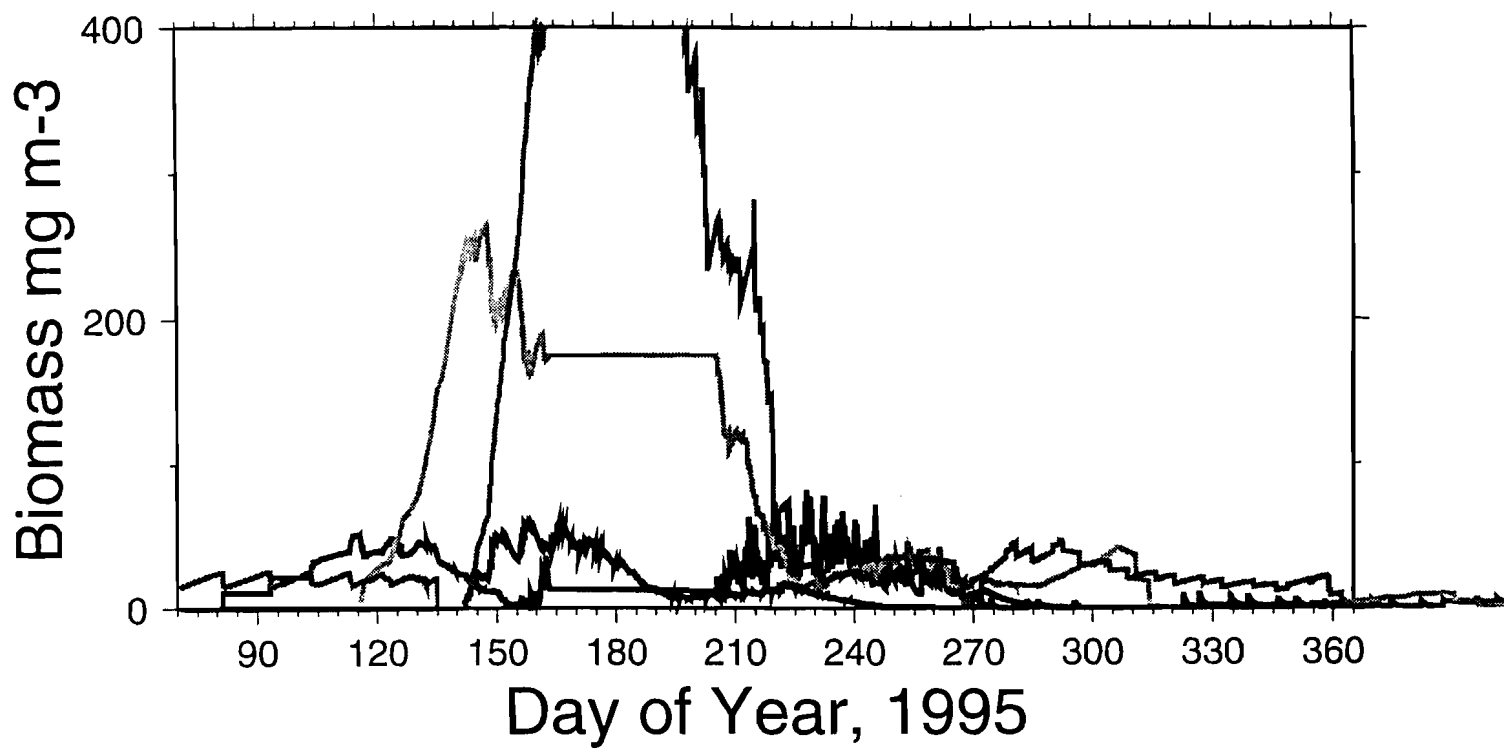


Figure A-2.



— Eggs+(N I - N VI) — C I - C V
 — Males — Females

Figure A-3

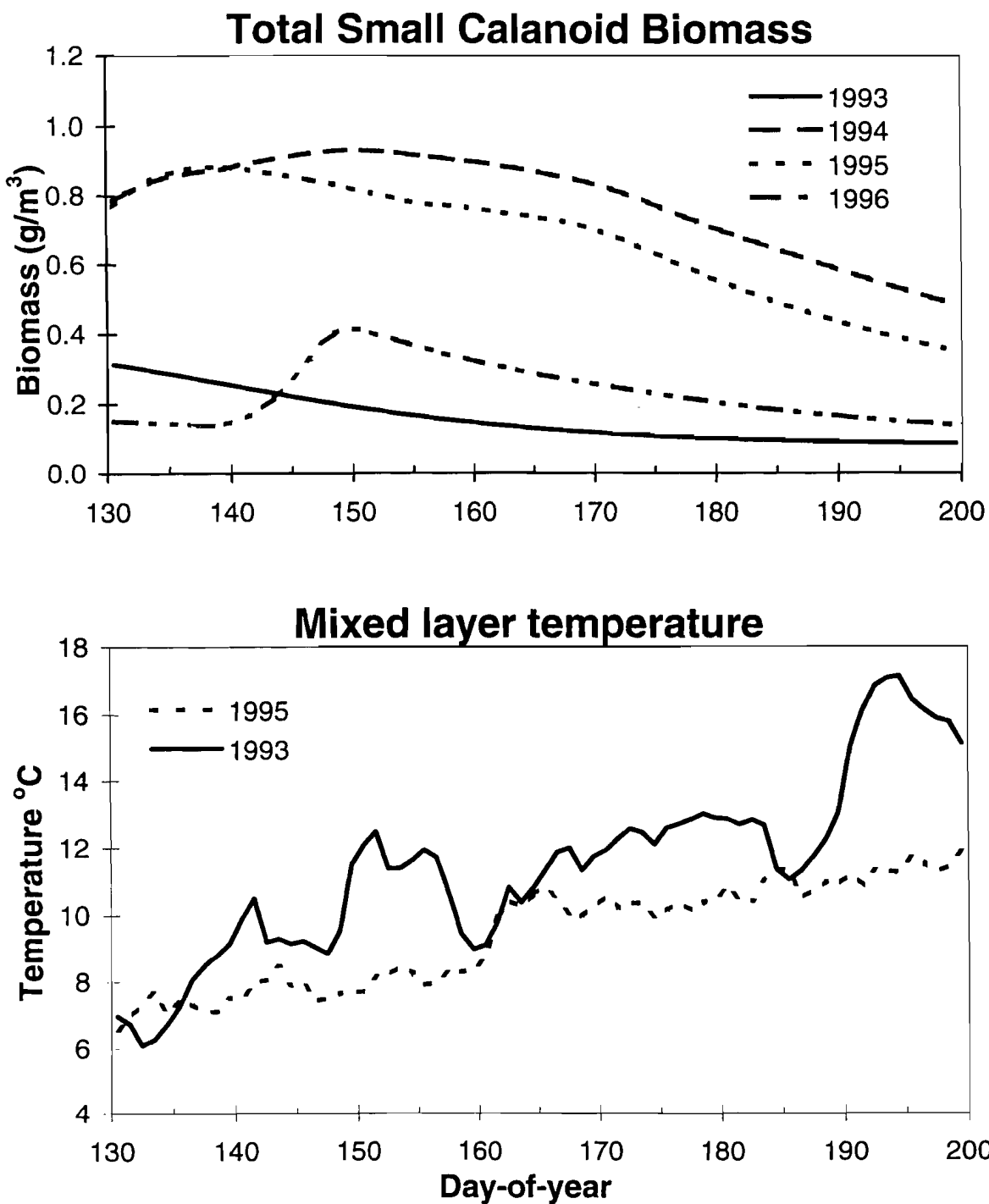


Figure B-1: Forcing data for the herring depth-integrated model. Top panel: Total small calanoid biomass in 1993 through 1996. Bottom panel: Mixed layer temperature. For clarity, only the extreme years are shown (warm 1993, cool 1995).

Length of larval Pacific herring

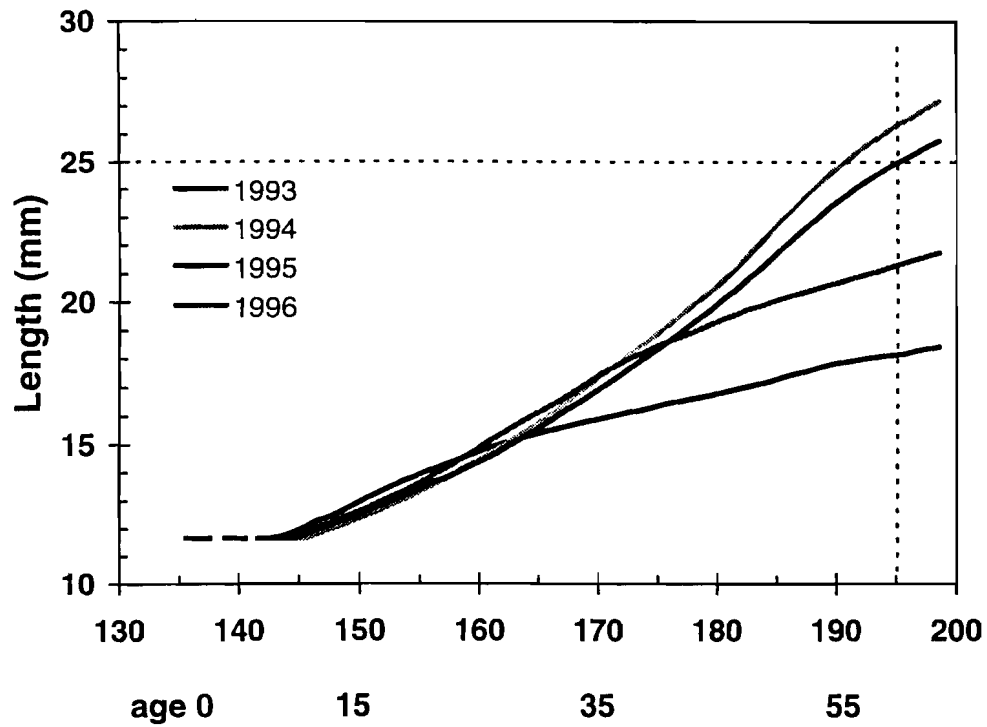


Figure B-2: Length (mm) of larval Pacific herring from depth-averaged model for 1993-1996. Dashed lines show 60 days and metamorphosis length (25mm).

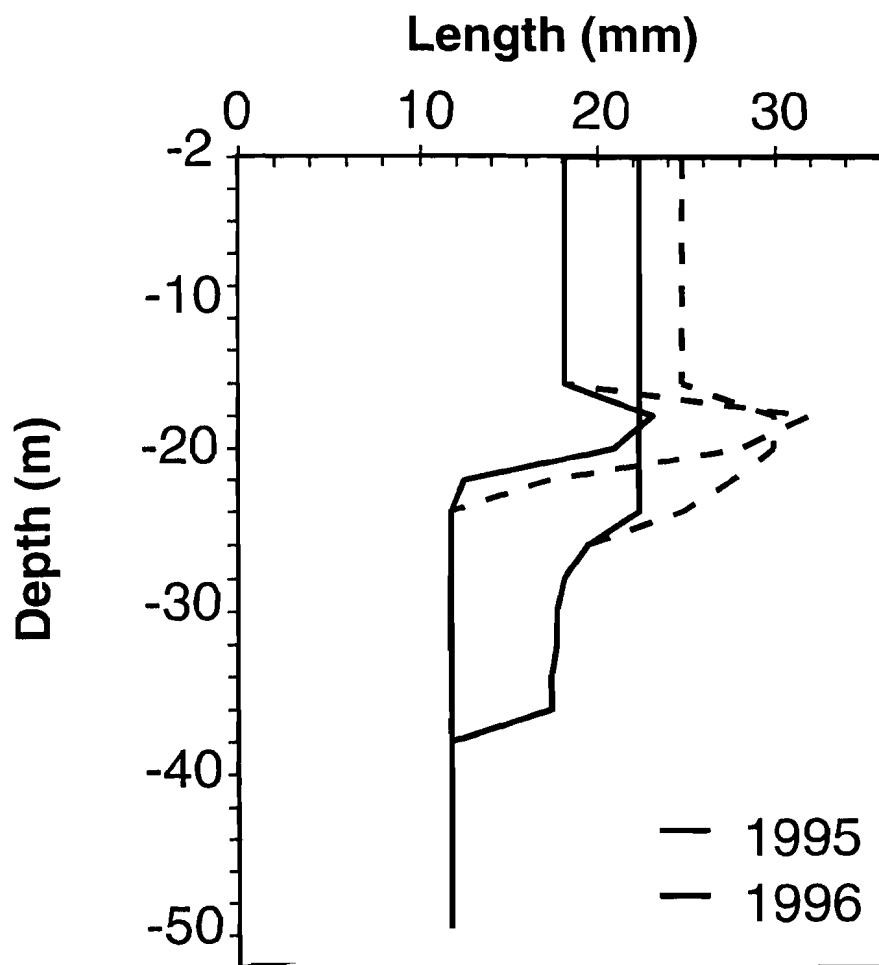


Figure B-3: Depth-resolving model results showing larval length after 60 days (solid) and 80 days (dashed) in the surface 50m. Note that lengths are greater in 1995 than 1996, and that fish grow at deeper depths in 1995.

Chapter 6

Stable Isotopes as Food-Web Tracers

Exxon Valdez Oil Spill
Restoration Project Annual Report

Sound Ecosystem Assessment: Confirming Fish Food Web Dependencies in the Prince
William Sound Ecosystem Using Natural Stable Isotope Tracers (SEA-FOOD).

Restoration Project 98320I
Annual Report

This annual report has been prepared for peer review as part of the *Exxon Valdez* Oil Spill Trustee Council restoration program for the purpose of assessing project progress. Peer review comments have not been addressed in this annual report.

Thomas C. Kline, Jr., Ph. D.

Prince William Sound Science Center, P. O. Box 705, Cordova, Alaska 99574

April 1998

Scales and Patterns of Temporal and Spatial Variability of $^{13}\text{C}/^{12}\text{C}$ and $^{15}\text{N}/^{14}\text{N}$ in Pelagic Biota

Thomas C. Kline, Jr. (Prince William Sound Science Center, P.O. Box 705, Cordova AK 99574; 907-424-5800 (tel), -5820 (fax); tkline@grizzly.pwssc.gen.ak.us)

In: Steve Brandt and Doran Mason (eds) Space, Time and Scale: New Perspectives in Fish Ecology and Management

Abstract

Stable isotope ratios of carbon and nitrogen are useful for reconstructing flow of biogenic materials in food webs when sources of production have contrasting isotopic signatures. Potential pelagic food sources of Prince William Sound (PWS), Alaska, were characterized isotopically at the secondary production level using two approaches, (1) bulk, 335 μ -mesh, net zooplankton samples, and (2) individuals of a single herbivorous copepod species, *Neocalanus cristatus*, at life-history stage copepodite IV to VI. The two approaches produced similar results in terms of correlation and graphical analyses. There was a strong ^{13}C gradient, but weak ^{15}N gradient within the PWS northern Gulf of Alaska (GOA) study area, suggesting a regional-scale spatial isotopic pattern. ^{15}N was positively correlated with ^{13}C only during the March to April phytoplankton bloom period. This is consistent with nutrient draw-down isotope effects and suggests a seasonal-scale temporal isotopic pattern. Little correlation of ^{15}N with ^{13}C during the May to June zooplankton bloom period was consistent with decoupling of N and C cycles, because N can be regenerated via zooplankton excretion whereas C is accumulated. Interannual isotopic patterns were suggested by relatively large differences in ^{13}C of juvenile herring, pollock, and diapausing copepods from 1994 and 1995. A consistency in the spatial distribution of plankton isotopic signatures suggests a diagnostic ^{13}C for GOA carbon. Large differences in ^{13}C of pelagic biota among years is ascribed to variation in cross-shelf transport of carbon from the GOA to PWS, which is postulated to effect recruitment and nutritional processes in fishes through their food base. The natural stable isotope tracer thus provides direct evidence of fluctuations in the transfer of carbon from the GOA to PWS.

Revised Draft, as of 29 March 1998
Incorporating changes suggested by the editor and two anonymous peer-reviewers

**Scales and Patterns of Temporal and Spatial Variability of $^{13}\text{C}/^{12}\text{C}$ and $^{15}\text{N}/^{14}\text{N}$ in
Pelagic Biota**

Thomas C. Kline, Jr.
Prince William Sound Science Center
P.O. Box 705, Cordova AK 99574
907-424-5800 (tel.), -5820 (fax)
tkline@grizzly.pwssc.gen.ak.us

For:
Steve Brandt and Doran Mason (eds)
Space, Time and Scale: New Perspectives in Fish Ecology and Management,
Canadian Journal of Fisheries and Aquatic Sciences

Introduction

Prince William Sound (PWS), Southcentral Alaska, is a fjordlike inland sea that receives oceanic water from the Gulf of Alaska via the Alaska Coastal Current (Niebauer et al. 1994). In PWS, Pacific herring (*Clupea pallasii*) populations have supported important commercial and subsistence fisheries. However, since 1993, herring have not been abundant enough to harvest. An ecosystem level study called Sound Ecosystem Assessment (SEA) is examining trophic interactions to see if the flow of energy through the food web is impeding recovery of herring stocks in PWS. The principal SEA hypothesis, known as the river-lake hypothesis, states that spatial and temporal variability in regional oceanographic conditions control production in PWS. Conditions are postulated to vary from lentic (lakelike) to lotic (riverlike) in relation to the strength and influence of the Alaska Coastal Current (Niebauer et al. 1994) on PWS. Physical oceanographic processes are further hypothesized to affect both bottom-up and top-down biological processes that in turn affect recruitment of exploited fish stocks. Of concern here is the bottom-up effects on Pacific herring and other fishes in PWS that are seasonal feeders, building up fat stores to sustain them when food is scarce during the winter months (Blaxter and Holiday 1963). The advective regime connecting the northern Gulf of Alaska (GOA) with Prince William Sound (PWS) is postulated to control recruitment and nutritional processes in fishes. Of special interest is the role of interzonal copepods in the zooplankton advected from the Gulf of Alaska towards the bordering continental shelf (Cooney 1988). The concomitant transfer of carbon from the GOA to PWS being demonstrated by using natural stable isotope tracers is providing direct evidence of these links.

The natural abundance of nitrogen (N) and carbon (C) stable isotope ratios measured in aquatic biota is useful for reconstructing the flow of organic material in food webs. There may be considerable C and N isotopic variability in the supply of organic material for marine pelagic food webs that is passed on to higher trophic levels with consistent enrichment of ^{13}C and ^{15}N effecting $\delta^{13}\text{C}$ and $\delta^{15}\text{N}$ increases of ~ 1 and 3.4 ‰ per trophic level, respectively (DeNiro and Epstein 1978, 1981, McConnaughey and McRoy 1979, Rau et al. 1983, Minagawa and Wada 1984, Fry and Sherr 1984, Fry 1988, Wada et al. 1991, Hobson and Welch 1992, Kling et al. 1992, Cabana and Rasmussen 1994, Vander Zanden and Rasmussen 1996). Determination of temporal and spatial patterns of C and N stable isotope variability at the food web base in an ecosystem study provides a context for tracing material flow to higher trophic levels (Fry 1988, Dunton et al. 1989, Goering et al. 1990). Isotopic signatures are generated by primary producers which are then transferred to consumers such as microcrustacea (Fry and Sherr 1984, Stephenson et al. 1986, Peterson and Howarth 1987, Fry 1988, Goering et al. 1990, Vander Zanden et al. 1997) that are an important forage base for fishes. Isotopic characterization of the food web base using herbivores provides a good

ecosystem baseline (Vander Zanden et al. 1997). For example, analysis of herbivorous zooplankton eliminates the compositional uncertainty associated with particulate organic material samples typically used as a proxy for phytoplankton and its consequential confounding effects on data (Owens 1987). Furthermore, an isotopic context based upon the temporal and spatial variability in zooplankton is appropriate for using isotope techniques to understand material flow in fish food webs that are dependent upon a zooplankton forage base.

The approach taken here was to examine net zooplankton collections made on research cruises before, during, and after the Spring zooplankton bloom (March through June) as well as late Summer (September), in order to characterize regional spatial and temporal variability in the isotopic composition of zooplankton, especially in relation to the spring bloom period. Although zooplankton sampling consisted principally of bulk net samples, single zooplankton species were supplemented when available, to assess effects of zooplankton species composition on isotopic signatures. Different zooplankton taxa were collected initially, later only a large interzonal (Miller and Terazaki 1989) copepod of the genus *Neocalanus*, an important taxon that dominates the zooplankton of the epipelagic North Pacific (Miller et al. 1984). These data were then compared with juvenile herring and pollock broadly sampled within the same geographical area to assess their linkages with carbon sources represented by zooplankton. The goal of this study was to assess the nature of temporal and spatial variability of ^{13}C and ^{15}N in the pelagic ecosystem given a broadscale sampling capability. This provided a context for assessing secondary production source dependencies by rapidly growing juvenile pelagic fishes, herring and pollock in Prince William Sound.

Materials and Methods

Field sampling

Zooplankton

Zooplankton were collected in 1994 (April, May, September, November) for western Prince William Sound, Alaska (PWS) and in 1995 (March, April, May, June, September, October) for PWS and adjacent Gulf of Alaska (Fig. 1) from the F/V *Alaska Beauty* and R/V *Bering Explorer*. Sampling techniques varied according to month, year, and target taxa. A 335 μ -mesh 0.5 m diameter ring was towed from 50m to the surface at 1 m s⁻¹ (at various times of day throughout each cruise, Appendix 1) to collect composite (bulk) zooplankton samples. Deep vertical tows (~20m above the bottom to the surface) were made during March to June 1995 immediately after, using the same net as, the 50m tows. Bulk samples collected from March to June 1995 were immediately inspected for *Neocalanus cristatus* and other large (length > ~7 mm) zooplankters for isotopic analysis of individuals. A deep beam trawl (~200 m depth, 5 mm mesh) was used at station SEA4 (Fig. 1) in April 1994 and deep horizontal tucker trawls (400 m depth; 1 mm mesh) were used at two locations (SEA22 and SEA27, Fig 1) in November 1994 to collect macrozooplankters. In September 1995, a closing “Puget Sound” net (Miller et al. 1984) was towed from ~ 20 above bottom to 200 m below surface to collect diapausing *N. cristatus*. Macrozooplankters were removed by forceps in the laboratory from the collections made in 1994.

Following removal of macrozooplankters, bulk zooplankton samples were frozen in shipboard freezers (-20 °C) in 125 mL polyethelene jars (VWR “Trace-clean”). *Neocalanus* and other macrozooplanker samples, that were individually removed from tows described above, were placed into polyethylene “Omni-vials” (Wheaton) and frozen in shipboard freezers (-20 °C). In the laboratory, frozen bulk samples were thawed, then rinsed in tap water while holding the sample in a 223 μ -mesh nitex sieve to remove salts. Rinsed samples were returned to their jars, frozen and then freeze-dried open, in a Labconco “Shelf Drier - 6 Liter Freeze Drier” unit. Bulk freeze-dried samples were ground to a fine powder using a dental amalgamator (Crescent Dental “Wig-L-Bug”) and returned to their jars. Omni-vial samples were placed directly into the freeze-drier without rinsing. Freeze-dried samples were shipped to the University of Alaska Fairbanks stable isotope facility for isotopic analysis.

Juvenile Pacific herring and walleye pollock

Juvenile Pacific herring (*Clupea pallasii*) and walleye pollock (*Theragra chalcogramma*) were collected throughout PWS during a multi-vessel broadscale survey conducted from October to November 1995 (Fig. 1). Additionally, opportunistic samples were obtained in 1994 (Table 6). During the broadscale survey, the lead acoustic vessel located concentrations of fishes which were sampled with a variety of gear. From seine (50 m diameter by 4 m deep with 3 mm mesh (stretched)) samplings, a random sample of 200 herring up to 150 mm in length (age 0 and 1) and a random sample of 200 pollock up to 100 mm in length (age 0) were saved for energetic (Paul et al. In Press) and isotopic analysis (this study) at each study site. Fish were immediately frozen (-20 °C) in seawater after capture and kept frozen until processing. Details of how the fish were handled in the laboratory is described in Paul et al. (In Press). Following energetic analysis (Paul et al. In Press), dried fish samples were sent from Seward to Cordova for isotopic analysis preparation that included additional grinding and homogenization. From each sampling area, 25 herring and 25 pollock were randomly selected, sealed in polyethylene LSC (Wheaton) vials, and shipped to the University of Alaska Fairbanks Stable Isotope Facility for isotopic analysis. In 1994, fish samples were obtained using similar gear and analysis techniques.

Isotopic analysis and data modeling

Replicate sub-samples of ~1.5 mg were made from all samples except individual macrozooplankters since the entire organism was required for one analysis. Sub-samples or whole zooplankters, as appropriate, were weighed to the nearest µg and loaded into combustion boats for mass spectrometric analysis at the Stable Isotope Facility at the University of Alaska Fairbanks. Isotopic analyses were performed using a semi-automated stable isotope analyzer (Europa Scientific 20/20 equipped with Roboprep sample combustion and purification unit). A single analysis produced $^{13}\text{C}/^{12}\text{C}$ and $^{15}\text{N}/^{14}\text{N}$ ratios in standard delta units, $\delta^{13}\text{C}$ and $\delta^{15}\text{N}$, respectively, and ‰C and ‰N. The conventional delta notation used to express stable isotope ratios are reported relative to international standards (air for N and Vienna Pee Dee belemnite (VPDB) for C) and defined by the following expression:

$$(1) \quad \delta^{15}\text{N} \text{ or } \delta^{13}\text{C} = \left(\frac{R_{\text{sample}}}{R_{\text{standard}}} - 1 \right) \times 1000 \text{ ‰}$$

where $R = {}^{15}\text{N}/{}^{14}\text{N}$ or ${}^{13}\text{C}/{}^{12}\text{C}$ (Craig 1957). The isotope standards have delta values of zero by definition, i.e. $\delta^{15}\text{N} = 0$ for atmospheric N_2 . Typically, replication is $< 0.2 \text{ ‰}$. The %C and %N data were used to calculate C/N atomic ratios. The data presented here consist of mean $\delta^{13}\text{C}$, $\delta^{15}\text{N}$ and C/N in the case of bulk zooplankton and fish samples, since they were replicated.

Removal of lipid (DeNiro and Epstein 1977) and trophic level (Rau et al. 1983) isotope effects from $\delta^{13}\text{C}$ values of nekton makes it possible to assess carbon source (Kline 1997). Kline (1997) found that PWS nekton ${}^{13}\text{C}$ content was correlated with C/N (a proxy for lipid content) unless lipid-normalized. The method of McConnaughey and McRoy (1979) was used to calculate lipid-normalized ${}^{13}\text{C}/{}^{12}\text{C}$ while $\delta^{15}\text{N}$ values were used to normalize for trophic level (Kline 1997). The McConnaughey and McRoy (1979) normalization is based upon the C/N ratio using a $\text{C/N} = 4$ as the base level. Kline (1997) used the herbivore, *Neocalanus*, as the trophic level baseline (Vander Zanden et al. 1997) for PWS nekton. The trophic level normalization converts ${}^{13}\text{C}/{}^{12}\text{C}$ of all samples as if they were at the same trophic level as *Neocalanus*. Thus ${}^{13}\text{C}/{}^{12}\text{C}$ values of fishes can be compared directly with herbivores.

The expressions $\delta^{13}\text{C}$, $\delta^{13}\text{C}'$, $\delta^{13}\text{C}_{\text{TL}}$, or $\delta^{13}\text{C}'_{\text{TL}}$ are used to denote ${}^{13}\text{C}$ abundance in relation to the international standard, normalized for lipid content, normalized for trophic level, and normalized for lipid content and trophic level, respectively. The normalizations are used according to the context of a particular data analysis. “ ${}^{13}\text{C}$ ” is used to reflect generic ${}^{13}\text{C}/{}^{12}\text{C}$ isotopic trends irrespective of normalization.

Data mapping

Areal distribution of isotopic data were mapped and contoured using the Generic Mapping Tools computer program (Smith and Wessel 1990, Wessel and Smith 1995).

Results

Zooplankton species- and within-station variability

Bulk Plankton

The within-station variability $\delta^{15}\text{N}$, $\delta^{13}\text{C}$, and $\delta^{13}\text{C}'$ measured in upper 50 m net zooplankton (1994-5) suggested by the standard deviation (*SD*) value for each station was on the order of 1 to 2 ‰ while annual mean isotopic value differences (Table 1) ranged up to 3.4 ‰ at individual stations. The values and ranges of the isotopic composition of net zooplankton sampled over the water column were comparable to upper 50 m samples (Appendix 1). The collective bloom period (March through June) water column and upper 50m zooplankton data were compared statistically. The water column net zooplankton $\delta^{15}\text{N}$ values were not significantly correlated ($r^2 = 0.1$) with 50 m tows from the same station and date. Correlations between $\delta^{13}\text{C}$ and $\delta^{13}\text{C}'$ were significant, however ($r^2 = 0.3$ and 0.5 , respectively, Table 2).

Macrozooplankton

Macrozooplankton consisting of various taxa extracted from plankton tows made in 1994 and individually isotopically analyzed are shown in Table 3. These macrozooplankters consisted largely of diel migrators, as they were found in 50 m tows when conducted at night, as well as tows made over the water column. Macrozooplankters other than interzonal copepods had $\delta^{15}\text{N}$ values (Table 3) that were more positive than was typical of bulk net samples (Table 1). Interzonal copepods were consistently lower in $\delta^{15}\text{N}$ than other taxa, with a mean value slightly greater than +8. Euphausiids (*Euphausia pacifica* and several *Thysanoessa* spp.) had $\delta^{15}\text{N}$ of about + 10, whereas amphipods (principally *Cyphocaris challengerii*) and decapods (principally unspecified larval stages) were about + 11. Carnivorous copepods (*Euchaeta elongata*) had the most positive macrozooplankter $\delta^{15}\text{N}$ value of about +12.

Unlike $\delta^{15}\text{N}$ values, macrozooplankter $\delta^{13}\text{C}$ and $\delta^{13}\text{C}'$ values were similar to bulk sample means. $\delta^{13}\text{C}$ values, which ranged from about -19 to -23, were reduced in range to -18 to -21, when normalized to $\delta^{13}\text{C}'$. The only macrozooplankters with mean $\delta^{13}\text{C}'$ values less than -20 were interzonal copepods. Differences in trophic level (note that carnivorous copepods had the highest $\delta^{15}\text{N}$ values) and lipid storage abilities (note that lipid normalization changed ^{13}C values of copepods more than other taxa; Table 3) among the taxa comprising bulk zooplankton samples probably contributed to much of their isotopic variability. Trophic level differences among species found in bulk samples (e.g., Table 3) is conjectured to explain the poor correlation of 50 m and water

column zooplankton $\delta^{15}\text{N}$ values since higher trophic level taxa were more commonly collected in deep tows.

Neocalanus cristatus

To eliminate confounding effects of higher trophic level macrozooplankton taxa (Table 3), expanded isotopic analysis of macrozooplankters focused on the large interzonal copepod *Neocalanus cristatus*. *N. cristatus* were found in both water column and 50 m net plankton tows (Tables 4 and 5). These data are presented separately due to the fact that those sampled from the upper 50m were limited to those actively feeding, whereas those found in the water column included copepods undergoing diapause at depth as well as those actively feeding near the surface (the later principally in May, Table 4).

Copepodite IV and V stage *Neocalanus cristatus* were most abundant in the upper 50m in May (Table 4). The isotopic values of *N. cristatus* from 50 m tows were compared statistically with the bulk net samples from which they were collected (Table 2). Although, the monthly mean $\delta^{13}\text{C}$ and $\delta^{13}\text{C}'$ values of net zooplankton and *N. cristatus* collected from March through June 1995 were correlated ($r^2 = 0.4$ and 0.5 , respectively), the $\delta^{15}\text{N}$ were not significant ($r^2 < 0.1$). Restricting the data to mean $\delta^{15}\text{N}$, $\delta^{13}\text{C}$ and $\delta^{13}\text{C}'$ values of net zooplankton and *N. cristatus* collected in May 1995 altered the correlations to $r^2 = 0.3$, 0.7 and 0.7 , respectively. The correlation of $\delta^{15}\text{N}$, $\delta^{13}\text{C}$ and $\delta^{13}\text{C}'$ of *N. cristatus* with bulk samples was thus strongest during the peak zooplankton bloom. Varying trophic level composition of bulk samples (herbivore contribution peaked in May) probably contributed to the reduced $\delta^{15}\text{N}$ correlations. Four tows of collections made for *N. cristatus* from the upper 50 m produced large samples ($N \geq 12$, Table 4). The SD of these samples were small; 0.5 to 0.7 for $\delta^{15}\text{N}$, 0.3 to 1.4 for $\delta^{13}\text{C}$, and 0.4 to 1.3 for $\delta^{13}\text{C}'$.

Unlike the 50 m samples, the $\delta^{15}\text{N}$ values of *N. cristatus* from the water column were similar to the bulk net samples from which they were collected. The mean $\delta^{15}\text{N}$ value of *N. cristatus* and net plankton samples collected at each station were used to make X,Y pairs and regressed (Table 2). However when the same approach was used for $\delta^{13}\text{C}$ and $\delta^{13}\text{C}'$, the regressions were weak (Table 2). Furthermore, unlike upper 50m samples, the $\delta^{15}\text{N}$ and $\delta^{13}\text{C}$ values of *N. cristatus* from the water column were not significantly correlated (Table 2). A number of the deep *N. cristatus* tows had large N (Table 5). The SD of these were greater than from 50 m samples with $N \geq 12$, ranging in SD up to 4.3 .

Mean values (1994-5) of upper 50 m *N. cristatus*, upper 50 m bulk zooplankton, and water column bulk zooplankton collected at each station yielded very similar plots (Fig. 5). Taxonomic variation

(and hence trophic level) as well as temporal effects on isotopic variability of bulk samples were reduced by integrating over time. Correlations among sample types were better during the peak *Neocalanus* abundance when bulk samples consisted of mainly interzonal copepods. Seasonally, diapausing interzonal copepods form a large portion of the deep bulk zooplankton in PWS and thus should have been correlated at time of sampling. However, only $\delta^{15}\text{N}$ was correlated. Poor correlation in ^{13}C could only be explained when the bimodal nature of the variability was revealed in dual-isotope plots (Fig. 4) discussed in the Gulf of Alaska signature section, below. That is, a portion of the diapausing samples had ^{13}C inconsistent with other zooplankton from the same location. This was probably the case for the Fall 1994 interzonal copepod sample as well (Table 3). Bimodality also explains the greater SD values obtained for deep *N. cristatus* compared with 50 m if the deep tows reflected a mixture of the two modes while 50 m samples consisted of only one mode.

Zooplankton temporal variability

Bulk zooplankton

Isotopic values of bulk net zooplankton samples from individual stations sampled from 1994-5 varied by as much as 3.4‰ (Table 1). Much of this variance can be ascribed to stations only sampled in Fall 1994 since those stations sampled both in the Spring and Fall of 1994 as well as in 1995 differed by less than 1 ‰ (Table 1). Fall 1994 zooplankton had an east-west $\delta^{15}\text{N}$ gradient with higher values to the east, suggesting that eastern samples consisted of a proportion of higher trophic level zooplankters. There were several locations where $\delta^{13}\text{C}$ was isotopically higher, particularly in Montague Strait. The Fall samples reflected secondary production long after the Spring phytoplankton bloom that accounts for most of the pelagic productivity in PWS (Goering et al. 1973). Accordingly, the high variability may reflect where littoral carbon was pumped into the pelagic area by tidal action. This is a possibility in this tidally dominated system (Niebauer et al. 1994). Enriched ^{13}C is consistent with isotopic signature of littoral carbon sources such as eelgrass (Cooper 1989, McConnaughey and McRoy 1979) and macroalgae (Dunton and Schell 1987, Stephenson et al. 1986). A consistency in pelagic productivity isotopic signature, was thus more effectively assessed using only Spring bloom data as suggested by the similarity of isotopic data collected at stations CFOS13, SEA11, SEA25, SEA32, and SEA4 in early 1994 with data collected at these stations in 1995 (Appendix 1). During the PWS phytoplankton (April) and zooplankton (May) biomass peak periods the $\delta^{15}\text{N}$ within PWS was uniform (though higher in May than April) when compared with March and the previous Fall (Fig. 2) consistent with a composition principally of herbivores at this time.

Goering et al. (1990) found that during the Spring bloom period, zooplankton $\delta^{15}\text{N}$ shift to higher values following a similar shift in phytoplankton which was driven by NO_3^- depletion. Prince William Sound (PWS) zooplankton $\delta^{15}\text{N}$ values were similar to Auke Bay (Southeast Alaska near Juneau). Correlations in isotopic shifts occurring during the Spring bloom followed those by Goering et al. (1990) using $\delta^{13}\text{C}$ vs. $\delta^{15}\text{N}$ regressions. All 1995 data (Appendix 1) were regressed collectively and by month (Table 2). All $\delta^{13}\text{C}$ vs. $\delta^{15}\text{N}$ regressions were significant except May. Zooplankton $\delta^{13}\text{C}$ was correlated with $\delta^{15}\text{N}$ from April to May in Auke Bay (Goering et al. 1990) but only in March and April in PWS (Table 2) since May and June PWS zooplankton $\delta^{13}\text{C}$ and $\delta^{15}\text{N}$ values were poorly correlated. Goering et al. (1990) found the following relationship for Auke Bay zooplankton: $\delta^{13}\text{C} = 1.8\delta^{15}\text{N} - 34.2$ ($r^2 = 0.46$), which was comparable to that found here for PWS zooplankton: $\delta^{13}\text{C} = 0.8\delta^{15}\text{N} - 28.3$ ($r^2 = 0.49$) (collectively over the Spring bloom period). The reduced correlation in May and June suggests that phytoplankton isotopic fractionation effects on ^{15}N and ^{13}C become decoupled in zooplankton as the Spring bloom winds down. This may be due, in part, to recycling of N via the regenerated N pool (Dugdale and Goering 1967). Since zooplankton, and calanoid copepods in particular, build energy reserves by storing C, C and N turnover rates within the organisms must differ. Additionally, zooplankton regenerate the N pool (Dugdale and Goering 1967) with ^{15}N -depleted N (Checkley and Miller 1989) serving to counteract the N-uptake isotopic distillation process (e.g., Owens 1987). This N source became available as the zooplankton bloom developed, lagging approximately one month behind the phytoplankton.

Macrozooplankton

Variability (expressed as *SD*, Table 3) of macrozooplankton isotopic composition was greater in the Fall than Spring (except the $\delta^{15}\text{N}$ values of interzonal copepods, *Neocalanus* spp., which decreased slightly). The increase in *SD* of $\delta^{15}\text{N}$ values suggests a greater degree in omnivory (Kline and Pauly 1998) for zooplankton species during the late season.

Neocalanus cristatus

Neocalanus cristatus were more abundant in water column net tows than those made in the upper 50m (Tables 4 and 5). Abundance at particular stations varied with time (Table 5), with greatest springtime abundance in March at stations NWS4, PW1, SEA11, SEA22, and SEA27, which were deep enough to provide diapause habitat (Fig. 1). In May 1995, there were far fewer at station SEA22 with only 18 sampled compared to > 100 sampled in March (only 33 of these were analyzed, while at other stations all were analyzed). In May however, *N. cristatus* were more

broadly distributed than earlier, e.g., occurring in greater number at stations CS9, HE12, HE13, PV1, SEA25, where only few had been collected before. There was a gradual isotopic shift in water column collected *N. cristatus* to more positive $\delta^{13}\text{C}'$ values in May. The mean isotopic values of *N. cristatus* sampled in March to April throughout PWS as well as those from station SEA22 were comparable to the 20 *N. cristatus* sampled with the Tucker trawl at SEA 22 in the Fall of 1994 (Tables 3 and 5). However, *N. cristatus* sampled with a closing net in the Fall of 1995 differed considerably in $\delta^{13}\text{C}'$ value, from both the Fall 1994 and Spring 1995 water column samples. The variability, expressed as *SD*, was higher for the collective Fall 1995 sample compared with previous data as were the *SD* of each station. The mean $\delta^{13}\text{C}'$ of the Fall 1995 copepods of -22.4 fell between the -23.2 and -20.6 mean $\delta^{13}\text{C}'$ values of *N. cristatus* feeding (i.e., upper 50 m samples) in the GOA and PWS, respectively, during the March to June period (Tables 5 and 6).

Zooplankton Spatial variability

Data from stations that were sampled more than one time in the period, 1994 to 1995, were pooled by station (time-integrated) to reveal the average isotopic spatial pattern occurring in the region by method of sampling (bulk net zooplankton from upper 50m and entire water column and individual *N. cristatus* from the upper 50m) in Fig. 5. Fig. 5A suggests that zooplankton $\delta^{15}\text{N}$ values were relatively uniform at $\sim +8 \pm 1 \text{‰}$ while Fig. 5B suggests a ^{13}C isotopic gradient of ~ 3 to 4‰ between the GOA and PWS independent of sampling method, though more distinct for *N. cristatus* with more negative values occurring in the GOA.

The most ^{13}C -depleted signatures in bulk zooplankton occurred at station GOA6 in June when peak zooplankton abundance occurred in the Gulf (R. T. Cooney, Univ. Alaska, Fairbanks, pers. comm.) (Appendix 1). The June GOA values were also more depleted than any value obtained from the Fall of 1994. Furthermore, the $\delta^{13}\text{C}$ and $\delta^{13}\text{C}'$ throughout the 1995 Spring sampling series were consistently more depleted at GOA6 than at PWS stations (Fig. 2). Unlike the Spring, the spatial variability in September 1994, though considerable, suggests no definitive pattern in $\delta^{13}\text{C}$ or $\delta^{13}\text{C}'$ (Fig. 2). There was, however, a $\delta^{15}\text{N}$ gradient with more positive values to the east and south. In September 1994, the $\delta^{15}\text{N}$ of zooplankton was more positive than during the 1995 Spring period (Fig. 2) than suggested by the 0.6‰ difference of repeated stations (Table 1). The $\delta^{15}\text{N}$ values were lower in the GOA than PWS in the Spring of 1995 by $\sim 1 \text{‰}$ (Fig. 2). This difference is much less than the ~ 3 for ^{13}C values. The greater ^{13}C gradient takes on more significance when trophic fractionation factors are taken into account, e.g., if the ^{13}C difference was due to trophic level

differences (i.e., ~ 3 trophic levels), an ~ 10 ‰ $\delta^{15}\text{N}$ gradient would be expected. Therefore other processes are more relevant for explaining the ^{13}C spatial variation.

Neocalanus cristatus from upper 50m in PWS when compared with data from station GOA6 suggest differences in $\delta^{13}\text{C}'$ values of 3.5 and 3.6 ‰ seasonally, and in May, respectively, between PWS and GOA (Table 4). These same PWS vs. GOA comparisons when made for $\delta^{13}\text{C}$ were similar, 4.1 and 3.9 ‰. However, $\delta^{15}\text{N}$ differed by only 1.3 and 0.8 ‰, seasonally, and in May, respectively. The $\delta^{15}\text{N}$ is suggested to be relatively uniform in the region (PWS vs. adjacent GOA) in May since the difference was $< 1\text{ SD}$ (Table 4). Thus *Neocalanus cristatus* reflected the same regional isotopic spatial variability observed in bulk samples though with a more distinctive $\delta^{13}\text{C}'$ gradient (Fig. 5A).

Zooplankton bloom period spatial and temporal variability model

The availability of a large isotopic dataset based upon bulk net zooplankton samples collected throughout the March-June period (Appendix 1) over the study area enabled a broad-scale assessment of Spring bloom spatial and temporal variability in PWS. A simple numerical model was devised to integrate spatial and temporal variability utilizing statistical data derived from third order polynomial regressions made of $\delta^{13}\text{C}$, $\delta^{13}\text{C}'$ and $\delta^{15}\text{N}$ values of upper 50 m bulk zooplankton against time (in terms of Julian day) during the Spring of 1995 (Fig. 3). The shifts in values were similar, with peak values occurring in April (Fig. 3) while normalization of $\delta^{13}\text{C}$ to $\delta^{13}\text{C}'$ doubled the time-dependent correlation to 40%. The regression analyses correlation coefficients (r^2) were incorporated into a simple variability model:

$$(2) \quad V_s + V_t + V_o = V_b$$

where V_s is the spatial variability, V_t is the temporal variability, V_o are sources of variability not otherwise accounted for (e.g., isotopic variability due to species composition), and V_b is the total bloom period (broadscale) variability. The similarity in the correlations of both $\delta^{15}\text{N}$ and $\delta^{13}\text{C}'$ (Fig. 3A and C; both $r^2 \sim 0.4$) suggested that temporal variability was 0.4. The remaining variability is unknown. Based on eq. (2), spatial variability could be as high as 60% of V_b , given $V_o = 0$. This 60/40 split should differ among annual Spring blooms depending upon the relative strengths of the processes affecting isotopic composition such as the strength of physical processes controlling horizontal and vertical mixing. A lack of horizontal mixing may have contributed to the observed spatial variability whereas the

vertical mixing indirectly affected zooplankton isotopic composition by controlling photic zone nutrient fluxes affecting fractionation by phytoplankton. The lower correlation of $\delta^{13}\text{C}$ with time (compared with $\delta^{13}\text{C}'$), which implied a V_t of about 20% (Fig. 3B.), suggested that lipid (carbon storage) effects accounted for about 20% of V_b .

Diagnostic signatures for GOA and PWS production

The variability model analysis suggests that spatial variability in the isotopic composition of upper 50m net zooplankton may have accounted for as much as 60% of the total bloom period variability in bulk plankton samples. Spatial variability assessed by contouring the mapped data from each cruise (Fig 2) as well as time-integrated from 1994-5 (Fig. 5) suggested an isotope gradient occurring between PWS and the adjacent GOA. Figure 2 also indicated a temporal shift to more positive isotopic values from March to May and a return to lower values in June 1995 while maintaining the isotopic gradient. This gradient was evident in single species as well as mixed species bulk net samples (Fig. 5), but was particularly well-defined for the former.

Combination scatterplots with histograms (Fig. 4) suggested that $\delta^{13}\text{C}'$ values were bimodal, whereas $\delta^{15}\text{N}$ were unimodal, but slightly skewed to more positive values. These plots are distinguished by sampling method and inferred life history stage (Fig. 4). March and April 1995 water column samples consisted principally of copepods in diapause phase from the 1994 year class (the calendar year when they were actively feeding), as very few *N. cristatus* were found in the upper 50m during that period (Table 4). Since the May 1995 water column sample was more similar to the upper 50 m sample than the March or April sample, these copepods were from the 1995 year class, either feeding or just entering diapause (Fig. 4). The Fall 1995 sample (Fig. 4) was taken at depth and at the time of year when the population is in diapause. Reference lines at $\delta^{15}\text{N} = 8$, $\delta^{13}\text{C}' = -23$ and -19 are shown in each panel of Fig. 5 which aided in comparisons, suggest a consistency in occurrence of values near the intersections of the lines. These “cross-hairs” fall near the centers of the two clusters of diapausing copepods from the 1994 year class and the single dominant cluster of diapausing copepods from the 1995 year class. This latter cluster departs significantly from both the upper 50m copepods sampled throughout the Spring of 1995 as well as the May, 1995 water column data that were dominated by the $\delta^{13}\text{C}'$ values near -19 . Based on the $\delta^{13}\text{C}'$ values copepods during their feeding phase stages in Spring in the GOA and PWS (Table 4), it is conjectured that the crosshairs in Fig. 5 approximate centers of the isotopic value distribution for GOA copepods on the left and PWS copepods on the right of each plot.

Juvenile herring and pollock

Age-0 and -1 herring (*Clupea pallasii*) and age-0 walleye pollock (*Theragra chalcogramma*) were found in abundance at 10 and 7 sites (Table 7), respectively, during the Fall 1995 broad-scale fish survey (Norcross et al. 1996). Pollock were consistently elevated in $\delta^{15}\text{N}$ values when compared with herring, with a difference of 0.4 ‰ corresponding to an approximately 0.1 trophic level difference. Normalization reduced ^{13}C variability enabling comparisons among species without the confounding effects of trophic level and lipid content (Kline 1997). Trophic level normalization reduced the difference in $\delta^{13}\text{C}'_{\text{TL}}$ between the species in 1995 to 0.7 ‰, a value twice the *SD* and thus significant. Note that the $\delta^{13}\text{C}'_{\text{TL}}$ values of juvenile fishes in 1995 were quite different than those obtained in 1994 (Table 6). Interannual differences of 1.4 ‰ for pollock and 2.0 ‰ for herring were greater than the species differences each year.

Juvenile fishes change isotopic composition rapidly, reflecting isotopic changes in diet at temporal scales only slightly longer than zooplankton (Hesslein 1993). Isotopic spatial variability of fish may differ from large zooplankton, since they have the potential to integrate food sources of varying isotopic composition from different locations in proportion to their foraging range. This was revealed in the data (Table 6) as the differences in mean values among locations were small compared to bulk plankton samples during any one sampling period.

Discussion

The $\delta^{13}\text{C}'$ values of GOA bulk net zooplankton and *Neocalanus cristatus* sampled from the upper 50 m and bulk net zooplankton sampled from the entire water column consistently demonstrated higher levels of depletion than those in PWS, whether based on time-averaged data or based on monthly Spring bloom data. This consistency suggests that during the period of this study, 1994-5, that $\delta^{13}\text{C}'$ values less than -22, when measured at the herbivore trophic level, were diagnostic of GOA carbon. PWS production in the form of herbivore carbon, had $\delta^{13}\text{C}'$ values greater than ~ -21. This dichotomy in pelagic carbon source ^{13}C is not unlike that observed in Atlantic Ocean mesopelagic shrimp (Rau et al. 1989). Pelagic ^{13}C gradients have also been observed across the continental shelf of New England (Fry 1988), across Drake Passage (Rau et al. 1991), near Cape Hope (Rau 1989), and between the Beaufort, Chukchi, and Bering Seas off Alaska (Saupe et al. 1989). The PWS zooplankton carbon isotope range observed here

confirms an isotope source effect postulated on $\delta^{13}\text{C}'_{\text{TL}}$ of ~ 1700 fish collected from PWS (Kline 1997).

The variability and distinct patterns of isotopic data that when identified with an underlying process can be used to trace variability of that process in the ecosystem. Of particular interest here is the connection of isotopic signatures with oceanographic processes that have been postulated to control the strength of secondary production which is important as fish forage within Prince William Sound (Cooney 1993, 1997). Lateral movement of interzonal copepods from the GOA continental shelf adjacent to PWS (Cooney 1986), is postulated to drive PWS zooplankton abundance (Cooney 1997), is conjectured to cause a mixture of zooplankton populations in PWS with bimodal $\delta^{13}\text{C}'$ (Fig. 4).

The 1995 low $\delta^{13}\text{C}'$ value mode of *Neocalanus cristatus* diapausing in PWS were inconsistent with those sampled when they were feeding earlier in the year (Spring) within PWS. Instead, these values were very similar to those sampled in the Spring from the GOA. In comparison, those copepods sampled in the Spring in PWS were predominantly affiliated with the high $\delta^{13}\text{C}'$ value mode, particularly in May during their peak abundance. Thus many of the diapausing copepods found in PWS were affiliated with the low $\delta^{13}\text{C}'$ value mode of GOA origin copepods. It is also apparent that 1995 had a higher representation of GOA-origin copepods than diapausing copepods from the 1994 cohort. Most copepods collected in diapause during the Fall of 1995 were from the GOA, whereas only about half of the 1994 cohort originated there. The few ($N = 20$) diapaused *N. cristatus* that were collected in 1994 were similar to those sampled in Spring of 1995. Though not enough to histogram, their low mean $\delta^{13}\text{C}'$ value of -21 and large SD of 1.8 is consistent with the Spring 1995 sample shown in Fig. 4A. The timing of the collection early in the diapause period was therefore not important (the bottom row of Table 3 compares favorably with Fig. 4A), confirming the differences between the 1994 and 1995 cohorts diapausing within PWS.

The differences to the contribution of the diapaused copepod populations from the GOA mirrors differences seen in PWS juvenile herring and pollock in 1994 and 1995. In 1995, these fishes reflected the GOA isotopic signature to a much greater extent than in 1994 - much like the copepods. A probable explanation for the observed phenomenon of coincident isotopic shift is that of variable horizontal transport of production from the GOA affecting each species each year to a similar extent. Ekman transport of zooplankton is estimated to deliver 10 million metric tons per year over the 1000 km northern GOA continental shelf;

and into the Alaska Coastal Current and coastal waters during periods of relaxed downwelling in the late Spring and Summer (Cooney 1986, 1988). The late Spring to Summer period is also the period of deep water renewal of PWS (Niebauer et al. 1994) and large tidal fluctuations. The isotopic shift suggests that these processes may vary markedly from year to year.

An alternative explanation is that the fishes carried the GOA signature into PWS. This may seem plausible but is inconsistent with what is known of herring populations in the NE Pacific (E. Brown, Univ. Alaska, Fairbanks, pers. comm.). The nearest upstream (Alaska Coastal Current) source of herring is in southeastern Alaska. This source of herring would have acquired their Gulf signature enroute to PWS. Another alternative would be to have virtually all juvenile herring and pollock leave PWS, feed in the Gulf, then each species return as a group to explain the 1995 within-species isotopic uniformity. Such a mass migration has never been noted. These scenarios seem less likely than fishes acquiring the GOA signature from their plankton diet. Since plankton are by definition drifters, their inflow into PWS is passive and thus dependent on physical processes as were the diapausing copepods. Thus, year-to-year differences in advection provides the most consistent explanation for the isotopic shifts observed in this study (Table 7).

Sample effects

Bulk zooplankton samples typically consist of a mixture of different species and life-history stages, each with potentially different trophic levels. The complex nature of bulk net plankton samples may confound interpretations because of multiple processes with attendant isotopic effects (e.g., mixing due to lateral movement and nutrient depletion related to bloom dynamics) are involved. Extensive stable isotope analysis was performed on individuals of a single copepod species as an alternative approach to reduce the confounding effects of multiple factors associated with bulk net zooplankton samples. Analysis of individual copepods was directed at copepodite - IV and - V *Neocalanus cristatus* for the following reasons: 1) they are large in size at ~7 to 10 mm in length, ~ 1 to 5 mg in weight, thus large enough for one animal per analysis, 2) they are easy to identify while fresh and at sea, 3) they have a described life history pattern (Miller et al. 1984), and 4) they are principally herbivorous (Gifford 1993), giving them a well-defined trophic level (herbivore, TL = 2). Although these copepods are consumed by herring less than 150 mm in length (B. Foy, Univ. Alaska, Fairbanks, pers. comm., including age-1 fish) and other fishes (Willette, et al. 1997) in PWS, they are probably not the prey of age-0 fishes because of gape-size limitations.

However, since *N. cristatus* and bulk net zooplankton sample $\delta^{13}\text{C}$ were strongly correlated (Table 2) and had a similar ^{13}C spatial distribution (Fig. 5B), they appear to be a good proxy for each other and for carbon source. There was no relation between $\delta^{15}\text{N}$ of *N. cristatus* and bulk net zooplankton. This may have been due, in part, to the mixed species assemblage, and therefore mixed trophic level nature of bulk samples with consequential isotope effects. *N. cristatus* ^{13}C was more strongly correlated to $\delta^{15}\text{N}$ in May than bulk samples and also had y-intercept values more similar to earlier net plankton (Table 2), possibly because *N. cristatus* reflected a greater proportion of carbon that was previously assimilated. This is consistent with their storage of carbon integrating longer time scales. Their values may reflect an averaging of the carbon isotopic variation of phytoplankton to a greater extent than nitrogen, providing further evidence of N and C decoupling in zooplankton.

N. cristatus isotopic data shown as scatterplots with frequency histograms revealed the bimodal distribution of ^{13}C in a way that was not available in the bulk net zooplankton sample analysis. The latter yielded a homogenized effect. The analyses of a large number of individual zooplankters, particularly during diapause when a large number of individuals were obtainable, revealed the bimodality. However, since bulk net zooplankton sample analysis provided a single datum for each time and place, it was more practical for assessment of spatio-temporal factors.

Scales of Variability

The data presented in this paper suggest that mesoscale spatial (e.g., ~ 100 km, the length dimension of PWS) and mesoscale temporal (seasonal to annual) scales predominated; were thus effectively the predominant isotopic variability modes (Fig. 6). Zooplankton had both spatial and temporal variability. Although there was a moderate seasonal shift in ^{15}N and ^{13}C , the spatial gradient occurring between the GOA and PWS was the principal source of ^{13}C variability and was the predominant isotopic variability mode (Fig. 6). The variability in the physical processes that drives the advection mediating the transfer of carbon in the form of zooplankton between the GOA and PWS, resulting in interannual differences in ^{13}C abundance in juvenile fishes and diapausing copepods in PWS, forms second and third variability modes. Spatial variability in fishes was negligible when the GOA transfer was great, but was present when the GOA and PWS carbon were in near balance in 1994, thus forming a weak fourth mode in ^{13}C variability (Fig. 6).

Proxy Sampling

The large interannual differences in ^{13}C measured in diapausing copepods and juvenile fishes ascribed to oceanographic processes that transfer carbon in the form of zooplankton from the GOA

to PWS suggests the use of this tool as a proxy for carbon transport in long-term studies. An isotopic time series (when compared with upwelling indices and fishery statistics) could resolve a hypothetical relationship of oceanographic processes with fluctuations in fisheries, which in the northern GOA region appear to undergo regime shifts (Brodeur and Ware 1992, Francis and Hare 1994). Such sampling would require a confirmation of the isotopic gradient as well as sampling of diapaused copepods and fishes. The simplicity of single zooplankton species analysis appears to yield clearer results than bulk net sampling and may be the best sampling approach for long-term studies. *Neocalanus cristatus* consistently had low mean $\delta^{15}\text{N}$ values of ~ 8 , confirming their herbivorous ecological role (Gifford 1993) and making them an ideal candidate as a carbon proxy. Although the bulk net zooplankton samples are more likely to include the small zooplankton prey of early-stage juvenile herring and pollock, the use of *N. cristatus*, an herbivorous species, in the analysis, eliminates species composition, life history stage, and trophic level as sources of variability. The PWS setting includes an area of deep water to (> 700 m depths) that provides an isolated and well-defined diapausing habitat for *Neocalanus* sp. that could be easily sampled on a consistent basis to determine if changes in source of diapausing copepods occurred in cycles like those postulated for zooplankton abundance in the subarctic Pacific ocean (Brodeur and Ware 1992).

Fishes dependent on GOA carbon would be subject to vagaries of carbon flow that fall under the domain of physical oceanographic processes connecting the GOA with PWS. If fishes were wholly dependent on PWS carbon, they would be more directly affected by internal PWS processes. However, increased competition for PWS carbon by all species could occur if GOA carbon was less available to those that normally use it. Shifting to increased dependency on PWS carbon by species with normal affinity for GOA carbon during years of poor GOA carbon availability would provide evidence of competition for a limited carbon supply by the increasing overlap in their ^{13}C . Decadal cyclity in fish populations in the Northeast Pacific is postulated to results from decadal changes in the ring of zooplankton around the Gulf of Alaska (Francis and Hare 1994). This study suggests that zooplankton stocks are further transported, into PWS, being detectable by changes in ^{13}C abundance. Time series measurements of natural stable isotopes in zooplankton and fishes in conjunction with population indices and physical oceanographic measurements could thus enable a new understanding of how climatically-driven bottom-up processes affect fish recruitment and interaction.

Acknowledgments: This project was funded by the Exxon Valdez Oil Spill Trustee Council through the Sound Ecosystem Assessment project. However, the findings presented by the author are his own and not necessarily the Trustee Council's position. SEA colleagues collected fish

specimens. Evelyn Brown oversaw aging of the fish. J. M. Paul and P. Shoemaker did the initial fish sample preparation. Captain Mike Gaegel, the crew of the *R/V Bering Explorer*, E. Stockmar, J. Murphy, B. Barnett, and T. Cooney assisted with *Neocalanus cristatus* sampling. Kim Antonucci did the laboratory processing of samples for stable isotope analysis. Bruce Barnett at the University of Alaska Fairbanks Stable Isotope Facility performed the stable isotope analysis. John Williams made the station map and contour plots. We thank Paul Wessel and others in the GMT discussion group for assisting with Fig. 1. Kate Williams assisted with editing the first draft.

Literature Cited

- Blaxter J. H. and F. G. Holiday. 1963. The behavior and physiology of herring and other clupeids. *Adv. Mar. Biol.* 1: 261-393.
- Brodeur, R.D. and D.M. Ware. 1994. Long-term variability in zooplankton biomass in the subarctic Pacific Ocean. *Fish. Oceanogr.* 1:32-38.
- Cabana, G. and J. B. Rasmussen. 1994. Modeling food chain structure and contaminant bioaccumulation using stable nitrogen isotopes. *Nature* 372:255-257.
- Checkley, D. M., Jr. and C. A. Miller. 1989. Nitrogen isotopic fractionation by oceanic zooplankton. *Deep-Sea Res.* 36:1449-1456.
- Cooney, R.T. 1986. The seasonal occurrence of *Neocalanus cristatus*, *Neocalanus plumchrus*, and *Eucalanus bungii* over the shelf of the northern Gulf of Alaska. *Cont. Shelf Res.* 5:541-553.
- Cooney, R. T. 1988. Distribution and ecology of zooplankton in the Gulf of Alaska: a synopsis. *In:* (Nemoto, T. and W.G. Pearcy (eds.) *The biology of the subarctic Pacific, proceedings of the Japan-United States of America seminar on the biology of micronekton of the subarctic Pacific, Part I*. Bull. Ocean Res. Inst., University of Tokyo. p. 27-41.
- Cooney, R. T. 1993. A theoretical evaluation of the carrying capacity of Prince William Sound, Alaska, for juvenile Pacific salmon. *Fish. Res.* 18:77-87.
- Cooney, R. T. and K. O. Coyle. 1996. Sound Ecosystem Assessment: The role of zooplankton in the Prince William Sound Ecosystem. *Exxon Valdez Oil Spill Restoration Project Annual Report*

(Restoration Project 95320-H), Institute of Marine Science, University of Alaska, Fairbanks, Alaska 99775-1080.

Cooney, R. T. 1997. Sound Ecosystem Assessment (SEA): A science plan for the restoration of injured species in Prince William Sound, Alaska. *Exxon Valdez* Oil Spill Restoration Project Annual Report (Restoration Project 96320), Institute of Marine Science, University of Alaska Fairbanks, Fairbanks, Alaska 99775-7220.

Cooper, L. W. 1989. Patterns of carbon isotopic variability in eelgrass, *Zostera marina* L., from Izembek Lagoon, Alaska. *Aquat. Bot.* 34:329-339.

Craig, H. 1957. Isotopic standards for carbon and oxygen and correction factors for mass-spectrometric analysis of carbon dioxide. *Geochim. Cosmochim. Acta* 12:133-149.

DeNiro, M. J. and S. Epstein. 1977. Mechanism of carbon isotope fractionation associated with lipid synthesis. *Science*. 197:261-263.

DeNiro, M. J. and S. Epstein. 1978. Influence of diet on the distribution of carbon isotopes in animals. *Geochim. Cosmochim. Acta* 42:495-506.

DeNiro, M. J. and S. Epstein. 1981. Influence of diet on the distribution of nitrogen isotopes in animals. *Geochim. Cosmochim. Acta* . 45:341-353.

Dugdale, R. C. and J. J. Goering. 1967. Uptake of new and regenerated forms of nitrogen in primary productivity. *Limnol. Oceanogr.* 9:507-510.

Dunton, K. H. and D. M. Schell. 1987. Dependence of consumers on macroalgal (*Laminaria solidungula*) carbon in an Arctic kelp community: $\delta^{13}\text{C}$ evidence. *Mar. Biol.* 93:615-625.

Dunton, K. H., S. M. Saupe, A. N. Golikov, D. M. Schell, and S. V. Schonberg. 1989. Trophic relationships and isotopic gradients among Arctic and subarctic marine fauna. *Mar. Ecol. Progr. Ser.* 56:89-97.

Francis, R.C. and S.R. Hare. 1994. Decadal-scale regime shifts in the large marine ecosystems of the northeast Pacific: a case for historical science. *Fish. Oceanogr.* 3:279-291.

- Fry, B. and E. B. Sherr. 1984. $\delta^{13}\text{C}$ measurements as indicators of carbon flow in marine and freshwater ecosystems. *Contr. Mar. Sci.* 27:13-47.
- Fry, B. 1988. Food web structure on Georges Bank from stable C, N, and S isotopic compositions. *Limnol. Oceanogr.* 33:1182-1190.
- Gifford, D. J. 1993. Protozoa in the diets of *Neocalanus* spp. in the oceanic subarctic Pacific. *Prog. Oceanogr.* 32:223-237.
- Goering, J. V. Alexander, and N. Haubenstock. 1990. Seasonal variability of stable carbon and nitrogen isotope ratios of organisms in a north Pacific bay. *Estuar. Coast. Shelf Sci.* 30:239-260.
- Goering, J. J., C. J. Patton and W. E. Shiels. 1973. Primary Production *In*: D. W. Hood, W. E. Shiels, and E. . Kelley (eds), *Environmental Studies of Port Valdez*. Inst. Mar. Sci. Occ. Pub. No. 3. University of Alaska Fairbanks. P. 253-279.
- Hesslein, R. H., K. A. Hallard, and P. Ramlal. 1993. Replacement of sulfur, carbon, and nitrogen in tissue of growing broad whitefish (*Coregonus nasus*) in response to a change in diet traced by $\delta^{34}\text{S}$, $\delta^{13}\text{C}$, and $\delta^{15}\text{N}$. *Can. J. Fish. Aquat. Sci.* 50:2071-2076.
- Hobson, K. A. and H. E. Welch. 1992. Determination of trophic relationships within a high Arctic marine food web using $\delta^{13}\text{C}$ and $\delta^{15}\text{N}$ analysis. *Mar. Ecol. Prog. Ser.* 84:9-18.
- Kline, T. C. 1997. Confirming forage fish food web dependencies in the Prince William Sound ecosystem using natural stable isotope tracers. *Proceedings of the International Symposium on the Role of Forage Fishes in Marine Ecosystems*. Alaska Sea Grant College Program Report No. 9701. University of Alaska Fairbanks. P. 257 - 269.
- Kline, T.C. and D. Pauly. 1998. Cross-validation of trophic level estimates from a mass-balance model of, and $^{15}\text{N}/^{14}\text{N}$ data from, Prince William Sound. *Proceedings of the International Symposium on Fishery Stock Assessment Models for the 21st Century -- Combining Multiple Data Sources*. Alaska Sea Grant College Program Report. University of Alaska Fairbanks. In Press.
- Kling, G. W., B. Fry, and W. J. O'Brien. 1992. Stable isotopes and planktonic trophic structure in Arctic lakes. *Ecology* 73:561-566.

- McConnaughey, T. and C. P. McRoy. 1979. Food-web structure and the fractionation of carbon isotopes in the Bering Sea. *Mar. Biol.* 53:257-262.
- Miller, C. B., B. W. Frost, H. P. Batchelder, M. J. Clemons, and R. E. Conway. 1984. Life histories of large, grazing copepods in a subarctic ocean gyre: *Neocalanus plumchrus*, *Neocalanus cristatus*, and *Eucalanus bungii*. *Progr. Oceanogr.*, 13:201-243.
- Miller, C. B. and M. Terazaki. 1989. The life histories of *Neocalanus flemingeri* and *Neocalanus plumchrus* in the Sea of Japan. *Bull. Plankton Soc. Japan* 36:27-41.
- Minagawa, M., and E. Wada. 1984. Stepwise enrichment of ^{15}N along food chains: Further evidence and the relation between $\delta^{15}\text{N}$ and animal age. *Geochim. Cosmochim. Acta* 48:1135-1140.
- Niebauer, H.J., T.C. Royer, and T.J. Weingartner. 1994. Circulation of Prince William Sound, Alaska. *J. Geophys. Res.* 99:113-126.
- Norcross, B. L., E. D. Brown, K. D. E. Stokesbury, and M. Frandsen. 1996. Juvenile herring growth and habitat, *Exxon Valdez* Oil Spill Restoration Project Annual Report (Restoration Project 95320T), University of Alaska Fairbanks, Institute of Marine Science, Fairbanks, Alaska.
- Owens, N. J. P. 1987. Natural variations in ^{15}N in the marine environment. *Advances in Marine Biology* 24:389-451.
- Patrick, V. et al. 1997. Sound Ecosystem Assessment: information systems and model development. *Exxon Valdez* oil spill restoration project annual report (Restoration project 96320J), Prince William Sound Science Center, Cordova, Alaska.
- Paul, A. J., J. M. Paul and E. Brown. Fall and Spring somatic energy content for Alaskan Pacific herring (*Clupea pallasii* Valenciennes 1847) relative to age, size and sex. *J.Exp. Mar. Biol. Ecol.* In Press.
- Peterson, B. J. and R. W. Howarth. 1987. Sulfur, carbon and nitrogen isotopes used to trace organic matter flow in the salt-marsh estuaries of Sapelo Island, Georgia. *Limnol. Oceanogr.* 32:1195-1213.

- Rau, G.H. 1989. AMERIEZ 1986: Carbon-13 and Nitrogen-15 natural abundances in Southern Ocean biota collected during AMERIEZ 1986. *Antarct. J. of the U.S.* 24:168-169.
- Rau, G.H., M. Heyraud, and R.D. Cherry. 1989. $^{15}\text{N}/^{14}\text{N}$ and $^{13}\text{C}/^{12}\text{C}$ in mesopelagic shrimp from the northeast Atlantic Ocean: evidence for differences in diet. *Deep-Sea Res.* 36:1103-1110.
- Rau, G.H., T. Takahasi, D.J. Des Marais, and C.W. Sullivan. 1991. Particulate organic matter $\delta^{13}\text{C}$ variations across the Drake Passage. *J. Geophys. Res.* 96:131-135.
- Rau, G.H., A.J. Mearns, D.R. Young, R.J. Olson, H.A. Schafer, and I.R. Kaplan. 1983. Animal $^{13}\text{C}/^{12}\text{C}$ correlates with trophic level in epipelagic food webs. *Ecol.* 64:1314-1318.
- Saupe, S.M., D.M. Schell, and E.W. Griffiths. 1989. Carbon isotope ratio gradients in western Arctic zooplankton. *Mar. Biol.* 103:427-433.
- Smith, W. H. F., and P. Wessel. 1990. Gridding with continuous curvature splines in tension. *Geophys.* 55:293-305.
- Stephenson, R. L., F. C. Tan, and K. H. Mann. 1986. Use of stable carbon isotope ratios to compare plant material and potential consumers in a seagrass bed and kelp bed in Nova Scotia, Canada. *Mar. Ecol. Progr. Ser.* 30:1-7.
- Vander Zanden, M.J. and J.B. Rasmussen. 1996. A trophic position model of pelagic food webs: impact on contaminant bioaccumulation in lake trout. *Ecol. Monogr.* 66:451-477.
- Vander Zanden, M.J., G. Cabana, and J.B. Rasmussen. 1997. Comparing trophic position of freshwater fish calculated using stable nitrogen isotope ratios ($\delta^{15}\text{N}$) and literature dietary data. *Can. J. Fish. Aquat. Sci.* 54:1142-1158.
- Wada, E., H. Mizutani, and M. Minagawa. 1991. The use of stable isotopes for food web analysis. *Crit. Rev. Food Sci. Nutr.* 30:361-371.
- Wessel, P. and W.H.F. Smith. 1995. New version of the Generic Mapping Tools released. *EOS Trans. Amer. Geophys. U.* 72:441, 445-446.

Willette, M., M. Clapsadl, P. Saddler, M. Powell. 1997. Sound ecosystem assessment: salmon and herring integration. *Exxon Valdez* Oil Spill Restoration Project Annual Report (Restoration Project 96320E), Alaska Department of Fish and Game, Cordova, Alaska.

Wu, J. S.E. Calvert, and C.S. Wong. 1997. Nitrogen isotope variations in the subarctic Pacific: relationships to nitrate utilization and trophic structure. *Deep Sea Res* 44:287-314.

Table 1. Interannual differences of Prince William Sound, Alaska net zooplankton isotopic composition by oceanographic station; 1994 vs. 1995.

Station	1994			1995			(1994 - 1995)		
	$\delta^{15}\text{N}$	$\delta^{13}\text{C}$	$\delta^{13}\text{C}'$	$\delta^{15}\text{N}$	$\delta^{13}\text{C}$	$\delta^{13}\text{C}'$	$\delta^{15}\text{N}$	$\delta^{13}\text{C}$	$\delta^{13}\text{C}'$
CFOS13	8.2	-21.2	-19.6	7.6	-22.1	-19.5	0.5	0.9	-0.1
CS3	9.4	-21.2	-17.2	8.4	-21.7	-19.1	1.0	0.6	1.8
HE12	9.6	-21.0	-17.5	7.5	-23.0	-20.9	2.1	2.0	3.4
MS3	9.1	-22.3	-19.4	7.5	-22.3	-19.7	1.5	0.0	0.3
MS6	8.6	-21.6	-18.8	8.6	-21.5	-19.0	0.0	-0.1	0.2
NS1	9.6	-23.2	-20.1	8.4	-22.2	-19.7	1.1	-1.0	-0.4
NWS4	10.0	-22.8	-20.1	8.5	-21.7	-19.1	1.5	-1.1	-1.1
SEA11	8.7	-22.0	-19.6	8.9	-22.0	-19.3	-0.1	0.0	-0.2
SEA22	5.6	-23.2	-20.6	8.3	-21.0	-18.6	-2.7	-2.2	-2.0
SEA25	9.0	-22.4	-20.4	8.4	-21.9	-19.5	0.6	-0.5	-0.9
SEA27	9.1	-22.4	-20.4	8.4	-21.7	-18.9	0.8	-0.7	-1.5
SEA32	9.3	-22.0	-20.0	8.1	-22.2	-19.8	1.2	0.2	-0.2
SEA37	9.1	-21.3	-17.5	7.9	-22.9	-20.8	1.2	1.6	3.3
SEA4	7.7	-22.7	-20.0	8.4	-22.3	-19.4	-0.7	-0.4	-0.6
						mean	0.6	-0.1	0.1

Table 2. Regression analyses: their correlation, intercept and slope values with probabilities.

Data	Fixed Parameter	Variable 1	Variable 2	r ²	P	Intercept	P	Slope	P	N
<u>Net Zooplankton</u>										
Spring 95	Upper 50m	$\delta^{15}\text{N}$	$\delta^{13}\text{C}$	0.4420	<.0001	-28.2920	<.0001	0.7770	<.0001	79
Mar-95	Upper 50m	$\delta^{15}\text{N}$	$\delta^{13}\text{C}$	0.5690	0.0070	-29.8010	<.0001	0.9880	0.0007	16
Apr-95	Upper 50m	$\delta^{15}\text{N}$	$\delta^{13}\text{C}$	0.7440	<.0001	-28.4750	<.0001	0.8410	<.0001	22
May-95	Upper 50m	$\delta^{15}\text{N}$	$\delta^{13}\text{C}$	0.1290	0.1314	-25.0520	<.0001	0.4310	0.1314	19
Jun-95	Upper 50m	$\delta^{15}\text{N}$	$\delta^{13}\text{C}$	0.1770	0.0291	-29.6230	<.0001	0.8870	0.0291	22
Spring 95	Upper 50m	$\delta^{15}\text{N}$	$\delta^{13}\text{C}'$	0.4870	<.0001	-27.2490	<.0001	0.9480	<.0001	79
Mar-95	Upper 50m	$\delta^{15}\text{N}$	$\delta^{13}\text{C}'$	0.5420	0.0011	-28.3880	<.0001	1.0580	0.0011	16
Apr-95	Upper 50m	$\delta^{15}\text{N}$	$\delta^{13}\text{C}'$	0.5480	<.0001	-25.2310	<.0001	0.7440	<.0001	22
May-95	Upper 50m	$\delta^{15}\text{N}$	$\delta^{13}\text{C}'$	0.1880	0.0639	-22.4440	<.0001	0.4720	0.0639	19
Jun-95	Upper 50m	$\delta^{15}\text{N}$	$\delta^{13}\text{C}'$	0.1680	0.0582	-26.1440	<.0001	0.7290	0.0582	22
<u>Temporal comparisons</u>										
	Upper 50m	Julian Date (Apr & May)	Auke $\delta^{15}\text{N}$	0.8670	0.0069	4.5980	0.0019	0.0250	0.0069	6
	Upper 50m	Julian Date (Apr & May)	PWS $\delta^{15}\text{N}$	0.5860	<.0001	0.4490	0.5473	0.0690	<.0001	82
	Upper 50m	Julian Date (Apr & May)	Auke $\delta^{13}\text{C}$	0.7290	0.0304	-26.8740	0.0002	0.0530	0.0304	6
	Upper 50m	Julian Date (Apr & May)	PWS $\delta^{13}\text{C}$	0.3570	<.0001	-26.7640	<.0001	0.0450	<.0001	82
<u>Net zooplankton, Spring 1995</u>										
	$\delta^{15}\text{N}$	Water column	Upper 50m	0.1040	0.0330	5.5020	<.0001	0.2990	0.0330	44
	$\delta^{13}\text{C}$	Water column	Upper 50m	0.3290	<.0001	-10.2450	0.0004	0.5440	<.0001	43
	$\delta^{13}\text{C}'$	Water column	Upper 50m	0.5100	0.0003	-6.3630	0.0520	0.7200	0.0003	43
<u>Neocalanus vs. Net Zooplankton</u>										
		<u>Upper 50m</u>	<u>Upper 50m</u>							
Spring 95	$\delta^{15}\text{N}$	Net zooplankton	<i>Neocalanus cristatus</i>	0.0030	0.8220	7.9440	0.0117	0.0730	0.8220	18
Spring 95	$\delta^{13}\text{C}$	Net zooplankton	<i>Neocalanus cristatus</i>	0.4260	0.0013	-1.6160	0.7564	0.8910	0.0013	21
Spring 95	$\delta^{13}\text{C}'$	Net zooplankton	<i>Neocalanus cristatus</i>	0.5100	0.0003	-6.3630	0.0520	0.7200	0.0003	21
May-95	$\delta^{15}\text{N}$	Net zooplankton	<i>Neocalanus cristatus</i>	0.0300	0.6118	6.9980	0.0175	0.1360	0.6118	11
May-95	$\delta^{13}\text{C}$	Net zooplankton	<i>Neocalanus cristatus</i>	0.2040	0.1408	-6.1190	0.5128	0.6790	0.1408	12
May-95	$\delta^{13}\text{C}'$	Net zooplankton	<i>Neocalanus cristatus</i>	0.5240	0.0078	-0.6840	0.9074	1.0400	0.0078	12
		<u>Water column</u>	<u>Upper 50m</u>							
Spring 95	$\delta^{15}\text{N}$	Net zooplankton	<i>Neocalanus cristatus</i>	0.1100	0.0688	5.7160	0.0002	0.2790	0.0688	31
Spring 95	$\delta^{13}\text{C}$	Net zooplankton	<i>Neocalanus cristatus</i>	0.1160	0.0564	-15.5910	<.0001	0.2650	0.0564	32
Spring 95	$\delta^{13}\text{C}'$	Net zooplankton	<i>Neocalanus cristatus</i>	0.0360	0.2983	-16.7420	<.0001	0.1690	0.2983	32
<u>Neocalanus cristatus</u>										
Spring 95	Upper 50m	$\delta^{15}\text{N}$	$\delta^{13}\text{C}$	0.2620	<.0001	-29.3380	<.0001	0.9890	<.0001	124
May-95	Upper 50m	$\delta^{15}\text{N}$	$\delta^{13}\text{C}$	0.2060	<.0001	-29.6210	<.0001	1.0670	<.0001	72
Spring 95	Upper 50m	$\delta^{15}\text{N}$	$\delta^{13}\text{C}'$	0.3510	<.0001	-28.0150	<.0001	0.9050	<.0001	124
May-95	Upper 50m	$\delta^{15}\text{N}$	$\delta^{13}\text{C}'$	0.3380	<.0001	-29.9510	<.0001	1.1760	<.0001	72
Spring 95	Water column	$\delta^{15}\text{N}$	$\delta^{13}\text{C}$	0.0790	<.0001	-24.3770	<.0001	0.3640	<.0001	420
Spring 95	Water column	$\delta^{15}\text{N}$	$\delta^{13}\text{C}'$	0.0060	0.1003	-20.9130	<.0001	0.0920	0.1003	420

Table 3. Macro-zooplankton: isotopic data of individual zooplankters by taxon collected in Prince William Sound, Alaska in 1994. Copepods were distinguished as carnivorous (C) or interzonal (I). Fall 1994 interzonal copepods consisted of *Neocalanus cristatus* in diapause.

Taxon/Season	$\delta^{15}\text{N}$	SD	$\delta^{13}\text{C}$	SD	$\delta^{13}\text{C}'$	SD	N
<u>Amphipods</u>							
Spring	11.58	0.79	-20.25	1.10	-18.46	0.81	23
Fall	10.58	2.02	-21.55	1.19	-18.94	1.14	85
<u>Decapods</u>							
Spring	11.39	1.52	-20.42	0.46	-19.53	0.28	38
Fall	11.22	1.92	-20.56	0.88	-19.04	0.67	20
<u>Euphausiids</u>							
Spring	10.53	0.57	-19.36	0.56	-18.71	0.53	55
Summer	9.36	0.28	-19.76	0.63	-19.34	0.62	20
Fall	10.72	1.90	-21.24	1.13	-19.70	0.81	95
<u>Copepods(C)</u>							
Spring	12.00	0.24	-21.38	0.40	-19.98	0.39	6
Fall	11.91	0.62	-22.43	0.67	-19.92	0.33	23
<u>Copepods(I)</u>							
Spring	8.64	1.20	-22.96	0.96	-19.81	1.18	59
Fall	8.33	1.07	-22.89	2.12	-20.95	1.75	20

Table 4. Isotopic composition of copepodite IV and V *Neocalanus cristatus* sampled from upper 50 m at indicated oceanographic stations in Prince William Sound and northern Gulf of Alaska where at least one individual was found in March to June, 1995, except no monthly table is given for March since only 8 were found in total. Zeros indicate that none were found while NS indicate that station was not sampled. Mean $\delta^{13}\text{C}$, $\delta^{15}\text{N}$, and $\delta^{13}\text{C}$, their *SD*, and *N* of total sample collected from each station given. The *N* for some $\delta^{15}\text{N}$ analyses are less than the station sample total when copepods contained too little N for the analysis (B. Barnett, mass. spec. technician, pers. comm.). The total means for only Prince William Sound (PWS) stations just above Gulf of Alaska station GOA6 to facilitate comparison of mean PWS values with GOA values.

April									May									
Station	$\delta^{15}\text{N}$	<i>SD</i>	<i>N</i>	$\delta^{13}\text{C}$	<i>SD</i>	<i>N</i>	$\delta^{13}\text{C}$	<i>SD</i>	<i>N</i>	$\delta^{15}\text{N}$	<i>SD</i>	<i>N</i>	$\delta^{13}\text{C}$	<i>SD</i>	<i>N</i>	$\delta^{13}\text{C}$	<i>SD</i>	<i>N</i>
CFOS 13			0			0			0	8.7		1	-19.8		1	-19.3		1
CFOSBY			0			0			0	8.3	0.5	21	-19.7	0.3	21	-19.7	0.4	21
CS3			0			0			0	7.8	0.8	11	-20.0	0.3	11	-19.9	0.6	11
CS9			0			0			0			0			0			0
HE12			0			0			0	8.2	0.3	2	-19.7	0.0	2	-19.4	0.5	2
NS1	7.9		1	-23.1		1	-20.8		1	8.6	0.2	2	-19.2	0.8	2	-18.8	0.7	2
NWS4			0			0			0	9.3	0.6	4	-20.2	0.5	4	-18.6	0.5	4
OB1	7.1		1	-20.8		1	-18.7		1			0			0			0
OB2	9.1		1	-22.9		1	-20.9		1			0			0			0
PV1			0			0			0	8.7	0.2	2	-19.2	0.9	2	-18.9	0.9	2
PW1			0	-20.2		1	-20.3		1			0			0			0
SEA11			0			0			0	8.4	1.1	10	-20.4	1.1	10	-19.4	0.6	10
SEA22	9.1		0	-20.3	1.5	3	-19.3	1.6	3			0			0			0
SEA25	8.8	1.5	8	-21.7	1.4	8	-19.4	1.3	8			0			0			0
SEA4			0			0			0	8.3	0.6	3	-20.5	0.5	3	-19.4	0.9	3
all PWS	8.6	1.4	12	-21.5	1.4	15	-19.6	1.2	15	8.3	0.8	56	-19.9	0.7	56	-19.5	0.6	56
GOA6			NS			NS			NS	7.5	0.7	20	-23.8	1.4	20	-23.1	1.3	20

June									Mar-Jun									
Station	$\delta^{15}\text{N}$	<i>SD</i>	<i>N</i>	$\delta^{13}\text{C}$	<i>SD</i>	<i>N</i>	$\delta^{13}\text{C}$	<i>SD</i>	<i>N</i>	$\delta^{15}\text{N}$	<i>SD</i>	<i>N</i>	$\delta^{13}\text{C}$	<i>SD</i>	<i>N</i>	$\delta^{13}\text{C}$	<i>SD</i>	<i>N</i>
CFOS 13			0			0			0	8.7		1	-19.8		1	-19.3		1
CFOSBY			0			0			0	8.3	0.5	21	-19.7	0.3	21	-19.7	0.4	21
CS3			0			0			0	7.8	0.8	9	-20.0	0.3	11	-19.9	0.6	11
CS9	8.7	0.5	14	-20.1	0.6	14	-20.3	0.6	14	8.7	0.5	14	-20.1	0.6	14	-20.3	0.6	14
HE12			0			0			0	8.2	0.3	2	-19.7	0.0	2	-19.4	0.5	2
NS1			0			0			0	8.4	0.4	3	-20.5	2.3	3	-19.5	1.3	3
NWS4			0			0			0	9.3	0.6	4	-20.7	1.1	5	-19.1	1.1	5
OB1			0			0			0			0	-20.8		1	-18.7		1
OB2	8.3	1.2	8	-19.4	0.6	8	-19.9	0.8	8	8.2	1.2	9	-19.8	1.3	9	-20.0	0.8	9
PV1			0			0			0	8.7	0.2	2	-19.2	0.9	2	-18.9	0.9	2
PW1			0			0			0	9.5	1.5	6	-20.3	2.1	7	-19.8	1.5	7
SEA11			0			0			0	8.8	1.9	11	-20.3	1.2	11	-19.4	0.6	11
SEA22			0			0			0	9.1		1	-20.3	1.5	3	-19.3	1.6	3
SEA25			0			0			0	8.8	1.5	8	-21.7	1.4	8	-19.4	1.3	8
SEA4			0			0			0	8.3	0.6	3	-20.5	0.5	3	-19.4	0.9	3
all PWS	8.6	0.8	22	-19.8	0.7	22	-20.2	0.7	22	8.6	1.1	94	-20.2	1.1	101	-19.7	0.9	101
GOA6	7.0	0.5	12	-25.1	0.9	12	-23.5	0.6	12	7.3	0.7	30	-24.3	1.4	32	-23.2	1.1	32

Table 5. Isotopic composition of copepodite V and VI *Neocalanus cristatus* sampled from the water column at indicated oceanographic stations in Prince William Sound and northern Gulf of Alaska where at least one individual was found in March to June, 1995. Number of copepods collected at each station each month are given. Zeros indicate that none were found while NS indicates that the station was not sampled. ND indicates "no data" while an N less than the station sample total reflect copepods containing too little nitrogen for the analysis (B. Barnett, mass. spec. technician, pers. comm.). Data for the Fall cruise which started in September and ended in October are given in the Sept-Oct block. Means for the March to April and March to May period are given at the bottom.

Station	March									April								
	$\delta^{15}\text{N}$	SD	N	$\delta^{13}\text{C}$	SD	N	$\delta^{13}\text{C}$	SD	N	$\delta^{15}\text{N}$	SD	N	$\delta^{13}\text{C}$	SD	N	$\delta^{13}\text{C}$	SD	N
CFOS 13	10.6	0.8	7	-20.7	2.0	7	-20.0	1.9	7			ND	-20.0	1.0	2	-17.6	0.4	2
CS4			NS			NS			NS			NS			NS			NS
CS9			ND	-21.1	2.4	4	-19.6	2.4	4	8.1	0.6	2	-21.4	0.4	3	-20.0	1.1	3
HE11	6.8		1	-23.2		1	-21.4		1			NS			NS			NS
HE12			0			0			0			0			0			0
HE13	8.6	1.8	9	-20.3	1.4	9	-20.0	1.6	9	6.8		1			ND			ND
NS2			NS			NS			NS			NS			NS			NS
NWS4	9.0	1.5	20	-21.5	2.3	20	-20.7	1.8	20	9.5	1.1	16	-21.6	1.8	16	-20.5	1.6	16
PB1			NS			NS			NS	7.1	0.7	2	-21.2	1.2	3	-19.8	1.1	3
PV1			NS			NS			NS	9.0		1	-22.1	1.2	3	-20.4	1.0	3
PW1	8.8	2.3	21	-22.0	2.3	21	-21.1	1.9	21	9.1	1.7	17	-21.4	2.1	17	-20.8	1.9	17
SEA11	8.9	1.5	20	-21.5	2.1	20	-20.6	1.9	20	8.0	0.9	15	-22.5	1.8	18	-20.5	1.8	18
SEA22	8.0	0.9	31	-21.6	2.4	33	-20.4	2.1	33	7.8	1.4	30	-22.2	2.4	33	-20.2	2.0	33
SEA25			NS			NS			NS	8.7	2.3	8	-23.1	1.1	8	-21.6	1.2	8
SEA27	9.3	2.1	22	-22.1	2.1	26	-21.2	1.7	26	8.9	1.0	12	-21.2	1.6	17	-20.0	1.4	17
SEA4	9.4		1	-21.4	0.8	2	-21.2	1.9	2	8.3	1.0	11	-21.2	1.5	14	-19.7	1.3	14
all PWS	8.8	1.7	132	-21.6	2.2	143	-20.7	1.9	143	8.5	1.5	115	-21.8	1.9	134	-20.3	1.7	134

Station	May									Sept-Oct								
	$\delta^{15}\text{N}$	SD	N	$\delta^{13}\text{C}$	SD	N	$\delta^{13}\text{C}$	SD	N	$\delta^{15}\text{N}$	SD	N	$\delta^{13}\text{C}$	SD	N	$\delta^{13}\text{C}$	SD	N
CFOS 13	8.2	0.1	3	-20.9	0.1	3	-18.5	0.3	3	7.1	1.9	24	-24.4	1.6	24	-22.4	1.6	24
CS4	8.6	0.7	19	-20.2	0.5	20	-19.4	1.0	20			NS			NS			NS
CS9	8.9	1.0	12	-20.6	0.8	13	-19.6	0.8	13			NS			NS			NS
HE11			NS			NS			NS			NS			NS			NS
HE12	8.0	0.5	20	-20.1	0.3	21	-19.7	0.6	21			NS			NS			NS
HE13	8.0	0.9	18	-21.3	1.2	20	-21.1	1.2	20	8.5	2.6	12	-23.0	1.7	12	-21.7	1.7	12
NS2			NS			NS			NS	8.9	3.0	25	-24.3	1.7	25	-22.6	1.7	25
NWS4	8.3	0.9	8	-20.8	1.2	12	-19.4	0.9	12	6.9	1.7	26	-23.6	1.1	26	-22.3	1.1	26
PB1			NS			NS			NS			NS			NS			NS
PV1	8.2	0.7	19	-20.4	1.1	19	-19.3	0.9	19			NS			NS			NS
PW1	7.5	1.2	13	-21.2	1.2	13	-19.5	0.8	13			NS			NS			NS
SEA11	7.6	1.1	13	-20.5	0.8	18	-19.0	0.4	18	7.9	1.7	25	-24.3	1.3	25	-22.5	1.3	25
SEA22	6.8	0.9	17	-22.0	1.8	18	-19.7	1.7	18	6.8	1.8	50	-24.5	1.2	50	-22.5	1.2	50
SEA25	7.6	1.0	10	-21.0	2.2	12	-19.7	1.8	12	7.1	1.9	25	-24.0	1.2	25	-22.3	1.2	25
SEA27	7.8	1.3	11	-20.9	0.5	11	-19.1	0.8	11	11.5	4.3	22	-23.0	1.2	22	-22.3	1.2	22
SEA4	8.0	0.7	11	-20.9	1.0	12	-19.6	0.6	12			NS			NS			NS
all PWS	7.9	1.0	174	-20.8	1.8	192	-19.6	1.1	192	7.8	2.8	209	-24.0	1.6	209	-22.4	1.4	209

all PWS	Mar-Apr									Mar-May								
	$\delta^{15}\text{N}$	SD	N	$\delta^{13}\text{C}$	SD	N	$\delta^{13}\text{C}$	SD	N	$\delta^{15}\text{N}$	SD	N	$\delta^{13}\text{C}$	SD	N	$\delta^{13}\text{C}$	SD	N
	8.7	1.6	247	-21.7	2.1	277	-20.5	1.8	277	8.4	1.4	421	-21.3	1.8	469	-20.1	1.6	469

Table 6. Juvenile herring (Age 0 and 1) and pollock (age 0) isotopic data from indicated Prince William Sound sampling sites (Map codes refer to site location symbols in Fig. 1) sampled from 1994 to 1995. Annual means are given for each species on top line of their respective data blocks.

1994								
<u>Age 0 and 1 Herring</u>								
	Map code	$\delta^{15}\text{N}$		$\delta^{13}\text{C}$		$\delta^{13}\text{C}'_{\text{TL}}$		N
		Mean	SD	Mean	SD	Mean	SD	
Total		12.3	0.93	-20.9	1.12	-20.8	0.80	110
Apr-Wells Passage	H	12.1	1.86	-20.5	0.69	-19.9	0.54	20
Jun-Knight Is. Pass.	I	13.1	0.21	-19.8	0.57	-20.8	0.50	9
Oct-Port Gravina	C	12.0	0.49	-22.0	0.76	-21.5	0.49	31
Oct-Knowles Head	D	13.1	0.18	-19.5	0.34	-20.8	0.35	13
Oct- Windy Bay	B	12.2	0.26	-20.9	0.90	-20.8	0.74	37
<u>Age 0 Pollock</u>								
		$\delta^{15}\text{N}$		$\delta^{13}\text{C}$		$\delta^{13}\text{C}'_{\text{TL}}$		N
		Mean	SD	Mean	SD	Mean	SD	
Total		11.3	0.88	-20.3	1.00	-20.7	0.51	116
Jul-Knight Is.Pass.	I	10.6	0.20	-21.1	0.23	-20.8	0.15	59
Sep-Redhead/Gravina	C	11.4	0.15	-19.4	0.23	-20.3	0.22	20
Oct-Redhead/Gravina	C	12.4	0.64	-18.9	1.49	-20.3	1.33	11
Oct-Windy Bay	B	12.5	0.20	-19.7	0.41	-20.6	0.43	26

Fall 1995								
<u>Age 0 and 1 Herring</u>								
		$\delta^{15}\text{N}$		$\delta^{13}\text{C}$		$\delta^{13}\text{C}'_{\text{TL}}$		N
		Mean	SD	Mean	SD	Mean	SD	
Total		12.7	0.34	-22.7	0.62	-22.8	0.37	250
Eaglek Bay	G	12.7	0.35	-22.9	0.73	-22.8	0.52	25
Green Island	M	12.7	0.22	-22.5	0.40	-22.6	0.23	25
Hogg Bay	K	12.7	0.32	-22.3	0.46	-22.7	0.18	25
Jack Bay	F	12.6	0.33	-22.5	0.51	-22.7	0.29	25
Knowles Head	D	12.7	0.36	-23.4	0.71	-22.9	0.58	25
Sawmill Bay	L	12.8	0.27	-22.9	0.39	-22.9	0.26	25
Simpson Bay	A	12.7	0.24	-22.6	0.67	-22.8	0.43	25
Snug Corner Cove	E	12.8	0.35	-22.5	0.59	-22.9	0.37	25
Whale Bay	J	12.3	0.22	-23.0	0.34	-23.2	0.20	25
Zaikof Bay	N	12.8	0.35	-22.3	0.40	-22.7	0.19	25
<u>Age 0 Pollock</u>								
		$\delta^{15}\text{N}$		$\delta^{13}\text{C}$		$\delta^{13}\text{C}'_{\text{TL}}$		N
		Mean	SD	Mean	SD	Mean	SD	
Total		13.1	0.32	-20.9	0.45	-22.1	0.37	171
Eaglek Bay	G	12.9	0.20	-21.2	0.59	-22.0	0.48	25
Hogg Bay	K	13.0	0.25	-20.9	0.31	-22.1	0.26	25
Knowles Head	D	13.4	0.27	-20.6	0.38	-22.0	0.33	25
Sawmill Bay	L	13.1	0.36	-21.1	0.34	-22.2	0.30	25
Simpson Bay	A	13.2	0.35	-20.9	0.43	-22.1	0.41	25
Whale Bay	J	12.9	0.26	-20.9	0.44	-22.0	0.41	25
Zaikof Bay	N	13.1	0.28	-20.6	0.40	-22.1	0.33	21

Table7

	1994	1995
<u>Observations</u>		
Source of diapaused copepods in PWS	GOA & PWS	GOA
Carbon source in PWS juvenile fishes	GOA & PWS	GOA
Advection deduced to be:	Moderate	Strong

FIGURE CAPTIONS

1. Sampling Stations and potential copepod diapause habitat in Prince William Sound Alaska.

Zooplankton were sampled at designated oceanographic stations which had alphanumeric names (listed in Appendix 1). Fishes were sampled near map symbols consisting of single Roman characters (A - N). Names of these sites are given in Table 5. Potential diapause habitat is the area of Prince William Sound deeper than 400 m as indicated by shading.

2. Areal distribution of net zooplankton $\delta^{15}\text{N}$ and $\delta^{13}\text{C}$ (columns) in the PWS study area during September 1994, March, April, May, and June 1995 (rows), from upper 50 m in the PWS study area.

3. Temporal shift in zooplankton $\delta^{15}\text{N}$ (A) , $\delta^{13}\text{C}$ (B) and $\delta^{13}\text{C}'$ (C) in the PWS study area during March to June 1995. A. Regression is: $\delta^{15}\text{N} = -1.2249J + 0.011J^2 - 0.0000315J^3$, all P values < 0.0001, $r^2 = 0.412$, where J is the Julian date. B. Regression is: $\delta^{13}\text{C} = -0.638J + 0.006J^2 - 0.0000176J^3 - 0.453$, P values are 0.0068, 0.0029, 0.0013, and 0.959 for the J, J^2 , J^3 coefficients and Y-intercept, respectively, $r^2 = 0.209$, where J is the Julian date. C. Regression is $\delta^{13}\text{C}' = -0.749J + 0.007J^2 - 0.0000228J^3 + 3.25$, P values are 0.0021, 0.0003, < 0.0001, and 0.720 for the J, J^2 , J^3 coefficients and Y-intercept, respectively, $r^2 = 0.423$, where J is the Julian date.

4. Scatterplots with histograms of copepodite IV and V *Neocalanus cristatus* collected from the water column in March to April, 1995 (A), and May, 1995 (B), below 200m in Fall, 1995 (C), and from the upper 50m in the Spring, 1995 (D). "Cross-hairs" positioned near center of distribution of inferred GOA and PWS isotopic signatures to aid in comparisons of plots. Inferred life history stage shown in parentheses. A and C suggest large differences in source of copepods in diapause each year. Diapaused copepods in late 1995 differed considerably from those completing feeding and entering diapause phase in Spring (B), instead, resembling copepods sampled in the GOA (left cluster in D).

5. Mean areal distribution of (A) $\delta^{15}\text{N}$ and, (B) $\delta^{13}\text{C}$ and $\delta^{13}\text{C}'$ in: (1) feeding copepodite IV and V *Neocalanus cristatus* (top row); (2) upper 50m net zooplankton (second row); and (3) water column net zooplankton (bottom row) in the PWS study area in 1994-5.

6. Scales of ^{13}C variability in the PWS pelagic system. Relative strength suggested by this study is ranked and reflected by the number of asterisks (greater number of asterisks, the higher the rank). Physical forcing mediates (lines) the transfer of spatial variability on biota at annual scaling.

Figure 1

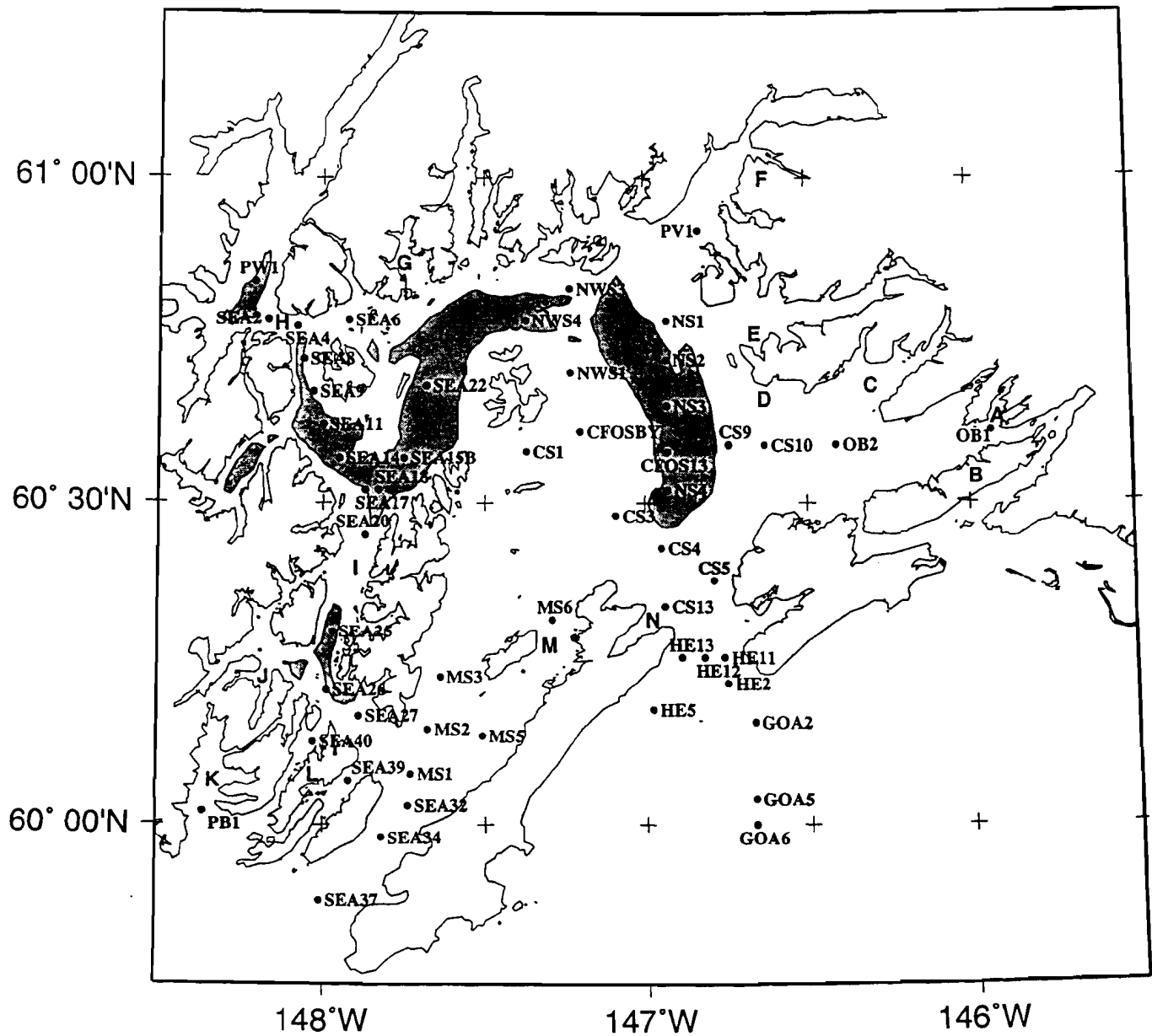


Figure. 2

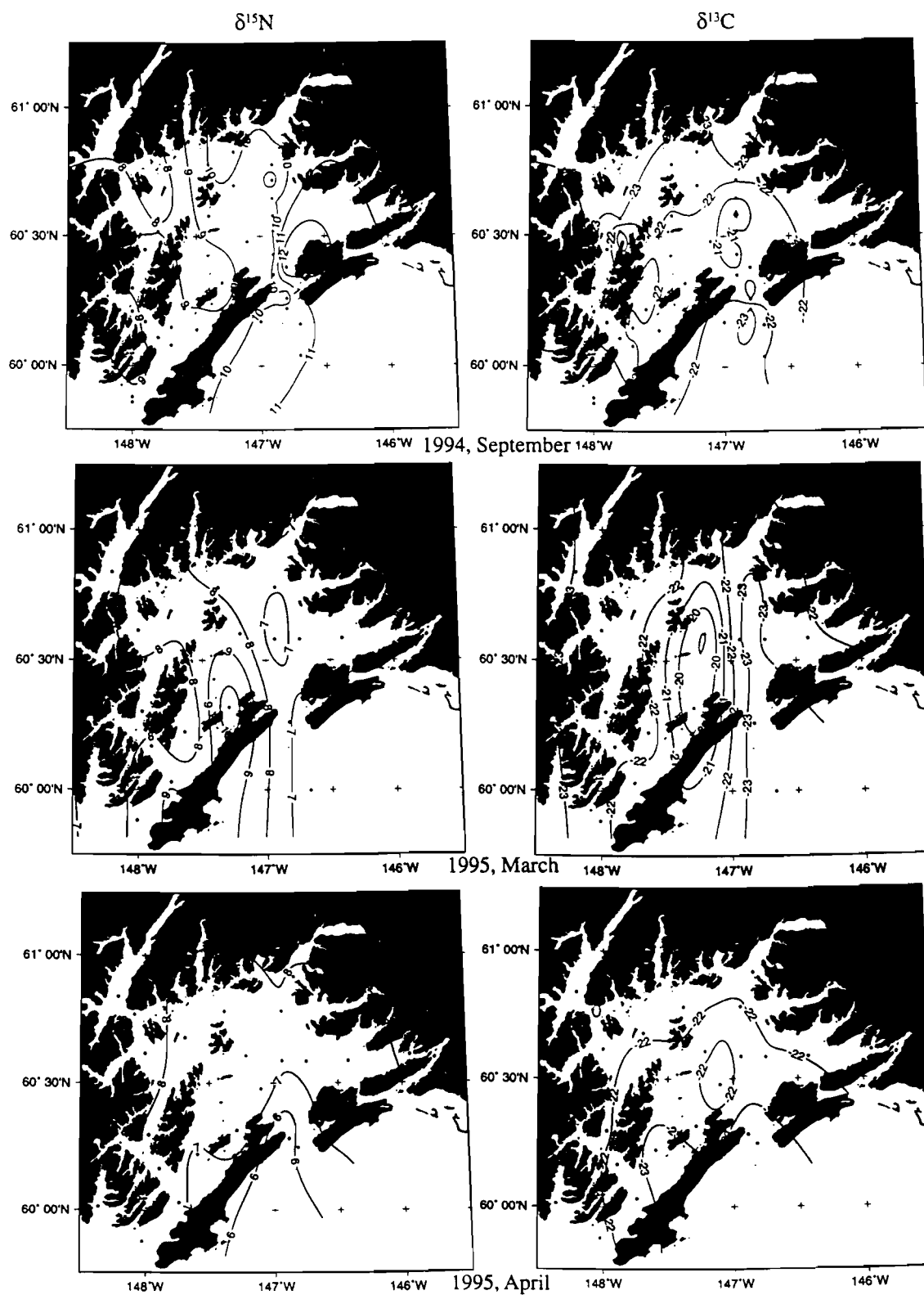
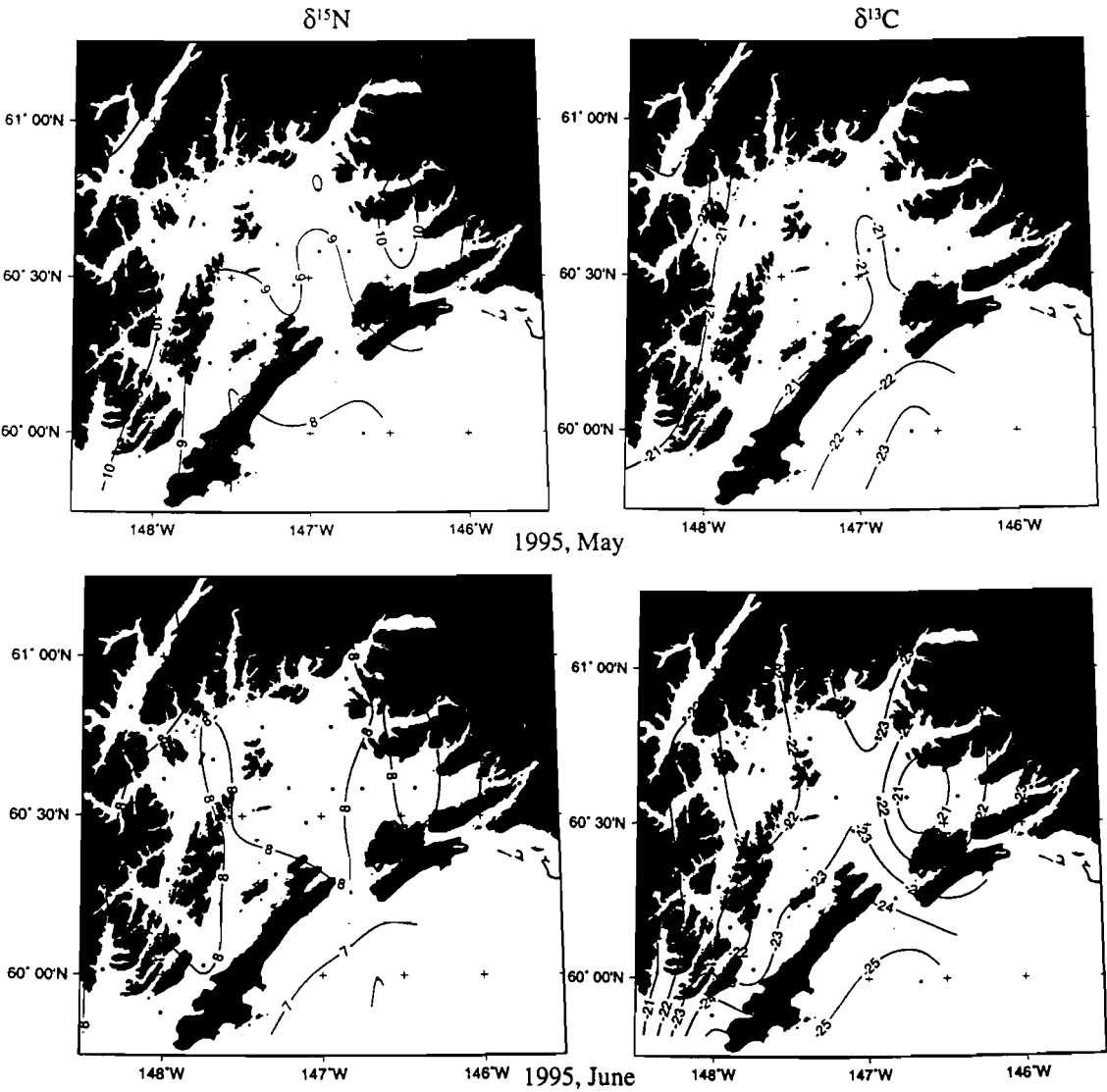


Figure. 2 continued



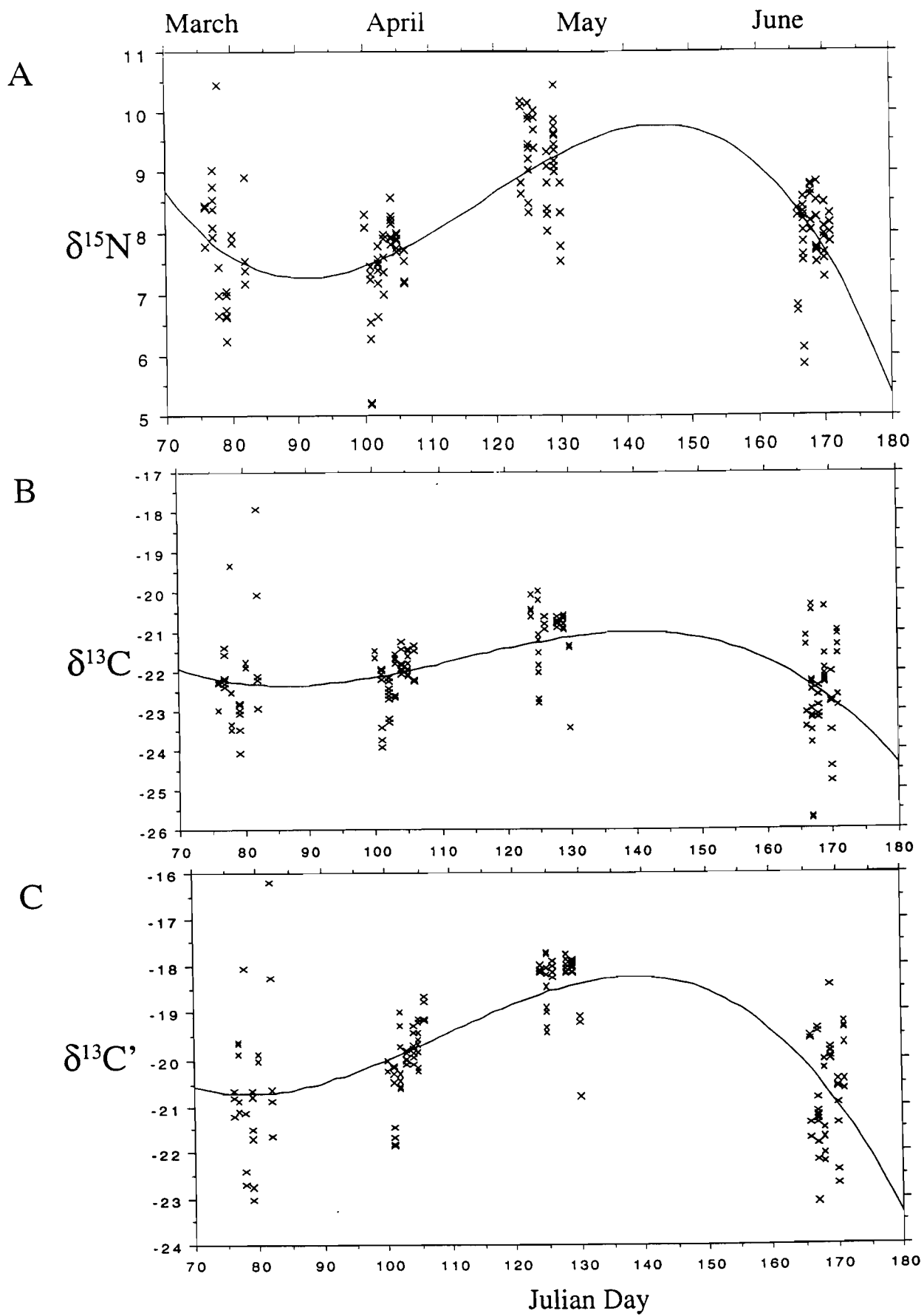


Figure 3

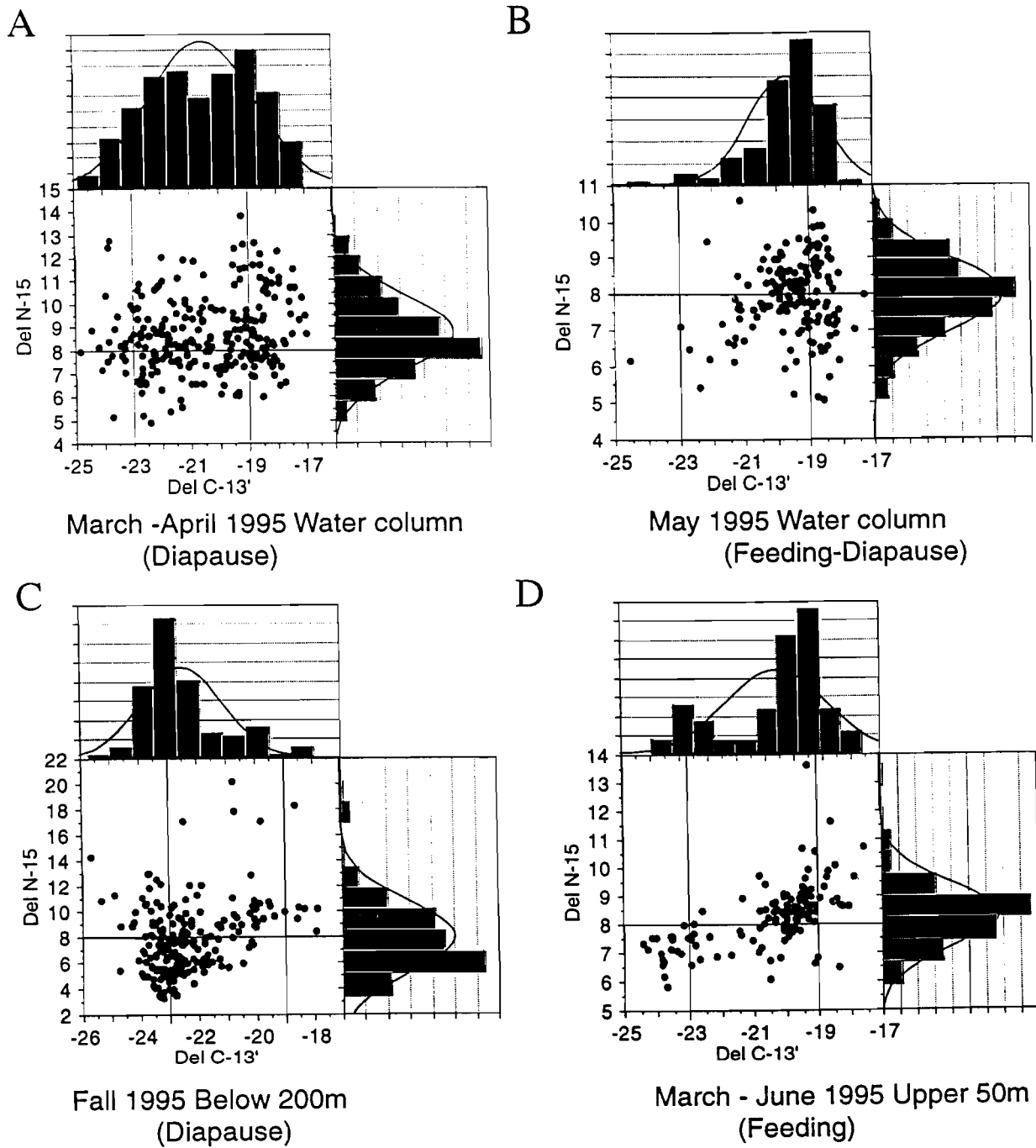


Figure 4

Figure. 5A

A

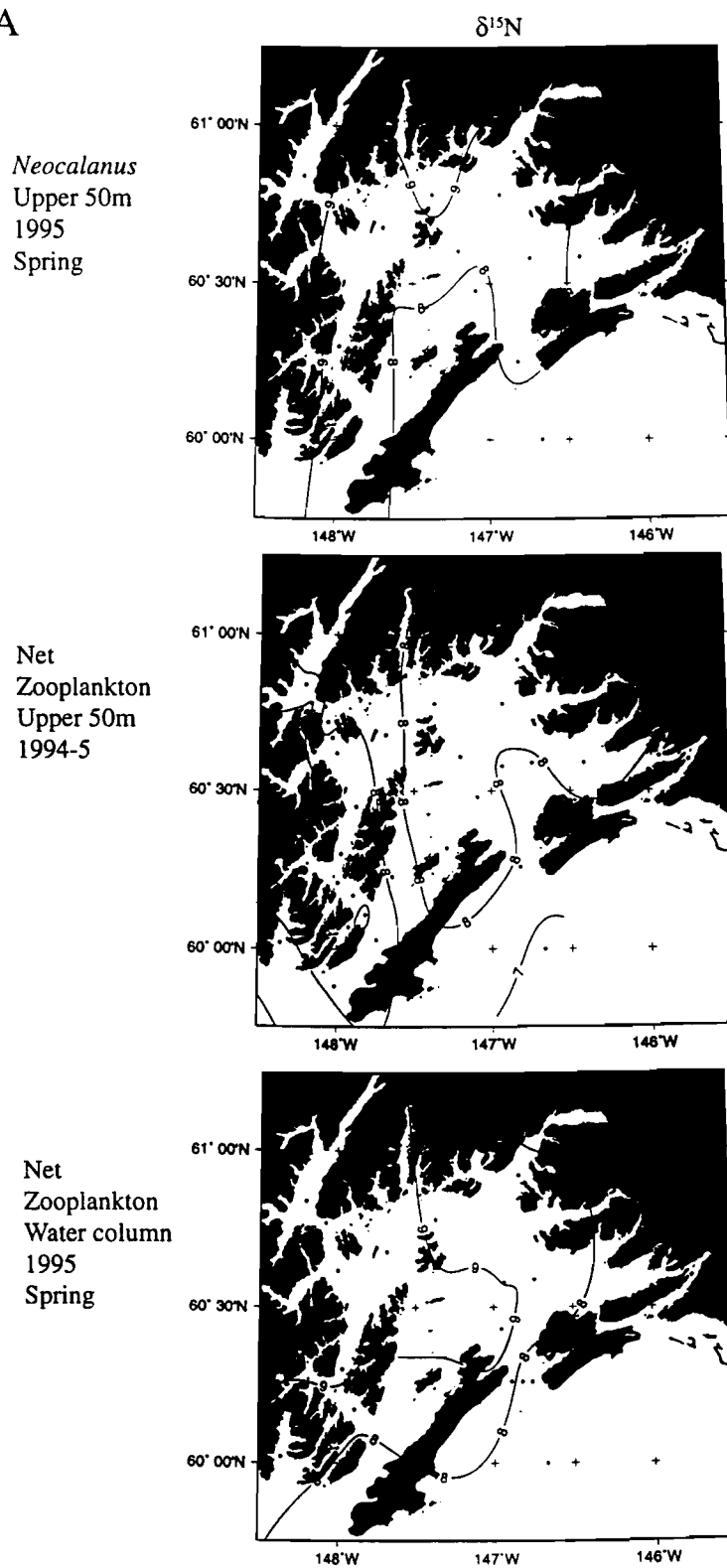
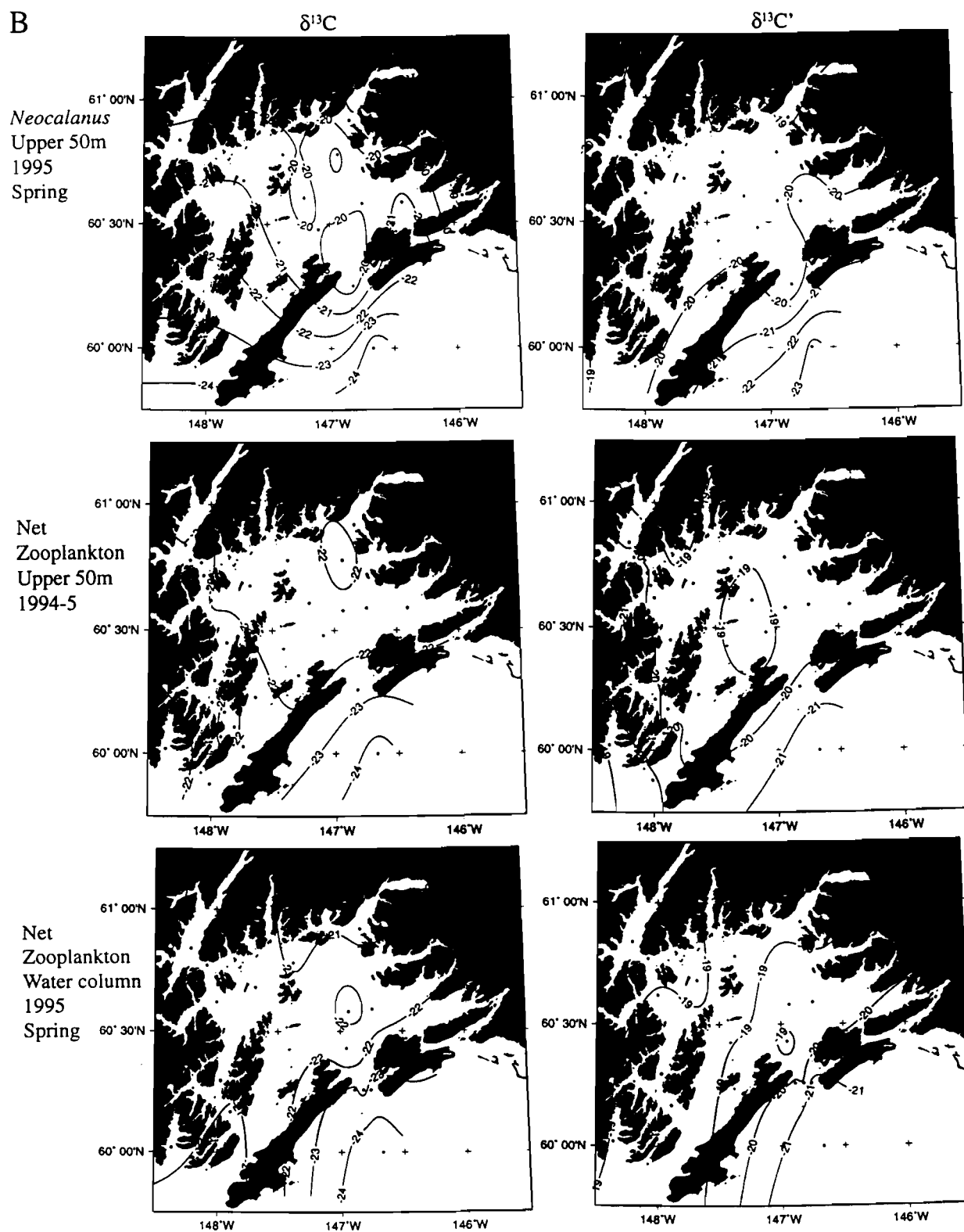


Figure. 5B

B



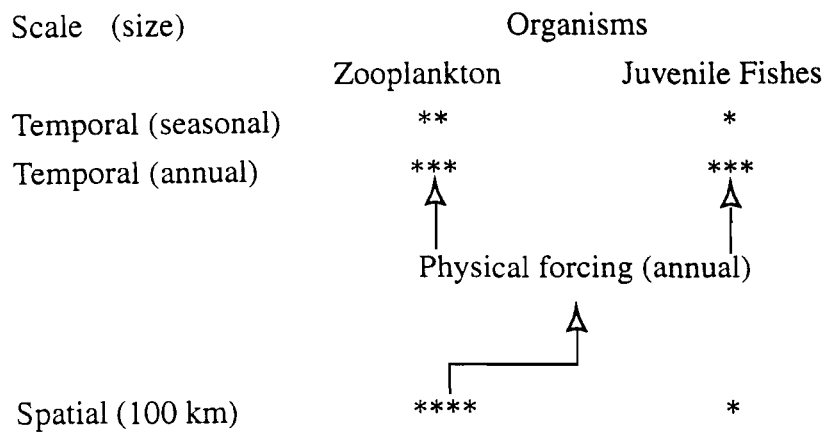


Figure 6

Appendix 1. Bulk net (335 μ -mesh, 0.5 m ring net) zooplankton isotopic and C/N data (replicate means) from indicated Prince William Sound and adjacent Gulf of Alaska oceanographic stations (Fig. 1) sampled from 1994 to 1995 by cast type (either upper 50 m or entire water column).

Date (YMD)	Time	Station	$\delta^{15}\text{N}$	$\delta^{13}\text{C}$	C/N (atoms)	$\delta^{13}\text{C}'$	Cast type
940421	19:58	CFOS13	6.42	-21.81	5.15	-20.79	Upper 50m
940623	13:45	CFOS13	8.66	-21.90	6.30	-20.24	Upper 50m
940927	17:08	CFOS13	9.42	-19.83	6.99	-17.89	Upper 50m
950320	14:00	CFOS13	6.66	-22.91	9.07	-20.38	Upper 50m
950416	13:38	CFOS13	7.20	-22.23	14.55	-18.96	Upper 50m
950505	23:57	CFOS13	8.42	-21.11	13.80	-17.91	Upper 50m
950616	4:13	CFOS13	8.33	-22.26	6.04	-20.72	Upper 50m
950323	10:05	CFOSBY	8.24	-18.97	7.52	-16.84	Upper 50m
950412	20:13	CFOSBY	7.58	-22.19	14.39	-18.93	Upper 50m
950509	1:00	CFOSBY	9.09	-20.82	11.87	-17.82	Upper 50m
950616	6:42	CFOSBY	8.51	-22.82	7.50	-20.70	Upper 50m
940924	22:01	CS1	9.44	-21.92	7.17	-19.91	Upper 50m
940623	11:26	CS10	7.66	-21.89	5.33	-20.76	Upper 50m
940925	23:29	CS13	10.20	-21.21	6.39	-19.51	Upper 50m
940924	18:05	CS3	9.40	-21.17	32.70	-17.22	Upper 50m
950416	17:43	CS3	7.65	-21.39	11.39	-18.46	Upper 50m
950508	21:50	CS3	9.22	-20.68	10.64	-17.86	Upper 50m
950616	9:19	CS3	8.24	-23.09	7.94	-20.84	Upper 50m
940927	13:51	CS4	9.78	-20.71	6.24	-19.08	Upper 50m
940925	21:52	CS5	12.81	-21.53	6.81	-19.65	Upper 50m
950323	14:15	CS9	7.40	-22.89	6.45	-21.17	Upper 50m
950411	5:45	CS9	7.35	-22.12	7.52	-19.99	Upper 50m
950509	18:10	CS9	9.37	-20.85	13.87	-17.64	Upper 50m
950616	1:40	CS9	7.60	-20.41	5.99	-18.90	Upper 50m
940926	23:41	GOA2	10.40	-22.27	9.99	-19.56	Upper 50m
940927	1:27	GOA5	10.84	-22.02	6.64	-20.21	Upper 50m
950320	5:45	GOA6	6.50	-23.75	5.77	-22.35	Upper 50m
950510	21:18	GOA6	7.67	-23.41	11.16	-20.51	Upper 50m
950616	21:46	GOA6	5.98	-25.72	11.16	-22.82	Upper 50m
940926	14:15	HE12	9.56	-21.02	17.70	-17.53	Upper 50m
950319	22:35	HE12	7.05	-23.39	5.75	-22.00	Upper 50m
950411	13:10	HE12	6.41	-23.56	8.12	-21.26	Upper 50m
950510	15:20	HE12	8.58	-21.36	9.13	-18.81	Upper 50m
950616	16:20	HE12	7.94	-23.68	7.40	-21.59	Upper 50m
950411		HE13	5.19	-23.80	8.48	-21.41	Upper 50m
940926	22:10	HE2	10.34	-23.03	8.06	-20.74	Upper 50m
940926	18:25	HE5	10.20	-22.46	7.29	-20.41	Upper 50m
940923	13:15	MS1	9.29	-22.11	7.43	-20.02	Upper 50m
940923	19:11	MS2	9.59	-21.74	7.76	-19.55	Upper 50m
940923	21:11	MS3	9.06	-22.35	11.34	-19.42	Upper 50m
950319	9:20	MS3	7.00	-22.51	6.68	-20.69	Upper 50m
950412	13:50	MS3	6.92	-23.23	12.72	-20.13	Upper 50m
950508	14:31	MS3	8.16	-20.75	12.17	-17.71	Upper 50m
950619	11:08	MS3	8.00	-22.75	9.19	-20.19	Upper 50m
940923	17:30	MS5	9.37	-21.16	17.47	-17.68	Upper 50m
940924	14:06	MS6	8.65	-21.57	10.08	-18.84	Upper 50m
950319	14:40	MS6	10.44	-19.36	6.55	-17.59	Upper 50m
950412	10:50	MS6	7.55	-22.66	8.63	-20.23	Upper 50m
950508	18:55	MS6	8.61	-20.77	13.09	-17.63	Upper 50m
950619	7:42	MS6	7.89	-23.13	8.90	-20.63	Upper 50m
940927	21:30	NS1	9.55	-23.24	12.98	-20.12	Upper 50m
950320	18:45	NS1	7.04	-22.93	6.67	-21.11	Upper 50m
950415	18:25	NS1	7.92	-22.07	13.08	-18.93	Upper 50m
950509	14:35	NS1	10.03	-20.87	12.72	-17.77	Upper 50m
950617	10:19	NS1	8.77	-23.11	7.00	-21.16	Upper 50m

940927	20:06	NS2	8.58	-22.08	7.63	-19.92	Upper 50m
940927	18:30	NS3	9.96	-21.08	6.21	-19.46	Upper 50m
940927	16:01	NS4	9.97	-21.15	6.47	-19.41	Upper 50m
940928	21:21	NWS1	9.86	-22.77	9.21	-20.21	Upper 50m
940928	23:52	NWS3	10.17	-22.71	9.20	-20.15	Upper 50m
940929	1:45	NWS4	10.00	-22.83	9.89	-20.13	Upper 50m
950321	0:15	NWS4	7.92	-21.82	7.90	-19.58	Upper 50m
950415	6:52	NWS4	7.73	-21.72	9.03	-19.19	Upper 50m
950509	4:45	NWS4	9.83	-20.74	12.51	-17.67	Upper 50m
950617	22:01	NWS4	8.63	-22.51	9.89	-19.81	Upper 50m
950410	21:40	OB1	8.19	-21.55	6.78	-19.69	Upper 50m
950504	14:40	OB1	8.73	-20.52	9.91	-17.82	Upper 50m
950615	18:37	OB1	6.78	-23.25	7.46	-21.15	Upper 50m
950323	16:45	OB2	7.17	-22.19	6.60	-20.40	Upper 50m
950411	2:30	OB2	7.39	-21.96	7.78	-19.75	Upper 50m
950504	19:02	OB2	10.14	-20.27	9.19	-17.71	Upper 50m
950615	22:01	OB2	8.33	-21.23	7.35	-19.16	Upper 50m
950413	0:00	PB1	7.62	-21.60	7.47	-19.49	Upper 50m
950620	23:59	PB1	7.92	-21.01	7.54	-18.88	Upper 50m
950415	15:26	PV1	7.96	-21.45	7.48	-19.34	Upper 50m
950509	12:00	PV1	9.41	-20.58	10.43	-17.79	Upper 50m
950617	13:07	PV1	8.11	-23.03	5.83	-21.60	Upper 50m
950317	16:40	PW1	7.78	-22.96	7.69	-20.79	Upper 50m
950414	16:50	PW1	8.24	-21.33	6.42	-19.62	Upper 50m
950505	17:05	PW1	9.21	-21.92	13.68	-18.73	Upper 50m
950618	14:03	PW1	7.74	-21.97	8.40	-19.59	Upper 50m
940423	17:18	SEA11	8.72	-21.98	8.55	-19.57	Upper 50m
950317	20:45	SEA11	8.44	-22.25	7.02	-20.30	Upper 50m
950414	9:55	SEA11	8.39	-21.82	10.21	-19.07	Upper 50m
950505	22:00	SEA11	9.92	-21.53	14.50	-18.26	Upper 50m
950618	7:55	SEA11	8.68	-22.21	9.22	-19.64	Upper 50m
940423	22:42	SEA14	7.52	-22.93	10.52	-20.12	Upper 50m
940920	16:39	SEA15B	7.53	-23.05	20.95	-19.41	Upper 50m
940424	8:55	SEA17	6.49	-22.60	12.55	-19.52	Upper 50m
940920	17:53	SEA18	8.93	-20.97	7.75	-18.78	Upper 50m
940422	14:27	SEA2	9.56	-23.39	9.35	-20.81	Upper 50m
940602	10:30	SEA2	8.56	-22.27	7.45	-20.17	Upper 50m
940424	12:55	SEA20	7.30	-22.30	10.47	-19.51	Upper 50m
940920	20:02	SEA20	9.43	-22.55	8.35	-20.19	Upper 50m
940421	23:46	SEA22	5.63	-23.18	9.28	-20.61	Upper 50m
950415	22:50	SEA22	7.70	-21.93	7.51	-19.81	Upper 50m
950505	9:00	SEA22	9.33	-20.10	9.79	-17.42	Upper 50m
950618	2:17	SEA22	7.97	-20.97	7.99	-18.71	Upper 50m
940613	12:32	SEA25	8.86	-21.80	5.84	-20.37	Upper 50m
940921	0:07	SEA25	9.09	-22.90	8.88	-20.41	Upper 50m
950323	14:00	SEA25	7.40	-22.10	6.90	-20.19	Upper 50m
950414	22:50	SEA25	7.89	-21.86	8.17	-19.54	Upper 50m
950506	15:34	SEA25	9.98	-20.90	11.67	-17.93	Upper 50m
950620	19:24	SEA25	8.23	-22.73	8.98	-20.21	Upper 50m
940613	17:37	SEA26	8.58	-22.36	6.19	-20.75	Upper 50m
940921	11:34	SEA26	8.85	-22.52	6.83	-20.63	Upper 50m
940921	14:54	SEA27	9.12	-22.40	7.17	-20.39	Upper 50m
950318	16:30	SEA27	8.24	-22.21	10.82	-19.36	Upper 50m
950412	18:00	SEA27	7.54	-22.46	11.72	-19.48	Upper 50m
950506	18:25	SEA27	9.55	-20.72	12.02	-17.71	Upper 50m
950620	15:31	SEA27	8.15	-21.43	8.17	-19.12	Upper 50m
940613	19:52	SEA29	9.16	-21.66	6.85	-19.77	Upper 50m
940921	17:02	SEA29	9.17	-22.18	6.79	-20.31	Upper 50m
940614	11:34	SEA32	9.29	-21.98	6.96	-20.05	Upper 50m
950318	19:10	SEA32	8.90	-21.47	7.53	-19.34	Upper 50m
950413	10:15	SEA32	7.19	-22.63	10.90	-19.77	Upper 50m
950619	14:06	SEA32	8.22	-22.39	7.28	-20.34	Upper 50m
940613	13:41	SEA34	7.89	-22.71	6.84	-20.83	Upper 50m

940922	16:22	SEA37	9.06	-21.28	26.38	-17.46	Upper 50m
950318	23:20	SEA37	8.24	-22.28	6.54	-20.51	Upper 50m
950413	5:20	SEA37	7.93	-21.74	7.80	-19.53	Upper 50m
950619	18:54	SEA37	7.43	-24.60	8.48	-22.21	Upper 50m
940614	9:45	SEA39	8.80	-22.23	6.86	-20.33	Upper 50m
940923	11:15	SEA39	9.10	-21.63	6.20	-20.01	Upper 50m
940422	17:00	SEA4	7.59	-22.79	8.52	-20.39	Upper 50m
940425	10:24	SEA4	6.40	-23.74	12.57	-20.66	Upper 50m
940425	14:43	SEA4	7.36	-22.94	11.02	-20.06	Upper 50m
940425	18:48	SEA4	5.73	-22.71	9.86	-20.02	Upper 50m
940425	22:43	SEA4	8.47	-22.42	9.45	-19.81	Upper 50m
940426	2:40	SEA4	8.89	-22.02	8.88	-19.53	Upper 50m
940426	7:26	SEA4	8.23	-22.93	11.82	-19.94	Upper 50m
940602	13:15	SEA4	8.85	-21.93	8.00	-19.66	Upper 50m
950414	14:35	SEA4	8.03	-22.01	9.36	-19.42	Upper 50m
950505	14:20	SEA4	9.59	-22.75	18.36	-19.23	Upper 50m
950618	11:44	SEA4	7.61	-22.22	9.87	-19.53	Upper 50m
940615	15:39	SEA40	7.98	-22.72	4.83	-21.93	Upper 50m
940422	20:43	SEA6	9.18	-22.07	6.90	-20.16	Upper 50m
940423	9:52	SEA8	6.00	-22.98	7.76	-20.78	Upper 50m
940604	9:39	SEA8	8.77	-21.71	7.50	-19.59	Upper 50m
940423	12:24	SEA9	8.07	-22.39	10.82	-19.54	Upper 50m
940604	11:58	SEA9	8.63	-21.77	6.94	-19.84	Upper 50m
950315		CFOS13	11.10	-21.20	6.29	-19.54	Water column
950416		CFOS13	8.61	-21.62	7.48	-19.51	Water column
950505		CFOS13	8.11	-25.22	13.65	-22.03	Water column
950616		CFOS13	8.11	-21.34	12.37	-18.29	Water column
950509		CS4	10.52	-20.29	6.93	-18.37	Water column
950617		CS4	8.08	-22.43	14.79	-19.14	Water column
950323		CS9	10.71	-21.57	6.20	-19.95	Water column
950411		CS9	8.08	-22.35	8.04	-20.07	Water column
950509		CS9	9.14	-20.76	10.35	-17.99	Water column
950616		CS9	7.87	-22.55	12.24	-19.51	Water column
950510		GOA6	8.50	-23.87	11.18	-20.97	Water column
950616		GOA6	5.94	-25.00	7.21	-22.98	Water column
950319		HE11	7.19	-23.45	8.05	-21.17	Water column
950319		HE12	7.08	-23.08	7.76	-20.89	Water column
950411		HE12	6.02	-23.28	7.51	-21.16	Water column
950510		HE12	8.97	-20.99	11.46	-18.05	Water column
950615		HE12	7.59	-23.16	12.45	-20.09	Water column
950419		HE13	6.59	-24.76	13.96	-21.54	Water column
950510		HE13	10.15	-22.05	11.72	-19.07	Water column
950616		HE13	8.19	-22.70	11.15	-19.80	Water column
950321		NWS4	9.09	-21.50	7.42	-19.41	Water column
950415		NWS4	8.34	-21.19	7.29	-19.14	Water column
950509		NWS4	8.82	-20.02	8.12	-17.72	Water column
950617		NWS4	8.68	-21.01	10.67	-18.18	Water column
950413		PB1	8.71	-21.96	9.33	-19.37	Water column
950413		PB1	9.03	-20.33	5.10	-19.34	Water column
950620		PB1	7.71	-21.22	12.53	-18.14	Water column
950415		PV1	7.90	-21.15	6.46	-19.42	Water column
950509		PV1	9.05	-19.86	7.08	-17.89	Water column
950617		PV1	7.66	-21.23	8.91	-18.74	Water column
950317		PW1	10.47	-21.68	8.62	-19.25	Water column
950414		PW1	8.84	-21.70	6.19	-20.09	Water column
950505		PW1	10.32	-21.61	10.26	-18.85	Water column
950618		PW1	8.49	-22.50	9.98	-19.79	Water column
950317		SEA11	8.92	-21.74	7.30	-19.69	Water column
950414		SEA11	9.64	-21.81	8.58	-19.39	Water column
950505		SEA11	9.57	-21.10	10.55	-18.29	Water column
950618		SEA11	7.95	-21.16	10.37	-18.38	Water column
950317		SEA22	10.97	-20.97	6.50	-19.22	Water column
950414		SEA23	9.44	-21.87	8.11	-19.59	Water column

950505	SEA22	9.11	-21.15	12.58	-18.07	Water column
950618	SEA22	9.74		8.91		Water column
950414	SEA25	9.62	-21.60	8.22	-19.27	Water column
950506	SEA25	9.76	-21.06	11.15	-18.16	Water column
950620	SEA25	8.37	-21.21	12.98	-18.09	Water column
950412	SEA27	8.36	-21.74	7.76	-19.54	Water column
950506	SEA27	8.65	-20.45	8.04	-18.17	Water column
950620	SEA27	7.76	-20.62	10.06	-17.90	Water column
950317	SEA4	9.77	-21.65	8.26	-19.31	Water column
950414	SEA4	8.76	-21.85	7.79	-19.64	Water column
950505	SEA4	9.70	-22.27	14.73	-18.99	Water column
950618	SEA4	8.10	-21.55	7.76	-19.36	Water column

Cross-validation of trophic level estimates from a mass-balance model of, and $^{15}\text{N}/^{14}\text{N}$
data from, Prince William Sound

by

Thomas C. Kline Jr.₁ and Daniel Pauly₂

(1)

Prince William Sound Science Center

P. O. Box 705

Cordova, AK 99574, USA

(corresponding author)

907-424-5800 (phone)

907-424-5820 (fax)

tkline@grizzly.pwssc.gen.ak.us

(2)

Fisheries Centre

2204 Main Mall

University of British Columbia

Vancouver, B.C., Canada V6T 1Z4

Proceedings of the International Symposium on Fishery Stock Assessment Models for the
21st Century -- Combining Multiple Data Sources. Alaska Sea Grant College Program
Report. University of Alaska Fairbanks. (In Press)

Cross-validation of trophic level estimates from a mass-balance model of, and $^{15}\text{N}/^{14}\text{N}$ data from, Prince William Sound

Thomas C. Kline Jr. and Daniel Pauly

*Abstract

Trophic mass-balance models of ecosystems constructed using the Ecopath approach and software include the diet composition of functional groups as model inputs, and trophic level estimates for these same groups as a model outputs. The well-documented 0.34% enrichment of $^{15}\text{N}/^{14}\text{N}$ that occurs at each feeding step in food webs can be used to determine trophic level as well. This contribution is the first to ever examine the relation between trophic levels estimated by these two independent methods. This was achieved by using a published Ecopath model of Prince William Sound (PWS) as reference, i.e., estimating $^{15}\text{N}/^{14}\text{N}$ ratios for each of the model's functional groups. Re-expression of these ratios as absolute estimate of trophic levels (TL) was done following calibration using the herbivorous copepods *Neocalanus cristatus*, for which $\text{TL} = 2$. The correlation between both sets of TL values ($n = 7$) was extremely high ($r = 0.986$), with the points evenly distributed about the 1:1 line. Also, the magnitude of the standard errors of the TL estimates based on $^{15}\text{N}/^{14}\text{N}$ data was similar to those of the Ecopath estimates. Applying $^{15}\text{N}/^{14}\text{N}$ data from PWS to an Ecopath model of the Alaska Gyre System resulted in a reduced correlation ($r = 0.755$, for $n = 16$), suggesting that TL estimates may be transferred between ecosystems, though at the cost of reduced precision. These encouraging results warrant further exploration.

*Introduction

While the trophic level concept existed since the beginning of ecosystem research (Golley 1993), controversy has raged as to its operational validity. Particularly, some ecologists could not reconcile this concept, articulated in form of integers (primary producers = 1; first order consumers = 2, etc.), with the observation that many organisms derive their food from widely different parts of food webs (see e.g., Rigler 1975). This problem was overcome by the introduction, through Odum and Heald (1975), of fractional trophic levels (TLs). These are computed as weighted means from disparate diet compositions, and their variance can be interpreted as an omnivory index (OI), in agreement with Pimm (1982), who defined omnivory as “feeding on more than one trophic level” (Pauly et al. 1993, Pauly and Christensen 1995). Until the late 1980’s, however, estimation of trophic levels continued to be largely definitional for lower levels (see above), or based on crude, and often grossly erroneous guesses for higher levels. (See Pauly 1996 for a discussion of such guesses by Ryther 1972 and other authors).

In recent years, two methods have emerged that are capable of reliably estimating TL and related statistics: (1) the $^{15}\text{N}/^{14}\text{N}$ method (DeNiro and Epstein 1981, Fry 1988, Wada et al. 1991, and see below), and (2) the construction of mass-balance trophic models of ecosystems (Christensen and Pauly 1992, and see below). The former estimates are identified as TL_N , the latter as TL_E . In this study, we present a first comparison of results obtained by these two approaches, using a preliminary mass balance model of the Prince William Sound (PWS) ecosystem (Dalsgaard and Pauly 1997) as a starting point. Another model, describing the Alaska Gyre System (AGS; Pauly and Christensen 1996) is then used to test whether estimates of TL and OI may be transferred from one ecosystem to the other.

*Materials and Methods

The trophic mass-balance models of PWS used here was constructed using the Ecopath approach of Polovina (1984) and Christensen and Pauly (1992); this are based on the system of linear equations

$$(1) \quad B_i \times (P/B)_i \times EE_i = Y_i + \sum B_j \times (Q/B)_j \times DC_{ij}$$

where, for any conventional period without massive change of system structure:

B_i is the mean biomass of functional group i (e.g., a group species with similar vital statistics, diet compositions and consumers); B_j is the mean biomass of the consumers of i ; $(P/B)_i$ is the production/biomass ratio of i (equivalent to its instantaneous rate of mortality; Allen 1971); EE_i is the fraction of production $\{P_i = B_i \times (P/B)_i\}$ that is consumed within the system; Y_i is the catch of i by the fishery, if any; $(Q/B)_j$ the consumption per unit biomass of j ; and DC_{ij} is the contribution of i to the diet of j .

The Ecopath software (Christensen and Pauly 1992) was used to solve this system of equations, after estimation of values of B , P/B , etc, from the literature on PWS and related systems. The assumptions made when estimating the inputs, and for their subsequent adjustment when establishing mass-balance, are documented in Dalgaard and Pauly (1997). The other trophic mass-balance model used here, representing the Alaska Gyre system was constructed in similar fashion, and is documented in Pauly and Christensen (1996).

For both models, estimation of the TL values was performed by Ecopath, based on

$$(2) \quad TL_{Ei} = (1 + \text{mean trophic level of prey})$$

Omnivory indices (OI_{Ei}) were computed as the variance of the TL_{Ei} estimates (Christensen and Pauly 1992); the square root of the OI_{Ei} values was then treated as standard error of the TL_{Ei} estimates ($S.E._{Ei}$).

Further details on Ecopath, including its ability to account for uncertainty in input values through a Monte-Carlo resampling scheme interpreted in a Bayesian context, are provided in Walters (1996) and other contributions in Pauly and Christensen (1996).

Stable isotope measurements are unique in that they trace assimilated material. Nitrogen stable isotope ratios provide excellent definition of relative trophic level (Fry 1988, Wada et al. 1991, Hobson and Welch 1992, Kiriluk et al. 1995). The heavy isotope of nitrogen, ^{15}N , is enriched by about 0.34 % (or 3.4 ‰ in conventional delta units with each trophic level (DeNiro and Epstein 1981, Minagawa and Wada 1984) and has been shown to accurately indicate the “realized” trophic level of species within an ecosystem (Kling et al. 1992, Cabana and Rasmussen 1994). Thus, the set of TL_N values used for comparison was derived from samples collected in 1994-1995 in PWS (Kline 1997), and based upon the trophic bioconcentration of ^{15}N .

The conventional delta notation used to express a stable isotope ratio is reported relative to international standards (air for N) and defined by the following expression:

$$(3) \quad \delta^{15}N = (R_{\text{sample}} / R_{\text{standard}} - 1) \times 1000 \text{ ‰}$$

where $R = ^{15}N/^{14}N$. The isotope standard has a delta value of zero by definition, i.e., $\delta^{15}N = 0$ for atmospheric N_2 . Naturally occurring $\delta^{15}N$ values observed in biota range from ~ 0 to $\sim +20$.

TL_N are estimated by relating observed $\delta^{15}N$ values to a reference value (TL_{ref}), and to the trophic enrichment factor, 3.4 (Minagawa and Wada 1984, Kline 1997), via:

$$(4) \quad TL_{Ni} = 1 + (\delta^{15}N_i - \delta^{15}N_{ref}) / 3.4$$

Where TL_{Ni} is the trophic level of group i , $\delta^{15}N_i$ is the mean $\delta^{15}N$ of group i , and $\delta^{15}N_{ref}$ is the mean $\delta^{15}N$ value of the herbivorous copepod (with $TL = 2$, by definition) used as reference, here *Neocalanus cristatus* (Kline 1997). The standard deviations of the $\delta^{15}N_i$, $S.D._{Ni}$ were multiplied by the trophic enrichment factor, 3.4 (Minagawa and Wada 1984, Kline 1997), to estimate $\delta^{15}N$ -based omnivory indices, OI_{Ni} . Given their relative magnitudes, we compared the OI_{Ni} estimates with the $S.E._{Ei}$, rather than with the OI_{Ei} .

Isotope sampling and data acquisition procedures were described elsewhere (Kline et al. 1993, Kline 1997). To account for the different definitions of the functional groups in the two ecosystem models (PWS and AGS), the available isotopic database were arranged differently for each comparison. For example, in the PWS model, herring are considered separately (Table 1), while they are included in the small pelagics group of the AGS (Table 2).

*Results and Discussion

Table 1 presents our results for PWS, i.e., the estimates of TL and $S.E.$ derived by the two methods under comparison. As might be seen, the fit between the estimates of TL_E and TL_N is very tight, even if one omits the reference data point, pertaining to *Neocalanus*, and for which $TL_E = TL_N = 2$ by definition (see arrow in Figure 1A). Moreover, the data points are close to the 1:1 line, as they should if TL_E and TL_N measure the same underlying quantity. Figure 1B shows that the magnitude of the omnivory index estimates are similar for both methods compared here, except for the reference group (see arrow), which cannot, by definition, take a value of $S.E._E$ other than zero, while the estimate of OI_N can be quite large. This feature precludes correlation analysis.

The good match between the two types of TL estimates for functional groups in the PWS model is due, we believe, to the taxonomic correspondence between the Ecopath groups and the groups for which $\delta^{15}\text{N}$ were available. Another factor is scope of the sampling for stable isotope data, which involved numerous samples (Table 1) and which was very broad for all groups except birds. (Bird isotopic data were collected within a limited spatial and temporal range and included few of the common duck-like shorebirds; M.A. Bishop, U.S.F.S., pers. comm.).

The Ecopath model of PWS was based almost exclusively on data collected prior to the 1989 *Exxon Valdez* oil spill, while the $\delta^{15}\text{N}$ data were collected after the spill. The good match between the two data sets implies that the basic structure of the food web has not been modified by the spill, at least as far as can be detected within the scope of this comparison. On the other hand, $\delta^{15}\text{N}$ data are not available for marine mammals and many bird species that experienced large mortalities, and this conclusion may thus change when the issue is revisited.

Table 2 and Figure 1C show that using $\delta^{15}\text{N}$ data from one system (PWS) to estimate trophic levels in another, adjacent system (AGS), leads to predictions that are less precise than when inferences are drawn within the same system. Moreover, the omnivory index values become completely uncorrelated (Figure 1D), partly because of overaggregation of functional prey groups, which leads to predators that appear to feed at only one trophic level.

A likely reason for the differences between TL_E in AGS and TL_N estimates from PWS is the shoe-horning of taxa with $\delta^{15}\text{N}$ data into the “boxes” of the AGS model. For example, the TL_N estimate for demersal fish in PWS is compared with a TL_E estimate for “large fish” in the AGS, though these consist of large pelagic fish (Pauly and Christensen 1996).

The $\delta^{15}\text{N}$ data on salmonids in Table 2 refer to adult specimens collected during their return migration through PWS and/or the Copper River, of which all would have done most of their feeding on the Gulf of Alaska shelf and/or in the AGS. However,

having broadly similar life histories may not be sufficient for their TL values to be similar: the iteroparous salmonid, Dolly Varden (*Salvelinus malma*) had an estimated TL_N much lower than another iteroparous salmonid, steelhead (*Oncorhynchus mykiss*; Table 2), but close to the value of $TL_N = 3.54 \pm 0.21$ estimated for semelparous coho salmon (*O. kisutch*; $n = 12$). Thus, caution needs to be used when selecting “analog” species for cross-validation.

Still, we view the cross-validation exercise presented here as encouraging, in that the data we assembled led to coherent results, fully validating the independent, within-system estimates of TL. We also think that the lower correlation between the TL values from PWS and AGS were largely due to the lack of correspondence between the species included in the functional groups that were compared.

The next step is to refine our analyses, based on ecosystem models that are more detailed, thus requiring less “shoehorning”, making better use of the available $\delta^{15}N$ data, and reducing the occurrence of misleadingly low estimates of S.E._E. Also, an important test will be to verify the high trophic level ($TL_E \sim 5$; Pauly and Christensen 1996) estimated for transient killer whales. Future work by both authors will be devoted to these and related issues, important in view of the recent demonstration (Pauly et al. 1998) that the trophic levels of global fisheries catches have been steadily declining in the last decades.

****Acknowledgments**

This project was funded by the Exxon Valdez Oil Spill Trustee Council through the Sound Ecosystem Assessment (SEA) and the Mass Balance Modeling (MBM) projects. However the findings presented by the authors are their own and do not necessarily represent the Trustee Council’s position. John Williams assisted with the translation of incompatible computer files between DP and TCK. Two anonymous reviewers provided useful improvements to our first draft.

* References Cited

Allen, K.R. 1971. Relation between production and biomass. J. Fish. Res. Board Can. 28:1573-1581.

Cabana, G. and J. B. Rasmussen, 1994. Modeling food chain structure and contaminant bioaccumulation using stable nitrogen isotopes. Nature 372:255-257.

Christensen, V. and D. Pauly 1992. Ecopath II: a system for balancing steady-state ecosystem models and calculating network characteristics. Ecol. Model. 61: 169-185.

Christensen, V. and D. Pauly 1995. Primary production required to sustain global fisheries. Nature 374:255-257.

Dalgaard and Pauly. 1997. A tentative mass-balance trophic model of Prince William Sound, Alaska, for the period 1980-1989, prior to the Exxon Valdez Oil Spill. University of British Columbia. Fisheries Centre Research Reports. Vol. 5(2). 33 pp.

DeNiro, M. J. and S. Epstein. 1981. Influence of diet on the distribution of nitrogen isotopes in animals. Geochim. Cosmochim. Acta. 45:341-353.

Fry, B. 1988. Food web structure on the Georges Bank from stable C, N, and S isotopic compositions. Limnol. Oceanogr. 33:1182-1190.

Golley, F.B. 1993. A history of the ecosystem concept in ecology: more than the sum of its part. Yale University Press. New Haven, 254 pp.

Hobson, K. A. and H. E. Welch. 1992. Determination of trophic relationships within a high Arctic marine food web using $\delta^{13}\text{C}$ and $\delta^{15}\text{N}$ analysis. *Mar. Ecol. Progr. Ser.* 84:9-18.

Hobson, K.A., J.L. Sease, R.L. Merrick, and J.F. Piatt. 1997. Investigating trophic relationships of pinnipeds in Alaska and Washington using stable isotope ratios of nitrogen and carbon. *Mar. Mammal Sci.* 13:114-13.

Kiriluk, R. M., M. R. Servos, D. M. Whittle, G. Cabana, J. B. Rasmussen. 1995. Using ratios of stable nitrogen and carbon isotopes to characterize the biomagnification of DDE, mirex, and PCB in a Lake Ontario pelagic food web. *Can. J. Fish. Aquat. Sci.* 52:2660-2674.

Kline, T.C. Jr., J.J. Goering, O.A. Mathisen, P.H. Poe, P.L. Parker, and R.S. Scalan. 1993. Recycling of elements transported upstream by runs of Pacific salmon: II. $\delta^{15}\text{N}$ and $\delta^{13}\text{C}$ evidence in the Kvichak River watershed, southwestern Alaska. *Can. J. Fish. Aquat. Sci.* 50:2350-2365.

Kline, T. C. 1997. Confirming forage fish food web dependencies in the Prince William Sound ecosystem using natural stable isotope tracers. In: *Forage Fishes in Marine Ecosystems. Proceedings of the International Symposium on the Role of Forage Fishes in Marine Ecosystems.* Alaska Sea Grant College Program Report No. 97-01. University of Alaska Fairbanks. pp.257-269.

Kline, T.C. Scales and Patterns of Temporal and Spatial Variability of $^{13}\text{C}/^{12}\text{C}$ and $^{15}\text{N}/^{14}\text{N}$ in Pelagic Biota. In: S. Brandt and D. Mason (eds.) *Space, Time and Scale: New Perspectives in Fish Ecology and Management.* *Can. J. Fish. Aquat. Sci.* (in review)]

Kling, G.W., B. Fry, and W.J. O'Brien. 1992. Stable isotopes and plankton trophic structure in arctic lakes. *Ecology* 73:561-566.

Minagawa, M., and E. Wada. 1984. Stepwise enrichment of ^{15}N along food chains: Further evidence and the relation between $\delta^{15}\text{N}$ and animal age. *Geochim. Cosmochim. Acta* 48:1135-1140.

Odum, W.E. and Heald, 1975. The detritus-based food web of an estuarine mangrove community. In: L.E. Cronin (ed.) *Estuarine Research*. Vol. 1. Academic Press, New York. pp. 265-286.

Pauly, D. 1996. One million tonnes of fish and fisheries research. *Fisheries Research* 25(1):25-38.

Pauly, D. and V. Christensen, 1995. Primary production required to sustain global fish catches. *Nature* 374:255-257.

Pauly, D. and V. Christensen (editors). 1996. Mass-balance models of north-eastern Pacific ecosystems. Univ. British Columbia. Fisheries Centre Reports 4(1). 131pp.

Pauly, D., M. Soriano-Bartz and M.L. Palomares. 1993. Improved construction, parameterization and interpretation of steady-state ecosystem models. In: D. Pauly and V. Christensen (eds.) *Trophic models of aquatic ecosystems*. ICLARM Conf. Proc. 26. pp. 1-13.

Pauly, D., V. Christensen, J. Dalsgaard, R. Froese and F.C. Torres Jr. 1998. Fishing down marine food webs. *Science* 279: 860-863.

Pimm, S.L. 1982. Food Webs. Chapman and Hall, London. 219 pp.

Polovina, J.J. 1984. Model of a coral reef system. I. The ECOPATH model and its application to French Frigate Shoals. Coral Reefs 3:1-11.

Rigler, F.H. 1975. The concepts of energy flow and nutrient flow between trophic levels. In: W.H. Van Dobben and R.H. Lowe-McConnel (eds.) Unifying concepts in ecology. Dr. W. Junk Publishers, The Hague. pp. 15-26.

Ryther, J.H. 1972. Photosynthesis and fish production in the sea. Science 166: 72-76.

Wada, E., H. Mizutani, and M. Minagawa. 1991. The use of stable isotopes for food web analysis. Crit. Rev. Food Sci. Nutr. 30:361-371.

Walters, C. 1996. Suggested improvements for the Ecopath model. In: D. Pauly and V. Christensen (eds.). 1996. Mass-balance models of north-eastern Pacific ecosystems. Univ. British Columbia. Fisheries Centre Reports 4(1). pp. 82-87.

Table 1. Comparison of trophic level (TL) and omnivory index (S.E._E and OI_N) estimates for seven functional groups in the Prince William Sound ecosystem.

<u>Ecopath group</u> _a	<u>Corresponding taxa with $\delta^{15}\text{N}$ data</u>	<u>data source</u> _b	<u>n</u> _c	<u>TL_E</u> _d	<u>TL_N</u>	<u>S.E._E</u> _e	<u>OI_N</u>
Mesozooplankton	<i>Neocalanus cristatus</i> _f	1	938	2	2	0	0.54
Macrozooplankton	Euphausiids, amphipods, chaetognaths, etc.	1,2	329	2.8	2.81	0.43	0.49
Salmon fry	Young-of the year chum, sockeye and pink salmon	3	285	3.2	3.18	0.32	0.31
Herring	<i>Clupeapallasi</i> (Pacific herring)	1,3	385	3.3	3.33	0.37	0.21
Small pelagics	Smelts, juvenile gadids	3	273	3.3	3.08	0.34	0.32
Demersal fishes	Flatfish, rockfishes, greelings, gadids, cottids.	3	459	3.9	3.88	0.53	0.40
Birds	Seabirds	4	191	4.1	3.81	0.45	0.44

a. model is described in Dalgaard and Pauly (1997), including details of species included in each functional group; b. numbers in this column indicate sources of $\delta^{15}\text{N}$ data, viz. 1 = Kline (in press?); 2 = Kline (unpublished data) ; 3 = Kline (1997); 4 = M.A. Bishop (U.S.F.S., Cordova, unpublished data); c. number of $\delta^{15}\text{N}$ measurements; d. as given on Table 23 of Dalgaard and Pauly (1997); e. from Ecopath file of PWS, available from second author; f. reference group for $^{15}\text{N}/^{14}\text{N}$ as discussed in text.

Table 2. Comparison of estimates of TL_E and $S.E._E$ for functional groups in the Alaska Gyre system with TL_N and OI_N estimates derived from Prince William Sound organisms.

<u>Ecopath group</u> _a	<u>Corresponding taxa with $\delta^{15}N$ data</u>	<u>data source</u> _b	<u>n</u> _c	<u>TL_E</u>	<u>TL_N</u>	<u>$S.E._E$</u>	<u>OI_N</u>
Small herb. zoopl.	<i>Neocalanus cristatus</i> _e	1	938	2	2	0	0.54
Microzooplankton	Bulk net samples	1	195	2	2.17	0	0.34
Carnivorous zoopl.	Amphipods, chaetognaths, decapod larvae, etc.	1,2	159	3	2.89	0	0.52
Jellies _f	Gelatinous zooplankton	2	4	3	2.35	0	0.35
Krill	Euphausiids	1	170	2.05	2.74	0.22	0.45
Squids	Squids	3	104	3.15	3.44	0.37	0.25
Small pelagics	Herring, smelts, juvenile gadids	1,3	545	3.16	3.24	0.36	0.27
Sockeye salmon	Sockeye salmon	4	118	3.91	2.88	0.45	0.13
Chum salmon	Chum salmon	2	1	4	3.05	0	
Pink salmon	Pink salmon	2	4	3.99	2.94	0.38	0.18
Steelhead	Dolly Varden _g	2	6	4.12	3.46	0.2	0.31
Mesopelagics	Myctophids, smoothtongue, glass shrimp, snailfish	3	73	3.04	3.12	0.05	0.39
Large fish	Flatfishes, rockfishes, greenlings,	2	459	4.04	3.88	0.3	0.4

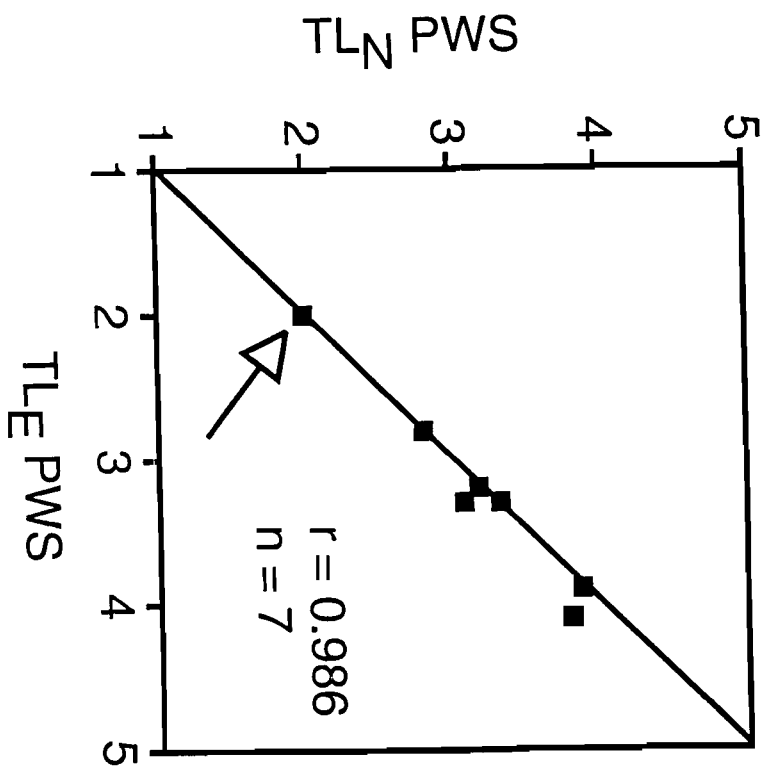
	gadids, etc.						
Sharks	Dogfish, salmon shark	2	5	4.49	3.66	0.45	0.4
Pinnipeds	Copper R. Delta Harbor seals & Steller	5	22	4.33	4.92	0.36	0.08
	Sealions						
Marine birds	Seabirds	6	191	4.08	3.81	0.28	0.44

a. model described in Pauly and Christensen (1996), including details of species included in each functional group; b. numbers in this column indicate sources of $\delta^{15}\text{N}$ data, viz. 1 = Kline (in press?); 2 = Kline (unpublished data) ; 3 = Kline (1997); 4 = Kline and Ewald (unpublished data); 5 = Hobson et al. (1997); 6 = M.A. Bishop (U.S.F.S., Cordova, unpublished data); c. number of $\delta^{15}\text{N}$ measurements; d. from Ecopath file of Alaska gyre, available from the second author; e. reference group for $\delta^{15}\text{N}$; f. diet composition, omitted in Pauly and Christensen (1996), consisted of 88 % herbivorous zooplanton, and 12 % microzooplanton; g. presumed analogous to steelhead because both are iteroparous salmonids; see text.

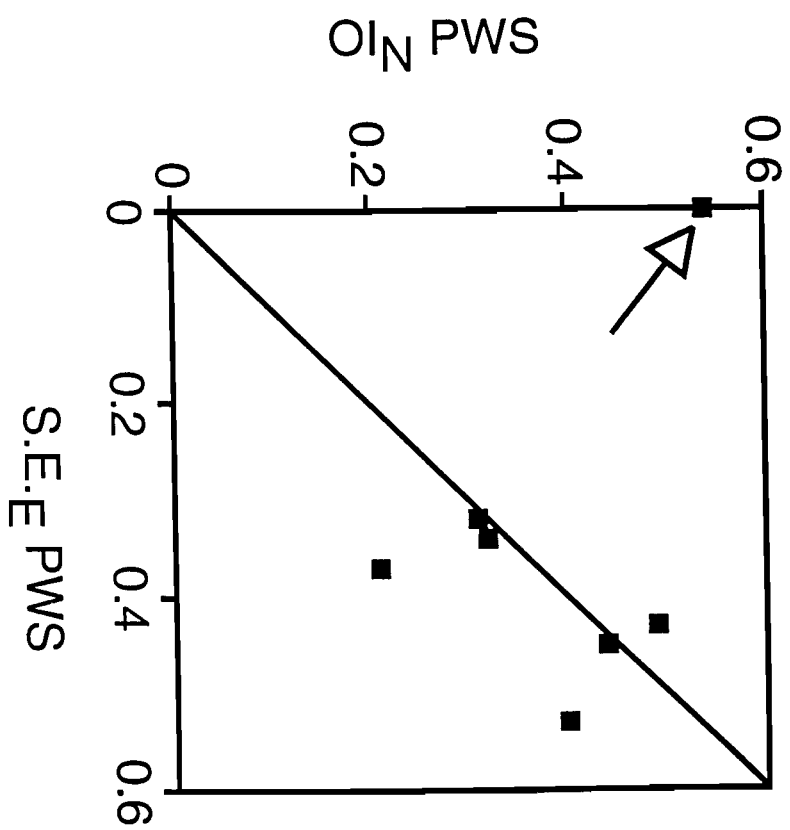
FIGURE CAPTIONS:

Figure 1. Relationships between estimates of trophic level derived from $\delta^{15}\text{N}$ data (TL_N) and Ecopath modeling (TL_E), and between the corresponding standard errors, for functional groups in Prince William Sound (PWS) and the Alaska Gyre System (AGS). [Arrows indicate reference group (*Neocalanus cristatus*); see Table 1 and 2 for details] A: Correlation between TL_N and TL_E estimates from PWS; B: Relationship between OE_N and S.E._E estimates from PWS; C: Correlation between TL_N estimates from PWS and TL_E estimates from AGS; D: Lack of relationship between OE_N estimates from PWS and S.E._E estimates from AGS.

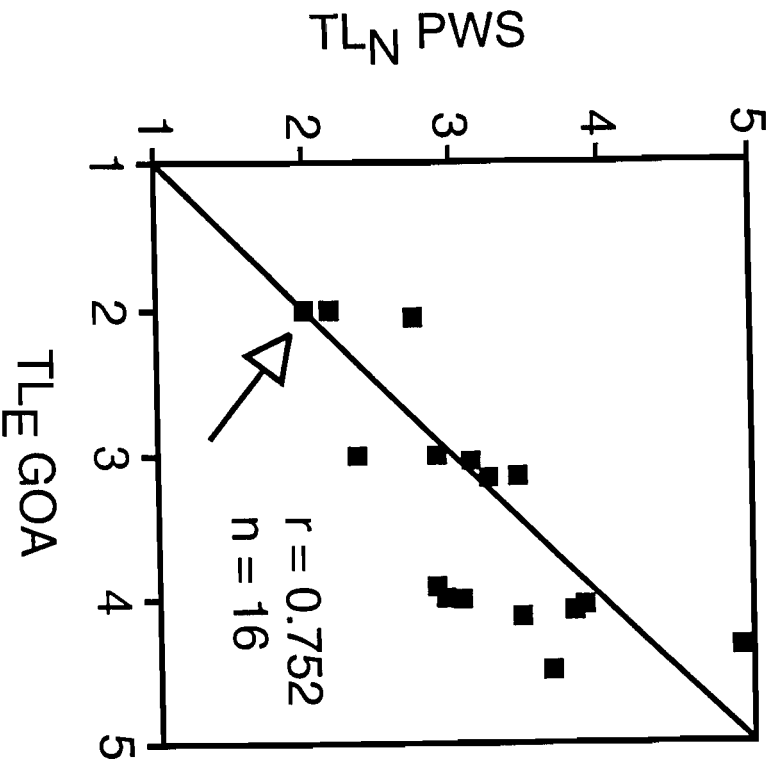
A



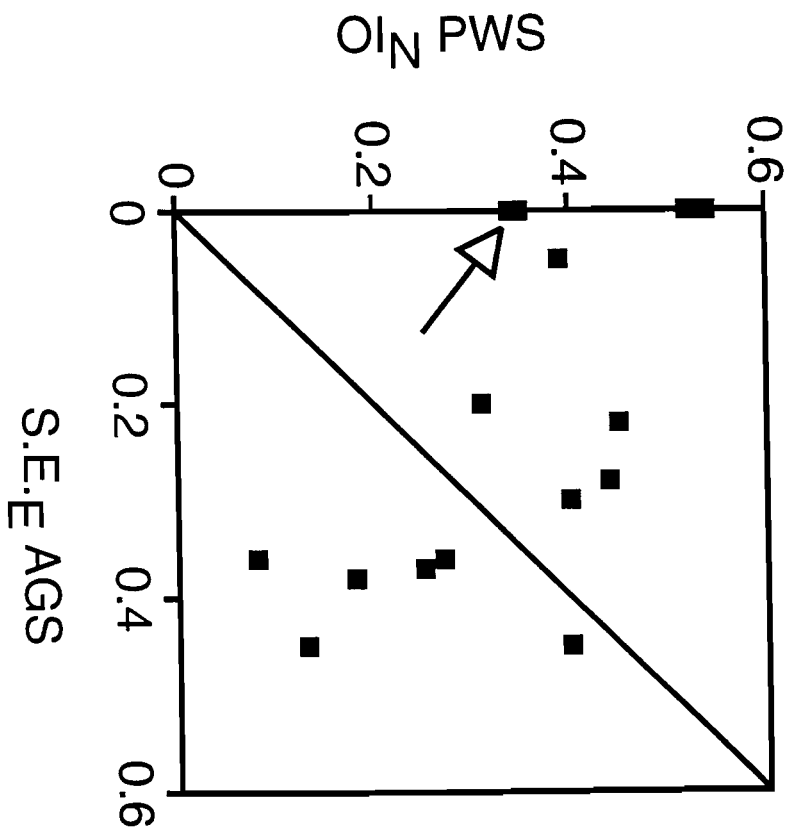
B



C



D



Chapter 7

Information Systems and Model Development

Exxon Valdez Oil Spill
Restoration Project Annual Report

Information Systems and Model Development

Restoration Project 97320-J (SEADATA)
Annual Report

This annual report has been prepared for peer review as part of the *Exxon Valdez* Oil Spill Trustee Council restoration program for the purpose of assessing project progress. Peer review comments have not been addressed in this annual report.

Principal Investigator:	Vincent Patrick	Prince William Sound Science Center
	Jennifer R. Allen	Prince William Sound Science Center
	Stephen Bodnar	Prince William Sound Science Center
	Charles S. Falkenberg	Adv. Visualization Lab., U. of Maryland
	Ravi Kulkarni	Prince William Sound Science Center & Adv. Visualiz. Lab., U. of Maryland
	Doran M. Mason	Prince William Sound Science Center & Purdue University
Pr. Investigator, Circulation Model	Christopher N. K. Mooers	Dir., Ocean Pollution Research Center, Rosenstiel Schl. Marine & Atmos. Sci., U. of Miami
	Roy Murray	Prince William Sound Science Center & Utah State University
	Ricardo H. Nochetto	Prince William Sound Science Center & Mathematics Dept., U. of Maryland
	Jia Wang	OPRC, Rosenstiel School, U. of Miami

Prince William Sound Science Center
PO Box 705
300 Breakwater Avenue
Cordova, AK 99574

April 1997

Information Systems and Model Development

Restoration Project 97320-J Annual Report

Study History: The Sound Ecosystem Assessment (SEA) Program is based upon the *Sound Ecosystem Assessment Initial Science Plan and Monitoring Program*, Rpt No. 1, Nov. 24, 1993. It began April 1994 (Restoration Project 94320) and has continued through FY97 (Projects 95-, 96- and 97320). The Information Systems and Model Development Project (SEADATA) is Restoration Project 9x320-J within the SEA Program. Prior progress is described in the SEA Annual Reports to EVOS for FY94 (Ch6), FY95 (Ch7), and FY96 (Ch7). During this reporting period the journal *Continental Shelf Research* accepted for publication in the JONSMOD '96 Special Issue the manuscript "A two-compartment model for understanding the simulated three-dimensional circulation in Prince William Sound, Alaska" by E. Dellersnijder, C. N. K. Mooers and Jia Wang. Also, the paper "A three-dimensional tidal model for Prince William Sound, Alaska" by J. Wang, C. N. K. Mooers, and V. Patrick was accepted for presentation and will appear in the forthcoming volume *Computer Modelling of Seas and Coastal Regions III*.

Abstract: There were seven task areas. **Pink salmon fry survival.** In the previous year all features of the model had been implemented, the design "frozen," and the design tested regarding prey switching. During 1997 the priority was the processes prior to, during, and after the macrozooplankton event that induces switching. The effort produced new extensions that significantly increase the model end-use value. **Overwinter survival of juvenile herring.** Model objectives presented at the February 1997 herring review were completed; models were documented and distributed for testing. **Princeton ocean model for PWS.** Fresh-water input, albeit in coarse form, was added, and the consequences for model realism are extremely promising. Validation testing continues. **Observing system specifications and operations.** Increased effort was allocated to formalizing the inputs and output of the SEA models. This task involves all of SEA. This project collects near realtime meteorological data from all sources. It maintains the met station at Applegate Rock, now at 18 months continuous, once daily transmission by repeater network. Products are published on the World Wide Web. This project is co-developer of the "subjective analysis" for surface winds **Database.** The catalog of datasets with full schemas is such that maintaining currency is a significant task. New additions are all acoustic survey data performed for ADFG and the first year of the comprehensive fishery field and laboratory database developed by Willette and Saddler. **Intranet.** The SEA project intranet continued to provide inter-project information and coordination. Emphasis turned to final year synthesis. **Applications.** Significant progress resulted from initiatives begun in response to review criteria of the EVOS Chief Scientist and review panel to demonstrate rapid transition of model development into applications.

Key Words: bioenergetics, circulation model, collaborative software, database, diffusion-taxis, dispersion, *Exxon Valdez*, Mellor-Blumberg, Pacific herring, packet-radio, pink salmon, Prince William Sound, Princeton Model, SEA, Sound Ecosystem Assessment, visualization, World Wide Web

Citation: Patrick, E. V., J. R. Allen, S. Bodnar, C. S. Falkenberg, D. M. Mason, C. N. K. Mooers, R. Murray, R. H. Nochetto, and J. Wang. 1998. Information Systems and Model Development Project (SEADATA) of the Sound Ecosystem Assessment Program, *Exxon Valdez* Oil Spill Restoration Project Annual Report (Restoration Project 97320-J), Prince William Sound Science Center, Cordova, Alaska.

Table of Contents

Study History	i
Abstract	i
Key Words	i
Citation	i
Table of Contents	ii
List of Figures	iv
EXECUTIVE SUMMARY	1
INTRODUCTION	2
OBJECTIVES	5
METHODS	5
RESULTS and DISCUSSION: In-depth Reports	6
RESULTS: Summary Reports	11
FIGURES	15
APPENDIX 1	16
Part I-A	
Technical note to SEA	
1997 findings from the EVOS-ADFG-PWSAC fry marking programs and	
from models for survival of pink salmon fry during migration thorough PWS	
.....	22
Part I-B	
Technical note to SEA	
Lower bounds for survival of juvenile pink salmon	
during migration as fry through PWS	33
Part I-C	
Summary of 1997 progress	
The pink salmon fry survival model with 1997 extensions:	
ecosystem production processes and their record in code-group survival . . .	80

Part II	
Report on 1997 progress	
Database	
C. S. Falkenberg	83
Part III-A	
Report on 1997 progress	
Web-based Communications	
J. R. Allen	86
Part III-B	
Scientific Visualization Methods for Marine Ecosystem Research:	
Case Studies Using AVS for Display of Hydroacoustic Data	
J. R. Allen, E. V. Patrick, R. Kulkarni, G. L. Thomas, and J. Kirsch	89
Part IV	
Report on 1997 progress	
Weather Data Systems	
S. Bodnar	92
APPENDIX 2	93
A three-dimensional tidal model for Prince William Sound, Alaska	
J. Wang, C. N. K. Mooers, V. Patrick	
to appear in <i>Computer Modelling of Seas and Coastal Regions III</i>	96
A two-compartment model for understanding	
the simulated three-dimensional circulation	
in Prince William Sound, Alaska	
E. Deleersnijder, Université catholique de Louvain, Belgium	
J. Wang and C. N. K. Mooers, RSMAS, University of Miami	
to appear in <i>Continental Shelf Research JONSMOD '96 Special Issue</i>	99

List of Figures

Figure 1.
Figure 2.
Figure 3.
Figure 4.
Figure 6.
Figure 7.
Figure 8.
Figure 9.
Figure 11.
Figure 12.
Figure 13.
Figure 14.
Figure 15.

EXECUTIVE SUMMARY

There were seven task areas. **Pink salmon fry survival.** In the previous year all features of the model had been implemented, the design “frozen,” and the design tested regarding prey switching. During 1997 the priority was the processes prior to, during, and after the macrozooplankton event that induces switching. The effort produced new extensions that significantly increase the model end-use value. **Overwinter survival of juvenile herring.** Model objectives presented at the February 1997 herring review were completed; models were documented and distributed for testing. **Princeton ocean model for PWS.** Fresh-water input, albeit in coarse form, was added, and the consequences for model realism are extremely promising. Validation testing continues. **Observing system specifications and operations.** Increased effort was allocated to formalizing the inputs and output of the SEA models. This task involves all of SEA. This project collects near realtime meteorological data from all sources. It maintains the met station at Applegate Rock, now at 18 months continuous, once daily transmission by repeater network. Products are published on the World Wide Web. This project is co-developer of the “subjective analysis” for surface winds **Database.** The catalog of datasets with full schemas is such that maintaining currency is a significant task. New additions are all acoustic survey data performed for ADFG and the first year of the comprehensive fishery field and laboratory database developed by Willette and Saddler. **Intranet.** The SEA project intranet continued to provide inter-project information and coordination. Emphasis turned to final year synthesis. **Applications.** Significant progress resulted from new initiatives begun in response to review criteria of the EVOS Chief Scientist and review panel to demonstrate rapid transition of model development into applications. As many end-user public meetings as possible have been attended to understand fully pressing problems, needs, and conditions imposed on possible solutions. In addition numerous presentations and application development sessions have been held with as many end-user groups as possible, and intranets were set up with ADFG and RCAC.

INTRODUCTION

The *1998 Status Report* of the *Exxon Valdez* Oil Spill Trustee Council (EVOS) notes

The Sound Ecosystem Assessment (SEA) project ... was initiated by commercial fishers and scientists in Cordova concerned about the longterm health of Prince William Sound fisheries. SEA focuses on the factors that influence the production of adult pink salmon and Pacific herring, both of which were injured by the 1989 oil spill...

The spill had brought into strong relief the problem of major missing pieces in the understanding of the marine production processes of Prince William Sound (PWS). These production processes were the basis of principle economies of the region, yet were understood largely descriptively and not in the quantitative manner typically associated with production systems. To whatever degree that understanding had been adequate, it was not following the spill. The ecosystem was now widely and carefully watched, and each observation highlighted the limited abilities to answer questions about an observed event such as "Why did this happen? How did it happen? What would happen next?"

The objective of the SEA program is the ability to answer those questions for that part of the PWS ecosystem that determines the production processes for pink salmon fry and juvenile Pacific herring. The approach is the development of numerical models, observing systems and procedures whereby the production processes can be "tracked" as well as projected ahead for some short time interval. This tracking and short term projection is the result of "continuously running" observations and numerical model simulations. In meteorology and oceanography this operation has a careful definition and is referred to as *nowcasting* and *forecasting*. Our biological models are but early and primitive in terms of nowcast/forecast, but with apologies we borrow the terminology, for it precisely conveys the goals and the methods.

Toward this objective the Information Systems and Model Development Project (SEADATA) was organized to provide the numerical models, a database, and information resources required by SEA, and also to provide the computing, communications, and certain observation system resources maintained at the PWS regional center for SEA. That center, the Prince William Sound Science Center, is the organizational home for four of the projects, the site for the primary SEA data and information servers, and the means by which SEA has continuous access to and is continuously accessible by the community served by the project.

The project history and highlights are available at the SEA Web site at URL
<http://www.pwssc.gen.ak.us/sea/sea.html>

SEADATA is responsible for the following items. The progress and status of each is described in this report.

1. Numerical model for survival of pink salmon fry during outmigration in PWS.
2. Numerical model for survival of juvenile Pacific herring during winter fasting in PWS.
3. SEA circulation model (C. N. K. Mooers, RSMAS).
4. Information system supporting collection, analysis, and distribution of near realtime data required for nowcast/forecast. This includes independently sited and maintained meteorological stations and repeater network providing near realtime data.
5. SEA scientific database.
6. SEA project intranet.
7. Initiatives for rapid transition of model development to applications; this includes intranets supporting model application development conducted jointly with region resource managers and community organizations such as ADFG and RCAC.

For the year prior to this reporting period (i.e., FY96) the principle concern was the completion of the development and implementations needed to address the project objectives (e.g., the model modules, intranet software, and database configurations—all of them developed, coded, debugged, tested, etc.)

In contrast, at the beginning of this reporting period, the scope and function established for the six of the seven areas above (excluding herring) were “frozen,” that is, there would be minimal further development for the remainder of the project. The focus became the development of model applications in preparation for the final year in which these applications would be tested against the project objectives.

The modelling tasks of the year were still diagnostic, not yet a full, final configuration. However, the models and the diagnostic scenarios for this year had the benefit of much greater realism and completeness. Consequently, results are significant to overall objectives in ways not fully anticipated. The summaries of the project activities and results that follow illustrate several such cases.

The tasks in the areas of database, intranets, and meteorological stations and repeaters also more frequently addressed the use of existing designs and developments rather than requirements for new designs and development. It was a year of providing the needed functions, performance, and services with the present set of resources. For example, a major accomplishment this year was the incorporation of the relational database for fish developed by Willette and Saddler into the SEA database. This is described by Falkenberg in Part II of the Appendix. The SEA intranet expanded to address the new functions required by the SEA synthesis effort, and it responded to never ending demands from this office for faster and more efficient information publishing and exchange. This progress is described by Allen in Part III

of the Appendix. The meteorological station at Applegate Rock is approaching the end of its second year of nearly uninterrupted measurement of one of the regions of the sound needed for the models but not within the coverage of the NOAA navigation aid stations along the tanker lanes. In Part IV Bodnar provides an update on the system, the repeaters, and the archive.

One measure for the year is the degree to which the shape and form of the outcome of this final year of SEA has moved into clearer and sharper focus. The progress described here for the seven areas shows that during 1997 each area has by a large measure moved from open issues and pending development to well-defined functions with specifications that are increasingly stable. The pink salmon fry area closes this period with major enhancements to the problem statement, major additions to the scope of the data used with the model, a reconfiguration of the model, and good evidence that fry model simulations are providing the why and how of previously unexplained features in hatchery net pen survival data.

Pacific herring tasks have not moved fully from development, since the project schedule for herring is delayed by one year relative to pink salmon. Instead, that work has moved from the implementation plan described in January 1997 to a point at which development is nearing completion: the two development milestones for overwinter survival modelling presented in January have been completed, with documentation and algorithms distributed throughout SEA and to ADFG.

The report on the status of the circulation modelling work benefits from the graphical display of recent simulations and the important contributions from the SEA oceanography project.

The natural complement to the foregoing progress is increased efforts to maximally relate the results and progress to the end-users and resource managers. In particular, the EVOS Chief Scientist and the scientific review committee established the rapid prototyping of applications from the model development as a project objective. Therefore, this additional project area has received steadily increasing effort throughout the year. By the end of the year the benefits to the project from the increased contact with stakeholders have begun to accrue, and these exchanges have contributed substantially to wider applicability and relevance and to sharper problem statements in all areas.

Most of this report will be devoted to specific results or milestones. Taken together, however, the collection of these specifics is a source for some optimism and a positive assessment regarding prospects for seeing in one year hence an outcome that fulfills the promise of the efforts begun in the fall of 1993.

OBJECTIVES

1. Numerical model for survival of pink salmon fry during outmigration in PWS.
2. Numerical model for survival of juvenile Pacific herring during winter fasting in PWS.
3. Numerical ocean circulation model (C. N. K. Mooers, RSMAS).
4. Information system supporting collection, analysis, and distribution of the near realtime data required for nowcast/forecast. This includes independently sited and maintained meteorological stations and repeater network providing near realtime data.
5. SEA scientific database.
6. SEA project intraet.
7. Initiatives for rapid transition of model development to applications; this includes intranets supporting model application development conducted jointly with region resource managers and community organizations such as ADFG and RCAC.

METHODS

The methods differ widely among the various objectives, hence information on methods is contained in the sections reporting results for each of the seven objectives.

RESULTS and DISCUSSION: In-depth Reports

In-depth reports are presented for the pink salmon fry model, database, web systems, and weather systems. These reports are covered in individual documents, and these are summarized below. The reports for herring overwinter modelling and for circulation modelling are given in brief summary form in the next section. The in-depth reports are presented in four parts of Appendix 1.

Part I 1997 Progress toward the PWS juvenile fish production models

1997 results for models of pink salmon fry survival in PWS

The results regarding pink salmon fry models for 1997 will be in the form of technical notes. Many of these were prepared throughout the year for distribution of information. Typically the notes were distributed by the SEA intranet. Many were then also published on the SEA-ADFG_Management_Exchange web site, an test intranet used by SEA, John Wilcock, James Brady, and Bill Hauser in an effort to find topics and communication approaches that result in faster movement of findings from independent investigators to agency mission operations.

The following are summaries of the contents of those technical notes, with those items of some note in bold font.

Part I-A The **fry survival model has undergone substantial evolution** and at the end of 1997 is quite different from what it was one year ago. It is sufficiently different that **it is convenient to refer to “1997 extensions”** for there are things covered now that had not been considered prior to this past year. This report is a combination of pieces from earlier in the year and some new development and descriptions.

The first topic is a review of the issue that was the initial catalyst for much of the new developments of the past year. To that end, results are shown from model simulations from earlier in the year run specifically to demonstrate the **sensitivity of fry survival to predator abundance**.

Part I-B (described below) is included by reference. Part I-B is the Technical Note to SEA in which the predation sensitivity was resolved analytically and the nature of the system whereby that effect occurs is characterized.

The EVOS-ADFG-PWSAC fry marking program provides an invaluable window into the ecological production system for fry in PWS. **The fry model with the 1997 extensions makes much greater use of this data resource and in fact is dependent upon it.** . This is reviewed in this note, in part by borrowing liberally from a Hatchery Data Review to SEA that was prepared as a web

the development of the zooplankton bloom and the occurrence of a large increase in alternative prey.

It is not uncommon to have a survival **maximum in the middle of the release series. This maximum occurs in model simulations** when preceding and following pre-releases overlap in space during outmigration providing fry self-sheltering as alternative prey, i.e., the so-called **predator swamping**.

During the last quarter of the year the process was begun that will provide end-users with a **specification for the data and the data analysis needed to accomplish the “tracking” objectives**. This notion of “analyzed data”—data wherein substantial value is added by an analysis, data fusion, or an application of a model—can be useful in this context once adequately defined. During the last quarter of 1997 several investigators set out to prepare prototypes of such data sets for use with the simulations described in this report. **Willette provided several such analyzed datasets for 1994: i) temperature for the upper 20m of the water column in the western passages; ii) adult fish species, density, size, and length by space-time strata from the predator net-sampling; and iii) diet data for predators. Cooney and Coyle prepared analyzed datasets for 1994 and 1995 based on a new analysis of the hatchery-watch time series. This provided hitherto unavailable high sampling frequency information on biomass, timing, and stage for euphausiids and pteropods. A third analyzed data set for herring was provided by Stokesbury but has not yet been incorporated into the model.**

1997 progress toward the SEA database

Part II Database. C. S. Falkenberg

C. S. Falkenberg provides a report on the database. The continuing updates and maintenance of those parts of the database that have complete schemas and documentation is an easily overlooked and underappreciated responsibility. More visible are the two new additions. The acoustic surveys conducted with ADFG for the herring and pollock fishery have been included in the SEA database. These data are a key contributor to an analyzed data product regarding predator pressures on fry. Now that data is integrated into the data system. Second, the fish database from M. Willette has been included. This is a major contribution to the data system for that archive had the benefit of many years of refinement and development by Willette and Saddler. The goal is to retain all of the functionality they developed, plus have it compatible with the additional query capabilities of the SEA database system.

1997 results and contributions from the SEA intranet

Part III-A Web-based Communications. J. R. Allen

There is one feature that is common to the numerical models, the database, and the SEA intranet: all three are “containers” in which to preserve, present, and make relevant and functional the work of each of the SEA projects. All of us that work on these “containers” have the responsibility to ensure that it is always evident that what is contained is the important contribution. The containers are successful only if the things contained become saved and retrievable in coordinated ways, seen and known in their cumulative, interrelated context, and used to solve problems through their quantitative representation in models. A project management lesson learned from SEA is the value this common feature has as a measure of project performance and status for multi-component projects.

J. R. Allen reports on the progress of the SEA intranet as the inter- and intra-project communication “container” of project results. The report provides a good snapshot of the status of the web on the three key issues at the close of the fourth year: synthesis, models, and relevance. In September the first components were begun for the web resources to “contain” and communicate the development the synthesis document. The model “containers” are increasing in number. Lastly, the means for co-development with the end-users served by SEA has been underway in test mode for some time; The status with that effort is described.

Part III-B Draft manuscript based in part on the paper presented at the 127th Annual Meeting of the American Fisheries Society, Monterey, CA, August 27, 1997: Scientific Visualization Methods for Marine Ecosystem Research: Case Studies Using AVS for Display of Hydroacoustic Data, J. R. Allen, E. V. Patrick, R. Kulkarni, G. L. Thomas, and J. Kirsch.

1997 progress toward the SEA observing system

Part IV Weather Data Systems.

The term “observing system” is another of those terms that has been adopted from another field. It is used in meteorology and oceanography to refer collectively to all observations that must be made and then delivered on some pre-determined schedule to sustain some modelling or analysis objective. The meteorological observing system is the first component of an observing system suitable for the “tracking” models from SEA. This component has gotten first attention because of the immediate need for the support of the circulation. It is also the easiest component to tackle first since near realtime data is a very well established practice in meteorology: for example, all instrument observations from NOAA buoys in PWS are available via the Internet within 30 minutes. Our own Applegate Rock station data is posted via the web every 24 hours solely because of cost and power constraints. S. Bodnar provides the technical update for 1997 on the

operation, maintenance, and performance of Applegate Rock and on related work to automate the data collection from all contributing stations.

RESULTS: Summary Reports

1997 results for models for survival of Pacific herring in PWS during winter fasting.

The model development had two parts. The first of the two was one of the first tasks of 1997, for there was a need to directly resolve a program planning question: Could historical herring fishery data together with historical climate information be useful in a statistical review of overwinter fasting and herring population formation? A second question was addressed in the last part of the year, the question of the model form most appropriate for the task of projecting the impact of a specific winter scenario given a specific measurement protocol.

The problem statement is that prepared for the EVOS Review of SEA-herring in February, 1997. In particular, the model work addressed **first a satisfactory formulation for the simpler problem of inactive fasting.**

An existing Wisconsin-type bioenergetics model for juvenile Baltic herring was used to estimate the consequences of deviation of winter mean ocean temperature from climatological winter mean temperature on the fasting basal metabolism of juvenile Pacific herring. Estimated relative change in metabolism is 5% per degree centigrade. For example, a 2 C increase in the winter mean water temperature results in a decrease in fasting survival time of approximately 10%. Based on this result it is conjectured that climate and winter fasting survival alone, in the absence of information on energy reserves, would exhibit poor correlation.

The linear regression of model of Paul and Paul (1996) can be used as is for a first estimate of the effects of fasting. The question then is what second order effects, if any, need consideration to achieve the SEA objectives. The adjustment to tackle first appears to be the underestimation of overall time for survival. For example, all fish were less than 6.0kJ/gm(wwt). The regression estimate for basal metabolic losses during the 56 day winter test series was 23.3J/gm/da. This implies 100% mortality at 120 days. The companion test for survival time had 38% alive at 120 days. The same loss rate applied to the mean of 5.2KJ/gm(wwt) and the minimum 4.3KJ/gm(wwt) predicts 50% mortality at 86 days and the onset of mortality at 47 days. The study had the first fatality at 50 days, and 80% surviving at 86 days.

The task was to find the suitable next generation formulation for losses during inactive winter fasts. **Models of inactive fasting for juvenile herring were developed using a range of approaches, from the basic Wisconsin model to the two-mass (e.g., structure and reserve mass, or protein and lipids) bioenergetics models of N. Broekhuizen *et al* (1994) and W. S. C. Gurney *et al* (1990).**

1997 results for a Princeton ocean model for Prince William Sound

At the conclusion of 1997 simulations based on 1996 data were being conducted. These were full year simulations using monthly mean forcing. This is one of several validation steps, and brings the validation sequence to about the halfway point. The most recent **runs have for the first time included fresh water input**. This addition has contributed significantly to the model findings. Completion of a suitable freshwater submodel is a first priority in the coming months.

Recent progress has been made with the addition of fresh water input. There is additional progress toward completion of the full complement of forcing data with the design and development of a **“subjective” interpolation method for a gridded analysis of surface wind fields using the existing PWS meteorological stations**. This interpolation is based on local knowledge of the wind field structure for given seasons and atmospheric conditions. An initial set of specifications was provided by Patrick Kearney, pilot with Cordova Air. The longer term requirement is for a much more contemporary approach to surface winds. These longer term considerations benefited from discussions with Dr. J. Tilley of the GeoPhysical Institute at UAF. This is joint work of this project and D. Eslinger.

Two manuscripts accepted during 1997 are attached in Appendix 2.

The paper “A three-dimensional tidal model for Prince William Sound, Alaska” by J. Wang, C. N. K. Mooers, and V. Patrick was accepted for presentation and will appear in the forthcoming volume *Computer Modelling of Seas and Coastal Regions III*.

The journal *Continental Shelf Research* accepted for publication in the JONSMOD '96 Special Issue the manuscript “A two-compartment model for understanding the simulated three-dimensional circulation in Prince William Sound, Alaska” by E. Dellersnijder, C. N. K. Mooers and Jia Wang.

PROJECT BIBLIOGRAPHY

See also bibliographies of manuscripts included as Appendices

Blumberg, A. F. and G. L. Mellor, 1987. A description of a 3-D coastal ocean circulation model. In *Coastal and Estuarine Sciences 4*, N.S. Heaps, ed., Amer. Geophys. Union, Washington D.C. pp 1-16.

Brandt, S. B., D. M. Mason, and E. V. Patrick. 1992. Spatially-explicit models of fish growth rate. *Fisheries*, 17(2) pp 23-35.

Deleersnijder, E., J. Wang and C. N. K. Mooers, 1997. A two compartment model for understanding the simulated three-dimensional circulation in Prince William Sound, Alaska. *Continental Shelf Research*, JONSMOD '96 Special Issue (to appear).

Eslinger, D. L., 1990. The effects of convective and wind-driven mixing on springtime phytoplankton dynamics as simulated by a mixed-layer model, 127pp., Ph. D. Dissertation, Florida State University.

Falkenberg C. S. and R. Kulkarni 1995. Using Spatial Access Methods to Support the Visualization of Environmental Data. In *Proceedings of Visualization '95*, Atlanta GA, November 1995, IEEE Computer Society Press, pp 400-403.

Gallacher, P. C. and P. A. Rochford, 1995. Numerical simulations of the Arabian Sea using tracers as proxies for phytoplankton biomass. *J. Geophys. Res.*, 100, pp 18,565-18,579.

Gerritsen, J., and J. R. Strickler. 1977. Encounter probabilities and community structure in zooplankton: a mathematical model. *J. Fish. Res. Board Can.* 34 pp 73-82.

Godin, J.-G. J. 1981a. Effect of hunger on the daily pattern of feeding rates in juvenile pink salmon, *Oncorhynchus gorbuscha* Walbaum. *J. Fish Biol.* 19 pp 63-71.

Godin, J.-G. J. 1981b. Daily patterns of feeding behavior, daily rations, and diets of juvenile pink salmon (*Oncorhynchus gorbuscha*) in two marine bays of British Columbia. *CJFAS* 38 pp 10-15.

Godin, J.-G. J. 1984. Temporal variation in daily patterns of swimming activity and vertical distribution in juvenile pink salmon (*Oncorhynchus gorbuscha*). *Can. J. Zool.* 62 pp 72-79.

Howick, G. L., and W. J. O'Brien. 1983. Piscivorous feeding behavior of largemouth bass: an experimental analysis. *Trans. Am. Fish. Soc.* 112 pp 508-516.

Mason, D. M., and S. B. Brandt. 1996. Effects of spatial scale, capture efficiency, and the spatial distribution of predators on the predictions made by spatially-explicit models of fish growth rate. *Environmental Biology of Fishes*, 45(3) pp 283-298.

Mason, D. M. and E. V. Patrick. 1993. A model for the space-time dependence of feeding for pelagic fish populations. *Trans. Am. Fisheries Soc.*, 122(5) pp 884-901.

Mooers, C. N. K. and D.-S. Ko. 1994. Nowcast system development for the straits of Florida. *Estuarine and Coastal Modelling III, Proc. of the 3rd Intern. Conf.*, pp 158-171.

Mooers, C. N. K. and Wang, J., 1996. The second generation of the Straits of Florida nowcast/forecast system. In *Conference on Coastal Oceanic and Atmospheric Prediction*, Atlanta, Jan. 28-Feb. 2, American Meteorological Society, Boston, pp 28-35.

Mooers, C. N. K. and Wang, J., 1997. On the Development of a Three-Dimensional Circulation Model for Prince William Sound, Alaska. *Continental Shelf Research*, in press.

Niebauer, H. J., T. C. Royer and T. J. Weingartner, 1994. Circulation of Prince William Sound, Alaska. *J. of Geophysical Research*, 99, pp 14,113-14,126.

Stonebreaker, M. 1994. Sequoia 2000: A Reflection on the First Three Years. *IEEE Computational Science & Engineering* Winter 1994, pp 63-72.

Wang, J. and C. N. K. Mooers, 1996. Modelling Prince William Sound ocean circulation. In *Conference on Coastal Oceanic and Atmospheric Prediction*, Atlanta, Jan. 28-Feb. 2, American Meteorological Society, Boston, pp 36-43.

Wang, J., L.A. Mysak and R.G. Ingram, 1994. A 3-D numerical simulation of Hudson Bay summer circulation: Topographic gyres, separations and coastal jets. *J. Phys. Oceanogr.*, 24, pp 2496-2514.

Wang, J., C. N. .K. Mooers and V. Patrick, (to appear) A Three-dimensional Tidal Model for Prince William Sound, Alaska. *Computer Modelling of Seas and Coastal Regions III*, Proceedings of the third international conference, Computational Mechanics Publications, Southampton.

FIGURES

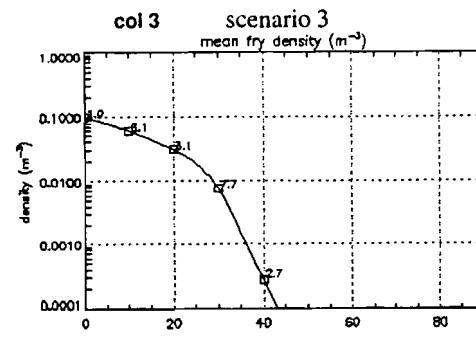
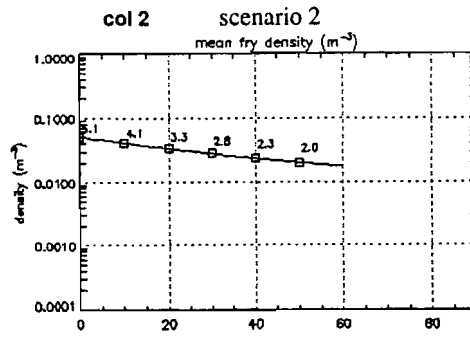
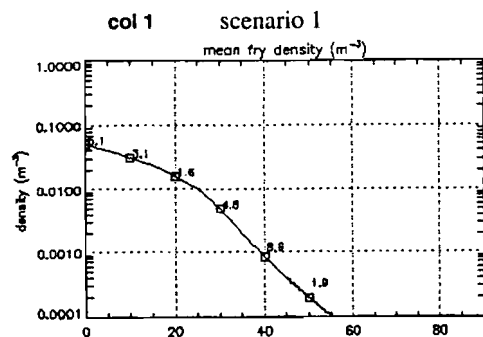
Figure 1.
Figure 2.
Figure 3.
Figure 4.
Figure 6.
Figure 7.
Figure 8.
Figure 9.
Figure 11.
Figure 12.
Figure 13.
Figure 14.
Figure 15.

initial conditions common for all scenarios: temperature = 9C, fry growth rate = .03 gm/gm, pseudocalanus density is constant = 200 m^{-3}

double both fry and pollock densities

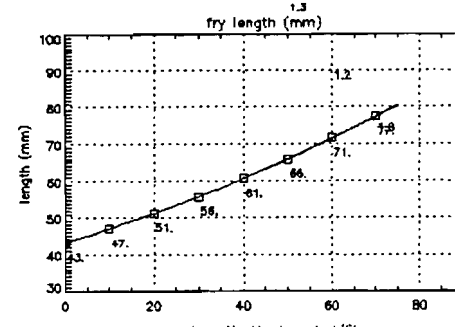
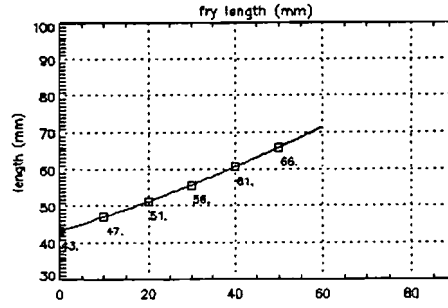
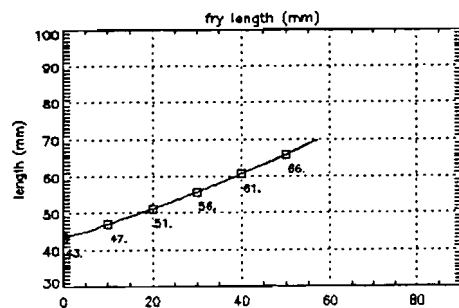
fry density = $0.5 \times 10^{-1} \text{ m}^{-3}$ → same → fry density = $0.5 \times 10^{-1} \text{ m}^{-3}$
 pollock density = $0.9 \times 10^{-4} \text{ m}^{-3}$ → 50% → pollock density = $0.45 \times 10^{-4} \text{ m}^{-3}$

fry density = $2 \times 0.5 \times 10^{-1} \text{ m}^{-3}$
 pollock density = $2 \times 0.9 \times 10^{-4} \text{ m}^{-3}$



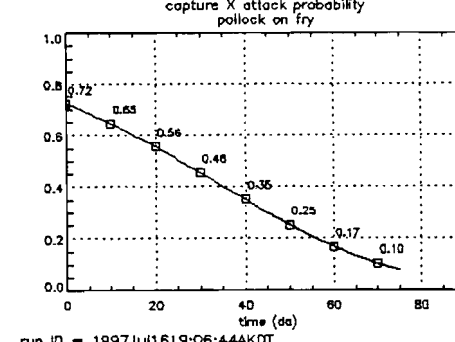
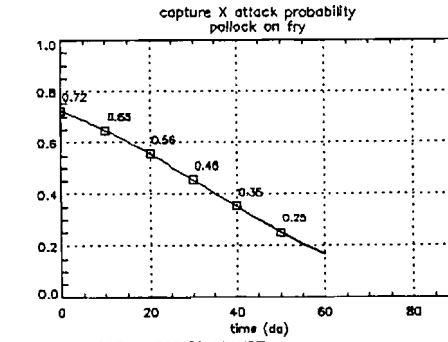
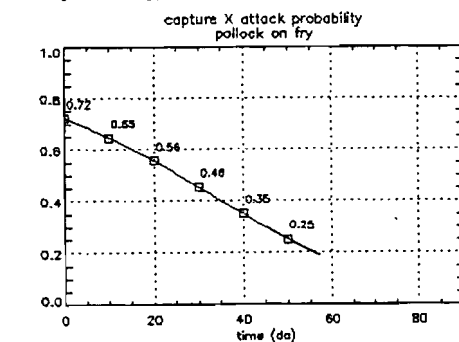
row 1

fry density at days since release



row 2

length of fry at day n



row 3

probability of capture times probability of attack

run ID = 1997Jul1615:56:35AKDT
 IDL code = mn_combi12_98h.pro

run ID = 1997Jul1700:55:45AKDT
 IDL code = mn_combi12_98j.pro

run ID = 1997Jul1619:06:44AKDT
 IDL code = mn_combi12_98i.pro

Figure 1. Three diagnostic runs for adult pollock predation on fry. The scenario assumes no prey for pollock other than pink salmon fry. Fry feed on pseudocalanus.

temp = 9C

coupled populations
time(hr): start = 120.75: interval = 0.25
present time = 240.00hr = 10.00da
nodes = 5
dx = 750.0m

mass = 0.416 length = 47.1

PINK_FRY

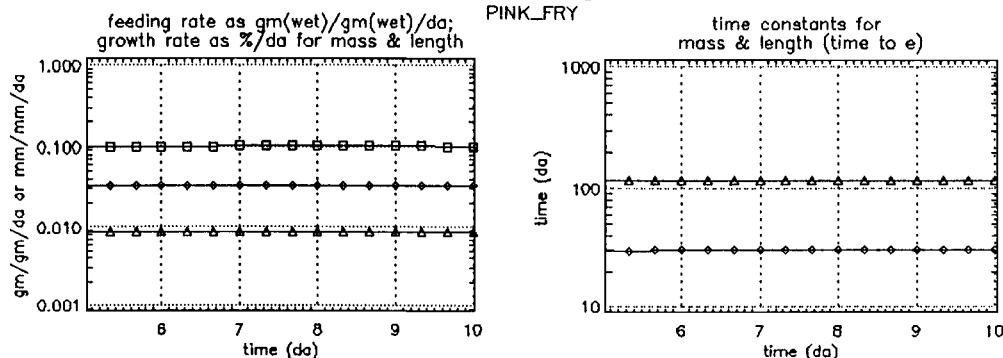
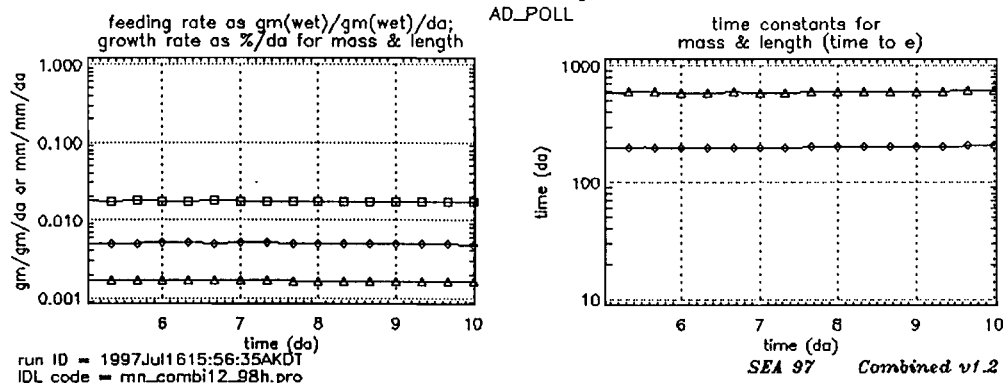


Figure 2.

Rates for
consumption,
mass change,
length change

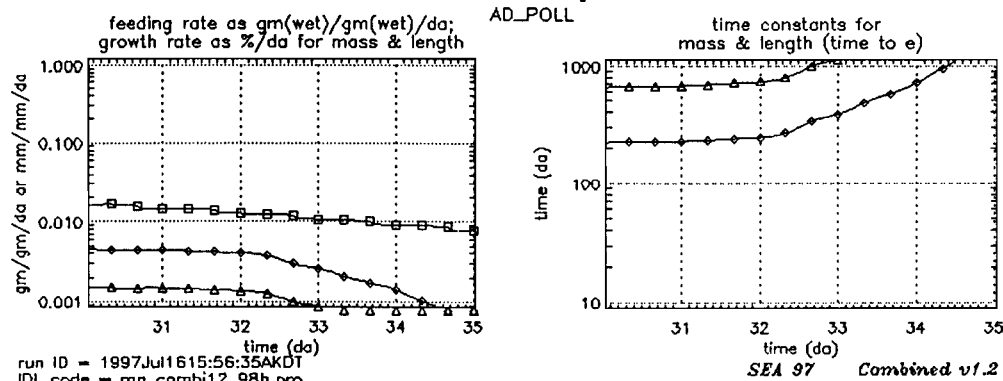
mass = 463. length = 407.

AD_POLL



mass = 520. length = 423.

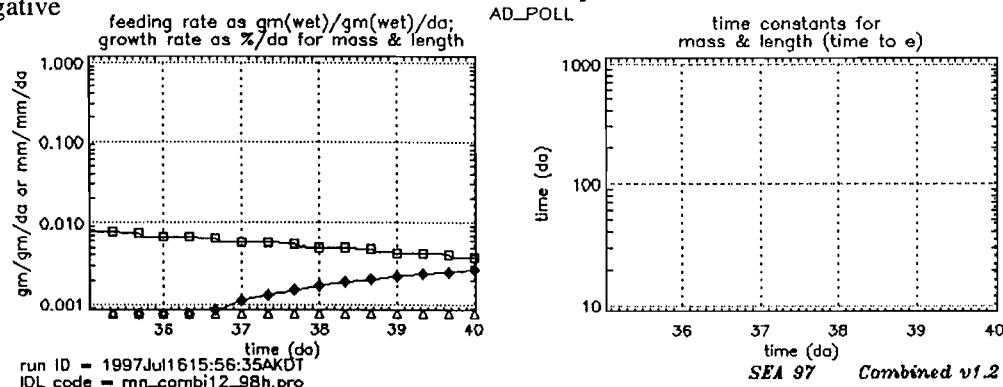
AD_POLL



Note fry density
in Figure 1
corresponding to
day at which the
mass gain goes negative

mass = 516. length = 423.

AD_POLL



The SEA problem statement for pink salmon: Survival during outmigration through PWS; Survival in GOA

Fri Sep 5 04:21:47 AKDT 1997

Some recent issues with the fry model, recent discussions regarding synthesis, reminders about sponsor's expectations, and a bit of prior mathematics conditioning all bring to mind the need to continually reexamine and refine the problem statement.

The following is my understanding of the problem statement for pink salmon, and this version should be corrected as needed.

The SEA problem statement for pink salmon is

to forecast the survival of hatchery pink salmon fry during their period of outmigration in PWS using initial conditions for hatchery fry releases provided by the hatcheries and the combined contributions from all of the collaborating disciplines in SEA. These latter provide the physical conditions and the population densities for prey, alternative prey, and predators during outmigration sufficient for the forcing and boundary conditions of the combined model for nowcasting of fry survival.

A further part of the problem statement is

to apply an estimate for survival for the ocean (GOA) phase of pink salmon and thereby forecast an upper bound for adult salmon returns for the following year.

Spatial context of the problem statement

The map at the right shows the spatial context for the problem statement. This map and several companion maps were prepared to describe specific space-time survival issues (hatchery interactions, aggregation in the south in late August, fry density). It is shown here since it seems a simple reminder of both spatial and multidisciplinary aspects of the problem statement. The symbols N_s , N_c , N_w , N_a refer to the total released at Solomon Gulch, Cannery Creek, WHN (Ester), and AFK. The symbols S_{pws} and S_{ocn} refer to survival during PWS and the oceanic periods, respectively.

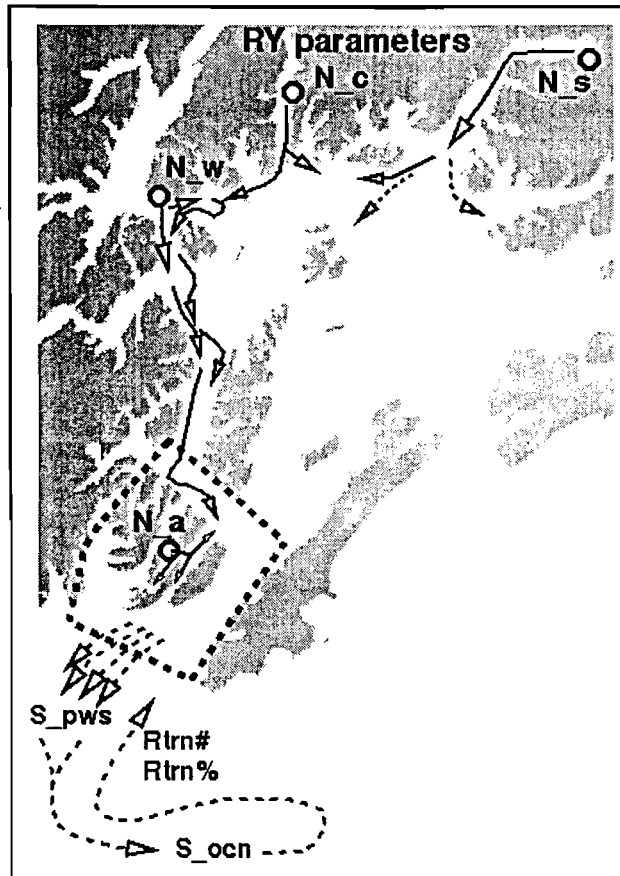


Figure 3. Revisiting the problem statement for pink salmon.

PWS hatchery data

a brief review of data prior to and data since 1994

Fri Sep 5 03:50:00 A KDT 1997

The four pink salmon hatcheries in Prince William Sound provide ADF&G with datasets for their fry releases and the resulting adult returns. Since 1989 a single data record is associated with a unique coded-wire tag group code. Each record has fields for time of release (day, month, year), mean mass at release (gm), duration of release (days), number of fry released, and the percentage of released fry that return the following year.

The SEA problem statement for pink salmon fry is inherently dependent upon the hatchery data for

- a. initial conditions for time, number, and individual mass for hatchery fry released into the system;
- b. accurate survival information for the hatchery component of the fry population, information which is to serve as the final arbitrator of the efficacy and reliability of the SEA coupled models.

This review was motivated initially by modelling issues. During the review, however, the statement above regarding the role of the hatchery data in determining the success of SEA came into greater relief, in part because of recent planning and discussion regarding synthesis. This "report to SEA" is in part shaped by the possible utility in the emerging discussions.

The data reviewed has been provided by Mark Willette. This review is a straightforward assessment of scope and those aspects of the content that (seemingly) require no subtle statistics. Mark has carried out statistical analyses that are not described here. It is hoped that we can get these posted on the web in the near future.

There are two periods to the data. Data for release years 76 through 87 consist solely of release numbers, returns, and survival for the year for each of the four hatcheries based upon estimates without the use of coded wire tags. Data for 88 through 95 is substantially more complex because of the introduction of coded wire tags.

Possibly the greatest motivation for a review is the fact that (to my knowledge) the hatchery data for release years 94 and 95 -- data which became available since the preparation of the SEA Science Plan -- has not been widely reviewed within SEA.

This review of PWS hatchery data consists of:

- Part 1: yearly means Sat Sep 6 18:37:54 A KDT 1997
 - cumulative variables for the entire PWS-system;
 - variables for each hatchery;
- variables by *release-day* and by *tag-group*
 - Part 2a: data summaries; opportunities for synthesis Sun Sep 7 12:50:09 A KDT 1997
 - Part 2b: background & misc reviews Sun Sep 7 22:15:56 A KDT 1997
 - cumulative for the entire PWS-system;
 - variables for each hatchery;
- Part 3: one view of PWS and GOA survival Mon Sep 8 07:16:18 A KDT 1997
 - progress of each tag-group under one set of (too simple) assumptions regarding
 - time from release to return
 - the "development time" for observed survival differences.
- QC Notes: Remarks, further information, clarifications, requested fixes Thu Sep 11 16:53:57 A KDT 1997

Figure 4. Opening page for web-published overview of PWS hatchery data.

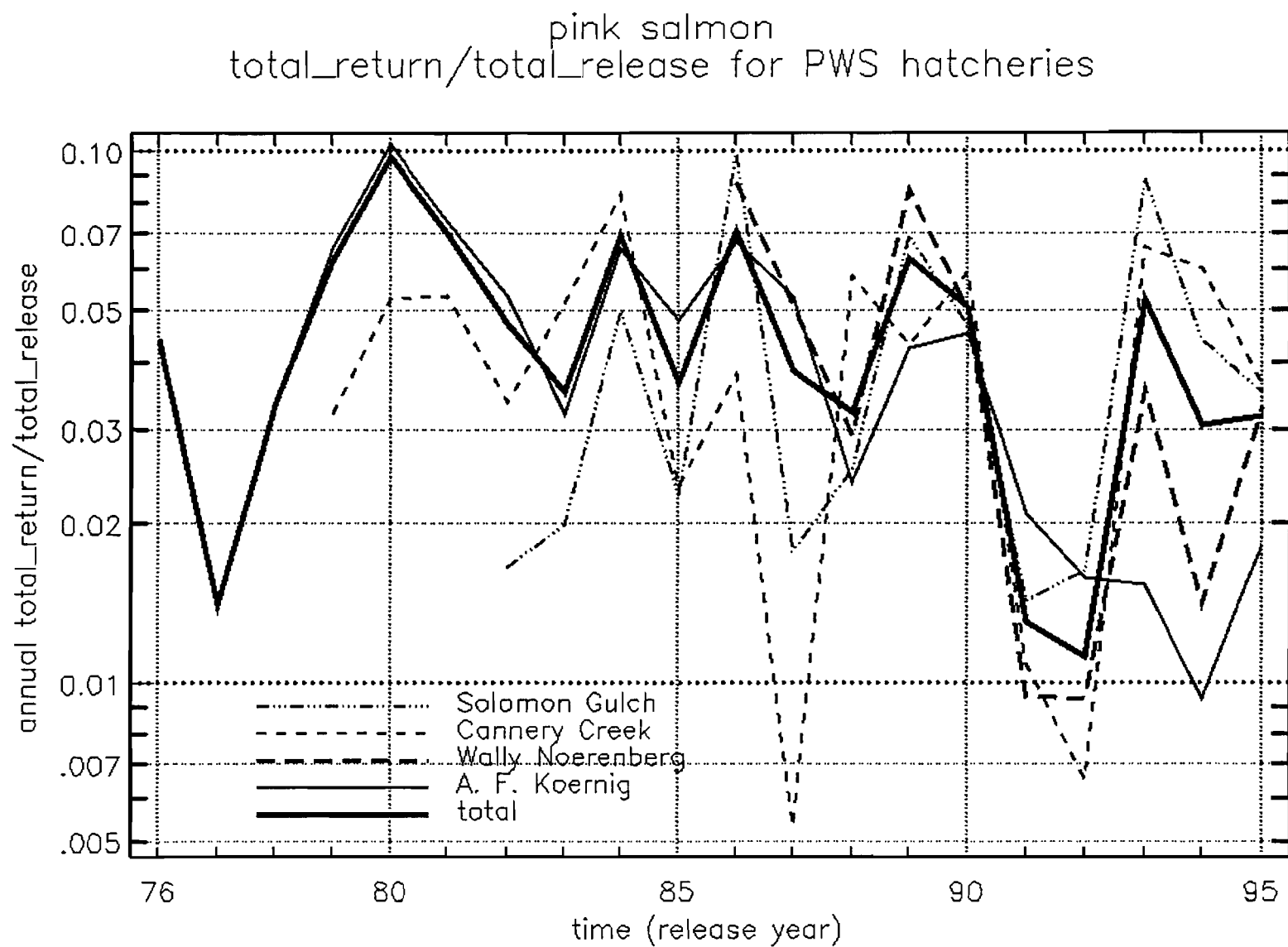


Figure 5. Annual total_return/total_release for each hatchery and for the four PWS hatcheries combined.

Release variables and release/return (for day) for

○ Solomon Gulch

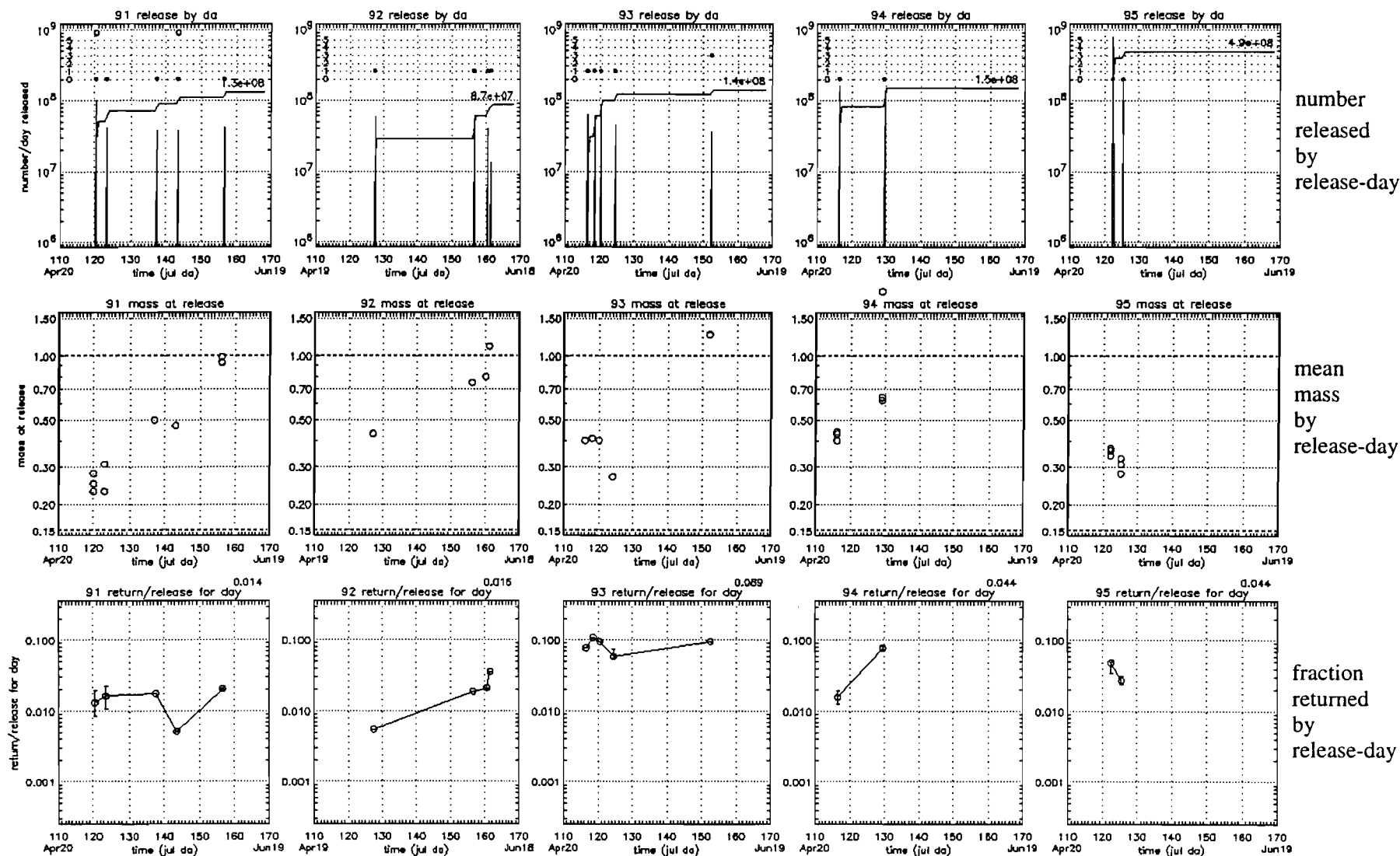


Figure 6. Number released, mass at release, fraction returned for Solomon Gulch, 91-95 release years

Release variables and release/return (for day) for

□ Cannery Creek

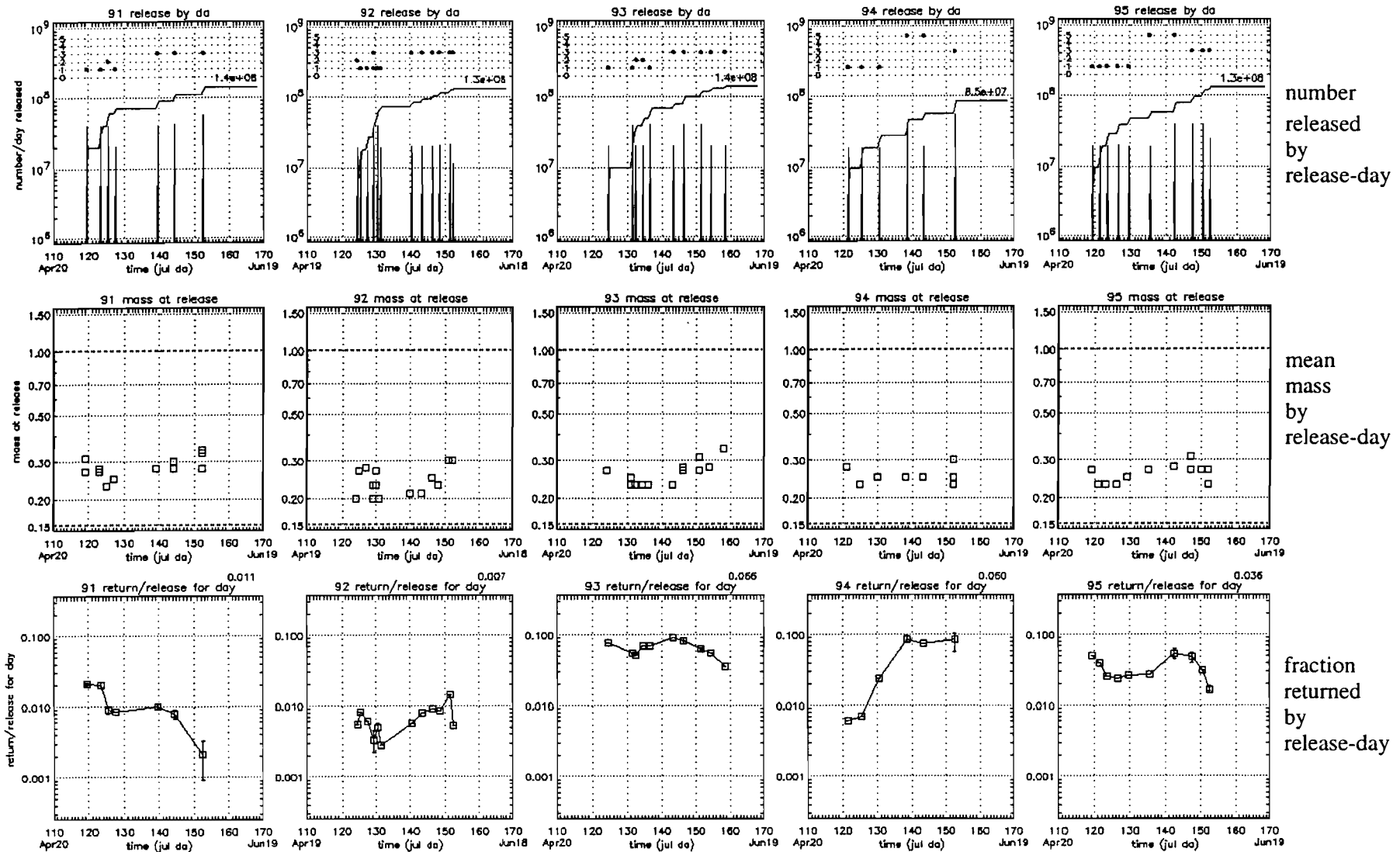


Figure 7. Number released, mass at release, fraction returned for Cannery Creek, 91-95 release years

Release variables and release/return (for day) for
 Δ Wally Noerenberg

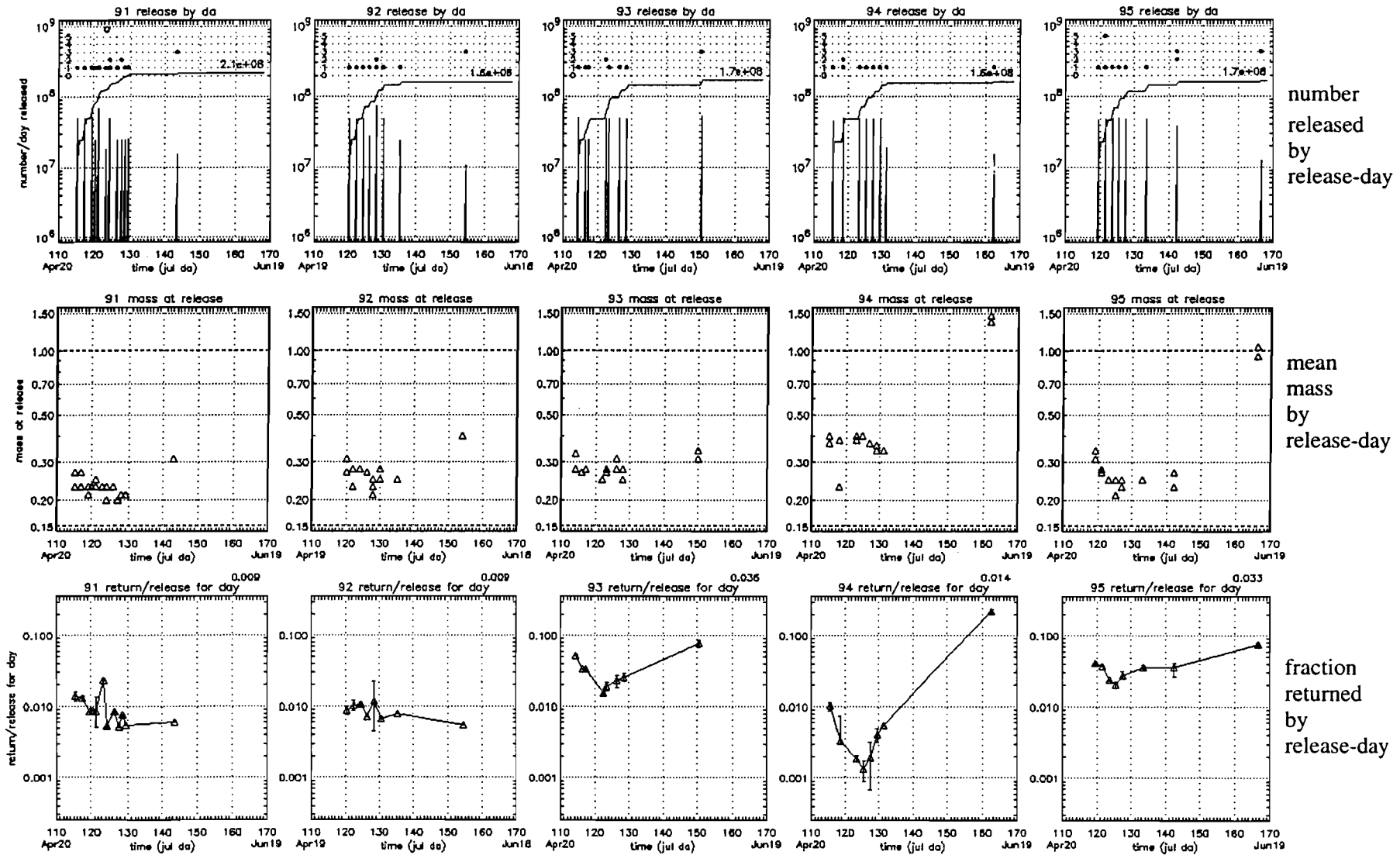


Figure 8. Number released, mass at release, fraction returned for WHN, 91-95 release years

Release variables and release/return (for day) for
 ▽ A. F. Koernig

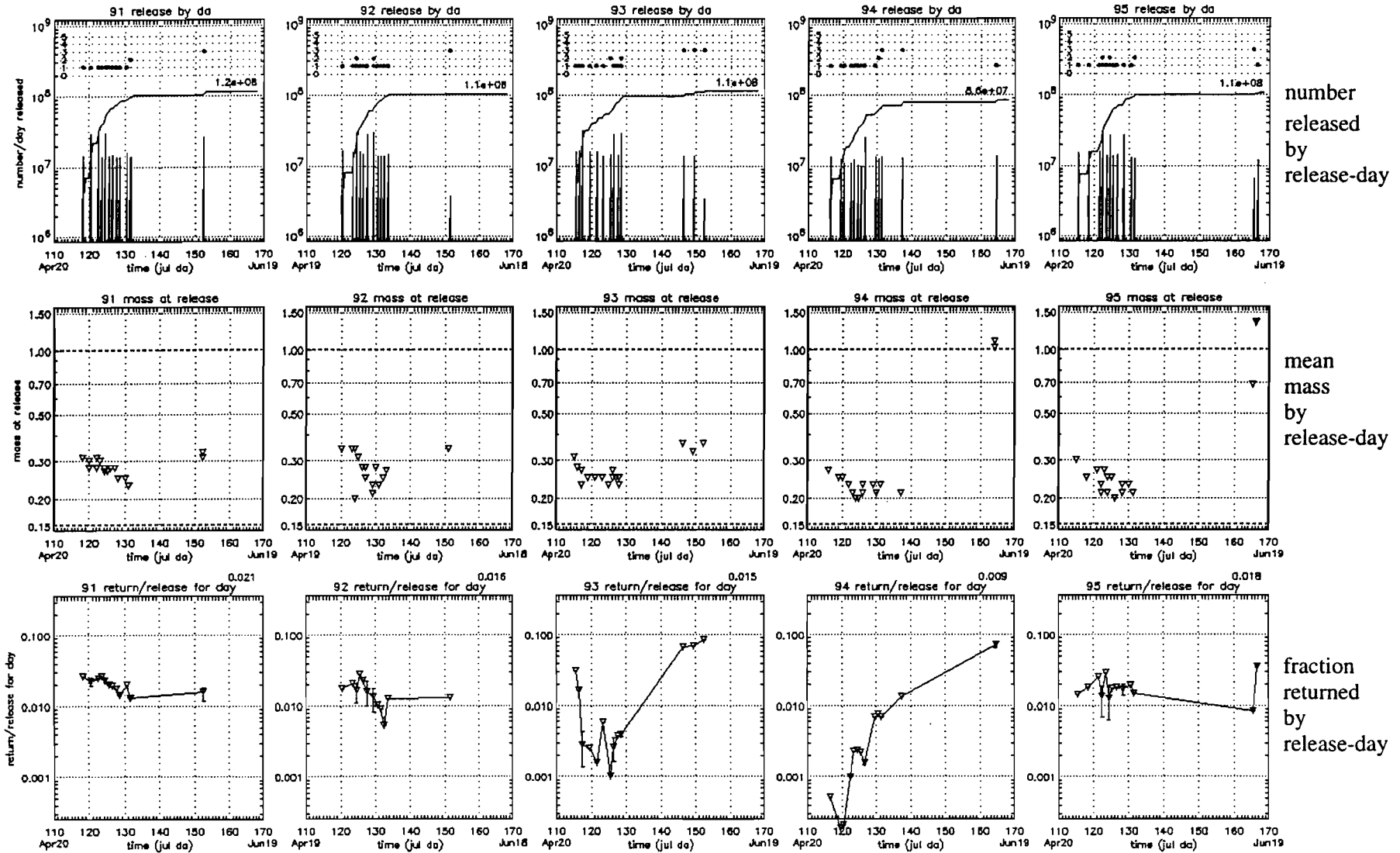


Figure 9. Number released, mass at release, fraction returned for AFK, 91-95 release years

pink salmon hatchery fry
 return/release for return & release summed over day
 error bar indicates day with multiple releases, height corresponds to observed survival range

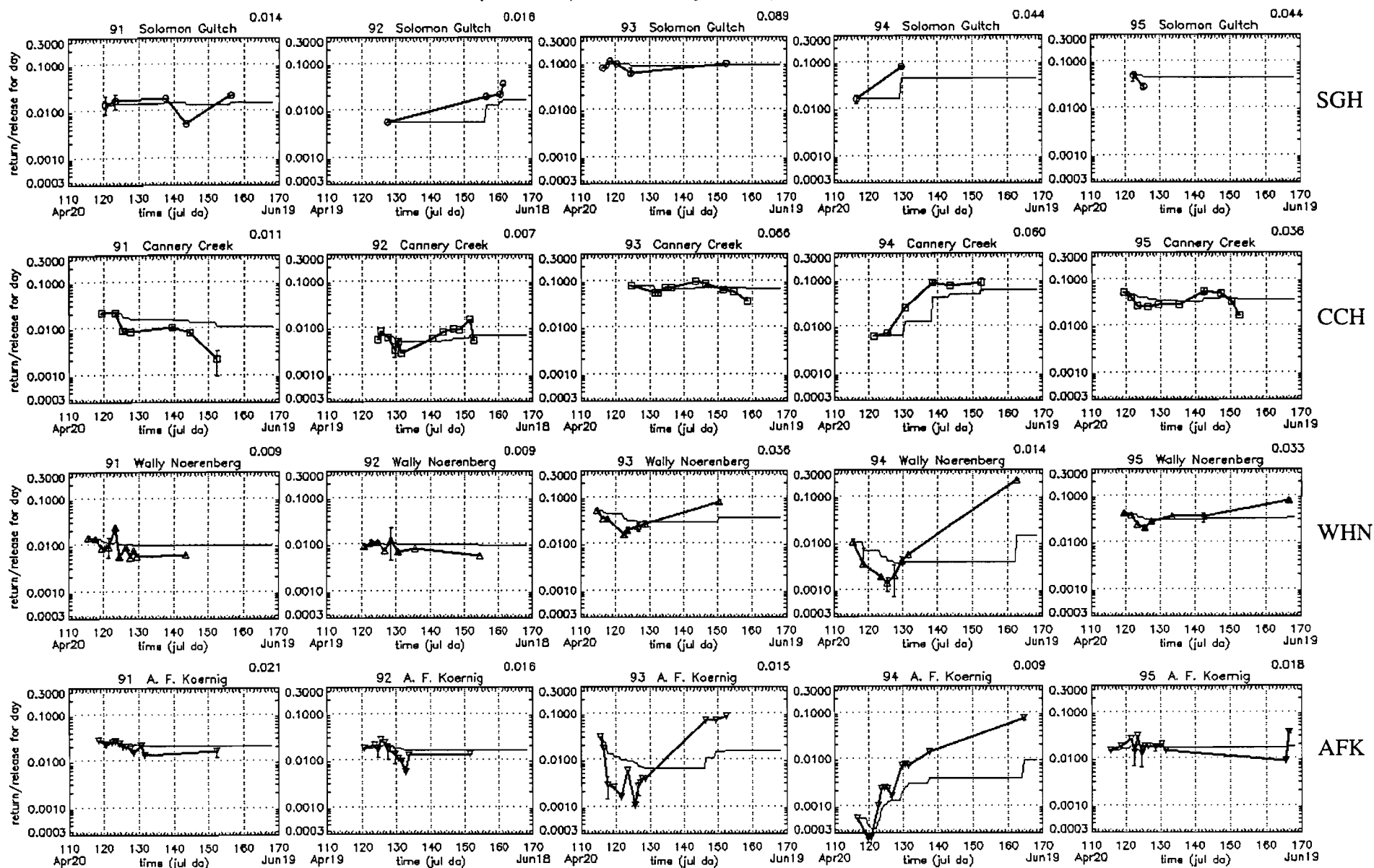


Figure 10. Fraction returned by release-day (bold line between data pairs)
 Running tally of returns/released up through release date (faint line)
 91-95 release-years arranged: north to south = top to bottom

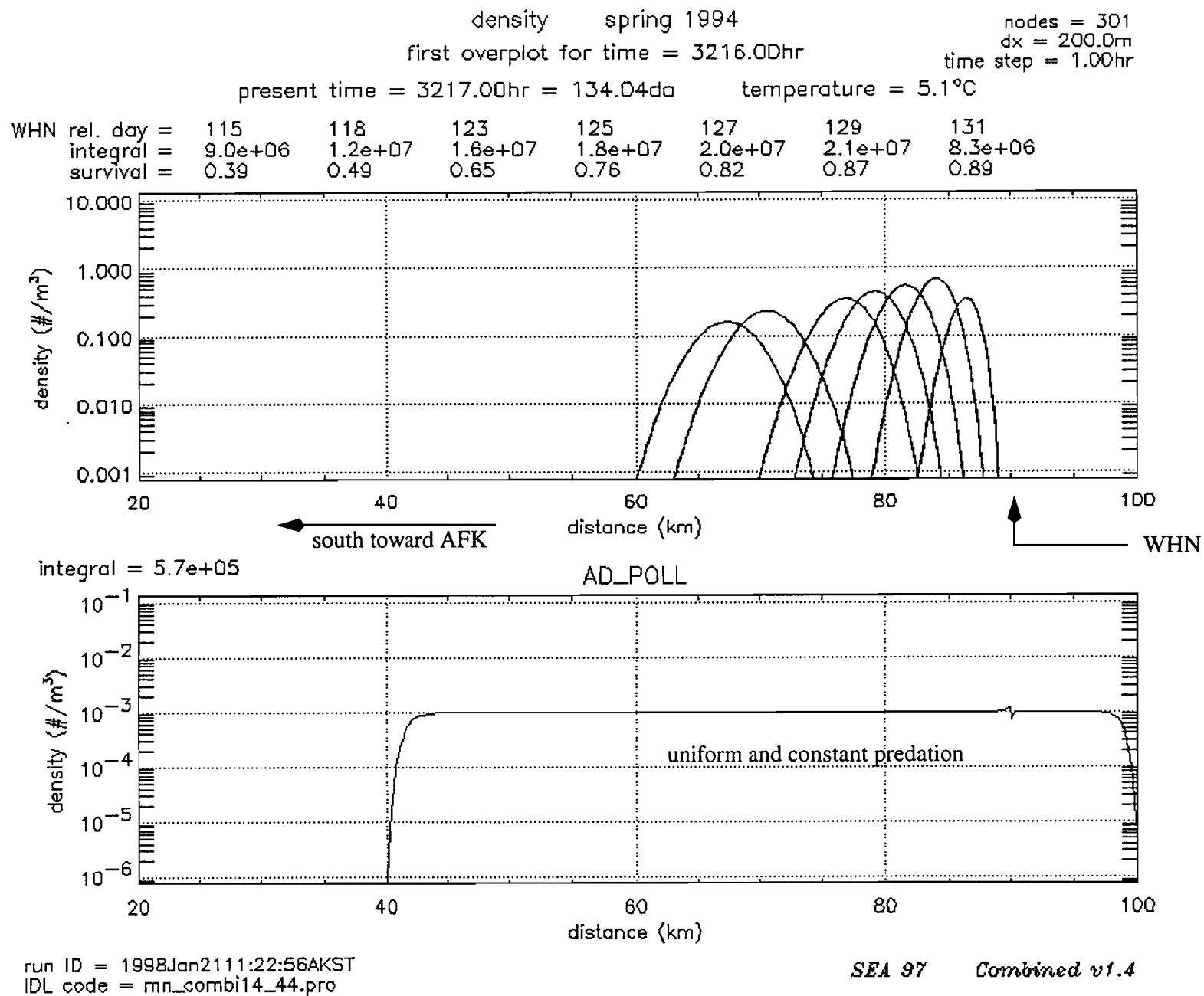


Figure 11. Snapshot of fry survival model "tracking" each group of pens with common release-day.

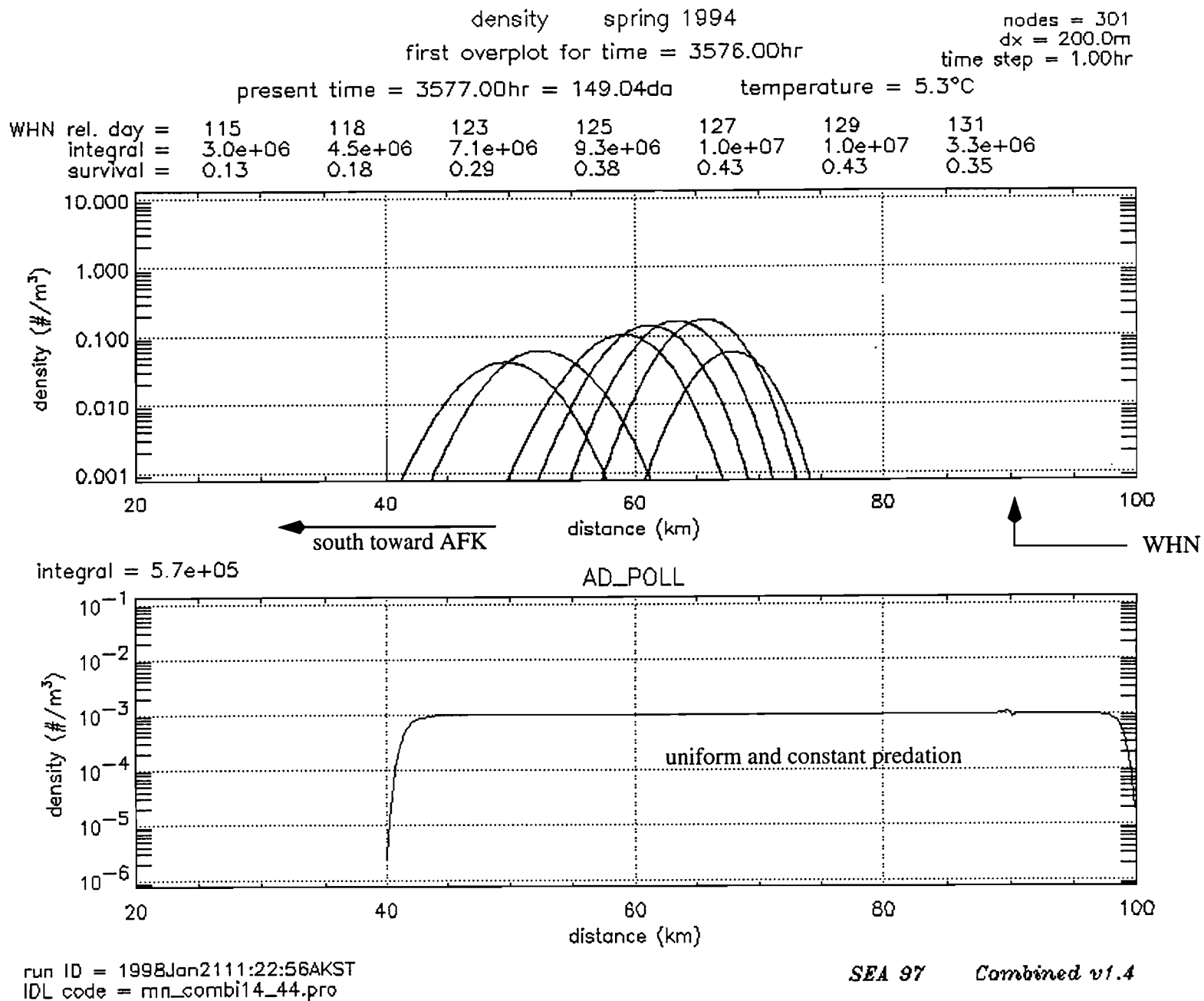


Figure 12. Snapshot of fry survival model "tracking" each group of pens with common release-day.
At Julian day 149

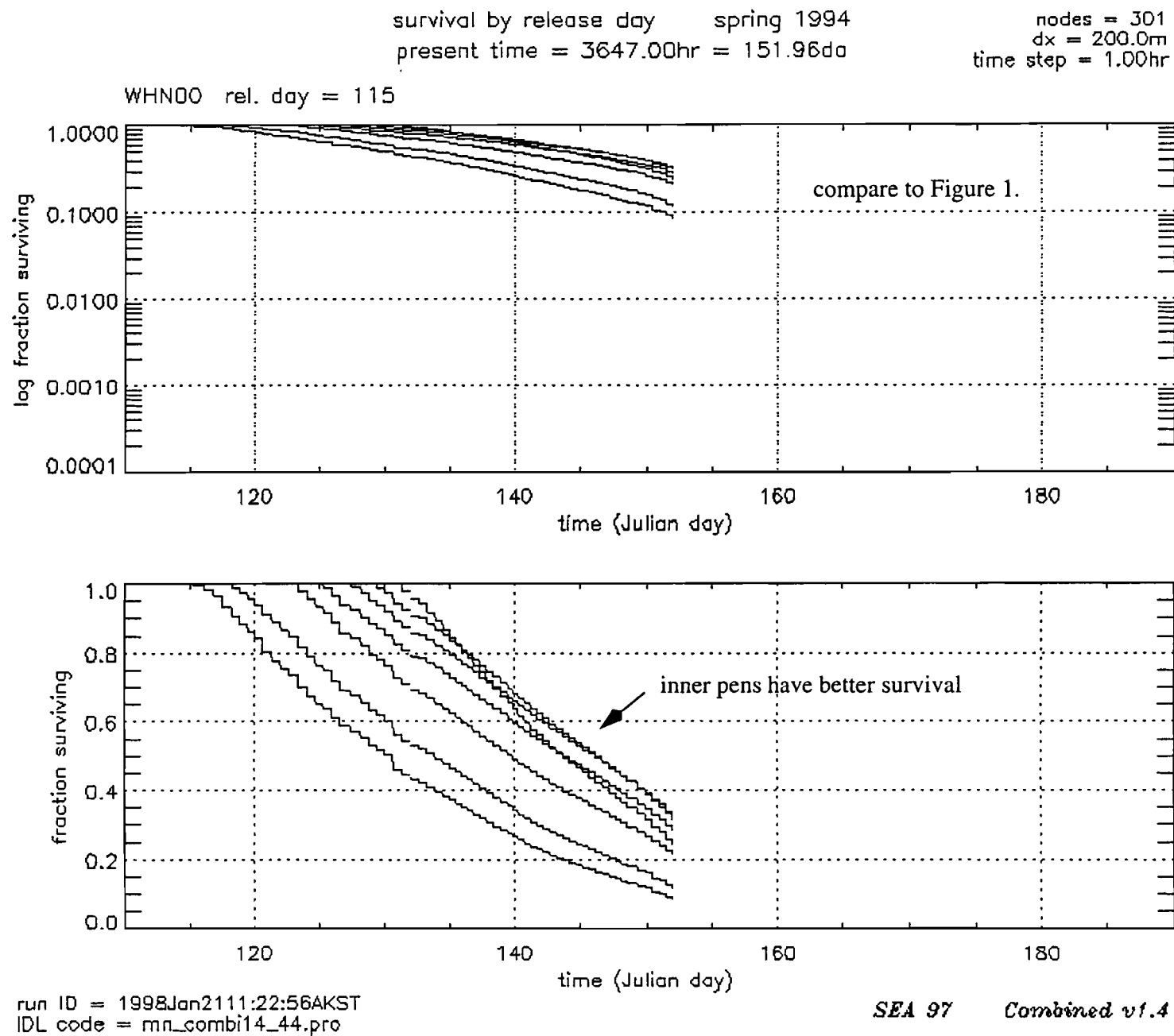


Figure 13. The same as Figure 1, but with tracking of each release-day.

Configuration of Systems used in simulations

Initial conditions according to

WHN 1994

8 distinct release days

115, 118, 123, 125, 127, 129, 131, 162

fry stock structure = release days

8 discrete fry stocks

initial stock abundance =
number released

initial individual mass =
mean individual mass at
release day.

Scenario for simulations

release site: WHN (at 90km mark)

duration of release: instantaneous

fry diffusivity: $0.088 \text{ m}^2 \text{ sec}^{-1}$

fry forage: pseudocalanus 200 m^{-3}

fry predator(s): equiv. of:

adult pollock 475mm, 700gm

distribution: uniform

(wrt. model domain)

diffusivity: $0 \text{ m}^2 \text{ sec}^{-1}$

fry predator forage: fry (only)

(assumes no alternative prey)

Neocalanus: 0 m^{-3}

model manifold: 1d space x time

model 1d coordinate represents:

shore to 500m offshore

upper 20m

along

1d path from Solomon Gulch to AFK

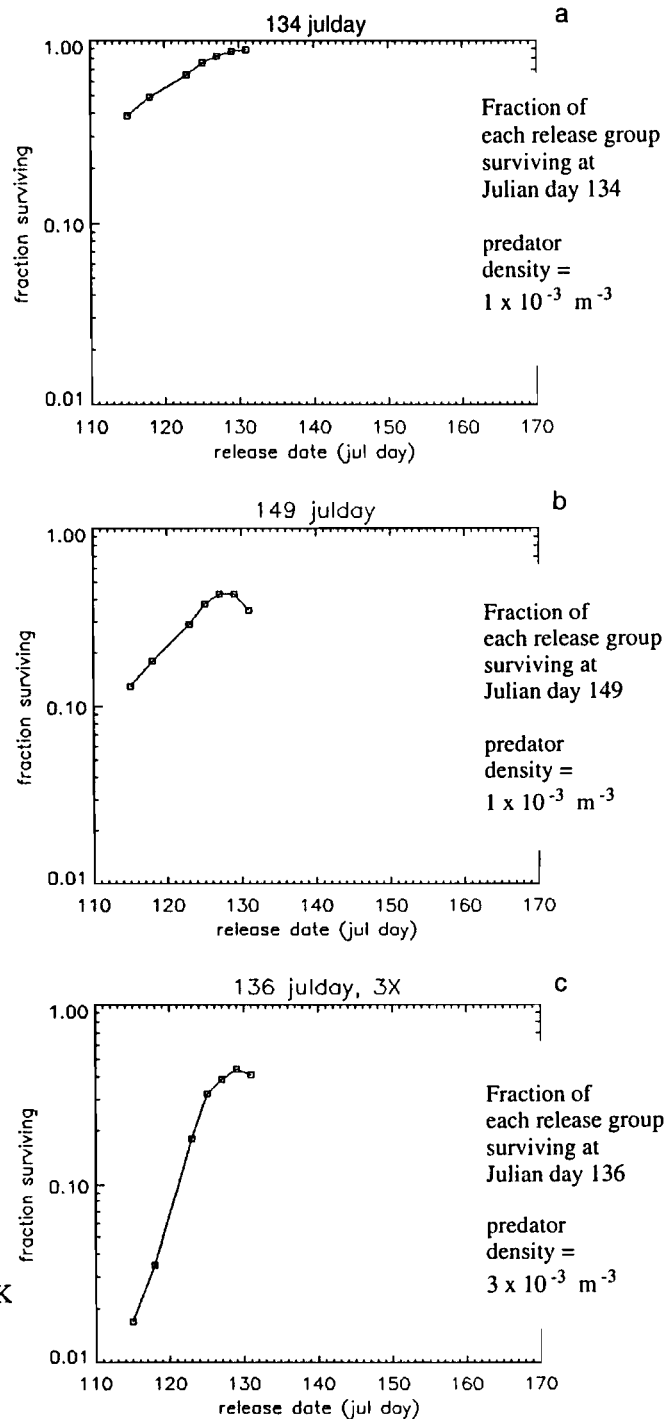


Figure 14. Simulation results from the SEA pink salmon fry model with 1997 extensions.

With 1997 extensions the models are capable of tracking production processes for any and all partitions and groupings of fry releases. The 1997 extensions enable production tracking at the maximum resolving power of contemporary fry marking and tagging technologies.

This figure illustrates the function of the new 1998 extensions: PWS ecosystem production processes and PWSAC pre-release hatchery production are modelled jointly, i.e., as a single "plant." With 1998 extensions optimal value problems requiring optimization across both the ecosystem and the hatchery can be considered.

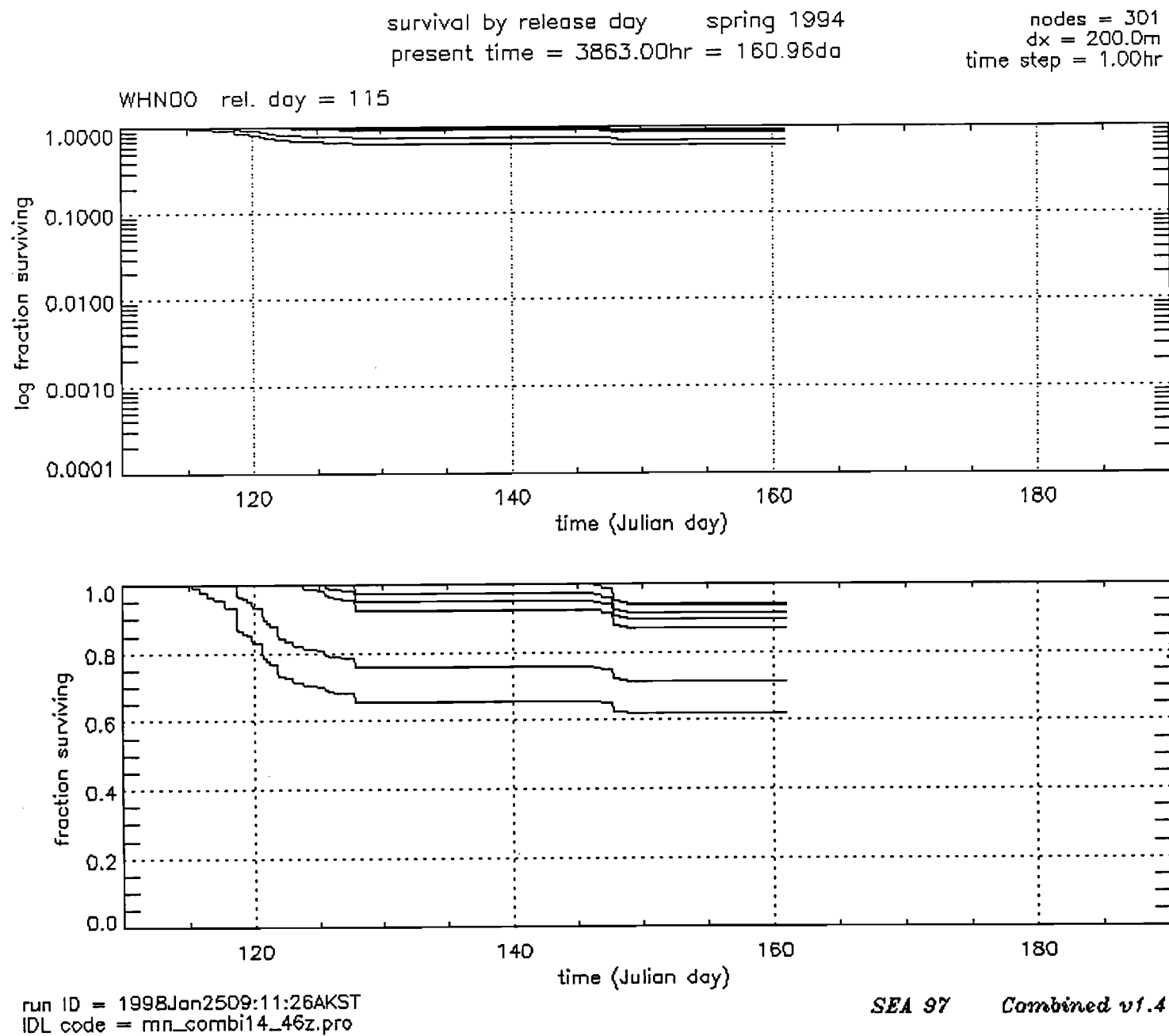


Figure 15. The same as Figure 1, but with diversion of predation due to zooplankton bloom development

APPENDIX 1

Part I-A

Technical note to SEA

**1997 findings from the EVOS-ADFG-PWSAC fry marking programs and
from models for survival of pink salmon fry during migration thorough PWS**

Technical note from SEA
1997 findings from
the EVOS-ADFG-PWSAC fry marking programs
and results from
the models for survival of pink salmon fry
during migration through Prince William Sound, AK *

J. E. H. SEA and M. N. R. SEA¹

Summary

The SEA Project is developing physical-plankton-nekton models for the survival of juvenile fish in Prince William Sound. This reports results from the nekton model for juvenile pink salmon. The model is a space-time model in which models for foraging, gut evaluation, and bioenergetics are embedded within diffusion-taxis models for the dispersion of all interacting nektonic species of the subsystem.

During model testing at the end of 1996, fry survival was found to be non-linearly related to predator density. The nature of this dependence was the starting point of work in 1997, for this dependence is the foundation upon which prey-switching occurs.

This note reports first on how the non-linearity shows up in a simulation of survival. A companion document provides an analysis whereby an approximation is established that explains the behavior. Next, the available data is reviewed for evidence of this effect. The result of that search brings to light new factors that have guided the addition of new extensions to the way the model is used.

* Sponsored by The *Exxon Valdez* Oil Spill Trustee Council, Anchorage, AK
Restoration Project 97320

¹ J, E. H, M, N, and R identify projects of the Sound Ecosystem Assessment (SEA) Program.
www.pwssc.gen.ak.us/sea/sea.html

1 Fry survival trials with the 1996 SEA model

Fry survival and macrozooplankton

By the end of 1996 all of the nekton responses identified in the SEA hypotheses had been written as model components of the fry survival model. Each of the components had been tested during development. Earlier in the year the numerical solutions for the overall system of equations had been rewritten and recoded and had undergone substantial checking and testing. The newly added model components were relatively straightforward functions within the overall system. With this confidence in the system code and in the code for the new modules, it remained only to begin simulations with all of the parts in place. A full chronology of this period is described in the SEA *FY96 Annual Report*, Ch 7, pp 11-14.

There was much changed within the model during 1996—bioenergetics and dispersion models were combined, it underwent rewrites to allow an arbitrary number of trophic structures, and a hybrid solver replaced the earlier mixed method solver. From the outside, however, the form by which the model represented the PWS ecosystem had changed very little. The model representation that would be used was identical to the representation described by Figures 19–31 of the annual report from a year earlier, from SEA *FY95 Annual Report* (Ch7). The testing domain would be small domains such as the cross-channel domains of Figure 20. The trophic structure was the simple four or five species structure shown in Figure 22: one or two zooplankton species, possibly a juvenile fish other than salmon fry as an alternative prey, a single fry trophic level, and one or two predator species. A frequently used basic test set consisted of pseudocalanus, Neocalanus C4, Neocalanus C5, pink salmon fry, and adult pollock.

A major theme of the model development at the end of 1996 was to insure that the developed model was sufficient to capture in simulation the diet and the shifts in diet seen in the stomach data. Both Willette and Cooney were interested in the diet performance of the model simulations and had made recommendations regarding fry schooling and pollock feeding behavior that should be covered by the model. In effect, the concern was that the model be complete in its representation of pollock foraging in order to accurately represent the observed sensitivity of adult pollock predation to changes in macrozooplankton density.

The typical test of the model began with some choice of initial densities (along a one-dimensional coordinate) for each of the species. These initial densities were then allowed to interact for up to 100 days. Here, of course, there are five things to change. Some have lesser effects on survival. Pseudocalanus are important primarily as food for fry; they are not prey for pollock. The pseudocalanus density for initial tests can be fixed. Also, for a model run late in the bloom, Neocalanus C4 could be lumped with Neocalanus C5.

The model trials at the end of 1996 demonstrated that the models did have sufficient structure for fry survival to be significantly enhanced through the “diversion” or “switching” of pollock predation from juvenile fish to macrozooplankton. A summary of this sensitivity is presented in a table in the SEA *FY96 Annual Report* (Ch 7, p 15). The capability to capture this sensitivity in the combined dispersion-bioenergetics model accomplished a core milestone that was over two years in the making.

Fry survival and predator density

There was a second sensitivity that was first noticed during this testing period at the end of 1996, that of fry survival to changes in the predator density or abundance. This was not anticipated and the information was solely from the model experiments. Because the nature of the sensitivity was not understood, it was necessary to conduct the initial zooplankton tests using a limited range of predator densities. In the SEA *FY96 Annual Report* Ch 7, p14, this fact was noted in the last paragraph:

Throughout these tests the total pollock population “in the domain” is assumed constant, though free to redistribute along the domain. That is, total predator abundance is not changed.

The sensitivity of fry survival to the predator abundance or density was as great, if not greater, than the sensitivity of fry survival to zooplankton density. Unlike the case of zooplankton, there was no prior considerations of the effects of predator density as a source of some non-linear or switching behavior. The properties exhibited by the model with respect to predator density had to be understood hence this issue was the first priority for 1997.

Spatially uniform software option

The sensitivity was almost certainly in the temporal component of the solution solely. Therefore, it would be advantageous to look again at the bioenergetics and foraging parts of the model without the overhead of the diffusion-taxis parts. However, much work had gone into merging the models. Separating them would be additional work, plus additional overhead in tracking two versions. Therefore, the combined code was modified whereby an option flag is used to setup the algorithm at the outset to execute with the smallest possible spatial grid and with all variables identical on this minimal spatial grid. This still retains some of the additional calculations of the spatial code, but with the advantage that the foraging and growth code retain a single revision path with the spatial parts.

The results of three simulations (with the software set for “uniform option on”) are shown in Figure 1. The three columns correspond to three different scenarios, labeled 1, 2, and 3. The rows contain differing data reports from the simulation. It is the first row that is of primary interest, for that row contains the record of the fry survival over time. The second row shows the growth of the fry in millimeters. Here this simply documents that the three simulations were identical in terms of fry condition, and that pseudocalanus at a density of 200 m^{-3} are sufficient for essentially optimal growth. The last row contains the graph of the product of the probability of attack and the probability of capture given an attack. This too is solely to show that there is no difference between the fry of the three scenarios.

Significance

In Figure 1 pink salmon fry are the only prey for an adult pollock. (The size of the fry and the pollock at 10 days after fry release is shown in Figure 2.) This situation must obviously be seen as a limit and not a typical situation. In this limiting scenario in column 1, the fry are seemingly reduced to less than 1% of the initial density in less than two months. Figure

2 shows that just after 35 days the energy gain for the predator is negative. Hence, this limit is not so unrealistic, for there is a limiting factor that constrains the fry losses. Still, the fry survival is only 4% after only 35 days—not so good.

In scenario 3, the computer experiment says that the system would respond the same if both fry and predator densities were doubled. Since the predator loses interest at some absolute density, here the survival for the fry would be only about 2% at somewhere after 35 days.

The point of this note is the change seen in scenario 2 for only a decrease of the predator density to 50% of the density in scenario 1. (A doubling of the fry density also works.) That change results in fry survival of 40% at 60 days.

This “swing” from very low survival to extremely good survival in response solely to the predator prey relationship adds another issue in addition to the zooplankton role in predator diversion. Scenario 2 seems to be capable of producing good survival with no need for other mechanisms.

From this limiting case experiment, three factors appeared.

- 1 Although this really is a minimum absolute value with some additional qualifiers, for purposes here it suffices to note that if the “real” interest of predators is part of any model, then things cannot go entirely to zero. Here, adult pollock were not able make a daily ration for fry approaching 60 mm length and at a density of less than $.0015 \text{ m}^{-3}$. Without benefit of consumption information one can see in scenarios 1 and 3 that the fry losses show an inflection at 35 days that is a useful cue to the minimum.
- 2 For densities that seem quite reasonable, the trajectory for the fry density makes very large swings for relatively small changes in the relative abundances of predator and fry; the end points of these swings seem very low and very high.
- 3 If we recall the historical behavior of salmon survival, it would appear that the salmon production system must have some remarkable feedback features that keep the system from exhibiting the range of values in this example. On the contrary, is it the case that one or the other of the two scenarios never occurs? Is there really only one of the cases that must be “smoothed out?” Is it always the case of “over” predation as in scenario 1? Or is scenario 2 the case except in very rare circumstances.

Much of this could be answered with a better estimate of the actual densities for fry and predators along the outmigration routes. Figure 3 is an effort to focus on the regions that would be the priorities in an effort to get a better estimate of densities.

2 Analysis

The behavior of the model in Figure 1 is the subject of the document in Part 1-B, “Lower bounds for survival of juvenile pink salmon during migration as fry through Prince William Sound, AK.” That analysis provides the relationships between fry and predator densities, fry and predator size, and fry and predator growth rates whereby the survival behaves as scenario 1 or 2 in Figure 1. In that document scenario 1 is referred to as a “crash” condition,

and scenario 2 as a "bloom" condition, and precise definitions are given.

The document also argues on the basis of some rough estimates that scenario 1 is the likely situation that would obtain in the absence of a diverting prey such as macrozooplankton. If this is the case then the system is susceptible to a low survival, this being the underlying situation. The issue then is why values for survival seem so consistent.

3 Review of hatchery data

The question of the potentially low survival in the absence of any predator diversion was good reason to thoroughly review the available hatchery data to fully define the targets for the model. A review with numerous graphical summaries was completed and published on the SEA Intranet. The first page of that review is shown in Figure 4.

The annual survival viewpoint

The driving factor in the review is the picture conveyed in Figure 5, a graph of the annual average survival by hatchery and for all four PWS combined. The survival values sound-wide are remarkable in their consistency. A note in the web-published review points out that the sound-wide annual survival rate is between 0.03 and 0.07 for every year from 1976 to 1995 except for four: 1977, 1980, 1991, and 1992. This consistency seems incompatible with the "crash" or "bloom" scenarios of Figure 1.

On the otherhand, the returns by hatchery are much less consistent. This has several implications that are now part of the modelling effort, but their description cannot be developed in time for this report. It suffices here to note that the individual hatcheries follow the general pattern of the sound-wide survival, but also have considerable individual differences. The immediate conclusion is that the modelling must be on a per-hatchery basis for it seems inappropriate to use one alone to represent "PWS survival."

The hatchery operator viewpoint

Figures 6–9 show just how misleading Figure 5 is. The first row of each of the four figures shows the release schedule each hatchery operator uses. These differ dramatically between hatcheries. The second row shows the mass at release. Once again, huge differences. The third row shows the survival by release-day. If more than one pen or code-group was released in a day then there is an error bar showing the range of survival, and a symbol shows the survival for the release of that day combined.

The most important observation is the degree to which survival can only be computed from a knowledge of the release schedule. To make this more apparent, the survivals for the four hatcheries are plotted together in Figure 10. Along with the survival the cumulative survival is plotted using a faint line. For example, at AFK in 1993, after the first release, the cumulative survival dropped from steadily from 0.03 to about 0.006 due to each release after the first having lower returns than that first one. It was only the late releases that then brought the annual return up to 0.015. In 1994 at AFK each release after Julian day 120 had

increasingly better survival, but things started from a minimum of 0.0003. (All survivals are in fractions, not percentage.)

The consistency in the annual survival plots does not characterize well the processes controlling production of fry in the sound.

The smoking gun

At least tentatively, the EVOS-ADFG-PWSAC coded wire tag data has provided the smoking gun regarding the question of evidence for "crash" occurring in PWS, that is, the low survival values indicated as possible by scenario 1 of Figure 1. The returns for AFK and WHN in 1993 and 1994 certainly have survival values for individual release-days that are consistent with the "crash" conditions. Since the "crash" condition does not persist—prey switching, as indicated in the lower bound analysis—the annual mean does not contain the crash-type survival values.

Part I-B
Technical note to SEA
Lower bounds for survival of juvenile pink salmon
during migration as fry through PWS

Technical note to SEA

Lower bounds for survival of juvenile pink salmon during migration as fry through Prince William Sound, AK *

J. E. H. SEA and M. N. R. SEA¹

Summary

The SEA Project is developing physical-plankton-nekton models for the survival of juvenile fish in Prince William Sound. This reports results from the nekton model for juvenile pink salmon. The model is a space-time model in which models for foraging, gut evaluation, and bioenergetics are embedded within diffusion-taxis models for the dispersion of all interacting nektonic species of the subsystem.

Initial simulations with the nekton model exhibited anticipated time interval of population movement followed by time intervals of reduced movement with sustained, regular population interactions. Based upon these simulations results, the model equations were studied with the intent of identifying the properties of the solutions that were responsible for the interactions during periods of relatively stable distribution. It is assumed here that the realizable foraging rates for all nektonic species exceeds gut evacuation rates, hence consumption is independent of prey density.

Lower bounds for survival of juvenile pink salmon are presented for two cases of prey populations and for arbitrary time-varying physical environments. The first case is that of juvenile pink salmon (or any single prey species) with an arbitrary number of predators. The second case is juvenile pink salmon with a group of alternative prey, again for arbitrary predators. A corollary of the analysis is the classification of conditions in which prey populations either "bloom" or "crash," that is, the prey populations approach limits with either positive values in infinite time or approach zero in finite time, respectively.

* Sponsored by The Exxon Valdez Oil Spill Trustee Council, Anchorage, AK
Restoration Project 97320

¹ J, E, H, M, N, and R identify projects of the Sound Ecosystem Assessment (SEA) Program.
www.pwssc.gen.ak.us/sea/sea.html

1 Brief and initial note on results

Starting assumptions; comments on starting assumptions

To be brief and to move quickly to the results, this initial note begins with relationships and distinctions that are specific to the area of application. In particular, the starting point incorporates the assumptions

- 1 smoothed mass intake rate (smoothed meaning averaged over a containing interval of several days) for each predator is
 - 1.1 independent of prey density,
 - 1.2 linear in predator mass, and
 - 1.3 nonlinear in temperature, the temperature dependence having a single maximum.
- 2 temperature is assumed to remain either sufficiently near the maximum or sufficiently constant so that the temperature effects on predator feeding rate can be neglected throughout the time interval in question.

In a separate note these assumed relationships are described using the properties of the forage-bioenergetics model. The assumed relationships develop in the limit as prey densities increase for both episodic and continuous foragers.

Predator foraging

Let φ_f^q denote the foraging rate—that is, the mass flux due for foraging, with units mass per unit time—of predator q on prey type f . A spatial domain is assumed wherein the prey density is everywhere sufficiently high that assumption 1.1 holds everywhere in that domain. For such a spatial domain it follows that, at most, φ_f^q varies with time. By assumptions 1.2 and 2 this time dependence is due exclusively to the time evolution of the mass of the predator. The total foraging mass flux for predator q is

$$\varphi^q = \sum_f \varphi_f^q$$

A routine and general partitioning of feeding conditions consists of the following.

- P-1 $\int_{1\text{ da}} \varphi^q dt$ is less than that required to meet whole body energy requirements for the 1 da time interval specified in the integral;
- P-2 $\int_{1\text{ da}} \varphi^q dt$ meets energy requirements but φ^q is insufficient to have the gut attain its maximum capacity;
- P-3 $\int_{1\text{ da}} \varphi^q dt$ is sufficiently large that the gut reaches capacity and foraging is then either reduced or stopped entirely in order to balance the smoothed mass intake rate and the smoothed assimilative throughput rate.

Throughout the following P-3 is assumed.

A standard approximation for the smoothed mass intake rate $\overline{\varphi^q}$ occurring under assumption P-3 is

$$\overline{\varphi^q}(t) = \frac{1}{\|\mathcal{I}_t\|} \int_{\mathcal{I}_t} \varphi^q(s) ds = \rho_q m_q(t) \quad (1)$$

where \mathcal{I}_t is a time interval of length $\|\mathcal{I}_t\| = (1 + \epsilon) da$, $\epsilon > 0$, with $t \in \mathcal{I}_t$, and where ρ_q depends at most on temperature (hence, possibly on time, but here it does not because of assumptions in 2) and m_q is the time-varying mass of predator type q .

Case 1: single prey population

Let m_f denote the mass of prey species f . By the assumptions in P-3 and by (1), the number of prey of type f consumed per day by any of the type q predators is $\frac{\rho_q m_q}{m_f}$.

The number of individuals of type f per unit volume consumed is $\frac{u_q m_q \rho_q}{m_f}$, where u_q is the density (units are number · meter⁻³) of predators of type q . Both f and q are considered to be growing hence m_f and m_q are time dependent; but u_q and ρ_q are assumed constant.

Let u_f denote the population density of the single prey species f for predator q . Combining all of the foregoing provides

$$\frac{du_f}{dt} = - \frac{u_q m_q \rho_q}{m_f} \quad (2)$$

This special case of a single prey is approximately the situation for fry relative to their predators before and after the macrozooplankton bloom. Hence, (2) contains the essential behavior of that predator-prey system for two time intervals during outmigration. We note this by the following lemma for the fry system.

Lemma 1. *For interactions between prey type f and its predator of type q during some time interval \mathcal{I} , if the predator q has only f as prey during \mathcal{I} , and the density of f alone throughout some spatial domain is sufficient for (1) to hold for predator q , then the decline of f during \mathcal{I} is given by (2). In particular, foraging of q and mortality of f are nonlinear in u_f and the decline of u_f is determined by the predator population structure (i.e., number (density u_q) and age and size (mass m_q)) and by the size of individuals in f (i.e., m_f).*

Since the interest is in time intervals of a few to several weeks, the standard approximation for growth suffices, namely

$$\frac{dm_f}{dt} = \gamma_f m_f, \quad \frac{dm_q}{dt} = \gamma_q m_q, \quad \gamma_f \text{ and } \gamma_q \text{ constants, with } \gamma_f > \gamma_q \quad (3)$$

Only $\gamma_f > \gamma_q$ is considered in this Note.*

* It is left as an exercise to determine whether these results suffice to determine the consequences for f if a predator q occurs with $\gamma_f < \gamma_q$.

Let $t = 0$ be the initial time and let $u_f(0)$ denote the initial density for prey f . (2) and (3) provide

$$\frac{d}{dt} \left(\frac{u_f}{u_f(0)} \right) = + \frac{u_q m_q(0)}{u_f(0) m_f(0)} \frac{\rho_q}{(\gamma_f - \gamma_q)} \frac{d}{dt} \left(e^{-(\gamma_f - \gamma_q)t} \right) \quad (4a)$$

$$= K_f^q \frac{d}{dt} \left(e^{-(\gamma_f - \gamma_q)t} \right) \quad (4b)$$

where

$$K_f^q = \frac{u_q m_q(0)}{u_f(0) m_f(0)} \frac{\rho_q}{(\gamma_f - \gamma_q)}. \quad (4c)$$

For reasons that will be apparent, K_f^q is called here the “crash” constant. It is convenient to distinguish two functions appearing in (4): U and E are defined to be

$$U(t) = \frac{u_f(t)}{u_f(0)} \quad \text{and} \quad E(t) = e^{-(\gamma_f - \gamma_q)t}, \quad (5a)$$

and the significance of (4) is the relationship between U and E ,

$$\begin{aligned} U(0) &= E(0) = 1 \\ \dot{U} &= K_f^q \dot{E} \end{aligned} \quad (5b)$$

Only predation mortality for f is considered. That is, changes to u_f due to population flux into or out of the spatial domain are not included. The results, then, are applicable to each of a series of bounded time intervals such that during any one the “zero flux” assumption is suitable. It is with this approximation in mind that we can state that “by construction” $\dot{U} < 0$.

From (3) and (5) $\dot{E} < 0$ by construction, E is decreasing exponentially at the rate $-(\gamma_f - \gamma_q)$, that is, declining somewhat less fast than the rate at which the mass of members of f are growing. If $K_f^q = 1$ then $U = E$ by the basic uniqueness theorem of ODEs. A short calculation shows that the “biomass” $m_f(t) u_f(0) U(t)$ of f is not constant but rather increasing at a rate that just keeps up with the increase of the biomass of q , for the case $K_f^q = 1$.

But if $K_f^q \neq 1$, then by (4) U is decreasing either faster or more slowly than E . Precisely how the evolution of U differs from E for $K_f^q \neq 1$ is the subject of Lemma 2. Lemma 2 is the most important result of this Note. Everything that follows is an application or extension of this simple “Crash-Bloom Lemma.” The “crash or bloom” response is exhibited by the prey for any system wherein prey are sufficient to keep predator consumption in the neighborhood of its upper bound. Predator consumption so constrained then satisfies (1) which in turn is the source of the nonlinear relation (2) and the consequent “crash-bloom” response.

Lemma 2. (Crash-Bloom Lemma) Let f denote a single prey population and q its predator population as in Lemma 1. Restrict considerations to a time interval \mathcal{I} for which (1) holds. Let K_f^q , U , and E be as defined in (4) and (5). Then, the trajectory of $U(t)$, $t \in \mathcal{I}$ “crashes” or “blooms” according to whether K_f^q is greater or less than 1, with the trajectory of U following paths described by the following summary.

$$\begin{aligned}
 K_f^q > 1 &\implies U(t) < E(t), \quad U(t^*) = 0, \quad t^* = \frac{1}{(\gamma_f - \gamma_q)} \ln \left(\frac{K_f^q}{K_f^q - 1} \right) && \text{crash} \\
 K_f^q = 1 &\implies U(t) = E(t), \quad U(t) = e^{-(\gamma_f - \gamma_q)t} \xrightarrow{t \rightarrow \infty} 0 && \text{predatn} \leq \text{productn} \\
 K_f^q < 1 &\implies U(t) > E(t), \quad U(t) > \lim_{t \rightarrow \infty} U(t) = 1 - K_f^q > 0 && \text{bloom}
 \end{aligned}$$

Proof: The analytic solution to (4) or (5) is straightforward.

$$U(t) = \frac{u_f(t)}{u_f(0)} = 1 - K_f^q \left(1 - e^{-(\gamma_f - \gamma_q)t} \right) = 1 - K_f^q (1 - E(t)) \quad (6)$$

□

Corollary to Lemma 2. In the “crash-bloom” system of Lemma 2, the prey population f declines according to the scaling and affine shift of a single exponential,

$$\frac{u_f(t)}{u_f(0)} = (1 - K_f^q) + K_f^q e^{-(\gamma_f - \gamma_q)t}.$$

In particular, the decline is a family of functions parameterized by the “crash” constant K_f^q .

The prey population never declines exponentially for some approximately constant mortality rate. In particular, mortality rate μ is never constant but rather is related to the “crash” constant by

$$\mu(t) = \frac{d \ln(u_f)}{dt} = - \frac{(\gamma_f - \gamma_q) K_f^q E(t)}{1 - K_f^q + K_f^q E(t)};$$

$\mu(0) = -(\gamma_f - \gamma_q)$ initially; thereafter μ is monotonically increasing to ∞ or decreasing to 0 according to whether $K_f^q > 1$ or $K_f^q < 1$, respectively.

The foregoing closed form solutions, the limits, and the zero crossings must all be viewed as indicative of the shape and trend but not the actual outcome. The density u_f does not actually approach 0 in the sense of a zero-crossing, for as u_f gets small the assumption regarding predator foraging described in P-3 no longer holds. Similarly, for time t large the mass m_f gets sufficiently large so that prey f is no longer within the predation range of q . These two, prey density and prey size, act jointly in the sense that increasing individual size increases the threshold density that f must exceed to sustain predation in P-3 mode and functioning according to (1).

In contrast to the limits shown in Lemma 2, the inequality relationships between U and E presented in Lemma 2 do not require the foregoing precautions. The inequalities develop instantaneously. Whether U is above or below E can be used to characterize the “crash” and “bloom” scenarios without appealing to the limits.

Case 1 applied to pink salmon fry in PWS: Case 1 for fry is “crash”

Conjecture 1. Available evidence indicates that for time intervals in which pink salmon fry are a single prey for one or more of their predators and occurring at densities sufficient for predator foraging according to assumption P-3 and (1), then they will be in “crash” mode. Attaining fry densities or growth sufficient for “bloom” seems problematic.

The following numerical examples provide the basis for Conjecture 1. Briefly we consider fry as single prey for any of adult pollock, adult salmon, and juvenile pollock. The following parameters for K_f^q are used for all three predators.

temp (C)	γ_f	m_f (g)
9	0.04	0.03

adult pollock A range of mass for adult pollock is 300–440 g. For $\gamma_q = 0.005$ and $\rho_q = 0.02$ then

$$K_f^q \leq 1 \iff u_f \geq \frac{300}{0.3} \frac{0.02}{0.035} u_q \approx 570 u_q$$

A pollock biomass of 30 kM, with mean mass $m_q = 300$ g, is equivalent to 10^7 predators. Wild and hatchery fry combined are approximately 10^9 . Hence, $u_f/u_q \approx 100$. This estimate places u_f substantially below the value needed to be at the threshold of “bloom”.

For $u_f/u_q = 100$, then $5.7 < K_f^q < 8.4$, and $3.6 < t^* < 5.7$, where t^* is the time-to-zero during a “crash”.

adult salmon Returning adult pink salmon are typically greater than 3% of the released fry, and of those returning approximately 25% are early (June) returning pink salmon. Here again $u_f/u_q \approx 100$ using only early returning adults.

Mass for a returning adult pink is approximately 1500 g. For $\gamma_q = 0.0$ and $\rho_q = 0.01$ then

$$K_f^q \leq 1 \iff u_f \geq \frac{1500}{0.3} \frac{0.01}{0.04} u_q \approx 1250 u_q$$

This is an upper bound, for it uses the fry release mass. For fry growth to .6 g or even to 1.0 g the $400 < u_f/u_q < 600$. If the full 25% of the 3% returning adults constitutes a predator population, then u_f/u_q is at least a factor of 4 above the switch to “bloom.” The involvement of returning adult salmon is not well developed.

juvenile pollock For juvenile pollock (age 1,2) of, say, 55 g, then

$$K_f^q \leq 1 \iff u_f \geq 105 g.$$

This illustrates that the “depth” of the “crash” condition can be substantially less for equivalent population densities with differing population structures.

Case 1: single prey, multiple predators

Only a minor change is needed to extend Case 1 to multiple predators. For this case q is now a set of indices $\{q_j, j = 1, \dots, n\}$. Summations over the predators is denoted by summation over the set q of indices.

For a set of predators, the rate of decline for f is simply the result obtained by linear superposition applied to the right side of (2). Results analogous to (4) and (5) follow directly,

$$\frac{d}{dt} \left(\frac{u_f}{u_f(0)} \right) = \sum_q K_f^q \frac{d}{dt} \left(e^{-(\gamma_f - \gamma_q)t} \right) \quad (7a)$$

which has the solution

$$\frac{u_f(t)}{u_f(0)} = 1 - \sum_q K_f^q \left(1 - e^{-(\gamma_f - \gamma_q)t} \right). \quad (7b)$$

The foregoing definition of “crash” and “bloom” is used: the scenario is “crash” if u_f goes to zero in finite time and “bloom” if $\lim_{t \rightarrow \infty} u_f = u_0 > 0$. From (7b) “crash” is the case for $\sum_q K_f^q > 1$ and “bloom” for $\sum_q K_f^q < 1$.

An approximation for (7a) in the form of (4b) can be useful. Let $\bar{\gamma}_q = \max_q \{\gamma_q\}$ and $\underline{\gamma}_q = \min_q \{\gamma_q\}$. Then from (7a)

$$\left(\sum_q K_f^q \right) \frac{d}{dt} \left(e^{-(\gamma_f - \bar{\gamma}_q)t} \right) > \frac{d}{dt} \left(\frac{u_f}{u_f(0)} \right) > \left(\sum_q K_f^q \right) \frac{d}{dt} \left(e^{-(\gamma_f - \underline{\gamma}_q)t} \right). \quad (8)$$

Neocalanus in PWS: testing the consequences of macrozooplankton as a single prey having multiple predators.

It is a SEA conjecture that during the macrozooplankton bloom *Neocalanus spp.* C4 and C5 instars become the preferred or dominant prey for all predators that feed upon both zooplankton and fish. To the extent this holds, the *Neocalanus* meet the criteria for the foregoing case of one prey, many predators.

For *Neocalanus* in PWS, the mass changes by a factor of approximately 3 during the C4 instar. For an interval of 15 days between molts, the growth rate per unit mass during C4 is approximately 0.20. The initial mass is estimated as 8×10^{-4} g. With these and previous values for pink salmon fry and for adult pollock, estimates for the conditions needed for $K_f^q < 1$ are

$$\begin{aligned} \text{adult pollock } K_z^q \leq 1 &\iff u_z \geq \frac{440}{8 \times 10^{-4}} \frac{0.02}{0.2} u_q \approx 55 \times 10^3 u_q \\ \text{pink salmon fry } K_z^f \leq 1 &\iff u_z \geq \frac{0.3}{8 \times 10^{-4}} \frac{0.10}{0.16} u_f \approx 235 u_f \end{aligned}$$

This suggests that for $u_q \approx 10^{-3}$ and $u_f \approx 0.1$ then $K_z^q + K_z^f < 1$. However, if $u_f \rightarrow 1.0$ or $u_q \rightarrow 10^{-2}$, then, at least locally, the density for macrozooplankton will approach zero.

In the following it will be assumed that $\sum_q K_z^q < 1$ and, hence

$$\frac{d}{dt} \left(\frac{u_z}{u_z(0)} \right) > \frac{d}{dt} \left(e^{-(\gamma_z - \min_q \gamma_q)t} \right) ,$$

at least during some interval during the (apparent) zooplankton bloom.

3 Bibliography

Part I-C
Summary of 1997 progress
The pink salmon fry survival model with 1997 extensions:
ecosystem production processes and their record in code-group survival

Technical note from SEA

The pink salmon fry survival model
with 1997 extensions:
ecosystem production processes
and
their record in code-group survival *

J. E. H. SEA and M. N. R. SEA¹

Summary

The SEA Project is developing physical-plankton-nekton models for the survival of juvenile fish in Prince William Sound. This reports results from the nekton model for juvenile pink salmon. The model is a space-time model in which models for foraging, gut evaluation, and bioenergetics are embedded within diffusion-taxis models for the dispersion of all interacting nektonic species of the subsystem.

Analyses of both the models and the coded wire tag data for Prince William Sound hatcheries have shown that successful tracking of the production processes requires the tracking of each release group. There is no "mean" fry outmigration.

The SEA fry model has been extended in the sense that each release group for each hatchery is modeled as a separate stock. The model specification fully encompasses this extension. The model is configured with a taxis providing the migration velocity, with calibration provided by 1994 measurements from Willette.

This reports on a simulation of WHN for 1994 with eight separate release days and the results from the model for the case of no macrozooplankton. This case is to simulate a pre-bloom condition and a multiple release version of previous simulations.

A second simulation is shown wherein analyzed data sets, one from Willette and one from Cooney and Coyle, were used to simulate the actual bloom onset.

* Sponsored by The Exxon Valdez Oil Spill Trustee Council, Anchorage, AK
Restoration Project 97320

¹ J, E, H, M, N, and R identify projects of the Sound Ecosystem Assessment (SEA) Program.
www.pwssc.gen.ak.us/sea/sea.html

1 An example with 1997 extensions

1994 WHN and the model configuration

The release schedule for WHN for 1994 is shown in Figure 8. The actual release days are shown along the top of Figure 11. The focus will be on the first seven release days for this discussion.

The model holds each "pen" until the release day, and then deposits instantaneously all fry into a one dimensional domain representing the outmigration path from WHN to the southwest entrance to the sound. The one dimensional domain represents a 500m wide by 20m deep shoreline domain of 90km length. The one-dimensional coordinate is oriented so that 0km is at the southwest entrance just south of AFK, WHN is at 90km, Cannery Creek is at a greater distance, and Solomon Gulch at the end, essentially as shown in Figure 3. Upon a release at WHN, there is a pulse at 90km with area equal to the release for the day.

The diffusion-taxis model is configured for a constant southward migration by advection plus a diffusive spreading. The diffusivity and the advection velocity were jointly calibrated so that the leading edge of the pulse was consistent with the measurements of Willette. At this time no further migration responses are included, such as zooplankton density, tidal velocity, and the like.

Two scenarios for predators have been tested. First, the predators were configured to move in response to releases. This had several consequences of interest in terms of processes, but the magnitude of the impact warranted using the simpler uniform predation shown in Figure 11. This uniform predation density is used to begin an "inverse" assessment of predation densities consistent with recorded survivals, especially the release-day sequence of survival values.

Progress of outmigration

Figure 11 is a snapshot of the release-day groups on day 134, that is, 3 days after the seventh release-day (131) and 19 days after the first release-day (115). The plot shows the extent of spreading of each of the releases in the time since release, the distance southward traveled by the group, and the extent of the mortality to the group. The actual integral of each group is shown across the top, along with the survival, that is the ratio of the integral to the initial release.

The example in Figure 11 has the same predator density as Figure 1, however, it uses more realistic values from the data analysis provided by Willette: the temperature at day 134 was 5.1C for the upper 20m, and the predator size is 475mm, 700g. See also Figure 14 for values.

A second snapshot at day 149 is shown in Figure 12. The first release group after 34 days has its leading edge approximately 45km south from WHN.

2 Results from a test case

Crash or Bloom?

To compare the simulation with Figure 1, the survival for each group is plotted in Figure 13 in a manner similar to that used in Figure 1. However, the results of the Lower Bound note cannot be applied directly for now each of the groups is acting as alternative prey for each of the other groups. However, in general, the shape of the plots in Figure 13 indicate that in finite time survival will tend toward zero, hence this is crash.

In addition to the alternative prey issue, the diffusion of fry reduces the fry density during the migration. This spreading, in terms of the lower bound, moves them closer to crash.

The point here is that the lower bound is the qualitative description but the actual simulation is needed for any specific case. Even this simple scenario has numerous examples of how many factors contribute to a specific outcome.

Predator swamping

An often mentioned "rule" is that more fry should yield better survival due to "predator swamping." This is precisely the content of the lower bound lemmas.

However, the simulation reveals that in addition to a general effect there is a local effect due to fry as self-alternative prey. The linear plot of Figure 13 shows that the last release is dropping faster than the ones preceding it, and indeed is approaching the earlier releases, even though the last has been out for a very much shorter time period. This is because the pen releases in the middle are the ones with self-alternatives, whereas the first and the last are short changed. This "dooming" or local maximum for survival in the middle pen releases occurs in the hatchery data

Pre-bloom predation

The last result from this simulation without *Neocalanus* is to approximate the consequences of predation during a period prior to the development of a significant diversion due to macrozooplankton. In Figure 14 the survival shown in Figure 11 is simply plotted against the day of release—precisely as was done with the PWS hatchery data in Figure 10. The resulting survival vs. release-day curve would have resulted if the WHN release had progressed to the state in Figure 11 and thereafter the predation was substantially reduced by the bloom. The survival pattern due to the first period without refuge would still be retained in the population, and would appear as shown in the top panel of Figure 14.

If instead the bloom did not cease predation until day 149, then the pattern in Figure 12 would be retained—as shown in the middle panel of Figure 14. If the predation were three times greater and stopped at day 136, the pattern in the lower panel would be obtained.

Tentatively, this identifies how one of the system production processes is recorded in the coded wire tag records of survival, and the records for 1994 for all hatcheries have records with this pattern.

3 Results from test case with analyzed data

A first simulation with analyzed data sets provided by Willette (temperature and predators) and Cooney and Coyle (zooplankton) was completed during 1997. The results plotted in the manner of Figure 13 are shown in Figure 15. Although it appears that predation is not adequate or zooplankton switching too great relative to the record for WHN for 1994, the pattern of initial predation decline in the manner reflecting the crash scenario followed by the sharp reduction of predation losses is clear.

Part II
Report on 1997 progress
Database
C. S. Falkenberg



Project 97320-J: Information Systems and Model Development
FY97 Report to the *Exxon-Valdez* Oil Spill Trustee Council

Part II: DATABASE

Charles S. Falkenberg
April 15, 1998

Summary

As with FY96 the database development effort in FY97 was split between data management activities and the development of the software tools to access those data. However, with the successful implementation of the web based retrieval tools in FY96, the focus of FY97 was on data management and ingestion in order to expand the data content of the SEA DataWeb. This included adding new datasets or "data types" as well as augmenting the data archived in for existing datasets. Several special project were also undertaken in FY97 to reformat existing data to make it more usable by the researchers within SEA. Together these data management tasks combined to form the bulk of the FY97 database development.

Although software tool development was secondary, the usability of the existing tools was improved and new user interfaces were added to support the added datasets. Part of this work included the initial development of an interface to the predator fish data. This web based interface is more elaborate then the ones used for the other SEA datasets. In addition to the integrated retrieval with other SEA datasets, this interface allows a small, specific, subset of the predator fish data to be displayed and downloaded.

The funding for the database effort in FY97 was .5 FTE or six months. Of this time nearly 40% was allocated to data management and ingestion, 30% was devoted to software tool development and 20% was devoted to EVOS reporting requirements and conference attendance. This last 20% included the AAAS conference in Valdez and the EVOS annual workshop. In addition several unfunded activities in FY97 bore an impact on the development of the SEA DataWeb. These included an investigation of the NASA EOS data archiving system and the development of the Shepard Point Region Environmental Assessment Database (SPREAD) for the Prince William Sound Science Center.

Expanding the content of the SEA DataWeb

The primary focus of FY97 was to expand the data content of the DataWeb and to provide data reformatting where it was needed. This included three basic activities: adding new types of data, reformatting existing data so it was more usable, and augmenting existing datasets with data from recent field seasons. Some of these new data types required the development of new retrieval tools which will be discussed in the next section.

Two new SEA datasets were ingested into the SEA DataWeb. Echo acoustic data on herring

abundance was ingested over the summer and predator fish data was ingested in the fall. The CTD and zooplankton datasets were augmented with data from recent field season and the zooplankton data was reformatted for use by the cross channel nekton modeling application.

The data ingestion process includes creating a description of the data and constructing the necessary database tables to allow the data to be retrieved. In the case of the herring acoustic data these tables look similar to the tables which are used by other SEA datasets. The predator fish data has a much more complicated structure, however, and required new processing and indexing techniques. These fish data are imported from another DBMS and although the volume is not high, multiple database tables are needed to capture all of the information. In the SEA DataWeb, the basic schema of the original tables is augmented with new data elements that allow these fish data to be viewed in an integrated way with the other DataWeb datasets.

Reformatting existing data was a secondary but important data management task for FY97. This is a data preparation step which allows data from the DataWeb to be made available to users in a more accessible format. Three different datasets were reformatted, the ocean circulation data, the bathymetry data and the herring acoustic data.

Of these the ocean circulation reformat was perhaps the most significant. In order to make these large data files available for the variety of platforms used by SEA researches, the circulation data were reformatted into the HDF scientific file format. This is a self-describing, transportable data format which keeps data in a binary representation and which can be read by programs running on different workstations architectures like SGI, Sun, or DEC or on PC's running Windows. The reformatting utility included several routines which can be used by the SEA researchers to read the data in the HDF file. Once reformatted these data were made available to various SEA researchers.

The bathymetry data of Prince William Sound was reformatted and converted to allow the creation of contour maps of the Sound and to integrate depth into several of the modeling applications. These bathymetry data were reprojected and subsampled into the required grids and coordinate system. Finally, several acoustic datasets were reformatted for use with the SEA visualization software.

Part of the FY97 data management activity was the acquisition and reformatting of external data which is relevant to the SEA project. These external data include both weather and tide data collected at stations around Prince William Sound and archived by NOAA. Software utilities which can automatically download both types of data from NOAA were created. The tide data have been downloaded, reformatted and are available through the DataWeb. The weather data are highly coded and need additional work but are currently being downloaded and archived.

Improving the DataWeb Software

The focus of FY96 was the implementation of the WWW software for the SEA DataWeb. This was a secondary focus for FY97 but several improvements were made in the basic tools, and the functionality was extended to incorporate new datasets. The interface to Directory Services was improved and expanded, and a new interface was created for both the echo acoustic data and the

predator fish data. In addition, several improvements were made in the software development environment in order to support the DataWeb mirroring.

A limited file name search capability was added to Directory Services as well as the ability to download a single zip file containing multiple data files. The new bathymetry data and the tide data were added to Directory Services in addition to the zooplankton and CTD data from the new field seasons. The initial choice page was also modified to allow access to Directory Services, Query Services, and Modeling Services.

Query Services was updated with a new user interface to the echo acoustic and predator fish data. The interface to echo acoustic data is similar to the other dataset selection pages but allows for echo acoustic specific selection criteria to be entered. A new page was also added for displaying all of the columns of echo acoustic data from the tables in the database.

Accessing the predator fish data is somewhat different than the other SEA datasets. The predator fish data is contained in eight different database tables that could be considered eight different datasets. However, the data from the different tables is linked closely and so it being made available together in Query Services. The interface to the predator fish data allows the entry of selection criteria and then a subset of the data matching those criteria from all selected tables is displayed. This required new utilities and display pages and is a new paradigm for retrieving SEA data.

The predator fish data are also available, in an integrated way, along with the other SEA datasets through the standard, cross dataset, selection page. The location of the fish catches will be displayed on the interactive map tool along with the other SEA datasets and a dataset containing the length and weight of the predator fish in a single catch can be downloaded along with the other SEA datasets in the group. Work on the final interface to the predator fish data will continue into FY98.

The utility used to download the tide data is not part of the access tools for the SEA DataWeb but the development of this tool has potential long term value for SEA. This utility is written in the Java programming language and uses the features built into this language to open a connection to a web site, download data and write out a local archive file without using a browser interface. The advantage of this utility is that it can be triggered on a regular basis to retrieve external data into a local archive.

One of the features of this utility is that it bypasses the form fill-in page and supplies all of the parameters which would the web server expects from that page. The server then responds by supplying the data which is normally returned in response to the submission of the HTML form. Although this utility was written to download tide data several of the objects which make up this utility can be reused for downloading data from similar web site. Taken together these changes represent a significant improvement in the capability of the DataWeb Tools.

Conferences and Related Projects

In addition to expanding the data content and extending the functionality of the SEA DataWeb

several related activities were undertaken during FY97. These included the attendance at several relevant conferences and the creation of a data system similar to the SEA DataWeb. Some of these activities, although relevant to the long term mission of building a the SEA DataWeb, were not funded as part of FY97 EVOS funding. The funded activities included a presentation at the AAAS conference in Valdez and attendance at the EVOS yearly workshop. Unfunded activities include involvement with the data archiving systems for the NASA Earth Observing System NASA-EOS, updates to the Informix DBMS, and a data system for the Shepard Point regional environmental assessment.

Two conferences were included in the FY97 database development funding. The first was the AAAS conference in Valdez and the second was the EVOS annual restoration workshop. The content and structure of the DataWeb was presented at the AAAS conference and the feedback was positive. This status of the SEA DataWeb was also presented at the associated SEA planning meeting in Valdez.

Unfunded activities which are of particular importance to the evolution of the SEA DataWeb included participation in the NASA workshop devoted to the data archiving tools needed to support the large volume EOS database. Several tools which allow spatial selection and reformatting of EOS data may be available and quite useful to the SEA DataWeb.

In addition, insight into the evolution of the Informix DBMS was gained during a multi-day meeting at the headquarters of the Informix technical team in Oakland Ca. Informix remains committed to the concept of extensible database management systems and it has greatly expanded its spatial data management offerings. These offerings come from partnerships with two GIS vendors, ESRI who makes the Arc/Info product and MapInfo. It is clear from these different partnerships, and from the spatial products that are supported by Informix itself, that Informix will continue to support several options for the management of spatial data.

Finally a data system similar in some aspects to the SEA DataWeb was developed to support the Shepard Point Road Environmental Impact Statement. This work was funded by the Prince William Sound Science Center is designed to allow public access to the data collected as part of the environmental impact statement. The data system supported a the selection and display of data from a wide range of database tables using time, date, location and species as possible selection data. This system provided some of the concepts used to implement the interface to the predator fish data.

Future work on the DataWeb

The goals for FY98 will again include both the management and ingest of the SEA data and the development of user tools to retrieve those data. FY98 will see the wrap up of the tool development into a final user interface to SEA data. This will include some significant improvements to the spatial selection and display and should include a new map display. Additional datasets will also be added to the DataWeb as the individual projects wrap up the processing that is necessary before the data are submitted to the archive.

Part III-A
Report on 1997 progress
Web-based Communications
J. R. Allen



Part III: WEB-BASED COMMUNICATIONS

Jennifer R. Allen
April 15, 1998

ABSTRACT

The SEA internal web site (Intranet) has been functional since September, 1995, providing electronic mechanisms to facilitate collaborative interactions critical to the mission of SEA. This annual report addresses features added or expanded in the last year. These include a Synthesis work area; Modeling Progress area; Management Collaboration area; and the State of the Sound report, which is a compilation of near realtime data for Prince William Sound. Detailed usage statistics for the system are also presented.

INTRODUCTION

The rationale and design of the SEA internal web site (Intranet) were reported to EVOSTC last year (Allen et al., 1997) and were the subject of a presentation to the AAAS Arctic Division Science Conference in Valdez, AK, in September 1997 (Allen and Patrick, 1997). Briefly, the purpose of this work is to provide electronic collaboration mechanisms to the multi-disciplinary, geographically dispersed SEA research team. Tasks served include scheduling, data sharing, joint assessment of data across disciplinary boundaries; preparation of joint presentations and manuscripts; and liaison between the field and modeling efforts. The ongoing quest is to help integrate the observations, expertise and knowledge of each investigator into a joint system-wide synthesis, with translation into management and monitoring applications.

Previously reported features include a dynamic results archive, threaded discussion server, interactive papers collaboration work area, platform-independent file upload and exchange tools, as well as general informational documents such as calendars, maps, cruise plans, cruise reports, and announcements. The present report addresses new developments made during FY97. Detailed usage statistics for the internal web site are also presented (Appendix 1).

FY97 ACTIVITIES

In addition to maintenance of existing Intranet functions, development work continued during FY97. The new additions and expanded features reflect the shifting emphasis in SEA from field work to synthesis activities. Areas in the Intranet that were new or expanded during FY97 include:

1. Synthesis work area
2. Modeling Progress area
3. Management Collaboration area
4. Near Realtime Data delivery work

Each of these will be described individually, following a brief synopsis of general activities.

General Activities

The areas and their relationships within the SEA Intranet are diagramed in Figure 1. A new feature, this diagram is posted on the web site in the form of a clickable map and gives direct access to each of the named regions. The map is instantly reachable via the "SITEMAP" icon found on every page.

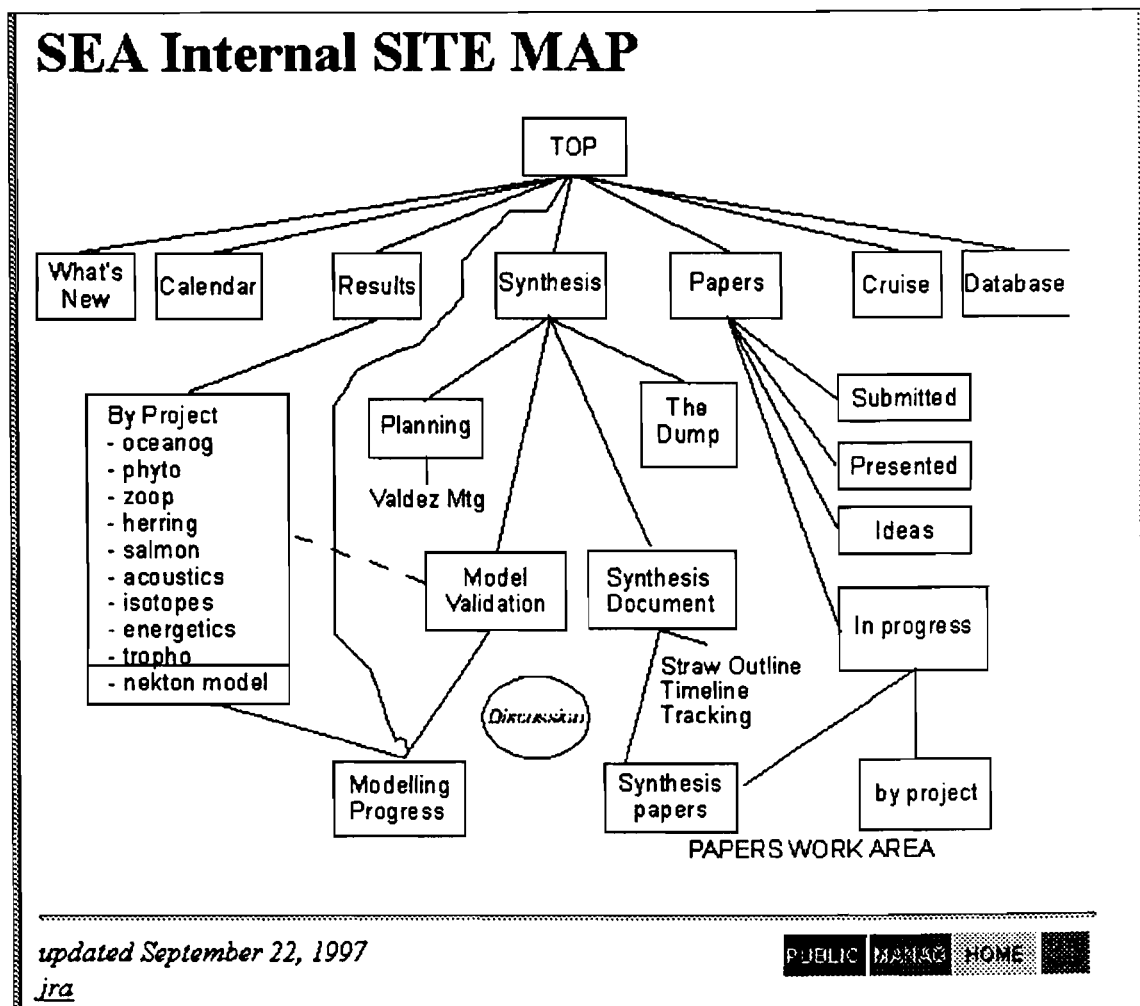


Figure 1: Layout and area relationships in the SEA Intranet

The opening page of the SEA Intranet (Figure 2) is password-protected and provides secure access to the rest of the internal functions, including the database. The structure and functionality of this opening page was updated in FY97 to reflect the increasing emphasis on modeling and synthesis and to promote interrelationship between the SEA internal areas and the Management Collaboration area.

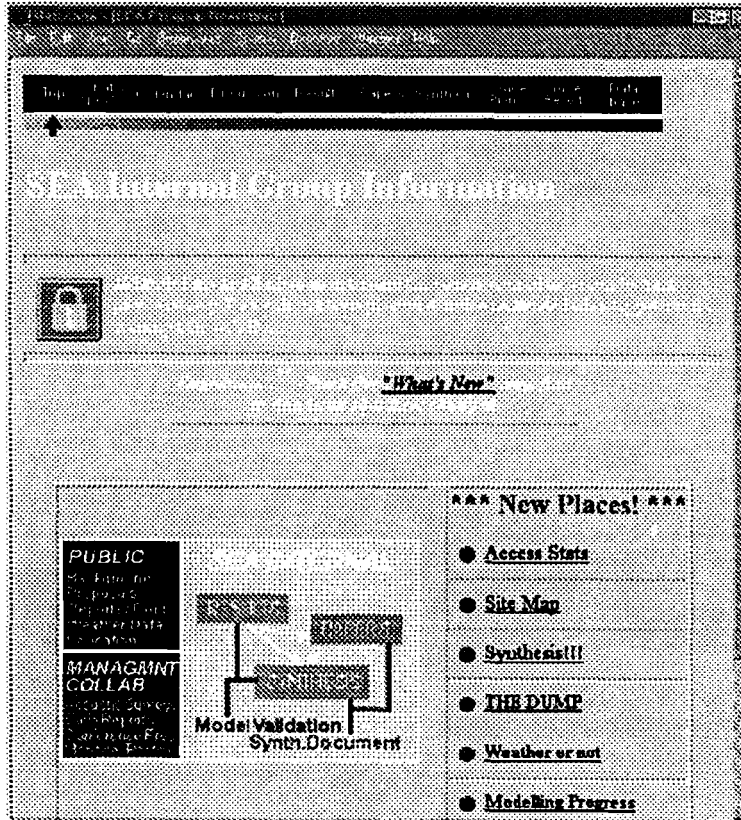


Figure 2. SEA Internal Web - reorganized opening page

The schematic in the lower left quadrant (Figure 2) is a simplified version of the sitemap, showing the Intranet divisions into major areas. This diagram also is hyperlinked and clickable, providing quick access to the various work areas. The text list at lower right is used to introduce new features as they are added to the site. The clickable cross-site menu bar, visible at the top of Figure 2, is present on most pages of the web site and incorporates a graphic indicator of current location.

Other changes in FY97 included an expansion of the number of draft papers online, and an increase in web authoring by individual researchers and staff, and improvement in access tracking. Software was obtained (Analog v2.11 for Unix) and written (PERL scripts) to allow convenient analysis of access logs with summaries both by user and by area accessed. Daily updates of these

summaries are automatically posted to the internal website. Finally, the file upload area or “dump” site has proven successful and is a frequently used mechanism of file exchange, particularly in the case of files that are too large to transmit as email attachments or which are of general interest to multiple SEA team members. This application, which was written in the PERL language, was described in more detail in the FY96 report.

Synthesis Work Area

The SEA Synthesis Work Area was established as a result of a SEA synthesis planning meeting held in September 1997. Its purpose is to support the dual ongoing tasks related to synthesis: model validation and preparation of a joint multi-chapter report detailing the new ecosystem level results and understanding which have resulted from SEA research. The site was also used for assembly of materials during preparation of the 1997 SEA presentation made to the January 1998 Restoration Workshop. Figure 3 shows the entry page to the synthesis area.

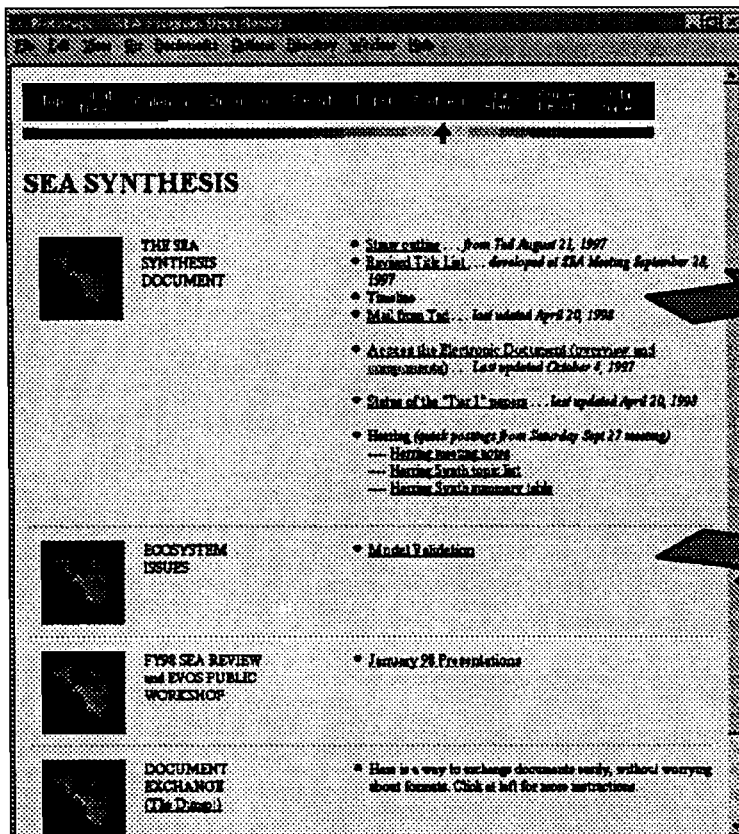





Figure 3 (left)
SEA Synthesis area opening page

A. Synthesis document work area (detail below)

B. Model validation work area (detail in following section)

Figure 4 (below)
SEA Synthesis Document Work Area
(first row of 12 rows)

SEA SYNTHESIS DOCUMENT							
Monday, 27-Apr-98 18:52:17 AKDT							
HELP ... How This Page Works ... Display help file in: This Window Separate Window							
<div>  Look </div> <div> Bold/red "Look" in the table indicates component has web-browsable material available for online viewing. </div>							
Overview Table							
CHAPTER	WHO	Key "Tier 1" Papers to be cited	TARGET/STATUS				Comments
			Data	Outline or Key Points	Draft	Figures	
I. Introduction: What is SEA?	Cooney, Thomas, Torie Baker, et al.		Data Target date: Status: completed	Outline Target date: Status: first draft done	Draft Target date: Status:	Figures Target date: Status:	<div>  Add a Comment </div> <div>  Print Comments </div> <div> Number of messages: 1 </div>
			<input type="checkbox"/> STATUS UPDATE	<input type="checkbox"/> SEND A FILE	<input type="checkbox"/> GET A FILE		

The Synthesis Document work area (Figure 4, previous page) is laid out as a table, in which each row is a chapter and each column is an attribute or target for that chapter. The basic structure is shown in Figure 4, which has been cropped to display the layout for the first row only. This table provides an at a glance summary of the status of work and also gives entry to deeper levels of detail on each chapter. Hyperlinks in each row provide access to related papers in preparation, bibliographies, data summaries where applicable, drafts and figures. The three buttons below each row deliver a status update or allow users to send and retrieve binary files, respectively. The two buttons in the right-hand column provide access to notes and discussion on the chapter: users can add comments to the dialog as well as review previous comments which are logged chronologically. It is anticipated that this work area will be heavily used during the final synthesis year of the SEA program.

The synthesis entry page (Figure 3) also gives entry (arrow B) to a new section for model validation work (Figure 5, at left). This area has been built to house model simulation output and corresponding comparative field data during the model validation and refinement process. It is also a repository for results of a planned set of scenario simulations under selected realistic input parameter settings, and will provide an online focus for emerging findings and discussion. This page also links to the extensive Modeling Progress area maintained by Vince Patrick (see next section).

TOCD	NRSC	BDYR	SPCD	ALNO	RLWT	BOHN	BODY	ENHNS	ENBY	ALYR	S
1301010104	114	87	440	89280153	0.21	4	25	5	17	88	
1301010105	114	87	440	9239753	0.21	5	10	5	10	88	
1301010106	114	87	440	11622113	0.23	5	31	6	1	88	
310000	118	87	440	1513	-9.99	5	16	3	16	88	
1301010109	115	87	440	35322711	0.21	5	10	6	5	88	
1301010114	115	87	440	40251430	0.21	5	9	5	16	88	
1301010110	120	87	440	37200196	0.25	5	6	5	6	88	
1301010111	120	87	440	17002558	0.37	5	17	5	17	88	
1301010112	120	87	440	33213406	0.33	5	14	5	14	88	
1301010113	120	87	440	43414107	0.37	5	17	5	17	88	
1301010107	122	87	440	184277200	0.25	5	1	5	14	88	
1301010106	122	87	440	11342361	0.23	4	29	5	16	88	
1301010301	114	88	440	40793295	0.25	4	24	4	29	89	
1301010302	114	88	440	32598861	0.28	5	15	5	25	89	
1301010303	114	88	440	43331812	0.23	4	27	5	15	89	
1301010309	114	88	440	43772606	0.25	5	1	5	31	89	
1301010306	115	88	440	10033836	0.21	5	5	5	5	89	
1301010307	115	88	440	20702880	0.23	5	5	5	7	89	
1301010308	115	88	440	28235320	0.25	5	25	6	1	89	
1301010207	120	88	440	21405470	0.31	4	23	4	25	89	
1301010208	120	88	440	19903146	0.34	4	28	4	28	89	
1301010209	120	88	440	20284352	0.81	5	19	5	19	89	
1301010210	120	88	440	14412130	0.28	4	28	4	28	89	
1301010211	120	88	440	32610684	0.50	5	16	5	16	89	
1301010212	120	88	440	9208873	0.40	5	4	5	4	89	
1301010213	120	88	440	10693597	0.40	5	4	5	4	89	
1301010304	122	88	440	112241525	0.23	4	23	4	30	89	

Figure 5. Model Validation work area

Modeling Progress area

The Modeling Progress area is an extensive subsection of the Intranet which is maintained by Vince Patrick and modeling colleagues as a medium for communication of emerging modeling findings to other SEA researchers. It can be accessed directly from the top level page as well as from the synthesis page and model validation sections. Maintained in chronological order, this section traces findings and posts items for review and discussion. A few representative posting examples are illustrated below (Figure 6a-c).

Most recent result from the qualitative analysis of fry model equations

Simulations with the full space-time fry survival model had shown that fry survival could be quite sensitive to initial values for predator and fry population densities. The source of this sensitivity was not immediately obvious.

During the last months a priority has been a qualitative analysis of the solutions to the model equations sufficient for an explanation of the properties exhibited by those simulations. The most recent result of that analysis is presented.

The simulations typically show a first time interval of population movement, then a second time interval with locally homogeneous populations.

The conditions assumed are spatially uniform, constant populations, with each population assumed to remain invulnerable to the other.

A corollary of the analysis is that a population either "blows up" or "goes extinct" within a few days).

An unanticipated finding is that populations in established states have a mean length of population persistence.

The report is a sequence of pages:

- [title page](#)
- [abstract pg 1](#)
- [abstract pg 2](#)
- [page 1](#)
- [page 2](#)
- [page 3](#)
- [page 4](#)
- [page 5](#)
- [page 6](#)
- [page 7](#)

Brief report of results ("flash" report)

This brief report will use relationships that are recent in the applied disciplines and will forego the linking of relationships to the SEA foraging - bioenergetics model (units of gm/dm²).

Let ϕ_f^q denote the foraging rate of predator q on f .

~~Let ϕ_f^q denote the foraging rate of predator q on f .~~ A spatial domain of approximately uniform density is assumed so that, at most, ϕ_f^q varies with

Figure 6a. Use of Intranet for posting of emerging findings in real time, allowing rapid dissemination of results for feedback and discussion.

A further part of the problem statement is

to apply an estimate for survival for the ocean (OOA) phase of pink salmon and thereby forecast an upper bound for adult salmon returns for the following year.

Spatial context of the problem statement

The map at the right shows the spatial context for the problem statement. This map and several companion maps were prepared to describe specific space-time survival issues (hatchery interactions, aggregation in the south in late August, fry density). It is shown here since it seems a simple reminder of both spatial and multidisciplinary aspects of the problem statement. The symbols N_s, N_c, N_w, N_e refer to the total released at Solomon Gulch, Cannery Creek, WHN (Ester), and AFK. The symbols S_pws and S_ooc refer to survival during PWS and the oceanic periods, respectively.

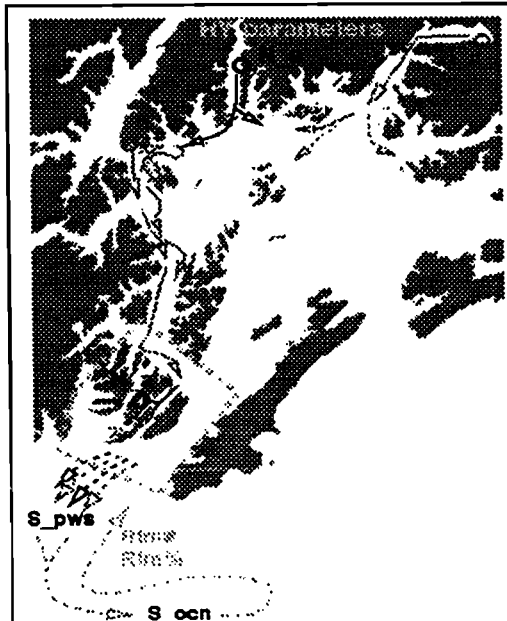


Figure 6b (left)
Use of Intranet for archival postings of SEA's developing description of the system

returns, and survival for the year for each of the four hatcheries based upon estimates without the use of coded wire tags. Data for 88 through 95 is substantially more complex because of the introduction of coded wire tags.

Possibly the greatest in years 94 and 95 - data widely reviewed within

This review of PWS has

- Part 1: yearly
 - cumulative
 - variable
- variables by rel.
 - Part 2: data
 - Part 3: tracks
 - cumulative
 - variable
- Part 3: summary progress of each
 - time from
 - the "dev"
- QC Notes: Res 1997

Tue Aug 26 08:

Model for over First formulat

The text is not yet "Te

first formulation

Tue Sep 16 16:5

Most recent re

Simulations with the fu

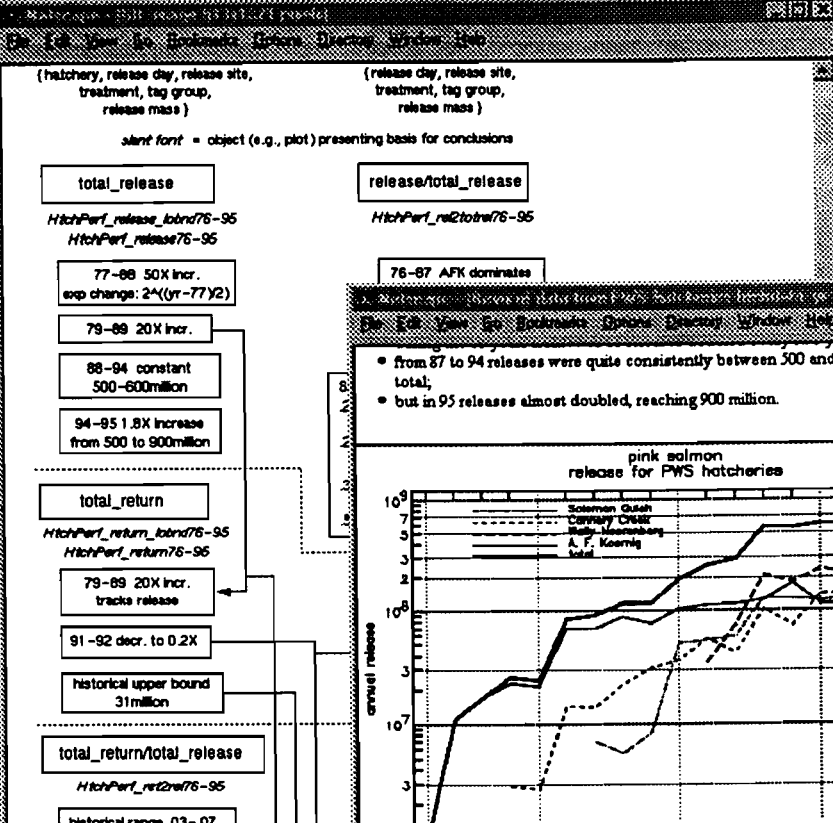


Figure 6c (below)
Use of Intranet for sharing in-depth reviews of data relevant to modeling results

Management Collaboration work area

The management collaboration work area was established with the intent of providing an online forum for exchange between SEA researchers and PWS resource managers. It currently exists in functional prototype form although is not yet in routine use. Features to date include postings of early release data, compilations of acoustic survey results, pre-release draft reports, and an index to abstracts presentations of all SEA presentations. There are also facilities for upload of postings from managers and for email feedback.

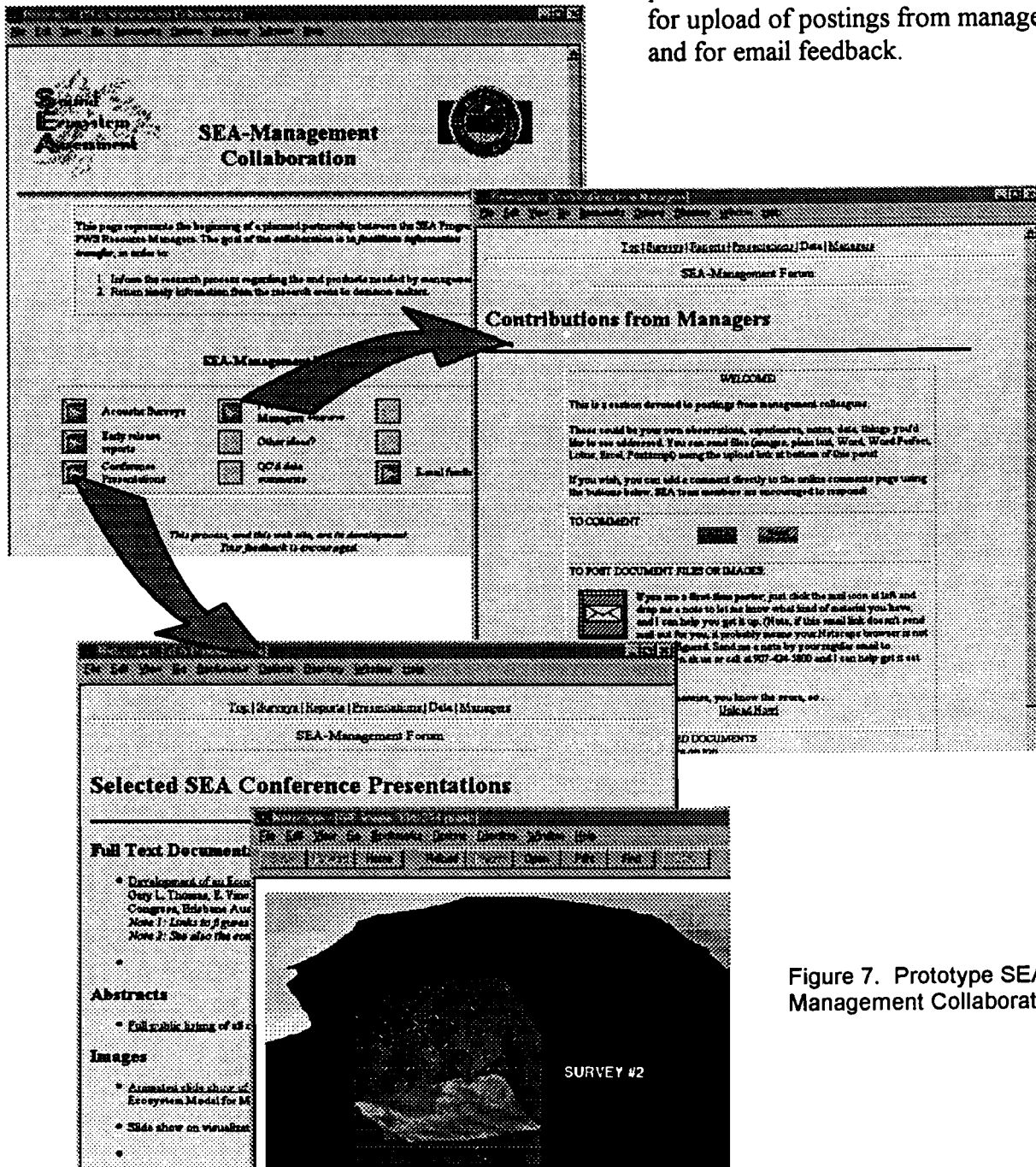


Figure 7. Prototype SEA-Management Collaboration area

REFERENCES

Allen, J.R., Patrick, E.V. and Cooney, R.T. (1997) The SEA Intranet: Scientific collaboration in a shared information space by a multidisciplinary, geographically distributed research team. In preparation.

Allen, J.R. and Patrick E.V. (1997) The SEA Intranet: Story of a long-distance collaboration. Presented at 48th AAAS Arctic Division Science Conference, Valdez Alaska, September, 1997.

Stein, L. D. (1998) Web Security: Reference Guide. Addison Wesley Longman, Inc., Reading Massachusetts. Part II: Client side security. Part III: Server side security.

APPENDIX 1: Usage Statistics for SEA Internal Web Site

- A. June 96 to present, summary of accesses by Investigator
- B. June 96 to October 97: detailed report.
- C. October 97 to present: detailed report.

Please note: these reports cover the SEA internal (restricted access) area only.

Activity in the public SEA web site will be tabulated separately.

A. Usage Statistics for SEA Internal Web Site, by Investigator

Please note: this report tabulates only whole pages accessed. It does not count multiple items retrieved from a single page. This was a design decision intended to best capture actual usage intensity. The numbers below are therefore lower than produced by standard access counters which log every mouse click and every graphic logo, line or button delivered as a "hit".

[Image]

[Image]

Back to Stats Menu

SEA Intranet Access Statistics ANALYSIS BY USER

- o June 96 to Today
- o Last 30 Days
- o Last 24 Hours

=====

REPORT PREPARED: Sat Apr 25 04:00:35 AKDT 1998

=====

Total Requests

FOR PERIOD: June 1996 to TODAY

Person	# of Pages Accessed	
-----	-----	(* = 23 accesses or part thereof)
allen	3727	*****//
baker	44	**
bishop	34	**
bodnar	34	**
brady	2	*
brown	72	****
clapsadl	140	*****
cooney	172	*****
eslinger	212	*****
falkenberg	127	*****
foy	92	****
gay	17	*
guest	5	*
hauser	52	***
kirsch	189	*****
cline	138	*****
mason	608	*****
mcroy	68	***
mooers	11	*
osgood	358	*****
patrick	580	*****
peters	185	*****
scheel	25	**
seitz	60	***
steinhart	365	*****
stokesbury	85	****
thomas	57	***
thornton	426	*****
tuttle	897	*****
vaughan	252	*****
wilcock	46	**
willette	46	**
williams	395	*****

Back to top

/continued....

=====

REPORT PREPARED: Sat Apr 25 04:00:35 AKDT 1998

=====

Last 30 Days

FOR PERIOD: Mar 25 1998 to Apr 25 1998

Person	# of Pages Accessed	
-----	-----	
allen	78	*****
baker		
bishop		
bodnar		
brady		
brown		
clapsadl		
cooney	15	***
eslinger	10	**
falkenberg	3	*
foy	37	*****
gay	9	**
guest		
gunther		
hauser	36	*****
kirsch		
kline	37	*****
mason	119	*****
mcroy	38	*****
mooers		
osgood	48	*****
patrick	38	*****
peters	10	**
scheel	6	**
seitz		
steinhart	107	*****
stokesbury	4	*
thomas		
thornton	14	***
tuttle	154	*****
vaughan		
wilcock		
willette		
williams	70	*****

Back to top

=====

Access counts are for HTML pages and menu requests.
GIF files are not counted.

Analysis by in-house SEA software, code available on request [Image]
jra October 10, 1997

B. Detailed Usage Statistics for SEA Internal Web Site 6-19-96 to 10-15-97

(file-level tabulation is omitted from this printout)

Program started at Thu-16-Oct-1997 14:38 local time.
Analysed requests from Wed-19-Jun-1996 18:03 to Wed-15-Oct-1997 17:59
(483.0 days).

Total successful requests: 30 167 (628)
Average successful requests per day: 63 (89)
Total successful requests for pages: 20 916 (361)
Average successful requests for pages per day: 43 (51)
Total failed requests: 3 557 (73)
Total redirected requests: 3 060 (91)
Number of distinct files requested: 2 420 (90)
Number of distinct hosts served: 89 (11)
Number of new hosts served in last 7 days: 0
Corrupt logfile lines: 8
Unwanted logfile entries: 470 500
Total data transferred: 443 836 kbytes (5 788 kbytes)
Average data transferred per day: 940 973 bytes (846 644 bytes)
(Figures in parentheses refer to the last 7 days).

(Go To: Monthly Report: Daily Summary: Hourly Summary: Domain Report: Host
Report: Directory Report: Request Report)

Monthly Report

(Go To: Top: Daily Summary: Hourly Summary: Domain Report: Host Report:
Directory Report: Request Report)

Each unit ([+]) represents 60 requests for pages, or part thereof.

month:	pages:
Jun 1996:	63: [++]
Jul 1996:	160: [+++]
Aug 1996:	919: [+++++]
Sep 1996:	738: [+++++]
Oct 1996:	2249: [+++++]
Nov 1996:	2326: [+++++]
Dec 1996:	2131: [+++++]
Jan 1997:	2555: [+++++]
Feb 1997:	192: [++++]
Mar 1997:	1581: [+++++]
Apr 1997:	1289: [+++++]
May 1997:	431: [+++++]
Jun 1997:	850: [+++++]
Jul 1997:	1405: [+++++]
Aug 1997:	475: [+++++]
Sep 1997:	1568: [+++++]
Oct 1997:	1984: [+++++]

Daily Summary

(Go To: Top: Monthly Report: Hourly Summary: Domain Report: Host Report:
Directory Report: Request Report)

Each unit ([+]) represents 100 requests for pages, or part thereof.

day:	pages:
Sun:	2982: [+++++]

Mon: 4888: [+++++]
Tue: 3218: [+++++]
Wed: 2980: [+++++]
Thu: 2861: [+++++]
Fri: 2335: [+++++]
Sat: 1652: [+++++]

Hourly Summary

(Go To: Top: Monthly Report: Daily Summary: Domain Report: Host Report:
Directory Report: Request Report)

Each unit ([+]) represents 30 requests for pages, or part thereof.

hr: pages:

-- --
0: 871: [+++++]
1: 873: [+++++]
2: 606: [+++++]
3: 499: [+++++]
4: 246: [+++++]
5: 471: [+++++]
6: 224: [+++++]
7: 220: [+++++]
8: 483: [+++++]
9: 647: [+++++]
10: 826: [+++++]
11: 960: [+++++]
12: 1339: [+++++]
13: 1315: [+++++]
14: 1484: [+++++]
15: 1584: [+++++]
16: 1367: [+++++]
17: 1032: [+++++]
18: 1109: [+++++]
19: 1095: [+++++]
20: 885: [+++++]
21: 968: [+++++]
22: 1011: [+++++]
23: 801: [+++++]

Domain Report

(Go To: Top: Monthly Report: Daily Summary: Hourly Summary: Host Report:
Directory Report: Request Report)

Printing all domains with at least 20 requests, sorted by number of requests.

#reqs: %bytes: domain

25469: 84.30%: .us (United States)
4010: 14.68%: .edu (USA Educational)
334: 0.52%: .ca (Canada)
185: 0.31%: [unresolved numerical addresses]
142: 0.14%: .net (Network)
27: 0.05%: .com (Commercial, mainly USA)

Host Report

(Go To: Top: Monthly Report: Daily Summary: Hourly Summary: Domain Report: Directory Report: Request Report)

Printing all hosts with at least 20 requests, sorted alphabetically.

#reqs:	%bytes:	host
302:	0.45%:	cyclops.erin.utoronto.ca
62:	0.17%:	banana.ims.alaska.edu
658:	1.70%:	cooney.ims.alaska.edu
29:	0.03%:	filth.ims.alaska.edu
49:	0.18%:	halibut.ims.alaska.edu
27:	0.04%:	murre.ims.alaska.edu
79:	0.21%:	sarah.ims.alaska.edu
78:	0.54%:	scoter.ims.alaska.edu
528:	1.71%:	skua.ims.alaska.edu
134:	0.21%:	sole.ims.alaska.edu
86:	0.31%:	twister.rsmas.miami.edu
62:	0.09%:	venus.rsmas.miami.edu
71:	0.12%:	blackbirch.fnr.purdue.edu
88:	0.24%:	norspruce.fnr.purdue.edu
46:	0.23%:	cooney.ims.uaf.edu
46:	0.05%:	ebrown.ims.uaf.edu
22:	0.03%:	foy.ims.uaf.edu
91:	0.77%:	iron.ims.uaf.edu
49:	0.26%:	murre.ims.uaf.edu
42:	0.08%:	pppl.ims.uaf.edu
52:	0.20%:	sarah.ims.uaf.edu
101:	0.26%:	skua.ims.uaf.edu
34:	0.09%:	sole.ims.uaf.edu
630:	3.21%:	europa.avl.umd.edu
303:	2.21%:	io.avl.umd.edu
487:	1.43%:	limnosun.limnology.wisc.edu
47:	0.08%:	f181-184.net.wisc.edu
21:	0.09%:	f181-196.net.wisc.edu
112:	0.10%:	pwssc.alaska.net
485:	1.25%:	abot.pwssc.gen.ak.us
404:	0.88%:	clupea.pwssc.gen.ak.us
168:	0.56%:	copepod.pwssc.gen.ak.us
25:	0.02%:	curly.pwssc.gen.ak.us
2340:	1.53%:	daffy.pwssc.gen.ak.us
74:	0.22%:	donald.pwssc.gen.ak.us
303:	3.16%:	eagle.pwssc.gen.ak.us
11250:	34.70%:	grizzly.pwssc.gen.ak.us
431:	2.69%:	husky.pwssc.gen.ak.us
411:	1.00%:	ichthys.pwssc.gen.ak.us
111:	0.06%:	larry.pwssc.gen.ak.us
473:	1.58%:	lumpsucker.pwssc.gen.ak.us
316:	0.96%:	marmot.pwssc.gen.ak.us
54:	0.14%:	moose.pwssc.gen.ak.us
509:	1.12%:	nemo.pwssc.gen.ak.us
1316:	6.39%:	onerka.pwssc.gen.ak.us
40:	0.13%:	ophiodon.pwssc.gen.ak.us
139:	0.34%:	orca.pwssc.gen.ak.us
94:	0.11%:	sea6.pwssc.gen.ak.us
6351:	27.30%:	sebastes.pwssc.gen.ak.us
133:	0.08%:	wolverine.pwssc.gen.ak.us
101:	0.21%:	137.229.41.61
23:	0.04%:	146.63.245.240
37:	0.05%:	152.163.195.240

Directory Report

(Go To: Top: Monthly Report: Daily Summary: Hourly Summary: Domain Report: Directory Report: Request Report)

Host Report: Request Report)

Printing all directories with at least 20 requests, sorted alphabetically.
Printing directories to depth 4.

#reqs: %bytes: directory

```
-----
2215:  1.04%: /sea/block/
 500:  0.24%: /sea/block/progop/cal/
 817:  1.49%: /sea/block/progop/cruise/
1278:  6.39%: /sea/block/progop/dump/
  77:  0.26%: /sea/block/progop/misc_collab/
  20:  0.05%: /sea/block/progop/mysterypic/
9542: 15.14%: /sea/block/progop/papers.inprog/
  21:  0.01%: /sea/block/progop/proposals.inprog/
5252: 27.53%: /sea/block/progop/rslts_disc/
1927:  2.89%: /sea/block/progop/synthesis/
 735:  1.92%: /sea/block/progop/whatsnew/
1611:  8.23%: /sea/block/progop/wip/
1260:  9.94%: /seaDB/
  29:  0.07%: /seaDB/Webdriver/
  30:  0.05%: /seaDB/cspARFile/ctd/cruise.hdr/
  85:  0.25%: /seaDB/cspARFile/ctd/datafiles/
  86:  0.38%: /seaDB/cspARFile/zoops/datafiles/
132:  0.02%: /seaDB/cspARFile/zoops/modelfiles/
  34:  1.63%: /seaDB/cspARZipFile/
  38:  0.05%: /seaDB/page/
252:  0.13%: /seaDBH/
137:  0.06%: /seaDBHtest/
2830: 16.53%: /seaDBtest/
  34:  0.24%: /seaDBtest/cspARFile/tide/OLLD/
  34:  0.88%: /seaDBtest/cspARFile/zoops/datafiles/
  34:  0.01%: /seaDBtest/cspARFile/zoops/modelfiles/
  50:  0.37%: /seaDBtest/cspARZipFile/
168:  0.17%: /seaDBtest/page/
306:  1.03%: /synthdoc/
160:  0.02%: /synthdoc/comments/
166:  0.08%: /synthdoc/update/
  30:  0.02%: /synthdoc/update/ch01/
  30:      : /synthdraft/ch01/
  24:  0.01%: /synthdraft/ch06/
-----
```

This analysis was produced by analog2.11/Unix.
Running time: 45 seconds.

(Go To: Top: Monthly Report: Daily Summary: Hourly Summary: Domain Report:
Host Report: Directory Report: Request Report)

C. Detailed Usage Statistics for SEA Internal Web Site 10-6-97 to 4-20-98

(file-level tabulation is omitted from this printout)

Program started at Tue-21-Apr-1998 00:16 local time.
Analysed requests from Mon-06-Oct-1997 13:56 to Mon-20-Apr-1998 16:41
(196.1 days).

Total successful requests: 8 285 (78)
Average successful requests per day: 42 (11)
Total successful requests for pages: 4 594 (65)
Average successful requests for pages per day: 24 (9)
Total failed requests: 1 472 (18)
Total redirected requests: 965 (7)
Number of distinct files requested: 725 (37)
Number of distinct hosts served: 59 (7)
Number of new hosts served in last 7 days: 1
Corrupt logfile lines: 33
Total data transferred: 208 651 kbytes (643 481 bytes)
Average data transferred per day: 1 064 kbytes (91 926 bytes)
(Figures in parentheses refer to the last 7 days).

(Go To: Monthly Report: Daily Summary: Hourly Summary: Domain Report: Host
Report: Directory Report: Request Report)

Monthly Report

(Go To: Top: Daily Summary: Hourly Summary: Domain Report: Host Report:
Directory Report: Request Report)

Each unit ([+]) represents 25 requests for pages, or part thereof.

month:	pages:	
-----	-----	
Oct 1997:	1089:	[+++++++]
Nov 1997:	1070:	[+++++++]
Dec 1997:	775:	[+++++++]
Jan 1998:	759:	[+++++++]
Feb 1998:	239:	[+++++++]
Mar 1998:	425:	[+++++++]
Apr 1998:	237:	[+++++++]

Daily Summary

(Go To: Top: Monthly Report: Hourly Summary: Domain Report: Host Report:
Directory Report: Request Report)

Each unit ([+]) represents 20 requests for pages, or part thereof.

day:	pages:	
---	-----	
Sun:	346:	[+++++++]
Mon:	1005:	[+++++++]
Tue:	970:	[+++++++]
Wed:	784:	[+++++++]
Thu:	838:	[+++++++]
Fri:	454:	[+++++++]
Sat:	197:	[+++++++]

Hourly Summary

(Go To: Top: Monthly Report: Daily Summary: Domain Report: Host Report:

Directory Report: Request Report)

Each unit ([+]) represents 8 requests for pages, or part thereof.

hr: pages:

```
--  -----
0:    47: [++++++]
1:     8: [+ ]
2:    96: [+++++]
3:   129: [+++++]
4:    71: [+++++]
5:    65: [+++++]
6:    62: [+++++]
7:    55: [+++++]
8:   126: [+++++]
9:   264: [+++++]
10:  358: [+++++]
11:  259: [+++++]
12:  294: [+++++]
13:  296: [+++++]
14:  401: [+++++]
15:  399: [+++++]
16:  330: [+++++]
17:  290: [+++++]
18:  200: [+++++]
19:  168: [+++++]
20:  260: [+++++]
21:  149: [+++++]
22:  113: [+++++]
23:  154: [+++++]
-----
```

Domain Report

(Go To: Top: Monthly Report: Daily Summary: Hourly Summary: Host Report:
Directory Report: Request Report)

Printing all domains with at least 20 requests, sorted by number of requests.

```
#reqs: %bytes: domain
-----
6402: 73.25%: .us (United States)
1695: 25.64%: .edu (USA Educational)
  72:  0.23%: .net (Network)
  65:  0.60%: [unresolved numerical addresses]
  34:  0.24%: .com (Commercial, mainly USA)
-----
```

Host Report

(Go To: Top: Monthly Report: Daily Summary: Hourly Summary: Domain Report:
Directory Report: Request Report)

Printing all hosts with at least 20 requests, sorted alphabetically.

```
#reqs: %bytes: host
-----
  28:  0.76%:      idfix.rsmas.miami.edu
568: 10.29%: blackbirch.fnr.purdue.edu
  27:  0.44%:      auklet.ims.uaf.edu
  35:  0.33%:      banana.ims.uaf.edu
163:  3.65%:      cooney.ims.uaf.edu
  66:  0.38%:      ebrown.ims.uaf.edu
  32:  0.20%:      engle.ims.uaf.edu
  89:  0.35%:      foy.ims.uaf.edu
  52:  0.35%:      pppl.ims.uaf.edu
345:  3.68%:      sarah.ims.uaf.edu
```

```

100: 0.90%: skua.ims.uaf.edu
55: 0.15%: sole.ims.uaf.edu
109: 4.03%: europa.avl.umd.edu
25: 0.11%: anc-p29-165.alaska.net
31: 0.10%: dialups-31.cordova.ptialaska.net
25: 0.04%: abot.pwssc.gen.ak.us
23: 0.05%: commfish.pwssc.gen.ak.us
737: 5.57%: copepod.pwssc.gen.ak.us
299: 0.71%: daffy.pwssc.gen.ak.us
121: 0.82%: eagle.pwssc.gen.ak.us
47: 0.26%: evelyn.pwssc.gen.ak.us
2235: 11.29%: grizzly.pwssc.gen.ak.us
381: 4.33%: husky.pwssc.gen.ak.us
246: 1.75%: ictchys.pwssc.gen.ak.us
236: 1.08%: larry.pwssc.gen.ak.us
112: 1.12%: lumpsucker.pwssc.gen.ak.us
41: 0.23%: mark.pwssc.gen.ak.us
209: 9.84%: marmot.pwssc.gen.ak.us
134: 0.84%: nemo.pwssc.gen.ak.us
553: 11.59%: onerka.pwssc.gen.ak.us
55: 0.19%: ophiodon.pwssc.gen.ak.us
155: 2.21%: orca.pwssc.gen.ak.us
49: 0.25%: pwssc-01.pwssc.gen.ak.us
306: 7.92%: sea6.pwssc.gen.ak.us
404: 12.86%: sebastes.pwssc.gen.ak.us
22: 0.09%: 146.63.245.240

```

Directory Report

(Go To: Top: Monthly Report: Daily Summary: Hourly Summary: Domain Report:
Host Report: Request Report)

Printing all directories with at least 20 requests, sorted alphabetically.
Printing directories to depth 4.

```

#reqs: %bytes: directory
-----
875: 0.84%: /sea/block/
56: 0.06%: /sea/block/progop/cal/
127: 0.48%: /sea/block/progop/cruise/
562: 31.91%: /sea/block/progop/dump/
470: 2.99%: /sea/block/progop/papers.inprog/
287: 2.74%: /sea/block/progop/rslts_disc/
3641: 32.73%: /sea/block/progop/synthesis/
217: 1.83%: /sea/block/progop/whatsnew/
384: 2.62%: /sea/block/progop/wip/
586: 12.61%: /seaDB/
42: 0.32%: /seaDB/cspARFile/echodens/datafiles/
63: 6.54%: /seaDB/cspARFile/zoops/datafiles/
23: 0.07%: /seaDB/page/
127: 0.17%: /seaDBH/
323: 2.29%: /synthdoc/
82: 0.03%: /synthdoc/comments/
40: 0.03%: /synthdoc/draft/ch01/
162: 0.16%: /synthdoc/update/
33: 0.05%: /synthdoc/update/ch01/

```

(Go To: Top: Monthly Report: Daily Summary: Hourly Summary: Domain Report:
Host Report: Directory Report)

This analysis was produced by analog2.11/Unix.
Running time: 24 seconds.

Part III-B
Scientific Visualization Methods for Marine Ecosystem Research:
Case Studies Using AVS for Display of Hydroacoustic Data
J. R. Allen, E. V. Patrick, R. Kulkarni, G. L. Thomas, and J. Kirsch

Scientific Visualization Methods for Marine Ecosystem Research:

Case Studies Using AVS for Display of Hydroacoustic Data

**Jennifer R. Allen¹, E.V. Patrick¹, R. Kulkarni²,
G.L. Thomas¹ and J. Kirsch¹**

¹ Prince William Sound Science Center
P.O. Box 705, Cordova AK 99574

² Advanced Visualization Laboratory
University of Maryland
College Park, MD 20746

Running title: Visualization of Marine Systems

Partial Text of a Paper Presented at the
127th Annual Meeting of the American Fisheries Society
Monterey CA, August 27, 1997

INTRODUCTION

Background

The Sound Ecosystem Assessment (SEA) program is a five year, multidisciplinary study initiated in 1994 to examine pink salmon and Pacific herring populations in Prince William Sound (PWS), Alaska. At that time pink salmon and herring were classified as injured and non-recovering species following the 1989 *Exxon Valdez* oil spill. The SEA objective is to develop predictive models of juvenile survival and to separate natural from anthropogenic causes of population fluctuations. The research team includes investigators from the fields of oceanography, remote sensing, phytoplankton, zooplankton, herring and salmon biology, energetics, isotope tracing of foodwebs, and numerical modeling. The ecosystem approach taken by SEA depends upon gaining insight into sound-wide physical processes, as well as an understanding of the spatial and temporal distributions of the fish, their predators, prey, and the biological processes that occur in the areas of overlap. The value of computer visualization in aiding communication of individual results during such efforts at building an ecosystem understanding has been recognized (Lam et al., 1994).

Role of Visualization

Scientific visualization is a form of communication involving both cognitive and computing elements. Functionally it is the process of re-mapping numeric data into a visual representation, in order to facilitate improved understanding of the data structure. This process takes advantage of analytical and pattern recognition capabilities of the human eye-brain system in ways not possible with purely numeric data (DeFanti et al., 1989). In most cases, the visual representation has been found to be more intuitive or accessible than numerical or mathematical portrayals of the same data (Arrott, 1992). The ability to visualize complex datasets, models and results from simulations is increasingly regarded as essential in provoking insights, enabling communication to colleagues, and confirming the integrity of observations (Kaufman, 1994). Figure 1 shows an example with a marine systems application which illustrates the power of the visual approach. Figure 1a is a partial table of data from an acoustic Doppler current profiler (ADCP). This is a 15-line snapshot from a data set which is over 8,000 lines long and occupies several megabytes. Figure 1b shows a 3-dimensional (3-D) still shot from a 4-D tide cycle animation of this data. After re-mapping the 3-D vector data into 3-space and animating it over time, it is possible to visualize current flow patterns in eastern PWS in a way that is not possible from the table of data or even 2-D cross sections or profile plots. The full animation is available for viewing at <http://www.pwssc.gen.ak.us/sea/movies/adcp.mpeg>.

In SEA, high level visualization procedures are being used to help assess dynamic distributions, give some insight into patterns of overlap, and facilitate joint representation of cross-disciplinary observations. The aim is to assist in a visual understanding of the structure of the data as a tool for gaining insight into the underlying biological phenomena. The present communication summarizes visualization techniques employed in this effort and presents some specific examples of hydroacoustics applications.

METHODS

Visualization Software

Most of the visualizations in SEA are performed using the Application Visualization System (AVS) (Advanced Visual Systems, Inc., Waltham, MA). This system uses a data flow paradigm and graphical programming interface to provide an extensible and customizable visualization environment. Libraries of interchangeable modular components are assembled into flow networks. Flow networks are constructed via a graphical user interface (GUI) known as the Network Editor (Figure 2). Additional user-authored modules can be written in either C or FORTRAN, with optional assistance from the AVS module generator. For the SEA work, some customized modules for displaying individual transect data were coded in C. Animations were created using the AVS animator, which provides sophisticated and efficient key-frame interpolation. Animated output was converted to MPEG format for portable, platform-independent, web capable display of dynamic products.

Pixel-based versus Geometry-based Visualization.

Pixel-based visualization is a 2-D process based on a relatively direct one-to-one representation of each data point as a color-coded pixel in an image. By contrast, the work described in this report concerns multidimensional, geometry-based visualization. In geometry-based visualization, data points are mapped into the vertices of geometric objects, and the data values are used to assign color and other characteristics to the geometry. Using AVS, low level graphics software and rendering hardware then render the objects for display to the screen in the AVS geometry viewer. Advanced features available include transparency, texture mapping, volume rendering, particle advection, isosurfaces and slice planes. In addition, use of geometry-based techniques provides a display that is not static, but can be interrogated interactively. Objects in the geometry viewer can be viewed dynamically using the mouse to pan, zoom, rotate the object, change the viewing angle, lighting direction, perspective and other attributes. An animation showing the power of these features is available for viewing on the web at <http://www.pwssc.gen.ak.us/sea/movies/flyby1.mpeg>

Data Model

The data model provides the rules for mapping of the data array into the display coordinate space. The AVS data model supports a number of aggregate data types, of which two were used in the work reported here: unstructured cell data (UCD) and field data. UCD is based on representation of data by a geometric model built from individual cells that are defined by nodes. It provides a useful mechanism for representing volume data that is not sufficiently structured to be represented as a field data type. The UCD data type was employed for some of the acoustic visualization processes, particularly those involving interpolation.

The field structure is typically used for image and volume data. Field Data are in the form of an n-dimensional array with an m-dimensional vector of observations at each location. AVS recognizes uniform, rectilinear and irregular fields. These differ primarily in the method of mapping from the computational space into the coordinate space (see Figure 3). In uniform fields, the elements are equally spaced; in rectilinear fields the between-element spacing can vary but is constant along each axis; whereas in irregular fields there is no implicit mapping between the computational space and the coordinate space, and no restriction that the number of dimensions in the coordinate space be the same as the number of dimensions in the computational space. Because of these useful properties of irregular fields, much of the SEA data is handled as the irregular field type. Figure 3 shows some examples of AVS mappings of irregular fields, showing 1-D data that is re-mapped into 1-, 2- or 3-space, as might occur in visualizing a CTD cast, a single acoustic transect, or a series of acoustic transects, respectively.

Figure 4 shows a composite example in which 2-D acoustic transects re-mapped into 3-D coordinate space; along with several examples of 1-D data sets: CTD casts showing temperature, aerial survey flight paths, and a 1-D data stream from an towed aquashuttle measuring zooplankton counts.

Bathymetry Data

The PWS bathymetry data renderings used as the basis for all visualizations presented here are a product of the SEADATA group from FY94 and also involved collaboration beyond SEA. The original data source was the National Ocean Service (NOS) database, obtained on tape in both raw and 15' gridded versions. Substantial processing performed at the Alaska Department of Natural Resources (ADNR) helped remedy the patchiness of the original NOS coverage. This work yielded several Arcinfo coverages that included 20m depth contours. The present gridded data set was created by David Scheel and Vince Patrick using the 20m contour coverages and Arcinfo coastlines provided by Randal Hagenstein, formerly of Pacific GIS. The last conversion used Delauney triangulation and quintic interpolation in the Arc procedures TIN and GRID, respectively. Additional documentation on this data set is available on request.

Acoustics Data

The data for the acoustic visualization examples presented here are drawn from acoustic surveys in PWS performed by Gary Thomas and Jay Kirsch as part of the SEA program and in stock assessment work with the Alaska Department of Fish and Game (ADF&G). Surveys used a dual beam echo sounder with echo integrator. Accompanying trawl or seine samples provided species composition and size distribution. Post-processing was performed using in-house software developed by Jay Kirsch. Species of interest were identified and separated interactively based on a priori knowledge of acoustic appearance and behavior plus information from the catch data. An estimate of mean backscattering cross-section (target strength) was computed from length/weight measurements in the catch data. Biomass density was then calculated by multiplying the acoustic backscatter (echosquare integration, calibrated) by the target constant of average weight divided by the mean backscattering cross-section. Georeferenced arrays of either volume backscatter (dB) or biomass (kg/m³) were exported for re-mapping and visualization.

CASE STUDIES

1. Spatial distribution patterns of pollock in western PWS.

Re-mapping of acoustic data into 3-space as described above provided early insights into the nature of the time-varying spatial distribution of pollock, an important system predator. Figure 6 shows data from multiple surveys during the spring and summer of 1994 in the western corridor of PWS. Figure 6a shows survey transect locations in May (red) and July (blue); Figure 6b shows the locations where pollock were present. Figure 6b is zoomed and rotated to about 45 degrees from the vertical to reveal the depth distribution. This method of display makes it easy to discern that pollock are collected at the northern and southern ends of the passage at both observation times, but that in July the distribution is more aggregated or contagious than in May. There is also a tendency for pollock in the southern areas (lower Knight Island Passage and Montague Strait) to be deeper in the water column, particularly in July, compared with the northern end where they are concentrated near the surface. This pattern could be related to food

supply, as pollock in the north are likely feeding on newly released fry from the Wally Noerenberg hatchery. In contrast, by the time they reach the southern end of the migration corridor the fry are more dispersed and larger, and the pollock may be turning to alternative sources of food. It should be noted that this picture is just showing presence or absence, i.e. the pattern of the distribution, but gives no indication of density. Figure 7 shows the same pollock distribution data enhanced by addition of a quantitative representation. Here biomass density is coded by color. In this and all subsequent images, density scales range from blue (lowest density) to red (highest). This figure confirms that in the northern part of the channel the pollock aggregation was concentrated near the surface, while moving down the channel the densities decrease and the higher concentrations were deeper in the water column.

2. Case Study: Pollock and Plankton Co-Distribution

This set of figures provides an example of overlaying distributions of organisms from two different trophic levels, in this case pollock and zooplankton, in order to examine their codistribution patterns in time and space. Figures 8a and 8b show pollock and plankton densities assessed acoustically in the same region of PWS as the preceding case. In these figures, pollock density is indicated by color on a scale of 10^{-6} to 10^{-3} kg/m³. The slightly compressed scale is used to shorten the scale of contrast and thereby highlight patches in the pollock distribution. Zooplankton are indicated by black dots, classified here on a 4-point qualitative scale from 0 to 3. Only levels 3 and 4 are plotted; the larger black dots indicate the highest density level. The inset in Figure 8a shows an example of an AVS widget: in this case the color map interface. The viewer can use these controls to adjust the lower and upper bounds, and other properties, of the color scale, in order to narrow or broaden the focus on the density region of interest. Similar dynamic techniques are used in medical imaging to interrogate density-based 2-dimensional images such as CT and MRI scans. From these data, in May, there appears to be some concordance between the high density pollock and the plankton clumps, but only imperfect agreement. It is easy to find aggregations of pollock where not associated with plankton aggregations. On the other hand, in July, the remaining dense clumps of pollock are associated fairly consistently with high density zooplankton patches.

3. Case Study: School characteristics of adult herring and pollock and repeatability of herring acoustic surveys.

The third example illustrates some more advanced visualization techniques and ways they can be applied to acoustic data once it has been re-gridded into 3D coordinate space. The example focuses on repeated surveys of herring schools, conducted on a pre-spawning aggregation of tightly grouped adult herring in Stockdale harbor in March 1996. Stockdale harbor is a shallow bay with a sloping shore (Figure 9). This enables the herring to move onshore into quite shallow water and can make covering a school with an acoustic survey difficult.

a. 1-D Remapping into 3-space (scatter dot cloud)

Figure 10a shows a top-down view giving the orientation of the survey transects. Figures 10b through d show progressive rotation of the geometry about the vertical axis from 20 to about 85

degrees (d), by which point the viewpoint is into the bay at an angle almost perpendicular to the horizontal face of the transects. Each colored dot in this image corresponds to an actual data point from the echo-integration data. Viewed together, the 3-D dispersion of the from all transects forms a “scatter dot cloud” that to the human eye takes on the appearance of an almost solid object.

b. Volume interpolation

In Figure 11a, the size of the dots has been reduced and a semitransparent interpolated volume has been overlaid. The boundaries of this colored volume represents the actual sampled water volume in the survey and its colors correspond to the log of fish density (expressed here as volume backscatter in dB). The volume interpolation in this study was achieved by reconfiguring the data into a UCD format and then applying an interpolation by Delauney triangulation using several UCD-processing module from the AVS libraries. The fuzzy 3-D region delimited by the red-orange-yellow region within the interpolated volume corresponds to the most dense area of the herring school.

c. Slice planes and Isosurfaces

Having achieved a volume interpolation of herring density, two further manipulations are useful for assessing school distribution. The first is to pass a slice plane through the volume (Figure 11b). This plane can be placed at any orientation and at any depth within the volume. In this case a horizontal plane, i.e. parallel to the water surface, has been positioned at a depth of about 15m. The colors on the slice correspond to herring density encountered at that slice plane, ranging from blue (empty water) to red (highest herring density). The widget illustrated in Figure 11b is a control panel that allows the viewer to interactively position the plane. Plane angle, offset and depth are all user adjustable. The viewer can thus dynamically interrogate the data, by moving the slice plane through the volume and visualizing the changing shape of the density pattern. Doing this rapidly on a live screen gives the viewer a good “feel” for the structure of the fish school. Figure 12a-12d shows a series of 4 such horizontal slices passing through the school at progressively increasing depths. This series indicates that the herring are crowded towards the shoreline at the inner margin of the surveyed volume. The last slice in the series contains blue-green densities only, indicating that the school was, however, fully encompassed in the vertical direction in this survey.

The second useful manipulation is to delineate sub-volume structure by means of isosurfaces. The AVS isosurface module takes UCD data as input and produces a 3-D surface passing through all points at the specified density level and enclosing points at higher densities. Figure 13a and b show two representative surfaces at -45 and -37 dB respectively. Again, interactive widgets enable the viewer to dynamically interrogate the data by sweeping the isosurface threshold through a range of values, thereby visually delineating the shape of the school. The image movement which accompanies dynamic use at the computer also facilitates appreciation of the 3-D orientation of the school which is more difficult to convey in 2-D still shots here. In this survey the herring school has a single center of aggregation and this core is located relatively deep within the sampled volume. Although the school depth and location are variable, this pattern of

unifocal aggregation is typical of adults in the prespawning period. However the schooling patterns differ among species. For example, Figure 14a and 14b show results of a survey of adult prespawning pollock in March 1997 in Port Bainbridge. This visualization was generated in the same way as described above. The color scale indicates biomass, with bounds set to encompass the range from empty water to densest fish aggregations seen. In this survey the pollock isosurfaces tend to be rather fragmented, indicating that these pollock were not aggregated into a single concentrated school were dispersed more diffusely. (It should be noted that this is not a constant finding for pollock, since a survey the preceding year did not show this appearance but instead revealed more aggregation, with the pollock isosurfaces enclosing large coalesced volumes that appeared more like the herring pictures.) The visualization techniques used in this example are providing information about the fish schooling behavior that is difficult to discern simply from looking at the individual 2-D transects.

d. Time animation of herring school movements

The fourth component of this study consisted of repeating the above procedures for each of five surveys conducted over the Stockdale harbor herring school during a single night. In particular, the isosurface demarcating the body of the herring school was generated for each survey. The results were then animated over time, yielding a display which illustrates the temporal and spatial dynamics of this single large school. In addition, visualization results for each survey were used to assess the completeness of coverage of the school by the survey. This technique thereby provides information that can be used to (a) assess the repeatability of survey methods, and (b) help determine the validity of inclusion of particular surveys in biomass estimate determinations, by means of providing a visual assessment of the degree of truncation of the school. In this case, the herring school was found to be quite mobile, with both its depth and its concentration on or off shore varying during the course of the night. Of the five surveys, #2 and #3 were considered successful in capturing the bulk of the school, whereas #1, #4 and #5 all exhibited varying degrees of truncation of the school. The animation showing school movements is available for viewing at <http://www.pwssc.gen.ak.us/sea/movies/herring1.mpeg>

DISCUSSION

The exponentially increasing power of computers and graphics systems has made it possible for computer scientists and engineers to exploit advanced data visualization techniques using realtime interactive display. It was predicted early in this decade that interactive visualization would “offer the possibility of profoundly changing the way we assimilate and process new information” (Arrott, 1992) and to a great degree that has proven true. However the high level of programming expertise required has tended to limit the use of these techniques by scientists in general. In this respect AVS is a compromise which allows the scientist to develop powerful customized visualization applications, but at the same time reduces the programming required. This combination is beginning to bring visualization techniques into more generalist use. For example, Socha et al. (1996) developed a customized data-handling module as part of a post-processing system for AVS-based analysis of acoustic data, with display in 2-D image format. The

extendability of AVS have been investigated by Pagendarm and Choudry (1993), who found creation of user modules for AVS to be feasible and comfortable. In addition, large numbers of modules are available for the system, both in the marketed application and via the international user group web site.

The present work with multidisciplinary data from a marine ecosystem study confirms the some of the usefulness of visualization applications that has been reported from other fields. In the present study, many relationships of interest involve multidimensional quantities both in domain and range; variables measured at multiple spatial scales, changing over both space and time. In addition, many measurement technologies, such as remote sensing, hydroacoustic and many oceanographic techniques, give rise to extremely large volumes of digital data. While such large collections of numerical values contain great deal of information, effectively conveying the information requires a form of communication with a high bandwidth and an effective interface (Nielson, 1989). Visualization techniques such as those described here provided a means of conveying information compactly and effectively. Although the display is somewhat subjective, it nevertheless was useful in revealing patterns that often suggested avenues of further analysis or further questions to be addressed. The value of interactivity for evaluating visually presented data has been stressed repeatedly by others (Nielson, 1989; Arrott, 1992; Kaufman, 1994) and this was also borne out by the present work using such interrogation operators as the slice plane and isosurface threshold to delineate fish school boundaries. Interactivity, and its consequence, motion, were particularly valuable in enhancing three-dimensional comprehension of the data structure. Abilities in 3-D perception were noticeably variable between individuals, but in all cases lack of 3-D comprehension was overcome by the introduction of movement, as this enabled the viewer to establish 3-D reference points and relationships. Interactivity also, as reported by Neilson (1989), "allows the researcher to cooperate with the computer, increasing the chance for insight and understanding". Animation sequences were also found to be effective at revealing the time evolution of changes and also were particularly valuable in communicating results.

Advanced visualization methods have not previously been reported in application to fisheries acoustics data. Greene et al. (1996) described the use of visualization methods for assessment of patchiness in plankton populations. They found that interactive exploration of 3-D acoustic datasets provided enhanced insights into zooplankton and micronekton dynamics and spatial structure. The present work suggests similar benefits arise from application of visualization procedures to fisheries acoustics data. Active areas of visualization research, continuing both in SEA and elsewhere, include development of graphical computer interfaces to design simulation and modeling environments that are more accessible to decision-makers (Wagner et al., 1996); integration of scientific visualization systems with geographic information systems in order to realize simultaneously the complementary strengths of each (Hay and Knapp, 1996); and use of the Java language and web-based protocols to permit platform-independent data visualization across collaborative groups (Byeongseob and Klasky, 1997).

ACKNOWLEDGMENTS

We thank Mark Willette, Kevin Stokesbury, and John Wilcock for assistance in data interpretation. This work was performed as part of the Sound Ecosystem Assessment (SEA) Program funded by the *Exxon-Valdez* Oil Spill Trustee Council.

REFERENCES

- Arrott, M. and Latta, Sara (1992) Perspectives on visualization. *IEEE Spectrum*, September 1992, pp. 61-65.
- Byeongseob, K. and Klasky, S. (1997) Collaborative scientific data visualization. *Concurrency Pract. Exp.* 9(11):1249-1259.
- DeFanti, A., Brown, M.D. and McCormick, B.H. (1989) Visualization: Expanding scientific and engineering research opportunities. *IEEE Computer* 22:12-25.
- Domik, G. (1996) Computer visualization: Concepts, trends and current research. *Proceedings 23rd International Symposium on Current Trends in Theory and Practice of Informatics*. Milovy, Czechoslovakia, November 1996.
- Globus, A. and Raible, E. (1994) Fourteen ways to say nothing with scientific visualization. *IEEE Computer* 27(7):86-88.
- Hay, L. and Knapp, L. (1996) Integrating a geographic information system, a scientific visualization system, and an orographic precipitation model. *Proceedings of International Conference on Application of Geographic Information Systems in Hydrology and Water Resources Management*, Vienna, Austria, April 1996. pp. 123-131.
- Greene, C.H., Wiebe, P.H. and Zamon, J.E. (1994) Acoustic visualization of patch dynamics in oceanic ecosystems. *Oceanography* 7(1): 4-12.
- Kaufman, A.E. (1994) Visualization (guest editorial). *IEEE Computer* 27:18-19.
- Lam, D.C.L., Wong, I., Swayne, D.A. and Fong, P. (1994) Data and knowledge visualization in an environmental information system. *J. Biol. Syst.* 2(4):481-497.
- Nielson, G.M. (1989) Visualization in Scientific Computing. *IEEE Computer*, 22:10-11.
- Pagendarm, H.-G. and Choudry, S.I. (1993) Visualization of hypersonic flows: Exploring the opportunities to extend AVS. *Proc. 4th EuroGraphics Workshop in Visualization in Scientific Computing*, Abington, UK, April 1993.
- Socha, D.G., Watkins, J.L and Brierly, A.S. (1996) A visualization-based post-processing system for analysis of acoustic data. *ICES Journal of Marine Sciences* 53(2):335.
- Wagner, P.R., Freitas, C.M.D.S. and Wagner, F.R. (1996) A new paradigm for visual interactive modeling and simulation. *8th European Simulation Symposium*, Genoa, Italy, October 1996. Vol.1 pp. 142-145.

FIGURES

All figures and animations accompanying this report are available for viewing on the web at <http://www.pwssc.gen.ak.us/evos97rpt/>

FIGURES

Figure 1: Acoustic Doppler current profiler (ADCP) vector animation in eastern PWS. **A.** Form of the stored data; first 15 lines of a multi thousand line file. **B.** The 3-D visualization. This view looks north in PWS through Hinchinbrook Entrance. The arrows indicate direction and magnitude of current flow. Red arrows are closest to the surface, blue arrows to the bottom. The data are animated over 8 stages of the tide. Full animation available for viewing at <http://www.pwssc.gen.ak.us/sea/movies/adcp.mpeg>.

Figure 2: AVS network editor interface. This example shows the AVS network that generated one of the visualizations presented in Case Study #3. The screen consists of a library of modules (top) and a work area for flow network construction (below). Each box in the work area is a module which performs a specific function data handling or graphic manipulation function. The point-and click interface allows the user to select modules from the libraries, drag them to the work area, and connect them together to specify routes of data flow through the network. Data enter the network at the top, pass through being acted upon by each module in turn under control of the flow executive, finally being output as the graphic product. AVS also provides for co-routines (modules that act spontaneously) and upstream flow control for specialized feedback loop requirements. In addition to the data input and output ports for data flow, most modules accept input parameters to adjust functional settings at run-time. These are presented in the form of graphical widgets: dials, buttons, slider bars, that allow the user to configure or interactively adjust the visualization during the data display process.

Figure 3: Steps in generation of geometry-based visualization using AVS. Georeferenced data are acted on by “filter” modules to produce representations in terms of the AVS data model, and then passed through “mapper” modules to create geometric objects which in turn can be acted upon in various manipulations such as slicing and contouring.

Figure 4: Examples of AVS mappings for irregular fields. Computational space refers to the dimensionality of the data (AVS assumes that the computational space is logically rectangular, with each dimension forming a perpendicular axis beginning at the origin, with the interval between elements equal to 1 for each element in the array). Coordinate space is the physical space into which the data array is mapped. Regridding is accomplished by explicitly defining the mapping that translates each data point into a specific location in physical space. This allows, for example, a 2D plane such as an acoustic transect to be re-mapped into 3D space. Because of the nature of the sparse sampling in large marine systems, it can often be convenient to handle data as a 1D array of points remapped into 3-space, as this avoids the requirement of having an observation for every possible combination of x,y,and z locations within the data array.

Figure 5: Simultaneous display of multidisciplinary ecosystem data sampled at different spatial scales. This example includes 2-D acoustic transects re-mapped into 3-D coordinate space (the vertical planes); along with several examples of 1-D data sets: CTD casts showing temperature, (cylinders); aerial survey flight paths (red lines), and a 1-D data stream from an towed aquashuttle measuring zooplankton counts (sinusoidal track).

Figure 6: Pollock surveys 1994. **A.** Location of survey transects in May (red) and July (blue). **B.** Location of pollock. For more explanation, see text - Case Study #1.

Figure 7: Quantitative representation of pollock distribution in northwestern PWS, May. Wally Noerenberg hatchery is at top left of image. For more explanation, see text - Case Study #1.

Figure 8: Co-distribution of plankton (black dots) and pollock (colored areas) in northwestern PWS in May (**A**) and July (**B**). This figure also shows AVS widgets for interactive adjustment of color scale. For more explanation, see text - Case Study #2.

Figure 9: Location and bathymetric features of Stockdale Harbor, a prominent location for aggregation of pre-spawning adult herring in PWS.

Figure 10: Preliminary step in herring survey visualization in Stockdale Harbor. **A.** Top-down view of transect locations. **B.** through **D.** progressive rotation toward a front-on view, illustrating the appearance of the “scatter dot cloud”. For more explanation, see text - Case Study #3.

Figure 11: Volume interpolation used in herring survey visualization in Stockdale Harbor. **A.** The interpolated volume is displayed as the semitransparent structure seen here, color coded by herring biomass density. **B.** A horizontal slice passed through the interpolated volume at approximately 15 m depth. The widget shown in this figure allows interactive movement of the plane through the region of the herring school. For more explanation, see text - Case Study #3.

Figure 12: Sequence of 4 slices moving through the interpolated volume, beginning near the surface and passing through the herring school. For more explanation, see text - Case Study #3.

Figure 13: Isosurfaces through interpolated volume in herring survey visualization. **A.** Surface at -45dB **B.** Surface at -37dB, delineating the core of the herring school. For more explanation, see text - Case Study #3.

Figure 14: Isosurfaces through interpolated volume in pollock survey visualization, showing more fragmented distribution than seen for the herring. For more explanation, see text - Case Study #3.

A.

400	400	400	30	8	47	4						
94	9	19	19	21	39	96	1	6	5.680	-1.400	58.320	11.630
-207.90		-111.10		-0.90				0.10	-32768	-32768	-32768	-32768
205.80		209.88		196.81								199.79
191.66		81.23		91.03					168.64		191.64	
60.5840625		-145.9955711		-201.60					-66.30		173.9	
-1571.0		-82.5		-228.5					0.0		0.0	0.0
	0.0	0.0	0.0									
30 cm BT dB	0.43	0.038										
13.98	7.57	224.465	-5.3	-5.4	2.6	2.2	75.8	77.1	76.3	7		
5.4 100	-5.51											
17.98	15.68	238.033	-13.3	-8.3	1.3	6.4	76.8	80.2	78.1	7		
5.9 100	-2.65											
21.98	18.98	227.990	-14.1	-12.7	1.0	3.7	76.8	79.4	77.7	7		
6.4 100	-6.88											
25.98	24.47	224.669	-17.2	-17.4	1.4	-1.0	77.7	79.4	79.0	7		
6.8 100	-10.75											
29.98	26.05	234.846	-21.3	-15.0	1.1	3.1	77.0	78.7	78.3	7		
6.5 100	-4.84											
9.0 100	-14.01	223.708	-19.5	-20.4	1.2	6.9	77.7	79.9	77.7	7		
37.98	31.76	226.148	-22.9	-22.0	0.6	5.9	80.0	85.2	82.2	8		
3.9 100	-11.78											
41.98	44.83	209.539	-22.1	-39.0	2.6	11.6	82.2	90.8	86.5	8		
8.2 100	-33.42											
45.98	28.00	225.000	-19.8	-19.8	-1.6	-1.0	86.4	97.6	90.7	9		
2.4 83	-4.28											
49.98	10.15	212.125	-5.4	-8.6	-0.3	0.2	93.1	97.0	93.6	9		
5.3 100	-7.99											
53.98	7.44	120.700	6.4	-3.8	0.6	2.3	97.2	99.4	95.9	10		
1.1 100	-11.40											
57.98	15.48	127.388	12.3	-9.4	-0.4	3.9	99.5	101.7	100.4	10		
1.7 100	-20.63											
61.98	14.45	152.371	6.7	-12.8	-0.4	-0.6	99.6	100.5	103.9	9		
8.7 100	-19.66											
65.98	13.10	138.403	8.7	-9.8	0.2	6.9	98.4	100.1	100.1	10		
0.1 100	-18.76											
69.98	17.40	109.477	16.4	-5.8	0.9	5.6	99.7	101.8	101.4	9		
9.2 100	-18.41											
73.98	15.34	85.888	15.3	1.1	0.7	5.0	97.1	100.1	100.9	9		
4.5 100	-8.16											
77.98	11.85	78.311	11.6	2.4	0.6	5.8	94.9	97.9	97.9			

B.

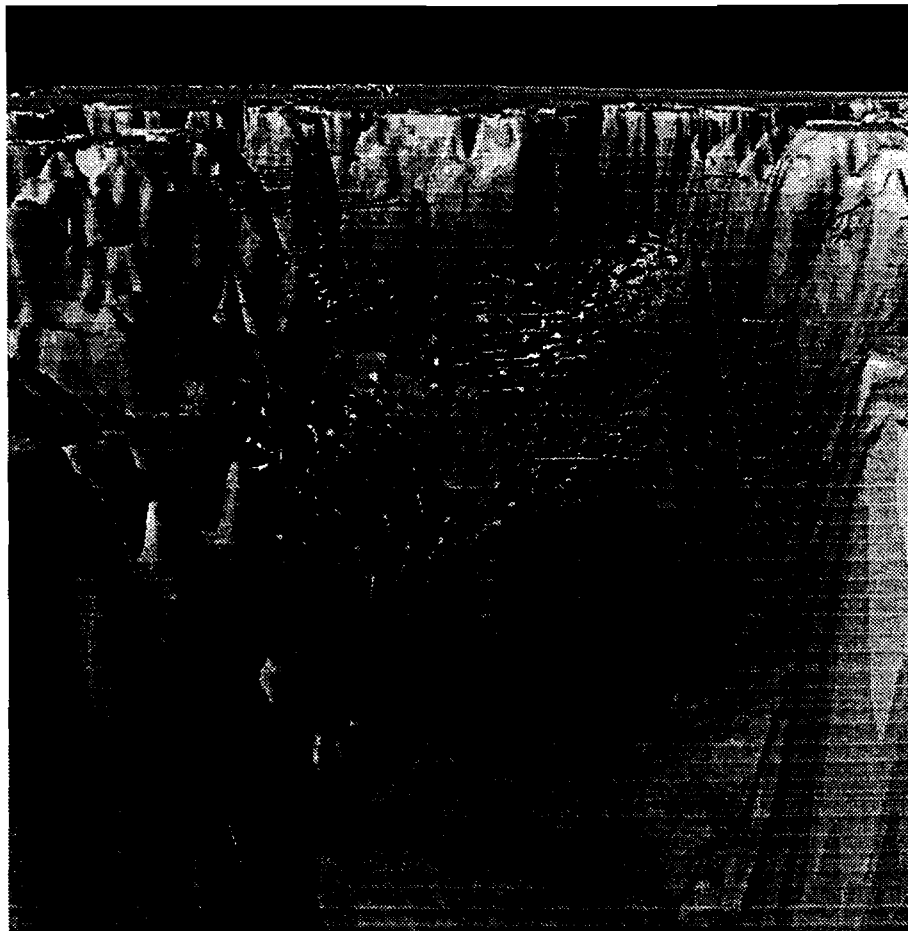


Figure 1.

Color versions are available for viewing at www.pwssc.gen.ak.us/evos97rpt/

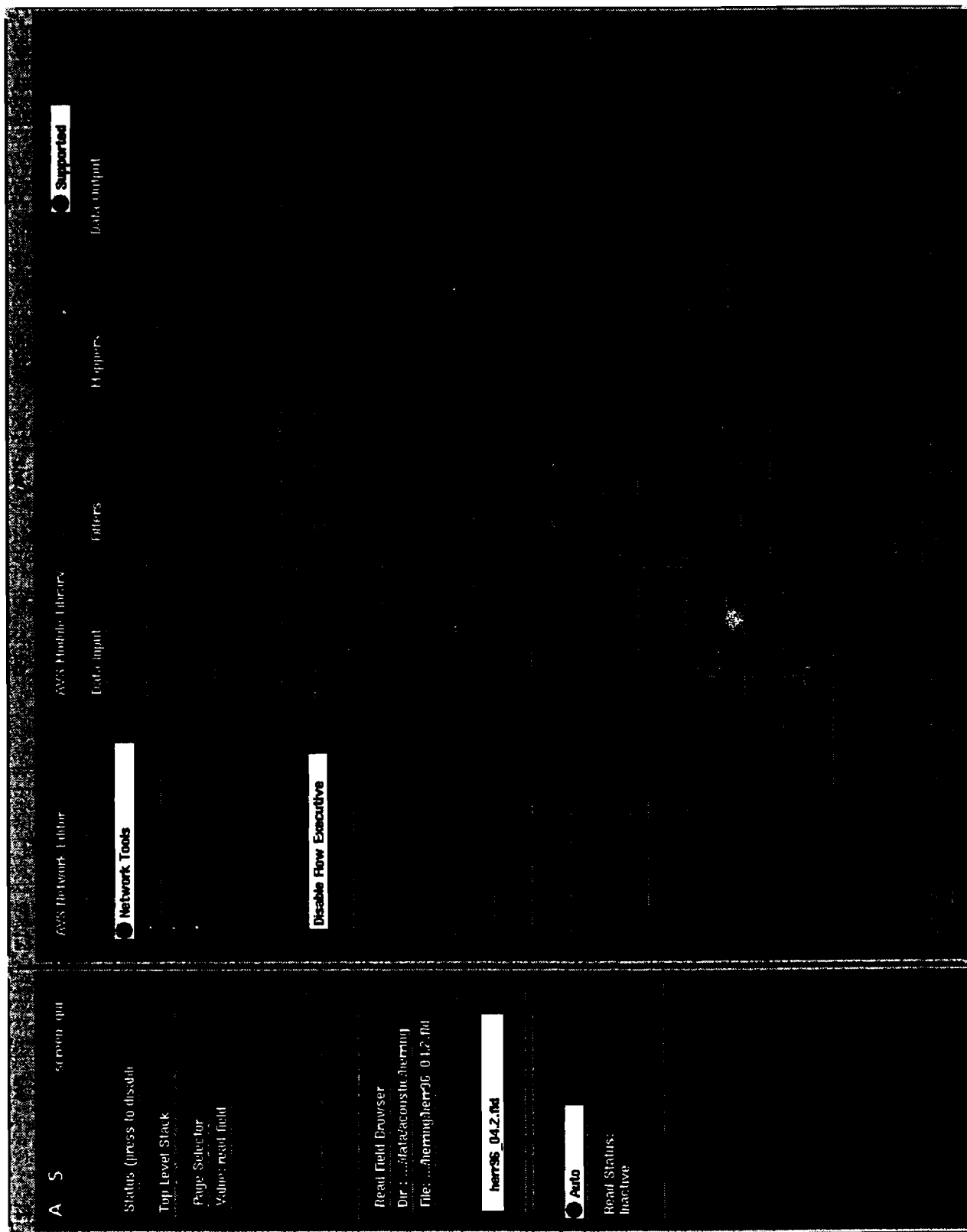


Figure 2.

Color versions available for viewing at www.pwssc.gen.ak.us/sea/evos97rpt/

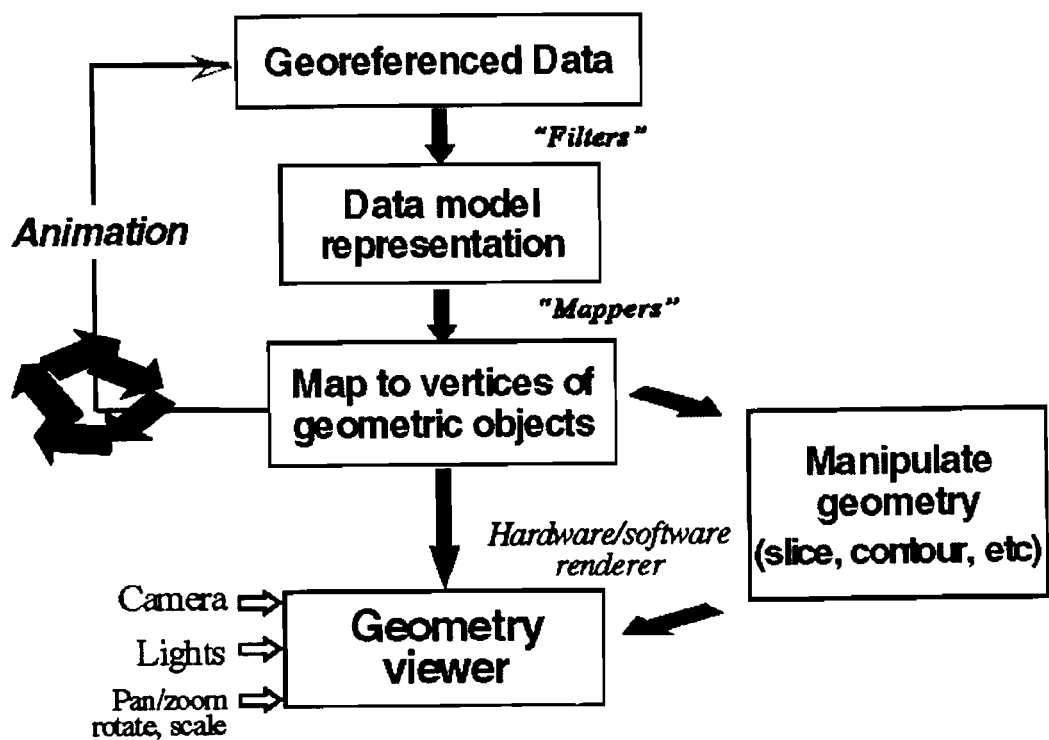


Figure 3

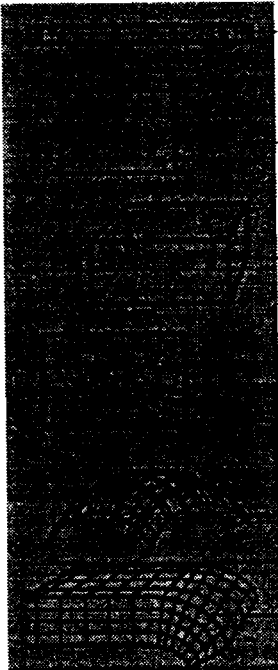
Examples of AVS Mapping for Irregular Fields		Computational Space	Coordinate Space
	1	1	1
	1	2	2
	1	3 *	3 *
	2	2	2
	2	3 *	3 *
	3	3 *	3 *

Figure 4

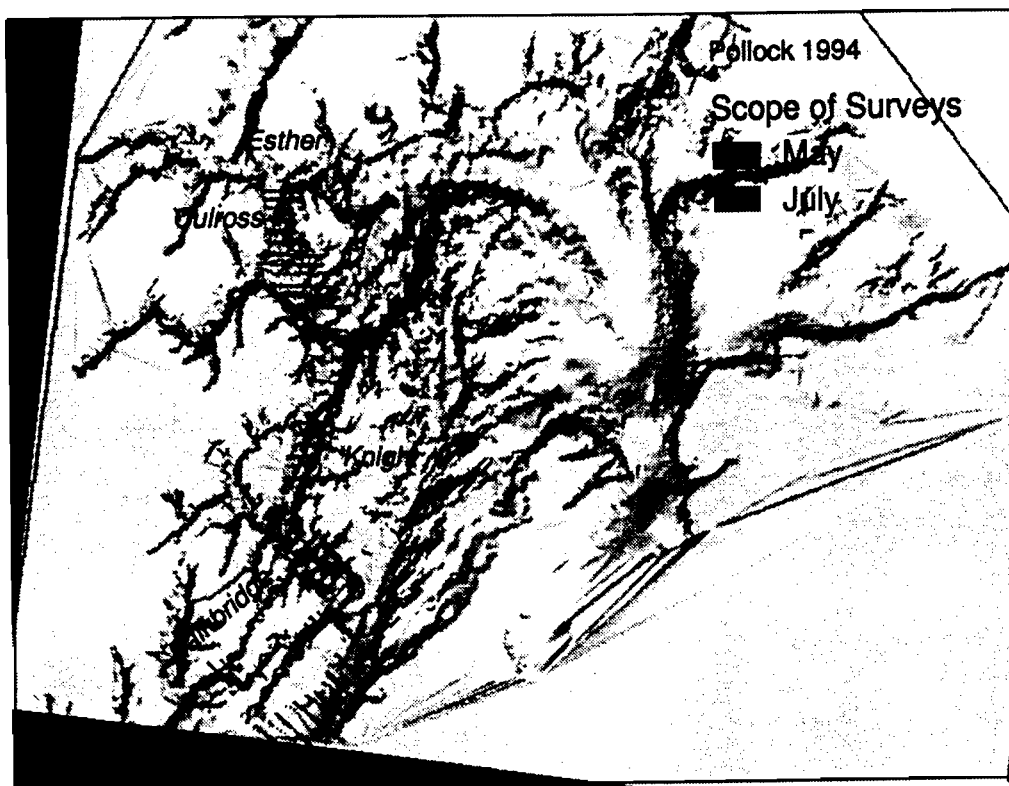
Color versions available for viewing at www.pwssc.gen.ak.us/sea/evos97rpt/



Figure 5.

Color versions available for viewing at www.pwssc.gen.ak.us/sea/evos97rpt/

A



B



Figure 6

Color versions available for viewing at www.pwssc.gen.ak.us/sea/evos97rpt/



Figure 7.

Color versions available for viewing at www.pwssc.gen.ak.us/sea/evos97rpt/



A



B

Figure 8

Color versions available for viewing at www.pwssc.gen.ak.us/sea/evos97rpt/

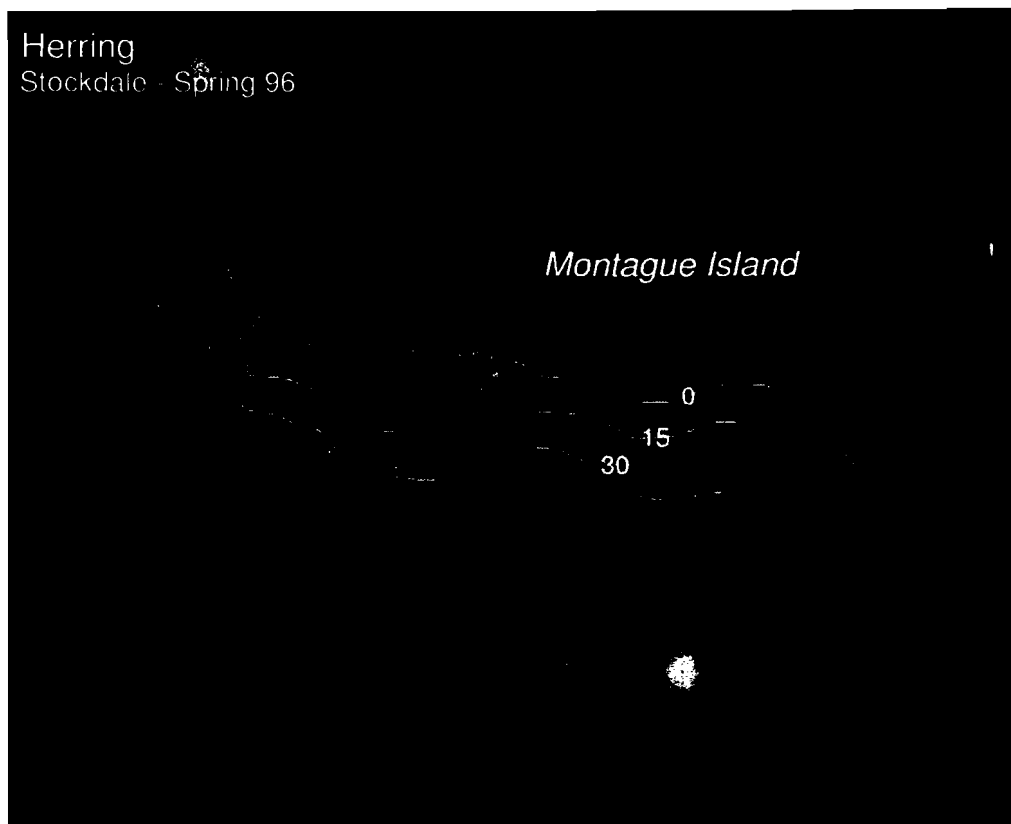
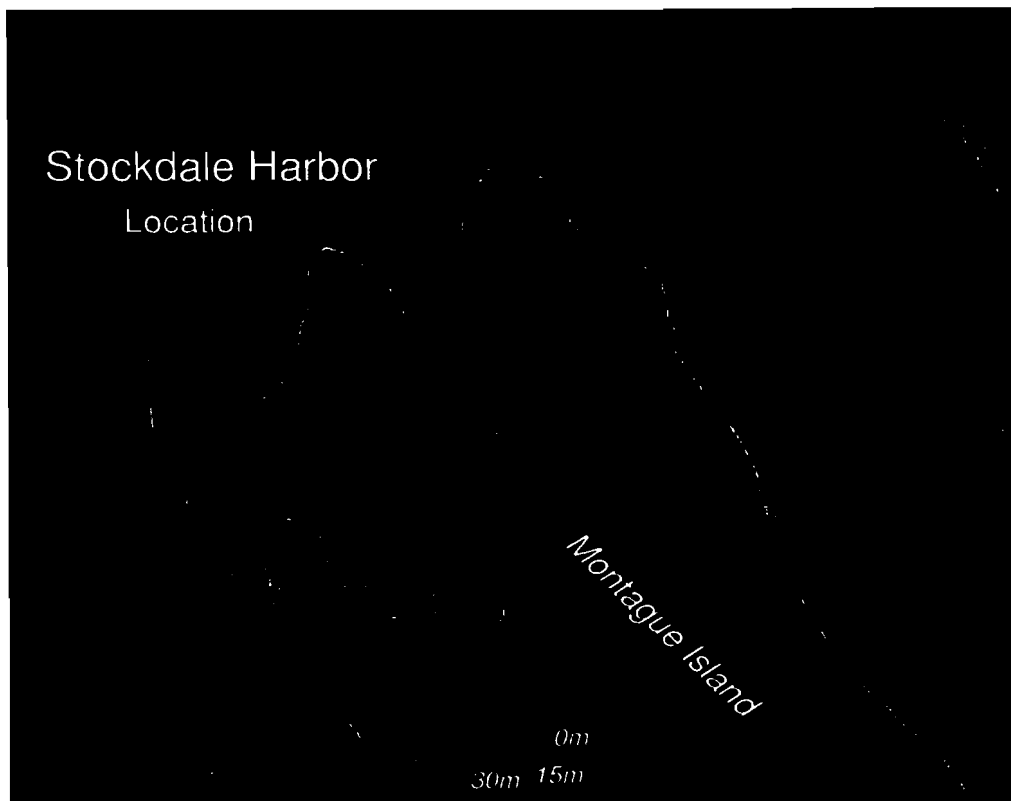
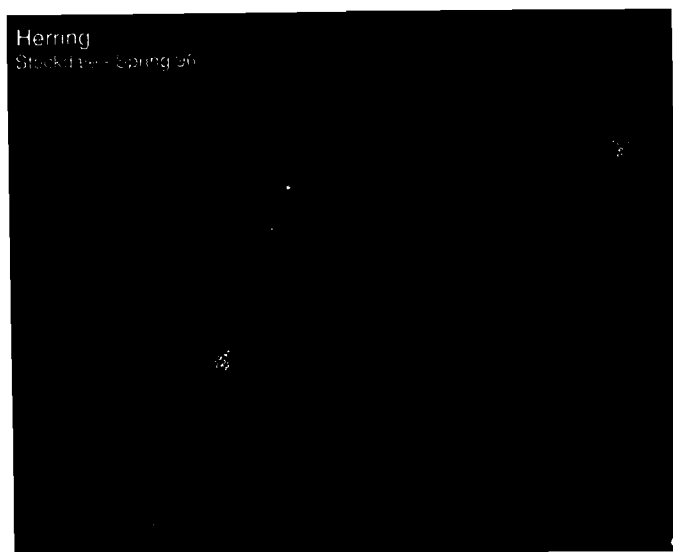
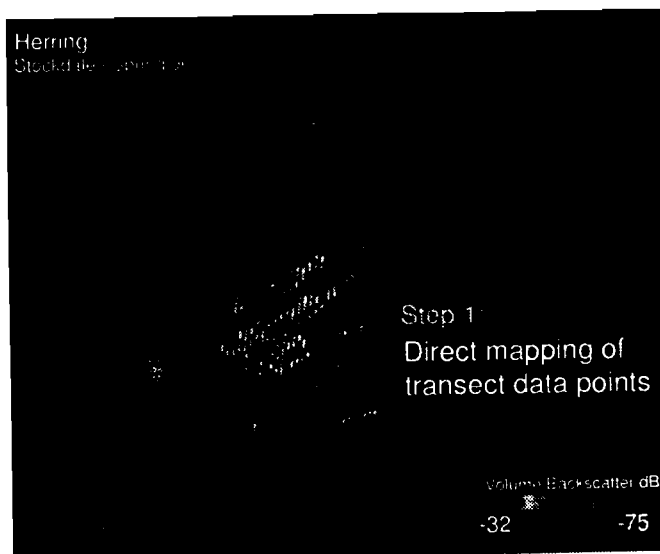


Figure 9

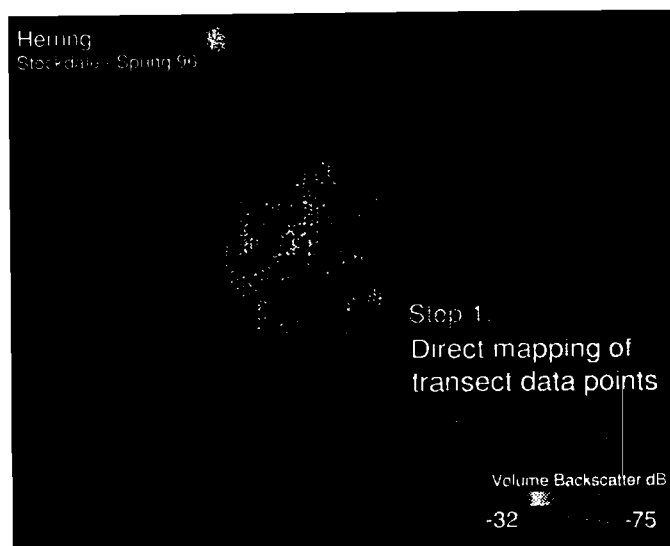
Color versions available for viewing at www.pwssc.gen.ak.us/sea/evos97rpt/



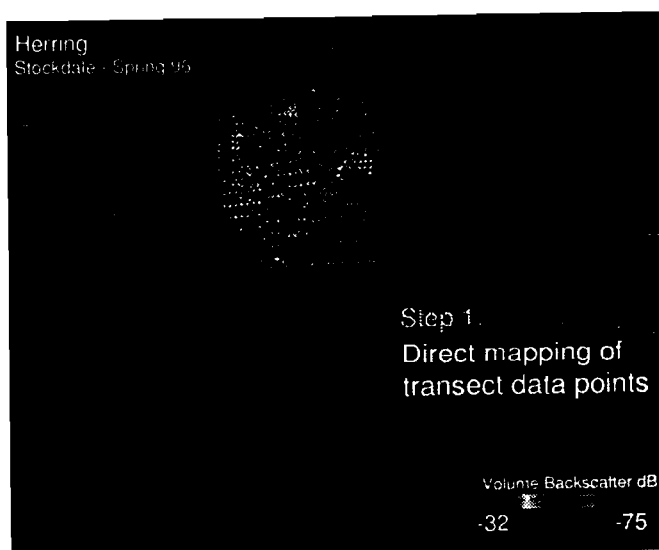
A



B



C



D

Figure 10

Color versions available for viewing at www.pwssc.gen.ak.us/sea/evos97rpt/

A

Herring
Stockdale - Spring 96

Step 2:
Volume interpolation

Volume Backscatter dB

-32 -75

B

Herring
Stockdale - Spring 96

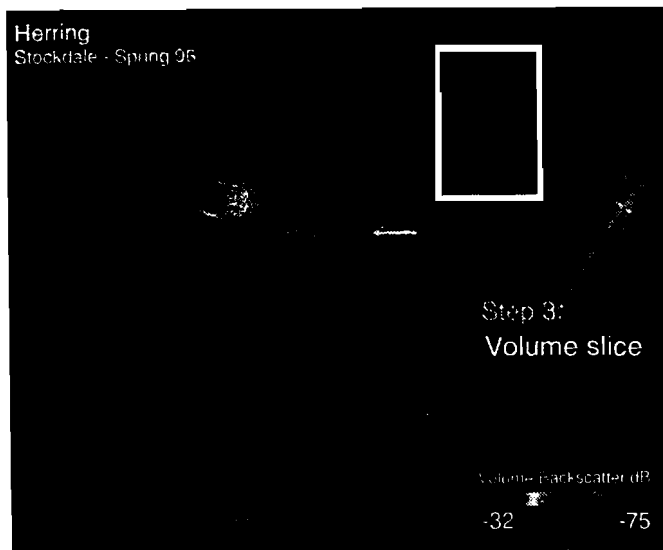
Step 3:
Volume slice

Volume Backscatter dB

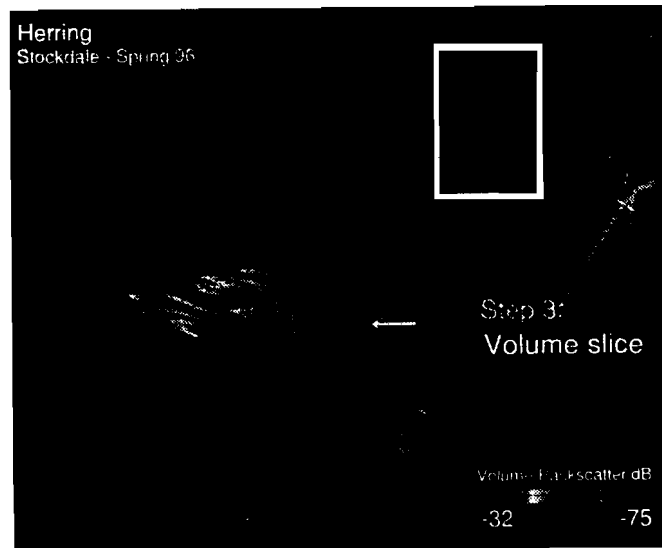
-32 -75

Figure 11

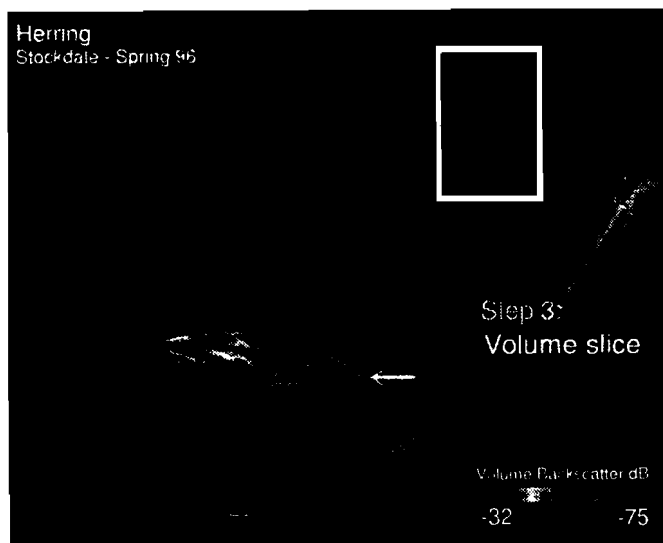
Color versions available for viewing at www.pwssc.gen.ak.us/sea/evos97rpt/



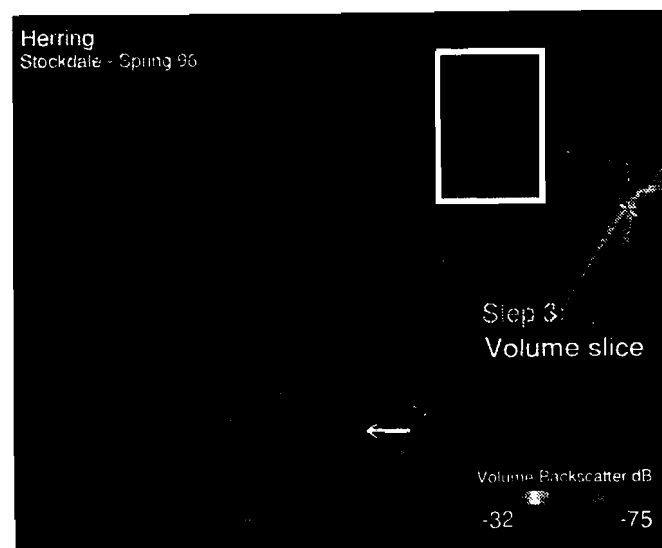
A



B



C



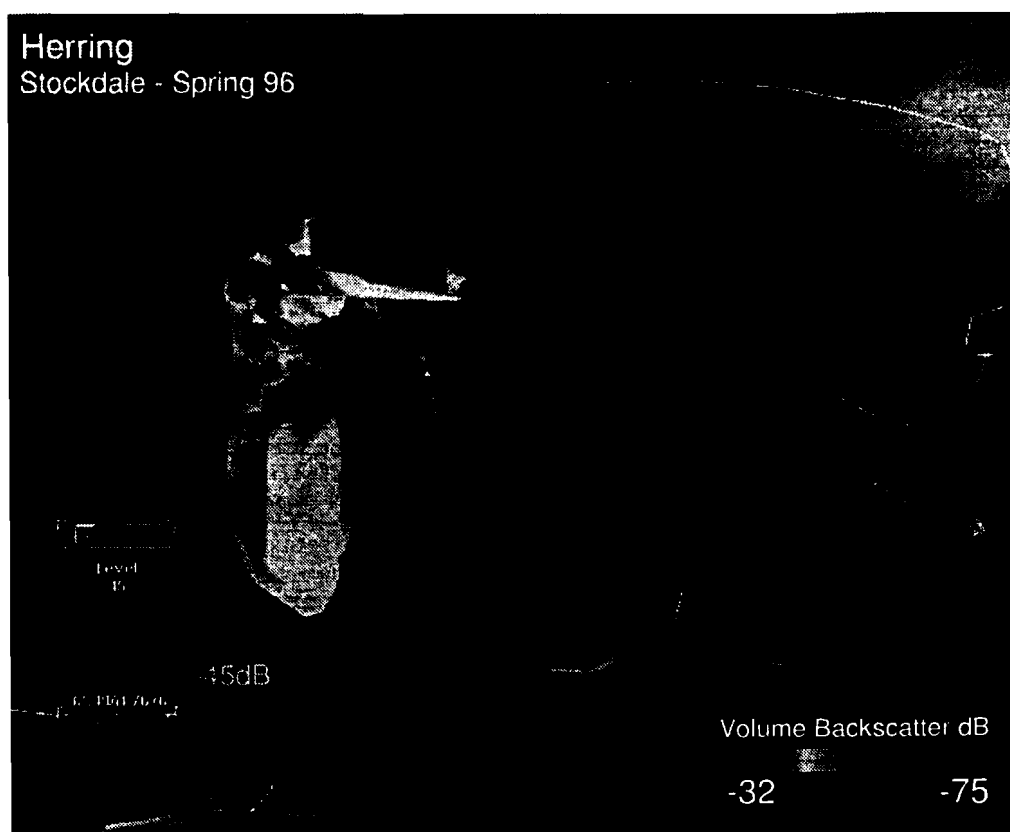
D

Figure 12

Color versions available for viewing at www.pwssc.gen.ak.us/sea/evos97rpt/

A

Herring
Stockdale - Spring 96



B

Herring
Stockdale - Spring 96

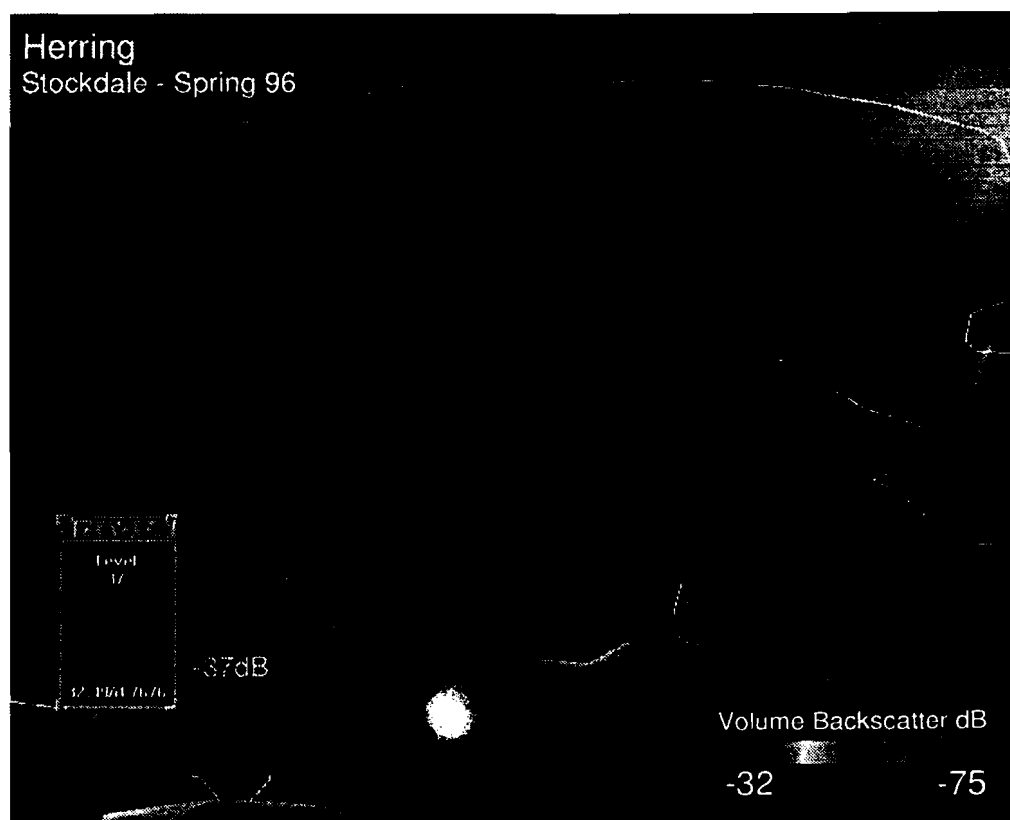
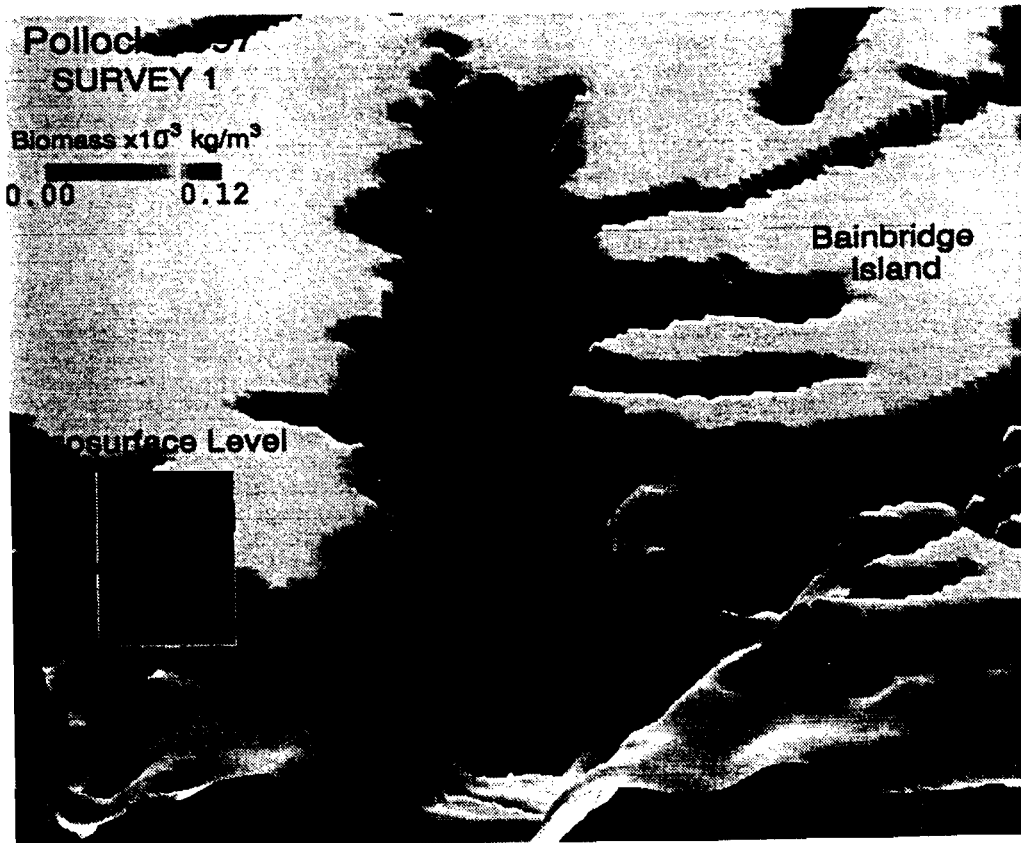


Figure 13

Color versions available for viewing at www.pwssc.gen.ak.us/sca/evos97rpt/

A



B

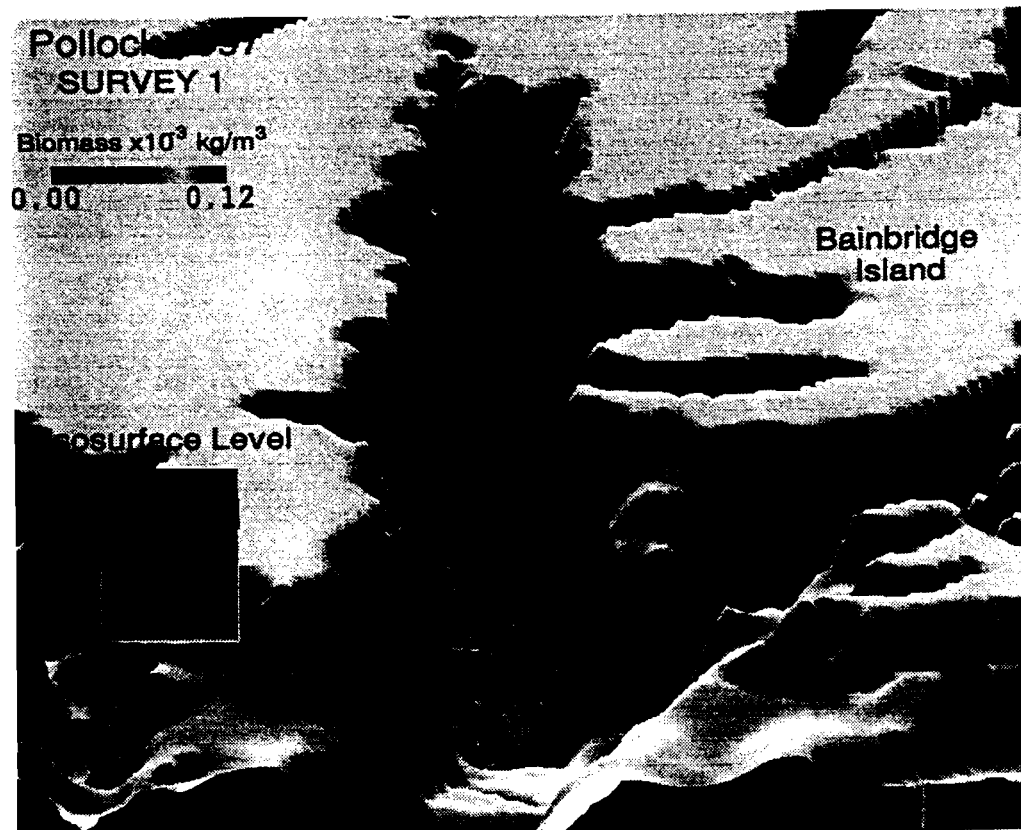


Figure 14

Color versions available for viewing at www.pwssc.gen.ak.us/sea/evos97rpt/

Part IV
Report on 1997 progress
Weather Data Systems
S. Bodnar



Part IV: WEATHER DATA SYSTEMS

Stephen Bodnar
April 15, 1998

The Applegate Weather Station operated through calendar year 1997 with a 95% data coverage, 16673 records out of a possible 17520. The station is recording wind speed, wind direction, air temperature, solar radiation, and barometric pressure at 30 minute intervals, and data is downloaded via radio-modem to the PWS Science Center on a daily basis.

Work is underway to upgrade the station for near-realtime data download. The current custom DOS download software is being tested under a DOS shell on a linux computer, and is being ported to run under linux. When the Applegate station is capable of reliable communications under all atmospheric conditions, it will be reprogrammed for continuous realtime data transmission to the Science Center.

An interface has been developed to post the most recent Applegate data to the Science Center web page, and to plot the last 24 hours of data in an easily accessible format. The data is archived, along with that from a small weather station located at the Science Center. Software is being written and tested to continuously download realtime weather data from all METAR stations in the Prince William Sound and near-coastal region. It will also download NOAA buoy data, and other relevant climatic datasets to a local master archive for use by researchers in Prince William Sound. This will replace the current manually updated archive.

The Heney Ridge repeater was replaced with an updated radio-modem, removing the last NETROM node from the system. The Naked Island repeater had a similar upgrade last year. The new modems will allow faster, more flexible network routing, as well as the ability to connect RS232 capable equipment at the mountaintop repeater sites. It also adds redundancy as all modems in the network are now identical.

The radio network has been operating successfully with a minor atmospheric related reception problem. During periods of heavy weather (heavy snow, heavy rain, high SE winds), the system operates well above design and theoretical parameters. It has been possible to send data 40 miles with a 2 watt radio under these conditions. Six miles is the theoretical maximum; design parameters state that signals in the uhf band (our operating frequency is 464.425 mhz) are often blocked by heavy precipitation. In our network, the exact opposite has proved true. The Applegate weather station is 21 miles from the Naked Island repeater and has maintained reliable communications with a 2 watt radio and newly installed yagi (directional) antenna. Only during periods of high barometric pressure and cloudless skies does the system lose connectivity. Reasons are as yet unclear, but replacing the existing 2 watt radio with a 5 watt transceiver is expected to alleviate the problem.

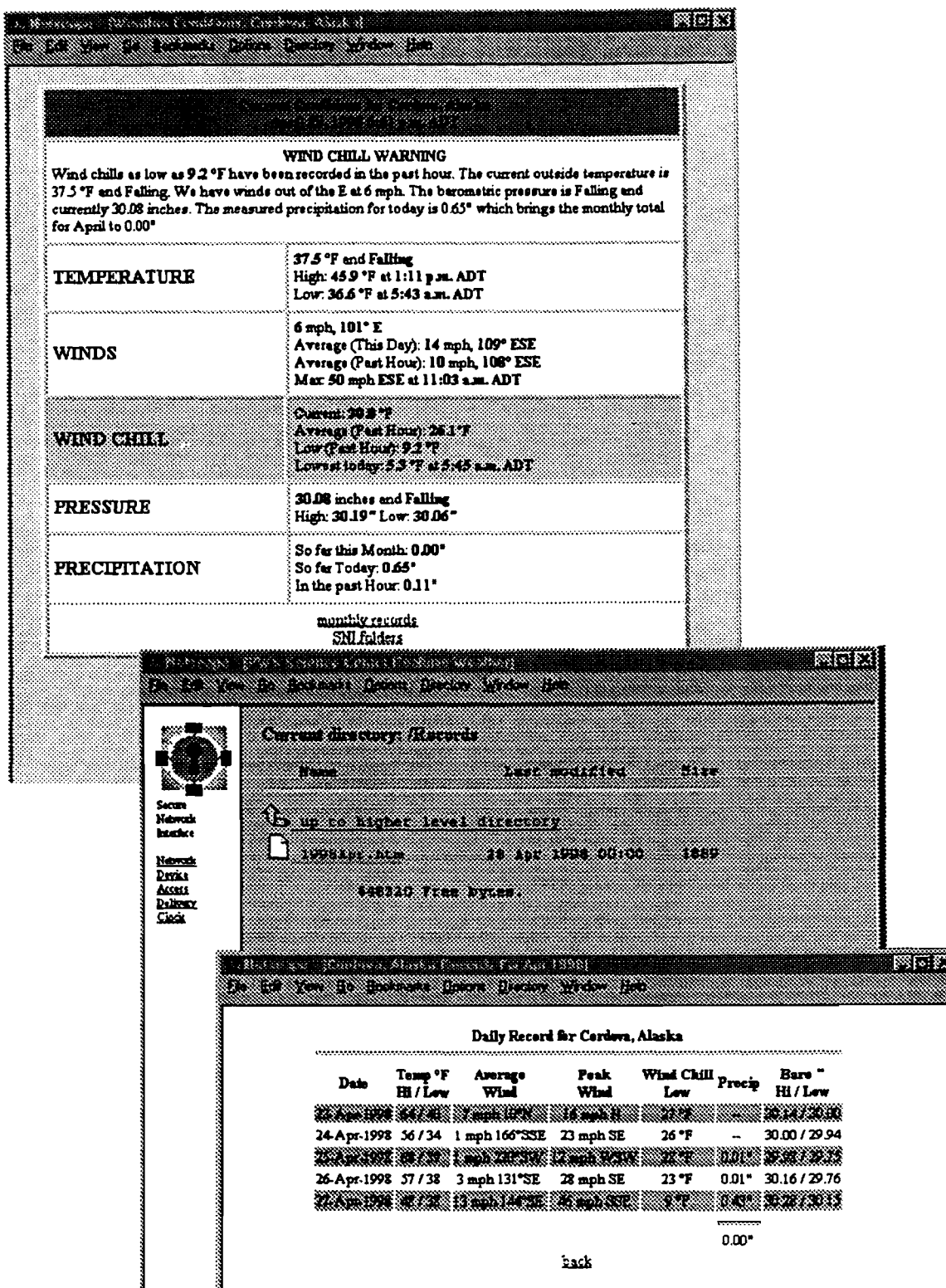


Figure 1. Secure Network Interface configured for realtime delivery of Cordova weather data

APPENDIX 2

A three-dimensional tidal model for Prince William Sound, Alaska
J. Wang, C. N. K. Mooers, V. Patrick
to appear in *Computer Modelling of Seas and Coastal Regions III*

A three-dimensional tidal model for Prince William Sound, Alaska

J. Wang^a, C.N.K. Mooers^a, V. Patrick^b

^a Ocean Prediction Experimental Laboratory and Division of Applied Marine Physics, Rosenstiel School of Marine and Atmospheric Science, University of Miami, Miami, Florida 33149 USA ^b Prince William Sound Science Center, P.O. Box 705, Cordova, Alaska 99574 USA

Email: jia.wang@rsmas.miami.edu

Abstract

A three-dimensional, primitive equation model is used to simulate the ocean tides in Prince William Sound (the Sound), Alaska. Six tidal constituents (M_2 , N_2 , S_2 , K_1 , O_1 , and P_1) are specified on the open boundaries with a partially clamped condition. The model is used to simulate the tidal heights, tidal currents, and residual current. The tide is mixed, mainly semidiurnal. The tidal current vector fields compare reasonably with towed ADCP (Acoustic Doppler Current Profiler) measurements conducted during 1994. The tidal residual current pattern is significant relative to the mean throughflow circulation.

1 Introduction

Prince William Sound (the Sound) is a combination of multiple basins, fjords, channels, islands, inlets, and estuaries along the coast of Alaska. Its area, including estuaries and arms, is approximately $120 \times 120 \text{ km}^2$ (about 70% covered by water) with an average depth of about 190m. It has several deep basins (with a maximum depth of about 750m in the northwestern Sound) and channels.

Ocean tides entering the Sound from the Gulf of Alaska are a major dynamical feature, although they have not been much studied. Because North America's largest oil spill (by T/V Exxon Valdez on 24 March 1989) seriously impacted the ecosystem of the Sound and the adjacent downstream waters⁶, a large

number of studies have been conducted to address impact, recovery, and restoration. The SEA (Sound Ecosystem Assessment) Program is a restoration project of the Exxon Valdez Oil Spill Trustee Council. The program objective is a quantitative characterization of those components of the ecosystem driving the recovery of the two primary commercial fish species, pink salmon and Pacific herring. The method of approach involves the development of a coupled physical-biological model for critical juvenile stages of the two species. The physical oceanography component consists of a field project and a circulation modeling project. This paper presents numerical simulations of tides and tidal currents in the Sound to assess their influence on the mean circulation. The progress of the SEA Program has been summarized³.

A 3-D ocean circulation model has been developed for Prince William Sound and studies of the circulation patterns due to throughflow and wind-forcing have been described⁴. However, tidal flows were not included. Thus, the purpose of this study is to 1) implement a 3-D numerical model for simulating tides and tidal current and 2) examine the tidal residual currents.

Section 2 briefly describes the 3-D numerical model, plus the model configuration, model parameters, initial and boundary conditions, and forcing. Section 3 presents the simulation results. Finally, section 4 summarizes the results and outlines the future effort.

2 Description and Implementation of the Model

A version of the Princeton Ocean Model (POM²), which has been successfully applied to the circulation of Hudson Bay¹¹, is utilized. It is based on the primitive equations (with hydrostatic and Boussinesq approximations) and has the following features: (1) horizontal curvilinear coordinates (not used here); (2) an Arakawa C grid; (3) sigma (terrain-following) coordinates in the vertical with realistic bottom topography; (4) a free surface; (5) the Mellor-Yamada level 2.5 turbulence closure model for vertical viscosity and diffusivity; (6) the Smagorinsky parameterization for horizontal viscosity and diffusivity; (7) a semi-implicit scheme for the shallow water equations^{1,11}; and (8) a predictor-corrector scheme for the time integration to avoid inertial instability^{9,10}.

The model domain includes the entire Sound with two open boundaries

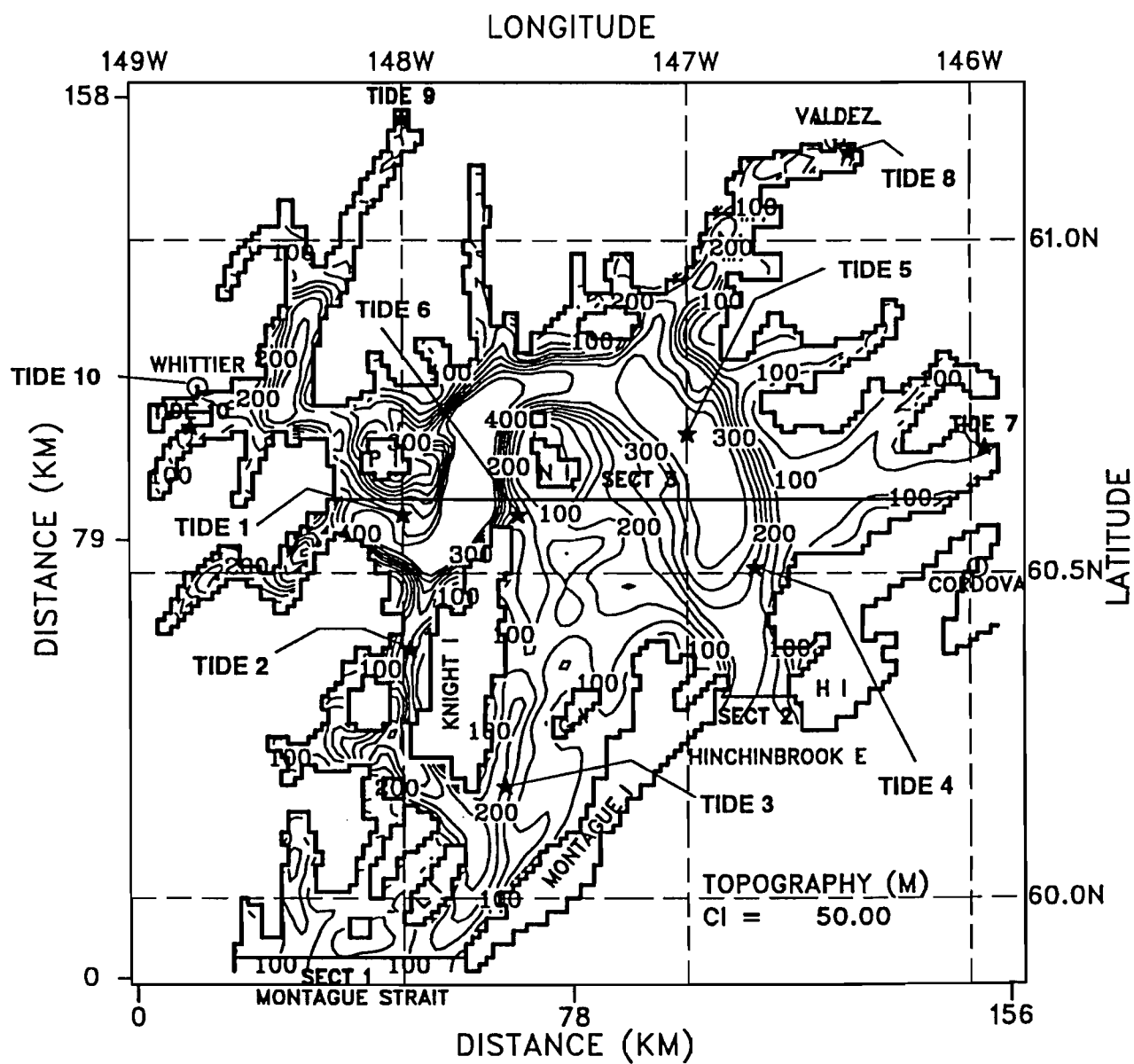


Figure 1, Model domain and topography with depths in meters. Stations, Tide 1 to Tide 10, indicate the stations from which tidal height time series are extracted.

(Hinchinbrook Entrance and Montague Strait, Fig 1), allowing water exchange with the Alaskan coastal waters⁷. The model grid spacing is 1.2 km, which is eddy-resolving because the internal Rossby radius of deformation is about 5km⁵. There are 11 vertical sigma levels. The integration time step is 62.1 seconds, which is about six times the CFL (Courant-Friedrichs-Lewy) constraint because a semi-implicit scheme has been used for the shallow water equations¹¹.

The open lateral boundary conditions are determined by a partially clamped radiation condition in which the sea surface elevation, η , at the boundary is time dependent:

$$\frac{\partial \eta}{\partial t} + C \frac{\partial \eta}{\partial n} - \frac{\eta_k - \eta}{T_f} = 0, \quad (1)$$

where η_k is the tide's elevation, $C=(gH)^{1/2}$ is the surface gravity wave phase speed, and T_f is a time scale for the clamped/radiation boundary condition. The partially clamped condition of this study uses $T_f=10s$ (clamped being the limit for $T_f \rightarrow 0$). [In contrast, a radiation condition would be obtained by using, for example, $T_f=4$ days (pure radiation being the limit for $T_f \rightarrow \infty$ which is not used here)]. For the normal component of throughflow, the 2-D normal velocity (or transport) is defined following Wang et al.¹¹. Furthermore, the 3-D normal velocity (or transport) into/out of the Sound is equal to the 2-D transport and the total transport is conserved when averaged over a tidal cycle.

The initial temperature and salinity fields used are based on typical early summer profiles in the central Sound for late summer 1994, and are specified to be horizontally uniform. The mean throughflow was specified at Hinchinbrook Entrance; two cases were considered: $0.15 \times 10^6 \text{ m}^3\text{s}^{-1}$ corresponding to a case treated in Mooers and Wang⁴ and $0.05 \times 10^6 \text{ m}^3\text{s}^{-1}$ corresponding to the conditions in the fall of 1994. The model was spun-up for 10 M_2 cycles (about 5 days) to reach a dynamically steady state. The vertical viscosity is determined from the Mellor-Yamada level 2.5 turbulence closure model with a background viscosity of $10^{-5} \text{ m}^2\text{s}^{-1}$ (i.e., the value used if the calculated viscosity is smaller than this minimum value). The horizontal viscosity is determined from the Smagorinsky horizontal turbulence closure with the mixing coefficient $C=0.2$.

3 Simulation Results

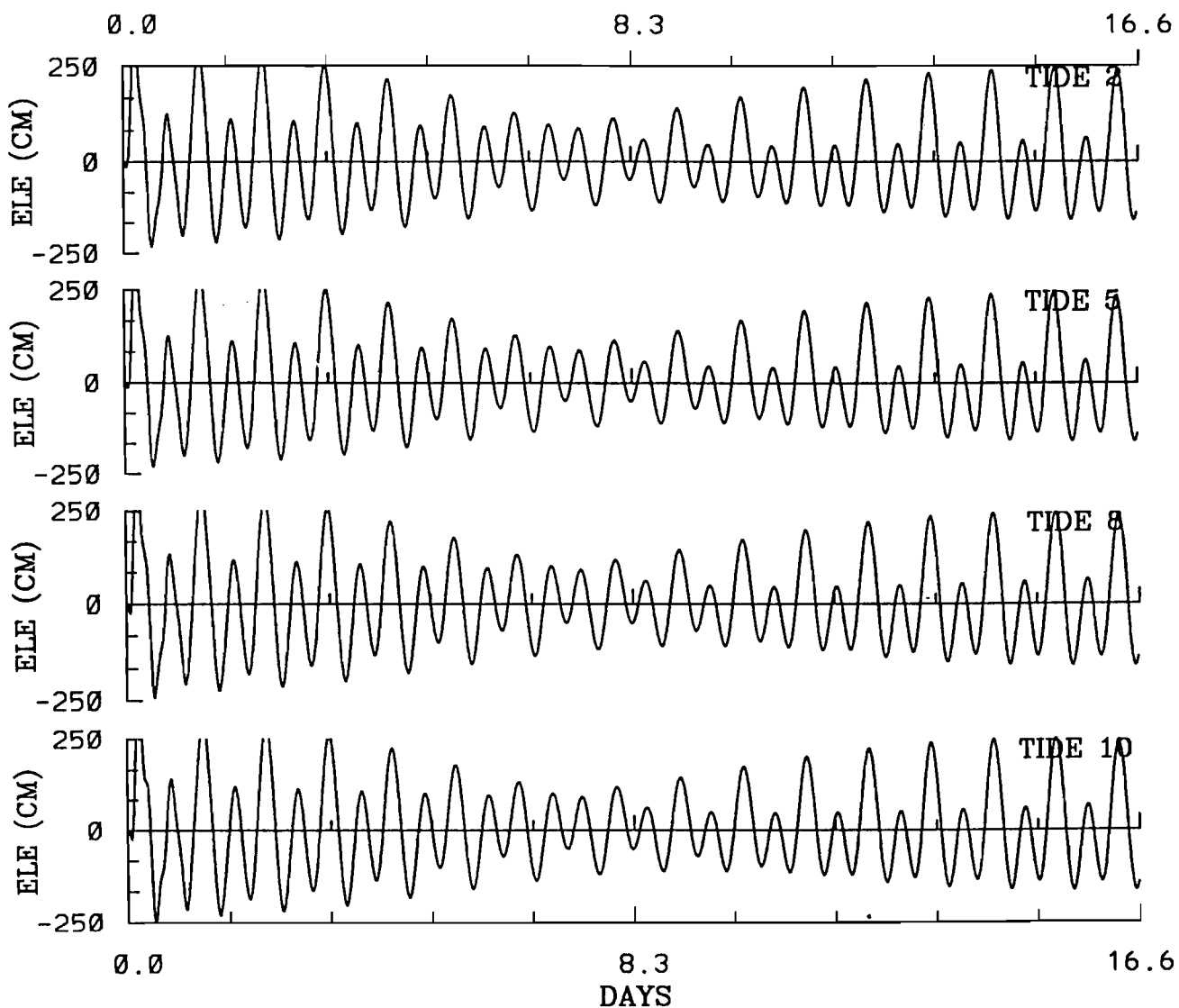


Figure 2. Sixteen-day tidal height time series from stations Tide 2 (Knight Island Passage), Tide 5 (Central Sound), Tide 8 (Valdez), and Tide 10 (Whittier) under forcing of six tidal constituents and throughflow of $0.15 \times 10^6 \text{ m}^3\text{s}^{-1}$.

The harmonic constants of the six tidal constituents [with amplitudes (in meters) and phases (in degrees) for M_2 (1.16m, 286), N_2 (0.24m, 264), S_2 (0.4m, 321), K_1 (0.5m, 274), O_1 (0.28m, 257), and P_1 (0.16m, 273)] were obtained from Schwiderski⁸. The tide type factor, $F=(K_1+O_1)/(M_2+S_2)$, is 0.5, indicating a mixed, mainly semidiurnal tide type.

The simulated tidal heights (Fig. 2) for about 16 days at four stations [Knight Island Passage (Tide 2), Central Sound (Tide 5), Valdez (Tide 8), and Whittier (Tide 10)] demonstrate that the average tidal range (peak-to-peak) is about 5m during spring tide and about 3m during neap tide.

The first experiment was conducted using a throughflow of $0.05 \times 10^6 \text{ m}^3\text{s}^{-1}$ corresponding to the conditions in the fall of 1994. The simulated tidal currents on seven different stages (maximum flood, high tide, maximum ebb, low tide, etc.) can be examined and compared with available observations. The towed ADCP tidal current fields (acquired by Prince William Sound Science Center during the fall of 1994 under the SEA Program) were also grouped into the seven tidal stages. For example, the tidal current field at 17m, during early ebb when there is a spring tide (Fig. 3), is compared with the towed ADCP measurements at 17m during the same tidal stage (Fig. 4). The overall pattern (magnitude and direction) is similar, except in the northern Sound (around 60.8N and 147.3W).

For this project it is important to estimate the possible mean circulation pattern induced by the throughflow and tides (residual current) in the Sound, which may modify the dispersal patterns and times of biota (fish eggs and larva and plankton) and pollutants. The second experiment was conducted using a throughflow of $0.15 \times 10^6 \text{ m}^3\text{s}^{-1}$ and the six tidal constituents. The tidal residual current averaged over two M_2 tidal cycles (Fig. 5), which can be compared to the mean flow only under the throughflow forcing (Fig. 3 of Mooers and Wang⁴). The overall throughflow pattern is similar; however, the anticyclonic circulation in the Central Sound is very prominent, and there is also an anticyclonic circulation in the northwestern Sound (over the deepest basin). These two mean circulation cells differ in strength and location from those occurring in the absence of the tides, indicating that the tidal residual current is an important factor in the Sound, particularly in the Central Sound and in the northwestern Sound.

4 Concluding Remarks

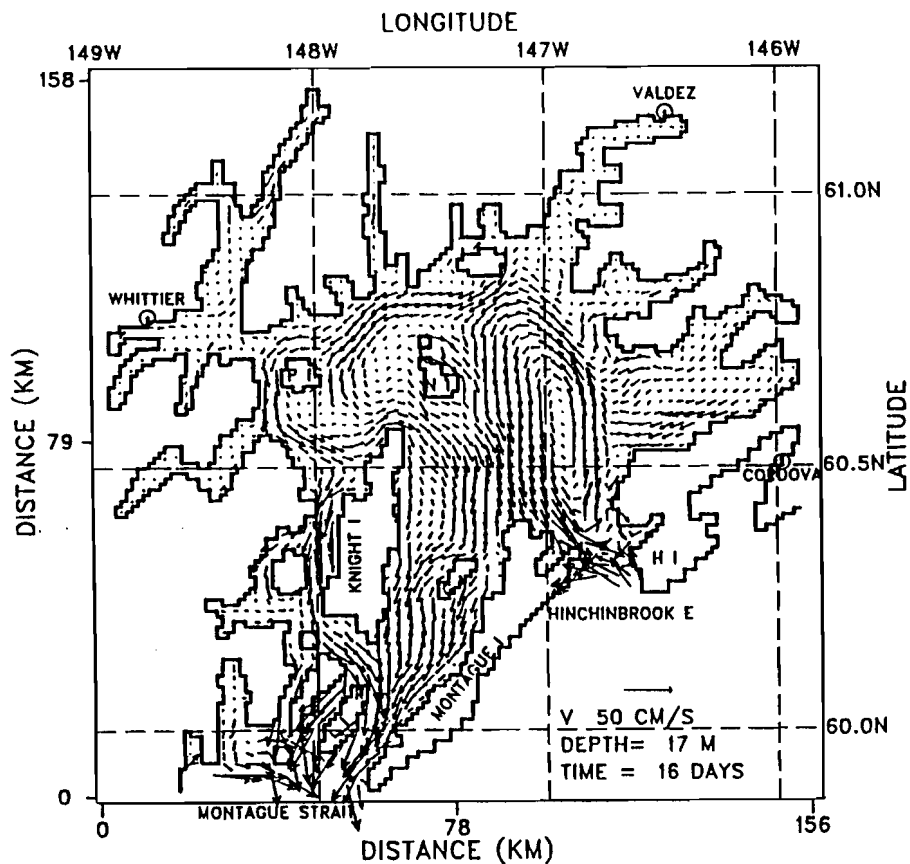


Figure 3. Simulated subsurface (17m) tidal current field at early ebb tide on day 16 (spring tide) with the throughflow of $0.05 \times 10^6 \text{ m}^3 \text{ s}^{-1}$.

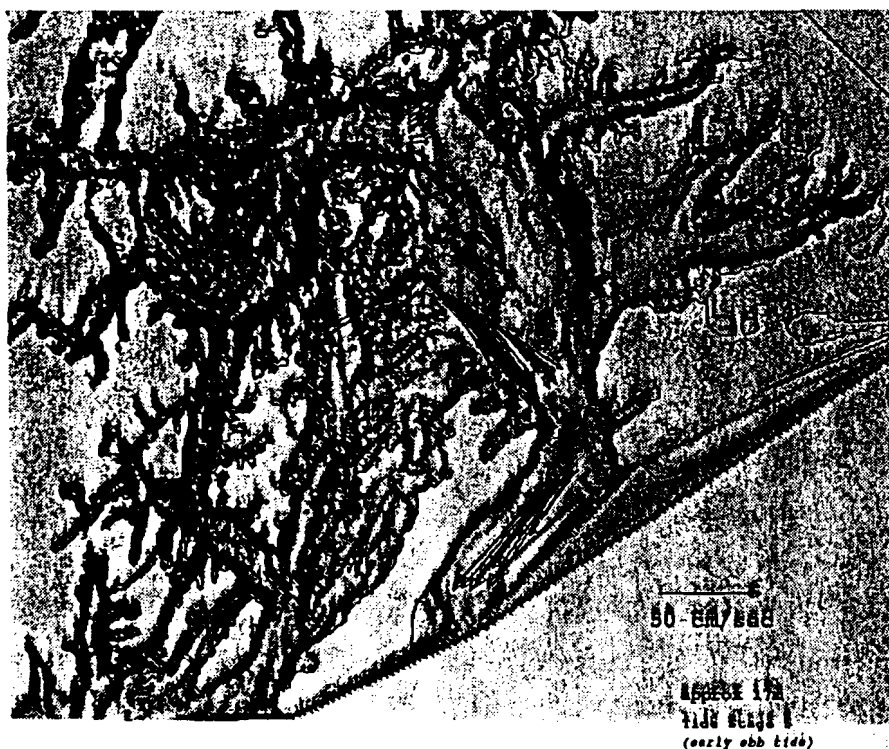


Figure 4. Observed subsurface (17m) tidal current field at early ebb tide using a towed ADCP in the fall of 1994.

The tidal currents play a significant role in the mean and transient circulation of Prince William Sound. The tide is mixed, mainly semi-diurnal. The tidal currents may reach 0.5 ms^{-1} ; hence, they may be influential in the mixing regime. The tidal range is as high as about 5m during spring tide and as low as about 3m during neap tide. The residual currents in the Central Sound and the northwestern Sound are about 3 to 5 cm s^{-1} and will influence the dispersal of suspended, dissolved, and particulate matter. Thus, they may impact the location and residence times of the biological retention zones.

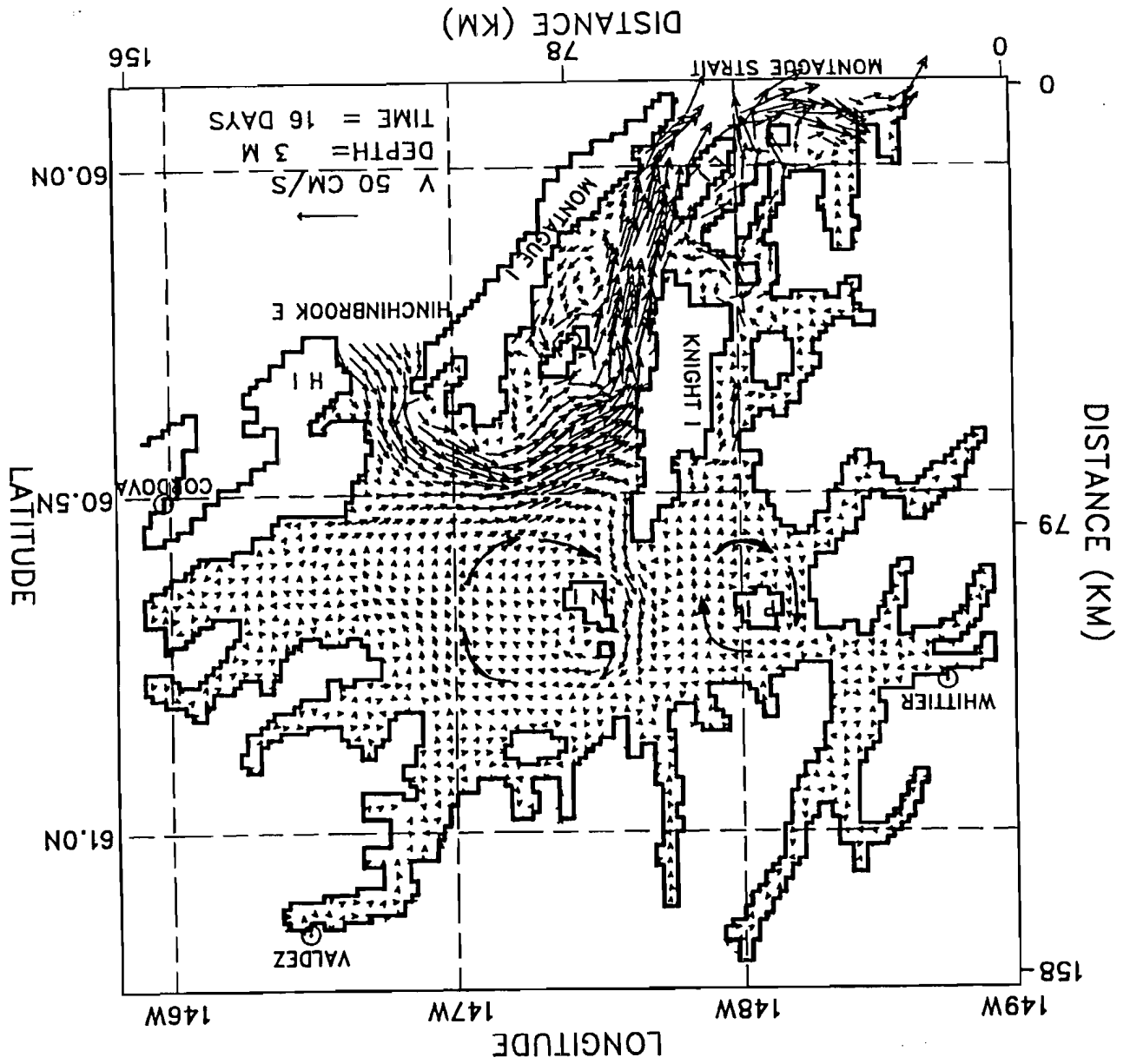
The simulated tidal velocity fields are generally consistent with those from the towed ADCP measurements. The simulated mean circulation pattern under tidal and throughflow forcing differs from the mean circulation pattern induced by a throughflow only. Obviously, the significance of the differences will depend upon the strength of the throughflow. The tidal residual current pattern includes anticyclonic gyres in the Central Sound and an anticyclonic gyre in the northwestern Sound. These two residual current gyres will influence the dispersal properties of the Sound.

Acknowledgements: Financial support from the SEA Program of the Exxon Valdez Oil Spill (EVOS) Trustees Council administered through Prince William Sound Science Center, Alaska, is appreciated. Discussions of the PWS circulation with Drs. T.C. Royer and Z. Kowalik are gratefully acknowledged. We also thank Mr. J. Murphy, Ms. J.R. Allen, and Dr. D.K. Salmon of PWSSC for the analysis of the ADCP data.

References

1. Blumberg, A.F., 1991. A primer for ECOM-si. Technical Report for HydroQual, Inc., Mahwah, NJ, 66 pp.
2. Blumberg, A.F. and G.L. Mellor, 1987. A description of a three-dimensional coastal ocean circulation model. In: Coastal and Estuarine Sciences 4: Three-Dimensional Coastal Ocean Models, N.S. Heaps, ed., American Geophysical Union, Washington D.C.: 1-16. 18: 775-787.

Figure 5. Simulated surface (3m) residual current field averaged over two M_2 tidal cycles under forcing of both the six tidal constituents and throughflow of $0.15 \times 10^6 \text{ m}^3 \text{ s}^{-1}$.



3. Cooney, R.T. 1996. Sound Ecosystem Assessment (SEA): A Science Plan for the Restoration of Injured Species in Prince William Sound, Alaska. Exxon Valdez Oil Spill Restoration Project Annual Report (Restoration Project 95320). Alaska Depart. of Fish and Game, Anchorage, Alaska.
4. Mooers, C.N.K. and J. Wang, 1997. On the development of a 3-D circulation model for Prince William Sound, Alaska, **Cont. Shelf Res.** (in press).
5. Niebauer, H.J., T.C. Royer and T.J. Weingartner, 1994. Circulation of Prince William Sound, Alaska. **J. Geophys. Res.**, 99: 14,113-14,126.
6. Royer, T.C., J.A. Vermersch, T.J. Weingartner, H.J. Niebauer and R.D. Muench, 1990. Ocean circulation influencing the Exxon Valdez oil spill. **Oceanography**, 3-10.
7. Schmidt, G.M., 1977. The exchange of water between Prince William Sound and the Gulf of Alaska, M.S. thesis, Univ. of Alaska, Fairbanks, 116 pp.
8. Schwiderski, E.W. 1980. On charting global ocean tides. **Rev. Geophys. Space Phys.**, 18: 243-268.
9. Wang, J. and M. Ikeda, 1996. A 3-D ocean general circulation model for mesoscale eddies-I: Meander simulation and linear growth rate. **Acta Oceanologica Sinica**, 15: 31-58.
10. Wang, J. and M. Ikeda, 1997. On inertial stability and phase error of time integration schemes in ocean general circulation models. **Mon. Wea. Rev.** (in press).
11. Wang, J., L.A. Mysak and R.G. Ingram, 1994. A 3-D numerical simulation of Hudson Bay summer circulation: topographic gyres, separations and coastal jets. **J. Phys. Oceanogr.**, 24: 2496-2514.

**A two-compartment model for understanding
the simulated three-dimensional circulation
in Prince William Sound, Alaska**

E. Deleersnijder, Université catholique de Louvain, Belgium

J. Wang and C. N. K. Mooers, RSMAS, University of Miami

to appear in *Continental Shelf Research* JONSMOD '96 Special Issue

A two-compartment model for understanding
the simulated three-dimensional circulation
in Prince William Sound, Alaska

by

Eric DELEERSNIJDER

Institut d'Astronomie et de Géophysique G. Lemaître,
Université catholique de Louvain,
2 Chemin du Cyclotron, B-1348 Louvain-la-Neuve, Belgium

Jia WANG and Christopher N.K. MOOERS

Ocean Prediction Experimental Laboratory and Division of Applied Marine Physics,
Rosenstiel School of Marine and Atmospheric Science, University of Miami,
4600 Rickenbacker Causeway, Miami, Florida 33149-1098, USA

(accepted)

corresponding author address:

Eric Deleersnijder Unité ASTR - UCL
--

to be submitted to *Continental Shelf Research*
(JONSMOD '96 Special Issue)
July 1997

2 Chemin du Cyclotron
B-1348 Louvain-la-Neuve, Belgium
Tel: +32-10-472.676 or +32-10-473.297
Fax: +32-10-474.722
E-mail: ericd@astr.ucl.ac.be

ABSTRACT

A two-compartment model of Prince William Sound (PWS), Alaska, is developed. One compartment, corresponding to the southern part of the Sound, represents advective phenomena, while the other is dominated by diffusion. This simple model is shown to reproduce rather well the temporal evolution of the mass of a passive tracer contained in PWS simulated by a complex, three-dimensional model under five types of surface forcing. The three parameters of the box-model have clear physical meanings, which helps to understand the hydrodynamics of PWS. In particular, the fraction of the flow entering the northern PWS is estimated, as well as the turnover time of the two regions considered.

INTRODUCTION

One of the largest oil spills onto the seas occurred in Prince William Sound (PWS), Alaska, on 24 March 1989, as the result of a navigation error of the Exxon Valdez. Since then, considerable efforts have been devoted to the study of the ecosystem of this region. In this framework, Mooers and Wang (1997) — hereafter referred to as MW — used a version of the three-dimensional Princeton Ocean Model (*e.g.* Blumberg and Mellor, 1987) to simulate the water circulation in PWS.

For details about the topography of the domain of interest, refer to MW. Herein, it is sufficient to mention that the lateral computational boundary is impermeable, except for two narrow passages in the southern part of PWS, Hinchinbrook Entrance and Montague Strait. Moreover, it must be underscored that, in general, water originating from the Gulf of Alaska enters PWS through the former and leaves through the latter.

MW conducted a sensitivity analysis of the PWS circulation to the surface stress. In the control run, no wind forcing was applied. Four additional simulations were carried out in which the wind was assumed to be blowing with the same speed toward the east, the north, the west, and the south, respectively. For each type of forcing, a flow in a statistical equilibrium was obtained. The latter was then used to simulate the fate of a passive tracer released at a constant rate for four days by a line source located in Hinchinbrook Entrance.

In each model run, the source released tracer in the upper 40 m at the constant rate Φ from time $t=0$ until it was cut off, at time $t=T$, with $T=4$ days. Thus, the total amount of tracer injected into PWS was $M=\Phi T$. The tracer content of PWS, m_s , was simulated for 33 days by MW (Fig. 1).

The temporal evolution of the tracer mass present in PWS exhibits four distinct phases which are qualitatively similar in every model run (Fig. 2). First, from $t=0$ until $t=T$, m_s grows approximately linearly, since almost no tracer parcel has yet left PWS

through Montague Strait. Then, as long as the outgoing tracer flux is negligible, the tracer mass remains virtually constant. This regime lasts until $t = \tau$, which is the time period that a tracer parcel needs to travel from Hinchinbrook Entrance to Montague Strait following the most direct pathway. Then, the tracer mass diminishes monotonically. During the third phase, the tracer mass decreases approximately linearly as time progresses. The transition from the third to the fourth phase is characterised by an abrupt change in the pace at which the mass diminishes. Finally, during the final phase, the rate of decrease of the mass is much smaller.

The processes which are at work during the first two phases are readily understood. That the mass must decrease during the subsequent phases is obvious too. However, explaining why the rate of decrease of the mass changes is not straightforward. To do so, a simple, compartmental model is established, which will help infer major properties of the PWS circulation, as well as reveal the influence of the wind on them.

A TWO-COMPARTMENT MODEL

An attempt will be made to represent the evolution of PWS tracer content by means of an elementary model. The tracer mass estimated therefrom will be denoted m so as to distinguish it from its counterpart, m_s , simulated by MW using a complex, three-dimensional model.

The tracer mass obeys

$$\frac{d}{dt}m(t) = \phi^{in}(t) - \phi^{out}(t), \quad (1)$$

where ϕ^{in} is the tracer flux entering PWS through Hinchinbrook Entrance while ϕ^{out} represents the rate at which tracer leaves PWS through Montague Strait. The flux ϕ^{in} is due

to the tracer source, while the outgoing flux depends on the tracer content of the Sound and the hydrodynamic processes occurring in it, the major features of which must be understood for a suitable parameterization to be devised.

A tracer parcel behaves like a water parcel, since the tracer considered is passive.

The MW modelled current maps clearly suggest that a tracer parcel may follow two distinct types of path leading from Hinchinbrook Entrance to Montague Strait. The largest current speeds occur between Knight Island and Montague Island, implying that the quickest pathway is associated with advection through this region. The second route is that of parcels going further north into the Sound, where the circulation is much slower and intricate, partly because of numerous topographic features, such as islands, fjords, or headlands. At the scale of the northern PWS, these advective processes may amount to diffusion.

This description provides a basis for dividing PWS into two parts, the southern PWS — also termed “region 1” below — dominated by advection and the northern PWS — also called “region 2” hereafter — where diffusive mechanisms prevail. Therefore, the tracer mass present in PWS at a given time, $m(t)$, may be regarded as the sum of $m_1(t)$ and $m_2(t)$, where $m_i(t)$ ($i = 1, 2$) is the tracer mass contained in region i . If ϕ_i^{in} and ϕ_i^{out} denote the fluxes entering and leaving region i , respectively, m_i obeys

$$\frac{d}{dt}m_i(t) = \phi_i^{in}(t) - \phi_i^{out}(t), \quad i = 1, 2. \quad (2)$$

Since region 1 is assumed to be dominated by advection,

$$\phi_1^{out}(t) = \phi_1^{in}(t - \tau), \quad (3)$$

where the time lag τ , as already mentioned in the preceding section, is the period of time that a tracer parcel, following the quickest path, needs to transit from Hinchinbrook Entrance to Montague Strait.

If the diffusive processes taking place in region 2 are rather strong, then the tracer concentration therein may be assumed to be sufficiently homogeneous for the tracer flux leaving this region to be proportional to the tracer mass present in it, *i.e.*,

$$\phi_2^{out}(t) = \frac{m_2(t)}{\theta} , \quad (4)$$

where the time scale θ is the turnover time of region 2. The latter is defined to be the average over the northern PWS of the residence time — which, at a given point of region 2, is the period of time that a water parcel, initially located at the point considered, needs to leave the northern PWS. Additional explanations and appropriate references on such hydrodynamic time scales, as well as parameterizations similar to (4), may be found in Bolin and Rodhe (1973) and Tartinvill *et al.* (1997).

Let α denote the fraction of the tracer flux entering PWS that goes directly into region (2). Hence,

$$\phi_2^{in}(t) = \alpha \phi^{in}(t) . \quad (5)$$

The tracer flux leaving region 2 may be assumed to join that exiting the southern PWS. However, it is readily seen that such a flux arrangement would prevent the PWS tracer content from growing linearly during the first phase of the tracer mass evolution. In addition, m could not remain almost constant for a certain period of time after the source is cut off. To circumvent these problems, the tracer pathway involving region 2 must include an appropriate time lag. For the sake of simplicity, it is decided that the flux leaving region 2 enters the southern PWS (Fig. 3), *i.e.*,

$$\phi_1^{in}(t) = (1-\alpha)\phi^{in}(t) + \phi_2^{out}(t). \quad (6)$$

This is a modelling choice which does not require introducing a time lag specific to the northern PWS, since use is made of that associated with region 1.

The two-compartment model meant to represent the major features of the tracer evolution in PWS consists of equations (1) to (6), the solution of which reads

$$m(t) = \int_0^t [\phi^{in}(\mu) - (1 - \alpha e^{\frac{\mu-t}{\theta}}) \phi^{in}(\mu-\tau)] d\mu, \quad (7)$$

if $m(0)=0$. In the case considered above, $\phi^{in} = \Phi$ if $0 \leq t \leq T$ ($=4$ days), and $\phi^{in}=0$ otherwise. Therefore, if $T < \tau$,

$$m(t) = \Phi t, \quad 0 \leq t \leq T, \quad (8a)$$

$$m(t) = \Phi T, \quad T \leq t \leq T + \tau, \quad (8a)$$

$$m(t) = \Phi(T + \tau - t) + \alpha \Phi \theta (1 - e^{\frac{\tau-t}{\theta}}), \quad T + \tau \leq t \leq T + \tau + \theta, \quad (8a)$$

and

$$m(t) = \alpha \Phi \theta (e^{\frac{T}{\theta}} - 1) e^{\frac{\tau-t}{\theta}}, \quad T + \tau + \theta \leq t. \quad (8a)$$

ASSESSMENT AND DISCUSSION

As expected, the solution above exhibits four different phases. It remains to be seen whether or not the three parameters τ , θ and α may be calibrated in such a way that the evolution of the tracer content predicted by the compartmental model, m , is close to that simulated by MW, m_s .

The dimensionless distance between m and m_s may be defined as

$$\varepsilon = \frac{\left[\int_0^{t_{max}} (m - m_s)^2 dt \right]^{\frac{1}{2}}}{\Phi T (t_{max})^{\frac{1}{2}}}, \quad (9)$$

where $t_{max} = 33$ days is the duration of MW's three-dimensional simulations. Obviously, the values of the parameters τ , θ , and α to be considered are those that minimise ε . They are obtained by means of a simple, iterative algorithm. As may be seen in Table 1, for every type of surface forcing, ε is rather small, indicating that there is an excellent agreement between the evolution of the tracer mass simulated by MW and that derived from the present compartmental model, which is clearly confirmed by the similarity of Fig. 1 and Fig. 4.

The parameters of the simple model are such that $\tau - t \ll \theta$ during the third phase of the tracer mass evolution, *i.e.*, during the time interval $\tau \leq t \leq T + \tau$. As a result, m admits the following asymptotic expansion

$$m(t) \approx \Phi [T - (1 - \alpha)(t - \tau)], \quad \tau \leq t \leq T + \tau, \quad (10)$$

which is the reason why the tracer mass decreases almost linearly during the third phase, as may be seen in Fig. 1 and Fig. 4.

It is clear that the turnover time of the southern PWS, as modelled above, is equal to $\tau/2$. That, in all cases, the turnover time of region 1 is much smaller than that of region 2 enables suggesting the following scenario: during the third phase, the outgoing flux at Montague Strait is essentially due to the tracer parcels that followed the quickest route, *i.e.*, those that did not enter region 2; most of the tracer parcels which penetrated into the northern PWS leave PWS during the final phase.

The fraction of the tracer parcels entering the northern PWS, α , is largest, or smallest, when the wind is northward, or southward, respectively. This is no surprise!

When the wind is northward or westward — which induces a net northward Ekman transport —, it is conceivable that tracer parcels leave the northern PWS less frequently to enter the southern region, so that it is in such circumstances that the turnover time of region 2, θ , is largest (Table 1). Conversely, θ is smallest when the wind is southward or eastward.

For reasons which are still unclear, the advective time lag τ depends weakly on the surface forcing considered (Table 1). However, it may be that τ is dominated by the specified constant throughflow and not much influenced by the Ekman flow which varies from case-to-case, a hypothesis consistent with MW's modelled current fields.

It would be foolhardy to assert that the simple model above is more realistic than the three-dimensional Princeton Ocean Model applied by MW to PWS. That the compartmental model provides at almost no cost an estimate of the tracer transport through PWS is marginally interesting, since most three-dimensional models may now be run routinely in domains like PWS. The most appealing feature of the two-compartment model is that it involves only three parameters, which all have a clear physical meaning, helping to understand the hydrodynamics of PWS — since the passive tracer and water parcels behave similarly. So, it has been possible to estimate, for every type of surface forcing considered, the fraction of the water flux crossing Hinchinbrook Entrance which first goes northward, instead of flowing directly toward Montague Strait. In addition, the turnover times of the southern and the northern regions have been evaluated. Finally, it has been suggested that the hydrodynamic processes taking place in the latter region amount to diffusion, while the former is dominated by mere advective mechanisms.

To design the two-compartment model, it has not been necessary to precisely mark out the limit between the two regions considered. In fact, the only clear-cut difference between

the two boxes is that they are dominated by hydrodynamic processes of a different nature, which does not prevent them from overlapping geographically. In other words, it is hydrodynamics rather than topography that allows distinguishing the two compartments. Therefore, it would be difficult to validate the simple model by direct comparison with fluxes computed, or measured *in situ*, through a given section of PWS. This consideration is why an inverse approach has been — and should continue to be — preferred.

In spite of the excellent agreement between the evolution of the tracer mass simulated by MW's complex three-dimensional model and that predicted by the present simple model, the latter may not be deemed to be fully validated. In fact, it would be necessary to compare the predictions of the compartmental model to those of the three-dimensional model over periods of time larger than the largest turnover time, *i.e.*, at least 100 days. On the other hand, for every type of flow, only one tracer release scenario has been considered so far, which is not sufficient. Therefore, for a given flow in PWS, it should be verified that the same set of parameters enables the two-box model to represent the evolution of the tracer mass in a satisfactory way throughout a series of tracer releases. For instance, a constant source located at Hinchinbrook Entrance of magnitude Φ may be considered, in which case the tracer mass should tend to $(\tau + \alpha\theta)\Phi$. Another interesting example consists of a source releasing an amount M of tracer in an arbitrarily short period of time, which corresponds to the case detailed above in the limit $T \rightarrow 0$. In this case, according to the simple model, the tracer mass should remain equal to M until $t = \tau$, then m should undergo a discontinuity, and finally decrease as $\alpha \exp[(\tau - t) / \theta]$ for $\tau < t$.

ACKNOWLEDGEMENTS

ED is a Research Associate with the National Fund for Scientific Research of Belgium. JW and CNKM appreciate the financial support of the Sound Ecosystem Assessment (SEA) Program of the Exxon Valdez Oil Spill (EVOS) Trustees Council through Prince William Sound Science Center, Alaska. ED is indebted to Benoît Tartinville and Marian Scott for the comments they provided on various aspects of this work.

REFERENCES

- Blumberg A.F. and G.L. Mellor (1987) A description of a three-dimensional coastal ocean circulation model. In: *Three-Dimensional Coastal Ocean Models*, N.S. Heaps, editor, American Geophysical Union, Washington, D.C., pp. 1–16.
- Bolin B. and H. Rodhe (1973) A note on the concepts of age distribution and transit time in natural reservoirs. *Tellus*, **25**, 58–62.
- Mooers C.N.K. and J. Wang (1997) On the development of a three-dimensional circulation model for Prince William Sound, Alaska. *Continental Shelf Research* (in press).
- Tartinville B., E. Deleersnijder and J. Rancher (1997) The water residence time in the Mururoa atoll lagoon: sensitivity analysis of a three-dimensional model. *Coral Reefs* (in press).

TABLE AND FIGURE CAPTIONS

Table 1. The values of the parameters τ , θ and α minimising ε as determined for various surface forcings. The direction toward which the wind blows is indicated. The error bars related to these estimates are $(\Delta\tau, \Delta\theta, \Delta\alpha) = (0.1 \text{ day}, 1 \text{ day}, 0.01)$.

Figure 1. The evolution of the dimensionless tracer mass present in PWS, m_s / M , as simulated by MW using the three-dimensional Princeton Ocean Model with various surface forcings. The direction toward which the wind is blowing is indicated. (These curves are obtained by deleting the slight overshootings of the simulated mass, occurring for unidentified numerical reasons, after the source was cut off.)

Figure 2. Schematic illustration of the four phases, labelled I to IV, of the temporal evolution of the tracer mass present in PWS.

Figure 3. Schematic illustration of the tracer fluxes accounted for in the compartmental model.

Figure 4. The evolution of the dimensionless tracer mass present in PWS, m / M , obtained from the compartmental model with various surface forcings. The direction toward which the wind is blowing is indicated.

Table 1. The values of the parameters τ , θ and α minimising ε as determined for various surface forcings. The direction toward which the wind blows is indicated. The error bars related to these estimates are $(\Delta\tau, \Delta\theta, \Delta\alpha) = (0.1 \text{ day}, 1 \text{ day}, 0.01)$.

	no wind	westward	southward	eastward	northward
τ (days)	7.1	7.8	7.4	7.1	7.5
θ (days)	48	80	32	42	97
α	0.68	0.78	0.62	0.62	0.78
ε	0.065	0.066	0.067	0.066	0.066

Figure 1. The evolution of the dimensionless tracer mass present in PWS, m_s/M , as simulated by MW using the three-dimensional Princeton Ocean Model with various surface forcings. The direction toward which the wind is blowing is indicated. (These curves are obtained by deleting the slight overshootings of the simulated mass, occurring for unidentified numerical reasons, after the source was cut off.)

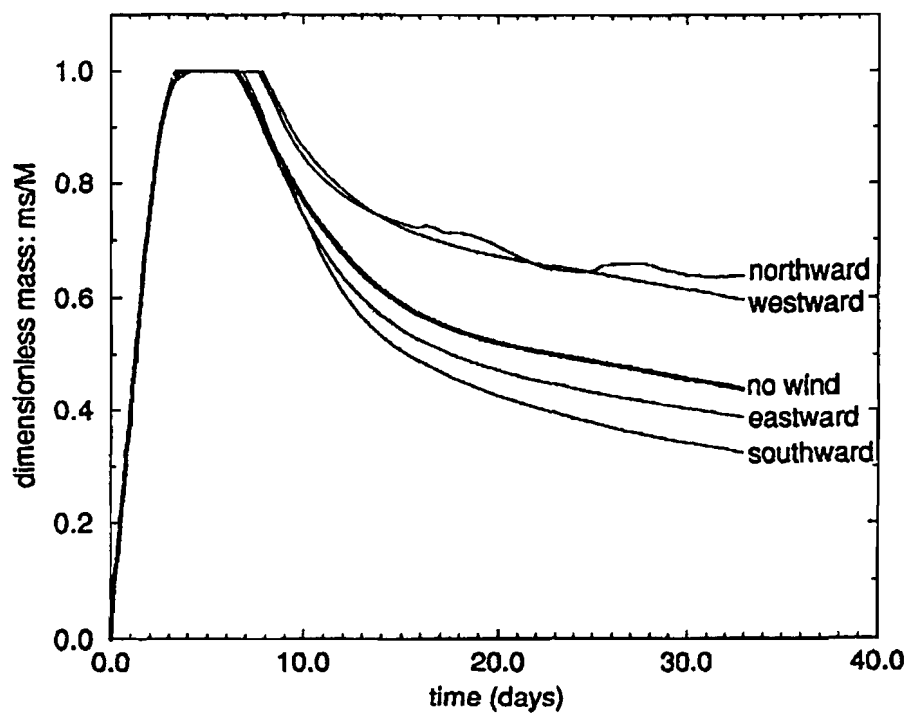


Figure 2. Schematic illustration of the four phases, labelled I to IV, of the temporal evolution of the tracer mass present in PWS.

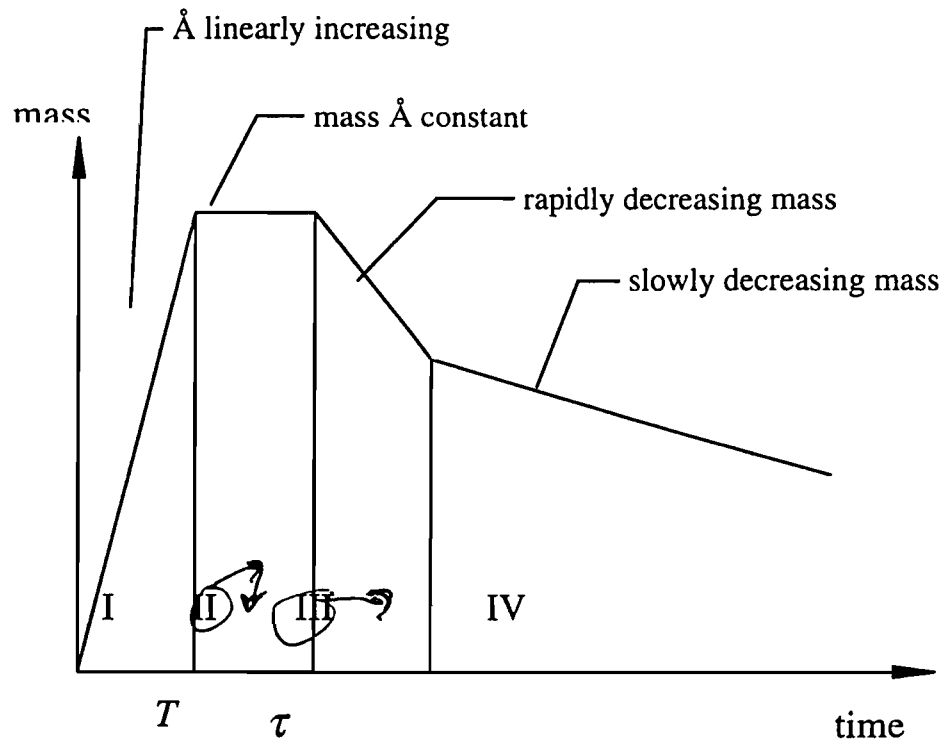


Figure 3. Schematic illustration of the tracer fluxes accounted for in the compartmental model.

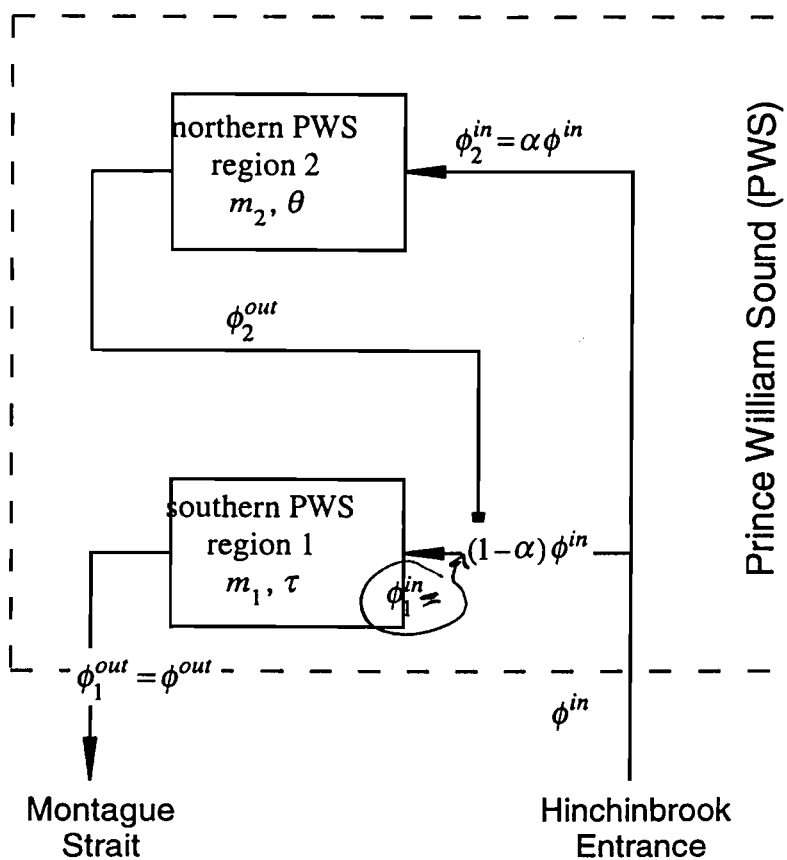
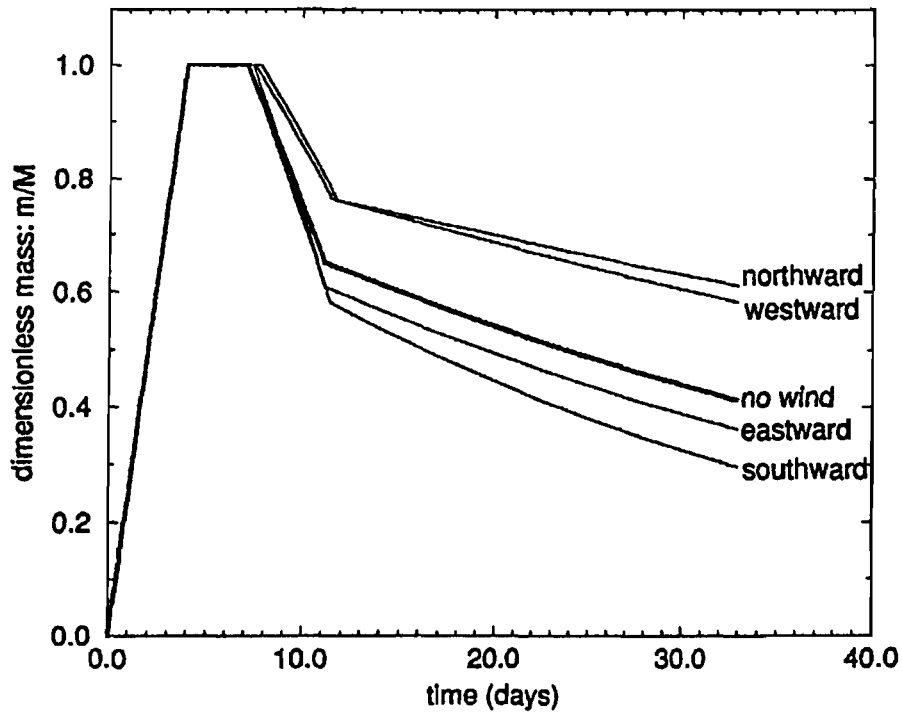


Figure 4. The evolution of the dimensionless tracer mass present in PWS, m/M , obtained from the compartmental model with various surface forcings. The direction toward which the wind is blowing is indicated.



Chapter 8

Observational Physical Oceanography

Exxon Valdez Oil Spill
Restoration Project Annual Report

SEA: Observational Oceanography in Prince William Sound

Restoration Project 96320-M
Annual Report

This annual report has been prepared for peer review as part of the *Exxon Valdez* Oil Spill Trustee Council restoration program for the purpose of assessing project progress. Peer review comments have not been addressed in this annual report.

Shari L. Vaughan
Shelton M. Gay III
Loren B. Tuttle
Kenric E. Osgood

Prince William Sound Science Center
P. O. Box 705
Cordova, Alaska 99574

April 1998

SEA: Observational Oceanography in Prince William Sound
Restoration Project 96320-M
Annual Report

Study History: Unexpectedly small Prince William Sound pink salmon runs in 1992 and 1993, and the almost complete collapse of the herring fishery in 1993, prompted the EVOS Trustee Council to initiate ecosystem-level studies of the region to investigate possible environmental reasons for these disasters. A collaborative effort involving the University of Alaska Fairbanks, the Prince William Sound Science Center, the Prince William Sound Aquaculture Corporation, and Alaska Department of Fish and Game resulted in the development of a coordinated plan in the fall of 1993. After substantial review, Sound Ecosystem Assessment (SEA) was approved for funding April 11, 1994. A scope of work for SEA was projected over 5-8 years at that time. Annual reports were issued in 1995 by D. K. Salmon entitled Descriptive Physical Oceanography (project number 94320-M), in 1996 by S. L. Vaughan entitled Observational Physical Oceanography in Prince William Sound and the Gulf of Alaska (project number 95320-M), and in 1997 by S. L. Vaughan entitled Water Mass Variability and Circulation of PWS (project number 96320-M), all as chapter contributions to the single compiled report of all SEA FY94, FY95 and FY96 projects. Project results were presented in 1996-1998 at several professional meetings. A journal article was submitted for publication in 1996 (Gay, S.M., 1996: Seasonal Changes in Hydrography of Embayments and Fjords of Prince William Sound, Alaska during Spring and Summer 1994, Fall 1995, and Late Winter 1996. In IAPSO Conference Proceedings).

Abstract: Hydrographic surveys and current velocity measurements in 1994 through 1997 show significant seasonal and interannual variability in water mass properties and circulation patterns in central Prince William Sound (PWS), and in the PWS nearshore areas. Intrusion of Gulf of Alaska (GOA) water into PWS was indicated in June 1996, but not in June 1994 or 1995. In September, the Sound seems to be sealed off from the GOA entirely. The dominant circulation feature in September is the cyclonic gyre in the central Sound. A mooring deployed at Hinchinbrook Entrance showed that the summer months were characterized by outflow above 150m and inflow below. The fall and early winter months were characterized by inflow above 150m and weak outflow below. Late winter and early spring months were characterized by more barotropic flows. Spring of 1996 was the most productive year for zooplankton in the Sound. Warming and stratification started earlier in 1996 than in 1995. Stratification was greater in May 1996 than in May of either 1995 or 1997. In May 1996, there were greater numbers of zooplankton and less fluorescence than in May 1997. In the nearshore regions of PWS, fjords generally exhibited greater vertical stratification from both heat and freshwater input, while bays became only partially stratified. Tidal currents within bays and fjords appear to be influenced by the relative strength of tidal flows within passes outside the respective basins. Locations with strong surface inflows from these sources may exhibit frontal zones caused by convergence with outflows from within the bay.

Key Words: physical oceanography, temperature, salinity, circulation, Prince William Sound.

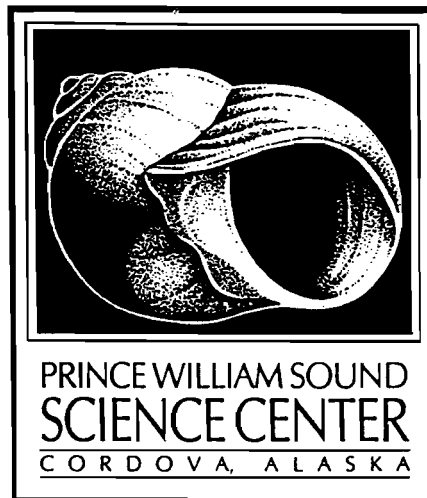
Citation: Vaughan, S.L., S.M. Gay, L.B. Tuttle, and K.E. Osgood. 1998: SEA: Observational Oceanography in Prince William Sound. *Exxon Valdez* Oil Spill Restoration Project Annual Report (Restoration Project 96320-M), Prince William Sound Science Center, Cordova, Alaska. 99574.

Circulation in Prince William Sound from Satellite Tracked Drifting Buoys

by

Shari L. Vaughan

Presented at the AAAS 48th Arctic Division Science Conference
September 24-27, 1997 in Valdez, Alaska



Prince William Sound Science Center
P. O. Box 705
Cordova, Alaska 99574

February 1998

Technical Report No. 9801

Introduction

ARGOS satellite tracked drogued drifting buoys provide near real time visualization of ocean current velocity structure. Other advantages include autonomous data collection (no vessel requirements), and unambiguous interpretation of results. Five ARGOS drifters were deployed in Prince William Sound (PWS), Alaska, as part of the Sound Ecosystem Assessment program sponsored by the Exxon-Valdez Oil Spill (EVOS) Trustee Council. Two were released near Hinchinbrook Entrance (Figure 1) in 1996, and three were released in the central Sound in 1997. While many more than 5 trajectories are required to make statistically sound conclusions about probable flow patterns, these drifter paths document some interesting features of the circulation, which are presented here.

The drifters are ClearSat-GPS WOCE drifters manufactured by Clearwater Instrumentation, Inc. They consist of a roughly 20 inch diameter surface float with a radio antenna mounted on top, and a canvas drogue connected to the bottom (Figure 2). The buoy houses the electronics and provides floatation. The antenna communicates the buoy's position to a satellite (operated by the French company ARGOS), which relays the information to an ARGOS service and data distribution center. Roughly hourly position updates are delivered by the service center to the user via email. A roughly 7 meter long, 1 meter diameter hollow cylindrical drogue is connected to the underside of the surface buoy by a roughly 9 meter long coated wire cable and a 2.5 meter long tether. A smaller shock absorbing buoy is connected in between. This design allows the drifter to follow currents at depths of roughly 9 to 16 meters (about 30 to 50 feet) without contamination by near surface wind induced flow.

In this report, 4 of the 5 drifter paths are presented. One of the two 1996 releases (25651) stopped transmitting a few days after deployment, probably due to damage from a collision with a vessel. For clarity in the trajectory figures, positions are plotted approximately every 12 hours (about 1200 and 2400 GMT), although many more positions are available. This means the spacing between positions is roughly proportional to the speed of the drifter (farther spacing means faster flow). The initial release position is shown as a larger, lighter colored dot. Release dates, the date of the last transmission, and the approximate record length are shown in the table below.

Drifter	Released	End of Record	Length of Record
25651	August 2, 1996	August 5, 1996	3 days
25652	August 2, 1996	September 12, 1996	6 weeks
25653	May 8, 1997	November 24, 1997	6.5 months
25654	May 8, 1997	September 30, 1997	4.7 months
25655	July 15, 1997	October 23, 1997	3.2 months

Results

Drifter 25652 deployed in Hinchinbrook Entrance (Figure 3) in August 1996 exited PWS about 3 days after deployment. It moved southwestward then westward past southern Montague Island. It continued moving southwestward past the Kenai Peninsula, making a large anticyclonic loop south of Aialik Bay. It entered Cook Inlet at Stevenson Entrance, and continued moving southwestward. It stopped transmitting in Shelikof Strait near the southern end of Kodiak Island.

Drifter 25653 was released in central PWS in May 1997. The entire path is shown in Figure 4a. Due to the complexity of the trajectory, positions before and after September 17 are shown in Figure 4b and 4c. Drifter 25653 moved north initially and spent roughly 10 days in Valdez Arm (Figure 4b). It then returned to the central Sound and remained motionless for several days before curving in an anticyclonic path to the west. It moved slowly through the western Sound, being retained for several days in the nearshore regions of Perry Island, Dangerous Passage, Icy Bay, Whale Bay, and northern Latouche Passage. The drifter transited to southern Montague Strait east of Latouche Island, where it reversed direction and traveled north through Montague Strait (8/25 - 9/4). It crossed Hinchinbrook Entrance and moved north past Hinchinbrook Island to Orca Bay. After about 2 weeks in Orca Bay, the drifter moved northward again to Valdez Arm, stopping at Knowles Head, Bligh Island, and Rocky Point. From there it moved southwestward and quickly southward through Knight Island Passage. It entered Bainbridge Passage from the north and moved through to Port Bainbridge. It remain near the head of Port Bainbridge until it stopped transmitting on November 24, 1997.

Drifter 25654 was released in central PWS in May 1997 roughly 4 miles west of drifter 25653. The entire path is shown in Figure 5a, with paths before and after July 29 shown in Figures 5b and 5c for clarity. Drifter 25654 moved west initially passing south of Naked Island (Figure 5a). It made 2 cyclonic circulations over the deep basin known as the 'Black Hole'. From there it proceeded south through Knight Island Passage to southern Montague Strait where it, like drifter 25653, reversed direction and moved north through Montague Strait (6/21 - 6/26). Drifter 25654 exited the Sound on 6/27 and moved eastward south of the Copper River Flats, making two cyclonic revolutions before almost reaching Kayak Island. Just west of Kayak Island, it made 3 cyclonic revolutions, and a fourth revolution farther to the west. It started moving rapidly westward on about August 12. It passed southern Montague Island and then curved northward entering Montague Strait. It again traveled north through Montague Strait (8/23 - 9/4) and exited PWS at Hinchinbrook Entrance, but this time moved southwestward past Montague Island. It proceeded westward south of the Kenai Peninsula, similar to drifter 25652, and entered Cook Inlet at Kennedy Entrance (not shown). It stopped transmitting near Augustine Island in Cook Inlet on September 30, 1997.

Drifter 25655, released July 15, 1997 in the central Sound, moved westward and spent several days south of Naked Island (Figure 6). It then returned to the central Sound and made two cyclonic circulations. Afterward, it moved toward Smith Island and then south to Montague Point. It entered Zaikof Bay on September 9 and remained there until it was retrieved on October 23, 1997.

Discussion

Drifters 25651, 25652 and 25654 indicated that in the summer and early fall 1996 and 1997, southward flow is present in the upper (9 - 16 meter) layers at Hinchinbrook Entrance. Drifters 25653 and 25654 showed northward flow through Montague Strait in late August and early September 1997. Drifter 25654 also showed northward flow through Montague Strait in June 1997. Using data from 1977 to 1979, Niebauer et al (1994) found that in all months the vertically integrated mean monthly transports were into the Sound at Hinchinbrook Entrance and out of the Sound at Montague Strait. Closer inspection of their moored current meter velocities reveals periods of southward flow at Hinchinbrook Entrance

and northward flow at Montague Strait.

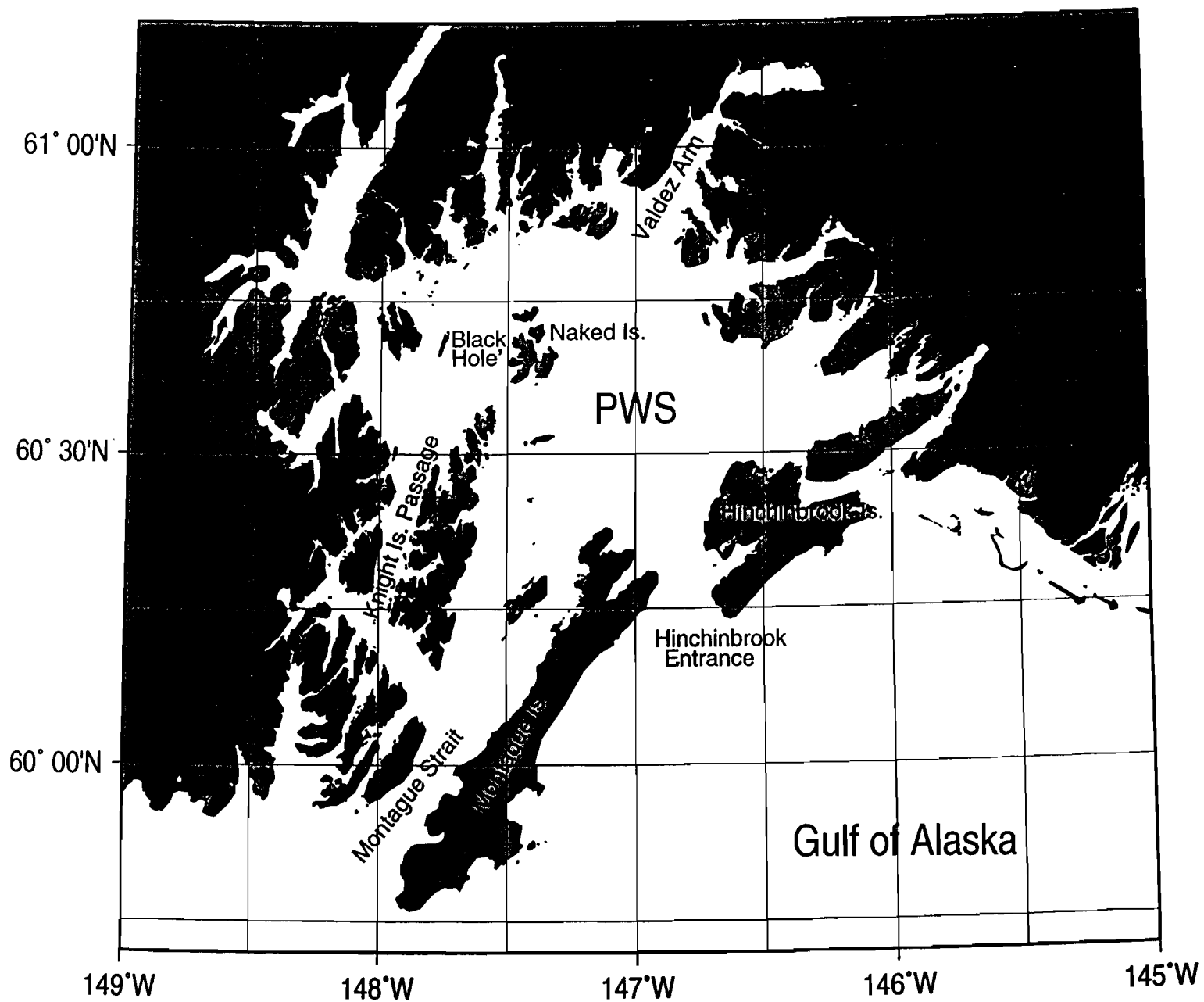
Drifters 25653 and 25655 suggest that cyclonic circulation was present in the central sound in the summer of 1997. Drifter 25654 showed cyclonic circulation over the 'Black Hole' in late spring and summer 1997. Retention in several nearshore areas (most strongly in Zaikof Bay) was suggested by drifters 25653 and 25655.

Although this experiment was designed to capture the circulation patterns of PWS, 2 drifters escaped and provided some information on the circulation outside the Sound. Westward flow past the Kenai Peninsula was documented by drifters 25652 and 25654. Drifter 25654 first showed eastward flow with some large eddies south of the Copper River Flats, and then flow to the west. This drifter also documented the existence of one or more cyclonic eddies west of Kayak Island. An eddy at this location has been documented previously using drifters and hydrography (e.g. Royer, Hansen, and Pashinski, 1979), but with anticyclonic rotation. Closer inspection of the drifter tracks in Royer, Hanson, and Pashinski does reveal cyclonic circulation in one case (their drifter 1142). Multiple dipole eddies shed from Kayak Island have also been observed in satellite images (Ahlnas, Royer, and George, 1987).

References

- Ahlnas, K., T.C. Royer, and T.H. George, 1987: Multiple Dipole Eddies in the Alaska Coastal Current Detected With Landsat Thematic Mapper Data. *J. Geophys. Res.*, **92**, C12, pp 13,041-13,047.
- Niebauer, H.J., T.C. Royer, and T.J. Weingartner, 1994: Circulation of Prince William Sound, Alaska. *J. Geophys. Res.*, **99**, C7, pp 14,113-14,126.
- Royer, T.C., D.V. Hansen, and D.J. Pashinski, 1979: Coastal Flow in the Northern Gulf of Alaska as Observed by Dynamic Topography and Satellite Tracked Drogued Drift Buoys. *J. Phys. Oceanog.*, **9**, 4, pp 785-801.

Figure 1: Map of Prince William Sound.



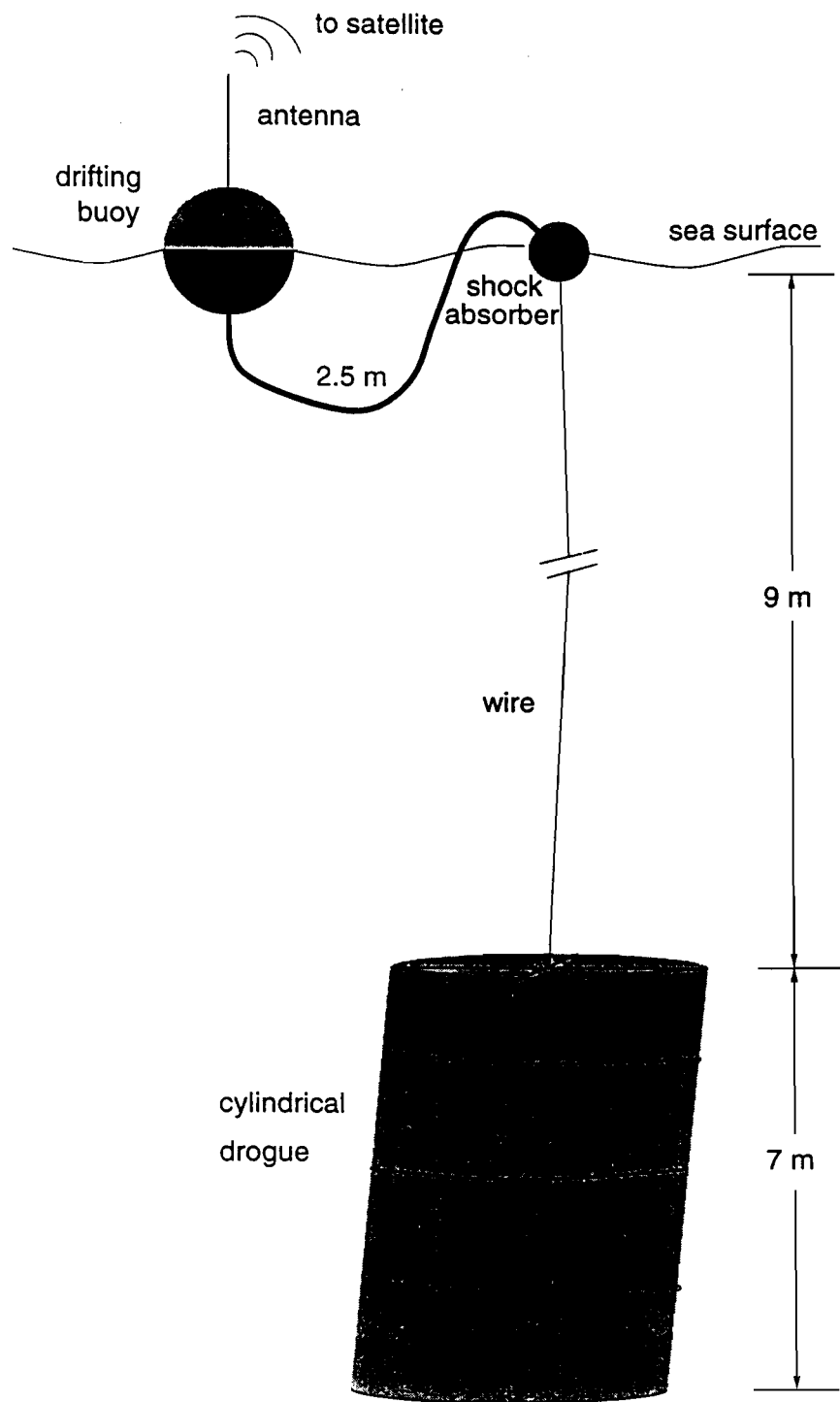


Figure 2: Schematic diagram of satellite tracked drifting buoy.

Drifter Track: 25652

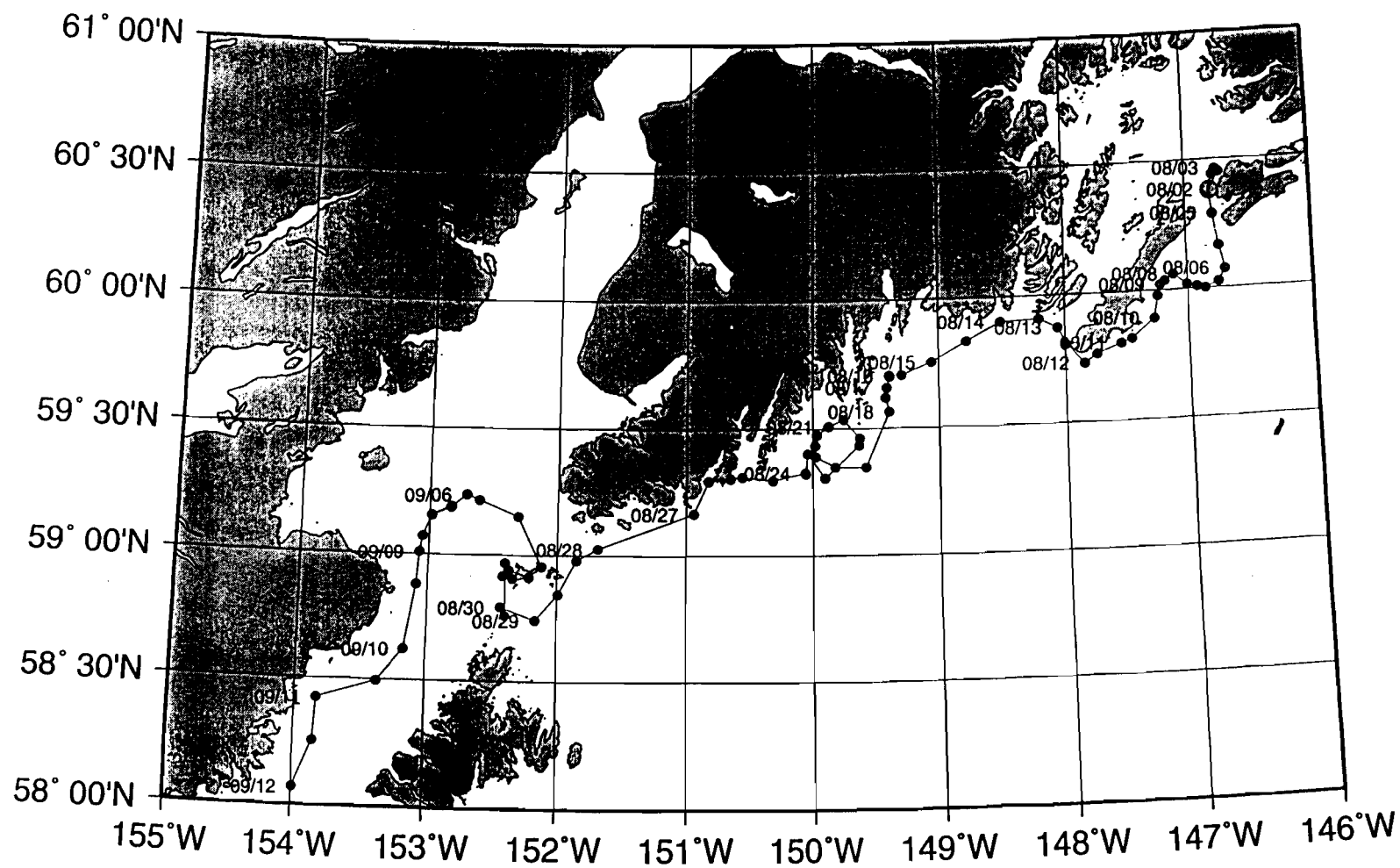


Figure 3: Entire track of drifting buoy 25652, drogued at 9 to 16 meters.
Positions are plotted approximately every 12 hours.

Drifter Track: 25653

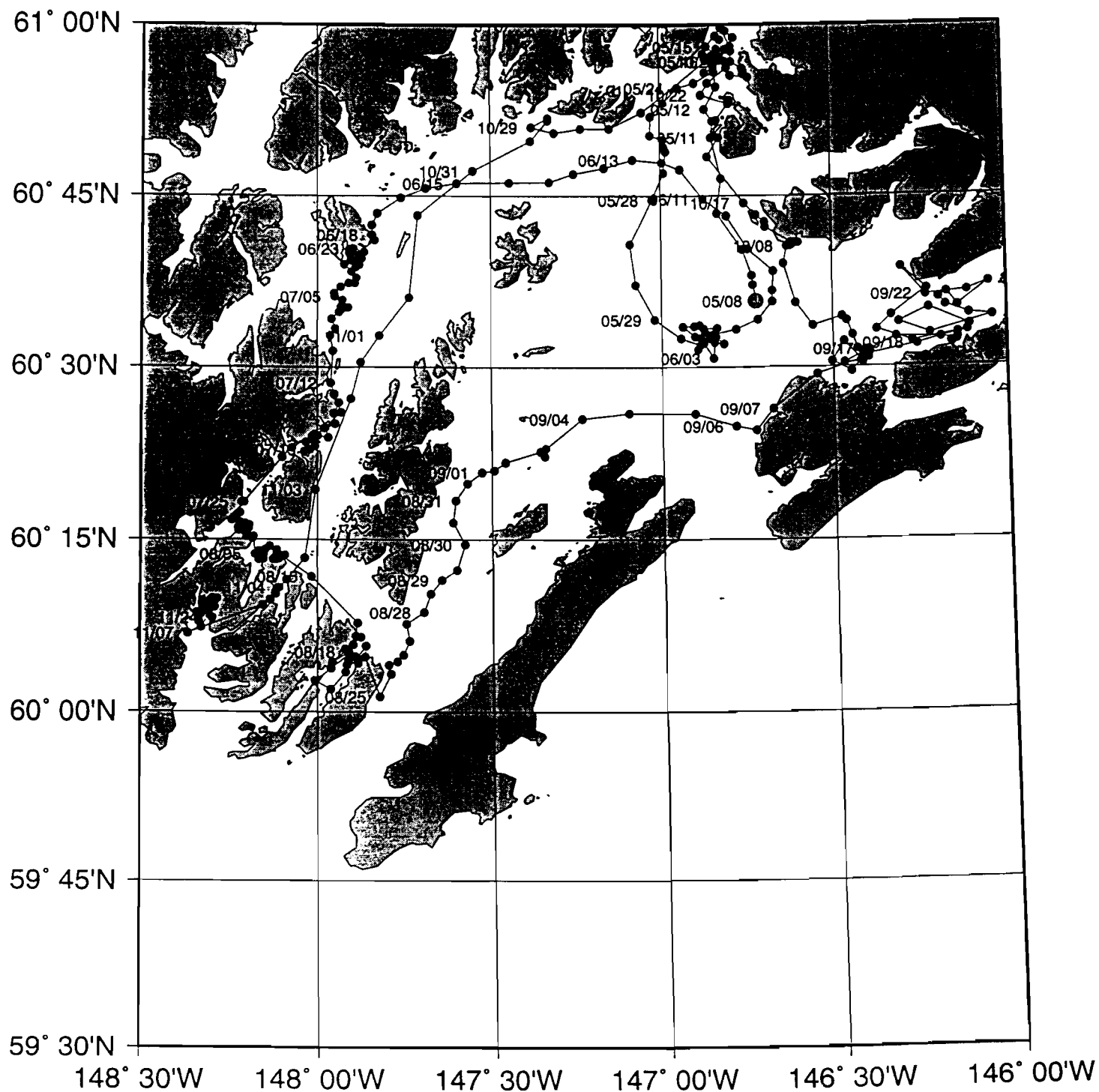


Figure 4a: Entire track of buoy 25653, drogued at 9 to 16 meters. Positions are plotted approximately every 12 hours.

Drifter Track: 25653

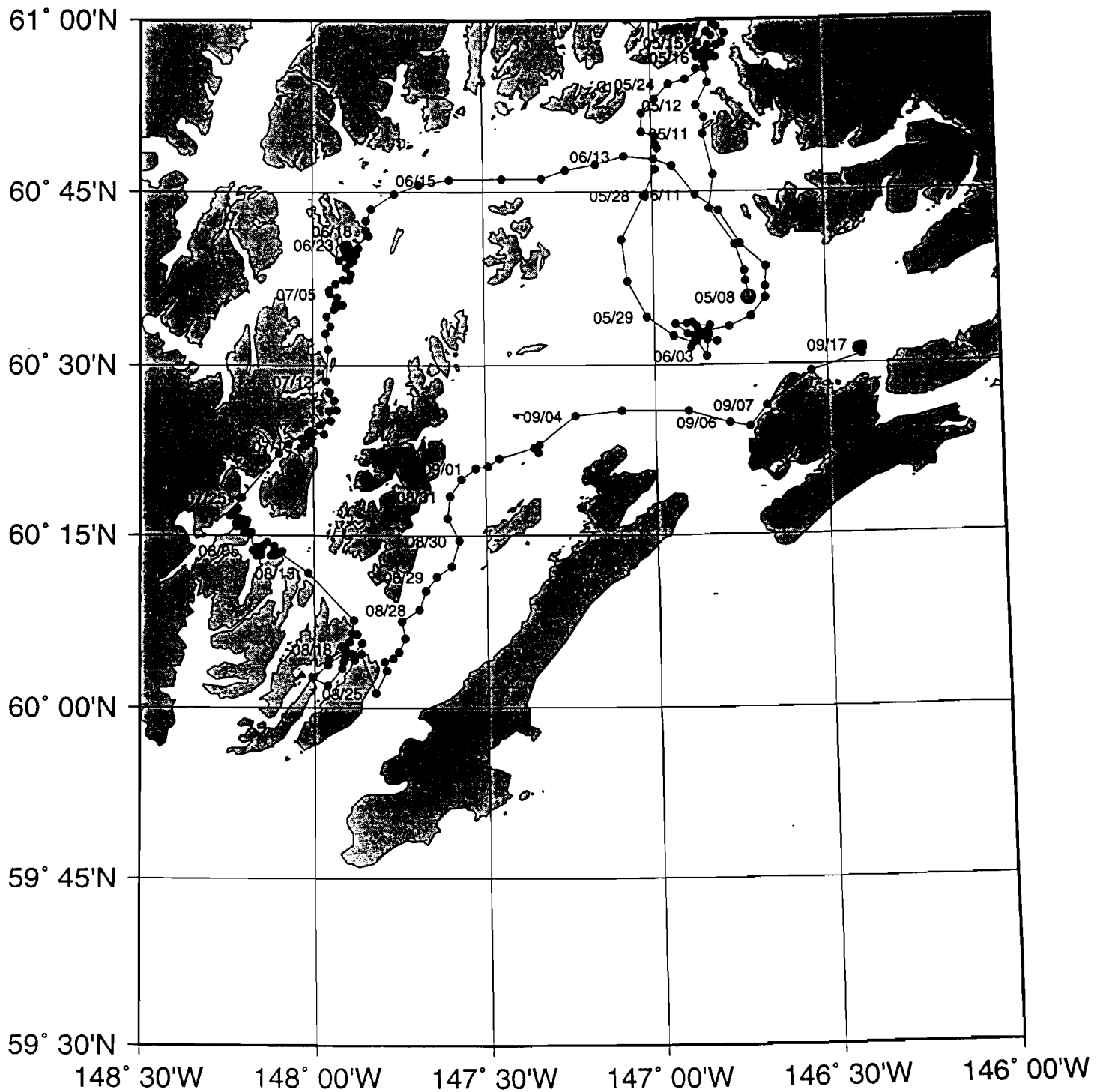


Figure 4b: Track of buoy 25653 from May 8 to September 17, 1997.
Positions are plotted approximately every 12 hours.

Drifter Track: 25653

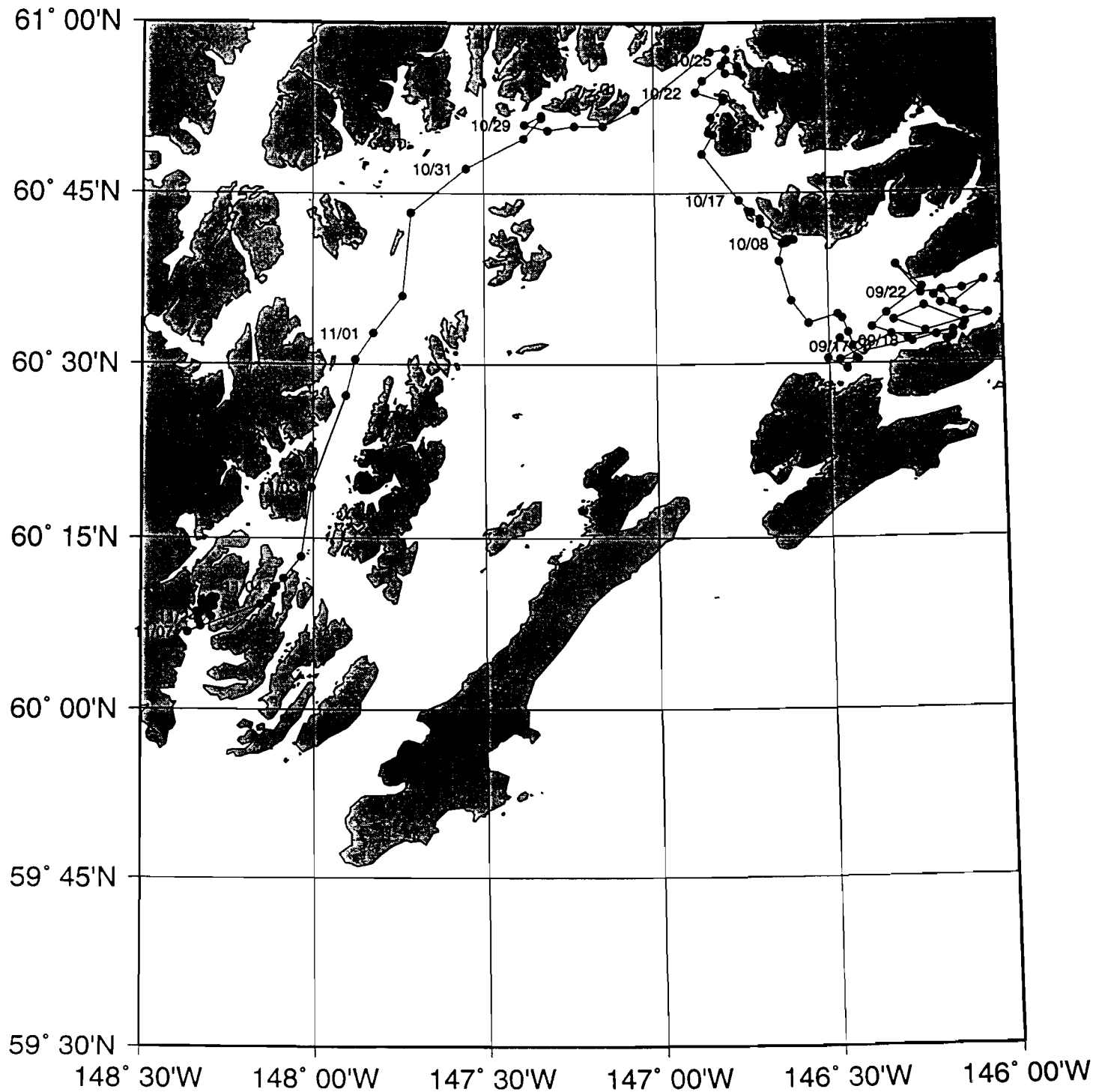


Figure 4c: Track of buoy 25653 from September 17 to November 24, 1997. Positions are plotted approximately every 12 hours.

Drifter Track: 25654

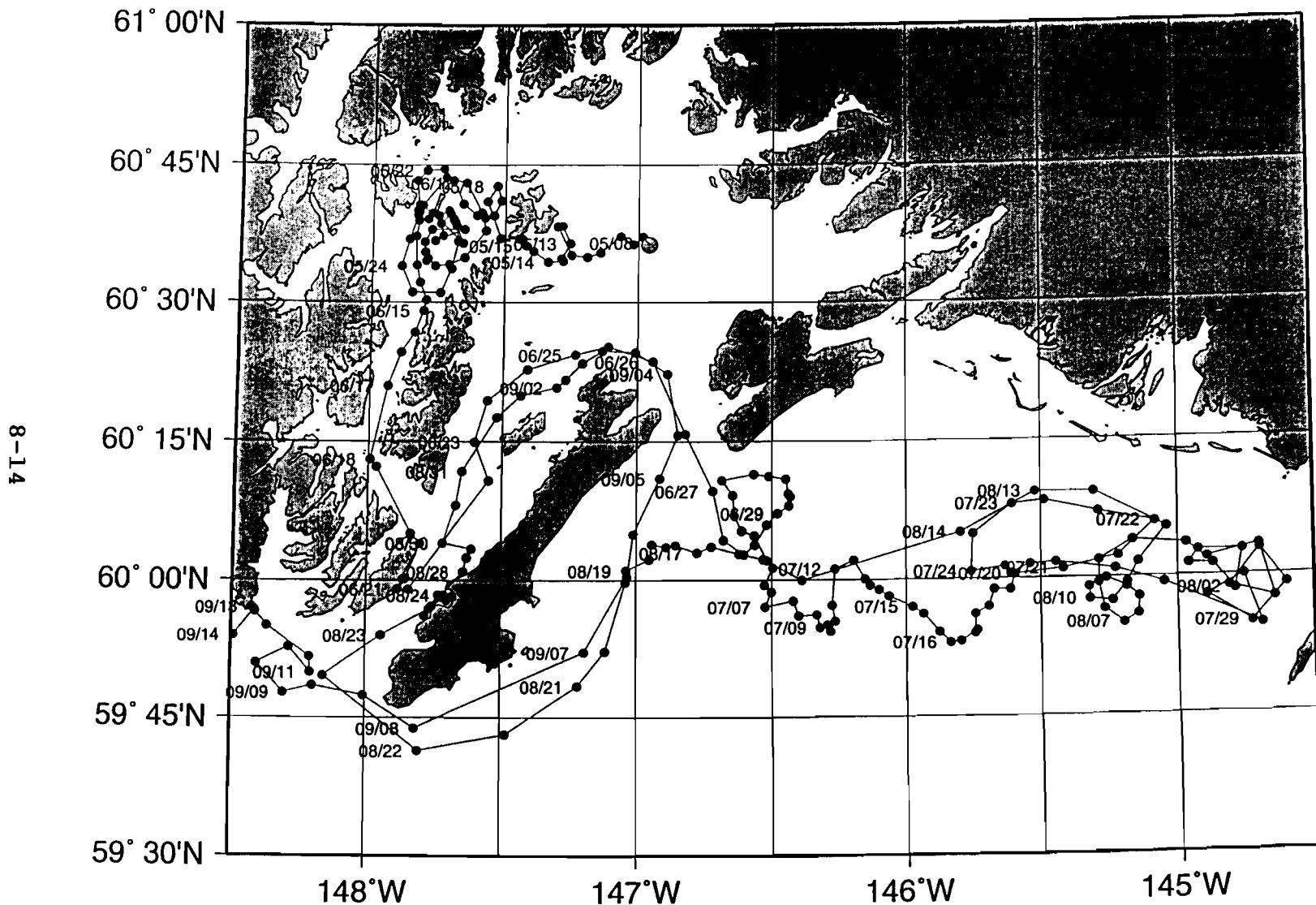


Figure 5a: Entire track of buoy 25654, drogued at 9 to 16 meters.
Positions are plotted approximately every 12 hours.

Drifter Track: 25654

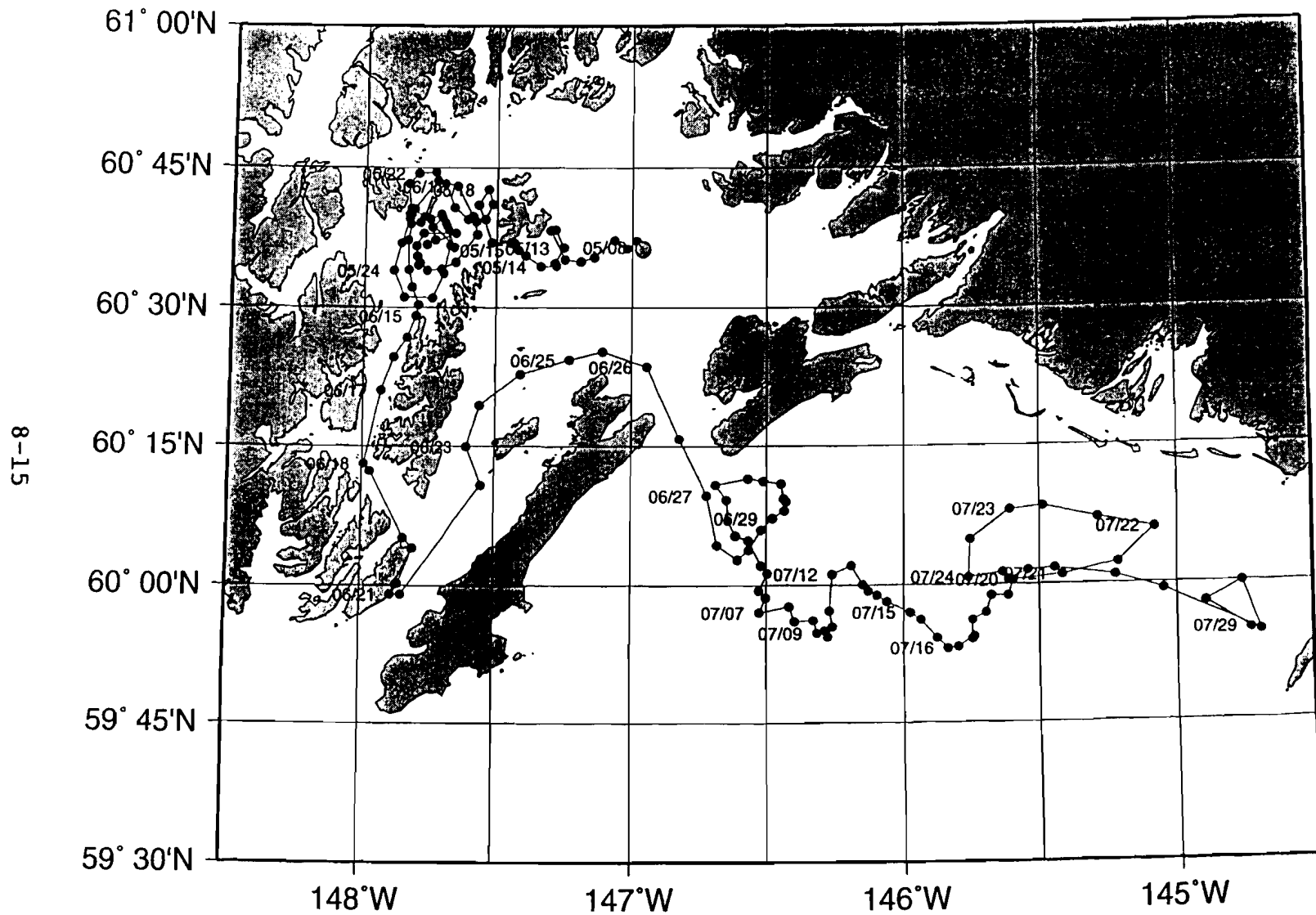


Figure 5b: Track of buoy 25654 from May 8 to July 29, 1997.
Positions are plotted approximately every 12 hours.

Drifter Track: 25654

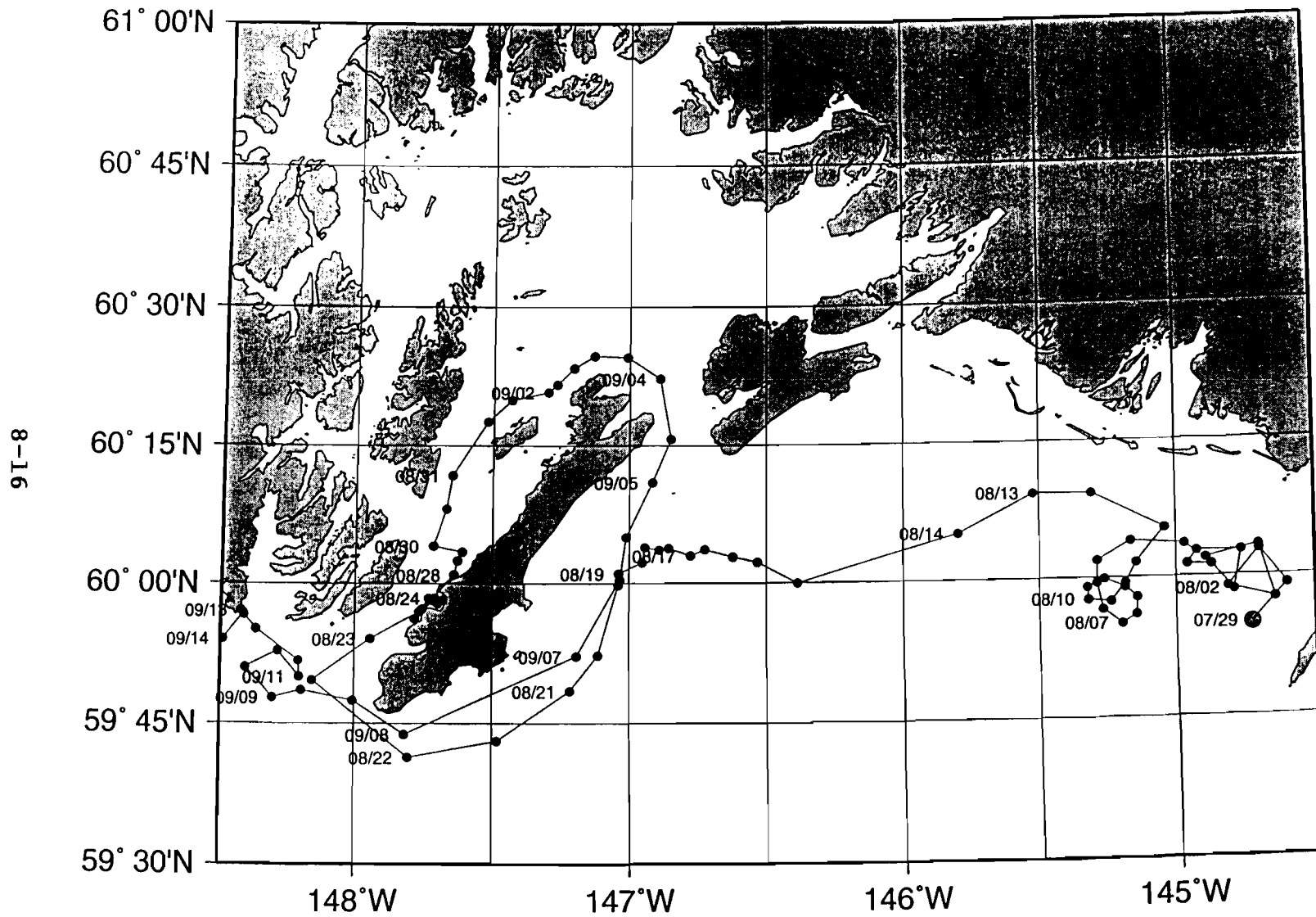


Figure 5c: Track of buoy 25654 from July 29 to September 14, 1997.
Positions are plotted approximately every 12 hours.

Drifter Track: 25655

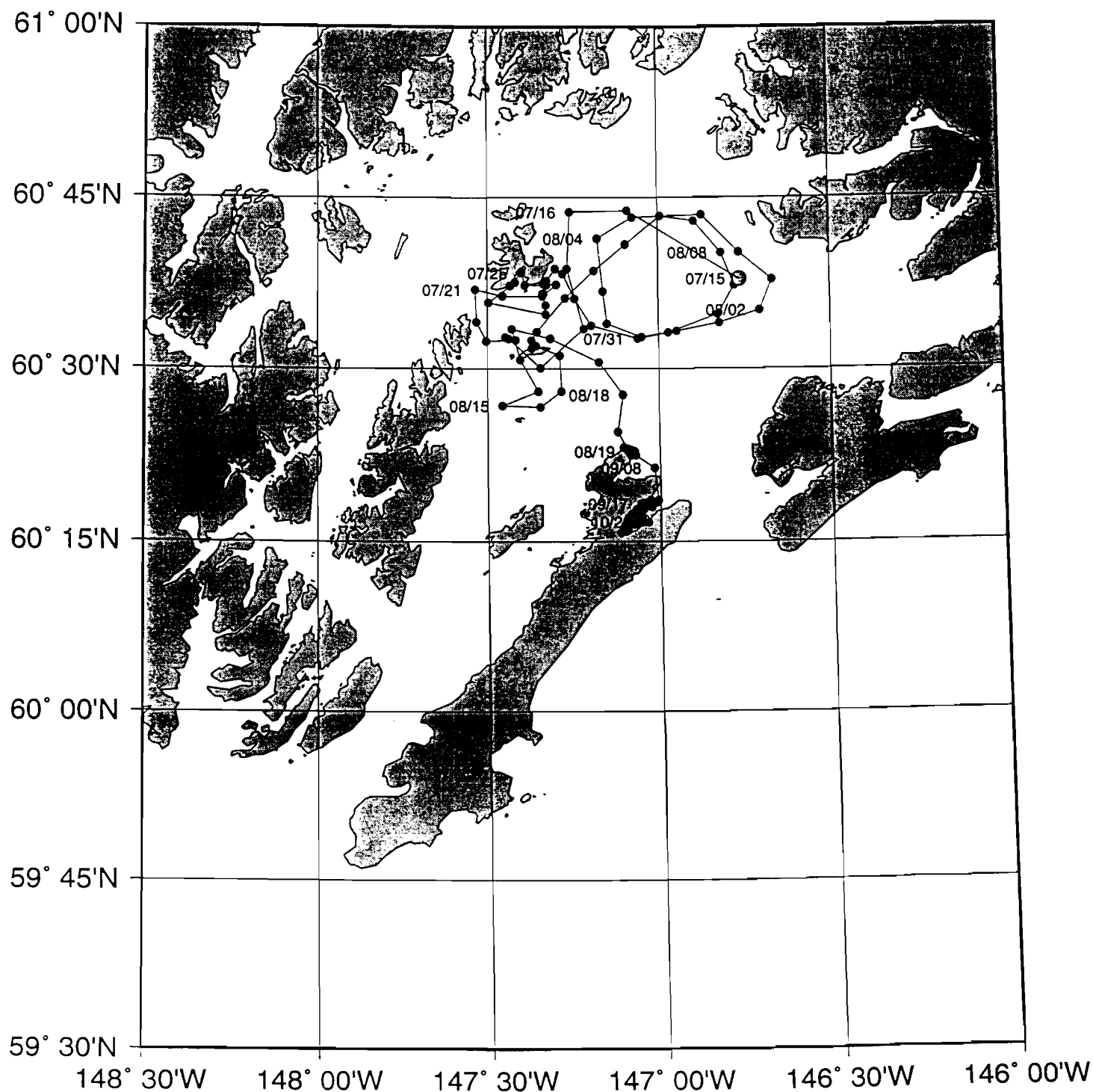


Figure 6: Entire track of buoy 25655, drogued at 9 to 16 meters.
Positions are plotted approximately every 12 hours.

DRAFT

Upper Layer Circulation and Water Mass Variability in Prince William Sound, Alaska

S.L. Vaughan, L.B. Tuttle, K.E. Osgood, and S.M. Gay
Prince William Sound Science Center

Introduction

Prince William Sound (PWS), Alaska is a shallow (mostly ≤ 350 m) estuarine, subarctic sea, surrounded by mountains, numerous fjords, and coastal rivers (e.g. Muench and Schmidt, 1975). The circulation within the Sound is generally cyclonic, with water entering from the Gulf of Alaska (GOA) through Hinchinbrook Entrance, and exiting through Montague Strait (Niebauer, Royer and Weingartner, 1994; Royer, Hansen and Pashinski, 1979). Seasonal changes in wind forcing and precipitation produce departures from this general pattern. Light westerly winds in the summer are replaced by strong easterlies in the winter. This reversal modulates the volume of Gulf of Alaska water entering Prince William Sound. Fresh water input, a combination of precipitation and snow melt/river runoff, reaches a maximum in fall and a minimum in spring (e.g. Royer, Hansen, and Pashinski, 1979). The upper layer density structure of the Sound responds to both types of variability.

PWS is also a region of high biological production, and supports a large Alaskan salmon fishery. Oil tankers transverse this region regularly and pose a finite risk in the event of a spill, yet little is known about the seasonal and interannual changes in the physical and biological conditions. The devastation caused by the 1989 Exxon-Valdez oil spill demonstrated the need for a comprehensive description of the seasonal variability of the circulation and water mass properties of PWS, in relation to plankton and nekton distributions.

In 1993, the Exxon-Valdez Oil Spill (EVOS) Trust Council funded a comprehensive ecosystem study called the Sound Ecosystem Assessment (SEA). A main goal of the physical oceanographic part of the SEA program was to identify the physical processes that influence the production of two commercially harvested species, pink salmon and Pacific herring. It was hypothesized that food (zooplankton) was the dominant limiting factor to growth and survival. Since phytoplankton and zooplankton biomass fields are closely coupled to the water mass properties of the surface layer, a specific goal was to document the monthly and seasonal upper layer water mass variability in Prince William Sound.

This paper examines the relation of the upper layer water mass properties and circulation to the fluorescence and zooplankton distributions in the spring and early summer of 1995 through 1997. Differences in the timing and intensity of vertical stratification formation appear to be the primary link.

Data

Large scale hydrographic cruises were conducted in PWS in spring and summer months of 1995, 1996 and 1997. Cruise dates are shown below.

1995	1996	1997
April 10-17	April 15-21	May 7-13
May 4-11	May 2-11	
June 15-20	June 15-21	

Station locations and transects for each cruise are shown in Figure 1. Measurements of temperature (T), salinity (S), oxygen, and current velocities were made with simultaneous measurements of fluorescence and zooplankton abundance. The hydrographic data was collected using a SeaBird 911 CTD. Conductivity, temperature, and oxygen as a function of pressure were recorded at 1 dbar intervals. Salinity was calculated from conductivity using standard SeaBird software. The CTD sensors were calibrated annually by SeaBird Electronics. The CTD salinities and oxygens were not calibrated with bottle samples because of minimal annual sensor drift rate. In December 1996 and May 1997, expendable CTDs (XCTDs) were used when conditions were too rough to use the CTD.

To relate temperature and salinity to zooplankton distributions and fluorescence (a proxy for phytoplankton), a combined instrument designed by Chelsea Instruments called an Aquashuttle was towed from the ship. The Aquashuttle consists of a Focal Technologies optical plankton counter (OPC), to count and size particles in the water, and a Chelsea Instruments Aquapack, which measures temperature, salinity, and fluorescence. The Aquashuttle is raised and lowered vertically from the surface to about 50 meters as it is towed, sampling continuously.

Instantaneous current velocity transects were collected using an RDI 150 kHz broadband acoustic Doppler current profiler (ADCP) deployed from the stern of the ship in a towed body. Most transects were in water less than 400 m depth so that bottom tracking was available. The bin length was 8 m for most of the data. The ADCP generally measured flows from about 20 m depth to the bottom.

The echo intensity data collected with the ADCP can be used to infer relative zooplankton abundance along the current velocity transects (e.g. Heywood et al. 1991; Roe and Griffiths. 1993). The ADCP measures the acoustic backscatter from particles in the water column. These particles are primarily zooplankton and micronekton. Due to the frequency of the ADCP, 150 kHz, the acoustic return is weighted towards larger zooplankton, including micronekton, euphausiids, amphipods and possibly large copepods. The range-corrected, relative backscatter intensity (Flagg and Smith, 1989) was calculated by averaging the echo intensity data for the ADCP's 4 beams and converting to relative backscatter intensity (dB) using the conversion factor supplied by RDI (San Diego, CA). The range correction was then applied, as described by Flagg and Smith (1989).

From an ADCP moored in Hinchinbrook Entrance it was observed that at times diel vertical migration contributed a large signal to the variability of the relative backscatter data. To segregate the effects of diel vertical migration from the relative backscatter data obtained with the towed ADCP, the data were categorized as day or night. Day was taken to be the period from 30 min after sunrise to 30 min before sunset. Night was considered

to be 30 min after sunset to 30 min before sunrise.

Meteorological data from C-MAN stations in PWS is available from the National Data Buoy Center (NDBC), and from a station at Middleton Island. The C-MAN stations are located at Bligh Reef, Potato Point, Seal Rocks, and Mid-Sound (in the central Sound). Wind speed, wind direction, wave height, barometric pressure, air temperature, water temperature, dew point temperature, and visibility are measured every 30 minutes. The C-MAN stations became operational in May 1995, but May and June records are incomplete. The Middleton Island data will be used for 1995, and the Mid-Sound data will be used for 1996 and 1997.

Physical Properties

April 1995 and 1996

South to north sections of temperature (T), salinity (S), potential density (σ), and Brunt-Vaisala frequency (N^2) are shown for April 1995 (Figure 2(a) and (b)) and April 1996 (Figure 3(a) and (b)). Upper layer stratification is present by April 1996 in the central and northern Sound, but 1995 still is well mixed down to 20m. The temperature minimum layer volume (3.8 isotherm) is larger in 1995 than in 1996. A density front is present between CS12 and NS4 in April 1996.

Contours of temperature and salinity averaged over the upper 20m layer are shown for April 1995 (Figure 4(a) and (b)) and April 1996 (Figure 5(a) and (b)). Since potential density is mainly determined by salinity at these latitudes, only salinity is shown here. Temperature is more uniform in April 1995, and no contours less than 4.0 degrees are present. In April 1996, the 3.8 isotherm outcrops in the northern Sound, west of the vertical section in Figure 3. Variability in salinity exists in 1995 (Figure 4b), but does not appear in the vertical section (Figure 2(a)) because of the narrow range of station locations. Freshening as shown by the 31.4 isohaline, extends much farther south in 1995 than in 1996. A weak density front at around $60^{\circ}30'N$ separates the cold, fresh northern waters from the warmer saltier southern waters (not shown). A dome of dense, high salinity water (31.8) is present north of Hinchinbrook Entrance in April 1996.

Wind speed and direction from April 1995 and April 1996 are shown in Figures 6(a) and (b). The cruise dates are highlighted. The April 1995 cruise had 2 wind bursts up to 15 m/s, while the April 1996 cruise was relatively calm. Wind forcing was at least partly responsible for the well mixed April 1995 structure.

May 1995, 1996, and 1997

South to north sections of temperature (T), salinity (S), potential density (σ), and Brunt-Vaisala frequency (N^2) are shown for May 1995, 1996, and 1997 in Figures 7, 8, and 9. May 1996 exhibits the warmest surface temperatures and the greatest stratification. The stratification is weaker in the south at CS12 (Figure 8(b)). Compared to 1995, the 25.2 isopycnal is much higher in the water column. The volume of the temperature minimum layer as indicated by the 4.0 isotherm, is the smallest of the 3 years in 1996.

A slight doming in the near surface ($< 20m$) isohalines and isopycnals appears in May

1995, centered around CFOS13 (Figure 7(a)). The stratification is weakest in the central Sound, with weak fronts to the south and north. The temperature minimum layer (4.0 isotherm) extends deeper than 100m.

In May 1997, a deep (30m) mixed layer exists in the central Sound (Figure 9(a)). Strong density fronts are present to the north and south. Maximum stratification is from 30-40m depth. This density structure is due to both temperature and salinity. The temperature minimum layer is warmer ($T \sim 4.2$) and is located between roughly 60 and 100m (not shown).

Contours of temperature and salinity averaged over the upper 20m layer are shown for May 1995, 1996 and 1997 in Figures 10, 11, and 12. Warm ($T \geq 6.0$), fresh ($S \leq 31.0$) surface water has intruded at Hinchinbrook Entrance in May 1995 and 1997. Density fronts are associated with these inflows. Salinity is fairly uniform in 1996. Temperatures in 1996 are warmest in the north, probably due to sensible heating. In May 1997, the densest water (coldest and saltiest) is north of northern Montague Island. Temperatures of 5.0 or less are not present in either 1995 or 1996. Salinities greater than 31.6 are not present in the Sound in 1995, and are only present at Hinchinbrook Entrance and southern Montague Strait in 1996. Whether this is Gulf of Alaska inflow or upwelled deep water is uncertain.

Wind speed and direction from May 1995, 1996, and 1997 are shown in Figures 13(a)-(c). The cruise dates are highlighted. Wind bursts in excess of 15m/s occurred during the 1995 and 1997 cruises. Conditions in 1996 were calm. Reduced wind forcing in May 1996 was undoubtedly responsible for the large thermal surface stratification.

June 1995 and 1996

South to north sections of temperature (T), salinity (S), and potential density (σ) are shown for June 1995 and June 1996 in Figures 14 and 15. The water column is well stratified in both years, but more in the northern Sound in 1996. A density front is present near NS4 in 1996. The 25.0 isopycnal is higher in the water column in 1996 than in 1995. The temperature minimum layer (4.5 isotherm) is still present in June 1995.

Contours of temperature and salinity averaged over the upper 20m layer are shown for June 1995 in Figure 16 and June 1996 in Figure 17. Warm, fresh water has intruded from the Gulf of Alaska at Hinchinbrook Entrance in both years. Another source of fresh water is in the northwest Sound. June 1995 is fresher and colder than June 1996. The coldest and saltiest water in both years occurred north of Montague Island, similar to what was seen in May 1997. It could be that conditions in 1997 were accelerated, with May 1997 resembling June months in other years.

Wind speed and direction from June 1995 and 1996 are shown in Figures 18(a) and (b). The cruise dates are highlighted. Conditions during both June cruises were calm.

Biological Properties

Contours of the relative backscatter from 20 m for April 1995 (Figure 19(a)) indicate generally higher relative backscatter, and hence inferred zooplankton biomass, in the northern and western parts of PWS. This corresponds to the regions of colder, fresher water (Figures 4(a) and (b)). In April 1996 there was a region of lower relative backscatter roughly

coinciding with the dome of high salinity water just north of Hinchinbrook Entrance (Figures 19(a) and 5(b)). There was also generally higher backscatter from 20 m in central PWS in April 1996 than in April 1995. This may have been due to the earlier onset of the phytoplankton bloom and the subsequent earlier zooplankton biomass increase in 1996 compared with 1995. Stratification formation started earlier (Figures 2(b) and 3(b)), and the wind forcing was less (Figures 6(a) and (b)) in April 1996 than April 1995.

During May 1995 levels of relative backscatter were reduced in the central portion of the sound at 20 m (Figure 19(b)). This region coincides with the region of uplifted isohalines and isopycnals (weakened stratification) in the central sound (Figure 7(a)). There were also generally higher levels of backscatter in May 1995 than in April 1995 (indicative of the increase of the zooplankton biomass with the progression of the zooplankton bloom). During May 1997, the relative backscatter levels were reduced over most of PWS compared to May 1995 (Figure 19(b)). This may have been due to conditions in 1997 being accelerated, and the peak of the zooplankton bloom having already passed. There was no indication in the backscatter data of the intrusion of water at Hinchinbrook Entrance that was apparent in the May 1995 and 1997 temperature and salinity data.

The relative backscatter data from June 1995 indicate generally lower levels of zooplankton at 20 m in the northern portion of central PWS compared with the southern portion of the central sound (Figure 19(c)). The higher backscatter levels correspond to the slightly less stratified region of the sound (Figure 14(a)). In June 1996 there were also generally higher backscatter values from the southern, less stratified portion of PWS (Figures 19(c) and 15(a)). Less stratification may have lead to higher primary production, and hence more zooplankton. There is a slight indication that the warm, fresh water intruded from the Gulf of Alaska at Hinchinbrook Entrance is also water of elevated relative backscatter. Whether in increased backscatter in the southern portion of the Sound was primarily due to weakened stratification, or GOA inflow is unclear.

Panels of temperature, salinity, and fluorescence derived from the Aquapack, and particle distribution derived from the OPC, for May 1996 and May 1997 are shown in Figures 20(a) and (b). The tow track in May 1996 (Figure 20(a)) runs from south to north (left to right), roughly from station NS4 to CFOS13. The temperatures and salinities agree with those in Figures 8(a) and 9(a). Maximum values of fluorescence are found at a depth of 20 to 25m along or just below the pycnocline, with largest values (0.89) closer to CFOS13. A greater number of *Neocalanus* sized (1-4mm) particles (maximum 6.87) were associated with regions of lower fluorescence, possibly due to grazing by the zooplankton on the phytoplankton.

The tow track in May 1997 (Figure 20(b)) runs from north to south (left to right), roughly from station CFOS13 to NS4. The surface temperatures were cooler than in May 1996. Fluorescence was greater (2.15) over all depths than in May 1996, with the maximum near CFOS13. Zooplankton were fewer in number (maximum 2.5) and were scattered through more of the water column in May 1997 compared to May 1996.

Conclusions

Warming and stratification started earlier in 1996 than in 1995. Stratification was greater in May 1996 than in May of either 1995 or 1997. In May 1996, there were greater numbers of zooplankton and less fluorescence than in May 1997. In May 1996, the low

numbers of phytoplankton in the stratified layer may have resulted from nutrients being depleted and not renewed. The deep mixed layer in May 1997 may have allowed phytoplankton growth and zooplankton dispersal.

The relative backscatter calculations also suggested that zooplankton abundance was reduced in May 1997, and that April 1996 values were increased. Backscatter was lower in the central Sound in May 1997 than in May 1995, and higher in April 1996 than in April 1995. Backscatter was also higher in May 1995 than in April 1995. Backscatter was high over the 'black hole' in the northwest Sound in June 1995. This maximum was not present in June 1996.

The spatial distribution of the zooplankton, as inferred from relative backscatter, changed seasonally. In April and especially May of both 1995 and 1997, more zooplankton were in the northern Sound, in regions of increased surface stratification. By June, more zooplankton were found in the southern Sound, in regions of reduced stratification. The movement of zooplankton from regions of high stratification to low stratification as the seasons progress is in agreement with theoretical primary productivity curve dynamics.

Spring of 1996 was the most productive year for zooplankton. May 1996 was unusually calm and warm. A strongly stratified surface layer formed. It is unclear whether the large number of zooplankton observed resulted from this mixed layer formation, or from favorable conditions in a prior season, like increased zooplankton abundance over the 'black hole' diapausing region in the previous June (1995).

References

- Flagg, C.N. and S.L. Smith, 1989: On the use of the acoustic Doppler current profiler to measure zooplankton abundance. *Deep-Sea Res.*, **36**, 3, pp 455-474.
- Heyward, K.J., S. Scrope-Howe, and E.D. Barton, 1991: Estimation of zooplankton abundance from shipboard ADCP backscatter. *Deep-Sea Res.*, **38**, 6, pp 677-691.
- Muench, R. D. and G. M. Schmidt, 1975: Variations in the Hydrographic Structure of Prince William Sound. IMS Report R75-1. 135pp.
- Niebauer, H.J., T.C. Royer, and T.J. Weingartner, 1994: Circulation of Prince William Sound, Alaska. *J. Geophys. Res.*, **99**, C7, pp 14,113-14,126.
- Roe, H.S.J. and G. Griffiths, 1993: Biological information from an Acoustic Doppler Current Profiler. *Mar. Biol.*, **115**, 339-346.
- Royer, T.C., D.V. Hansen, and D.J. Pashinski, 1979: Coastal Flow in the Northern Gulf of Alaska as Observed by Dynamic Topography and Satellite Tracked Drogued Drift Buoys. *J. Phys. Oceanogr.*, **9**, 4, pp 785-801.

List of Figures

Figure 1 : Cruise track and station locations.

Figure 2 : South to north sections through the central Sound of (a) temperature (T), salinity (S), and density (σ), and (b) density (σ) and Brunt-Vaisala frequency (N^2) from April 1995.

Figure 3 : South to north sections through the central Sound of (a) temperature (T), salinity (S), and density (σ), and (b) density (σ) and Brunt-Vaisala frequency (N^2) from April 1996.

Figure 4 : Mean (a) temperature and (b) salinity averaged over the upper 20m from April 1995.

Figure 5 : Mean (a) temperature and (b) salinity averaged over the upper 20m from April 1996.

Figure 6 : Wind speed and direction from (a) April 1995, and (b) April 1996.

Figure 7 : South to north sections through the central Sound of (a) temperature (T), salinity (S), and density (σ), and (b) density (σ) and Brunt-Vaisala frequency (N^2) from May 1995.

Figure 8 : South to north sections through the central Sound of (a) temperature (T), salinity (S), and density (σ), and (b) density (σ) and Brunt-Vaisala frequency (N^2) from May 1996.

Figure 9 : South to north sections through the central Sound of (a) temperature (T), salinity (S), and density (σ), and (b) density (σ) and Brunt-Vaisala frequency (N^2) from May 1997.

Figure 10 : Mean (a) temperature and (b) salinity averaged over the upper 20m from May 1995.

Figure 11 : Mean (a) temperature and (b) salinity averaged over the upper 20m from May 1996.

Figure 12 : Mean (a) temperature and (b) salinity averaged over the upper 20m from May 1997.

Figure 13 : Wind speed and direction from (a) May 1995, (b) May 1996, and (c) May 1997.

Figure 14 : South to north sections through the central Sound of (a) temperature (T), salinity (S), and density (σ), and (b) density (σ) and Brunt-Vaisala frequency (N^2) from June 1995.

Figure 15 : South to north sections through the central Sound of (a) temperature (T), salinity (S), and density (σ), and (b) density (σ) and Brunt-Vaisala frequency (N^2) from June 1996.

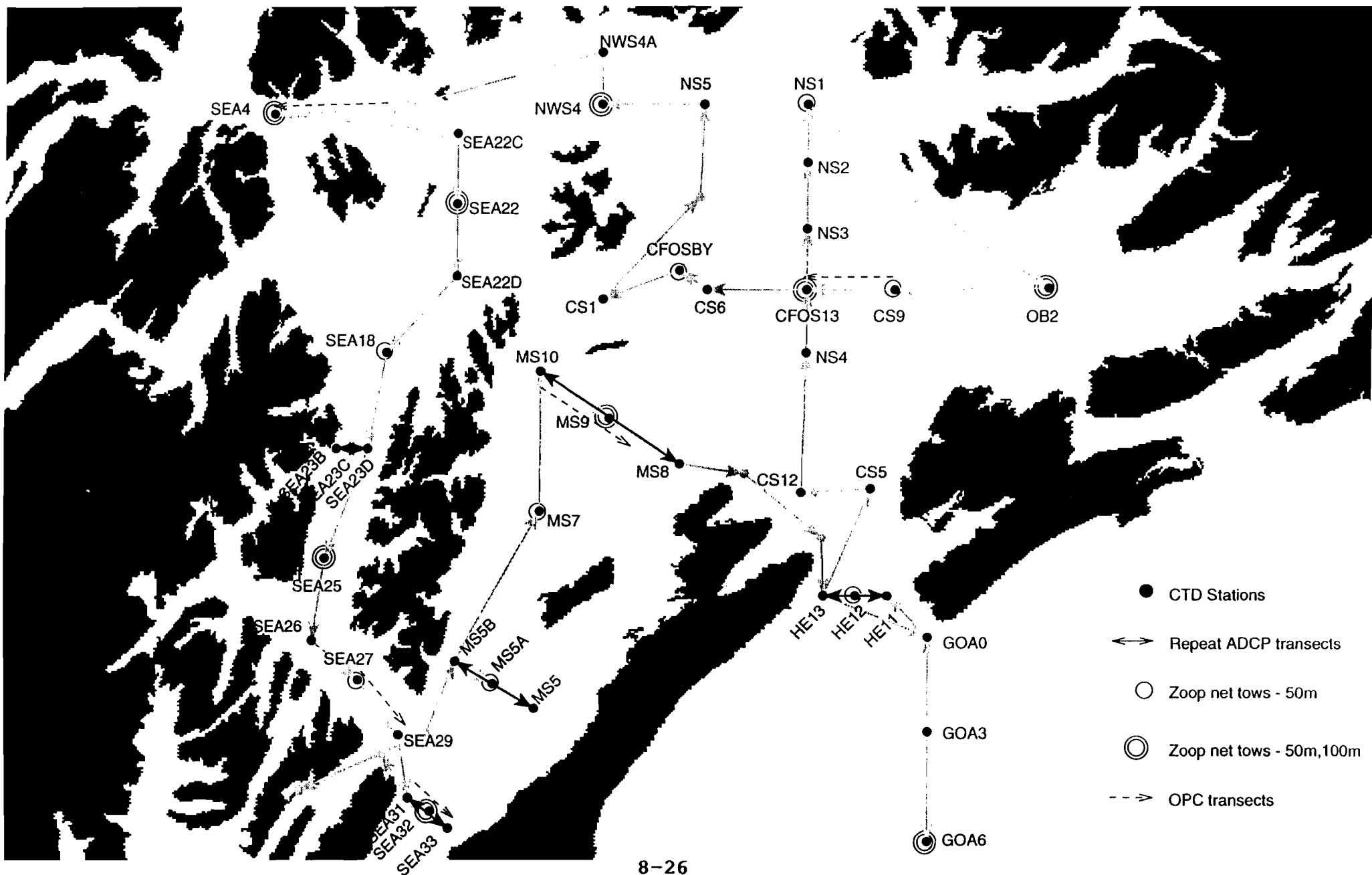
Figure 16 : Mean (a) temperature and (b) salinity averaged over the upper 20m from June 1995.

Figure 17 : Mean (a) temperature and (b) salinity averaged over the upper 20m from June 1996.

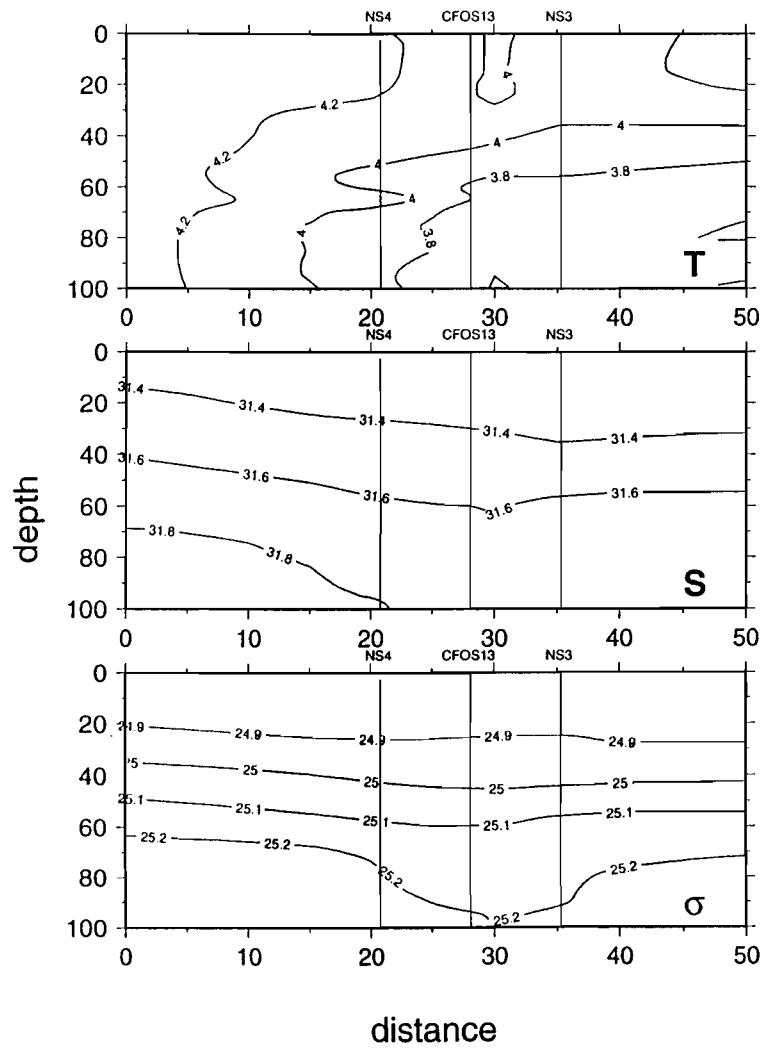
Figure 18 : Wind speed and direction from (a) June 1995. and (b) June 1996.

Figure 19 : Relative backscatter from 20m for (a) April 1995 and April 1996, (b) May 1995 and May 1997. and (c) June 1995 and June 1996.

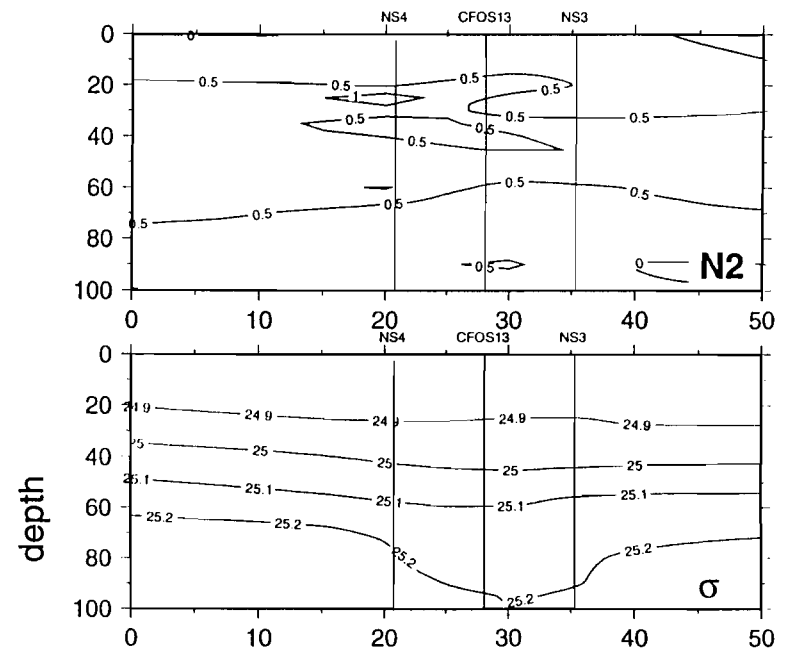
Figure 20 : Aquashuttle temperature, salinity, fluorescence, and particle size for (a) May 1996 and (b) May 1997.



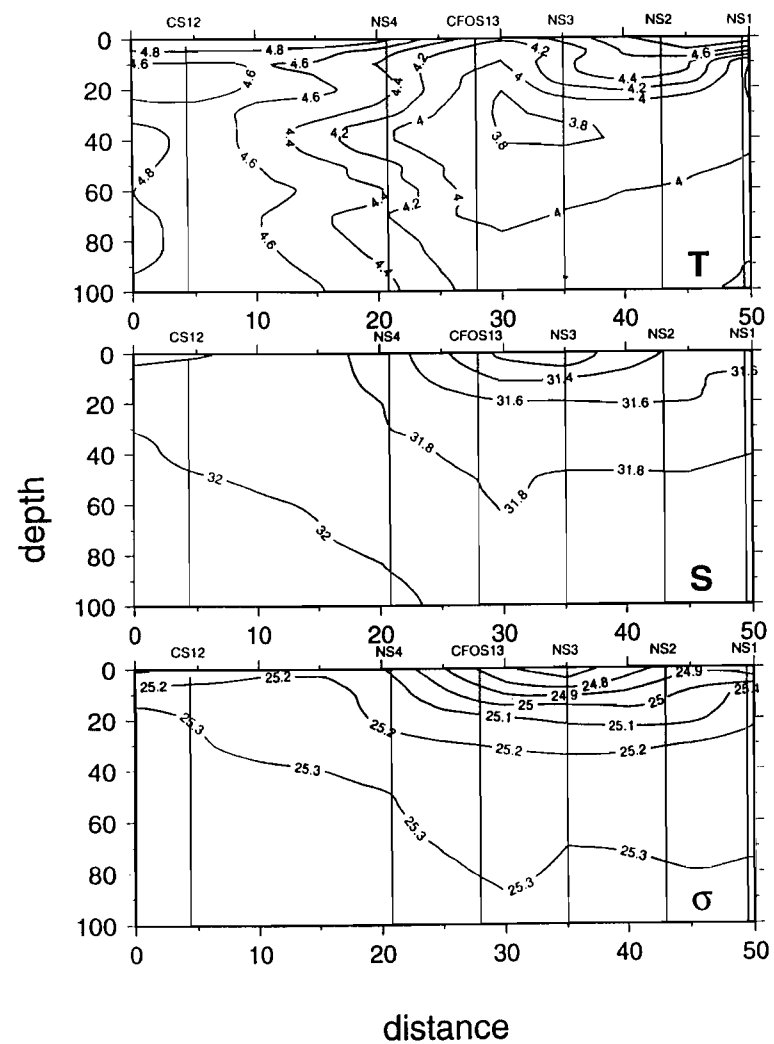
SNCS - be504



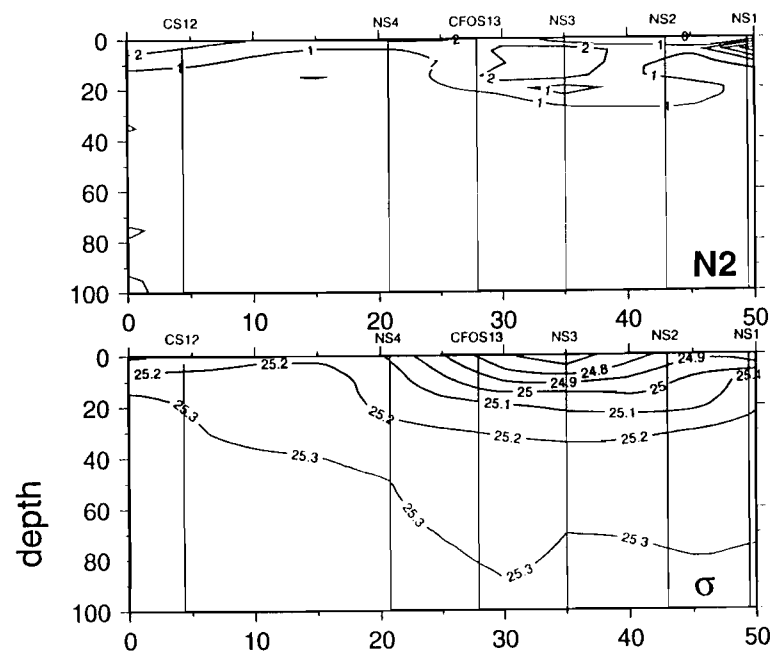
SNCS - be504



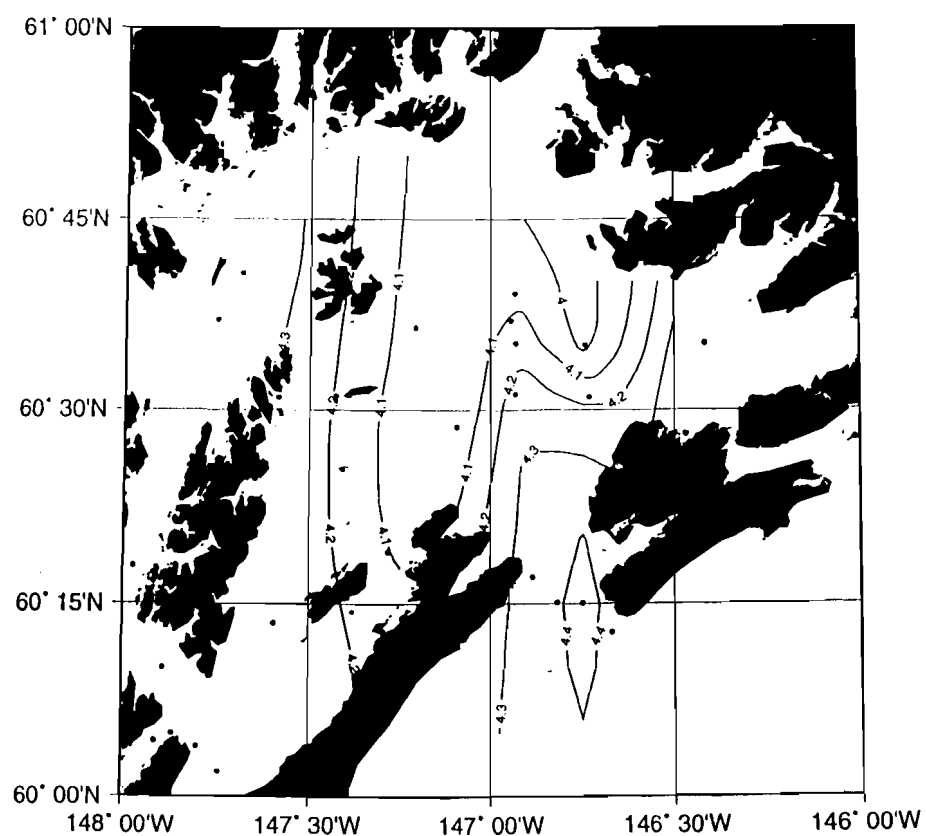
SNCS - be604



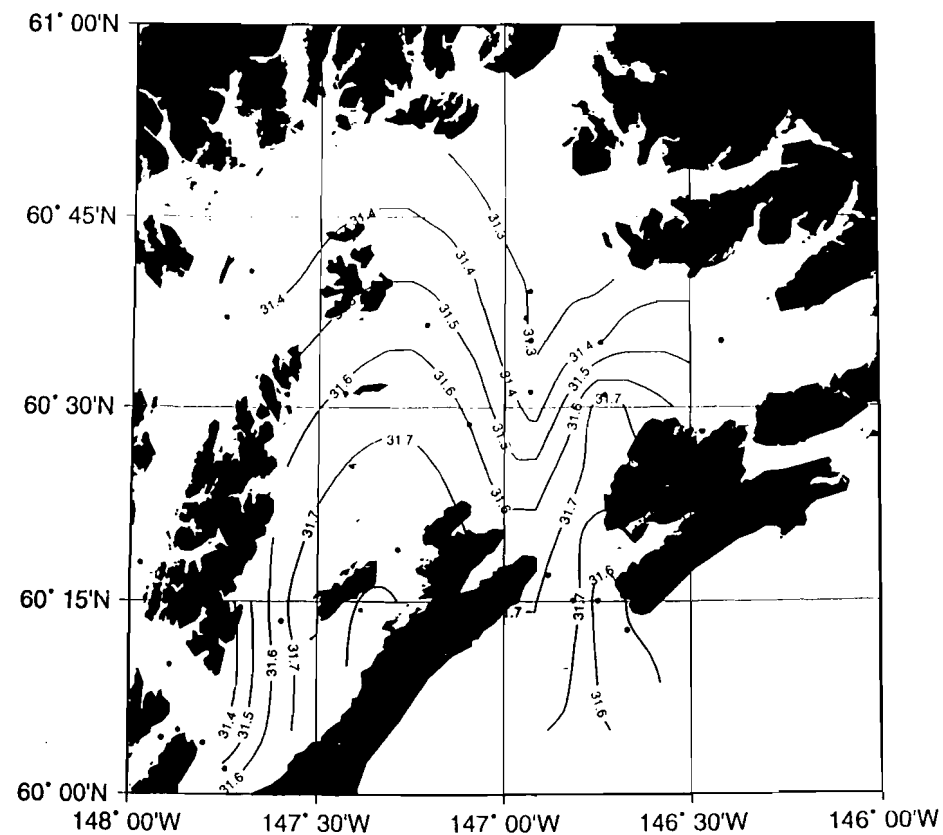
SNCS - be604



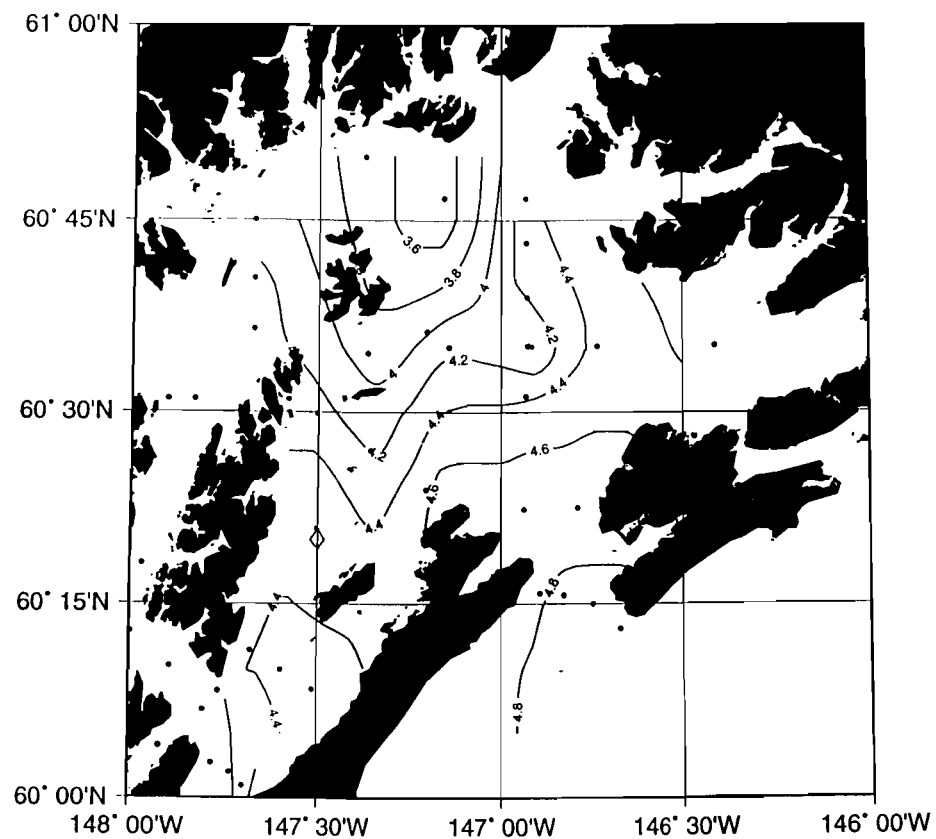
Mean Temperature (001to020m) - be504



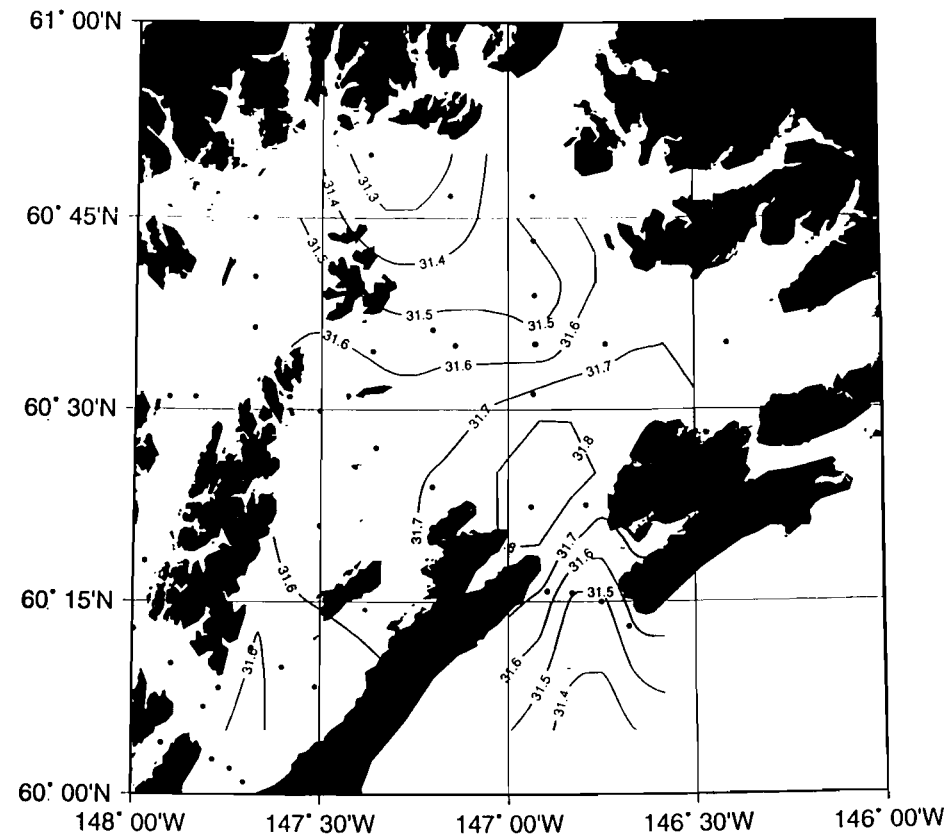
Mean Salinity (001to020m) - be504



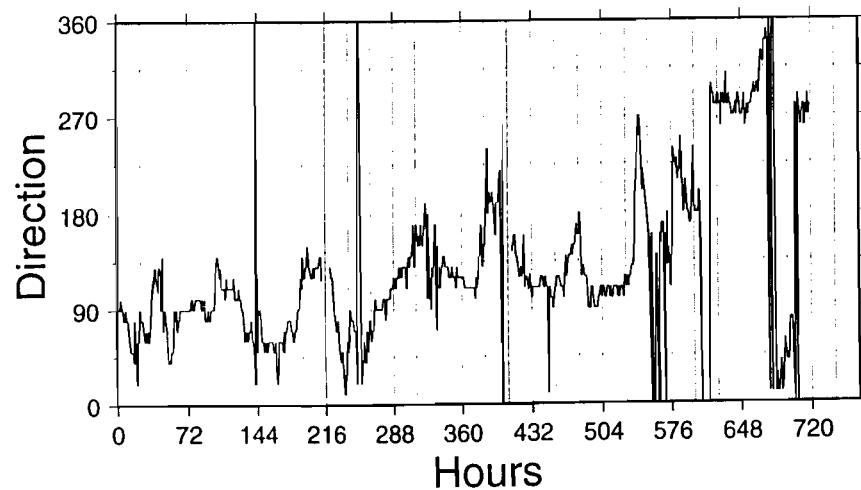
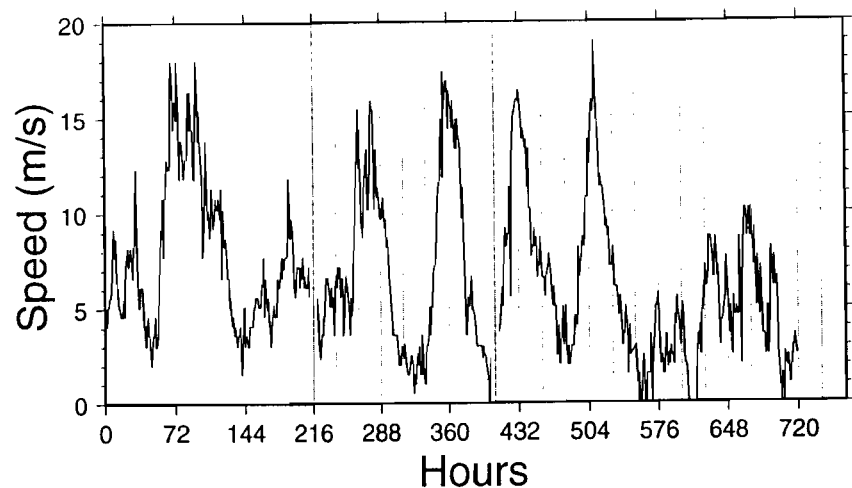
Mean Temperature (001to020m) - be604



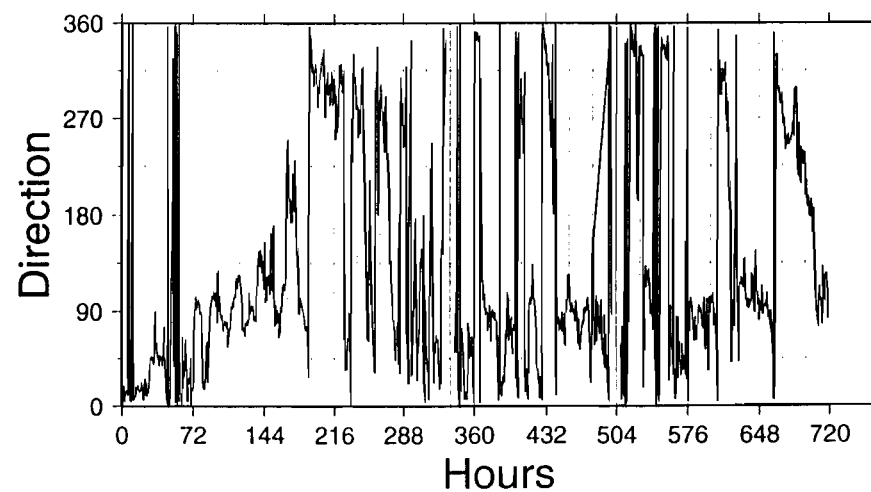
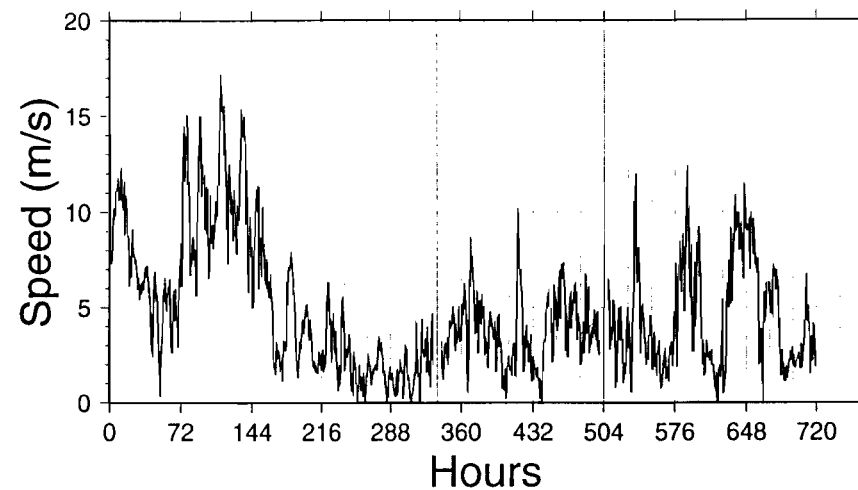
Mean Salinity (001to020m) - be604



Middleton Island Wind - April - 1995



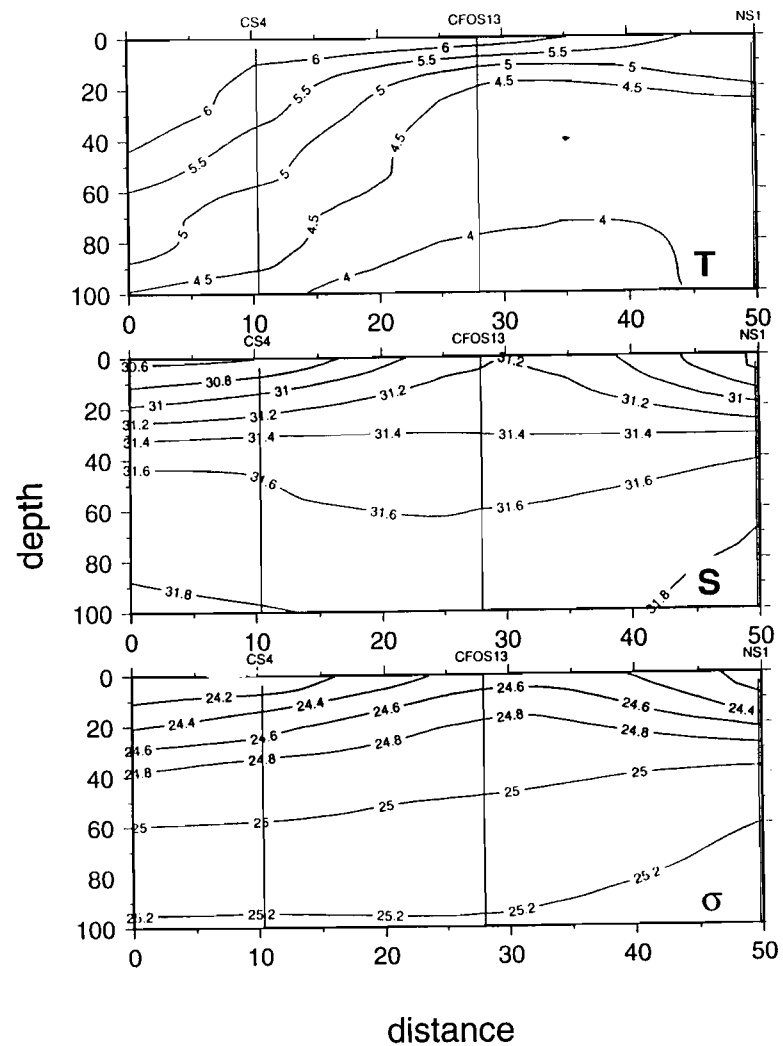
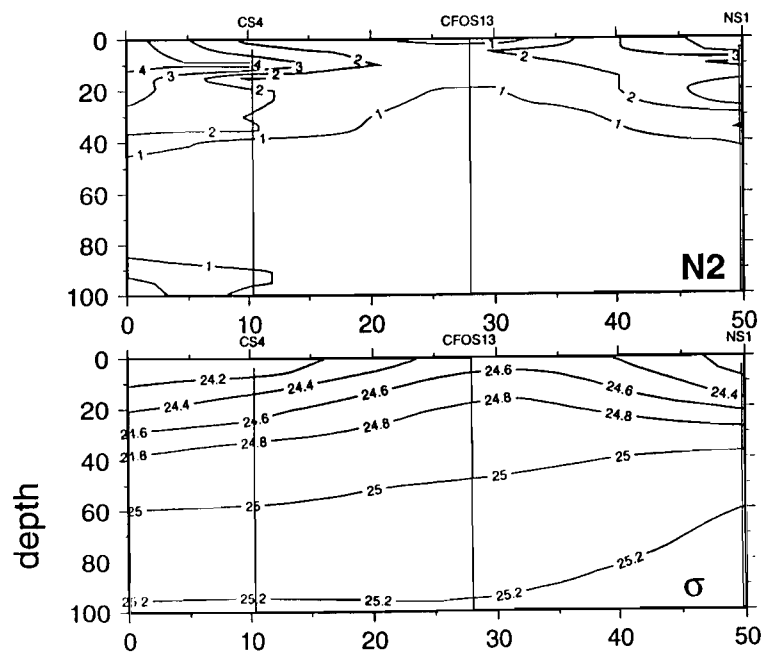
Mid-Sound Wind - April - 1996



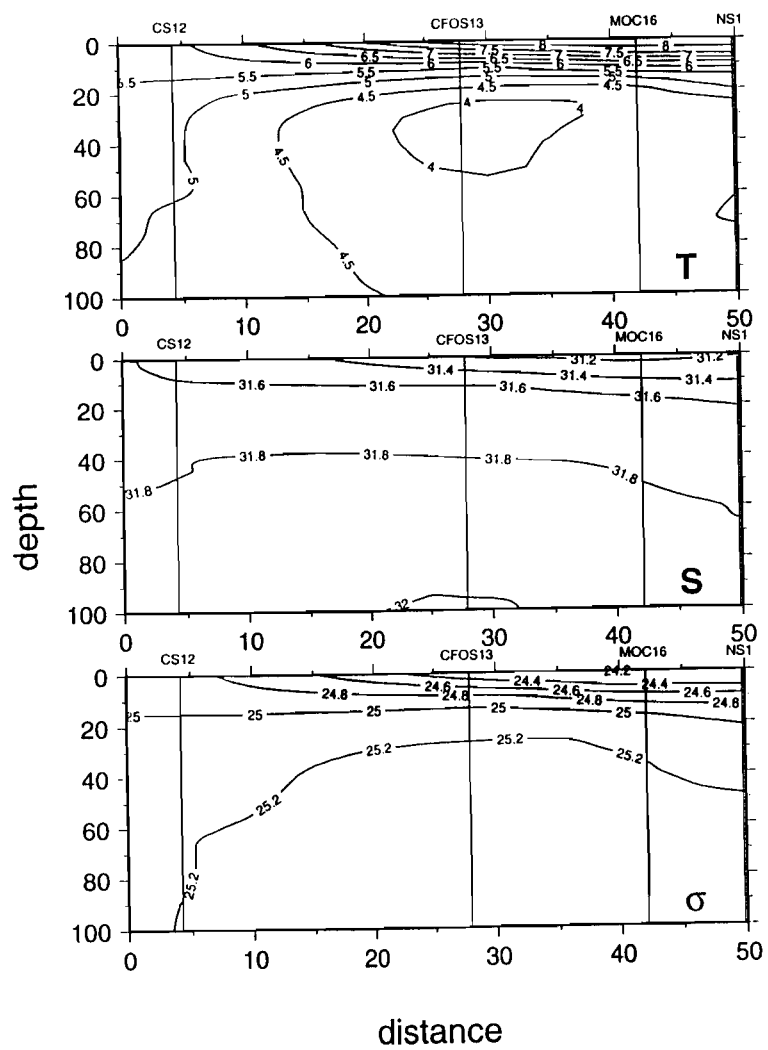
SNCS - be505

Fig. 7(b)

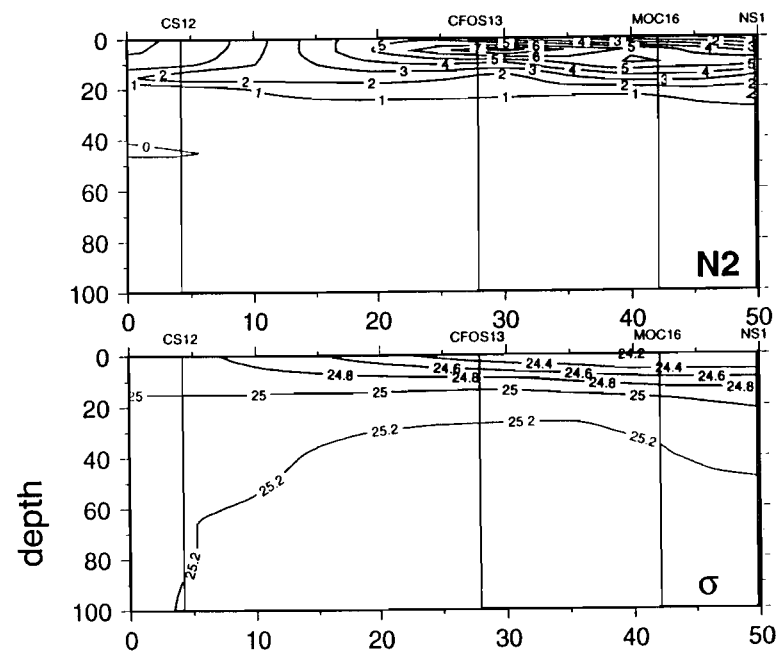
SNCS - be505



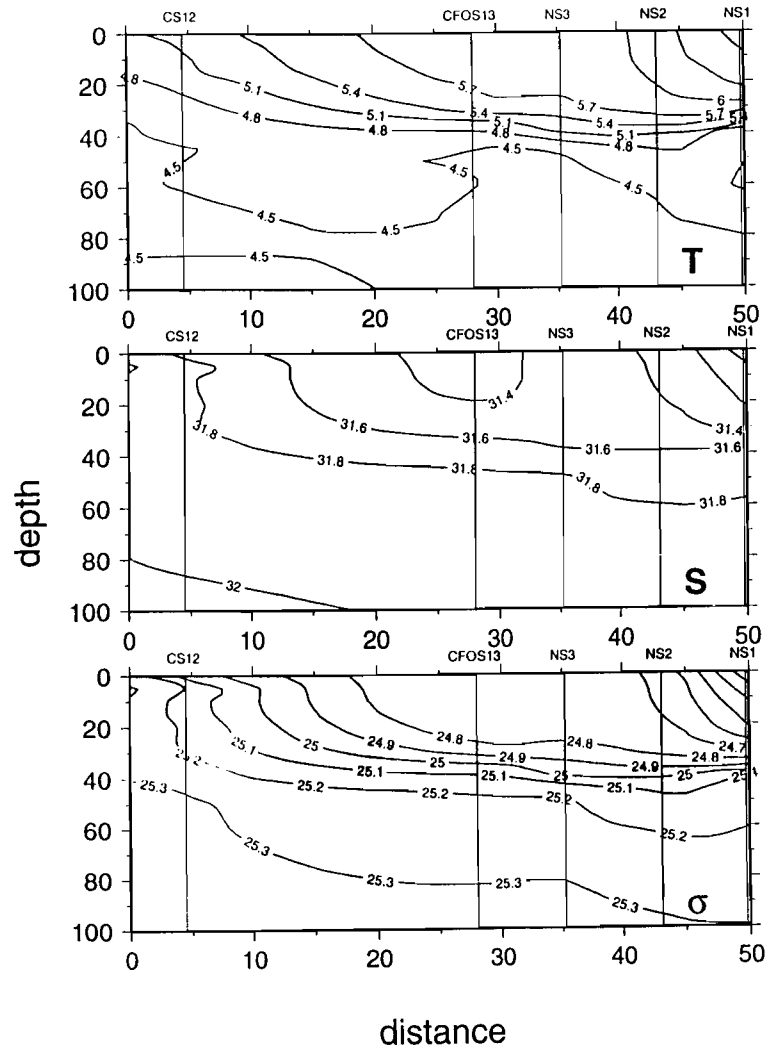
SNCS - hx605



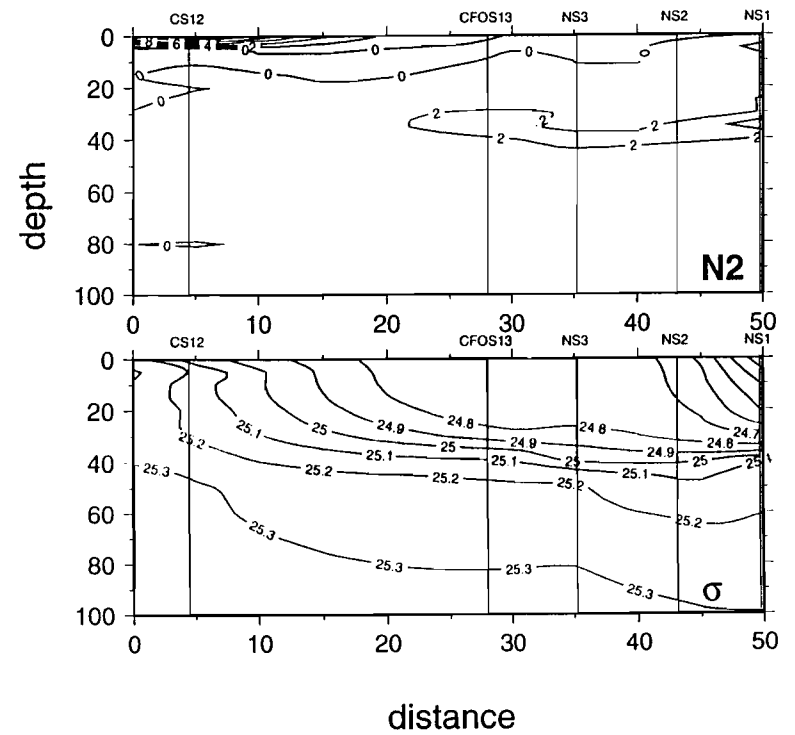
SNCS - hx605



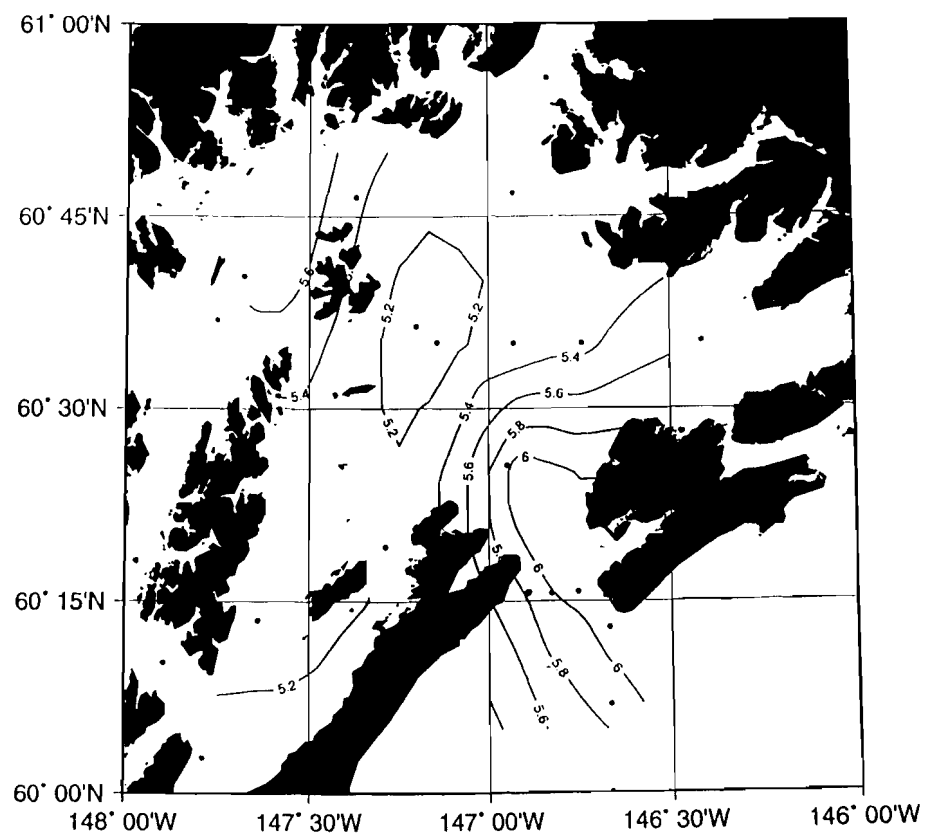
SNCS - be705



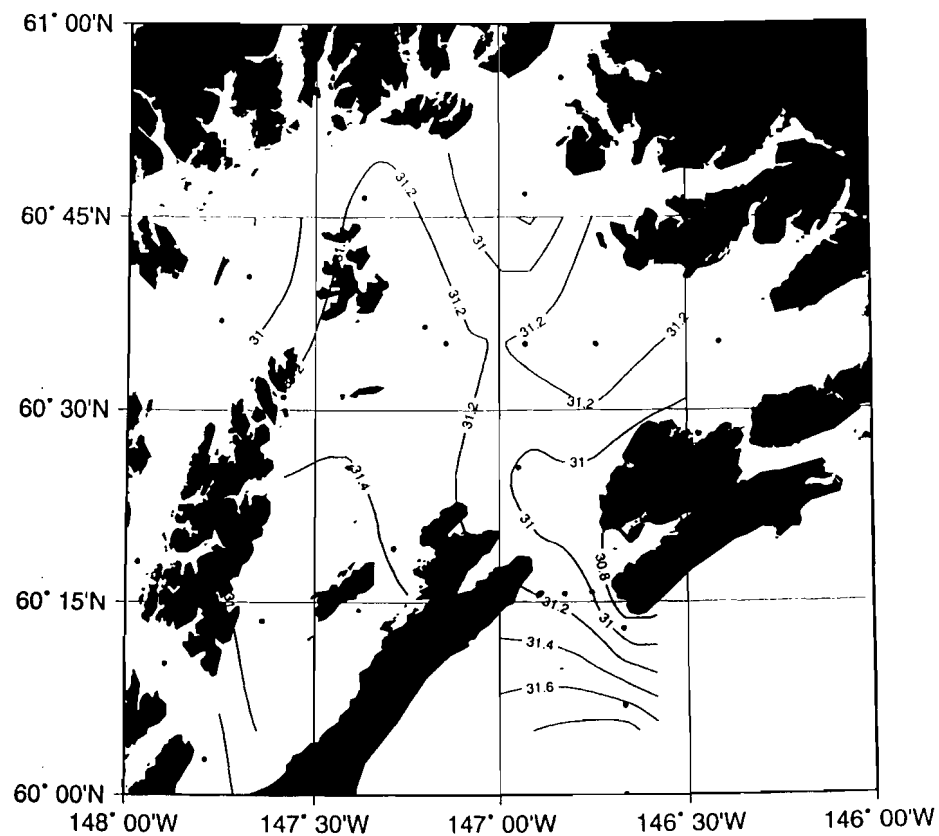
SNCS - be705



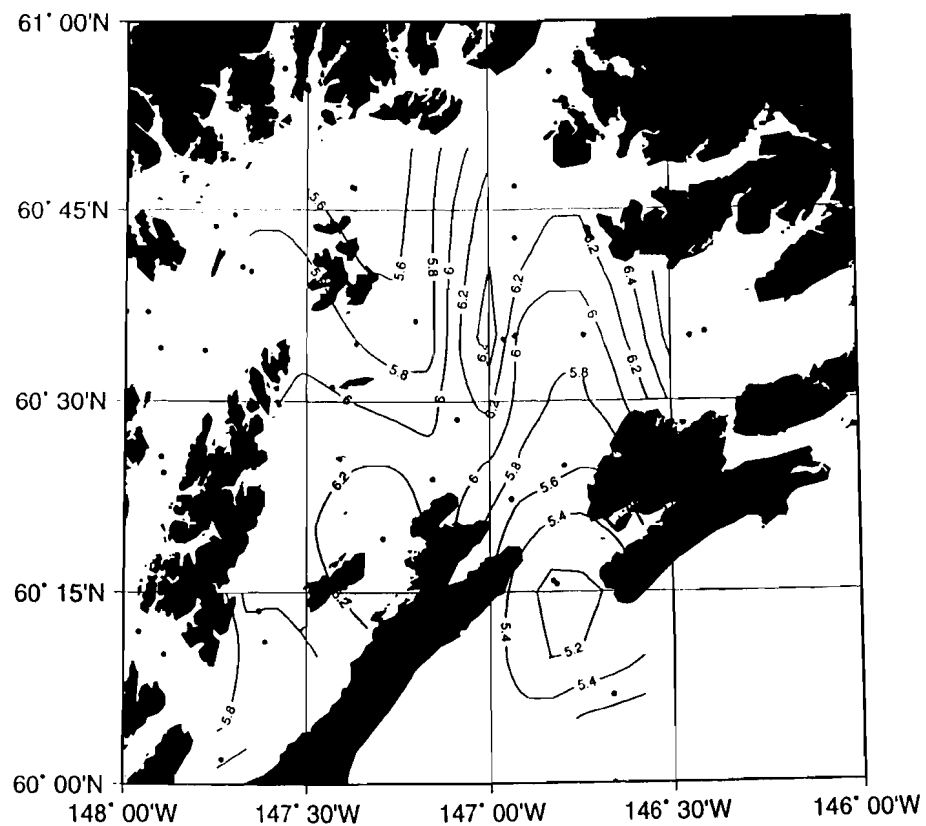
Mean Temperature (001to020m) - be505



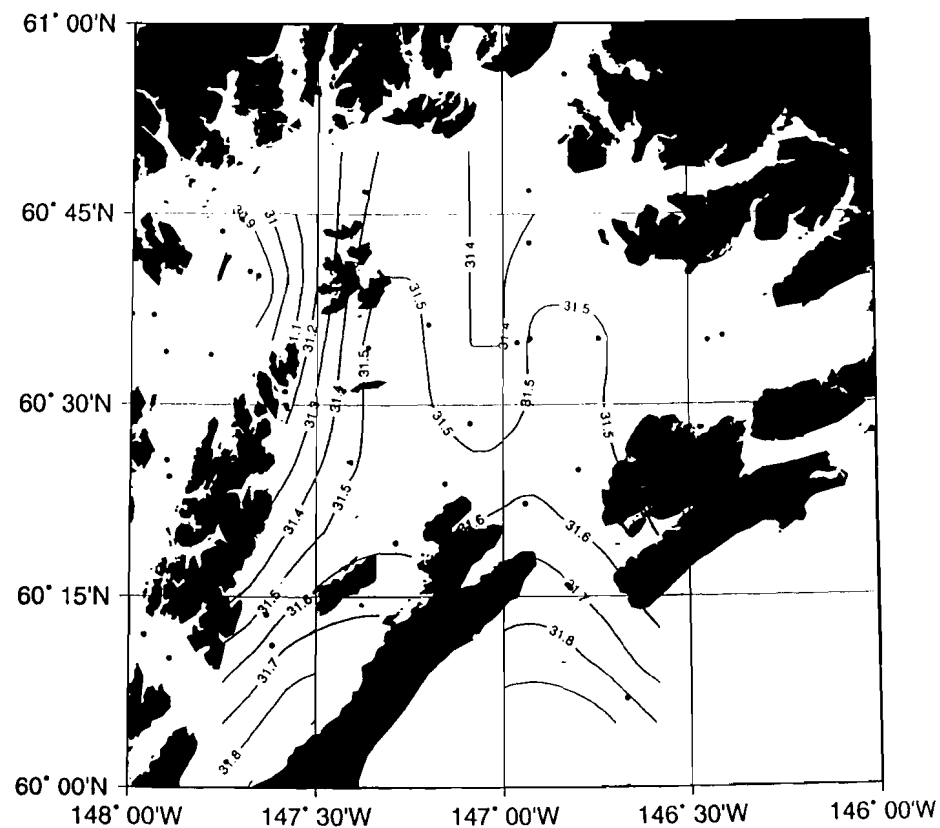
Mean Salinity (001to020m) - be505



Mean Temperature (001to020m) - hx605

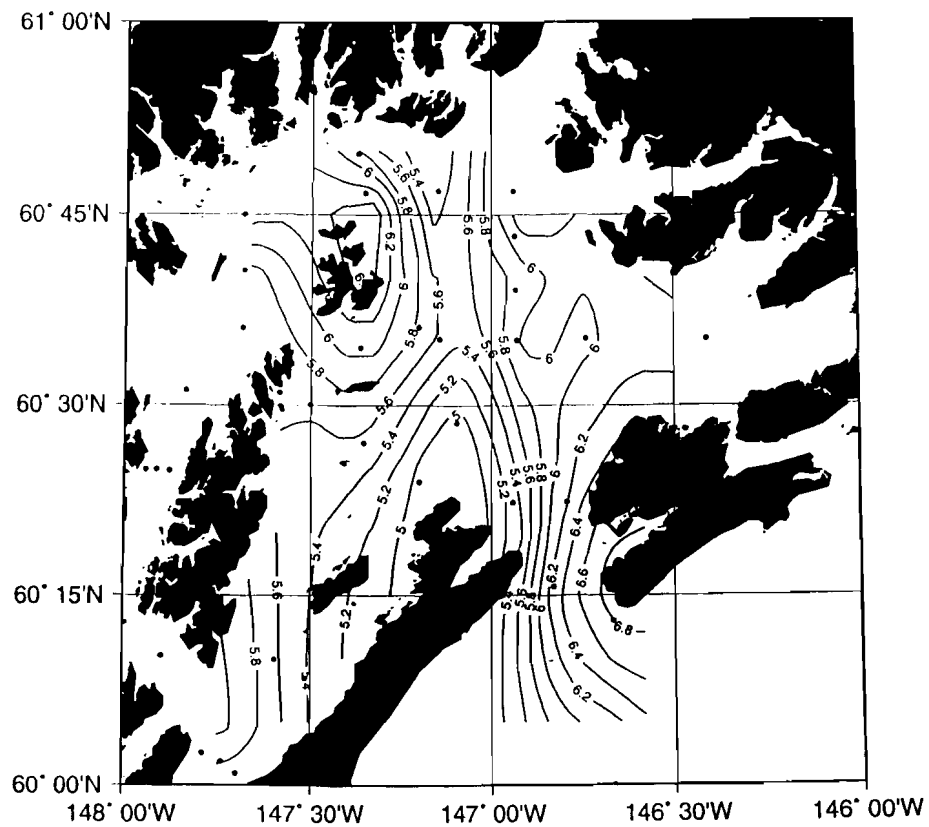


Mean Salinity (001to020m) - hx605

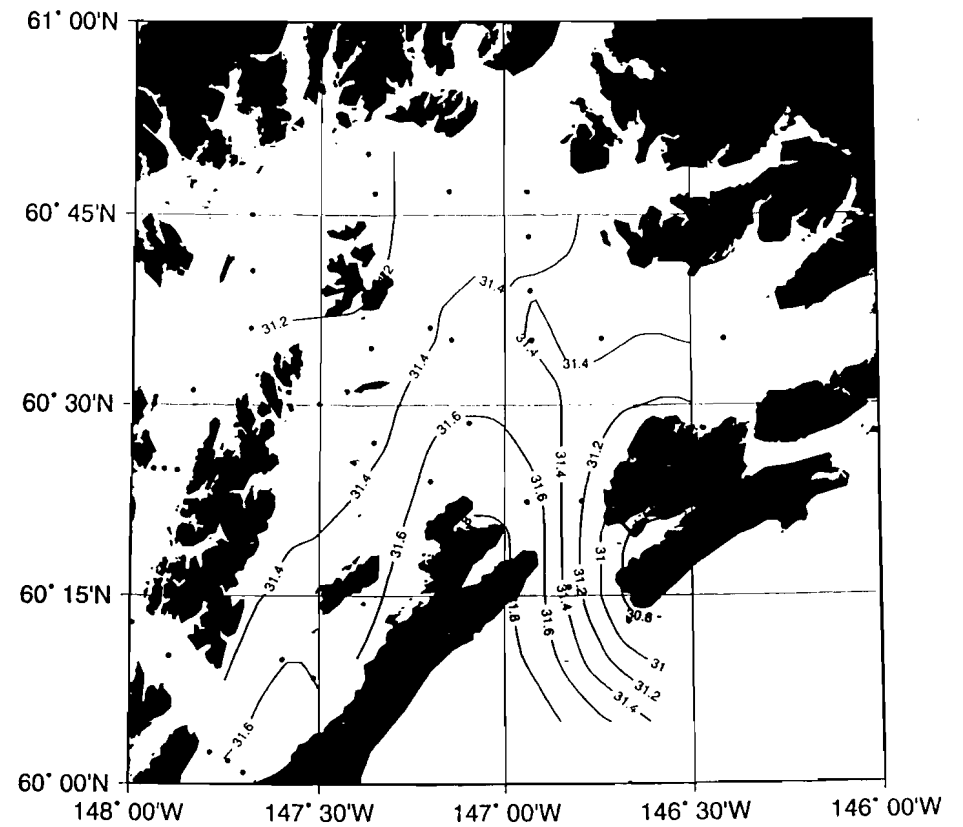


(1210)

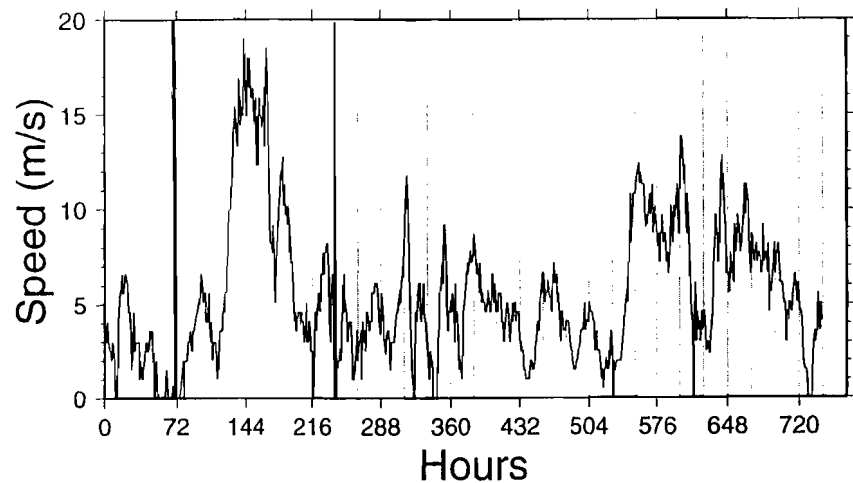
Mean Temperature (001to020m) - be705



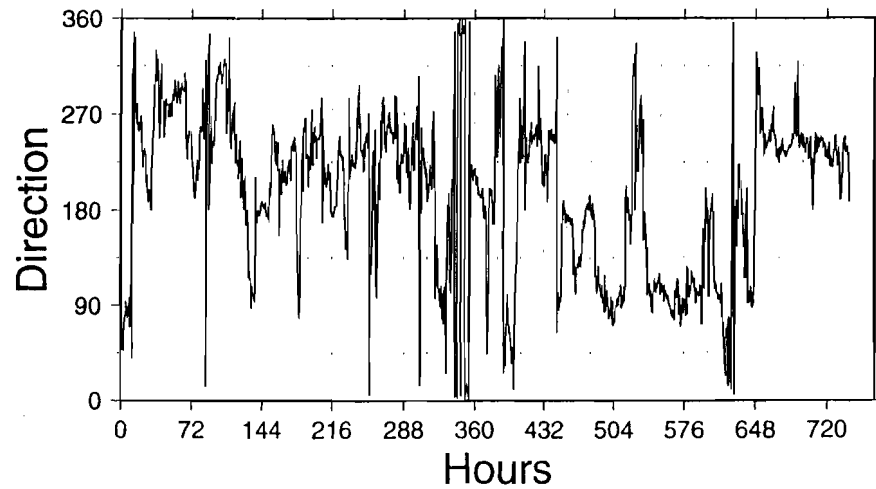
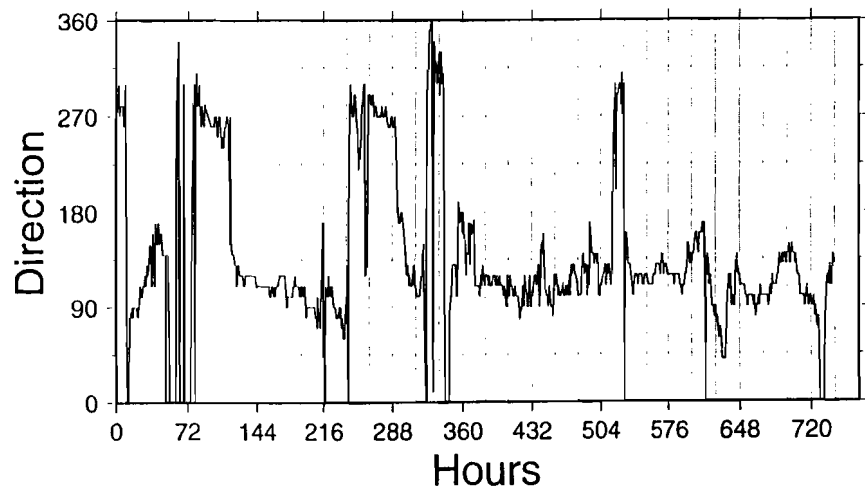
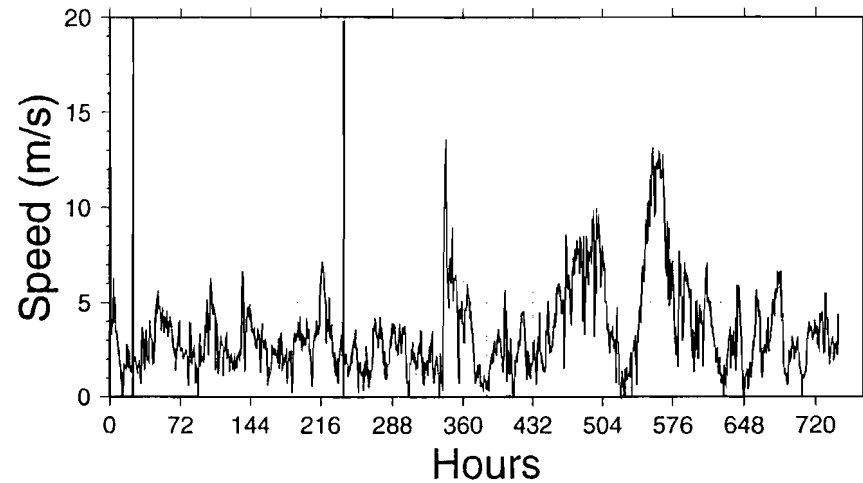
Mean Salinity (001to020m) - be705



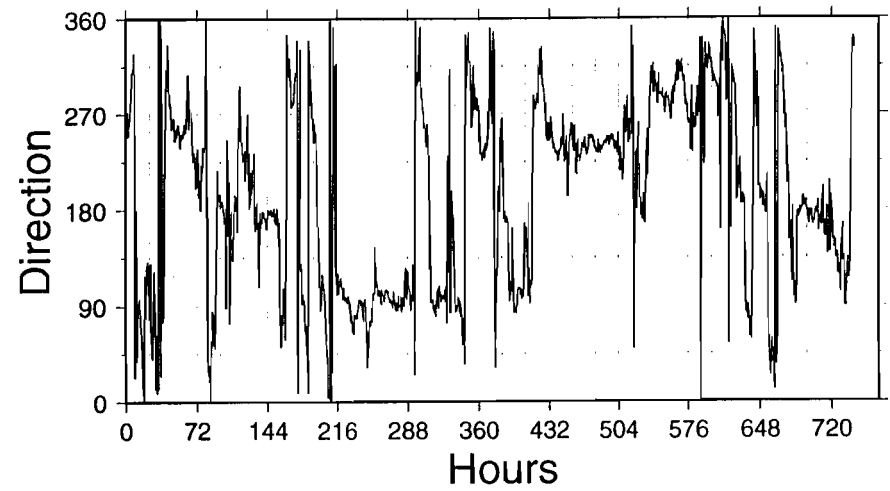
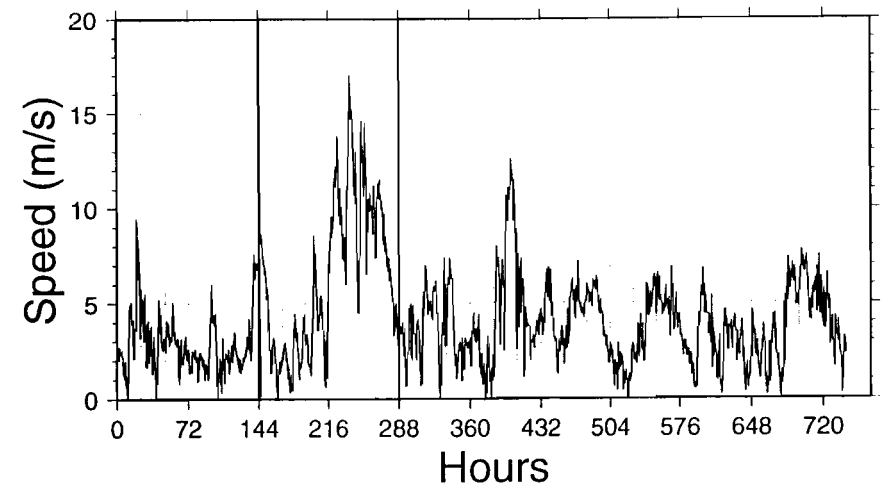
Middleton Island Wind - May - 1995



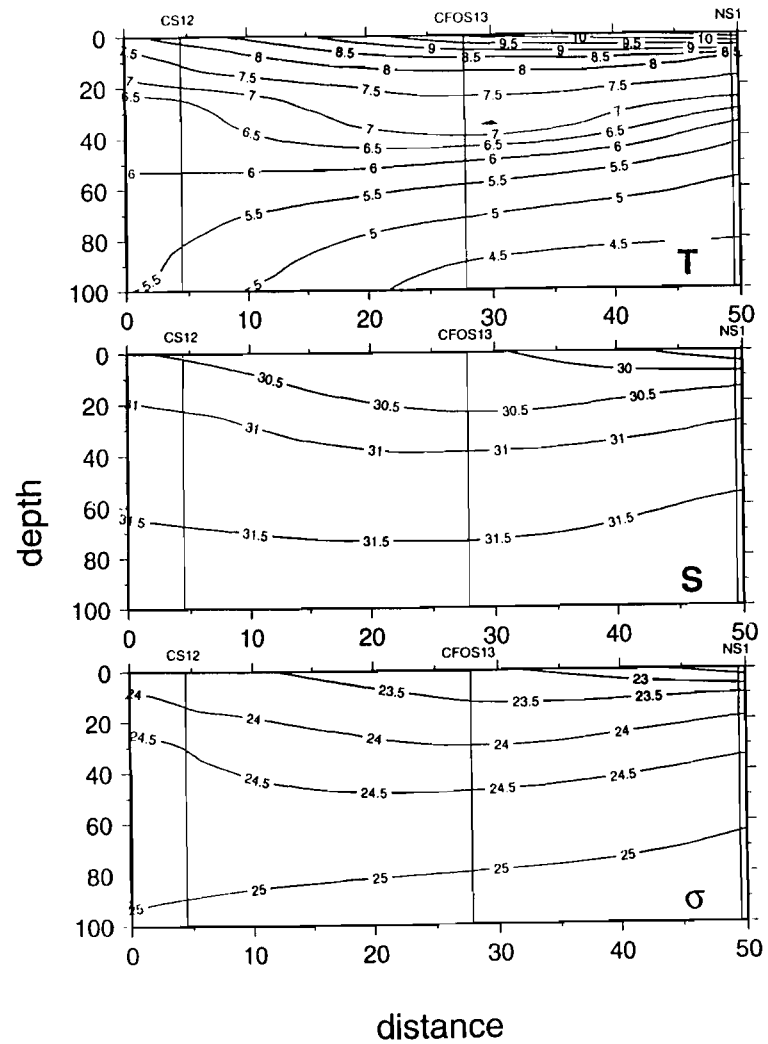
Mid-Sound Wind - May - 1996



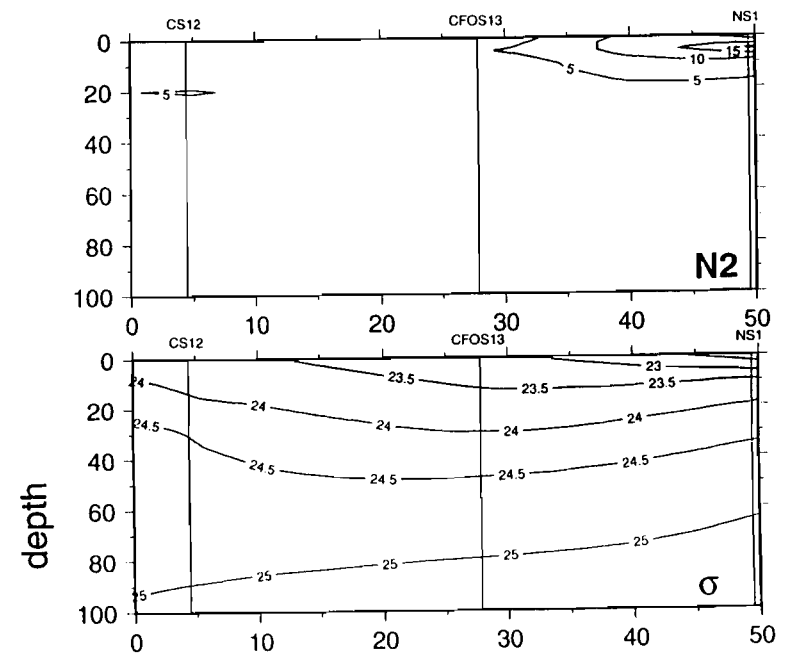
Mid-Sound Wind - May - 1997



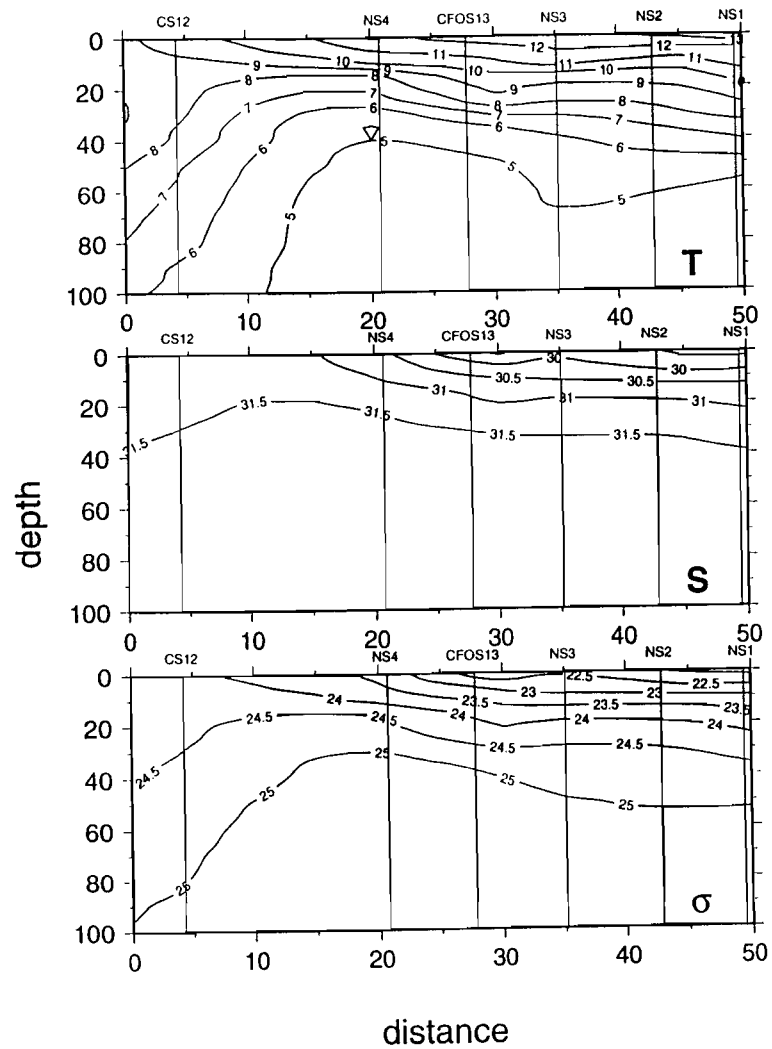
SNCS - be506



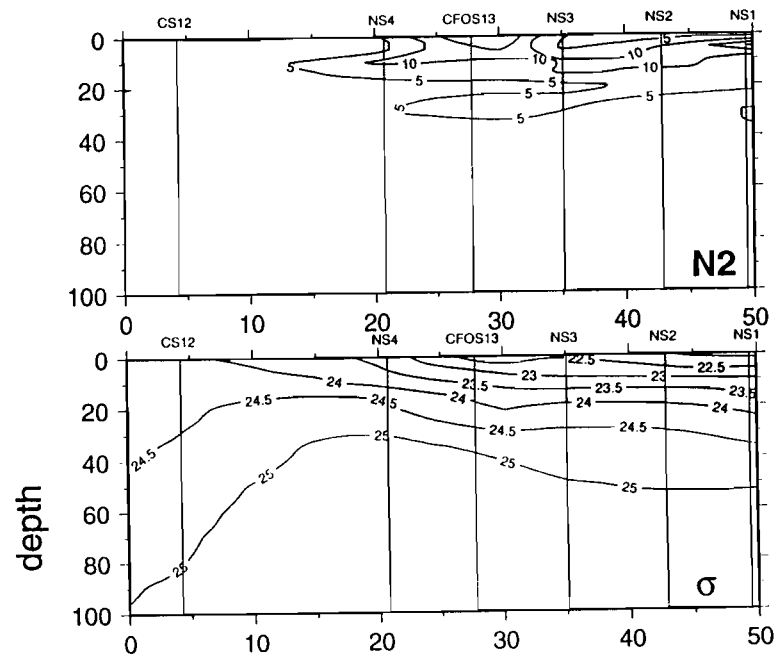
SNCS - be506



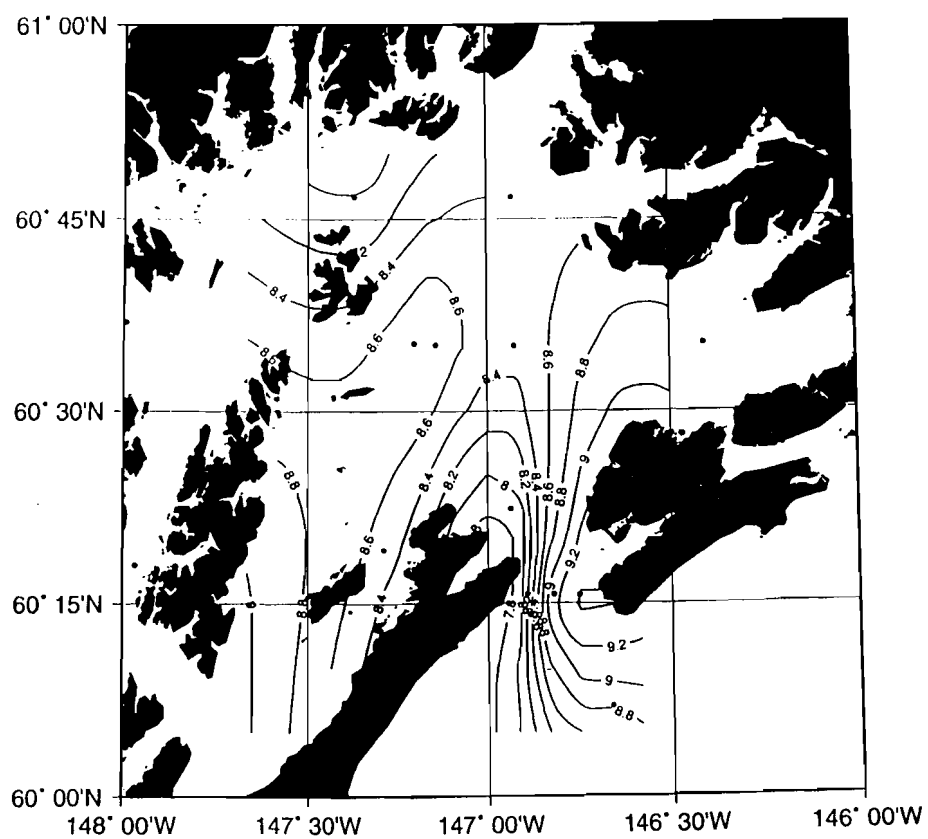
SNCS - be606



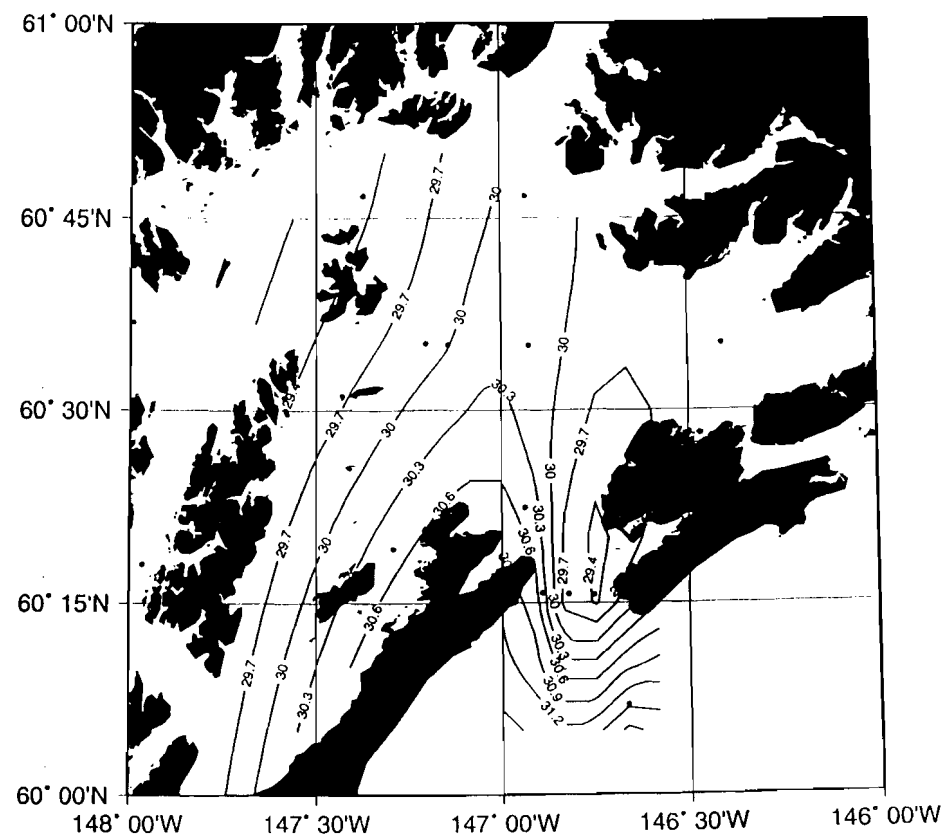
SNCS - be606



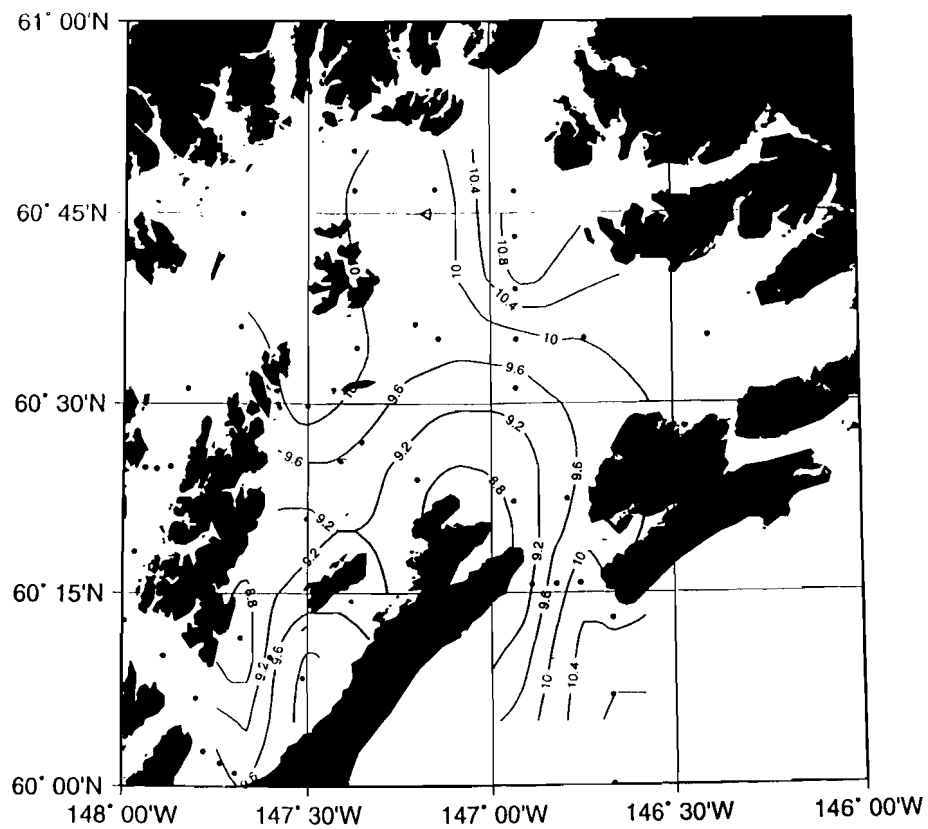
Mean Temperature (001to020m) - be506



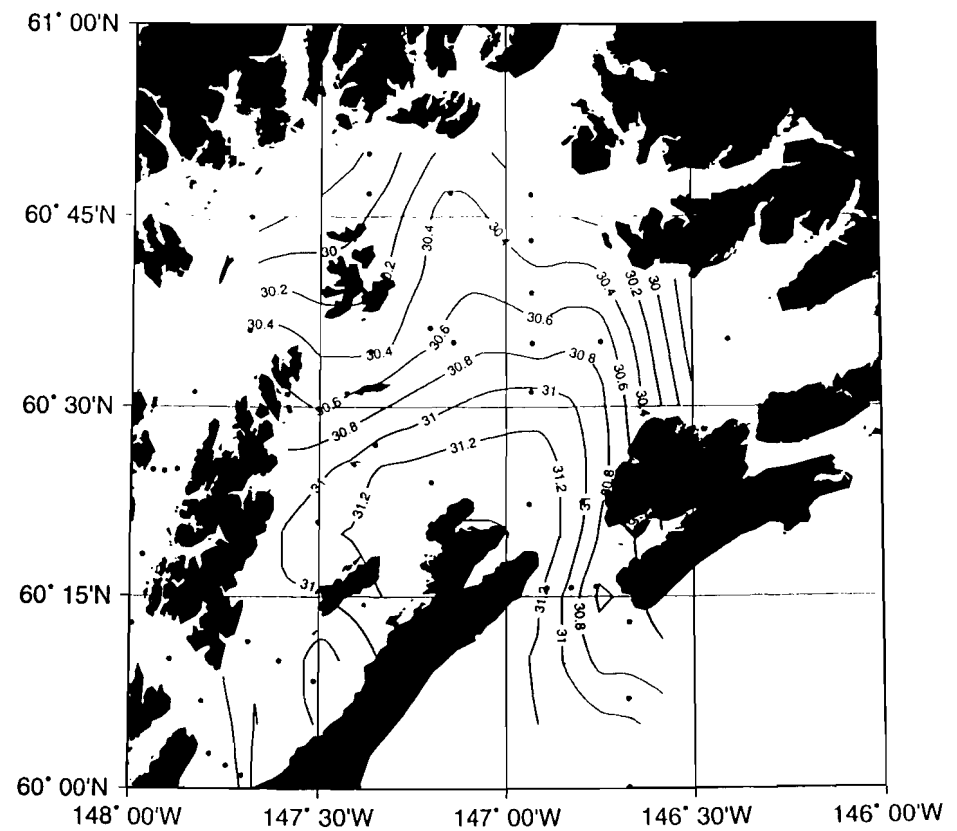
Mean Salinity (001to020m) - be506



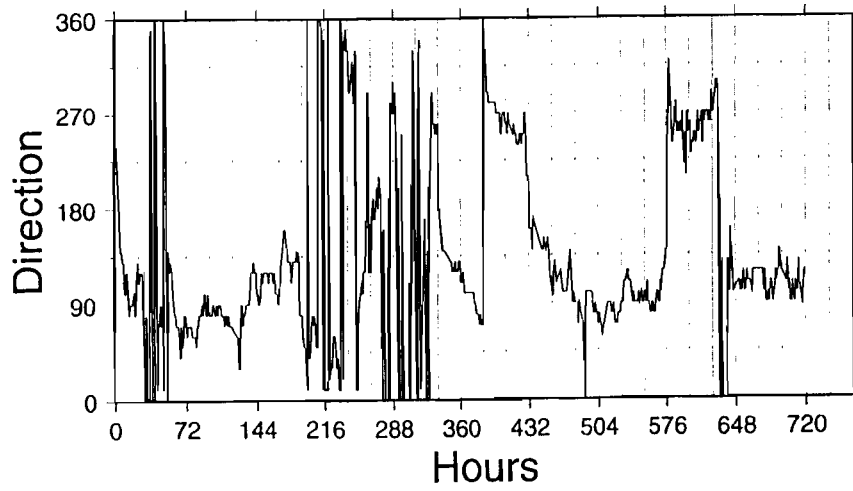
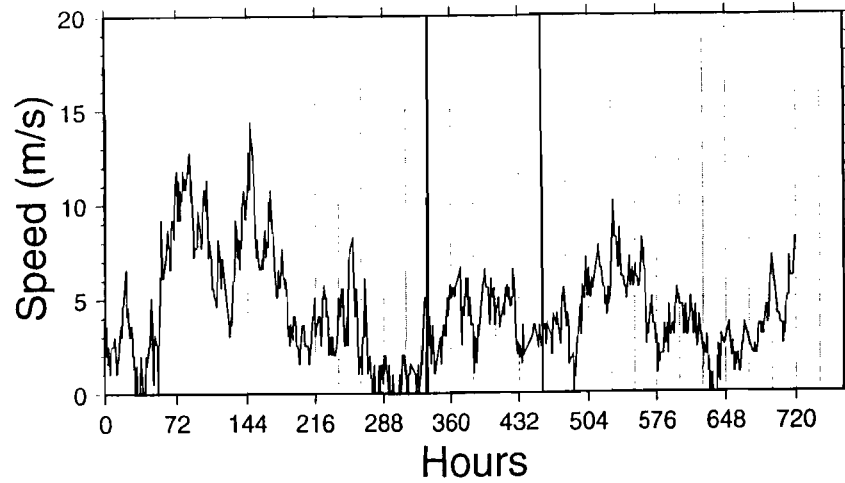
Mean Temperature (001to020m) - be606



Mean Salinity (001to020m) - be606



Middleton Island Wind - June - 1995



Mid-Sound Wind - June - 1996

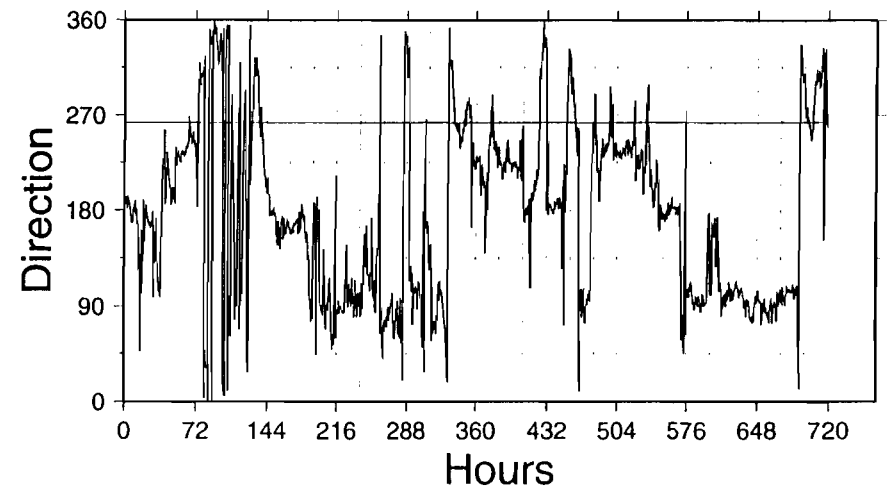
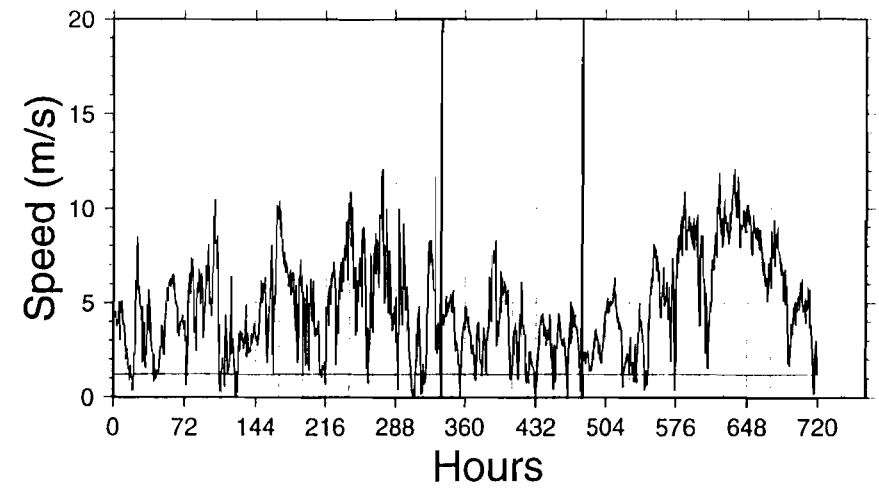


FIG. 19 (a)

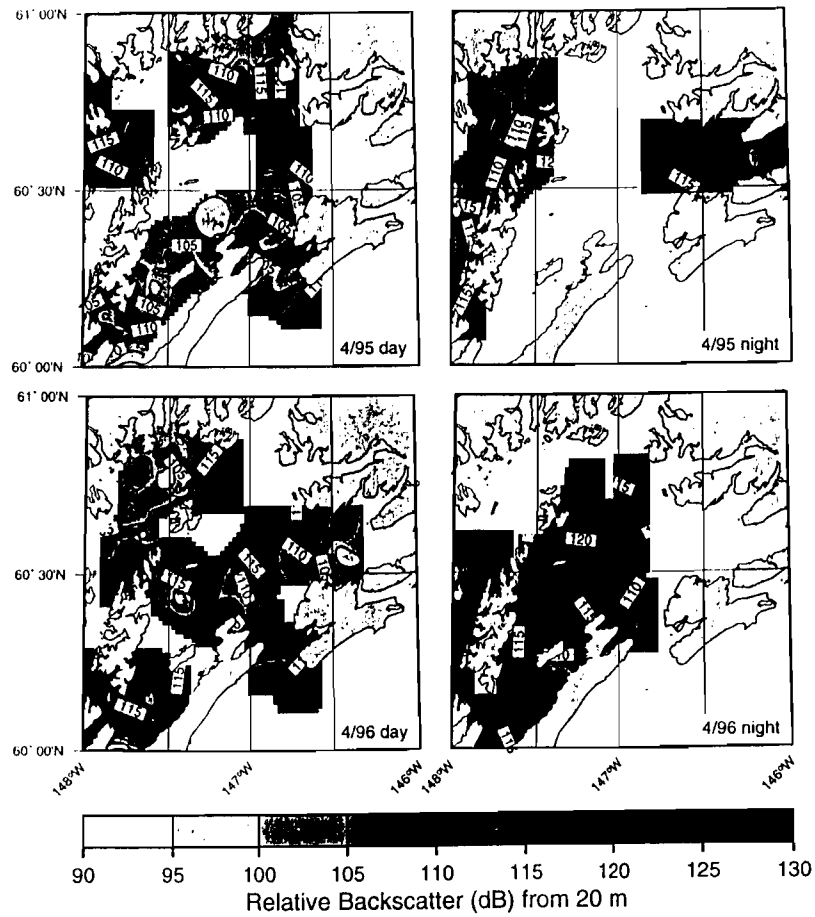
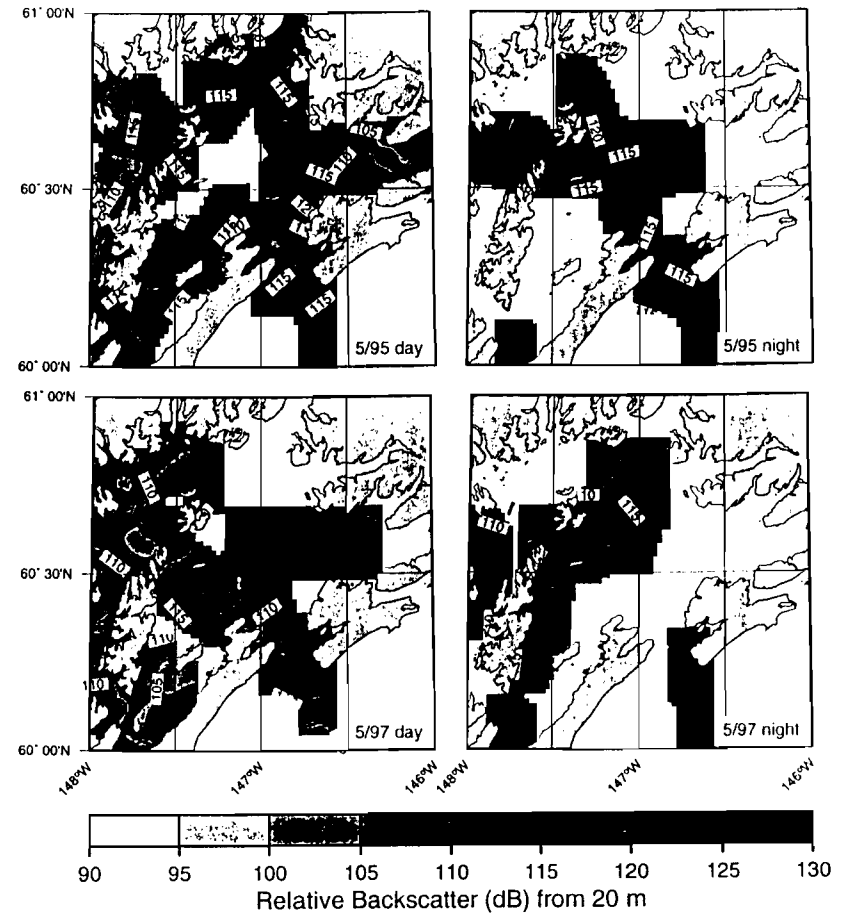


FIG. 19 (b)



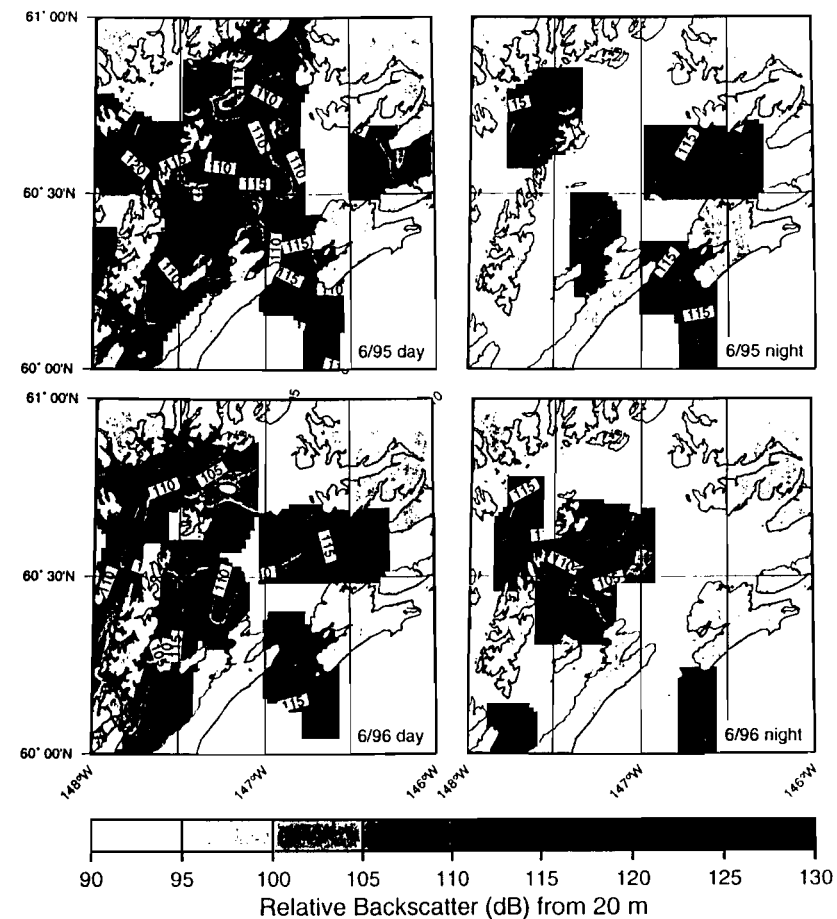


FIG. 20(a)

May 1996

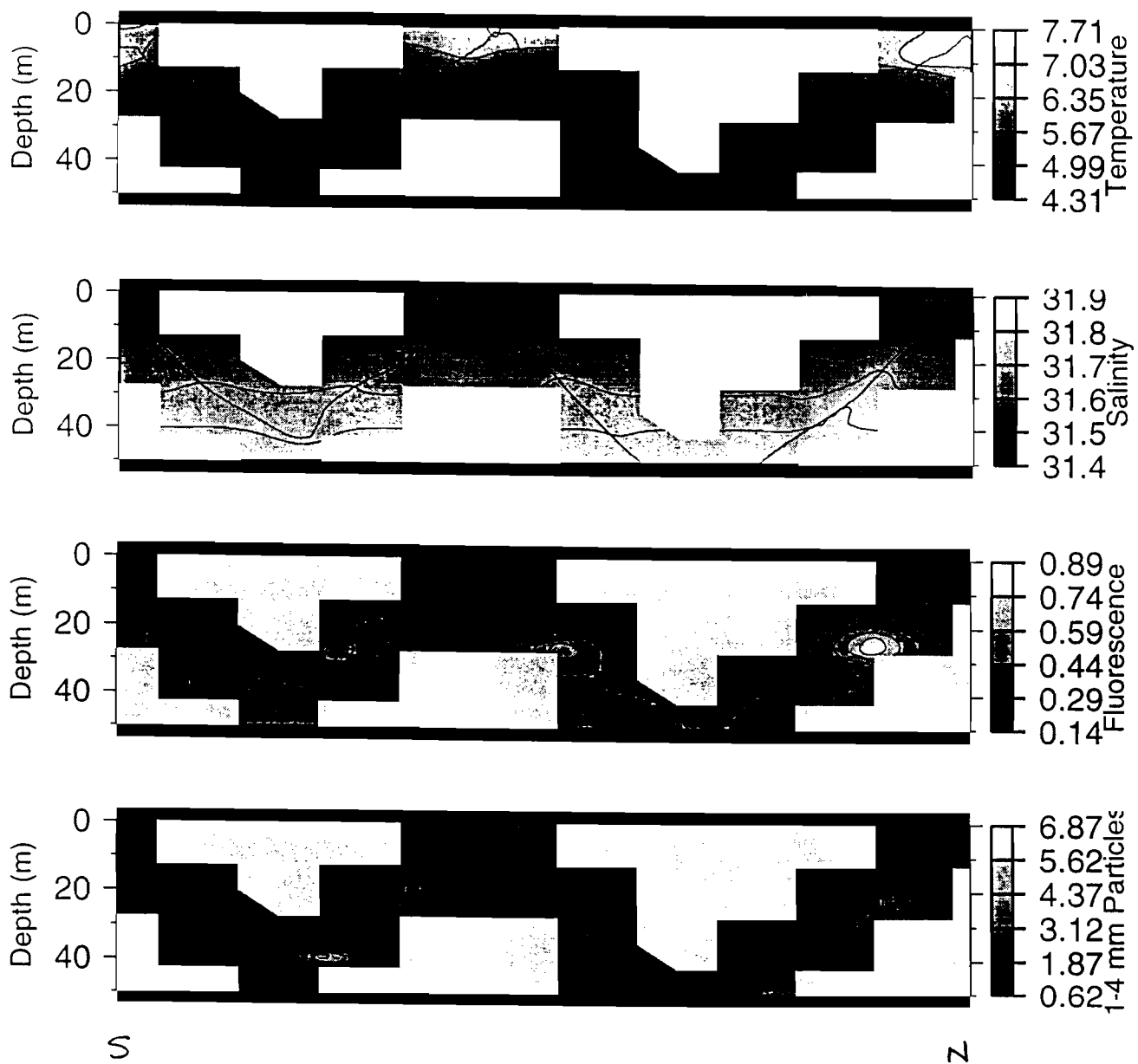
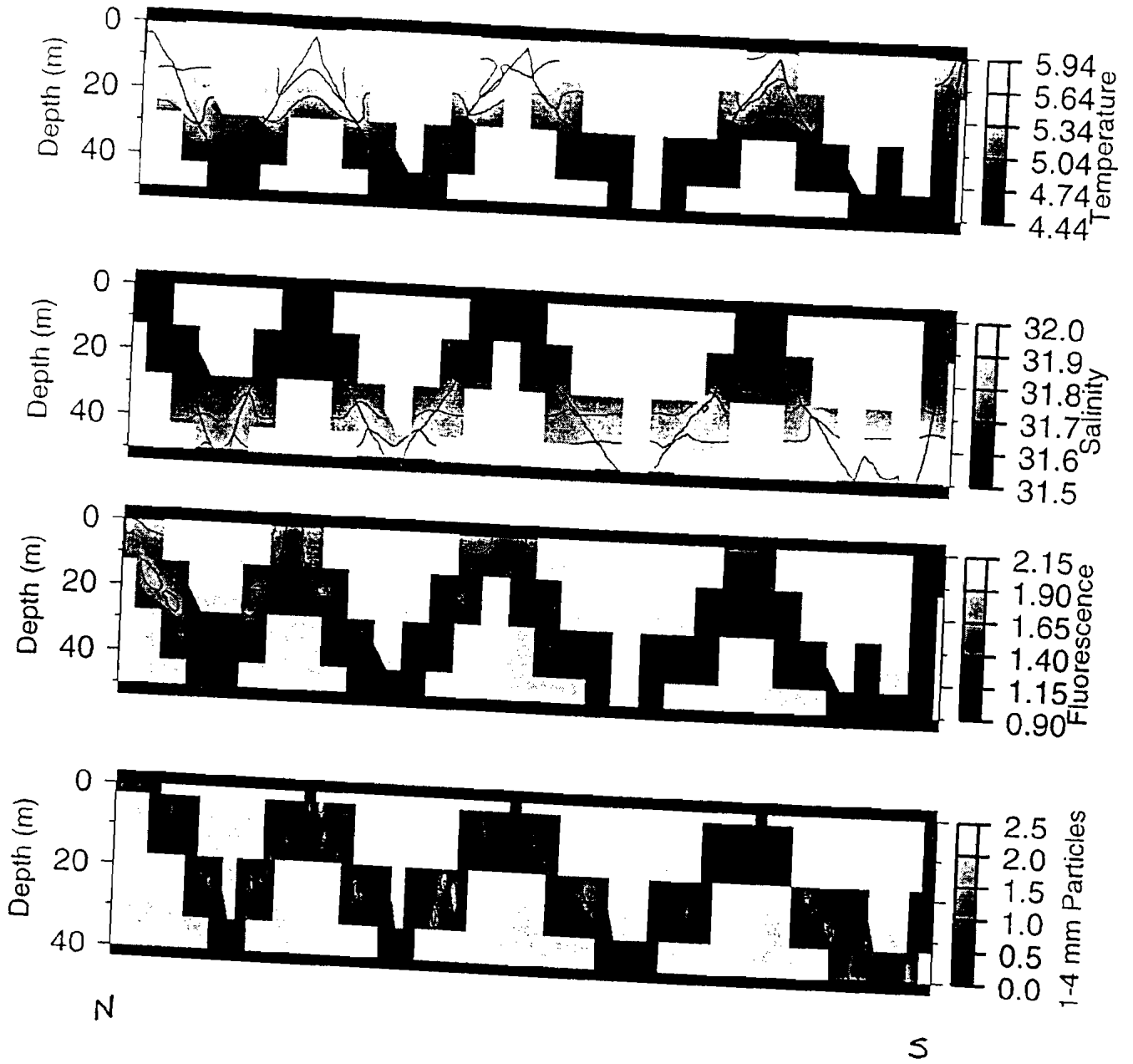


FIG. 20(b)

May 1997



DRAFT

Seasonal Variability of the Large Scale Circulation and Water Mass Variability in Prince William Sound, Alaska

S.L. Vaughan, K.E. Osgood, S.M. Gay, and L.B. Tuttle
Prince William Sound Science Center

Introduction

Prince William Sound (PWS), Alaska is a shallow, estuarine, subarctic sea, surrounded by mountains, numerous fjords, and coastal rivers (e.g. Muench and Schmidt, 1975). The central basin is roughly 350 m deep. A deep basin in the northwest Sound (the 'black hole') reaches depths of 730m. The main connections between the Sound and the northern Gulf of Alaska (GOA) are Hinchinbrook Entrance and Montague Strait. The flow is generally thought to be inward at Hinchinbrook Entrance and outward at Montague Strait (Niebauer, Royer and Weingartner, 1994; Royer, Hansen and Pashinski, 1979), but seasonal changes in wind forcing and precipitation produce departures from this general pattern. Instantaneous current velocities are dominated by tides.

Meteorological conditions in PWS are dominated by the strength and location of the Aleutian Low and the Siberian High (Wilson and Overland, 1986). Light westerly winds in the summer are replaced by strong easterlies in the winter, which produces downwelling along the north Gulf coast and inflow into PWS. Fresh water input, a combination of precipitation and snow melt/river runoff, reaches a maximum in fall and a minimum in spring (e.g. Royer, Hansen, and Pashinski, 1979).

Mid-depth temperature minima and maxima occur as a result of seasonal surface warming and cooling (Muench and Schmidt, 1975). Density is primarily determined by salinity. The coldest, saltiest, and most homogeneous water occurs in March. The warmest, freshest, and most stratified water occurs in September (e.g. Muench and Schmidt, 1975).

Niebauer et al (1994) presented hydrographic and current velocity data from the late 1970s and 1989. They calculated transports into and out of the Sound from current meter moorings deployed in Hinchinbrook Entrance and Montague Strait from November 1977 to February 1979. The total vertically integrated transport was inward at Hinchinbrook Entrance, and outward at Montague Strait in all months, with most of the transport occurring in winter. Based on these transport calculations, they estimated that roughly 40% of PWS was flushed during the summer months. From October to April, they estimated that the Sound was flushed at least twice.

PWS is a region of high biological production, and supports a large Alaskan salmon fishery. Oil tankers transverse this region regularly and pose a finite risk in the event of a spill, yet little is known about the seasonal and interannual changes in the circulation. In 1993, the Exxon-Valdez Oil Spill (EVOS) Trust Council funded a comprehensive, multidisciplinary ecosystem study called the Sound Ecosystem Assessment (SEA). A main goal of the physical oceanographic part of the SEA program was to identify the physical processes that influence the production of two commercially harvested species, pink salmon and Pa-

cific herring. The initial task was to document the seasonal dominant circulations patterns and water mass properties in PWS.

Data

Large scale hydrographic cruises were conducted in PWS in 1994 - 1997. Cruise dates are shown below.

1994	1995	1996	1997
	March 15-23		
	April 10-17	April 15-21	
	May 4-11	May 2-11	May 7-13
June 1-7, 10-18, 23-30	June 15-20	June 15-21	
July 6-12, 15-20			
September 20-29	Sept. 29-Oct. 3	Sept. 10-16	
		Dec. 5-11	

Station locations and transects for each cruise are shown in Figure 1. Measurements of temperature (T), salinity (S), oxygen, and current velocities were made with simultaneous measurements of fluorescence and zooplankton abundance. The hydrographic data was collected using a SeaBird 911 CTD. Conductivity, temperature, and oxygen as a function of pressure were recorded at 1 dbar intervals. Salinity was calculated from conductivity using standard SeaBird software. The CTD sensors were calibrated annually by SeaBird Electronics. The CTD salinities and oxygens were not calibrated with bottle samples because of minimal annual sensor drift rate. In December 1996 and May 1997, expendable CTDs (XCTDs) were used when conditions were too rough to use the CTD.

Instantaneous current velocity transects were collected using an RDI 150 kHz broadband acoustic Doppler current profiler (ADCP) deployed from the stern of the ship in a towed body. Most transects were in water less than 400 m depth so that bottom tracking was available. The bin length was 8 m for most of the data. The ADCP generally measured flows from about 20 m depth to the bottom.

To calculate a coarse approximation of the mean flow without the tidal component, repeat ADCP transects were made during periods of maximum flood and maximum ebb tide at critical transport regions in Hinchinbrook Entrance, Montague Strait, and Knight Island Passage in April, June, September, and December 1996 (see Figure 1). The tidal component was assumed to be barotropic and approximately equal during flood and ebb tides. Mean velocities were calculated by averaging over both tide stages. Vertical sections of along-channel and cross channel velocities were created for each cruise.

In addition to the large scale hydrographic cruises, an upward looking ADCP mooring (RDI 150 kHz broadband) was deployed in Hinchinbrook Entrance from June 1995 to October 1995, and from September 1996 to May 1997 (Figure 1). Velocities were recorded from a depth of about 300m to within roughly 50m of the surface using an 8 m bin length. The sampling interval was 30 minutes in 1995, and 2 hours in 1996-97.

Meteorological data from C-MAN stations in PWS is available from the National Data Buoy Center (NDBC). The stations are located at Bligh Reef, Potato Point, Seal Rocks,

and Mid-Sound buoy (in the central Sound). Wind speed, wind direction, wave height, barometric pressure, air temperature, water temperature, dew point temperature, and visibility are measured every 30 minutes. The buoys became operational in May 1995, and have collected mostly uninterrupted data since then. Meteorological data prior to 1995 is available from a station on Middleton Island, south of PWS. Upwelling indices were obtained from the NOAA Pacific Fisheries Environmental Group (PFEG) web page.

Oceanographic Cruises

March 1995

A T/S diagram with 4 stations in PWS and the GOA is shown in Figure 2. Station SEA32 is in southern Montague Strait, SEA22 is in the 'black hole' in the northwest Sound, CFOS13 is in the central Sound, and GOA3 (and other GOA stations) is located south of PWS on the GOA shelf. The surface temperatures are colder and fresher than those at depth. The densest water is in the central Sound (CFOS13) and in the 'black hole' (SEA22), with a density of 26.1. The deep water at CFOS13 and SEA22 has similar properties. The Montague Strait water (SEA32) is intermediate T/S properties, which may indicate it resulted from mixing of central and northwest Sound water. The GOA water is more homogeneous than the PWS water, and is slightly colder and fresher along isopycnals. Freshening of the very upper layers is apparent at SEA32. The GOA water is unlike any of the other types. The temperature minimum layer has not yet formed, but it is the surface water around $\sigma_\theta = 25.0$ that will become the temperature minimum.

Dynamic heights calculated from 0 to 100 m is shown in Figure 3. The station locations are shown as dots. Very weak geostrophic flow is indicated.

April 1994, 1995, and 1996

By April in all 3 years, the temperature minimum layer has started to form as a result of warming and freshening of the surface waters. An example is shown from April 1996 in Figure 4. The density of the coldest water is between 25.0 and 25.2. In all 3 years the water deeper than the temperature minimum is the same at SEA22 and CFOS13. In 1995 and 1996, the water mass properties in southern Montague Strait (SEA32) is the same as well. Figure 4 shows the shelf GOA water mass properties (GOA0) are warmer and slightly saltier along the same isopycnal (warmer and fresher at the surface) except at the very bottom. In April 1995, the deep GOA water coincides with the mid-depth Sound water.

Dynamic heights (0/100m) for April 1995 and 1996 are shown in Figures 5(a) and (b). Weak anticyclonic curvature is indicated in the central Sound in April 1995. Baroclinic (20-100m) velocity vectors from April 1995 (Figure 6) also indicate a weak anticyclonic circulation. In April 1996, the dynamic heights suggest a weak anticyclonic circulation at Hinchinbrook Entrance (Figure 5(b)). The vertical section of along-channel velocity, calculated from the repeat ADCP transects, from Hinchinbrook Entrance in April 1996 also indicate an anticyclonic circulation above about 150m (Figure 7(a) along channel). The flow pattern is also spatially variable at Montague Strait during April 1996 (Figure 7(b), with mostly inflow except for a small region of surface outflow in the west.

Neither the dynamic heights or the repeat ADCP sections show strong inflow at Hinchinbrook Entrance in April. The T/S plots show that the Sound has fairly uniform water mass properties throughout, even in the most remote northwest region. It is likely that the surface warming and freshening observed in April is due to sensible heating and precipitation rather than GOA intrusions.

May 1994-1997

Surface warming and freshening continues at all stations in all years (Figures 8(a)-(d)). The deepest water at SEA22 remained at a density of roughly 26.1 (the cast in May 1997 may not have reached the bottom). At CFOS13 in the central Sound, the density of the deepest water decreased primarily due to freshening. In all years except 1994 (no data available), the upper layer water mass properties at SEA32 resemble those at GOA0 more closely than those in PWS (CFOS13 and SEA22). Water mass properties in May 1997 are shown more clearly in Figures 9(a) and (b). Stations HE12 and SEA32 resemble GOA water at the surface and PWS water at depth (Figure 9(a)). Stations in the southern Sound (CS12) and in Montague Strait (MS8 and MS5A) exhibit PWS (CFOS13) properties at all depths (Figure 9(b)).

Repeat ADCP velocity transects in May 1997 at Hinchinbrook Entrance show northward velocities above about 50m and southward velocities below (Figure 10(a)). Meteorological data from Seal Rocks buoy shows a strong easterly wind burst (in excess of 15m/s occurred on May 10-13, 1997, which probably forced an inflow in the surface Ekman layer. The theoretical Ekman depth for latitude 60° and a wind speed of 15m/s is 69m. Repeat transects from Montague Strait (Figure 10(b)) do not show a surface inflow, but these transects were performed at the beginning of the wind burst. Repeat ADCP velocity transects from May 1995 are shown in Figure 10(c). A subsurface anticyclonic structure, similar to that in April 1996, was present.

Dynamic height contours for May 1995, 1996, and 1997 are shown in Figures 11(a)-(c). A weak anticyclonic circulation is suggested in the central Sound in 1995 and a weak cyclonic circulation is suggested in 1996. A strong inflow at Hinchinbrook Entrance is suggested in 1997 (Figure 11(c)), with cyclonic curvature around Montague Island and outflow in Montague Strait. None of these features are verified by the baroclinic velocity vectors (not shown). It may be that geostrophic balance is not a good assumption in May, or that the density gradients are too weak or too recently formed to set up a geostrophic flow.

June and July 1994, June 1995 and 1996

T/S diagrams from June 1994, July 1994, June 1995, and June 1996 are shown in Figures 12(a)-(d). By June, the temperature minimum layer is well defined at all PWS station. The isopycnal where the minimum occurs varies from 25.0 in 1994 (Figures 12(a) and (b)), to 25.2 in 1995 and 1996. The density of the bottom water in the 'black hole' (SEA22) is still about 26.1, with the CFOS13 bottom water density slightly less (26.0). The difference between PWS and GOA water mass properties is more pronounced than in previous months. In 1994 and 1995, the GOA water is both warmer and saltier along isopycnals, except at the very near surface. Properties at SEA32 more closely resemble PWS properties than GOA. In June 1996, the water mass properties at SEA32 and GOA0

are similar to each other, and to the other PWS stations.

Comparison of Figures 12(a), (c) and (d) show that in June 1996 it was the PWS water above the temperature minimum layer that became warmer and saltier, rather than a change in the GOA water mass that resulted in the similarity. In June 1996, the temperature minimum layer T/S signature is sharper, and the overlying PWS water mass properties are between the 1995 PWS properties and the 1996 GOA. Intrusion and mixing of GOA water into PWS probably occurred in June 1996.

Dynamic height contours from June 1996 also show evidence of inflow from the GOA at Hinchinbrook Entrance, and a basin scale cyclonic circulation (Figure 13(a)). Some agreement between the dynamic heights and the baroclinic velocity vectors (Figure 13(b)) can be seen in the central and northwest Sound, and at Hinchinbrook Entrance. Dynamic heights in June 1995 indicate very weak flow (Figure 13 (c)), which is not verified by observed baroclinic velocities.

September 1994, 1995 and 1996

T/S diagrams for September 1994, 1995 and 1996 are shown in Figures 14(a)-(c). By September of all years, the temperature minimum layer, while still detectable, has become much less pronounced. The surface waters are the warmest and freshest in September. The density of the deepest water at CFOS13 and SEA22 is still roughly 26.0-26.1. In 1995 and 1996, the PWS stations (CFOS13, SEA22, and SEA32) have similar water mass properties, which differ from the shelf GOA. In 1994, stations CFOS13 and SEA22 are similar and differ from the GOA, but the water mass properties of station SEA32 are inbetween.

Dynamic height contours from September of each year show cyclonic circulation in the central Sound (Figures 15(a)-(c)). Outflow at Montague Strait is indicated in September 1994 and 1995. Baroclinic velocity vectors from 1994, 1995 and 1996 (Figures 16(a)-(c)) also indicate cyclonic circulation in the central Sound. The baroclinic velocities show some outflow at Montague Strait in 1994 (Figure 16(a)), and inflow in 1996 (Figure 16(c)). Repeat ADCP velocity sections also show inflow at Montague Strait at the surface (Figure 17). The transects coincided with an easterly wind burst on September 15-16, 1996, which may have pushed water in the surface Ekman layer into the Sound.

December 1996

The T/S diagram for December 1996 shows a temperature maximum layer at a density of roughly 24.8 (Figure 18). The density of the bottom water is slightly less than in March 1995, and throughout the entire observation period. Stations SEA22 and CFOS13 no longer closely resemble each other as they did in September. CFOS13 is warmer and fresher along isopycnals, and SEA22 is fresher at the surface by ~ 0.5 . The water mass properties at SEA32 more closely resemble CFOS13.

Dynamic height contours from December 1996 show a cyclonic curvature around the central Sound basin, and outflow Montague Strait (Figure 19(a)). The baroclinic velocity vectors confirm this general circulation (Figure 19(b)). Repeat ADCP velocity sections show inflow at Hinchinbrook Entrance above about 150m, and outflow below ((Figure 20).

ADCP Mooring Velocity Time Series

Time series of north-south (v-component) velocities at Hinchinbrook Entrance, 40 hour low-pass filtered, for the summer 1995 deployment are shown in Figure 21(a). The flow was generally out of the Sound (southward) above about 150m. and inward (northward) below. This pattern was interrupted by high velocity bursts of inflow at the surface. Inspection of wind speed and direction time series show that these inflow bursts are correlated with easterly wind speed bursts, as indicated by the arrows at the top of the figure. An example from September (the last 2 bursts) is shown in Figure 21(b). For a wind speed of 20m/s (the second event in Figure 21(b)), the theoretical Ekman depth is 90m, in agreement with the observed inflow depth. Associated with the upper layer inflow bursts are periods of outflow in the deeper layers. The upper bin depth is about 44m. and even when the inward surface burst is not visible, the deeper outflow is (arrows in July).

The 40 hour low-pass filtered velocity time series from the 1996-1997 deployment are shown in Figures 22(a) and (b). From September 1996 to the end of December the summer inflow/outflow pattern was reversed with inflow generally above 150m and outflow below. The transition depth increased as the season progressed. The bursts of inflow at the surface, corresponding to strong easterly wind events, is apparent until January. From roughly January to May 1997 the velocity was nearly barotropic. After mid-February, the flow was mostly inward except for periods in early April and in early May.

Volume transports were calculated using mean monthly velocities, for the portion of the water column above and below 150m. The channel width, measured at its greatest constriction between the 50 fathom depth contours, was approximately 10 km. The mooring was actually located about 5km north of this point. The width at the actual mooring location was not used because of the broad shelf regions on either side. The total depth at the mooring location was 280m. The area above 150m used in the calculation was then $1.5 \times 10^6 m^2$, and the area below 150m used was $1.3 \times 10^6 m^2$.

It was assumed that (1) there was no horizontal variability, (2) that the ADCP mooring velocities were representative of velocities farther south, and (3) the the velocities from 50m depth to the surface (in the ADCP shadow zone) did not change the mean significantly. The assumption of no horizontal variability was shown by the repeat ADCP sections to be valid in most seasons. but invalid in April for example. Comparison of the repeat ADCP velocities from the cruises with the moored velocities showed that the second assumption is fairly good. Some repeat ADCP sections show increased velocities near the surface, which were not captured by the mooring. The velocities from the upper 50m layer were assumed to be equal to the mean.

Transports during the 1995 and 1996-1997 deployments are shown in Figures 23(a) and (b). In summer 1995, the upper and lower layer transports roughly balanced each other. The net flow was close to zero. In fall and early winter 1996, the upper layer transport reached a maximum of 0.2 Sv (Figure 23(b)). Niebauer et al (1994) found maximums in excess of 0.3 Sv in 1978. The standard deviations of these averages was often close to 0.1 Sv. so this difference may not be significant. From January 1997 on, transports were either positive or close to zero.

To compare the 1996-1997 transports to those calculated by Niebauer et al. the 1978-1979 tranports were summed into layers above and below 150m. and plotted along with the 1995-1997 values in Figures 24(a)-(d). The maximum upper layer transport at Hinchinbrook

Entrance peaked in October and December of both 1978 and 1996, although the magnitudes in 1996 were less. The seasonal trends in transports both above and below 150m were similar.

Monthly mean upwelling indices from 60°N, 146°W for the periods 1975 - 1979 and 1993 - 1997 are shown in Figure 25. Except for 1979, mean meteorological conditions were approximately the same during both time periods. Unfortunately, the Niebauer et al mooring was retrieved before the intense downwelling event in February 1979.

Summary

Densest water is constant at $\sigma_\theta = 26.0 - 26.1$ for all seasons of all years. The density of the temperature minimum layer varies interannually from 25 to 25.2. In T/S space, the dip of the temperature minimum layer becomes more shallow as the seasons progress, from maximum in June to a minimum in December, and is non-existent in March. During most of the year, the water properties of the central Sound (CFOS13) and the northwestern Sound (SEA22) deeper than the temperature minimum layer are similar.

The water mass properties in March are the coldest and saltiest of all the seasons observed, and the most spatially uniform. In April, the surface waters start to warm and freshen, probably due to heating and precipitation rather than GOA inflow, so that a temperature minimum layer is formed. An anticyclonic baroclinic eddy present in the central Sound in April 1995 is not present in April 1996. Inflow and outflow at Hinchinbrook Entrance and Montague Strait have both horizontal and vertical shears.

By May the deepest water in the central Sound has freshened compared to April. The deepest water in the 'black hole' remains unchanged. In May 1997, the water at both Montague Strait and Hinchinbrook Entrance resembled the GOA water at the surface and PWS water at depth. T/S plots for stations throughout Montague Strait show that the exchange took place at southern Montague Strait and Hinchinbrook Entrance, rather than in through Hinchinbrook, around Montague Island, and out through Montague Strait. An easterly wind burst occurred during this time that may have pushed water in the surface Ekman layer into the Sound.

Some intrusion from the GOA into PWS through both Montague Strait and Hinchinbrook Entrance is indicated in June 1996. Water mass properties between the shelf GOA water and PWS are separate in summer 1994 and 1995, and in September of all years. A closed basin scale cyclonic circulation was present in the central Sound in September 1994, 1995, and 1996. Dynamic heights from Niebauer et al (1994) also indicated a cyclonic circulation was present in September 1978. September of all years exhibited the warmest and freshest surface waters.

In December, in addition to the temperature maximum layer formation, warming and freshening penetrated down to the bottom water at both CFOS13 and SEA22. The central Sound and northwestern Sound deep water mass properties were much less similar in December. Whether this was due to vertical exchange or GOA influence is unclear. A basin scale cyclonic circulation was observed, with outflow at Montague Strait.

Geostrophic balance may be a good assumption during seasons when the density gradients are strongest. The Rossby number $\epsilon = U/fL$ for velocity $U \sim 25\text{cm/s}$, Coriolis parameter $f = 1.26 \times 10^{-4}\text{s}^{-1}$, and length scale $L \sim 20\text{km}$ is $O(0.1)$. While other process

certainly effect the circulation, the influence from the geostrophic component should be fairly large.

Conclusions

No indication of intrusion of GOA water into the central Sound was found in April or May. Intrusion was indicated in June 1996, but not in June 1994 or 1995. In September, the Sound seems to be sealed off from the GOA entirely. The dominant circulation feature in September is the cyclonic gyre in the central Sound. In December, several processes seem to be acting simultaneously. Identifying these processes will require further investigation.

The T/S plots indicate 4 water masses are present in PWS. The bottom water with $\sigma_\theta \sim 26.0 - 26.1$, is present most of the year (except maybe December) throughout the Sound with constant $T \sim 5.9^\circ\text{C}$ and $S \sim 33.0$. Deep water, defined from the density of the temperature minimum to the bottom, or $25.2 \leq \sigma_\theta \leq 26.0$, is present from March to at least September. The temperature minimum in April and May is defined by roughly $T \sim 4.0$, $S \sim 31.8$, and $\sigma_\theta \sim 25.2$. Warming and salinification along isopycnals occurs from March to December, where the layer becomes less well defined. In September, the temperature minimum is defined by $T \sim 5.0$, $S \sim 32.0$, and $\sigma_\theta \sim 25.2$. Intermediate water, resulting from upper layer warming, at roughly $24.8 \leq \sigma_\theta \leq 25.2$, starts to form in April. The upper limit of this layer (24.8) corresponds roughly to the density of the temperature maximum observed in December. The stratified upper layer water with $\sigma_\theta \leq 24.8$ changes T/S properties seasonally.

Comparisons between the transports calculated by Niebauer et al (1994) and those presented here, and the upwelling indices for both periods, suggest that conditions during the late 1970s and mid-1990s were similar. At Hinchinbrook Entrance the summer months were characterized by outflow above 150m and inflow below. The fall and early winter months were characterized by inflow above 150m and weak outflow below. Late winter and early spring months were characterized by more barotropic flows. Finally, strong easterly wind events in 1996 and 1997 caused upper layer inflow velocity bursts down to the Ekman depth. Associated with the Ekman layer inflow, were periods of outflow at deeper depths. It is not clear if the surface inflow penetrated far into the central or northern Sound, or if it was limited to just north of Hinchinbrook Entrance. Without this information, accurate flushing rates and residence times can not be calculated.

In some seasons, some aspects of the circulation and water mass properties of PWS are fairly predictable and geostrophic. Especially in the fall and winter (September through March), the dynamics of the Sound seem fairly stable. More variability exists in April, May and June. These transition months correspond to the period of highest biological activity, and even small changes may effect phytoplankton and zooplankton growth rates and distributions. The next step is to examine the effect of the seasonal and interannual variability on the biological components of the Sound.

References

- Muench, R. D. and G. M. Schmidt. 1975: Variations in the Hydrographic Structure of Prince William Sound. IMS Report R75-1. 135pp.
- Niebauer, H.J., T.C. Royer, and T.J. Weingartner. 1994: Circulation of Prince William Sound, Alaska. *J. Geophys. Res.*, **99**, C7, pp 14,113-14,126.
- Royer, T.C., D.V. Hansen, and D.J. Pashinski. 1979: Coastal Flow in the Northern Gulf of Alaska as Observed by Dynamic Topography and Satellite Tracked Drogued Drift Buoys. *J. Phys. Oceanog.*, **9**, 4, pp 785-801.
- Wilson, J.G. and J.E. Overland. 1986: Meteorology, in The Gulf of Alaska. Physical and Biological Resources. Hood, D.W. and S. T. Zimmerman, eds. Alaska Office, Ocean Assessments Div., NOAA. 655pp.

List of Figures

Figure 1 : Cruise tracks and station locations, with repeat ADCP transects highlighted and the ADCP mooring location.

Figure 2 : T/S diagram from March 1995.

Figure 3 : Dynamic heights (0/100m) from March 1995.

Figure 4 : T/S diagram from April 1996.

Figure 5 : Dynamic heights (0/100m) from (a) April 1995 and (b) April 1996.

Figure 6 : Baroclinic (20-100m) velocities from April 1995.

Figure 7 : Along channel and cross channel velocities with tides removed from April 1996 from (a) Hinchinbrook Entrance and (b) Montague Strait. Distance is from west to east.

Figure 8 : T/S diagram from (a) May 1994, (b) May 1995, (c) May 1996, and (d) May 1997.

Figure 9 : T/S diagram from May 1997 for standard stations plus stations in (a) Hinchinbrook Entrance, and (b) Montague Strait.

Figure 10 : Along channel and cross channel velocities with tides removed from (a) Hinchinbrook Entrance in May 1997, (b) Montague Strait in May 1997, and (c) Hinchinbrook Entrance in May 1995. Distance is from west to east.

Figure 11 : Dynamic heights (0/100m) from (a) May 1995, (b) May 1996, and (c) May 1997.

Figure 12 : T/S diagram from (a) June 1994, (b) July 1994, (c) June 1995, and (d) June 1996.

Figure 13 : Dynamic heights (0/100m) from (a) June 1996, (c) June 1995, and (b) baroclinic (20-100m) velocities from June 1996.

Figure 14 : T/S diagram from (a) September 1994, (b) September 1995, (c) September 1996.

Figure 15 : Dynamic heights (0/100m) from (a) September 1994, (b) September 1995, and (c) September 1996.

Figure 16 : Baroclinic (20-100m) velocities from (a) September 1994, (b) September 1995, and (c) September 1996.

Figure 17 : Along channel and cross channel velocities with tides removed from September 1996 from Montague Strait.

Figure 18 : T/S diagram from December 1996.

Figure 19 : Dynamic heights (0/100m) from (a) December 1996 and (b) baroclinic (20-100m) velocities from December 1996.

Figure 20 : Along channel and cross channel velocities with tides removed from Hinchinbrook Entrance in December 1996.

Figure 21 : (a) ADCP mooring velocities (v-component, 40 hour low-passed filter) from June to September 1995 and (b) wind speed and direction from Mid-Sound buoy in September 1995.

Figure 22 : ADCP mooring velocities (v-component, 40 hour low-passed filter) from (a) September 1996 to January 1997 and (b) January to May 1997.

Figure 23 : Upper and lower layer transports in Sv from (a) 1995 deployment and (b) 1996-1997 deployment.

Figure 24 : Comparison of transports to 1978-1979 mooring deployment from (a) 1995 above 150m, (b) 1996-97 above 150m, (c) 1995 below 150m, and (d) 1996-97 below 150m.

Figure 25 : Upwelling Index from 1975 to 1979 and from 1993 to 1997.

Oceanography Cruise - May 1997

FIG. 1

971

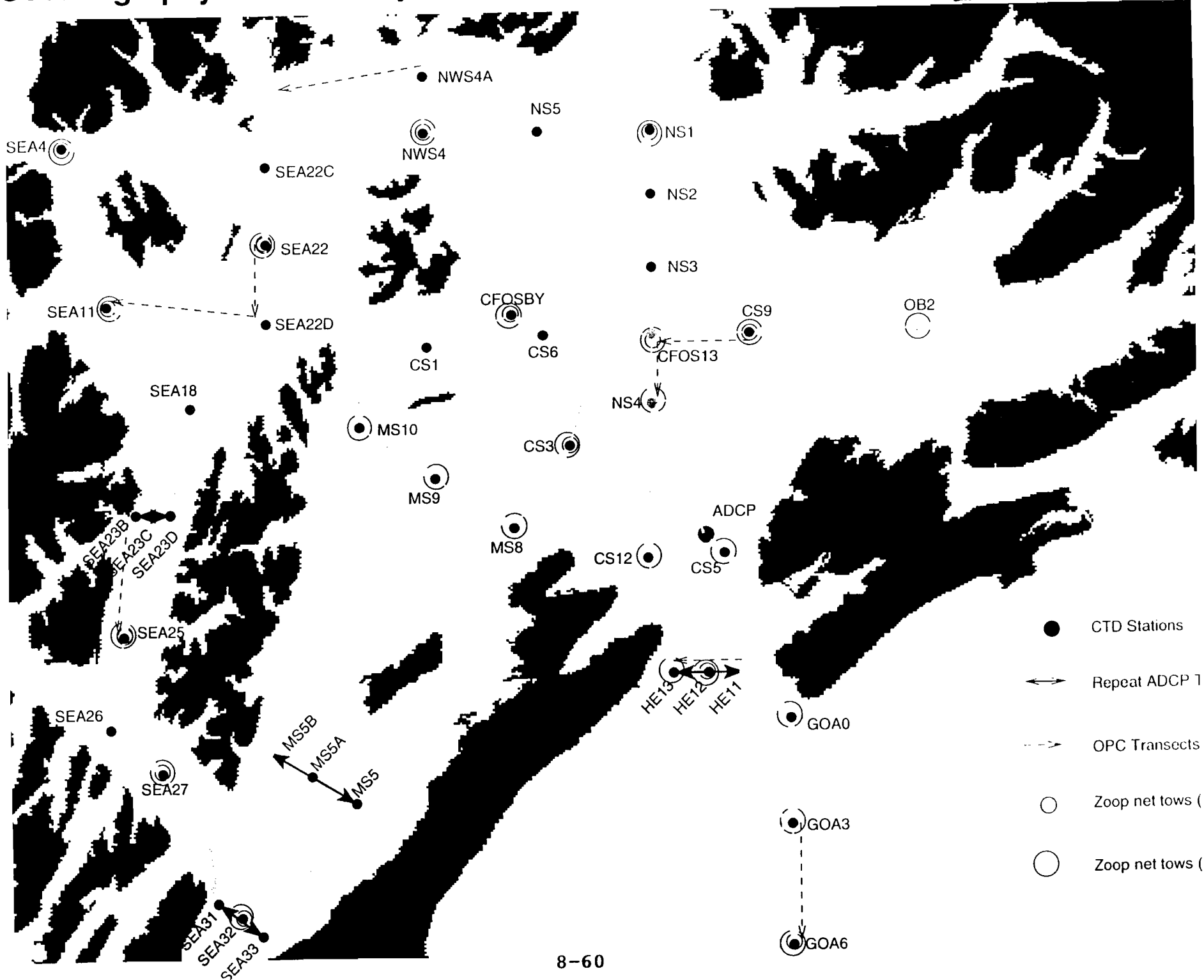


FIG 2

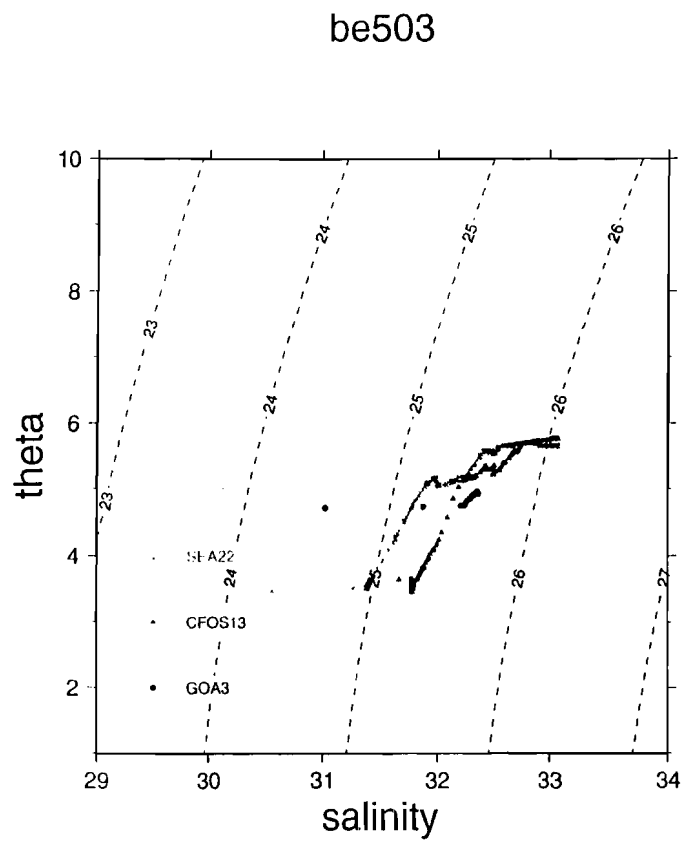


FIG 3

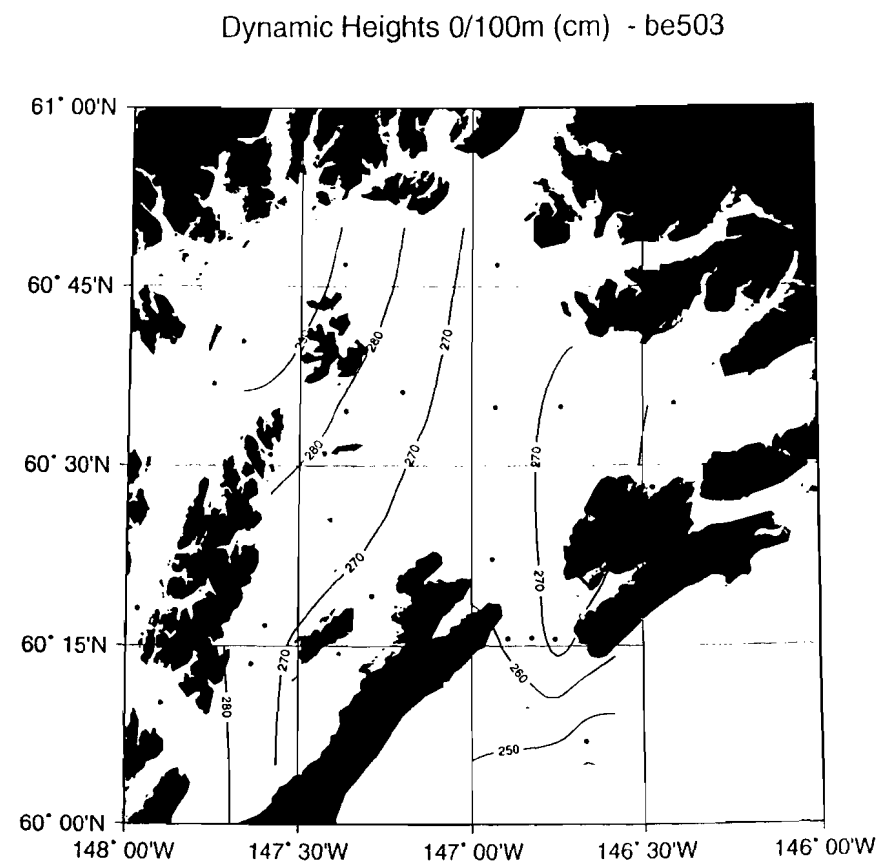


FIG 4

be604

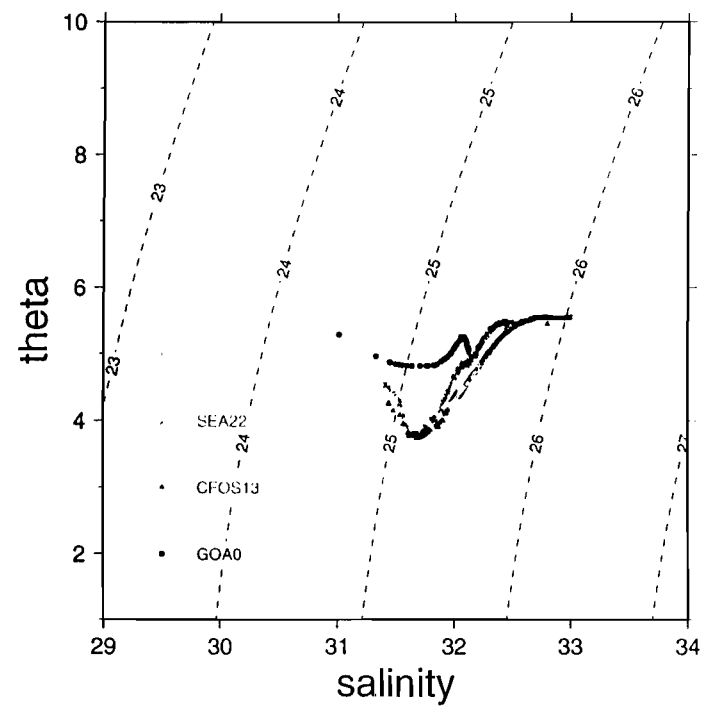


FIG 5(a)

Dynamic Heights 0/100m (cm) - be504

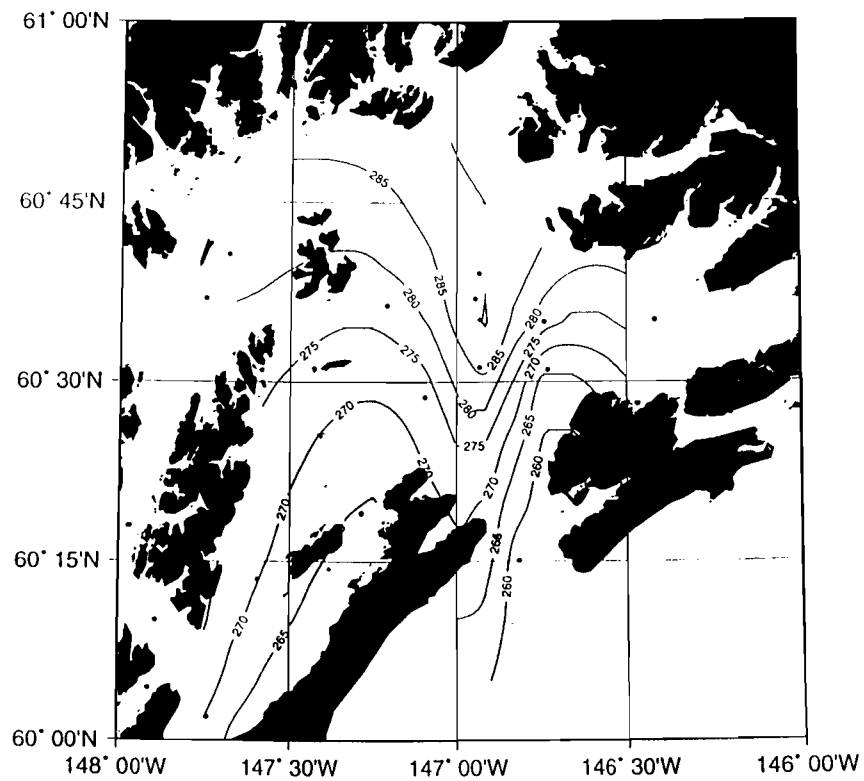


FIG 5(b)

Dynamic Heights 0/100m (cm) - be604

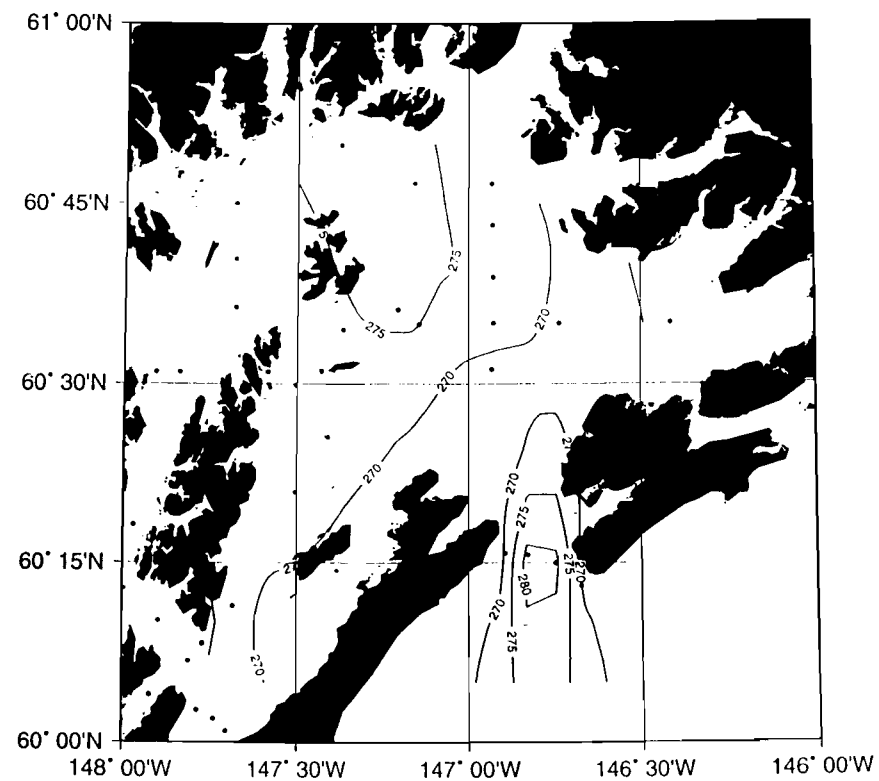


FIG 6

April 1995

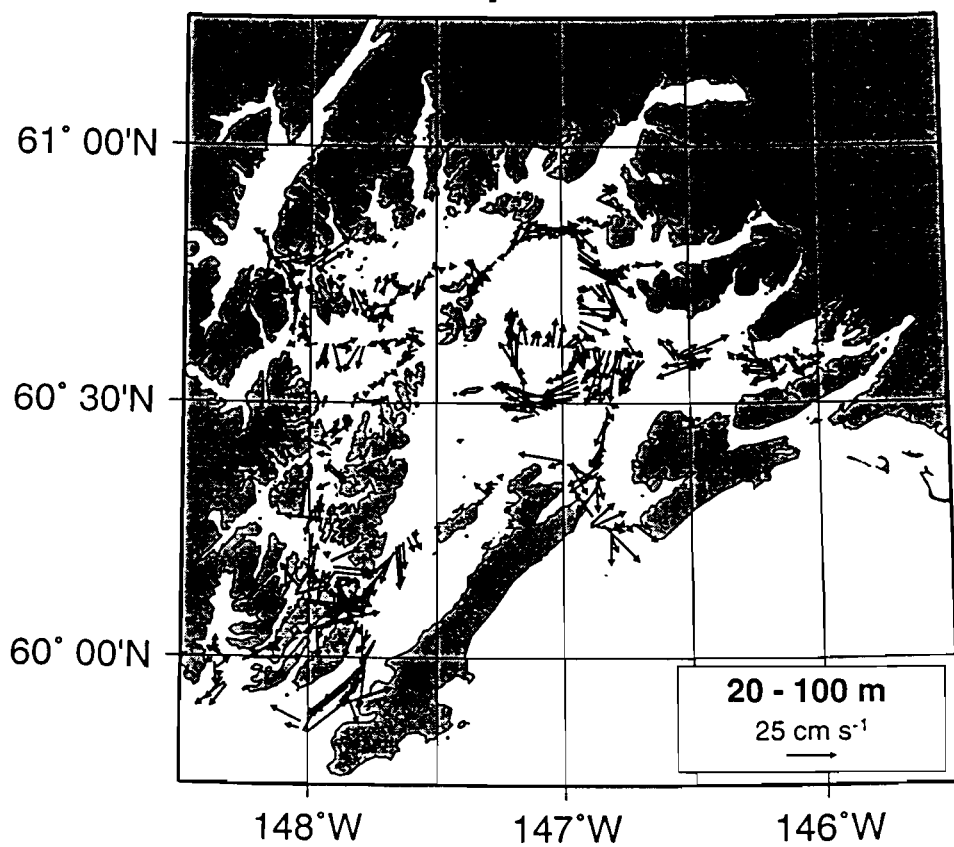
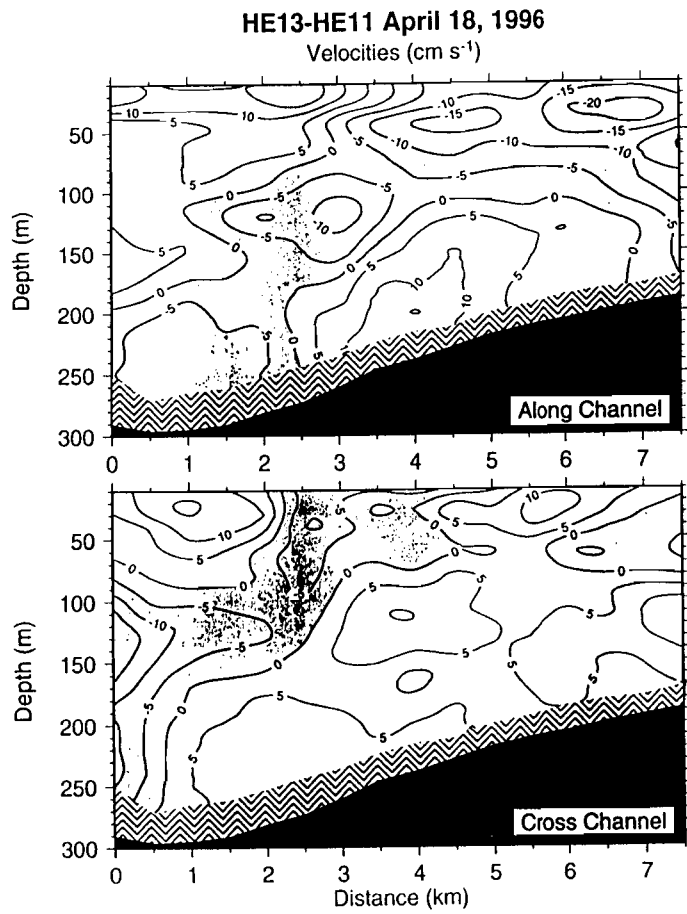
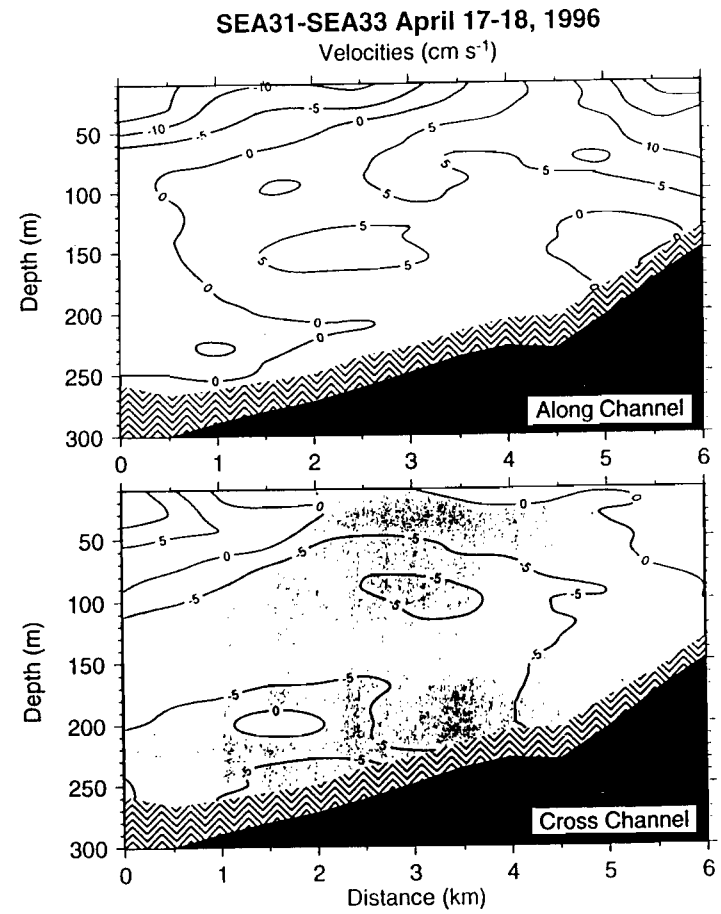


FIG 7(a)



be46044, 46, 49
(avg flood + ebb)/2

FIG 7(b)



be46037, 38, 40, 41
avg of 2 flood and 2 ebb tides

FIG 8(a)

ab405

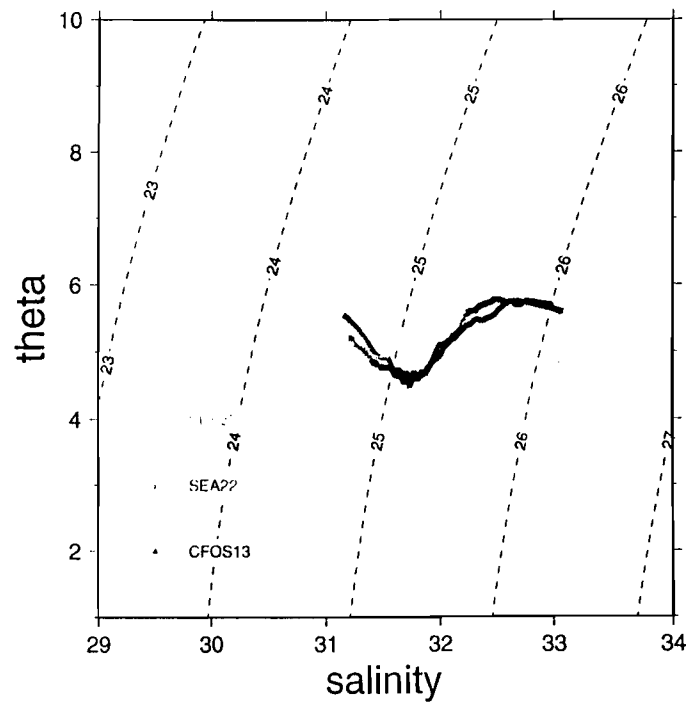


FIG 8(b)

be505

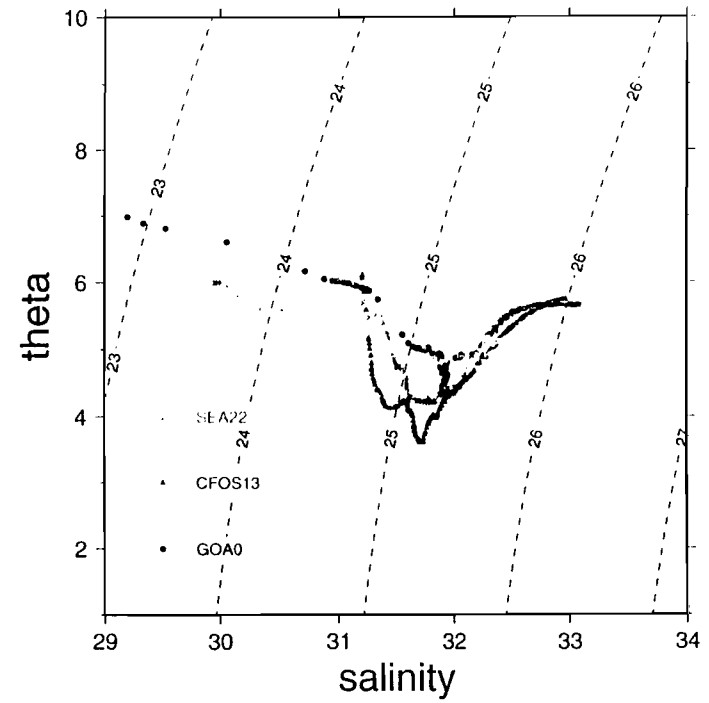


Fig 8(c)

hx605

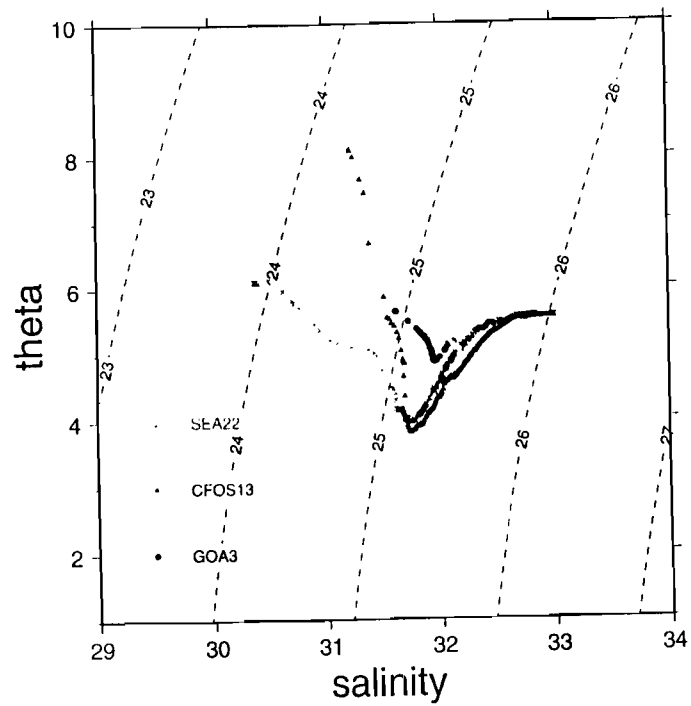


Fig 8(d)

be705

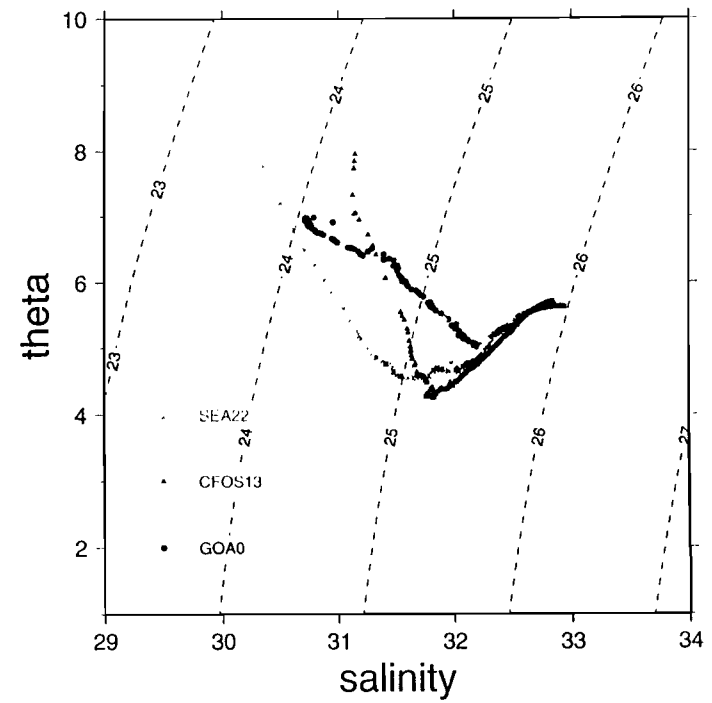


FIG9(a)

be705

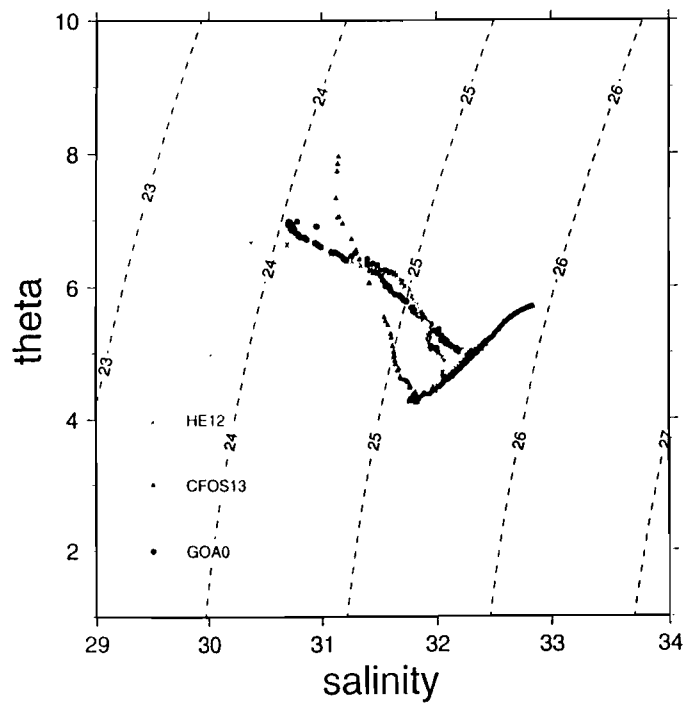


FIG9(b)

be705

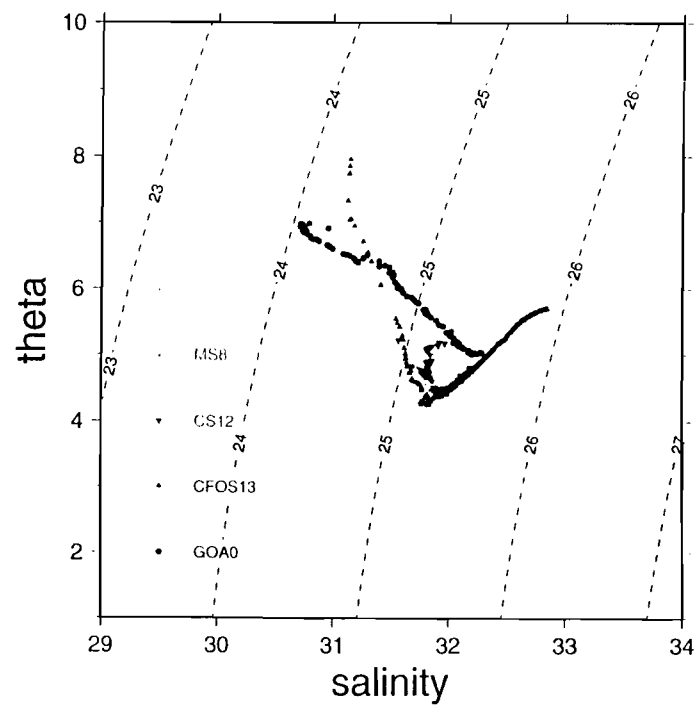
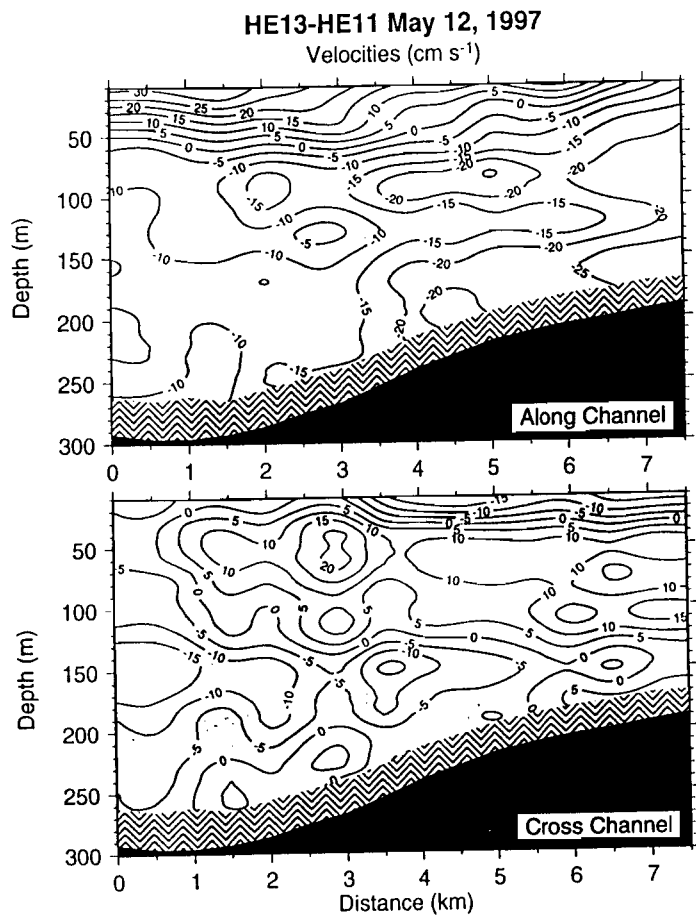
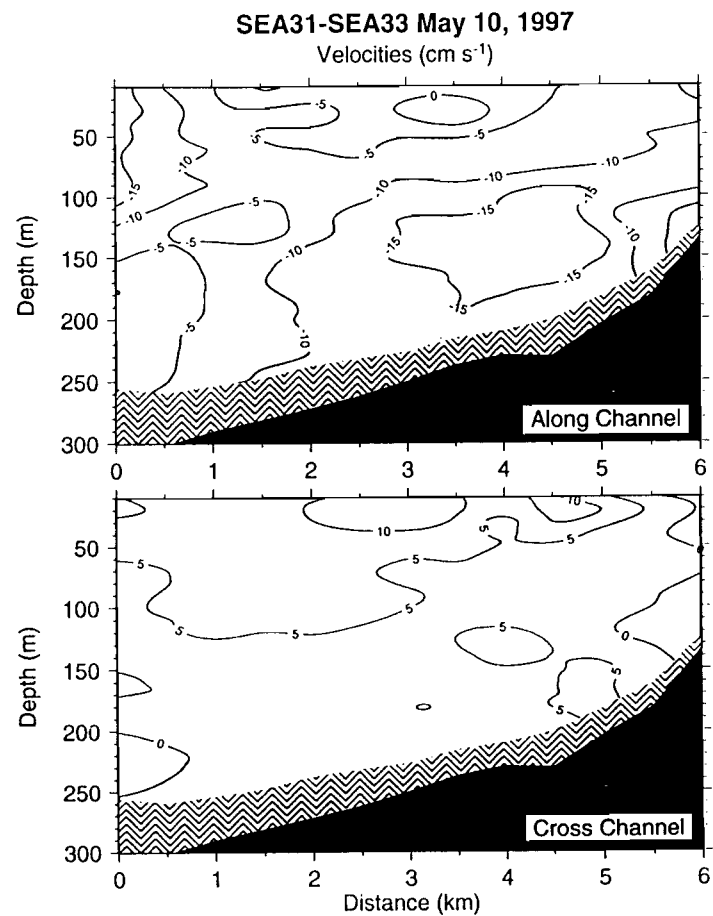


FIG 10(a)



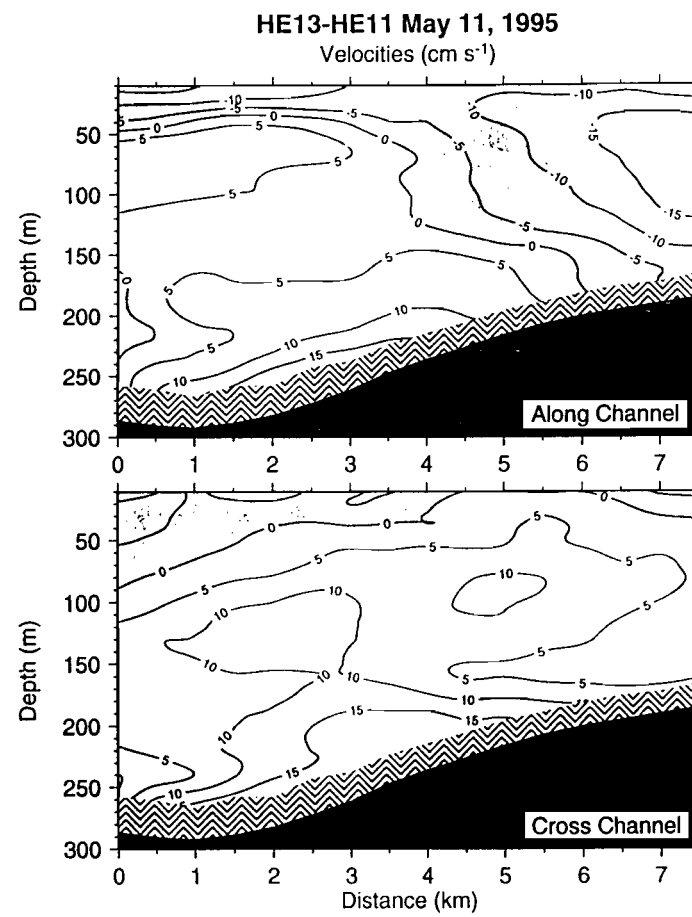
be57046, 47, 49, 50
avg of 2 flood and 2 ebb tides

FIG 10(b)



be57022, 23, 24, 25
avg of 2 flood and 2 ebb tides

FIG 10(c)



be95073a, c, d, e, g, h
avg of 3 flood and 3 ebb tides

FIG 11(a)

Dynamic Heights 0/100m (cm) - be505

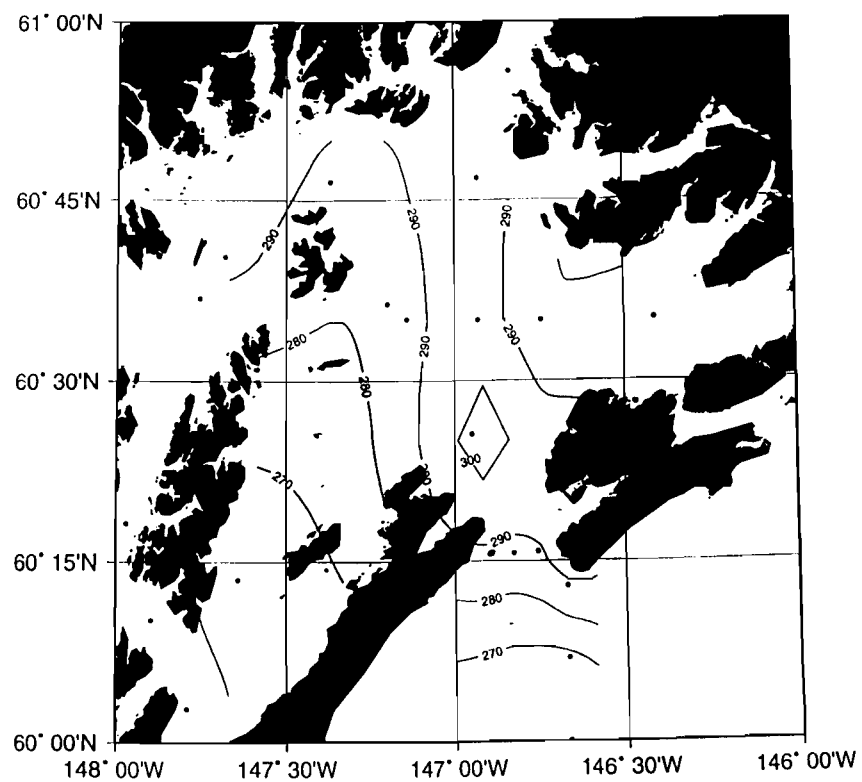


FIG 11(b)

Dynamic Heights 0/100m (cm) - hx605

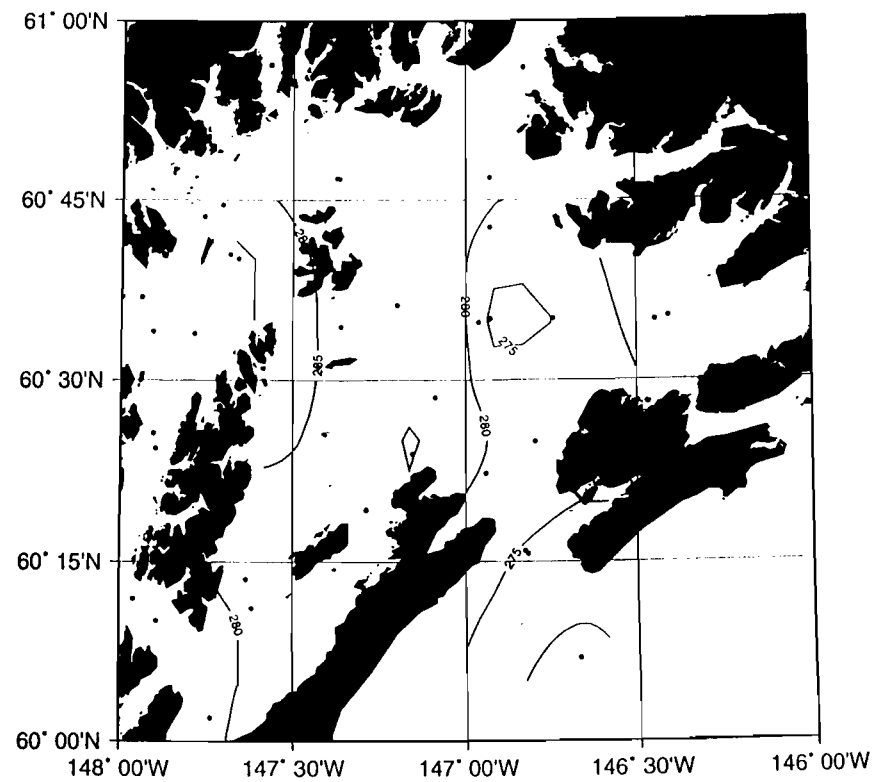


FIG. 11 (C)

Dynamic Heights 0/100m (cm) - be705

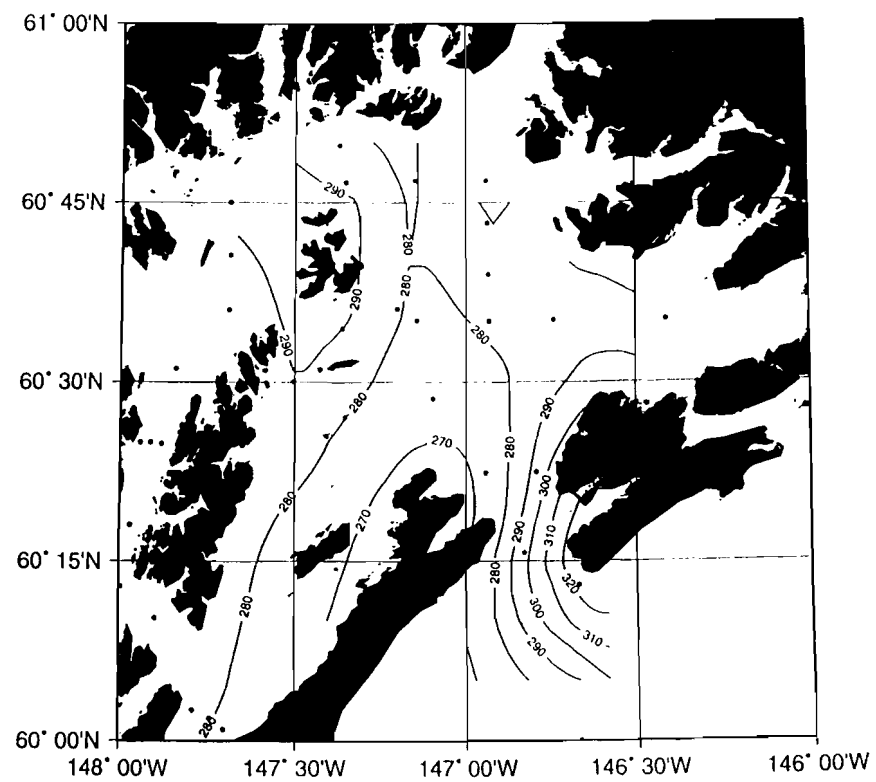


FIG 12(a)

ab406

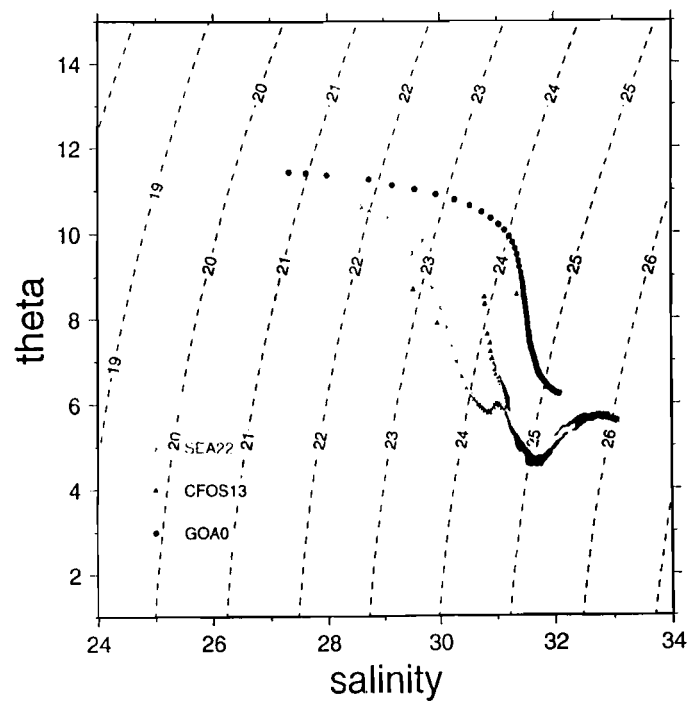


FIG 12(b)

ab407

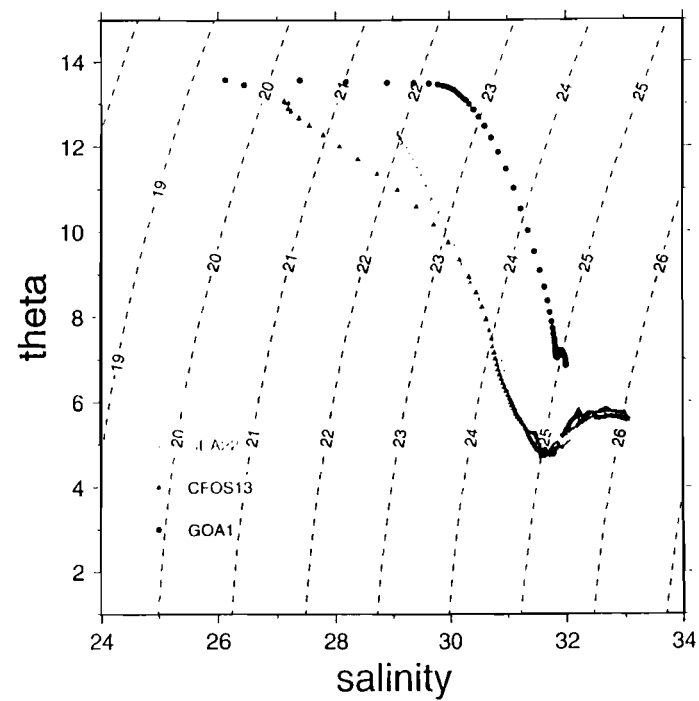


FIG 12 (c)

be506

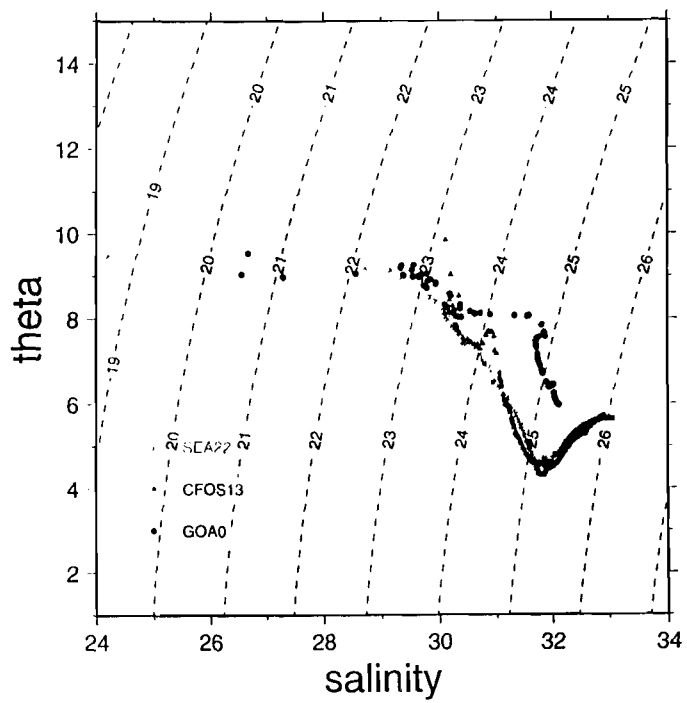


FIG 12 (d)

be606

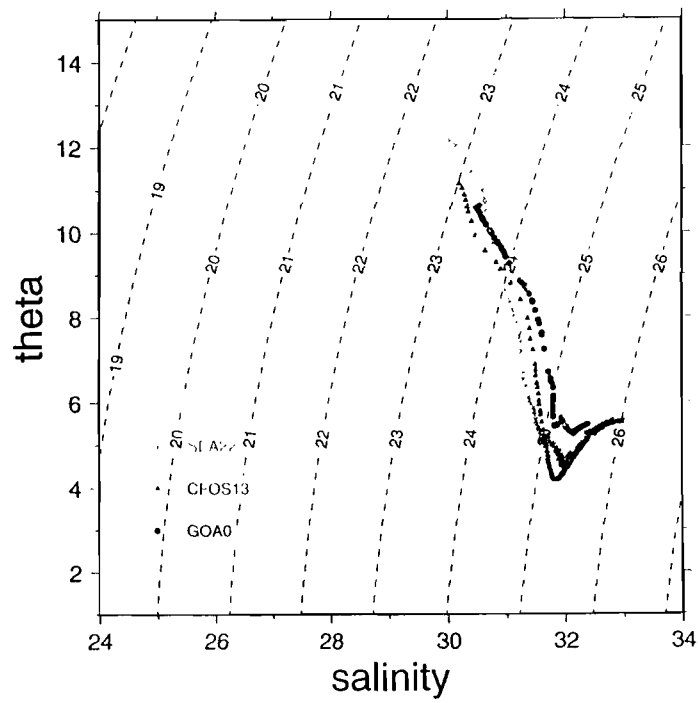


FIG. 13(a)

Dynamic Heights 0/100m (cm) - be606

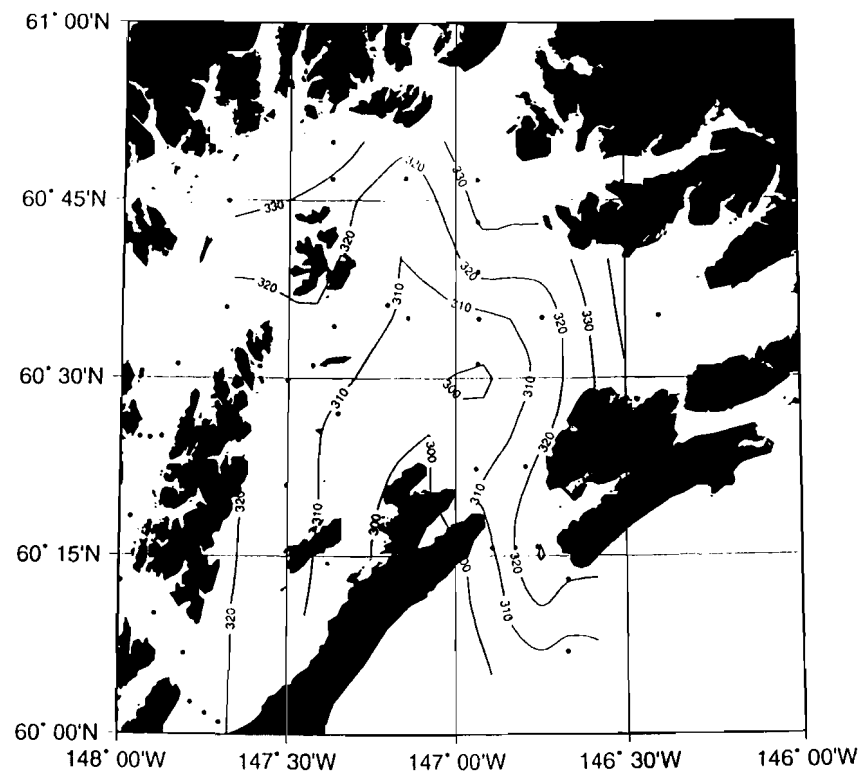


FIG. 13(c)

Dynamic Heights 0/100m (cm) - be506

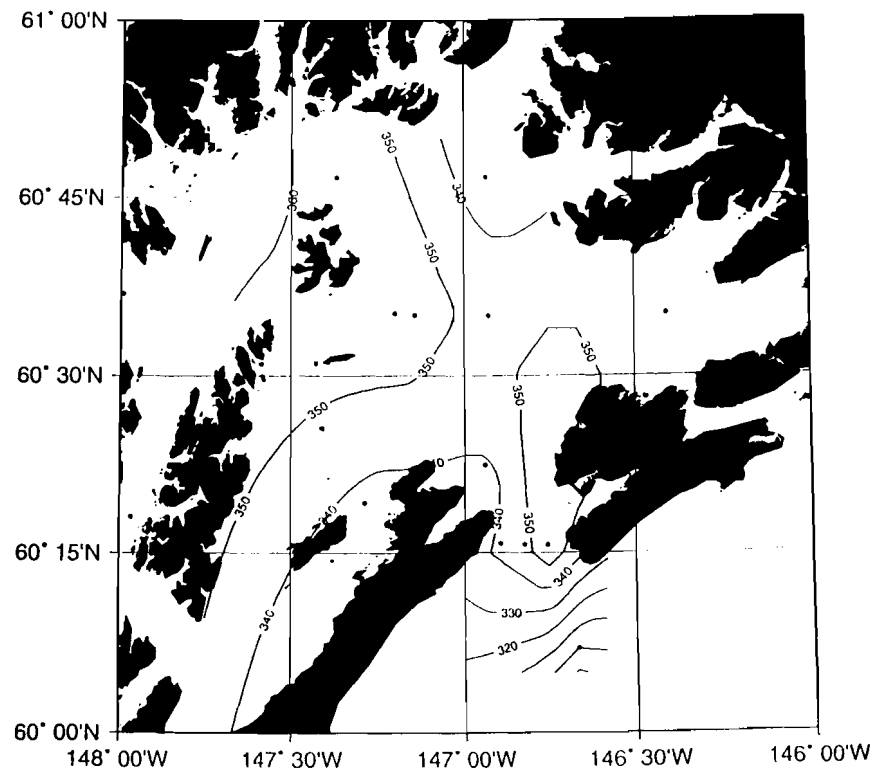


FIG. 13(b)

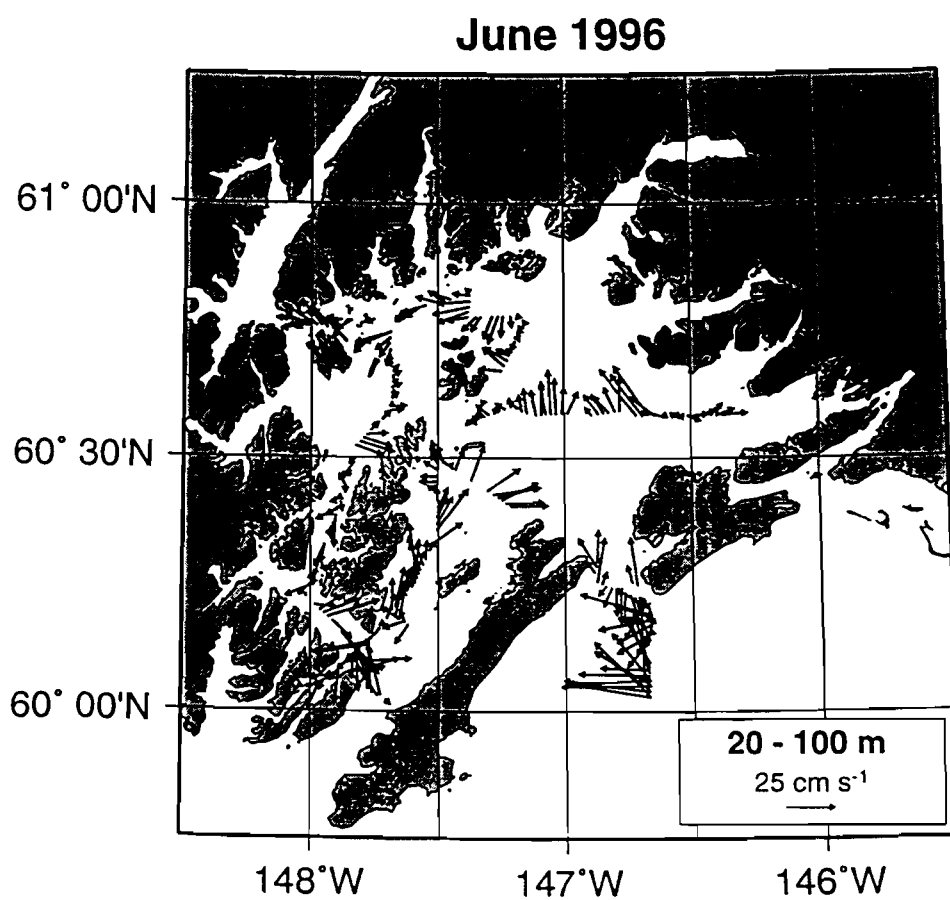


FIG. 14(a)

be409

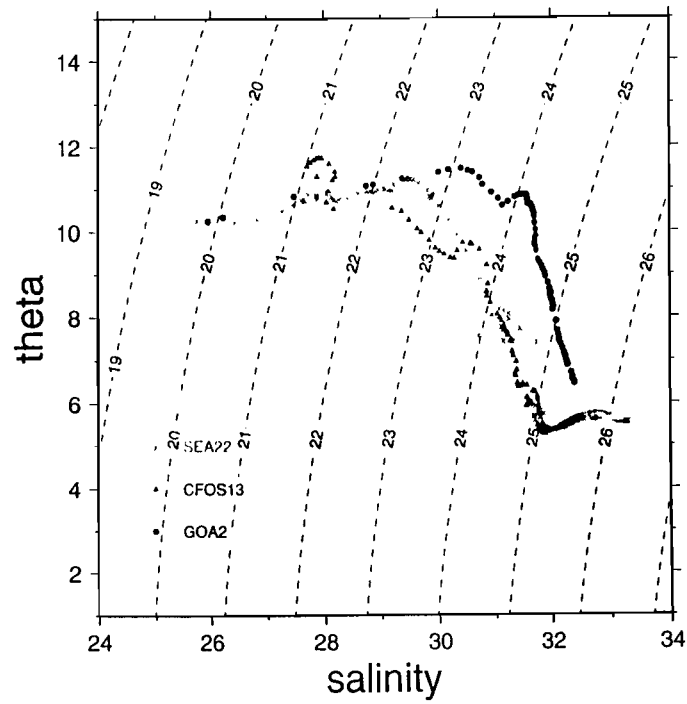


FIG. 14(b)

be509

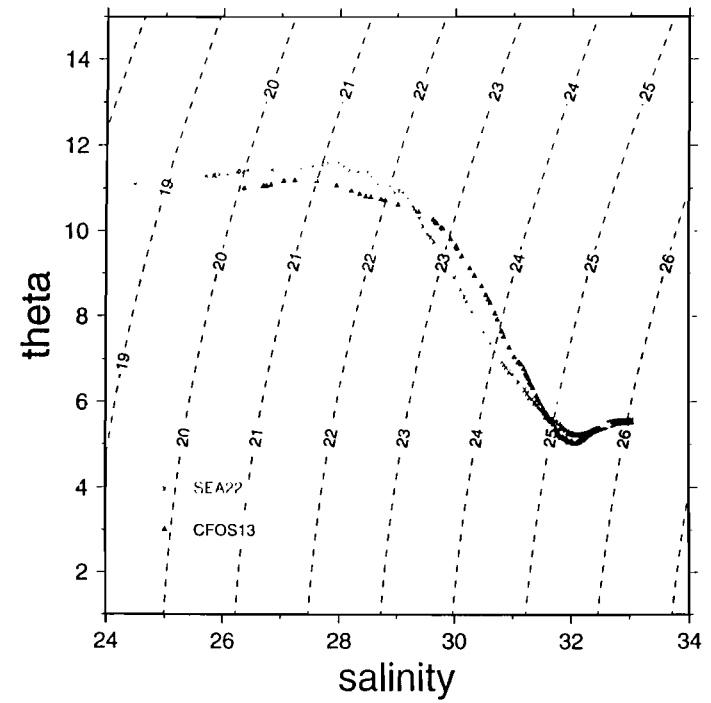


FIG. 14(c)

be609

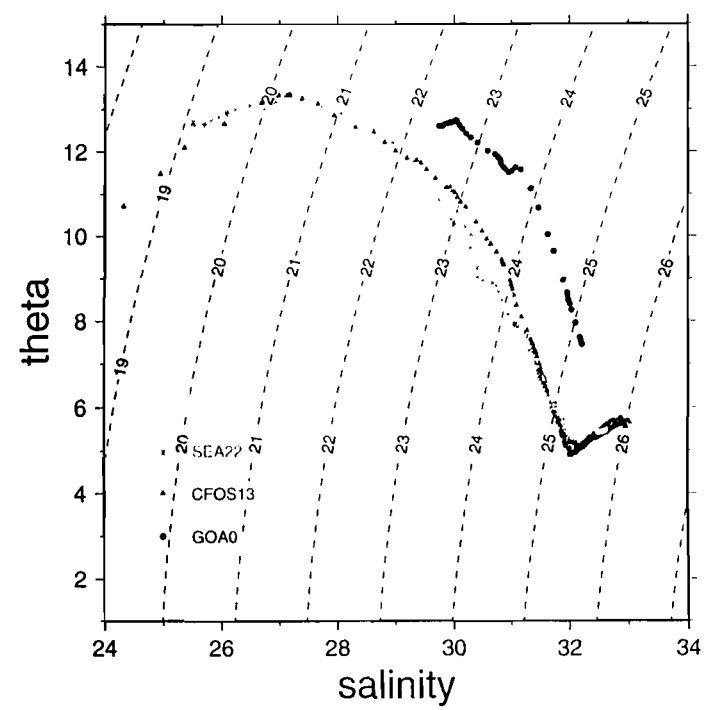


FIG. 15(a)

Dynamic Heights 0/100m (cm) - be409

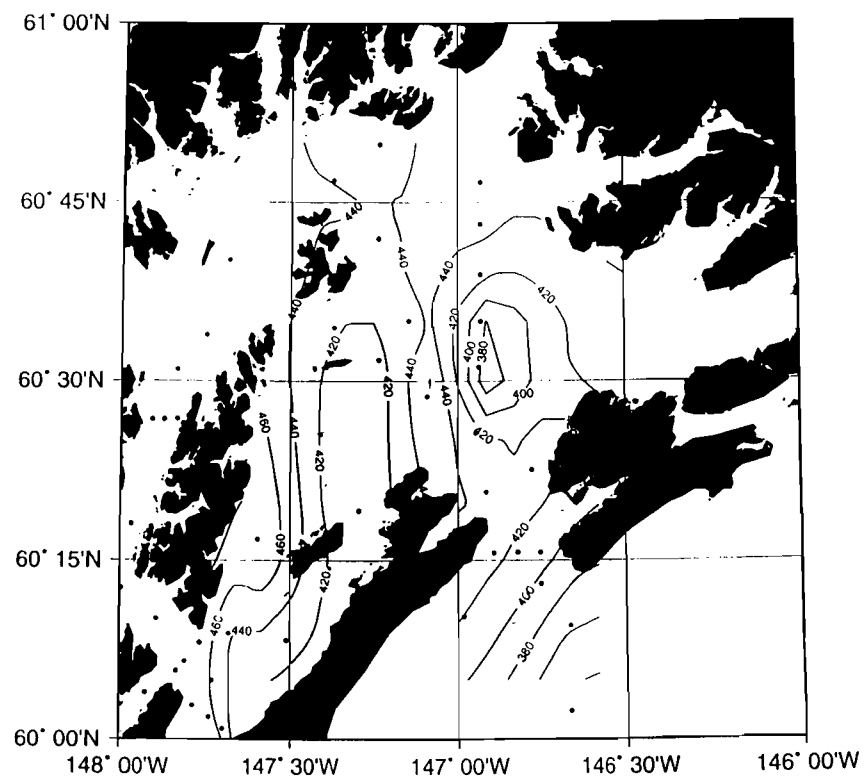


FIG. 15(b)

Dynamic Heights 0/100m (cm) - be509

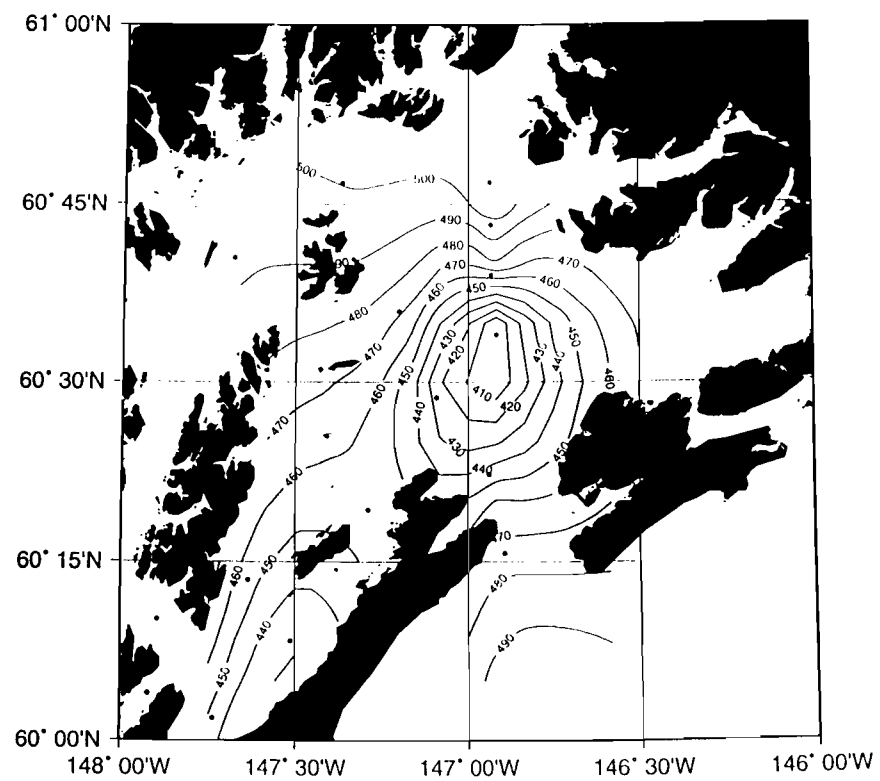


FIG 15(c)

Dynamic Heights 0/100m (cm) - be609

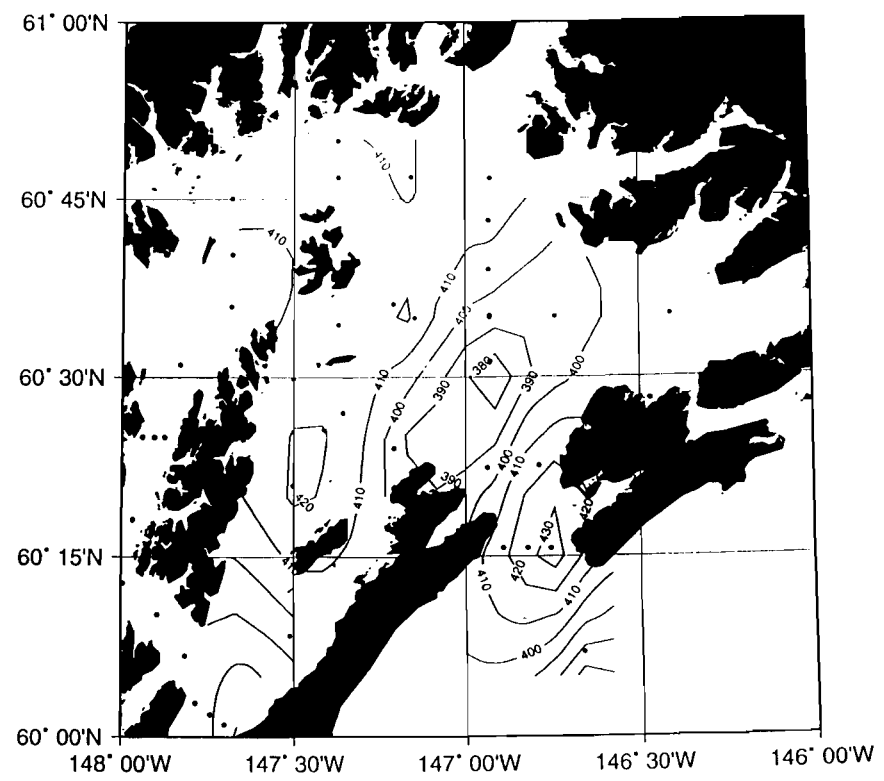


FIG. 16(a)

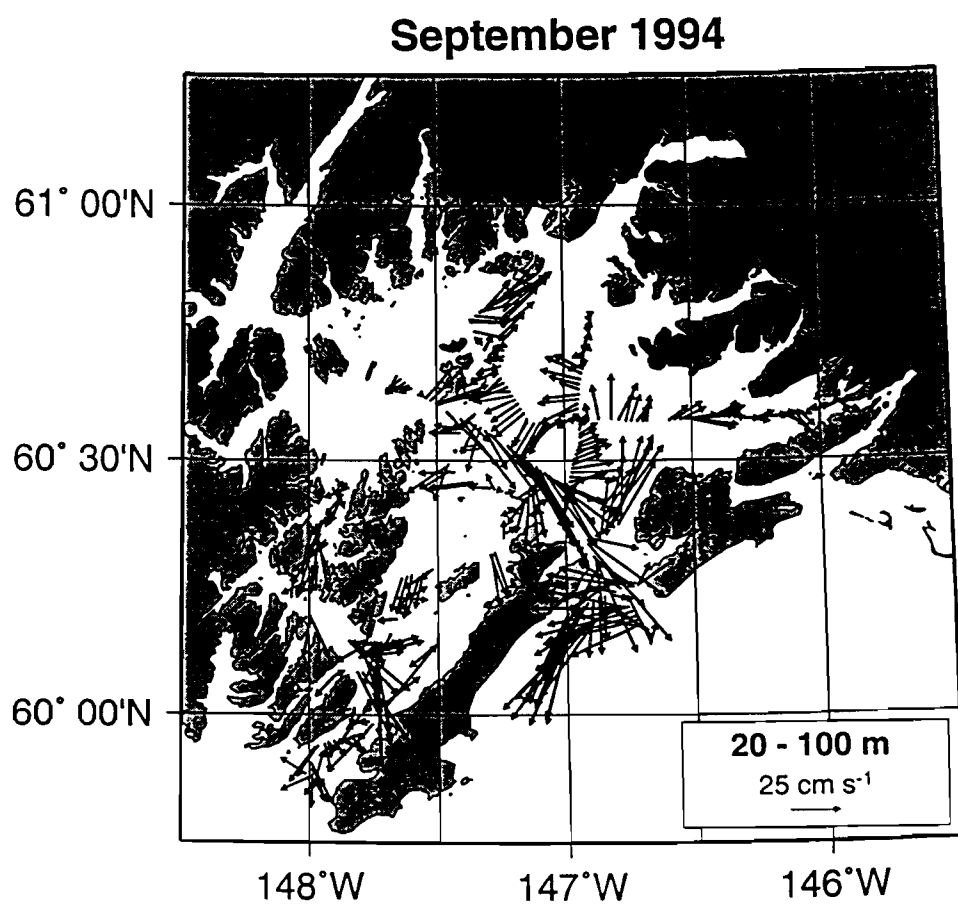


FIG. 16(b)

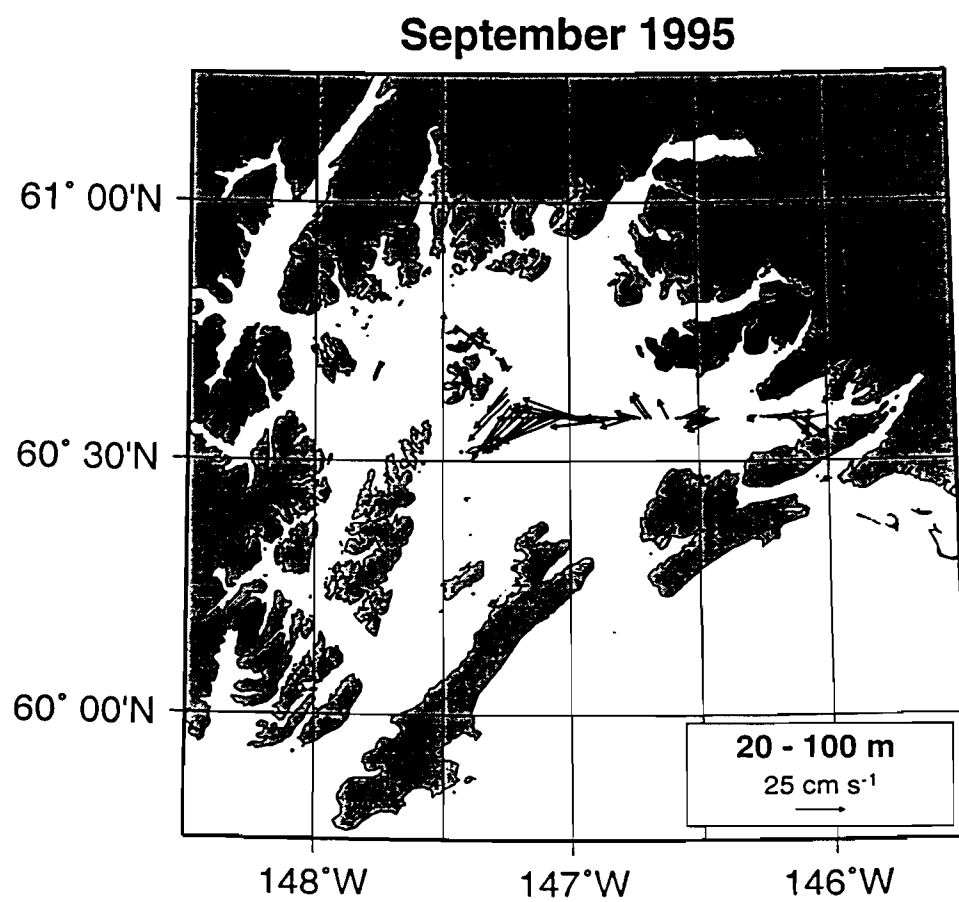


FIG. 16(c)

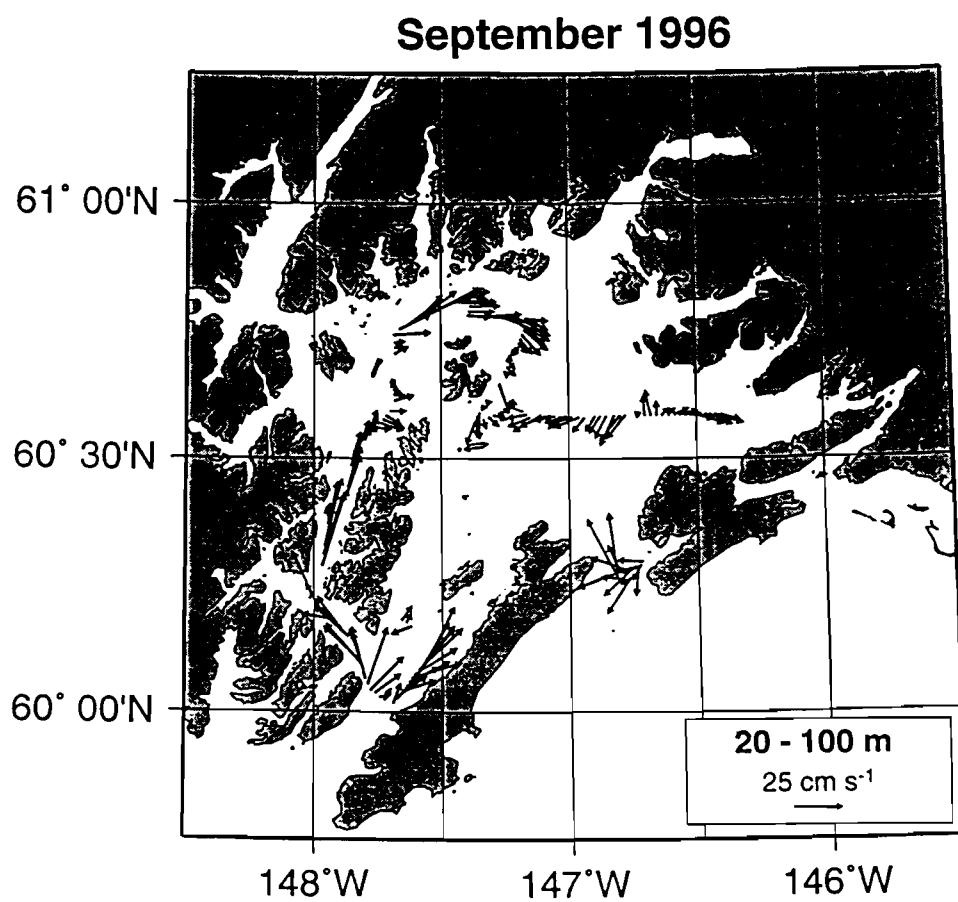
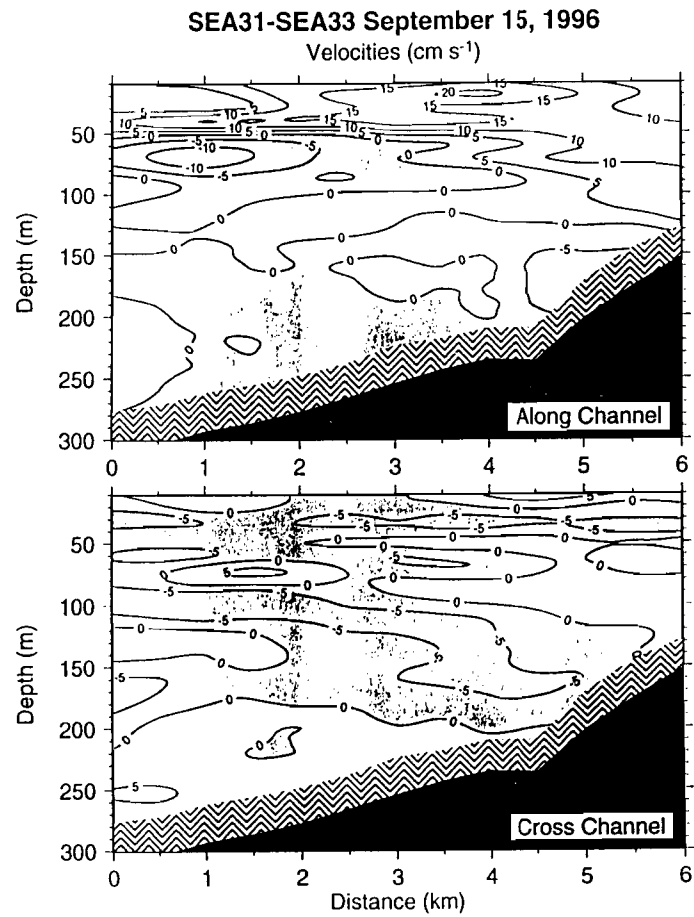


FIG. 17



be96038, 39, 40, 41
avg of 2 flood and 2 ebb tides

FIG. 18

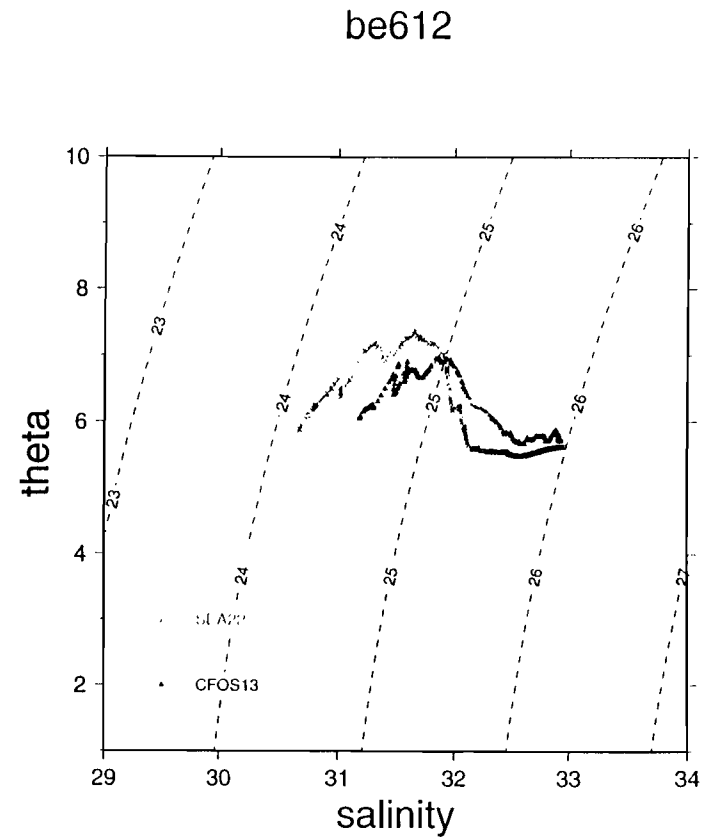


FIG. 19(a)

Dynamic Heights 0/100m (cm) - be612

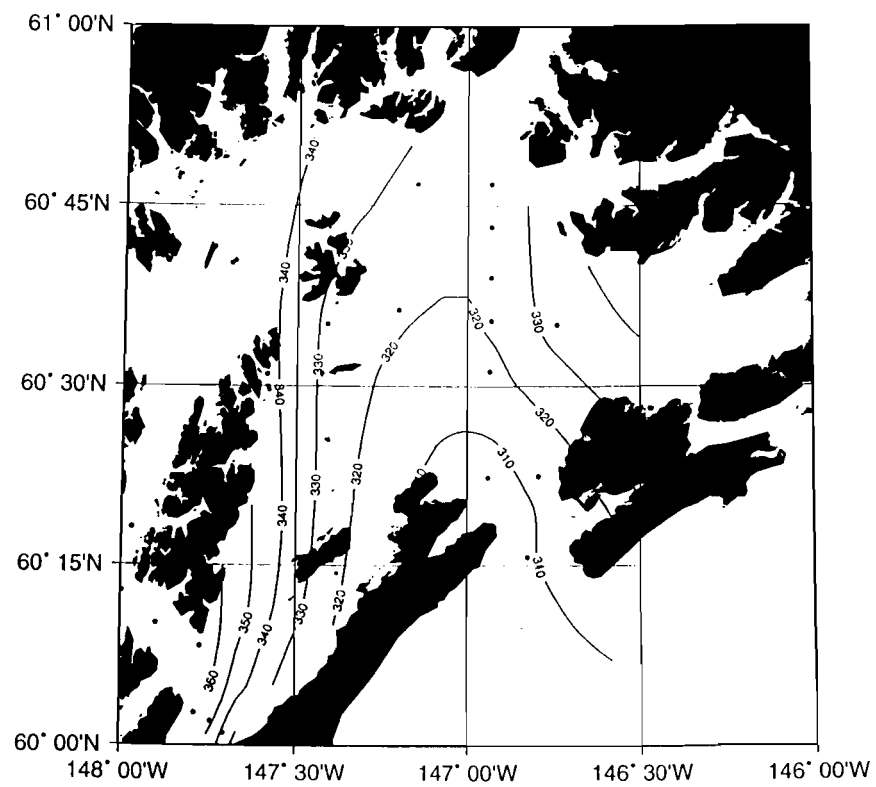
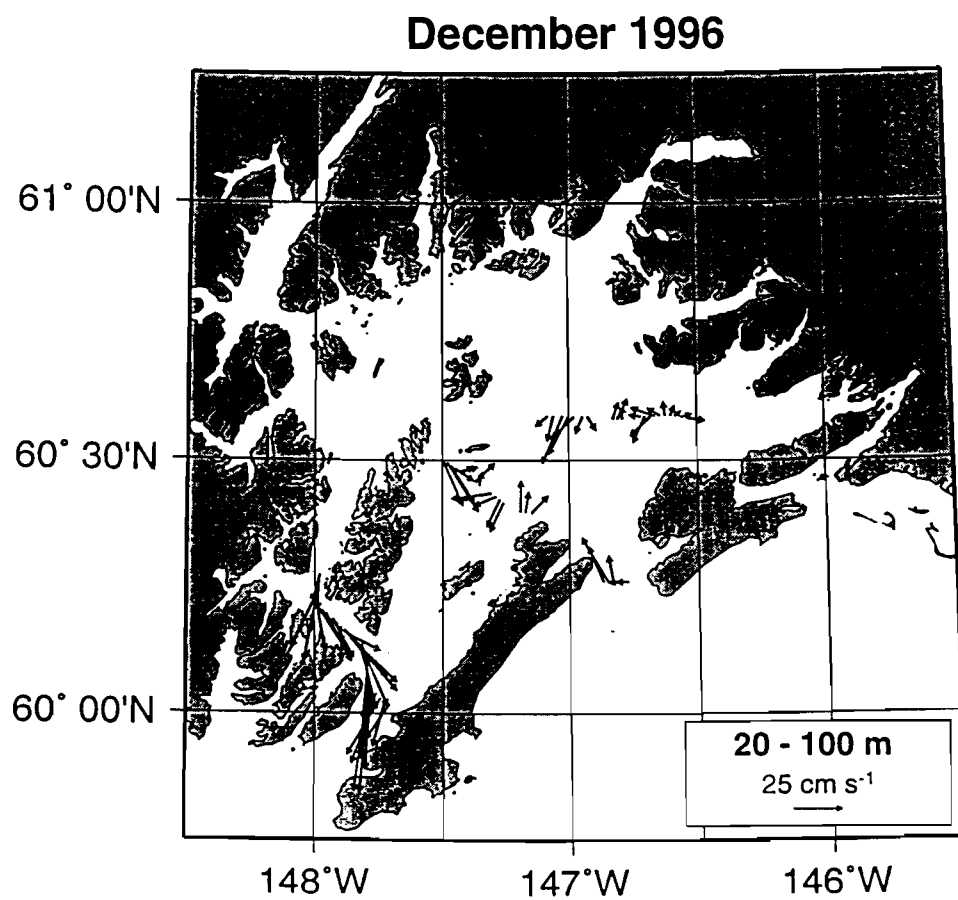


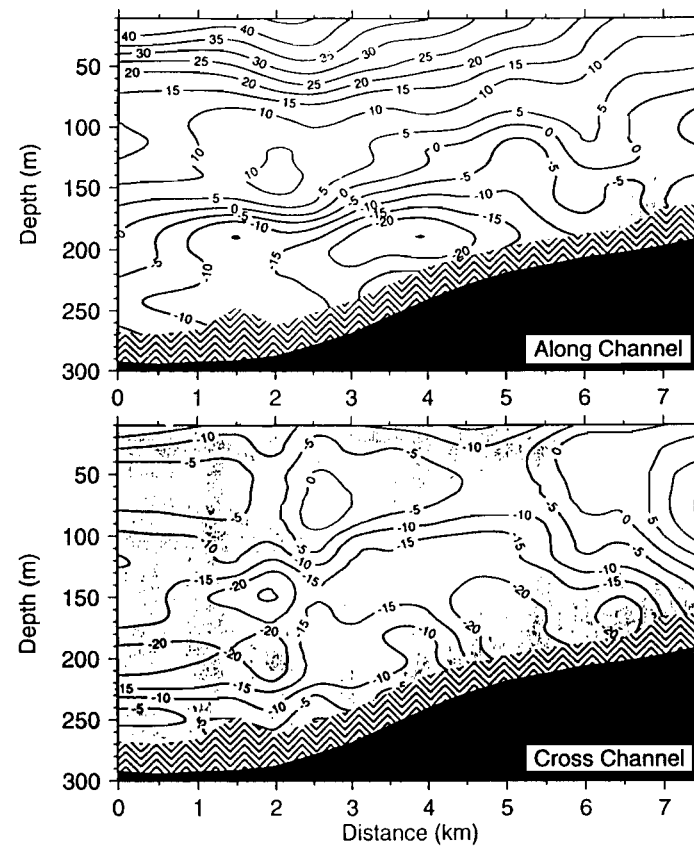
FIG. 19(b)



F16.20

HE13-HE11 December 10, 1996

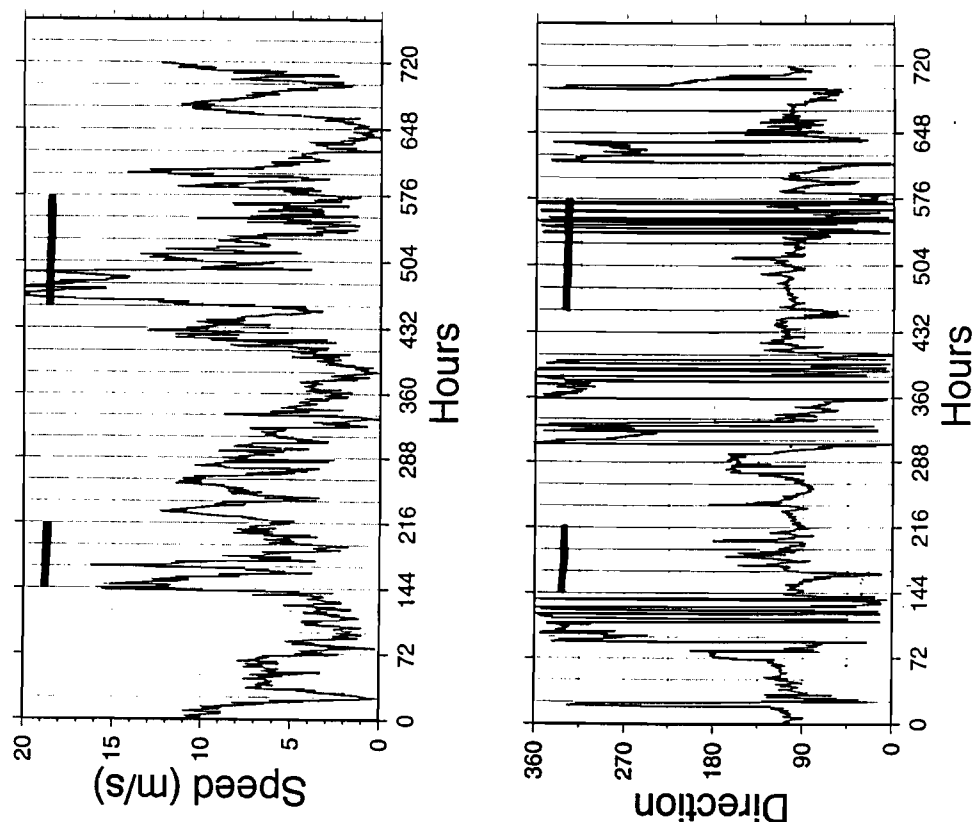
Velocities (cm s^{-1})



be12026, 27
avg of 1 flood and 1 ebb tide

F(6.21(b))

Mid-Sound Wind - September - 1995



F(6.21(a))

HE mooring (6/22-10/3/95) - v comp. (cm/s) - 40 hlp

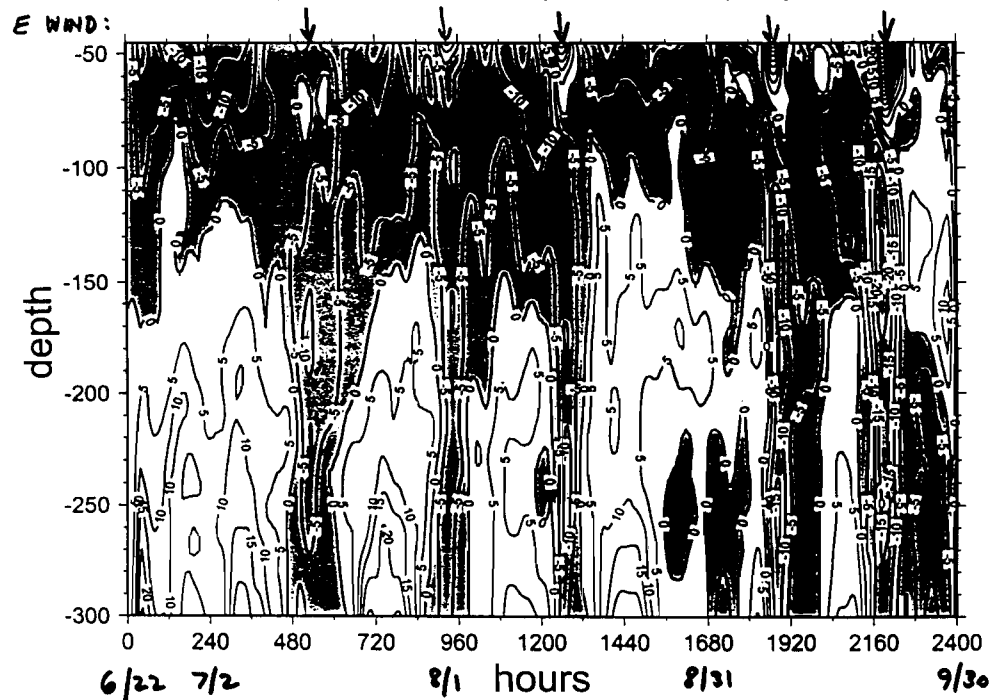


FIG 22 (a)
HE mooring (9/15-5/13/97) - v comp. (cm/s) - 40 hlp

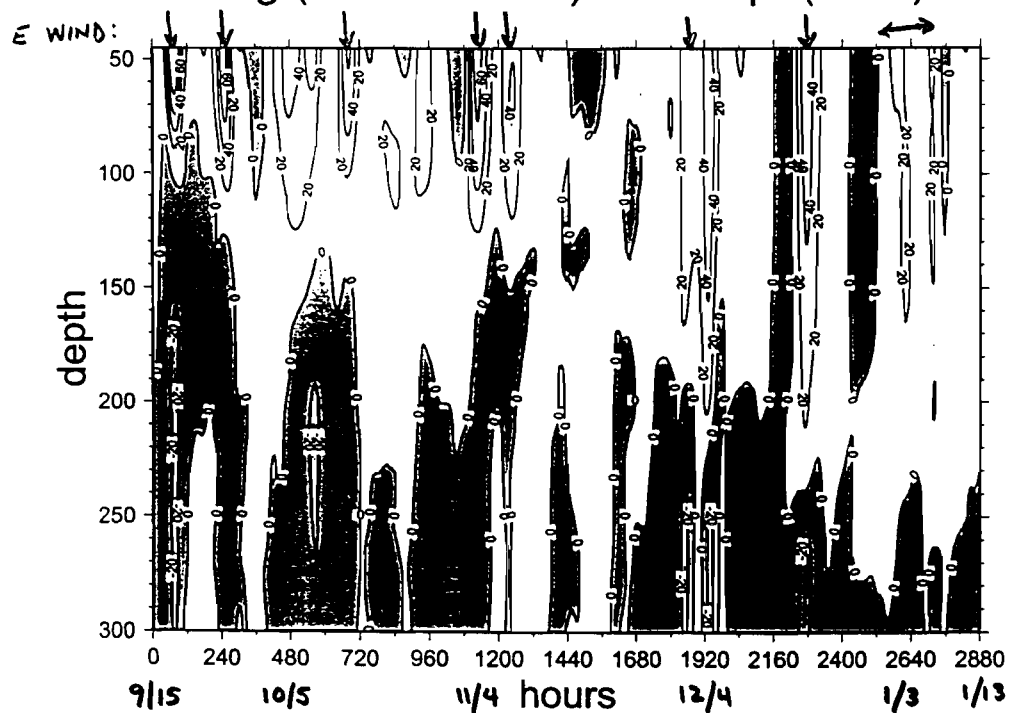


FIG. 22 (b)
HE mooring (9/15-5/13/97) - v comp. (cm/s) - 40 hlp

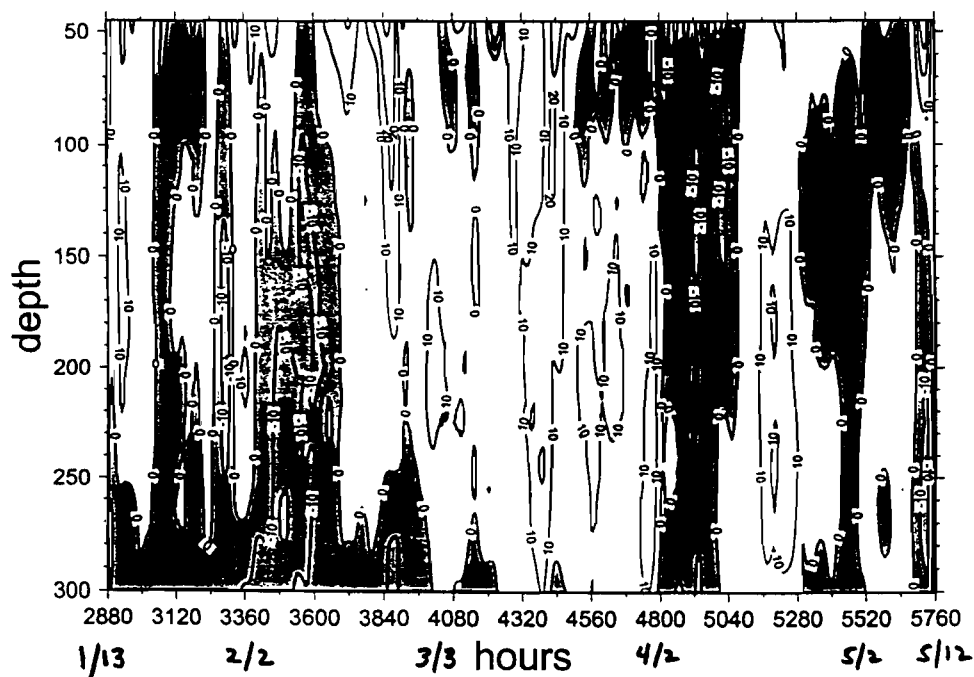


FIG. 23(a)

1995

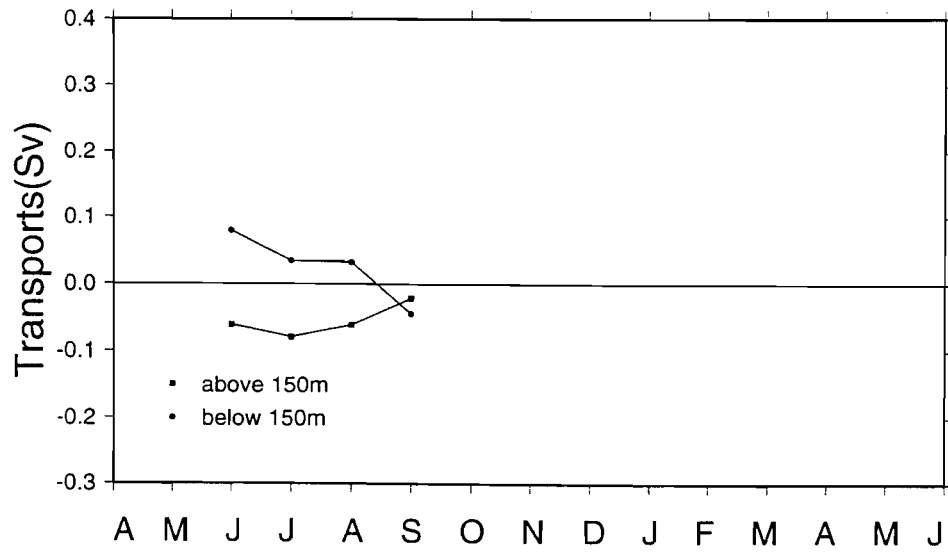


FIG. 23(b)

1996-1997

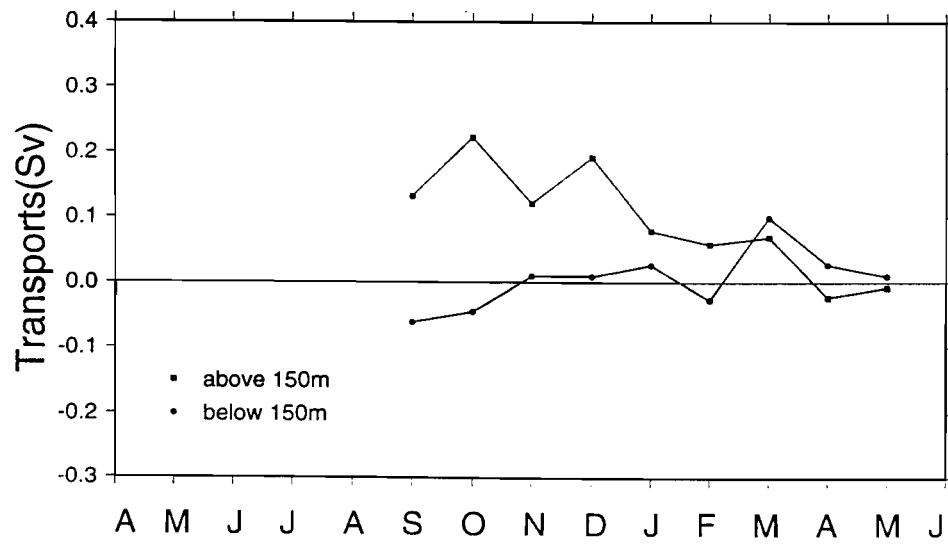


FIG. 24(a)

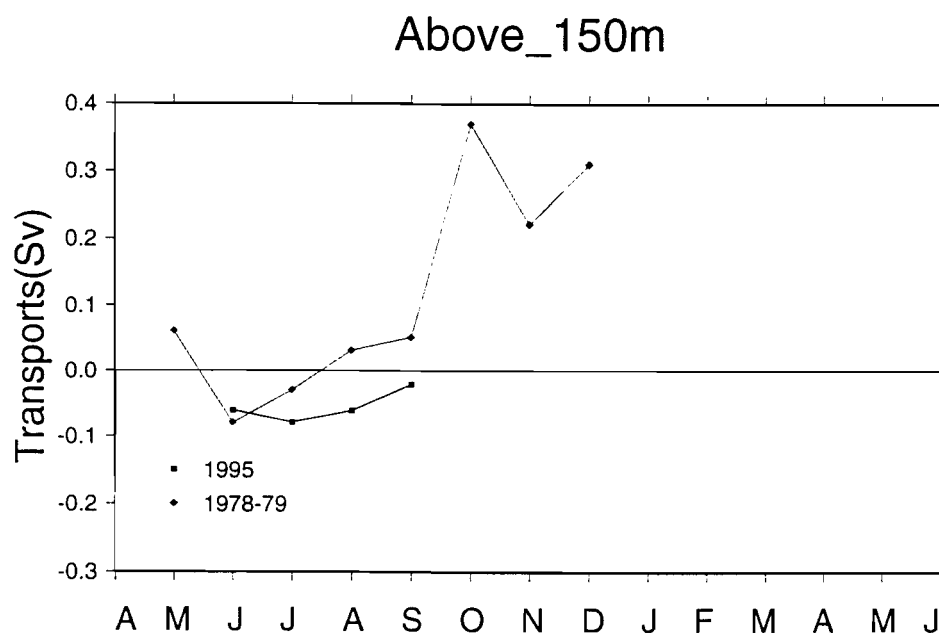


FIG. 24(b)

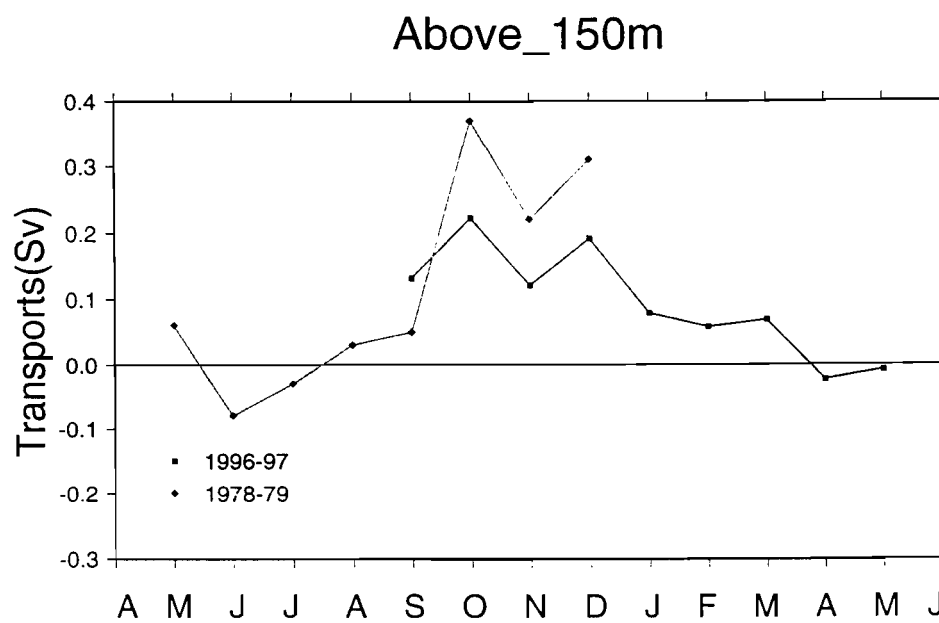


FIG 24(c)

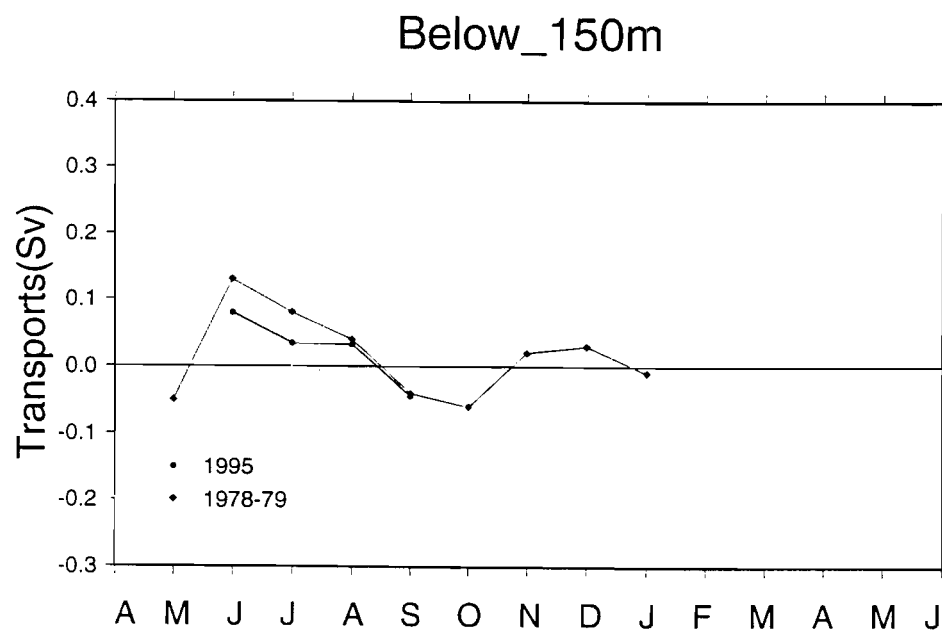
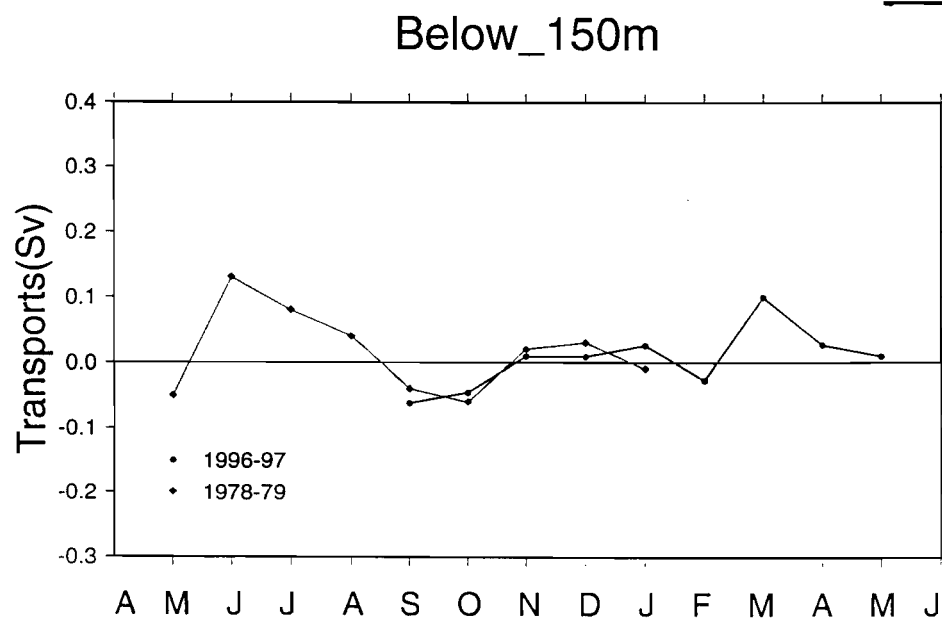
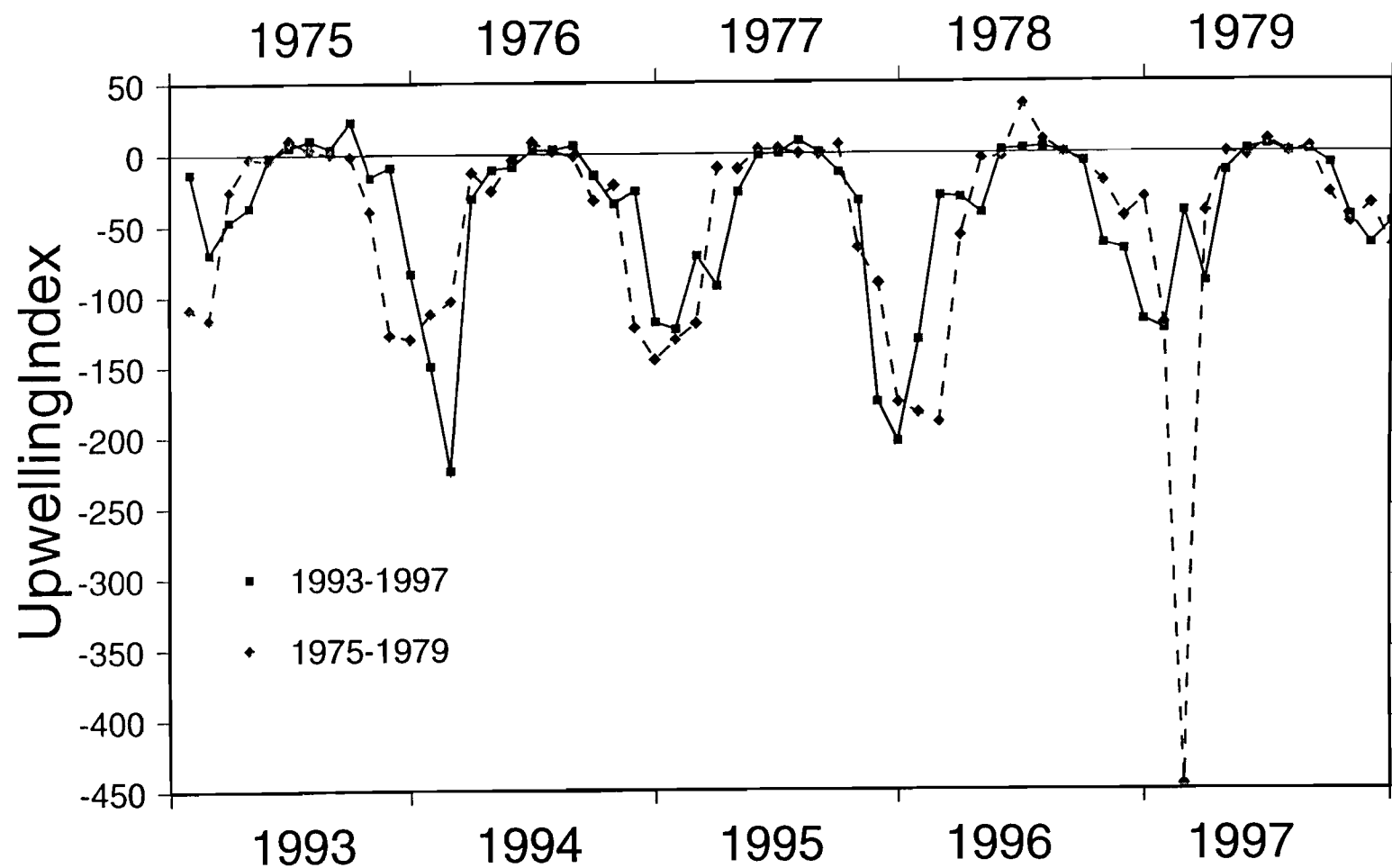


FIG. 24(d)



F16.25



Exxon Valdez Oil Spill
Restoration Project Annual Report

**DESCRIPTIVE PHYSICAL OCEANOGRAPHY OF BAYS AND FJORDS IN
PRINCE WILLIAM SOUND, ALASKA USED AS NURSERY HABITAT BY
JUVENILE PACIFIC HERRING (*Clupea pallasii*)**

Shelton M. Gay III and Shari L. Vaughan

Prince William Sound Science Center
P.O. Box 705
Cordova, Alaska

April 1998

Descriptive Oceanography of Bays and Fjords in Prince William Sound, Alaska used as Nursery
Habitat by Juvenile Pacific Herring (*Clupea pallasii*)

Abstract: Hydrographic surveys performed between spring, 1994 and late winter, 1998 revealed regional variability in the profiles of thermal and haline stratification both seasonally and annually for various bays, fjords and shallow passes within Prince William Sound (PWS), Alaska. Observations in 1994 revealed regional patterns in surface estuarine conditions during spring and summer that were associated directly with the relative sizes (i.e. surface area ratios) of the basins and their respective watersheds. The general hydrographic conditions in the spring showed substantial thermal and haline stratification in comparison to more uniform T/S profiles of late winter. These were a result of both rapid initial surface heating as air temperatures increased during April and May, 1994 and substantial increases in surface freshwater content resulting from higher precipitation rates and melting of lower elevation snow-pack. Precipitation rates appeared to decline during the summer of 1994, and climatic conditions were relatively mild from June through August. However, certain fjords showed disproportionate increases in estuarine conditions in relation to their watershed:basin size ratios. This additional runoff was presumably caused by discharge from higher elevation snow fields. At this time most locations also exhibited maximal summer vertical temperature and salinity gradients within the upper 10 to 20 m. The degree of vertical stratification varied between bays and fjords during the summer, with bays tending to be only partially stratified in comparison with fjords which exhibited prominent vertical T/S gradients in the surface layers. During the summer of 1994, the degree of vertical stratification among bays varied sub-regionally within the southwestern portion of PWS, and during later years certain bays exhibited brief periods during summer in which the T/S conditions were more like fjords. These conditions were short-lived within shallow bays, however, and by the fall these basins typically exhibited partially mixed T/S profiles. Observations within fjords during the fall revealed a general cooling of the upper 20 to 30 m as air temperatures rapidly diminished from October to November, and certain basins exhibited maximum seasonal haloclines at this time. T/S conditions tended to be the most variable at this transitional time of year, and apparently reflected differences in mixing and heat loss due to variable affects of winds geographically. However, this situation was probably further complicated within certain fjords by additional inputs of freshwater from late seasonal snow melt, and mixing. Tidal currents also exhibited varied patterns seasonally and between successive ebb-flood cycles for certain locations. Currents tended to be highest in general at the mouth of bays, with evidence of considerable horizontal shear during both ebb and flood tides at Zaikof Bay, and during ebb tides at Whale Bay. Simpson and Eaglek Bays had much more variable patterns in the currents, which were generally lower in magnitude. Frontal regions associated with the tidal flows were observed in the spacial distribution of the horizontal gradients in temperature, salinity and density. These occurred consistently within Zaikof Bay and Whale Bay, and to a varying extent within Simpson Bay and Eaglek Bay.

Introduction

The following report describes the results of physical oceanographic surveys of bays and fjords which comprise nursery habitats of juvenile fish species in Prince William Sound (PWS). This research is a part of Sound Ecosystem Assessment (SEA), an ecosystem study of Pacific herring (*Clupea pallasii*) and pink salmon (*Oncorhynchus gorbuscha*) in PWS sponsored by SEA project no.320-M in support of SEA Herring project no. 320-T. The objectives of this portion of SEA included determining the seasonal distribution of young herring within PWS, and measuring characteristics of their nursery habitats that might influence recruitment of juvenile fish into the adult populations. In this regard, the main purpose of the physical oceanographic surveys was to quantify the changes in temperature, salinity and density within bays on both annual and seasonal time scales to provide part of the habitat descriptions. A secondary objective involved measuring tidal currents synoptically with high resolution profiles of temperature (T) and salinity (S) in an attempt to identify eddies and frontal zones within bays. Such zones may form where surface currents converge, and tend to be ephemeral in nature, shifting in location within bays during the course of the tidal cycle. The role of tidal currents in the mixing of water masses and drift or retention of larval fish within bays of PWS is unknown and thus identifying such features of circulation would be of value in describing the physical aspects of the habitats.

Background

Past research of oceanographic characteristics within PWS has focused mainly on the influence of the Northern Gulf of Alaska (GOA) on the circulation and seasonal variation of the physical properties of water masses within the main basins of the sound. This work is summarized within the preceding chapter on broadscale physical oceanography. Studies within the bays and fjords, however, are very limited and much of the past work focused on the hydrography and circulation within Port Valdez, due to the location of the oil pipeline terminal within this fjord (Meunch and Niebert, 1973; Colonell, 1981). The circulation within Port Valdez was found to vary seasonally between 2 and 3 layered flow, modified by factors such as local winds, barometric pressure gradients and estuarine surface flows. Additional work was done between 1968 and 1972 by the Institute of Marine Science, UAF in which the characteristics of deep water exchange in relation to sill depths were described for fjords located along the northern gulf coast (Meunch and Heggie, 1978). These included two fjords within PWS: Unakwik Inlet and Port Valdez. Results of this work revealed that sill depth in relation to the level of minimum annual density variation within the water column is important in influencing the timing and extent of advection of dense marine source water into fjord basins. This process is crucial in preventing anoxic conditions from developing within the deep water layer, particularly within fjords with very shallow sills (< 20 m).

Study of the recently formed fjord in Columbia Bay was conducted in 1982 by Walters et. al. (1988) in which a form of estuarine circulation that is unique to fjords with tidewater glaciers is described. This circulation occurs during the summer when glacial runoff is at a maximum, and is governed principally by the massive inflow of fresh water entering from the bottom of the glacier. This subglacial river rises vertically upon entering the estuary and mixes with the higher salinity basin water to form a subsurface buoyant layer, that moves seaward in a manner believed to be similar to entrainment type estuarine flow. The latter form of circulation has been well documented for fjords of British Columbia and Southeast Alaska that have very large inflows of

runoff from fluvial sources at the head of the basins (Pickard 1961 and 1967). The motion of the subsurface estuarine layer across the sill at Columbia Bay was evident from both increased current velocities and a temperature minimum occurring between 3 and 10 m. depth. Its presence in water below the sill was detected in the form of a prominent temperature minimum and maximum occurring respectively at about 10 and 20 m. depth.

Hydrographic surveys measuring T/S profiles within bays, fjords, and nearshore zones, were conducted by the Prince William Sound Science Center (PWSSC) during joint cruises with the Alaska Dept. of Fish and Game in the spring and summer of 1994. This research was expanded to include measurements of tidal currents and high resolution T/S profiles within the upper 50 m. of the water column during joint cruises with the University of Alaska at Fairbanks (UAF), from the fall of 1995 to early spring of 1998. At this time acoustic surveys of fish density and biomass were also conducted by PWSSC while samples of fish for age, length, weight and stomach contents were collected by UAF. Samples of zooplankton and larval fish were also collected by UAF, and additional T/S profiles were collected at selected stations to augment the data from the physical oceanographic surveys.

The results from the initial oceanographic surveys from spring, 1994 to late winter, 1996 were described in a paper submitted for publication to the Journal of Marine Systems (Elsevier Publ.) (Gay - in review). This work revealed regional variability in the T/S conditions within bays and fjords during all seasons that was related to local topography, hydrology and climatic conditions. A summary of this work is included in the present report along with the results of work conducted through FY96.

Methods

Hydrography data were collected using a SeaBird Electronics 19.03 CTD while occupying oceanographic stations established in bays, fjords and passes during the various surveys (Fig. 1). In addition to individual casts, high resolution CTD samples were also collected using either a Chelsea Instruments Aquack CTDF or a SBE 19.03 profiler mounted to a Chelsea Instruments Aquashuttle.. The Aquapack data (which included fluorometry) were collected in real time via a conductive tow cable, whereas data collected with the SBE instrument were saved to a buffer and uploaded following the deployments.

During all cruises in which the Aquashuttle was deployed, particles within the water column were also enumerated using an Optical Plankton Counter (OPC). In August and October, 1996, however, the Aquapack was mounted to a Biosonics sled, modified for towing with the conductive cable used with the Aquashuttle; OPC data were not collected on these occasions. In all deployments, the tow-body (or sled) was lowered and raised manually via a deck winch (housing the conductive cable) while the vessel was underway.

Measurements of the tidal currents were made using an RDInstruments 150 khz Acoustic Doppler Current Profiler (ADCP) which was mounted to the hull of the survey vessel. These data were collected in March, August and October 1996, October 1997, and March 1998. The high resolution CTD data were collected synoptically over the ADCP transects, and all data were georeferenced from Global Positioning System (GPS) data collected by a Magellan 5000 .

Study Area Description

The shoreline of PWS is quite rugged and complex due to its past glacial and tectonic history (Fig 1a). The bays and inlets of this region reflect this diversity, ranging from small, shallow basins with average depths of less than 50 m. to deep fjords, some exceeding 400 m. in depth. The Chugach mountains form a massif bordering the northern and western portions of PWS, and elevations rise abruptly to almost 1000 m at the coast to heights of up to 4000 m within 60 km of the shore. The orographic effect of this barrier has created extensive ice fields within the region, and numerous alpine and tidewater glaciers frequently extend into fjords located along the mainland from Port Valdez to Port Bainbridge. Glacial streams also enter into various bays located along the northern and western regions of the mainland.

The general physiography of the bays and fjords sampled during this study is shown in Table 1. Most locations were surveyed in 1994 and during the three broadscale cruises conducted in the fall, 1995, late winter, 1996 and summer, 1996. From these surveys four bays representing habitats within four regions of PWS were selected to be sampled regularly: Simpson Bay (Eastern PWS), Zaikof Bay (South Central PWS), Whale Bay (Southwest PWS), and Eaglek Bay (North Central PWS).

The majority of the bays sampled as juvenile herring habitats conformed to the standard definition of fjords (Pickard 1961, Pritchard 1967; Rattray 1967), in that they have steep-sided basins and are typically highly stratified during periods of freshwater runoff. However, cross-sections of the basins vary significantly in shape, and some locations can have considerable vertical structure in the form of ridges and pinnacles. Sills of varying depth may be present as well (Table 1), and these local bathymetric characteristics within each basin undoubtedly affected the patterns of hydrography and tidal currents that were observed during the surveys.

As a rule, the locations in Table 1 may be classified as either a bay or a fjord depending on the average basin depths: maximum depths of 100 m. or less would be associated with bays (e.g. Simpson, Zaikof, Paddy and Ewan Bays) and depths over 100 m. tend to occur in fjords (e.g. Herring, Lower Herring, Drier and Whale Bays). The fjords with tidewater glaciers included Unakwik Inlet, Icy Bay, and Nassau Fjord, which are classified separately due to their unique hydrography. Note that all the glacial fjords have sills ranging in depth from moderately shallow (20 - 30 m.) to extremely shallow (4 m.).

Tides. Tides within PWS are semidiurnal (M_2) with velocities ranging from 30 to 50 cm sec⁻¹ (Niebauer et. al. 1994). Tidal prisms in Cordova and Valdez range from less than 3 m. during neap tides to over 5 m. during spring tides, however, maximum tidal amplitudes have been reported for Unakik Inlet ranging from 6 to 8 m. (Meunch and Heggie 1978). The monthly pattern in tidal amplitudes for PWS tends to cycle between periods of neap or "hold-up" tides to periods of high tidal prisms or spring tides; the latter reaching a maximum of almost 6 m. in early spring. Pickard (1961) describes semidiurnal tides within fjords of British Columbia as being declinational, in that tidal prisms vary considerably between each successive cycle of flood and ebb tides. This pattern also occurs within PWS and influenced the timing of oceanographic surveys in order to sample the largest volume changes during the tidal period.

Climatic and Oceanographic Conditions. The climatic conditions of the Northern Gulf of Alaska Coast have been well documented by Royer (1979, 1982) in which he reported a substantial variability in average air temperatures and total precipitation both annually and regionally. Meteorological conditions within PWS during 1994 to early 1996 were described from data provided by hatcheries located at Main Bay, Lake Bay, Unakwik Inlet, and data from the CFOS buoy located in central PWS (Gay, 1996). The data from this paper are included in Figure 2 which shows annual differences in total precipitation and mean monthly air temperatures. Wind speed and direction measured at the CFOS buoy are shown for the same time period in Figure 3. Marked annual differences in air temperatures can be seen between years during winter, and most locations exhibited cooler mean temperatures during the summer of 1995 in comparison to 1994. There is also a greater degree of sub-regional variation in mean air temperatures in 1995. Although precipitation records at Main Bay and Lake Bay exhibited substantial monthly differences in 1995, the annual totals at the two locations were comparable (5.2 vs. 5.4 m.). Winds during the fall through the spring tend to cycle between southeasterly directions to northerly directions, reflecting the passage of low pressure systems from Gulf of Alaska, followed by a predominance of high pressure from the interior of Alaska (Fig. 3). Summer climatic conditions can sometimes be dominated by prolonged periods winds from the southwest.

The general oceanographic conditions within PWS tend to be influenced greatly by climatic conditions from the Gulf of Alaska. However, this effect within bays and fjords may vary depending upon the geographical location. Topographic channeling of winds along the Chugach Mountain Range and geographical gradients in air temperature across PWS create differential physical conditions within various bays, particularly during the winter months. For example, basins located within the northern and western regions along the Chugach Mountains tend to be affected more by cold winter temperatures than are bays located in the eastern side of PWS and along the main islands, such as Montague or Knight Island. Observations of sea-ice formation exclusively within the northern and western regions directly reflects the effects of this temperature gradient. Katabatic winds during periods of high pressure during winter have a differential effect across the northern regions of PWS, and have been observed to be predominate in locations such as Valdez Arm and Wells Pass (entrance to College Fjord) during fall and late winter cruises. These conditions create a complex pattern of winds and climate within PWS, and conditions within a given bay or fjord are governed by both the local topography and the geographical location within PWS.

To summarize, PWS's climate is influenced primarily by the location of the Aleutian Low during the fall through the spring, and the formation of high barometric pressure over the Northern Pacific during summer. Variability in this pattern directly affects the pattern of winds and air temperatures seasonally, and can thus result in substantial interannual variation in oceanographic conditions generally throughout PWS. Anomalous weather patterns caused by ENSO² events may also influence local climate, causing unusually warm years whenever a strong El Nino persists into the winter months, however, this effect needs to be more fully documented.

² ENSO - El Nino and the Southern Oscillation

Results and Discussion

The results of the oceanographic surveys will be divided into three main sections: 1) a comparison of physical conditions sound-wide among the various bays sampled during the broad scale surveys, 2) seasonal and annual variations in physical conditions among the four bays selected for long term measurements; and 3) the patterns of tidal currents within the four bays, and the fine scale T/S conditions observed during flood and ebb tides.

Broadscale Surveys

The locations within the western and southwestern portions of PWS, sampled during the spring and summer of 1994 were grouped into five primary subregions according to geography and similarities in hydrography (Fig. 1b). These regions are defined as follows: region 1- the west side of Knight Island; region 2- Perry Island, Culross Island and Ester Island; region 3- the mainland south of Port Nelly Juan to Dangerous Passage; region 4- the mainland from Whale Bay to Bainbridge Pass, and the northern locations of Prince of Wales Pass to Shelter Bay; and region 5- the extreme southwest portions of PWS, including the lower portions of Prince of Wales, and Elrington Passes.

During the fall survey of 1995 Hogg Bay and lower Bainbridge Pass were added to region 5, and in March, 1996 Icy Bay, Ewan Bay and Paddy Bay were added to region 3. The remaining basins were grouped according to their general locations within PWS (Table 1). The locations designated as glacial refer to fjords that are directly affected by tidewater glaciers.

Spring and Summer, 1994

Seasonal changes in temperature and salinity over the spring and summer of 1994 are presented for regions 1 to 5 to show the differences between these areas in terms of timing and magnitude of physical property changes (Figs. 4 to 7). Plots of T/S data are means calculated for all casts at each basin for the following standard depths: 1,3,5,10,15,20,30,40,50,....100,120,140, 160,....300 m.

The relationship between estuarine conditions within embayments and the sizes of the respective watersheds was examined to determine if differences in surface freshwater between locations during given months could be attributed to relative concentrations of runoff. Higher ratios of watershed to bay surface area would theoretically predict greater concentrations of runoff and vice versa. These results are summarized in Table 2 and from here on the surface area ratios will be referred to as watershed ratios.

In spring of 1994 many locations exhibited marked inputs of both heat and freshwater relative to late winter conditions (indicated by data shown below for March 1996 and winter 1997. This was due to warming air temperatures in April and early May and initial runoff from both snow melt at lower elevations and direct precipitation (Fig. 2). However, the average surface temperature and salinity at Main Bay (region 3) and Culross Bay (region 2) was much lower in comparison to all other locations. These cold, fresh surface layers indicated that high initial runoff from snow melt was being concentrated in these bays (Fig. 4c). This would be expected for these bays on the basis that the watershed ratios were generally higher than in other regions

(Table 2). Eshamy Bay was exceptional, however, in that it did not exhibit the same surface freshening as either Culross Bay or Main Bay despite its high watershed ratio. Other notable differences occurred between bays in region 2 and the various nearshore locations (Fig. 4). The two locations in the northern portion of region 2 (Fig. 4f) appeared to still exhibit effects of surface cooling with minimal increases in runoff, whereas the locations along the south side of Perry Island had warmed, but remained fairly high in salinity. One exceptional nearshore location was West Crafton Island, which exhibited conditions similar to the hydrography of Main Bay.

In June all locations continued to rapidly gain heat within the surface layers in response to the prominent rise in average air temperatures (Fig. 2), and seasonal vertical temperature gradients were well developed (Fig. 5). The freshwater input evident in the surface salinities showed a disparity between bays in region 3 and all other regions, and the locations around the south side of Perry Island exhibited prominent increases in estuarine conditions relative to May with salinity decreases of -4.0 psu on average. The most notable changes, however, occurred in Eshamy Bay and West Crafton Island which decreased by almost -6.3 and -6.5 psu respectively (Fig. 5c and f). The lower surface salinities within region 3 would be expected on the basis of the higher watershed ratios relative to other regions, however, the prominent surface freshening exhibited behind Crafton Island in both May and June indicated that nearshore zones on the west side of Knight Island Pass were influenced by the marked estuarine conditions that affected the fjords of this region.

The two locations sampled in June from region 4, Whale Bay and Bainbridge Pass, exhibited relatively low surface salinities at this time, but Whale Bay appeared to have an exceptionally low value relative to its watershed ratio indicating that this fjord either had relatively greater amounts of runoff from within its watershed or was affected by advection of low salinity water from outside the bay. Measurements of tidal currents and high resolution upper layer hydrography in 1996 and 1997 indicated that the latter process occurs within Whale Bay and that glacial water from Icy Bay affects the upper layer temperatures. This glacial water apparently disperses southwestward towards Knight Island Pass and can be seen in the unique T/S signatures both within this fjord and the outer basin of Bainbridge Pass (Fig. 5d). In both locations the temperature drops rapidly within the upper 20 m, forming a temperature minimum at about 15 m depth. This signature is very similar to the hydrography of subsurface glacial water described by Walters et.al.(1988) flowing across the sill from Columbia Bay. Vertical sections (Fig. 6) also show that subtle variations in the temperature persist below the thermocline to depths of 50 m, within the outer portion of Bainbridge Pass, near the mouth, and across the main basin of Whale Bay. This is discussed further in the sections below regarding tidal currents and upper layer hydrography.

The nearshore locations and passes all exhibited more limited ranges of temperature and salinity relative to the bays and fjords. This may reflect a greater amount of mixing due to higher tidal flows observed within the passes from adcp transects.

Hydrographic conditions in July 1994 (Fig. 7) showed additional heating of the surface layers for bays within regions 1 and 4 as average air temperatures continued to increase in July (Fig. 2). However, salinity changes tended to vary within all regions. For example, within region 1, Drier Bay exhibited the largest decrease in salinity (-1.21 psu) and was significantly warmer and fresher than either Herring Bay or Lower Herring Bay (Fig. 7a). The additional freshwater inputs into these bays that occurred during July were likely from melting of higher elevation snow fields. This was consistent with both the warm, sunny weather conditions observed during the

cruise in July and weather conditions measured at Main Bay in July 1994 (Fig. 2). The pass in Long Channel and the two shallow bays along the southwest portion of Knight Island, however, all exhibited lower ranges of temperature than the fjords along the west side of the island, and one location, Mummy Bay, had a much lower range in salinity as well.

Whale Bay and Bainbridge Pass both had very minor increases in heat at the surface ($< 0.2^{\circ}\text{C}$), however, the average surface salinities also increased by 0.72 psu and 0.08 psu respectively and indicated a drop in freshwater input in July (Fig. 8c). The shallow temperature minimum was still present in Whale Bay, but did not appear in the TS plot for Bainbridge Pass. The stations located in the outer mouth of Bainbridge (stns. 11 - 14 in Fig. 11) were not resampled in July due to time constraints and this may be the reason that the minimum was not observed. The two other locations in region 4, upper Prince of Wales Pass and Flemming Island both exhibited increases in heat and freshwater content in the upper layers (Fig. 7d).

Four additional locations were sampled within the extreme southwestern portion of PWS (region 5) which included Elrington Pass, Sawmill Bay, lower Prince of Wales Pass, and Twin Bays. This region exhibited much different conditions of hydrography than the other regions, apparently due to the effects of higher tidal currents within the narrow passes on mixing within the water column (Fig. 7e and f). The extremely small ranges in T/S conditions exhibited in lower Prince of Wales Pass and N. and S. Twin bays, located at the mouth of Port Bainbridge, were possibly influenced by mixing from both winds or tides and may also exhibit properties derived from exchange with Gulf of Alaska waters. However, this region of PWS will require further study to identify the actual processes affecting the hydrography.

Fall, 1995 and Late Winter, 1996

The hydrography of bays and fjords in mid October to early November, 1995 (Fig. 8) reflected a wide range of conditions that occurred at that time of year, following the period of maximum precipitation and fresh water input in September and October (Fig. 2). Although the amounts of fresh water and heat within the upper 40 m. layer appeared to vary significantly among locations, the T/S profiles tended to reflect the relative degree of surface cooling and mixing that had occurred among the various basins; deeper fjords tending to remain stratified and shallow bays and passes exhibiting more mixed profiles. Differences within these groups was most likely due to the variable effect of winds within bays, depending upon their geographical location and local topography.

Examples of locations that were apparently sheltered included Herring Bay and Whale Bay. In these cases stratification persisted well into the fall and surface cooling had resulted in the formation of a prominent temperature maximum located at about 20 m. in both fjords (Fig. 8a). Eaglek Bay and Jack Bay, both fjords, exhibited varying effects of wind mixing within their basins (Fig. 8d). Although the temperature maximum within Eaglek Bay was located at about 40 m. depth its T/S profiles indicated that it still remained stratified. Jack Bay, however, exhibited an erosion of both the seasonal thermocline and halocline. (This fjord was observed later to be highly stratified in July, 1996.) During the sampling within Jack Bay in early November, strong katabatic winds from the mainland were observed to blow down this fjord and also down Port Valdez for days. These wind events were episodic during the fall months of 1995, and were the most likely cause of the unusual T/S signature within this bay (Fig. 8d).

The varied conditions of hydrography within bays and fjords in late fall probably reflected both a subregional variability in precipitation and wind effects due to differences in geographical location, orientation (aspect) to the prevailing wind directions, and topographic effects on channeling winds into their basins. The combination of protection from prevailing winds and the stabilizing effect of large amounts of fresh water at Herring Bay and Whale Bay may prevent mixing of the upper water column of these fjords until later in the winter when very low temperatures may start the process of thermohaline convection.

Late Winter, 1996

In March, 1996 most locations exhibited well mixed profiles with minimal ranges in temperature and salinity as expected for this time of year in PWS (Meunch and Schmidt 1975). However, a minor amount of cold runoff from early snow melt appeared to have begun to enter into two fjords: Eaglek Bay and Whale Bay (Fig. 9a and d). Eaglek Bay has a number of tributaries, such as Cascade Falls, that were observed to provide early input of freshwater, and although this was not observed directly for tributaries into Whale Bay the air temperatures were quite warmer during early spring in comparison to previous years indicating that an early snow melt was occurring at lower elevations (Fig. 2). It is possible that the main basin of Whale Bay was also affected by glacial water from Icy Bay at this time, where the T/S profiles also indicated some early input of meltwater (Fig. 9b). However, the profiles of water beyond the shallow sill were well mixed and this can be seen in the differences in T/S signatures between the inner basin and Knight Island Pass in Figures 9b and c.

The combined effects of thermohaline convection and wind induced circulation was likely to have created the more uniform conditions observed within the other fjords (Drier Bay, Jack Bay, and Galena Bay) and most shallow bays (Fig. 9). A southeast gale prevented immediate sampling of stations in Drier Bay and winds were observed to be channeled and accelerated into this bay by the topography of Knight Island. This storm was evident in the weather records for the central sound in the later part of March, followed by a second storm event in early April immediately following the March 1996 cruise (Fig. 3). The mixed T/S conditions within Jack and Galena Bay were not related to this storm activity, however, and were probably caused by local katabatic winds similar to those observed during the fall. This weather pattern was reported to occur frequently within Port Valdez during the winter (Meunch and Nebert 1973), and was also observed within PWS in March 1996 (personal observation).

The two glacial fjords surveyed in late winter, Icy Bay and Unakwik Inlet, exhibited very uniform conditions below 10 m depth, and with the exceptions of whale Bay and Eaglek Bay the surface layers tended to be colder and fresher than all other locations (Fig. 9b). The water below the sills at these fjords tended to be warmer at the surface, but more saline in general indicating a marked difference in density between the basins. The thoroughly mixed profiles within the upper basins were most likely related to strong thermohaline convection, as evident from sea-ice covering their entire basins over the winter (personal observation). Although air temperatures well below 0° C typically occur during the winter along the coastal regions of the Chugach Mountains, and were observed at Main Bay in January, 1996 (Fig. 2), the extent of annual sea-ice formation is apparently quite variable. For example, conditions occurring during the winter of 1972 described by Meunch and Heggie included slush ice and growler ice bergs, however, no mention was made of extensive sea-ice formation. The T/S conditions within these fjords were

found to be similar to those measured 24 years prior by the Institute of Marine Science, UAF, and the density variation of water located above and below the shallow sill was conducive to deep water exchange (Gay, 1996).

Summer, 1996

In June, 1996 the two bays and one fjord that were surveyed varied considerably in ranges of temperature and salinity, with Zaikof Bay still exhibiting very mixed conditions (Fig. 10a). By July, however, all locations showed marked increases in heat and fresh water within the surface layer, with varying degrees of stratification (Fig. 10b to i). The fjords tended to exhibit more shallow vertical temperature and salinity gradients (i.e. thermoclines and haloclines) and rather isothermal and isohaline deep layers in comparison to the bays and two larger basins located in the eastern sound: Port Gravina and Port Fidalgo (Fig. 10h). Both Elrington Pass (southwest: region 5) and the nearshore location at Green Island remained more mixed, and exhibited deep temperature gradients. The T/S signature at Green Island appeared much colder than North Elrington Pass partly because ctd casts were made to greater depths at Green Island (~ 120 m. vs 60 m.). However, Elrington Pass has strong tidal currents (observed in 1995) which apparently account for the consistently more uniform conditions observed there since the summer of 1994.

The other basins which had exceptional T/S conditions during the summer included the two glacial fjords, Icy Bay and Unakwik Inlet, and Whale Bay (Fig. 10b,c and d). The cold brackish layer in the upper 10 to 15 m. within the glacial locations reflects the substantial cooling caused by the melting of ice calved from Chenega Glacier in Nassau Fjord and the Meares Glacier in Unakwik Inlet. These same conditions were described by Walters et.al. (1988) for Columbia Bay, in which the heat sink created by the latent heat of fusion required to melt the glacial ice overcomes solar heating, thus creating the excessive cold, fresh conditions in the surface layer. The substantially colder surface conditions within Whale Bay appeared to reflect the exchange of this glacial water during summer from Knight Island Pass. The T/S depth profiles within this bay showed both a shallow minimum and subsurface maximum unlike any other nonglacial fjord, but similar to temperature anomalies that occurred in water below the sills at Icy Bay and Unakwik Inlet (Fig. 10c). The surface currents in Whale Bay flow into the mouth during both the ebb and the flood tides and the effect of this circulation on the upper layer hydrography is discussed in the sections below regarding tidal currents.

Seasonal Hydrography of Selected Bays and Fjords

In the following section the seasonal patterns in water mass physical properties are presented for two bays, Simpson Bay and Zaikof Bay, and two fjords, Whale Bay and Eaglek Bay. The data cover the period beginning in August, 1996 and ending in March, 1998, with winter ctd measurements occurring in 1996-97 only.

Late Summer and Fall, 1996

The physical conditions within the bays and fjords in August, 1996 showed varying degrees of vertical stratification, with well developed thermoclines and haloclines occurring in all fjords and in Simpson Bay (Fig. 11). Zaikof Bay exhibited a limited amount of stratification, but the

vertical gradients in temperature and salinity penetrate almost to the bottom (60 to 100 m.). This bay exhibits only a very short duration in summer stratification and by fall both bays have become much more isothermal and isohaline in comparison with the fjords which, remained stratified (Fig. 11d and e).

The surface temperatures in Whale Bay continued to remain much cooler than Eaglek Bay, with the same minima and maxima within the surface layer as in July. This pattern occurs within the deep, main basin only, and the shallow southern arm exhibits thermoclines without minima and maxima. The fall conditions for these two fjords were quite interesting in that the seasonal cooling of the average surface layer to 20 m. was much greater in Eaglek Bay than the cooling observed at Whale Bay ($\Delta T_{\text{bar}} \sim -5.5^{\circ}\text{C}$ vs. -1.5°C). Again, the effect of glacial water in moderating the heat gain and loss at Whale Bay may have caused the disparity between these fjords, however, this remains to be investigated further.

The glacial fjord, Unakwik Inlet was also resurveyed in August, and the T/S signatures of water masses above and below the shallow sill revealed that separate conditions persist between these two basins between winter and summer (Fig. 11 b).

By late fall the two bays exhibited partially mixed T/S profiles with minor temperature and salinity gradients in the surface layers, whereas the one fjord, Whale Bay still showed some vertical stratification (Fig. 12 a). All locations exhibited continued cooling at the surface in November, and by December both bays were well mixed with minimal vertical T/S gradients (Fig. 12 b). The physical conditions in Whale Bay in November showed a significant erosion of both the fall temperature maximum and the seasonal thermocline that developed during the previous summer. Because of the sheltered nature of this fjord, it is presumed that most vertical mixing occurs there due to thermohaline convection caused by strong surface cooling from late fall through early spring.

Winter, 1997

T/S conditions within Simpson Bay during winter showed a gradual trend towards very isothermal conditions in January and February, 1997 with gradual cooling of the water column during this period by almost 1°C on average (Fig. 13a and b). Zaikof Bay also was very isothermal within the deeper layers, however, there was a marked reduction in the surface salinity within this bay in February, that corresponded with a period of warmer temperatures and slight runoff from low elevation snow-pack (personal observation). This moderation of the winter climate appears to have affected watersheds of Zaikof much more than those of Simpson Bay, in that the reduction in surface salinity was very minor in the latter. This was not unexpected since the bulk of the watershed for Simpson Bay is comprised of high elevation snow-fields and alpine glaciers and it was not affected by the milder air temperatures as much as the lower elevations of Zaikof Bay's watershed. By late winter (March 1997) both bays were well mixed with only very minor T/S gradients within the surface layers (Fig. 13c).

Whale Bay also exhibited moderate vertical temperature and salinity gradients in February, 1997 (Fig. 13b), and although the temperatures continued to cool within the water column in March, the salinity gradient appeared to continue to degrade further, indicating that mixing did not stabilize until late winter (Fig. 13c). It appears that this fjord remains partly stratified during all seasons, however, a more thorough time series during the winter would help to confirm this. At this time it is unknown if the reduction in salinity relative to bays observed during February resulted from early snow-melt or was a remnant of the fall halocline.

Spring and Summer, 1997

The spring pattern in hydrography among the bays and fjords reflected the relative amounts of initial heating and freshwater runoff that occurred at the various locations (Fig. 13d and e). With the exception of Zaikof Bay all locations exhibited early thermal stratification, but both fjords appeared to receive greater amounts of runoff relative to the bays. Zaikof remained fairly well mixed despite the warming and surface freshening typical at this time of year. This may be partly due to the early runoff that occurred within this bay in February which precluded the contribution of low elevation snow-pack from runoff later in spring. However, the action of wind and tides within this bay appeared to also cause the water column to remain relatively well mixed until late summer, at which time heating and freshwater runoff created enough vertical stability to allow a minimal amount of stratification, albeit the vertical gradients extend through the entire water column (Figs. 14b and d). Note that in Figure 14b and d, a cluster of points can be seen at the top of the T/S plot. These reflect a shallow wind mixed layer that occurred in both July and August to depths of about 8 m. This bay is prone to the effects of wind mixing during any season.

Simpson Bay showed a T/S signature similar to the Whale Bay in late summer, 1997 (Fig. 14d). This resulted from a significant release of glacial water from its watershed sometime between the July and August survey. This bays watershed area is approximately 6 times the area of the bay (Table 2), and any large discharge of freshwater would be expected to concentrate within the upper arm of this bay. Such was the case as salinity at 1 m. depth ranged from 13 psu in the upper arm to 21psu at the mouth.

The two fjords exhibited differing T/S signatures throughout the spring and summer (Figs.13d, 14a and c). Whale was consistently cooler than Eaglek within the upper layer (40 to 50 m.). This fjord also showed a substantially different pattern in surface layer temperatures in 1997 than in either 1996 or 1994. The surface temperatures were higher in 1997 by almost 3.5°C, but decreased rapidly within the subsurface layers to a value close to 6°C by 50 m. depth, which is similar to prior years. The T/S signature for this bay exhibited the subsurface temperature maximum in 1997, indicating that input of glacial water had still affected the hydrography of this bay. However, this effect may have been moderated by warming of the glacially derived water prior to its entering Whale Bay, caused by atypically high summer air temperatures in 1997. Eaglek Bay also showed significant differences in the surface layer hydrography between 1996 and 1997, in which the highest temperatures occurred as a subsurface maximum in July at 10 m. depth. This maximum had eroded by August and a temperature minimum occurred instead at 5 m. depth. These features were probably also a response to much warmer air temperatures that occurred during the summer of 1997, and the minimum temperatures which occurred at 3 m. during both months may reflect greater releases of stored glacial water from Cascade Bay, which drains a high elevation alpine region.

Fall, 1997 and Late Winter, 1998

T/S conditions during the fall of 1997 were similar to 1996 with certain exceptions (Fig. 15). Eaglek Bay exhibited a higher surface salinity and warmer upper layer temperatures in 1997 than in 1996, and although Whale Bay exhibited similar salinities to 1996, increased cooling occurred within the upper 20 m. in 1997. Zaikof Bay exhibited a substantially greater deep vertical salinity gradient in 1997 in comparison to the previous fall. This may have been a remnant of the

deep stratification in August, 1997 which was greater on average throughout the water column that year ($\Delta S_{bar} \sim -5.3$ psu over 100 m. in 1997 vs. -3.2 psu over 80 m. in 1996). However, this may also have been moderated by the milder climatic conditions that occurred during October, 1997, which would have possibly prolonged more thorough mixing until later in the season. Simpson Bay exhibited opposite trends between years with a vertical salinity gradient being higher in the fall of 1996 than in 1997, despite the substantial surface freshening that occurred in August, 1997.

These trends again indicate that fall is a period of high variability in terms of climatic effects across the sound, and bays and fjords exhibit trends in hydrography that are inconsistent with general weather patterns, and reflect the effects of local factors which moderate or intensify the climatic influences during this season.

Over three separate winters between 1996 and 1998, some long-term trends in average temperature were evident among the four locations. With only one exception in 1997, all bays and fjords exhibited a consistent warming throughout the deeper water column from 1996 to 1997, indicating that deep temperatures track the changes in annual atmospheric temperatures over time. The surface layers were more variable, but if averaged vertically they appeared to also exhibit a gradual increase over time as well. The one exception occurred at Whale Bay in the winter of 1997 in which the upper 3 m. layer average decreased by almost 1°C and the deep layer decreased by 0.7°C (Figs. 9.13, and 15). The most striking increases occurred over the winter in 1998 and temperatures are summarized over all years in the following table. Values are degrees C and the depth is the level at which the deep average basin temperature was taken.

	<i>1996</i>		<i>1997</i>		<i>1998</i>		
	<i>deep</i>	<i>surface</i>	<i>deep</i>	<i>surface</i>	<i>deep</i>	<i>surface</i>	<i>depth</i>
Whale Bay	5.5	3.2	5.2	2.5	6.5	4.5	160 m.
Eaglek Bay	4.7	3.0	5.2	3.2	6.5	5.0	140 m.
Simpson Bay	~ 4.3	~ 4.3	5.0	4.5	6.2	5.7	80 m.
Zaikof Bay	4.0	3.7	4.7	4.2	5.9	5.8	80 m.

These values are approximate and were taken from the T/S profiles. Further analysis needs to be done to determine more accurate long-term trends, however, these values serve as examples of the of the general trends of increasing mean annual air temperatures within the PWS region.

Long-term changes in average salinity did not follow a particular trend, and varied in the pattern between years at the two fjords. The long-term salinity of the two bays, however, appeared to remain consistent between years. The trend in more highly mixed profiles within the bays in comparison to the fjords over winter remained consistent (Fig.15).

Stations located within Nassau Fjord and Icy Bay were also resurveyed during late winter, 1997. The results indicated that the deeper layers of both fjords were warmer on average in 1998 in comparison to measurements taken in 1996. The increase was most evident in Icy Bay which went from about 4.6°C in 1996 to almost 6.0°C in 1998. The surface temperatures in Nassau Fjord were similar ($\sim 1.0^{\circ}\text{C}$) due to the melting of ice in both years, however, the profiles in 1998 appeared to be slightly colder down to 5 m. Below this layer the temperatures became warmer in 1998. Although the salinity of the water just below the sill at Icy Bay appeared to be higher than the water inside the sill, the density difference is less than that observed in 1996, and further analysis will be needed to determine if deep water exchange had occurred in 1998.

Seasonal Tidal Currents

In this section of the report, examples of seasonal variability in tidal currents is presented for selected locations, and discussed in relation to general patterns observed between ebb and flood tide stages and features of circulation such as fronts and eddies. References to bathymetric effects will be limited, as these are beyond the scope of this initial report and will be reserved for future analysis.

Zaikof Bay

Tidal circulation for Zaikof Bay is presented in Figures 16 to 19 for all months that adcp data were collected. One consistent feature in the currents was the strong flow at the mouth of the bay and across the shallow shelf that extends north and eastward from Montague Island. The adcp transects followed this shelf almost to its edge, where the depths drop from less than 100 m. to over 300 m. within Hinchinbrook Entrance. Variability in the direction and strength of this flow occurred both seasonally and also between successive flood or ebb tide stages within a given semidiurnal period. For example, the general direction of the flood currents across this shelf was from the east in all months except August, in which the direction is out of the north and west. The motion of the ebb tide, however, seemed to consistently occur from the north and west during all months, and with the exception of March, 1996 there appeared to be an acceleration in this flow to the southeast across the east peninsula at Schooner Rocks.

The relative strength and direction of the shelf flow appeared to influence the circulation within the lower reaches inside the mouth of Zaikof Bay. Inflows at the surface during both ebb and flood tides created areas of velocity shear and convergence of the tidal currents, which may enhance turbulent mixing and the development of frontal zones respectively. The latter were a consistent feature observed at the mouth of this bay during all cruises, and were evident in the form of flotsam lines with varying surface water properties appearing on either side (i.e. slicks vs. ripples). Currents located along certain areas of the shoreline in this part of the bay also exhibited a consistent direction regardless of the tide stage. One such area is located along the eastern side where currents appear to be either forced back out of the bay (eastward) during strong flood tides (Figs. 16a, 17b, and 19b), or deflected eastward during the ebb tide (Figs. 17a, 17c, 18a, 18c, and 19a, 19c). Another area is located along the northwest shoreline where the direction of currents is to the north or northeast during both ebb and flood tides. This flow may be either forced out of the bay during the flood tide or drawn into the cross shelf flow during the ebb tide (Fig. 17 and 18). The strength and direction of the inflow during the ebb tide appears to be important in the formation of an anticyclonic eddy which was observed during October, 1996. This appeared to be more prominent during the first ebb tide, but it may have also remained in a reduced form during the second ebb tide (Fig. 18a and c).

The horizontal vectors of the deeper currents are shown for the 22 to 30 m. depth layer in Figures 16 and 19. In general, the high velocity flow at the mouth tended to be barotropic, and the u and v components were observed to be consistently high throughout the water column during data acquisition in all months. The currents within the remainder of Zaikof Bay, however, tended to be of low magnitude and generally more variable in direction. August, 1996 was somewhat exceptional in that stronger surface currents occurred farther into the bay on both flood tide 1 and ebb tide 2 (Fig 17b and c). These two stages may have had the highest tidal prisms of

the semidiurnal tidal period, however, this was also the only season in which Zaikof Bay became partially stratified in density due to freshwater input, and this may affect the baroclinic tidal flow creating greater vertical shear in the current.

Simpson Bay

The tidal currents at Simpson Bay were highly variable and did not exhibit the consistent velocities at the mouth, as were observed for Zaikof Bay (Figs. 20 to 23). For this reason, separating seasonal and declinational effects on flow patterns will be difficult. Like Zaikof, Simpson Bay is also shallow and certain features of the morphometry (topography and bathymetry) may influence the circulation. The basin of this bay is formed by a shallow shelf, which rises from depths of over 200 m. in Orca Bay (to the south) to depths ranging from 40 to 50 m. inside the mouth. A shallow reef separates the upper arm from the main basin, and depths drop to 70 m. just north of this reef. Although the highest velocities tended to occur at the mouth of the bay during most months, this pattern was not observed for all months or tide stages.

In March, 1996, the tidal currents across the shelf from Hanks Island (west) to the mouth of Simpson Bay were very low in magnitude (Fig. 20). Surface flows during flood tides appeared to accelerate slightly into the mouth, but this diminished with depth. The opposite situation occurred within the upper arm, however, in which subsurface flows at 25 m. were stronger than the surface flows (Fig. 20a and c). The highest velocities during this month occurred during the ebb tide within the upper northern arm. Here there appeared to be an acceleration in outflow caused by the narrows and shallow reef (Fig 20b).

Surface tidal currents in August, 1996 exhibited marked differences between the two successive flood tides and the two ebb tides (Fig. 21). The currents in the first flood stage indicated an outflow at the mouth and east arm, cross channel flow in the main basin, and inflow within the northern arm (Fig. 21a). The deeper currents, however, showed the inflow expected during the flood tide, resulting in a two layer flow. This type of circulation was most likely related to the strong estuarine conditions that prevailed within the surface layer to about 20 m. depth (Fig. 11c). At all other times of the year the density of the water column was not stratified. The only case during August in which surface and subsurface flows were strongly unidirectional was during flood tide 2 within the main basin (Fig. 21c). Here there is evidence of formation of an anticyclonic eddy resulting when the outflow from the east arm converges with the stronger inflow to the west. Although currents at 25 m. are not shown for this bay, replay of the data revealed that a two layer pattern in the circulation occurred within the east arm and northern arm. A similar situation existed during the ebb tides as well, however, during ebb tide 2 the outflows along the west side near the mouth extended into the subsurface circulation.

In both October, 1996 and 1997 the tidal currents were more similar in pattern than during the other months (Figs. 22 and 23). Surface flows tended to conform with outflow during the ebb tides and inflow during the flood stages, particularly at the mouth of the bay. Although reversals in the direction of the currents are evident, the differences between the surface and subsurface velocities appeared to be caused more by changes in magnitude and some change in direction. However, the strong two layer flow observed in August, 1996 was not evident. Again, this change in pattern was probably a partial response to the return to lower gradients in density that typically occurred during the fall (see Figs. 8f, 11e, and 15c).

Whale Bay

The magnitude of the tidal currents at Whale Bay were generally low (<25 cm/sec) during all months this location was surveyed (Figs. 24 to 27). Whale Bay is a deep fjord with depths exceeding 300 m. within the main basin (Table 1). The two arms are much shallower and silled at about 60 m. depth, however, the main basin has no sill. Depths within the southern arm are over 100 m. inside the sill, but shoal rapidly in the lower portion of the basin. This fjord remains stratified in density through most of the year and currents exhibited varied velocities at depths below the surface layer.

During late winter (March, 1996) the water column was the most uniform in density (Fig. 9a) and the surface currents, though very limited in magnitude, tend to exhibit inflow and outflow with the respective ebb and flood tide stages (Fig. 24). The subsurface flow at 25 m. is primarily into the bay at the mouth, but is highly variable elsewhere over the basin. These data appear to need more processing as well to determine if some vectors are actually bad. In August, 1996 and October of both 1996 and 1997, however, the patterns in the currents are much different, and a moderately strong surface inflow occurred during the ebb tide. This appeared to be the strongest in August, and may be correlated with the period of maximum discharge of glacial water from Icy Bay. The spacial variability in the hydrography within the surface layer was affected by these patterns in tide flow and is discussed below in the final section of this paper.

Surface inflows occurred at the mouth of the bay during the flood tides as well during all three months (Aug.96-Oct.97), but the flow was much reduced in comparison to the inflows of the ebb tide (Figs. 25, 26, and 27). The deeper flows at 25 m. at the mouth showed either outflow or deflection of the stronger ebb currents moving down Knight Island Pass (Figs. 25e, 26e, and 27c). The convergence of currents that occurred at the mouth during both tides apparently was responsible for the formation of ephemeral tidal fronts which were observed to trap flotsam and ice bergs along the convergence lines. Another interesting feature of the circulation on the ebb tide was the tendency for the surface inflow to turn to the right as it enters the lower portion of the main basin. This westward flow was evident at 25 m. depth during the ebb tides for August and October, 1996 (Figs. 25e, 26e, and 27c), but appeared mostly in the surface flow in October, 1997 (Fig. 27c). From the T/S profiles this water appeared to be glacial in origin and tended to be much cooler and slightly lower in salinity. Since its density was less than the surface water outflowing from the southern arm, it probably sinks beneath the outflowing water, forming a frontal zone. Evidence of a convergence zone was observed along the lower portion of the main basin during the cruises and was also evident in the spacial distribution of the hydrography. Individual cast profiles indicated that the cold, fresher layer existed within the main basin only, and this formed a prominent temperature maximum in the profiles where it overlaid the seasonal thermocline.

During the flood tides in August, 1996 and October, 1997, the circulation appeared to reverse between the western and eastern sides of the bay, in which surface currents were outflowing from the western arm and inflowing into the southern arm (Figs. 25b and d, 27b). There was a tendency for this same pattern in October, 1996, however, it was not a very prominent flow (Fig. 26a and d).

Eaglek Bay

The most variable tidal currents from among all four locations occurred within Eaglek Bay (Figs. 28, 29 and 30). During all months and between successive tide stages the currents exhibited strong directional changes which initially raised questions regarding data quality. However, the adcp measured substantially different patterns in the flow field and most of the anomalous vectors are not isolated but occurred in groups, therefore, suggesting that localized characteristics unique to this bay were responsible for what at first appeared to be random motion over many locations of the basin.

In general, the magnitude of the currents was fairly low (10-15 cm/sec), with the exceptions occurring at locations where acceleration of the currents to velocities exceeding 50 cm/sec was evident. These anomalies were possibly caused by both local factors in the bathymetry and differential effects of winds within this bay. The winds were observed to be channeled by the surrounding topography and thus affecting certain regions of the bay strongly and leaving other areas such as the head becalmed. For example, wind directions from the north or northwest typically caused wind to flow only out from the two western arms, creating strong plumes across the bay. Southeasterly winds, however, were observed to be channeled across and down the bay.

The direction of the currents during the ebb and the flood tides tended to vary in both March and October, 1996 (Fig. 28 and 29), with some general inflow for flood tide 3 in March and ebb tide 2 in October. In certain areas of the bay the general direction appeared to change and may correspond with zones of convergence and possibly divergence. This was observed in ebb tide 1 in March, 1996 (Fig. 28b) and also in both the ebb and flood tides in October, 1997 (Fig. 30). Examples of the spacial variability in the surface layer hydrography are presented below, and these provide evidence of horizontal gradients possibly reflecting the downwelling and upwelling associated with the changes in direction in the currents. This bay also exhibited the strongest vertical velocity components as well, and these were mostly negative and associated with downwelling.

Spacial Gradients in the Hydrography Associated with Tidal Currents

This section of the paper involves recent analysis of hydrography data sets collected with the Aquashuttle and Biosonics tow-sled described above in the methods. These instruments were deployed continuously while the vessel was underway conducting surveys of tidal currents, and the resulting continuous profiles were geo-referenced by synchronizing sample time and gps time, then layer averaged for each cast. The midpoint gps coordinates of each depth layer average were used as the latitude and longitude of each cast. Temperature, salinity, fluorescence, and density were averaged over 5 to 10 m, and 20 to 30 m, in depth. Examples of these data will be presented for the surface layer from selected locations to illustrate the effect of the tidal currents in enhancing spacial variability in the surface layer hydrography and the formation of fronts within various regions of the bays.

Late Winter-Early Spring, 1996

In March, 1996 the horizontal gradients of average temperature within the upper 5 to 10 m, were limited due to the highly mixed T/S conditions that typically occur by late winter. However, the ranges in both temperature and salinity varied between most locations, reflecting

the differences in local conditions during winter (Figs. 31 to 34). Eaglek Bay exhibited the lowest temperature and salinity, and also the widest range (2.6 to 3.8 C and 30.7 to 31.7 psu). Simpson Bay had the highest values, but the lowest variance (4 to 4.4 C and 31.5 to 31.8 psu). Whale and Zaikof Bay were similar in temperature range (3.3 to 4.3 C), but Whale was similar to Eaglek in terms of salinity (30.8 to 31.5 psu) which reflects the differences in general between fjords and bays. With the exception of Zaikof Bay, all locations had moderately high fluorescence indicating that the spring phytoplankton bloom had started within most of the nearshore regions.

The spacial distributions in the horizontal T/S gradients within bays and fjords varied substantially, and apparently reflected the unique patterns of the tidal currents within each location. These distributions also changed temporally at Zaikof and Eaglek Bays from a generally less complex gradient from the head to the mouth during ebb tide, to a more complicated distribution on the flood tide (Fig. 31 and 34). This apparently occurs whenever there is inflow of water from outside the basins, which can take place on either tide stage (see previous section on tidal currents). Both of these bays exhibited some evidence of pooling of water with differing T/S properties that may be associated with frontal formation (i.e. divergence and convergence). The marked regions of high to low fluorescence within Eaglek Bay reflected the significant changes in water mass property distribution between tides.

Summer, 1996

The effects of seasonal increases in heat and freshwater were observed in the horizontal T/S gradients of all locations in August, 1996 (Figs. 32, 33, and 35), however, there was also a wide range in these values among locations. The fjord, Whale Bay, exhibited the widest range in average temperature, but also the lowest values in both variables in comparison to the bays (7.5 to 11.0 C, and 25.5 to 27.5 psu). Simpson Bay, as in March, had the lowest overall range in horizontal T/S gradient (12.6 to 13.6 C, and 27.5 to 27.8 psu), however, Zaikof Bay exhibited relatively high values for both variables (12.5 to 14.8 C and 28 to 30 psu). Although Zaikof had a relatively well developed vertical temperature gradient in August, haline stratification was much more limited in comparison to Simpson Bay (Fig. 11c). The well developed halocline in Simpson indicated that vertical stability was higher within this Bay than in Zaikof Bay, which may have contributed to the low range in horizontal gradients observed there. Zaikof Bay, however, tended to remain more mixed seasonally, and the lower stability which results from this fact probably acts to promote more vertical motion within the water column due to the greater amount of current shear that occurs there. Higher vertical velocities were observed within this bay in comparison to either Whale or Simpson Bays.

The spacial distribution of the T/S properties in Whale Bay showed that gradients in both temperature and salinity occurred within the lower portion of the main basin (Fig. 33d and e). This was apparently the edge of a frontal region that results from the surface inflow of cold, lower salinity water from Knight Island Pass (Fig. 25a). The data do not cover the entire transects within the lower reaches of this fjord, and therefore, this phenomenon will be discussed in later months when the data are more complete. Pooling of water with varying T/S properties was evident within Zaikof Bay (Fig. 35). Two adjacent regions appear in which water with opposite properties occurs; one with warmer, less saline conditions indicative of surface water, and one with cooler, more saline conditions indicative of deeper water. These zones possibly

correspond with convergence and divergence of tidal flow respectively, in which deeper water would be upwelled and surface water would be pooled. The higher values of fluorescence are also correlated with the area of potential upwelling (Fig. 35c).

Fall, 1996

In the fall of 1996, the fjord, Whale Bay, exhibited a higher range in horizontal temperature than the two bays (Figs. 35,36 and 37), but of lower values (8.8 to 10 C vs 9.6 to 10 C for Zaikof, and 9.8 to 10.3 C for Simpson). The horizontal salinity values were also lower than those within the bays (25.2 to 25.8 psu), and the highest range occurred within Zaikof Bay (29.2 to 30.2 psu). Simpson Bay was intermediate in terms of horizontal salinity range (28.8 to 29.5 psu), and was the only location to exhibit high values of fluorescence, indicating a fall phytoplankton bloom was occurring there (Fig. 36c).

The data for Zaikof Bay were not complete beyond the mouth of the bay, however, the spacial distribution shows some cross-channel gradients on the ebb tide as were observed in March. The areas of higher salinity evident along the northern side of this bay (Fig. 35e) were also observed in October, 1997, but the pattern was somewhat different (Fig. 38). These may be associated with diverging currents and this possibility will be discussed for October, 1997, when the data were completed for both ebb and flood tides.

Simpson Bay exhibited a change in T/S gradients between the tide stages in which a cross-channel gradient in salinity occurred on the ebb, but became a longitudinal gradient during the flood tide (Fig. 36b and e). The currents associated with these tides are shown in Figure 22a and b. From the vectors there appeared to be some horizontal shear on the west side during both tides, and this seemed to create a consistent cross-channel gradient in temperature, but not salinity. Why this occurred is uncertain, however, the gradient that forms on the ebb tide must be related to water mass properties within the main basin, as this is where the strongest flow occurred.

At Whale Bay the temperature gradient showed a gradual increase in temperature from the mouth inward, however, the gradient in salinity was concentrated along the northeast shore (Fig. 37a and b). These gradients appeared to be related to the inflow at the mouth of the bay, which occurred during both tide stages.

Fall, 1997

In October, 1997 the ranges of the horizontal T/S gradients were greater at all locations than those occurring in the fall, 1996 (Figs. 37,38,39 and 40). The fjords exhibited the highest values of temperature (8.3 to 10.1 C for Whale and 9.0 to 11.0 C for Eaglek). Temperatures were lower in range at the two bays, but tended to be warmer at Simpson than at Zaikof (9.3 to 10 C at Simpson, vs. 8.7 to 9.5 C at Zaikof). The salinity range at Simpson Bay was narrower and the values higher than at Zaikof Bay (29.2 to 29.6 psu vs. 27.4 to 28.6 psu). The two fjords exhibited relatively wider ranges in salinity (25.2 to 26.4 psu for Whale and 27.6 to 29.4 psu for Eaglek). These differences reflect the various conditions occurring locally within the fjords and bays. For example, the wider range in the horizontal salinity gradient at Zaikof Bay in comparison to that of Simpson Bay agrees with the differences in average vertical salinity gradients over the respective basins. The vertical salinity gradient at Simpson Bay was much more uniform (i.e.

more mixed) than that of Zaikof Bay, and thus the higher values and narrower range would be expected there (Fig. 15b). In this same regard, the differences in horizontal T/S gradient values observed between Whale Bay and Eaglek Bay were also apparent from the variance in the hydrography (Fig. 15a). Whale Bay was much cooler and less saline on average within the surface layer than was Eaglek Bay.

The spacial distribution of the horizontal T/S gradients exhibited substantial differences between the ebb and flood tide stages at both Zaikof Bay and Whale Bay (Figs. 38 and 39). In Zaikof Bay the higher salinity water located at mid basin along the north side of the bay during the ebb tide is also slightly warmer, indicating that it is of deeper origin. This would occur over an area of diverging flow, and the currents in this region of the bay show directional changes giving some evidence that this was the case (Fig. 19a). However, the low magnitude does not give a clear indication of flow separation, therefore, the inference was drawn more from the pattern in hydrography. A region of pooled water with lower average temperature and salinity occurred within an area where surface convergence should occur according to the pattern in the currents. Here the stronger inflow into the mouth appeared to converge with outflowing currents and an area of low flow results, which turns to the west (Fig. 19a). Evidence of a tidal front was typically observed within this area of the bay during most cruises.

The changes in spacial distribution of T/S conditions within Whale Bay also appeared related to the tidal currents. The inflow into the mouth of this bay during the ebb tide appeared to move glacially derived water, with much lower average temperature, into the main basin (Figs. 27a and 39a).

The average salinity of this water is slightly lower as well and the tidal currents apparently direct this water westward into the mouth of the west arm, however, the direction of the flow under this layer at 25 m. depth was outward (Fig. 27c). This water mass formed a frontal region located along the southern portion of the main basin, which appeared as both a temperature and salinity horizontal gradient in relation to the more uniform water mass properties occurring within the main basin. The changes occurring during the flood tide were less clear, however, the cross-channel gradients in both temperature and salinity (i.e. density) that occurred within the main basin appeared correlated with an outflow from the west arm and west basin to the mouth and a reciprocal inflow along the eastern basin (Fig. 27b). The inflow continued southward into the lower arm of the bay.

The horizontal T/S gradients for Simpson Bay are shown for the flood tide only (Fig. 37). The tidal flow within this bay appeared to have a considerable eastward tendency within the lower and upper regions of the bay. This pattern was even more evident in the deeper layer (Fig. 23b and d). These currents apparently affected the salinity, producing a cross-channel gradient, but the temperature gradient remained longitudinal (gradually increasing up the bay). A density front resulted from this gradient, particularly at the mouth of the east arm.

Tidal currents within Eaglek bay were very low in magnitude, however, they did exhibit directional changes that indicated possible convergence within the main basin (Fig. 30.). The changes in horizontal distribution of temperature and salinity between the tide stages did not show the marked variability that was observed in late winter, possibly because of the vertical stratification that existed in conjunction with the very small tidal flows (Fig. 15a and 30). There was some evidence at mid basin of a front developing during both tide stages, in which there is a slight gradient in salinity (i.e. density). This is a region of the bay where an inflow appeared to converge with outflow during both the ebb and the flood tides.

Summary and Conclusions

Bays and fjords within Prince William Sound exhibited marked seasonal changes in heat and freshwater content that generally reflected the extremes of the Subarctic climate between summer and winter. Inter-annual variability in the seasonal extremes of the physical water mass properties occurred between 1994 and 1998 at all locations surveyed, and this tended to reflect the general climatic trends towards warmer, drier summers and milder winters, particularly from the summer of 1996 to the spring of 1998. The temperatures of the deep water of both bays and fjords increased over the above time period in response to the increased average air temperatures. However, the most striking changes occurred seasonally in the surface layer temperatures of fjords, which developed much greater vertical temperature gradients than bays during the warmest period in summer of 1997.

General trends in hydrography observed among most locations during the spring and summer of 1994 showed initial surface heating as average air temperatures increased during April and May, however, this was moderated by substantial variance in cold, freshwater input from melting of the lower elevation snowpack along with higher precipitation rates. These factors contributed to the observations of strong sub-regional patterns in freshwater input, especially evident within fjords with high watershed to bay surface area ratios. During the summer of 1994 certain fjords continued to show high rates of surface freshening relative to other regions despite a general drop in the precipitation rate. These increases were presumably from continued melting of higher elevation snow fields, and therefore, watershed characteristics played a large part in influencing seasonal differences in physical properties.

Other factors affecting the hydrography sub-regionally included general differences in basin morphometry and proximity to sources of water derived from fjords with tidewater glaciers. For example, many of the locations within the extreme southwestern part of the sound are narrow, shallow passes which tend to have higher tidal current velocities than most bays and fjords. These areas exhibited much lower vertical T/S gradients during the summer presumably as a result of increased mixing, and this appeared to affect the hydrography within the bays of this sub-region as well which have connections with these passes. Fjords located near the glacial region of Icy Bay exhibited unique temperature characteristics in the T/S signatures which indicated advection of glacially derived water into their main basins.

In the fall and winter the general loss of heat through surface cooling was evident in all bays and fjords, however, the process of vertical mixing occurred much earlier within the bays. Fjords tended to remain stratified well into the late fall, but by late winter the water column of all locations typically became nearly vertically homogeneous.

The tidal current velocities varied substantially among the two bays and two fjords surveyed in 1996 and 1997. The only location which exhibited consistently higher velocities of over 50 cm/sec was Zaikof Bay. Inflows observed during the ebb tides were barotropic, but also exhibited horizontal shear. The portions of the mouth where these flows occurred showed the presence of frontal zones due to convergence with outflows from the bay. Tidal front were also observed during the flood tide where strong inflows tended to create reversals in currents out of the basin along the shoreline. Patterns in the horizontal T/S gradients also indicated formation of zones of convergence and possibly divergence in which water with surface and deeper T/S properties tended to form sequential gradients. The patterns at Simpson and Eaglek Bays were much more variable, however, horizontal T/S gradients occurred on various tides seasonally and indicated the formation of fronts episodically. The patterns in the currents and hydrography at

Whale Bay exhibited surface inflows during both the ebb and flood during all seasons except late winter. However, these flows were baroclinic and varied with depth, showing outflow in the deeper layers during the ebb tide and weak subsurface inflow during the flood tide. Reverse flow was also observed occasionally at 25 m. under the surface flows at ebb tide within both the main basin and the lower arm. The horizontal T/S gradients exhibited evidence of tidal fronts forming at the mouth and lower portions of the deep main basin during the ebb tide and a cross-channel gradient forming during the flood tide: these forming in response to changes in the surface flow between tides.

Conclusions. From this research we can conclude that estuarine conditions within bays and fjords of Prince William Sound generally follow the annual cycles of air temperature and precipitation and as such, would be expected to vary considerably from year to year, similar to annual variation in hydrography within PWS and the North Gulf Coast. However, smaller scale local factors also appear to play a prominent role in determining the relative extent and timing of both surface heating and estuarine conditions. These local factors include the following: 1) relative sizes of bays and fjords and their respective watersheds, 2) topography and aspect, 3) sub-regional variation in precipitation and winds, and 4) proximity to glacial regions.

The sub-regional variability in T/S conditions and circulation patterns of the bays, fjords and smaller passes within PWS may have important implications in the distribution of larval fish species. These areas serve as nursery habitats for salmonid smolts and larval Pacific herring during spring and summer, and as over-wintering areas for juvenile herring. Circulation patterns and their affect on seasonal hydrography and formation of tidal fronts may have influence the biological productivity among these bays and fjords, and serve as mechanisms in either the retention of locally produced larval fish or advection of larval fish into nursery areas. Comparisons of larval and juvenile fish distribution with the physical characteristics of these habitats is the focus of future research on Pacific herring.

Acknowledgments. Weather data from the C-Lab Buoy were provided by Dr. Dave Eslinger with IMS/UAF and data from the PWSAC hatcheries were provided by both Dr. Ted Cooney with IMS/UAF and Mark Summerville with PWSAC. Also I would like to especially thank Dave Janka, Captain of the M/V Auklet, his wife Annette and the crew of the F/V Miss Kayley for their generous assistance and support during the field portions of this project. Funding support for this study was provided by the EVOS Trustee Council as part of the Sound Ecosystem Assessment Project No. 97320M .

REFERENCES

- Colonell, J. M. 1981. Deep Water Renewal in a Subarctic Fjord. *Journal of the Waterway, Port, Coastal and Ocean Division, Proceedings of the Society of Civil Engineers*, Vol. 107, No. WW4, pp. 223 - 231.
- Gay, S.M. III (In review). Seasonal changes in hydrography of embayments and fjords of Prince William Sound, Alaska during spring and summer 1994, fall 1995, and late winter 1996. Submitted in 1996 to *Journal of Marine Systems*.
- Meunch, R. D. and Nebert, D. L., 1973. Physical Oceanography, *Environmental Studies of Port Valdez*, D. W. Hood, W. E. Shiels, and E. J. Kelly, eds., University of Alaska, Fairbanks, Alaska, pp. 103-149.
- Meunch, R. D. and G. M. Schmidt. 1975. Variations in the hydrographic structure of Prince Sound. *Sea Grant Report R75-1*. Institute of Marine Science Report, R75-1, University of Alaska, Fairbanks, 135 pp.
- Meunch, R. D. and D.T. Heggie. 1978. Deep Water Exchange in Alaskan Subarctic Fjords. In *Estuarine Transport Processes*. (Kjerfve, B., ed.) The Belle W. Baruch Library in Marine Science, No. 7, pp. 239-267.
- Niebauer, H. J., T. C. Royer, and T. J. Weingartner 1994. Circulation of Prince William Sound, Alaska. *Journal of Geophysical Research*, Vol. 99, No. C7, pp. 14,113-14,126.
- Pickard, G. L. 1961. Oceanographic Features of Inlets in the British Columbia Mainland Coast.. *J. Fish. Res. Bd. Canada*, 18(6), pp 907- 999.
- Pickard, G. L. 1967. Some oceanographic characteristics of the larger inlets of Southeast Alaska. *J. Fish. Res. Bd. Canada*, 24, pp 1475-1505.
- Pritchard, D. W. 1967. What is an estuary: physical viewpoint. In *Estuaries*: 3-5. G. H. Lauff (editor). American Association for the Advancement of Science Publication No. 83.
- Rattray, M. Jr. 1967. Some aspects of the dynamics of circulations in fjords. In *Estuaries* (ed. G. H. Lauff), American Association for the Advancement of Science pp. 53-62.
- Royer, T. C. 1979. On the effect of precipitation and runoff on coastal circulation in the Gulf of Alaska, *Journal of Physical Oceanography*, 9, 555-563.
- Royer, T. C. 1982. Coastal fresh water discharge in the northeast Pacific. *Journal of Geophysical Research* 87: 2017-2021.
- Walters, R.A., E.G. Josberger and C.L. Driedger. 1988. Columbia Bay, Alaska: an 'Upside Down' Estuary. *Estuarine, Coastal and Shelf Science* 26: 607-617.

LIST OF TABLES AND FIGURES

Table 1. General physiography and observation dates of fjords, bays, and passes within Prince William Sound, Alaska surveyed from Spring 1994 through Late Winter, 1998.

Table 2. Watershed and fjord/bay surface areas, surface area ratios, and mean salinity at 1.0 m depth for 1994, 1995 and 1996.

Figure 1a. Location of Prince William Sound along the south-coastal region of Alaska showing the major geographical features and locations of bays, fjords and nearshore zones surveyed from 1994 to 1998.

Figure 1b. Detail of locations of fjords, bays and passes within subregions surveyed in May, June and July 1994, and locations added during broadscale cruises in fall, 1995 and Late winter, 1996.

Figure 2. Annual air temperature and precipitation cycles for stations within PWS, 1994-1996.

Figure 3. Wind directions and speeds measured at the C-Lab Buoy, 1994 to 1996. Directions and speeds are daily vector averages, low pass filtered by a running average using a 3 day window. Easterly directions are $+90^{\circ}$ and westerly directions are -90° .

Figure 4. Temperature vs. salinity plots for locations sampled in May 1994.

Figure 5. Temperature vs. salinity plots for locations sampled in June 1994.

Figure 6. Temperature contours for Whale Bay and Bainbridge Pass, June 1994 showing the fine scale sub-thermocline maxima and minima. Also shown is the deep temperature minimum below 70 m. depth.

Figure 7. Temperature vs. salinity plots for locations sampled in July 1994.

Figure 8. Temperature vs. salinity plots for locations sampled in October/November 1995.

Figure 9. Temperature vs. salinity plots for locations sampled in March 1996.

Figure 10. Temperature vs. salinity plots for locations sampled in June and July, 1996.

Figure 11. Temperature vs. salinity plots for locations sampled in August and October, 1996.

Figure 12. Temperature vs. salinity plots for locations sampled in November and December, 1996:

Figure 13. Temperature vs. salinity plots for locations sampled in January, February, March, and May.

1997.

Figure 14. Temperature vs. salinity plots for locations sampled in July and August, 1997.

Figure 15. Temperature vs. salinity plots for locations sampled in October, 1997 and March, 1998.

Figure 16. Tidal currents for Zaikof Bay, March 1996.

Figure 17. Tidal currents for Zaikof Bay, August 1996.

Figure 18. Tidal currents for Zaikof Bay, October, 1996

Figure 19. Tidal currents for Zaikof Bay, October, 1997.

Figure 20. Tidal currents for Simpson Bay, March, 1996.

Figure 21. Tidal currents for Simpson Bay, August, 1996.

Figure 22. Tidal currents for Simpson Bay, October, 1996.

Figure 23. Tidal currents for Simpson Bay, October, 1997.

Figure 24. Tidal currents for Whale Bay, March, 1996.

Figure 25. Tidal currents for Whale Bay, August, 1996.

Figure 26. Tidal currents for Whale Bay, October, 1996.

Figure 27. Tidal currents for Whale Bay, October, 1997.

Figure 28. Tidal currents for Eaglek Bay, March, 1996.

Figure 29. Tidal currents for Eaglek Bay, October, 1996.

Figure 30. Tidal currents for Eaglek Bay, October, 1997.

Figure 31. Horizontal contours of temperature, salinity and fluorescence averaged over 5 to 10 m. depth for Zaikof Bay, March, 1996.

Figure 32. Horizontal contours of temperature, salinity and fluorescence averaged over 5 to 10 m. depth for Simpson Bay, March, 1996 (top) and August, 1996 (bottom).

Figure 33. Horizontal contours of temperature, salinity and fluorescence averaged over 5 to 10 m. depth for Whale Bay, March, 1996 (top) and August, 1996 (bottom).

Figure 34. Horizontal contours of temperature, salinity and fluorescence averaged over 5 to 10 m. depth for Eaglek Bay, March, 1996.

Figure 35. Horizontal contours of temperature, salinity and fluorescence averaged over 5 to 10 m. depth for Zaikof Bay, August 1996 (top), and October, 1996 (bottom).

Figure 36. Horizontal contours of temperature, salinity and fluorescence averaged over 5 to 10 m. depth for Simpson Bay, October, 1996.

Figure 37. Horizontal contours of temperature, salinity, fluorescence, and density averaged over 5 to 10 m. depth for Whale Bay, October 1996 (top), and Simpson Bay, October, 1997 (bottom)

Figure 38. Horizontal contours of temperature, salinity and density averaged over 5 to 10 m. depth for Zaikof Bay, October, 1997.

Figure 39. Horizontal contours of temperature, salinity and density averaged over 5 to 10 m. depth for Whale Bay, October, 1997.

Figure 40. Horizontal contours of temperature, salinity and density averaged over 5 to 10 m. depth for Eaglek Bay, October, 1997.

Table 1. General physiography and observation dates of fjords, bays and passes within Prince William Sound, Alaska sampled from May 1994 through March, 1998.

<u>Location</u>	<u>Median Width (km)</u>	<u>Maximum Length (km)</u>	<u>Basin Depth (m)</u>	<u>Sill Depth (m)</u>	<u>Observation Period (month/year)</u>	<u>No. of Ctd Stations</u>
<i>Western and Northwestern PWS:</i>						
<i>Region 1.</i>						
Herring Bay	3.70	9.3	230	unsilled	May, June, July 94; Oct. 95	22
Drier Bay	2.80	11.1	180	40 - 60	June, July 94; Mar., July 96	16
Long Channel	0.75	7.5	50-200	unsilled	June, July 94	8
Mummy Bay	1.30	7.5	100	unsilled	July 94	9
Little Bay	0.90	1.8	50	unsilled	July 94	3
<i>Region 2.</i>						
South Bay	1.85	3.2	160	unsilled	May, June 94	9
Culross Bay	0.65	3.0	170	unsilled	May 94	8
N. Applegate I.	---	---	---	nearshore	May 94	5
W. Twin Bay	0.90	5.0	80	unsilled	May 94	6
Quillion Bay	0.37	2.8	60	unsilled	May 94	5
<i>Region 3.</i>						
Main Bay	1.40	5.2	160	50	May, June 94	8
Eshamy Bay	1.85	3.2	200	50 - 60	May, June 94	14
W. Crafton I.	---	---	---	nearshore	May, June 94	4
Ewan Bay	1.00	5.6	100	unsilled	Mar., July 96	3
Paddy Bay	0.74	4.1	100	unsilled	Mar., July 96	5
<i>Southwestern PWS:</i>						
<i>Region 4.</i>						
Whale Bay	2.80 ¹	4.2 ¹	280	unsilled	June, July 94; Oct. 95 Mar., July, Aug., Oct., Nov. 96 Feb., Mar., May, Jul., Aug., Oct. 97; Mar. 98	17
Bainbridge Pass	2.00 ²	6.3 ²	340	unsilled	June, July 94	14
Shelter Bay	0.70	3.7	100	unsilled	June 94	12
Flemming I.	---	---	120	nearshore	June, July 94	6
N. Prince of Wales P.	---	---	130	pass	June, July 94	14
<i>Region 5.</i>						
Sawmill Bay	0.70	4.8	160	60	Nov. 95	6
N. Elrington Pass	---	---	70	pass	July 94; Nov 95; July 96	9
Hogg Bay	8.33	1.8	120	unsilled	Nov 95	8
L. Bainbridge Pass	---	---	90	unsilled	Nov 95	3

Table 1. (Continued)

Northern PWS:

Jack Bay	0.93	10.2	200	30	Nov 95; Mar., Jul. 96	12
Galena Bay	1.50	8.3	200	25	Mar., Jul. 96	6
Eaglek Bay	3.70	14.4	200	unsilled	Nov 95; Mar., Jun., Jul., Aug., Oct. 96 Mar., May, Jul., Aug., Oct. 97; Mar. 98	16

Eastern PWS:

Sheep Bay	3.50	13.8	80	unsilled	Mar. 96; Jul 96	5
Port Gravina	---	---	80		Mar., Jul. 96	8
Port Fidalgo	---	---	100		Jul. 96	2
Knowles Head	---	---	60		Nov. 95	12
Snug Corner Cove	---	---	120		Nov. 95	11
Simpson Bay	1.70	9.5	90	unsilled	Oct 95; Mar., Jun., Jul., Aug., Oct., Nov., Dec. 96; Jan., Feb., Mar., May, Jul., Aug., Oct. 97; Mar. 98	9

South Central PWS:

Green Island	---	---	120		Oct. 95; Mar., Jul. 96	14
Zaikof Bay	3.00	12.9	100	unsilled	Oct 95; Mar., Jun., Aug., Oct., Nov., Dec. 96 Feb., Mar., May, Jul., Aug., Oct. 97; Mar. 98	

Glacial Fjords:

Unakwik Inlet	2.50	30.5	270	4	Mar., Jul., Aug. 96	6
Icy Bay	1.80	18.5	168	30	Mar., Jul. 96; Mar. 98	3
Nassau Fjord	1.90	5.4	350	20 - 30	Mar. 96; Mar. 98	2

1 Data for main basin only; widths of S arm and narrows at SW inlet are 1.5 and 0.7 km respectively, and lengths are 4.1 and 11 km.

2 Data for main basin only; widths of NW and S arms of the fjord are 1.3 and 1.5 km respectively, and lengths are 5.9 and 7.4 km.

Table 2. Watershed and fjord/bay surface areas, area ratios, and mean salinities at 1.0 m depth for 1994, 1995 and 1996.

<u>Location</u>	<u>Watershed Area (ha)</u>	<u>Fjord or Bay Surface Area (ha)</u>	<u>Ratio</u>	<u>May 94</u>	<u>June 94</u>	<u>July 94</u>	<u>Oct/Nov 95</u>	<u>March 96</u>
Herring Bay	2,541	2,088	1.2	27.89	27.49	27.03	25.08	---
Lower Herring	1,639	708	2.3	28.20	26.75	26.13	---	---
Drier Bay	5,091	1,906	2.7	---	26.25	25.04	---	31.50
South Bay	656	526	1.3	29.57	25.65	---	---	---
Culross Bay	3,497	538	6.5	23.37	---	---	---	---
Main Bay	2,732	664	4.1	24.77	22.28	---	---	---
Eshamy Bay	5,637	1,109	5.1	27.38	21.12	---	---	---
Whale Bay	5,411	2,566	2.1	---	23.44	24.16	19.64	30.32
Sawmill Bay	1,092	572	1.9	---	---	26.14	27.22	---
Twin Bays	489	635	0.8	---	---	29.03	---	---
Simpson Bay	16,980	2,792	6.1	---	---	---	27.50	31.20
Jack Bay	13,853	1,429	9.7	---	---	---	27.54	31.84
Zaikof Bay	5,488	2,614	2.1	---	---	---	29.41	31.38
Ewan Bay	2,590	676	3.8	---	---	---	---	31.09
Paddy Bay	1,295	457	2.8	---	---	---	---	31.15

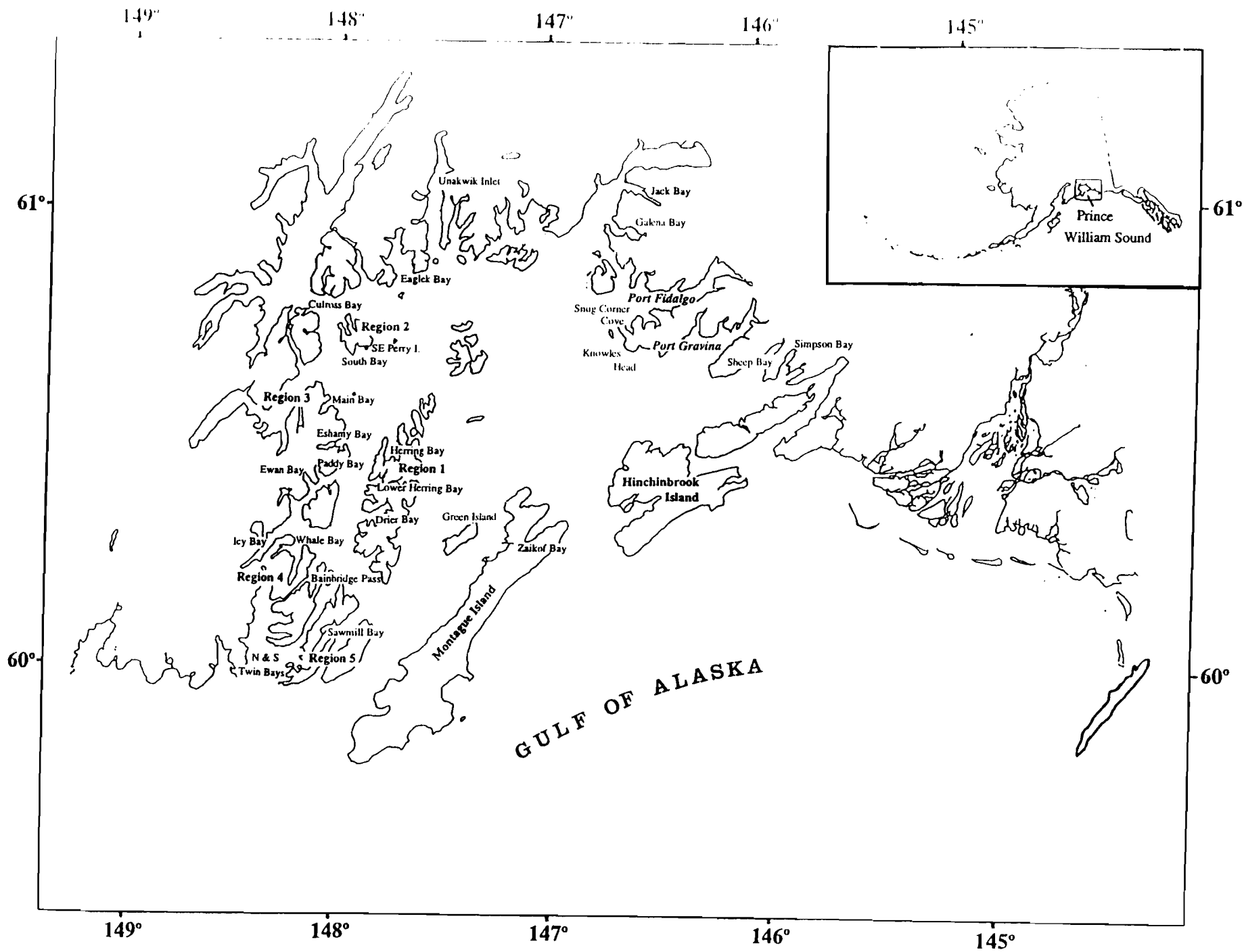


Figure 1a.

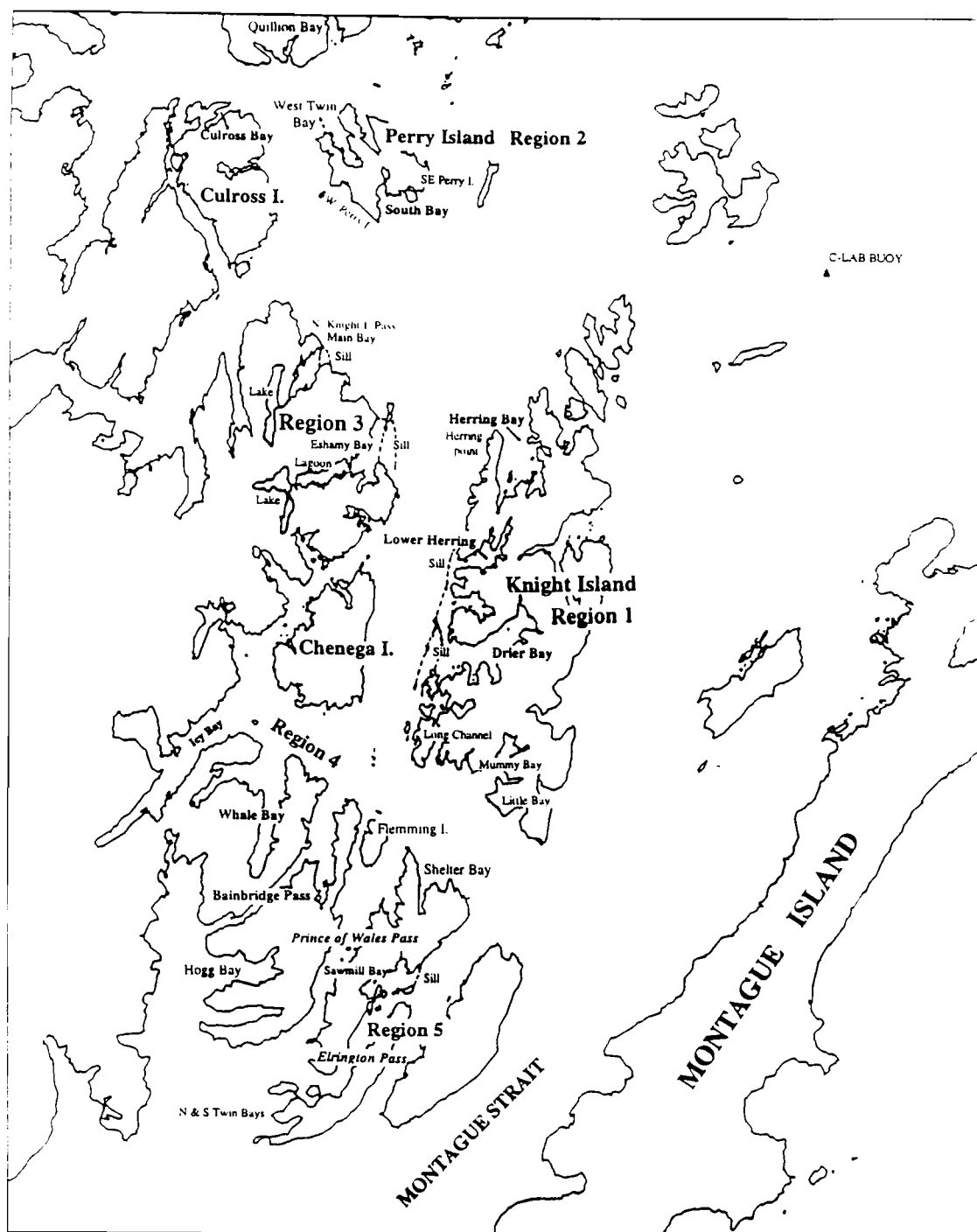


Figure 1b.

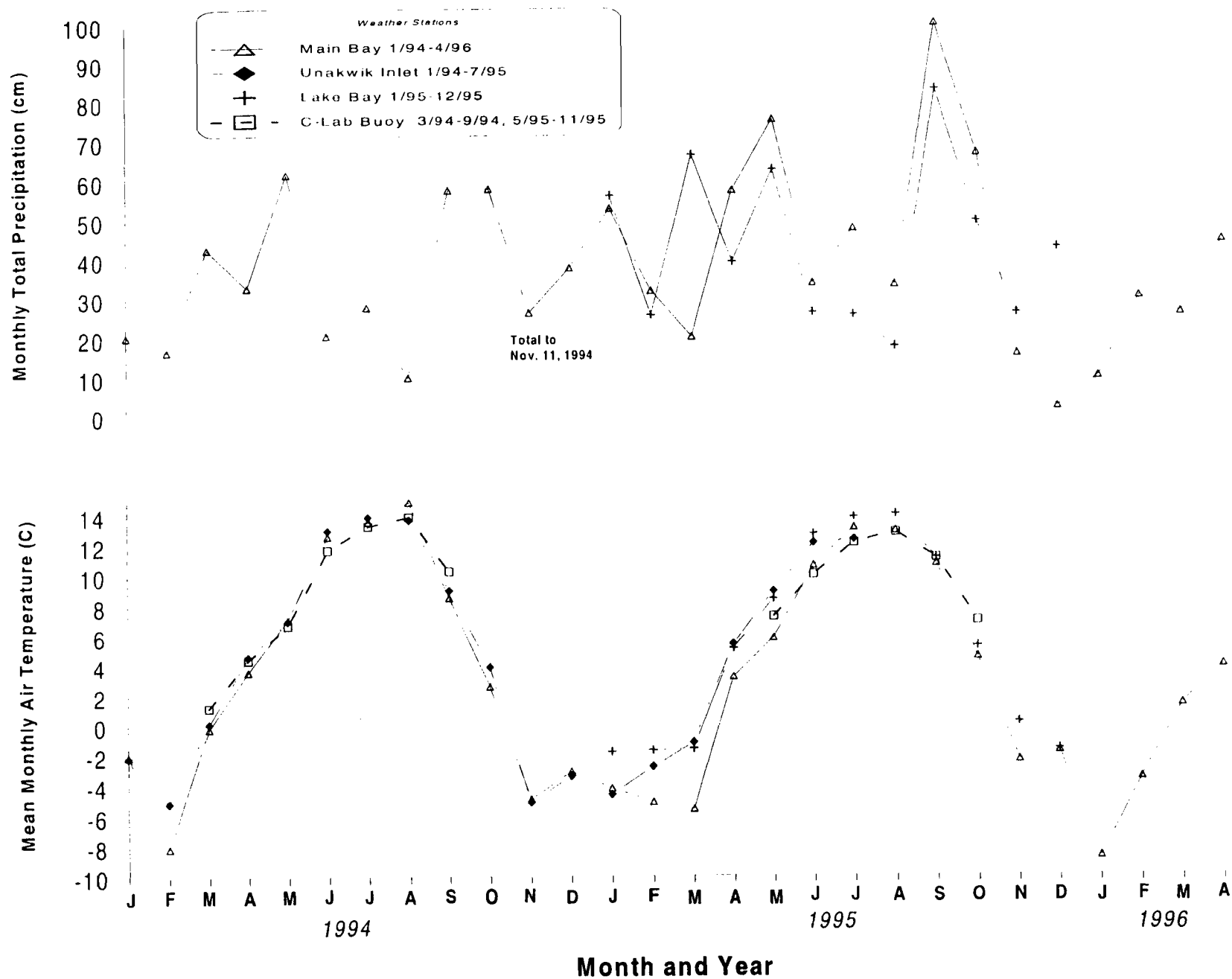


Fig. 2. Annual air temperature and precipitation cycles for stations within PWS. 1994-1996

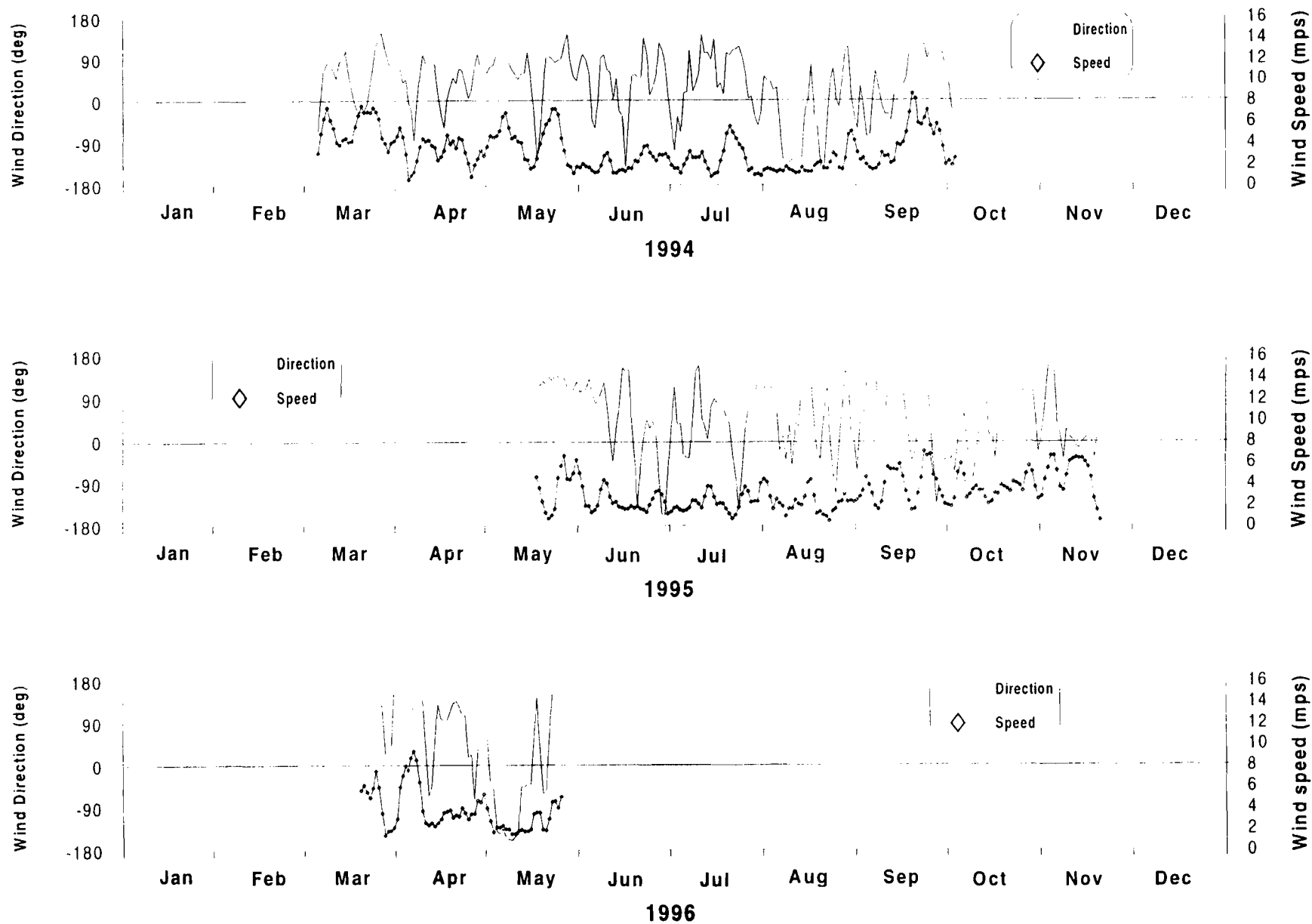


Figure 3. Wind directions and speeds measured at the C-Lab Buoy, 1994 to 1996. Directions and speeds are daily vector averages, low pass filtered by a running average using a 3 day window. Easterly directions are +90 and westerly directions are -90.

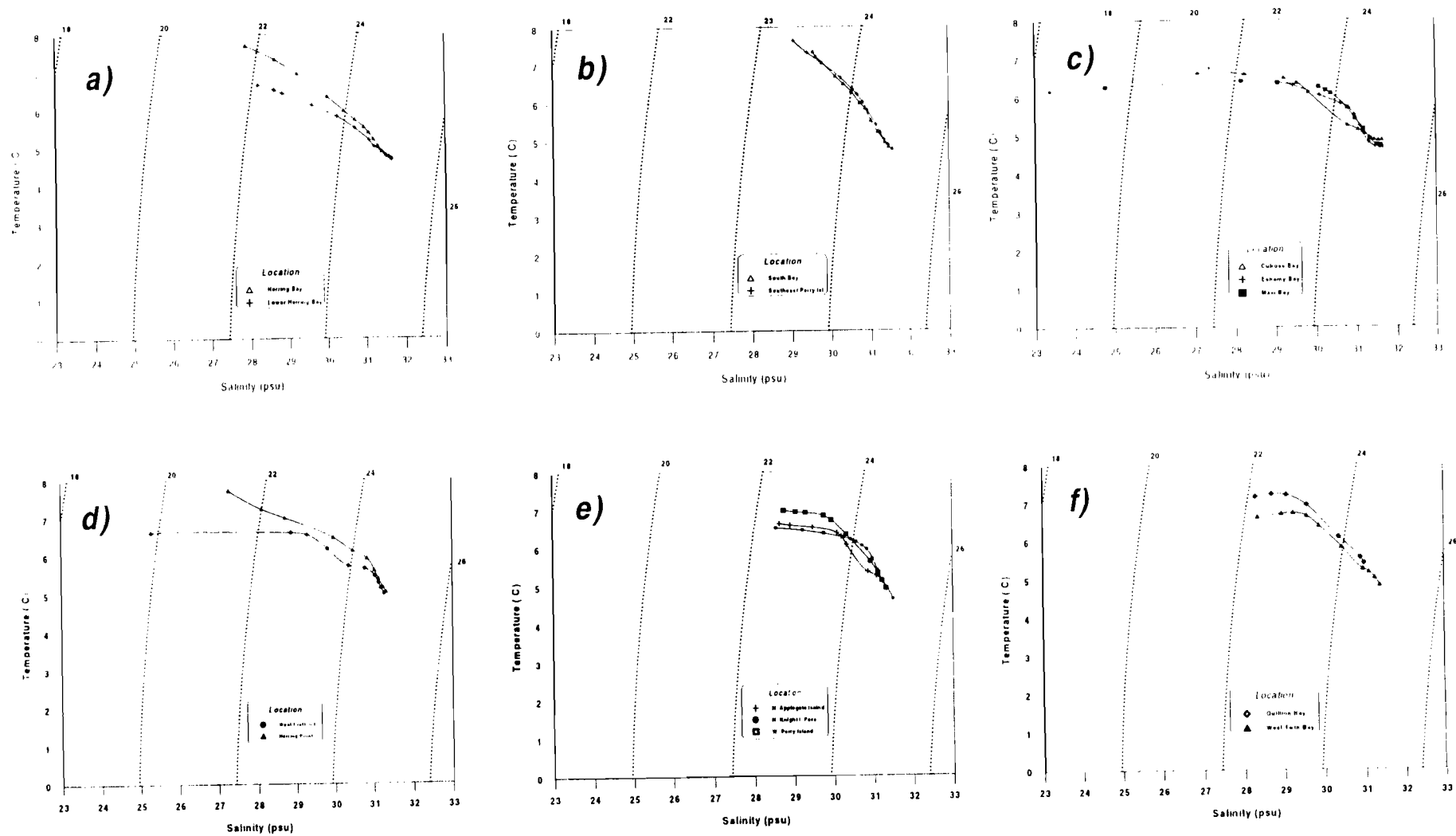


Figure 4

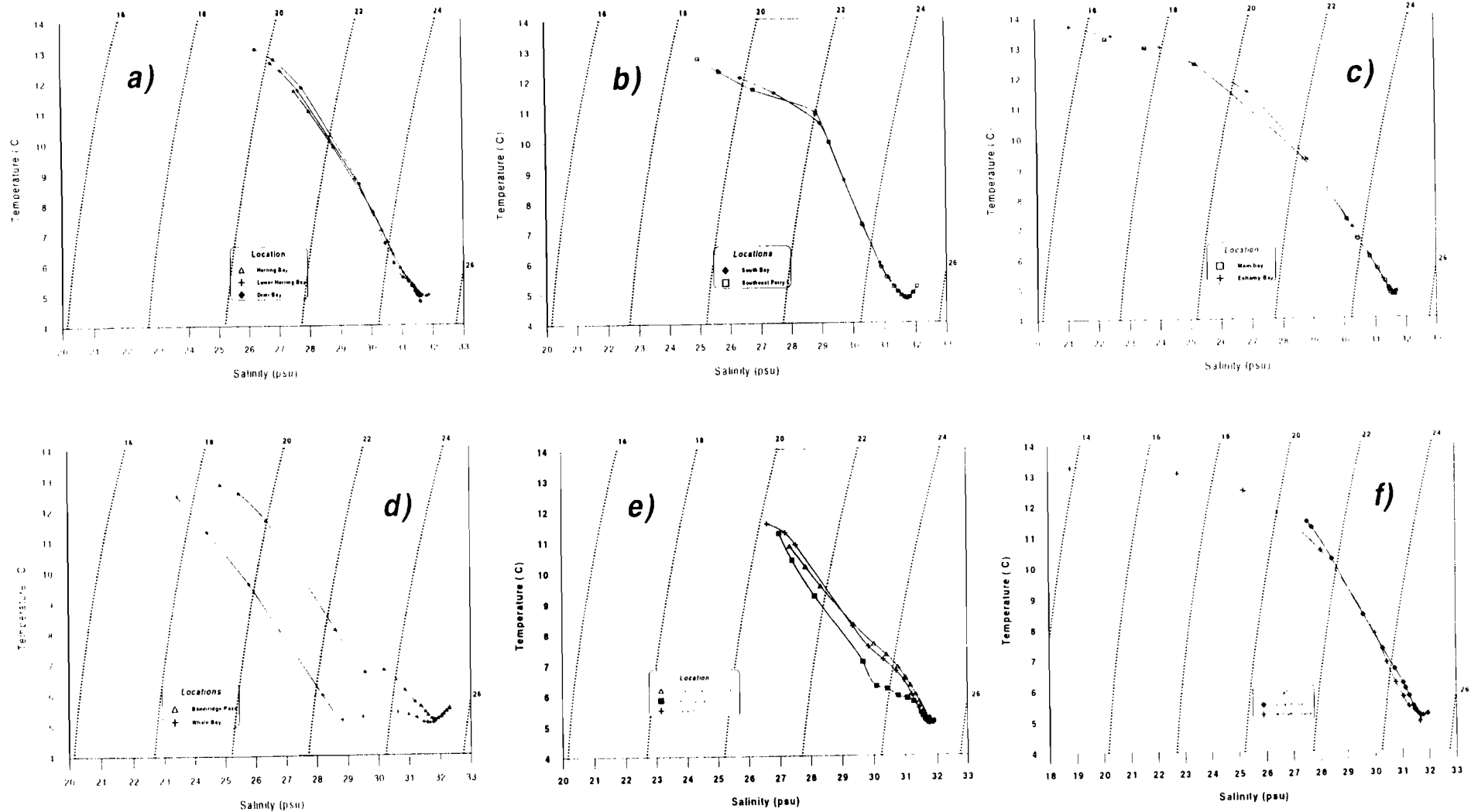


Figure 5.

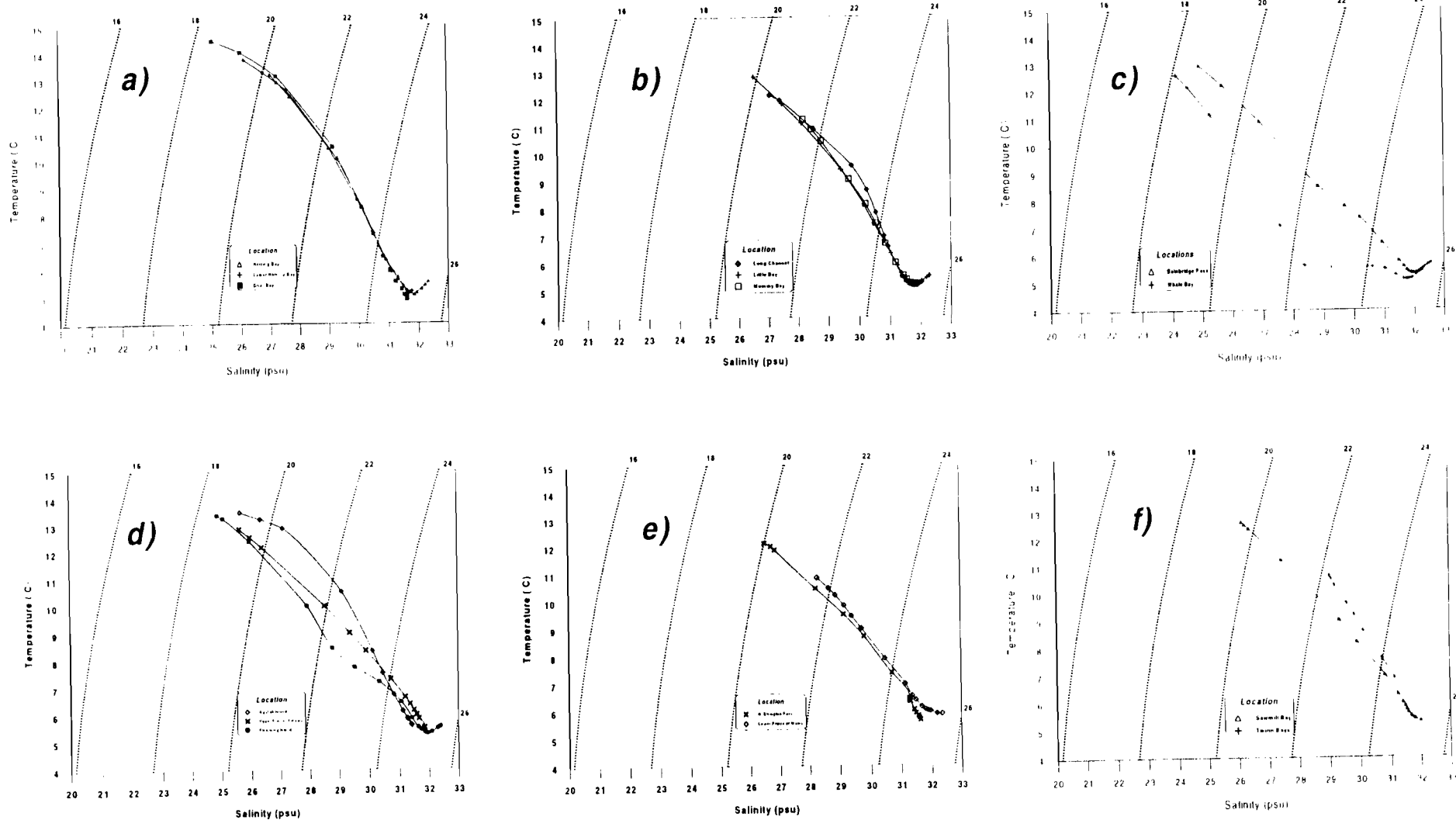


Figure 7.

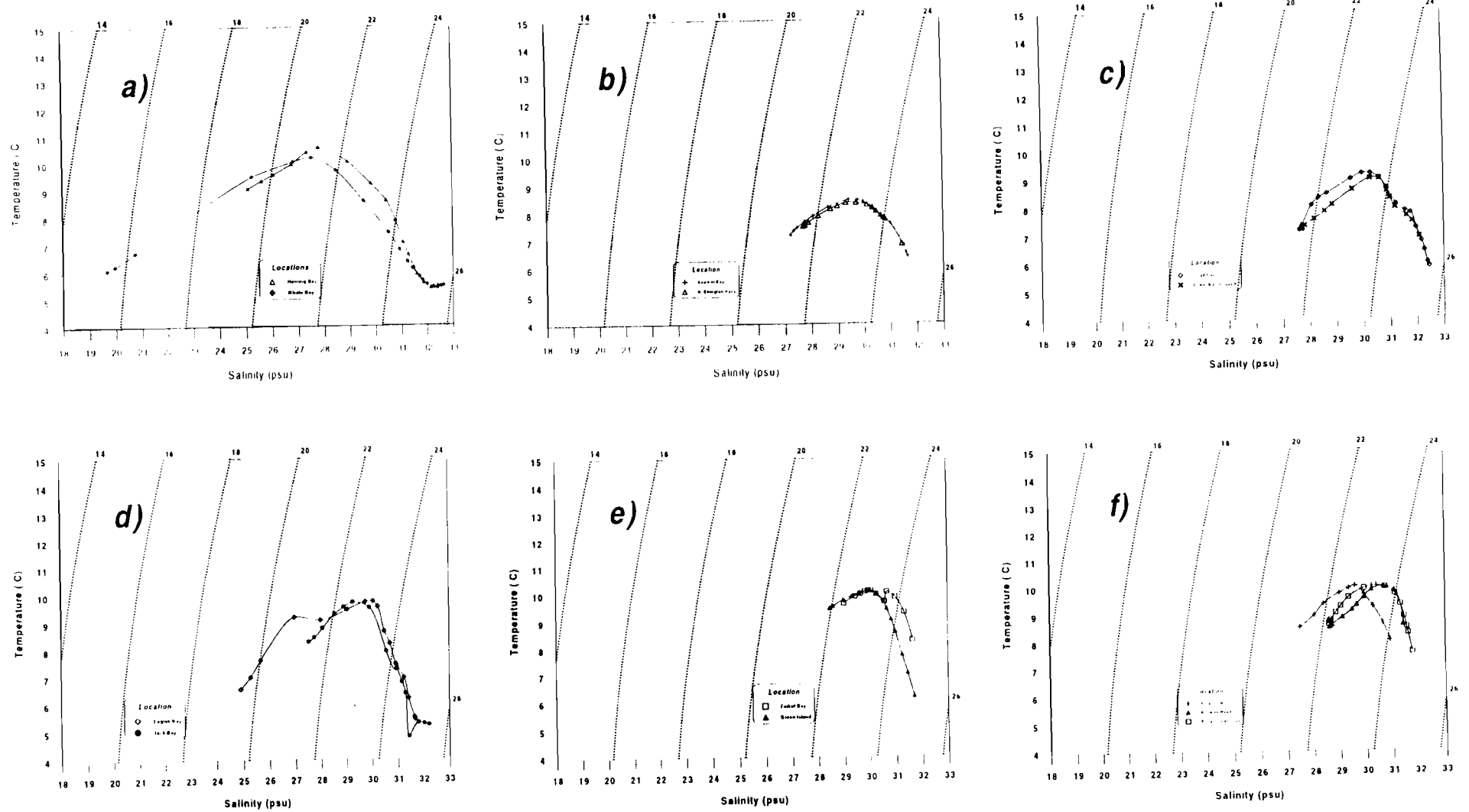


Figure 8.

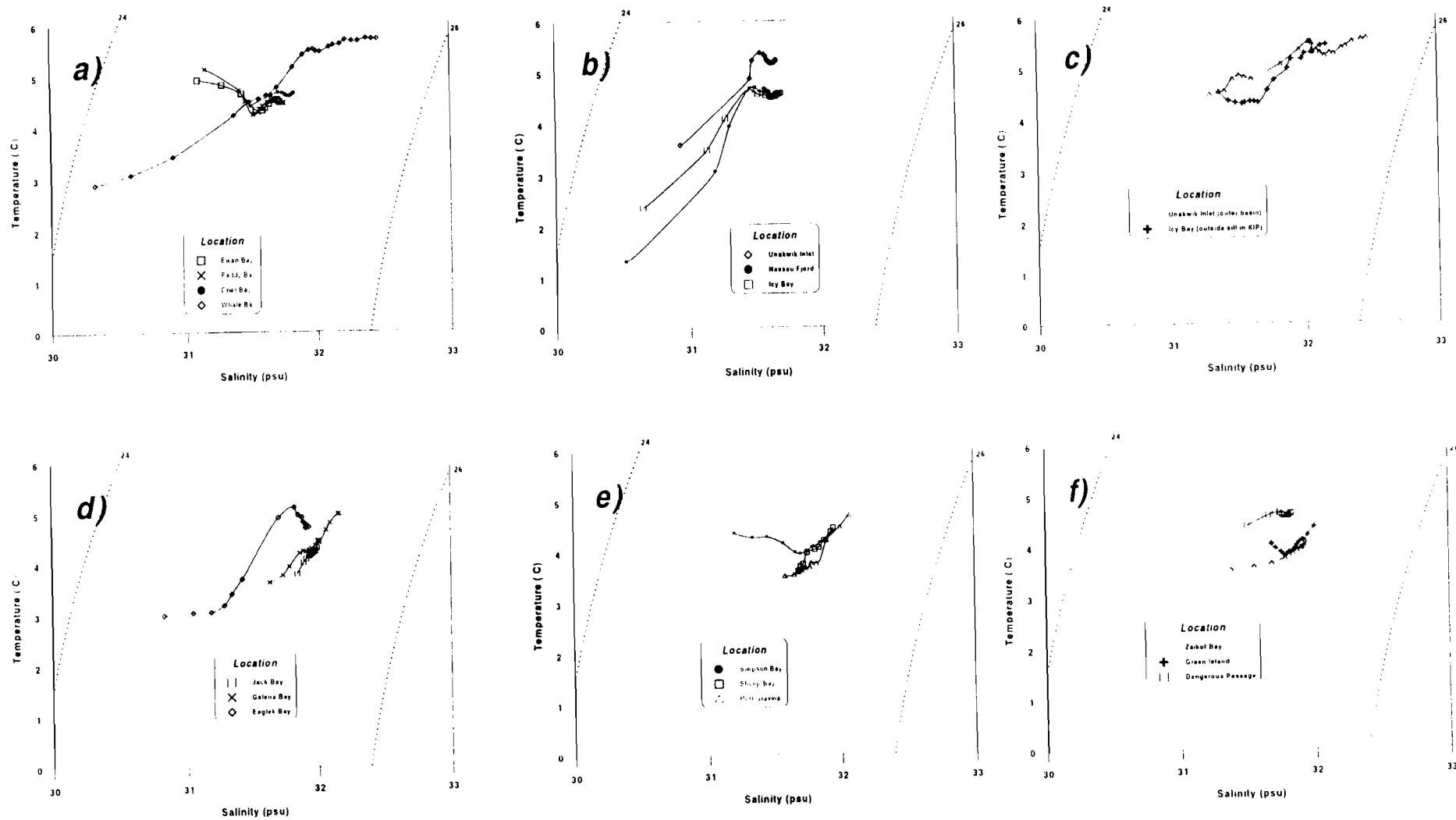


Figure 9.

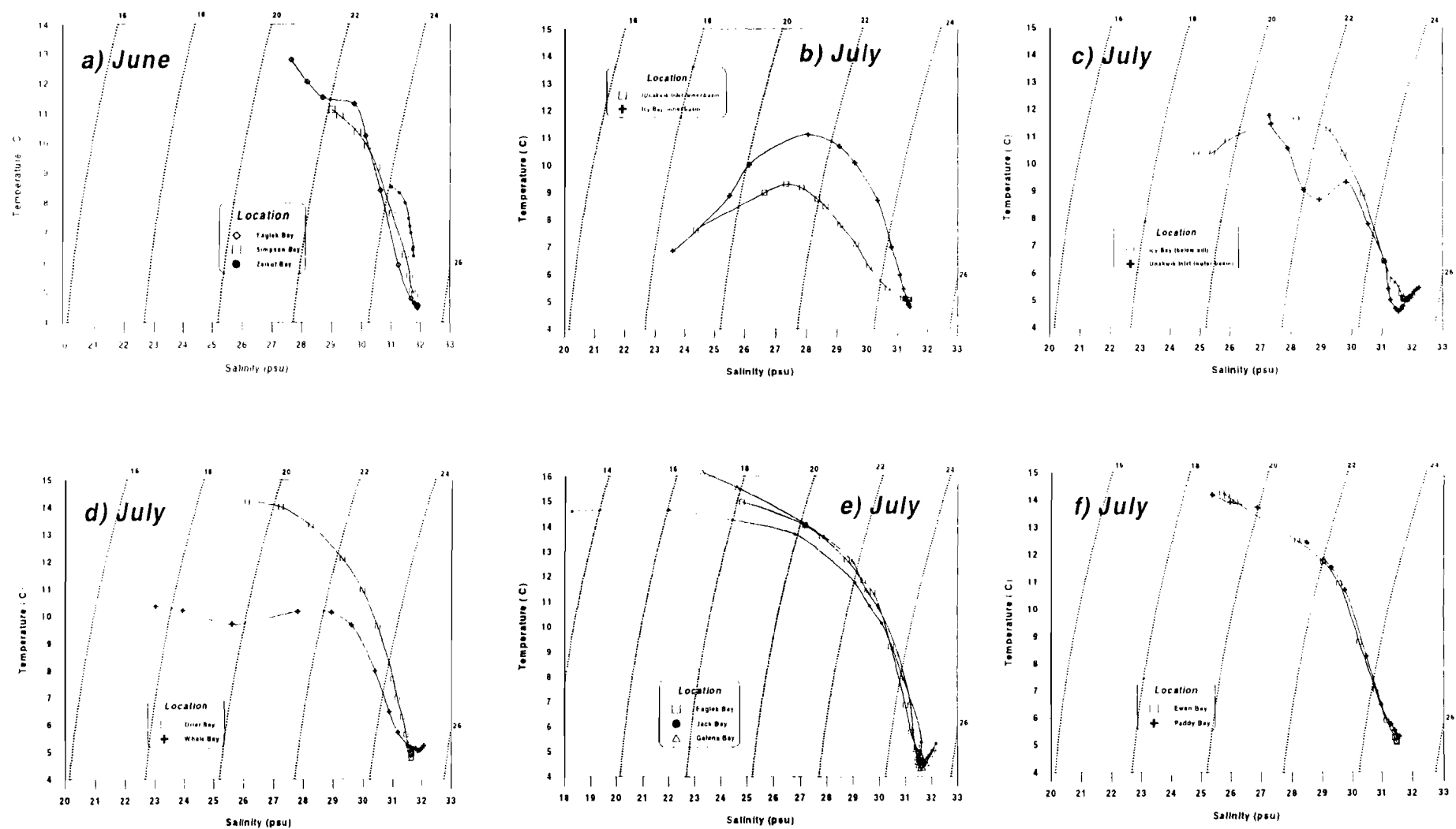


Figure 10.

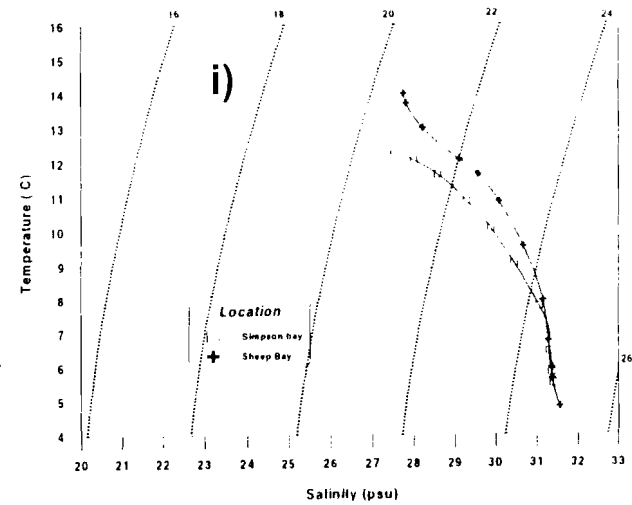
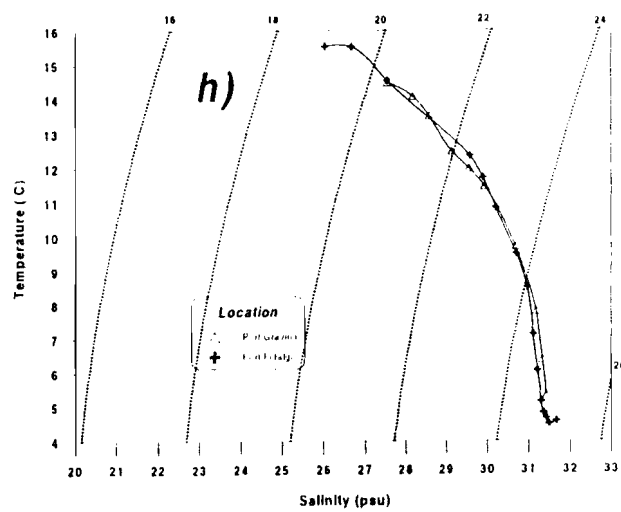
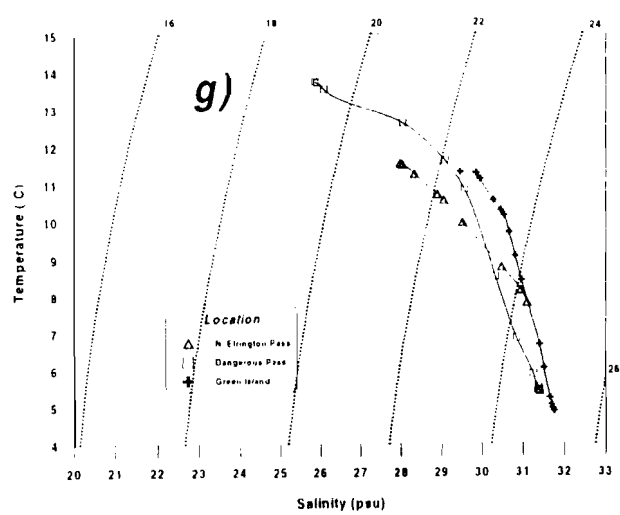


Figure 10 (Continued).

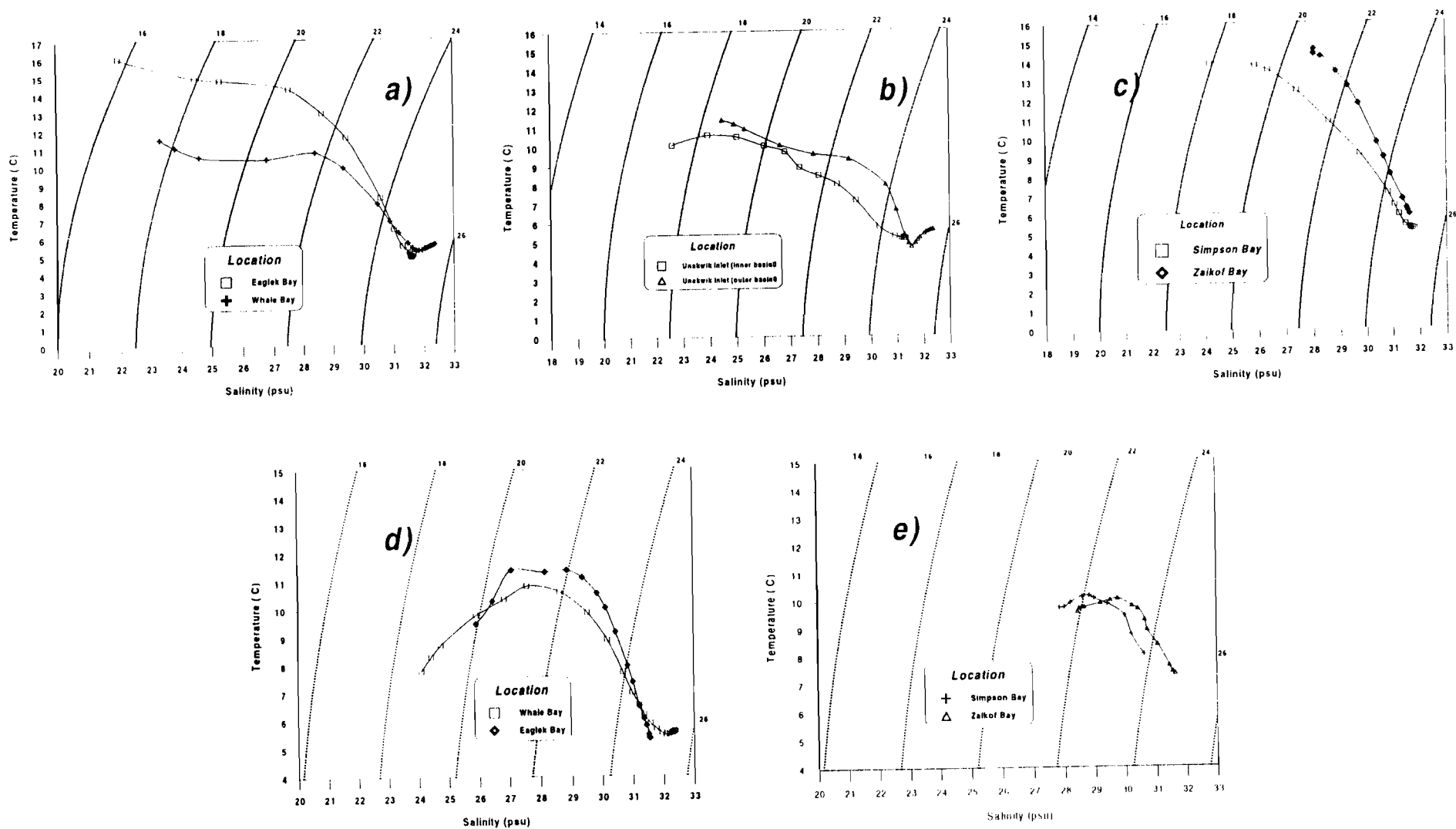


Figure 11.

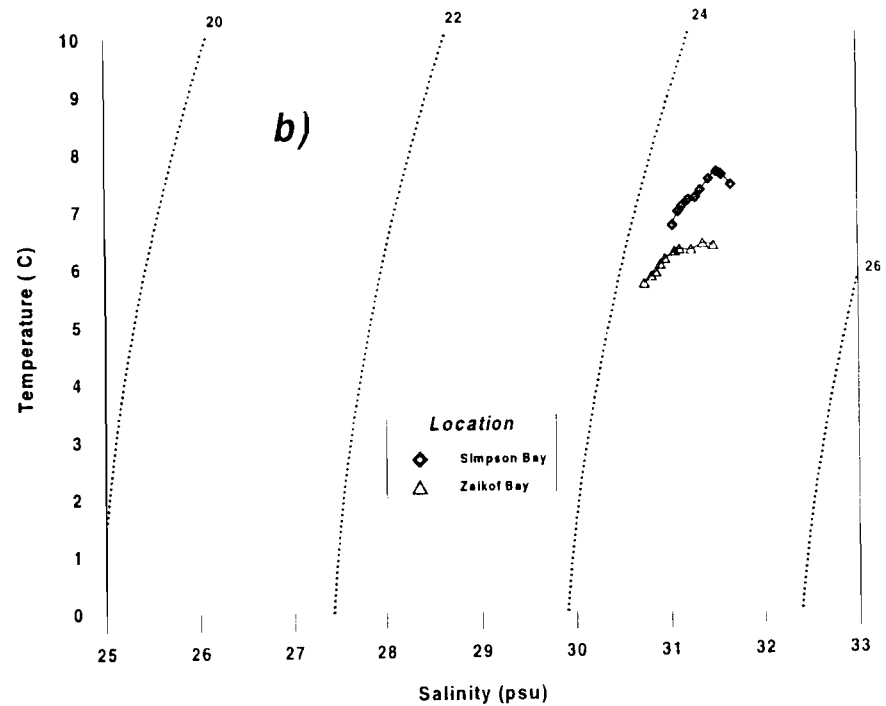
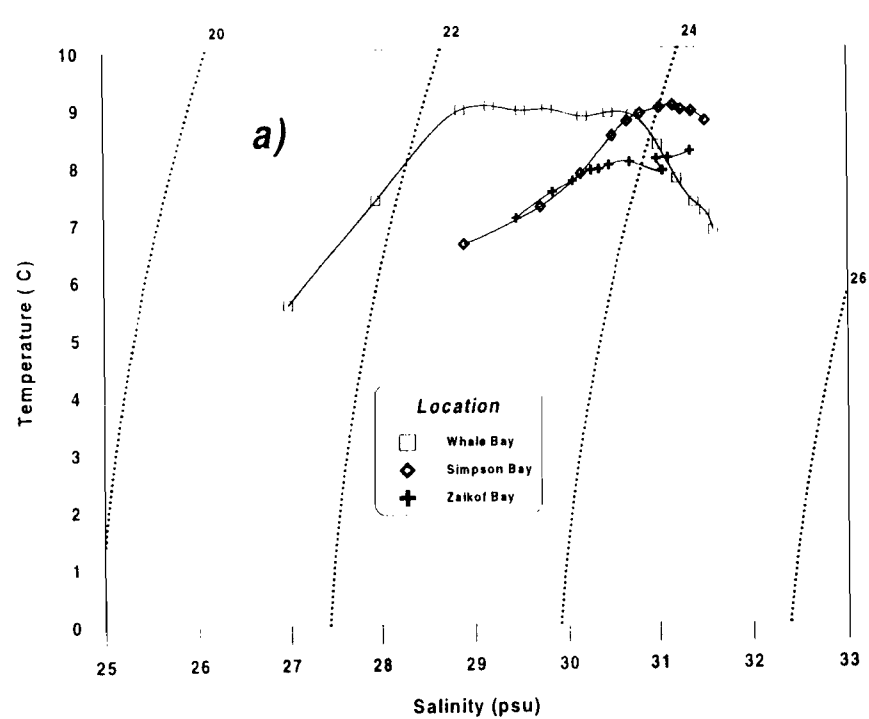


Figure 12.

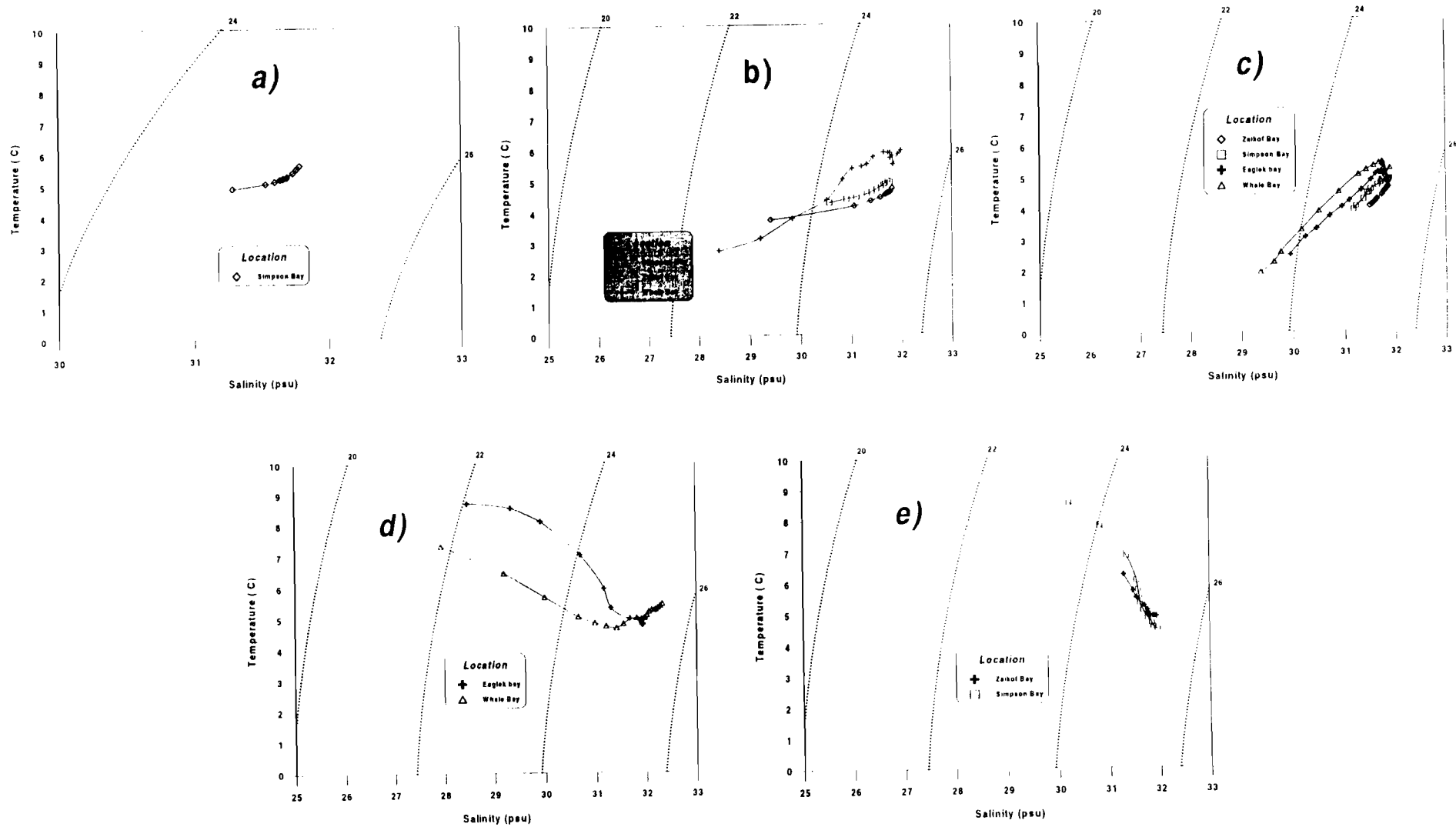


Figure 13.

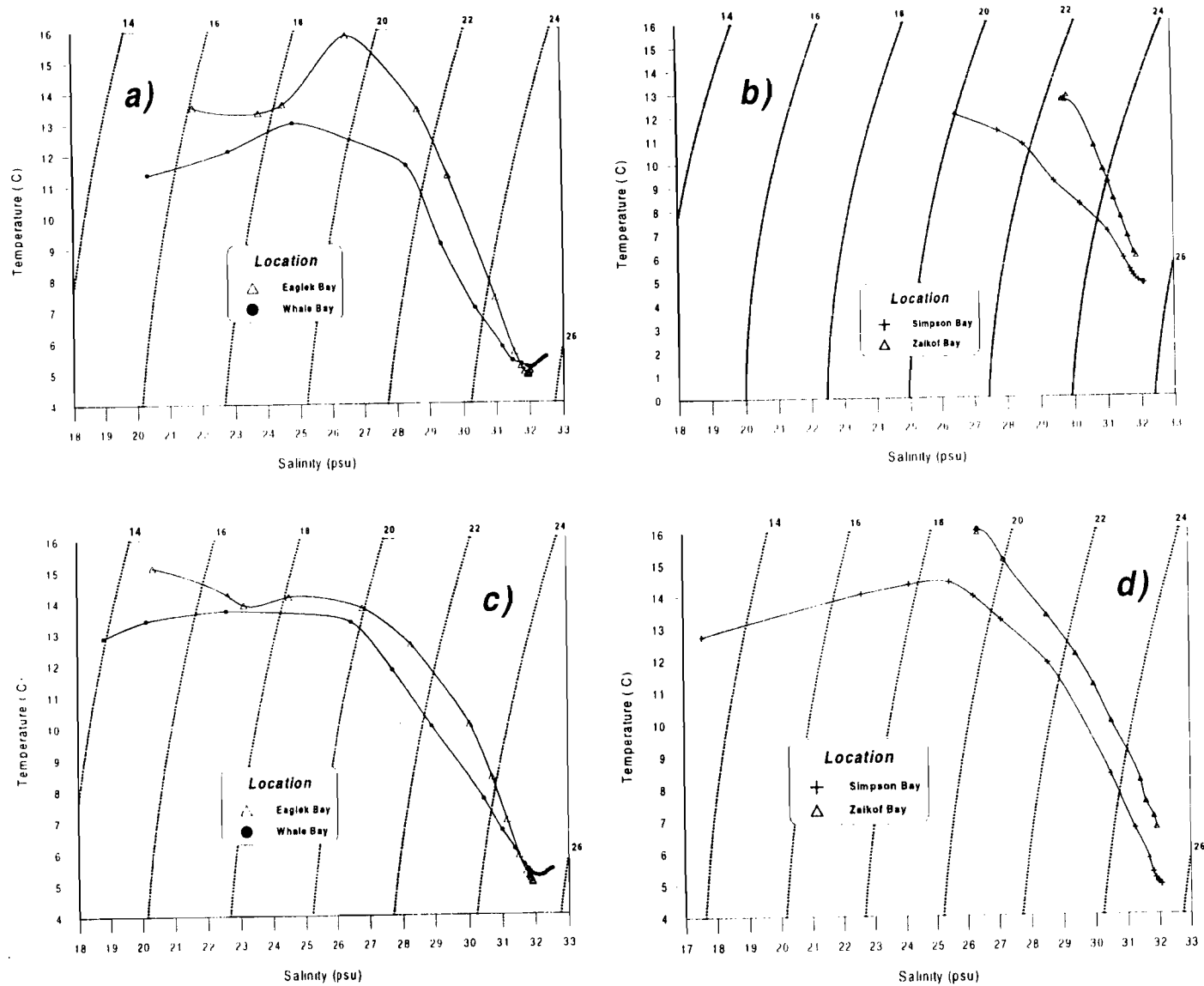


Figure 14.

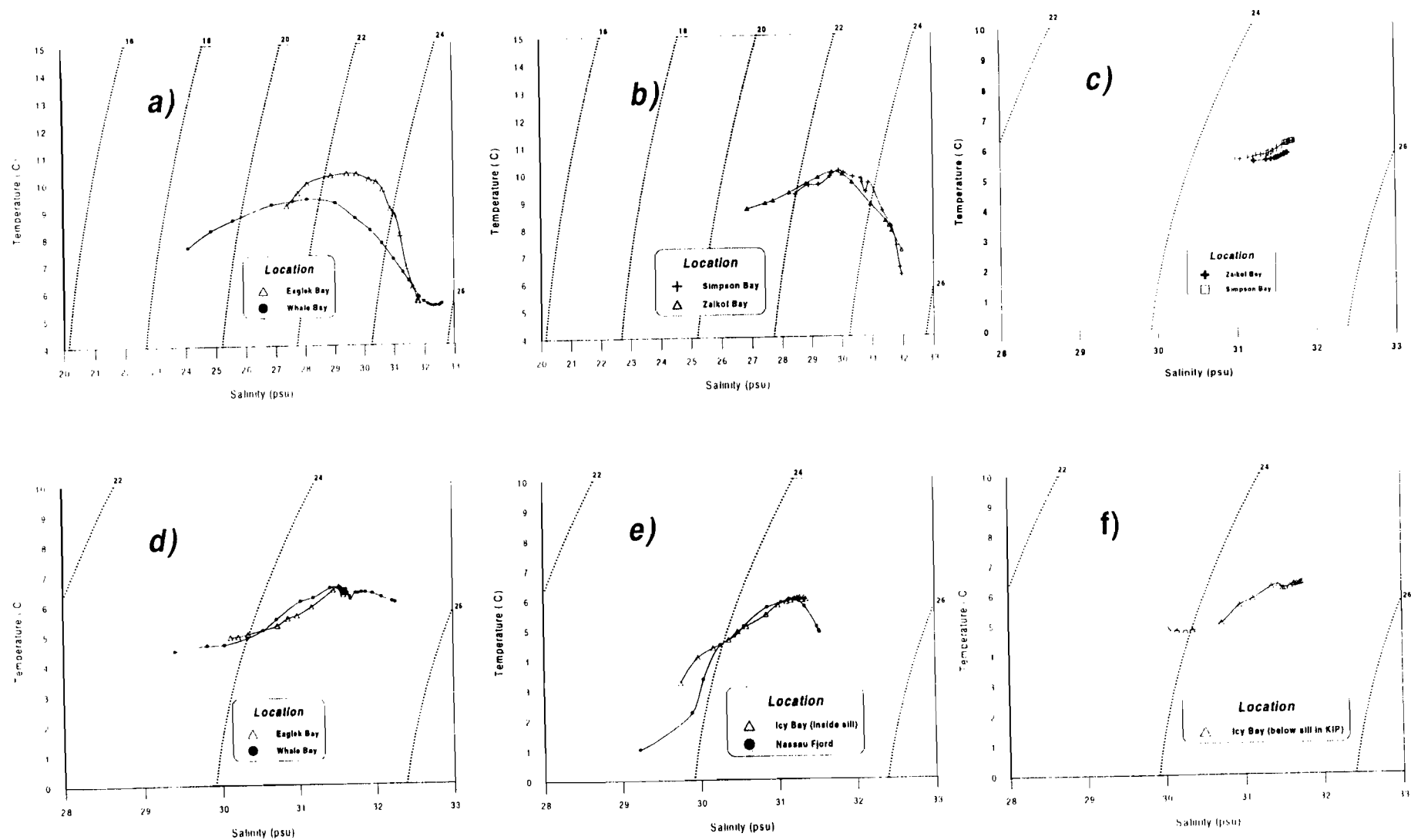


Figure 15.

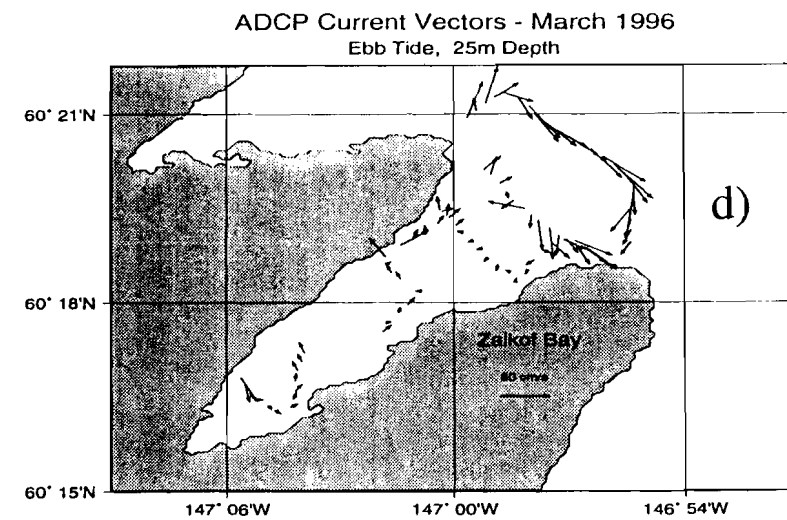
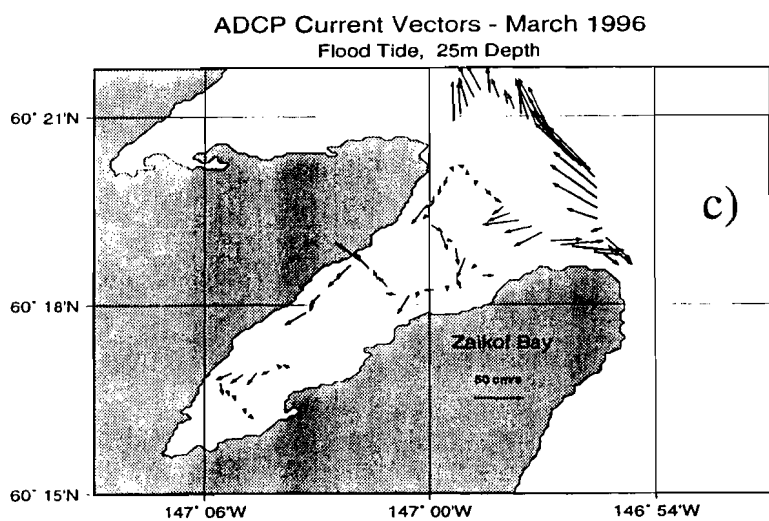
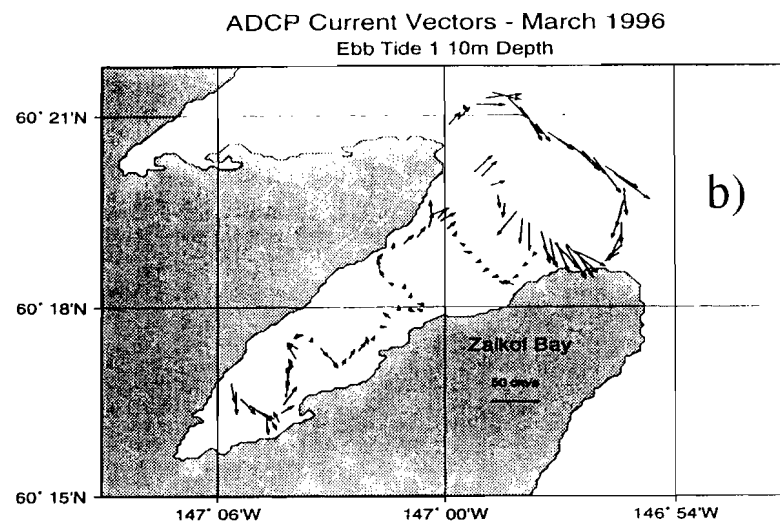
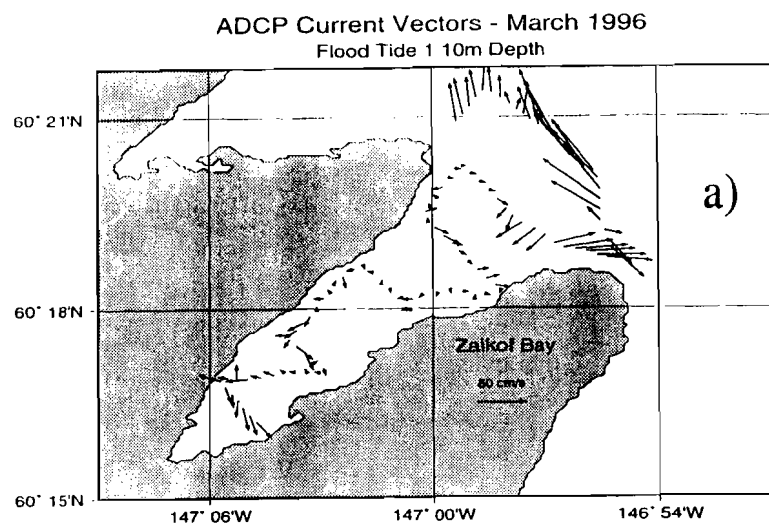


Figure 16. Tidal currents for Zaikof Bay, March 1996 averaged over 8 m. depth bins centered at 10 and 25 m. a) Flood tide, 10 m., b) ebb tide, 10 m., c) flood tide, 25 m., and d) ebb tide, 25 m.

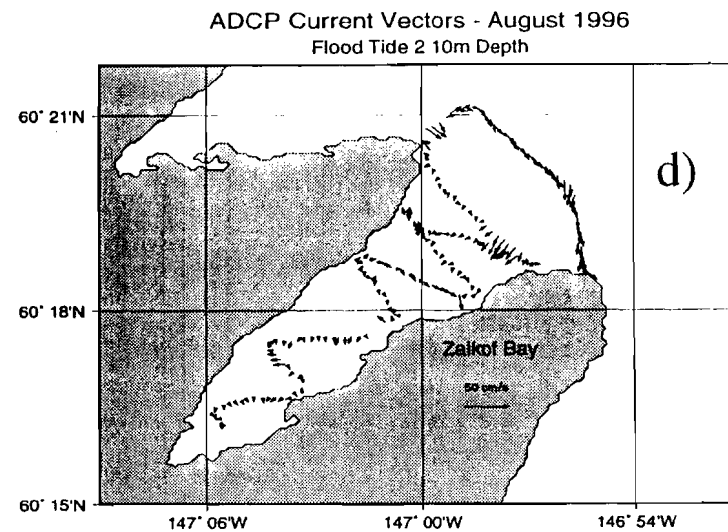
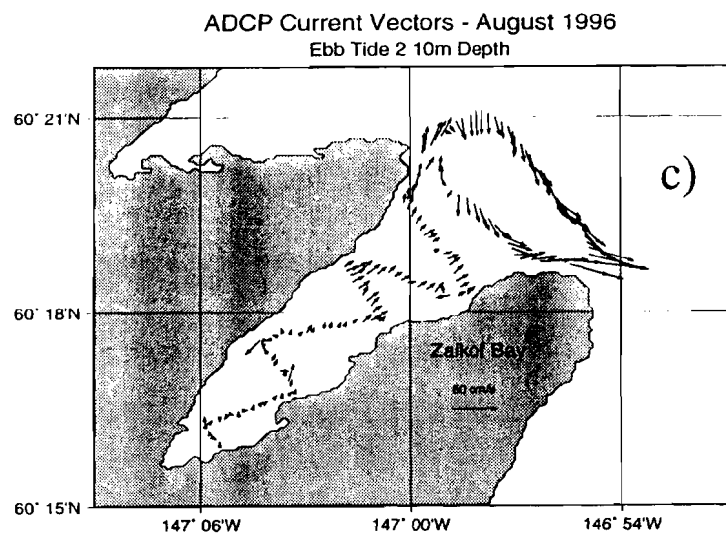
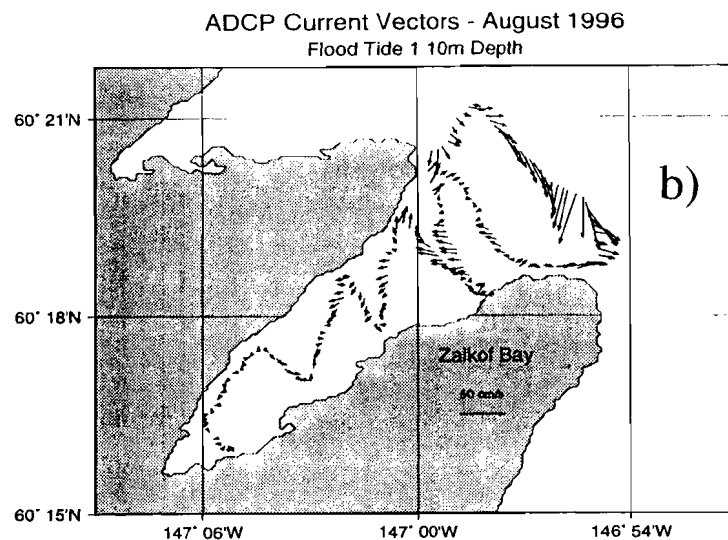
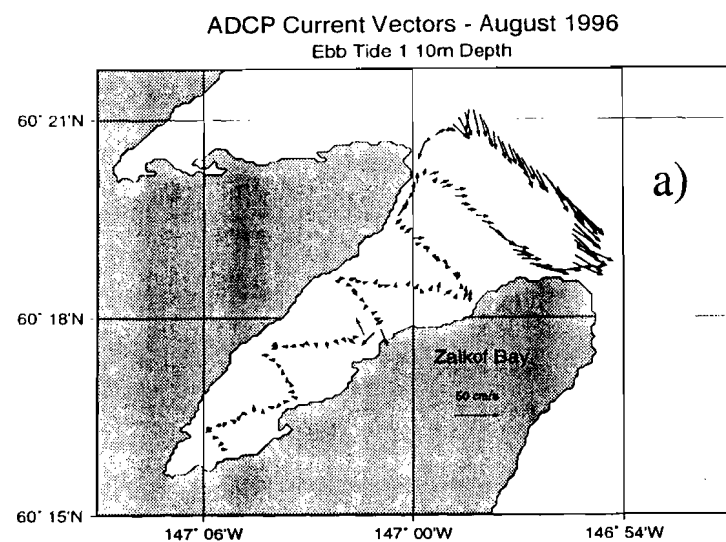


Figure 17. Tidal currents for Zaikof Bay, August 1996 averaged over 8 m. depth bins centered at 10 m. Complete semidiurnal cycle shown for first ebb and flood tides (a and b), and the second ebb and flood tides (c and d).

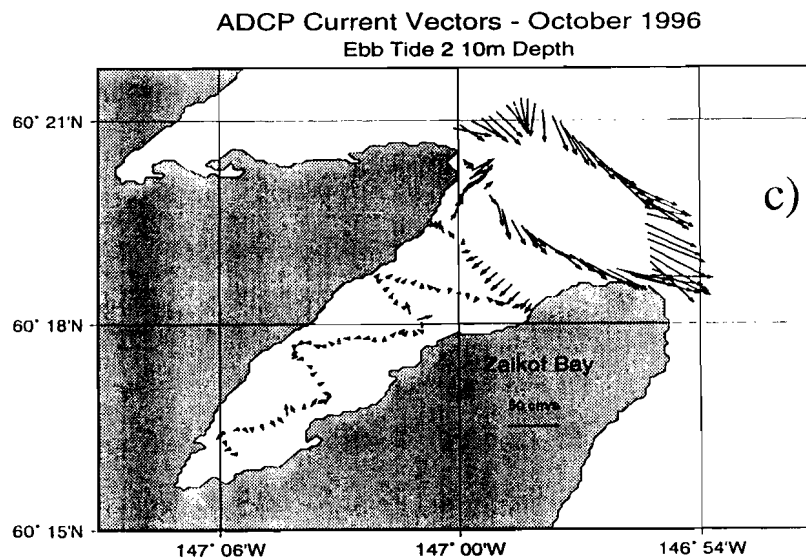
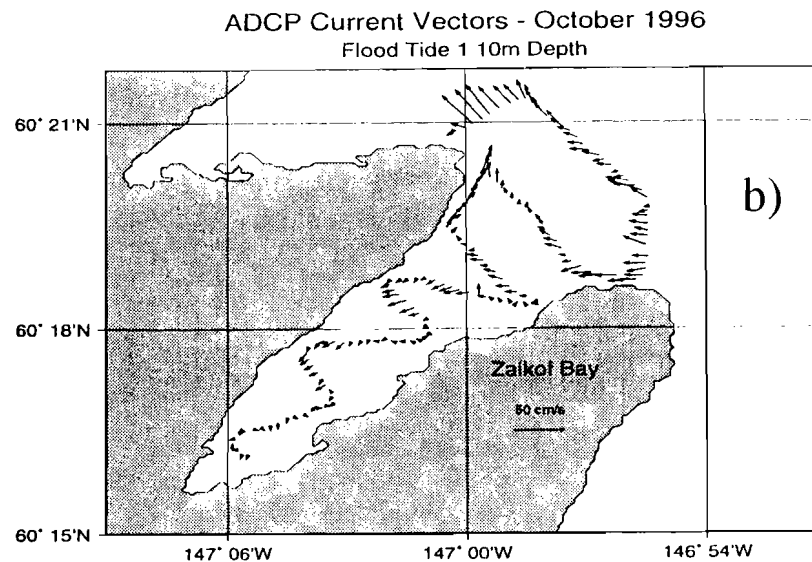
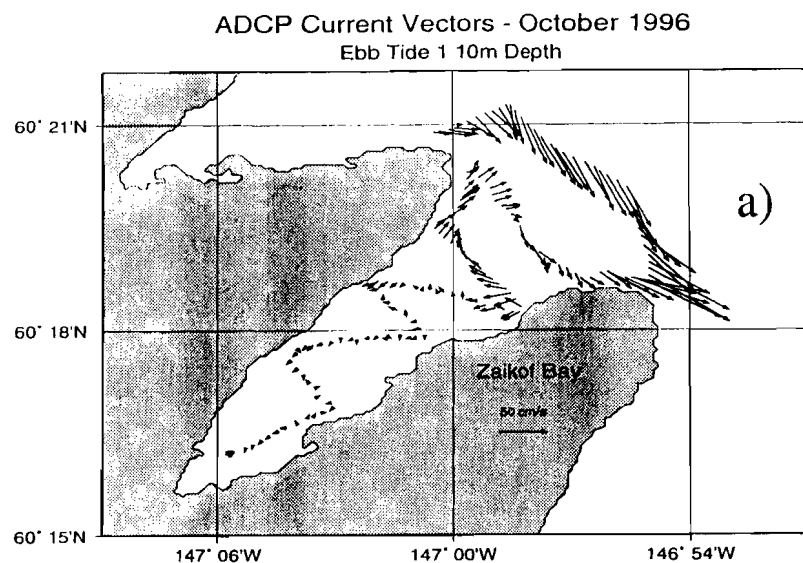


Figure 18. Tidal currents for Zaikof Bay, October 1996 averaged over 8 m. depth bins centered at 10 m. First part of the semidiurnal cycle shown for ebb and flood (a and b), and second ebb tide (c).

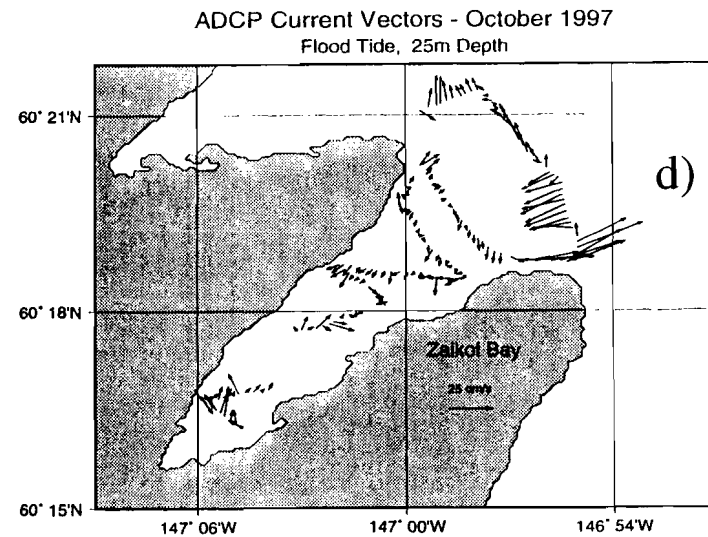
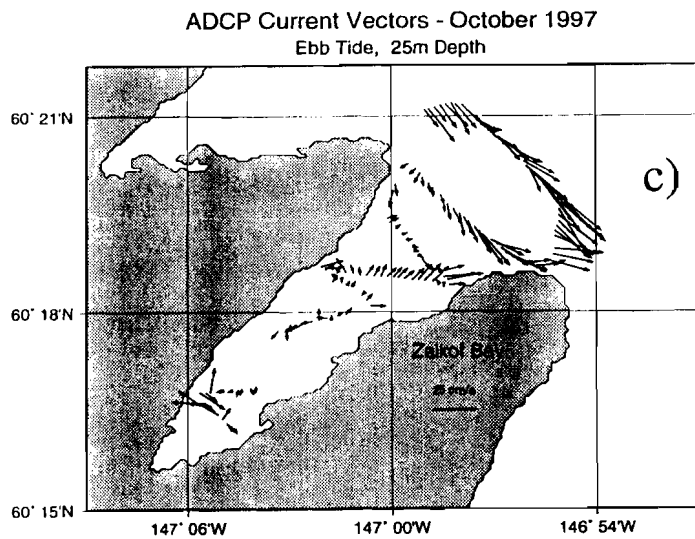
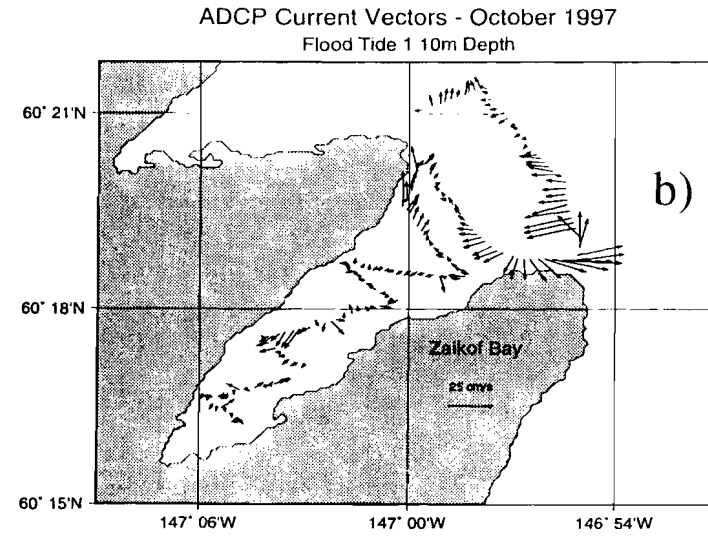
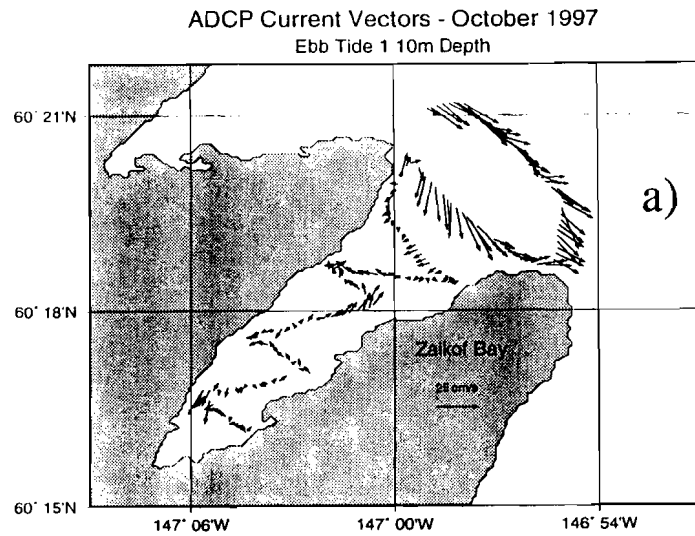
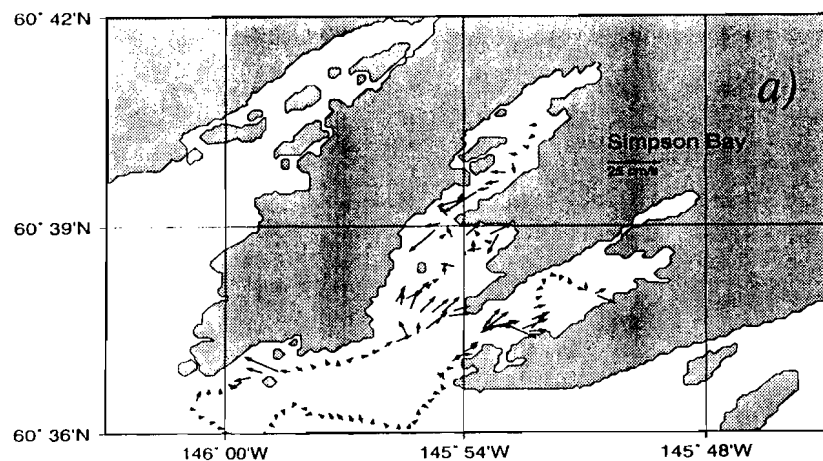


Figure 19. Tidal currents for Zaikof Bay, October 1997 averaged over 8 m. depth bins centered at 10 m. Second portion of the semidiurnal cycle shown for ebb and flood currents, at 10 m. (a and b), and at 25 m. (c and d).

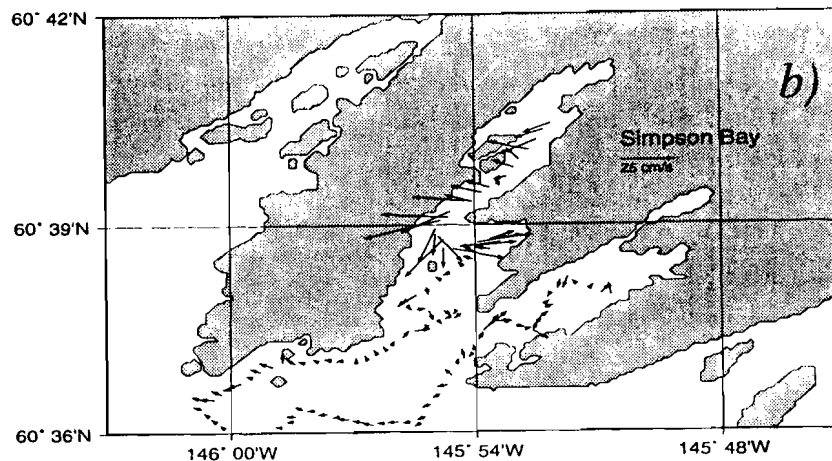
ADCP Current Vectors - March 1996

Flood Tide 1, 10m Depth



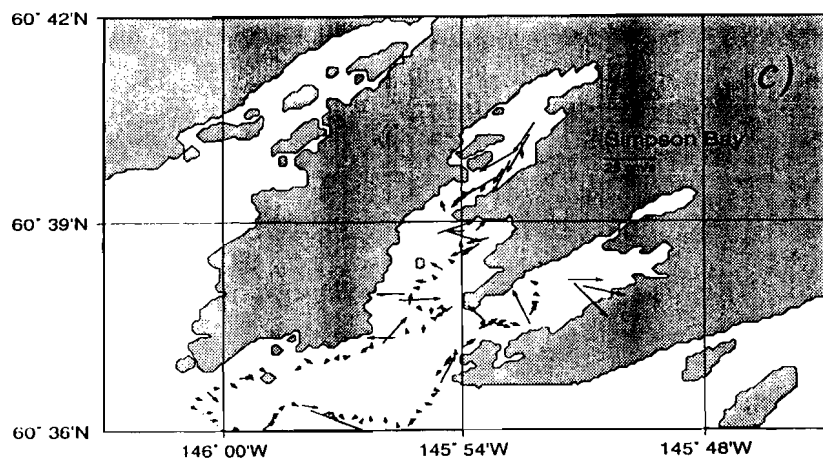
ADCP Current Vectors - March 1996

Ebb Tide 1, 10m Depth



ADCP Current Vectors - March 1996

Flood Tide, 25m Depth



ADCP Current Vectors - March 1996

Flood Tide 2 10m Depth

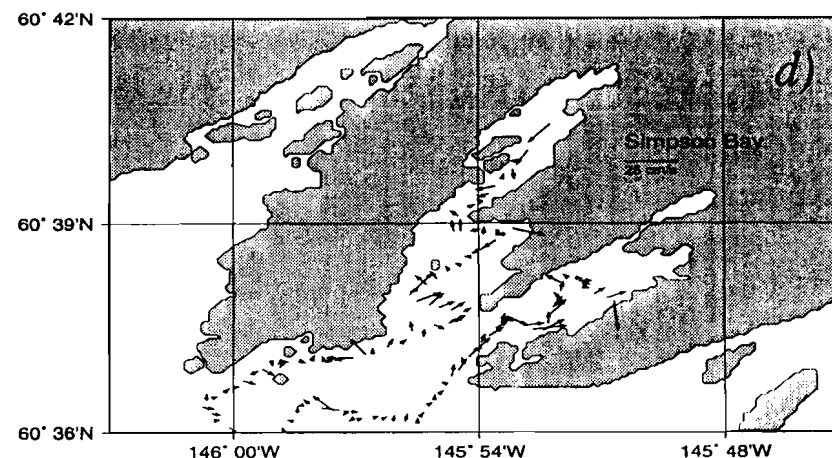
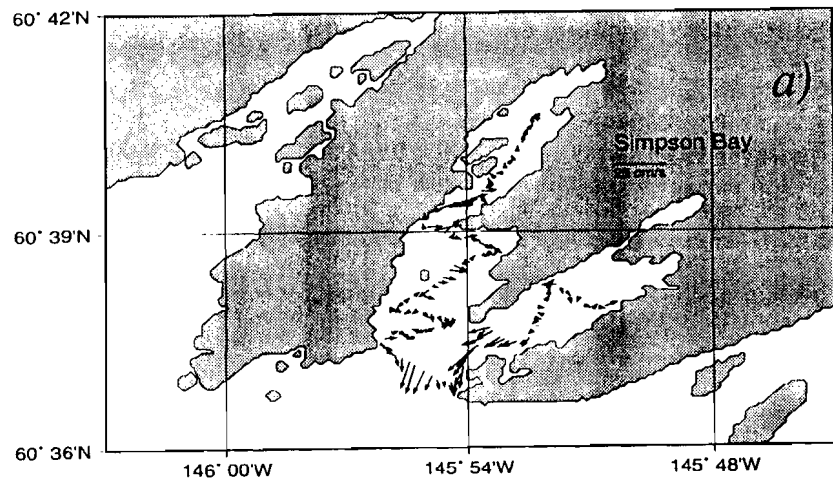


Figure 20. Tidal currents for Simpson Bay, March 1996 averaged over 8 m. depth bins centered at 10 and 25 m. First cycle of the semidiurnal period shown for 10 m currents in (a) and (b), first cycle, flood currents at 25 m. in (c), and second cycle flood currents shown in (d).

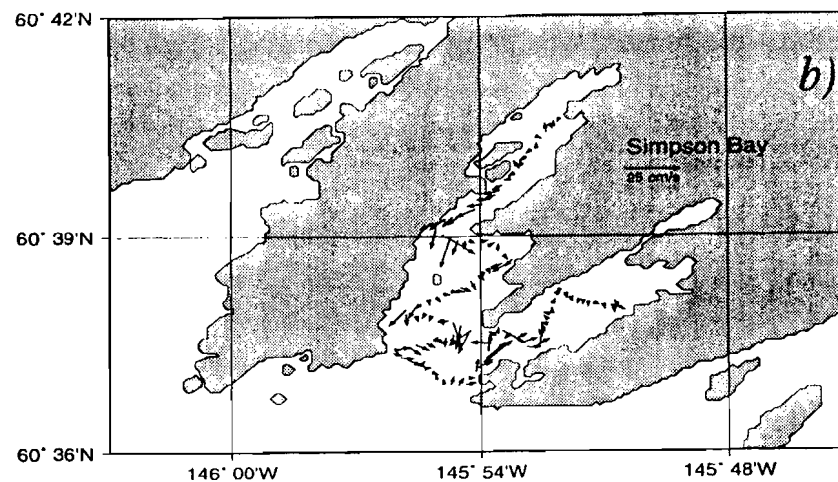
ADCP Current Vectors - August 1996

Flood Tide 1 10m Depth



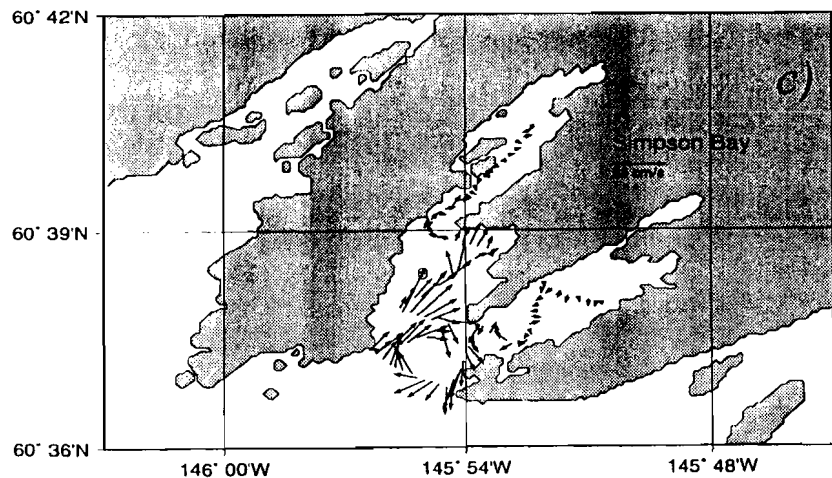
ADCP Current Vectors - August 1996

Ebb Tide 1 10m Depth



ADCP Current Vectors - August 1996

Flood Tide 2, 10m Depth



ADCP Current Vectors - August 1996

Ebb Tide 2, 10m Depth

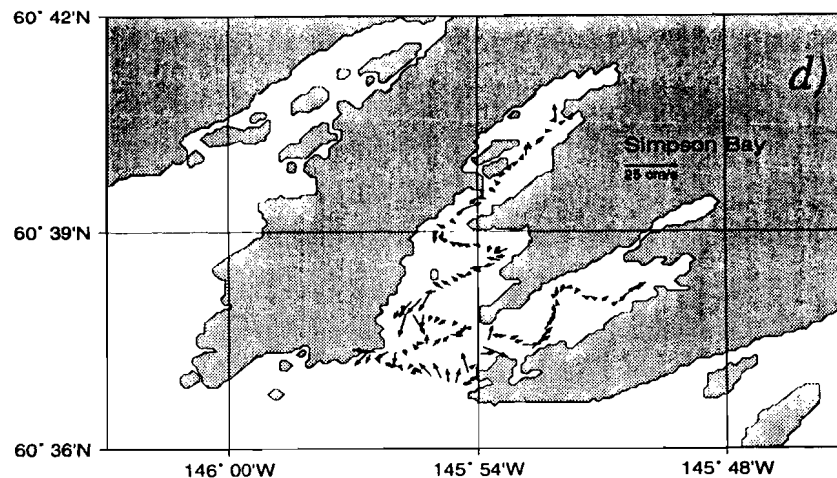


Figure 21. Tidal currents for Simpson Bay, August 1996 averaged over 8 m. depth bins centered at 10 m. Full semidiurnal period shown with first cycle flood and ebb in (a) and (b), and second cycle flood and ebb in (c) and (d) respectively.

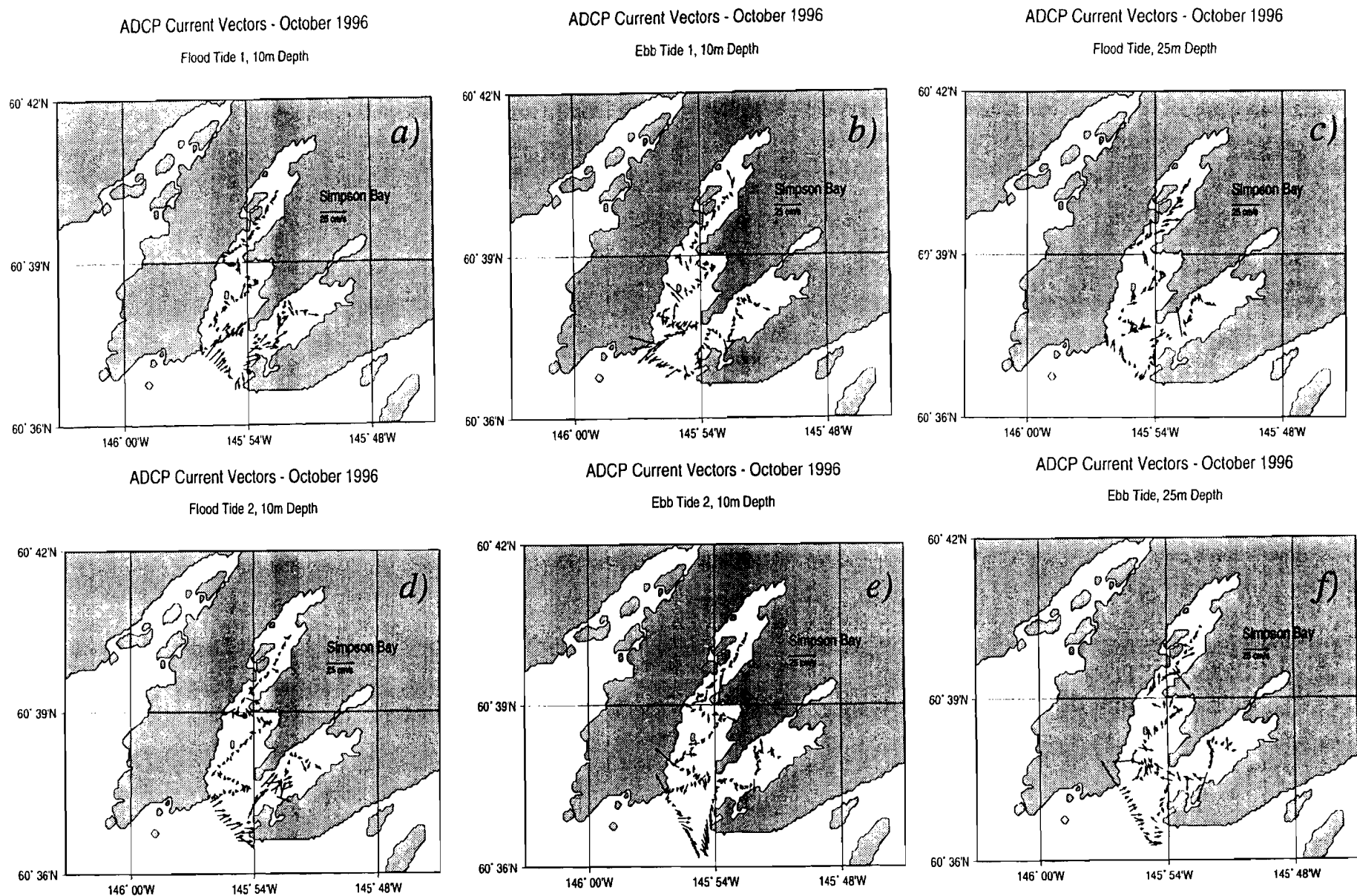


Figure 22. Tidal currents for Simpson Bsy, October 1996 averaged over 8 m. depth bins centered at 10 and 25 m. Full semidiurnal period shown with first cycle flood and ebb currents in (a) and (b), 25 m. currents for flood tide 1 in (c), second cycle in (d) and (e), and 25 m. currents for ebb tide 2 in (f).

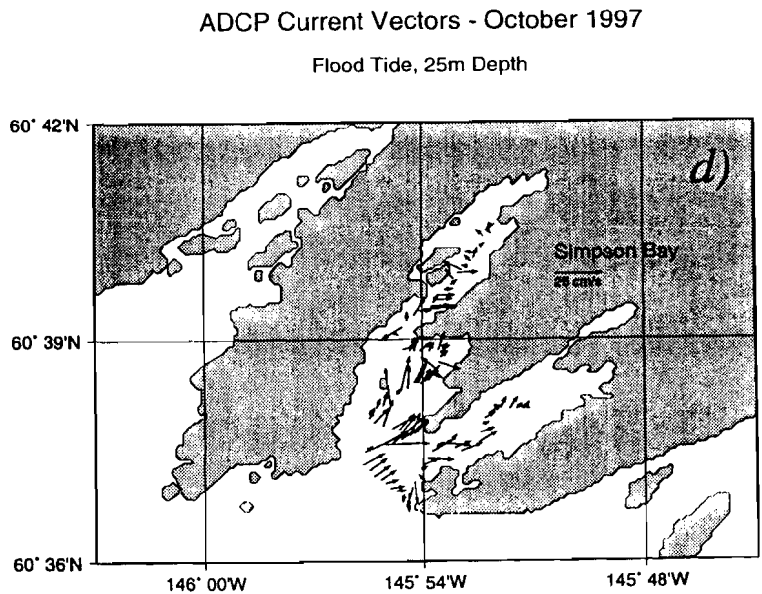
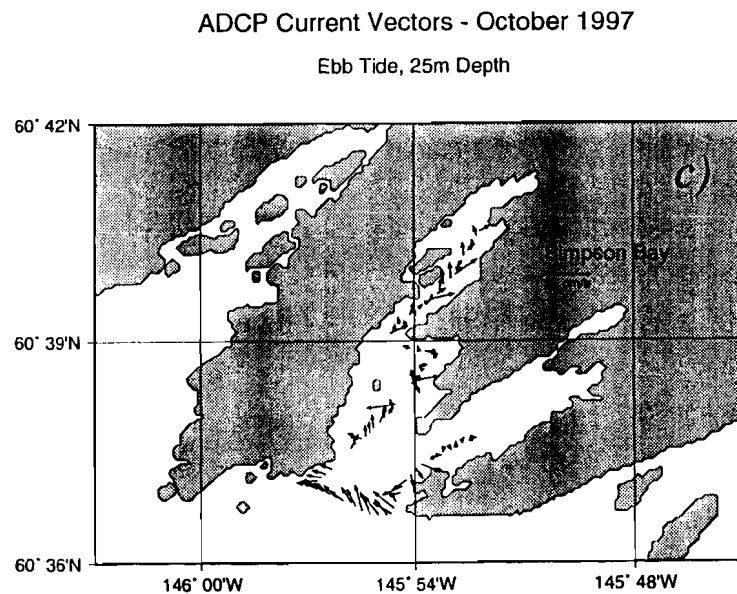
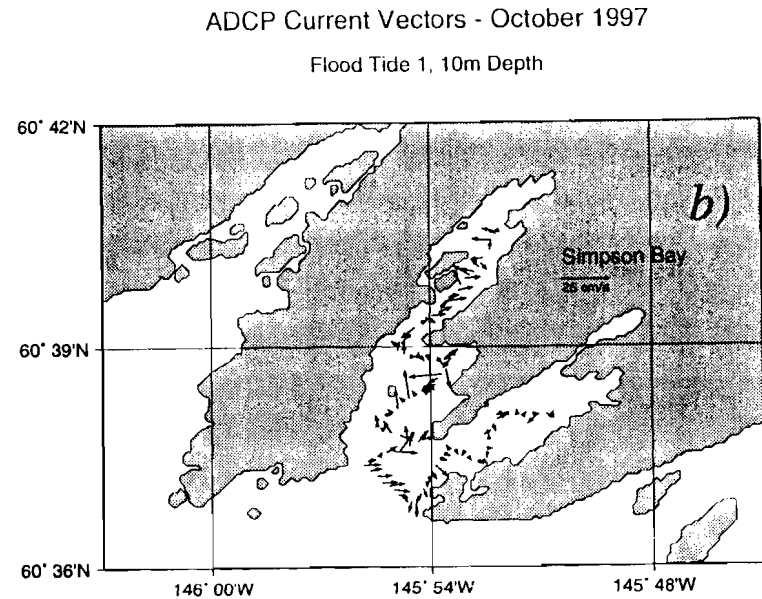
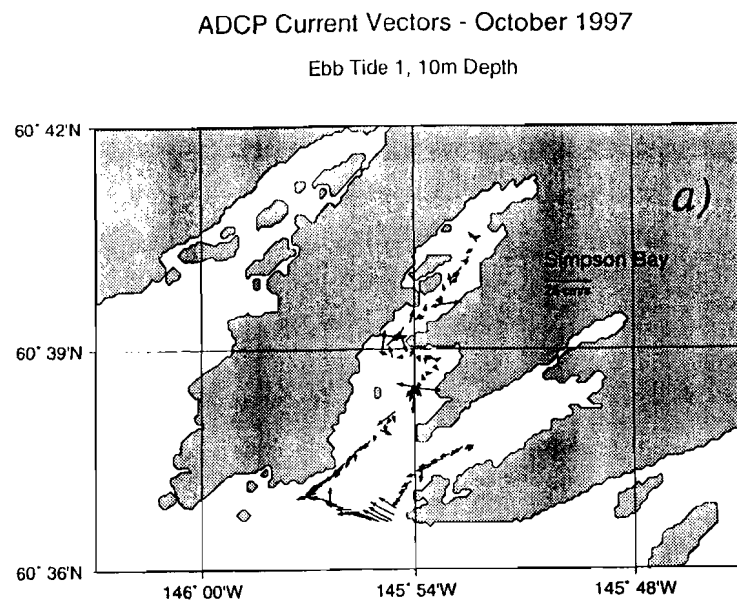


Figure 23. Tidal currents for Simpson Bay, October 1997 averaged over 8 m. depth bins centered at 10 and 25 m. Second cycle of the semidiurnal period is shown with ebb and flood currents at 10 m. in (a) and (b), and 25 m. currents in (c) and (d).

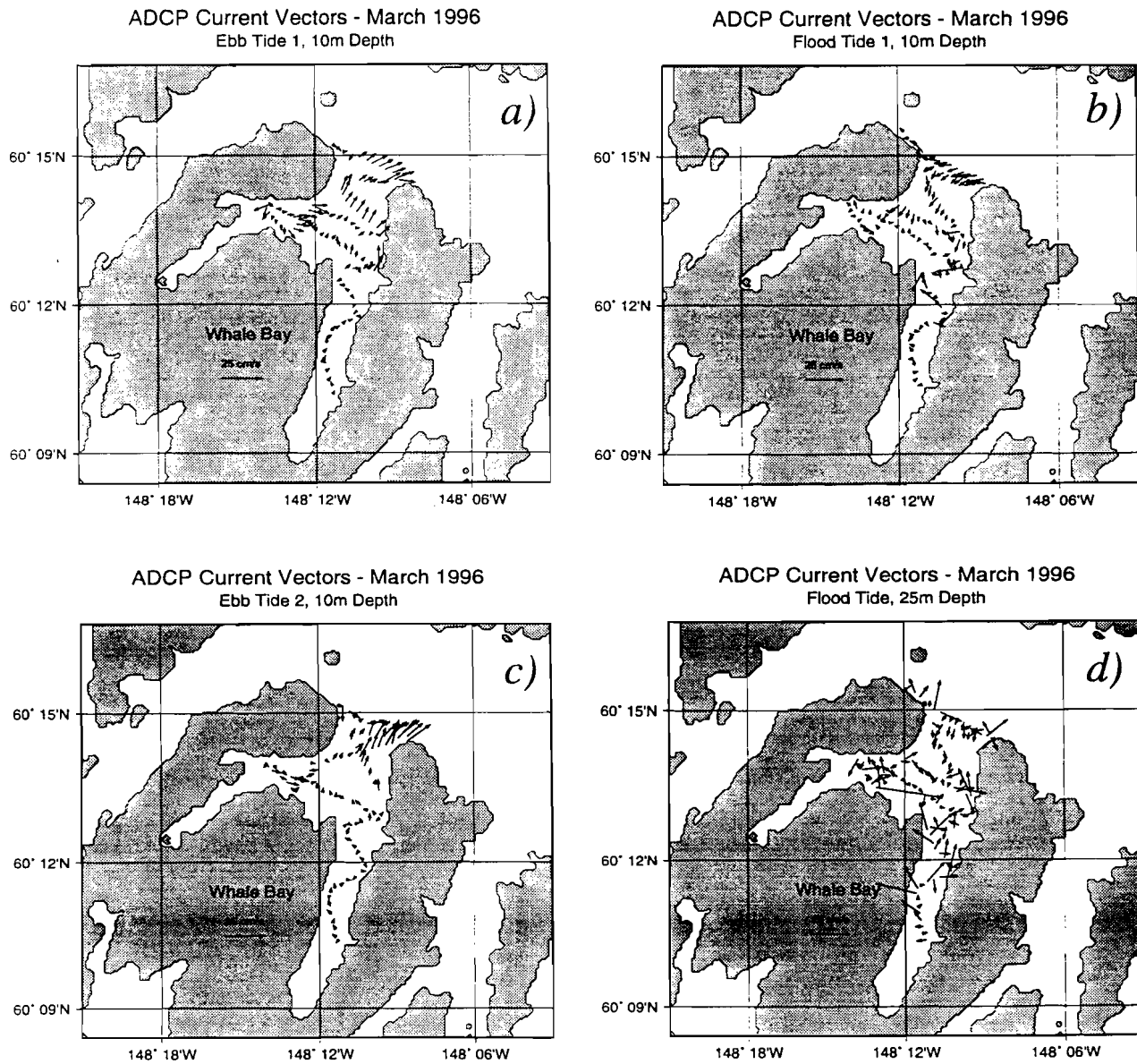


Figure 24. Tidal currents for Whale Bay, March 1996 averaged over 8 m. depth bins centered at 10 m. Currents for the first cycle of the semidiurnal period is shown for the ebb and flood tides (a and b), second ebb tide (c), and first flood at 25 m. depth (d).

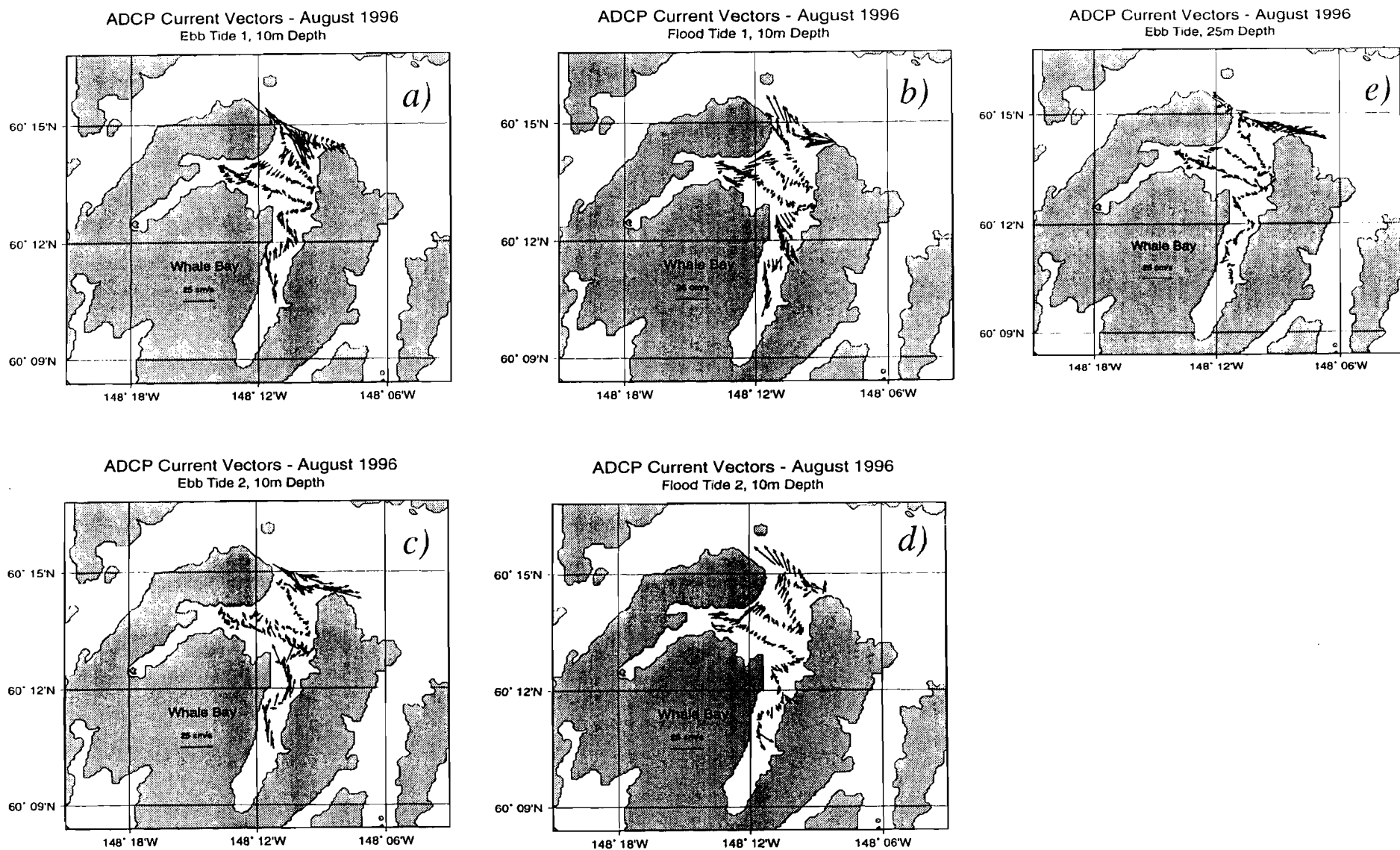


Figure 25. Tidal currents for Whale Bay, August 1996 averaged over 8 m. depth bins centered at 10 m. and 25 m. depth. First cycle of the semidiurnal period is shown for ebb and flood tides in (a) and (b); second cycle shown in (c) and (d); and 25 m. currents for the first ebb tide shown in (e).

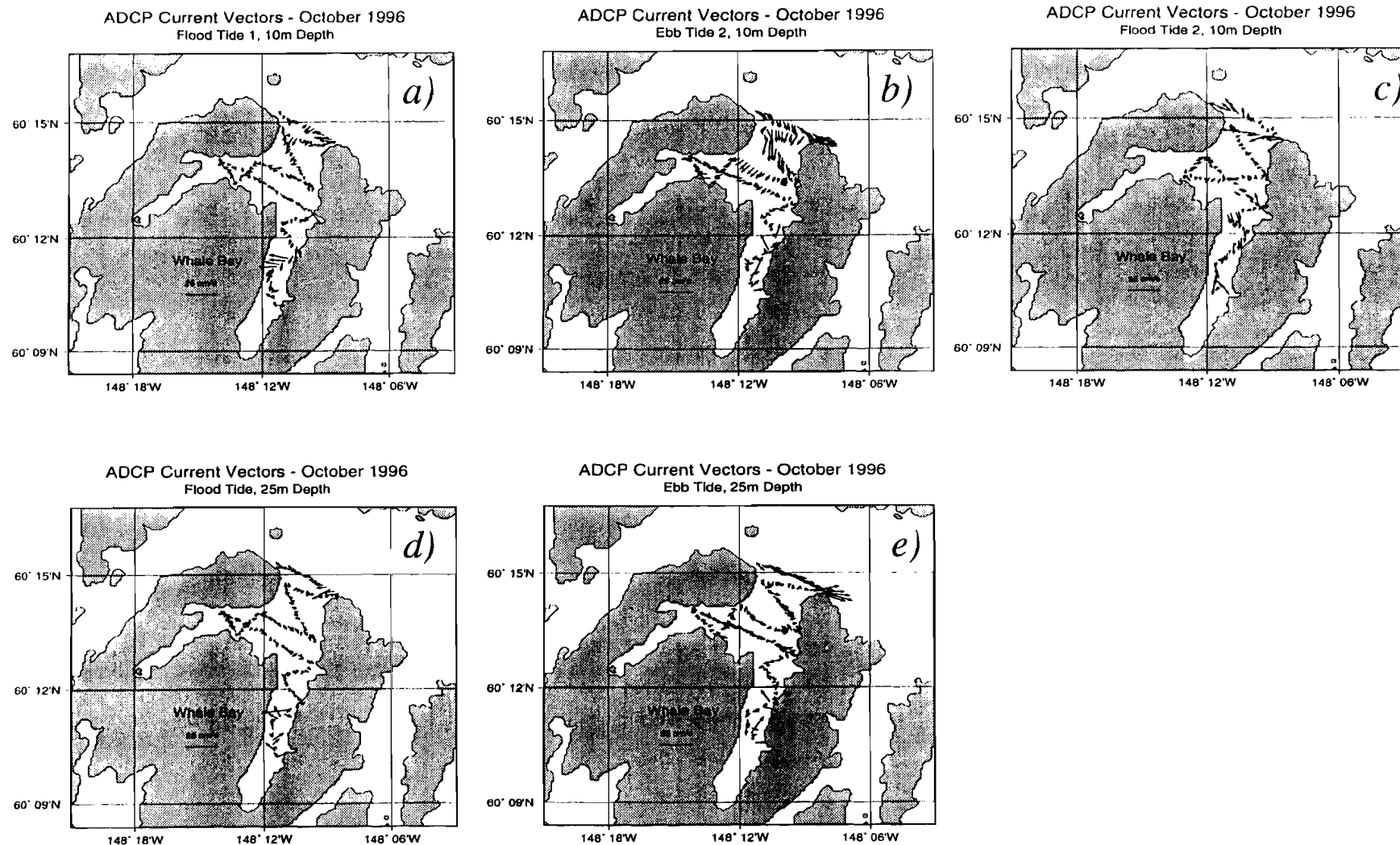


Figure 26. Tidal currents for Whale Bay, October 1996 averaged over 8 m. depth bins centered at 10 and 25 m. First cycle flood tide of the semidiurnal period is shown in (a), second cycle for ebb and flood phases in (b) and (c), and currents centered at 25 m. depth are shown for first cycle flood tide in (d) and second cycle ebb tide in (e).

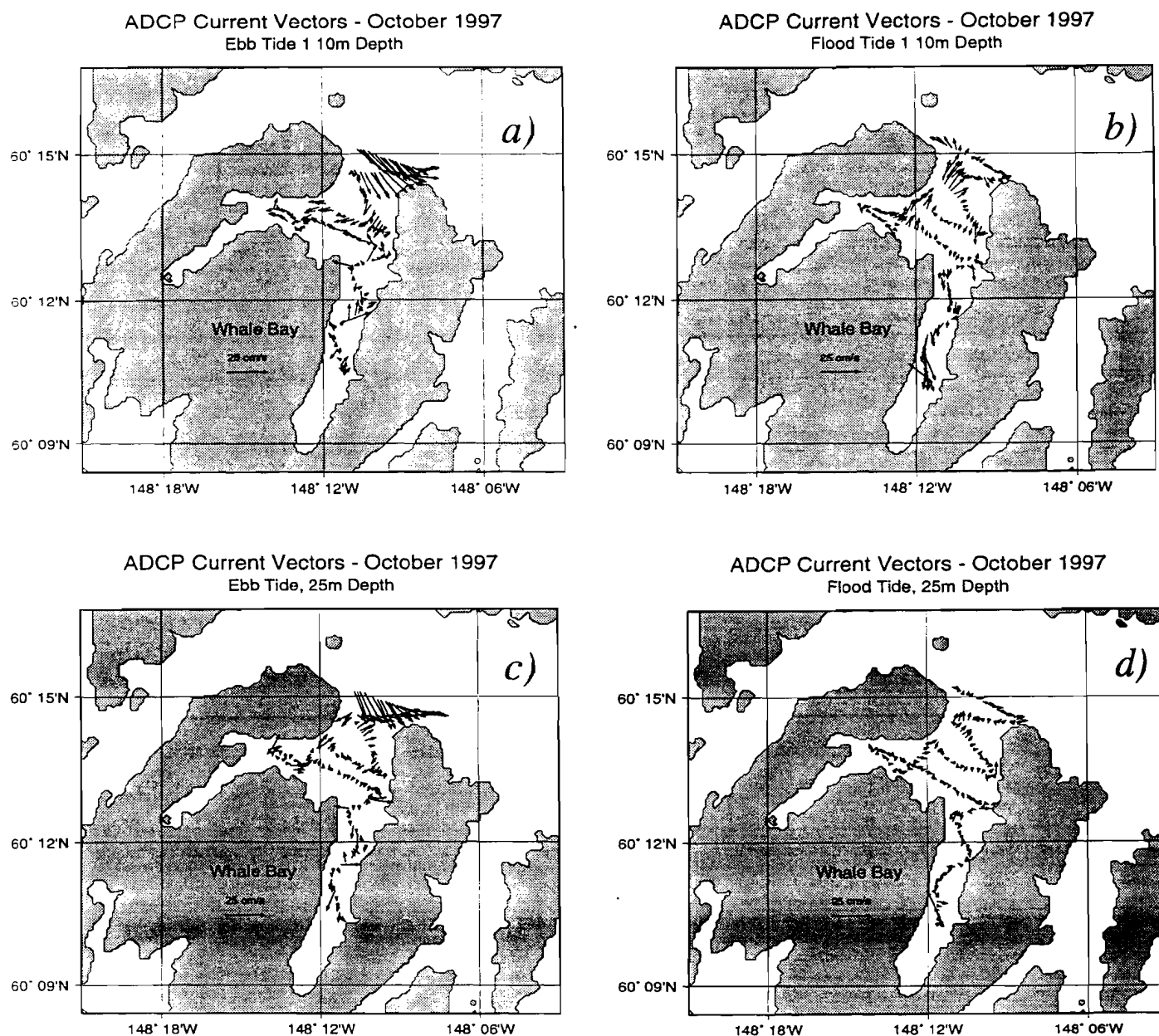


Figure 27. Tidal currents for Whale Bay, October 1997 averaged over 8 m. depth bins centered at 10 and 25 m. Second cycle of the semidiurnal period is shown for the ebb (a) and flood (b) currents at 10 m. and ebb (c) and flood (d) currents at 25 m.

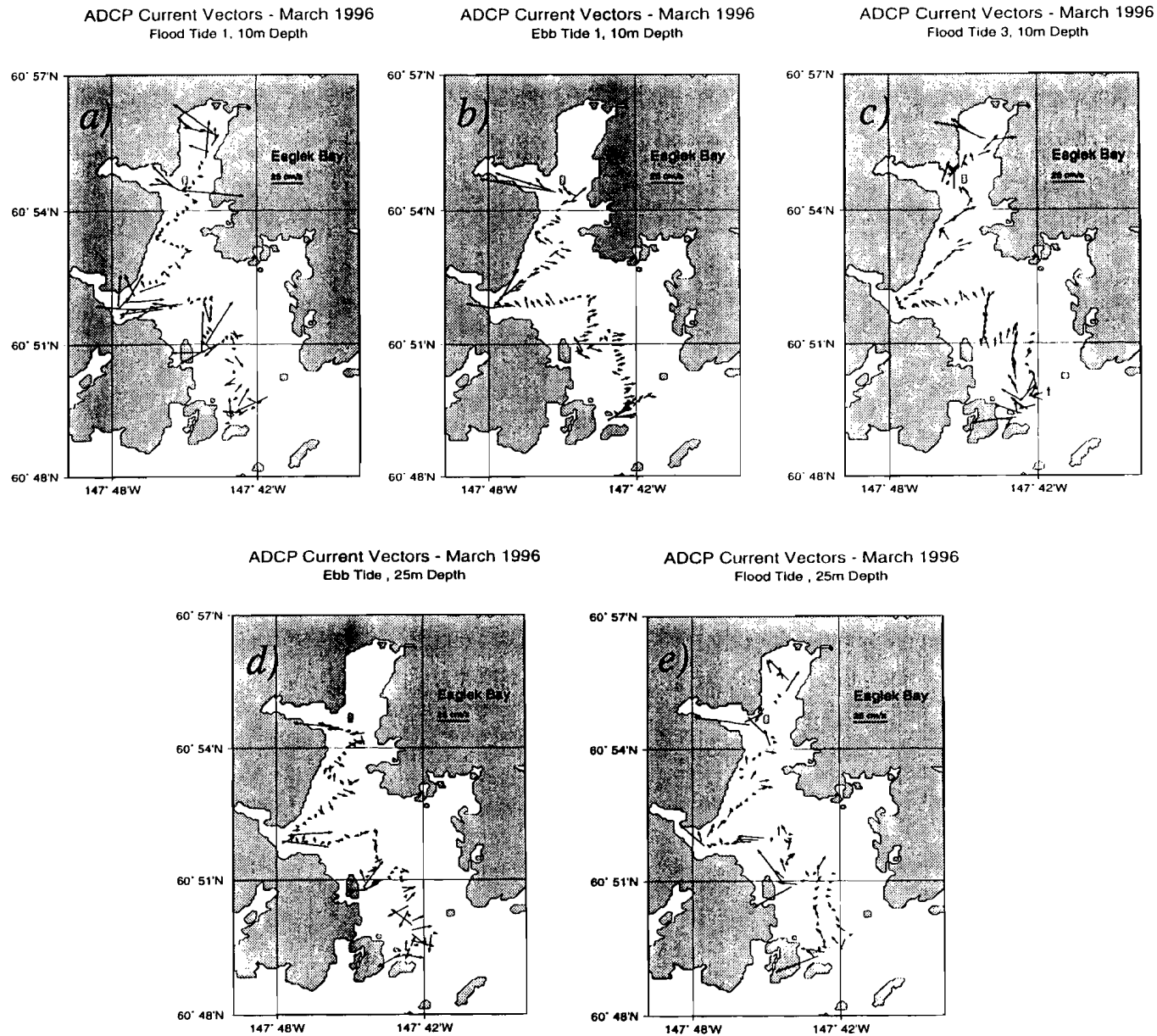


Figure 28. Tidal currents for Eaglek Bay, March 1996 averaged over 8 m. depth bins centered at 10 and 25 m. First cycle of the semi diurnal period shown in (a) and (b), first flood tide of the second semidiurnal period in (c), and currents at 25 m. for first ebb tide(d) and third flood tide (e).

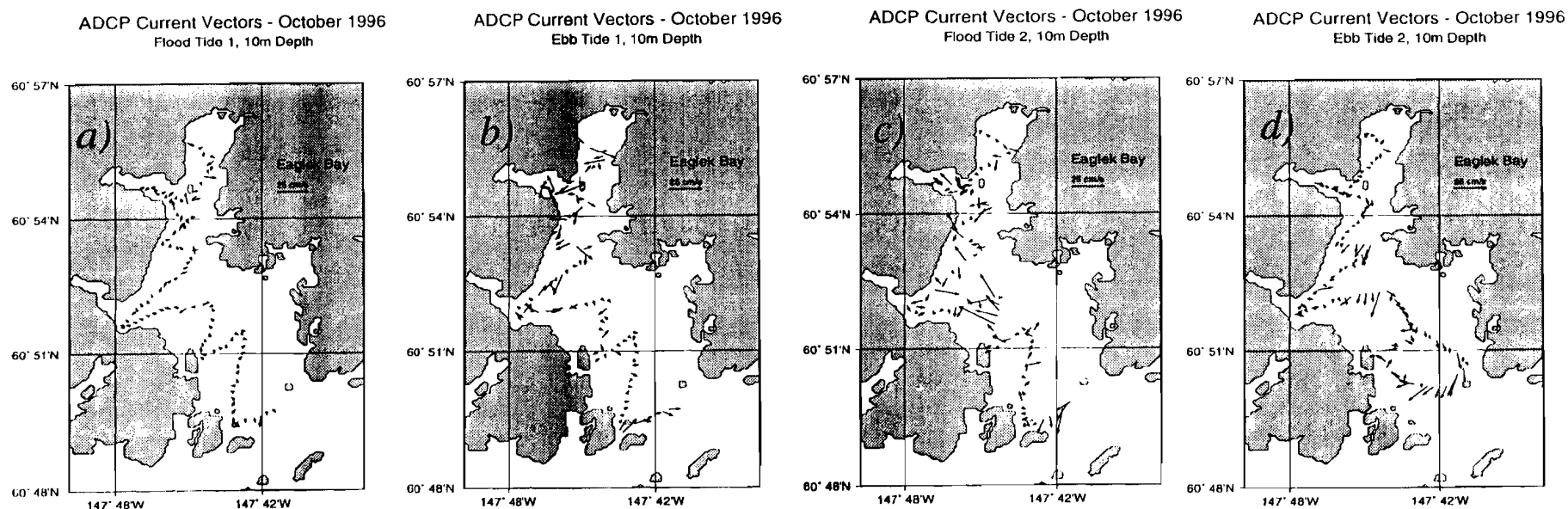


Figure 29. Tidal currents for Eaglek Bay, October 1996 averaged over 8 m. depth bins centered at 10 m. Full semidiurnal tidal period shown; first flood and ebb tides in (a) and (b), and second flood and ebb tides in (c) and (d).

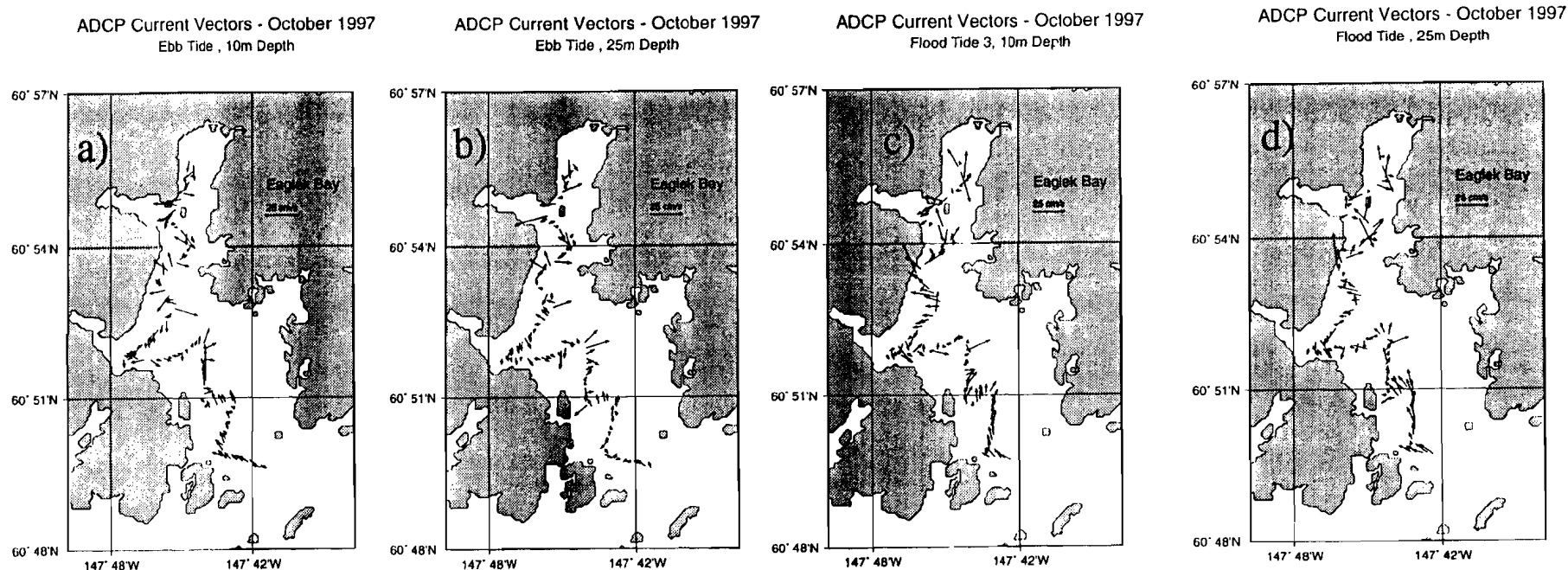


Figure 30 Tidal currents for Eaglek Bay, October 1997 averaged over 8 m. depth bins, centered at 10 and 25 m. Second cycle of the semidiurnal tidal period shown for ebb tide at 10 m, (a) and 25 m. (b), and flood tide at 10 m.. (c) and 25 m. (d).

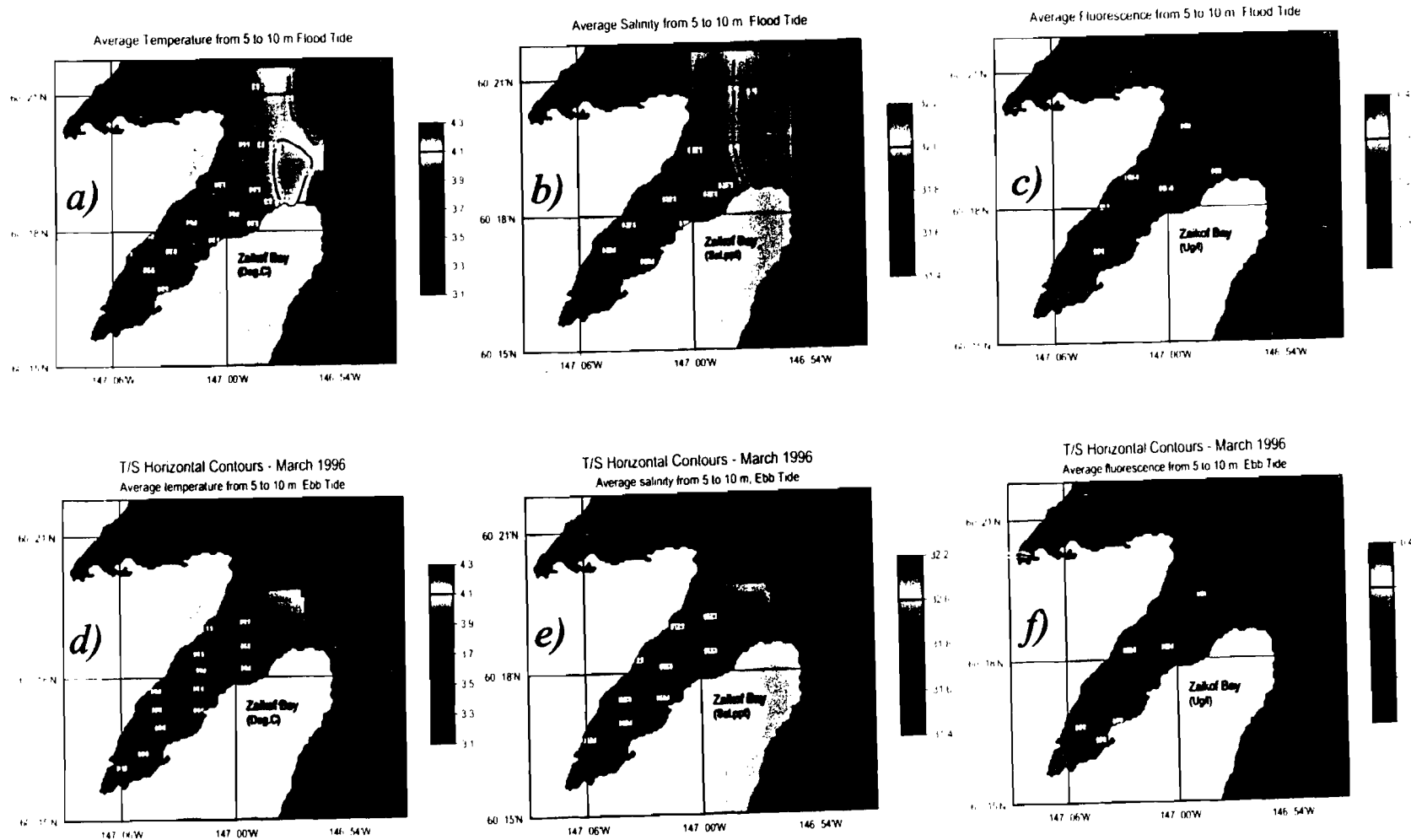
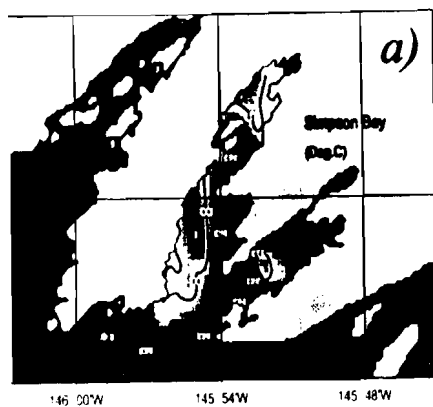
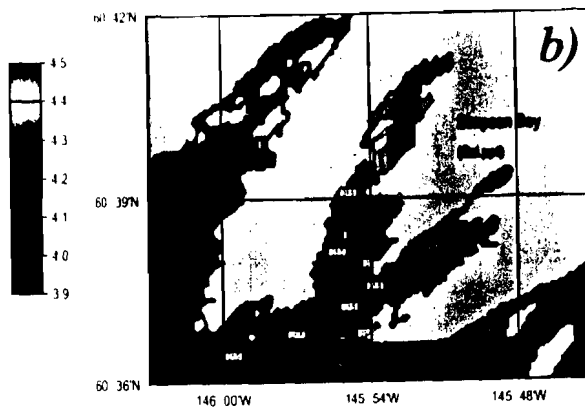


Figure 31.

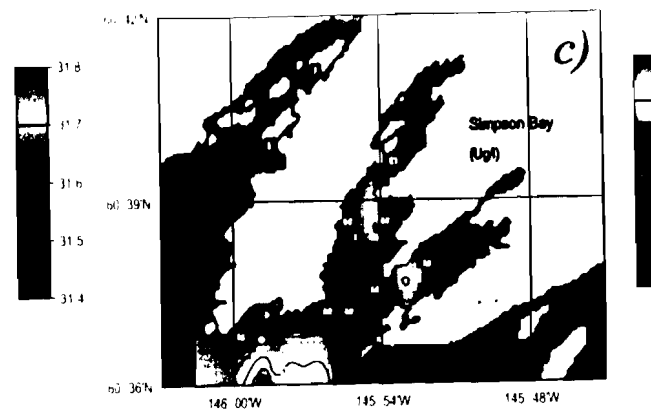
Average Temperature from 5 to 10 m. Flood Tide



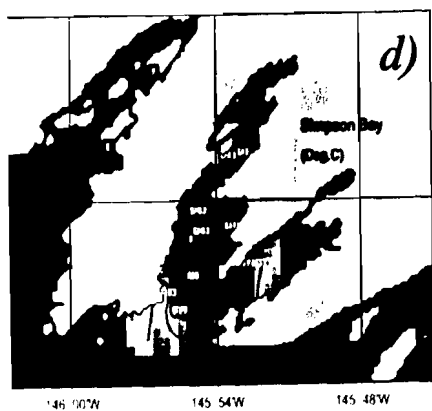
Average Salinity from 5 to 10 m. Flood Tide



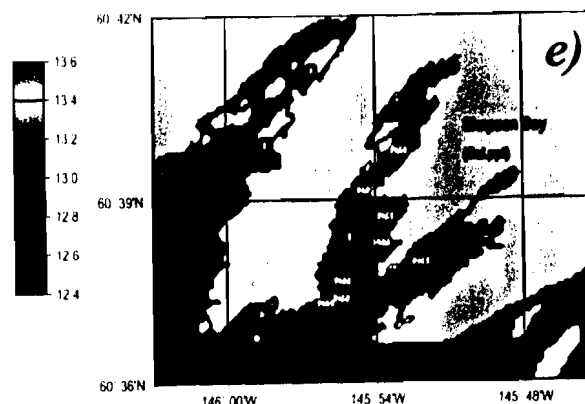
Average Fluorescence from 5 to 10 m. Flood Tide



Average Temperature from 5 to 10 m. Ebb Tide



Average Salinity from 5 to 10 m. Ebb Tide



Average Fluorescence from 5 to 10 m. Ebb Tide

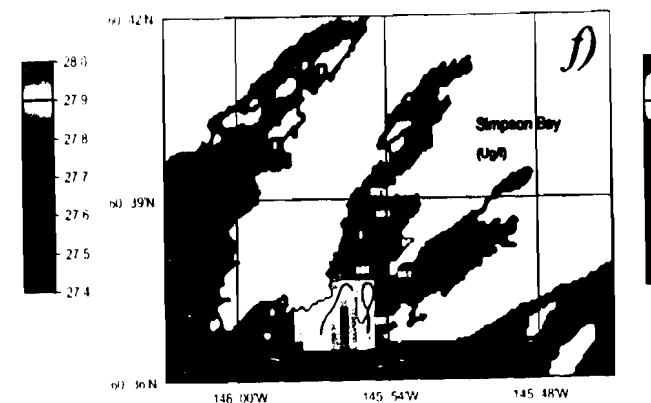


Figure 32.

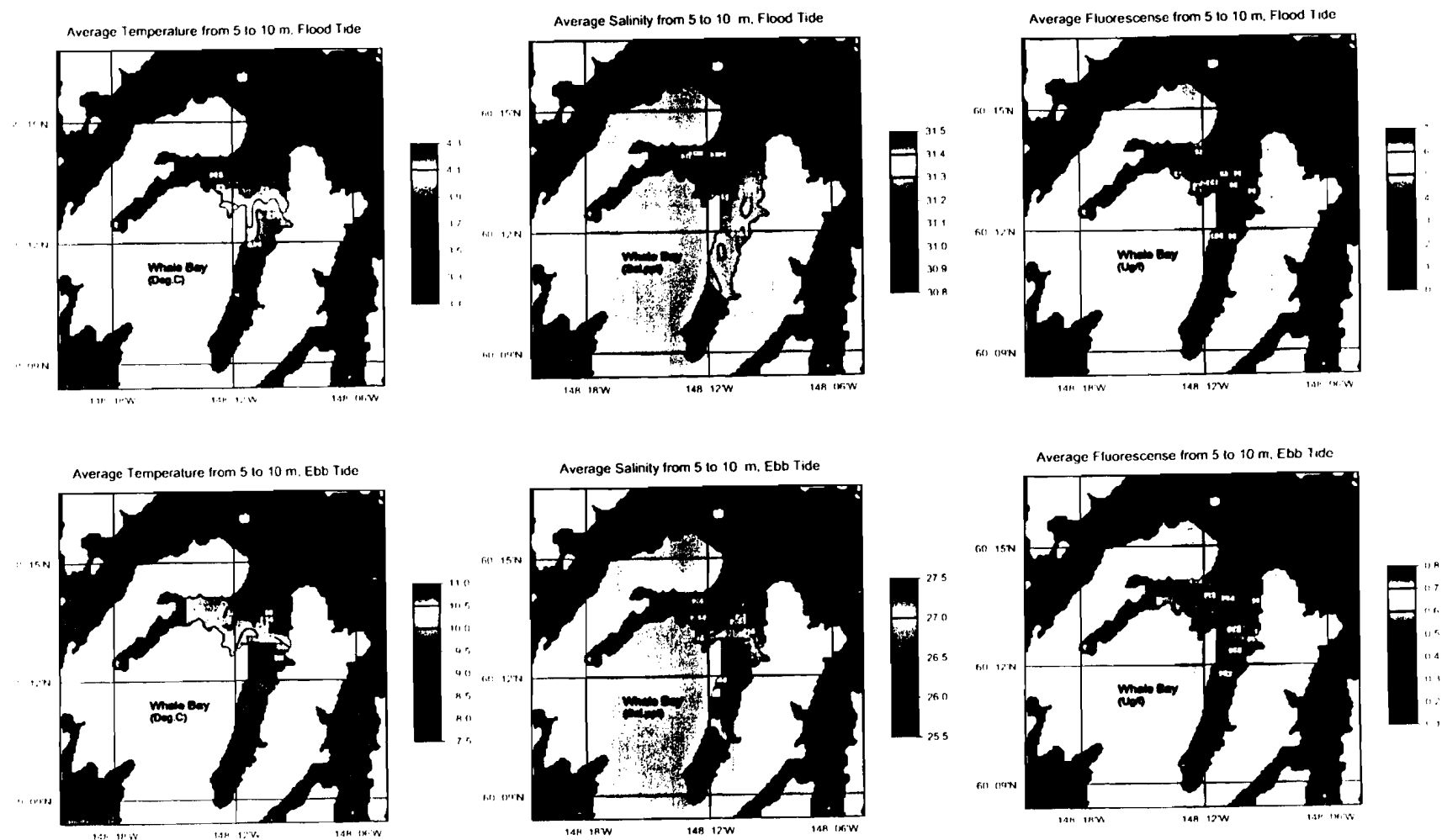


Figure 33.

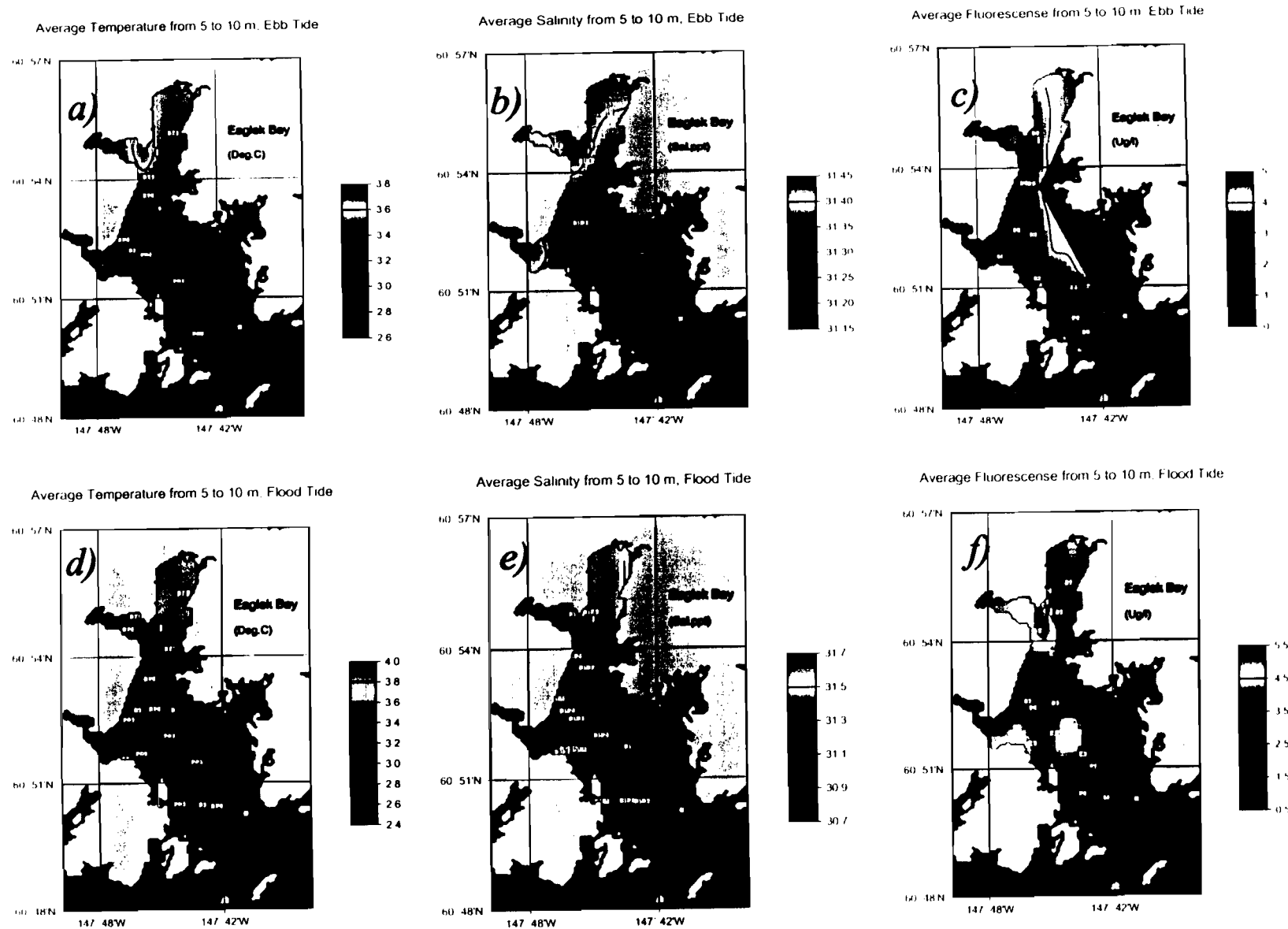


Figure 34.

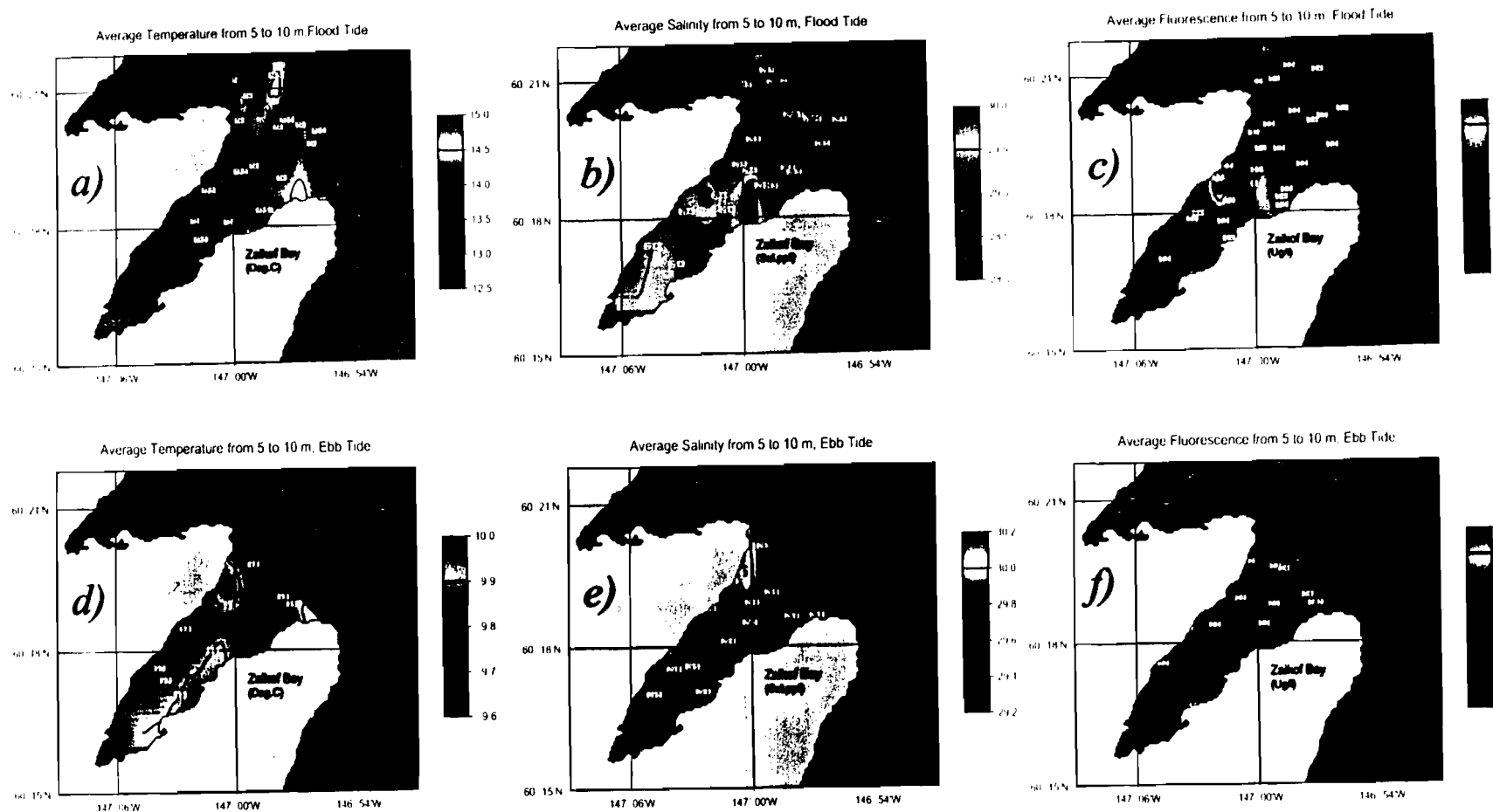


Figure 35.

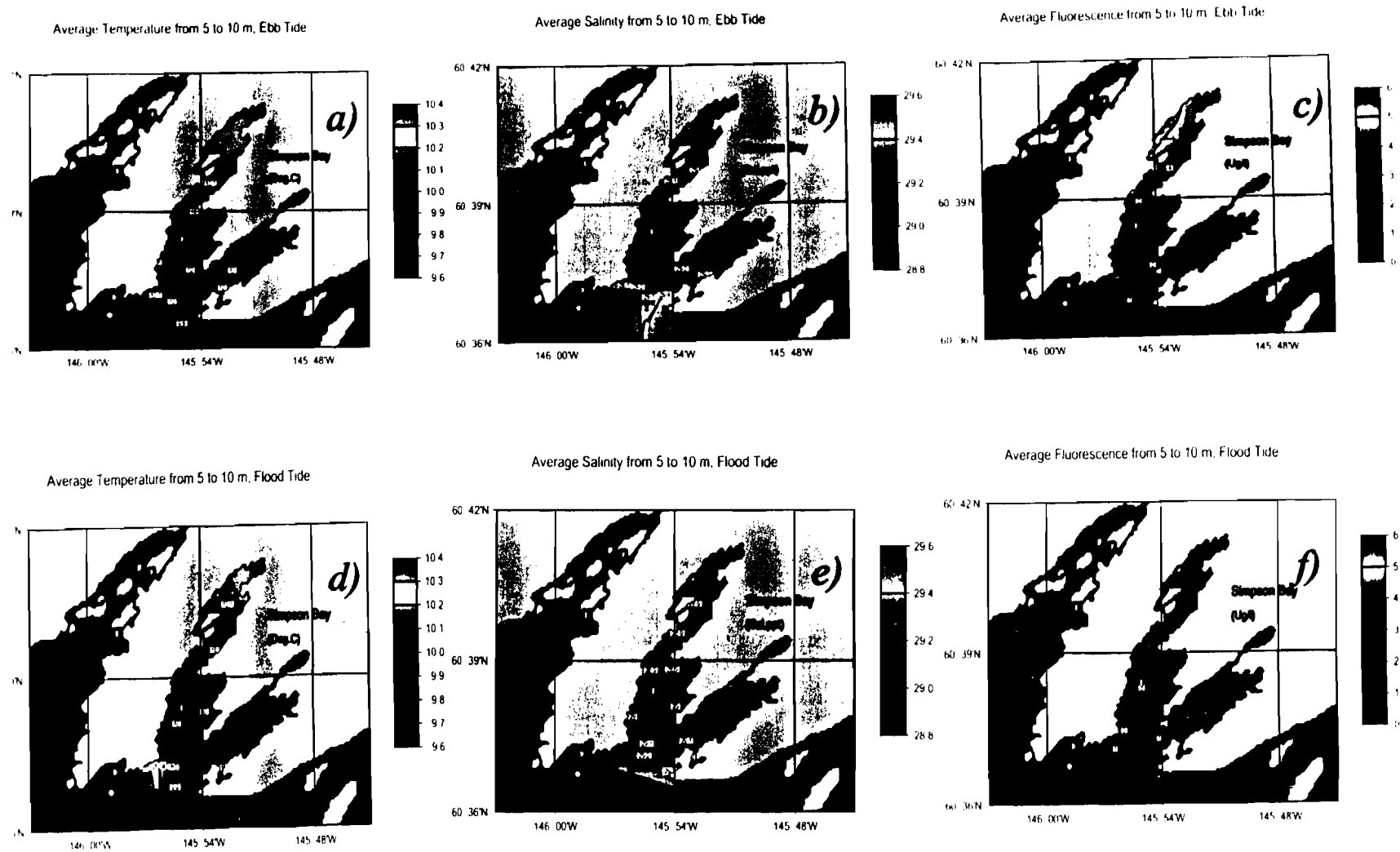


Figure 36.

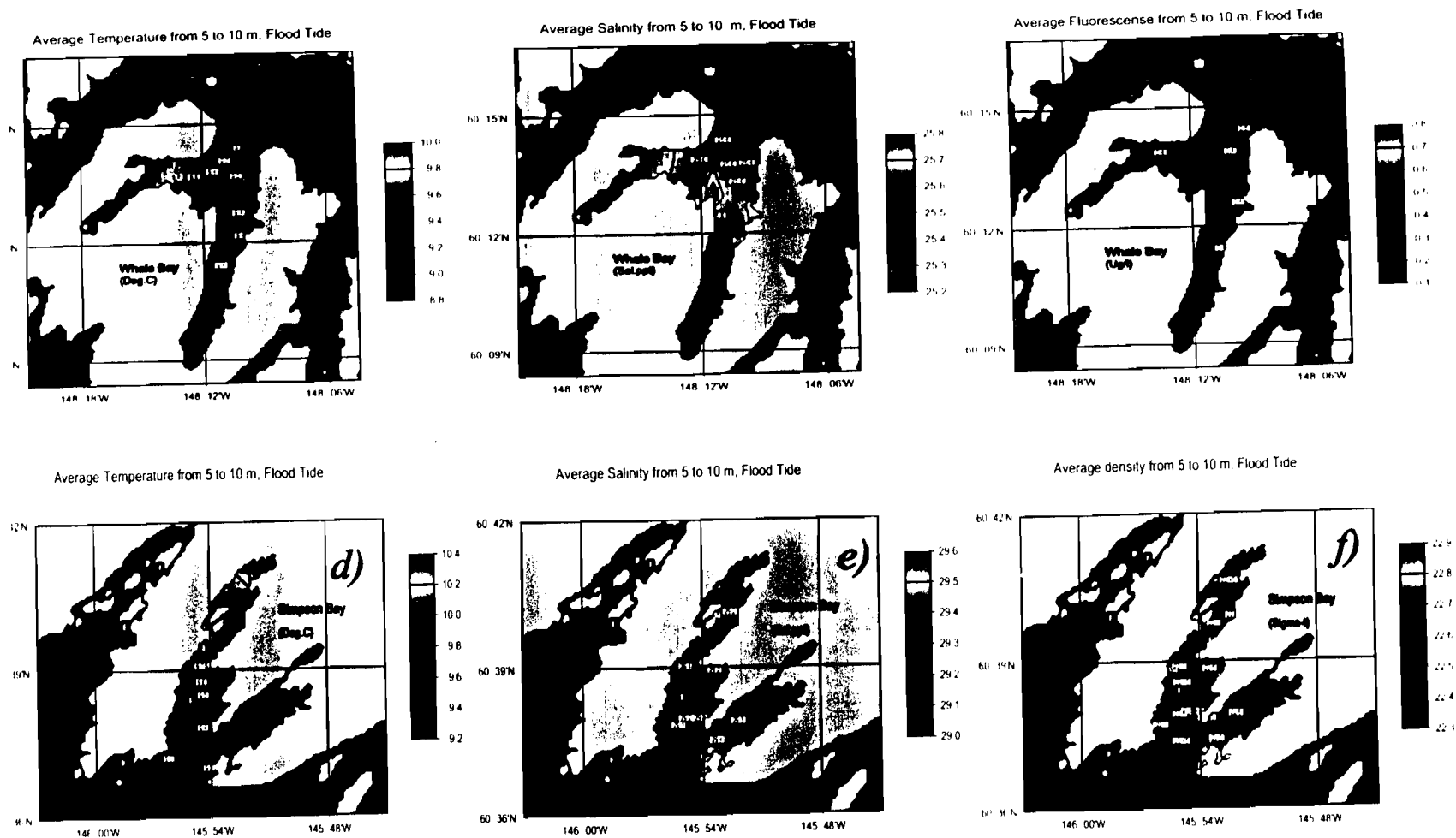


Figure 37.

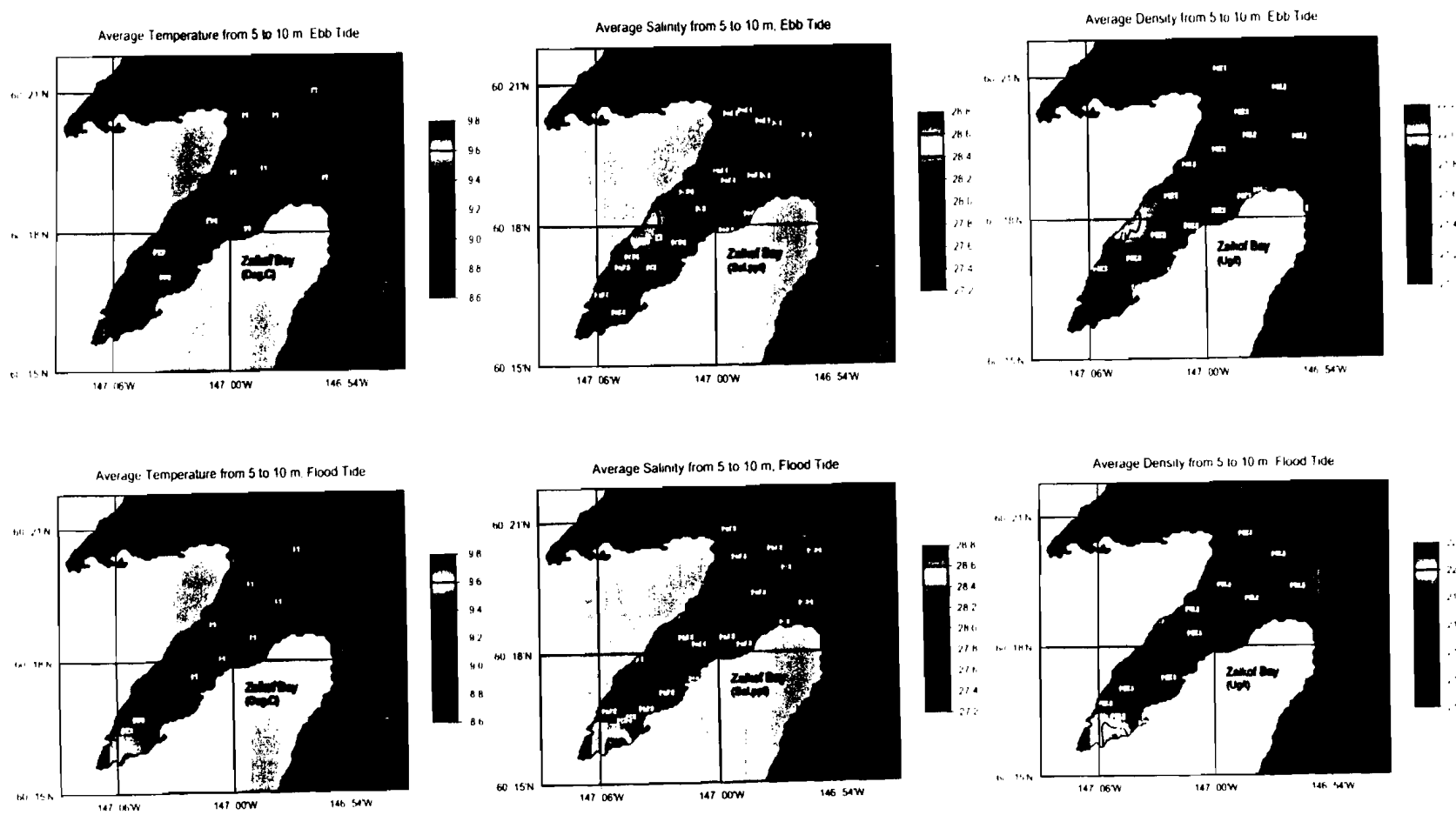


Figure 38.

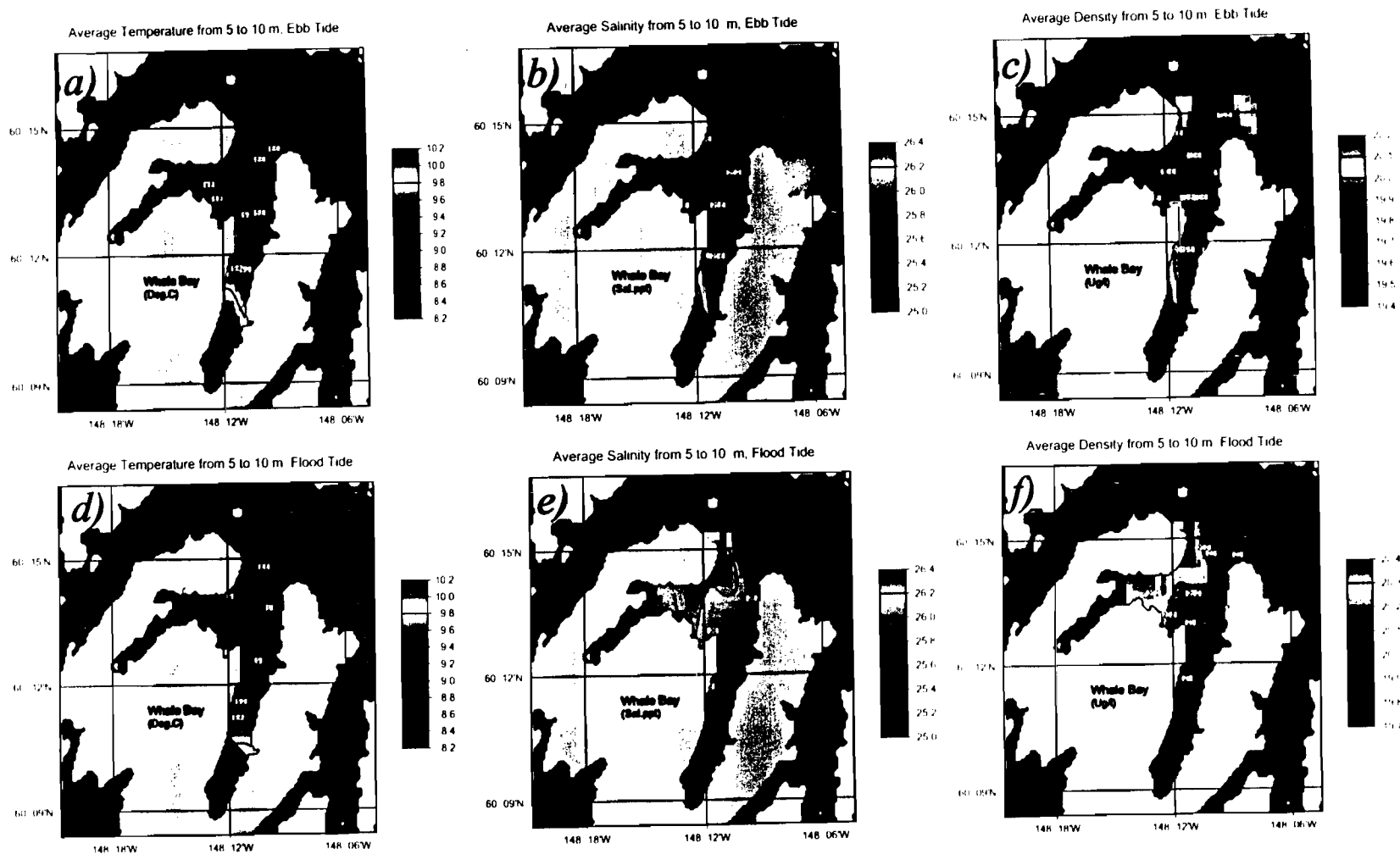


Figure 39.

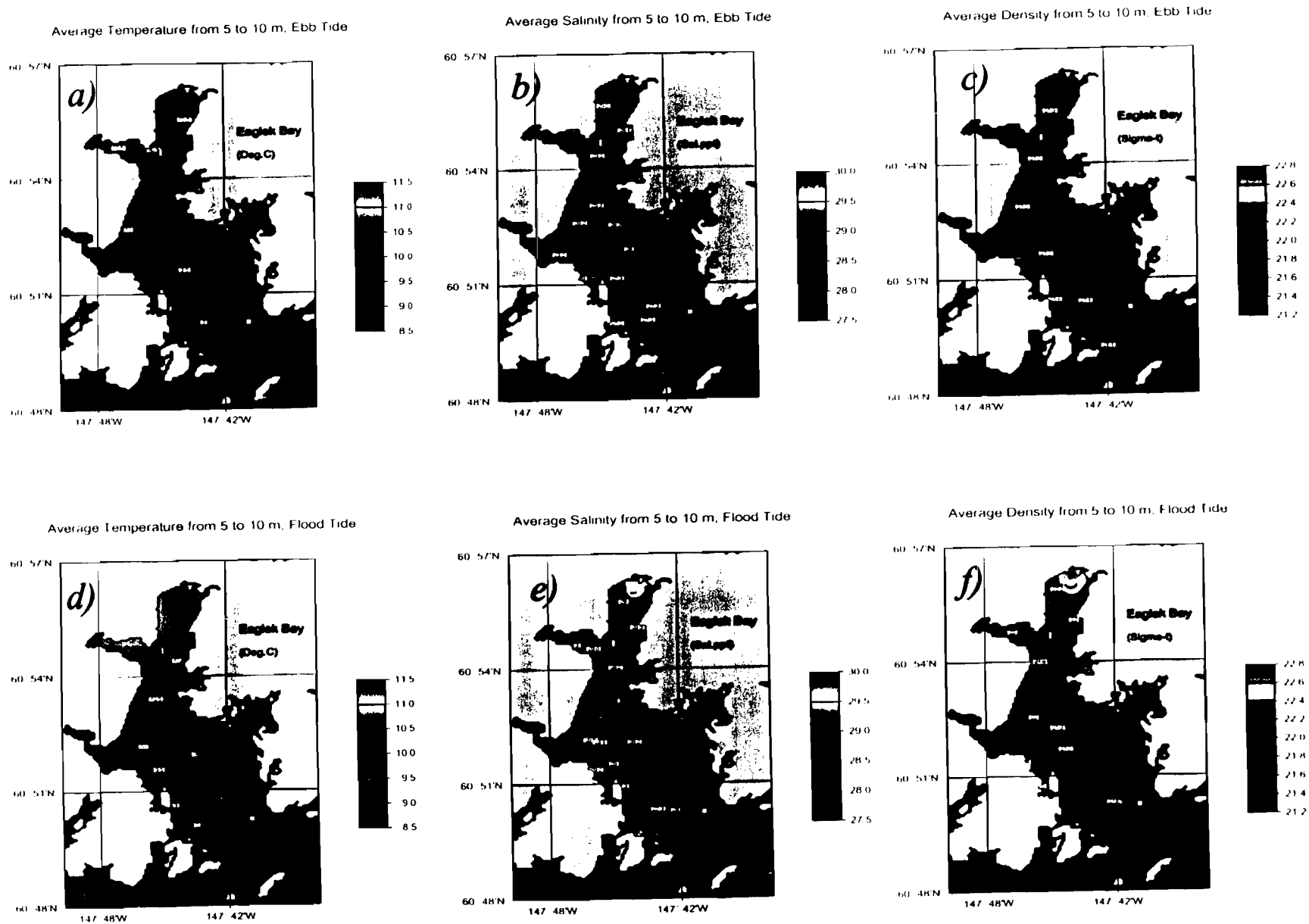


Figure 40.

Chapter 9

Plankton and Nekton Acoustics

Exxon Valdez Oil Spill
Restoration Project Annual Report
Nekton-Plankton Acoustics Project 97320N

Nekton-Plankton Acoustics
Restoration Project 97320N
Annual Report

This annual report has been prepared for peer review as part of the *Exxon Valdez* Oil Spill Trustee Council restoration program for the purpose of assessing project progress. Peer review comments have not been addressed in this annual report.

G.L. Thomas P.I., Jay Kirsch, P.L.
Geoffrey B. Steinhart and Nicholas Peters

Prince William Sound Science Center

P.O. Box 705

Cordova, AK 99574

Phone: (907)424-5800

Fax: (907)424-5820

e-mail: loon@grizzly.pwssc.gen.ak.us

April 15, 1998

Nekton-Plankton Acoustics (SEAFISH)
Restoration Project 97320N
Annual Report

Study History: The small runs of Prince William Sound pink salmon in 1992 and 1993, and the collapse of the herring population in 1993, prompted the EVOS Trustee Council to initiate the ecosystem-level studies to improve existing predictive tools. In 1993, the Sound Ecosystem Assessment science plan was developed using the GLOBEC program as a guide. Funding of research began in the spring of 1994. The Nekton-Plankton Acoustics project (SEAFISH) is evaluating and applying acoustic measurement technology to collect information on fish and macrozooplankton distribution and abundance.

This is the fourth annual report for the Nekton-Plankton Acoustic project. Six technical reports and seven abstracts have been published to date, including chapter 2 of this report, while the remaining chapters in this report are being prepared for submission to journals. Upon implementation, the Sound Ecosystem Assessment program was recommended by peer reviewers to be a 8-10 year program. Funding from the EVOS Trustee Council is committed for five years. Funding for the fifth year is in place and preliminary budgets have been projected through FY00 (six years). We envision a transition from the intense observational oceanography and modeling program (SEA), into a model-based monitoring program in years four through six. This second phase will focus on the implementation of monitoring to collect the data needed to initialize the SEA numerical models and to verify the model predictions. Developments in the plankton-nekton acoustics are essential to the design of a cost-effective monitoring program.

Abstract: In the first four years, the primary contribution of the Nekton-Plankton Acoustics project was to develop accurate estimation procedures for animal abundance and distribution information. These data were used for testing of the river-lake and prey-switching hypotheses and the development of predictive numerical models. The results are split between preliminary and completed products. The products are the estimates of nekton predators and macrozooplankton prey along the outmigration corridor for the pink salmon in the spring, and the fall and winter density and distribution of the juvenile and adult herring (*Clupea pallasii*), and pollock populations. The completed products are the stock assessments of adult pollock (*Theragra chalcogramma*), biomass in Feb-Mar 1995 and 1997 (37 and 38 thousand metric tonnes), and adult herring biomass in Sep 1993, Oct-Nov 1994, April 1995, Oct-Nov 1995, Mar-April 1996, April 1997 and April 1998 (20, 13, 13, 24, 23, 32, 24 thousand tonnes, respectively).

Key Words: *EXXON VALDEZ*, hydroacoustics, macrozooplankton assessment, marine instrumentation, salmon fry predators, Pacific herring, *Clupea pallasii*, pink salmon, *Oncorhynchus gorbuscha*, population trends, stock assessment, walleye pollock, *Theragra chalcogramma*.

Citation: Thomas, G. L., J. Kirsch, G.B. Steinhart and N.J. Peters. 1998. SEA: Nekton-plankton acoustics fourth annual report, 1998. Restoration Project 97320N. *EXXON VALDEZ* Trustee Council. Anchorage, Alaska. 119 pp.

TABLE OF CONTENTS

Executive Summary: Nekton-Plankton Acoustics - Project 97320N

G.L. Thomas (Principal Investigator), J. Kirsch (Project Leader), G. B. Steinhart and N.J. Peters, Prince William Sound Science Center.

Chapter One: Pollock distribution and abundance

Distribution and abundance of walleye pollock (*Theragra chalcogramma*) in Prince William Sound, 1994-1997. *G.B. Steinhart, G.L. Thomas, J. Kirsch and N. Peters*

Chapter Two: Predation potential on salmon fry

Co-occurring patches of walleye pollock (*Theragra chalcogramma*) and zooplankton in Prince William Sound, Alaska, USA. *G.B. Steinhart, G.L. Thomas, and J. Kirsch*

Chapter Three: Nearshore herring and rockfish

Preliminary analysis of nearshore distribution and abundance of Pacific herring (*Clupea pallasii*) and pelagic rockfish in western Prince William Sound. *G.B. Steinhart, G.L. Thomas, J. Kirsch, and M. Blair*

Chapter Four: Zooplankton instrumentation

The preliminary fusion of acoustical and optical data with net catch information to assess zooplankton distributions in Prince William Sound, Alaska. *L.B. Tuttle, J. Kirsch, R.T. Cooney (UAF/IIMS), and G.L. Thomas*

Chapter Five: Juvenile herring and plankton

Preliminary acoustic measurements of juvenile Pacific herring (*Clupea pallasii*) and plankton in selected bays in Prince William Sound. *N.J. Peters, G.B. Steinhart, J. Kirsch, and G.L. Thomas.*

1997 ANNUAL REPORT

Sound Ecosystem Assessment (SEA), Nekton-Plankton Acoustics

G.L. Thomas, Jay Kirsch, Geoffrey Steinhart and Nicholas Peters - PWS Science Center

EXECUTIVE SUMMARY

The Nekton-Plankton Acoustics Project (97320-N) is evaluating and applying acoustic measurement technology to collect accurate information on the distribution, density and size of specific animal populations. These data are essential for the development and operation of numerical models to improve the prediction of animal population change and the testing of the river-lake and prey switching hypotheses under the Sound Ecosystem Assessment Program (SEA). Improving the prediction of animal population change is a prerequisite for accurate assessment of anthropogenic influences and restoration from damage.

SEA is a multi-tasked project that relies on: (1) cooperative model development to assist in sampling design, data analysis, and interpretation, (2) shared vessel and facilities for data collection and logistical support, (3) data sharing with agency, university, public and commercial interests, and (4) remote sensing with acoustical and optical technologies. We used the existing knowledge and skills of commercial fishers in the design and implementation of surveys. Salmon hatcheries in the region provided support for field crews and the hatchery releases of pink salmon are treated as an experimental manipulation of the marine ecosystem. Because of the multi-tasking nature of this project, we have relied on partnerships with other funding sources to accomplish tasks to fill in some of the gaps between SEA projects.

This annual report includes five chapters: (1) distribution and abundance of walleye pollock in western Prince William Sound, (2) Co-occurring patches of walleye pollock and zooplankton distribution in Prince William Sound, (3) preliminary herring and rockfish

distribution, (4) data fusion for zooplankton assessment, and (5) juvenile herring. Predator and prey acoustic assessments are major components of the pink salmon investigations and annual stock assessments are a primary part of the herring research.

Pink Salmon:

Predators (walleye pollock):

We have used acoustics to measure abundance and distribution of walleye pollock (*Theragra chalcogramma*) in Prince William Sound (PWS) since 1994. We found that during the spring and summer, pollock abundance in the northwest PWS increased, while pollock density decreased in southwest passages. We believe that this increase in pollock may have been influenced by the timing and magnitude of the spring zooplankton bloom, one of the primary prey items of pollock in the Sound. In 1994, a year with a relatively late, and small, bloom of *Neocalanus* spp., pollock were more abundant near Esther Island than during any other year we sampled. We believe this observation supports the Prey-Switching hypothesis: in the absence of abundant plankton, pollock switch to other prey items, including salmon fry.

The Sound Ecosystem Assessment (SEA) program is a multi-disciplinary effort to acquire an ecosystem-level understanding of Prince William Sound (PWS), Alaska. A primary SEA hypothesis is that adult walleye pollock (*Theragra chalcogramma*) switch from their primary food source, fish, to macro-zooplankton when plankton densities are high. We examined this hypothesis by making acoustic observations of fish and zooplankton during the spring of 1995. We found patches of plankton 50 m to 5 km long in the top 50 m of water. Net tows showed that these patches were over 90% calanoid copepods. Walleye pollock abundance was positively correlated with zooplankton abundance ($r^2=0.26$). Furthermore, copepods dominated the diet of pollock at this time. These results showed that walleye pollock were feeding on, and were attracted to macro-zooplankton patches in PWS. Environmental conditions that result in low macro-zooplankton densities, or prohibit the formation of dense plankton patches, could reduce feeding opportunities for pollock. When macro-zooplankton

are not abundant, adult pollock may switch their diet to include more juvenile fish, which could reduce the survival of many important fish species.

Other Predators:

We used acoustics to measure abundance and distribution of many fish species in nearshore environments in western Prince William Sound (PWS) in 1994. We found that both pelagic rockfish (*Sebastes* spp.) and Pacific herring (*Clupea pallasii*) were present in many of the areas we surveyed. In addition, aggregations of these predacious fish were easily identifiable in the acoustic data as tall loosely aggregated targets above peaks and slopes (rockfish) and as dense school or balls in open water (herring). Since both rockfish and herring are predators of pink salmon (*Oncorhynchus gorbuscha*) fry, we analyzed the acoustic data to produce estimates of pelagic rockfish and herring. We found the highest number of rockfish in rocky areas along Culross Island and in the southwest passages. Herring were most abundant in the southwest passages.

Prey (macrozooplankton):

The Sound Ecosystem Assessment (SEA) is a multi-investigator project designed to identify the primary physical and biological factors that affect the production of pink salmon and Pacific herring in Prince William Sound (PWS), Alaska. As part of this assessment, research cruises were conducted to describe the abundance and patchiness of zooplankton in PWS using high-frequency acoustics, an optical plankton counter (OPC), and a multiple-sample zooplankton net, as well as instruments to measure temperature, salinity, and fluorescence. The high-resolution, continuous sampling provided by the acoustics and optics showed that zooplankton aggregate in layers and patches throughout PWS, and that Hinchinbrook entrance had relatively high densities in both 1995 and 1996. In regions where *Neocalanus* copepod dominates the biomass, the optics and acoustics showed similar patterns, but in regions with high pteropod biomass, the acoustics estimate more biomass than the optics.

Pacific herring:**Juveniles:**

Diel hydroacoustic surveys were conducted from June 1996 to August 1997, in Simpson, Zaikof, Whale and Eaglek bays, located in Prince William Sound, Alaska. Preliminary investigation of target strength (TS) information has detected seasonal variation in size classes and vertical changes in distribution of fish and plankton. Seasonal fluctuations in the relative frequency of detected targets below -60dB, indicating plankton size targets, mark the spring bloom of plankton. In addition, seasonal shifts in TS range may be due to the influx and growth of new herring recruits. Diel changes in depth distribution showed that some fish may be undergoing daily vertical migrations. Further investigation of the acoustic and catch data sets will be needed to expand on the observed changes. Improvements in hydroacoustic equipment and subsequent data processing are discussed, with suggestions for further research.

Multi-species management and restoration: Collectively, since harvest of all three species (pink salmon, herring, pollock) are being managed in PWS, we are already practicing a form of multispecies management; it is just not a coordinated effort (“ostrich management”). If all three species were independent of each other, this practice might be acceptable. However, SEA has shown that the pink salmon, herring and walleye pollock populations are dominant competitors and/or predators in the Sound. Since the EVOS Trustee Council is a unique entity in the fact that it represents the agencies that are responsible for establishing harvest strategies for pink salmon, Pacific herring and walleye pollock management, the continued investment in monitoring these populations creates an opportunity to evaluate the use of multi-species harvest strategies to assist the restoration of damaged species. The key to making multi-species management decisions is having reliable estimates of the abundance of each species and knowledge of how they interact. The next step is up to the three management teams to talk to each other about the information. The opportunity to evaluate a multiple-species approach to fisheries management in the Prince William Sound is unique and could be a major contribution to fisheries science by the EVOS Trustee Council.

CHAPTER 1

Distribution and abundance of walleye pollock (*Theragra chalcogramma*) in Prince William Sound, 1994 to 1997. G. B. Steinhart, G. L. Thomas, J. Kirsch, and N. Peters

ABSTRACT

We have used acoustics to measure abundance and distribution of walleye pollock (*Theragra chalcogramma*) in Prince William Sound (PWS) since 1994. We found that during the spring and summer, pollock abundance in the northwest PWS increased, while pollock density decreased in southwest passages. We believe that this increase in pollock may have been influenced by the timing and magnitude of the spring zooplankton bloom, one of the primary prey items of pollock in the Sound. In 1994, a year with a relatively late, and small, bloom of *Neocalanus spp.*, pollock were more abundant near Esther Island than during any other year we sampled. We believe this observation supports the Prey-Switching hypothesis: in the absence of abundant plankton, pollock switch to other prey items, including salmon fry.

INTRODUCTION

Walleye pollock (*Theragra chalcogramma*) are one of the most abundant and ecologically important fish species in Prince William Sound (PWS). Not only do they support a commercial fishery, but they play a large role in the food-web dynamics of the Sound. With over 30,000 tonnes of pollock in the Sound (Thomas and Stables 1996; Kirsch 1997), pollock could have dramatic effects on recruitment of juvenile fishes through predation and/or competition. The goal of this research is to describe the abundance and distribution of pollock in western Prince William Sound in order to better understand their role in the ecosystem.

Many previous studies have looked at the behavior, distribution, and abundance of walleye pollock in the North Pacific (Dwyer et al. 1987; Bailey 1989; Brodeur and Wilson 1996); however, some of these studies focused on juvenile pollock, and none looked at behavior of pollock in Prince William Sound. These earlier studies found that pollock ate mostly young fish, including juvenile walleye pollock. In PWS, however, adult pollock have been shown to eat mostly macro-zooplankton (Thomas et al. 1997a). The Prey Switching hypothesis (SEA 1993) predicts that as macro-zooplankton availability decreases, pollock will switch from eating primarily zooplankton to juvenile fish and other large invertebrate prey. Given their abundance, if pollock began to prey on salmon fry, they could dramatically affect the survival and recruitment of many fish species in the Sound, including commercially important pink salmon.

In this paper we present the results from four years of acoustic surveys in Prince William Sound. This work was part of the Sound Ecosystem Assessment Project (SEA): an ecosystem level study of PWS. An assumption of SEA that was adapted from GLOBEC is that fish fry do not die by starvation, but that all mortality is the result of being eaten. Pollock, being the most abundant pelagic fish, are considered to be the primary predator of pink salmon fry in the Sound (M. Willette, pers. com.). By looking at how pollock abundance and distribution have changed over various time and spatial scales, we increase our knowledge of how this predator behaves. The first step in determining if pollock are feeding on zooplankton and/or salmon is to show that there is co-occurrence of pollock with either zooplankton or salmon. Since pollock are one of the most abundant fish species in PWS, understanding their ecology will aid us in efforts to restore and protect the valuable resources of the Sound.

MATERIALS AND METHODS

Study site

Prince William Sound (PWS) is located at the northern edge of the Gulf of Alaska (Fig. 1). This large fjord/estuary covers an area of approximately 8800 km², and has about 3200 km of shoreline (Grant and Higgins 1910). Coastal rainforests, high mountains, and glaciers border the shoreline of PWS. The area receives seasonally intense storms moving up from the Gulf of Alaska, resulting in more than 7 m of annual rainfall.

Survey design

The survey designs differed during the four years of this project (Table 1). In 1994, offshore surveys were conducted during the day throughout western PWS (Fig. 2). There were 5 cruises where usable acoustic data were collected: 02a (5/4-5/16/94), 03a (5/17-5/24/94), 04a (6/2-6/15/94), 05a (6/24-6/30/94), and 06a (7/7-7/17/94). There were 88 different parallel transects in Wells, Perry, and Knight Island Passages, Montague Straight and the Southwest passages (Thomas et al. 1996). Many of these transects were repeated in the various cruises; however, not all cruises surveyed all transects. Data were collected with a BioSonics 101-120 kHz dual beam echosounder.

In 1995, there were two different survey designs (Table 1). There were two broadscale surveys of PWS, consisting of approximately 15 long transects throughout open, deep water areas all around the Sound. The broadscale surveys were conducted from 4/27-5/1/95, and from 5/23-5/27/95. Immediately following the broadscale surveys, we commenced sampling for the offshore (> 0.5 NM from shore) diel surveys. These surveys were concentrated in northwest portion of PWS (Fig. 3), and were designed to examine differences between nearshore and offshore distributions of fish (See Thomas et al. 1997a for nearshore survey methods and results). The tow offshore surveys were conducted from 5/2-5/18/95 (Cruise 07a) and 5/28-6/15/95 (Cruise 08a). The offshore

surveys were conducted aboard the F/V Alaska Beauty with a BioSonics 101-120 kHz dual beam echosounder, set to collect data to a depth of 250 m.

In 1996, sampling was limited to Wells and Perry Passages, Ester Island, and Unakwik and Kiniklik Inlet. Three cruises were conducted beginning in early May, and ending in early June: 11k (5/3-5/10/96), 12k (5/20-5/19/96), and 13k (6/1-6/8/96). The surveys were conducted nearshore ($< .05$ NM), and consisted of one long transect parallel to the shoreline, and 5 parallel transects perpendicular to the shoreline (Fig. 4). The surveys were repeated 4 times a night: 2000, 2300, 0200, and 0500. Data were collected with a down-looking BioSonics 101-120 kHz dual beam echosounder.

During 1997, sampling was conducted in the eastern portion of PWS, as well as some of the western sites surveyed in 1996. The eastern sites sampled included Sheep Bay, Port Gravina, and Fish Bay. Three cruises were conducted beginning in early May, and ending in early June. The surveys were conducted nearshore, and consisted of a long transect parallel to the shoreline, and 5 parallel transects perpendicular to the shoreline (Fig. 4). The surveys were repeated 4 times a night: 2000, 2300, 0200, and 0500. Data were collected with a down-looking 38 kHz digital transducer, however, these data are still being analyzed. The data presented here are from a down-looking BioSonics 101-120 kHz dual beam echosounder that used during the final cruise, 22m (11 June - 18 June, 1997).

For all surveys, transects were marked on paper and/or electronic charts to allow repetition of the same transect. At night, or during low tide, some transects were modified for safety purposes. Boat speed during transects was approximately 4-6 kn. The down-looking transducers were mounted on a fin towed alongside the boat at a depth of approximately 2 m.

Personnel from the Alaska Department of Fish and Game (ADF&G) collected numerous fish samples using a variety of fishing gear. Commercial seines and mid-water trawls were used for target verification of the acoustic data. In addition, small purse seines, pair trawls, bottom trawls, gillnets and longlines were used to collect fish. These fish were used for age/length/weight measurements and diet analyses.

Acoustic equipment

The acoustic data presented here was collected using a BioSonics 101-120 kHz dual-beam transducer. The data were processed in real-time using ESP software on a 486 laptop computer. A Magellan DLX-10 GPS receiver with an external antenna was used to geo-reference the data. Echo-square integration, dual-beam target strength (TS), and GPS data were stored on the computer hard disk, and backed up on tape drives. Raw acoustic signals were stored on Digital Audio Tape.

The acoustic systems were calibrated before most cruises, but at least once per year (Table 2). The transducers were attached to a floating platform, and a tungsten-carbide

standard target was carefully moved within the beam of the transducer until a large sample of target positions were collected. Using the known TS of the standard target, the peak target strength from the calibration was used to calculate the source level and receiver gains (Foote and MacLennan 1982). The calibration of the system was not different from 1995, 1996 and 1997.

Acoustic processing

Once the cruise was completed, the acoustic files were transferred to UNIX workstations where batch processing of files was performed. To facilitate reduction and processing of acoustic information, software was written in the Interactive Data Language (IDL) which corrected for physical parameters (temperature and salinity), and applied the acoustic calibrations. After initial processing, additional IDL software was used to interactively remove untracked bottom, and to calculate density and biomass estimates.

Echo-square integration has been shown to be an effective tool for estimating fish biomass when densities are high (Ehrenberg and Lytle 1972); however, pollock densities are relatively low in PWS. Therefore, we used an echo-counting technique to estimate pollock density and biomass. A test of our echo-counting technique was performed in 1995, and showed that for our data, echo-counting resulted in a small underestimate pollock density for most surveys (Thomas et al. 1996).

Our echo-counting consisted of two major steps: target classification and target counting (Fig. 5). First, we identified targets which were not pollock. These targets were identified using information on the paper echograms, electronic target echograms, net catch data, and knowledge of fish behavior and distribution. Targets that were identified as non-pollock, but potentially had a similar TS range as pollock, were interactively selected and removed. Examples of removed targets included: dense plankton aggregations and tightly schooled herring and capelin. Although these species generally have a TS range below that of adult pollock, when found in tight aggregations, coincident targets may sum to a yield a pollock-sized TS. In addition, rockfish, which were easily identifiable as clumps of targets on pinnacles and slopes, were removed since they are similar in TS to pollock, but are not vulnerable to sampling by mid-water trawl.

Once the remaining targets were selected, we counted all targets that fell within a specified TS range (-39 to -25 dB). We chose a TS range based on the observed size distribution of pollock captured in the mid-water trawls and the acoustic data (Figs. 6 and 7). We then expanded the range of counted targets in an attempt to compensate for the inherent variation in TS due to various factors, including: target tilt, target depth, and changes in body condition (Love 1997; Traynor and Ehrenberg 1979; Traynor and Williamson 1983; Mukai and Iida 1996). After counting all qualifying targets, we used the net data (mid-water trawl and pair-trawl only) to examine the species composition at the survey sites.

Since pollock made up almost of all trawl catches of fish greater than 350 mm (a couple salmon were captured, as were a couple large herring), we considered our selected and counted targets to be pollock. The sum of the echo-counted targets was divided by the sample volume of the acoustic beam to compute mean density for each transect. Mean pollock densities were calculated by taking the weighted mean of all transects at a particular site during a single survey. Transect length (the number of reports) was used as the weighting factor in 1994 and 1995. In 1996, due to the short length of the transects, and the repeated survey design, we used each sample period as the sample unit. The sum of reports for each sample period was used as the weighting factor in 1996. All statistical analyses were conducted using $\alpha=0.05$.

RESULTS

1994

Pollock distribution was seasonally variable in the western portion of Prince William Sound in 1994. Pollock densities increased in the northwest passages, but remained nearly constant in the middle passages, and declined in the southwest passages (Fig. 8). In Wells Pass (Site 13), pollock densities increased significantly from mid May to early June ($df=17$, $t=2.09$, $p=0.026$). In Perry Passage (Site 14), another northern area, there was initially a significant decrease in pollock density from early May to mid May ($df=18$, $t=4.64$, $p=0.00007$); however, pollock density significantly increased from early June to early July ($df=12$, $t=2.04$, $p=0.032$).

In the Middle passages, there was little change in pollock densities (Fig. 8). In southern Perry Passage (Site 15), there was a small, but significant decrease in pollock density from early May to late May ($df=12$, $t=1.89$, $p=0.042$). There were no other significant differences in density in this area of the Sound.

In contrast to the northwest passages, the southern passages tended to decrease in pollock density through the spring and summer (Fig. 8). In lower Knight Island Passage (Site 17), there was a significant decline in pollock density from mid May to late June ($df=16$, $t=3.14$, $p=0.003$), and from late June to mid July ($df=18$, $t=10.3$, $p<<0.05$). In Montague Strait (Site 18), there was a significantly higher density of pollock in late June than in late July ($df=26$, $t=6.25$, $p<<0.05$). There were no significant changes in the observed pollock densities near Elrington and Latouche Passages (Site 19).

The depth distribution of pollock changed during the spring and summer of 1994 (Fig. 9). More fish were found near the surface during the earlier cruises, and they appeared to move deeper as the year progressed. This was especially evident during the July cruise (06a), when pollock densities near the surface were 80% lower than the early May cruise (02a).

1995

Between the two broadscale surveys from 1995, there was a decrease in pollock density in each of four major areas in the Sound (Fig. 10) but none of the differences were significant. However, we did see a rather large change in the vertical distribution of targets (Fig. 11). In the late April broadscale (07a), more targets were found near the surface than in the May broadscale (08a). In addition, the number of pollock deep in the water increased from April to May.

During the 1995 offshore surveys, we saw an increase in pollock during the spring and summer (Fig. 12). There were significant increases in pollock density at Hodgkin Point (Site 502; $df=46$, $t=12.45$, $p<<0.05$), Tipping Point (Site 506; $df=111$, $t=10.35$, $p<<0.05$), and west Esther Island (525; $df=73$, $t=8.42$, $p<<0.05$). There were no significant differences at south Esther Island (501; $df=92$, $t=1.35$, $p=0.09$) or Perry Passage (531; $df=18$, $t=0.89$, $p=0.19$). All other sites did not have repeated surveys.

Most pollock were found in the top 50 m during the 1995 offshore surveys (Fig. 13). However, from April to May, the density of pollock below 40m increased dramatically, while numbers near the surface decreased slightly.

1996

Pollock densities increased in many of the nearshore areas surveyed in 1996, but only by the last cruise (Fig. 14). There were few sites that had data from both the early May and late May cruises, but at the one site where there were repeated surveys, west Esther Island (site 525), there was no significant difference in pollock numbers ($df=15$, $t=0.31$, $p=0.38$). There were significant increase in pollock density from early May to early June at south Esther Island (site 501; $df=15$, $t=6.18$, $p<<0.05$). From late May to early June, pollock densities increase significantly at Tipping Point (site 506; $df=6$, $t=2.48$, $p=0.024$), west Esther Island (site 525; $df=8$, $t=2.57$, $p=0.017$), at the mouth of Esther and Quillian Bays (site 526; $df=5$, $t=3.41$, $p=0.01$), and at Kiniklik (site 587; $df=5$, $t=2.19$, $p=0.04$); however, there was no significant difference in pollock density at Culross Island (site 504; $df=12$, $t=0.81$, $p=0.23$) and Unakwik (site 586; $df=5$, $t=1.6$, $p=0.085$).

The vertical distribution of pollock did not change as much in 1996 as in the other years (Fig. 15). By early June, however, there were more pollock deep in the water column than during the first two surveys. There was not a decline in pollock numbers near the surface, rather pollock densities were generally lower near the surface than in other years.

1997

Only some of the data has been processed from the 1997 cruises (Figs. 16 and 17). The highest pollock densities were found in Fish Bay (site 585), Sheep Bay (site 611), Kiniklik (site 587) and Culross Island (site 505). It should be noted, however, that we have no trawl data from this cruise, so the numbers should be considered adult pollock-sized

targets, and not necessarily as adult pollock. The vertical distribution showed a peak near the surface, and between 150 and 200 m.

DISCUSSION

Pollock in Prince William Sound displayed seasonal changes in abundance and vertical distribution. We believe this behavior is related to food resources in PWS, primarily zooplankton and salmon fry abundance. Our data show insight into how pollock populations behave in PWS, and when combined with oceanography and zooplankton data, will help determine the validity of the Lake/River and Prey Switching hypotheses (Cooney 1993).

Pollock migrated northward into Prince William Sound as the year progressed in 1994, 1995, and 1996. Commercial fisherman have long reported finding large concentrations of adult pollock in Port Bainbridge and the southwest Passages during winter (Thomas et al. 1996). Our own pollock surveys have also shown this (Kirsch 1997). These pollock probably begin migrating northward after the winter, eventually reaching as far north as Port Wells. Our data showed an increase in pollock densities in northwest PWS from May to June. Furthermore, as pollock numbers increased in the north, they often decreased in southern areas, while remaining nearly constant in the middle portion of western PWS (Fig. 8). These data all supports the hypothesis that the adult pollock migrate northward after the winter.

The one anomaly to the trend of increased pollock abundance in northwest PWS was seen in the 1995 broadscale data. Pollock densities were lower in the later cruise than in the first, although the difference was not statistically significant. The observed decline could be attributed to two factors. First, the broadscale surveys covered vast areas, including central and eastern PWS, but not in great detail, and with no repeated transects. The variability of pollock spatial distribution may therefore be a confounding factor. Second, pollock moved deeper in the water column from the first to the second broadscale survey. The areas covered were in very deep water, and it is very likely that some of the pollock had migrated deeper than 250 m, beyond the maximum range we collected data.

The pollock migration into the Sound is probably part of a seasonal feeding migration after spawning. We did see a strong positive correlation of pollock biomass with zooplankton density (see Chapter 2). One piece of evidence supporting the hypothesis that pollock abundance and migration patterns may be related to zooplankton is shown in the inter-annual differences in timing and magnitude of the spring zooplankton bloom. The Prey Switching hypothesis predicts that when plankton densities are low, pollock will switch to other prey, including salmon fry. In 1994, the *Neocalanus spp.* bloom appeared later, and was smaller, than in 1995 (Fig. 18). Late April/early May pollock densities in the northwest were higher in 1994 than 1995, before the observed peak in the bloom of *Neocalanus spp.*(Fig. 19). It is possible that the high densities

observed in this area in 1994 were pollock that had migrated northward more quickly, in order to feed on the salmon fry being released from Wally Noerenbuerg Hatchery. Conversely, in 1995, the late northward migration of pollock may be a result of the abundant plankton that year. With plenty of food available, there was no energetic need to migrate to other areas until later that year. Salmon fry released from Wally Noerenberg hatchery had lower survival in 1994 (low *Neocalanus spp.* densities and high pollock densities) than in 1995 (high *Neocalanus spp.* densities and low pollock densities). These data support the Prey Switching hypothesis; however, we have only 2 years of data from throughout the Sound (we do not have zooplankton numbers from 1996 or 1997), so this inter annual variability is not yet fully understood.

The vertical distribution of pollock also changed throughout the year. In general, as the year progressed, pollock tended to move deeper in the water column. This migration may be to follow the large marine copepods, who migrate down in spring to overwinter in deep waters (Cooney 1987; see Chapter 2). In 1994, the largest decrease in pollock abundance in the top 50 meters occurred between the cruise 02a (early May) and 03a (mid May), and between 05a (late June) and 06a (July). The biomass of *Neocalanus spp.* in the top 50 m dropped to nearly zero in mid June, approximately the same time that pollock migrated deeper in the Sound. In 1995, there was downward seasonal migration of the pollock. It was more evident in the offshore surveys than in the broadscale surveys, but in both cases, there were also large numbers of pollock near the surface. This may demonstrate how some pollock are feeding on plankton (those that migrate down later in the year), while others stay near the surface to feed on salmon fry, where they are present. The areas surveyed in the broadscale surveys were not likely to contain many salmon fry, since the transects were far from shore, this may explain why there was a large decrease in the number of pollock observed in the top 25 m. The 1995 offshore surveys (> 0.5 NM) were much closer to shore than the broadscale surveys, and were areas where one would expect to find salmon fry. In these surveys, pollock densities remained high near the surface, with only a portion of the population migrating deep.

Our present results may be confounded by statistical problems. The small sample volume of the acoustic beam in shallow water, combined with relatively low overall fish densities, lead to high variability in our density estimates. The addition of one target in the top 10 m of a transect can have a significant effect on the predicted biomass for a relatively short transect (e.g. the 1996 and 1997 nearshore surveys). In addition, target strengths of fish are highly variable and depend on many factors (Love 1977; Traynor and Williamson 1983; Mukai and Iida 1996). For example, a fish swimming up or down within the acoustic beam is tilted and thus presents a reduced cross-section to reflect the acoustic signal. The reduced acoustic return will lead to an underestimate of the total length of the fish. Furthermore, an echo from a fish that is only partially within the acoustic beam will also underestimate the target's size. In both these cases, the reduced signal return may result in a pollock-sized target being incorrectly classified as a non-pollock. Partially overlapped targets, which will occur more

frequently with depth, cause the target discriminator to omit targets. This will underestimate the number of targets in deep water. Also, dual beam target strength determination requires some tracking, but at short ranges there are insufficient sonifications to track a target. Future work will focus on overcoming the statistical problems of a small sample volume near the surface to improve our echo-counting procedure.

In conclusion, pollock behavior, abundance, and distribution are dynamic between and within the years of this study. Further analysis will be used to test the hypothesis the migrations are driven by food resources. If low zooplankton biomass results in more pollock in areas with high salmon fry abundance, it could lead to reduced survival of salmon fry. Conversely, when plankton are abundant, pollock may not migrate to areas with high fry numbers, instead choosing to feed on plankton, and undergoing a seasonal vertical migration that follows the seasonal copepod migration. Future work will focus on completing our comparison of pollock distribution with relation to plankton abundance, and comparing salmon fry survival to pollock density and distribution.

ACKNOWLEDGMENTS

We would like to thank all the captains and crews of all the fishing and research vessels that helped us collect these data. Without their knowledge and experience, this research would not have been possible. We would also like to thank the Alaska Department of Fish and Game, and the University of Alaska-Fairbanks, for they were responsible for the daunting task of analyzing the catch and zooplankton data. We would especially like to thank Mark Willette for his contributions to this research. This work was supported by the *Exxon Valdez* Trustee Council, Grant No. 97320-N.

REFERENCES CITED

- Bailey, K. M. 1989. Interaction between the vertical distribution of juvenile walleye pollock *Theragra chalcogramma* on the eastern Bering Sea, and cannibalism. Mar. Ecol. Prog. Ser. 53: 205-213.
- Brodeur, R. D., and M. T. Wilson. 1996. Meso-scale acoustic patterns of juvenile walleye pollock (*Theragra chalcogramma*) in the western Gulf of Alaska. Can. J. Fish. Aquat. Sci. 53: 1951-1963.
- Cooney, R. T. 1987. The seasonal occurrence of *Neocalanus cristatus*, *Neocalanus plumchrus* and *Eucalanus bungii* over the shelf of the northern Gulf of Alaska. Continental Shelf Res. 5: 541-553.
- Cooney, R. T. 1993. A theoretical evaluation of the carrying capacity of Prince William Sound, Alaska, for juvenile Pacific salmon. Fisheries Research, 18: 77-88.
- Dwyer, D. A., K. M. Bailey, and P. A. Livingston. 1987. Feeding habits and daily ration of walleye pollock (*Theragra chalcogramma*) in the eastern Bering Sea, with special reference to cannibalism. Can. J. Fish. Aquat. Sci. 44: 1972-1984.
- Ehrenberg, J. E. and D. W. Lytle. 1972. Acoustic techniques for estimating fish abundance. Trans. Geosci. Elec. GE-10: 138-145.
- Foote, K. G. and D. N. MacLennan. 1982. Use of elastic spheres as calibration targets. p. 52-58. In O. Nakken and S.C. Venema [ed.], Symposium on fisheries acoustics. ICES/FAO. Bergen, Norway.
- Grant, U. S. and K. F. Higgins. 1910. Reconnaissance of the geology and mineral resources of Prince William Sound, Alaska. U.S. Geological Survey Bulletin. No. 443. 89 pp.
- Kirsch, J. 1997. Acoustic biomass estimate of adult walleye pollock in Prince William Sound, Alaska, in winter 1997. Report to the Alaska Department of Fish and Game. Prince William Sound Science Center. Cordova, AK.
- Love, R. H. 1977. Target strength of an individual fish at any aspect. J. Acoust. Soc. Amer. 62: 1397-1493.
- Mukai, T. and K. Iida. 1996. Depth dependence of target strength of live kokanee salmon in accordance with Boyle's law. ICES J. of Marine Sci., 53: 245-248.
- PWSFERPG. 1993. SEA Plan: Initial science plan and monitoring program. 111 p.

Thomas, G. L., J. Kirsch, T. McLain. 1996. SEA: Nekton-plankton acoustics second annual report, 1995. Restoration Project 95320N. EXXON VALDEZ Trustee Council. Anchorage, Alaska. 120 pp.

Thomas, G. L. and T. B. Stables. 1996. Winter 1995 estimates of the prespawning biomass of walleye pollock in Prince William Sound, Alaska. Report to the Alaska Department of Fish and Game. Prince William Sound Science Center. Cordova, AK.

Thomas, G. L., J. Kirsch, G. B. Steinhart, and N. Peters. 1997. SEA: Nekton-plankton acoustics second annual report, 1996. Restoration Project 96320N. EXXON VALDEZ Trustee Council. Anchorage, Alaska. 120 pp.

Thomas, G. L., E. V. Patrick, J. Kirsch, and J. R. Allen. 1997. Development of an ecosystem model for managing the fisheries resources of Prince William Sound. pp . 606-613. D. C. Smith, A. Grant, and J. P. Beumer [eds.], Developing and sustaining world fisheries resources. CSIRO. Collingwood, Australia.

Traynor, J. J. and J. E. Ehrenberg. 1979. Evaluation of the dual-beam acoustic fish target strength method. J. Fish. Res. Bd. Can. 36: 1065-1071.

Traynor, J. J. and N. J. Williamson. 1983. Target strength measurements of walleye pollock (*Theragra chalcogramma*) and a simulation study of the dual-beam method. Proceedings of the Symposium on Fisheries Acoustics. FAO Fish. Rep. No. 300: 112-124.

Table 1. Survey location, design, and purpose for 1994-97 SEA Nekton-Plankton Acoustic cruises. Other cruises were conducted, and more data were collected, but this table describes the cruises where data presented in this report were collected.

Year	Surveys	Locations	Survey Design	Survey Purpose
1994	Offshore	Western PWS	Repeated same transects monthly	Examined monthly trends and patchiness of pollock distribution
1995	Offshore Broadscale	All PWS	Two repeated surveys covered vast distances	Examined summer trends and patchiness of pollock distribution
	Offshore Diels	NW PWS	Surveyed every 3 h for 24 h period at each site	Examined summer and daily changes in pollock abundance and distribution
1996	Nearshore	NW PWS	Surveyed each site four times at night Monthly repeated sampling at sites	Examined monthly and daily changes in pollock abundance and distribution in nearshore areas
1997	Nearshore	NW and NE PWS	Surveyed each site four times at night	Examined daily changes in pollock abundance and distribution in nearshore areas

Table 2. Parameters of the acoustic equipment used during sampling of Prince William Sound in 1997.

System	Frequency	Source Level	System Gain	Transducer Directivity	Pulse Duration
101	120 kHz	225.023	-159.282	0.0010718	0.4 ms
102	200 kHz	221.655	-155.765	0.0006515	0.4 ms

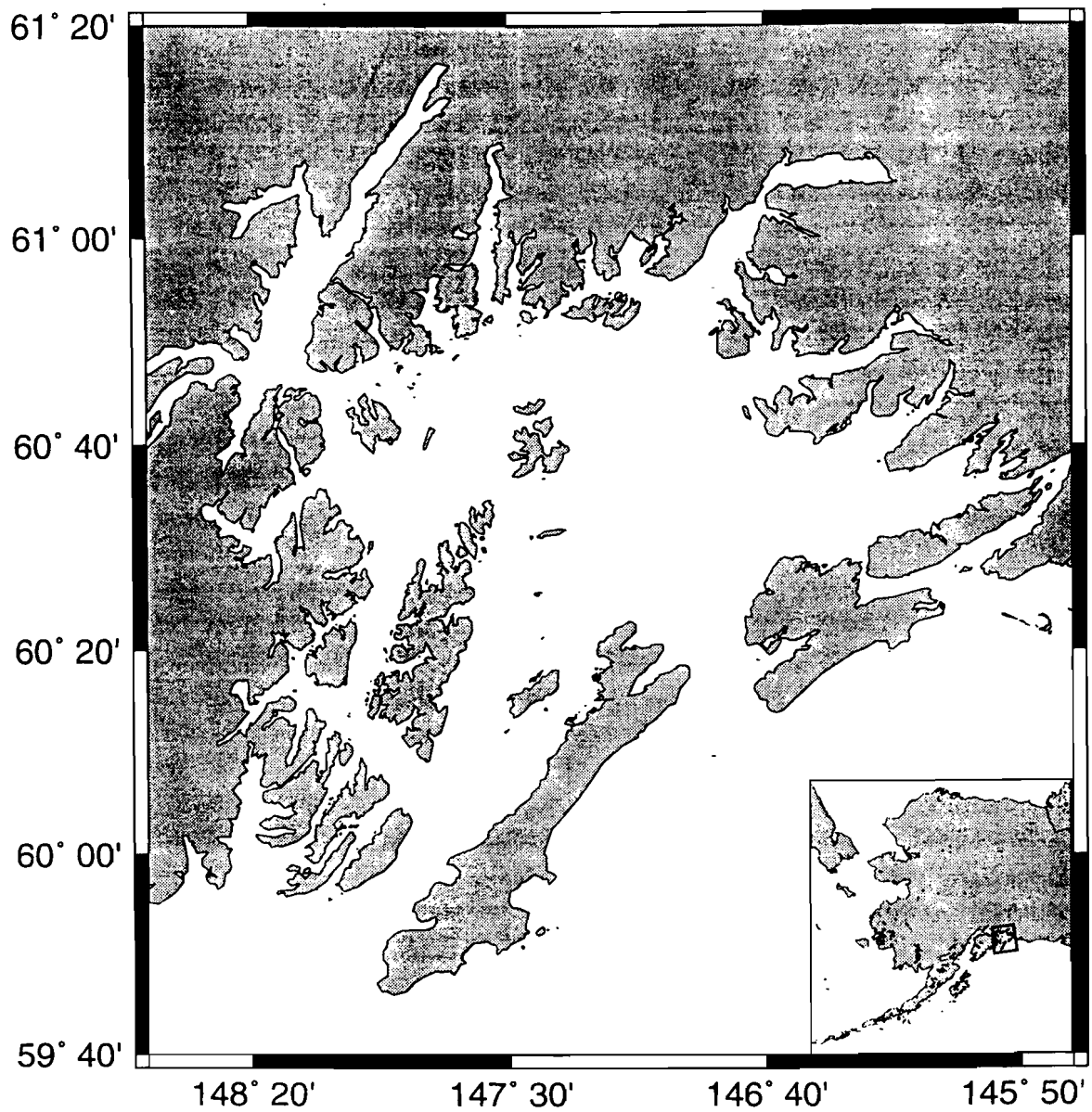


Fig. 1. Map of Prince William Sound, Alaska, USA.

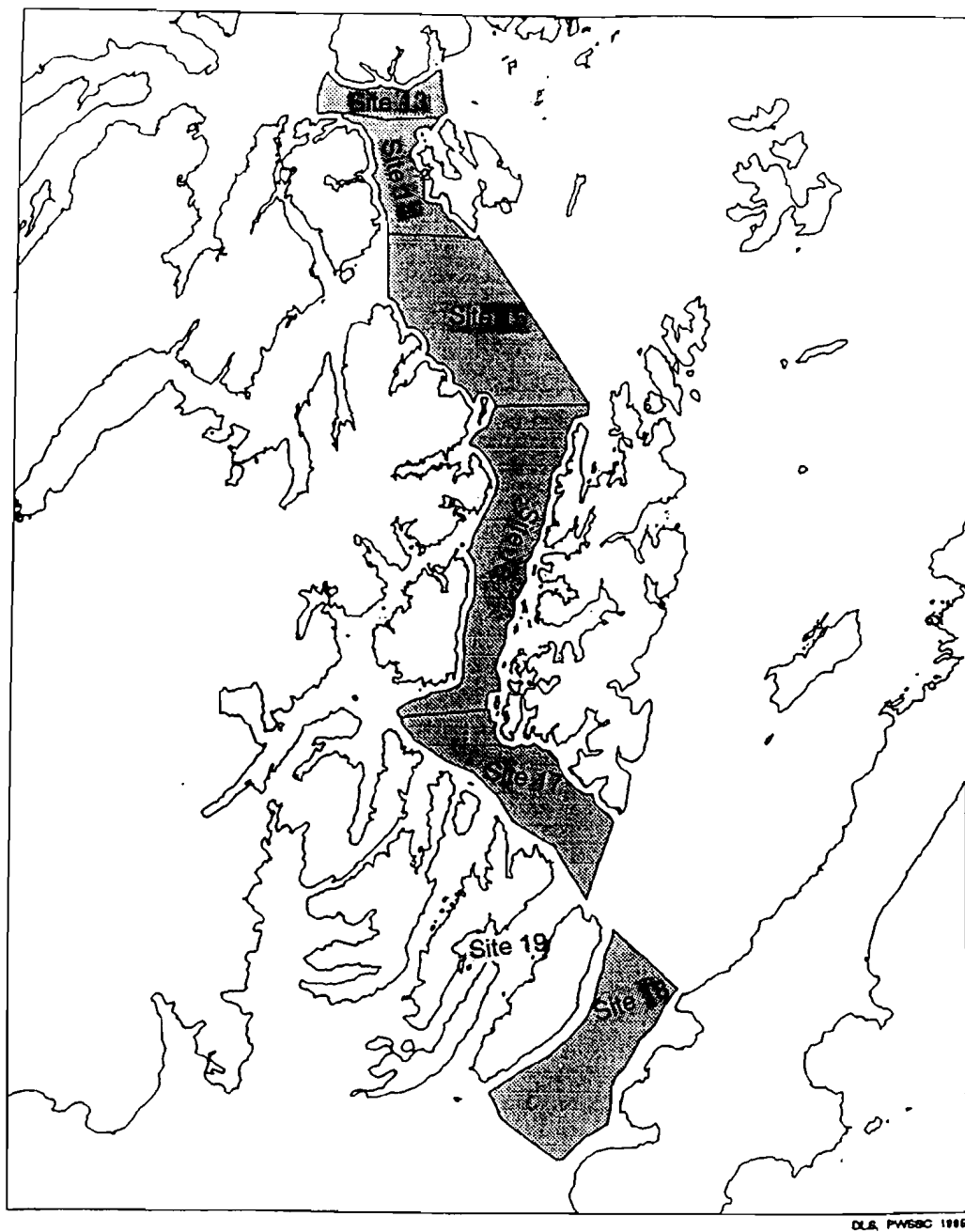


Fig. 2. Map of western Prince William Sound showing the offshore areas surveyed in 1994.

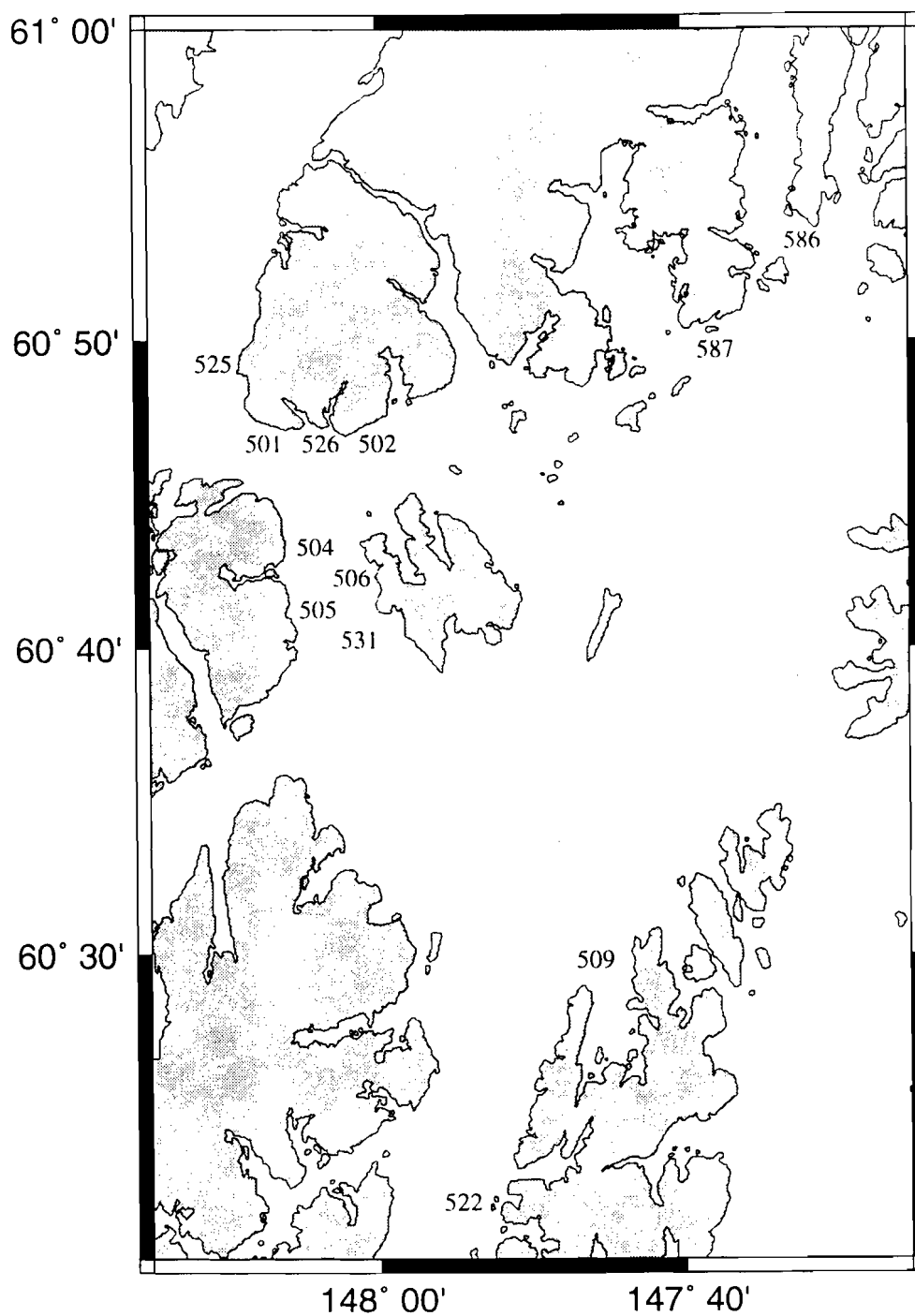


Fig. 3. Map of northwestern Prince William Sound showing where most of the sampling occurred in 1995, 1996, and 1997. The site numbers (from ADF&G) are in the approximate locations of sampling areas.

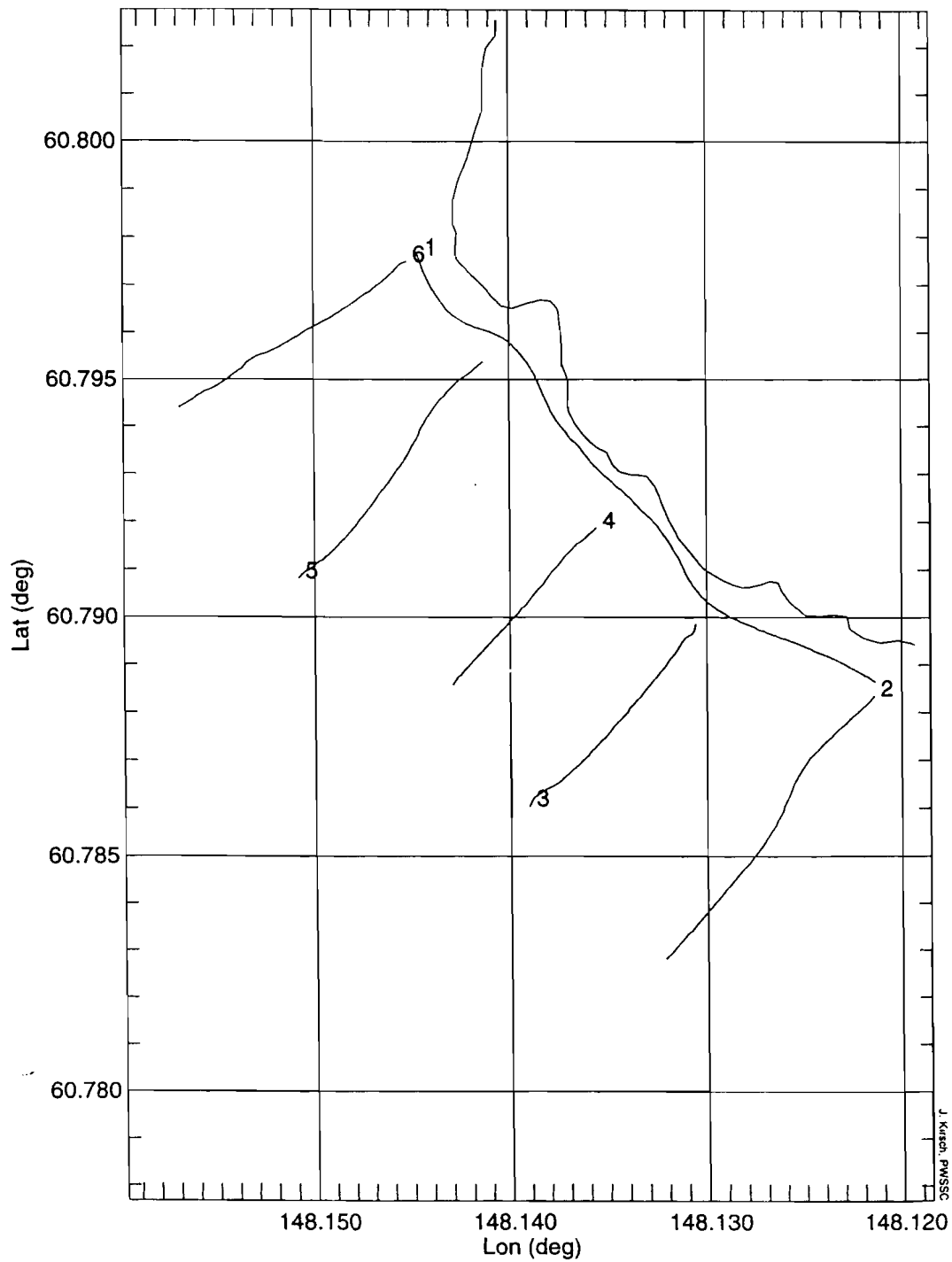


Fig. 4. Map of transect design used during 1996 and 1997 acoustic surveys: one along shore transect, followed by 5 perpendicular to shore transects.

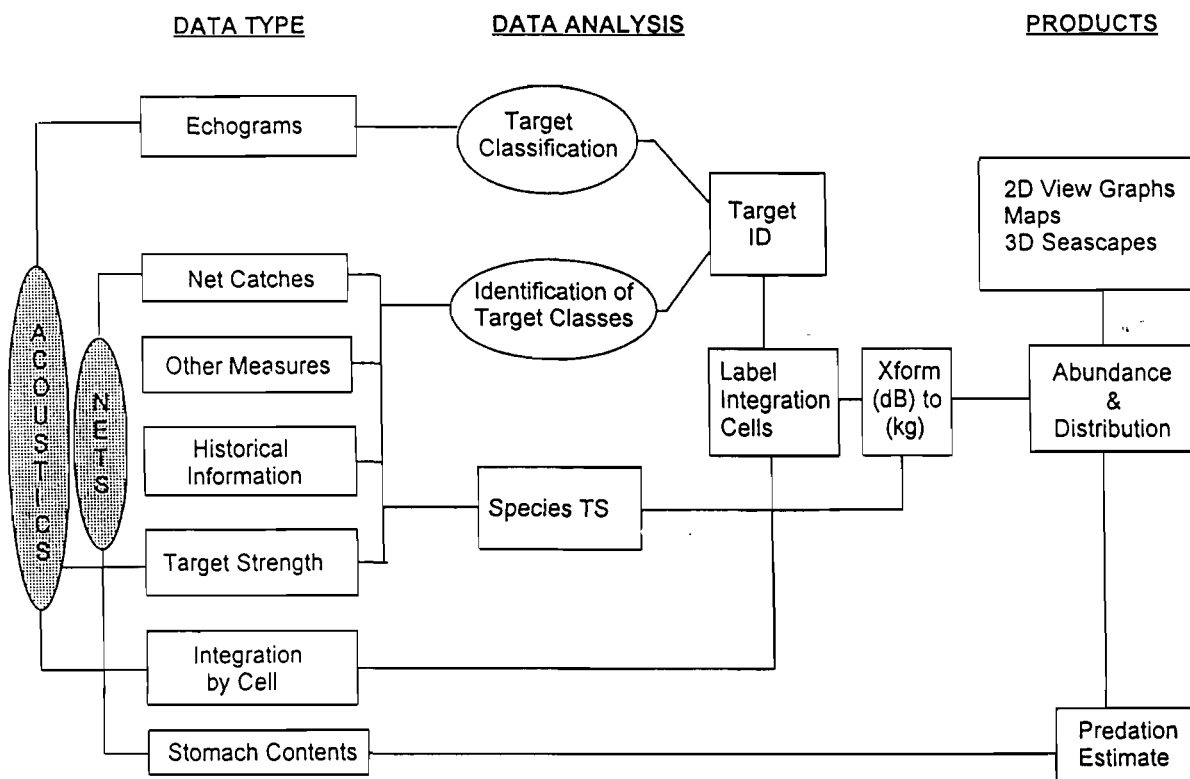


Fig. 5. Flow chart of data processing steps used in analysis of SEA acoustic data collected in 1994-97.

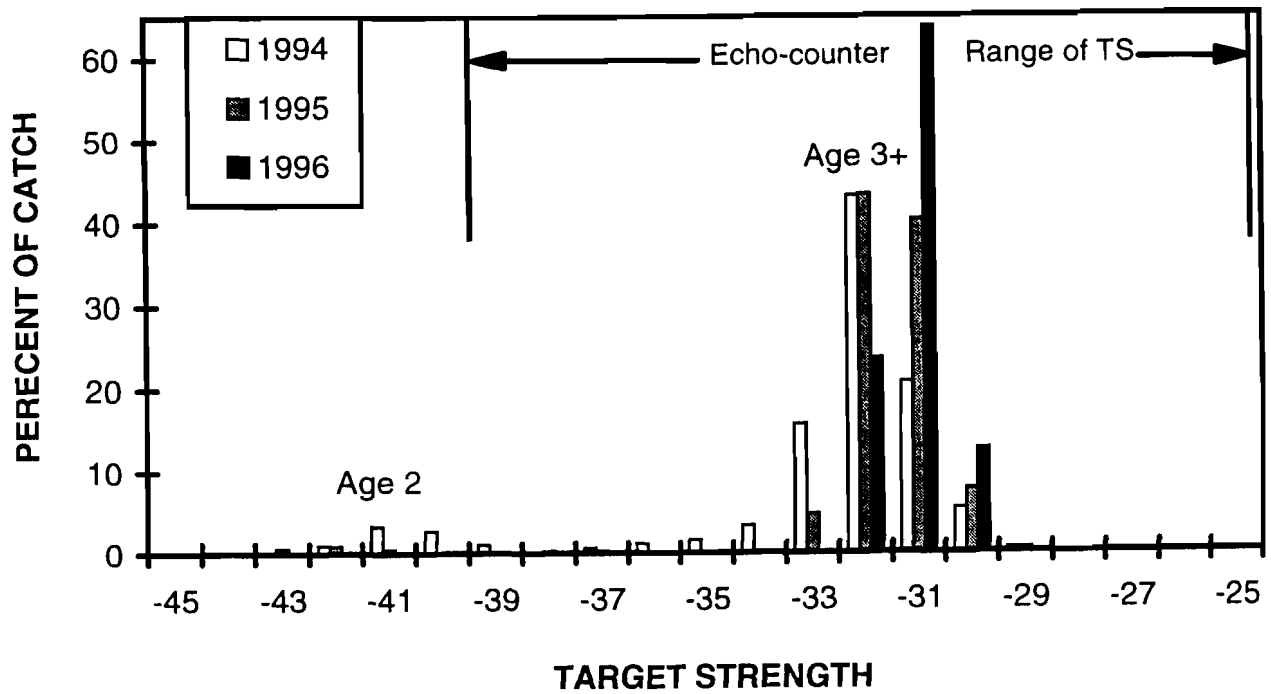


Fig. 6. Predicted target strength (TS) distribution of pollock captured in mid-water trawls in 1994, 1995, and 1996. TS values were calculated using the equation $20 \log(\text{Length} - 66)$ (Traynor 1978). Also shown is the range of TS values accepted by the echo-counter.

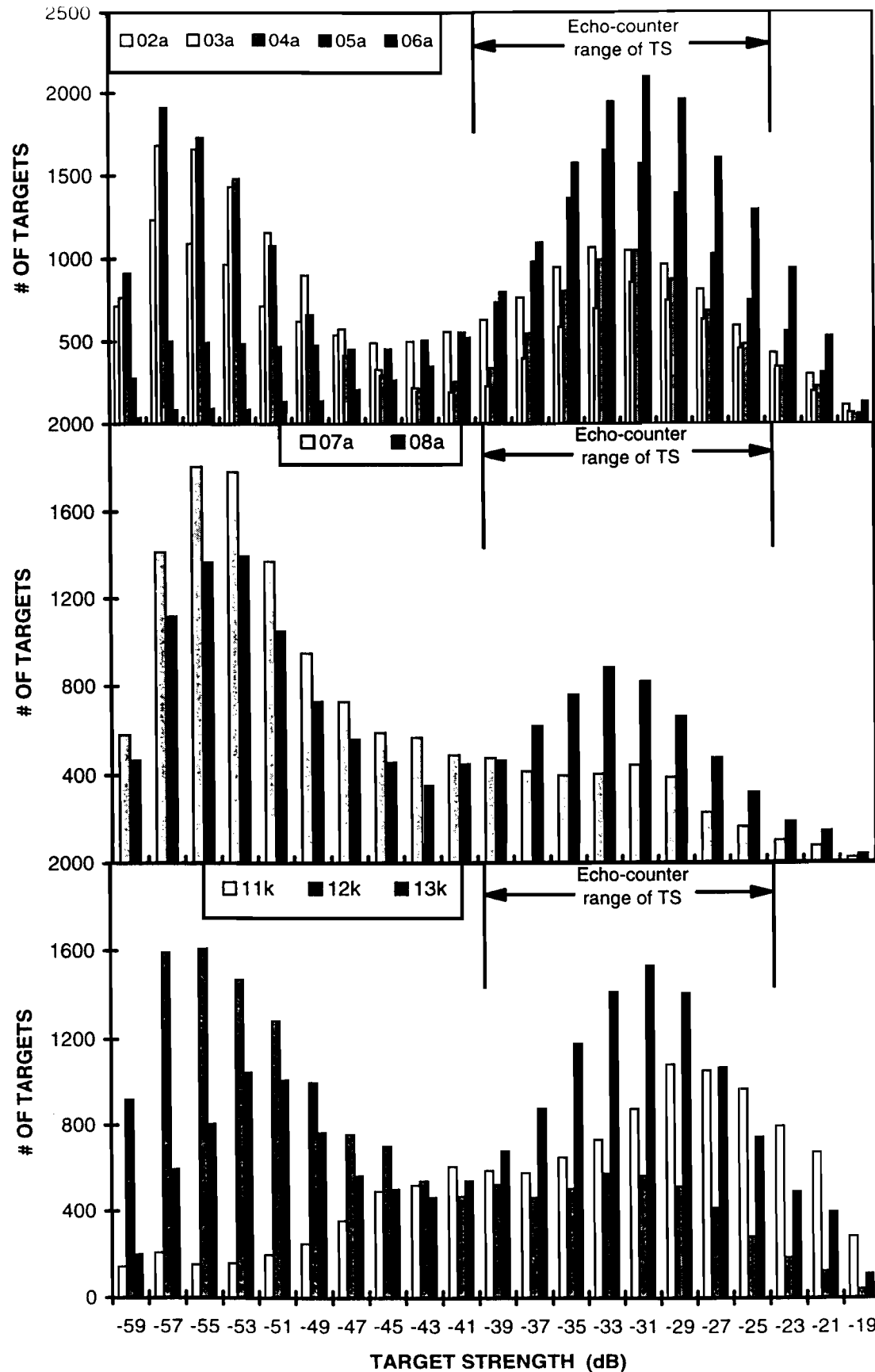


Fig. 7. Target strength (TS) distribution of acoustic data used in our echo-counting procedure from 1994 (02a-06a), 1995 (07a, 08a), and 1996 (11k-13k). Due to the huge amounts of data collected, the data graphed represent systematic random samples of approximately 15,000 targets per cruise. Also shown is the range of TS values accepted by the echo-counter.

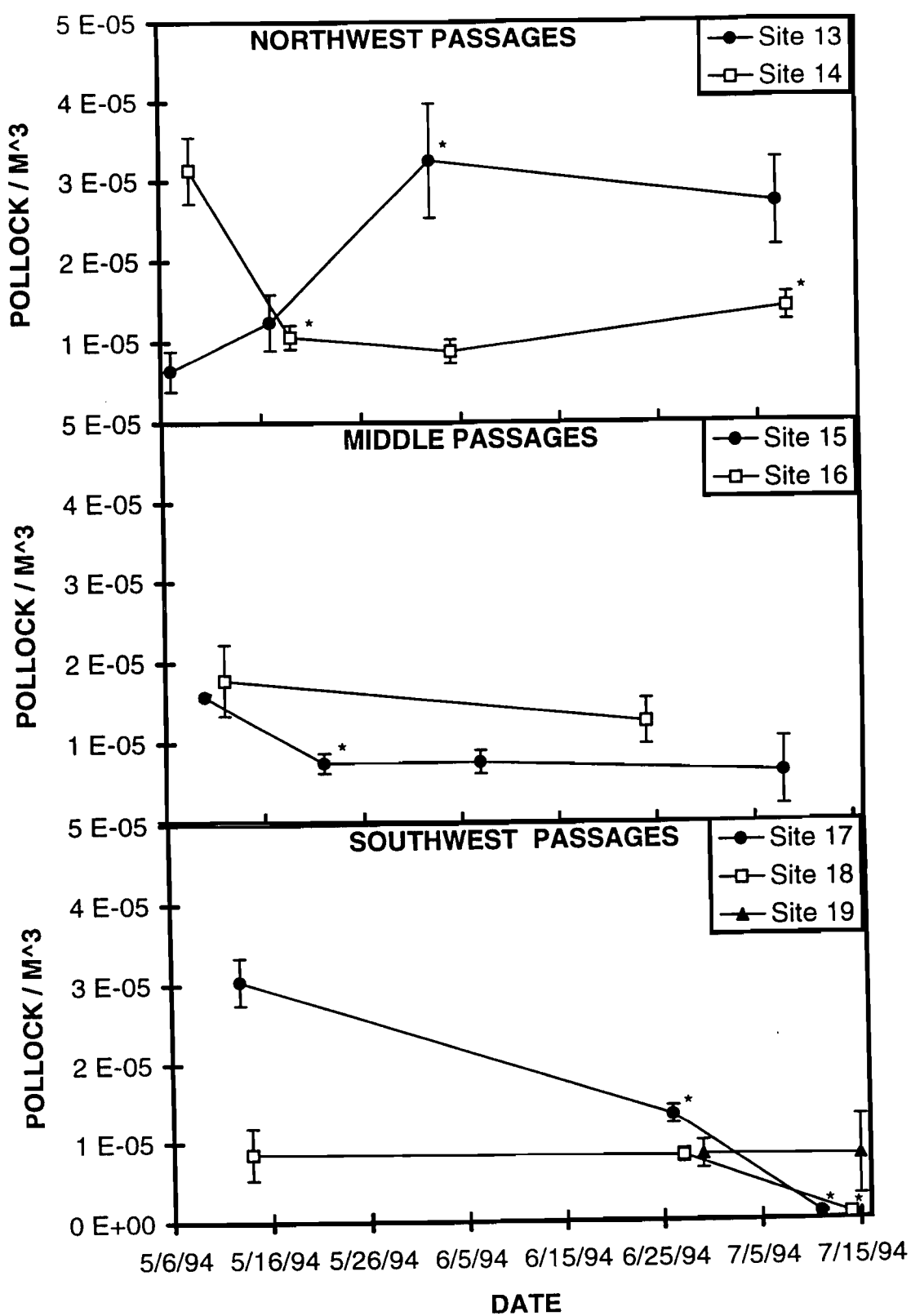


Fig. 8. Weighted mean pollock densities (± 1 S.D.) from 1994 offshore surveys. See Fig. 2 for exact site locations. The asterisks indicate a significant change in density from the previous sample.

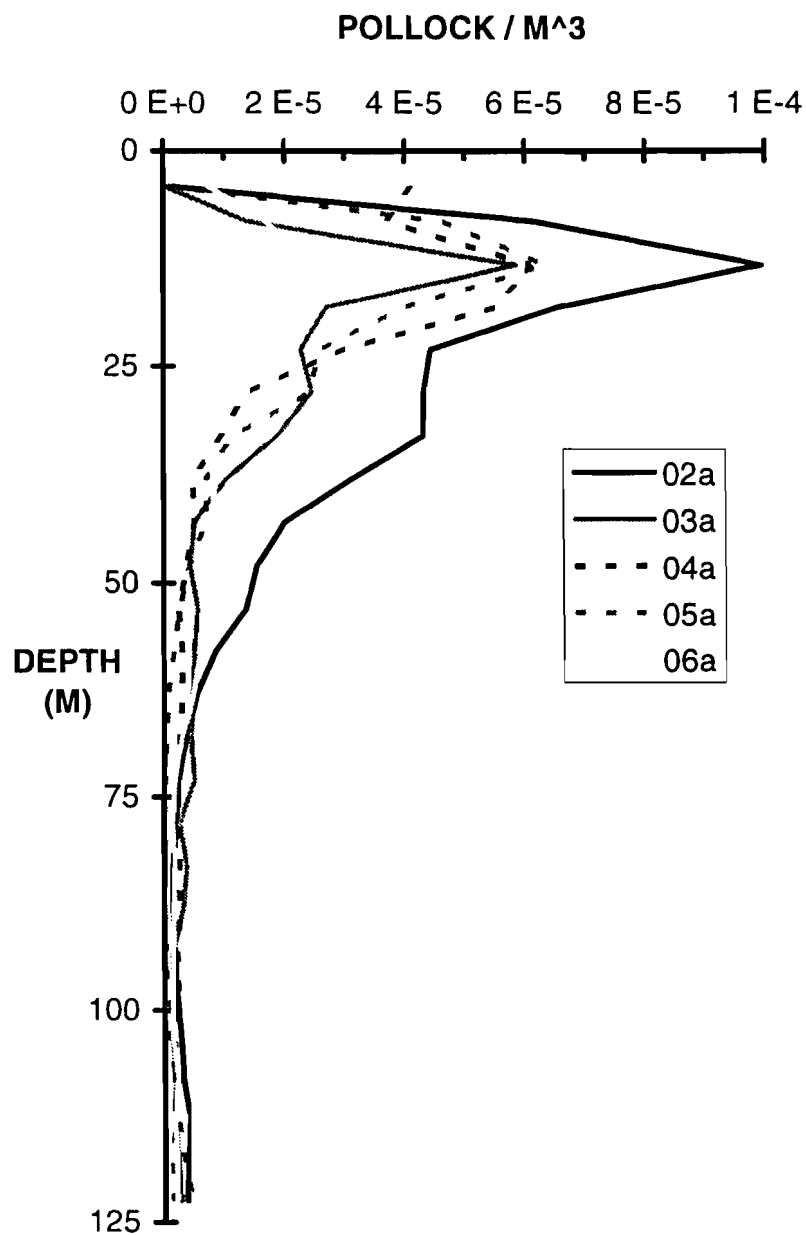


Fig. 9. Seasonal changes in pollock vertical distribution from 1994 offshore surveys in Prince William Sound.

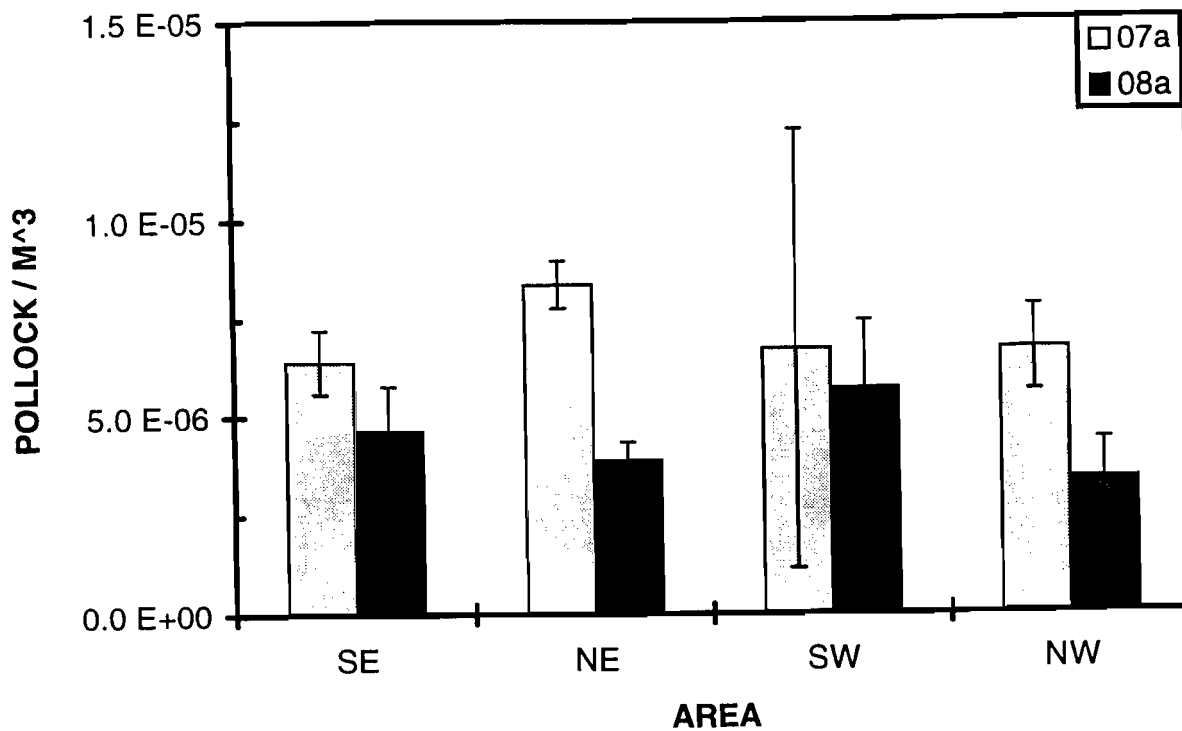


Fig. 10. Weighted mean pollock densities (± 1 S.D.) for offshore regions of Prince William Sound in May (07a) and June (08a) broadscale surveys in 1995.

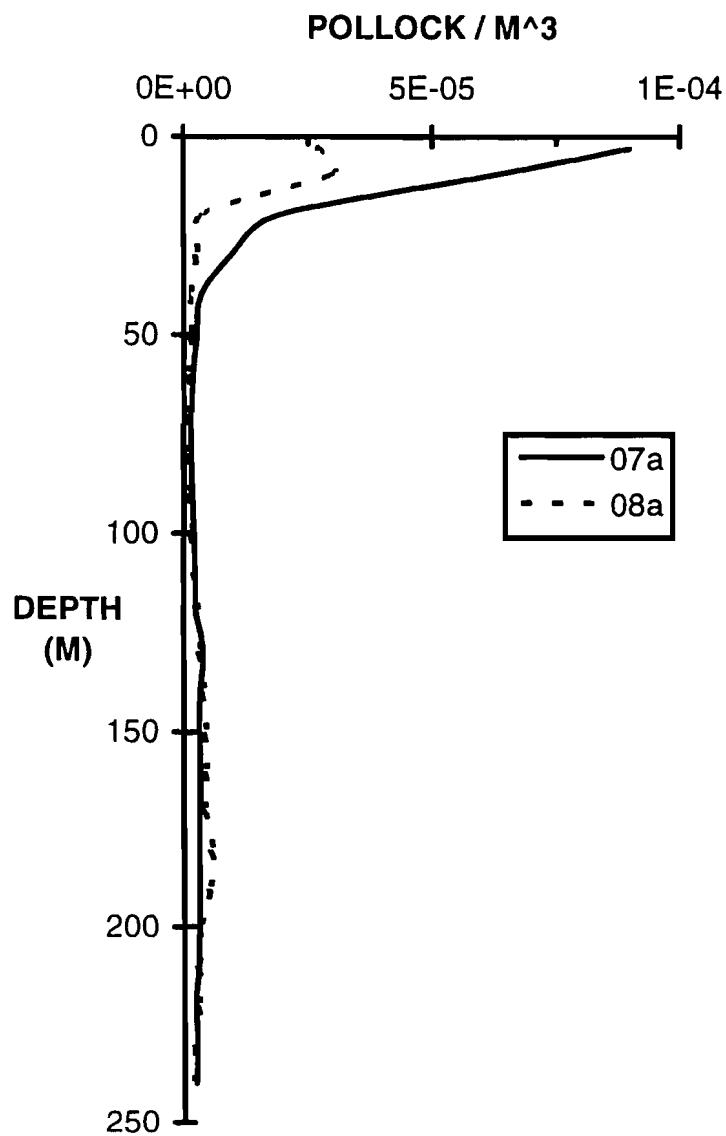


Fig. 11. Seasonal changes in pollock vertical distribution from 1995 broadscale offshore surveys in Prince William Sound.

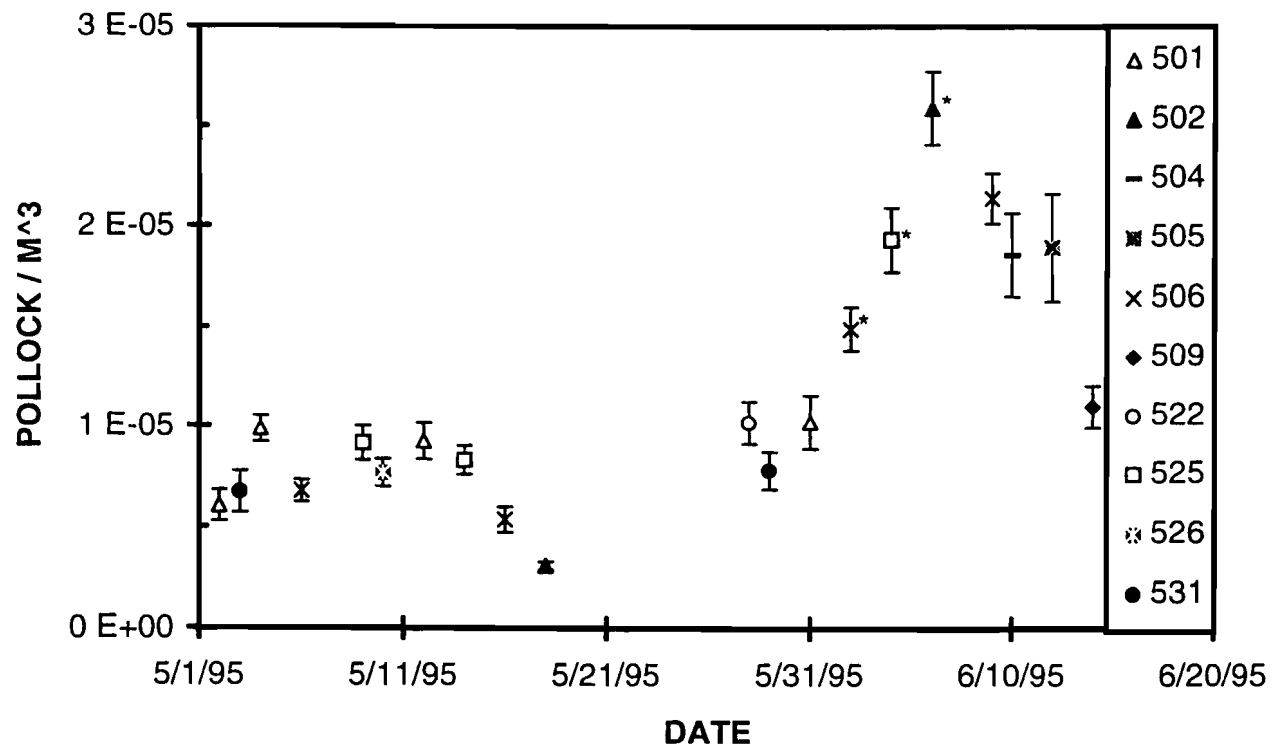


Fig. 12. Weighted mean pollock densities (± 1 S.D.) from 1995 offshore surveys. See Fig. 3 for exact site locations. The asterisks indicate a significant change in density from the previous sample.

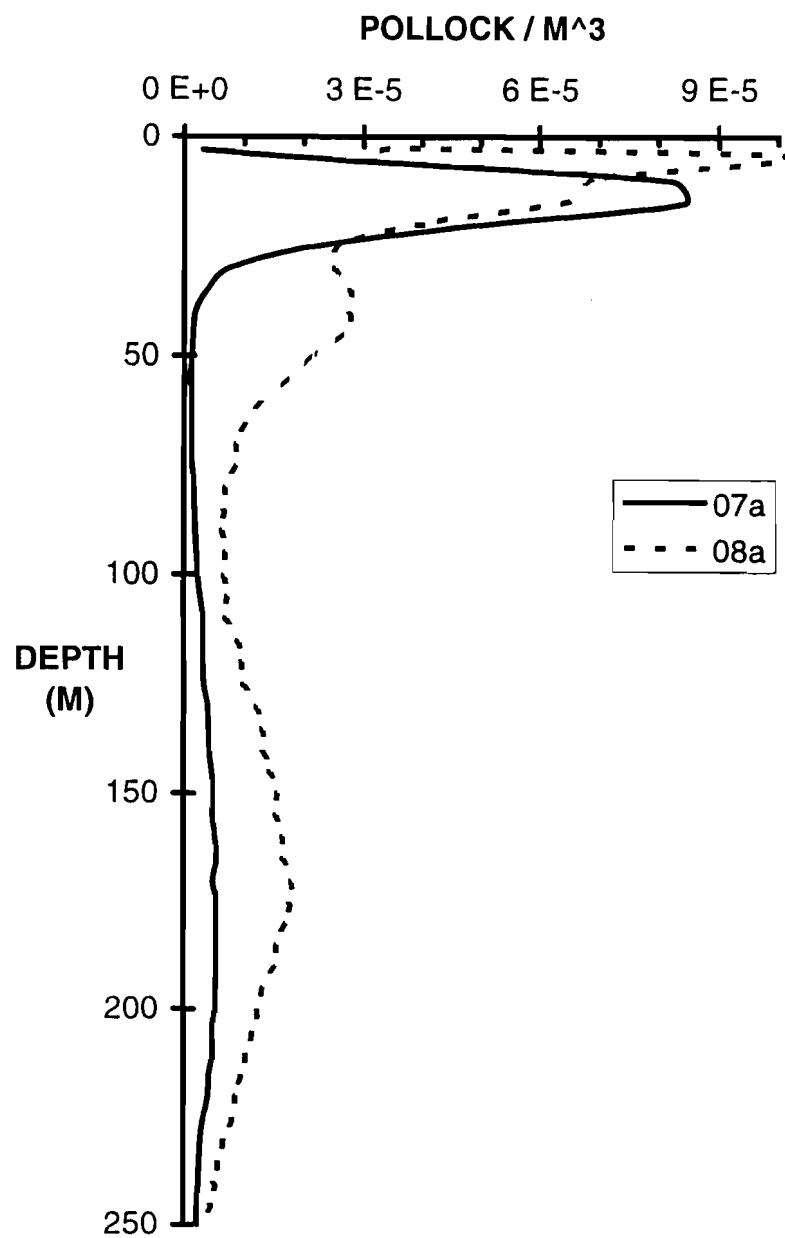


Fig. 13. Seasonal changes in pollock vertical distribution from 1995 offshore surveys in Prince William Sound.

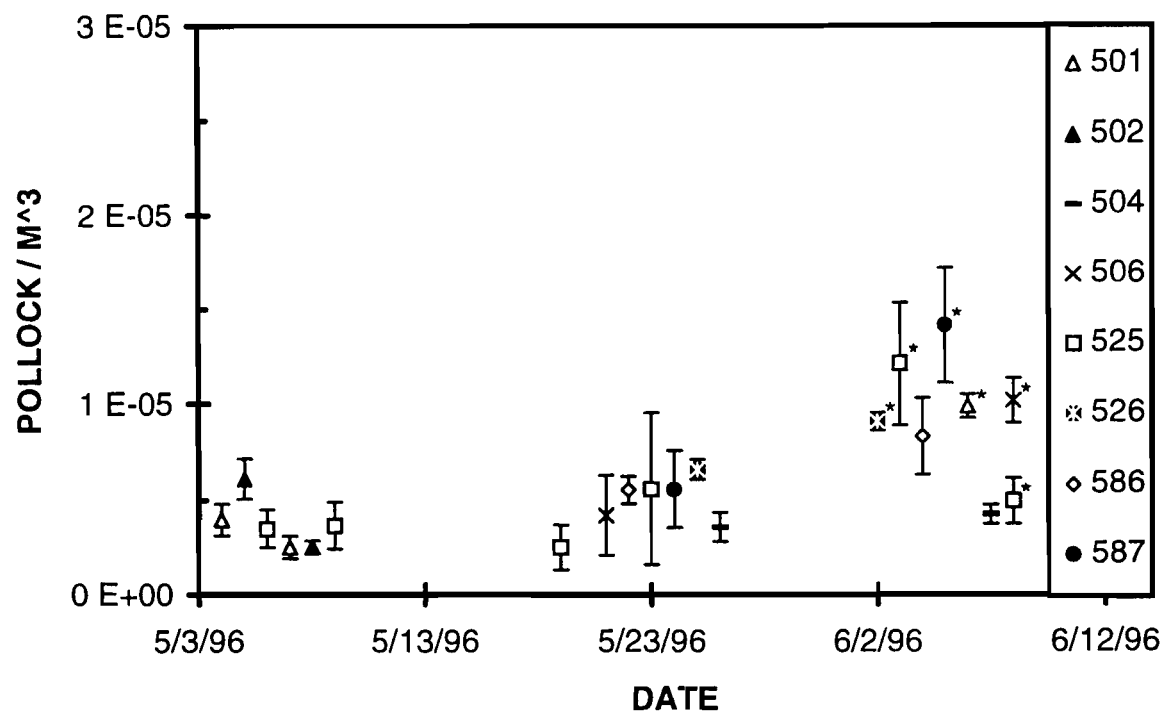


Fig. 14. Weighted mean pollock densities (± 1 S.D.) from 1996 nearshore surveys. See Fig. 3 for exact site locations. The asterisks indicate a significant change in density from the previous sample.

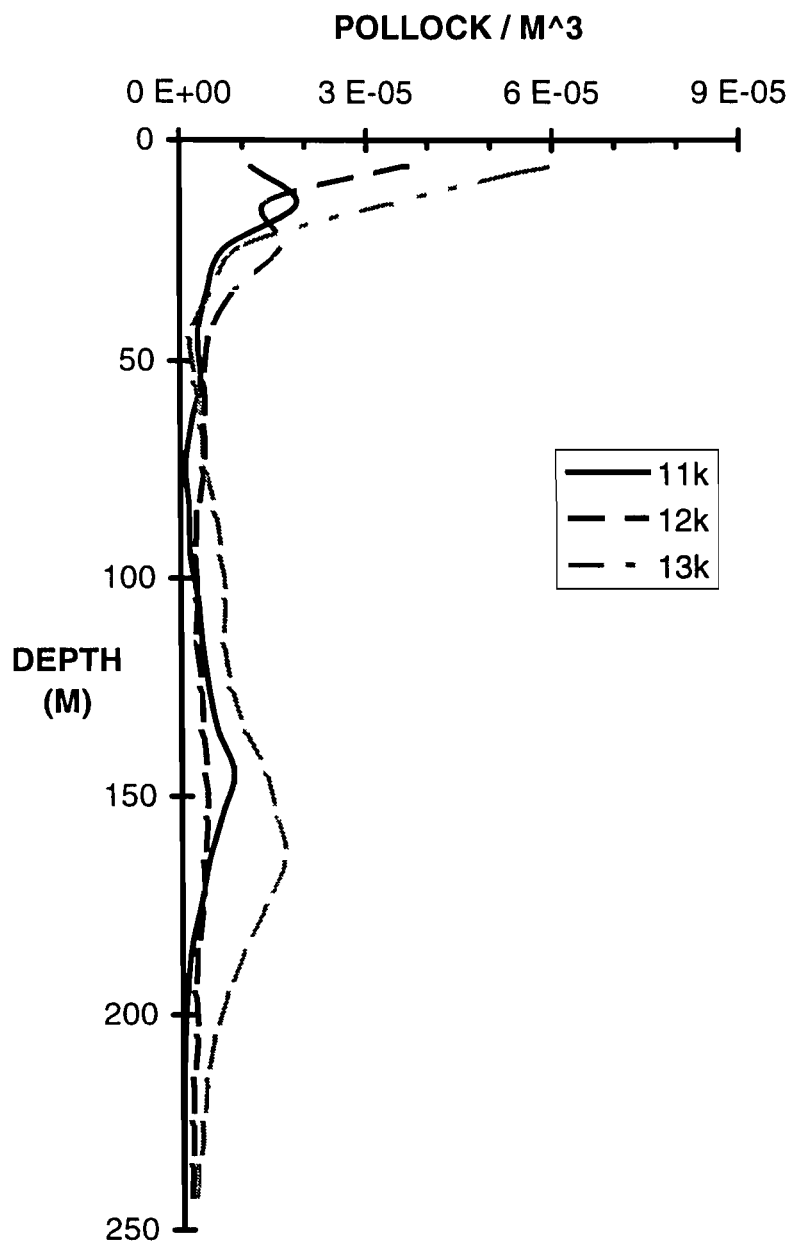


Fig. 15. Seasonal changes in pollock vertical distribution from 1996 nearshore surveys in Prince William Sound.

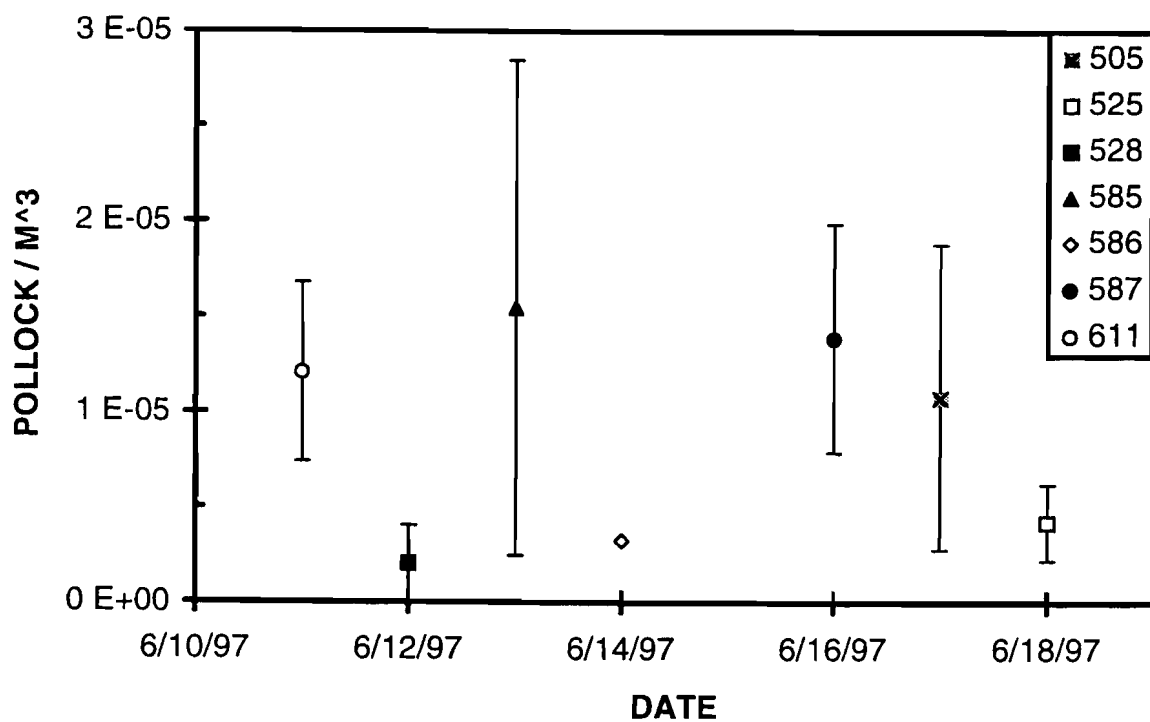


Fig. 16. Weighted mean pollock densities (± 1 S.D.) from 1997 nearshore surveys. Sites 528 (Port Gravina), 585 (Fish Bay), and 611 (Sheep Bay) are in Eastern Prince William Sound. For other site locations, see Fig. 3.

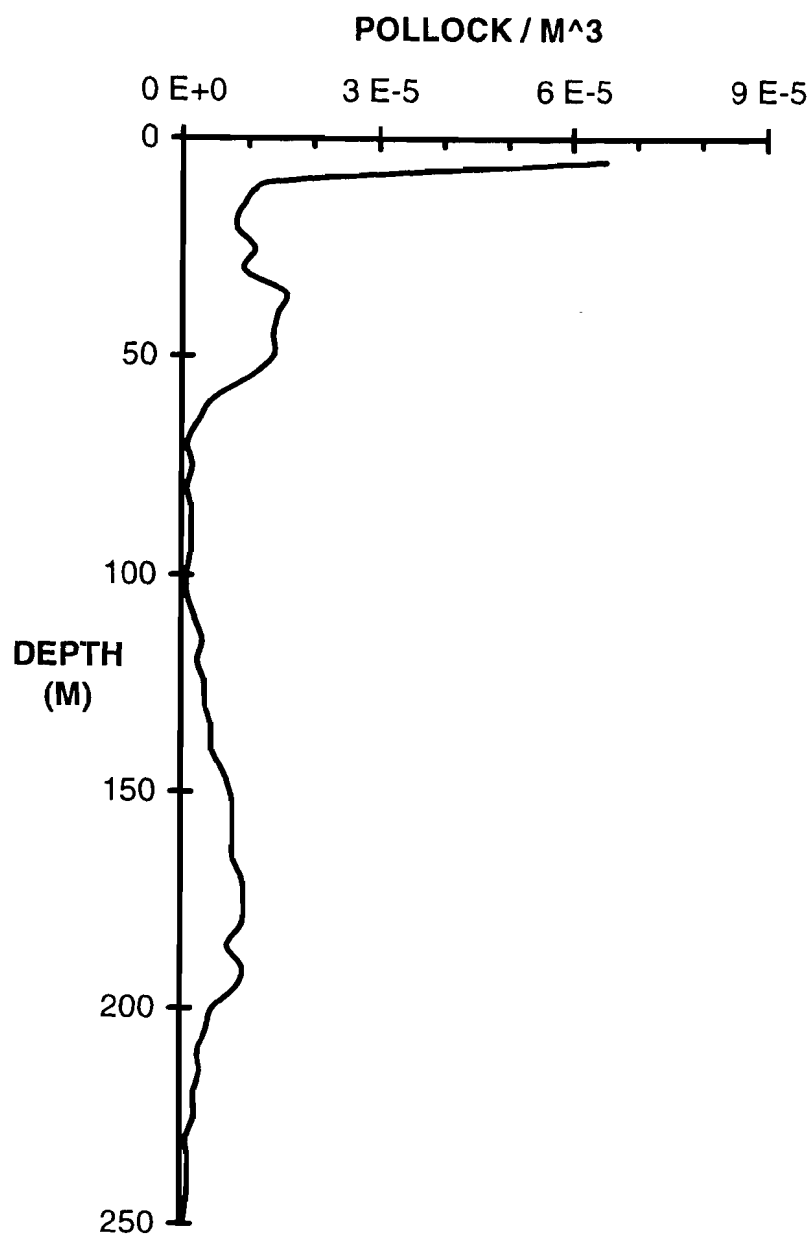


Fig. 17. Vertical distribution of pollock in Prince William Sound from nearshore acoustic surveys in June 1997.

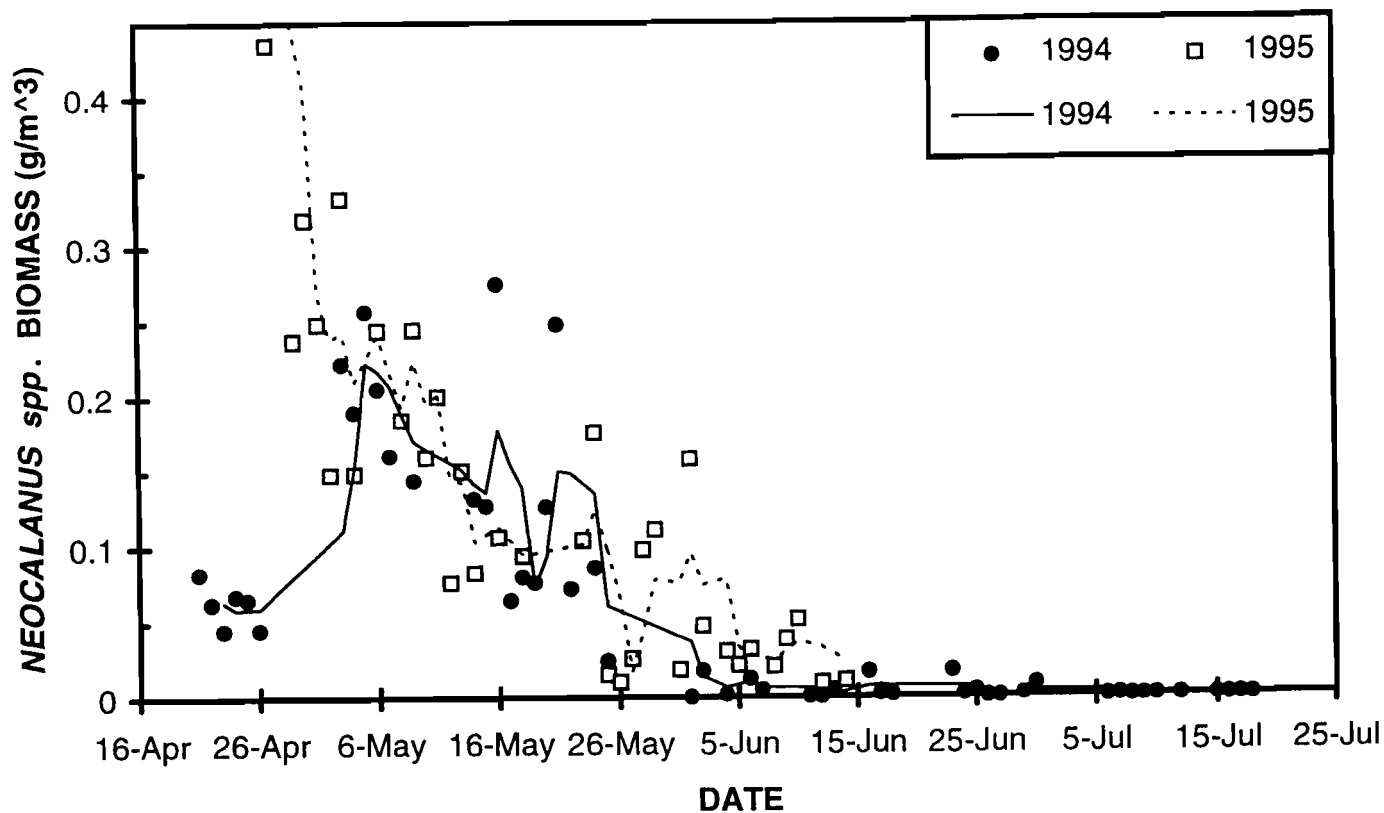


Fig. 18. Biomass of *Neocalanus* spp. in the top 50 m in Prince William Sound during 1994 and 1995. The lines are three-point running averages of 50 m vertical plankton tows (points).

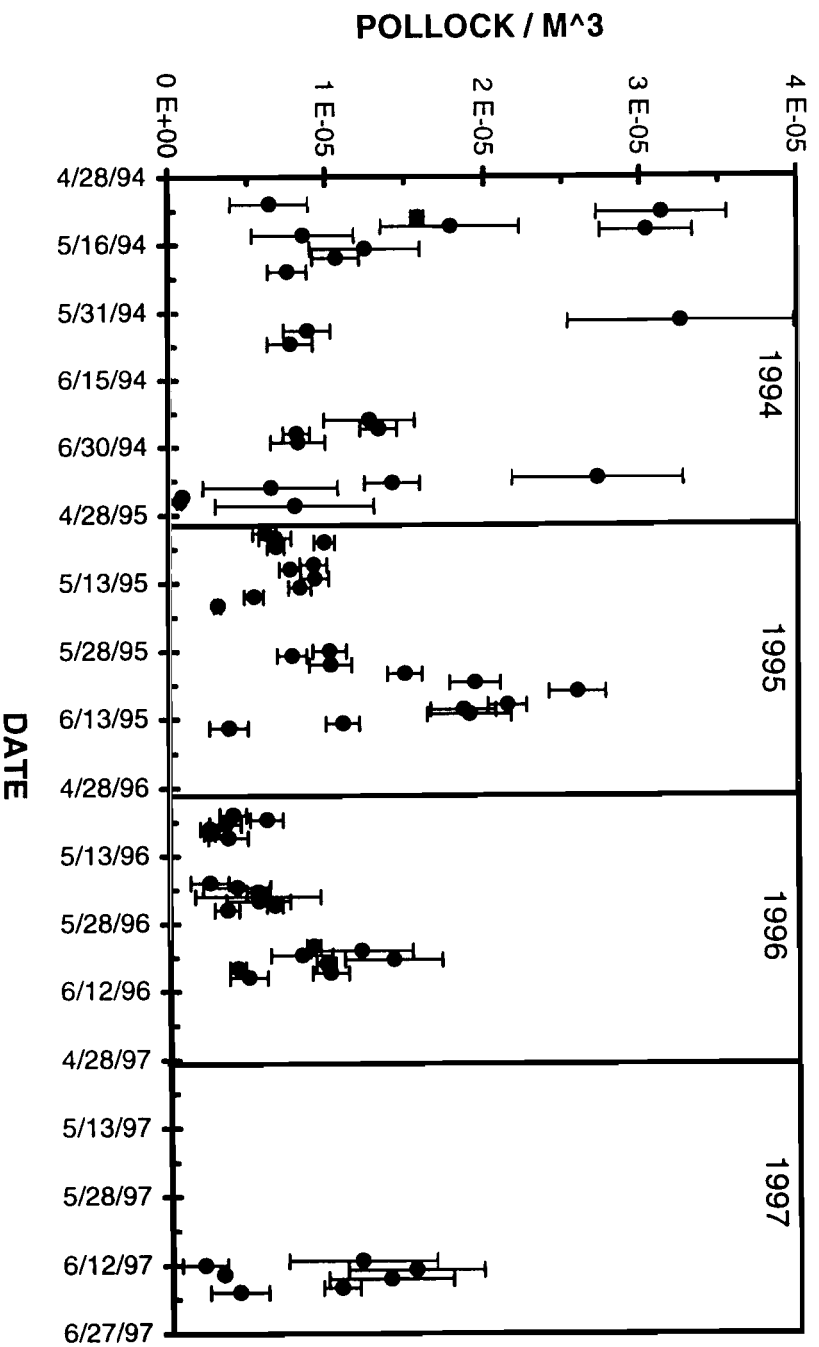


Fig. 19. Seasonal changes in pollock densities (± 1 S.D.) from 1994 to 1997. Note the general increase in pollock density within years, but the slight decline in pollock density between years.

CHAPTER 2

Co-occurring patches of walleye pollock (*Theragra chalcogramma*) and zooplankton in Prince William Sound, Alaska, USA. G. B. Steinhart, G. L. Thomas, and J. Kirsch.

ABSTRACT

The Sound Ecosystem Assessment (SEA) program is a multi-disciplinary effort to acquire an ecosystem-level understanding of Prince William Sound (PWS), Alaska. A primary SEA hypothesis is that adult walleye pollock (*Theragra chalcogramma*) switch from their primary food source, fish, to macro-zooplankton when plankton densities are high. We examined this hypothesis by making acoustic observations of fish and zooplankton during the spring of 1995. We found patches of plankton 50 m to 5 km long in the top 50 m of water. Net tows showed that these patches were over 90% calanoid copepods. Walleye pollock abundance was positively correlated with zooplankton abundance ($r^2=0.26$). Furthermore, copepods dominated the diet of pollock at this time. These results showed that walleye pollock were feeding on, and were attracted to macro-zooplankton patches in PWS. Environmental conditions that result in low macro-zooplankton densities, or prohibit the formation of dense plankton patches, could reduce feeding opportunities for pollock. When macro-zooplankton are not abundant, adult pollock may switch their diet to include more juvenile fish, which could reduce the survival of many important fish species.

INTRODUCTION

Walleye pollock (*Theragra chalcogramma*) are one of the most abundant fish species in Prince William Sound (Thomas et al. 1997). Acoustic surveys have estimated pre-spawning biomass of pollock at 38,000 to 44,000 tonnes (Thomas and Stables 1996; Kirsch 1997). Many previous studies have looked at the behavior, distribution, and abundance of pollock in the Gulf of Alaska (GOA) and the Bering Sea (Dwyer et al. 1987; Bailey 1989; Brodeur and Wilson 1996); however, little is known about the distribution and behavior of pollock in Prince William Sound (PWS). These previous studies have shown that pollock eat large numbers of young fish, including juvenile walleye pollock. Given their abundance in PWS, walleye pollock play a major role in the trophic structure of the Sound. As in the GOA and Bering Sea, juvenile pollock are important competitors with other planktivores and serve as a major food source for predators (Dwyer et al. 1987). Adult pollock are likely significant predators and could effect the recruitment success of other fish (Walters et al. 1986).

After the *Exxon Valdez* oil spill, stocks of pink salmon in Prince William Sound had highly variable recruitment success. Low returns of hatchery-released salmon in 1992 and 1993 were likely caused by poor survival during their outmigration from PWS (Willette et al. 1996). An assumption of Sound Ecosystem Assessment Program (SEA), that was adapted from GLOBEC, is that fish fry do not die by starvation, but that all mortality is the result of being eaten. Pollock, being one of the most abundant pelagic

fish in PWS, are likely the primary predator of pink salmon fry (Willette et al. 1994). If there are approximately 25 million adult pollock (Thomas and Stables 1996; Kirsch 1997), and 750 million salmon fry in PWS (Thomas and Mathisen 1993), then salmon survival will be negligible if each pollock eats only 30 salmon fry per year. Therefore, it is not hard to imagine that predation by adult pollock could have a profound impact on salmon survival. This paper focuses on the spatial distribution of predators (pollock) and their prey (juvenile fish and zooplankton) to improve our understanding of the trophic dynamics of PWS.

Developing a better understanding of predator/prey interactions is a primary goal of the SEA project. Two primary hypotheses of SEA that relate to these interactions are: the Lake/River hypothesis and the Prey Switching hypothesis (Thomas et al. 1997). The Lake/River hypothesis describes conditions as cold, stormy and turbulent "river" years with lower zooplankton abundance, and fewer dense patches of zooplankton than warmer, calmer "lake" years. The SEA Prey Switching hypothesis predicts that as macro-zooplankton availability decreases, pollock will switch from eating primarily macro-zooplankton to feeding heavily on other large invertebrate prey and juvenile fish. To test these hypotheses, we initiated investigations of pollock behavior in relation to zooplankton abundance and distribution in PWS.

In this paper, we describe the spatial distribution of pollock and macro-zooplankton in western Prince William Sound. This line of research should lead to an increase in knowledge of the roles of predation in the trophic structure of PWS. Understanding the role of predation on juvenile fish survival is a critical step in improvement of predicting changes in fish populations in Prince William Sound.

MATERIALS AND METHODS

Prince William Sound is located at the northern edge of the Gulf of Alaska (Fig. 1). This large fjord/estuary covers an area of approximately 8800 km², and has about 3200 km of shoreline (Grant and Higgins 1910). Coastal rainforests, high mountains, and glaciers border the shoreline of PWS. The area is exposed to seasonally intense storms moving in from the Gulf of Alaska, resulting in 5-7 m of annual rainfall.

In 1995, two surveys of PWS were conducted during 27 April to 1 May, and 23-27 May (Fig. 1). The cruises were designed to cover all major regions of the Sound. Sampling consisted of hydroacoustic surveys, mid-water trawls, and vertical plankton tows. All sampling was conducted during daylight hours.

Thirty vertical zooplankton tows were collected using a 0.5 m ring net with 333 μ m mesh. The net was towed vertically through the top 50 m at several SEA oceanographic stations. The samples were preserved in a formalin solution. In the lab, the zooplankton were enumerated, measured, and identified to species. The mean length of each species was used to calculate the mean weight, and then multiplied by the number of individuals in the sample to yield biomass estimates.

Nine mid-water trawls performed during the two broadscale surveys to provide target verification for the acoustic sampling and to collect pollock for length, weight,

and diet analyses. The trawl measured 40 m x 28 m and was equipped with a net. The cod end of the trawl was lined with 1.5 cm stretch-mesh to retain small specimens. The depth and location of the trawling was directed toward layers of fish to verify acoustic targets. The length of trawl hauls was approximately 30 min at depth. Fish from the catch were specified, weighed, measured, and had their stomachs removed and preserved in 10% buffered formaldehyde for later diet analysis.

Acoustic equipment

Acoustic data were collected using a BioSonics 101-120 kHz 6°/15° dual-beam echosounder. The transducer was mounted on a tow-body which was towed alongside the boat at a depth of 2 m at an approximate speed of 3 m/s. The parameters of the acoustic system were: source level = 225.023 dB; receiver gain = -159.282 dB; transducer directivity = 0.0010718; pulse width = 0.4 s. The acoustic system was calibrated before each cruise using a tungsten-carbide ball, of known target strength, suspended within the beam of the transducer (Foote and MacLennan 1982). The data were processed in real-time using BioSonics ESP software on a 486 computer and were geo-referenced and time-coded by a connection to a Magellan DLX-10 GPS receiver with an external antenna. Echo-square integration, dual-beam target strength (TS), and GPS data were stored on the computer hard disk, and backed up on a tape drive. Raw acoustic signals were stored on Digital Audio Tape and printed on paper echograms.

Acoustic processing

Once the cruise was completed, the acoustic files were transferred to UNIX workstations where batch processing of files was performed. To facilitate reduction and processing of acoustic information, software was written which applied the acoustic calibrations and corrected for absorption (temperature and salinity). After initial processing, we used software written to allow the user to interactively remove untracked bottom, calculate biomass estimates, and produce images of fish distributions.

Echo-counting of pollock-sized targets was chosen over echo-integration because the density of pollock was relatively low, so coincident targets would not cause the target discriminator to fail. Furthermore, dense plankton layers were present and by echo-counting we could easily remove acoustic scattering due to plankton layers from the acoustic data. Our echo-counting technique involved defining the range of possible target strengths that corresponded to an adult pollock-sized target. Targets between -39 dB and -28 dB were counted as pollock-sized targets. The echo-counting software then counted all qualifying targets, which were then divided by the sample volume of the acoustic beam, and averaged to yield densities in fish/m³.

Multiple targets in the acoustic beam can effect the reliability of any echo-counting technique (Foote 1996). Multiple targets may either overlap just enough to cause the target discriminator to fail to recognize any of the multiple targets, or they may sum their individual returns to yield an artificially high single target strength. A test between the target discriminator and manual counts of pollock-sized targets showed that auto-counting underestimated the number of targets by 13-28 %. A similar

comparison between echo-counting and echo-integration showed that echo-counting resulted in an underestimate of pollock density by 18-33 % for some surveys (Thomas et al. 1996).

To estimate zooplankton abundance from our acoustic data, we used echo-integration techniques. Mean backscatter for cells 5 m deep and approximately 50 m long (32 pings) were converted to zooplankton biomass after removing those cells that contained fish. To remove fish, we set a volume backscatter (Sv) threshold of -55 dB. This threshold was selected since there was an anti-mode in the Sv histogram around -55 dB. All cells above that threshold were assumed to contain fish, and were not included in our relative zooplankton estimate.

Once the acoustic data arrays for pollock-sized targets and plankton were generated, we analyzed the data from the top 50 m to look for spatial overlap between the two. A correlation between pollock-sized target densities and relative plankton biomass was performed. In addition, we looked at the differences in the range of densities and biomass between the patches.

RESULTS

Vertical net hauls revealed that the zooplankton community was comprised of several species, but was dominated by calanoid copepods: 87% in April and 68% in May (Fig. 2). *Neocalanus spp.* was the most abundant plankter during the April cruise, comprising over 70% of the total zooplankton biomass. By May, however, *Neocalanus spp.* accounted for only 24% of the total biomass and many other species contributed to the total biomass, most notably *Oikopleura spp.* (8%) and *Metridia spp.* (5%). Overall, zooplankton biomass declined significantly from April to May ($df=25$, $t=2.22$, $p=0.018$), largely due to the decline in *Neocalanus spp.* in the top 50 m.

Zooplankton not only were more abundant during the first cruise (Fig. 2), they were also more patchy. Zooplankton biomass estimates from net hauls ranged from 1.5-17 g/tow ($\sigma=16.6$) in April and 1.3- 14 g/tow ($\sigma=1.5$) in May. The variance in zooplankton biomass was significantly higher for the April cruise ($F=11.31$, $p=0.004$). In addition, the variance in acoustic backscatter due to zooplankton was significantly higher during April ($\sigma=389$) than during May ($\sigma=230$; $F=1.69$, $p<0.0001$).

The zooplankton patches seen with the hydroacoustic system (Fig. 3) varied in size and biomass. Zooplankton patches averaged 1.5 km across, while patches as small as 100m, and as large as 5 km, were seen during the surveys. Zooplankton biomass estimates varied by about an order of magnitude when sampled with vertical net tows. The hydroacoustics, which have a finer spatial resolution than nets, found up to two orders of magnitude difference in acoustic backscatter attributed to plankton.

To better describe the composition of these patches, we compared the species composition of the three highest biomass zooplankton tows and the three lowest biomass tows using χ^2 -tests and t-tests. During the April cruise, the mean species composition of the three high biomass tows was not significantly different from the mean of all the tows ($df=6$, $\chi^2=2.4$, $p>0.25$), but the mean composition of the three low

tows was significantly different from the mean ($df=6$, $\chi^2=14.5$, $p<0.02$). The high biomass tows had significantly more copepods ($df=4$, $t=2.55$, $p=0.03$), and also had a higher percentage of copepods (90% versus 81%) than did the low biomass tows. There were no other significant differences in abundance of the other major zooplankton taxa.

In May, the mean species composition of the high biomass tows was significantly different from the mean of all the tows ($df=6$, $\chi^2=40.3$, $p<0.0005$). The low biomass tows, however, were not significantly different from the mean tows ($df=6$, $\chi^2=10.4$, $p>0.05$). The largest contributor to the significant difference was the increased number of pteropods found in the high biomass tows over the mean tows. In addition the high tows had significantly more pteropods ($df=4$, $t=3.6$, $p=0.012$), copepods ($df=4$, $t=2.2$, $p=0.49$), and *Oikopleura* spp. ($df=4$, $t=7.9$, $p=0.007$) than in the low biomass tows. Although there were more copepods found in the high biomass tows, they made up a lower percentage of the total count (82% versus 94%).

The mid-water trawl caught almost exclusively adult walleye pollock. In total, 596 pollock were caught and comprised 93% of the total catch. Additional fish captured included 31 lantern fish (Family Myctophidae), 9 sculpin (Family Cottidae), 2 capelin (*Mallotus villosus*), and 1 chinook salmon (*Oncorhynchus tshawytscha*). The lantern fish were caught in only 1 trawl towed at 125 m depth. The pollock averaged 508 mm fork length and 870 g wet weight. The predicted TS of these pollock was determined using $TS=20\log(\text{length}) - 66$ (Traynor and Williamson 1983). The predicted TS of these pollock overlapped the TS that we used to count pollock-sized targets (Fig. 4). Since pollock dominated the catch, and the other fish captured in the trawl would have target strengths too small to be counted by our echo-counter, we assumed that all pollock-sized targets observed were adult pollock.

In general, there appeared to be two layers of pollock during these cruises: a shallow layer (less than 20 m deep), and a deep layer around 150 to 200 m. The mid-water trawl had the highest catch per unit effort above 20 m, and caught very few pollock below 70 m; however, the trawl was not fished below 140 m (Fig. 5). The acoustics also showed that the highest density of pollock-sized targets was in the top 20 m (Fig. 6). The depth distribution changed between the two surveys: pollock were more abundant near the surface during the April cruise than during the May cruise. The acoustics also showed that there were pollock-sized targets deep in the water column during both cruises, but there were more pollock-sized targets in the deep layer during May.

Pollock stomachs were found to contain nearly 99 % zooplankton (by weight) in April and May (Fig. 7). In April, calanoid copepods, primarily *Neocalanus* spp., comprised 65 % of the stomach contents. In May, however, pteropods were the dominant prey item (43%), while less than 25 % of the diet consisted of copepods. Fish made up less than 1 % of pollock diets during both cruises.

We saw pollock-like targets associated with plankton patches on echograms during both surveys (Fig. 3) and we found a positive correlation between pollock density and relative zooplankton density during both surveys in 1995 (Fig. 8). The correlation coefficient was higher for the May cruise, and both correlation coefficients were significantly different from 0, but they did not explain much of the variation in pollock density (April: $r^2=0.26$, $n=420$, $t=14.33$, $p<0.0005$; May: $r^2=0.27$, $n=145$, $t=8.5$, $p<0.0005$).

We calculated the correlation between pollock density and zooplankton acoustic backscatter at various spatial scales: cells approximately 50 m to 10 km long. The correlation coefficient was highest when we used cells that were approximately 5 km long.

DISCUSSION

The highest densities of adult walleye pollock in Prince William Sound were found in the top 50 m, and were positively correlated with zooplankton biomass. This behavior may not be unique, but most previous work has shown that adult pollock remain deep in the water column, with only juveniles commonly found near the surface (Traynor 1986; Bailey 1989). We believe that the bulk of adult pollock in PWS feed near the surface in order to exploit the food resources found in the epilimnetic waters in the Sound. Salmon fry are abundant in the top 50 m during their spring out-migration, and are found in pollock diets. However, walleye pollock are so abundant in PWS that feeding exclusively salmon fry cannot sustain the pollock population. Therefore, zooplankton, found to compose the bulk of pollock diets during this study, are also an important food resource. We believe that zooplankton density has a major influence on pollock distribution in PWS. Our data show insight into how pollock are distributed relative to plankton, and will help determine the validity of the Lake/River and Prey Switching hypotheses (Cooney 1993).

The hypothesized migration of adult pollock northward into the Sound after spawning in the southwest corner of PWS is thought to be related to zooplankton distribution (Steinhart et al. 1997). We found a positive correlation between pollock density and relative zooplankton biomass during this study. Correlations between predators and prey are common in the literature (Rose and Leggett 1989; Rose and Leggett 1990; Veit et al. 1993; Deblois and Rose 1995), but correlation analysis does not prove a casual relationship. Pollock diets, however, were dominated by zooplankton, especially *Neocalanus spp.*. This demonstrates that pollock were feeding on plankton during our surveys. In order to maximize food intake, pollock would be expected in the presence of high plankton biomass.

Although zooplankton abundance only explained about 27% of the variation in pollock density that was observed, this type of spatial relationship can be difficult to quantify using simple correlation. Spatial associations between predators and their prey are notoriously weak, with correlation coefficients often less than 0.5 (Veit et al. 1993). Rose and Leggett (1990) suggest that positive correlations between predator and prey densities would occur at scales greater than the dimensions of the predator and prey aggregations. Predators, such as pollock, may be found close to their prey (zooplankton), but not right on top of them. For example, strong currents may concentrate plankton in some areas, but fish may avoid the strongest currents and feed on the edges of the aggregation. Indeed, we did find that the best correlation was when we pooled our acoustic data into 5 km bins. The relatively poor correlation could also be due to other variables that we haven't examined yet. The abundance of other prey

items, such as fish, may also influence pollock distribution. Certain areas may also have physical conditions (temperature, oxygen, or currents) that may attract or repel pollock regardless of plankton abundance (Rose and Leggett 1990).

Observations during this study, as well as other research (Simard and Mackas 1989; Barange 1993), suggested that currents may influence zooplankton distribution and the co-occurrence of pollock and plankton. Currents encountered during the survey effected plankton distribution by concentrating plankton in some areas, and resulted in varying depth distributions (Fig. 3). The effects of large-scale circulation and turbulence are unknown at this time, but may aid in the formation of dense concentrations of plankton, or may flush plankton into and out of PWS, thereby increasing or reducing the amount of food available for pollock within the Sound.

Neocalanus spp., along with many other marine copepods, undergo a seasonal vertical migration (Cooney 1987). In spring, young copepods migrate up from great depths to respond to the spring phytoplankton bloom. In summer, the matured copepods migrate down to 400 m where they spend the winter. There is also evidence that oceanic copepods enter near-shore and coastal waters in the spring (Incze et al. 1997). Since adult pollock can exploit the copepods as a food source, the seasonal changes in plankton abundance are likely the cause of the observed shifts in the distribution and diet of walleye pollock.

As *Neocalanus spp.* densities in the top 50 m declined from April to May, pollock switched both their diet and their depth distribution in PWS. This behavior pattern has been observed in other years (Willette et al. 1995; Willette et al. 1996). In 1994, as copepod densities in the top 40 m declined, the percent of age-0 fish and salmon fry in pollock diets increased. In addition, pollock moved deeper in the water column as plankton densities near the surface declined. This switch in diet, and the change in vertical distribution, are hypothesized to be related to plankton abundance and distribution.

We not only saw a general decline in copepod abundance near the surface, but we also observed changes in zooplankton patch densities and species composition. During April, there were more dense patches of plankton, and more variability in plankton density, than in May. In April, the zooplankton patches were made up almost entirely of copepods. During May, however, there were fewer high density zooplankton patches, and less variability in plankton distribution. In May, the observed zooplankton patches may have been aggregations of species other than copepods, since there were lower percentages of copepods in high density tows than in low density tows. Pteropods, on the other hand, were much more abundant in the high density areas, and may have been forming the dense patches we observed during May.

The Prey Switching hypothesis states that in the absence of abundant zooplankton, pollock will switch to juvenile fishes, including salmon fry. During "lake" years, high zooplankton numbers and/or increased density of zooplankton patches may result in less predation pressure on juvenile fishes than during "river" years. However, even when zooplankton are abundant, or in dense patches, pollock may prefer to feed on small fish, including salmon fry but since there are relatively few of these prey, they don't show up as a significant proportion of the pollock diet. Although young fish

made up less than 1% of pollock diets during this study, it is important to remember that individual pollock don't need to eat many salmon fry to have a profound effect on salmon survival given the large number of pollock found in the Sound. These observations support prey-switching on a seasonal time scale. The relationship between pollock and zooplankton suggests that annual differences in zooplankton availability should affect the extent of seasonal prey switching, thus causing inter-annual variability. Tying the availability of macro-zooplankton to turbulence, primary production and migration/emigration, and observing inter-annual differences are the subject of the ongoing SEA research.

Our present results, however, may be confounded by several sources of error. The small sample volume of the acoustic beam at short ranges, combined with the near surface distribution of pollock may have underestimated pollock densities. In addition, target strengths of fish are highly variable and depend on many factors (Traynor and Williamson 1983; Mukai and Iida 1996). A fish swimming upward or downward within the acoustic beam may be tilted, and thus presents a smaller cross-section to reflect the acoustic signal. Furthermore, an echo from a fish that is only partially within the acoustic beam may also underestimate the target's size. The reduced acoustic backscatter would lead to an underestimate of pollock density since some fish would not meet the -39 dB criteria for a pollock-sized target. Coincident targets, which will increase in frequency with depth also cause the target discriminator to fail. Furthermore, boat avoidance by pollock near the surface may be a problem. These potential errors will all lead to underestimate the number of pollock-sized targets.

Further research is needed, and we are currently improving on our estimates of plankton and fish using acoustic technologies. We are using digital transducers to provide a much finer spatial resolution in our data. This will allow us to more easily remove fish from the echo-integration array, thus providing more accurate zooplankton estimates. Furthermore, we are using multiple frequencies to separate fish targets from plankton targets. The results of this work should clarify some of the results we saw during our April and May surveys in 1995. In addition, by sampling repeatedly over several years, we will be able to more completely examine the SEA hypotheses. How inter-year variability in climatic conditions relates to plankton abundance, pollock diets, and salmon survival will increase our ability to correctly manage and sustain the fisheries in Prince William Sound.

ACKNOWLEDGMENTS

We would like to thank all the crews of our research vessels for helping us to collect these data: without their knowledge and experience, this research would not have been possible. The Alaska Department of Fish and Game and the University of Alaska-Fairbanks were responsible for the daunting task of processing the zooplankton and trawl data. A special thanks goes to Mark Willette (ADF&G) for sharing his data on pollock diet and to R. Ted Cooney (UAF) for the plankton data. This work is supported by the Exxon Valdez Oil Spill Trustee Council, Grant No. 96320-N and 97320-N as part of the Sound Ecosystem Assessment project.

LITERATURE CITED

- Bailey, K. M. 1989. Interaction between the vertical distribution of juvenile walleye pollock *Theragra chalcogramma* on the eastern Bering Sea, and cannibalism. Mar. Ecol. Prog. Ser. 53: 205-213.
- Barange, M. 1993. Acoustic identification, classification and structure of biological patchiness on the edge of the Agulhas Bank and its relation to frontal features. S. Afr. J. Mar. Sci. 14: 333-347.
- Brodeur, R. D., and M. T. Wilson. 1996. Meso-scale acoustic patterns of juvenile walleye pollock (*Theragra chalcogramma*) in the western Gulf of Alaska. Can. J. Fish. Aquat. Sci. 53: 1951-1963.
- Cooney, R. T. 1987. The seasonal occurrence of *Neocalanus cristatus*, *Neocalanus plumchrus* and *Eucalanus bungii* over the shelf of the northern Gulf of Alaska. Continental Shelf Res. 5: 541-553.
- Cooney, R. T. 1993. A theoretical evaluation of the carrying capacity of Prince William Sound, Alaska, for juvenile Pacific salmon. Fisheries Research, 18: 77-88.
- DeBlois, E. M., and G. A. Rose. 1995. Effect of foraging activity on the shoal structure of cod (*Gadus morhua*). Can. J. Fish. Aquat. Sci. 52: 2377-2387.
- Dwyer, D. A., K. M. Bailey, and P. A. Livingston. 1987. Feeding habits and daily ration of walleye pollock (*Theragra chalcogramma*) in the eastern Bering Sea, with special reference to cannibalism. Can. J. Fish. Aquat. Sci. 44: 1972-1984.
- Ehrenberg, J. E., and D. W. Lytle. 1972. Acoustic techniques for estimating fish abundance. Trans. Geosci. Elec. GE-10: 138-145.
- Foote, K. G. 1996. Coincidence echo statistics. J. Acoust. Soc. Am. 99: 266-271.
- Foote, K. G., and D. N. MacLennan. 1982. Use of elastic spheres as calibration targets. p. 52-58. In O. Nakken and S. C. Venema [eds.], Symposium on fisheries acoustics. ICES/FAO. Bergen, Norway.
- Grant, U. S., and K. F. Higgins. 1910. Reconnaissance of the geology and mineral resources of Prince William Sound, Alaska. U.S. Geological Survey Bulletin. No. 443. 89 pp.
- Incze, L. S., D. W. Siefert, and J. M. Napp. 1997. Mesozooplankton of Shelikof Strait, Alaska: abundance and community composition. Continental Shelf Res. 36: 287-305.

Kirsch, J. 1997. Acoustic biomass estimate of adult walleye pollock in Prince William Sound, Alaska, in winter 1997. Report to the Alaska Department of Fish and Game. Prince William Sound Science Center. Cordova, AK.

Mukai, T. and K. Iida. 1996. Depth dependence of target strength of live kokanee salmon in accordance with Boyle's law. ICES J. of Marine Sci., **53**: 245-248.

Rose, G. A. and W. C. Leggett. 1989. Interactive effects of geo-physically forced sea temperatures and prey abundance on mesoscale coastal distributions of a marine predator, Atlantic cod (*Gadus morhua*). Can J. Fish. Aquat. Sci. **46**: 1904-1913.

Rose, G. A. and W. C. Leggett. 1990. The importance of scale to predator-prey spatial correlations: an example of Atlantic fishes. Ecology **71**: 33-43.

Simard, Y and D. L. Mackas. 1989. Mesoscale aggregations of euphausiid sound scattering layers on the continental shelf of Vancouver Island. Can. J. Fish. Aquat. Sci. **46**: 1238-1248.

Steinhart, G. B., G. L. Thomas, and J. Kirsch. 1997. Seasonal and diel movements of walleye pollock (*Theragra chalcogramma*) in western Prince William Sound. Restoration Project 95320N. Exxon Valdez Oil Spill Trustee Council. Anchorage, Alaska.

Thomas, G. L. and Mathisen. 1993. Biological interactions of natural and enhanced stocks of salmon in Alaska. Fish. Res. **18**: 1-18.

Thomas, G. L. and T. B. Stables. 1996. Winter 1995 estimates of the prespawning biomass of walleye pollock in Prince William Sound, Alaska. Report to the Alaska Department of Fish and Game. Prince William Sound Science Center. Cordova, AK.

Thomas, G. L., J. Kirsch, and T. McLain. 1996. Sound Ecosystem Assessment: nekton-plankton acoustics second annual report, 1996. Restoration Project 95320N. Exxon Valdez Oil Spill Trustee Council. Anchorage, Alaska.

Thomas, G. L., E. V. Patrick, J. Kirsch, and J. R. Allen. 1997. Development of an ecosystem model for managing the fisheries resources of Prince William Sound. pp . 606-613. D. C. Smith, A. Grant, and J. P. Beumer [eds.], Developing and sustaining world fisheries resources. CSIRO. Collingwood, Australia.

Traynor, J. J. 1986. Midwater abundance of walleye pollock in the eastern Bering Sea, 1979 and 1982. Int. North Pac. Fish. Comm. Bull. **45**: 121-135.

Traynor, J. J., and N. J. Williamson. 1983. Target strength measurements of walleye pollock (*Theragra chalcogramma*) and a simulation study of the dual-beam method.

Proceedings of the Symposium on Fisheries Acoustics. FAO Fish. Rep. No. 300: 112-124.

Walters, C. J., M. Stocker, A. V. Tyler and S. J. Westerheim. 1986. Interaction between pacific cod (*Gadus macrocephalus*) and herring (*Clupea harengus pallasii*) in the Hecate Strait, British Columbia. Can J. Fish. Aquat. Sci. **43**: 830-837.

Willette, T. M., G. Carpenter, P. Shields, and S. Carlson. 1994. Early marine salmon injury assessment in Prince William Sound. Exxon Valdez Natural Resource Damage Assessment Program, Final Report, Alaska Department of Fish and Game. Anchorage, AK.

Willette, T. M., E. Debevec, and J. Johnson. 1995. Sound ecosystem assessment: salmon predation. . Exxon Valdez Oil Spill Restoration Project Annual Report (Restoration Project 94320E). Alaska Department of Fish and Game. Anchorage, AK.

Willette, T. M., M. Clapsadl, P. Saddler, and M. Powell. 1996. Sound Ecosystem Assessment: salmon and herring integration. Restoration Project 95320E. Exxon Valdez Oil Spill Trustee Council. Anchorage, AK.

Veit, R. R., E. D. Silverman, and I. Everson. 1993. Aggregation patterns of pelagic predators and their principal prey, Antarctic krill, near South Georgia. J. Anim. Ecol. **62**: 551-564.

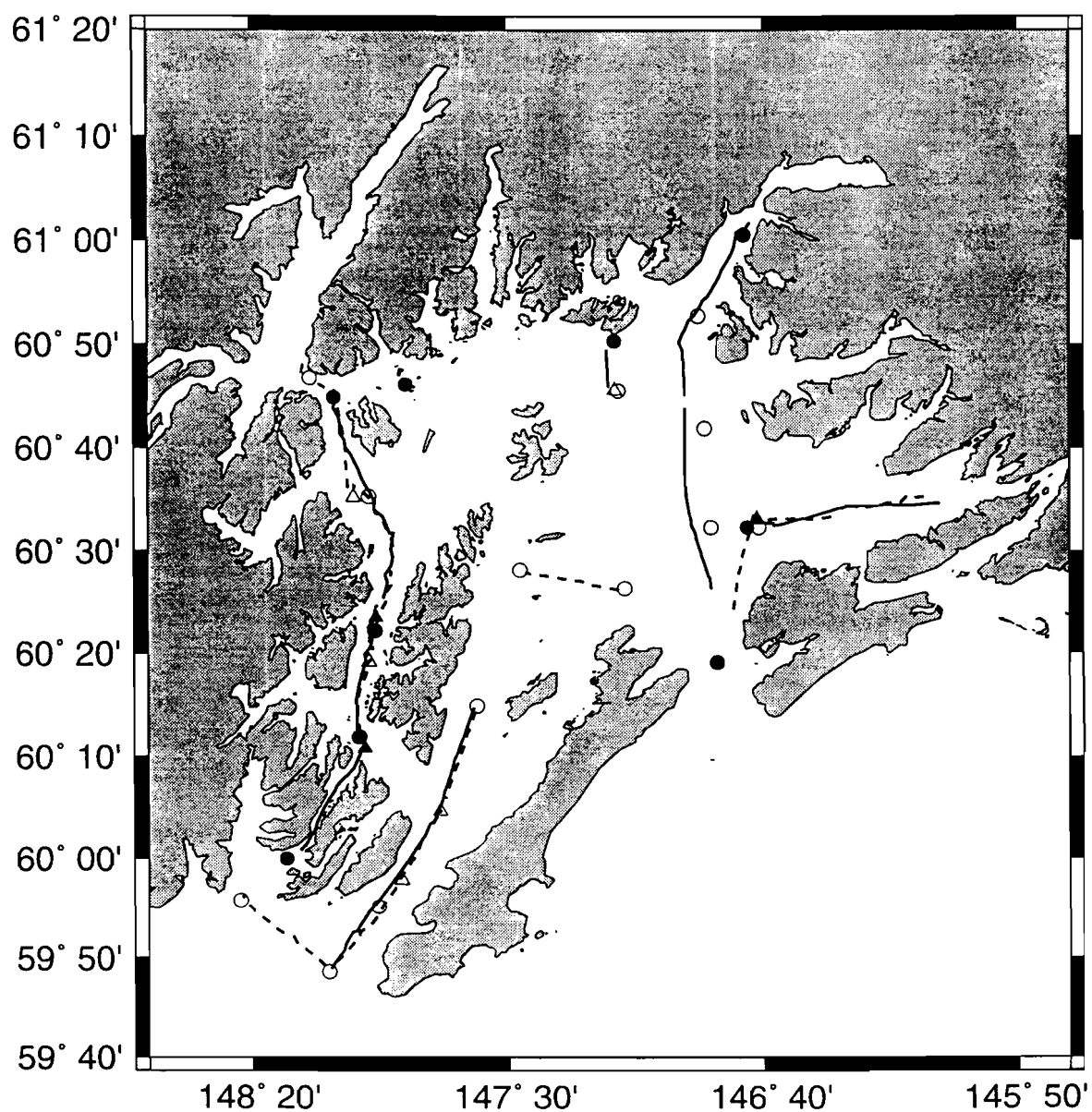


Fig. 1. Map of Prince William Sound showing sampling locations of acoustic transects from April (dashed lines) and May (solid lines) 1995. Also shown are zooplankton tows (circles) and trawls (triangles) from April (empty symbols) and May (filled symbols) 1995.

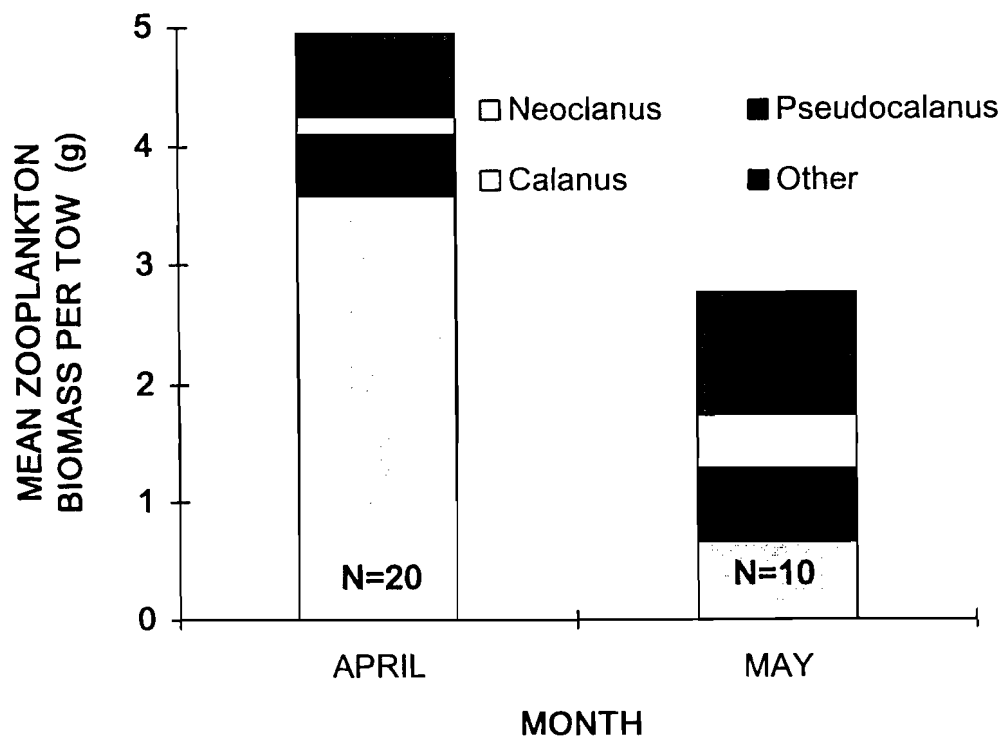


Fig. 2. Zooplankton biomass by species from the top 50 m of Prince William Sound for April and May 1995.

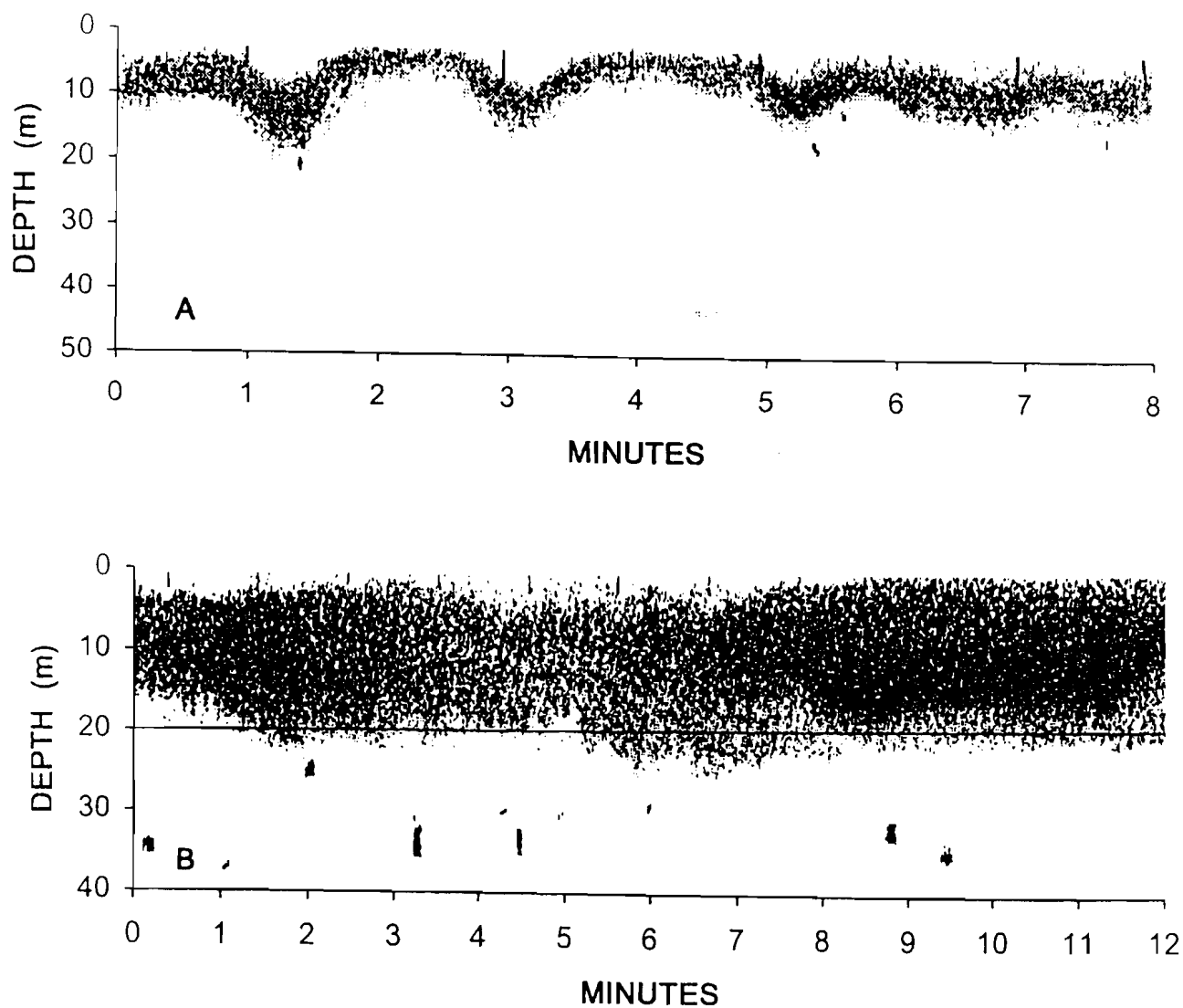


Fig. 3. Paper echograms from two transects during April 1995 showing: A) Plankton layer with varying depth and density due to localized currents; B) Plankton patch with pollock-sized targets associated with areas of high density.

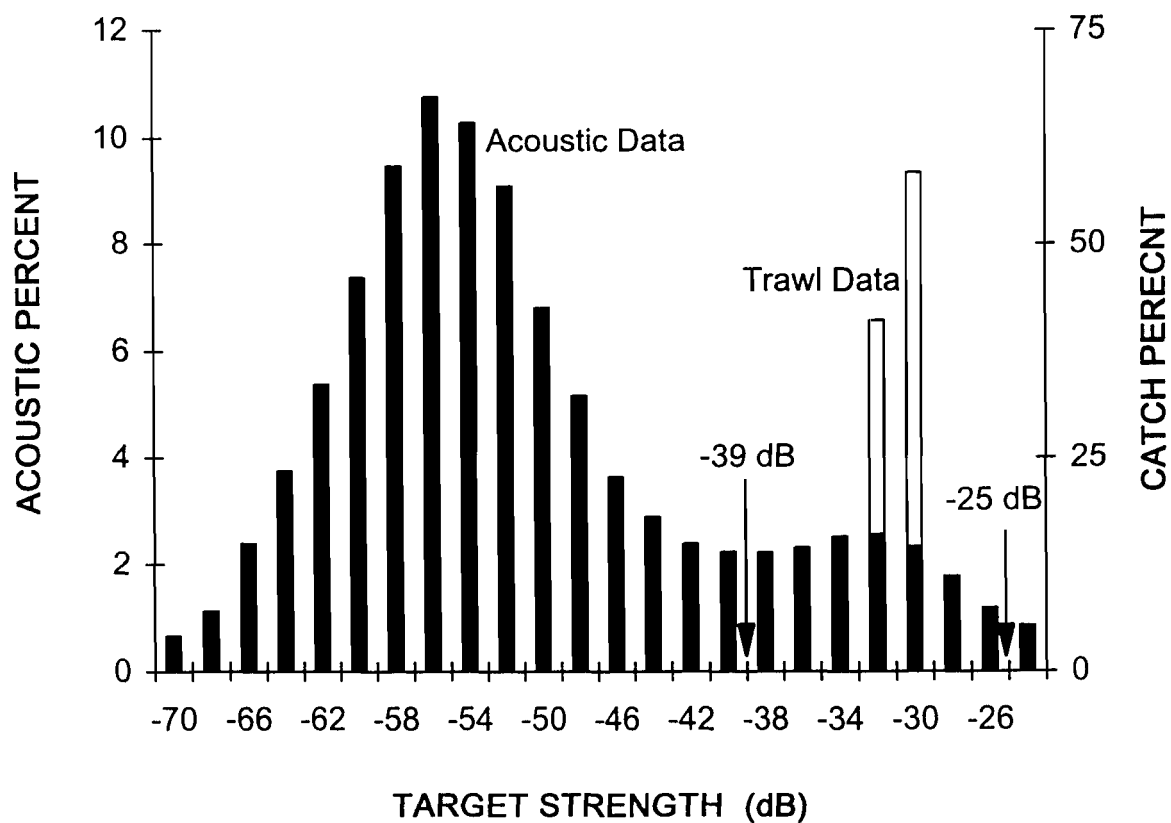


Fig. 4. Target strength (TS) frequencies from acoustic data files (black bars) and estimated TS from walleye pollock captured in the mid-water trawl in Prince William Sound during April and May 1995. Estimated TS were calculated using $20\log(\text{length}) - 66$ (Traynor and Williamson 1983). The arrows mark the range of TS values that were used to produce estimates of pollock density.

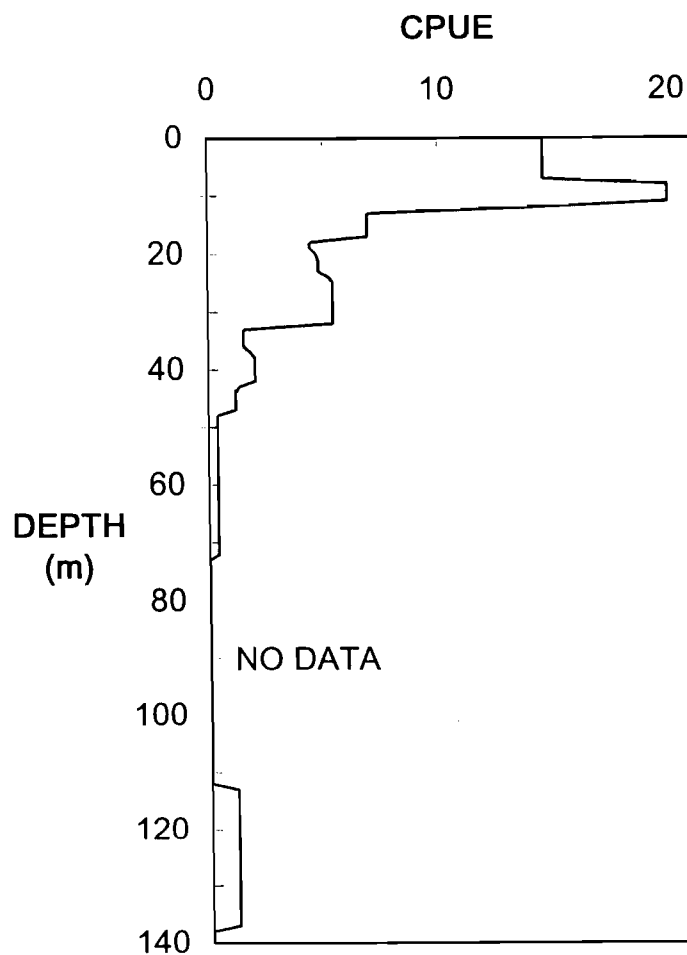


Fig. 5. Catch per unit effort of adult pollock from nine mid-water trawls performed in Prince William Sound in April and May 1995. There were no trawls between 73 and 122 m, or deeper than 138 m.

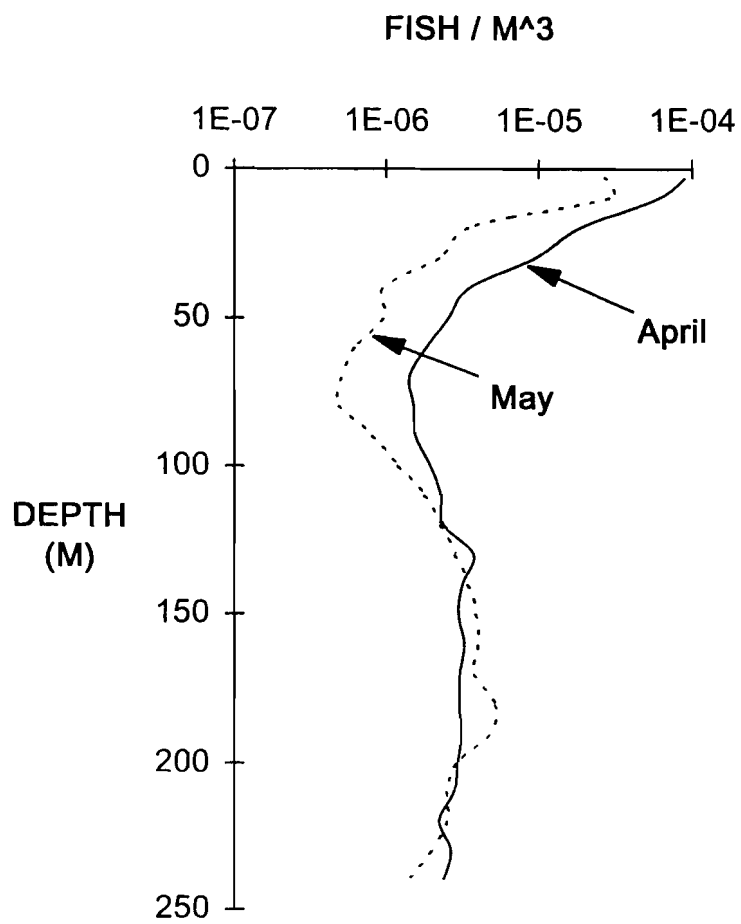


Fig. 6. Depth distribution of pollock-sized targets from acoustic data collected in Prince William Sound during April and May 1995.

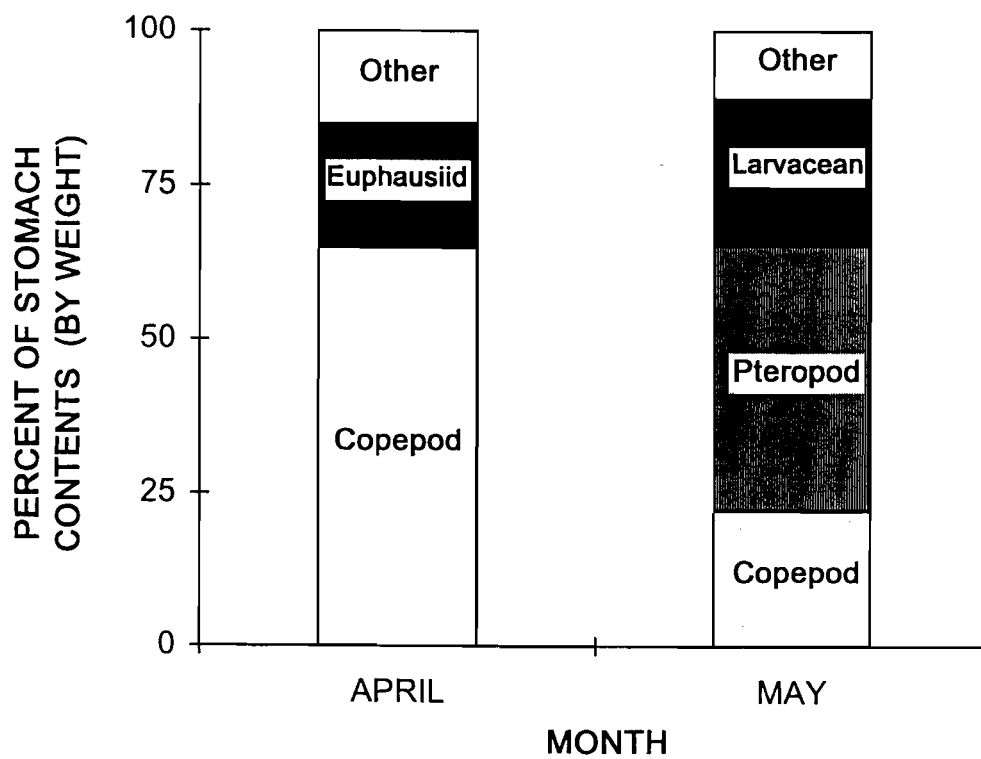


Fig. 7. Adult pollock diet composition (percent by weight) in April and May 1995 in Prince William Sound.

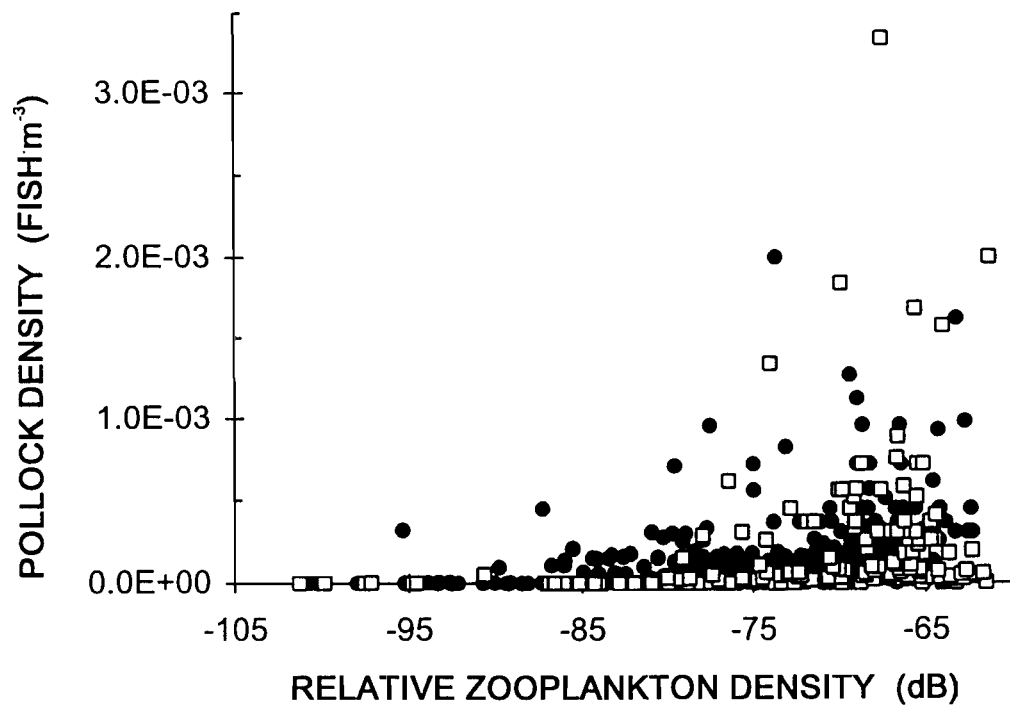


Fig. 8. Relationship between pollock density and relative zooplankton density (acoustic backscatter) in Prince William Sound from cruises in April (filled circles) and May (empty squares) 1995.

CHAPTER 3

Preliminary analysis of the nearshore distribution and abundance of Pacific herring (*Clupea pallasii*) and pelagic rockfish in western Prince William Sound. G. B. Steinhart, G. L. Thomas, J. Kirsch, and M. Blair

ABSTRACT

We used acoustics to measure abundance and distribution of many fish species in nearshore environments in western Prince William Sound (PWS) in 1994. We found that both pelagic rockfish (*Sebastes spp.*) and Pacific herring (*Clupea pallasii*) were present in many of the areas we surveyed. In addition, aggregations of these predacious fish were easily identifiable in the acoustic data as tall loosely aggregated targets above peaks and slopes (rockfish) and as dense school or balls in open water (herring). Since both rockfish and herring are predators of pink salmon (*Oncorhynchus gorbuscha*) fry, we analyzed the acoustic data to produce estimates of pelagic rockfish and herring. We found the highest number of rockfish in rocky areas along Culross Island and in the southwest passages. Herring were most abundant in the southwest passages.

INTRODUCTION

Stocks of pink salmon (*Oncorhynchus gorbuscha*) in Prince William Sound (PWS) have had highly variable recruitment success since the Exxon-Valdez oil spill. The cause of this variable recruitment is still under debate. One focus of the Sound Ecosystem Assessment (SEA) Project has been to model pink salmon survival. An assumption of SEA, that was adapted from GLOBEC, is that salmon fry do not die by starvation, but that all mortality is the result of being eaten. The Nekton/Plankton acoustics project has attempted to quantify the numbers various fish species in the Sound. Meanwhile, personnel at the Alaska Department of Fish and Game (ADF&G) have measured diet composition of these predators. Until recently, it was believed that most of the fry losses by predation have been due to predation by walleye pollock (*Theragra chalcogramma*). There is no doubt that pollock are one of the most abundant fish species in Prince William Sound; however, SEA research has not yet concluded that all salmon mortality is due to pollock predation. In fact, diet analysis on other fish species, such as rockfish and herring, have shown that many other fish species are eating salmon fry (Willette et al. 1997). The goal of this work was to re-analyze the acoustic data to quantify numbers of both pelagic rockfish and Pacific herring.

MATERIALS AND METHODS

Study site

Prince William Sound (PWS) is located at the northern edge of the Gulf of Alaska (Fig. 1). This large fjord/estuary covers an area of approximately 8800 km², and has about 3200 km of shoreline (Grant and Higgins 1910). Coastal rainforests, high mountains, and glaciers border the shoreline of PWS. The area receives seasonally intense storms moving up from the Gulf of Alaska, resulting in more than 7 m of annual rainfall.

Survey design

The data used for this analyses were from the 1994 nearshore surveys. The surveys were conducted during the day throughout western PWS (Fig. 2). There were 5 cruises where usable acoustic data were collected: 02o (5/5-5/9/94), 03o (5/19-5/25/94), 04o (6/2-6/11/94), 05o (6/18-6/29/94), and 06o (7/10-7/18/94). Zig-zag transects were made within 0.5 NM of the shoreline in Wells, Perry, and Knight Island Passages, Montague Straight and the Southwest passages (Thomas et al. 1996). Many of these transects were repeated in the various cruises; however, not all cruises surveyed all transects. Data were collected with a BioSonics 102-200 kHz dual beam echosounder.

For most surveys, transects were marked on paper and/or electronic charts to allow repetition of the same transect at a later date. At night, or during low tide, some transects were modified for safety purposes. Boat speed during transects was approximately 4-6 kn. The down-looking transducer was mounted on a fin towed alongside the boat at a depth of approximately 2 m.

Personnel from the Alaska Department of Fish and Game (ADF&G) collected numerous fish samples using a variety of fishing gear. Commercial seines and mid-water trawls were used for target verification of the acoustic data. In addition, small purse seines, pair trawls, bottom trawls, gillnets and longlines were used to collect fish. These fish were used for age/length/weight measurements and diet analyses.

Acoustic equipment

The acoustic data presented here was collected using a BioSonics 102-200 kHz dual-beam transducer. The data were processed in real-time using ESP software on a 486 laptop computer. A Magellan 5000 DX GPS receiver with an external antenna was used to geo-reference the data, or to record the cruise track in a separate database. Echo-square integration, dual-beam target strength (TS), and GPS data were stored on the computer hard disk, and backed up on tape drives. Raw acoustic signals were stored on Digital Audio Tape.

Acoustic processing

Once the cruise was completed, the acoustic files were transferred to UNIX workstations where batch processing of files was performed. To facilitate reduction and processing of acoustic information, software was written in the Interactive Data

Language (IDL) which corrected for physical parameters (temperature and salinity), and applied the acoustic calibrations. After initial processing, more IDL software was used to interactively remove untracked bottom, and to calculate density and biomass estimates.

Our data processing consisted of two major steps: target classification and target counting or echo-integration summing (Fig. 3). Hydroacoustic data can be successfully partitioned into different species based on knowledge of fish behavior, distribution and size (Rose and Leggett 1998; Richards et al. 1991). Rockfish were easily identifiable as clumps of targets on pinnacles and slopes (Wilkins, 1986; Starr et al. 1996; Fig. 4). Herring typically form tight schools, or balls, which were also easily identified (Fig. 5). We identified targets that appeared to be either rockfish or herring using information on the paper echograms, known fish behavior and distribution, electronic target echograms, and net catch data. We then interactively selected on those targets using software written by J. Kirsch in IDL (Fig. 6).

Due to differences in behavior and distribution, we processed the rockfish and herring acoustic data using different techniques. For the rockfish data, we used an echo-counting method that summed the number of identified targets in a transect, and then divided by the sample volume of the acoustic beam, to compute mean density for each transect. Herring biomass was calculated using echo-integration, since the target discriminator often failed to identify all targets in the dense herring schools (Thomas et al. 1997). We converted echo-integration voltages (V^2) to biomass density using mean herring length at each site, and the acoustic calibration (K_{equip}) using the following equations:

- [1] TS re: weight = $6\text{Log}_{10}\text{Length}_{(\text{mm})} - 18$ (Thorne 1983)
- [2] $\sigma/W = 10^{(\text{TS re: weight})/10}$
- [3] Biomass density = $(V^2/K_{\text{equip}})(W/\sigma)$.

Rockfish densities ($\#/m^3$) and herring biomass (kg/m^3) were then summed to the surface and to provide aerial densities ($\#/m^2$) and biomass (Kg/m^2). The mean rockfish density and mean herring biomass for each site were calculated by taking the weighted mean of all transects at a particular site during a single survey. Transect length (the number of reports) was used as the weighting factor. Once weighted rockfish densities and herring biomass were calculated for each site, the data were multiplied by the area sampled during the acoustic survey. This yielded estimates of the total number of rockfish, and the total tonnage of herring at each site.

RESULTS

Rockfish

Rockfish distribution was highly variable in the western portion of Prince William Sound in 1994 (Fig. 7). We found the most rockfish, an estimated 8750 fish, on the eastern shore of Culross Island in late May. The southwest passages (sites 8, 9, 10) and sections of Knight Island Passage (sites 13, 14, and 15) also had large numbers of pelagic rockfish. In contrast, few rockfish were found near Esther Island. When data from all sites were combined, we found mean rockfish densities of $9.3e^{-08}$ fish/m³ in late May, $1.4e^{-06}$ fish/m³ in early June, $4.4e^{-07}$ fish/m³ in late June, and $1.4e^{-06}$ fish/m³ in mid July. After accounting for the area surveyed during these cruises, we measured a total of approximately 400 rockfish in late May, 11,000 in early June, 7,000 in late June, and 21,000 in mid July, in the surveyed nearshore environments.

Herring

Herring abundance was also highest in the Southwest passages (Fig. 8). The largest concentrations of herring were seen in Prince of Wales Passage (sites 7 and 8), where we found approximately 3800 tonnes in late June and 1400 tonnes in mid July. Very few herring were seen north of Knight Island Passage. When all the data from each cruise were pooled, we estimated total herring biomass in the surveyed nearshore environments to be: 30 tonnes in early May, 200 tonnes in early June, 5,000 tonnes in late June, and 2,500 tonnes in mid July.

DISCUSSION

In general, there we found fewer rockfish and herring in the northwest portion of the Sound, than in the southwest passages. This distribution primarily reflects the habitat available in these areas, but since these surveys were not designed to specifically measure the abundance of these species, and therefore did not take habitat into consideration during their design.

There are several characteristics of rockfish distribution that make an accurate estimate of their numbers using acoustics difficult. First, rockfish are typically found over rocky substrates, often over pinnacles and slopes (Moulton 1975; Murie et al. 1994). In addition, rockfish do not often swim vast distances, instead opting to stay within a small, well defined area. The highly variable nature of rockfish distribution means intensive sampling relative to substrate must be conducted to insure an adequate number of samples (Adams et al. 1995). Although these surveys covered vast areas of shoreline, the actual percent of the shoreline and bottom sampled directly by the acoustic beam was relatively small and the surveys were only conducted once per cruise. This may result in misleading results, since a transect may just miss passing over several clumps of rockfish gathered above pinnacles. A subsequent survey may pass over the pinnacles, providing a more accurate sample of the rockfish population.

To overcome this problem, we propose to do a more in depth analysis of the data by defining suitable rockfish habitat, estimating the total amount of suitable habitat, and quantifying rockfish densities within those habitats. Future surveys should be designed with closely spaced repeated transects to reduce the error due to the discrete spatial variability of rockfish.

Many species of rockfish remain very close to the bottom (Starr et al. 1996). We believe the rockfish-like targets we identified were pelagic rockfish, such as the black rockfish (*Sebastes melanops*) and the widow rockfish (*S. entomelas*); however, even these pelagic species are also found close to the bottom, especially during high tidal flows (Moulton 1975). Current hydroacoustic equipment does not have the ability to resolve targets that are resting on, or extremely close, to the bottom. In combination acoustic and submersible surveys along the Oregon coast, it was estimated that the submersible surveys accounted for approximately one-third of the rockfish population (Starr et al. 1996). This portion of the population was missed by the acoustic surveys. Rockfish behavior, and the limitations of current acoustic systems, will generally result in an underestimation of rockfish abundance. This error may be minimized in the future by using digital echo-sounders, which have higher resolution, and by timing surveys so they do not take place during periods of high tidal flow.

Measuring herring abundance with acoustics can also be problematic. During the day, herring often form dense schools near the surface. These schools can be relatively small, and could have been missed in the small volume of water sampled. Furthermore, herring schools near the surface are very spooky, and often avoid approaching boats. This problem can be at least partially overcome by doing acoustic surveys at night, when herring are often not as densely schooled during the day. Boat avoidance can also be reduced during periods of low light, however the fish do respond to boat noise, which cannot be eliminated during nighttime surveys. The use of side-scanning sonar in future surveys will allow us to measure the degree of boat avoidance by herring,

In conclusion, our data from the 1994 nearshore surveys are some of the most intensive sampling of the western portion of Prince William Sound. From these surveys, it appears that rockfish and herring were more abundant in the southwest passages than near Esther Island. Rockfish were also abundant in Knight Island Passage. Numbers and biomass of these species appeared to increase later in the year. These data should be further analyzed to provide more accurate estimates of both rockfish and herring populations in order to more accurately quantify the potential losses of salmon fry to predation by these fishes.

ACKNOWLEDGMENTS

We would like to thank all the captains and crews of all the fishing and research vessels that helped us collect these data. Without their knowledge and experience, this research would not have been possible. Thanks to Tom McClain and Paul Salomone for their collection of the acoustic data. We would also like to thank the Alaska Department of Fish and Game, and the University of Alaska-Fairbanks, for they were responsible for analyzing the catch data. This work was supported by the *Exxon Valdez* Trustee Council, Grant Nos. 94320-N and 97320-N.

REFERENCES CITED

- Adams, P. B., J. L. Butler, C. H. Baxter, T. E. Laidig, K. A. Dahlin, and W. W. Wakefield. 1995. Population estimates of Pacific coast groundfishes from video transects and swept-area trawls. U. S. Fish. Bull. 93: 446-455.
- Grant, U. S. and K. F. Higgins. 1910. Reconnaissance of the geology and mineral resources of Prince William Sound, Alaska. U.S. Geological Survey Bulletin. No. 443. 89 pp.
- Murie, D. J., D. C. Parkyn, B. G. Clapp, and G. G. Krause. 1994. Observations on the distribution and activities of rockfish, *Sebastes* spp., in Saanich Inlet, British Columbia, from the *Pisces IV* submersible. U. S. Fish. Bull. 93: 313-323.
- Richard, L. J., R. Kieser, T. J. Mulligan, and J. R. Candy. Classification of fish assemblages based on echo integration surveys. Can. J. Fish. Aquat. Sci. 48: 1264-1272.
- Rose, G. A., and W. C. Leggett. 1988. Hydroacoustic signal classification of fish schools by species. Can. J. Fish. Aquat. Sci. 45: 597-604.
- Starr, R. M., D. S. Fox, M. A. Hixon, B. N. Tissot, G. E. Johnson, and W. H. Barss. 1996. Comparison of submersible-survey and hydroacoustic-survey estimates of fish density on a rocky bank. U.S. Fish. Bull. 94: 113-123.
- Thomas, G. L., J. Kirsch, G. B. Steinhart, and N. Peters. 1997. SEA: Nekton-plankton acoustics second annual report, 1996. Restoration Project 96320N. EXXON VALDEZ Trustee Council. Anchorage, Alaska. 120 pp.
- Thorne, R. E. 1983. Assessment of population abundance by hydroacoustics. Bio. Ocean. 2: 253-262.
- Wilkins, M. E. 1986. Development and evaluation of methodologies for assessing and monitoring the abundance of widow rockfish, *Sebastes entomelas*. U.S. Fish. Bull. 84: 287-310.
- Willette, M., M. Clapsadl, P. Saddler, and M. Powell. 1997. SEA: Juvenile Salmon Predation annual report, 1996. Restoration Project 96320E. EXXON VALDEZ Trustee Council. Anchorage, Alaska.

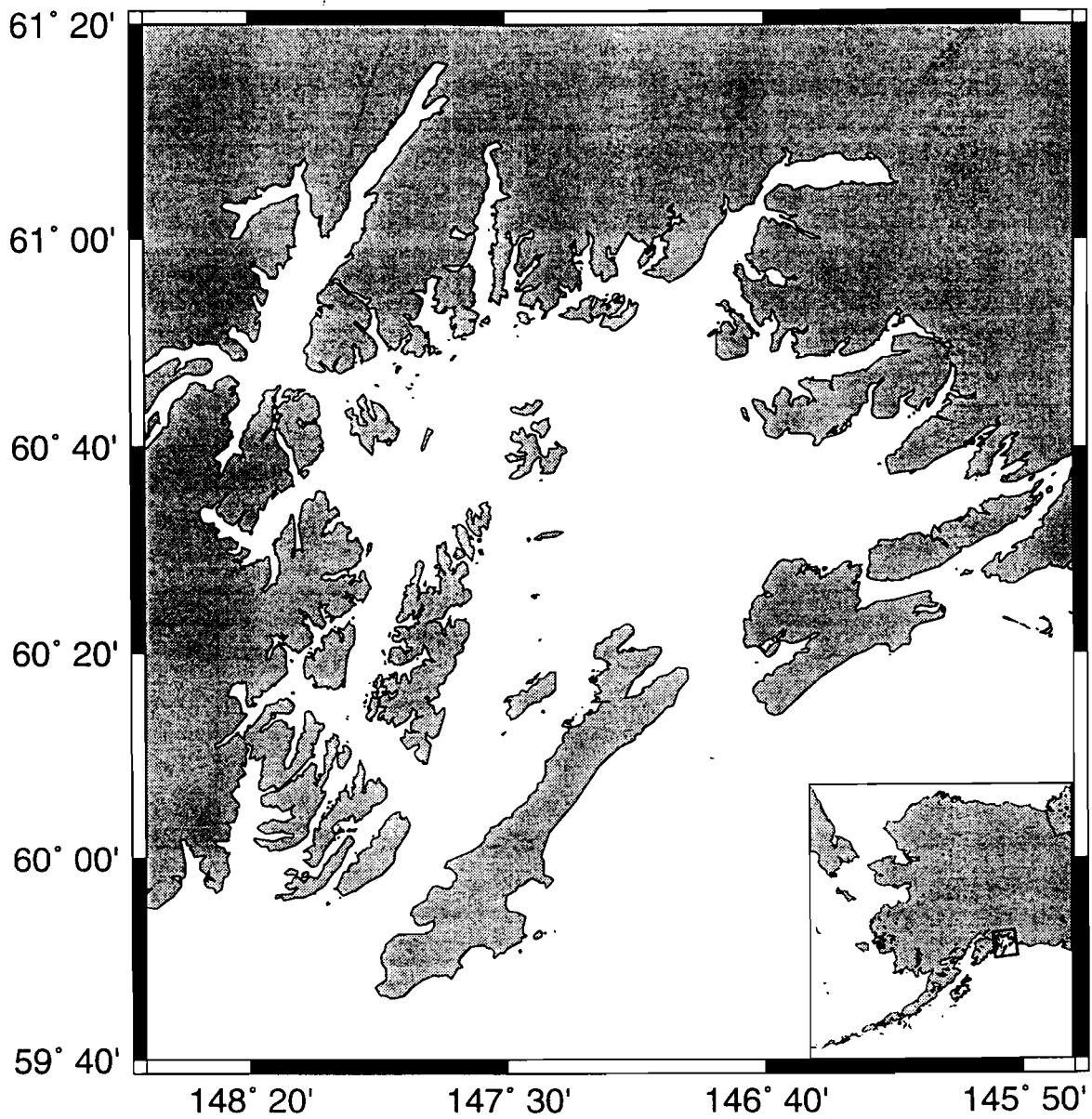


Fig. 1. Map of Prince William Sound, Alaska, USA.

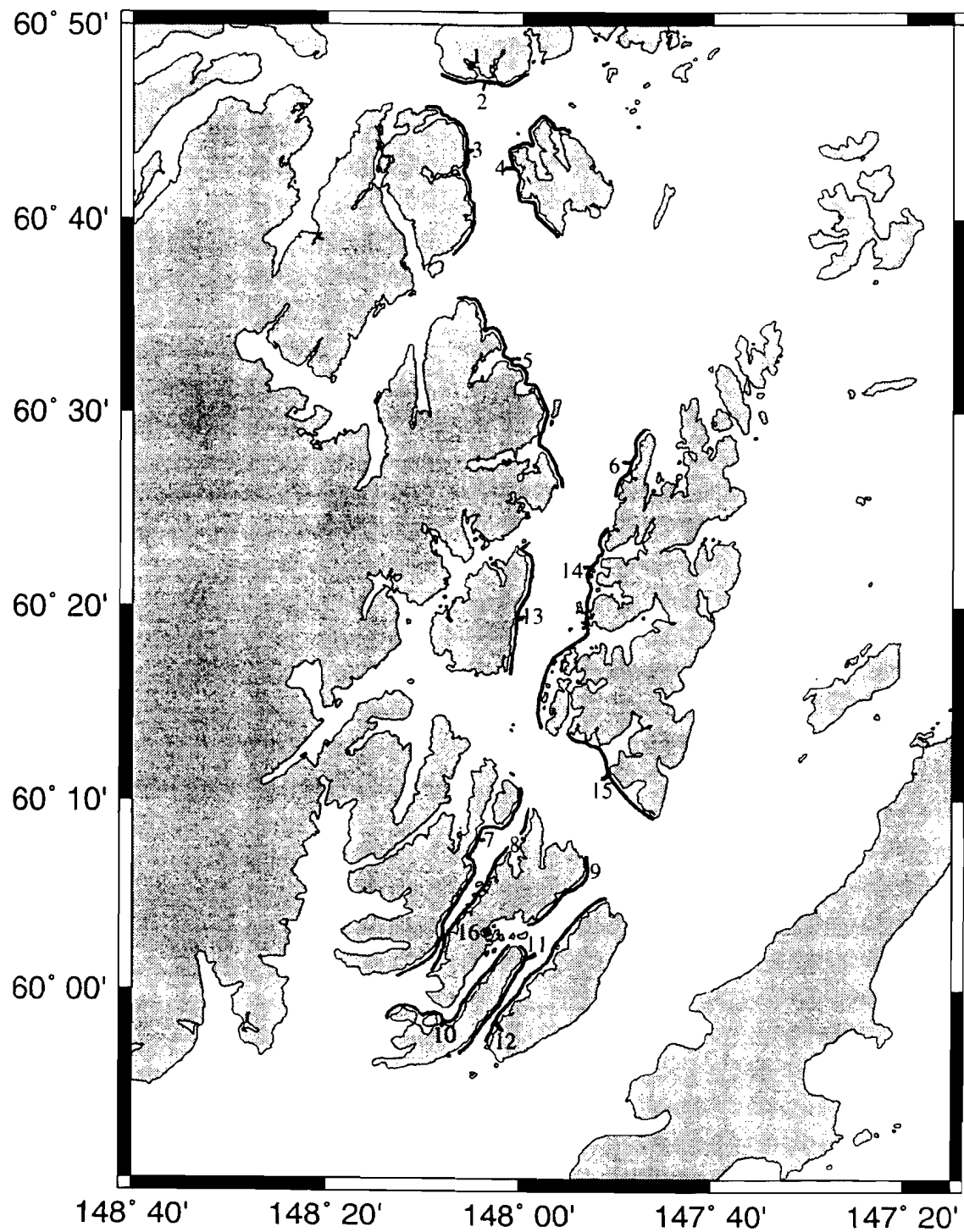


Fig. 2. Map of western Prince William Sound showing the nearshore areas surveyed in 1994.

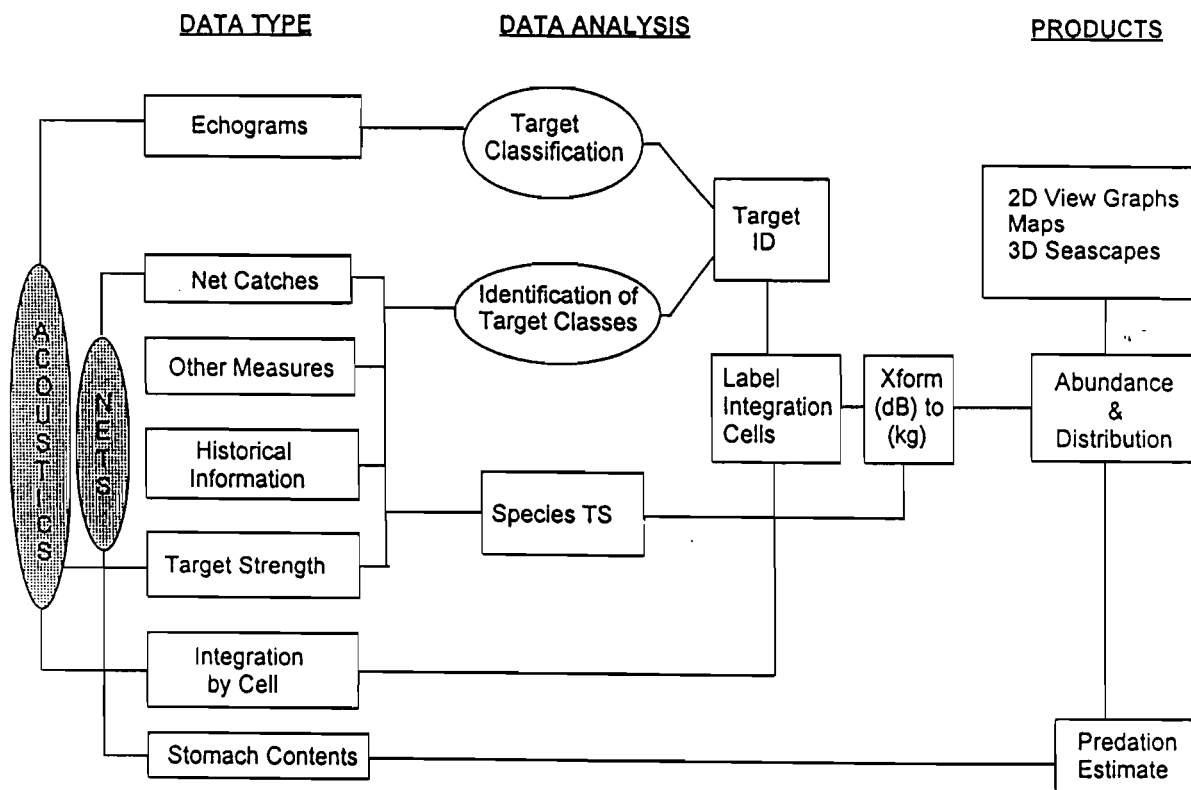


Fig. 3. Flow chart of data processing steps used in analysis of SEA acoustic data collected in 1994-97.

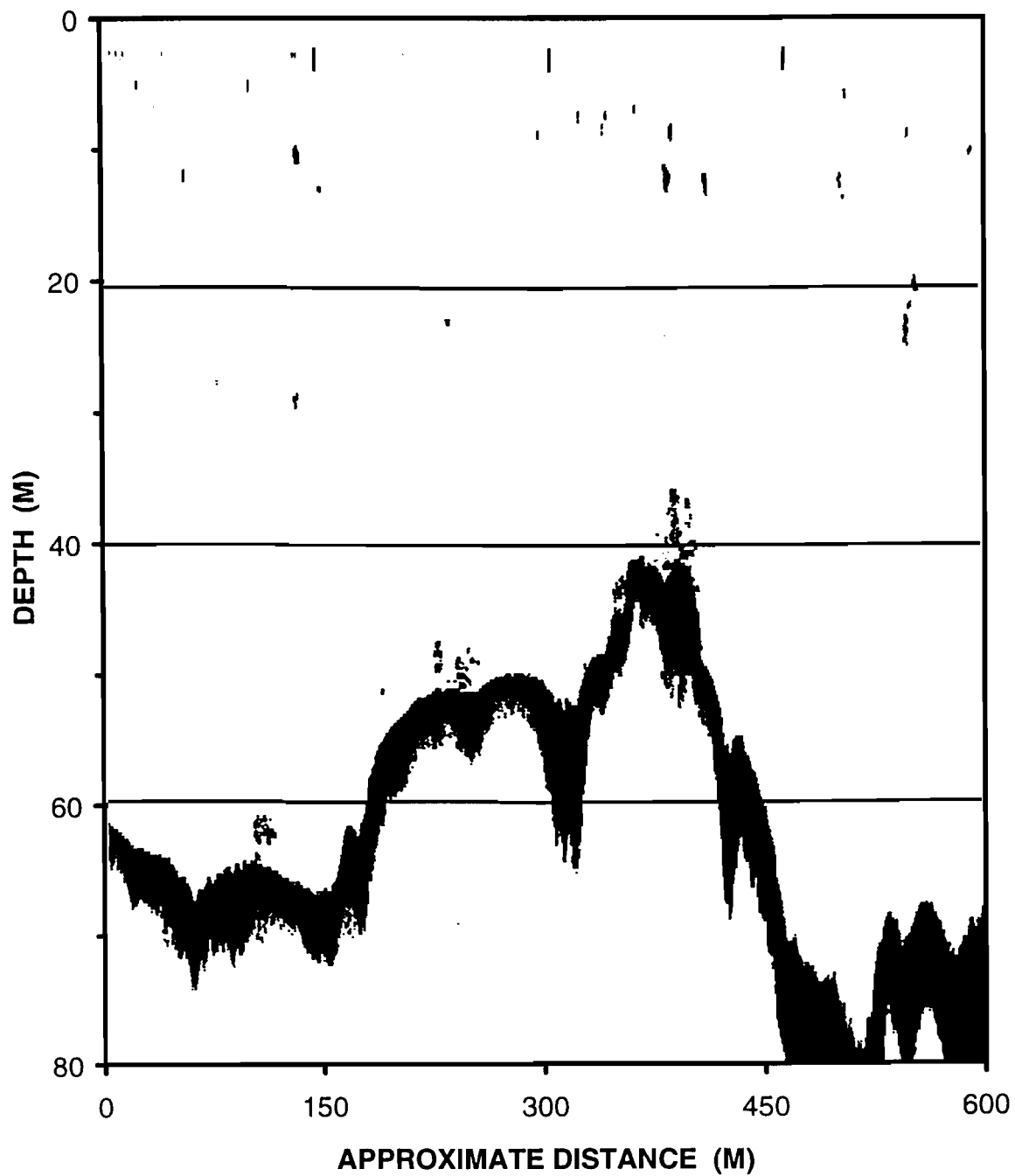


Fig. 4. A paper echogram showing several rockfish from an acoustic survey in Sawmill Bay, 1994. Rockfish are clearly visible as clumped targets 0-10 m above the bottom, especially near pinnacles and slopes.

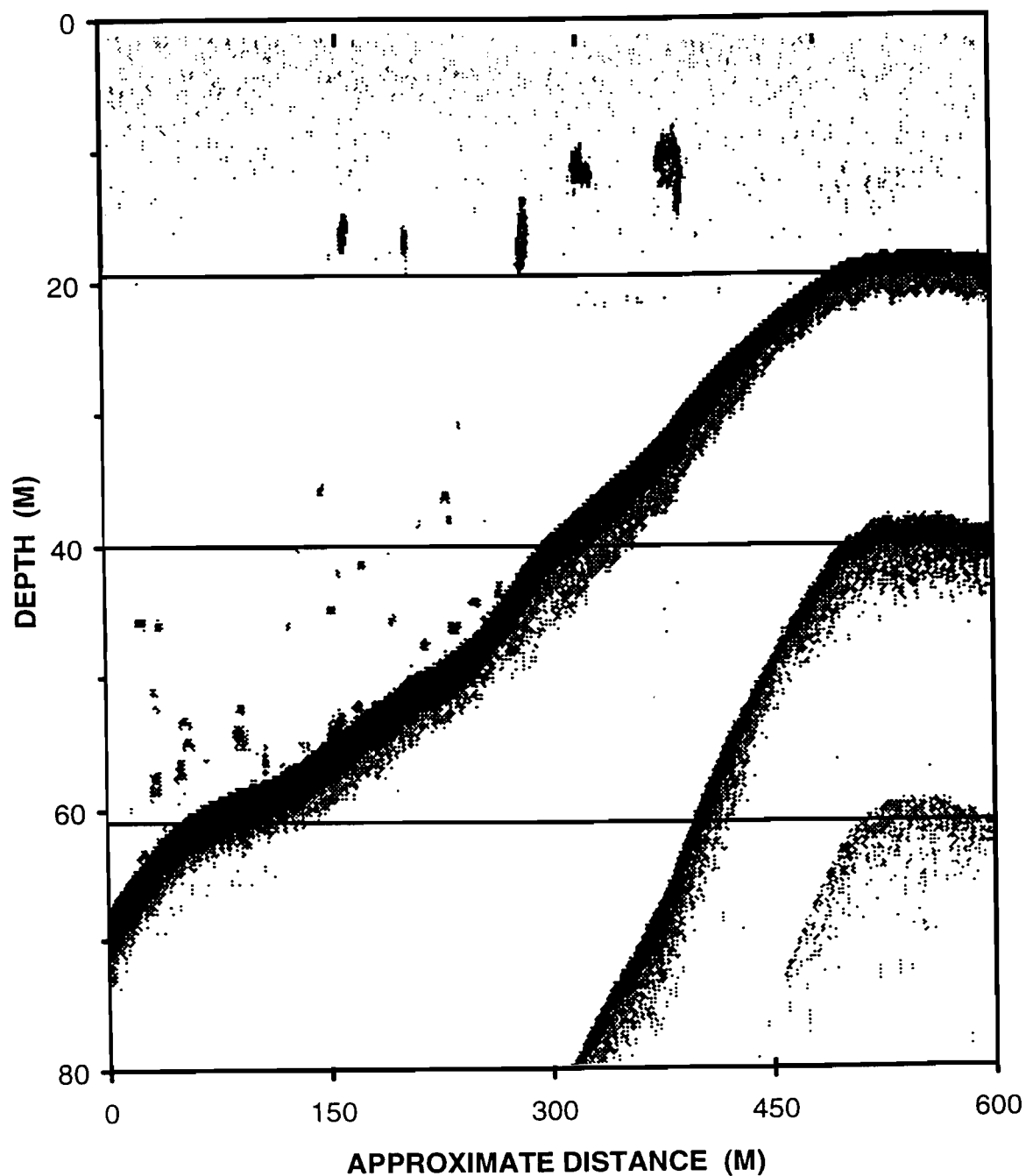


Fig. 5. A paper echogram showing several herring schools from an acoustic survey in Prince of Wales Passage, 1994. Herring typically form dense schools, as seen in the top 20 m of this transect.

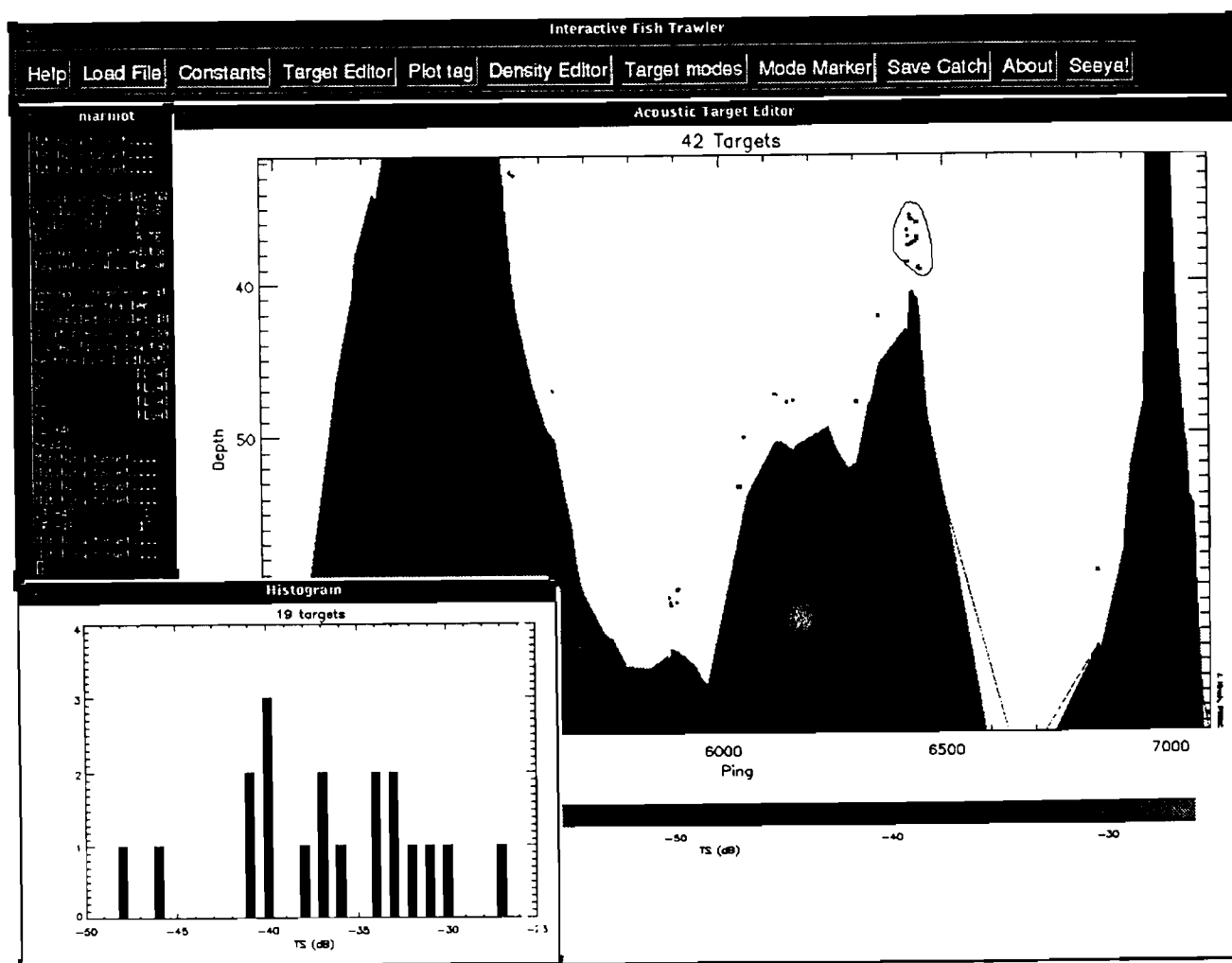


Fig. 6. We used software written by J. Kirsch to interactively select and classify targets. In this picture, the user has selected a group of rockfish swimming above a pinnacle. These data are from the same transect pictured in Fig. 4.

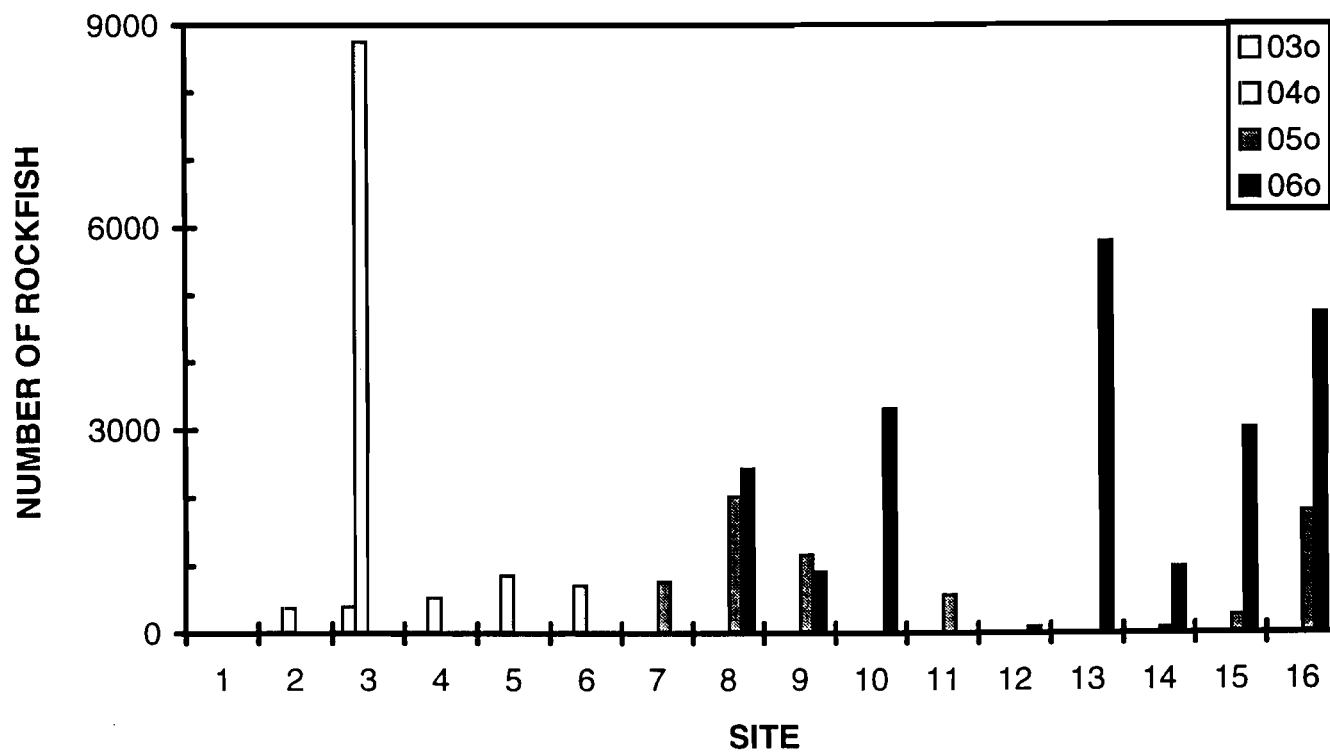


Fig. 7. Weighted mean rockfish numbers from 1994 nearshore surveys. See Fig. 2 for exact site locations.

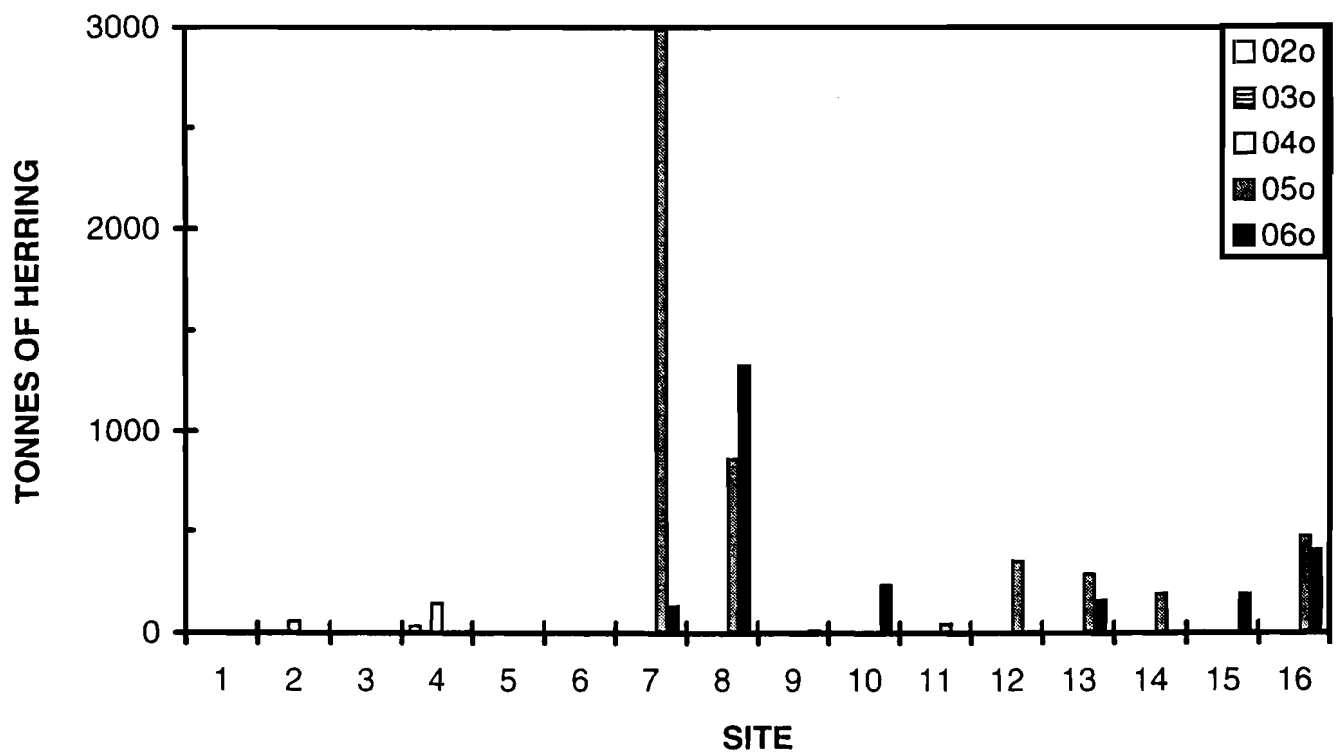


Fig. 8. Weighted mean herring tonnage from 1994 nearshore surveys. See Fig. 2 for exact site locations.

CHAPTER 4

The preliminary fusion of acoustical and optical data with net catch information to assess zooplankton distributions in Prince William Sound, Alaska. L.B. Tuttle, J. Kirsch, R.T. Cooney, and G.L. Thomas

ABSTRACT

The Sound Ecosystem Assessment (SEA) is a multi-investigator project designed to identify the primary physical and biological factors that affect the production of pink salmon and Pacific herring in Prince William Sound (PWS), Alaska. As part of this assessment, research cruises were conducted to describe the abundance and patchiness of zooplankton in PWS using high-frequency acoustics, an optical plankton counter (OPC), and a multiple-sample zooplankton net, as well as instruments to measure temperature, salinity, and fluorescence. The high-resolution, continuous sampling provided by the acoustics and optics showed that zooplankton aggregate in layers and patches throughout PWS, and that Hinchinbrook entrance had relatively high densities in both 1995 and 1996. In regions where *Neocalanus* copepod dominates the biomass, the optics and acoustics showed similar patterns, but in regions with high pteropod biomass, the acoustics estimate more biomass than the optics.

INTRODUCTION

The Sound Ecosystem Assessment (SEA) program was established to identify the primary factors that affect the production of pink salmon and Pacific herring in Prince William Sound (PWS). An understanding of how zooplankton production varies over space and time is important in achieving an ecosystem-level model of PWS since zooplankton is an important link between primary production and the upper trophic levels. The purpose of this research is to describe the abundance and patchiness of zooplankton using high-resolution, continuous-sampling methods. *Neocalanus* spp. constitutes much of the zooplankton biomass during the spring bloom in PWS.

In 1993 on the Scotian shelf, Herman et. al. used an OPC coupled with acoustics and a BIONESS multiple-net sampler to estimate euphausiid abundance. The acoustic and OPC abundances agreed within a factor of two or better. However, Herman (1992) found that in areas with high zooplankton species diversity, separation of individual species is difficult. Sensitivity to zooplankton below 0.5 mm is limited by marine snow, chain-forming phytoplankton, and other detritus in the water column. Because of these problems, the agreement of the OPC and nets was only 30%.

Recent advances in zooplankton scattering models allowed us to predict backscatter for a given species composition and density. Target strength is dependent on animal size, material,

orientation, and transducer frequency (Stanton et al 1993, Stanton et al 1994, Stanton et al 1996). These models allow us to compare net catch and acoustic backscatter quantitatively.

METHODS

Broadscale cruises were conducted in both 1995 and 1996 to survey zooplankton in Prince William Sound and north Gulf of Alaska (Figure 1).

1995

A BioSonics 101-120 kHz dual-beam sonar mounted on a tow fin measured scattering layers from 3 m to 50 m depth. Echo signals were acquired on a laptop computer, and were echo-integrated into arrays of volume backscatter S_v . A Chelsea Instruments Aquashuttle was undulated from surface to 50 m depth. The Aquashuttle includes a Chelsea CTD and fluorometer, and a Focal Instruments Optical Plankton Counter (OPC). The CTD collected temperature and salinity data, the fluorometer measured chlorophyll concentrations, and the OPC counted and measured particles in the water.

A ½ meter ring net with .333 mm mesh was deployed at oceanographic stations throughout PWS. At each site, the net collected zooplankton from 50 m to the surface.

1996

A BioSonics DT 420 kHz digital sonar mounted on a tow fin measured scattering layers from 3 m to 50 m depth. Echo signals were acquired on a laptop computer, and were later echo-integrated into arrays of volume backscatter S_v . Data were collected using a Chelsea Instruments Aquashuttle using the same methods as in 1995.

A Multiple Opening and Closing Net and Environmental Sensing System (MOCNESS) net with .333 mm mesh was deployed at 24 sites along the cruise track. At each site, 8 nets collected zooplankton at separate depths, from 50 m to the surface. A flow meter indicated sampled volume, allowing absolute density to be calculated.

RESULTS

The results here are preliminary, as work is still in progress. Acoustic and Aquashuttle data analysis is more complete for 1996 because of the refinement of sampling methods. Data for 1995 are currently being analyzed for comparison.

1995

Figure 2 shows the geographical distribution of acoustic backscatter in 1995. Highest scattering levels were found in the north-central PWS and Hinchinbrook Entrance.

Biomass data from vertical net stations for all zooplankton species are displayed in Figure 3.

Biomass is highest in north-central and northwest PWS in April 1995. In May, biomass remains high in north-central PWS, but the highest biomass is found in the Knight Island Pass region.

1996

Figure 4 presents data from a series of transects on May 2, 1996 in Knight Island Passage, heading from south to north. The top panel illustrates the high-resolution acoustic backscatter, showing patchy distribution of layers ranging from 3 to 25 m. The second and third panels show the oscillating tow track of the Aquashuttle, with layers of chlorophyll (second panel) and *Neocalanus*-sized particle counts (third panel), which correspond well with the acoustic backscatter layers.

Figure 5 presents a series of transects in Montague Strait, from north to south on May 6, 1996. The acoustic backscatter layer is strongest to the south, ranging from 3 to 20 m, on average. Conversely, the strongest chlorophyll layers are seen in northern Montague Strait, concentrated between 10 and 40 m, with a corresponding *Neocalanus*-sized particle layer.

Figure 6 shows the geographical distribution of acoustic backscatter. Highest scattering levels were found in the Gulf of Alaska, Hinchinbrook Entrance, and southern Montague Strait.

Biomass data from MOCNESS stations for stage 5 *Neocalanus*, the pteropod *Limacina helicina*, euphausiids, and stage 4 *Neocalanus* are displayed in Figures 7-10, respectively. *Neocalanus* biomass is highest in northwest PWS and from Hinchinbrook Entrance into the central sound. Euphausiid biomass is highest in Montague Strait and Orca Inlet, while the highest pteropod biomass is found at the south end of Montague Strait.

Although not discussed here, plots of the remainder of the 1996 data set (days 2,3,4,6,7,8,9) are printed as an appendix.

DISCUSSION

In 1996, regions where pteropod and euphausiid biomass was low, the high-frequency acoustics and the Optical Plankton Counter were able to detect the same patchy horizontal and vertical distributions of the plankton layers, which included concentrations of *Neocalanus*-sized particles. Conversely, in regions where pteropod or euphausiid densities were high, the acoustics and OPC were in disagreement. Target strengths (TS) of pteropods, because of their rigid shell, are much higher than copepod TS. The TS of euphausiids are also higher than copepods, due to their larger average sizes. Higher TS causes these species to be much more visible to the acoustics, while the OPC has difficulty seeing these species due to their larger sizes.

In most cases, there is a good correspondence between the layers of chlorophyll measured by the fluorometer, and the concentration of *Neocalanus*-sized particles. This is expected since *Neocalanus* must incorporate energy from the phytoplankton before it leaves the surface waters to enter diapause at depth in late spring.

Figure 11 shows a comparison of the distribution of volume backscatter S_v between 1995 and 1996. This higher acoustic backscatter indicates higher zooplankton densities in 1995, with increased variability. Also, differences in predicted target strength (TS) seen in figure 12 (Stanton) indicate that the 1995 acoustic density are actually higher than the estimates shown. More work will be required to resolve these differences as acoustical or ecological.

FUTURE WORK

We maintain that acoustic and optical instrumentation offers the promise of high-resolution, large-scale monitoring of patchy plankton populations in PWS. But there is further work to increase the accuracy of the instruments.

As an example, the flow of water through the opening of the OPC is affected by the pitch of the Aquashuttle. Figure 13 shows the density estimations plotted against the pitch for the 9 days of the Alpha Helix cruise. The slope is consistently negative, and the data points are bi-modal, indicating the high pitch may have reduced the water flow, and therefore particle flow, available to the OPC.

Alignment of these data over space and time, and synthesis with the species and density data from the nets, lead to an understanding of the biases of the instrumentation, and of the ecology of zooplankton in PWS. These data will then be assimilated into bio-physical models of PWS being developed as part of SEA.

ACKNOWLEDGEMENTS

This work would not have been possible without the captain and crew of the Alpha Helix. Ken Coyle and Elizabeth Stockmar counted and measured the MOCNESS samples. This work was supported by EVOSTC, through Sound Ecosystem Assessment (SEA) projects 9x320-N, 9x320-M, and 9x320-H.

REFERENCES

- Exxon Valdez* Trustee Council, Restoration Plan, 1995
- Grant, U.S., and D.F. Higgins. 1910. Reconnaissance of the geology and mineral resources of Prince Williams Sound, Alaska. U.S. Geological Survey Bulletin. 443:1-89.
- Herman, A.W. 1988. Simultaneous measurement of zooplankton and light attenuation with a new optical plankton counter. *Contin. Shelf Res.* 8:205-221.
- Herman, A.W. 1992. Design and calibration of a new optical plankton counter capable of sizing small zooplankton. *Deep Sea Res.* 39:395-415.

- Herman, A.W., N.A. Cochrane, D.D. Sameoto. 1993. Detection and abundance estimation of euphausiids using an optical plankton counter. *Mar Eco. Prog. Ser.* 94:161-173.
- Kirsch, J., G.L. Thomas, R.T. Cooney. 1997. Acoustic estimate of zooplankton distribution in Prince William Sound, spring 1996. SEA-FISH Annual report to EVOSTC.
- Kirsch, J. and G.L. Thomas. 1998. On the use of digital sonar systems for practical fisheries acoustics surveys. *Fisheries Oceanography*. In progress.
- MacLennan, D.N. and E. John Simmonds. 1992. *Fisheries Acoustics*. Chapman & Hall. London. 325pp.
- Medwin, H, and C.S. Clay. 1997. *Fundamentals of Acoustical Oceanography*. Academic Press.
- Schmidt, G.M. 1977. The exchange of water between Prince William Sound and the Gulf of Alaska. MS thesis. University of Alaska, Fairbanks. 116pp.
- Stanton, T.K., Chu, D., Wiebe, P.H., and Clay, C.S. 1993. Average echoes from randomly oriented random-length finite cylinders: zooplankton models. *Journal of the Acoustical Society of America*, 94: 3463-3472.
- Stanton, T.K., Wiebe, P.H., Chu, D., Benfield, M.C., Scanlon, L., Martin, L., and Eastwood, R.L. 1994. On acoustic estimates of zooplankton biomass. - *ICES J. Mar. Sci.*, 51: 505-512
- Stanton, T.K., Chu, D., and Wiebe, P.H. 1996. Acoustic scattering characteristics of several zooplankton groups. - *ICES Journal of Marine Science*, 53: 289-295
- Urick, Robert J. 1975. *Principles of underwater sound*. McGraw Hill. New York. 384 pp.

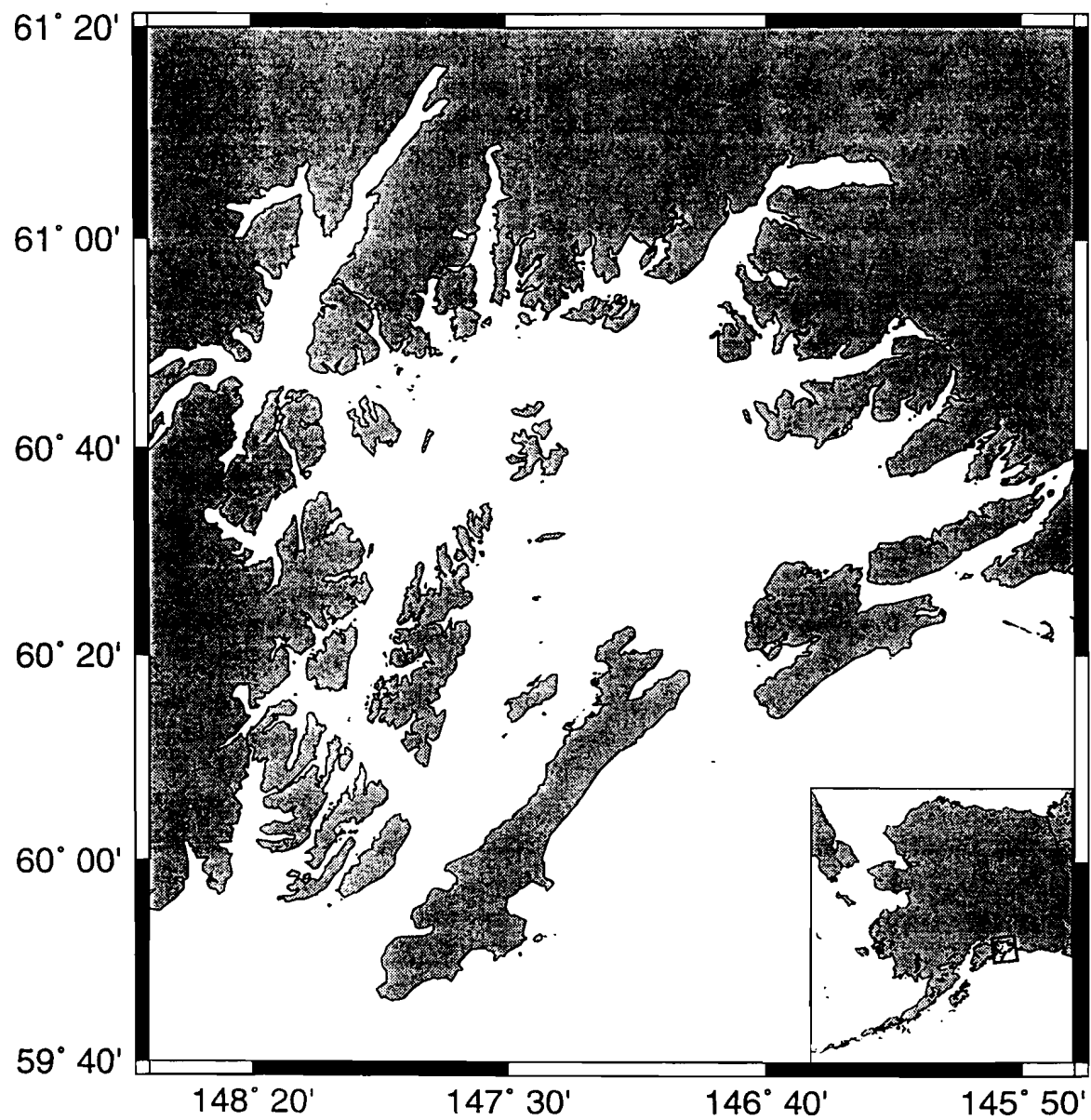


Fig. 1. Map of Prince William Sound, Alaska, USA.

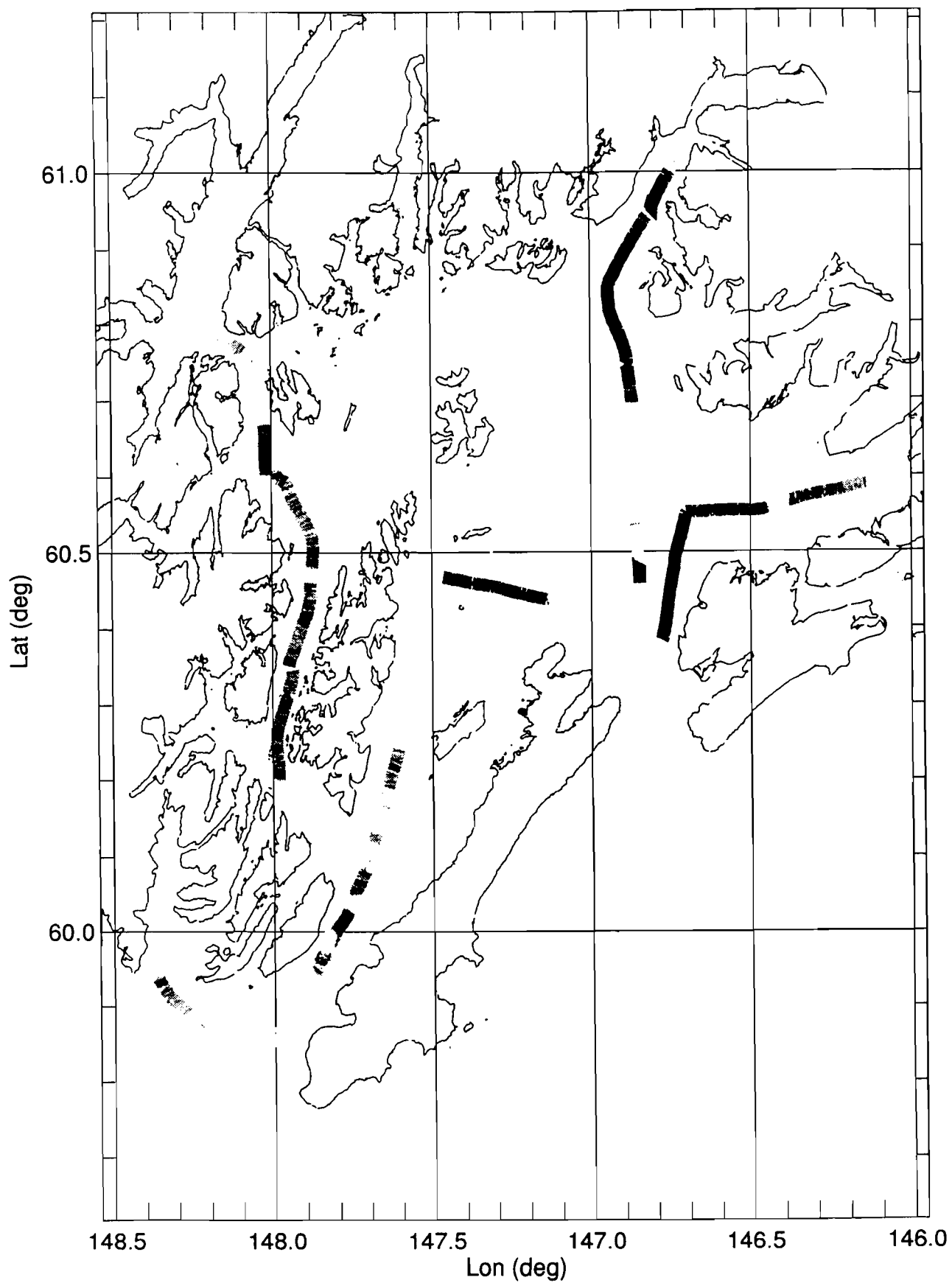


Figure 2. Geographical distribution of acoustic backscatter, 1995.

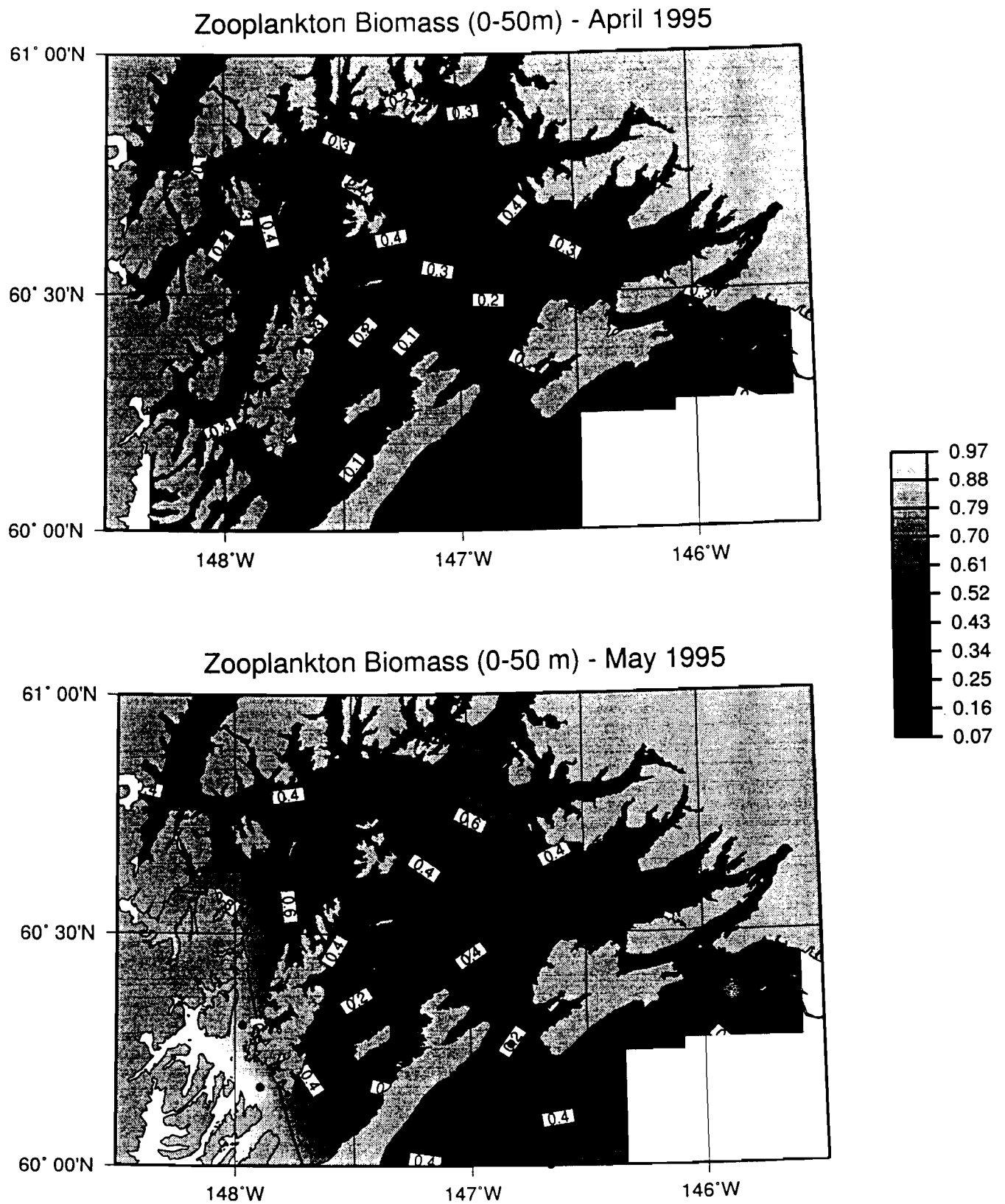


Figure 3. Vertical net zooplankton biomass, 1995.

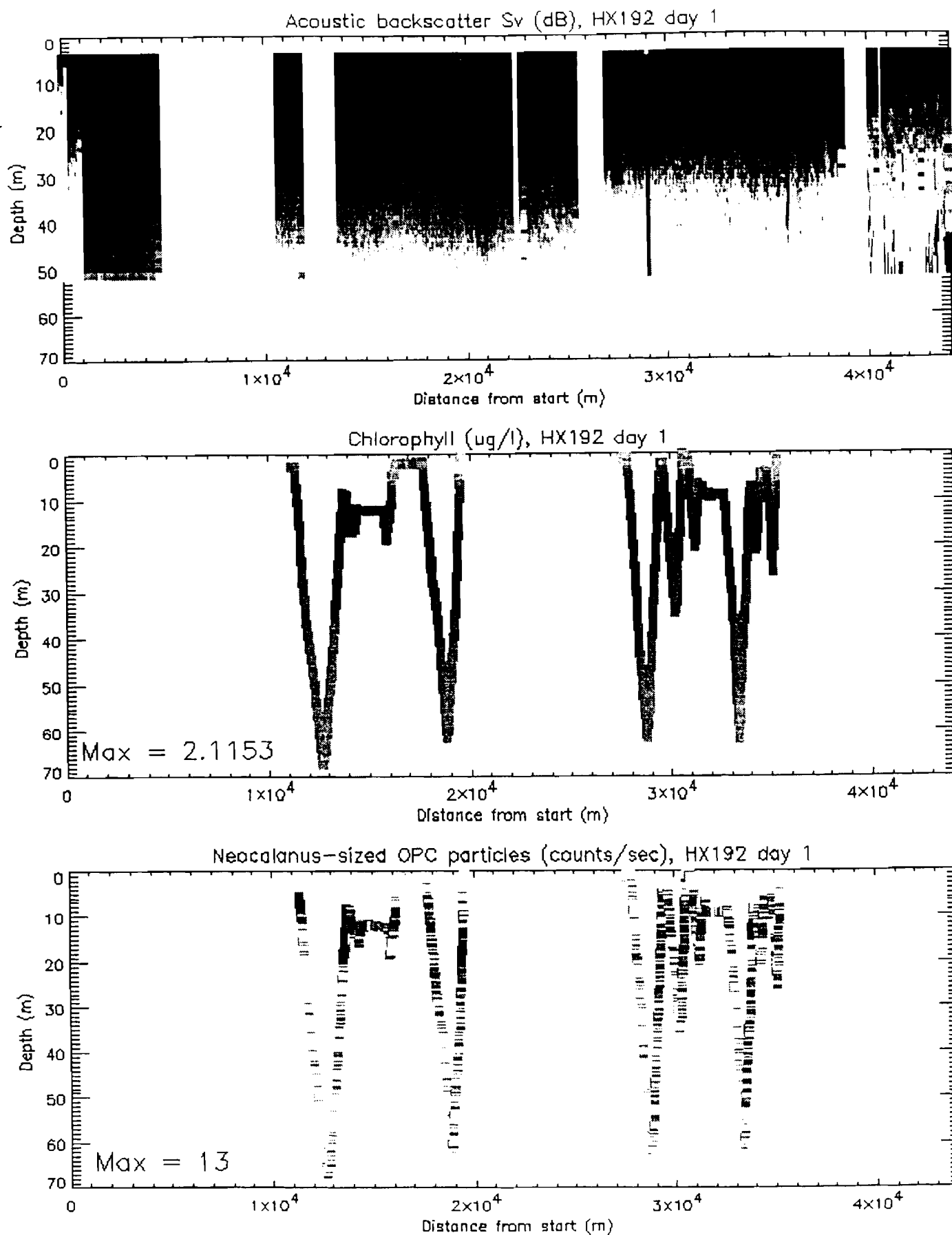


Figure 4. Knight Island Passage plankton distributions, May 1996.

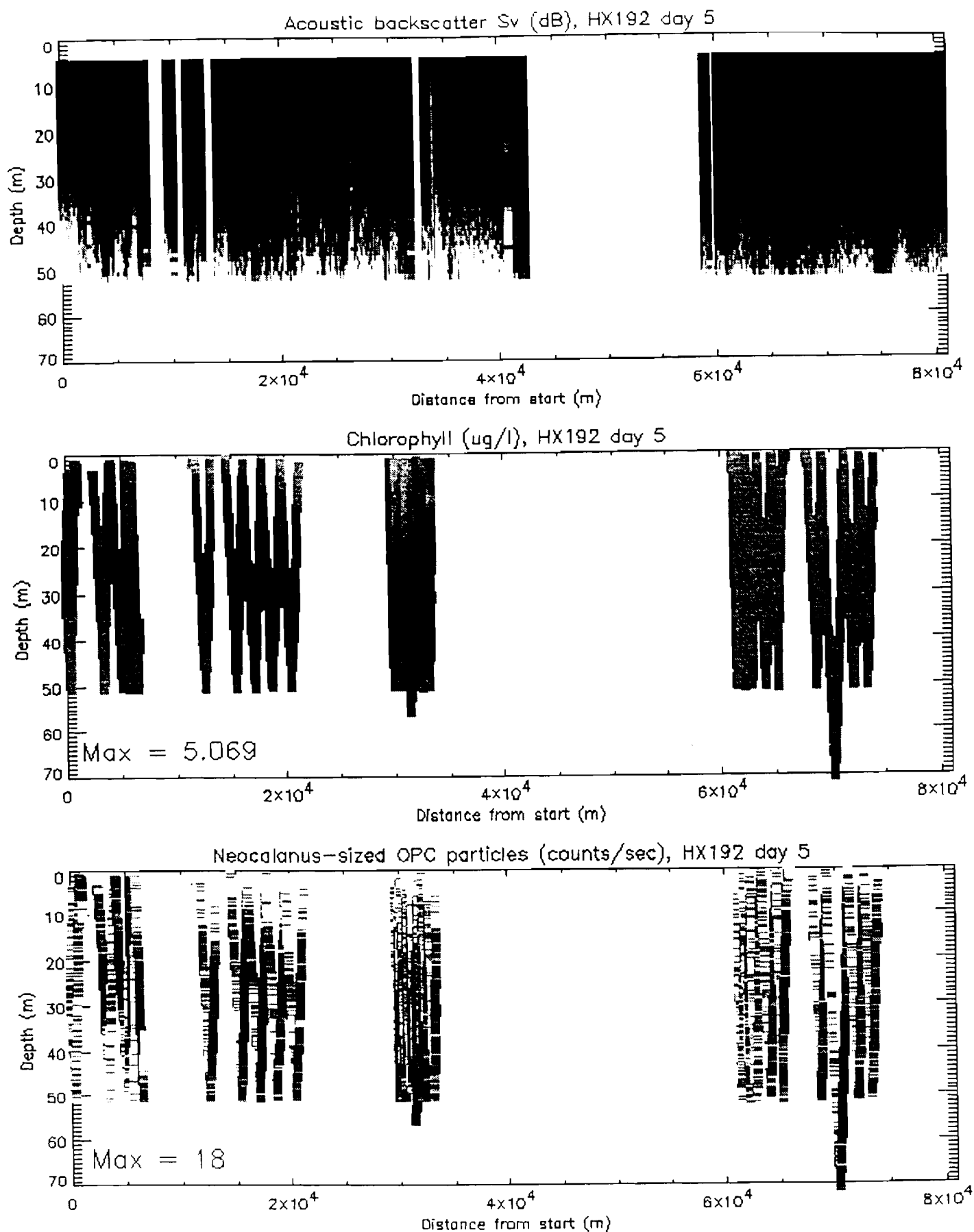


Figure 5. Montague Strait plankton distributions, May 1996.

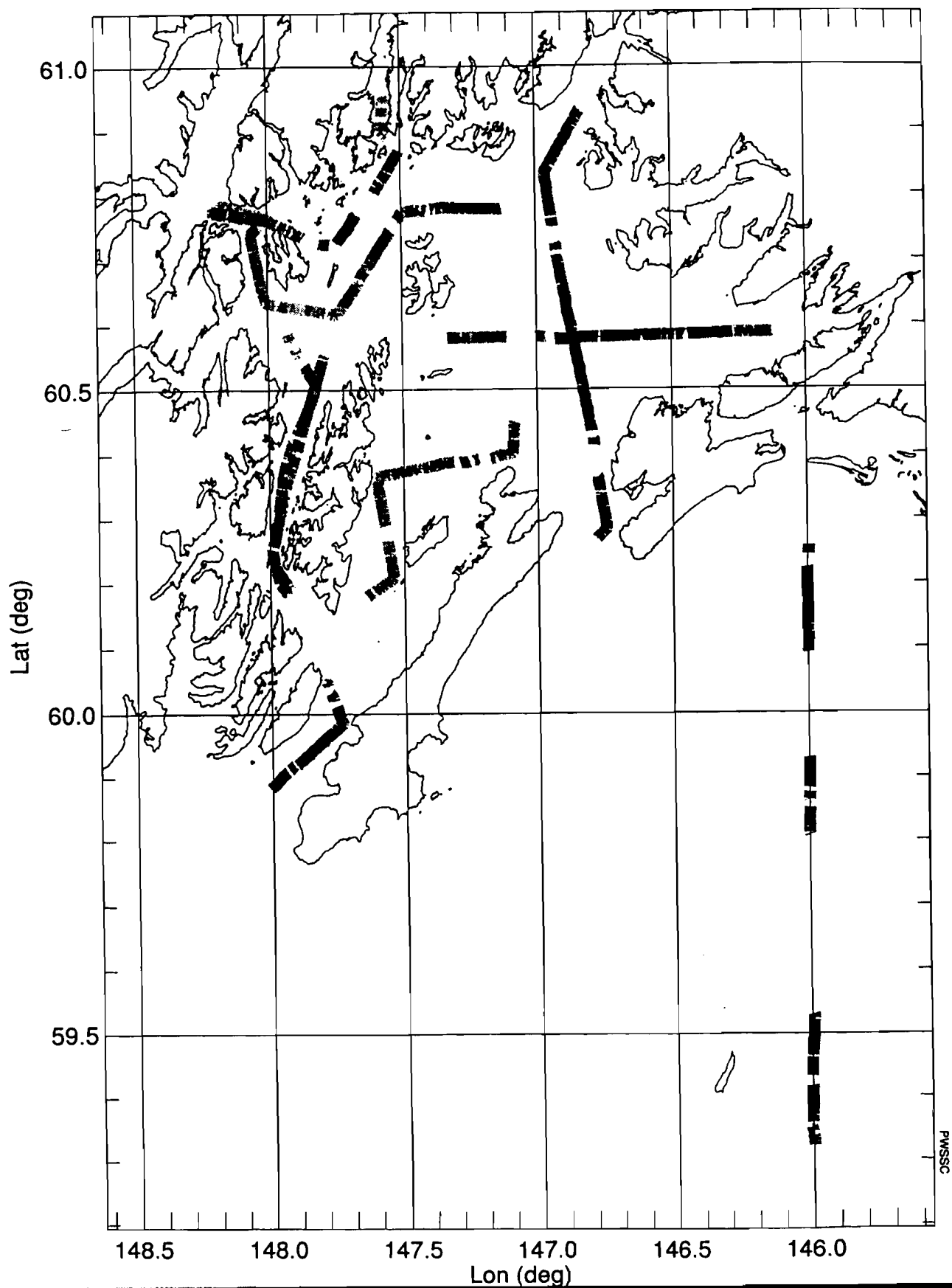


Figure 6, Geographical distribution of acoustic backscatter, May 1996.

HX192 - Neocalanus 5 Biomass - 0-50m

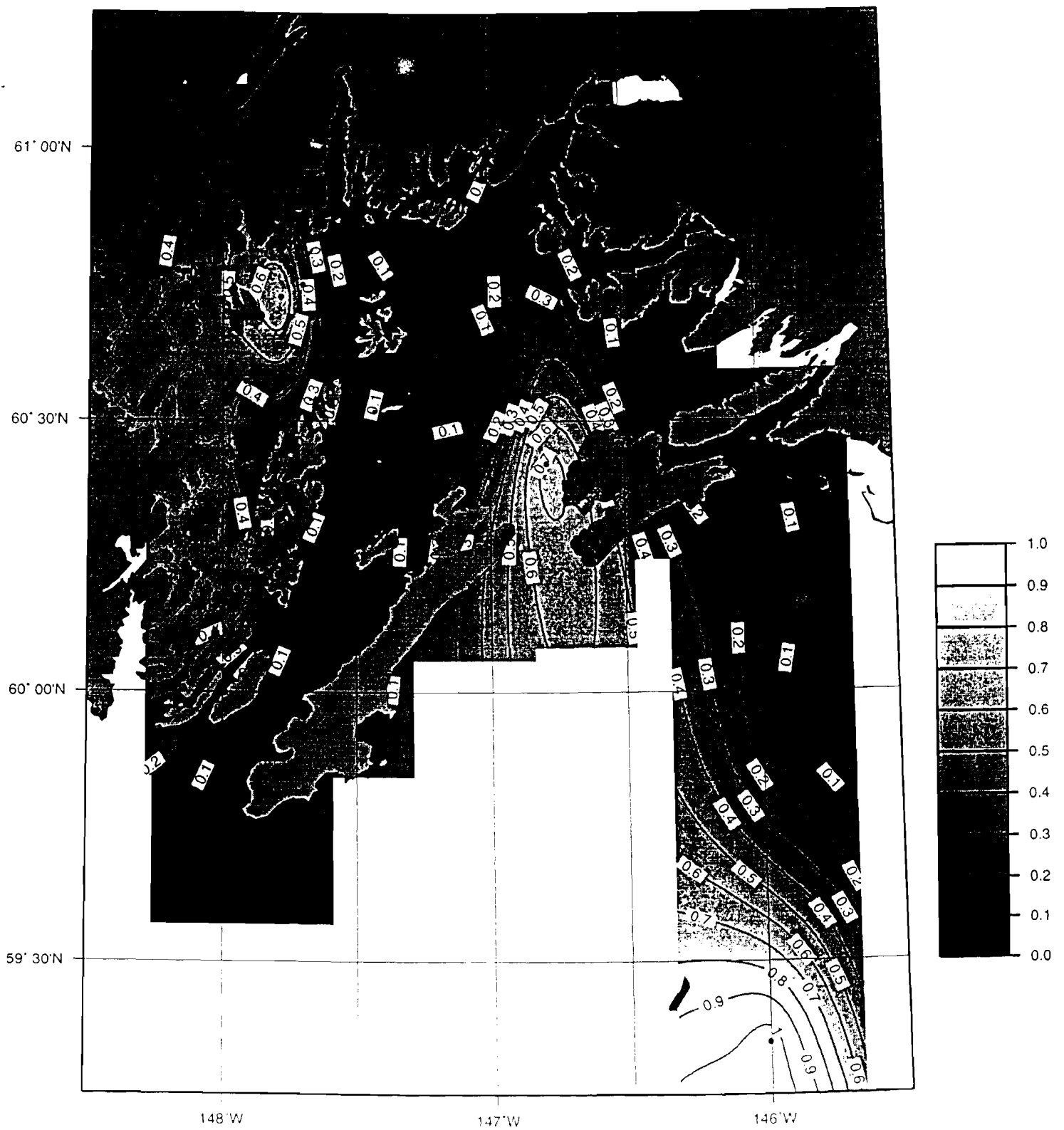


Figure 7. Neocalanus stage 5 biomass (g/m³), 1996

HX192 - Limacina Biomass - 0-50m

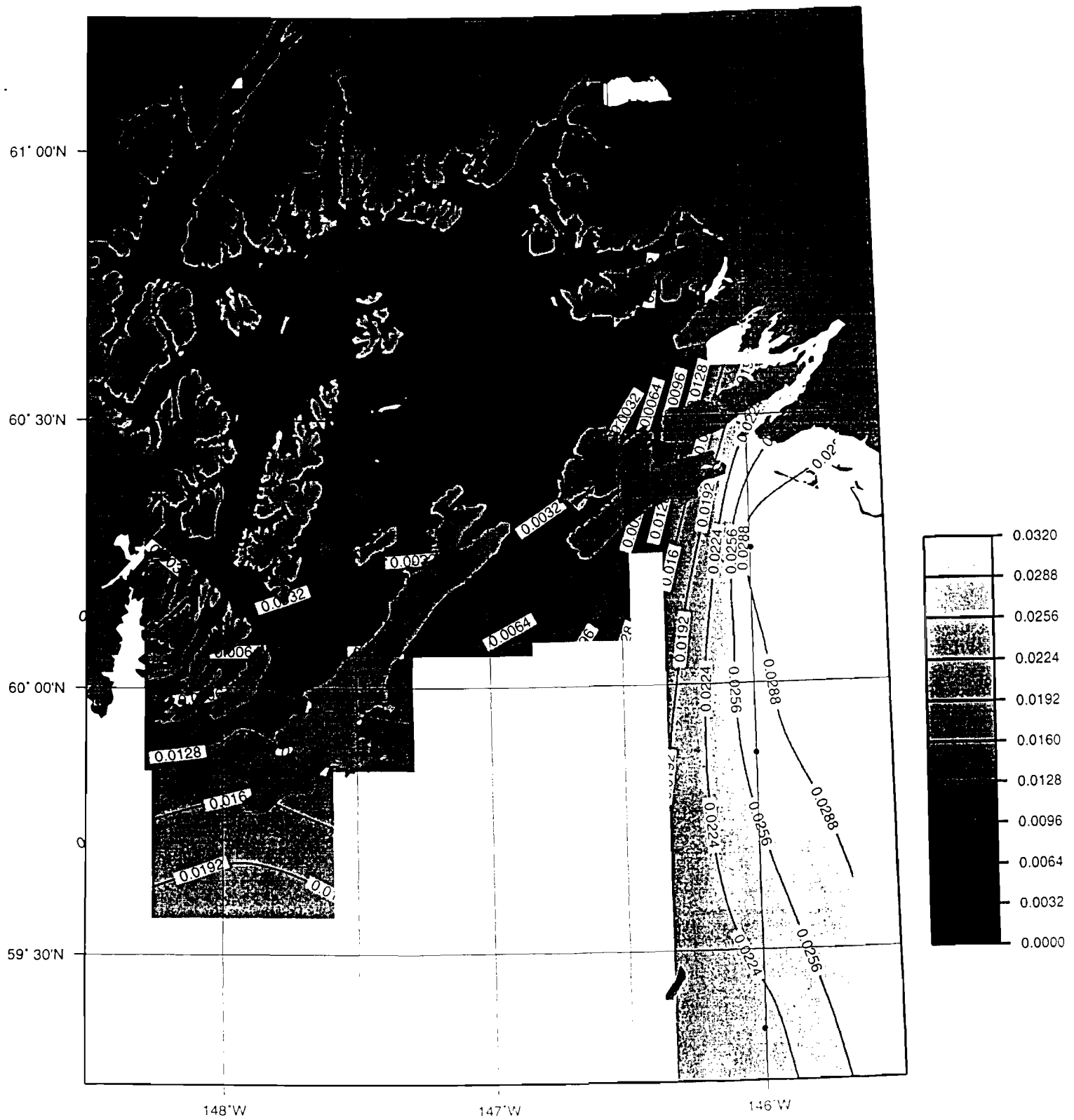


Figure 8. Limacina biomass (g/m³), 1996

HX192 - Euphausiid Biomass - 0-50m

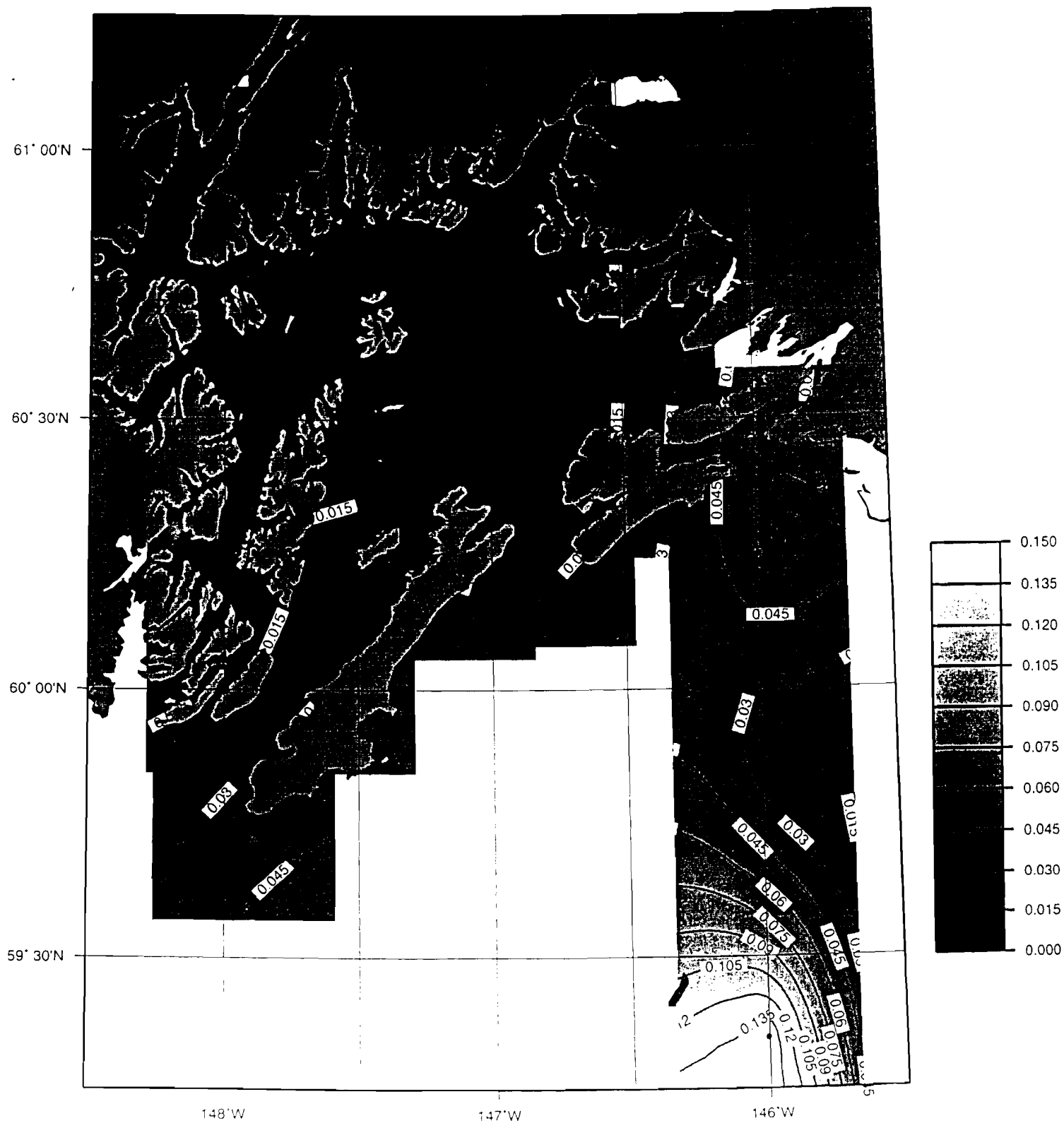


Figure 9. Euphausiid biomass (g/m³), 1996

HX192 - Neocalanus 4 Biomass - 0-50m

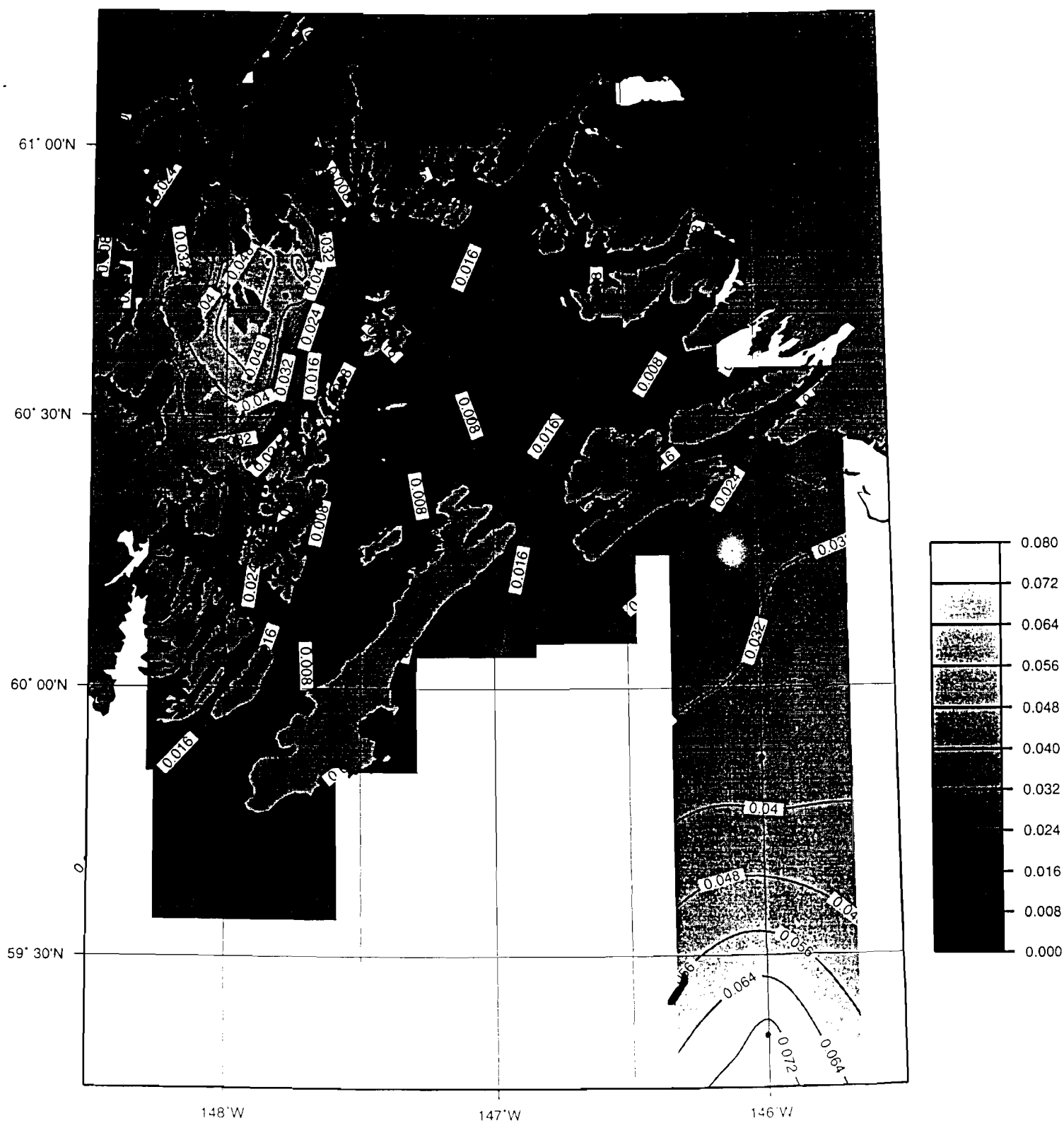


Figure 10. Neocalanus stage 4 biomass (g/m³), 1996

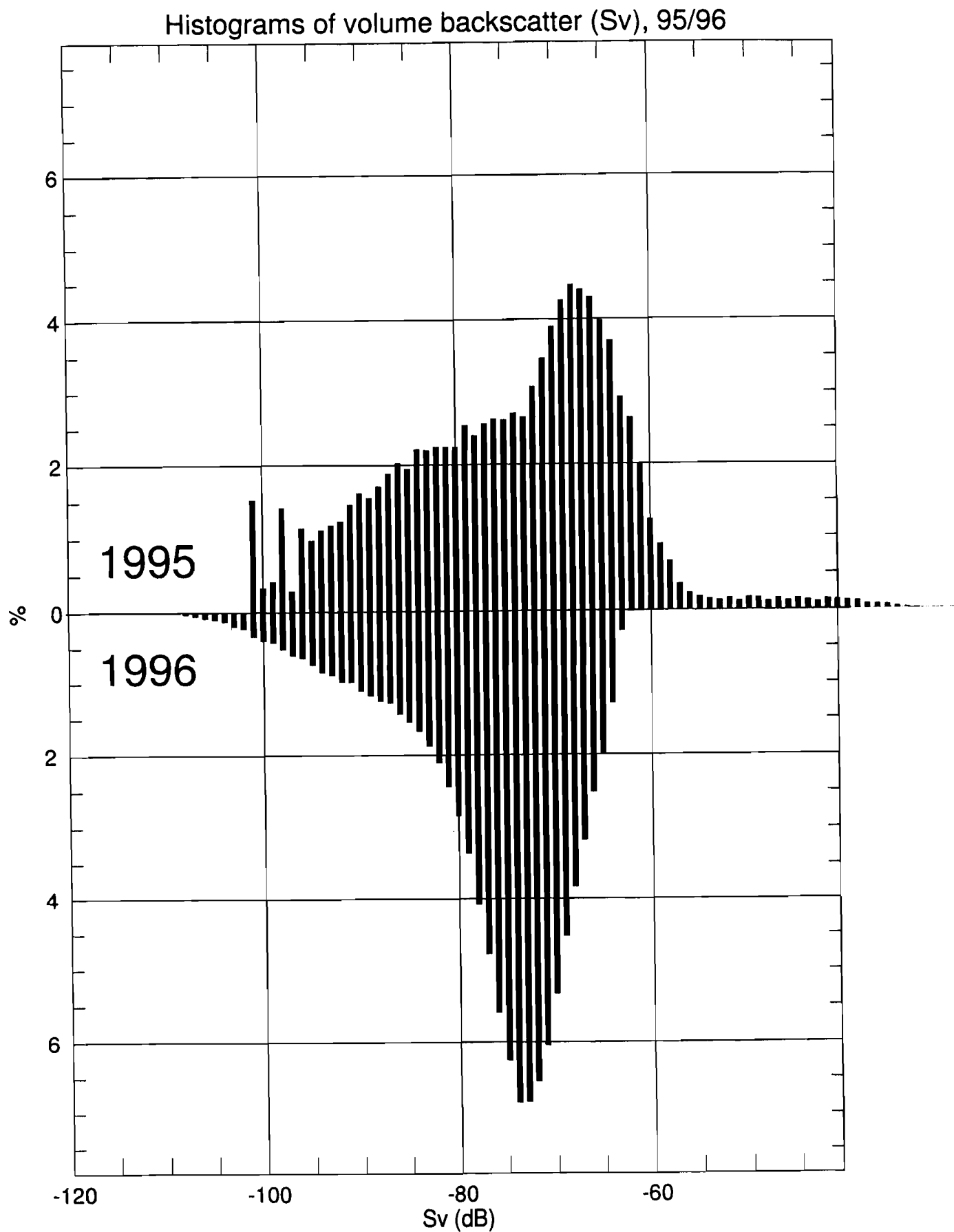
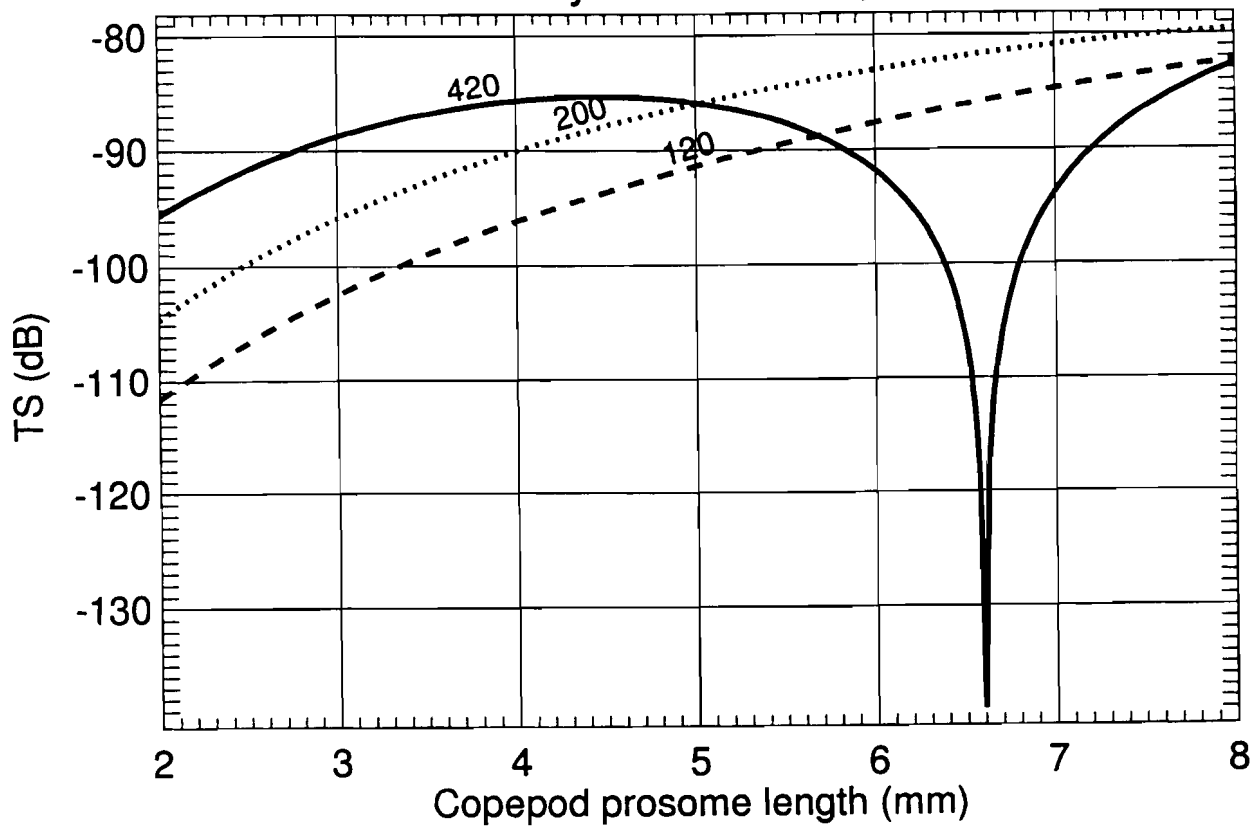


Figure 11. Comparison of volume backscatter, 1995 and 1996.

Frequency effects (Stanton, 1993)

Fluid bent cylinder model, $R = .058$



Elastic sphere model, $R=0.5$

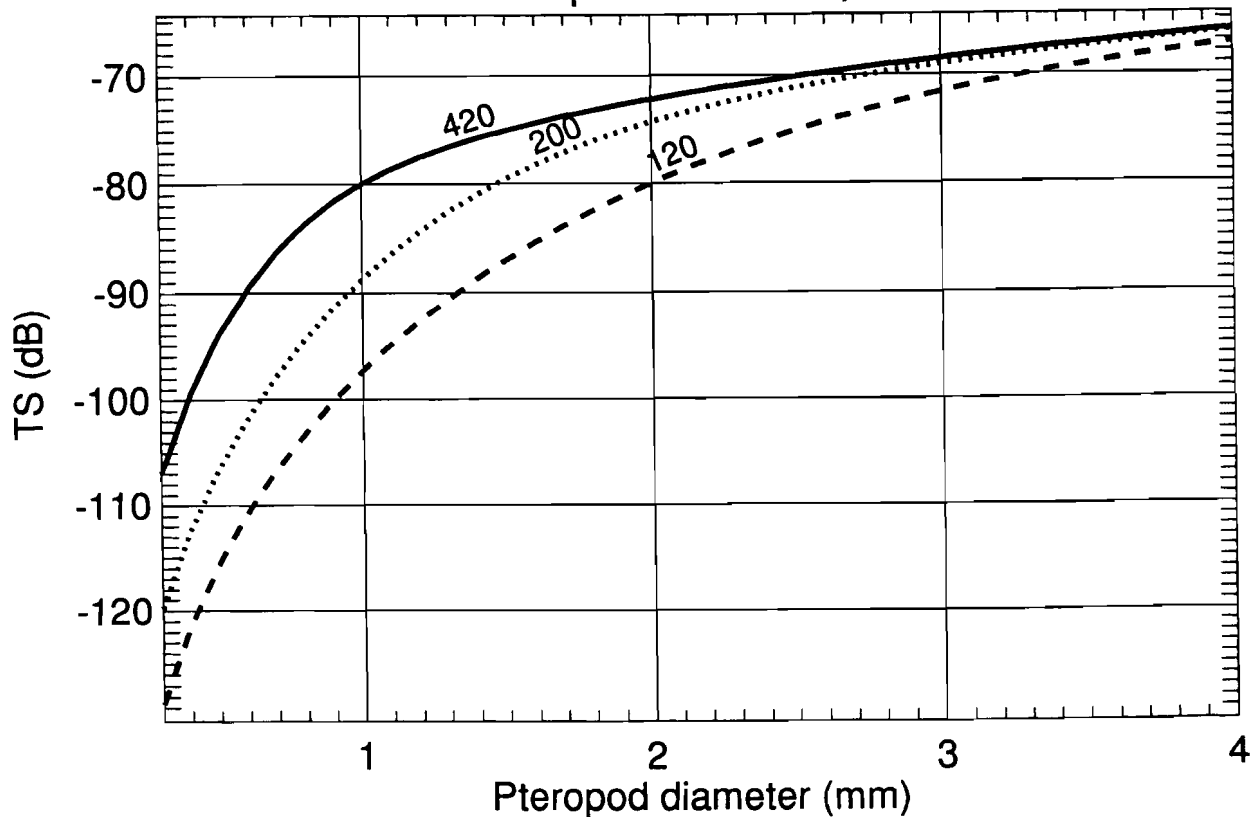


Figure 12. Comparison of frequency effects.

Effect of Aquashuttle pitch on OPC biomass estimate

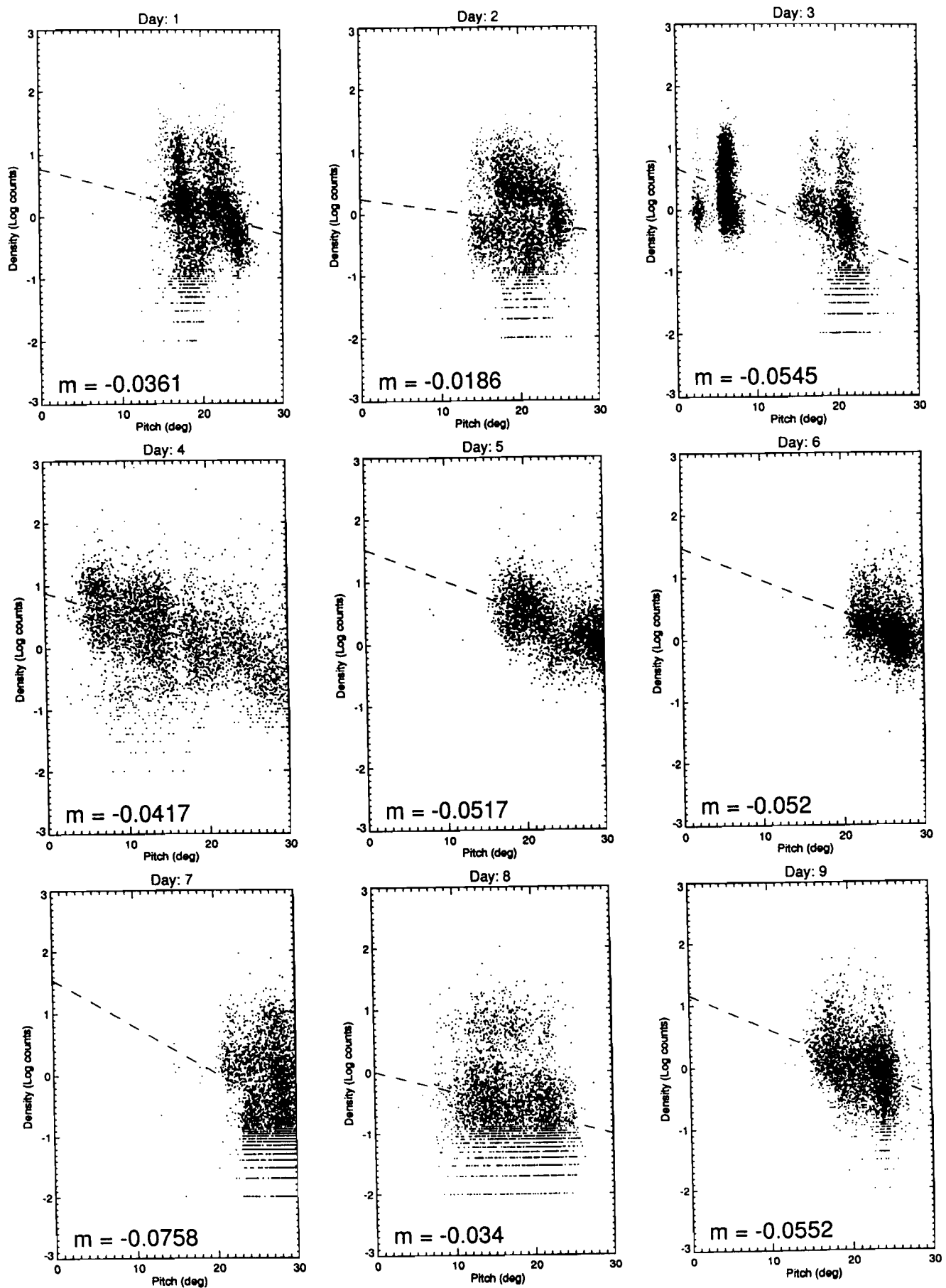


Figure 13. Comparison of Aquashuttle pitch and OPC counts density.

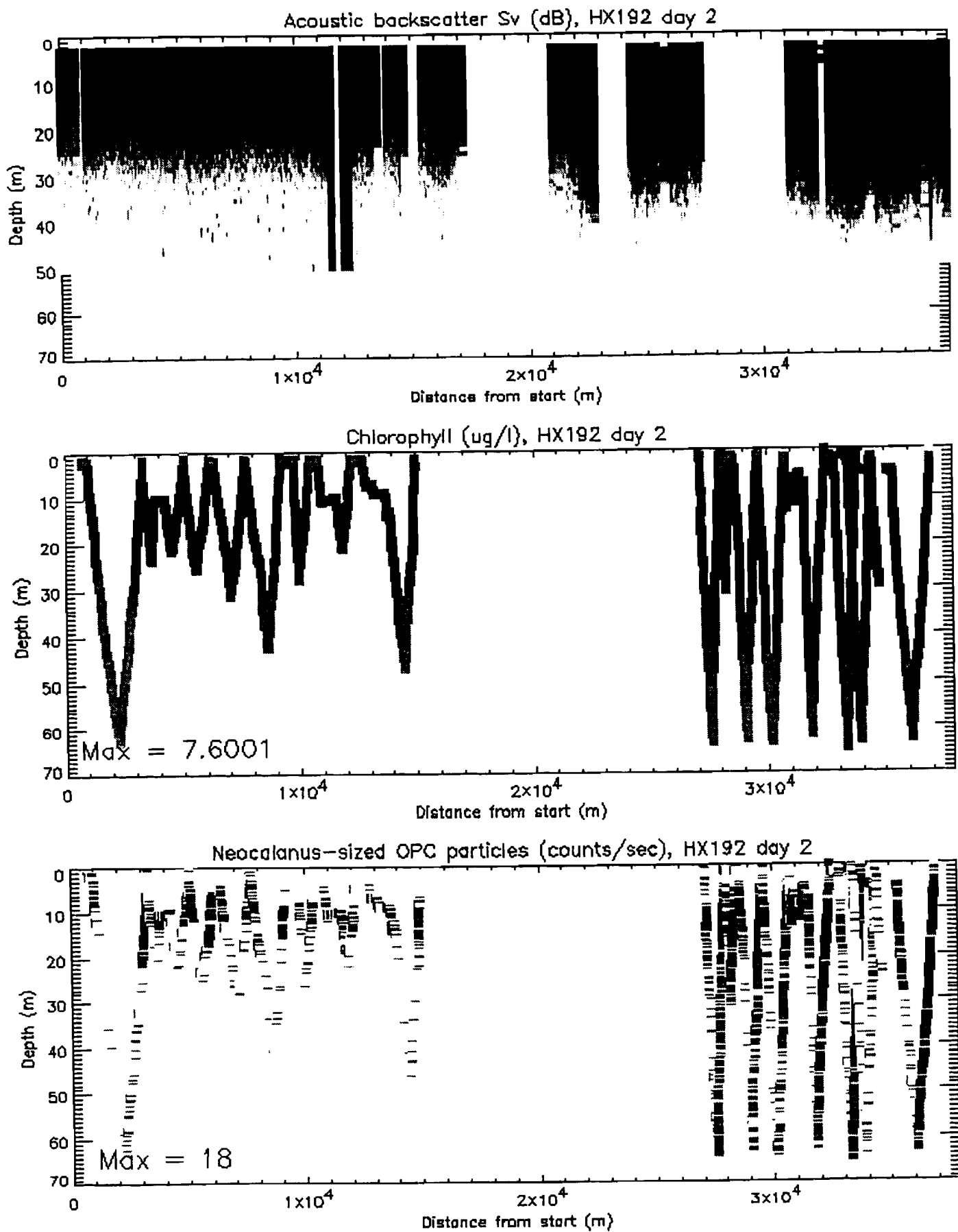


Figure A1. Wells Passage and Unakwik Inlet plankton distributions, day 2.

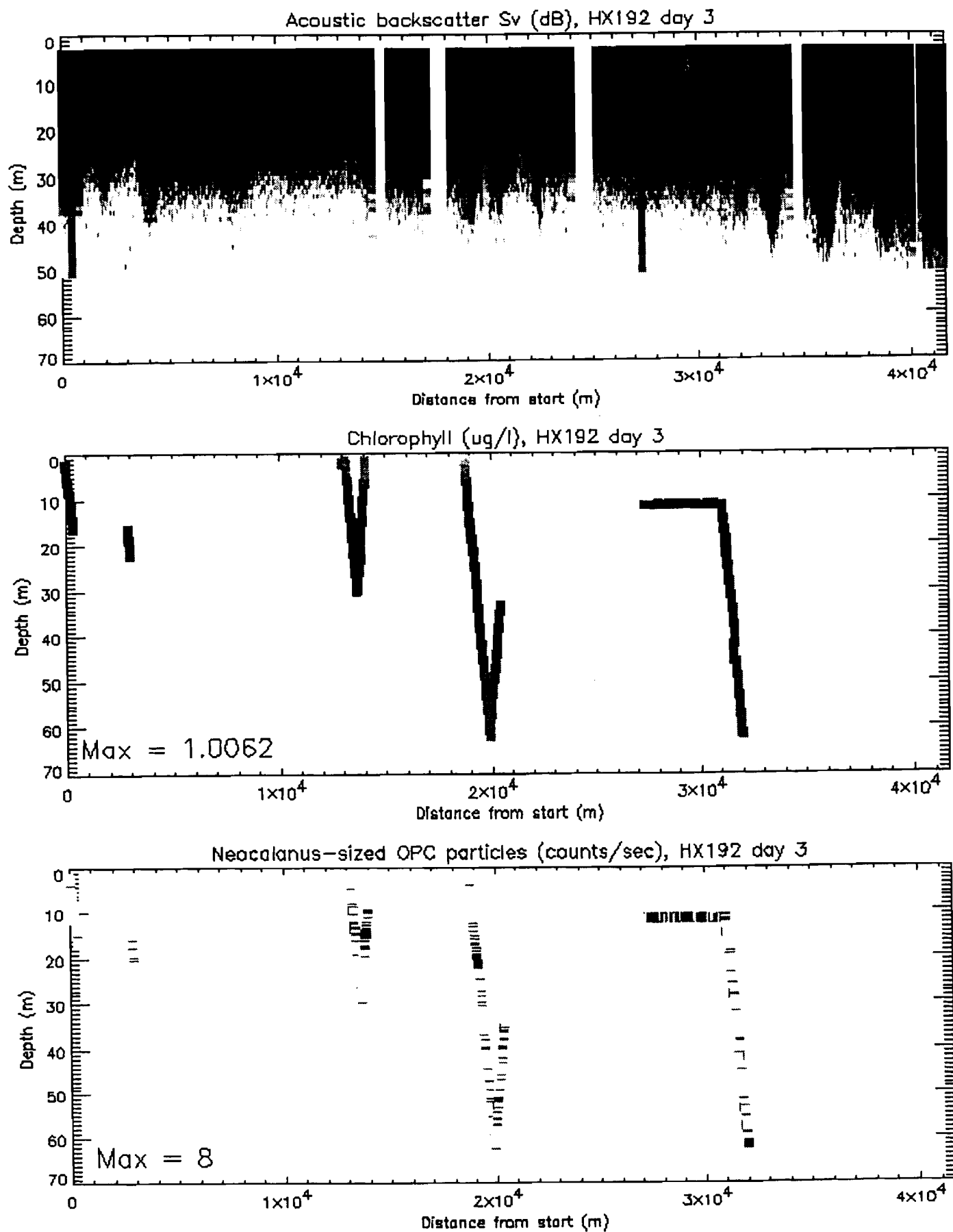


Figure A2. Knight Island Passage plankton distributions, day 3.

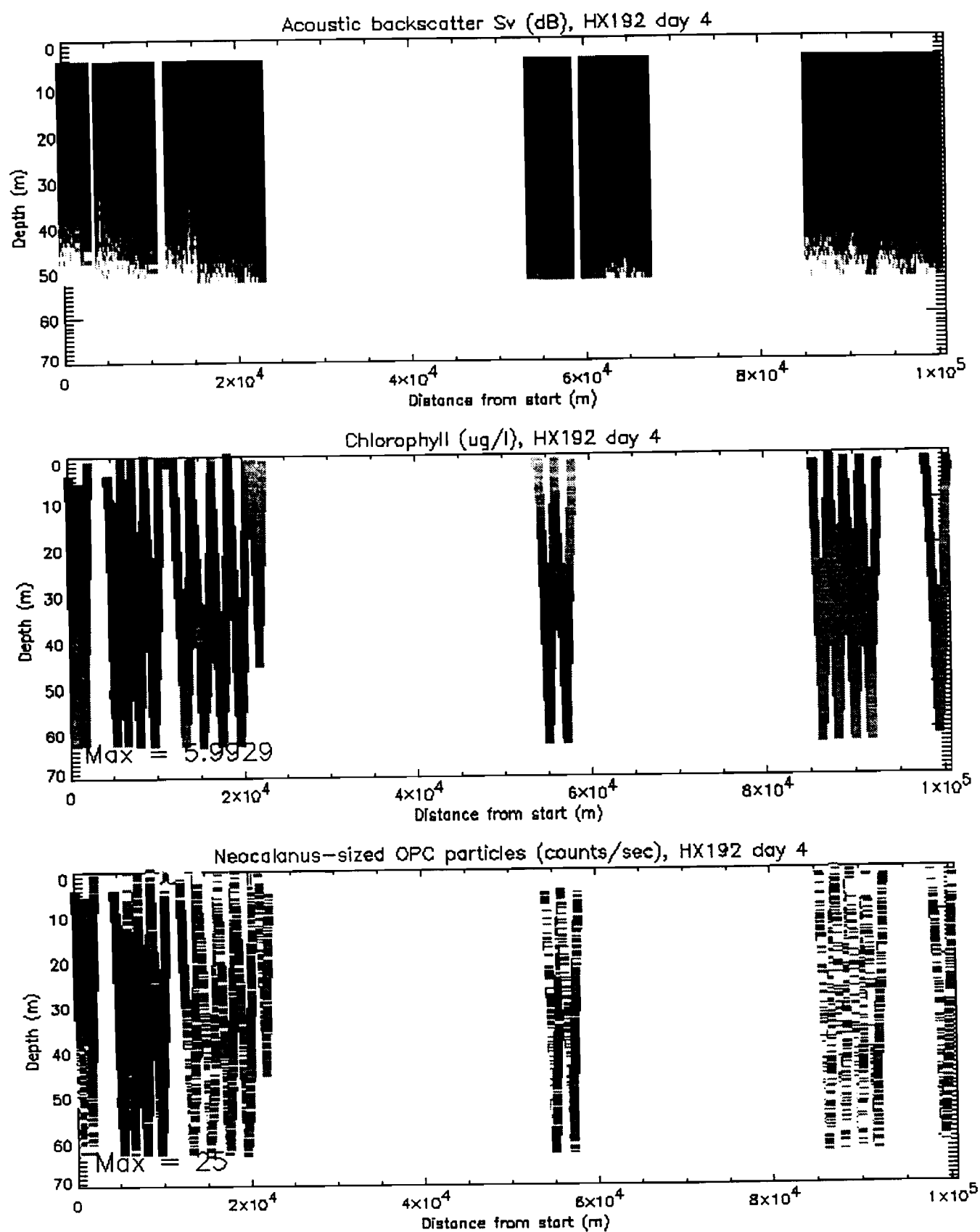


Figure A3. Gulf of Alaska plankton distributions, day 4.

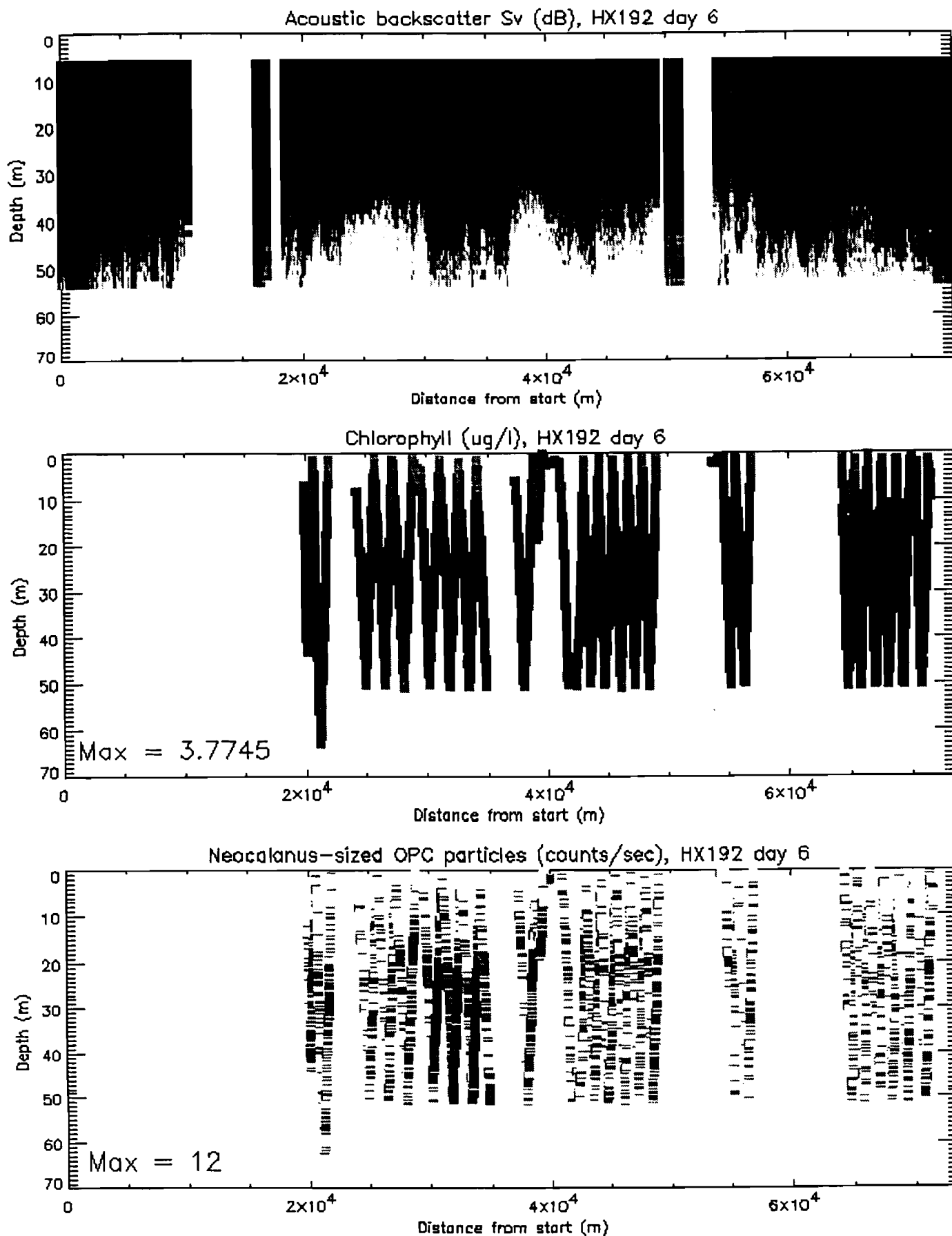


Figure A4. Hinchinbrook Entrance to Valdez Arm plankton distributions, day 6.

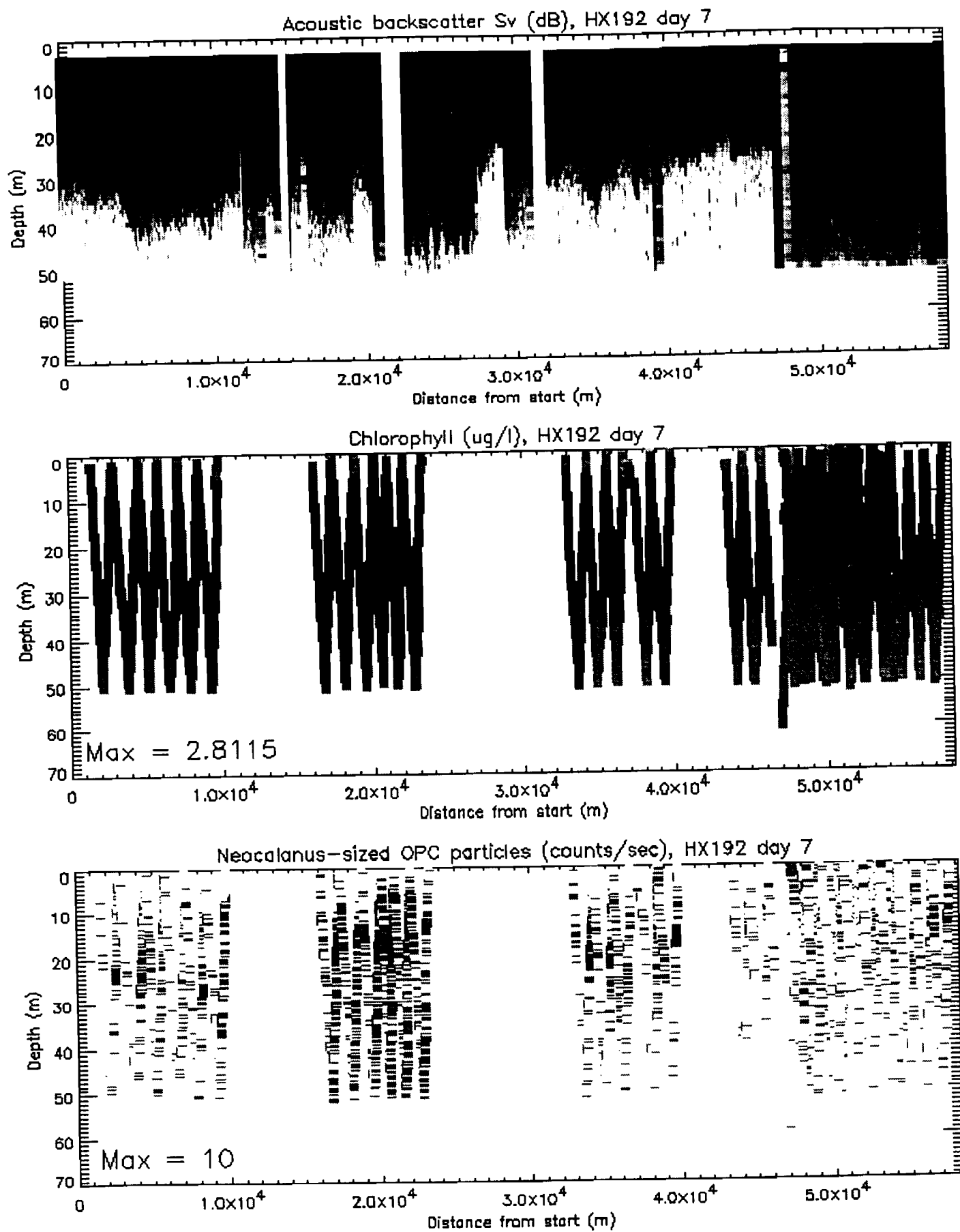


Figure A5. NW PWS plankton distributions, day 7.

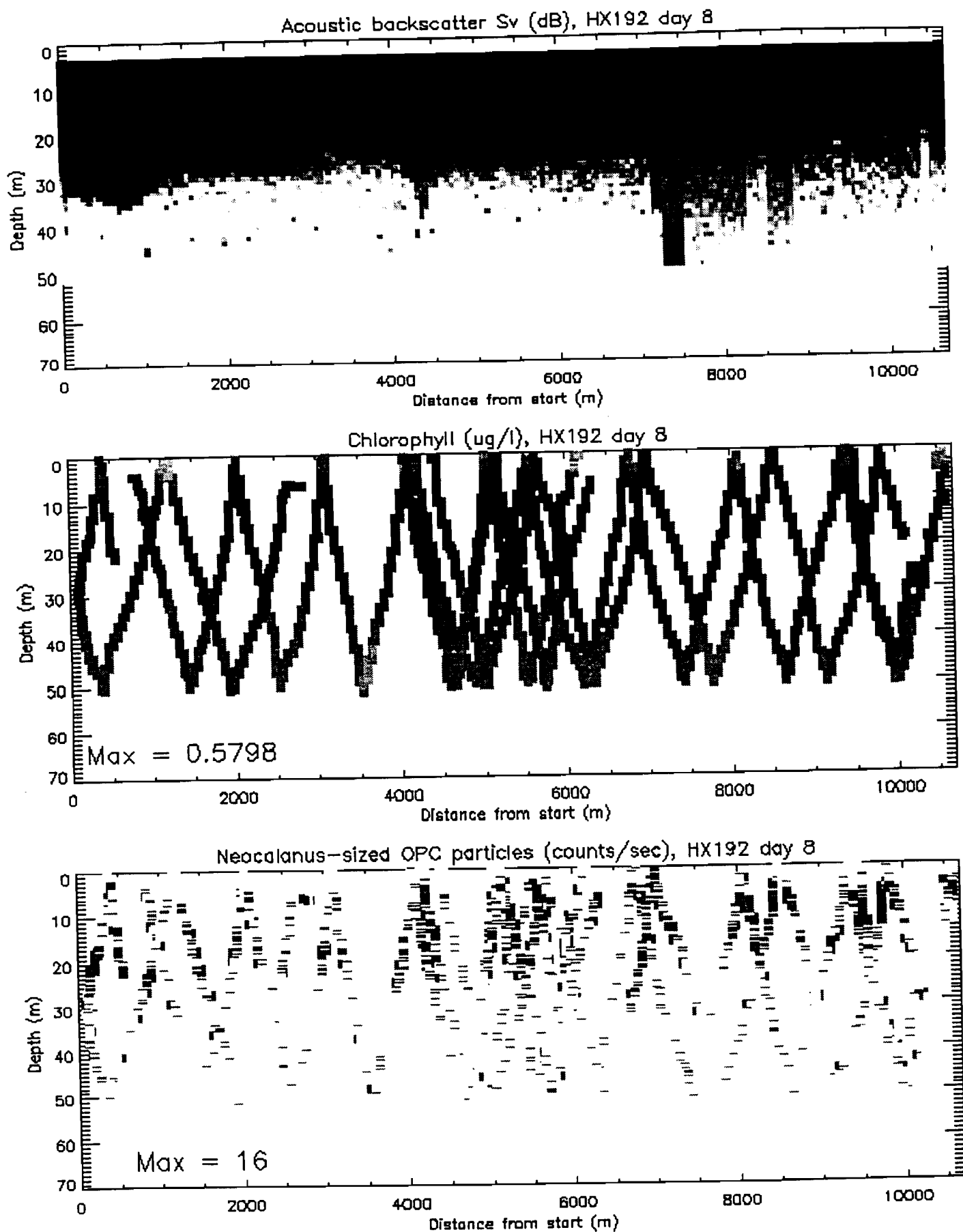


Figure A6. Wells Passage plankton distributions, day 8.

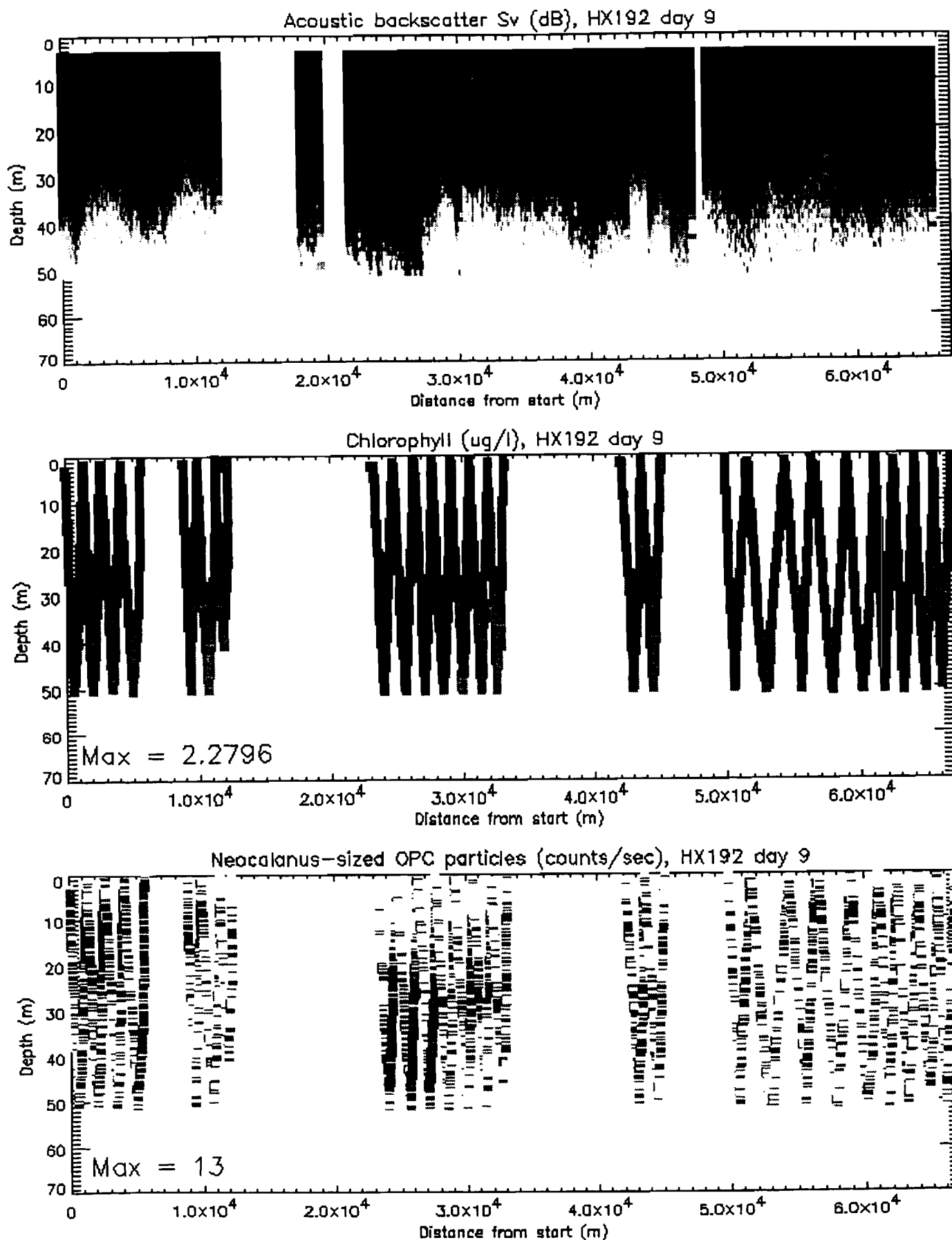


Figure A7. Naked Island to Orca Inlet plankton distributions, day 9.

CHAPTER 5

Preliminary acoustic measurements of juvenile Pacific herring (*Clupea pallasii*) and plankton in selected bays in Prince William Sound.

N. J. Peters, G. B. Steinhart, J. Kirsch, and G. L. Thomas.

ABSTRACT

Diel hydroacoustic surveys were conducted from June 1996 to August 1997 in Simpson, Zaikof, Whale and Eaglek bays, located in Prince William Sound, Alaska. Preliminary investigation of target strength (TS) information has detected seasonal variations in size classes, and vertical changes in distribution of fish and plankton. Seasonal fluctuations in the relative frequency of detected targets below -60 dB, indicating plankton sized targets, marked the spring bloom of plankton. In addition, seasonal shifts in TS range may be due to the influx and growth of new herring recruits. Diel changes in depth distribution showed that some fish may be undergoing daily vertical migrations. Further investigation of the acoustic and catch data sets will be needed to expand on the observed changes. Improvements in hydroacoustic equipment and subsequent data processing are discussed, with suggestions for further research.

INTRODUCTION

Pacific herring (*Clupea pallasii*) in Prince William Sound are important both biologically and commercially. The decrease in herring abundance after the 1989 Exxon Valdez oil spill has had wide reaching implications for the marine organisms depending of herring as a source of food, and for the fishing industry. There is little information available on the spatial distributions of the early life stages of herring, so it has been difficult to determine the cause of the decline, or to understand how the population is recovering. In order to facilitate the investigation into the juvenile herring abundance and distribution in Prince William Sound, four bays were selected for repeated acoustic and oceanographic surveys. The bays were selected as they are spatially segregated, have overwintering populations of herring, and evidence of spawning and recruitment. The data collected will be used in the overwintering survival model, summer habitat model, and for determination of a monitoring strategy.

A brief overview of new technologies and techniques in fisheries acoustics for species identification in multispecies environments. The methods discussed include changes in field data collection equipment, such as wideband sounders, to supplementary information, gathered by video cameras, and post processing techniques.

The data presented is a first look at the variation in the diel, seasonal and geographic distributions of nekton and plankton using target strength by depth and relative density. Since hydroacoustic sampling is nearly continuous, the utilization of target strength information

provides a better evaluation of spatial and temporal variation than net sampling. This paper presents the vertical and size structure of the fish and plankton assemblages seen in the four bays in Prince William Sound, along with the seasonal variations in the fish communities. Separation of the detected targets by depth and size, and the seasonal changes of this layering is evident. The seasonal aggregation of herring in the bays over the fall and winter periods is observed, with indication of acoustic discrimination of cohorts. Relative abundances between bays and seasonal changes in each bay are discussed.

METHODS

Four spatially separated bays in Prince William Sound were repeatedly sampled from June 1996 to August 1997. (Figure 1). The hydroacoustic information was collected using a 120 kHz BioSonic 101 echosounder. The transducer was mounted on a tow fin and towed at approximately 2.5 m/s, about 1 m below the ocean surface. The data was processed in real time with BioSonics ESP (echo signal processor) software. Echo-square integration, dual-beam target strength and concurrent GPS data were recorded. The raw acoustic signal was placed on Digital Audio Tape. Calibration of the transducer was performed using a standard target to obtain the source level and receive gain (Foote and MacLennan 1982). Equipment parameters were: source level = 255.023 dB; receiver gain = -159.28 dB; transducer directivity = 0.00107; pulse duration = 0.4 ms. The data was then archived and transferred to UNIX platforms for secondary processing.

Each Bay was hydroacoustically sampled three times in 24 hours. The dates of the survey were chosen to coincide with the new moon, reducing any light dependant behavioral pattern, (Luecke, C. and Wurtsbaugh, W. A. 1993). The three sampling periods began approximately at, 0800, 1600, and 0000, and lasted about four hours. The survey design called for parallel transects perpendicular to the shore separated by 1/4 Nm, connected by along-shore transects between. All surveys were marked on paper and/or electronic charts to allow repeated transects.

Net catch data was collected at each site. For each survey an anchovy seine (250 x 34 m and 20 m 25 mm stretch mesh) was deployed for target validation, length, weight, age analysis, and diet information. The location of the set was determined by the acoustic vessel, based on observed layers of targets. The seine vessel would also deploy a shallow fishing box trawl to capture small organisms. A mod-trawl was used to collect deep targets. (1.52 x 2.13 m Nor'Eastern Astoria V trawl doors, head rope 21.3 m, foot rope 29 m, estimated 3 x 20 m mouth, 10.2 cm mesh wings, 8.9 cm middle, and a 32.0 mm cod end liner). The location of the trawl set was determined by the acoustic vessel. In shallow water a 6 m skiff using a salmon fry seine (50 x 3 m, 3 mm stretch mesh) was used. The captured fish were sub-sampled into approximately 1000 individuals, then identified, these were then randomly sub-sampled and measured for length information. For the purposes of this paper related species were grouped together to aid in reading the graphs of net catches.

DATA PROCESSING

During post processing of the acoustic data, non-biological signals were removed. One common removed signals were surface bubbles: caused by either surface entrainment due to wave action, or by diving mammals and birds. We also removed bottom signals from the data. Loss of bottom tracking, where the ESP fails to recognize the floor signal return, will cause data corruption. This occurred in the presence of a dense schools near the bottom, and where the roll and pitch of the vessel caused the loss of the floor signal. Side lobe effects on sharply changes bathymetry can also reduce signal quality. Comparison of the electronic echo-grams with the paper echo-grams allowed the corrupted data to be removed manually.

Target validation was acquired for the acoustic data from the net catches. Species composition and length information were recorded. When geo-referenced with the acoustic survey, the relative acoustic backscatter for each caught species can be determined by use of target strength models and relative catch densities (see Thomas et al. 1996, for complete methods).

The target strength data were corrected for sampling effort and volumetric changes with depth due to the acoustic beam pattern. The volume V , is given by,

$$V = \frac{1}{12} \pi \phi^2 (r_2^3 - r_1^3) \quad (1)$$

where r_1 is the range to the top and r_2 the range to the bottom of the selected depth, and ϕ is the beamwidth in radians. The problem of coincident targets returning an increased signal was, in a first step, reduced by the removal of unrealistic TS values. The data were then binned into depth and target strength ranges producing a relative density of sampled targets over depth and TS value. Comparison with the net catch data which, where appropriate, were converted into target strength is included. The conversions used are, Thorne (1983), Eq. (2), for herring, and Traynor and Ehrenberg (1979), Eq. (3), for pollock (Figure 2). Here L_{cm} is the length of the appropriate fish species measured in centimeters.

$$TS \text{ re: } W = 6 \log_{10} L_{cm} - 24.2 \quad (2)$$

$$TS = 20 \log_{10} L_{cm} - 66 \quad (3)$$

The target strengths were calculated from the average lengths of the fish sampled. Also shown were the depths of catch and the estimated number for each species. There is no accounting for missed catches, or for the targeting of particular species, gear selectivity, or

any incurred bias in length measurements.

RESULTS

The data presented are an initial look at the target strength distributions within the water column of the four bays for the period of June 1996 to August 1997. All color scales are the same to allow for inter bay, and seasonal comparisons. However, the reported target strength distributions will have a bias towards higher values as the removal of coincident targets through extraction of unrealistic values is not a robust technique. Due to the duration of the surveys, about four hours per bay, the depth distribution of the detected targets may have changed over the sampling period. This may have lead to an increase in the depth range in which the targets are partitioned. The data were looked at in two ways: first each cruise was examined; then the inter-bay comparisons and the seasonal changes for a particular location are discussed.

June 1996

Simpson Bay

During the June 1996 Simpson Bay surveys, we saw numerous targets throughout the water column (Figure 3a, 3b). At 0800, there were many small targets (-70 to -58 dB) from 5 m to 40 m. In addition, there were two other distinct groups of targets: a peak centered at about -35 dB at 45 m, and a deep layer at 60 m, with two peaks at -30 and -55 dB. By the 1600 survey, there were fewer targets in the bay, but with a similar TS distribution as 0800. At night, however, there was a pronounced increase in the number of large targets (-44 dB found in the top 20 m. There was also an upward movement of large, deep targets from 100 m, at 0800, to 65 m at 0000. Net catches at this site were dominated by herring, which increased in size as the fishing depth increased (Figure 7).

Zaikof Bay

Zaikof Bay had fewer targets than Simpson, but had a large number of small (< -55 dB) targets in the top 40 m during all sample periods (Figure 4a, 4b). During the 0800 survey, there was a second peak of targets around -50 dB found at approximately 70 m. At midnight, there was a distinct increase and upward movement of large targets. This change was seen in the top 30 m, with increases of targets around -55 dB and -40 dB. In addition, there was a group of pollock-sized targets (-30 to -40 dB) at 80 m. The seines caught mostly herring, with larger fish caught at night than during the day (Figure 7). The trawls caught pollock, but in relatively low numbers except for the morning bottom trawl set.

Whale Bay

In June 1996, Whale Bay had few targets deep in the water, but many small and medium targets (-80 to -40 dB) were seen near the surface (Figure 5a, 5b). There was an increase in the number of medium and large-sized targets above 40 m during the 0000 sample period. Fewer adult herring were captured in the purse seine than in the other bays, but thousands of

young herring were captured near the surface in the fry seine (Figure 7).

Eaglek Bay

In Eaglek Bay, there was again a large concentration of targets near the surface (Figure 6a, 6b), but unlike the other bays, there were distinct TS modes of the surface targets. Two modes, one at -75 dB and one from -40 to -60 dB, were seen above 20 m during all sample periods. During the 0000 survey, there was a substantial increase in deep (40 to 100 m), large (-30 to -45 dB) targets. The purse seine caught numerous herring, and the deep trawls caught mostly pollock (Figure 7).

August 1996

Simpson Bay

During the day, there were far fewer targets seen than during the July cruise (Figure 3a, 3b). These targets were divided into two distinct groups: a shallow (< 30 m) group of small targets (< -60 dB), and a deep (50 m) layer of -30 to -45 dB targets. At night, however, there were many targets of all sizes throughout the top 80 m, plus additional targets to 120 m. The seines caught almost exclusively herring, again with the larger individuals found deeper than the smaller fish (Figure 8).

Zaikof Bay

The August data from Zaikof also show fewer targets than the July cruise, but with more distinct separation in distribution and TS (Figure 4a, 4b). The largest concentration of targets was in the top 40 m, and ranged from -55 to -80 dB. A second group of targets was seen at 40 m, and had a TS around -35 dB. At night, there were abundant targets from -30 to -80 dB in the top 40 m, again suggesting a vertical migration at night. Seine sets at this time caught adult herring and pollock in the top 20 m, while during the day, the seine caught herring and smelt (Figure 8).

Whale Bay

Whale Bay followed the same pattern as Simpson and Zaikof Bays: fewer targets than the previous cruise, with most targets found near the surface, and an increase in targets at night (Figure 5a, 5b). The targets tended to extend to deeper waters in Whale Bay than in the other bays. Daytime seine sets caught thousands of herring, while the night catches were dominated by pollock (Figure 8).

Eaglek Bay

Eaglek Bay had the fewest targets of the bays sampled during this cruise, but followed a similar diel pattern (Figure 6a, 6b). There were fewer targets greater than -40 dB detected in Eaglek Bay than in the other bays. Net catches were also lower in Eaglek than in the other bays, and were composed of mostly herring (Figure 8).

October 1996

Simpson Bay

In October, there were more targets than in August, and their numbers and distribution looked more comparable to June (Figure 3a, 3b). During these surveys, there was less separation among the peaks in TS: there were many targets of all sizes, at all but the deepest depths. There was a slight increase of TS with depth. During the morning, the seine caught all herring, while at 1600 and 0000, both pollock and herring were captured (Figure 9).

Zaikof Bay

The October data from Zaikof were almost identical to August, but with more large targets found deep at night (Figure 4a, 4b). The largest concentration of targets was again in the top 40 m. A second group of targets was seen at 40 m at 0800, 80 m at 1600, and from 40 to 100 m at 0000, the time when there were the most targets in the group. The TS of these targets ranged from -30 to -45 dB. The purse seine caught mostly herring, with larger fish caught at night (Figure 9). The mid-water trawl caught many pollock, but only at night.

Whale Bay

In Whale Bay, we saw fewer targets than in Simpson, but a similar amount to Zaikof (Figure 5a, 5b). During the day, there were many small targets (< -55 dB) extending from the surface to 80 m. This was a similar distribution of TS as we saw in August, however it extended deeper into the water column. Another difference was the increase in the number of deep targets at night. While this feature was common during most surveys, the increase was especially large during this cruise, and included targets from -25 to -60 dB. Net catches were also highest at night, with larger pollock caught from deep water and at night (Figure 9). Many herring were also caught by the seine at night, but few during the day.

Eaglek

Unlike the other bays, the number of targets in Eaglek was highest during the October cruise, although still lower than the other bays (Figure 6a, 6b). The distribution, however, was similar to Whale Bay in that there were many small targets (< -55 dB) extending from the surface to 80 m. There was a distinct group of targets around -45 dB seen at 20 m during the 1600 sampling. At night, there were more large (-30 to -55 dB) targets throughout the water column, but concentrated in the top 50 m. The purse seine caught numerous pollock and herring at 1600 and 0000, but little else (Figure 9).

March 1997

Simpson Bay

There were much fewer targets in Simpson Bay in March than during the previous three cruises, but still more targets than seen in the other bays (Figure 3a, 3b). There were two distinct modes of targets during these surveys: a mode seen at 0 to 40 m, and ranging from -60 to -60 dB; and a mode around -35 to -40 dB seen around 60 m. Although this second mode did not show a diel movement, the number of targets measured did increase

dramatically at night. The catch data generally agreed with the acoustic data: few fish were caught, except at night, when the purse seine caught mainly adult herring (Figure 10).

Zaikof Bay

There were relatively few targets detected in Zaikof Bay in March, 1997 (Figure 4a, 4b). This was especially true during the day, when only a few small (< -55 dB) targets were seen. At night, however, there was a high density of targets from -25 to -60 dB in the top 30 m. The purse seine caught adult herring near the surface at night, while the trawl only caught adult herring on the bottom during the day (Figure 10).

Whale Bay

Whale Bay had less targets detected in March 1997 than in any other month (Figure 5a, 5b). There were also fewer targets than the other bays, except Eaglek Bay. In daytime, the only TS mode was a small peak of targets less than -60 dB in the top 30 m. At night, there were small (-50 to -60 dB) targets to 50 m, and a second peak of -30 to -45 dB targets at 80 m. Net data were limited, but the bottom trawl caught pollock, herring and smelt (Figure 10).

Eaglek Bay

We found the fewest targets at any time, and in any bay, in Eaglek during March 1997 (Figure 6a, 6b). The targets were distributed in two distinct groups: a low TS surface group, and large (-30 to -45 dB) targets at 100 m. The bottom trawl caught adult herring, pollock, and flatfish during the day, but mostly flatfish at night (Figure 10).

May 1997

Simpson Bay

Simpson bay had fewer targets detected in May 1997 than during any other sampling (Figure 3a, 3b). The observed targets were primarily in the -25 to -25 dB range, and were found at 60 m during the day, but moved above 40 m at night. The number of small targets near the surface dramatically increased at night. During the day, the bottom trawl caught mainly herring, but at night, the highest catches were of herring in the purse seine (Figure 11).

Zaikof Bay

Like Simpson, there were few targets in Zaikof during this cruise (Figure 4a, 4b). During the day, there were some shallow small targets, plus a collection of -30 to -40 dB targets below 60 m. At night, these larger targets moved to the top 40 m, and the overall number of targets increased. A trawl at 100 m during the day caught a few adult herring and pollock, while the seine caught adult herring near the surface at night (Figure 11).

Whale Bay

Of the four bays, Whale Bay appeared to have the largest number of targets during this cruise (Figure 5a, 5b). The highest concentration of targets was above 30 m, and consisted of targets less than -55 dB. During the 0800 and 0000 surveys, there were also many large targets (-25 to -45 dB). At 0800, these large targets were found between 20 and 80 m, but at

night they were in two more distinct depths: 20 m, and 60 to 80 m. Like the other bays, daytime catches were highest in the bottom trawls and consisted of herring, pollock and flatfish (Figure 11). At night, the seine had high catches of herring and pollock.

Eaglek Bay

The TS distribution in Eaglek was similar to the other bays, but with more small targets near the surface, and fewer large (> -45 dB) targets (Figure 6a, 6b). There was a small peak of large targets at 60 m at night, but not many compared to the other bays. The nets caught mainly herring during both day and night, and caught a few pollock at night, by trawl (Figure 11).

July 1997

Simpson Bay

We found more targets in Simpson Bay in July than in March 1997 (Figure 3a, 3b). The biggest difference was the increase in small targets seen in the top 30 m. We also saw a diel increase in the number of large targets, which was similar to other cruises. During the day, small herring were captured in near the surface in the box trawl and fry seine (Figure 12). The large seine caught predominantly herring in the day, and pollock at night.

Zaikof Bay.

There were more small targets in Zaikof Bay in July than in March 1997, but fewer targets than the summer of 1996 (Figure 4a, 4b). During the 0800 survey, not many targets were seen; however, by 0000, the top 40 m was filled with targets ranging from -30 to -80 dB. Net catches at this time were low, but some adult herring were caught in the seine and bottom trawls during daytime sampling (Figure 12).

Whale Bay

Whale Bay had fewer targets in July than in May, or during the previous year (Figure 5a, 5b). In addition, there was a larger range of target strengths (-45 to -80 dB) than during the previous two cruises. Once again, there was an increase in the number of detected targets at night, especially of targets greater than -50 dB. Net catches were highest at night, when the seine caught mostly juvenile pollock (Figure 12).

Eaglek Bay

The distribution of detected targets in Eaglek Bay was similar in May and June 1997; however, the TS range of the observed targets was slightly larger in June 1997 (Figure 6a, 6b). The diel pattern of higher numbers of large targets near the surface was again seen, although not at the same magnitude as the previous summer. During the day, many small herring were captured by seine and a few pollock were caught in the bottom trawl (Figure 12).

August 1997

Simpson Bay

The number of detected targets in Simpson Bay increased dramatically from July to August 1997 (Figure 3a, 3b). This increase was apparent in the breadth of TS values, and an increase in the depth of their distribution. At night, there were abundant targets ranging from -25 to -80 dB from the surface to 75 m. Net catches were high during these surveys, and were dominated by young herring, with a few adult pollock (Figure 13).

Zaikof Bay

Sampling in Zaikof was limited to just one survey (1600) in August 1998. The distribution and range of target strengths appeared similar to July 1997, with many small target in the top 20 m, plus a few large deep targets (Figure 4a, 4b). Catch data were also limited, but the trawl did catch pollock at 40 m depth (Figure 13).

Whale Bay

The number and distribution of targets in Whale Bay was different from July to August 1997, but August 1997 and August 1998 were similar (Figure 5a, 5b). There were again two groups of targets detected in Whale Bay. The shallow, small targets had a smaller range of TS than in July 1997, but extended deep to 60 m. as seen the previous August. There was also a much larger increase in the number of large targets detected at night in August than in July 1997. Net catches were primarily pollock in Whale Bay (Figure 13).

Eaglek Bay

We found an larger range of TS values for detected targets in August than in July 1997 in Eaglek Bay (Figure 6a, 6b). This was most dramatic at night above 30 m, where we found large numbers of targets ranging from -30 to -80 dB in August, compared to a range of -50 to -80 in July. There were also more large, deep targets in August than in July 1997. Overall, this pattern was similar to August 1996. The highest net catches were in the seines, and were composed of young herring (Figure 13).

DISCUSSION

Inter-Bay Comparison

In June 1996 all the bays displayed plankton sized surface targets throughout the sampling period, (Cooney et al. 1995). A large range of TS values were acquired indicating the presence of a number of size classes, this includes small and large fish sized targets. Simpson and Zaikof displayed the greatest relative number of targets, and also showed a separation of different layers and target values. The increase in detected targets at night is a consistent feature in all bays, and has been in other studies. (Luecke and Wurtsbaugh, 1993). Whale and Eaglek did not display the deep fish sized targets evident in Simpson and Zaikof. In August 1996, the daylight samples displayed a grouping of small surface targets, again

plankton sized. The midnight period, however, had an increase in all targets of all sizes. Whale and Eagleks' surface structure of depth distribution and target strength are markedly different than that of the other bays. Both display a narrower range of TS values, and a greater range of depth. This may be due to different zooplankton species.

In October 1996, all the bays had large numbers of surface scatters around the TS value for plankton and fish, and increased in the number deep large targets during the night sampling period. The distinctive small target structure in Whale and Eaglek. Is more pronounced in its difference as compared to Simpson and Zaikof. In March 1997, Simpson showed the surface structure found in the Whale and Eaglek bays. All bays are again consistent, showing a large reduction in the detected surface targets. The presence of fish sized targets is indicated in the bays. At night, in Simpson and Zaikof Bays, the fish sized targets are found in two distinct layers, one at depth around 60 m, the other in the surface waters. This may be due to vertical migration for foraging. In May 1997, Simpson and Zaikof had relatively low surface scattering, whereas Whale and Eaglek had an increase in the plankton sized targets near the surface. All bays but Eaglek had large deep fish sized targets evident at night. In July 1997, the small surface targets were again in increased evidence in all the bays. Simpson and Zaikof also showed an increase in the deeper fish sized targets, as did Whale. Eaglek, however, had very few detected deep targets of that size range. In August 1997, the surface targets were numerous and evident throughout the sampling periods, for all the bays. Whale and Eaglek had the distinctive small target structure, Whale having the more pronounced narrow TS values and corresponding large depth range, and also showed larger targets deeper in the water column.

Seasonal Changes

A major feature evident was the consistency between the bays in the relative abundances of the targets. This is illustrated by the dramatic reduction in small surface plankton sized targets found in the March cruise, and the trends of increasing abundances in similar TS ranges that the bays follow throughout the year. This reduction in plankton sized targets over the winter may be due in part to the climatic conditions and predatory action. However, the five month hiatus of sampling means that the date of the reduction in detected surface targets of this size cannot be accurately determined. The observed increase in the target strengths could be attributed to increases in the length structure of the observed targets, and with further analysis this could yield information on the age structure throughout the sampling periods, thus identifying cohorts and following the changes in the population structure. The increase observed in all the bays of the small plankton sized targets could be indicative of the March plankton bloom. The delayed signature is due to the small initial size of plankton targets and to the frequency used in the surveys. As mentioned previously, the plankton sized surface targets found in Whale and Eaglek, have, throughout the year, a different vertical and horizontal structure which is appeared by August. The comparison of the observed acoustic changes in the plankton sized targets to the plankton net information, showing species break up, is ongoing.

All four bays displayed a strong seasonal change, Eaglek, however, had relatively the lowest abundance, with Simpson showing regularly relatively higher abundances. The increase in TS spread seen in all the bays after March could be attributed to length changes of the local fish populations. This increase continues throughout the year, culminating with August 1997. There is good similarity between the two surveys conducted in August 1996 and August 1997. The same relative larger abundances than in other months, and the comparison of the TS to depth distribution structure show a greater fidelity for the individual bays than in comparison to the other bays. This indicates a cyclic fluctuation in the fish populations.

There are numerous instances of the detected fish sized targets separating into distinct layers. There has been some preliminary indication these distributions are being influenced by the physical water mass properties, (unpublished data, Peters and Gay). The comparisons of the acoustic data with the oceanographic will lead into new insights on the distributions of both the juvenile and adult herring.

Although acoustics are the best source of information as yet available for fisheries management of populations, some of the sources of error can be dramatically reduced by the amalgamation of other investigative data sets. For instance the species and size make up of the acoustic targets can be found with net sampling. Nets, however, are selective, and will cause biases in the delivered data. In areas where the fish are separated enough that the frequency of coincident targets is small the target strength information can be used to described the size classes of the observed targets with a fair degree of accuracy. However, as the density of the aggregation increases, the rate of coincident targets also increases, and, as these are rejected by the target discriminator, the quality of the information as representative of the fish assemblage decreases.

Use of underwater cameras can provide species identification, and the ability to measure size of the target can give length comparison. Use of historic data in the form of long term monitoring of the same area will give a greater certainty to the identity of the acoustic signal. Knowing behavioral patterns, seasonal fluctuations and aggregations for the target species, can greatly enhance the ability of hydroacoustic surveys to accurately measure the fish biomass.

The uncertainty in the data interpretation is compounded in multi-species environments. Concentrations of fish can include more than one species and age class. If the size classes overlap in TS, acoustical separation of the species is extremely difficult or impossible. Hydroacoustics are virtually always used in conjunction with a type of capture technique. When dealing with the multispecies layering this becomes a vital source of additional information. It is, however, not always necessary to specifically identify the individuals in the acoustic return. Using the net catches to evaluate the amount of acoustic return that can be attributed to each species, allows the biomass composition to be determined (Thomas et al. 1996).

It is possible to augment the information collected by the acoustics with the use of video cameras. Gledhill et. al. (1996), showed that the differences in the sampling abilities of the

instruments can lead to large differences in the resulting abundance of fish species. For example the acoustic estimates of the near bottom species were lower than the video estimates. Whereas the increased sampling volume of acoustics estimated larger abundances of off bottom species. A highlighted difference was in the species identification: video yields precise information on the species, while acoustics produces initially no species specific information.

New techniques that are being implemented include the use of multi frequency and wideband acoustic surveys. Concurrently operating two or more transducers of different frequencies, affords measurement of the size of the gas bladder, due to the difference in frequency response this information can be used to discriminate between species. Wideband sounders are the next logical step in this area. They operate over a continuous frequency range. The returned frequency spectra is then analyzed. Species identification of the wideband signal has been shown to present recognition rates of 95%, Simmons et. al. (1996). Data were processed in eight continuous frequency bands from 27 kHz to 54 kHz, yielding the frequency spectra. Further analysis obtained a mean frequency spectra independent of absolute backscatter. Through the use of neural networks and discriminant analysis the aforementioned recognition rate was obtained. Zakharia et. al. (1996), also utilized a wideband system. Here the methodology of data processing was based on the frequency signature of the individual fish. Use of neural networks on the parameterized power spectrum, a standard technique in signal processing where resonant features occur, produced a classification success rate of 75%.

The two wideband analysis mentioned are independent of the physical surroundings of the fish; however, use of the physical characteristics can also be used to identify fish species. School shape and/or proximity to bathymetric features, has been used to successfully identify fish species. In Richards et. al. (1991), a technique discriminating between bottom habitats to characterize fish schools was implemented. Using such parameters as time of day, mean volume density, dispersion and mean bottom distance of the biomass, with subsequent nearest neighbor analysis on these features produced a 97% success rate.

Due to the constraints of time and survey design the data collected from acoustic transects tended to be separated in spatial measurements over distance. This coupled with the aggregations of the target species led to a few high density estimates with a larger number of low density measurements. If the fish are known to aggregations at certain times of the year, and it can be reasonably assumed that a large percentage of the population, for an area, is contained in these schools, then repeated acoustic surveys, can be used to accurately measure the relative biomass of the target species, when coupled with net catch information.

ONGOING RESEARCH

The preliminary look at this data shows promise in identifying age classes and the continual identification of the cohorts throughout the season. However, much work needs to be done

correcting for net biases, and on the post processing of acoustic target strength information. A more exacting methodology of removing the multiple returns on a single fish needs to be investigated, and the physical and positional changes of the fish targets resulting in changes of target strength of the individual warrant further evaluation. The target discriminator, which analysis the raw acoustic signal, needs improvement. Presently there is no information recorded on the coincident signals which are rejected. The improvement of the signal processing will lead to the ability to acoustically measure the size difference in high fish densities will allow the cohorts of the fish population to accurately determined.

The reported data highlights the complicated and highly dynamic nature of the environment. With only one year of this type of information (repeated acoustic and net sampling) it is hard to speculate on the relative importance of each bay, as this may very well change per season. It could be seen, however, that these areas were used for rearing of the juvenile herring. The overwintering populations of fish having been shown, in these areas, to be consisted of almost entirely of herring, the regular influx of larger fish, manifested in increased targets and TS and in net data, lends itself to the idea that, at least for the bays sampled, they have a returning spawning biomass.

ACKNOWLEDGMENTS

We would like to thank all the captains and crews of the fishing and research vessels in the collection of the data. Kevin Stokesbury who conceived the diel study. We would also like to thank the University of Alaska Fairbanks and the Alaskan Department of Fish and Game, as they were responsible for analyzing the net catch data. This work is funded by the Exxon Valdez Oil Spill Trustee Council.

FIGURE CAPTIONS

- Figure 1. Location of the four bays. Clockwise from top, Prince William Sound, Alaska. Eaglek, Simpson, Zaikof, Whale Bays.
- Figure 2. Variation of calculated target strength with length.
- Figure 3a. Relative frequency of detected acoustic targets by TS and depth. Simpson Bay June 1996 to March 1997.
- Figure 3b. Relative frequency of detected acoustic targets by TS and depth. Simpson Bay May 1997 to Aug 1997.
- Figure 4a. Relative frequency of detected acoustic targets by TS and depth. Zaikof Bay June 1996 to March 1997.
- Figure 4b. Relative frequency of detected acoustic targets by TS and depth. Zaikof Bay May 1997 to Aug 1997.
- Figure 5a. Relative frequency of detected acoustic targets by TS and depth. Whale Bay June 1996 to March 1997.
- Figure 5b. Relative frequency of detected acoustic targets by TS and depth. Whale Bay May 1997 to Aug 1997.
- Figure 6a. Relative frequency of detected acoustic targets by TS and depth. Eaglek Bay June 1996 to March 1997.
- Figure 6b. Relative frequency of detected acoustic targets by TS and depth. Eaglek Bay May 1997 to Aug 1997.
- Figure 7. Net catch data for Simpson, Zaikof, Whale, and Eaglek Bays. June 1996.
- Figure 8. Net catch data for Simpson, Zaikof, Whale, and Eaglek Bays. August 1996.
- Figure 9. Net catch data for Simpson, Zaikof, Whale, and Eaglek Bays. October 1996.
- Figure 10. Net catch data for Simpson, Zaikof, Whale, and Eaglek Bays. March 1997.
- Figure 11. Net catch data for Simpson, Zaikof, Whale, and Eaglek Bays. May 1997.
- Figure 12. Net catch data for Simpson, Zaikof, Whale, and Eaglek Bays. July 1997.
- Figure 13. Net catch data for Simpson, Zaikof, Whale, and Eaglek Bays. August 1997.

REFERENCES

- Cooney, R. T. and K. O. Coyle. 1995 The role of zooplankton in the Prince William Sound Ecosystem. Exxon Valdez Oil Spill Restoration Project annual report. Restoration Project 95332-H.
- Gledhill, C. T., Lyczkowski-Shultz, J., Rademacher, K., Kargard, E., Crist, G., and Grace, M. A. 1996. Evaluation of video and acoustic index methods for assessing reef-fish populations. *ICES Journal of Marine Science*, 53:483:485.
- Luecke, C. and Wurtsbaugh, W. A. 1993. Effects of moonlight and daylight on hydroacoustic estimates of pelagic fish abundance. *Trans. Am. Fish. Soc.* 122:112-120
- Richards, L. J., R. Kieser, T. J. Mulligan, and J. R. Candy. 1991. Classification of fish assemblages based on echo integration surveys. *Can. J. Fish. Aqua. Sc.* 48:1264-1272.
- Simmonds, E. J., Armstrong, F., and Copland, P. J. 1996. Species identification using wideband backscatter with neural network and discriminant analysis. *ICES Journal of Marine Science*, 53:189-195.
- Stokesbury, K. D. E., E. Brown, R. J. Foy, B. L. Norcross. 1996. Juvenile herring growth and habitats. Restoration project 95320T.
- Thomas, G. L., J. Kirsch, N. Peters. 1996 SEA: Acoustically determined juvenile herring distribution in Prince William Sound fall 1995. Nekton-plankton acoustics. 1996 Restoration Project 96320N.
- Thorne, R. E. 1983a. Assessment of population abundance by hydroacoustics. *Biol Oceanog* 2:253-262
- Thorne, R. E. 1983b. Hydroacoustics. In: Neilsen L. A., Johnson D. L., (ed) Fisheries techniques. *Am. Fish. Soc.*, Bethesda MD, p239-259.
- Traynor, J. J. and J. E. Ehrenberg. 1979. Evaluation of the dual-beam acoustic fish target strength method. *J. Fish. Res. Bd. Can.* 36: 1065-1071.
- Zakharia, M. E., Magand, F., Hetroit, F., and Diner, N. 1996. Wideband sounder for fish species identification at sea. *ICES Journal of Marine Science* 53:203-208

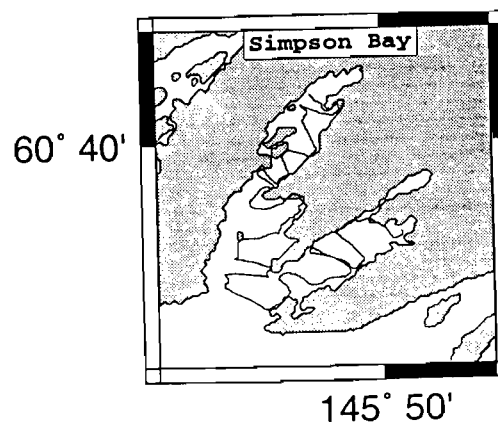
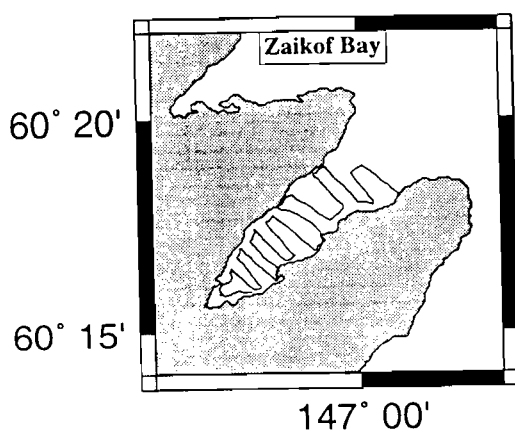
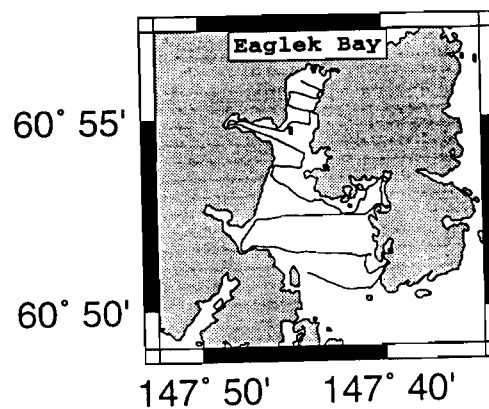
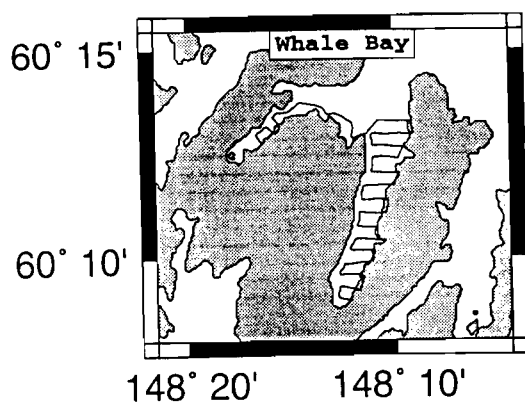
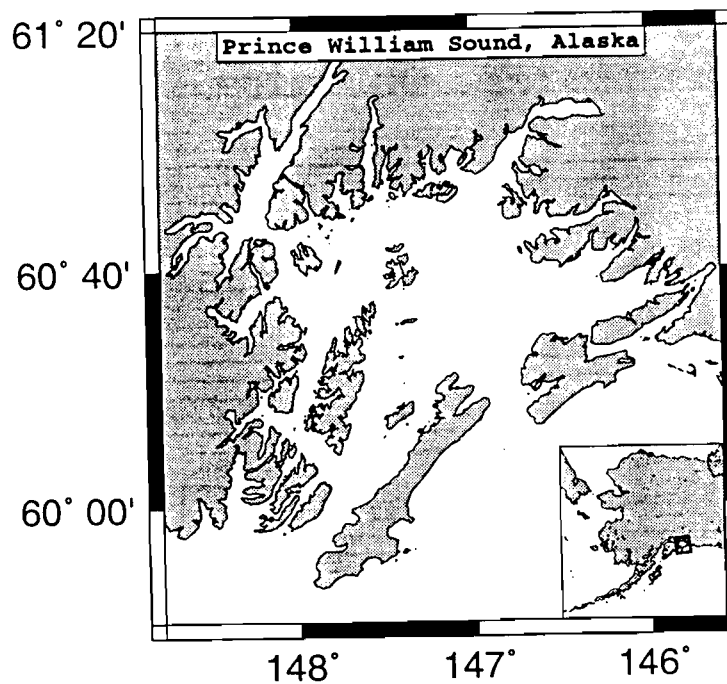


Figure 1.

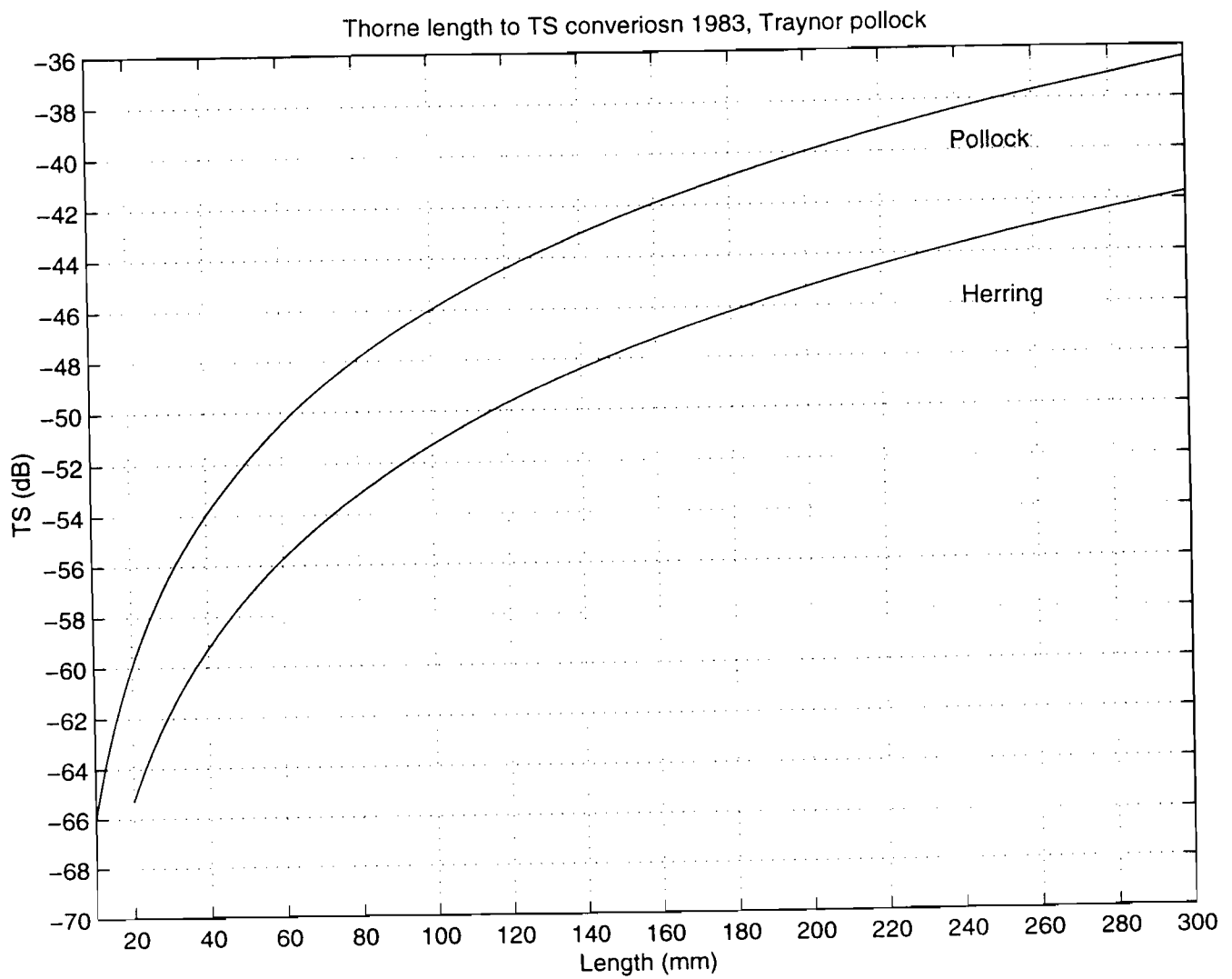


Figure 2.

SIMPSON BAY

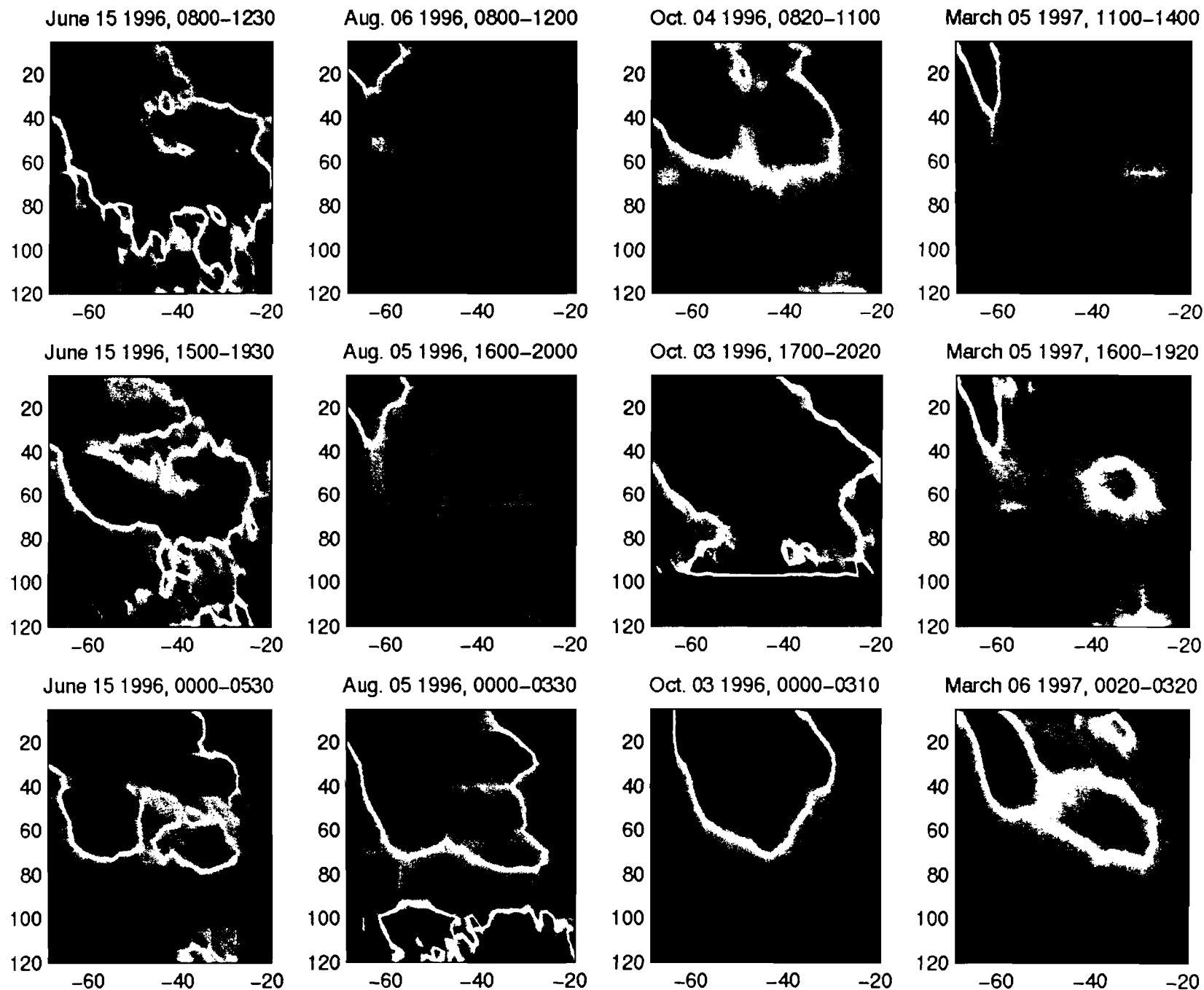


Figure 3a.
9-117

SIMPSON BAY

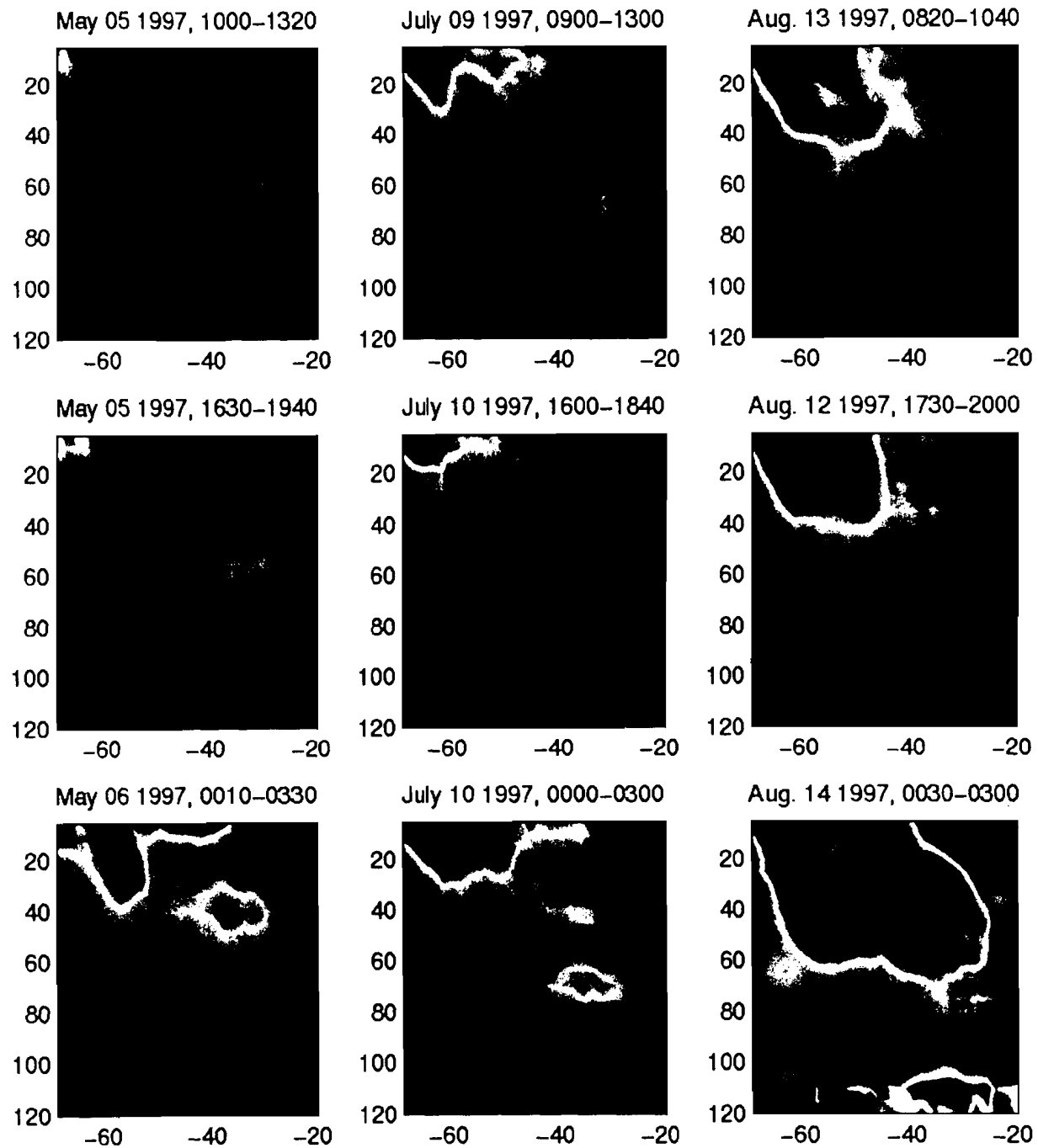


Figure 3b.

ZAIKOF BAY

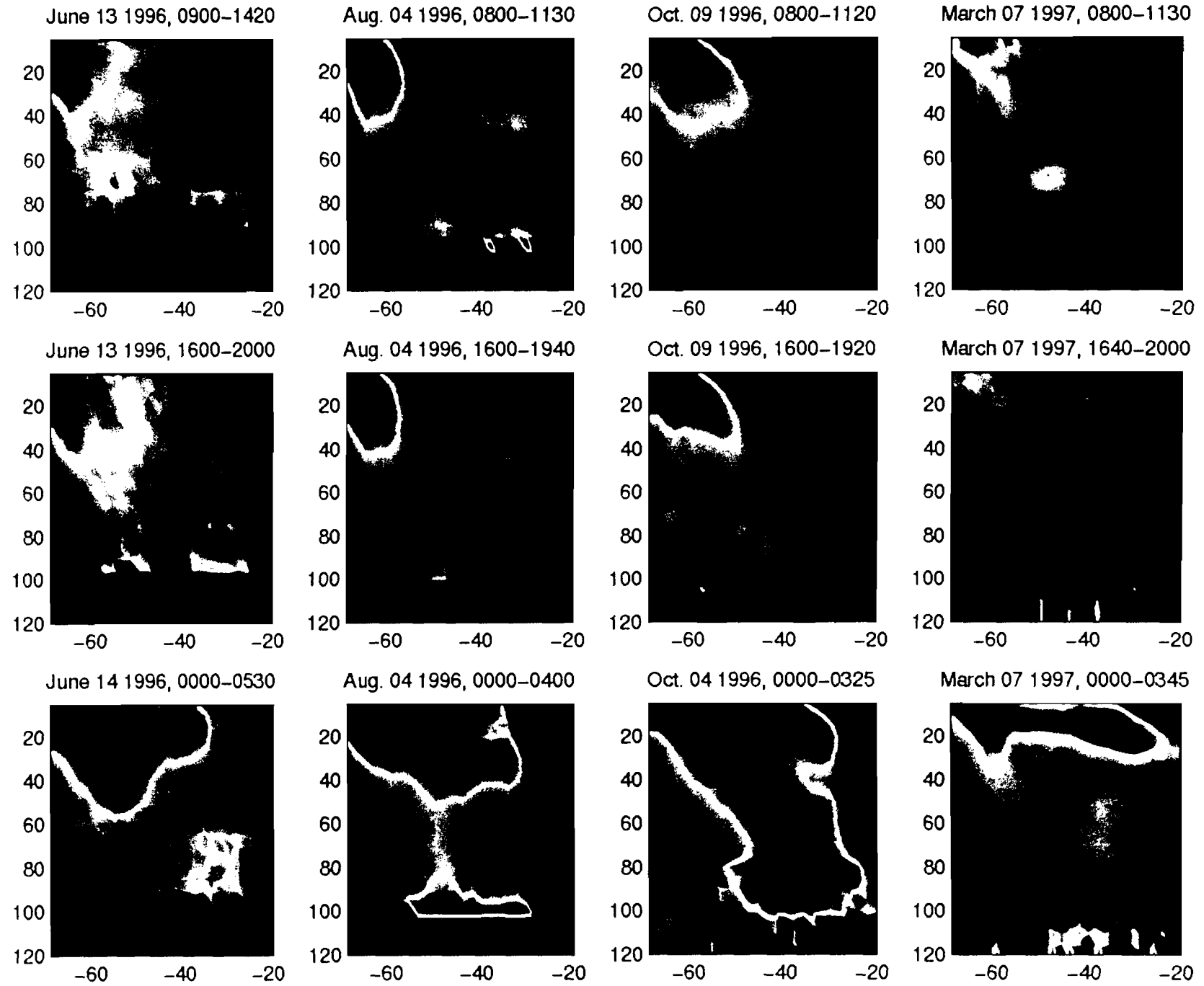


Figure 4a.

ZAİKOF BAY

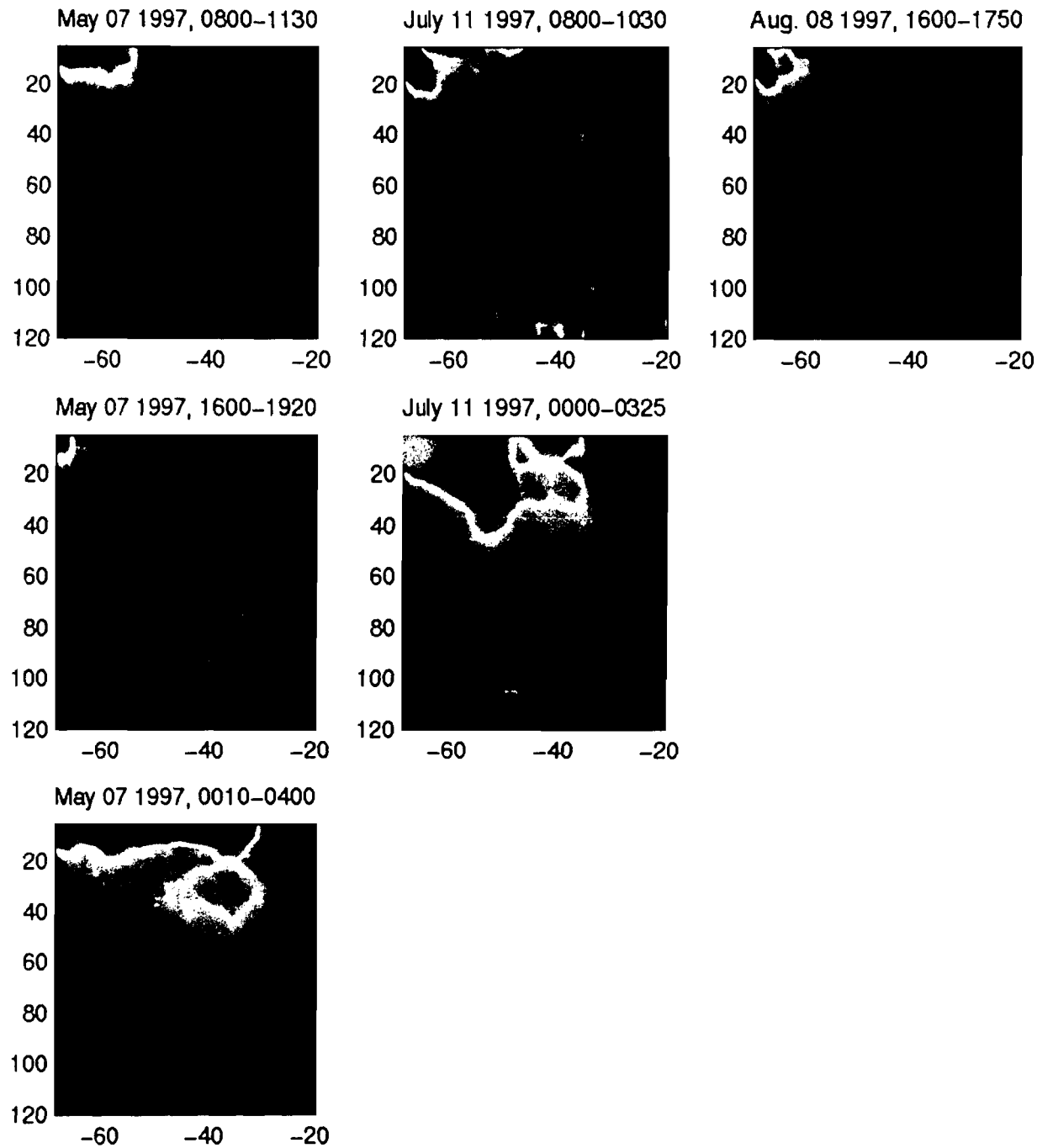


Figure 4b.
9-120

WHALE BAY

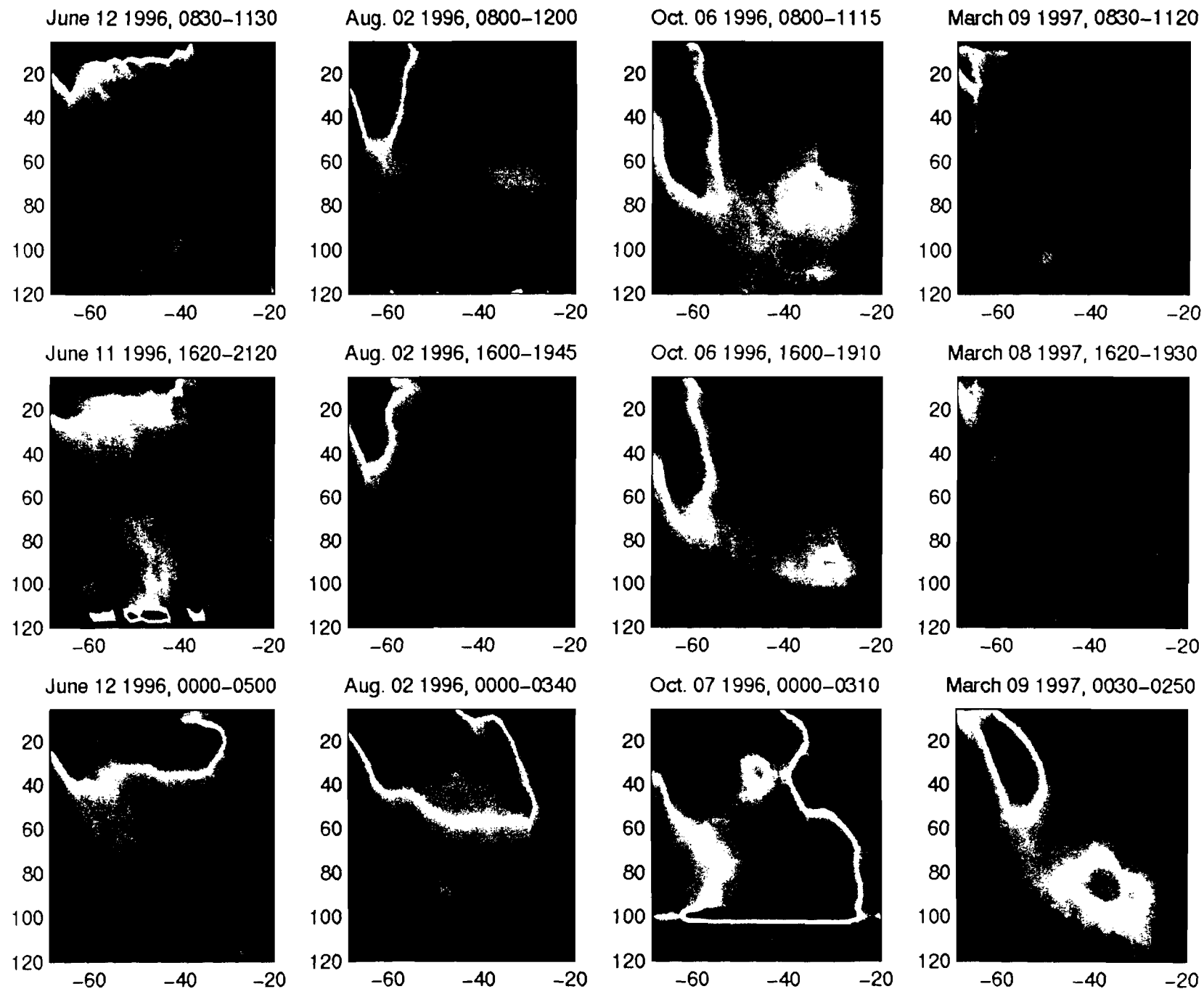


Figure 5a.
9-121

WHALE BAY

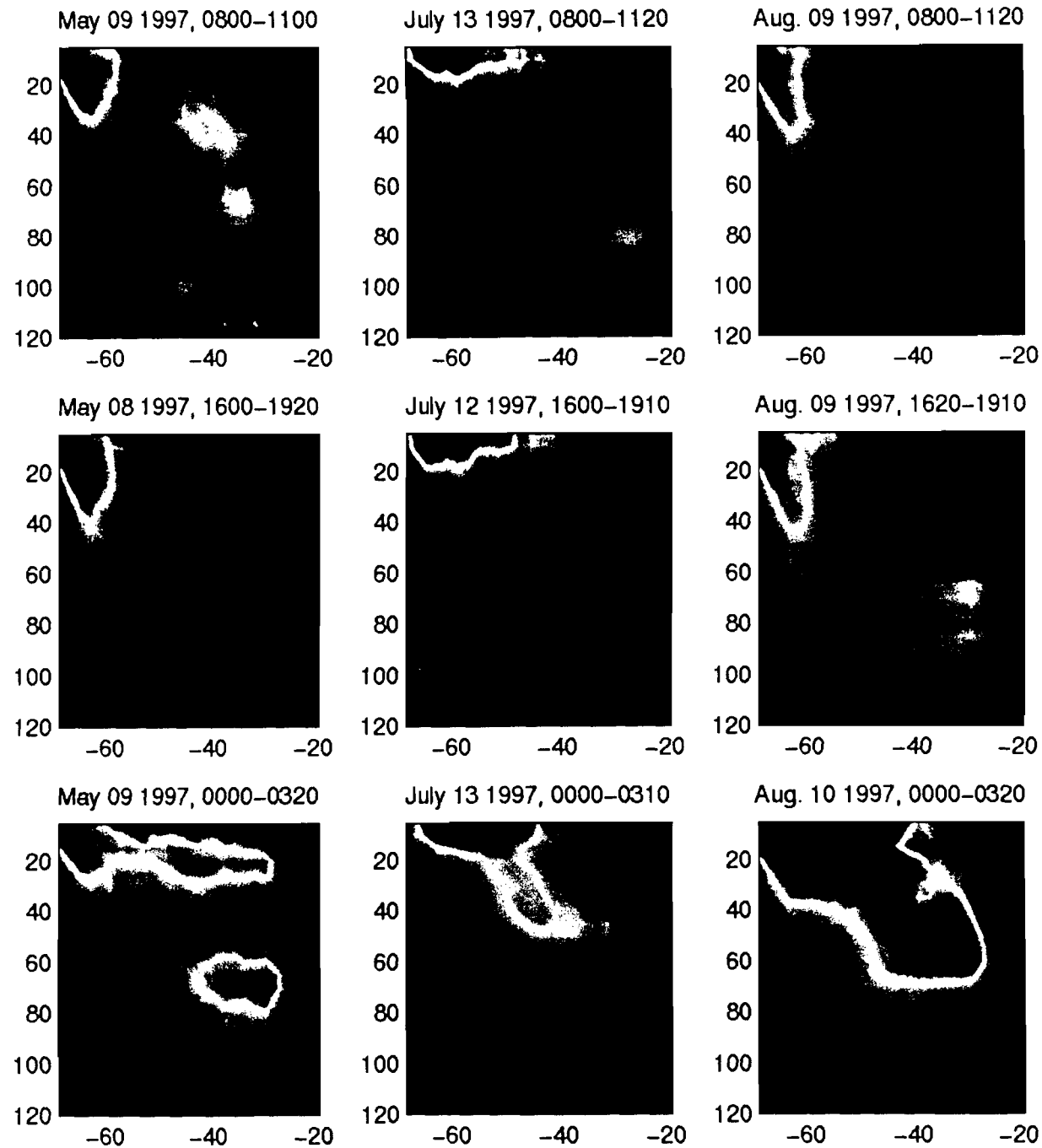


Figure 5b.
9-122

EAGLEK BAY

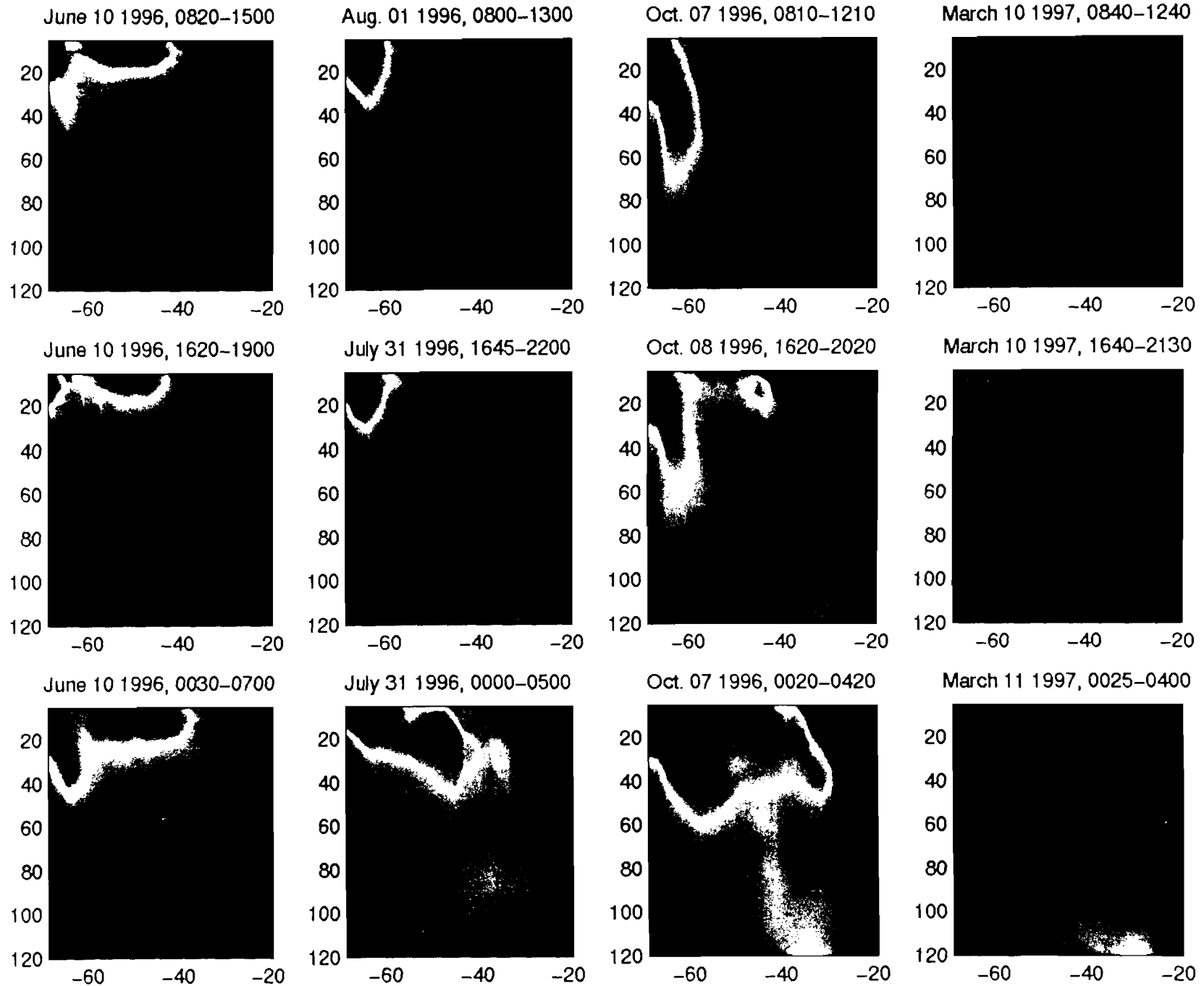


Figure 6a.
9-123

EAGLEK BAY

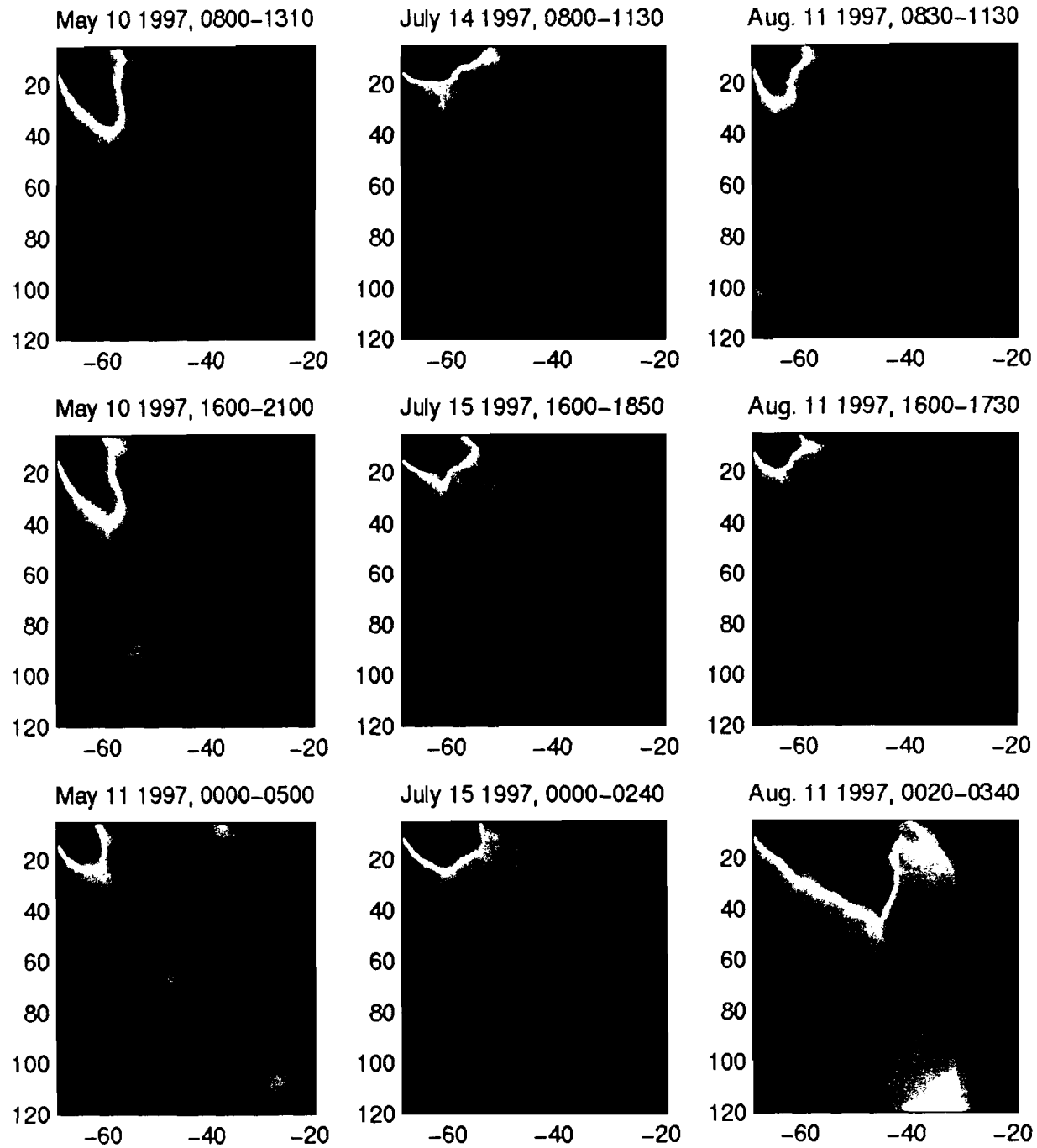


Figure 6b.
9-124

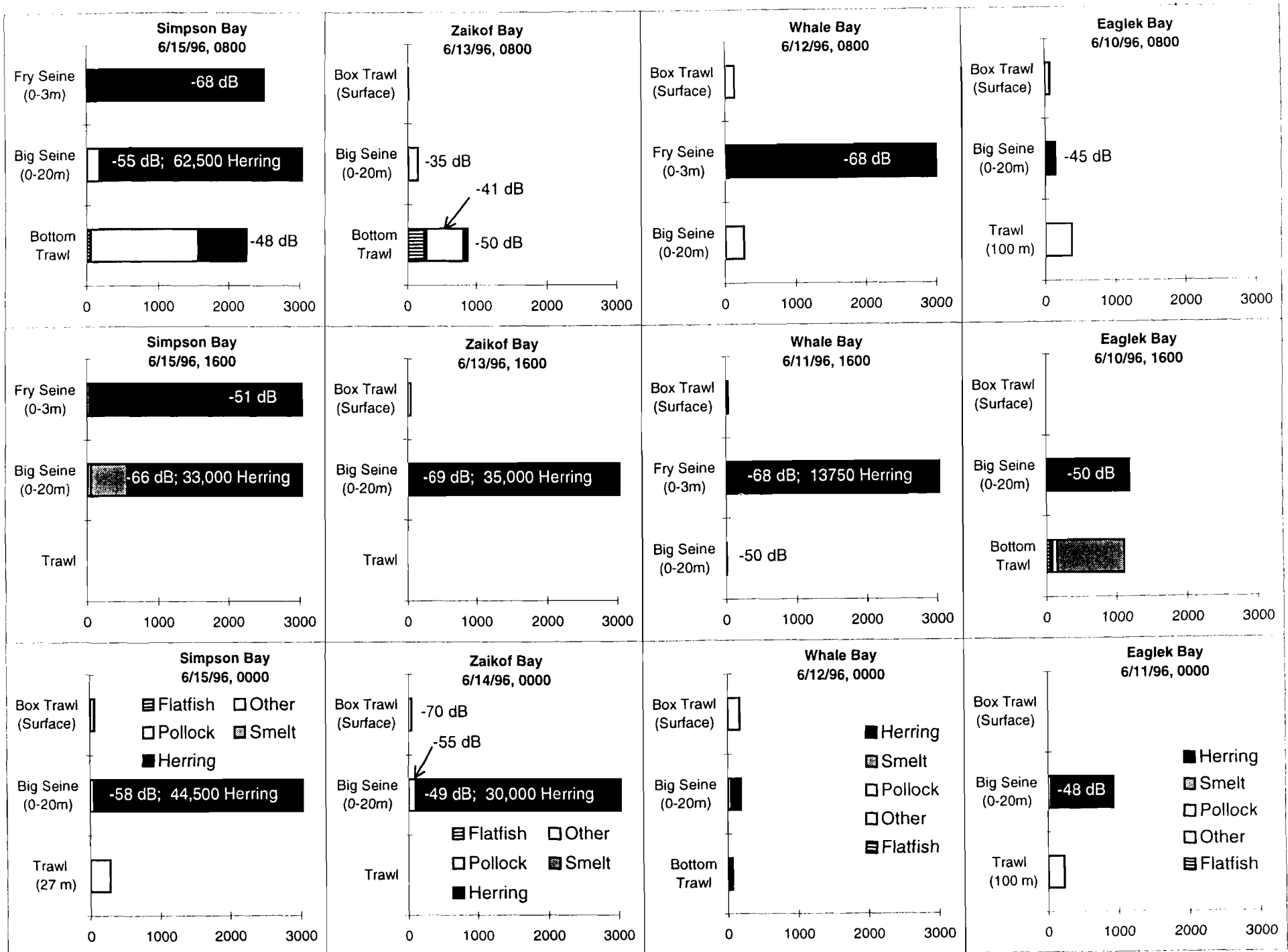


Figure 7.
9-125

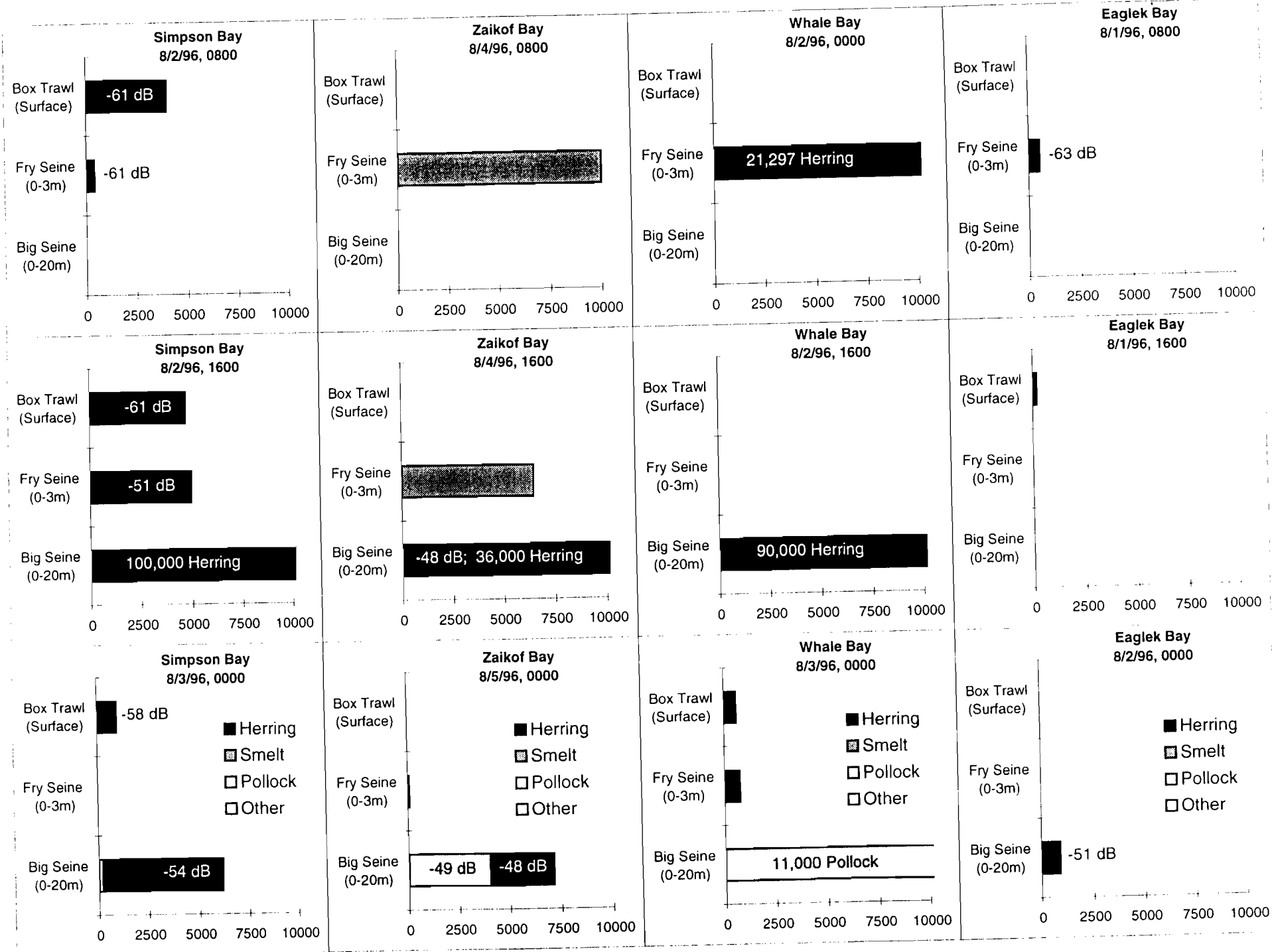


Figure 8.
9-126

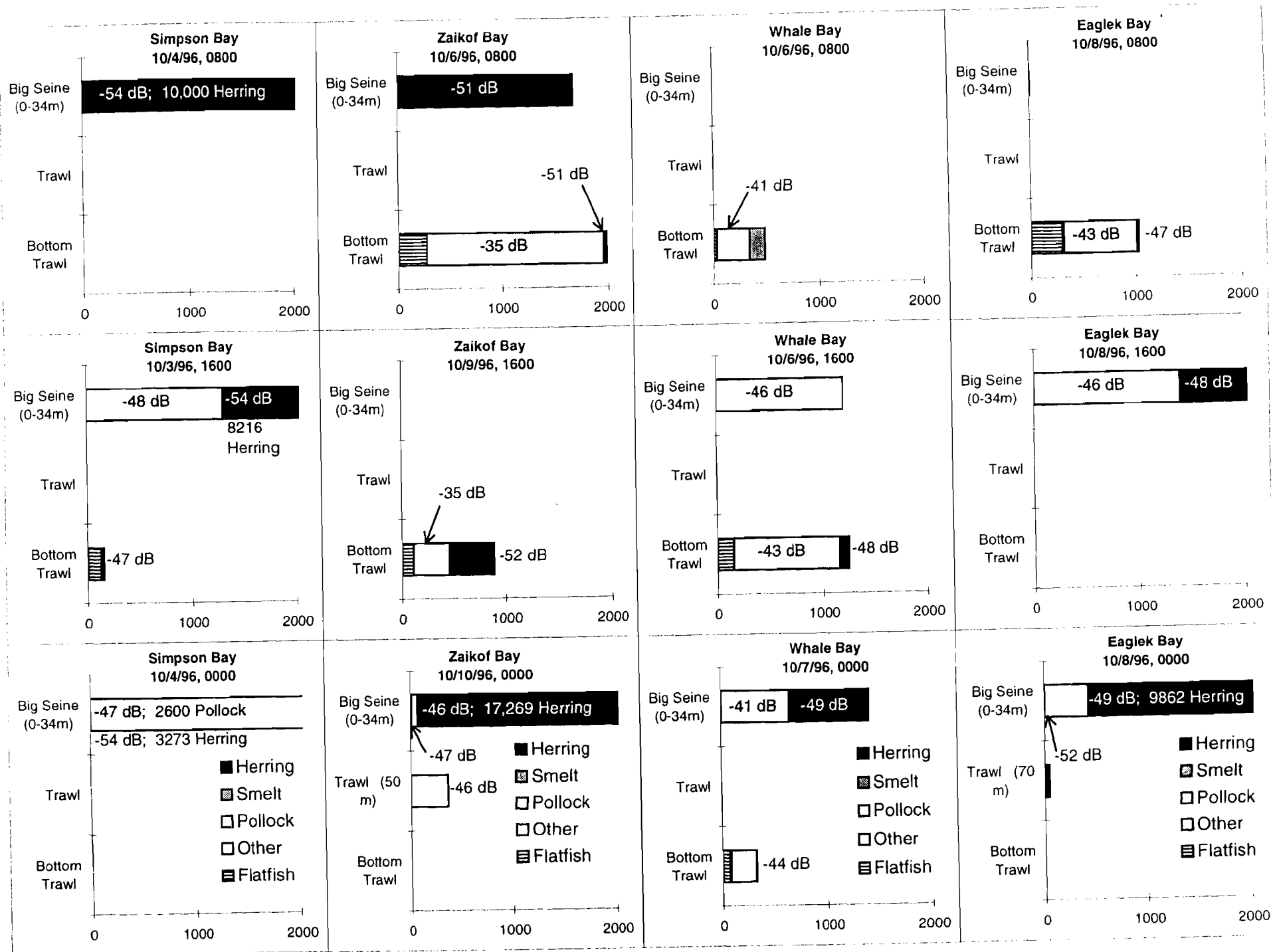


Figure 9.
9-127

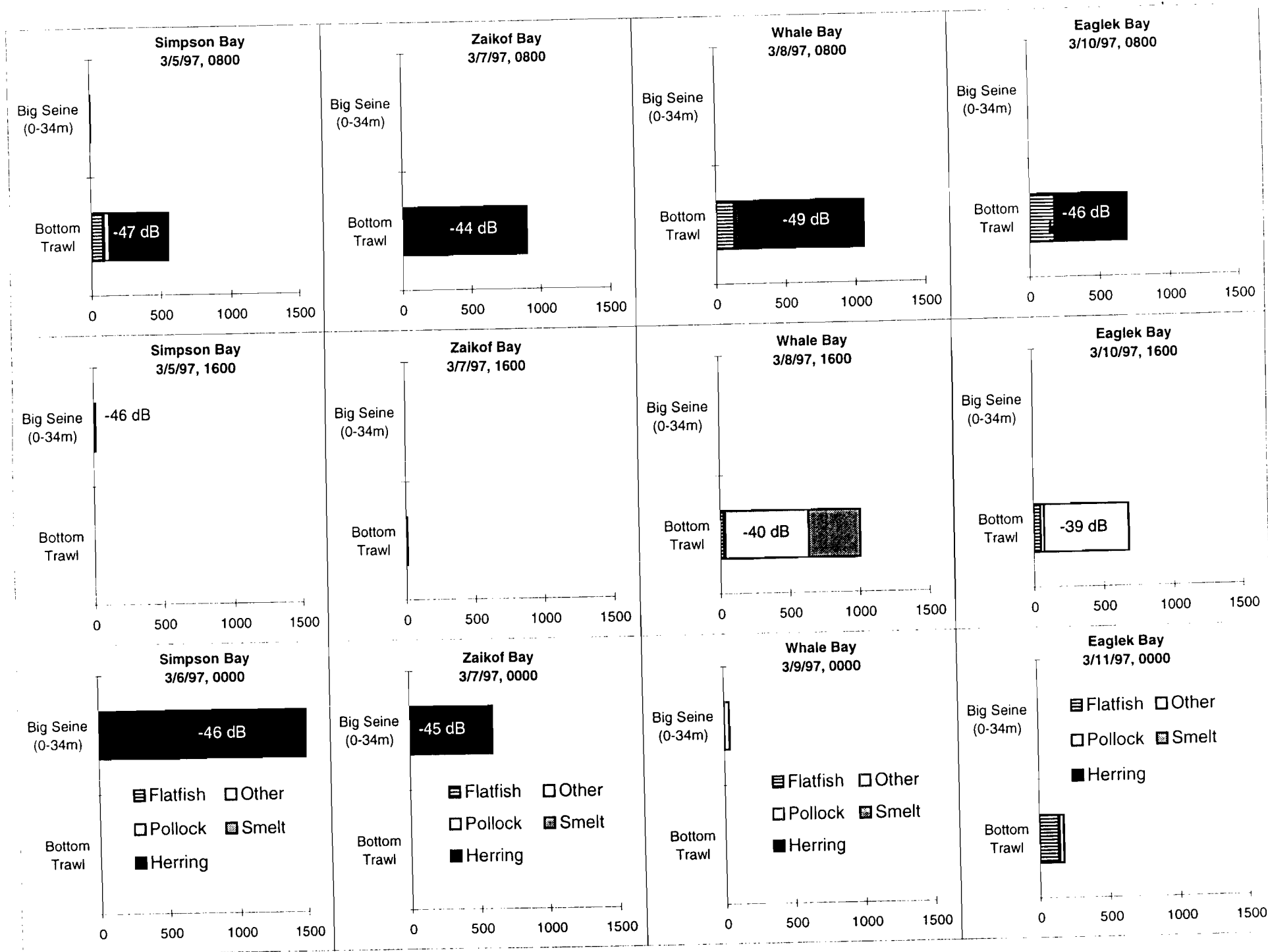


Figure 10.
9-128

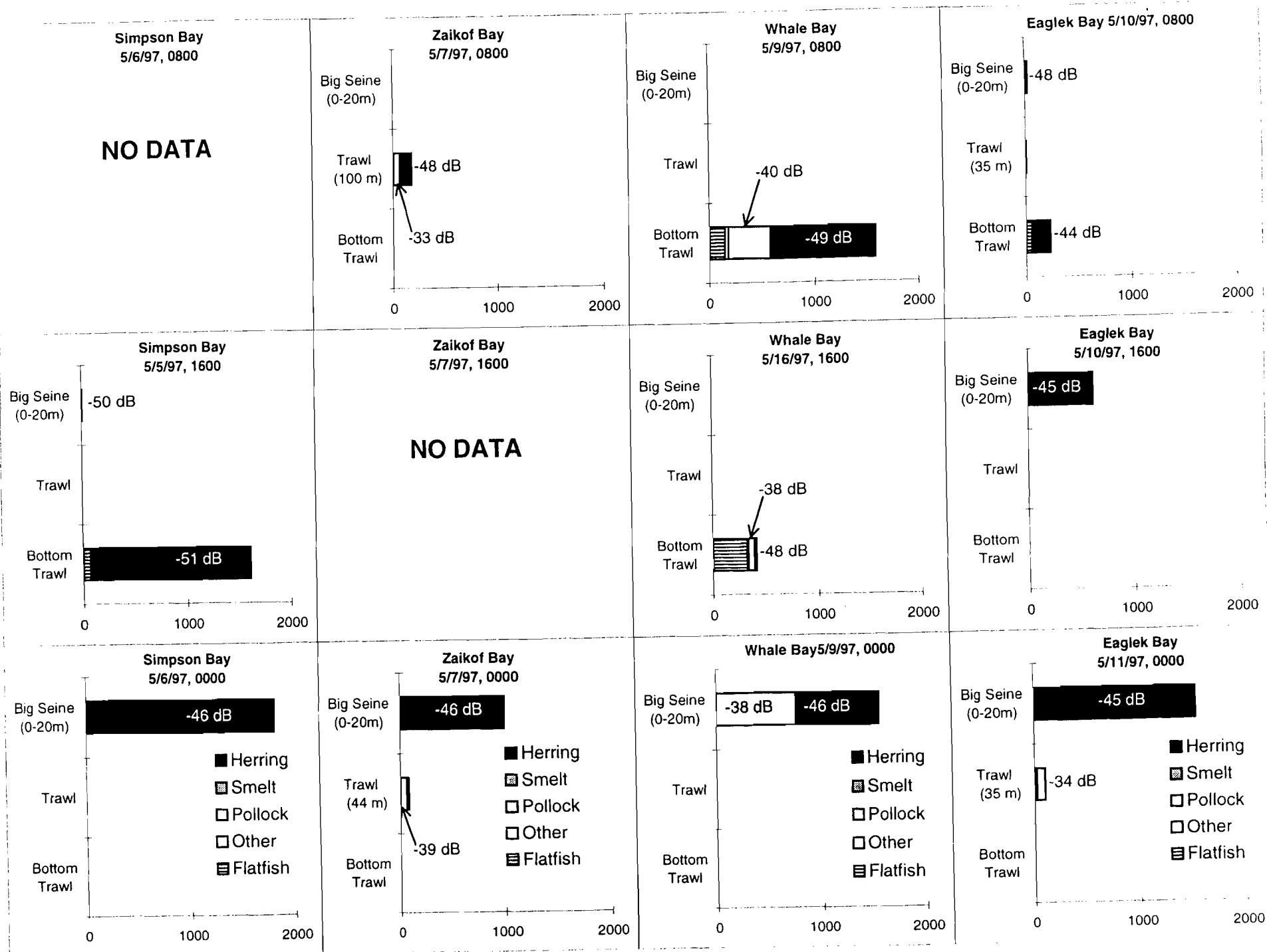


Figure 11.
9-129

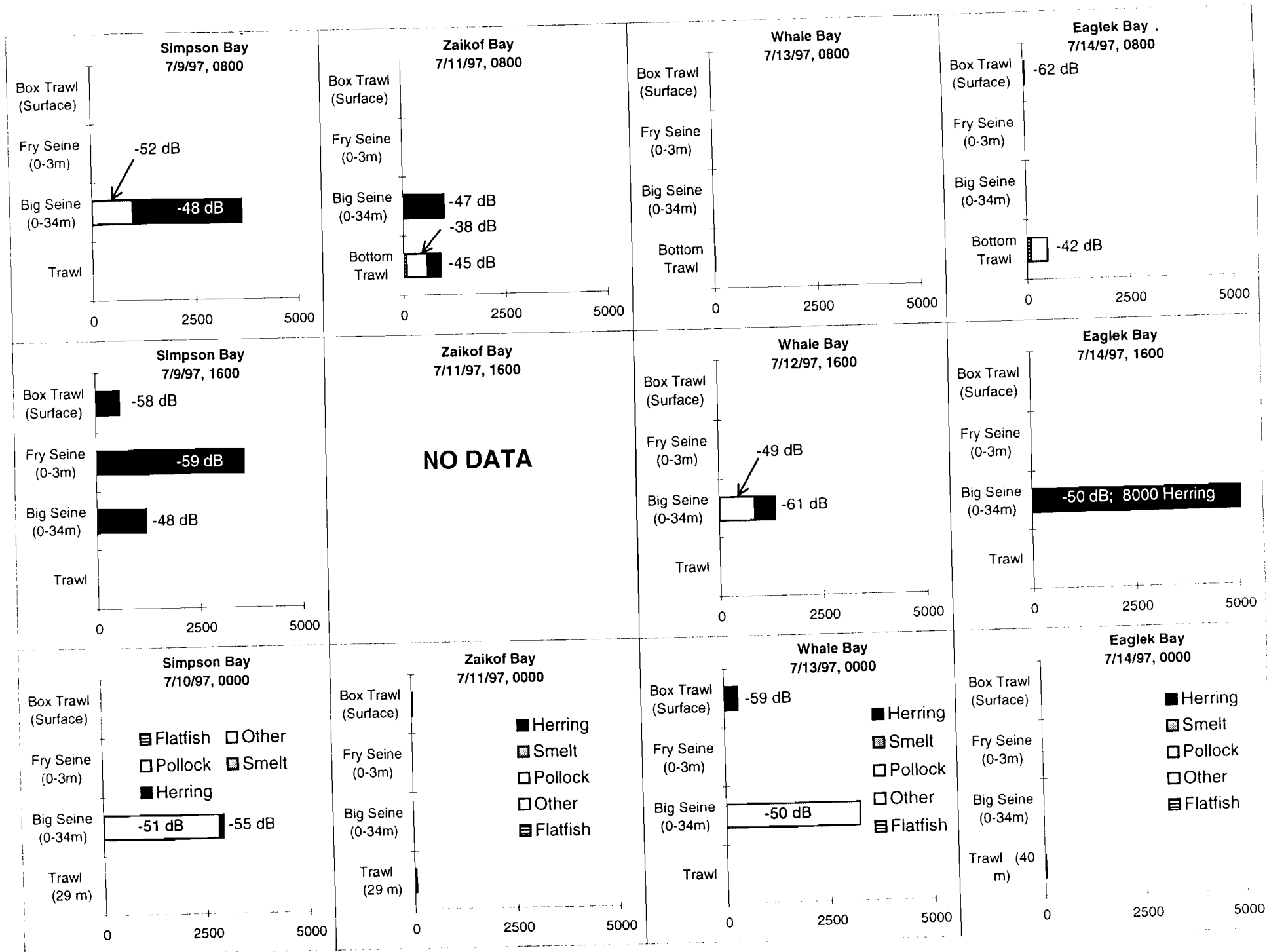


Figure 12.
9-130

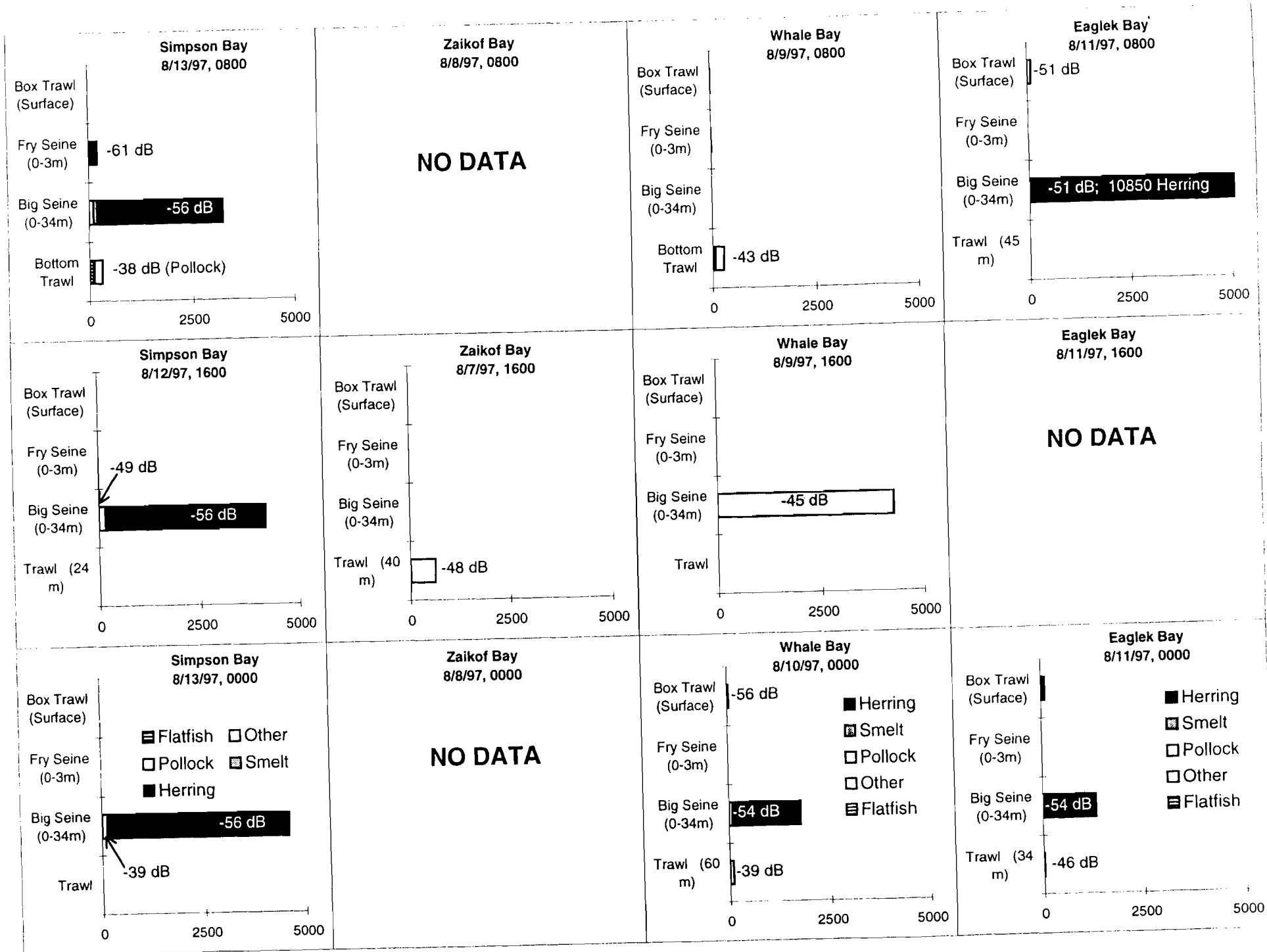


Figure 13.
9-131

Chapter 10

Juvenile Herring Growth and Habitats and Herring Traditional Ecological Knowledge (Project T Supplement)

Exxon Valdez Oil Spill
Restoration Project Annual Report

Juvenile Herring Growth and Habitats

Restoration Project 97320T
Annual Report

This annual report has been prepared for peer review as part of the *Exxon Valdez* oil Spill Trustee Council restoration program for the purpose of assessing project progress. Peer review comments have not been addressed in this annual report.

Kevin D.E. Stokesbury
Evelyn D. Brown
Robert J. Foy
Jody Seitz
Brenda L. Norcross

Institute of Marine Science
University of Alaska Fairbanks
Fairbanks, Alaska
99775-7220

April 1998

Juvenile Herring Growth and Habitats

Restoration Project 97320T Annual Report

Study history: Restoration Project 97320T is the core of the Herring Recruitment Dynamics Project, a multi-investigator ecosystem study and part of the Sound Ecosystem Assessment (SEA; PWSFERPG 1993) program in Prince William Sound (PWS). SEA was initiated because the lack of knowledge of the ecological processes affecting pink salmon and herring confounded the identification of damage caused by the *Exxon Valdez* oil spill. The PWS herring population crashed in 1993 possibly due to a viral infection (VHSV). This viral infection occurs more frequently in fish exposed to oil. Local residents, frustrated by the loss of valuable fisheries and the inability to accurately identify the causes, strongly voiced support for research. They formed a group, appealed to the EVOS Trustee Council, and as a result of their effort, SEA was created in 1994. Research on juvenile herring began in April 1995.

Abstract: The purpose of this project is to determine spatial distributions and habitats of age 0 to 2 year old Pacific herring (*Clupea pallasii*). In 1997 we completed 5 diel acoustic surveys, sampling Eaglek, Whale, Ziakof, and Simpson Bays in March, May, July, August and October. Aerial surveys were completed in June and July. As our field sampling effort decreased, our focus shifted to data analysis. The Prince William Sound Pacific herring population was made up of 3 size modes representing young of the year, juvenile (1-2 year old) and adult (sexually mature) herring. Herring of each size mode were contagiously distributed on different spatial scales. Cohorts (age/size) of herring were spatially segregated. Juvenile herring aggregated in Bays for the first 2 years of their life. Prey availability and herring prey selection varied spatially and temporally. These spatial distributions define the area where the physical and biological variables occur determining Pacific herring life history and population size in Prince William Sound.

Key Words: *Clupea pallasii*, Pacific herring, juvenile, habitat, Prince William Sound, distribution

Project Data: Spatial distribution (acoustic and aerial), length frequencies, zooplankton community structure, diet compositions and near shore ichthyofauna structure are part of the SEA data base (Project 97320-J Information Services and Modeling).

CITATION: Stokesbury, K.D.E., E.D. Brown, R.J. Foy, and B.L. Norcross. 1998. Juvenile Herring Growth and Habitats, *Exxon Valdez* Oil Spill Restoration Project Annual Report (Restoration Project 97320T), Institute of Marine Science, University of Alaska Fairbanks, Fairbanks, Alaska.

Table of Contents

Executive Summary.....	4
Introduction.....	5
Objectives.....	6
Methods.....	7
Results and Discussion.....	9
Literature Cited.....	12
Table 1. List of researchers.....	13
Figure 1.....	14
Figure 2.....	15
Appendix I.....	16
Stokesbury, K. D. E., J. Kirsch, E. D. Brown, G. L. Thomas, B. L. Norcross. 1998. Seasonal variability in Pacific herring (<i>Clupea pallasii</i>) and walleye pollock (<i>Theragra chalcogramma</i>) spatial distributions in Prince William Sound, Alaska.	
Appendix II.....	44
Brown, E. D. Preliminary Documentation of Temporal and Spatial Variability of Pacific Herring, Other Forage Fish, and Seabirds in Prince William Sound, Alaska	
Appendix III.....	60
Brown, E. D. and G. A. Borstad. Progress Report on Aerial Survey Development	
Appendix IV.....	79
Foy, R. J., and B. L. Norcross. 1998. Spatial and temporal differences in the diet of juvenile Pacific herring (<i>Clupea pallasii</i>) in Prince William Sound, Alaska.	
Appendix V.....	101
Seitz, J. Distribution of Herring and Other Forage Fish as Observed by Resource Users Restoration Project 97320T Supplement. Annual Report	

Executive Summary

This project is a component of the Herring Recruitment group of SEA, initiated to provide information on the herring population in Prince William Sound and restoration measures required after the *Exxon Valdez* oil spill. The Herring Recruitment group is examining the physical and biological mechanisms affecting the survival of juvenile Pacific herring (*Clupea pallasii*) and providing indices of recruitment into the fishing stock. To do this a conceptual model addressing three objectives: 1.) overwintering survival model, 2.) summer habitat model, 3.) monitoring strategy, has been created. The Growth and Habitat project is determining: 1.) horizontal and vertical distributions of juvenile herring, using hydroacoustic and aerial surveys, and the underlying biological (predator distribution, prey distribution) and physical variables (oceanographic conditions, substrata) influencing these distributions, 2.) survival rate of juvenile herring based on densities and yearclass distribution, 3.) summer growth rates in different areas, 4.) habitat quality, based on oceanographic conditions, energetics, growth rates and prey availability, 5.) larval drift based on the SEA oceanographic model, 6.) an overwintering survival model.

In 1997 we completed 5 diel surveys, sampling Eaglek, Whale, Ziakof, and Simpson Bays in March, May, July, August and October. During all but the latter survey four or five vessels were employed: an acoustic vessel, a trawler, a seiner, a processing boat which also supported the inshore fry skiff, and an oceanographic vessel. Aerial surveys were completed in June and July. One vessel was used during the October survey and focused on developing a cost-effective monitoring strategy combining hydroacoustic, zooplankton and fish collections with oceanographic measurements. As our field sampling effort decreased, our focus shifted to data analysis. Presently, the majority of acoustic survey data has been combined with fish collection data to extrapolate estimates of spatial distributions for pollock and herring. Diet composition of juvenile herring and prey availability within the four bays has been determined for 1995 and 1996, and work continues on the 1997 data.

The Prince William Sound Pacific herring population was made up of 3 size modes representing young of the year, juvenile (1-2 year old) and adult (sexually mature) herring. Herring of each size mode were contagiously distributed on different spatial scales. Cohorts (age/size) of herring were spatially segregated. Juvenile herring aggregated in Bays for the first two years of their life. They congregated in surface waters during June and July. Prey availability and herring prey selection varied spatially and temporally.

These spatial distributions define the area where the physical and biological variables occur determining Pacific herring life history and population size in Prince William Sound. The lack of information of these variables confounded the identification of damage caused by the *Exxon Valdez* oil spill and estimates of the population's recovery time. Our future work will focus on determining these variables.

Introduction

The purpose of this project is to determine spatial distributions and habitats of age 0 to 2 year old Pacific herring (*Clupea pallasii*). It is linked to the Herring Recruitment Dynamic subgroup of SEA and provides data for the three objectives (1. overwintering survival model, 2. summer habitat model, 3. monitoring strategy) which will determine the physical and biological mechanisms influencing the recovery of Pacific herring. Pacific herring is listed as “not recovered” in the “Resources and Services Injured by the Spill” *Exxon Valdez* Oil Spill Restoration Plan.

The Herring Recruitment Model is being developed as the integration of several submodels, each of which focuses on a stage in the early life history of Pacific herring (*Clupea pallasii*). We hypothesize that, like other clupeoids, year-class strength of Pacific herring in Prince William Sound (PWS) is determined during its early life history. All field work, laboratory experiments, and data analysis for all components of SEA relate to one or more of these submodels. Two major SEA hypotheses are the focus of these submodels and will be linked within the overall Herring Recruitment Model (Figure 1). The first is the Herring Overwinter Hypothesis which states that survival of herring through their first winter is critical to year-class strength and is dependent upon their condition when they enter winter. We will test this hypothesis by examining distribution and condition of herring in the fall, winter and spring. We expect to see changes in condition indices related to the physical and biological variables of different geographic locations. A bioenergetic model, combining SEA field and laboratory observations together with energetic information from Atlantic herring studies, is being constructed to predict overwinter survival for recruiting herring. In support of the herring Overwinter Hypothesis we will examine how the Lake/River hypothesis applies to transport and distribution of herring at the larval stage. We will employ larval drift simulations, using the Circulation and Transport Models for PWS being formulated by Mooers and Wang as part of the Ocean Dynamics Model, to determine the expected drift of larval herring within PWS and determine how that affects the distribution of summer juvenile nursery areas. We expect to examine various drift patterns in response to simulated lake (i.e. retention), river (i.e. rapid movement through the sound), and combinations of varying amounts of “lake” and “river” in accordance with the recent evolution of the lake/river hypothesis. The larval drift synthesis is a tool, which will link the Summer Habitat Model, which examines location and characteristics of summer nurseries utilized by juvenile herring, with the Overwintering Survival Model. The Summer Habitat Model will determine the survival and growth rates of juvenile herring and the quality of nursery areas by examining changes in herring distribution, density, length, weight, energy (kJg^{-1}), interspecific biological variables (prey abundance, predation) and physical variables (oceanographic conditions, bathymetry). These data will define the conditions of herring entering into the Overwintering Survival Model.

This project is a component of the SEA project; Dr. T. Cooney chief scientist. Within SEA, coordination exists between projects linking physical and biological data. Multiple authors on proposed publications reflect this integration. In addition, this project coordinates with

the APEX and NVP ecosystem projects via field logistics (vessels, equipment and samples), shared data (catch, aerial survey data, and acoustics results), and joint publications. Coordination with these groups increased during FY98 and we expect this to continue in FY99.

Objectives

The research objectives of this project are:

1. Develop an Overwinter Survival Model for juvenile herring.
2. Develop a Summer Habitat Model for juvenile herring.
3. Develop a Monitoring Strategy for juvenile herring.

For the Overwinter Survival Model:

Describe overwinter distribution, size, condition, energy needs, and relative abundance of juvenile herring, physical and biologic characteristics of herring nursery areas and overwintering bioenergetics.

Tasks:

1. Collect data on the whole body energy content of age 0 and 1 herring in the late fall and winter.
2. Determine changes in bioenergetics over the winter season using time sequence (monthly) sampling of juvenile herring from two or more index sites in 1996-97 and 1997-98.
3. Examine stomach contents of over-wintering recruits and make energetic estimates for consumption during the winter of 1996-97 and 1997-98.
4. Determine the energy need of fasting herring in the laboratory.
5. Develop a model to predict winter survivorship using field and laboratory measurements of over-winter energy needs and literature values for Atlantic herring.
6. Describe spring, pre-bloom biological and habitat conditions as an endpoint of Overwintering Survival Model and beginning of second year Summer Habitat Model.
7. Compile historic biological and physical data for the purpose of model verification

For Summer Habitat Model:

Describe summer and fall distribution, size, condition and relative abundance of juvenile herring (biological data), and physical and biological characteristics of herring nursery areas (habitat data) to evaluate quality of summer growth of herring and as initial conditions for the Overwintering Survival Model.

Tasks:

1. Use Circulation and Transport Models (Ocean Dynamics Model) to simulate drift of larval herring and distribution to summer nursery areas.
2. Determine distribution of juvenile herring during the spring, summer and fall using broad scale surveys that include simultaneous overflights, acoustics and net collections.
3. Determine physical (salinity, temperature, depth, currents, light levels, bathymetry) and biological (zooplankton, competitors) parameters which determine good vs. bad nursery areas measured by condition of herring (length, weight, age, growth rates, stomach contents, energetic condition and stable isotopes).
4. Develop maps of key habitats (nursery areas) for juvenile herring within PWS.
5. Describe the retention characteristics of herring nursery areas using information from the larval drift simulations, physical oceanographic measurements and biological data (spatial distributions, isotopes, and growth rates) indicating immigration or emigration.
6. Develop maps of possible retention areas with different historical spawning sites and transport conditions.
7. Compare historic distributions reported by local and traditional knowledge with distributions described by this study

For Monitoring Strategy:

Tasks:

1. Identify key index sites and develop monitoring techniques by relating aerial, acoustic and net sampling data during summer surveys to condition of juvenile herring.

Methods

To address the above objectives and tasks, we have formulated our approach into two component models, each with several subcomponents. These models and subcomponents are described in chronological order of herring life history (Figure 1).

The first subcomponent is embryo survival. This component is not a SEA program, but rather projects funded by EVOS outside of SEA. For the starting point of our Summer Habitat Model, we intend to combine the results of 1) the ADF&G spawn deposition survey, 2) the Haldorson, Quinn and Rooper egg loss model which predicts losses due to physical factors and predation, 3) estimates of baseline egg mortality, and 4) estimates of baseline levels of viable hatch (Hose et al. 1996; Kocan et al. 1996). From this we will know the location of spawning of herring, an estimate of the amount of spawn, and the expected percentage of viable larvae produced.

The output of that subcomponent is the input into the Larval Drift Model (Figure 1). We will examine the direction of transport without incorporating the population size component. We will run the Ocean Circulation and Transport Model with input at the locations of herring spawning and test observed distribution of particles. Distribution predicted by this subcomponent will be verified by the distribution of age-0 herring during the summer. We will compare the Larval Drift Model results to the transport and retention of larval Atlantic herring (*Clupea harengus*) in North Atlantic (Graham and Davis 1971, Graham and Townsend 1985, Sinclair and Iles 1985, Sinclair 1988). We will also use 1989 as a test case. By inputting location of spawning and physical conditions which we know occurred in 1989, we can test the model against the offshore distribution of larvae observed in May, June and July 1989 (Norcross and Frandsen 1996) and the nearshore distribution observed in May 1989 (McGurk 1990). We will also use spawning location information from 1995, 1996 and 1997 correlated with the distribution of larvae and the distribution of herring observed from the aerial and acoustic surveys. This simulation will be an iterative process.

The output of the larval drift simulation is the input for the Summer Habitat Model (Figure 1). From October 1995 to March 1998, acoustic and aerial surveys were conducted and these data will be processed, analyzed, interpreted and combined to determine herring nurseries. The broadscale distribution of age-0 herring was observed during October 1995, March and July 1996. These surveys covered most of PWS and adjacent waters to Resurrection Bay. The Sound is very large and resources were limited so the survey focused on regions where fishermen had observed juveniles and where earlier ADF&G surveys indicated high densities of herring (<1 km from shore). Sampling from the air provided approximately weekly estimates of horizontal distribution of herring across the Sound.

These broadscale surveys provided a preliminary estimate of oceanographic patterns and distribution of herring. However, the broadscale survey was a continuous transect along the coastline of Prince William Sound and there were several limitations associated with its design, for example, it was non-random, and it was a temporal point measurement while

fish distribution and oceanographic conditions are strongly effected on a short temporal scale by the tidal cycle and the diel (day/night) cycle.

We have addressed these limitations by employing a factorial design, based on Green's (1979) principles of sampling to derive the survival rate of juvenile herring from density changes using a life table. Densities must be estimated precisely and accurately on both spatial and temporal scales. In this factorial design each spatial replicate (bay) has 3 temporal replicate samples within 24 hours, allowing us to estimate the variability in densities caused by tidal and diel cycles and allow accurate measurements of the oceanographic conditions of each bay (Gunderson, 1993) (Figure 2). This design allows an overall estimate of changes in survival rates of Prince William Sound juvenile herring and comparisons between and within bays on different spatial and temporal scales, i.e. 24 hours, monthly, annually. The four bays are, Eaglek, Whale, Ziakof and Simpson. These bays were selected because:

1. herring overwinter in bays
2. spatially segregated; North South, East and West.
3. located at a distinct position along the prevailing PWS current, relating directly to the lake/river hypothesis (Cooney 1995: Chapter 7 Fig. 11-17; and Chapter 9).
4. strong evidence that herring spawn/recruitment in each of these bays

Each bay was surveyed three times in a 24 hour period using sidescan sonar (Figure 2). Net collections of herring were coupled with acoustics estimates of horizontal and vertical distribution and abundance, and aerial estimates of horizontal distribution. These net collections are used to ground-truth both acoustic and aerial estimates for species size and composition. Subsamples of herring were retained and later evaluated for size, age, stomach contents, condition (energetics and standard fisheries age-weight-length (AWL)), and stable isotopes (trophic analysis). Simultaneous with net collections for fish were vertical plankton tows to estimate availability of food for planktivorous herring. Oceanographic parameters collected include salinity and temperature at depth (CTD), estimates of current structure (ADCP), light levels and bathymetry at location. The main effort in 1998 will be to process, analyze and interpret these data.

Results and Discussion

Larval Drift Model

The Ocean Circulation and Transport Model is being developed and the first results are being published in the manuscript:

Mooers, C.N.K. and J. Wang. 1998. On the development of a three-dimensional circulation model for Prince William Sound, Alaska. Continental Shelf Research 17:000-000 in press.

This model will be the basis for the Larval Drift Model, which is presently being developed.

Summer Habitat Model

In this component we are determining the biological and physical variables influencing the spatial and temporal distribution of Pacific herring (*Clupea pallasii*) in Prince William Sound. This is a combined effort with support for acoustics and oceanography from PWSSC and technical support from Alaska Department of Fish and Game in Cordova.

The first manuscripts from this work are:

Stokesbury, K. D. E., J. Kirsch, E. D. Brown, G. L. Thomas, B. L. Norcross. 1998. Seasonal variability in Pacific herring (*Clupea pallasii*) and walleye pollock (*Theragra chalcogramma*) spatial distributions in Prince William Sound, Alaska.

Appendix I

Brown, E.D. , S. Vaughan, and B.L. Norcross. In prep. Annual and seasonal spatial variability of herring, other forage fish, and seabirds in relation to oceanographic regimes in Prince William Sound, Alaska *in* Ecosystem Considerations in Fisheries Management, Lowell-Wakefield Symposium. A preliminary look at data to be included in this publication is attached in **Appendix II**.

Brown, E.D., G.A. Borstad, and B.L. Norcross. In prep. Assessment of forage fish distribution, relative abundance, and ecology using aerial surveys: survey design and methodology. Ecological Applications draft. Chapter 11, Appendix I, SEA 1996 Annual Report. **Appendix III** is a progress report on this work.

Foy, R. J., and B. L. Norcross. 1998. Spatial and Temporal Differences in the Diet of Juvenile Pacific Herring (*Clupea pallasii*) in Prince William Sound, Alaska.

Appendix IV

Overwintering Survival Model

The Overwintering Survival Model evaluates distribution and condition of age 0 and 1 herring as they enter, pass through, and complete the winter. The objective of this sampling is to determine change in condition of herring over the course of winter in concert with the hypothesis that herring which enter winter in poor condition due to “bad” nursery habitats will not survive winter, while those from “good” habitats will successfully survive winter.

Dr. A.J. Paul is leading this effort, he and his co-authors have submitted the following manuscripts:

Paul, A.J., J.M. Paul, and E.D. Brown. 1997. Fall and spring somatic energy content for Alaskan Pacific herring (*Clupea pallasii* Valenciennes 1847) relative to age, size and sex. Journal of Experimental Marine Biology and Ecology. 000:000-000 in press.

Paul A.J., and J. M. Paul. 1997) Comparisons of whole body energy content of captive fasting age zero Alaskan Pacific herring (*Clupea pallasii* Valenciennes) and cohorts over-wintering in nature. Journal of Experimental Marine Biology and Ecology. 000:000-000 in press.

Refer to Dr. Paul's sections in this Annual report for more details on these manuscripts.

Alaska Predator Ecosystem Experiment (APEX) Project Support

Juvenile herring were determined to be an important forage fish in PWS (Haldorson et al. 1996). Thus there is considerable overlap between research conducted by SEA and APEX. In 1997, SEA herring researchers were requested to cooperate and share data with researchers within APEX. Overflights were coordinated with APEX acoustic surveys and ongoing sea bird research. The aerial database was shared with APEX to enhance modeling efforts linking fish distribution to bird foraging behavior and reproductive effort. In addition, SEA aerial and net catch data concerning jellyfish was shared with the APEX project for analysis and publication. We expect these cooperative efforts to continue as both programs move toward synthesis.

Historic Data Summary

An effort to capture local knowledge about herring and other forage fish continued, for its second year, as a supplement to this project. Presently thirty-nine individuals have been interviewed. Several observations were consistent among interviewees: juvenile herring are most abundance at the heads of bays in the summer, juvenile herring have a different distribution than adults, juvenile herring schools are smaller but more abundant than adult schools. These anecdotal observations are in general agreement with the results of this study. A separate annual report has been prepared for 97320T supplement **Appendix V**.

Literature Cited

- Graham, J.J. and C.E. Davis. 1971. Estimates of mortality and year class strength of larval herring in western Maine, 1964-67. ICES Rapp. R.-V. 160: 147-152.
- Graham, J.J. and D.W. Townsend. 1985. Mortality, growth, and transport of larval Atlantic herring *Clupea harengus* in Maine Coastal waters. Trans. Am. Fish. Soc. 114: 490-498.
- Gunderson R.D. 1993. Surveys of Fisheries Resources. John Wile & Sons, Inc., New York
- Haldorson, L., T. Shirley, K. Coyle, and R. Thorne. 1996. Alaska Predator Ecosystem Experiment Forage Species Studies in Prince William Sound Project 163A, 1996 Annual Report *prepared for Exxon Valdez Oil Spill Trustee Council*, Anchorage, Alaska. 93 pp.
- Hose, J.E., M.D. McGurk, G.D. Marty, D.E. Hinton, E.D. Brown, and T.T. Baker. 1996. Sublethal effects of the *Exxon Valdez* oil spill on herring embryos and larvae: morphologic, cytogenetic and histopathologic assessments, 1989-1991. Can. J. Fish. Aquat. Sci. 53: 2355-2365
- Kocan, R.M., J.E. Hose, E.D. Brown, T.T. Baker. 1996. Herring embryo (*Clupea pallasii*) sensitivity to Prudhoe Bay petroleum hydrocarbons: laboratory evaluation and *in situ* exposure at oiled and unoiled sites in Prince William Sound. Can. J. Fish. Aquat. Sci. 53: 2366-2375
- McGurk, M.D. 1990. Early life history of Pacific herring: Prince William Sound herring larvae survey. Final report to NOAA-NOS, Contract 50ABNC-7-00141, Anchorage, AK.
- Norcross, B.L. and M. Frandsen. 1996. Distribution and abundance of larval fishes in Prince William Sound, Alaska during 1989 after the *Exxon Valdez* oil spill. In S.D. Rice, R.B. Spies, D.A. Wolfe and B.A. Wright (eds.). *Exxon Valdez Oil Spill Symposium Proceedings*. Am. Fish. Soc. Symp.
- Sinclair, M. 1988. Marine Populations. Washing Sea Grant Program, Seattle, WA, 252p.
- Sinclair, M. and T.D. Iles. 1985. Atlantic herring (*Clupea harengus*) distributions in the Gulf of Maine-Scotian Shelf area in relation to oceanographic features. Can. J. Fish. Aquat. Sci. 41:1055-1065.

Table 1. List of researchers we collected samples for during the SEA Herring cruises.

1. Kathy Frost, ADF&G Fairbanks, AK.; Marine Mammal Ecosystem. Needed various size fish of any species.
2. Jeff Short, Auke Bay, Juneau AK.; Needed herring and pollock.
3. Molly Sturdavent, Auke Bay, Juneau AK.; Needed capelin, sandlance, eulachon and pollock.
4. Tom Kline, PWSSC, Cordova AK.; Isotopes
5. John Piatt, NBS, Anchorage AK.; Needed juvenile herring and pollock
6. A.J. Paul, Seward Marine Center, Energetics, herring and pollock.
7. James Raymond, Univ. of Nevada; Needed blood and liver samples from herring in the Gravina or Montague area.
8. Steve Moffitt and John Wilcox, ADF&G Cordova. Herring AWL.
9. Richard Kocan, UW; Disease; 60 juvenile herring from 5 sites, would like heart, liver and spleen removed, put in tubes, and kept cool.
10. Gary Marty, UC-Davis; Disease; Looking at herring from the Montague Is. area

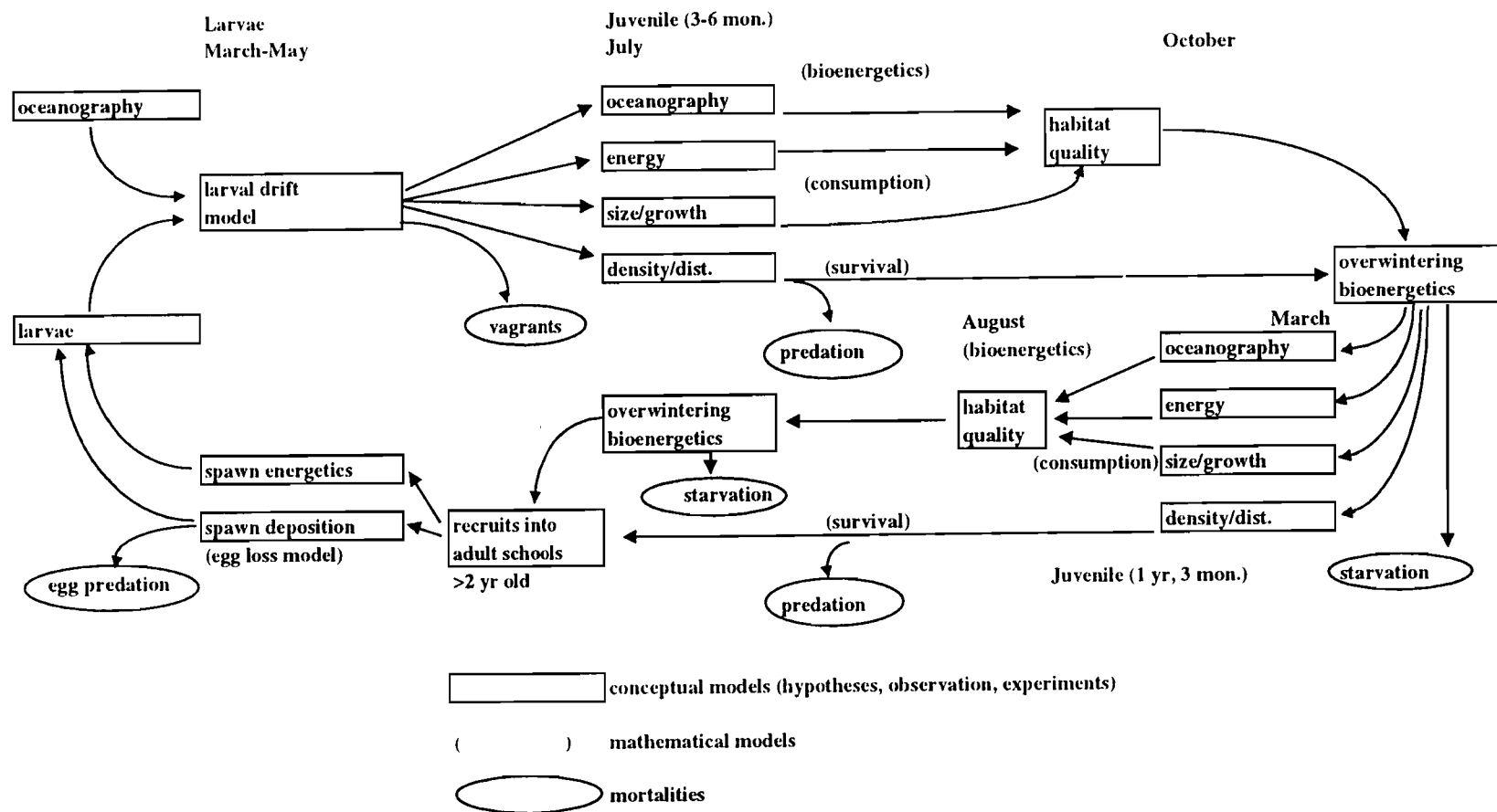


Figure 1. Herring Recruitment Model

SEA Herring Survival-Growth Sampling Design

7 day survey of Prince William Sound

Oct. 95 to Mar 98

	800	1600	2400	
Eaglek Bay				AWL, energetics, aerial survey
Whale Bay				AWL, energetics, aerial survey
Zaikof Bay				AWL, energetics, aerial survey
Simpson Bay				AWL, energetics, aerial survey

Sample Unit

Biological Factors		Environmental factors	
Y1	YOY herring	X1	Simpson/Hunter parameter
Y2	age 1 herring	X2	salinity
Y3	age 2 herring	X3	temperature
Y4	mature herring	X4	bathymetry
Y5	larval herring	X5	light intensity
Y5	juvenile pollock	X6	freshwater input
Y6	adult pollock	X7	tidal cycle
Y7	other species	X8	light
Y8	zooplankton		
Y9	jellyfish		
Y10	predators		

Y = dependent or independent variable

X = independent variable

Figure 2. 4-bay diel sampling design.

Appendix I

Stokesbury, K. D. E., J. Kirsch, E. D. Brown, G. L. Thomas, B. L. Norcross. 1998.
Seasonal variability in Pacific herring (*Clupea pallasii*) and walleye pollock (*Theragra
chalcogramma*) spatial distributions in Prince William Sound, Alaska. For submission to
Marine Ecology Progress Series.

Seasonal variability in Pacific herring (Clupea pallasii) and walleye pollock (Theragra chalcogramma) spatial distributions in Prince William Sound, Alaska.

Kevin D. E. Stokesbury¹

¹Institute of Marine Science,
University of Alaska-Fairbanks,
Fairbanks, Alaska, 99775-7220
Telephone: (907) 474-5184; Fax: (907) 474-1943
email: kstokes@ims.alaska.edu

Jay Kirsch²

²Prince William Sound Science Center
P.O. Box 705, Cordova, AK, 99574

Evelyn D. Brown¹

Gary L. Thomas²

Brenda L. Norcross¹

ABSTRACT: Pacific herring, Clupea pallasii, and walleye pollock, Theragra chalcogramma, spatial distributions were determined using acoustic surveys, with supporting net collections, in October 1995, March and July 1996 in Prince William Sound, Alaska. Of the 97 species of fish and macroinvertebrates collected, Pacific herring (65.0%) dominated the nearshore ichthyofauna, followed by walleye pollock (19.2%), Pacific sand lance (Ammodytes hexapterus; 2.6%), and capelin (Mallotus villosus; 1.9%). The Pacific herring population size structure was trimodal representing age 0, 1 to 2 year old, and adult fishes. The walleye pollock population size structure was bimodal representing age 0 and adult fishes. Large scale distributions of Pacific herring and walleye pollock were contagious, with aggregations occurring in the east-northeast and the west-southwest areas of the Sound. Pacific herring occupied the upper 30 m of the water column while walleye pollock were usually located near the bottom. Bays appeared to be nursery areas as age 0 and 1 to 2 Pacific herring were aggregated within them during all surveys. After their second winter juvenile herring joined the adult schools, leaving the bays at approximately the same time that new recruits enter the bays. Adult Pacific herring migrated seasonally, overwintering in Zaikof Bay and spending the summer in the west-southwest portion of the Sound.

Key words: Pacific herring, Clupea pallasii, walleye pollock, Theragra chalcogramma, acoustics, spatial distribution, nursery area, migration, size distribution, oil spill

Introduction

An organism's life history is its response to physical and biological variables allowing it to persist in a specific geographic area over time (Sinclair 1988). In Prince William Sound, Alaska, the Pacific herring (*Clupea pallasii* Valenciennes, 1847) population crashed in 1993 (Funk 1994, Paine et al. 1996). Prince William Sound contains a biologically rich, high latitude ecosystem and little is known of the physical and biological variables influencing Pacific herring life history (Paine et al. 1996). This lack of information confounded the identification of damage caused by the 24 March 1989 Exxon Valdez oil spill (36,000 metric tons of north Slope crude oil effecting 900 km of coast line in PWS), commercial fisheries (bait, sac-roë, and roë on kelp) and estimates of the population's recovery time (Paine et al. 1996, Spies et al. 1996). This is the second pulse perturbation effecting Prince William Sound's marine community in 34 years, the 27 March 1964 earthquake raised sections of the coast line by as much as 3 m (Hansen & Eckel 1971). A third pulse perturbation may be occurring with this year's large El Nino. Fish communities in other highly perturbed systems have shifted their species composition and abundance to new equilibrium levels, for example large sand eel, pollock and eel pout populations replaced herring and mackerel populations in the North Sea due to high fishing mortality on the latter species (Andersen & Ursin 1978, Auster 1988). Walleye pollock (*Theragra chalcogramma* Pallas, 1814) may be a competitor and predator of Pacific herring and may have filled the vacancy in the nearshore ecosystem that occurred due to the decrease in herring density (Willette et al. 1997).

Pacific herring usually begin to spawn in their third year when they have reached a size of about 185 mm and a weight of 95 g (Robinson 1988). Females can produce as many as 40,000 eggs each year until they reach an age of about 15 years (Robinson 1988). Pacific herring deposit their eggs in mid-April in the nearshore low intertidal or subtidal zone, primarily on marine vegetation (Wespestad & Moksness 1990, Brown et al. 1996). In early May, after approximately 2 weeks, the eggs hatch into larval herring. They metamorphose from the larval to juvenile form when they reach a size of 25 mm to 30 mm, which can take from 4 to 10 weeks (Wespestad & Moksness 1990). During this time larvae are transported away from the spawning areas, although studies in British Columbia, Canada, have found significant densities remaining nearshore (Robinson 1988).

Walleye pollock, (*Theragra chalcogramma*) are an important commercial species in Alaskan waters and a primary forage fish for sea birds, marine mammals and fish (Clausen 1983, Hatch & Sanger 1992, Livingston 1993). Walleye pollock congregate and spawn in deep water in late March and April and the larvae occupy the upper 50 m of the water column in late May (Hinckley et al. 1991, Kendall et al. 1996). Walleye pollock metamorphose into juveniles in August and September (Hinckley et al. 1991, Kendall et al. 1996).

Acoustic estimates of fish abundance are frequently used for stock assessment and fisheries management but infrequently for ecological and life history studies (Thorne 1983a, Thorne 1983b, MacLennan & Simmonds 1991, Thomas 1992, Gunderson 1993, Misund 1997). Acoustic surveys estimating Pacific herring fishing stocks have been conducted from Alaska to California, but relatively few have been conducted in Prince William Sound (Thorne 1977a, Thorne 1977b, Trumble et al. 1982, Thorne et al. 1983, Thorne & Thomas 1990).

We examined seasonal variability in Pacific herring, *Clupea pallasii*, and walleye pollock, *Theragra chalcogramma*, spatial distributions in Prince William Sound, Alaska. We hypothesized that: 1. Pacific herring and walleye pollock were contagiously distributed and this distribution varied seasonally; 2. Pacific herring and walleye pollock occurred in different areas of the water column; 3. cohorts (age/size) of Pacific herring were spatially segregated; 4. juvenile Pacific herring aggregated in bays rather than passages or along open coastline. To test these hypotheses we determined the spatial distributions of Pacific herring age cohorts and walleye pollock observed during three acoustic surveys of the Prince William Sound coastline in October 1995, March and July 1996.

Material and Methods.

Prince William Sound is a large body of water separated from the Gulf of Alaska by a series of mountainous islands and deep passages (Fig. 1). The rocky coastline is highly irregular with numerous islands, passages, bays and deep fjords. The Sound has a semi-diurnal tide with a maximum range 4.4 m during this study.

The Prince William Sound coastline was acoustically surveyed in October 1995, March and July 1996 (Fig. 1). Five vessels were used during each 10 day survey (12 hours per day); three commercial fishing vessels (≈ 16.8 m) which deployed the acoustic and oceanographic equipment and fished the seines, a trawler (Alaska Department of Fish and Game R/V *Pandalus*, ≈ 20 m trawler), a cruise vessel (≈ 25 m) where the samples were processed. Surveys were conducted during the night (2000 to 0800 h) in October 1995 and March 1996 and in daylight (0800 to 2000 h) during July 1996.

The acoustic vessel followed a zig-zag pattern along the shore to a distances of ≈ 1 km at a speed of 14 to 17 km h⁻¹. The vessels sonar (50 KHz, 46°) was used to locate schools along the transect. When a school of fish was encountered the acoustic vessel slowed to 9 to 11 km h⁻¹ and completed a series of parallel transects perpendicular to shore using a 120 kHz BioSonics 101 echosounder with a preamplifier dual-beam transducer. The transducer was mounted on a BioSonics 1.2 m BioFin and towed ≈ 1 m under the water surface. The acoustic signals were processed in real-time using the BioSonics ESP 221 Echo square integration software and ESP 281 Dual beam software, and stored on digital audio tape (Thorne 1983a, Thorne 1983b, MacLennan & Simmonds 1991). The acoustic system was calibrated both with a hydrophone and a standard target. Parameters of the acoustic system during the surveys were: source level = +225.023 dB; receiver gain = -159.28 dB; transducer directivity = 0.00107 and pulse duration = 0.4 ms. The signal to noise ratio exceeded that required to estimate the minimum fish densities. The acoustic survey vessel used a GPS navigational system, and coordinates were imported by the ESP software and C-MAP software to plot the survey tracks.

Once the acoustic vessel surveyed a fish school, one of three fishing vessel sampled it to determine species composition and size structure. Fish were sampled using a modified bottom trawl for deep water targets (1.52 x 2.13 m Nor'Eastern Astoria V trawl doors, head rope 21.3 m, foot rope 29.0 m, estimated 3 x 20.0 m mouth, 10.2 cm mesh wings, 8.9 cm middle and a 32.0 mm cod end liner), an anchovy seine for surface schools (250.0 x 34.0 m and 20.0 m, 25.0 mm stretch mesh) or, in shallow water, a small salmon fry seine (50.0 x 8.0 m, 3.0 mm stretch mesh deployed from a 6m skiff equipped with a 70 horsepower engine). Each collection was speciated and 1000 herring, or other dominant fish species in the catch, were randomly subsampled. Fork length (mm) and weight (g) were recorded

from 450 herring and remaining fish were measured to fork length. Seine collections were often very large, therefore once the subsample had been collected the remaining fish were released unharmed.

A length dependent scaling constant was used to convert the reflected acoustic energy into a biomass estimate:

$$TS_{re:w} (dB_{re:kg}) = -6.0 \log x - 24.2 \text{ dB}$$

where x is the mean fork length (cm) of the fish caught in the area (Thorne 1977b, Thorne 1983a, Thorne 1983b, Thorne & Thomas 1990). This equation differs from the more standard regression equation calculated by Foote (1987) as it derives the target strength as a proportion of weight. It was developed for echo integration primarily using Pacific herring surveys from Alaska and Puget Sound (Thorne 1983a). However, Thorne's equation was unsuitable for estimating walleye pollock target strength, due to the fish's morphology, therefore the more standard equation:

$$TS = 20 \log x - 66.0 \text{ dB}$$

was used (Foote & Traynor 1988, MacLennan & Simmonds 1991).

Echo integration measurements were converted into data cells with 120 to 40 m, 40 m or 20 m lengths (estimated from 2 ping s^{-1} with a surveying speed of 2.5 to 3.0 $m s^{-1}$ equals 60 or 32, 32, 16 pings $cell^{-1}$ respectively) and 1 m widths and depths, during the October 1995, March 1996, and July 1996 surveys, respectively. Latitude and longitude were recorded simultaneously with each data cell from the GPS. The acoustic files were transferred to a UNIX work station for batch processing. Software created in the Interactive Data Language (IDL) was used to apply the acoustic calibrations and enabled interactive image editing to remove untraced bottom and other non-biological scatter.

Species proportion and size modes per species were determined from the fish collections. The species proportions, based on the number individuals per fish species in the random subsample, were converted to biomass using length/weight regressions. Using these proportions the echo integration densities ($kg m^{-3}$) were converted into number of Pacific herring per size mode, or number of Walleye pollock. Walleye pollock were not divided into size modes because the standard deviations of the mean fork lengths for individual collections indicated that aggregations were primarily a single size mode. Based on frequency distributions of the data we assumed that cells containing the equivalent of $<0.5 \text{ fish } m^{-3}$ were probably zooplankton, so they were removed from the data set (MacLennan & Simmonds 1991, Gunderson 1993). Fish located near the bottom were difficult to distinguish acoustically, so if the signal appeared to be corrupted the bottom 5 m were removed. Visual examination of the echograms and fish collections agreed with these assumptions.

The hypotheses that Pacific herring and walleye pollock were contagiously distributed, were spatially segregated, and that Pacific herring cohorts (age/size) were spatially segregated were tested by determining the large scale spatial distributions of herring size modes, calculated from fork length frequencies, using circular statistics (Batschelet 1981). The angle (0° = true north) for each data cell, within each herring size mode, was determined from an origin in the center of Prince William Sound ($60^\circ 60.00'$, $146^\circ 90.00'$; Fig. 1). These angles represent distributions along the transect line and are influenced by inequalities in shore line distance and sampling bias. These angle frequency distributions were compared to random distributions and to the distributions of other

herring size modes along the same transect using a chi-squared test at the 5 % levels of significance (Batschelet 1981). Expected values were grouped according to Cochran's rule, which states that <20% of the expected frequencies should have a value <5 (Sokal & Rohlf 1981).

The hypothesis that juvenile herring aggregated within bays was tested by examining the relationship between the spatial distributions of herring and distances from shore. A group of data cells was considered to be a fish school if the sum of the differences between latitudes and longitudes of adjacent cells was $>0.009^\circ$. Visual examination of the echograms and plots of cells along transects supported this assumption. Bays were statistically defined from passages or open coast line by creating a parameter that is the sum of the three nearest shore distances ($\Sigma 3\text{NSD}$), each separated by 90° . This measurement was calculated at 12 bays and along 2 passages, 26 inside bays and 17 outside bays, to verify that it accurately defined bays, passages, and open coast line. The $\Sigma 3\text{NSD}$ for each herring school within each size mode was calculated and compared to the same measurements from randomly selected points along the transect for the three surveys using a chi-squared test. Expected values were grouped according to Cochran's rule (Sokal & Rohlf 1981). This technique corrected sampling and shoreline structure biases, for example 80 % of the shoreline may have been in bays or we may have surveyed bays more than open coastline or passages. Further to determine if there were physical differences in water mass and larval fish community structure at these locations vertical water profiles measuring temperature and salinity at 1 m intervals, using a SeaBird instrument, and two tucker trawl samples (1 m² mouth, 505 μ mesh nets) were collected at each of these sites. Tucker trawl samples were preserved in 10% formalin for >48 h, then transferred to 50% isopropyl alcohol and sorted to species and measured in the laboratory.

Results.

Ninety-seven species of fish and macroinvertebrates were collected during October 1995, March and July 1996 surveys. Pacific herring (*Clupea pallasii*; 65.0%) dominated the ichthyofauna; followed by walleye pollock (*Theragra chalcogramma*; 19.2%), Pacific sand lance (*Ammodytes hexapterus* Pallas, 1814; 2.6%), and capelin (*Mallotus villosus* Muller 1776; 2.0%) (Table 1). Pacific herring and walleye pollock were collected in all fishing gear during each survey while the majority of capelin and Pacific sand lance were collected in seines during March and July 1996, respectively (Table 1).

The Pacific herring population consisted of three size modes representing age 0, 1 - 2 year old, and adult fishes (Fig. 2). In October 1995 the first mode (0-110 mm) were the 5 months old 1995 cohort, the second mode (111 - 180 mm) were the 1 year 5 month old 1994 cohort and the third mode are mature adults. The March 1996 the first mode (0-120 mm) were the 10 months old 1995, the second mode (121 - 180 mm) were the 1 year 2 month old 1994 cohort and the third mode are mature adults. In July 1996 the first mode (0-80 mm) were the 3 months old 1996 cohort, the second mode (81 - 160 mm) were the 1 year 3 month old 1995 cohort and the 1994 cohort moved into the adult mode. The walleye pollock population was bimodal representing age 0 and adult fishes, in October 1995 and March 1996 while only age 0 fish were collected during July 1996 (Fig. 3).

Pacific herring and walleye pollock were contagiously distributed within Prince William Sound (Fig. 4). The general distribution of both species was bimodal with aggregations occurring in the east-northeast and the west-southwest (Fig. 1 and 4).

Location of age 0 and 1 - 2 herring and walleye pollock aggregations were relatively similar within this bimodal distribution during each survey (Fig. 4). Adult herring appeared to be aggregated in the southwest (210° - 240°) in October 1995, in the south (180°) and east (90°) in March 1996, and west (240° - 270°) in July 1996 (Fig. 4).

The distributions of the three size modes of Pacific herring differed from each other and from walleye pollock in October 1995, March, and July 1996 (Table 2; Fig. 4). Age 0 herring had a similar distribution to age 1 - 2 herring in October 1995 but differed in March and July 1996 (Table 2; Fig. 4). Age 0 herring distribution always differed from adult distribution (Table 2; Fig. 4). Age 1 - 2 and adult herring distributions were similar in March 1996 but differed during the other two surveys (Table 2; Fig. 4). Walleye pollock distribution differed from all three herring size mode distributions combined and from each size mode except for Age 0 herring in March 1996 (Table 2; Fig. 4).

Pacific herring schools had the lowest densities for all size modes in March 1996 and the highest densities in July 1996 (Table 3). Pacific herring schools had the highest average number of data cells in March 1996 (Table 3). Walleye pollock schools had low densities in October 1995 and March 1996 compared to very dense schools in July 1996 (Table 3).

Pacific herring were primarily distributed top half of the water column. Pacific herring were deeper in the water column in March 1996 (27.0 - 28.9 m) than in October 1995 (15.0 - 20.2 m) and July 1996 (14.1 - 16.7 m) which were similar (Table 4). Walleye pollock were distributed near the bottom during all three surveys (Table 4). There appeared to be little vertical overlap between Pacific herring and walleye pollock as the mean depths were separated by >29 m of water during all surveys (Table 4).

The proportion of herring schools consisting of a single size cohort varied among seasons. In October 1995, 49.0% of the herring schools sampled with the nets consisted of a single size class, primarily age 0 (21 schools of the 55 schools sampled). In March 1996, 38.9% of the herring schools sampled with the nets consisted of a single size, primarily age 1 - 2 (14 schools of the 72 schools sampled). In July 1996, 83.3% of the herring schools sampled with the nets consisted of a single size, primarily age 1-2 (21 schools of the 30 schools sampled).

The 26 sites located within the 12 bays had a mean $\Sigma 3\text{NSD}$ value of 3.8 km ($\text{SD} = 2.45$) which was significantly smaller than 9.8 km ($\text{SD} = 6.69$) for the 17 sites located in passages and along open coast line ($t\text{-test} = -3.61$, $\text{df} = 41$, $p < 0.001$, log transformed). The water conditions within bays generally differed from conditions in passages and along open coastlines (Table 5). The surface water temperatures (0 - 30 m) were colder inside than outside the bays by 0.32°C and 0.20°C in October 1995 and July 1996, respectively. The surface water inside the bays was also more saline in October 95 (0.52‰) but were similar inside and outside the bays in deeper water (31-60 m) and throughout the water columns in July 1996 (Table 5). Conversely, the water columns inside the bays were warmer than outside the bays by 0.08°C (0 - 30 m) and 0.28°C (31 - 60 m) in March 1996. Surface water salinities were similar but deeper waters (31-60 m) had higher salinities inside bays (0.284‰) in March 1996.

Greater numbers of Pacific herring larvae were collected inside the bays (CPUE 1 minute tow mean = 3.2, $\text{SD} = 11.39$) than in passages or along open coastline (mean = 0.21, $\text{SD} = 0.68$), (Mann-Whitney rank sum test $T = 980$, $p = 0.01$). Pacific herring larvae

were similar in length, with a mean of 13.6 mm (SD = 4.52) inside the bays and a mean of 13.4 mm (SD = 3.04) in passages and open coastline ($T = 1103$, $p = 0.66$).

Pacific herring and walleye pollock $\Sigma 3NSD$ distributions differed from randomly calculated $\Sigma 3NSD$ distributions during all three surveys. In October 1995, age 0 and 1 herring aggregated at the heads of bays with $\Sigma 3NSD$ values (<3 km) below the mean bay value (3.8 km). Adult herring were aggregated in passages or along open coastline with $\Sigma 3NSD$ values (>11 km) above the mean value calculated from sites outside of the bays (9.8 km; Table 6). Walleye pollock distribution was also significantly aggregated within bays but not as tightly as age 0 and 1 herring (Table 6). In March 1996, all size modes of Pacific herring and walleye pollock had greater than expected $\Sigma 3NSD$ values ranging between 4 and 10 km (Table 7). In July 1996, age 0 herring aggregated tightly into the heads of bays (57.1% of $\Sigma 3NSD < 1$ km). Age 1 herring were also aggregated at the head of bays (<2 km). Adult herring were aggregated within bays (< 2 km) but also more than expected had $\Sigma 3NSD$ values of 6 to 7 km. Walleye pollock were tightly aggregated within bays with the majority of $\Sigma 3NSD$ values < 3 km (Table 8).

Discussion.

The near shore ichthyofauna structure of Prince William Sound consisted of a few common species and a large number of relatively rare species. Pacific herring, Clupea pallasii, was the most abundant annual resident followed by walleye pollock, Theragra chalcogramma.

The size distribution of Pacific herring in Prince William Sound was trimodal with a strong annual mode during the juvenile phase, similar to Atlantic herring distributions. Atlantic herring complete 75 % of their somatic growth by the time they reach first maturity (Cushing 1967). Walleye pollock distribution was bimodal indicating a separation between the young of the year and mature fish. Walleye pollock feed year round and continue to grow after reaching sexual maturity (Clausen 1983, Livingston 1993).

Pacific herring and walleye pollock were aggregated in the east-northeast and west southwest areas of Prince William Sound. The cause of this distribution is unclear. This distribution may partially be explained by sampling bias. The southeast area were only surveyed during the July 1996 cruise. However the northwest area was thoroughly surveyed during all three cruises. Age 0 and 1-2 Pacific herring aggregations remained relatively constant within the bimodal distribution during all three surveys. Adult Pacific herring distribution appeared to shift seasonally from the east in March to the west in July.

The largest aggregations of walleye pollock occurred in the southern portion of Prince William Sound. This school partially dispersed in March when pollock were more evenly distributed throughout the Sound. The majority of age 0 pollock were collected in the east and in the south west in July 1996 and appeared to be spatially and temporally segregated from adult pollock. This segregation probably results from the strong cannibalistic behaviour of adult walleye pollock preying on age 0 pollock (Livingston 1993).

Our estimates of Pacific herring and walleye pollock school densities are dependent on the applied target strength equations. This is a limitation of acoustic surveys as many physical and biological variables effect target strength including, fish orientation, depth, fat content, gonadal development, vertical avoidance reaction, and morphology of the fish

(Thorne 1983b, Foote 1987, Rose & Leggett 1988, Thorne & Thomas 1990, MacLennan & Simmonds 1991, Misund et al. 1995, Huse & Ona 1996, McClatchie et al. 1996, Ona & Mitson 1996, Misund 1997).

Thorne's target strength equation differs from equations calculated for Atlantic herring (MacLennan & Simmonds 1991), however, our estimates of Pacific herring density (means ranging from 0.51 to 9.15 fish m^{-3}) were similar to many herring density estimates measured using similar techniques, for example Atlantic herring densities in a fjord in northern Norway ranging from 0.3 to 5.0 fish m^{-3} (Misund & Floen 1993) and in the North Sea from 2.94 to 6.68 fish m^{-3} (Misund et al. 1995). Our density estimates do not agree well with the theoretical density of schooling fish (volume = 0.7 herring body length³) (Pitcher & Partridge 1979, Pitcher & Parrish 1993). However, in the wild large variations in herring density occur within schools (Misund & Floen 1993) and between schools (Blaxter & Hunter 1982).

The number, density, age and depth of schools of Pacific herring varied seasonally. Pacific herring were tightly aggregated forming fewer, denser schools of a single size cohort near the surface in July. This pattern began to deteriorate in October when schools were slightly less cohesive, and at approximately the same depth. However, the number of schools increased, the number of data cells making up each school decreased and the majority of schools were made up of mixed age cohorts. Pacific herring formed many schools with low densities, and mixed size cohorts, in deeper water (<1 fish m^3 for herring), in March. The October and March surveys were conducted during the night while the July survey was conducted during daylight. Clupeid distribution is strongly effected on a short temporal scale by the diel (day/night) cycle (Blaxter & Hunter 1982, Scott & Scott 1988, Stokesbury & Dadswell 1989, Huse & Ona 1996). However, these observation appear to reflect the conditions in the natural habitat and are therefore comparable to each other because in this northern latitude there is very little daylight in March and practically no darkness during July.

The seasonal difference in the structure of herring schools may result from the availability of food, the physical condition of the fish, and the threat of predation. The inter-fish distance within schools increases with hunger, reducing cohesion, and causing lower mean densities (Robinson 1995). Competition within schools for food is reduced with independent and segregated behavior (Robinson & Pitcher 1989). Fish also increase their chance of encountering food by breaking into small groups or by reducing shoal compactness, thereby increasing the schools foraging area (Robinson 1995). In March herring appeared to be spreading out forming low density aggregations covering large areas. These herring have just survived the winter when prey abundance is minimal and the risk of starvation is high (Paul & Paul 1997, Paul et al. 1997).

The number, density and depths of schools of walleye pollock varied seasonally. Walleye pollock were highly aggregated forming fewer, very dense schools in July and many, low density schools in October and March. Walleye pollock schools were always deep in the water column, near the bottom, and probably less influenced by light conditions. This seasonal variation maybe related to different phases of the life cycle. The walleye pollock collected in July were age 0 and their dense schools seemed to be associated with large jellyfish, Aurelia aurita, aggregations. Large jelly fish, Cyanea capillata, were also frequently seen with several gadids, possibly walleye pollock,

continuously associated with them. The October and March pollock collections were larger juveniles or adult fish, were not associated with jelly fish, and seemed to be pre and post spawning aggregations, respectively.

Pacific herring and walleye pollock distributions were roughly similar, both were bimodal with high concentrations occurring in the northeast and southwest. However, there appeared to be little overlap as they occupied different portions of the water column, Pacific herring in surface waters and walleye pollock near the bottom. Further their morphologies and behavior are different. Therefore competition for prey between these species seems unlikely.

Bays in Prince William Sound appeared to be nursery areas for age 0 and 1 Pacific herring. Larval Pacific herring aggregated within bays in July just prior to metamorphosing into juveniles. Larval herring depend on their transparency to escape detection and capture by visual predators (Batty 1989, Gallego & Heath 1994). The ontogenetic changes from the larval to juvenile body morph (body length 31 - 38 mm) require switching to a different antipredator strategy and this is a critical period in terms of vulnerability to predation (Gallego & Heath 1994). As juvenile herring develops its camouflage of guanine reflecting platelets under the scales and black dorsum they also fill their swim bladder and bullae with air (Blaxter 1985). The coupling of the bullae and head lateral line allows herring to detect range as well as direction of sound source and is indispensable to forming and maintaining the schools (Blaxter et al. 1981, Blaxter 1985, Gallego & Heath 1994). Schooling becomes the herring's primary defense against predation for the remaining portion of its life cycle (Blaxter & Hunter 1982).

Age 0 herring were very tightly aggregated near the shore in shallow water at the heads of bays in July. This distribution continued through October but in March the schools had moved away from the shores, into deeper water, however they still remained within the bays. The age 1 herring were also aggregated into tight schools in shallow water near the heads of bays during July and October and dispersed into a scattered layer in March. After their second winter within these bays the juvenile herring appear to join the adult schools leaving the bays at approximately the same time as the new recruits enter the bays (in June-August).

There appears to be a physical difference in the water conditions within bays compared to the open Sound. In October 1995 and July 1996 water temperatures in the upper 30 m were cooler inside these bays than in the open Sound. In March this pattern was reversed and waters were warmer within the bays. What effect this has on juvenile herring metabolic rate is unclear. Juvenile herring require a critical amount of energy to survive the winter (Paul & Paul 1997, Paul et al. 1997) and there may be an advantage to overwintering in cooler waters. The effect these water conditions have on zooplankton production is also unclear. Juvenile herring tightly aggregating near the shore may be feeding on prey associated with the nearshore algae or using the algae as a shelter from predation. Other juvenile species utilize near shore algae in a similar manor (Rangeley & Kramer 1995a, Rangeley & Kramer 1995b). The shift to deeper water away from the shore in March may result from increased food supply being transported into these bays. Adult Pacific herring appear to seasonally migrate within Prince William Sound. A large school of adult herring was observed in Zaikof Bay in March 1996. Large adult schools have traditionally been observed and fished in this bay and a similar large school was observed

here in 1997 (author's unpublished data). These adults moved out of Zaikof Bay and spawned in the Green Island - Stockdale harbor area in April (John Wilcox, personal communication; Alaska Department of Fish and Game, Cordova). We observed them during the summer months feeding from the lower part of Green Island to the southern part of the Sound, in Latouche and Elrington Passages. There appears to be a great deal of food in this region as the waters leaving Prince William Sound mix with the Gulf of Alaska current. Large schools of Pacific sand lance, large flocks of foraging sea birds and many marine mammals were also observed here during July 1996. The adult herring then migrate back towards Zaikof and are in the Green Island area in late October, as we observed in 1995. The bait fishery traditionally occurs in this area in late October-early November, and occurred in 1996 and 1997 (John Wilcox, personal communication; Alaska Department of Fish and Game, Cordova).

The predictability in temporal and spatial distributions of herring populations in tidally energetic systems has contributed to overfishing (Sinclair et al. 1985). Further, herring do not exhibit the classic signs of overfishing, i.e. a decline in the catch per unit effort and a loss of larger fish. The dual characteristics of homing to natal spawning areas and larval retention severely restrict the ability of one spawning population to repopulate neighboring spawning areas that have been disrupted by overfishing or a major perturbation (Iles & Sinclair 1982, Sinclair et al. 1985, Sinclair 1988). It is therefore critical to determine the seasonal variability in spatial distributions of each phase of the Pacific herring life cycle in Prince William Sound to determine the potential for recovery of the population and its role in the ecosystem and effective future management.

Acknowledgments We thank R. Foy, M. McEwen, S. Gay and L. Tuttle for assistance with field collections. N. Peters and G. Steinhart assisted in collecting and processing the acoustic data. M. Frandsen assisted with larval fish identification. S. Moreland and M. Vallerino assisted with data analyses. We also thank the captains and crews of the F/V Temptation, F/V Miss Kayley, F/V Kyle David, M/V Pacific Star, F/V Pagan, R/V Pandalus and the Alaska Department of Fish and Game, Cordova, for their help and insights on Prince William Sound. This project was funded by the Exxon Valdez Oil Spill Trustee Council through the Sound Ecosystem Assessment (SEA) project. However the findings presented by the authors are their own and not necessarily the Trustee Council position.

LITERATURE CITED

- Andersen KP, Ursin E (1978) A multispecies analysis of the effects of variations of effort upon stock composition of eleven North Sea fish species. ICES Rapp Proc-Verb 172:286-291
- Auster PJ (1988) A review of the present state of understanding of marine fish communities. Northw Atl Fish Sci 8:67-75
- Batschelet E (1981) Circular statistics in biology. Academic Press, London
- Batty RS (1989) Escape responses of herring larvae to visual stimuli. J Mar Biol Assoc UK 69:647-654
- Blaxter JH, Denton EJ, Gray JAB (1981) Acoustico-lateralis system in clupeoid fishes. In: Tavalga WN, Popper AN, Fay RR (ed) Hearing and sound communication in fishes. Springer-Verlag, New York, p39-59
- Blaxter JHS (1985) The herring: a successful species? Can J Fish Aquat Sci 42 (Suppl. 1):21-30
- Blaxter JHS, Hunter JR (1982) The biology of clupeoid fishes. Adv Mar Biol 20:1-223
- Brown ED, Baker TT, Hose JE, Kocan RM, Marty GD, McGurk MD, Norcross BL, Short J (1996) Injury to the early life history stages of Pacific herring in Prince William Sound after the Exxon Valdez oil spill. Am Fish Soc Symp 18:448-462
- Clausen DM (1983) Food of walleye pollock, Theragra chalcogramma, in an embayment of southeastern Alaska. Fish Bull 81:637-642
- Cushing DH (1967) The grouping of herring populations. J mar biol Ass U K 47:193-208
- Foote KG (1987) Fish target strengths for use in echo intergrator surveys. J Acoust Soc Am 82:981-987
- Foote KG, Traynor JJ (1988) Comparison of walleye pollock target strength estimates determined from in situ measurements and calculations based in swimbladder form. J acoust Soc Am 83:9-17
- Funk F (1994) Preliminary summary of 1994 sac roe herring fisheries. Alaska Dept. Fish & Game, Juneau
- Gallego A, Heath MR (1994) The development of schooling behavior in Atlantic herring Clupea harengus. J Fish Biol 45:569-588
- Gunderson RD (1993) Surveys of Fisheries Resources. John Wilet & Sons, Inc., New York
- Hansen WR, Eckel EB (1971) Setting and effects of the earthquake. In: The great Alaska earthquake of 1964. National Academy of Science
- Hatch SA, Sanger GA (1992) Puffins as samplers of juvenile pollock and other forage fish in the Gulf of Alaska. Mar Ecol Prog Ser 80:1-14
- Hinckley S, Bailey KM, Picquelle SJ, Schumacher JD, Stabeno PJ (1991) Transport, distribution, and abundance of larval and juvenile walleye pollock (Theragra chalcogramma) in the western Gulf of Alaska. Can J Fish Aquat Sci 48:91-98
- Huse I, Ona E (1996) Tilt angle distribution and swimming speed of overwintering Norwegian spring spawning herring. ICES J mar Sci 53:863-873
- Iles TD, Sinclair M (1982) Atlantic herring: stock discreteness and abundance. Science 215:627-633
- Kendall AWJ, Schumacher JD, Kim S (1996) Walleye pollock recruitment in Shelikof Strait: applied fisheries oceanography. Fish Oceanogr 5 (Suppl. 1):4-18

- Livingston PA (1993) Importance of predation by groundfish, marine mammals and birds on walleye pollock Theragra chalcogramma and Pacific herring Clupea pallasii in the eastern Bering Sea. *Mar Ecol Prog Ser* 102:205-215
- MacLennan DN, Simmonds EJ (1991) *Fisheries Acoustics*. Chapman & Hall, London
- McClatchie S, Alsop J, Coombs RF (1996) A re-evaluation of relationships between fish size, acoustic frequency, and target strength. *ICES J mar Sci* 53:780-791
- Misund OA (1997) Underwater acoustics in marine fisheries and fisheries research. *Rev Fish Biol Fisher* 7:1-34
- Misund OA, Aglen A, Fronaes E (1995) Mapping the shape, size, and density of fish schools by echo integration and a high-resolution sonar. *ICES J mar Sci* 52:11-20
- Misund OA, Floen S (1993) Packing density structure of herring schools. *ICES mar Sci Symp* 196:26-29
- Ona E, Mitson RB (1996) Acoustic sampling and signal processing near the seabed: the deadzone revisited. *ICES J mar Sci* 53:677-690
- Paine RT, Ruesink JL, Sun A, Soulanille EL, Wonham MJ, Harley CDG, Brumbaugh DR, Secord DL (1996) Trouble on oiled waters: lessons from the Exxon Valdez oil spill. *Annu Rev Ecol Syst* 27:197-235
- Paul AJ, Paul JM (1997) Comparisons of whole body energy content of captive fasting age zero Alaskan Pacific herring (Clupea pallasii Valenciennes) and cohorts overwintering in nature. *J Exp Mar Biol Ecol* 000:000-000 in press
- Paul AJ, Paul JM, Brown ED (1997) Fall and spring somatic energy content for Alaskan Pacific herring (Clupea pallasii Valenciennes 1847) relative to age, size and sex. *J Exp Mar Biol Ecol* 000:000-000 in press
- Pitcher TJ, Parrish JK (1993) Functions of shoaling behavior in teleosts. In: Pitcher TJ (ed) *Behavior of teleost fishes*. Chapman & Hall, New York, p363-439
- Pitcher TJ, Partridge BL (1979) Fish school density and volume. *Mar Biol* 54:383-394
- Rangeley BW, Kramer DL (1995a) Tidal effects on habitat selection and aggregation by juvenile pollock Pollachius virens in the rocky intertidal zone. *Mar Ecol Prog Ser* 126:19-29
- Rangeley BW, Kramer DL (1995b) Use of rocky intertidal habitats by juvenile pollock Pollachius virens. *Mar Ecol Prog Ser* 126:9-17
- Robinson CJ (1995) Food competition in a shoal of herring: the role of hunger. *Mar Behav Physiol* 24:237-242
- Robinson CJ, Pitcher TJ (1989) Hunger motivation as a promoter of different behaviors within a shoal of herring: selection for homogeneity in fish shoal? *J Fish Biol* 35:459-460
- Robinson SMC (1988) Early life history characteristics of Pacific herring, Clupea harengus pallasii Valenciennes 1847, in the Strait of Georgia, British Columbia: hydrodynamics, dispersal, and analysis of growth rates. University of British Columbia, Ph.D. thesis, p 141
- Rose GA, Leggett WC (1988) Hydroacoustic signal classification of fish schools by species. *Can J Fish Aquat Sci* 45:597-604
- Scott WB, Scott MG (1988) Atlantic fishes of Canada. *Can Bull Fish Aquat Sci* 219:1-731
- Sinclair M (1988) Marine populations: an essay on population regulation and speciation. Washington Sea Grant Program, University of Washington Press, Seattle

- Sinclair M, Anthony VC, Iles TD, O'Boyle RN (1985) Stock assessment problems in Atlantic herring (Clupea harengus) in the Northwest Atlantic. *Can J Fish Aquat Sci* 42:888-898
- Sokal RR, Rohlf FJ (1981) Biometry - the principles and practice of statistics in biological research. Freeman, San Francisco
- Spies RB, Rice SD, Wolfe DA, Wright BA (1996) The effects of the Exxon Valdez oil spill on the Alaskan coastal environment. In: Rice SD, Spies RB, Wolfe DA, Wright BA (ed) Proceedings of the Exxon Valdez oil spill symposium. *Am Fish Soc Sympos.* 18:1-16
- Stokesbury KDE, Dadswell MJ (1989) Seaward migration of juveniles of three herring species, Alosa, from an estuary in the Annapolis River, Nova Scotia. *Can Field-Nat* 103:388-393
- Thomas GL (1992) Successes and failures of fisheries acoustics: an international, federal, and regional point of view. *Fish Res* 14:95-104
- Thorne RE (1977a) Acoustic assessment of hake and herring stocks in Puget Sound, Washington, and southeastern Alaska. In: ARM (ed) Hydroacoustics in fisheries research. *ICES Rap et Proc*, p265-278
- Thorne RE (1977b) A new digital hydroacoustic data processor and some observations on herring in Alaska. *J Fish Res Bd Can* 34:2288-2294
- Thorne RE (1983a) Assessment of population abundance by hydroacoustics. *Biol Oceanog* 2:253-262
- Thorne RE (1983b) Hydroacoustics. In: Nielsen LA, Johnson DL (ed) Fisheries techniques. *Am. Fish. Soc., Bethesda MD*, p239-259
- Thorne RE, Thomas GL (1990) Acoustic observations of gas bubble release by Pacific herring (Clupea harengus pallasii). *Can J Fish Aquat Sci* 47:1920-1928
- Thorne RE, Trumble R, Lemberg N, Blankenbeckler D (1983) Hydroacoustic assessment and management of herring fisheries in Washington and southeastern Alaska. *Fish Bull* 81:269-277
- Trumble R, Thorne RE, Lemberg N (1982) The Strait of Georgia herring fishery: a case of timely management aided by hydroacoustic surveys. *Fish Bull* 80:381-388
- Wespestad VG, Moksness E (1990) Observations on growth and survival during the early life history of Pacific herring, Clupea pallasii from Bristol Bay, Alaska, in a marine mesocosm. *Fish Bull* 88:191-200
- Willette M, Sturdevant M, Jewett S (1997) Prey resource partitioning among several species of forage fishes in Prince William Sound, Alaska. In: Forage fishes in marine ecosystems. Alaska sea grant program, AK-SG-97-01:11-29.

Table 1. Numbers of dominant fish species collected in Prince William Sound, Alaska in 1995 and 1996. The number of fish measured from seine collections are random subsamples (1000 individuals) of the total catch therefore the % reflect the subsample maximum.

		October 1995		March 1996		July 1996	
scientific name	common name	trawl	seine	trawl	seine	seine	%
<u>Clupea pallasii</u>	Pacific herring	1421	47803	11535	40588	22639	65.0
<u>Theragra chalcogramma</u>	walleye pollock	3308	13994	7319	3950	7929	19.2
<u>Ammodytes hexapterus</u>	Pacific sandlance		1		1	5000	2.6
<u>Mallotus villosus</u>	capelin		68	266	3406		2.0

Table 2. Clupea pallasii and Theragra chalcogramma. Chi-squared tests examining the polar angle distributions of the three size modes of Pacific herring and walleye pollock during three acoustic surveys of Prince William Sound, Alaska in 1995 and 1996; NS = no significant difference, $p > 0.05$.

	October 1995			March 1996			July 1996		
	df	χ^2	p =	df	χ^2	p =	df	χ^2	p =
herring age 0, 1 and adults	8	109	0.01	7	41.5	0.01	6	87.7	0.01
herring age 0 and 1	8	0.9	NS	7	20.9	0.01	6	18.2	0.05
herring age 0 and adults	8	85.0	0.01	7	40.1	0.01	6	87.9	0.01
herring age 1 and adults	8	80.8	0.01	7	9.7	NS	6	43.4	0.01
herring and pollock	8	227	0.01	7	65.8	0.01	6	240	0.01
herring age 0 and pollock	8	117	0.01	7	9.0	NS	4	90.2	0.01
herring age 1 and pollock	8	114	0.01	7	23.2	0.01	4	62.2	0.01
herring adults and pollock	7	29.6	0.01	7	31.7	0.01	6	67.1	0.01

Table 3 Clupea pallasii and Theragra chalcogramma. Estimated means and standard deviations (SD) of densities (fish m⁻³) and number of data cells for the three size modes of Pacific herring and walleye pollock aggregations observed during three acoustic surveys of Prince William Sound, Alaska in 1995 and 1996 (n = count).

	October 1995 fish m ⁻³			March 1996 fish m ⁻³			July 1996 fish m ⁻³		
	n	mean	SD	n	mean	SD	n	mean	SD
herring									
age 0	137	2.52	8.36	179	0.91	2.84	8	2.67	5.46
age 1	126	0.51	1.10	223	0.81	0.95	42	9.15	15.75
adult	54	1.35	3.21	147	0.51	0.95	32	3.62	0.86
pollock	119	3.14	8.68	148	4.20	14.59	31	267.87	72.05
k									
herring	cells (40-120 x 1m)			cells (40 x 1m)			cells (20 x 1m)		
age 0	137	15.55	39.58	179	22.50	65.11	8	98.25	155.28
age 1	126	13.77	37.42	223	25.00	82.82	42	31.55	85.97
adult	54	9.63	14.04	147	28.36	96.88	32	21.00	56.98
pollock	119	8.05	11.07	148	13.12	44.73	31	300.16	72.05
k									

Table 4 Clupea pallasii and Theragra chalcogramma. Estimated means and standard deviations (SD) of three size modes of Pacific herring and walleye pollock depth in the water column and sea bed depth during three acoustic surveys of Prince William Sound, Alaska in 1995 and 1996 (n = count).

depth of fish (m)									
	October 1995			March 1996			July 1996		
	n	mean	SD	n	mean	SD	n	mean	SD
herring									
age 0	2131	15.02	6.51	3675	27.48	15.82	780	14.14	9.38
age 1	1819	15.48	6.65	5463	27.04	13.83	1325	15.18	10.42
adult	520	20.24	7.72	4180	28.86	13.66	633	16.65	10.58
pollock	958	64.44	26.42	1942	57.88	25.27	6301	63.75	34.65
k									
bottom depth (m)									
herring									
age 0	2131	47.87	26.01	3420	47.08	20.69	723	34.49	21.62
age 1	1819	45.62	26.10	5016	47.46	19.46	1242	34.96	18.28
adult	520	45.96	24.95	4026	46.43	16.76	583	47.42	38.35
pollock	958	68.7	30.96	1872	63.09	22.46	5612	86.99	34.65
k									

Table 5 Mean and standard deviations (SD) of water columns inside bays and outside bays in passages and along open coastline during three surveys of Prince William Sound, Alaska in 1995 and 1996 (n = count). The Mann-Whitney rank sum test was used to determine differences between mean values (T).

water depth (m)			temperature (oC)			salinity (o/oo)		
		n	mean	SD		mean	SD	
October 1995								
0-30	inside	146	9.34	0.626	T=16135	28.77	1.111	T=18583
0-30	outside	180	9.66	0.821	p<0.001	29.29	1.063	p<0.001
31-60	inside	71	7.95	2.06	T=4212	30.62	0.749	T=8610
31-60	outside	186	9.87	0.393	p<0.001	30.36	0.21	p=0.303
March 1996								
0-30	inside	667	4.14	0.437	T=281130	31.65	0.225	T=305280
0-30	outside	509	4.06	0.357	p<0.001	31.66	0.219	p=0.320
31-60	inside	416	4.53	0.521	T=228192	31.83	0.106	T=209925
31-60	outside	512	4.25	0.344	p<0.001	31.80	0.106	p<0.001
July 1996								
0-30	inside	688	10.93	1.984	T=291730	28.98	1.772	T=287935
0-30	outside	480	11.10	1.569	p=0.049	29.09	1.642	p=0.194
31-60	inside	453	6.45	1.084	T=192162	31.02	0.479	T=213780
31-60	outside	492	6.94	1.238	p<0.001	31.08	0.265	p=0.911

Table 6. *Clupea pallasii* and *Theragra chalcogramma*. Chi-squared analysis comparing the percent frequency distributions of observed sum of the three near shore distances ($\Sigma 3NSD$) for Pacific herring and walleye pollock aggregations to values generated from a random distribution, during the October 1995 acoustic survey in Prince William Sound, Alaska; * $p < 0.05$, ** $p < 0.01$.

$\Sigma 3NSD$ (km)	Pacific herring (%)			walleye	
	age 0	age 1+	adult	pollock (%)	random (%)
1, 2	35.38	32.77	4.08	19.82	15.59
3	12.31	13.45	12.24	18.92	10.22
4	5.38	5.04	4.08	10.81	9.14
5	3.08	3.36	2.04	10.81	5.91
6	4.62	4.20	0.00	3.60	9.14
7, 8	3.08	3.36	2.04	1.80	9.14
9, 10, 11	3.85	4.20	6.12	7.21	6.45
12, 13, 14	14.62	15.13	26.53	3.60	5.91
15 - 18	3.08	2.52	6.12	3.60	6.99
19 - 23	6.92	7.56	16.33	4.50	5.91
24 - 28	3.08	3.36	8.16	5.41	5.38
29 - 35	1.54	1.68	4.08	5.41	5.38
>36	3.08	3.36	8.16	4.50	4.84
$\chi^2 =$	55.30**	51.41**	123.26**	25.16*	
df=	12	12	12	12	

Table 7. Clupea pallasii and Theragra chalcogramma. Chi-squared analysis comparing the percent frequency distributions of observed sum of the three near shore distances ($\Sigma 3NSD$) for Pacific herring and walleye pollock aggregations to values generated from a random distribution, during the March 1996 acoustic survey in Prince William Sound, Alaska; * $p < 0.05$, ** $p < 0.01$.

$\Sigma 3NSD$ (km)	Pacific herring (%)			walleye	random (%)
	age 0	age 1+	adult	pollock (%)	
1	7.74	8.00	3.10	3.13	11.18
2	22.58	20.00	17.83	15.63	26.71
3	18.71	18.86	17.83	21.09	18.01
4	14.84	15.43	16.28	14.06	9.32
5, 6	16.13	15.43	18.60	14.84	6.21
7 to 10	15.48	17.14	19.38	18.75	5.59
11,12,13	0.65	1.71	2.33	6.25	6.21
14 to 17	2.58	2.29	3.10	3.13	6.21
18 to 29	1.29	1.14	1.55	3.13	6.83
>30	0.00	0.00	0.00	0.00	3.73
$\chi^2 =$	53.68**	58.40**	84.55**	63.60**	
df=	9	9	9	9	

Table 8 Clupea pallasii and Theragra chalcogramma. Chi-squared analysis comparing the percent frequency distributions of observed sum of the three near shore distances ($\Sigma 3NSD$) for Pacific herring and walleye pollock aggregations to values generated from a random distribution, during the July 1996 acoustic survey in Prince William Sound, Alaska; * $p < 0.05$, ** $p < 0.01$.

3NSD (km)	Pacific herring			walleye	
	age 0	age 1+	adult	pollock (%)	random (%)
1	57.14	41.67	38.46	26.67	16.58
2	14.29	27.78	26.92	26.67	22.99
3	0.00	8.33	7.69	33.33	13.37
4	28.57	11.11	7.69	6.67	10.70
5	0.00	2.78	3.85	0.00	10.70
6,7	0.00	2.78	11.54	3.33	7.49
8,9,10	0.00	2.78	0.00	3.33	5.88
11 to 15	0.00	0.00	0.00	0.00	5.88
>16	0.00	2.78	3.85	0.00	6.42
$\chi^2 =$	182.17**	59.29**	52.18**	64.46**	
df=	8	8	8	8	

List of Figures.

1. Location of the October 1995 (solid line), March (dashed line) and July 1996 (dotted line) acoustic survey transects in Prince William Sound, Alaska; EP = Elrington Passage, LP = Latouche Passage, GI = Green Island, SH = Stockdale Harbor, ZB = Zaikof Bay; + was positioned at $60^{\circ} 60.00' \text{ N } 146^{\circ} 90.00' \text{ W}$, 0 = true north.
2. Clupea pallasii. Percent size frequency distributions of Pacific herring (fork length mm) collected during three acoustic surveys of Prince William Sound, Alaska, in 1995 and 1996 (n = count).
3. Theragra chalcogramma. Percent size frequency distributions of walleye pollock (fork length mm) collected during three acoustic surveys of Prince William Sound, Alaska, in 1995 and 1996 (n = count).
4. Clupea pallasii and Theragra chalcogramma. Polar angle percent frequency distributions of Pacific herring and walleye pollock observed during three acoustic surveys of Prince William Sound, Alaska, in 1995 and 1996.

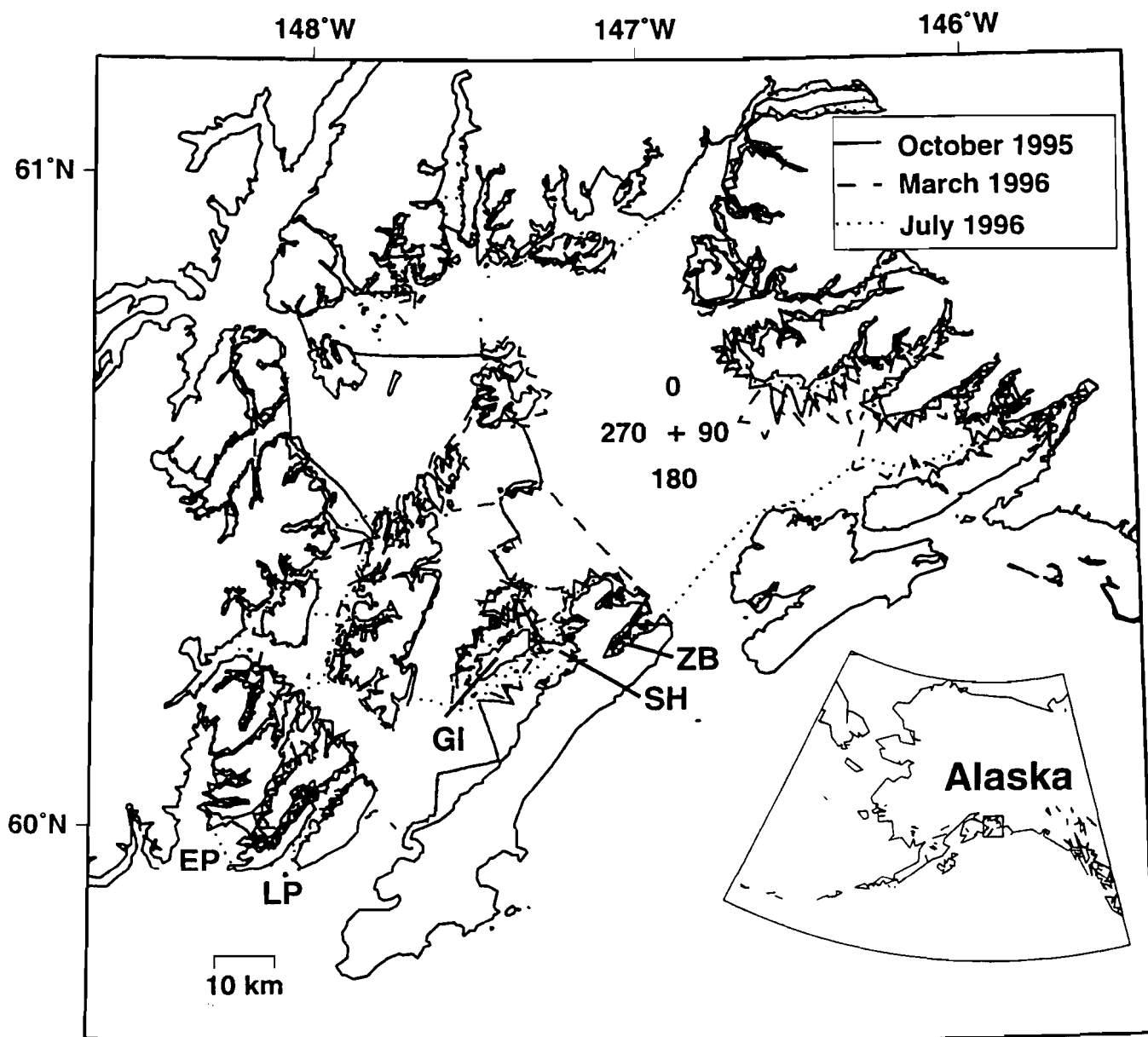


Fig. 1. Stokesbury et al.

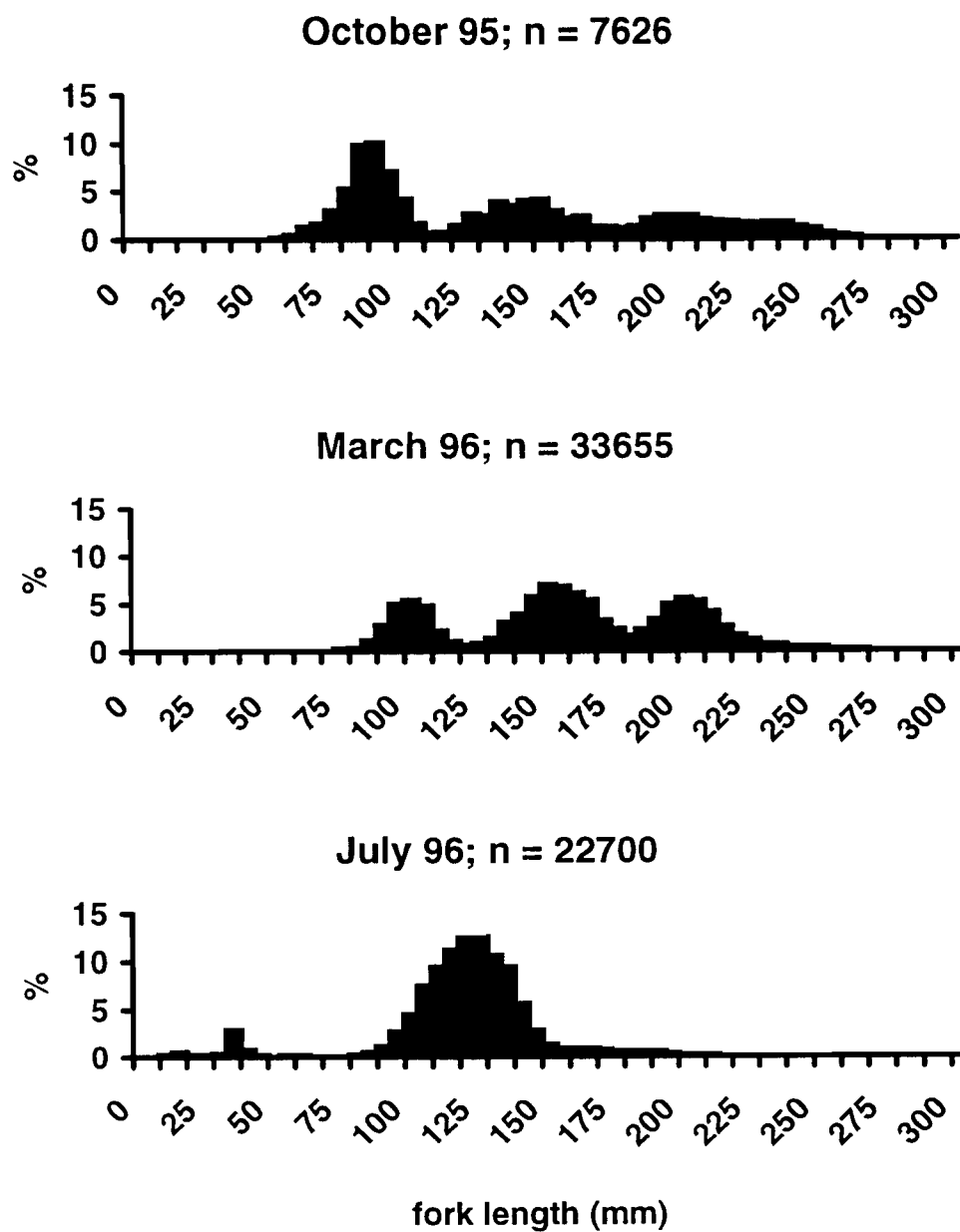


Fig. 2 Stokesbury et al.

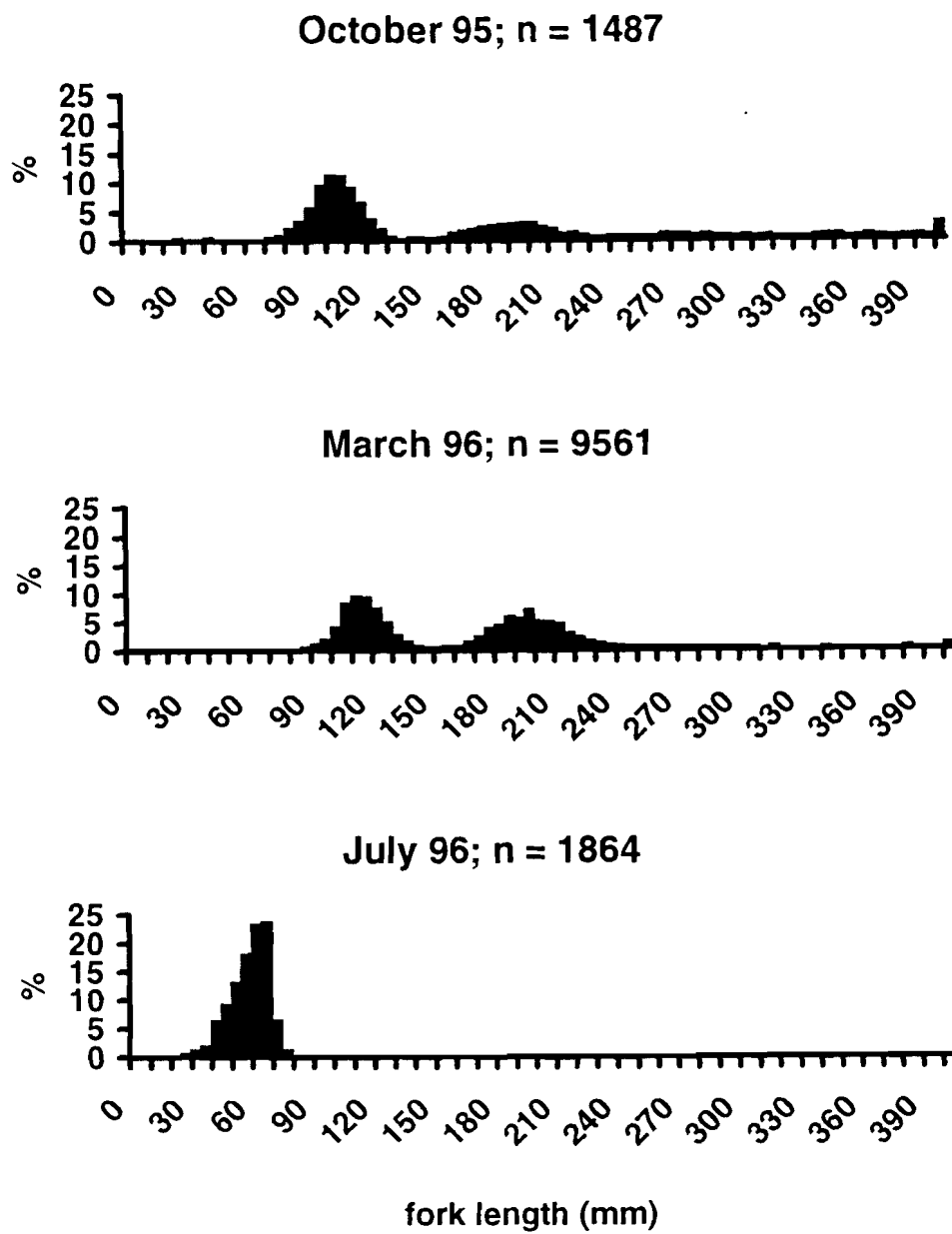


Fig. 3 Stokesbury et al.

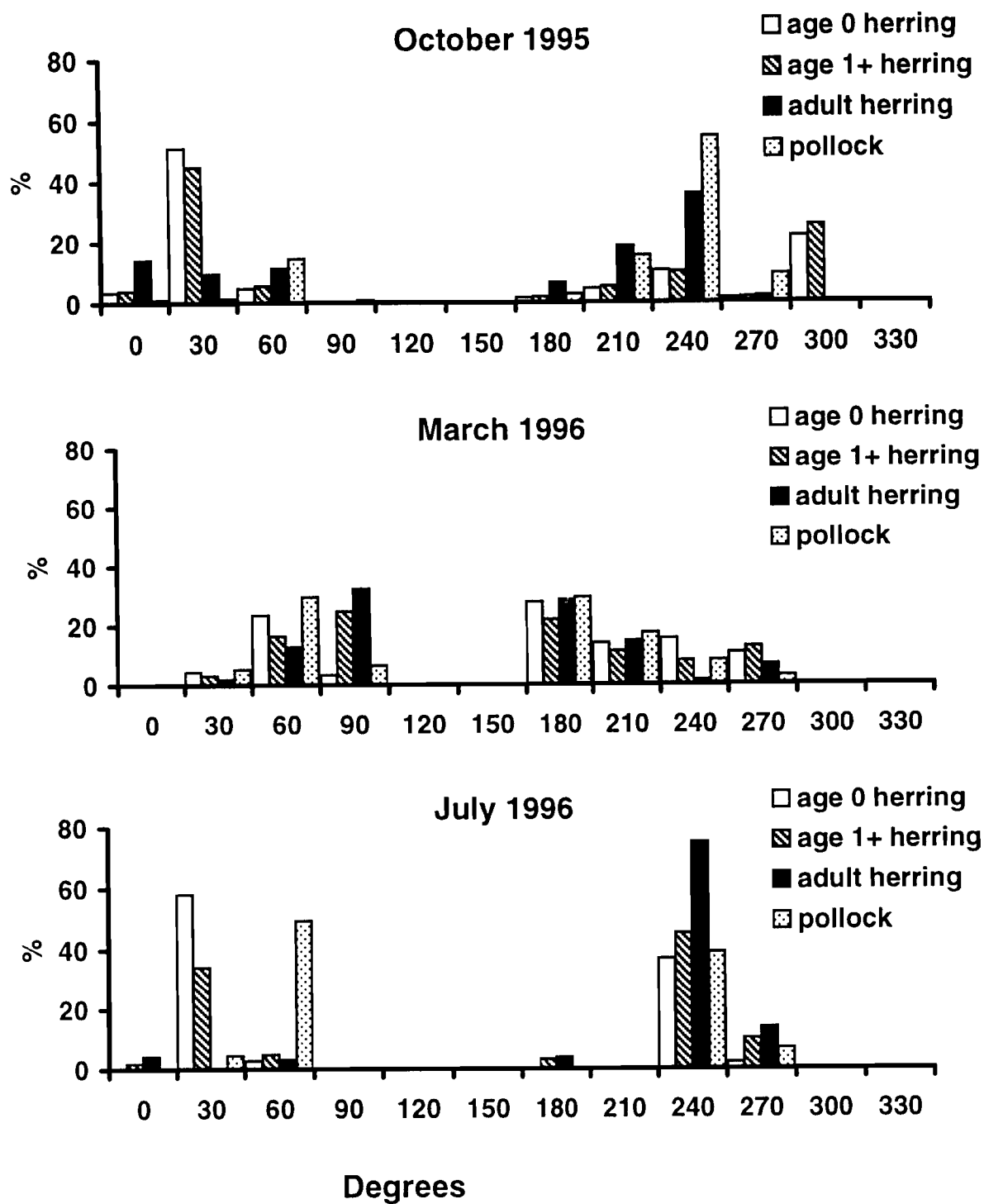


Fig. 4 Stokesbury et al.

Appendix II

Preliminary Documentation of Temporal and Spatial Variability of Pacific Herring, Other
Forage Fish, and Seabirds in Prince William Sound, Alaska

Evelyn D. Brown
April 7, 1998

Appendix II. Preliminary Documentation of Temporal and Spatial Variability of Pacific Herring, Other Forage Fish, and Seabirds in Prince William Sound, Alaska

Evelyn D. Brown

Introduction

This report covers preliminary aerial survey data presented at the annual science reviews for both the Sound Ecosystem Assessment (SEA) and Alaska Predator Ecosystem Experiment (APEX) projects funded by the *Exxon Valdez* Oil Spill Trustee Council (EVOS TC). From 1995 through 1997, monthly broadscale aerial surveys were flown in Prince William Sound (PWS) and the Outer Kenai (OK) over a 5-7 day period during May through August (see Appendix III and Stokesbury et al., 1997). Peak counts of fish schools were recorded in June and July. Less schools were observed in May and August. Increased counts observed in June and July were probably due to a change in fish distribution to shallow surface waters (see Stokesbury et. al., Appendix I this report) as the aerial survey is limited to observations of surface schooling fishes. Also, by July metamorphosis of larval Pacific herring (*Clupea pallasii*; Stokesbury et al., Appendix I) and sandlance (*Ammodytes hexapterus*) occurs and schooling behavior begins (evidenced by reductions in larval abundance, Norcross et al. 1996 and observations of large numbers of age-0 juvenile sandlance in the nearshore, APEX, unpublished data). Finally, pre-spawning capelin (*Mallotus villosus*) and post-spawning eulachon (*Thaleichthys pacificus*) form large visible schools in June in PWS and adjacent waters of the Gulf of Alaska (E. Brown, unpublished data).

I will present here the graphic results of the broadscale surveys during the months of June and July for PWS.

Methods

Methodology for the aerial survey technique is documented by Brown and Norcross (in prep) and in Appendix III of this report. For this report, the aerial survey database was queried for the broadscale survey data from June and July. Repeat surveys over herring nursery bays of interest to the SEA project were left out of the query. The data therefore represents a single pass over the entire area over the course of a week. The only shorelines not sampled were in the fiords of the extreme northwest corner of PWS (Port Wells, not labeled on the maps). Surface areas were estimated for all schools and total surface area estimates were plotted for each unique latitude and longitude by species (there were often several schools at a given location). The results were plotted using the GMT mapping software and the key for the shade-by-value school plots is given in Figure 1.

Seabird behavior codes are recorded easily from the air including plunging, milling tightly aggregated on the water, resting on the water (loose aggregation), resting on shore, broad-area search, and travelling. Therefore, a determination of the numbers of birds foraging (plunging, milling, tightly aggregated on the water) versus searching or other behaviors can be made. I can determine not only the degree to which birds are associated with surface

schools, but also what their behaviors are in association with schools. Therefore, the degree of spatial and temporal variability in foraging and school association can be determined.

The aerial database includes mainly white gulls (black-legged kittiwakes, mew gulls, and glaucous-winged gulls) which are easy to sight from the air. They also do not spend any time under the surface. Diving ducks and other seabirds are difficult to sight from the air. Therefore, the seabirds represented are gull species.

Results and Discussion

All forage species and seabirds or gulls were plotted by month and year (Figures 2-7). The notable features are discussed. The existence of large numbers of pre-spawning capelin schools were observed in June of 1995, but not in subsequent years (Figures 2-4). These sightings were validated by targeted catches on pre-spawning capelin sighted from the air. In June of 1997, following reports of excessive interceptions of spawning eulachon by Copper River drift net salmon fishermen (Copper River Fishermen's United, Cordova, Alaska, personal communication), large numbers of huge eulachon schools (about 1000 m²) were sighted mainly off Montague Island (Figure 4). These sightings were validated by examinations of stomach contents of predatory fish caught near the school groups and by interceptions of eulachon by salmon fishermen. No eulachon were observed in June of 1995 and 1996. Large numbers of juvenile herring schools were sighted all three years in June representing mainly age-1 herring (see Appendix III). However, interannual variability in abundance was evident with peak surface area estimates occurring in 1996 (Figures 2-4). This could represent differences in overall year-class strength. Only in June of 1997 were sandlance schools observed in significant numbers. Surface water temperatures were abnormally high in 1997 (SEA, unpublished data) and the anomalous numbers of sandlance sighted in June could represent early recruitment of post-metamorphic sandlance to nearshore beaches.

In June, broadscale seabird foraging activities were focused on the pre-spawning capelin and in eastern PWS in 1995 (Figure 2) and post-spawning eulachon in 1997 (Figure 4). In general, more foraging activity was observed in 1997 over the two previous years. In 1996, bird foraging activities were more numerous at nearshore beaches on outer Montague and western and northern Hinchinbrook Island. There was also large number of foraging flocks in northwestern PWS near the village of Tatitlek and associated with juvenile herring schools.

The notable features in July of each year were the absence of capelin and eulachon and peak annual counts of both juvenile herring and sandlance (except in 1995 when peak herring counts occurred in June) (Figures 5-7). The variability of herring counts in July probably represents changes in year-class strength for both age-1 and age-0 herring. However, changes in the depth distribution of juvenile herring as well as early departure of age-1+ herring from nursery bays could also explain the variability observed (see Stokesbury et al., Appendix I). Comparisons of acoustic and aerial data, planned for later

this spring, will document variability in distribution by depth, which will aid in correct interpretation of the aerial results (see Appendix III). No such comparisons are available for sandlance since they generally occur in waters too shallow for acoustic measurements (Appendix III). However, because of that characteristic, aerial counts are probably more conclusive for sandlance than for juvenile herring at this time. Sandlance appear to be in a state of population building as increasingly higher numbers of schools were observed from 1995 to 1997 (Figures 5-7).

Although there was considerably bird foraging activity associated with schools sighted from the air in July, flock size appeared to have decreased from June to July (compare the size of the triangles from Figures 2-4 to 5-7). There appears to be a species preference by the foraging seabirds for juvenile herring over sandlance. In 1996 and 1997, 35.7% (n=226) and 43.6% (n=326) respectively of the herrings schools were associated with seabirds. This compares to 18.3% (n=71) and 11.1% (n=180) of the sandlance schools in 1996 and 1997 respectively. There did not appear to be a preference for school size as the frequency distribution of school size was identical for schools with or without birds.

In all three years, the majority of the seabirds sighted from the air were involved in active foraging behaviors (41.0%) or search activities (27.0%). The remainder were either resting or travelling (15.7%) including counts at seabird colonies (mainly kittiwakes).

It appears from preliminary results of APEX chick diet studies, that PWS seabirds feeding primarily on pelagic fishes are targeting juvenile herring and sandlance. Since sandlance and juvenile herring are the most abundance surface schooling fishes observed in PWS, the birds appear to be feeding on what is available. I produced plots to show interannual variability of juvenile herring and sandlance in the months of June and July. The peak abundance estimates (total school surface areas) of juvenile herring (probably age-1) in June of 1996 are obvious in Figure 8. For sandlance, the 1997 peak June count is obvious (Figure 9). In July, both peak school counts and surface area estimates in 1996 and 1997 exceeded those in 1995 (Figure 10). There is also evidence of slight changes in distribution from year to year. In 1997, more herring schools were observed in waters outside bays than in 1996. I have no explanation for this. The population increase in sandlance is obvious in Figure 11 with an accompanying increase in spatial distribution from 1995 to 1997.

Now that the documentation of fish distribution is complete, I can proceed with ecological evaluations of those distributions. I can compare the distributions to oceanographic conditions and regimes occurring within and outside of PWS. I can compare the trends in abundance of the juvenile herring to resulting changes in the adult population size and distribution. I can examine regional and temporal changes in seabird or gull foraging activity as well as interannual fluctuations in colony size (on a broadscale). In short, the potential for use is broad-based. There are obvious monitoring advantages in the continuation of this data set over a longer period of time.

Literature Cited

Brown, E.D. and B.L Norcross. In prep. Assessment of forage fish distribution and abundance using aerial surveys: survey design and methodology. To be submitted to Ecological Applications.

**Shade by value of fish schools at
a given location, species by color**

◦ **1-10**

◦ **11-20**

◦ **21-30**

○ **31-50**

○ **51-100**

○ **101-200**

○ **201-500**

○ **501-1000**

○ **>1000**

**Total no. birds at
a given location**

△ **1-25**

△ **26-50**

△ **51-100**

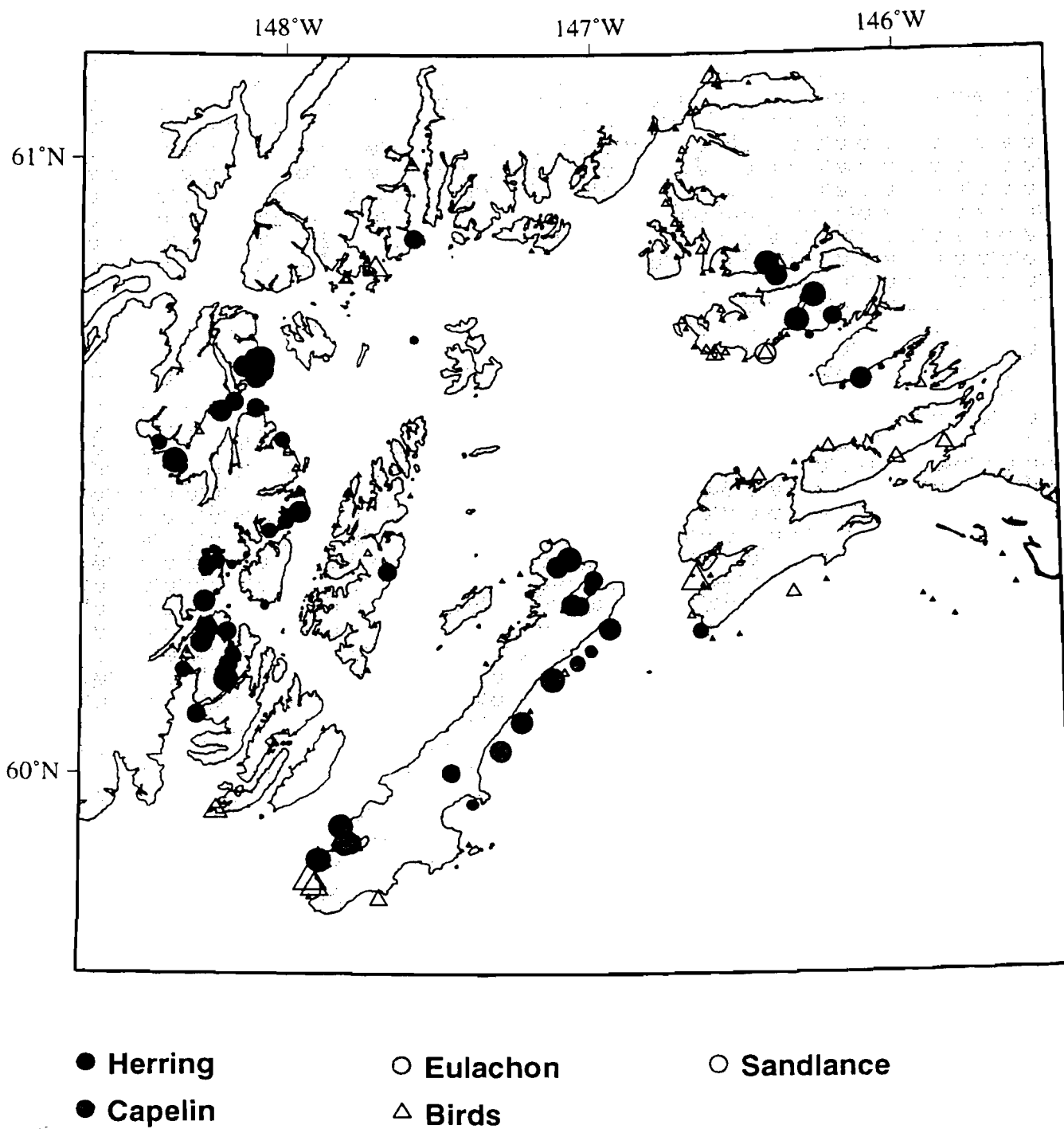
△ **101-200**

△ **201-500**

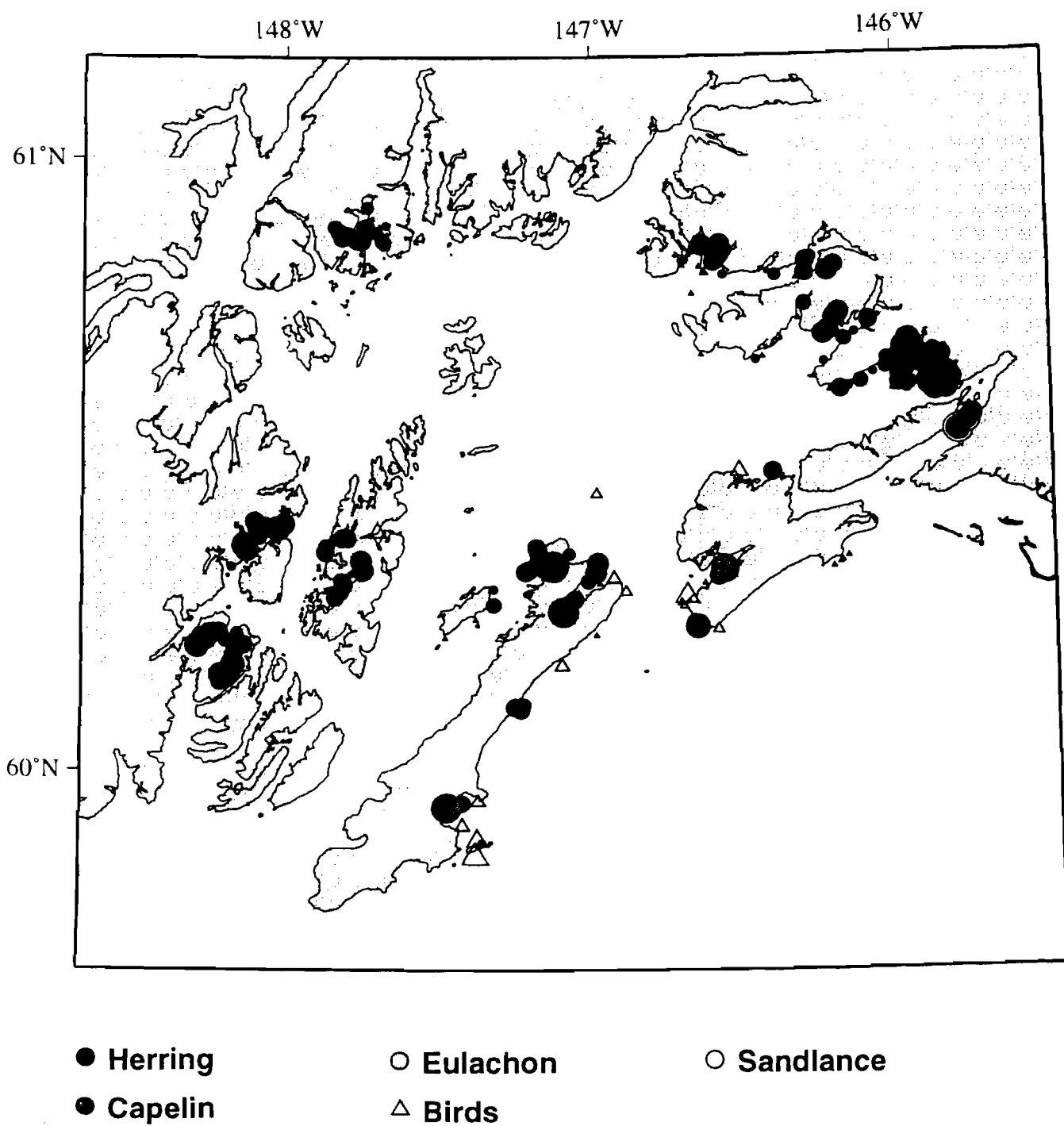
△ **501-1000**

△ **1001-5000**

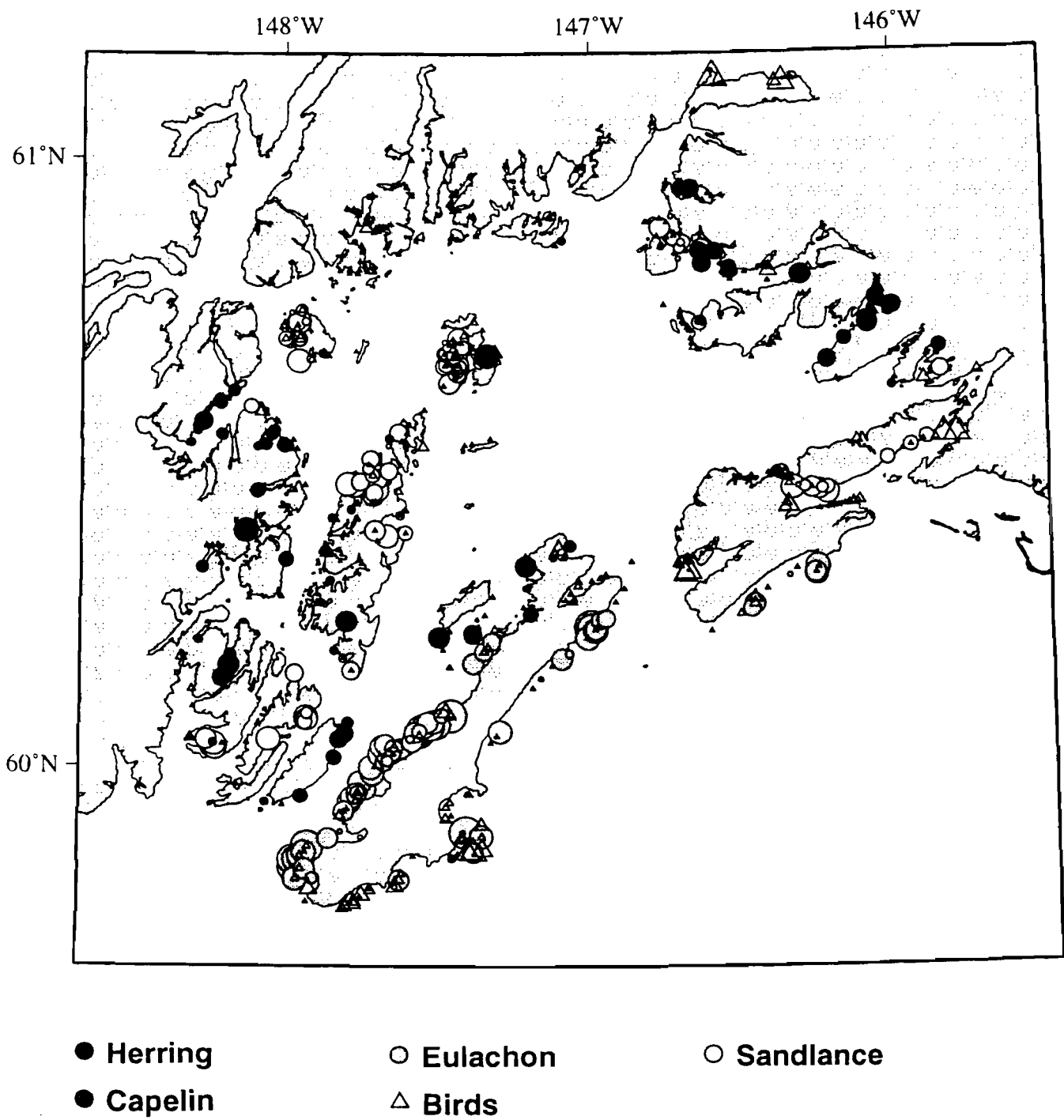
△ **>5001**



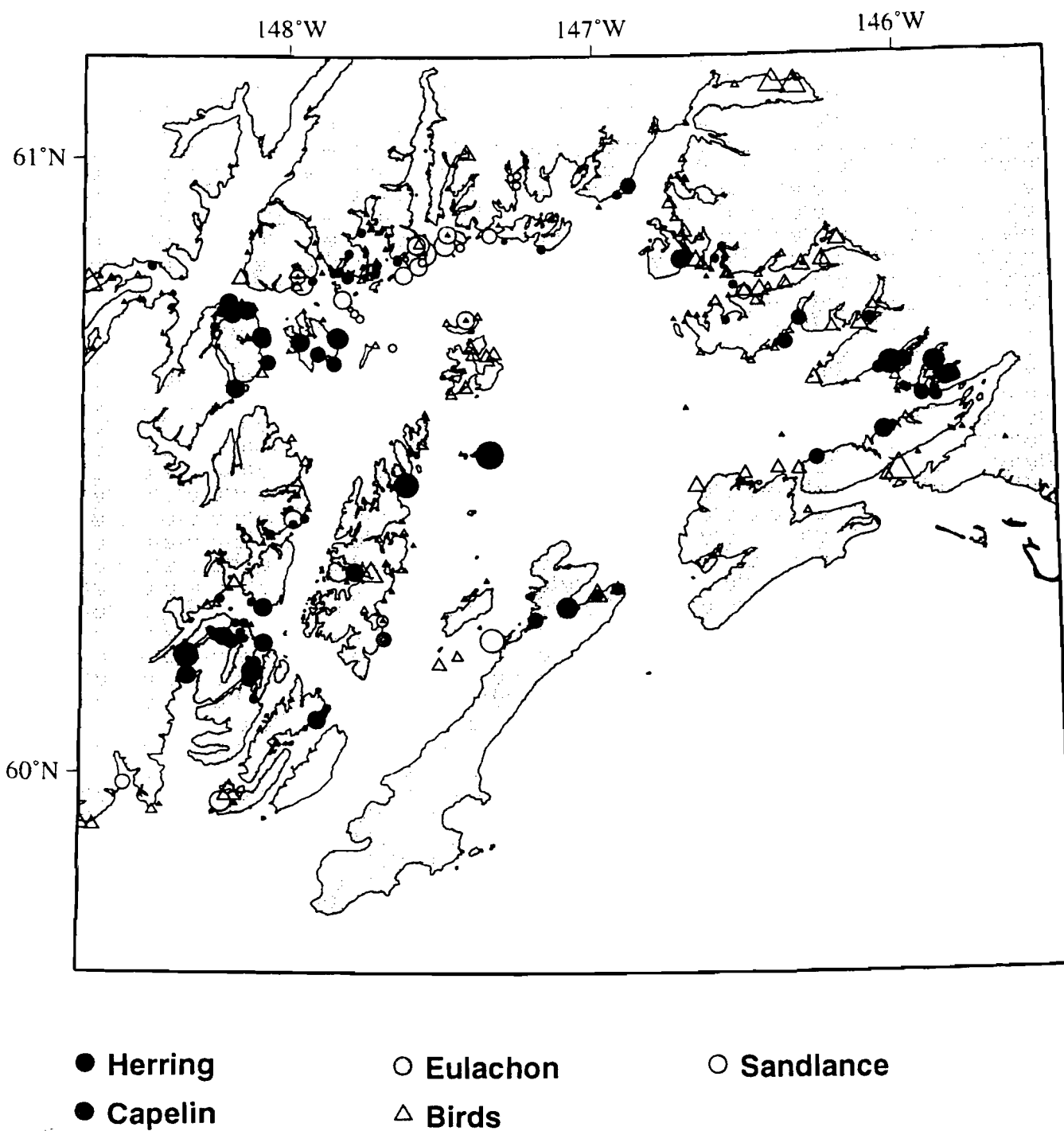
Appendix II Fig. 2. Distribution of Seabird and Forage Fish, in Prince William Sound, Alaska, June 1995. No eulachon were sighted.



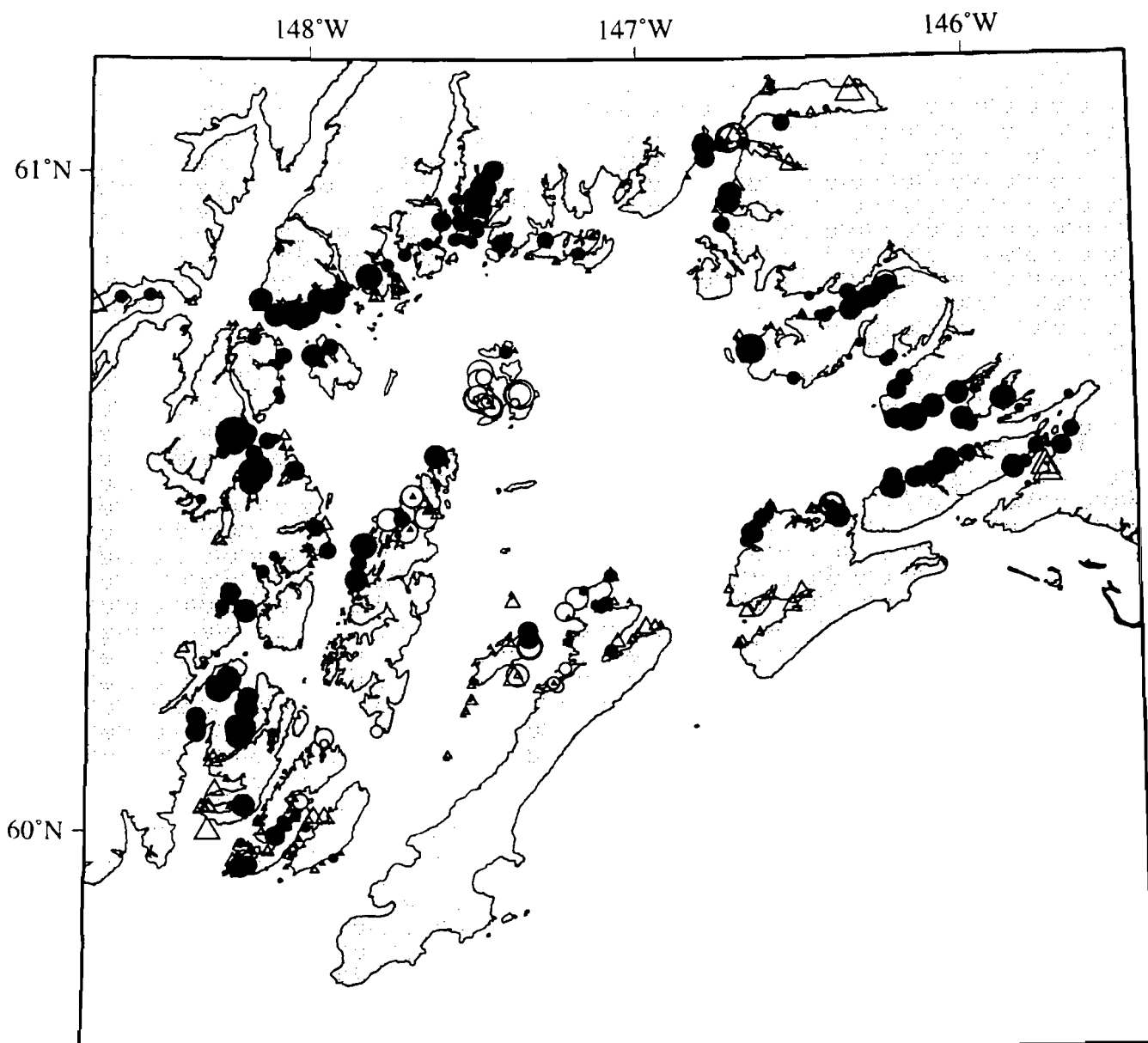
Appendix II Fig. 3. Distribution of Seabird and Forage Fish, in Prince William Sound, Alaska, June 1996. No eulachon were sighted.



Appendix II Fig. 4. Distribution of Seabird and Forage Fish, in Prince William Sound, Alaska. June 1997. No capelin were sighted.

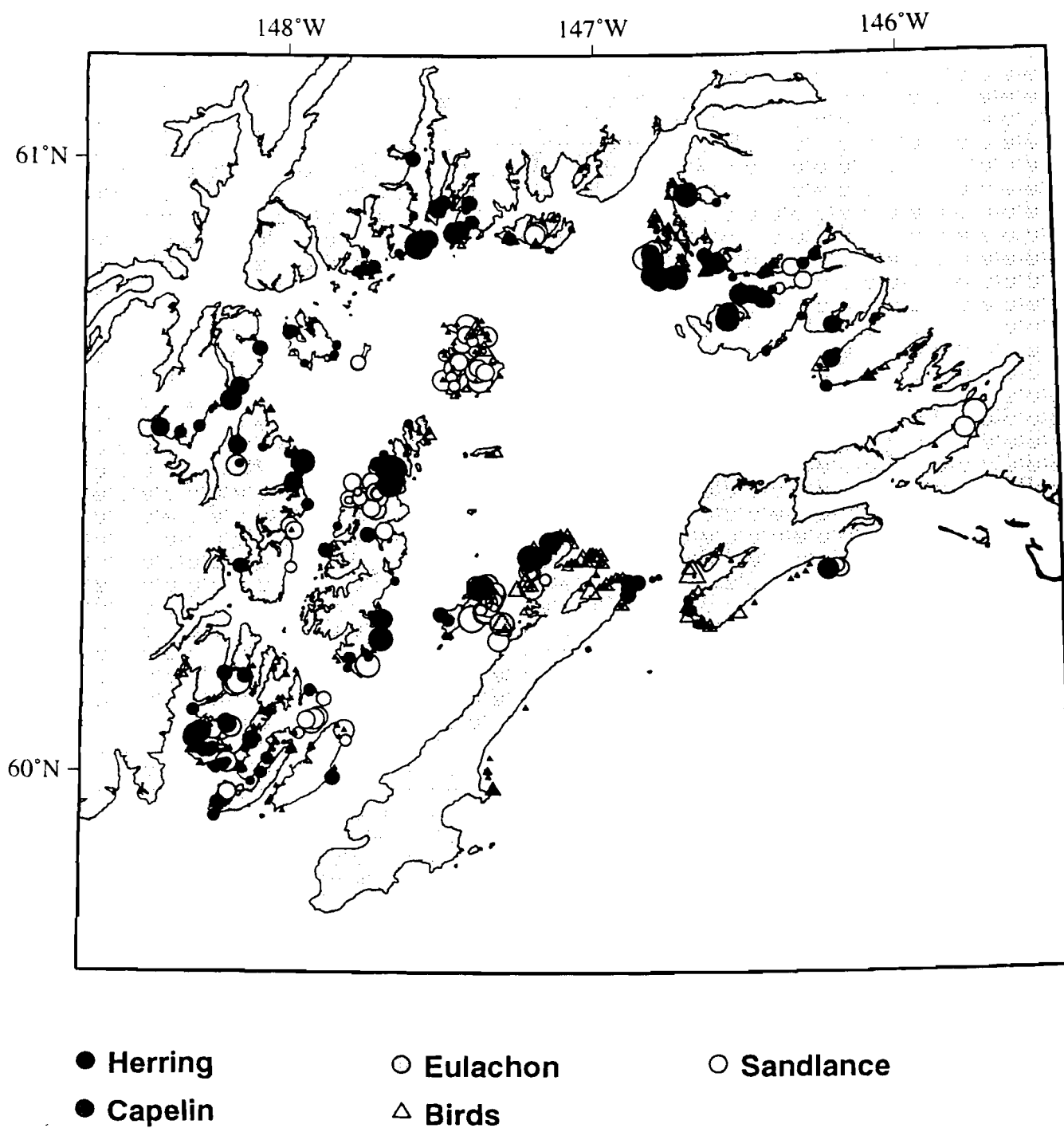


Appendix II Fig. 5. Distribution of Seabird and Forage Fish, in Prince William Sound, Alaska, July 1995. No eulachon were sighted.

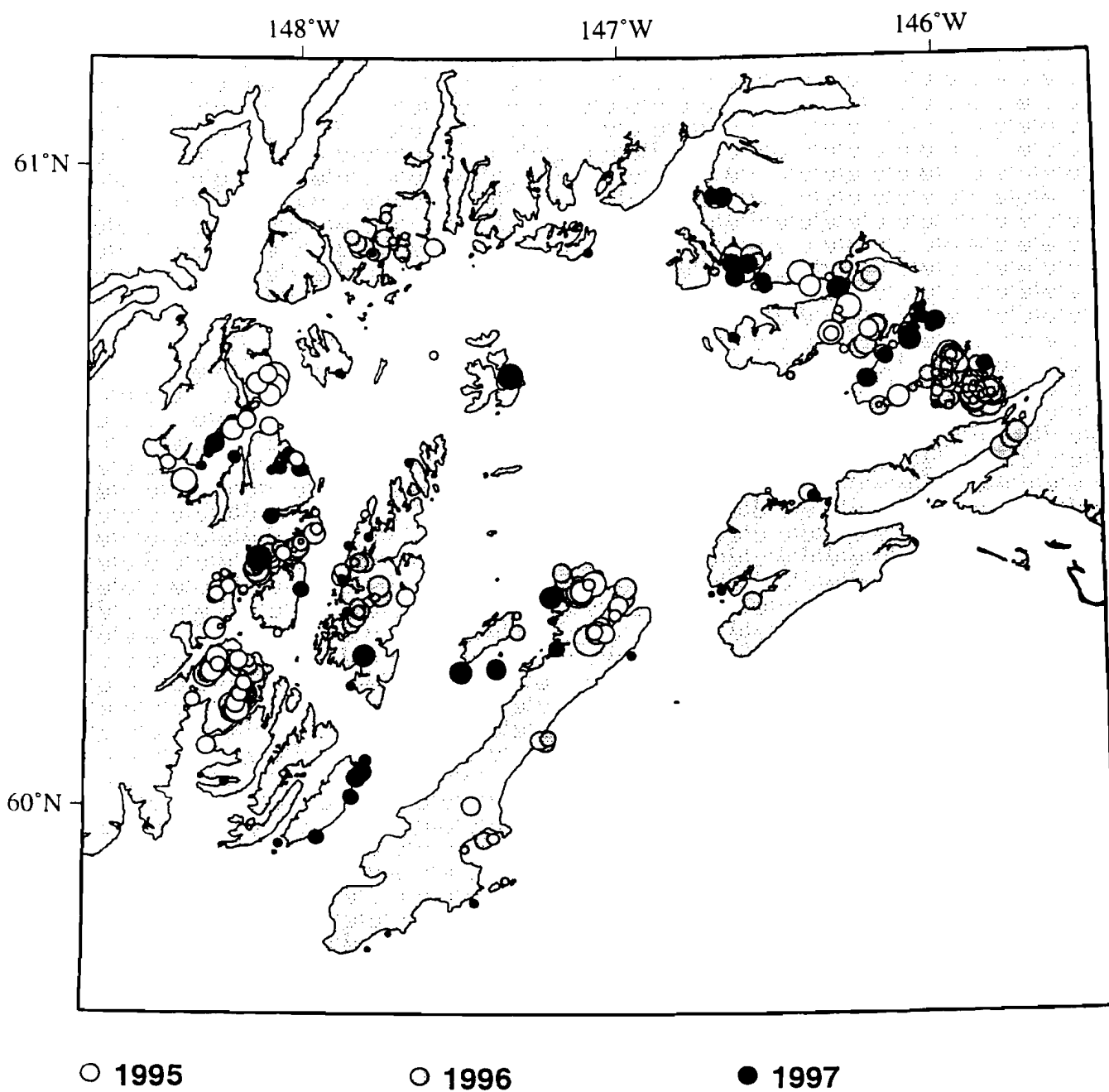


- Herring
- Eulachon
- Sandlance
- Capelin
- △ Birds

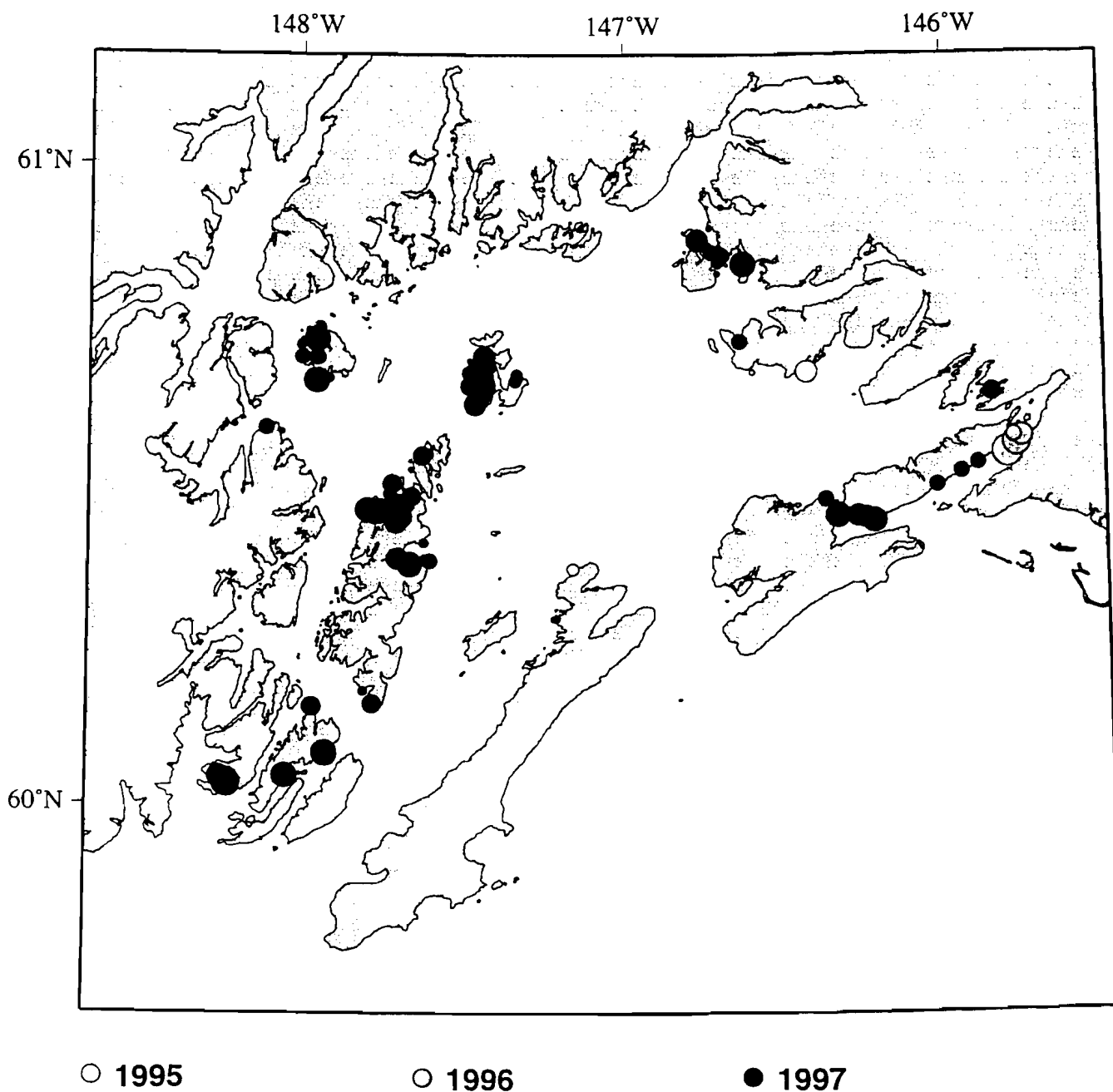
Appendix II Fig. 6. Distribution of Seabird and Forage Fish, in Prince William Sound, Alaska, July 1996. No capelin, or eulachon were sighted.



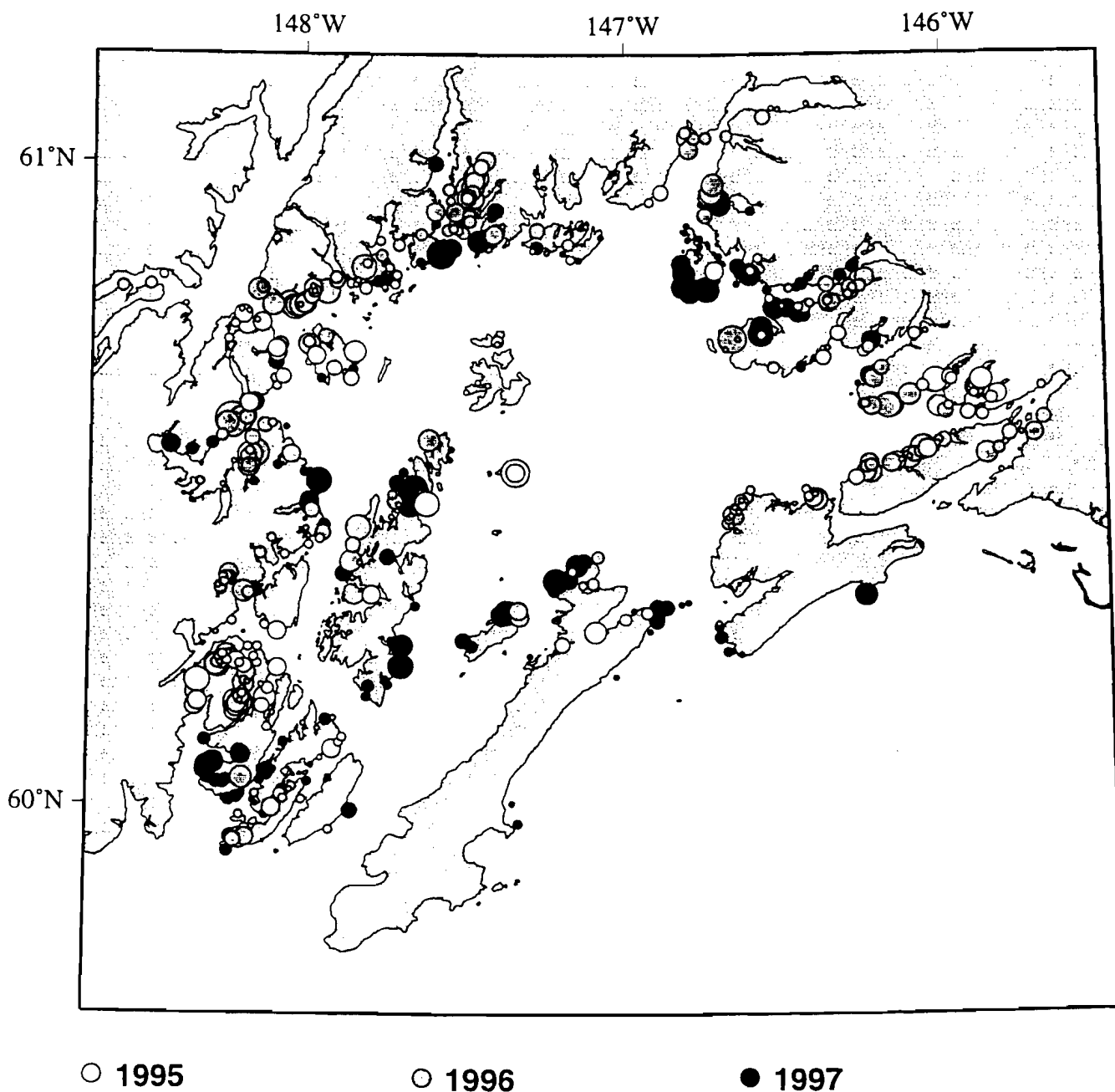
Appendix II Fig. 7. Distribution of Seabird and Forage Fish, in Prince William Sound. Alaska, July 1997. No capelin were sighted.



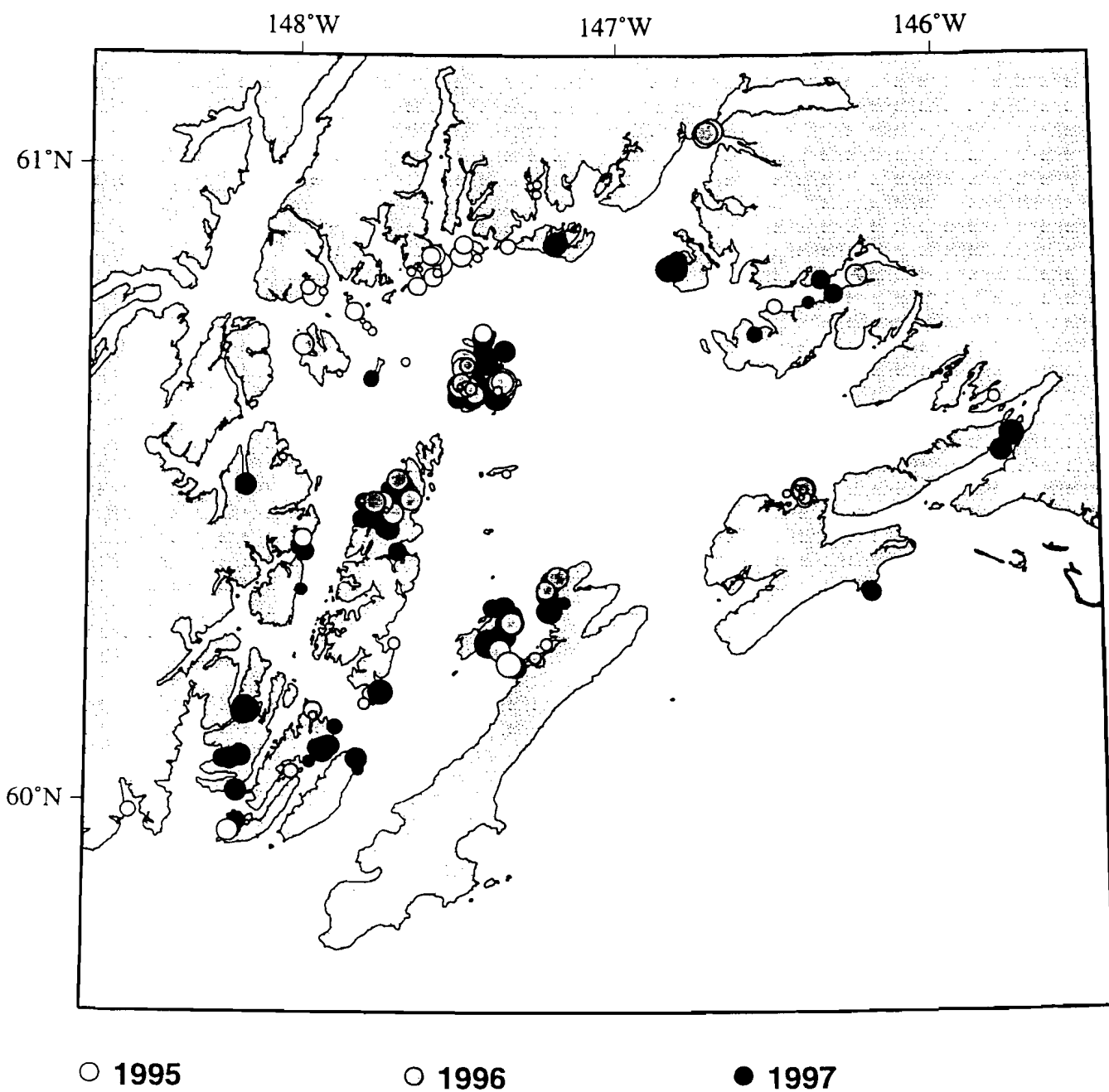
Appendix II Fig. 8. Interannual Variation in the Distribution of Herring, in Prince William Sound, Alaska, June 1995-1997.



Appendix II Fig. 9. Interannual Variation in the Distribution of Sandlance, in Prince William Sound, Alaska, June 1995-1997.



Appendix II Fig. 10. Interannual Variation in the Distribution of Herring, in Prince William Sound, Alaska, July 1995-1997.



Appendix II Fig. 11. Interannual Variation in the Distribution of Sandlance, in Prince William Sound, Alaska, July 1995-1997.

Appendix III

Progress Report on Aerial Survey Development

Evelyn D. Brown and Gary A. Borstad
April 7, 1998

Appendix III. Progress Report on Aerial Survey Development

Evelyn D. Brown and Gary A. Borstad

Introduction

This section of the SEA annual report (97320T) is an update on the development of aerial survey methodology used by the SEA project for the last three years. The original objective of aerial surveys was to provide an economic method of documenting broadscale distributions of juvenile herring. Because of the way surveys were conducted, a considerable amount of incidental data was collected that has now become pivotal for other EVOS projects. Information on the distribution of pre-spawning capelin (*Mallotus villosus*), juvenile and adult sandlance (*Ammodytes hexapterus*), eulachon (*Thaleichthys pacificus*), jellyfish aggregations, foraging gull distributions and behavior, and marine mammals (humpback whales, killer whales, sea lions, sea otters, and harbor seals) is included in the three-year database. Much of this incidental information has been shared with other EVOS projects and included in recent publications (Irons, Ostrand, Purcell, and Gotthardt from the APEX project). It is now clear, that this methodology is useful for a multiple array of research objectives and is cost effective.

We can now more clearly define research questions that can be answered with the aerial survey data in concert with other physical or biological data:

What is the distribution of juvenile herring, sandlance, capelin and other schooling forage fishes, and jellyfish aggregations?

How do those distributions relate interspecifically, to ocean conditions, and to distributions of predators?

What is the temporal and spatial variation of those distributions?

Current research objectives are also more clearly defined:

- 1) Measure the species-specific distribution and abundance of forage fish schools
- 2) Determine the precision, validity and accuracy of those measurements
- 3) Determine how those results relate to oceanic conditions or regimes and to the distributions of avian and mammalian predators.

In Appendix II of this report chapter, we document the distributions of all forage fish species observed in the last three years (objective 1). In this report section, we will focus on the progress toward measurement of error associated with the aerial survey methodology (objective 2).

Measurement of error falls into one of three categories: precision, validity and accuracy. Precision or variability of data introduced by the technique is determined via repeated measures, double counts, and comparison to independent measurements. Validity of aerial sightings is accomplished by species identification from net catches, ground identifications, or underwater videos of individual schools identified from the air. Accuracy or bias is measured by comparison of aerial survey results to independent measures such as acoustics and compact airborne spectrographic imager (CAST).

Finally, we will outline tasks yet to be accomplished for completion of the aerial survey methods publication (SEA Annual Report Chapter 11, Appendix I) and make recommendations for research direction in the future.

Methods

A detailed description of the methods was included in a chapter of the SEA 1996 Annual Report (Stokesbury et al., 1997), so this section will serve as a brief review.

For these methods a sighting tube is used which consists of a PVC tube with a mylar grid attached to the end. School diameters or dimensions were measured through the tube and converted to meters using a simple proportional equation (Brady 1987; Lebida and Whitmore, 1985):

$$X = A (L / F); A=\text{altitude}, L=\text{tube tick measurement}, F=\text{tube focal length}.$$

A preferred altitude range of 275-365 m (900-1200 ft) was established based on school size. Since many of the schools were smaller than 5 m², the altitude range selected is lower than for many other established aerial surveys that are looking at much larger, pre-spawning adult aggregations (Carscadden et al. 1994; Funk et al. 1995)

The survey design is a "narrow-strip" line transect within which uniform detection is assumed (Thompson 1992). The visual swath is equivalent to the area perpendicular to the transect where uniform detection occurs and is a function of altitude. The dimensions of the visual swath were developed by flying over a fixed object of known distance and area (an airport runway and helipad) within the range of altitudes used for data collection. The distance to a maximum sighting tube angle of 30 degrees (to the vertical), and within which the smallest detectable object (a single gull) could be discriminated, was identified as the edge of the swath.

In order to eliminate survey condition bias, introduced by variable meteorological conditions or aircraft, minimum criteria were established. We did not fly if the winds were over 25 knots (creating a sea state of over 1 beaufort scale or 1 m wave heights), if the average ceiling (cloud cover) was below 200m, or on rainy days. We also used the same

type of aircraft (Cessna 185) for each survey. Finally, where possible, we flew during the same tide stage and time of day.

In order to estimate the precision of the survey data produced, we used double counts (Rivest and Potvin, 1995). Two surveyors were independently counting and measuring schools simultaneously from the same side of the aircraft. For each map, bay, transect or survey day, counts were compared between the two. The residual distances represent an estimate of surveyor bias.

In order to measure repeatability of the survey results, we flew over the same bay several times within a 24-48 hr time period. The unit of measurement was a single bay or nursery site for juvenile herring (refer to the main body of this report).

Validation of schools was accomplished in several ways. The best validations were obtained when vessels or skiffs capable of catching fish or with divers were directed to specific schools spotted from the air. We also obtained validations by directing skiffs with underwater videos, although avoidance was a problem with this method. A priority for scheduling aerial surveys was to overfly acoustic vessel surveys whenever possible (for both APEX and SEA). Geocoded net catches were then matched to aerial sightings occurring during the same day and location. Finally, we landed at vessels where research diving activities were taking place (Steve Jewett, Nearshore Vertebrate Predator or NVP project, personal communication) and conferred with them about the identification of schools seen underwater that matched our school locations. In this case, latitudes and longitudes were also matched within a 24 hr time scale.

Validation of schools will be taken a step further in a modeling exercise. Species discrimination parameters were identified and measured for over 400 samples. The identification parameters will be used in a discriminate function analysis to separate species and age classes by their distinct characteristics.

For estimating the accuracy of the aerial survey results, we used both CASI and acoustic survey results. We only briefly discuss acoustic comparisons here (work in progress); see the body of this report and Appendix I of this annual report for more detail on acoustic methodology. For comparisons to CASI, two aircraft were used. We flew the visual surveys in the Cessna 185 as usual. The CASI equipment was mounted in a Dehavilland Beaver 216GB aircraft on floats with a hole cut in the bottom of the plane for the sensor array. The surveyors in the 185 performed a reconnaissance survey setting up straight line transect passes for the CASI. Then the two aircraft lined up and flew each transect simultaneously with the visual surveyors counting schools underneath the Beaver. The two aircraft were not always lined up perfectly in space or time, but exact school locations could be obtained later and compared within a defined geographic region rather than for each transect.

The CASI system acquired digital multispectral imagery of fish schools (Borstad et al. 1992). The resulting images were radiometrically calibrated (Borstad Associates. Program

CVTD3_3), corrected for aircraft roll, and scaled uniformly. Because the herring schools were small, the CASI instrument was configured to acquire data with the highest spatial resolution (small pixels) possible. The along-track pixel length was determined by the number of spectral channels and the aircraft speed. Only three channels were used (Table 1) allowing a 30 msec integration time. Wide spectral bands were defined, which gathered as much light as possible while still differentiating the schools from their surroundings. On some lines, the fore optics fstop were changed to f4 from 4 to 5.6 in order to further increase the signal levels.

Table 1. The Configuration File Bandset

CASI band #	Wavelengths (nm)
1	405 – 455
2	460 – 590
3	600 - 675

The settings resulted in single pixel dimensions of .3-.5 m wide and 1-2 m long. With these setting only a tiny school would be represented by a single pixel (as were gulls). For the vast majority of schools measured, the settings provided in excess of 10 pixels per school. The altitude flown affected the image swath, but generally at 305 m the CASI image was 200 m wide. In order to prevent the images from becoming too large to handle on the computer, transects were restricted to less than 10 km and preferably between 4-6 km long.

During post-processing, the 8 bit unsigned images were examined and the area for each school calculated. School dimensions and statistics were obtained using a custom program designed for the CASI on a Sun-Sparc5 Unix system. A full 512X1900 resolution window was used to process the images. Statistics were first recorded by transect line and checked for errors. Later, sections with concentrations of schools were extracted and geocoded so they could be linked in space with the visual sightings, since the two aircraft were not always lined up perfectly to record the same features at exactly the same time.

Results

In 1996-1997, 87 double counted surveys were conducted. Error was estimated for both total school counts and for surface area estimates within a given area (Figure 1a and 1b). The outliers in this relationship have not been checked; there is missing data that needs to be included. Once the corrections have been made, we expect the estimated surveyor bias to decrease. There is more error associated with making school surface area estimates than school counts. However, both relationships are currently close to one-to-one counts (slopes approximately equal to 1.0) with high correlation coefficients indicating that surveyor bias is a minor contributor to the total variability found in the data.

In 1996-1997, 11 repeat counts were conducted over individual juvenile herring nursery bays within a 24-48 hr time period (Figure 2). Residual analysis of this relationship indicates that normality may be a problem with increasing variability occurring when the delay between the repeat counts is increased. Despite that problem, the correlation coefficient (0.707) is relatively high and significant indicating that there is constancy in the number of surface herring schools observed in a given bay. The preliminary conclusion from this initial look at the data is that variability in school distribution over a 24-48 hr time period is probably not a significant contributor to overall variability in survey results.

During 1996-1997 over 350 validations of aerial survey observations were completed. Validations were collected from net catches, diver observations, and underwater videos of schools sighted from the air. Of the 309 herring schools identified on the ground (Figure 3), 96.1% were correctly identified as herring from the air. All of the misidentifications involved age-0 sandlance recorded as herring from the air. In addition, the vast majority (over 90%) of the validated herring schools were age 0-1. Of the 47 sandlance schools identified on the ground, 80.4% were correctly identified from the air. As with herring, all of the errors involved age-0 sandlance recorded as herring. Also, the vast majority (over 90%) of the validated sandlance schools were juveniles.

Ability to discriminate forage fish species from the air is an important objective for this project. In the initial definition of discrimination parameters, distance from shore, school shape, and school size are useful in separating herring and sandlance schools. Juvenile herring schools occur $31.8 \text{ m} \pm 2.26 \text{ m}$ (95% confidence) from shore in contrast to sandlance which occur $10.2 \text{ m} \pm 1.23 \text{ m}$. The vast majority of juvenile herring schools observed from the air in the summer are round (Figures 3 and 5) while the vast majority of sandlance schools are oval or irregular (Figures 4 and 5). Juvenile herring schools average $24 \text{ m}^2 \pm 3.64 \text{ m}^2$ in surface area while juvenile sandlance schools average $55.8 \text{ m}^2 \pm 7.23 \text{ m}^2$. Sample means of both distance from shore and school size between the two species are significantly different from one another ($p=0.000$).

In early July, we completed a series of 37 transects with visual and CASI counts performed simultaneously using two aircraft (25 transects shown in Figures 6-9). A single CASI image was obtained for each transect covering a surface area of 200m by up to 10 km (length of transect varied). Portions of the image with fish schools were saved as bitmaps (examples in Figure 5). We initially compared the visual counts and estimated of surface area with similar estimates derived from CASI images per transect ($n=33$). We found relatively good agreement with a regression analysis of \ln transformed school ($r^2 = 0.730$; slope = 0.75; d.f. = 36; $p = 0.0000$) (Figure 10). We had predicted that the visual method would result in undercounts and therefore expected a slope of less than one. However, when we examined the outliers, we found that geographic mis-alignment may have been responsible for some of the error (visual surveyor and CASI image not recorded the same area). The analysis of CASI versus visual counts is therefore incomplete at this time.

For an initial comparison of acoustic to aerial survey results, we compared the first available acoustic data set for July, 1996 (Figure 11). This was the date of the third and final broadscale acoustic survey of herring nursery areas in Prince William Sound (see Appendix I). Although there was general agreement in the breadth of distribution and the association with the shore, the number of schools documented by acoustics was significantly less. The analysis of the aerial visual counts versus acoustic estimates is incomplete at this time.

Discussion

There are some tasks remaining before the total variability due to survey technique can be quantified (accuracy and precision). Outliers occurring in the double count relationship need to be examined. There are more repeat counts that have not been processed and we plan to explore the relationship between variability and time. If the sample size is high enough, we will also examine the effect of tide stage on the counts.

For validation, we have more ground identifications to add since underwater video processing is incomplete. The analysis will be finalized at that point. The discriminate function analysis used to identify species in the aerial database without bias is incomplete. We are adding depth to the discrimination parameters of distance from shore, school shape, and school size and have recently acquired that data.

In order to correct the geographic discrepancies between the visual and CASI data, we completed additional processing of the CASI data to include latitudes and longitudes for fish schools identified in the image. The geocoded CASI data was available in January of this year. We plan to revisit the regression analysis of visual to CASI measurements using a number of geographic queries and comparing the counts within a defined geographic region. We will also compare surface area estimates from the two techniques. By comparing both school counts and surface area estimates, we will be able to calculate error in visual aerial assessments of fish relative abundance.

In our initial comparisons of acoustic and aerial survey data, we found a large discrepancy in the relative abundance estimates (Figure 11). The difference in measurement scale is obvious. The sonar beam is 6 degrees and directed at a 90 degrees to the water surface. If fish schools are relatively shallow (in this case, 15 m or less; Appendix I), then schools are being counted with the narrowest part of the beam. The width of the area measured is a few meters. Because of budget limitations, we had to limit the broadscale survey to approximately 10 days allowing a single pass through each area surveyed. The transect width of aerial measurements exceeds 200m and several passes can be made over an area to cover the entire surface area of the water. This results in approaching 100% coverage of the areas of interest (in this case nearshore waters of PWS and the Outer Kenai). The broadscale acoustic survey was accomplished for approximately \$60,000 in vessel charter while the broadscale aerial survey covering an extended area (including all waters surveyed

by boat) for approximately \$7,500 in aircraft charter. The advantage is obvious. Our recommendation is to use acoustics and net sampling in a random stratified design to subsample areas covered by air. This would maximize the utility of both techniques.

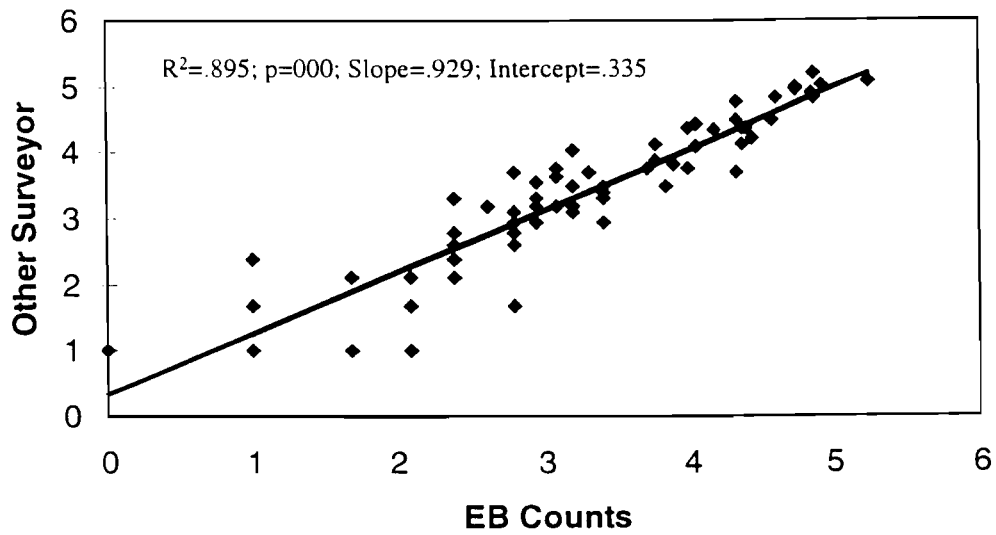
Acoustics will be an important source of data elucidating the relationship between variability in the three dimensional distribution of fish schools over a 24 hr to monthly time period and fish schools observed from the air during the same time periods. Acoustic data needed to complete this task have recently become available. This will add confidence to the aerial survey results, enable interpretation of aerial survey abundance estimates, and allow us to convert aerial estimates to biomass. We expect the comparison of aerial results to acoustics to be included in a separate publication.

We expect to complete these tasks and finalize the publication by May of 1998. This is a critical step in assimilating the aerial data for use by other projects and studies. Although the aerial data has been analyzed in relation to gull foraging activities (APEX review, 1998), our ability to publish the distributions hinges on documentation of the methodology. However, preliminary forage fish distributions have been presented in **Appendix II** of this SEA report chapter.

Literature Cited

- Borstad, G.A., D.A. Hill, R.C. Kerr, and B.S. Nakashima. 1992. Direct digital remote sensing of herring schools. *Int. J. Remote Sensing* 13(12): 2191-2198.
- Brady, J. A. 1987. Distribution, timing, relative biomass indices for Pacific herring as determined by aerial surveys in Prince William Sound 1978-1987. Prince William Sound Data Report No. 87-14. Alaska Department of Fish and Game, Div. of Commercial Fisheries, Juneau, AK. 11 pp.
- Carscadden, J., B. Nakashima, and D.S. Miller. 1994. An evaluation of trends in abundance of capelin (*Mallotus villosus*) from acoustics, aerial surveys and catch rates in NAFO Division 3L, 1982-89. *J. Northw. Atl. Fish. Sci.* 17: 45-57.
- Funk, F.C., G.A. Borstad, S.A. Akenhead. 1995. Imaging spectrometer detects and measures the surface area of Pacific herring schools in the Bering Sea. Third Thematic Conference on Remote Sensing for Marine and Coastal Environments, Seattle WA, September, 1995. pp II-833-844.
- Lebida, R.C. and D.C. Whitmore. 1985. Bering Sea herring aerial survey manual. Bristol Bay Data Report No. 85-2. Alaska Department of Fish and Game, Div. Commercial Fisheries, Anchorage AK.
- Rivest, L-P., F. Potvin, H. Crépeau, and G. Daigle. 1995. Statistical methods for aerial surveys using the double-count technique to correct visibility bias. *Biometrics* 51: 461-470.
- Stokesbury, K.D.E., E.D. Brown, R.J. Foy, and B.L. Norcross. 1997. Juvenile herring growth and habitats, Restoration Project 95320T Annual Report, Chapter 11 *in* Cooney, R.T. 1997. Sound Ecosystem Assessment (SEA) – an integrated science plan for the restoration of injured species in Prince William Sound. FY96 Annual Report for the Exxon Valdez Trustee Council, Anchorage, Alaska. 75 pp.
- Thompson, S.K. 1992. Sampling. John Wiley and Sons, New York, New York. pp. 176-204.

A. Ln Transformed School Counts



B. Ln Transformed Surface Area Estimates

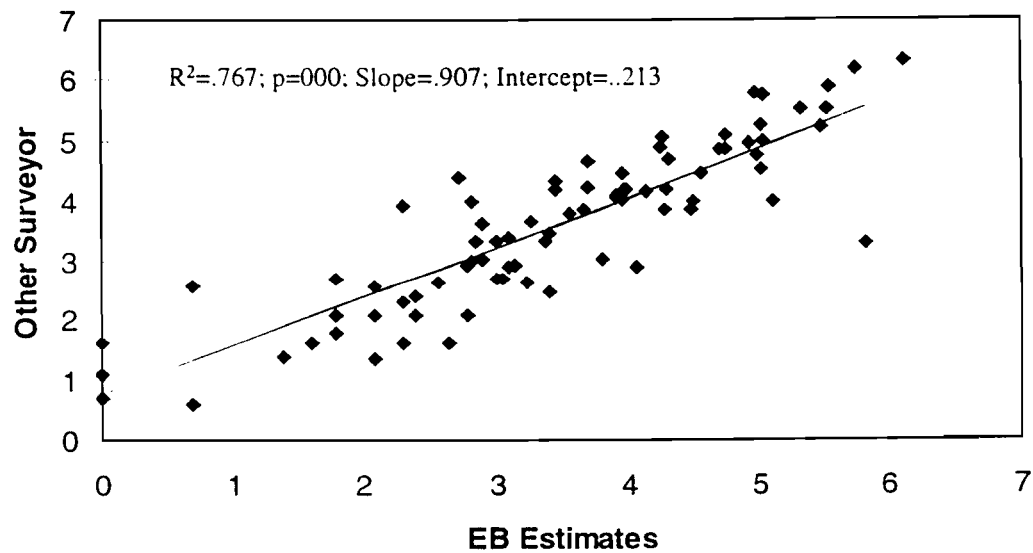


Figure 1. A. The regression between ln transformed simultaneous school counts for two surveyors. B. The regression between ln transformed simultaneous school surface area estimates for two surveyors.

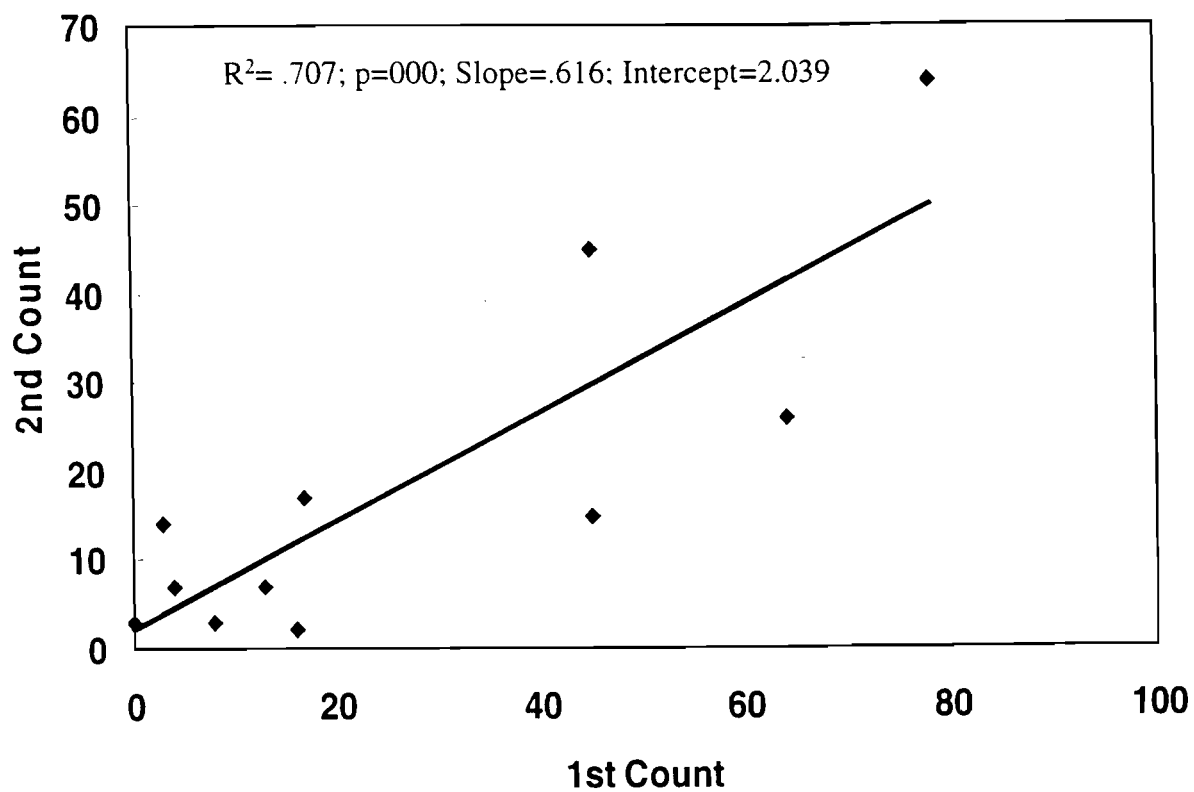


Figure 2. Repeat school counts conducted over a given bay between 24-48 hrs time difference.



Figure 3. Two age-1 herring schools in southwestern Prince William Sound (validated with net catches).



Figure 4. Age-0 sandlance school in shallow water in northeastern Prince William Sound (validated with underwater video mounted on R/V Predator).

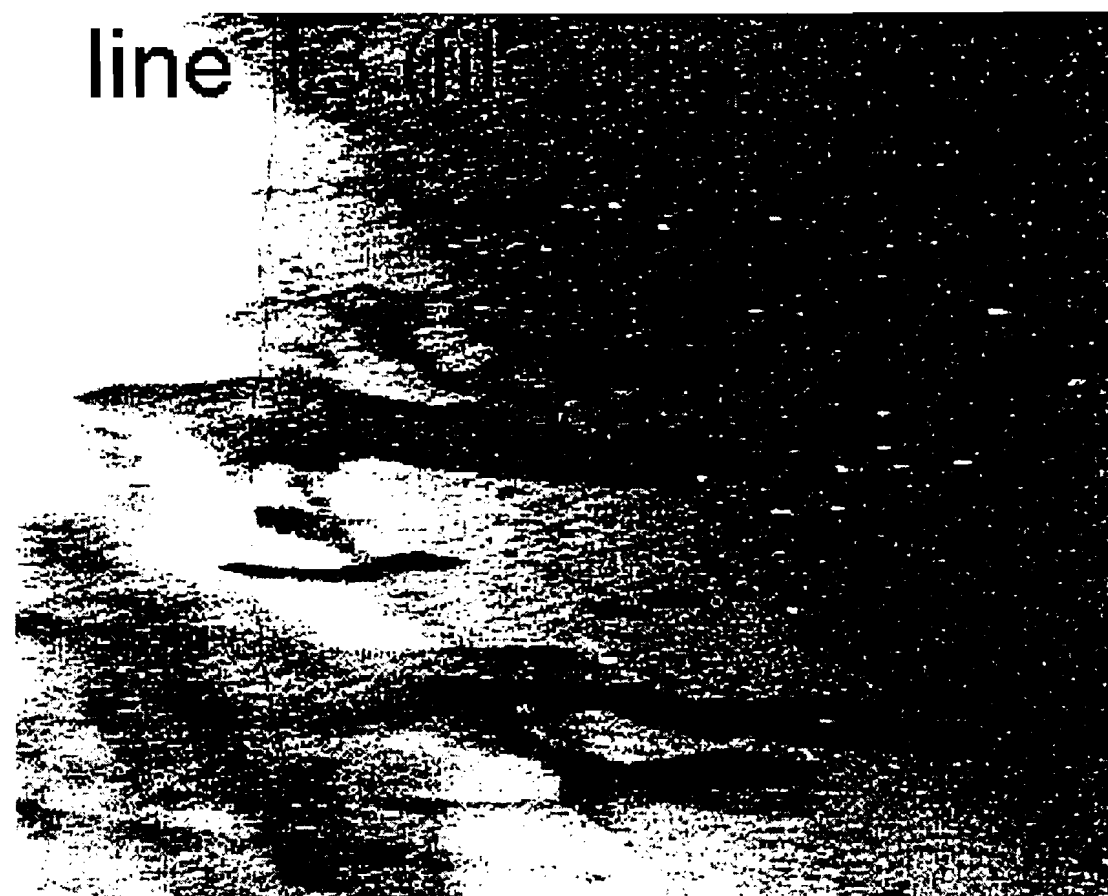
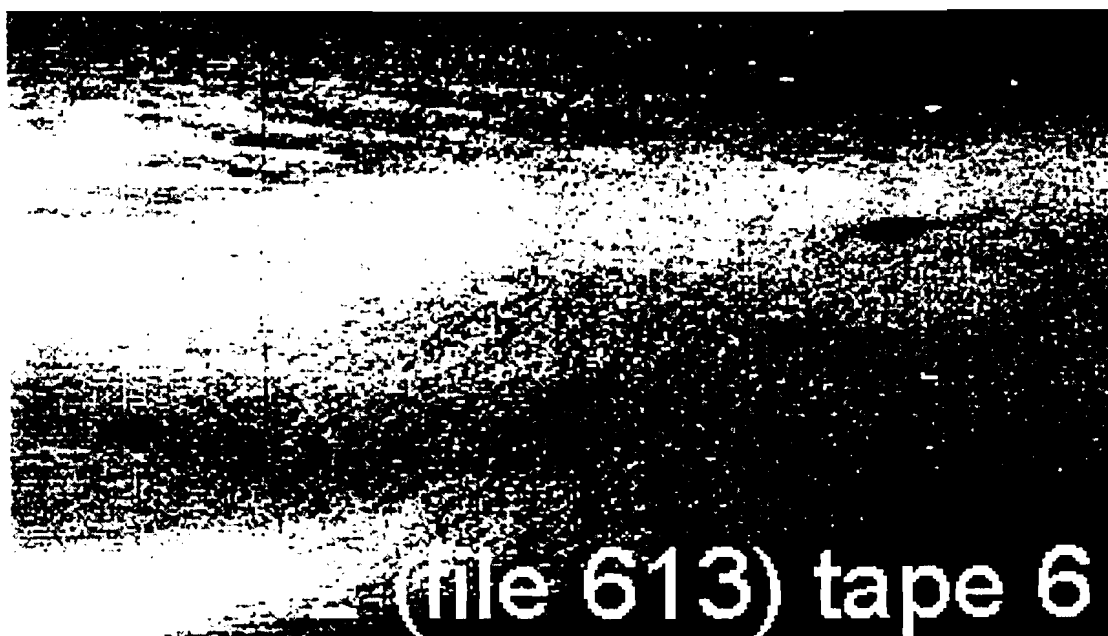
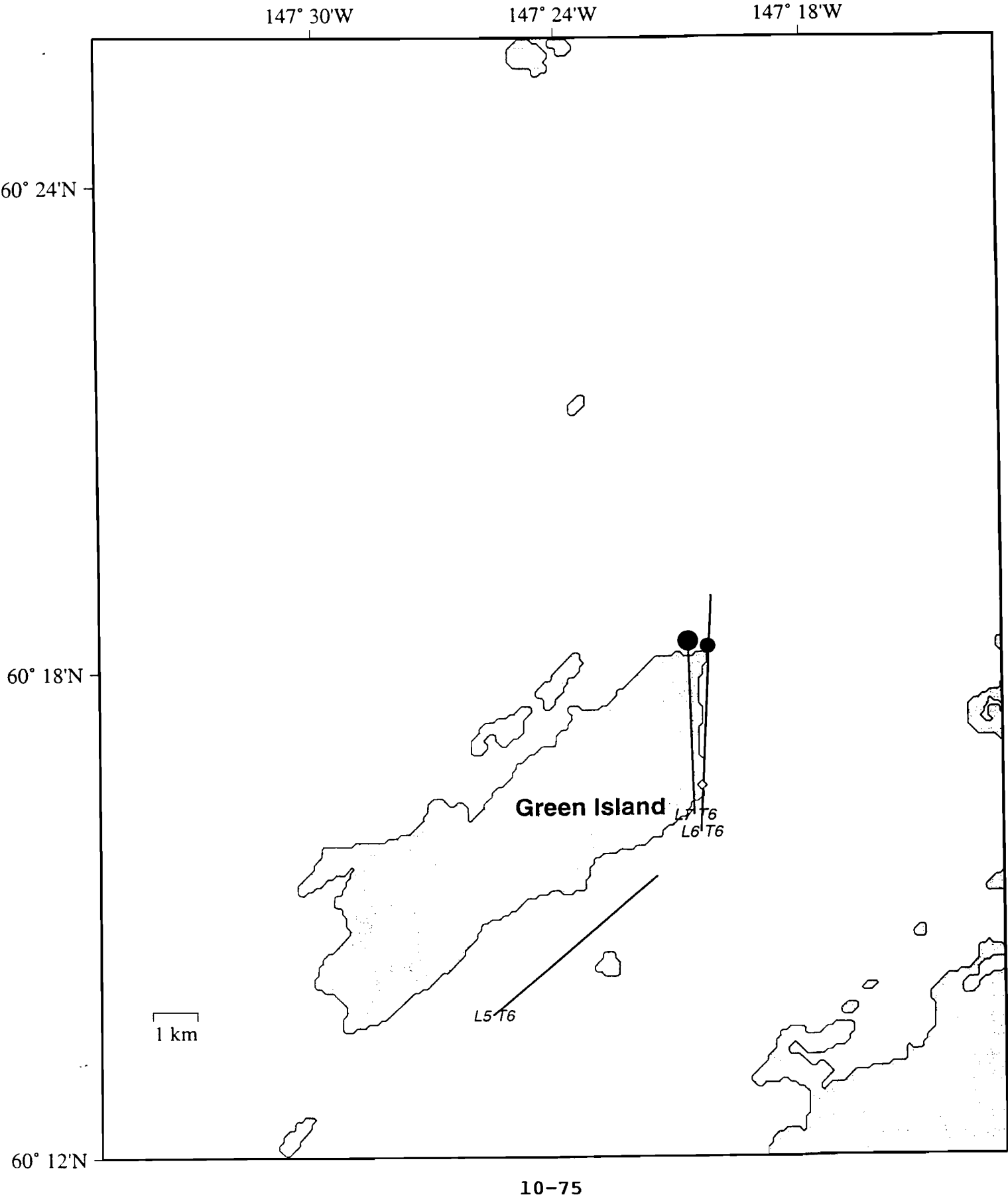


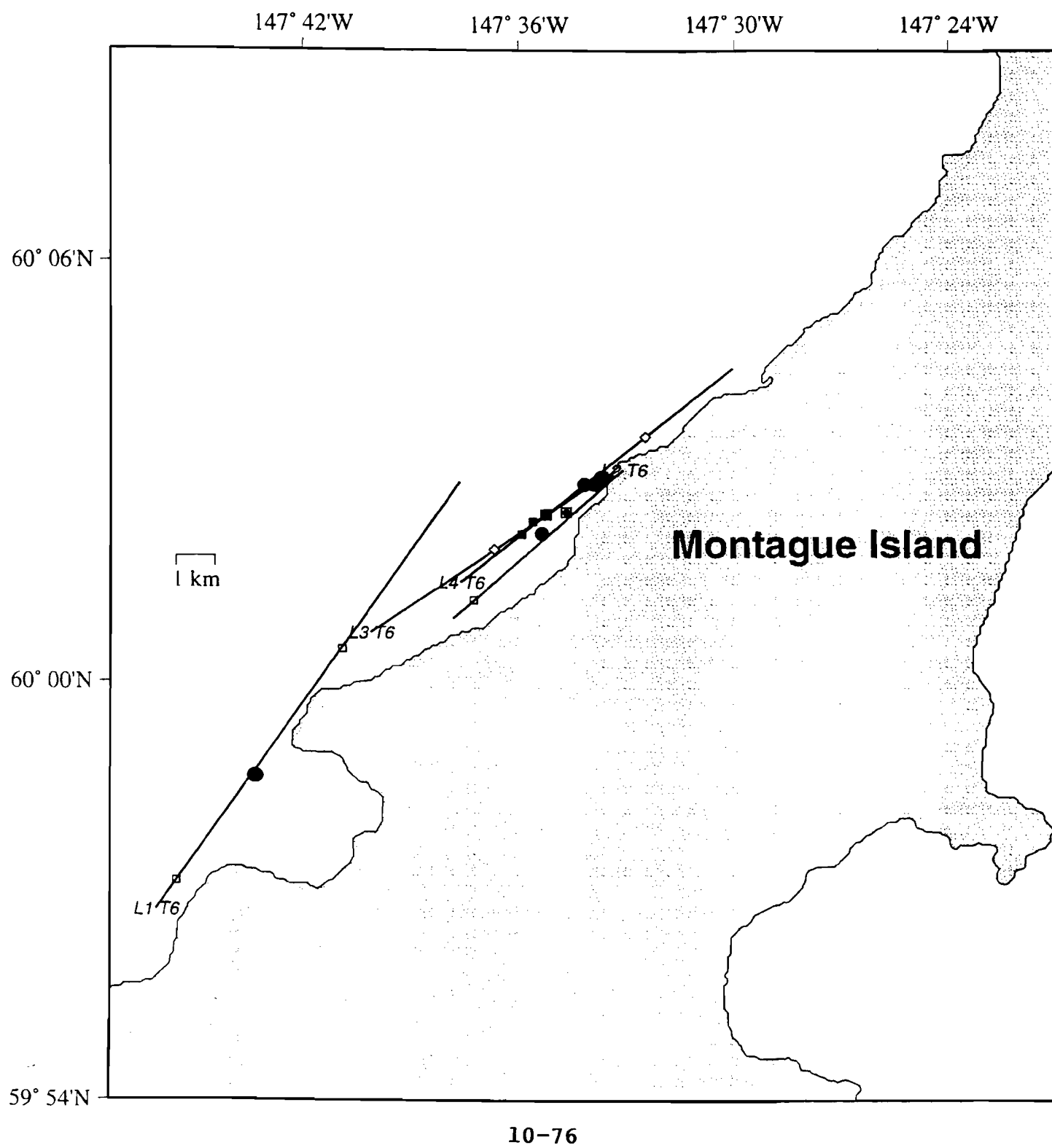
Figure 5. Images from the CASI system. The images have not been corrected for pixel distortion and appear compressed laterally as a result. The top image is herring schools on the northwestern shore of Hinchinbrook Island (eastern Prince William Sound). The bottom image is sandlance schools on the northeastern shore of Hinchinbrook Island. The white spots are individual gulls.

Shade by value (m ² surface area) of fish schools at a given location.	Total no. birds at a given location	Marine mammal(s) at a given location
• 1-10		
• 11-20	▣ 1-25	◇ 1-3
• 21-30	▣ 26-50	◇ >4
• 31-50	▣ 51-100	
● 51-100	▣ 101-200	
● 101-200	▣ 201-500	
● 201-500	▣ 501-1000	
● 501-1000	▣ 1001-5000	
● >1000	▣ >5001	

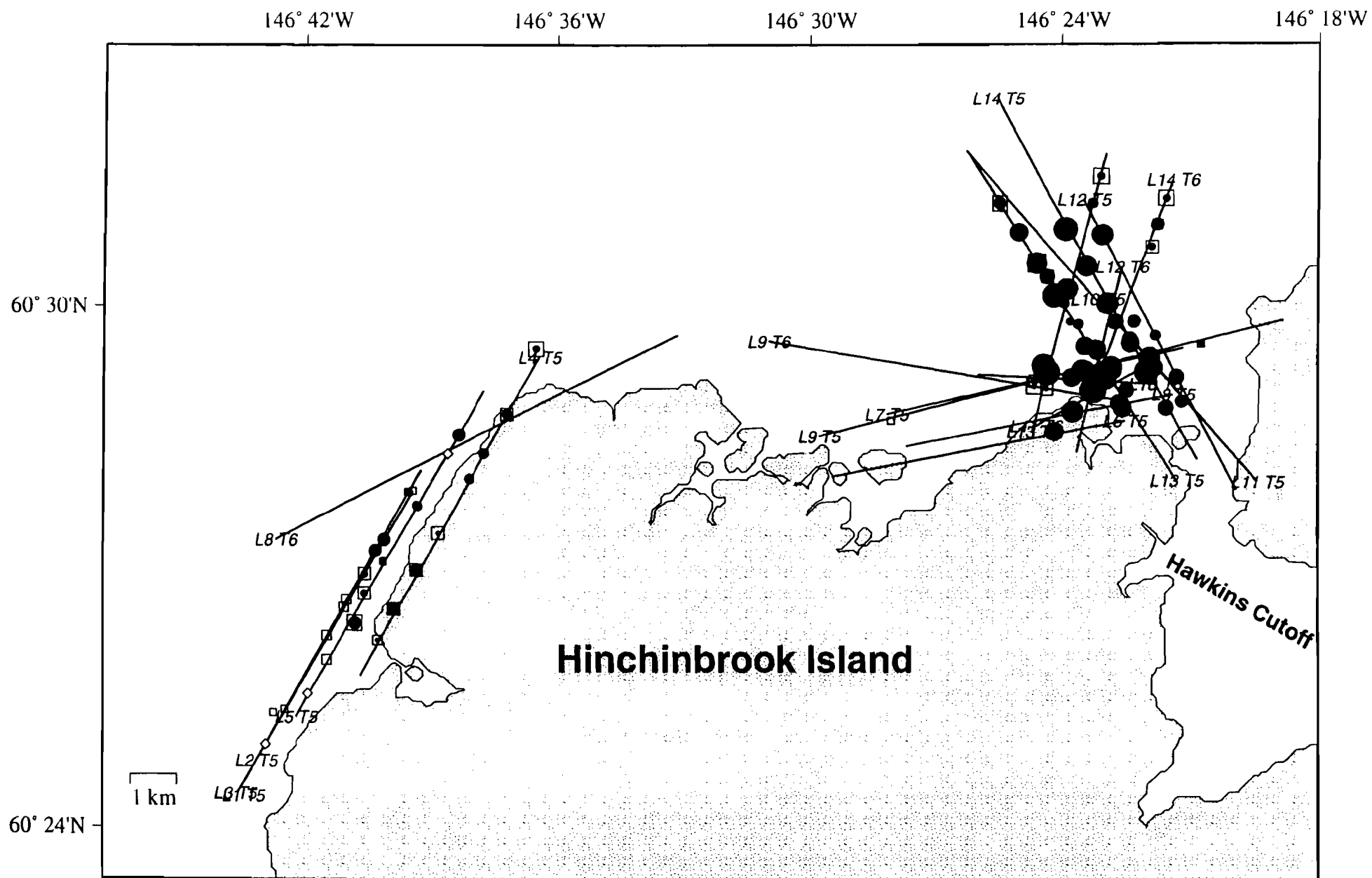
Appendix III Figure 7. CASI surveys at Green Island (low density).

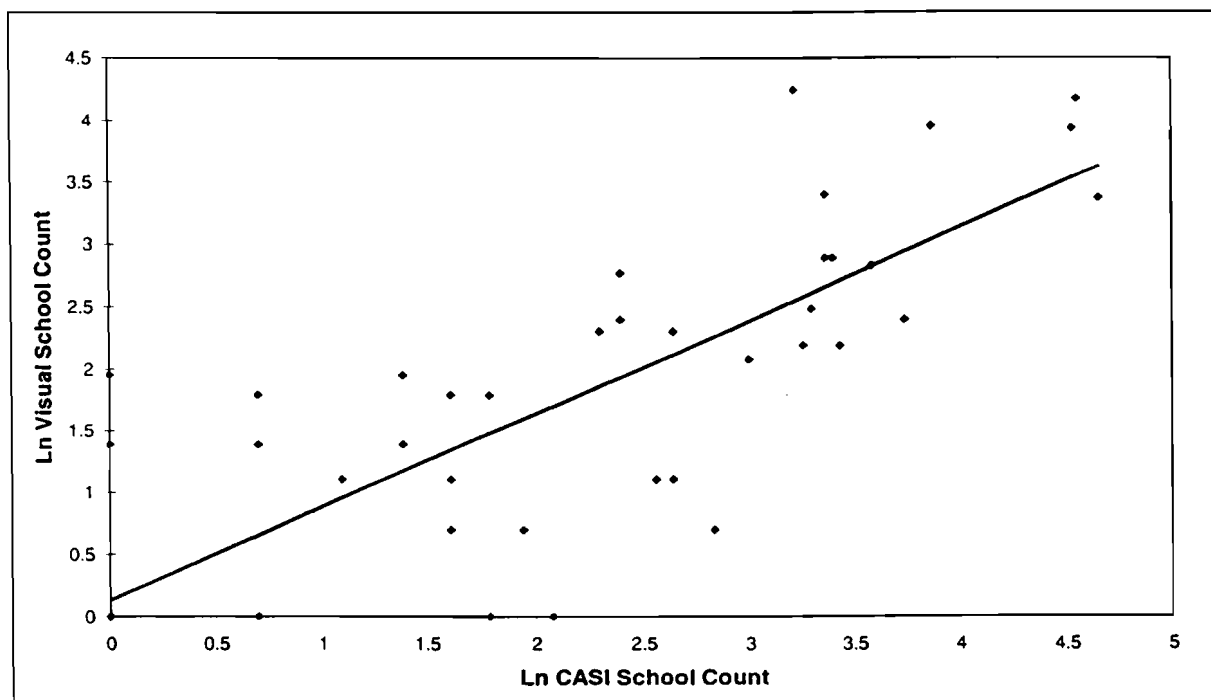


Appendix III Figure 8. CASI surveys at Montague Island (low density).



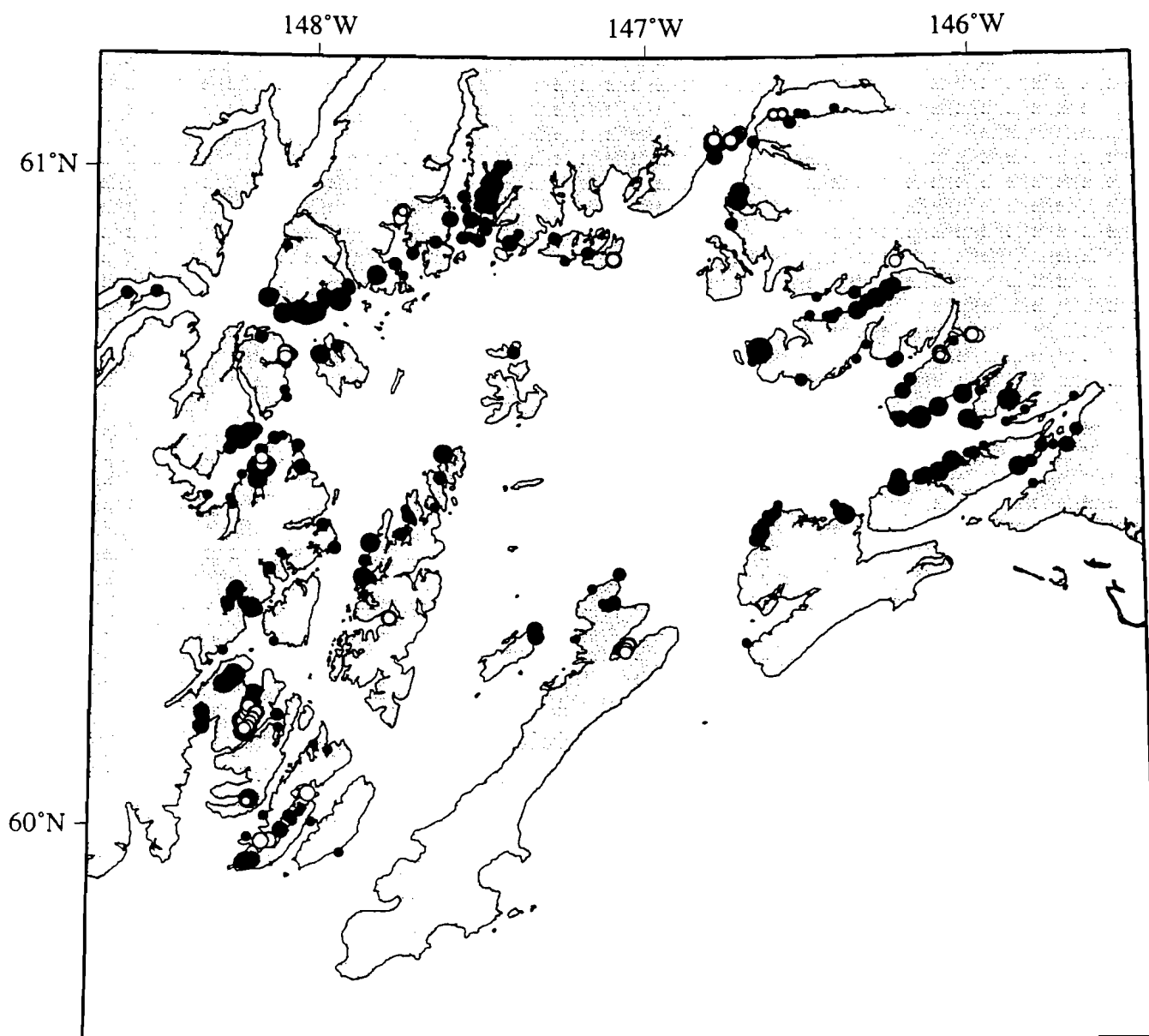
Appendix III Figure 9. CASI surveys at Hinchinbrook Island (medium and high densities).





$R^2=0.730$; $p=0.0000$; d.f.=36 (transects); slope=0.75

Figure 10. Regression analysis of ln transformed visual school counts versus CASI school counts by transect.



Acoustic Data

- YOY
- ◐ 1 year old
- Adult

Aerial Survey: Shoal surface area (m²)

- 1-50
- 51-100
- >100

Appendix III Figure 11. Comparison of broadscale aerial survey results to broadscale acoustic measurements.

Appendix IV

Foy, R. J., and B. L. Norcross. 1998. Spatial and temporal differences in the diet of juvenile Pacific herring (*Clupea pallasii*) in Prince William Sound, Alaska.

Spatial and Temporal Differences in the Diet of Juvenile Pacific Herring (Clupea pallasii) in Prince William Sound, Alaska

Robert J. Foy and Brenda L. Norcross

R. J. Foy. Institute of Marine Science, University of Alaska Fairbanks, P.O. Box 757220, Fairbanks, Alaska 99775-7220 USA. PHONE: 907-474-5801 FAX: 907-474-1943 email: foy@ims.alaska.edu

B. L. Norcross. Institute of Marine Science, University of Alaska Fairbanks, P.O. Box 757220, Fairbanks, Alaska 99775-7220 USA. PHONE: 907-474-7990 FAX: 907-474-1943 email: norcross@ims.alaska.edu

Abstract

The diet of juvenile Pacific herring, Clupea pallasii, from four bays in Prince William Sound, Alaska, differed spatially and seasonally. The stomach fullness and diversity indices of juvenile herring were significantly larger in May and declined through the following winter. Spatial and temporal trends were found among the most important prey species in the diet of juvenile herring. In March, fish eggs, Cirripedia nauplii, small Calanoida, and large Calanoida were the dominant prey in Eaglek, Simpson, Whale, and Zaikof Bay, respectively. In October, Oikopleura species of Larvacea were dominant in all bays sampled. In Zaikof Bay, large Calanoida dominated the prey taxa in May of 1995 and March of 1996. Small Calanoida and Larvacea were the highest prey biomass in summer and fall, respectively.

Introduction

Pacific herring, Clupea pallasii Valenciennes (1847), are distributed along the Asiatic and North American continental shelves in the Pacific Ocean. In Prince William Sound, Alaska, herring are a commercially important fishery. Reduced abundance, resulting in the closure of the commercial fishery in 1993, have led to questions about the recruitment processes in Prince William Sound. When studying recruitment it is important to understand mechanisms that create variation at particular stages in the fish's development (Houde 1987; Miller et al. 1991). For example, starvation or slow growth rates can lead to high mortality and decreased recruitment. Water temperature has been correlated to the density of zooplankton and subsequent abundant classes of herring (Maksimenkov 1982). An important aspect of herring recruitment variation, therefore, is that associated with the feeding behavior and success of larvae and juveniles prior to recruitment.

Most feeding studies and subsequent hypotheses regarding herring recruitment focus on larval stages and first feeding (Cushing 1975; Iles and Sinclair 1982; Sinclair and Tremblay 1984; Cushing 1990). However, recruitment may also be regulated during the juvenile stage of development (Houde 1987; Bollens et al. 1992). We hypothesize that the juvenile stage of Prince William Sound herring development incurs a significant amount of variation in mortality and therefore recruitment to older stages. This variation may be explained through the understanding the juvenile feeding ecology.

The spatial and temporal characteristics of the juvenile herring feeding ecology in Prince William Sound are poorly understood. Atlantic herring (Clupea harengus) are capable of filter and particulate feeding, depending on the size and concentrations of potential prey (Gibson and Ezzi 1985). Size dependent predation (Hrbáček et al. 1961; Brooks and Dodson 1965) suggests that herring would preferentially prey on the larger zooplankton. Densities of smaller zooplankton would then become greater due to decreased grazing pressure from larger zooplankton and, therefore, would become an available prey source to small fish such as juvenile herring. The prey of Baltic herring (Clupea harengus) increase in size with sampling date and fish size (Arrhenius 1996). Age 0+ Baltic herring feed on smaller zooplankton such as small copepods and cladocerans (Raid 1985; Rudstam et al. 1992; Mehner 1993; Arrhenius 1996) whereas larger juvenile herring prey on larger calanoid species when available (Pearcy et al. 1979; Sandstrom 1980). Cannibalism on larval herring by juveniles in the North Pacific has been found to occur (Hourston et al. 1981). Adult herring feed on euphausiids and larger copepod species (Pearcy et al. 1979), reproducing copepod and cladoceran species (Flinkman et al. 1991), and occasionally on pink salmon fry (Thorsteinson 1962) and chinook salmon fry (Ito and Parker 1971). Alternative fish feeding theories, which suggest the importance of the profitability of prey, take into account searching and handling time (optimal foraging) which may not favor the larger prey species (Werner and Hall 1974; Bence and Murdoch 1986). Selective feeding by Atlantic herring has been hypothesized to be dependent on prey escape capability, visibility, and possibly nutritional value (Checkley 1982).

Identification of seasonal prey species in herring diet is an important first step to understanding the trophic interactions of herring and its prey. We hypothesize that the diet of juvenile herring in Prince William Sound will temporally and spatially vary according to the abundance and species composition of available prey. Therefore, the objective of this

study is to describe the relative importance of prey categories in the diet of juvenile herring from four bays within Prince William Sound during the spring, summer, and fall.

Materials and Methods

Sample Collection

Prince William Sound is a coastal estuarine system located along the southern coast of Alaska. Four bays were chosen as study sites within the sound (Fig. 1). Eaglek and Whale Bays are deep fjords whereas Simpson and Zaikof Bays are relatively shallow estuaries. A total of 38 herring schools were sampled in May, June, and October 1995 and March 1996. Juvenile herring schools were targeted and caught using a purse seine vessel with a 250 m x 34 m or 250 m x 20 m, 150 mm stretch mesh anchovy net or a trawl vessel with a 40 m x 28 m, 150 mm mesh mid-water wing trawl net. From each catch, 15 fish were randomly sampled. Fish were measured (fork length mm) and preserved in a 10 % buffered formaldehyde solution. After 24 hours, samples were transferred to 50 % isopropanol for diet analysis.

Average weights of preserved zooplankton (Appendix 1) for prey biomass estimates were obtained from a database generated at the Institute of Marine Science at the University of Alaska Fairbanks. Seasonal zooplankton samples have been obtained from multiple sites in Prince William Sound and the upper North Pacific Ocean via 20 m vertical tows with a 333 μ m mesh net since 1987. Average weights of taxa are updated annually by weighing formalin preserved individuals (at least 15) until a representative weight distribution has been obtained and added to the database.

Diet analysis

Each fish was blotted dry, weighed to the nearest 0.01 g, and measured (fork and standard length) to the nearest 1.0 mm. The stomach was removed and weighed to the nearest 0.001 g. Stomach contents were removed and the empty stomach was reweighed to determine stomach content weight. Stomach fullness indices were calculated by dividing the stomach content weight by the total fish weight and were used to compare the temporal and spatial feeding activity of juvenile herring.

Prey in the stomach were enumerated and identified to the lowest possible taxonomic level. In some cases, due to digestion, it was only possible to identify prey to a broad taxonomic grouping (i.e. Calanoida > 2.5 mm). Prey biomass in the stomach was calculated by multiplying the database value of mean weight by the total stomach content number for each prey species. The distribution of prey biomass was compared to a logarithmic function in order to determine if a logarithmic series would be an appropriate measure of heterogeneity of prey found in the diet of herring. A logarithmic index of species diversity (α) of prey biomass in the stomach content was calculated for each site within each month (Fisher et al. 1943; Anscombe 1950; Krebs 1989). The logarithmic index of diversity is a function of the number of species in a sample and the number of individuals in a sample. For this study, however, the total biomass of a taxon was used instead of the number of individuals in a taxon. Spatial and temporal comparisons described the dominant prey taxa seasonally within each bay.

The percentage of stomach content number (% N), percentage of stomach content weight (% W), and percent frequency of occurrence among fish (% FO) was determined for each prey species in the stomach contents. The percent index of relative importance (% IRI

$= (\% N + \% W) * \% FO$; Pinkas et al. 1971) was calculated separately by site and by month and used to compare the relative importance of prey species taking into account the number of times a prey species was actually encountered in the diet of the herring sampled. Only IRI values above five percent are reported here to focus on the most important prey species.

Statistical analysis

Spatial analyses were conducted among all four sites from March, and among Zaikof Bay, Simpson Bay, and Whale Bay from October. Temporal analyses were conducted among the four months on samples from Zaikof Bay. Stomach fullness indices were arcsine transformed to satisfy the assumptions of normality by a Shapiro-Wilks' W test of normality prior to analysis. Mean stomach fullness indices were compared among sites and months using one-way analyses of variance. Significant differences between groups were analysed post hoc using an extended Tukey method when cases have unequal sample sizes (Spjøtvoll and Stoline 1973). Prey biomass distributions were compared to logarithmic functions using the coefficients of determination from the fitted equation.

Results

Sample sizes of herring used in the diet analysis within bays ranged from 12 to 146 fish (Table 1). Standard lengths of herring averaged 107 mm and ranged from 42 to 230 mm. The number of stomachs that contained prey items ranged from 12 to 114 fish.

Herring stomach fullness indices were significantly different among sites in October ($F=12.28$ $P<0.01$ $DF=2$) and March ($F=14.59$ $P<0.01$ $DF=3$). In October, stomach fullness indices from herring in Whale Bay were not significantly different from those in Zaikof Bay. In March, stomach fullness indices of herring from Simpson Bay were not significantly different from those in Zaikof Bay and Eaglek Bay (Table 1).

Stomach fullness indices from herring sampled for temporal analysis from Zaikof Bay were significantly different among months ($F=91.90$ $P<0.01$ $DF=3$), however, there was no significant difference in stomach content indices between October and March.

The logarithmic distribution described the distributions of prey species biomass described from the herring stomach contents in all months and sites; coefficients of determination ranged from 0.43 to 0.88 (Table 2). The logarithmic distribution also described the distributions of total biomass in October and March with coefficients of determination of 0.95 and 0.79, respectively (Figs. 2 and 3). In October, the five highest contributors to prey biomass were *Oikopleura* sp., *Euphausia* sp., Calanoida (<2.5 mm), Malacostraca, and *Metridia ochotensis*, respectively (Fig. 2). The five highest contributors to prey biomass in March were fish eggs, Calanoida (> 2.5 mm), Cirripedia nauplii, Calanoida (<2.5 mm), and Decapoda zoea, respectively (Fig. 3). The logarithmic indices of species diversity (α) ranged from 1.3 to 7.1 and had variances ranging from 0.18 to 2.20 (Table 2).

Indices of relative importance were calculated to determine spatial trends in the frequency of prey taxa in the diet of herring. In October, *Oikopleura* sp. of Larvacea was the dominant prey species in all three bays. In March, there were notable spatial differences in dominant prey taxa among the four bays (Fig. 4). Fish eggs were dominant in Eaglek Bay and were the second most important prey taxa in Simpson and Zaikof Bays. Cirripedia nauplii were the dominant prey taxa in Simpson Bay. As in March, Calanoida (< 2.5 mm)

were the dominant prey in Whale Bay whereas Calanoida (> 2.5 mm) were dominant in Zaikof Bay.

Indices of Relative Importance were also calculated to determine temporal differences in the dominant prey taxa in Zaikof Bay (Figs. 4 and 5). Calanoida (> 2.5 mm) were dominant in May. The June diet consisted of more species above an importance index of 5 % than any other period and Calanoida (< 2.5 mm) was the dominant taxa.

Discussion

Stomach fullness indices are applied to biomass data because we wanted to analyze both the number and weight of prey in each taxa identified. For instance, in October and March, herring from Whale Bay have significantly larger biomass of prey than any other site. In October, this is due to greater weights of prey species whereas the number of prey per fish is greater in March.

In Zaikof Bay, significantly larger prey biomass in May diets than later in the fall and the following spring is explained by the higher biomass of zooplankton common to Prince William Sound in April and May after the period of high productivity (Goering et al. 1973). The availability of prey after the high spring productivity is, therefore, limiting to the amount of food ingested by the herring sampled in this study. This assumes a positive linear relationship between the stomach capacity and weight of the fish, which has been found to be exponential for other species of fish (Knight and Margraf 1982).

The spatial and temporal variability observed in the stomach fullness indices suggests that the consumption rates in Prince William Sound may be variable. Trophodynamic models based on empirical models of copepod biomass estimate that juvenile herring on the southern British Columbia continental shelf need to ingest 3 % of their body weight of copepods per day (Robinson and Ware 1994). Consumption rates for Baltic herring are 10-20 % body weight per day for 0+ fish, 7-13 % for juvenile fish and 5 % for older fish (Rudstam et al. 1992). A 1.3 % body weight consumption rate for 0+ southern Baltic herring in May has been estimated (Mehner and Heerkloss 1994). In a controlled experiment, Atlantic herring are estimated to consume 5 % body weight at 6.5 °C, and 11 % body weight at 11 °C (DeSilva and Balbontin 1974). Consumption of 9.2 % per day is estimated for juvenile herring in the Baltic (Rudstam 1988). Much of the variation in these estimates may be due to the temperature and/or relative energetic value of the prey items encountered.

Fifty-three percent of the stomachs in Zaikof Bay in March were empty. The occurrence of empty stomachs was never higher than 27 % in any other bay in any month. Low consumption rates in Zaikof Bay during the winter suggests a potential effect on the survival of juveniles through the winter in this bay. Future studies of juvenile herring feeding in Prince William Sound should focus on annual consumption rates around the sound in order to compare seasonal growth with respect to survival prior to recruitment.

Diversity indices are a means of describing the species composition of a community (Krebs 1989). In this study, the logarithmic diversity index is used to compare the seasonal variation in prey species biomass found in the stomach contents of juvenile herring from the four bays. The biomass of prey from Eaglek Bay in March does not fit a logarithmic distribution due to the dominance of fish eggs in the herring diets; however, this does not significantly affect the value of the index of diversity.

The diversity of prey species in Zaikof Bay is largest in May followed by June due to the availability of different prey associated with the spring plankton bloom. Herring from Whale Bay, which have significantly higher stomach fullness indices, have lower prey diversity indices suggesting that juvenile herring can feed more when there is an increased biomass of fewer available prey taxa. Feeding more, however, does not mean an energetically better diet. It is possible that selective feeding during periods of low prey diversity and high density provides energetically “better” prey than feeding at times of high prey diversity and low density regardless of the level of stomach fullness achieved.

Comparisons of dominant prey species in the stomach content of juvenile herring account for the relative frequency of prey taxa occurrence with the index of relative importance. The spatial and temporal differences of the stomach fullness indices and diversity indices are exemplified by the distribution of most important prey species. Temporal differences are apparent in Zaikof Bay, indicating the seasonal importance of feeding to juvenile herring. In October, the dominant prey species in the diet was Oikopleura sp. in all three bays, which emphasizes the feeding strategy of herring when there is low prey diversity. A low diversity diet consisting of Copepoda, especially Eurytemora/Temora, dominates 0+ Baltic herring diet in October (Rudstam et al. 1992). The availability and energy density of prey may very well dictate which fish have enough energetic reserves to survive the winter, especially in the first year (Paul et al. ??).

Spatial differences in dominant prey taxa are especially evident in the spring. In March, when primary productivity is beginning to increase, the dominant prey species in the juvenile herring diet is different in each bay. This may represent a difference in prey composition or different herring feeding behavior. Variation among bays is controlled by the ecosystem response to the spring bloom oceanographic factors such as temperature, salinity, and nutrient availability as well as biological factors such as predation and competition among zooplankters.

Temporal differences of copepod presence in herring diets from this study are similar to variations in copepod abundance on the shelf near Kodiak Island, Alaska (Vogel and McMurray 1982) and the Gulf of Alaska (Cooney 1988). The diet of 0+ Baltic herring in the summer reflects the zooplankton availability, which consists mostly of Cladocera in the summer (Rudstam et al. 1992). In the fall of 1975, the dominant taxa of zooplankton in Prince William Sound were Copepoda, Amphipoda, and Euphausiacea (Damkaer 1977). Of the copepods, Acartia longiremis, Oithona similis, and Pseudocalanus sp. were the most abundant living in the upper waters. These species were present in low abundance in the herring diets in the fall of 1996. It is interesting to note that Larvacea were only in small abundance among the zooplankton in 1975, whereas in this study, they dominate the juvenile herring diet. Future analysis of the current zooplankton densities and composition in Prince William Sound will augment juvenile herring diet information with measures of prey availability.

Behavioral characteristics also have effects on the diet composition depending on whether the fish are filter or particulate feeding. Selective feeding by herring occurs in many locations. The size and abundance of prey of age-0 Baltic herring from 1978-1982 depend on the body size of the fish in the Gulf of Finland feeding mostly on Eurytemora sp. and Cladocera including Podon polyphemoides (Raid 1985). Baltic herring (150-220 mm) in Bothnian Bay select for the largest prey available which is Limnocalanus

grimaldi) in the early summer and switch to Eurytemora sp. and Cladocera after the L. grimaldi are gone (Sandstrom 1980). Similarly, in Zaikof Bay, the juvenile herring diets are dominated by large copepods available in the spring and then a mixture of other prey later in the season. The other three bays did not exhibit this trend, possibly due to the lack of availability of the larger zooplankton or to selection of different prey species. This is consistent 0+ Baltic herring which in April through June 1990 and 1991 consume Eurytemora affinis adults, nauplii, and eggs and to a small extent Harpacticoida in a bay in the southern Baltic Sea (Mehner 1993) and in the summer and fall 1992 and 1993 consume Acartia sp., Eurytemora sp., and Pseudocalanus sp. of Copepoda and Bosmina sp. and Pleopsis sp. of Cladocera (Arrhenius 1996). Bering Sea larval herring feed on smaller prey such as bivalve larvae and barnacle nauplii (Maksimenkov 1982), consistent with the juvenile herring diets from Simpson and Whale Bay in this study.

Diet composition will also be affected by the diel vertical migration of herring. For instance, the relatively small number of benthic and epibenthic invertebrate species found in the diet of herring in this study most likely represent feeding near the bottom during the day when feeding is at a minimum. Baltic herring prey on increased numbers of zoobenthic prey species, corresponding to the depth of capture (Ostrowski and Mackiewicz 1992). They hypothesize that this was due to the unavailability of preferred macro and mesozooplankton. It will be the goal of future work to elucidate such diel and ontogenetic shifts in juvenile herring feeding behavior.

Acknowledgments

We thank P. Lovely and C. Stark for sample sorting. Thanks to K. D. E. Stokesbury and A. Blanchard for advise with data analysis. This project was funded by the Exxon Valdez Oil Spill Trustee Council through the Sound Ecosystem Assessment (SEA) project. However, the findings presented by the authors are their own and not necessarily the Trustee Council position.

References

- Anscombe, F. J. 1950. Sampling theory of the negative binomial and logarithmic series distributions. *Biometrika*. **37**: 358-382.
- Arrhenius, F. 1996. Diet composition and food selectivity of 0-group herring (*Clupea harengus* L.) and sprat (*Sprattus sprattus* (L.)) in the northern Baltic Sea. *ICES Journal of Marine Science*. **53**: 701-712.
- Bence, J. R., and Murdoch, W. W. 1986. Prey size selection by the mosquitofish: relation to optimal diet theory. *Ecology*. **67**: 324-336.
- Bollens, S. M., Frost, B. W., Schwaniger, H. R., Davis, C. S., Way K. J., and Landsteiner, M. C. 1992. Seasonal plankton cycles in a temperate fjord and comments on the match-mismatch hypothesis. *Journal of Plankton Research*. **14**: 1279-1305.
- Brooks, J. L. and Dodson, S. I. 1965. Predation, body size, and composition of plankton. *Science*. **150**: 28-35.
- Checkley, D. M. J. 1982. Selective feeding by Atlantic herring (*Clupea harengus*) larvae on zooplankton in neutral assemblages. *Marine Ecology Progress Series*. **9**: 245-253.
- Cooney, R. T. 1988. Distribution and ecology of zooplankton in the Gulf of Alaska: a synopsis. *Bulletin of the Ocean Research Institute, University of Tokyo*. 27-41.
- Cushing, D. H. 1975. *Marine Ecology and Fisheries*. Cambridge University Press, Cambridge.
- Cushing, D. H. 1990. Plankton production and year-class strength in fish populations: an update of the match/mismatch hypothesis. *Advances in Marine Biology*. **26**: 250-293.
- Damkaer, D. M. 1977. Initial zooplankton investigations in Prince William Sound, Gulf of Alaska and Lower Cook Inlet. Pacific Marine Environmental Laboratory. National Oceanic and Atmospheric Administration. 3711 15th Avenue N.E. Seattle, Washington 98105. Research Unit #425: 137-274.
- DeSilva, S. S., and Balbontin, F. 1974. Laboratory studies of food intake, growth, and food conversion of young herring, *Clupea harengus* (L.). *J. Fish Biol.* **6**: 645-658.
- Fisher, R. A., Corbet, S. A., and Williams, C. B. 1943. The relation between the number of species and the number of individuals in a random sample of an animal population. *J. Animal Ecology*. **12**: 42-58.

- Flinkman, J., Vuorinen, I., and Aro, E.. 1991. Planktivorous Baltic herring (Clupea harengus) prey selectivity on reproducing copepods and cladocerans. Can. J. Fish. Aquatic. Sci. **48**: 73-77.
- Gibson, R. N., and Ezzi, I. A. 1985. Effect of particle concentration on filter- and particulate-feeding in the herring Clupea harengus. Marine Biology. **88**: 109-116.
- Goering, J. J., Shiels, W. E., and Patton, C. J. 1973. Primary production. Environmental studies of Port Valdez. Edited by D. W. Hood, W. E. Shiels, and E. J. Kelley. Institute of Marine Science. University of Alaska Fairbanks. Occasional Publication No. 3: 257-277.
- Houde, E. D. 1987. Fish early life dynamics and recruitment variability. American Fisheries Society Symposium. **2**: 17-29.
- Hourston, A. S., Rosenthal, H., and Kerr, S. 1981. Capacity of juvenile Pacific herring (Clupea harengus pallasii) to feed on larvae of their own species. Canadian Technical Report of Fisheries and Aquatic Sciences No. 1044. Department of Fisheries and Oceans. Resource Services Branch. Pacific Biological Station. Nanaimo, British Columbia, Canada.
- Hrbáček, J., Dvorakova, M., Korinek, V., and Prochazkova, L. 1961. Demonstration of the effect of the fish stock on the species composition of zooplankton and the intensity of metabolism of the whole plankton association. Verh. Internat. Verein. Limnol. **14**: 192-195.
- Iles, T. D., and Sinclair, M. 1982. Atlantic herring: Stock discreteness and abundance. Science. **215**: 627-633.
- Ito, J., and Parker, R.R. 1971. A record of Pacific Herring (Clupea harengus pallasii) feeding on juvenile chinook salmon (Oncorhynchus tshawytscha) in a British Columbia estuary. Journal of the Fisheries Research Board of Canada. **28**: 1921.
- Knight, R. L., and Margraf, F. J. 1982. Estimating stomach fullness in fishes. North American Journal of Fisheries Management. **4**: 412-414.
- Krebs, C. J. 1989. Ecological Methodology. HarperCollins, New York.
- Maksimenkov, V. V. 1982. Correlation of abundance of food (for herring larvae) zooplankton and water temperature in the Korfo-Karaginsk region of Bering Sea. The Soviet Journal of Marine Biology. **8**: 132-136.

- Mehner, T. 1993. Distribution and diet composition of 0+ herring (Clupea harengus L.) and perch (Perca fluviatilis L.) in a shallow estuary of the Southern Baltic. Arch. Hydrobiol. **128**: 309-316.
- Mehner, T. and Heerkloss, R. 1994. Direct estimate of food consumption of juvenile fish in a shallow inlet of the Southern Baltic. Int. Revue ges. Hydrobiol. **79**: 295-304.
- Miller, J. M., Burke, J. S., and Fitzhugh, G. R. 1991. Early life history patterns of Atlantic North American flatfish: likely (and unlikely) factors controlling recruitment. Netherlands Journal of Sea Research. **27**: 261-275.
- Munk, P., and Kiørboe, T. 1985. Feeding behavior and swimming activity of larval herring (Clupea harengus) in relation to density of copepod nauplii. Marine Ecology Progress Series. **24**: 15-21.
- Ostrowski, J., and Mackiewicz, A. 1992. Feeding of herring and cod in the southern Baltic in 1991. International Council for the Exploration of the Sea. 1-15.
- Paul, A. J., Paul, J. M., and Brown, E. D. 1997. Fall and spring somatic energy content for Alaskan Pacific herring (Clupea pallasii) relative to age, size and sex. Journal of Experimental Marine biology.
- Pearcy, W. G., Hopkins, C. C. E., Gronvik, S., and Evans, R. A. 1979. Feeding habits of cod, capelin, and herring in Balsfjorden, Northern Norway, July-August 1978: the importance of euphausiids. Sarsia. **64**: 269-277.
- Pinkas, L., Oliphant, M. S., and Iverson, I. L. K. 1971. Food habits of albacore, bluefin tuna, and bonito in California waters. Fish Bulletin 152:
- Raid, T. 1985. The reproduction areas and ecology of Baltic herring in the early stages of development found in the Soviet zone of the Gulf of Finland. Finnish Fisheries Research. **6**: 20-34.
- Robinson, C. L. K., and Ware, D. M. 1994. Modelling pelagic fish and plankton trophodynamics off southwestern Vancouver Island, British Columbia. Canadian Journal of Fisheries and Aquatic Sciences. **51**: 1737-1751.
- Rudstam, L. G. 1988. Exploring the dynamics of herring consumption in the Baltic: applications of an energetic model of fish growth. Kieler Meeresforschungen Sonderheft. **6**: 312-322.
- Rudstam, L. G., Hansson, S., Johansson, S., and Larsson, U. 1992. Dynamics of planktivory in a coastal area of the northern Baltic Sea. Mar. Ecol. Prog. Ser. **80**: 157-173.

- Sandstrom, O. 1980. Selective feeding by Baltic herring. *Hydrobiologia*. **69**: 199-207.
- Sinclair, M., and Tremblay, M. J. 1984. Timing of spawning of Atlantic herring (Clupea harengus harengus) populations and the match-mismatch theory. *Canadian Journal of Fisheries and Aquatic Sciences*. **41**: 1055-1065.
- Spjotvoll, E., and Stoline, M. R. 1973. An extension of the T-method of multiple comparison to include the cases with unequal sample sizes. *Journal of the American Statistical Association*. **68**: 975-978.
- Thorsteinson, F. V. 1962. Herring predation on pink salmon fry in a southeastern Alaska estuary. *Trans. Amer. Fish. Soc.* **91**: 321-323.
- Vogel, A. H., and McMurray, G. 1982. Seasonal population density distribution of copepods, euphausiids, amphipods and other holoplankton on the Kodiak shelf. VTN Oregon, Inc. Wilsonville, Oregon.
- Werner, E. E., and Hall, D. J. 1974. Optimal foraging and the size selection of prey by the bluegill sunfish (Lepomis macrochirus). *Ecology*. **55**: 1042-1052.

Table 1. Spatial and temporal distribution of juvenile herring lengths, the number (percent) of stomachs with prey, and stomach fullness indices of herring from Prince William Sound.

month	site	n	stomachs with prey (%)	<u>standard length (mm)</u>			<u>fullness index</u>	
				mean	SD	range	mean	SD
May	Zaikof Bay	12	12 (100)	101	3.3	95-107	0.30	0.027
June	Zaikof Bay	60	54 (90)	101	6.9	78-122	0.11	0.063
October	Simpson Bay	106	83 (78)	76	15.9	78-115	0.07	0.048
	Whale Bay	30	30 (100)	89	8.0	42-140	0.11	0.037
	Zaikof Bay	31	30 (97)	70	10.2	58-97	0.10	0.047
March	Eaglek Bay	146	114 (78)	133	26.8	84-191	0.10	0.075
	Simpson Bay	29	27 (93)	116	16.6	91-142	0.07	0.029
	Whale Bay	60	44 (73)	109	24.8	79-157	0.15	0.089
	Zaikof Bay	100	47 (100)	164	29.4	88-230	0.05	0.029

Table 2. Spatial and temporal distribution of juvenile herring prey diversity as well as coefficients of determination for fitting the data to logarithmic series.

Month	Bay	fish n	prey taxa n	r^2	diversity (\square)	\square variance
May	Zaikof	12	23	0.52	7.10	2.19
June	Zaikof	54	33	0.71	5.24	0.83
October	Simpson	83	26	0.56	4.21	0.68
	Whale	30	24	0.78	3.35	0.47
	Zaikof	30	15	0.82	2.10	0.29
March	Eaglek	114	29	0.43	4.38	0.66
	Simpson	27	10	0.75	1.33	0.18
	Whale	44	20	0.88	2.32	0.27
	Zaikof	47	27	0.61	4.18	0.65
Totals	March	232	41	0.79	5.44	0.72
	October	143	30	0.96	3.87	0.50

Figure captions

Fig. 1. Location of four bays sampled in Prince William Sound, Alaska.

Fig. 2. Distribution of juvenile herring prey biomass (g) fit to a logarithmic series from three bays in Prince William Sound in October 1995.

Fig. 3. Distribution of juvenile herring prey biomass (g) fit to a logarithmic series from four bays in Prince William Sound in March 1996.

Fig. 4. Spatial comparison of Indices of Relative Importance of juvenile herring prey in October and March.

Fig. 5. Temporal comparison of Indices of Relative Importance of juvenile herring prey in Zaikof Bay.

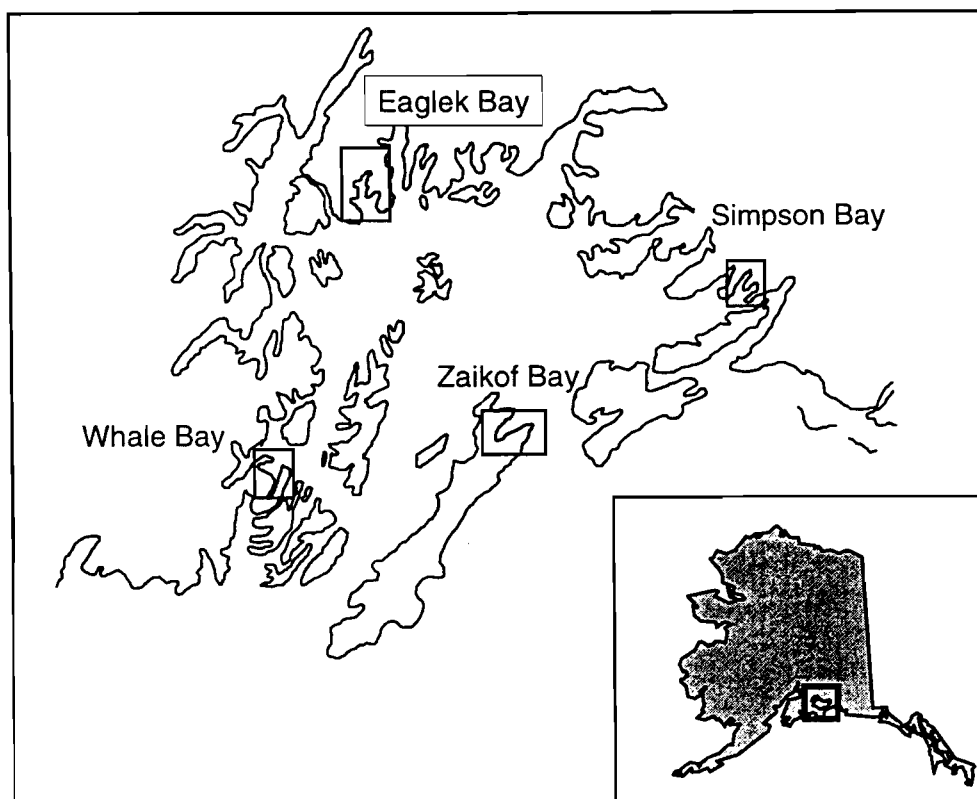


Fig. 1

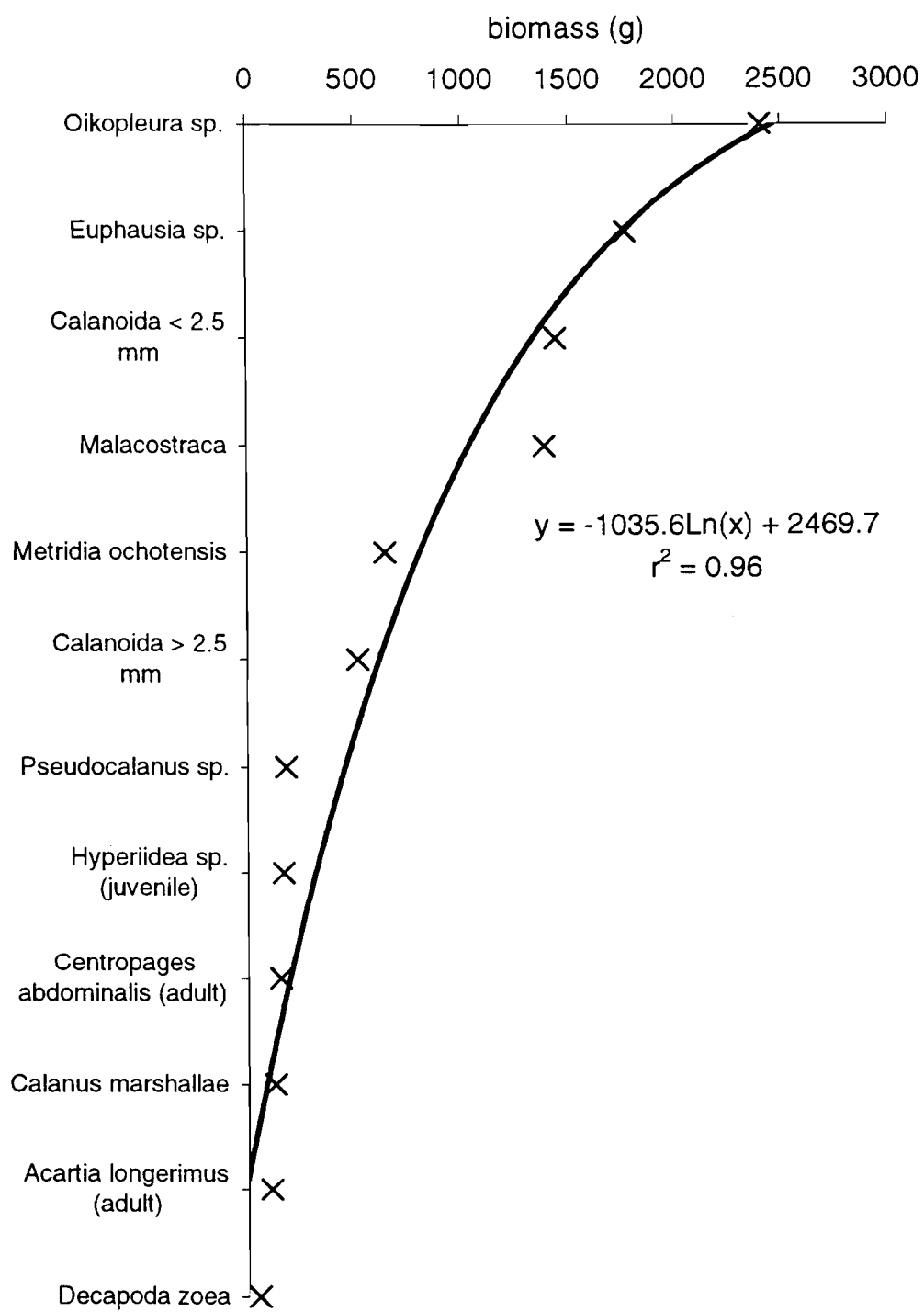


Fig. 2

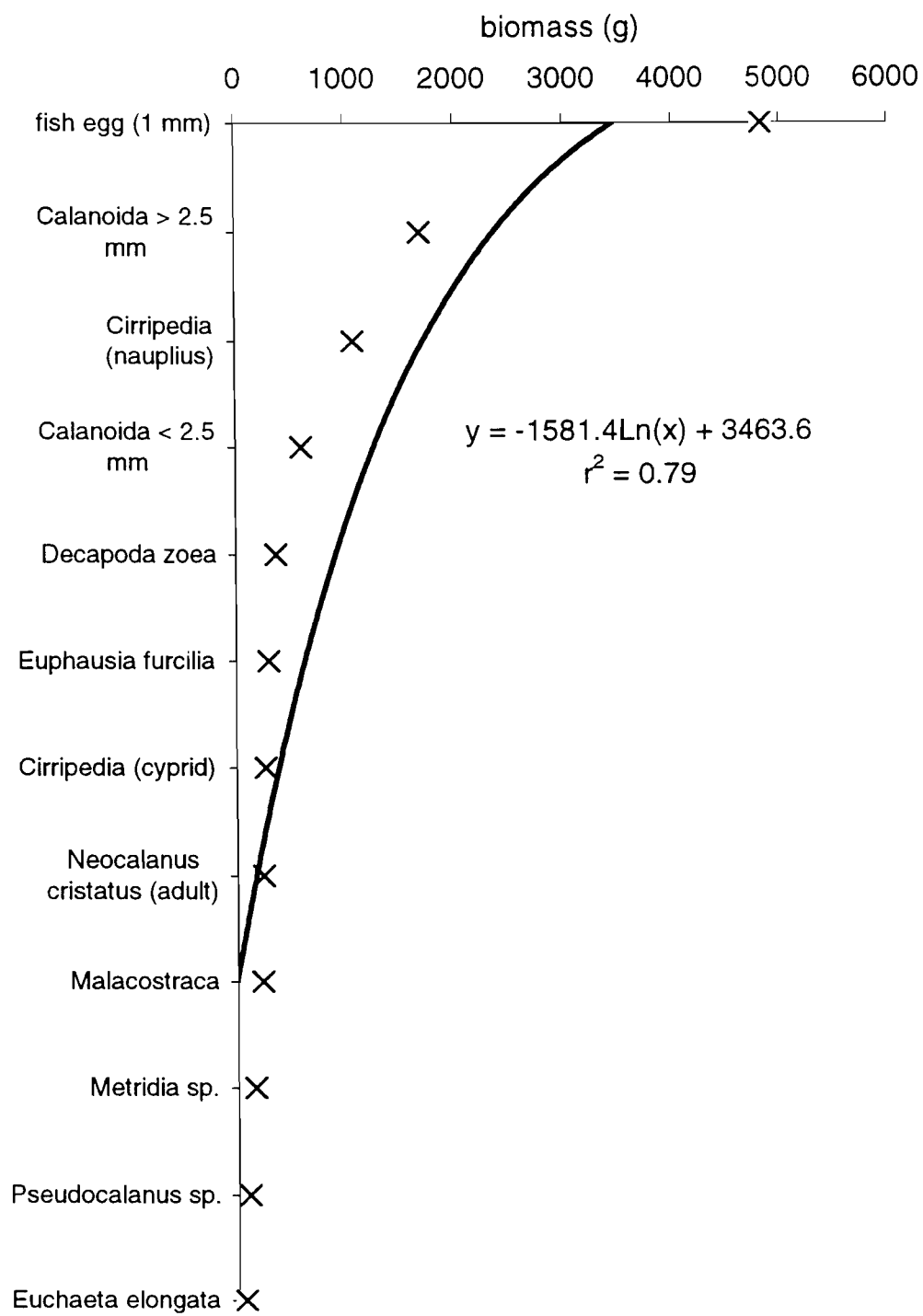
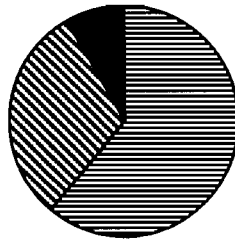


Fig. 3

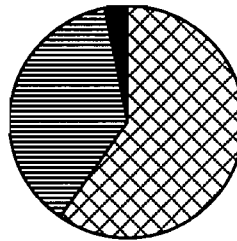
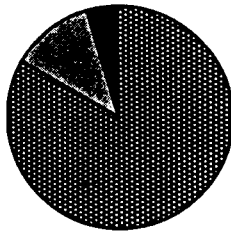
October 1995

March 1996

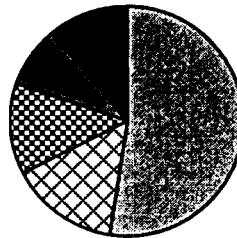
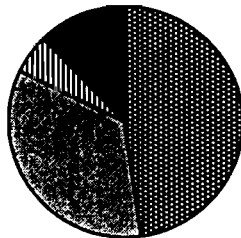
Eaglek Bay



Simpson Bay



Whale Bay



Zaikof Bay

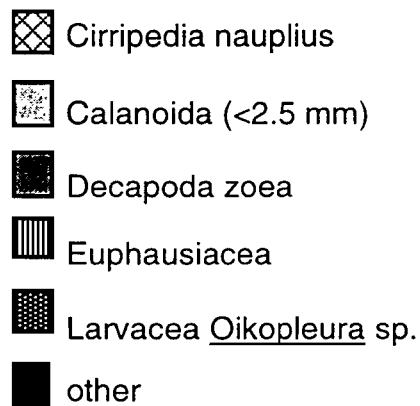
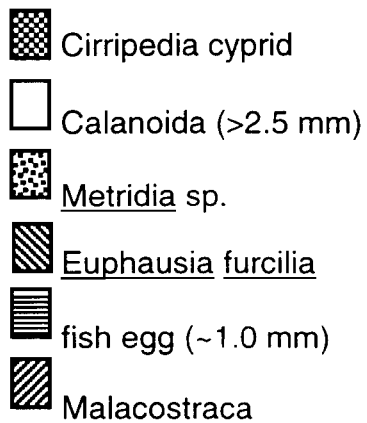
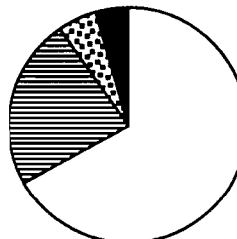
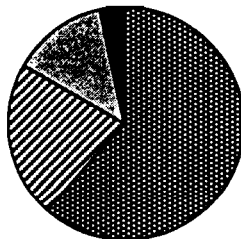


Fig. 4

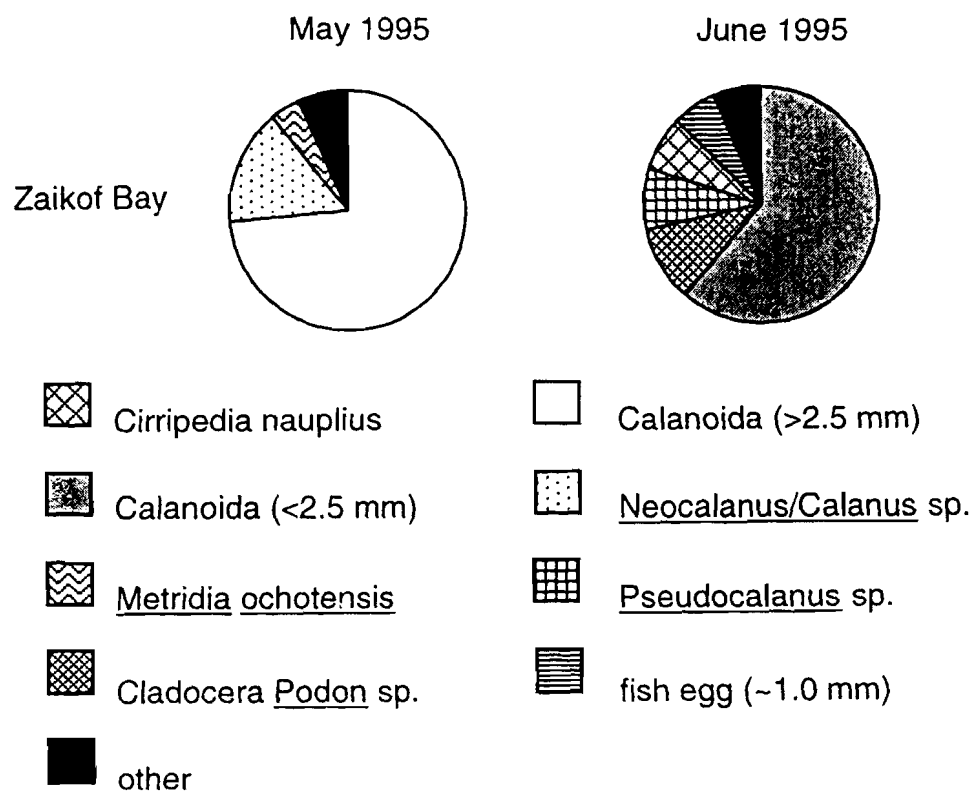


Fig. 5

Appendix 1. Average weights (mg) of invertebrate taxa from Prince William Sound used for biomass estimates.

taxon	wt (mg)	taxon	wt (mg)
<u>Acartia longiremus</u> adult	0.052	<u>Euphausia calyptopis</u>	0.165
<u>Acartia</u> sp.	0.028	fish egg (~1.0 mm)	6.590
Amphipoda Gammaridea	0.650	fish larvae	50.000
Amphipoda Hyperiidea (juvenile)	7.860	fish scales	0.001
Bivalvia (larvae)	0.005	<u>Gadius variabilis</u>	1.610
Brachyura zoea	2.620	Gammaridea <u>Ischyocerus</u> sp.	1.340
Bryozoa cyphonautes larva	0.020	Gastropoda (juvenile)	0.160
Calanoida (<2.5 mm)	0.075	Harpacticoida	0.090
Calanoida (>2.5 mm)	2.262	Hyperiidea <u>Primno macropa</u>	3.990
Calanoida <u>Metridia ochotensis</u>	1.480	invertebrate egg <0.2mm	0.000
Calanoida <u>Metridia pacifica</u> (adult female)	0.789	Isopoda	2.740
<u>Calanus marshallae</u>	1.430	Isopoda Epicaridea larva	0.190
<u>Calanus pacificus</u>	0.487	<u>Limacina helicina</u> (juvenile)	0.043
<u>Candacia columbiae</u>	2.150	Malacostraca	12.060
<u>Centropages abdominalis</u> (adult)	0.144	<u>Metridia ochotensis</u> (adult female)	1.883
Chaetognatha	0.440	<u>Metridia pacifica</u>	0.489
Chaetognatha <u>Sagitta</u> sp.	0.440	<u>Metridia</u> sp.	0.717
Cirripedia cyprid	0.288	<u>Neocalanus cristatus</u> adult	12.200
Cirripedia nauplius	0.190	<u>Neocalanus/Calanus</u> sp.	2.262
Cladocera	0.039	<u>Oncea</u> sp.	0.012
Cladocera <u>Evadne</u> sp.	0.039	<u>Oikopleura</u> sp.	0.033
Cladocera <u>Podon</u> sp.	0.039	Ostracod <u>Conchoecia</u> sp.	1.175
Cyclopoida <u>Oithona similis</u>	0.012	Paguridae zoea	1.590
Decapoda zoea	2.739	Pisinae zoea	0.330
diatom	0.000	Polychaeta (juvenile)	0.087
<u>Epilabidocera longipedata</u>	1.800	<u>Pseudocalanus</u> (adult male)	0.066
<u>Euchaeta elongata</u>	3.850	<u>Pseudocalanus</u> sp.	0.142
<u>Euphausia furcilia</u>	0.390	unknown egg mass	0.021
Euphausiacea	10.65	unknown nauplius	0.011
Euphausiacea egg	0.002		

Appendix V

Exxon Valdez Oil Spill
Restoration Project Interim Report

Distribution of Herring and Other Forage Fish as Observed by Resource Users

Restoration Project 98320T supplement
Annual Report

This annual report has been prepared for the
Exxon Valdez Oil Spill Trustee Council.

Jody Seitz

School of Fisheries and Ocean Sciences
University of Alaska Fairbanks
200 O'Neill Building
Fairbanks, Alaska 99775-7220

March 1998

Distribution of Herring and Other Forage Fish as Observed by Resource Users
Restoration Project 97320T Supplement
Annual Report

Study History: The project was initiated in 1997. The project was designed to document the historical distribution of forage fish such as juvenile herring, sandlance, capelin, and eulachon through qualitative interviews with key respondents in several communities. The information will be mapped and indexed by subject and provided to researchers with the Alaska Predator Ecosystem Experiment (APEX) and Sound Ecosystem Assessment (SEA). It is designed to provide researchers with population and habitat use information over a longer period and broader area than can be known through existing records and current data collection efforts.

Abstract: The researchers used a combination of key respondent interviews and mapping to document the locations of juvenile herring, herring of unknown age (unknown herring), mixed adult and juvenile herring (mixed herring), herring spawn, unidentified small fish (small fish), capelin, sand lance, eulachon and pollock. Researchers concentrated on recording information about juvenile herring and small fishes other than juvenile herring, such as sand lance and capelin. A total of thirty-nine respondents were interviewed in thirty-seven interviews (two couples were interviewed jointly). Ten interviews were carried out in Homer; twenty-six interviews were conducted in Cordova; and three interviews were carried out in Tatitlek. Most interviews were tape recorded. Respondents and researchers marked locations of fish schools on charts overlaid with mylar. Fish schools were color-coded by species for later reference. Maps of juvenile herring distribution in Prince William Sound were produced using the computer software mapping programs GMT for this report.

Key Words: *Exxon Valdez*, nursery areas, juvenile herring, forage fish, small fish, sand lance, capelin, traditional ecological knowledge, local knowledge, distribution.

Introduction

The Prince William Sound ecosystem, on the northern rim of the Gulf of Alaska, supports many ecologically important species, several of which are listed as threatened or endangered. Salmon and herring are two of the most important resources in the region, supporting both commercial fishing communities and wildlife populations. The 1989 Exxon Valdez oil spill occurred in the Sound at the most productive season of the year, early spring. Herring were returning to spawn, in record numbers.

Brown et al. (1996) reported that about half of the egg biomass was deposited within the oil trajectory, and an estimated 40 to 50 percent sustained oil exposure during early development. The 1989 year class was a minority of the 1993 spawning population, one of the smallest cohorts observed in the Sound. In 1993, only one third of the herring population expected to spawn were observed (Meyers et al. 1994). Viral hemorrhagic septicemia virus was identified in the population and later determined to be the primary disease related reason for the population crash.

In 1994, as part of a larger effort to understand the productivity of pink salmon and herring within the Prince William Sound ecosystem, fisheries oceanographers began a project to understand the factors contributing to the survival of juvenile herring. A focus of that project was an effort to learn more about the habitats of herring early life history stages from hatch up until the time they recruit to the adult population.

Locations of herring nursery areas have never been the subject of research in Prince William Sound prior to this effort. Herring research concerning distribution has primarily consisted of documentation of spawning areas, adult spawning aggregations, and concentrations of overwintering adult herring. This research has been focused in support of commercial fishing activities in early spring, fall and winter. Juvenile herring were sometimes caught with adult herring, but there did not seem to be complete overlap and catch-age sampling targeted adults. On the other hand, there seemed to be a large amount of anecdotal information available about distribution of small schooling fishes during times and places in Prince William Sound outside of commercial herring fishing seasons and areas.

The human presence in Prince William Sound dates back thousands of years. There are still people living in the sound who have lived in areas or who worked in areas of the sound which are no longer occupied. There are still people alive who remember and participated in the reduction fisheries and who sampled the herring in the catch for scientific analyses. Then, and more recently residents have had the opportunity to observe herring in the course of a variety of activities, including: subsistence hunting and fishing, aerial surveys of resource populations, herring or salmon spotting, fishing for bait herring or crab, or even delivering the mail by boat. Compiling and summarizing the large body of human knowledge about small herring and other schooling fishes provide researchers invaluable and often the only clues to past trends.

The goal of this project is to document historic knowledge about herring, especially during life stages and seasons when little other information is available. Since information about other schooling forage fishes can be readily obtained as well for no extra cost, the goal was expanded to include documentation of historic knowledge about all small schooling fishes. Specific objectives included the development of an appropriate interview guide, development of a historic knowledge data base, mapping and analyzing historic trends and providing this information in a format that is readily accessible to researchers. Finally, recommendations are provided in this report concerning the direction and continuation of this project.

Objectives

1. Develop an appropriate method for collection of historical and contemporary ecological knowledge about herring and other forage fish held by residents of the region.
2. Collect, organize, and map these data.
3. Disseminate these data.

Methods

TEK Protocol: The project followed the Traditional Ecological Knowledge protocols as outlined by the *Exxon Valdez* Oil Spill Trustee Council TEK advisory group. In Cordova, letters were written to the Traditional Village of Eyak and Cordova District Fishermen United was contacted regarding the project.

The first contacts were initiated from a list of potential respondents created by 97320T Project Leader, Evelyn Brown. CDFU contributed a list of potential participants. Following the first interview, other respondents were contacted through chain referral. Letters and project descriptions were sent to potential respondents. Written requests for permission to carry out the project were submitted to the IRA councils of Chenega Bay and Tatitlek. The Valdez Native Association was contacted by letter and by phone. In Homer individual respondents were recommended by chain referral and were contacted by phone, letter, and in person. An example of the interview guide is attached (Appendix A).

Community Approval:

The project leader sought approval by the IRA Councils of Chenega Bay and Tatitlek. Tatitlek approved the project May 10, 1997. The Tatitlek IRA Council recommended several elders. Two older men and a couple were interviewed.

Due to May weather, followed by summer activities; Chenega Bay's annual meeting was postponed until August. I was given approval to conduct the study in Chenega Bay on September 30, 1997.

Interview method:

All participants were given project descriptions and asked to read and sign a statement regarding the anonymity of their information, which the interviewer also signed. The statement assures the respondent that their information will be presented as part of compiled responses in a manner that protects their identity.

The interviews were carried out following Ives (1980) and Weiss (1994). All respondents were asked for permission to record the interview. Most of the interviews were tape-recorded. The interview guide was developed with the assistance of the herring researchers and was adapted over several interviews. I also referred to the interview design used by Ames and Watson in their study of cod and haddock spawning areas in the Gulf of Maine Ames (1966, unpublished manuscript). In the initial seven interviews I asked for detailed

information on the respondent's use of the Sound. The interview guide was revised after the seventh interview.

The revised interview asked less detail about respondents' use of the sound and got right to the questions about juvenile herring and forage fish. I maintained questions on commercial fishing history, and for pilots, their flight path. When these are combined with a review of ADF&G's commercial fishing seasons and history should provide much of the relevant information about patterns of use of the sound.

Responses for all interviews were recorded on a data sheet and on a chart overlaid with mylar. Following the interviews, the tapes were later reviewed, and used to check the datasheets and charts. The notes from the interviews have yet to be entered into the notes database.

Data was entered into Excel spreadsheets and digitized using a mapping software designed as a cruise planner for SEA by Charles Falkenberg, Prince William Sound Science Center, Cordova. The Homer and Seward data will be digitized using NavMaster software, since the Planner does not cover the outer Kenai Peninsula. GMT software was used to create the maps for this report.

Participants were asked to record where they had seen juvenile herring – herring less than four inches long. They were asked the year, or time frame, during which they had seen the fish schools, and asked to use colored pens to mark these schools on a chart covered with mylar. If they could not recall the exact year, they were asked to recall the range of years when they were in the area and how they saw the fish, whether they were caught, or “seen” on a sonar, or seen on the surface of the water. If respondents could not recall seeing juvenile herring they were asked to recall seeing herring in general, or small fish, at different times of the year. Information was also sought on sand lance, capelin, and eulachon, under the general category of small fish other than herring.

Respondents were asked to judge how often they saw juvenile herring in the places they had seen them, especially if they had seen them over the course of a season, or a range of years. They were asked to judge if they had seen them consistently, occasionally, or rarely.

C - CONSISTENTLY - "I'd see them almost every time I went there this time of year.

O - OCCASIONALLY - "I'd see them once in a while this time of year."

R - RARELY - "I remember them showing up there once or twice."

We also sought information about the presence of animals associated with the fish schools, but found it difficult to record much about their presence or absence over multiple years.

The Data

The Prince William Sound mapped database consists of data from interviews with twenty-five Cordova residents, four Tatitlek residents, and eight Homer residents who fished along the outer Kenai Peninsula and Prince William Sound. The notes database comprises these interviews and additional phone conversations and interviews where no observations were actually mapped. The observations are from 1938 to 1997. The Chenega Bay and Seward data has not been entered yet.

Ten Homer residents contributed observations to the database on the outer Kenai Peninsula. The observations of fishes in the bays and coastal areas of the Kenai Peninsula are from 1952 to 1997.

The Maps

The maps of juvenile herring observations in Prince William Sound were created using GMT software at the University of Alaska Fairbanks, Institute of Marine Science. Maps of juvenile herring observations in Prince William Sound for 1970, 1980, and 1990 are enclosed.

These maps group observations from a range of years into the decades which they overlap. For example, if someone saw juvenile herring in Eaglek Bay from 1970 through 1985, their observations would be represented in both the 1970s and in the 1980s. The same process was followed for observations on the outer Kenai. If a respondent had one observation in one decade, it was lumped into that decade for the purposes of this series of maps.

Notes

An additional source of information about the observations is the notes database, in preparation. Notes are being indexed using ASKSAM, which is compatible with ADF&G's marine mammal notes database. The notes concern a variety of topics: how respondents saw the fish; how they identified the fish; where the fish were in relation to the shore, or to depth; adult herring migrations; abnormal events – such as a large number of dead juveniles; and respondent's theories about herring.

Here is an example of the response to a question about how the respondent recognized juvenile herring. The notes database has not been completed. This is only an example.

To tell schools of fish in the summer, he notes that herring have, generally speaking, round schools. The schools of juveniles have soft edges. They are hard to tell from bait fish or needle fish (sandlance) in cloudy conditions with flat light. With enough light you can see the fish "flash". The herring flash is bright silver, but the bait fish looks brown and gold. The herring flash is much larger than the bait fish.

“Juveniles and bait fish are out there eating and growing. They are schooled up in round schools, for protection. They stay off the beach, and can be found on top of a cone of adults. They will be usually one to three fathoms from the surface and rarely against a beach. They like calm water with low currents, such as the backwaters of bays. If he were looking for juveniles while out flying he'd fly transects across the bays. However, he mainly looks for salmon. Their fry go into shallow water.

Sac roe fish are adults that have a mission. They are traveling and will be seen as a ball with a tail coming out ahead of it.”

One year he saw a lot of juvenile herring around Naked Island and Perry Island.

Describe for me, if you could, what it looked like to see a lot of fish:

“In terms of thousands of tons, we're not talking about tens of thousands of tons, but you've got to remember -we're not looking for herring. We're looking for salmon, and you're flying along the beaches.

The schools typically were 10 to 30 ton schools and if they were less than 10 tons, you'd have to be careful about calling them bait or herring. You'd have to have some light, because a lot of the bait fish were in little 2 to 5 ton schools. In terms of numbers, putting a number on it as far as of biomass, I don't know if I could do that.

Eaglek's always been a good producer of juveniles. And if you flew around in there you'd see 15 schools, 20 schools at a peak, and at a lull you might see one.”

Results

Respondents

Respondents included 28 salmon fishermen, of whom 21 were also herring fishermen and eight of whom were also pilots and had spotted salmon. Five individuals had had other occupations as professional biologists, cannery watchmen, and mail carriers. The average age of respondents was 54 years, the youngest was 34 and the oldest person interviewed was 86 years old. They ranged in years of commercial fishing experience from one year to sixty-eight years, with an average of 30 years of experience.

Herring spotter pilots ranged in experience from eight to thirty-six years, with an average of thirteen years experience. Several of the respondents were pilots by occupation. Several had worked both in the fishing industry and as charter pilots. Professional and non-professional pilots had a range of experience from four to 36 years, and averaged eighteen

years of experience. The averaged experience of persons in other occupations was twenty years.

Maps and Tables

The enclosed tables present some of the data upon which the maps are based. They list the places where observations occurred, and the range of years and number of respondents who saw fish in a group of neighboring areas or in one place. These tables show the overlap in time, and number of people making the observations.

The dots plotted on these maps are merely coordinates along the lines, points and polygons marked by respondents. We were restricted by our software and hardware to these size maps, and unless the coordinates are adjusted, lines cannot be plotted on top of each other and still be distinguished. Therefore, all the areas marked are represented by dots on these larger scale maps. To see if we could produce better representations of the lines, points, and polygons marked by respondents we produced regional maps of the sound as well (Figures A-C for all maps). The sound was divided into eastern, northern and southwestern regions, and areas with observations were represented as lines or polygons. The technician was unable to shade the polygons.

The locations where juvenile herring were seen in the spring (March, April, or May) during the 1970s, 80s, and 90s were listed (Table 1) and mapped (Figure 1). The number of respondents was listed below each decade. In the seventies observations from four respondents were concentrated along the northern shore, Valdez Arm - Galena Bay, Port Fidalgo, and the head of Port Gravina.

In several areas respondents saw herring over a range of several years (Table 1). In order to maintain the anonymity of respondents' information, the tables include the range of years and number of different observers for each area, but no way to attach individual respondents to the information. For example, four respondents saw juvenile herring in Eaglek Bay during the 1980s and 1990s.

Eight respondents' observations from spring of the 1980s were concentrated along the northern shore, the eastern side of the sound, and the northern end of Montague Island.

In the 1990s, four respondents observed juvenile herring in all of the above areas and along the western shore and the southeastern end of Montague Island. For somewhat finer scale views of these observations, please see the regional illustrations.

The number of observers and locations juvenile herring were seen in summer was mapped (Figure 2), and the range of years in which they were seen was listed by each place (Table 2). Over the seventies and eighties three respondents saw juveniles at Culross Island. More respondents saw juveniles in the summer than at any other time of year.

Seven respondents saw juvenile herring in Eaglek Bay between 1970 and 1997 -- two observers in the seventies, five in the eighties, and three in the nineties. Two respondents saw juvenile herring in Landlocked Bay in the summer in the seventies. During the eighties and nineties four observers saw summer juvenile herring in St. Mathew's Bay, Port Gravina, and Sheep Bay and Landlocked Bay. Fairmount Island is another place where juveniles were often seen in summer -one observer in the seventies is followed by three observers in the eighties, and two in the nineties. Polygons encircling Perry and Naked Islands are correctly represented. The respondent saw huge schools of juveniles around both islands in the late 80s.

In both spring and summer juvenile herring were observed near Fairmount Island, in Port Fidalgo, Port Gravina, Montague, Sheep and Simpson Bays (Tables 1 and 2; Figures 1 and 2).

Figures 3 and 4 illustrate the information gathered for fall and winter. The fall and winter information reflects the exploration in the early 70s of the sound for the bait fishery. Fishermen had taken some fish for bait all through the 1960s. It is said that the harvests were small, and not reported to the ADF&G.

In the early 70s local Cordova fishermen experimented with fishing for bait, and searched the sound for herring. Reported harvests were small until fishermen figured out how to catch the herring more efficiently, using a pair trawl and deep seines. In 1977, the Northern District and Montague Districts were established for the sac roe fishery. The Eastern District, consisting of Port Gravina and Orca Bay was established in 1980. After the sac roe districts were established, bait fishing was not allowed within them.

From 1978 until 1981 pair trawling and seiners were used to harvest bait outside the sac roe districts. The pair trawl users reported that they "got so they wouldn't go up into the bays, because they didn't want to run into juvenile herring." Table 3 reports juvenile herring that were caught with shrimp trawls and smelt nets in Simpson Bay. Table 4 reports in the notes for Simpson Bay, they "plugged the trawl." The respondents reported they spent hours scraping juvenile herring out of the trawl with flat-bladed snow shovels. They made the mistake a couple of times and didn't investigate the heads of bays again.

Although some information gathered about small fish, capelin and sand lance has been mapped (Figure 5) the tables for these figures have not been prepared yet.

The differences in the distribution of juvenile herring observations between the years can not be solely explained by respondents' participation in commercial fishing. The majority of the respondents who fish (18 out of 28) began fishing prior to 1970, only five of the fishermen interviewed were no longer fishing in the 1990s. Nine herring spotter pilots' experience bridges all three decades.

Experience spotting salmon is difficult to assess. Fishermen charter planes together to fly the sound looking for schools of fish. The pilots fly the plane, the fishermen look for fish.

This practice was made illegal in 1994, and prior to that it's difficult to say how many fishermen participated in this. However, at that time of year, the juvenile herring would have been most visible to people engaged in this type of activity.

Summary

This report was prepared after the first round of data was entered into the computer and is the first representation of the information. More interviews have been completed since then. The final report will be greatly refined.

The interview schedule for Valdez has been slightly delayed. We expect to finish interviewing respondents by the end of April.

Due to the short cycle of the grant and administrative procedures, hiring of a data entry technician was delayed by four months in FY97. This seriously compromised our ability to get other work done on the project. We are now caught up with data entry, but behind in other areas – such as interviews in Valdez, and notes transcription. We are in the process now of hiring another person to help with data analysis and GIS.

The mapping software which will be used to complete the project is ARC INFO, rather than GMT. This program is a relational database and has much more power to assist researchers in geographic analysis of the data than GMT.

REFERENCES

- Alaska Department of Fish and Game. 1979. Prince William Sound Area Annual Finfish Management Report - 1978. Cordova.
- Alaska Department of Fish and Game. 1980. Prince William Sound Area Annual Finfish Management Report - 1979. Cordova.
- Alaska Department of Fish and Game. 1981. Prince William Sound Area Annual Finfish Management Report - 1980. Cordova.
- Alaska Department of Fish and Game. 1983. Prince William Sound Area Annual Finfish Management Report - 1982. Cordova.
- Alaska Department of Fish and Game. 1984. Prince William Sound Area Annual Finfish Management Report - 1983. Cordova.
- Ames, E.P. 1996. Survey of Cod and Haddock Spawning Grounds within the Gulf of Maine: from Grand Manan Channel to Ipswich Bay. The Island Institute. Rockland, Maine. Unpublished manuscript.
- Barber, W. E., McDonald, L. L., Erickson, W. P., Vallarino, M. 1995. Effect of the *Exxon Valdez* Oil Spill on Intertidal Fish: A Field Study. Transactions of the American Fisheries Society 124:461-476.
- Brook, L. F. The Participation of Indigenous Peoples and the Application of their Environmental and Ecological Knowledge in the Arctic Environmental Protection Strategy, Inuit Circumpolar Conference.
- Brown, E. D., Baker, T. T., Hose, J. E., Kocan, R. M., Marty, G. D., McGurk, M. D., Norcross, B. L., Short, J. 1996. Injury to the Early Life History Stages of Pacific Herring in Prince William Sound after the *Exxon Valdez* Oil Spill. American Fisheries Society Symposium 18:448-462.
- Brush, S. 1993. "Indigenous Knowledge of Biological Resources and Intellectual Property Rights: The Role of Anthropology," in American Anthropologist 95(3):653-686.
- Fowler, F.J. Jr. 1995. Improving Survey Questions: Design and Evaluation. Sage Publications.
- Gjertz, I. and Wiig, O. 1994. "Past and Present Distribution of Walruses in Svalbard," Arctic. Vol.47, No.1. March. 34-42.

- Huntington, H.P. 1994. Traditional Ecological Knowledge of Beluga Whales, An Indigenous Knowledge Pilot Project in the Chukchi and Northern Bering Seas. Project Description, July 29, 1994.
- Hviding, E. 1991. "Traditional Institutions and Their Role in the Contemporary Coastal Resource Management in the Pacific Islands," in NAGA, the International center for Living Aquatic Resources Management (ICLARM) Quarterly. October. Manila.
- DeWalt, B. 1994. "Using Indigenous Knowledge to Improve Agriculture and Natural Resource Management," Human Organization Vol. 53, No.2.
- Flora, C.B. 1992. "Reconstructing Agriculture: The Case for Local Knowledge," Rural Sociology 57(1):92-97.
- Ives, E.D. 1980. The Tape Recorded Interview: A Manual for Fieldworkers in Folklore and Oral History. University of Tennessee Press, Knoxville.
- Johanness, R.E. 1989. Traditional Ecological Knowledge: A Collection of Essays, IUCN. The World Conservation Union. November.
- Ibid, 1994. "Science of Pacific Island Peoples and Marine Resource Management," Chapter 7, in Science of Pacific Island Peoples, V1, pp. 81-90. Institute of Pacific Studies.
- Ibid, 1993. "Integrating Traditional Ecological Knowledge and Management with Environmental Impact Assessment," In Traditional Ecological Knowledge: Concepts and Cases. Ottawa, International Program on Traditional Ecological Knowledge and International Development. International development Research Centre.
- Ibid, 1994. "Design of Tropical Nearshore Fisheries Extension Work Beyond the 1990s," in Traditional Marine Tenure and Sustainable Management of Marine Resources in Asia and the Pacific, Proceedings of the International Workshop, July 4-8, 1994. G. Robin South, Denis Goulet, Seremaia Tuqiri, Marguerite Church, Eds.
- Ibid, 1988. "Spawning Aggregation of the Grouper, *Plecctropomus areolatus* (Ruppel) in the Solomon Islands," in Proceedings of the Sixth International Coral Reef Symposium, Australia, Vol. 2.
- Johnson, M., ed. 1992. Lore: Capturing Traditional Environmental Knowledge. The Dene Cultural Institute. Hay River, NWT, Canada.
- Lamb, R. 1993. "Designs on Life," New Scientist, 30 October.

- Meyers, T.R., Short, S., Lipson, K., Batts, W.N., Winton, J.R., Wilcock, J., Brown, E.
1994. Association of Viral Hemorrhagic Septicemia Virus with Epizootic Hemorrhages of the Skin in Pacific Herring *Clupea harengus pallasii* from Prince William Sound and Kodiak Island, Alaska, USA. Diseases of Aquatic Organisms. Vol. 19: 27-37.
- Rounsefell, G.A. 1930. Contribution to the Biology of the Pacific Herring, *Clupea pallasii*, and the Condition of the Fishery in Alaska, Fisheries Document No. 1080, U.S. Department of Commerce.
- Rounsefell, G. A., and Dahlgren, E. H. 1932. Fluctuations in the Supply of Herring, *Clupea pallasii*, in Prince William Sound, Alaska. Bulletin No. 9.
- Weiss, S. R. 1994. Learning from Strangers: The Art and Method of Qualitative Interview Studies. The Free Press. New York.
- Wolfe, R.J. and Mishler, C. 1995. The Subsistence Harvest of Harbor Seal and Sea Lion by Alaska Natives in 1992. Technical Paper No. 229. Division of Subsistence, Alaska Department of Fish and Game.

Table 1. Spring Juvenile Herring in Prince William Sound

DRAFT

<u>PLACE</u>	<u>AREA</u>	<u>RANGE</u>	<u>n=12</u>	<u>FREQ</u>	<u>ID</u>	<u>NOTES</u>
Bainbridge Passage	614	1994-1996	1	n.d.	y	< 20 feet deep, within 20 meters of shore
Blackstone Bay	560	1987-1988	1	once	y	
Cochrane Bay	558	1987-1988	1	once	y	
Columbia Bay	554	1978	2	n.d.	Y	
Columbia Bay, Granite Cove	554	1975		once	y	50-100 grams, not quite gilling in the net
Dangerous Passage, Paddy Bay	610	1994	1	occs	y	
Dangerous Passage, Paddy Bay	610	1995		occs	y	
Dangerous Passage, Paddy Bay	610	1996		occs	y	
Eaglek Bay	584	1981-1987	4	n.d.	n	called juveniles because wouldn't set a seine on them, estimated depth 1 to 3 feet
Eaglek Bay	584	1987-1988		once	y	
Eaglek Bay	584	1987-1988		n.d.	n	
Eaglek Bay	584	1989-1996		cons	n	< 20 feet deep, within 20 meters of shore
Eaglek Bay	584	1990		n.d.	n	
Eleanor Island	537	1972	1	n.d.	y	
Eleanor Island, Ingot Island	537	1972		n.d.	y	
Esther Bay	502	1987-1988	2	once	y	
Esther Island, Point Esther	501	1987-1988		once	y	
Esther Island, Quillion/Lake Bays	526	1987-1988		once	y	
Esther Island, west side	525	1987-1988		once	y	
Esther Passage	499	1987-1988		once	y	
Esther Passage	499	1989-1996		occs	n	< 20 feet deep, within 20 meters of shore
Fairmount Island	545	1981-1987	2	n.d.	n	called juveniles because wouldn't set a seine on them, estimated depth 1 to 3 feet
Fairmount Island	545	1987-1988		n.d.	n	
Fairmount Island	545	1990		n.d.	n	
Glacier Island	629	1970-1973	3	n.d.	y	
Glacier Island	629	1978		n.d.	y	
Glacier Island	629	1985		once	y	
Glacier Island, Growler Bay	629	1979		n.d.	y	some sets on shrimp

<u>PLACE</u>	<u>AREA</u>	<u>RANGE</u>	<u>n=12</u>	<u>FREQ</u>	<u>ID</u>	<u>NOTES</u>
Green Island	630	1989-1996	1	occs	n	< 20 feet deep, within 20 meters of shore
Icy Bay	652	1994-1996	1	cons	y	< 20 feet deep, within 20 meters of shore
Jackpot Bay	671	1994-1996	1	cons	y	< 20 feet deep, within 20 meters of shore
Kiniklik	587	1987-1988	2	once	y	
Kiniklik	587	1989-1996		occs	n	< 20 feet deep, within 20 meters of shore
Knight Island, east side	556	-1989	1	once	y	during oil spill
Long Bay	553	1978-1979	1	n.d.	y	
Montague Island, Jeanie Cove	541	1994-1996	1	occs	n	< 20 feet deep, within 20 meters of shore
Montague Island, Patton Bay	540	1994-1996		occs	n	< 20 feet deep, within 20 meters of shore
Montague Island, Port Chalmers	529	1989-1993	3	cons	n	< 20 feet deep, within 20 meters of shore
Montague Island, Port Chalmers	529	1993		rare	y	pollock had adult herring in their stomachs
Montague Island, Port Chalmers	529	1994-1996		cons	y	< 20 feet deep, within 20 meters of shore
Montague Island, Rocky Bay	583	1989-1993		occs	n	< 20 feet deep, within 20 meters of shore
Montague Island, Rocky Bay	583	1990		rare	y	pollock had adult herring in their stomachs
Montague Island, Rocky Bay	583	1994-1996		occs	y	< 20 feet deep, within 20 meters of shore
Montague Island, Graveyard Point	631	1993		rare	y	pollock had adult herring in their stomachs
Montague Island, Stockdale Harbor	631	1983		n.d.	y	
Montague Island, Stockdale Harbor	631	1989-1993		cons	n	< 20 feet deep, within 20 meters of shore
Montague Island, Stockdale Harbor	631	1994-1996		cons	y	< 20 feet deep, within 20 meters of shore
Montague Island, Zaikof Bay	521	1989-1993		occs	n	< 20 feet deep, within 20 meters of shore
Montague Island, Zaikof Bay	521	1994-1996		occs	y	< 20 feet deep, within 20 meters of shore
Naked Island	520	1989-1996	2	occs	n	< 20 feet deep, within 20 meters of shore
Naked Island, Cabin Bay	520	1989-1996		occs	n	< 20 feet deep, within 20 meters of shore
Naked Island, north shore	520	1987-1988		n.d.	n	
Naked Island, north shore	520	1990		n.d.	n	
Olsen Island	586	1989-1996	1	occs	n	< 20 feet deep, within 20 meters of shore
Port Fidalgo	544	1978-1991	3	cons	n	juv like these places, Deep Bays with shallow estuaries at the back of the bay
Port Fidalgo, Fish Bay	585	1987-1988		occ	n	

<u>PLACE</u>	<u>AREA</u>	<u>RANGE</u>	<u>n=12</u>	<u>FREQ</u>	<u>ID</u>	<u>NOTES</u>
Port Fidalgo, Fish Bay	585	1990		occ	n	
Port Fidalgo, Irish Cove	585	1981-1992		n.d.	n	
Port Fidalgo, Landlocked Bay	625	1987-1988		n.d.	n	
Port Fidalgo, Landlocked Bay	625	1990		n.d.	n	
Port Fidalgo, Snug Corner Cove	603	1987-1988		n.d.	n	
Port Fidalgo, Snug Corner Cove	603	1990		n.d.	n	
Port Gravina	621	1978-1991	3	cons	n	juv like these places, Deep Bays with shallow estuaries at the back of the bay
Port Gravina, Red Head	628	1989-1996		occs	n	< 20 feet deep, within 20 meters of shore
Port Gravina, Hell's Hole	518	1989-1996		occs	n	< 20 feet deep, within 20 meters of shore
Port Gravina, Olsen Bay	586	1989-1993		occs	n	
Port Gravina, Olsen Bay	586	1994-1996		occs	y	
Port Gravina, St. Mathew's Bay	528	1989-1993		occs	n	< 20 feet deep, within 20 meters of shore
Port Gravina, St. Mathew's Bay	528	1994-1996		occs	y	< 20 feet deep, within 20 meters of shore
Port Gravina, St. Matthew's Bay	528	1981		n.d.	y	
Port Nellie Juan, Kings Bay	655	1970-1972	1	n.d.	y	
Port Wells, Coghill Bay	656	1973	1	n.d.	y	3-4 inch long, < 100 grams
Sheep Bay	611	1987-1988	3	n.d.	n	
Sheep Bay	611	1987-1989		cons	n	0-2, some spot spawn
Sheep Bay	611	1989-1993		occs	n	
Sheep Bay	611	1990		n.d.	n	
Sheep Bay	611	1994-1996		occs	y	
Simpson Bay	601	1987-1988	2	n.d.	n	
Simpson Bay	601	1989-1993		occs	n	
Simpson Bay	601	1990		n.d.	n	
Simpson Bay	601	1994-1996		occs	y	
Storey Island	532	1987-1988	1	n.d.	n	
Storey Island	532	1990		n.d.	n	
Tatitlek Narrows	623	1997	2	once	y	
Tatitlek Narrows Black Point	623	1979		cons	y	

<u>PLACE</u>	<u>AREA</u>	<u>RANGE</u>	<u>n=12</u>	<u>FREQ</u>	<u>ID</u>	<u>NOTES</u>
Valdez Arm, Galena Bay	624	1978-1991	4	cons	n	juv like these places, Deep Bays with shallow estuaries at the back of the bay
Valdez Arm, Galena Bay	624	1986-1988		once	y	while pounding
Valdez Arm, Galena Bay	624	1987-1988		n.d.	n	
Valdez Arm, Galena Bay	624	1987-1989		cons	n	too small to market 0-2 yr olds
Valdez Arm, Galena Bay	624	1990		n.d.	n	
Valdez Arm, Jack Bay	604	1978-1991	1	cons	n	juv like these places, Deep Bays with shallow estuaries at the back of the bay
Wells Bay	626	1978-1991	3	cons	n	juv like these places, Deep Bays with shallow estuaries at the back of the bay
Wells Bay	626	1987-1988		n.d.	n	
Wells Bay	626	1990		n.d.	n	
Wells Passage	559	1987-1988		once	y	
Whale Bay	602	1994-1996	1	occs	y	

Table 2. Summer Juvenile Herring in Prince William Sound

DRAFT

<u>PLACE</u>	<u>AREA</u>	<u>R/YR</u>	<u>RANGE</u>	<u>n=17</u>	<u>ID</u>	<u>FREQ</u>	<u>NOTES</u>
Bainbridge Passage	614	y	1994-1996	2	y	occs	< 20 feet deep, within 20 meters of shore
Bainbridge Point	511	r	1970-1985		n.d.	cons	
Chenega Island, east side	510	r	1970-1985	2	n	cons	Balls and schools
Chenega Island, east side	510	r	1985-1991		n	cons	
Chenega Island, south side	539	r	1970-1985		n	cons	
Cochrane Bay	558	y	1985		y	n.d.	
Crafton Island	507	r	1967-1975	2	y	cons	age zeros moving south, saw them when he was set netting
Crafton Island	507	r	1970-1985		n	cons	
Culross Island	504	r	1970-1985	4	n	cons	lots of juveniles here
Culross Island	505	r	1970-1985		n	cons	
Culross Island	505	y	1982		n	once	
Culross Passage	605	y	1985		y	n.d.	
Culross Point	504	y	1982		n	once	
Dangerous Passage, Paddy Bay	610	y	1994-1996	1	y	cons	
Eaglek Bay	584	r	1970-1985	7	n	cons	called juveniles because wouldn't set a seine on them, estimated depth 1 to 3 feet
Eaglek Bay	584	r	1972-1978		n	occ	
Eaglek Bay	584	r	1981-1987		n	cons	
Eaglek Bay	584	y	1982		n	once	
Eaglek Bay	584	r	1982-1996		n.d.	occ	
Eaglek Bay	584	y	1987-1988		n	n.d.	< 20 feet deep, within 20 meters of shore
Eaglek Bay	584	y	1989-1996		n	cons	
Eaglek Bay	584	y	1990		n	n.d.	< 20 feet deep, within 20 meters of shore
Eaglek Bay	584	y	1994-1996		y	cons	
Eleanor Island	537	r	1970-1985	2	n.d.	cons	
Eleanor Island, Point Eleanor	537	r	1974-1987		no	cons	
Elrington Island, Bettles Island	516	r	1970-1985	2	y	cons	
Elrington Passage	516	r	1971-1991		y	occ	
Elrington Passage	616	r	1971-1991		y	occ	
Eshamy Bay	617	r	1967-1975	2	y	cons	age zeros moving south, saw them when he was set netting
Eshamy Bay	617	r	1970-1985		n	cons	

Esther Bay	502	y	1982	3	n	once	
Esther Passage	499	r	1972-1978		n	occ	
Esther Passage	499	y	1982		n	once	
Esther Passage	499	y	1989-1993		n	cons	< 20 feet deep, within 20 meters of shore
Esther Passage	499	y	1994-1996		y	cons	< 20 feet deep, within 20 meters of shore
Prince of Wales Passage, Aluklik B.	513	r	1970-1985		y	cons	
Evans Island, northwest side	512	r	1970-1985	2	y	cons	
Evans Island, Shelter Bay	512	y	1990		y	once	a lot of jh tight on beach, 10 to 20 feet off beach <10 m deep
Fairmount Island	545	r	1970-1985	4	n	cons	
Fairmount Island	545	r	1981-1987		n	cons	called juveniles because wouldn't set a seine on them, estimated depth 1 to 3 feet
Fairmount Island	545	r	1982-1996		n.d.	cons	
Fairmount Island	545	y	1987-1988		n	n.d.	
Fairmount Island	545	y	1990		n	n.d.	
Glacier Island	629	r	1982-1996	1	n.d.	occ	
Green Island	630	y	1989-1996	2	n	cons	< 20 feet deep, within 20 meters of shore
Green Island, north west side	630	r	1982-1996		n.d.	occ	
Hawkins Island, Canoe Pass, Windy	548	y	1987-1988	2	n	n.d.	
Hawkins Island, north side	548	r	1970-1985		n	cons	
Hawkins Island, Windy Bay	548	y	1990		n	n.d.	
Hinchinbrook Island, north side	527	r	1970-1985		n	cons	
Icy Bay	652	y	1994-1996	1	y	cons	< 20 feet deep, within 20 meters of shore
Jackpot Bay	671	y	1994-1996	1	y	cons	< 20 feet deep, within 20 meters of shore
Kiniklik	587	r	1970-1985	3	n	cons	
Kiniklik	587	y	1982		n	once	
Kiniklik	587	y	1989-1993		n	cons	< 20 feet deep, within 20 meters of shore
Kiniklik	587	y	1994-1996		y	cons	< 20 feet deep, within 20 meters of shore
Knight Island, Drier Bay	622	r	1970-1985	3	n	cons	
Knight Island, Drier Bay	622	r	1980-1983		n	cons	
Knight Island, Drier Bay	622	r	1985-1991		n	cons	Balls and schools

Knight Island, Herring Bay	609	r	1970-1985	3	n.d.	cons	
Knight Island, Herring Bay	609	r	1974-1987		no	cons	
Knight Island, Herring Point	509	r	1970-1985		n.d.	cons	
Knight Island, Herring Point	509	r	1985-1991		n	cons	Balls and schools
Knight Island, Lower Herring and Jol	612	r	1985-1991	2	n	cons	Balls and schools
Knight Island, Lower Herring Bay	612	r	1970-1985		n.d.	cons	
Knight Island, west	555	r	1970-1985		n	cons	
Knight Island, Squire Island	522	r	1970-1985	3	n	cons	
Knight Island, Squire Island	522	r	1985-1988		y	once	scattered rocks among the rocks < 10 m deep
Knight Island, Squire Island	522	r	1985-1991		n	cons	Balls and schools
Knight Island, Snug Harbor to Point	555	r	1974-1987	1	no	cons	
Latouche Island, east side	619	y	1994	2	y	once	large concentration of herring
Latouche Passage, northwest	581	r	1970-1985		y	cons	
Latouche Passage, south	619	r	1970-1985		y	cons	
Long Bay	553	r	1970-1985	2	n	cons	
Long Bay	553	r	1982-1996		n.d.	occ	
Main Bay	608	r	1967-1975	2	y	cons	age zeros moving south, saw them when he was set netting
Main Bay	608	r	1970-1985		n	cons	
Montague Island, Graveyard Point t	631	r	1980-1983	2	y	cons	
Montague Island, Jeanie Cove	541	y	1994-1996		n	cons	< 20 feet deep, within 20 meters of shore
Montague Island, middle west side	566	r	1980-1983		y	cons	
Montague Island, Patton Bay	540	y	1994-1996	1	n	cons	< 20 feet deep, within 20 meters of shore
Montague Island, Port Chalmers	529	y	1989-1996	3	n	cons	< 20 feet deep, within 20 meters of shore
Montague Island, Port Chalmers	529	y	1994-1996		y	cons	< 20 feet deep, within 20 meters of shore
Montague Island, Port Chalmers	529	r	1980-1983		y	cons	
Montague Island, Port Chalmers	529	r	1981-1987		n	cons	called juveniles because wouldn't set a seine on them, estimated depth 1 to 3 feet
Montague Island, Port Chalmers	529	y	1991-1992		n	cons	called juveniles because wouldn't set a seine on them, estimated depth 1 to 3 feet
Montague Island, Rocky Bay	583	r	1980-1983	3	y	cons	

Montague Island, Rocky Bay	583	r	1982-1996	n.d.	cons	
Montague Island, Rocky Bay	583	y	1989-1993	n	cons	< 20 feet deep, within 20 meters of shore
Montague Island, Rocky Bay	583	y	1994-1996	y	cons	< 20 feet deep, within 20 meters of shore
Montague Island, Stockdale Harbor	631	r	1981-1987	3	n	cons called juveniles because wouldn't set a seine on them, estimated depth 1 to 3 feet
Montague Island, Stockdale Harbor	631	r	1982-1996	n.d.	occ	
Montague Island, Stockdale Harbor	631	y	1989-1993	n	cons	< 20 feet deep, within 20 meters of shore
Montague Island, Stockdale Harbor	631	y	1994-1996	y	cons	< 20 feet deep, within 20 meters of shore
Montague Island, Zaikof Bay	521	r	1980-1983	3	y	cons
Montague Island, Zaikof Bay	521	r	1982-1996	n.d.	cons	
Montague Island, Zaikof Bay	521	y	1989-1993	n	cons	< 20 feet deep, within 20 meters of shore
Montague Island, Zaikof Bay	521	y	1994-1996	y	cons	< 20 feet deep, within 20 meters of shore
Montague Strait, west lower	530	r	1970-1985	2	y	cons
Montague Trench	566	r	1982-1996	n.d.	occ	
Montague Trench	653	r	1982-1996	n.d.	occ	
Naked Island	520	r	1982-1996	3	n.d.	occ
Naked Island	546	r	1987-1989	n	once	once in late 1980s
Naked Island	520	y	1989-1996	n	cons	< 20 feet deep, within 20 meters of shore
Naked Island, north shore	520	y	1987-1988	n	n.d.	
Naked Island, north shore	520	y	1990	n	n.d.	
Olsen Island	586	r	1972-1978	2	n	occ
Olsen Island	586	y	1989-1993	n	cons	< 20 feet deep, within 20 meters of shore
Olsen Island	586	y	1994-1996	y	cons	< 20 feet deep, within 20 meters of shore
Orca Bay	563	r	1972-1978	2	n	cons one years in 1970s saw bay loaded with juv
Orca Inlet, Cordova Harbor	517	n.d.	n.d.	y	cons	
Perry Island	547	r	1987-1989	1	n	once once in late 1980s
Port Fidalgo, Fish Bay	585	r	1972-1978	3	n	cons
Port Fidalgo, Fish Bay	585	r	1972-1978	y	cons	
Port Fidalgo, Fish Bay	585	r	1981-1987	n	occ	called juveniles because wouldn't set a seine on them, estimated depth 1 to 3 feet
Port Fidalgo, Fish Bay	585	y	1987-1988	n	occ	
Port Fidalgo, Fish Bay	585	y	1990	n	occ	
Port Fidalgo, head	544	r	1970-1985	2	n	cons
Port Fidalgo, head	544	r	1981-1987	n	cons	called juveniles because wouldn't set a seine on them, estimated depth 1 to 3 feet

Port Fidalgo, head	544	r	1981-1987	n	occ	called juveniles because wouldn't set a seine on them, estimated depth 1 to 3 feet
Port Fidalgo, Irish Cove	585	r	1970-1985	n	cons	
Port Fidalgo, Landlocked Bay	625	r	1972-1978	4	n	cons
Port Fidalgo, Landlocked Bay	625	r	1982-1996	n.d.	occ	
Port Fidalgo, Landlocked Bay	625	y	1987-1988	n	n.d.	
Port Fidalgo, Landlocked Bay	625	y	1990	n	n.d.	
Port Fidalgo, Landlocked Bay	625	r	1970-1985	n	cons	
Port Fidalgo, Snug Corner Cove	603	r	1970-1985	4	n	cons
Port Fidalgo, Snug Corner Cove	603	y	1987-1988	n	n.d.	
Port Fidalgo, Snug Corner Cove	603	y	1990	n	n.d.	
Port Fidalgo, Two Moon Bay	603	r	1972-1978	y	cons	
Port Fidalgo, Two Moon Bay	603	r	1982-1996	n.d.	occ	
Port Fidalgo, Whalen Bay	544	r	1972-1978	y	cons	
Port Gravina, Gravina Rocks	562	r	1970-1985	1	n	cons
Port Gravina, head	621	r	1970-1985	1	n	cons
Port Gravina, Hell's Hole	518	r	1970-1985	3	n	cons
Port Gravina, Hell's Hole	518	r	1982-1996	n.d.	occ	
Port Gravina, Hell's Hole	518	y	1989-1993	n	cons	< 20 feet deep, within 20 meters of shore
Port Gravina, Hell's Hole	518	y	1994-1996	y	cons	< 20 feet deep, within 20 meters of shore
Port Gravina, Olsen Bay	621	r	1982-1996	2	n.d.	occ
Port Gravina, Olsen Bay	586	y	1989-1993	n	cons	
Port Gravina, Olsen Bay	586	y	1994-1996	y	cons	
Port Gravina, Knowles Head	632	r	1970-1985	3	n	cons
Port Gravina, Knowles Head to Red	628	r	1982-1996	n.d.	occ	
Port Gravina, Red Head	628	r	1970-1985	n	cons	
Port Gravina, Red Head	628	y	1989-1993	n	cons	< 20 feet deep, within 20 meters of shore
Port Gravina, Red Head	628	y	1994-1996	y	cons	< 20 feet deep, within 20 meters of shore
Port Gravina, St. Mathew's Bay	528	r	1970-1985	5	n	cons
Port Gravina, St. Mathew's Bay	528	r	1981-1987	n	occ	called juveniles because wouldn't set a seine on them, estimated depth 1 to 3 feet
Port Gravina, St. Mathew's Bay	528	r	1982-1996	n.d.	occ	
Port Gravina, St. Mathew's Bay	528	y	1989-1993	n	cons	< 20 feet deep, within 20 meters of shore
Port Gravina, St. Mathew's Bay	528	y	1994-1996	y	cons	< 20 feet deep, within 20 meters of shore
Port Gravina, St. Matthews Bay	628	r	n.d.	y	n.d.	

Port Nellie Juan, Kings Bay	655	r	1970-1972	1	y	n.d.	
Port Wells, middle	565	r	1938-1988	2	y	cons	n.d.
Port Wells, middle	565	r	1972-1978		n	occ	
Port Wells, south	564	r	1938-1988		y	cons	n.d.
Port Wells, south	564	r	1970-1978		n	occ	
Port Wells, south	564	r	1972-1978		n	occ	
Prince of Wales Pass	615	r	1970-1985	1	y	cons	
Prince of Wales Passage, Aluklik Bay	513	r	1970-1985		y	cons	
Sheep Bay	611	r	1970-1985	4	n	cons	
Sheep Bay	611	r	1982-1996		n.d.	occ	
Sheep Bay	611	y	1987-1988		n	n.d.	
Sheep Bay	611	y	1989-1993		n	cons	
Sheep Bay	611	y	1994-1996		y	cons	
Simpson Bay	601	r	1970-1985	3	n	cons	
Simpson Bay	601	y	1987-1988		n	n.d.	
Simpson Bay	601	y	1989-1993		n	cons	
Simpson Bay	601	y	1994-1996		y	cons	
Squaw Bay	498	r	1970-1985	2	n	cons	
Squaw Bay	498	y	1982		n	once	
Storey Island	532	y	1987-1988	1	n	n.d.	
Storey Island	532	y	1990		n	n.d.	
Tatitlek Narrows	623	r	1934-1996	3	y	cons	
Tatitlek Narrows, Boulder Bay	623	r	1967-1975		y	cons	
Tatitlek Narrows, Boulder Bay	623	r	1982-1996		n.d.	occ	
Valdez Arm	534	r	1980-1983	2	y	once	one time
Valdez Arm	523	r	1982-1996		n.d.	occ	
Valdez Arm, Galena Bay	624	r	1967-1975	4	y	cons	75% of the time not uncommon
Valdez Arm, Galena Bay	624	r	1970-1988		y	once	little balls of 1 years
Valdez Arm, Galena Bay	624	r	1972-1978		n	occs	
Valdez Arm, Galena Bay	624	y	1987-1988		n	n.d.	
Valdez Arm, Galena Bay	624	y	1990		n	n.d.	

Valdez Arm, Jack Bay	604	r	1970-1973	2	y	n.d.	saw balls of fish
Valdez Arm, Jack Bay	604	r	1982-1996		n.d.	occ	
Wells Bay, Cedar Bay	626	r	1982-1996	4	n.d.	cons	
Wells Bay	626	r	1970-1985		n	cons	
Wells Bay	626	r	1972-1978		n	occ	
Wells Bay	626	y	1987-1988		n	n.d.	
Wells Bay	626	y	1990		n	n.d.	
Wells Bay, Granite Bay	508	r	1970-1985		n	cons	
Whale Bay	602	y	1994-1996	2	y	cons	
Whale Bay, mouth	602	r	1970-1985		y	cons	

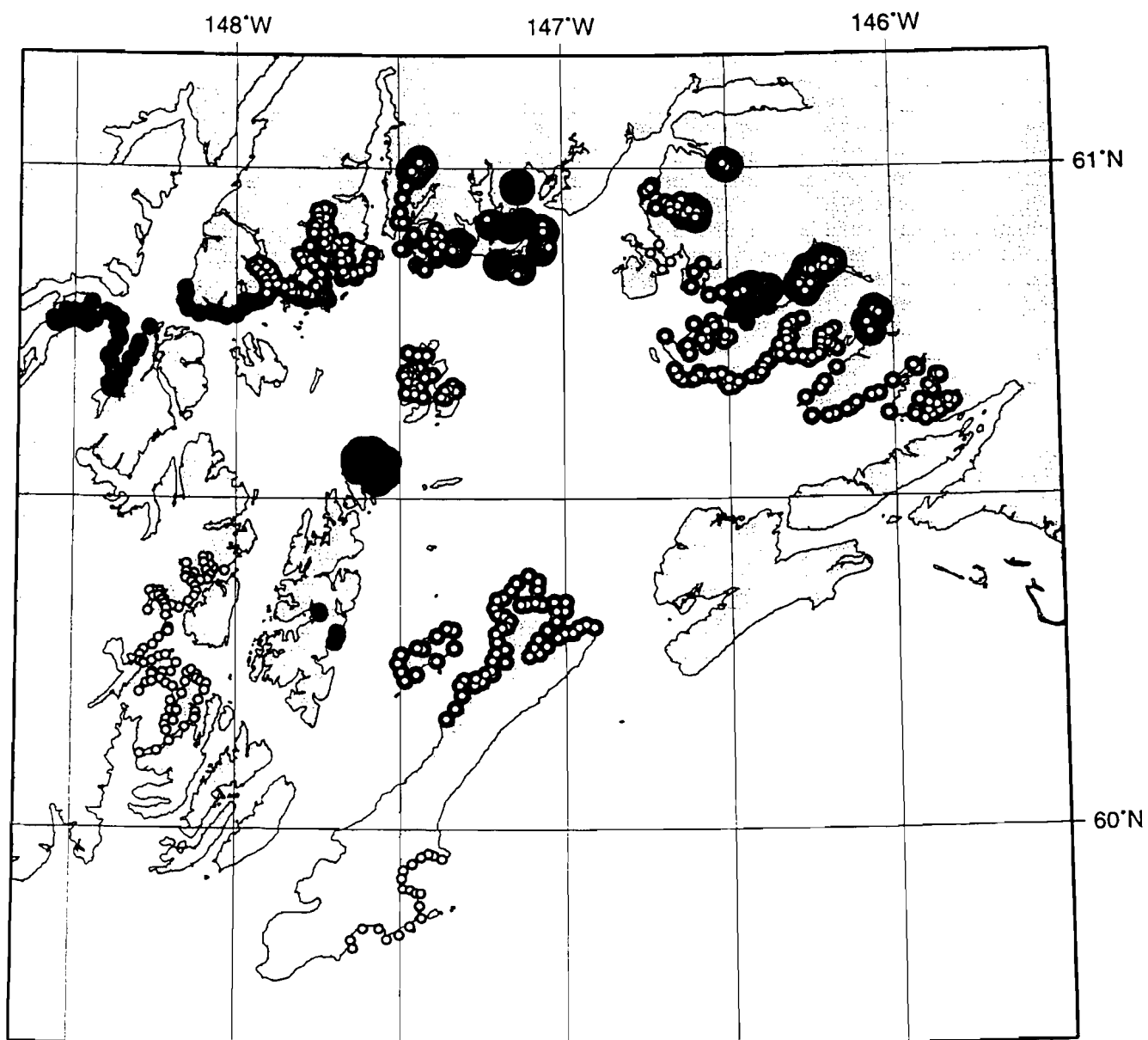
REGION	PLACE	AREA	RANGE	COUNT	
1	Esther Passage	499	1989-1996	2	
1	Eaglek Bay	584	1989-1996		
1	Kiniklik	587	1989-1996		
1	Olsen Island	586	1989-1996		
1	Wells Bay, Granite Bay	626	1996		
1	Naked Island	520	1989-1996	1	< 20 feet deep, within 20 meters of shore
2	Nelson Bay	517	1985-1995	2	caught with smelt nets, herring where 4" to 5" long
2	Orca Inlet	517	n.d.		
2	Orca Inlet	517	n.d.		
2	Port Fidalgo	542	n.d.	2	
2	Port Fidalgo, Fish Bay	585	1992		went trapping, could see from boat lights while anchored
2	Port Gravina, Beartrap Bay	621	1977-1981	3	5-20 fathoms on sonar
2	Port Gravina, Red Head	628	1989-1996		
2	Port Gravina, Hell's Hole	518	1989-1996		
2	Port Gravina, Olsen Bay	586	1989-1996		
2	Port Gravina, St Mathews Bay	528	1989-1996		
2	Port Gravina	621	1992		
2	Sheep Bay	611	1989-1996	1	
2	Simpson Bay	601	1977-1981	5	5-20 fathoms on sonar
2	Simpson Bay, head	601	1978-1981		midchannel
2	Simpson Bay	601	1985-1989		saw one time 1985-1989, on sonar
2	Simpson Bay	601	1985-1995		dragging for shrimp in '94; in '95 caught 4-5" herring with smelt nets
2	Simpson Bay	601	1989-1996		
3	Dangerous Passage, Paddy Bay	610	1994-1996	1	
3	Jackpot Bay	671	1994-1996	1	
3	Icy Bay	652	1994-1996	1	
3	Bainbridge Point	511	1970-1985	2	
3	Bainbridge Passage	614	1994-1996		
3	Prince of Wales Passage, Aluklik Bay	513	1970-1985	1	
3	Prince of Wales Passage	615	1970-1985		
3	Evans Island, northwest side	512	1970-1985	1	

REGION	PLACE	AREA	RANGE	COUNT	
	3 Elrington Island, Bettles Island	516	1970-1985	1	
	3 Latouche Passage, northwest	581	1970-1985	1	
	3 Latouche Passage, south	619	1970-1985		
	3 Knight Island, Mummy/Little Bays to Point Helen	613	1985-1991	1	Thin Bands
	3 Green Island	630	1989-1996	1	
	3 Montague Island, Port Chalmers	529	1981-1987	3	called juveniles because wouldn't set a seine on them, estimated depth 1 to 3 feet
	3 Montague Island, Port Chalmers	529	1981-1987		called juveniles because wouldn't set a seine on them, estimated depth 1 to 3 feet
	3 Montague Island, Port Chalmers	529	1985-1991		
	3 Montague Island, Port Chalmers	529	1989-1996		< 20 feet deep, within 20 meters of shore
	3 Montague Island, Port Chalmers	529	1991-1992		called juveniles because wouldn't set a seine on them, estimated depth 1 to 3 feet
	3 Montague Island, Gilmour Point	529	1991-1992		called juveniles because wouldn't set a seine on them, estimated depth 1 to 3 feet
	3 Montague Island, Stockdale Harbor	631	1981-1987	4	called juveniles because wouldn't set a seine on them, estimated depth 1 to 3 feet
	3 Montague Island, Stockdale Harbor	631	1989-1996		
	3 Montague Island, Stockdale Harbor	631	1991-1992		
	3 Montague Island, Stockdale Harbor	631	1992		tide went out, found a lot of juv herring dead on shore
	3 Montague Island, Graveyard Point	631	1989		1/4 mesh by 5.6 fathoms deep net
	3 Montague Point	583	1989	2	1/4 mesh by 5.6 fathoms deep net
	3 Montague Island, Rocky Bay	583	1989-1996		< 20 feet deep, within 20 meters of shore
	3 Montague Island, Zaikof Bay	521	1989-1996	2	< 20 feet deep, within 20 meters of shore
	3 Montague Island, Zaikof Point	521	1993		50 gram fish
	3 Whale Bay	602	1994-1996	1	

<u>PLACE</u>	<u>AREA</u>	<u>RANGE</u>	<u>n=4</u>	<u>FREQ</u>	<u>ID</u>	<u>NOTES</u>
Bainbridge Point	614	1971-1972	1	cons	n	
Chenega Island	510	1971-1972	1	cons	n	
Chenega Point	539	1971-1972		cons	n	
Crafton Island	507	1971-1972	1	cons	n	
Dangerous Passage, Ewan Bay	610	1971-1972	1	cons	n	
Elrington Passage	516	1971-1972	1	cons	n	
Eshamy Bay	617	1971-1972	1	cons	n	
Evans Island	616	1971-1972	1	cons	n	
Evans Island, Shelter Bay	512	1971-1972		cons	n	
Flemming Island	511	1971-1972	1	cons	n	
Knight Island, Herring Bay	609	1971-1972	1	cons	n	
Latouche Passage	619	1971-1972	1	cons	n	
Main Bay	608	1971-1972	1	cons	n	
Orca Inlet	517	n.d.	3	n.d.	n.d.	
Orca Inlet, Cordova Harbor	517	-1989		rare	y	sometime before oil spill
Orca Inlet, Cordova Harbor	517	n.d.		cons	y	
Orca Inlet, Mud Bay	517	-1989		rare	n	sometime before oil spill
Orca Inlet, Salmo Point	517	-1989		rare	n	sometime before oil spill
Port Gravina	562	1978-1981	1	cons	y	that's where they grow
Port Gravina, head	621	1978-1981		cons	y	plugged the trawl
Port Gravina, Hell's Hole	518	1978-1981		cons	y	
Port Gravina, St. Mathew's Bay	528	1978-1981		cons	y	

<u>PLACE</u>	<u>AREA .</u>	<u>RANGE</u>	<u>n=4</u>	<u>FREQ</u>	<u>ID</u>	<u>NOTES</u>
Port Nellie Juan, mouth	654	1971-1972	1	cons	n	
Sheep Bay, head	611	1978-1981	1	cons	y	midchannel
Wells Bay, Granite Bay	508	1971-1972	1	cons	n	
Whale Bay, mouth	672	1971-1972	1	cons	n	

PRINCE WILLIAM SOUND



JUVENILE HERRING DISTRIBUTION: SPRING

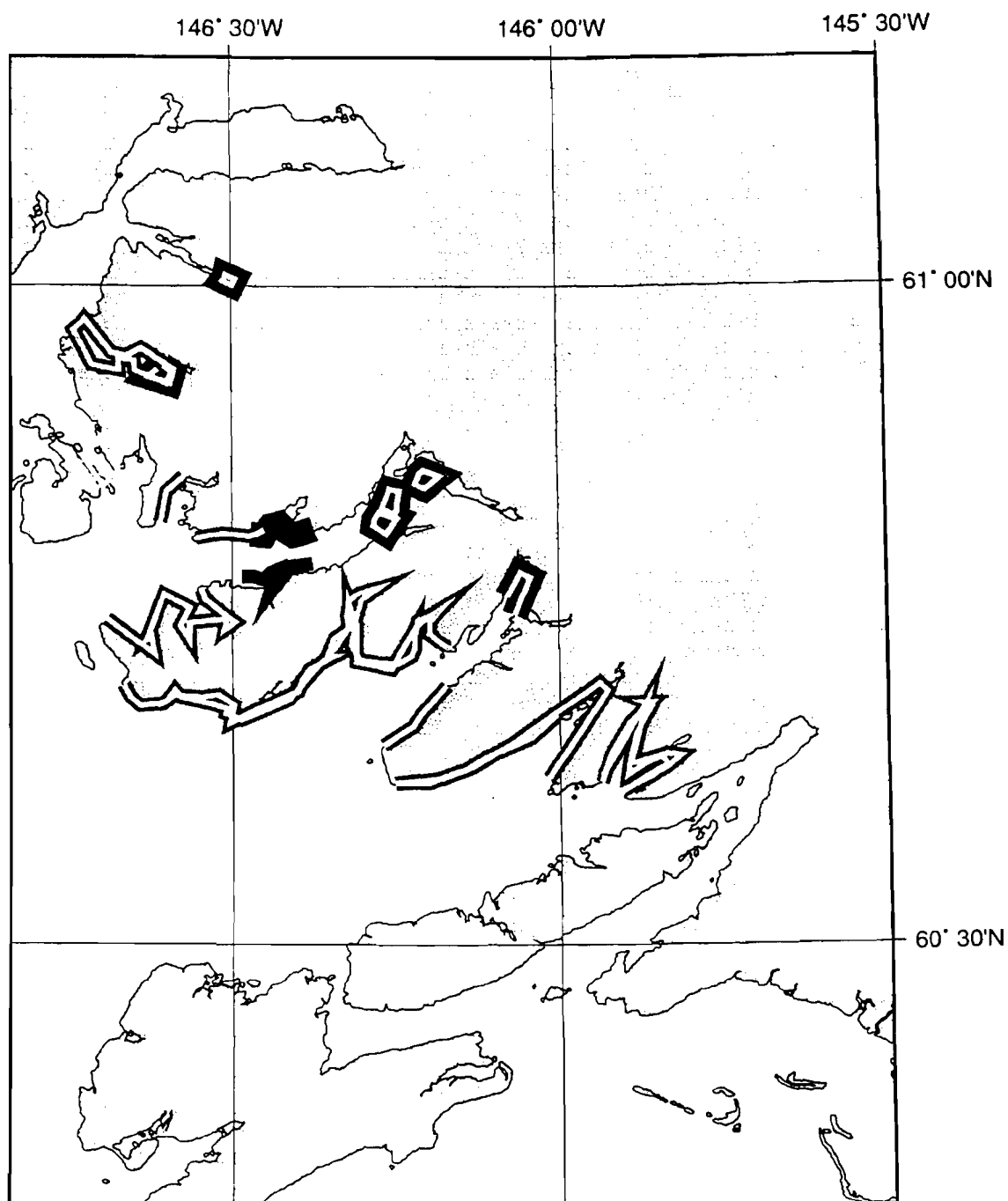
● 1970s
n = 4

● 1980s
n = 8

○ 1990s
n = 4

Figure 1.

PRINCE WILLIAM SOUND



JUVENILE HERRING DISTRIBUTION: SPRING

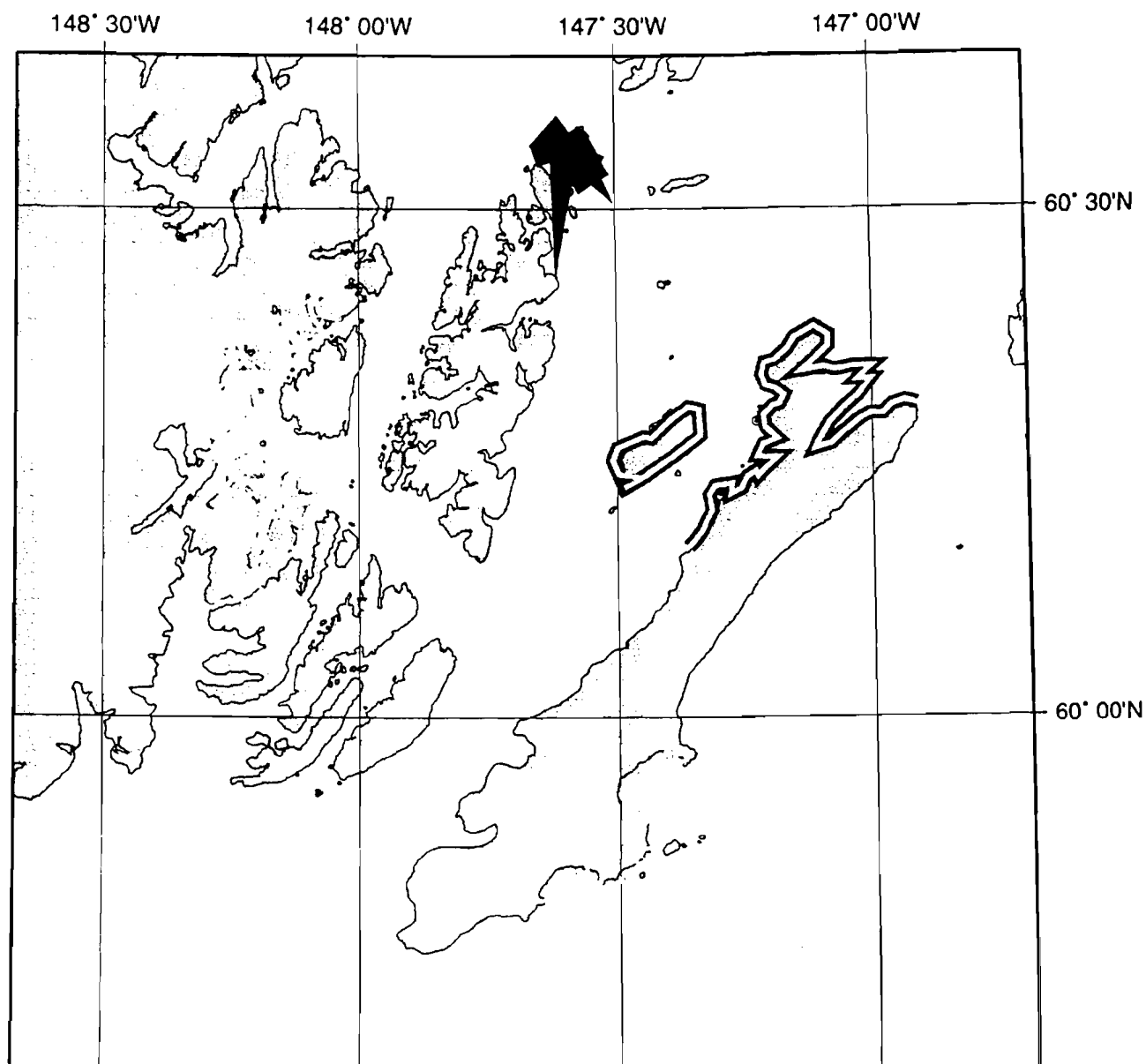
● 1970s

● 1980s

○ 1990s

Figure 1A.

PRINCE WILLIAM SOUND



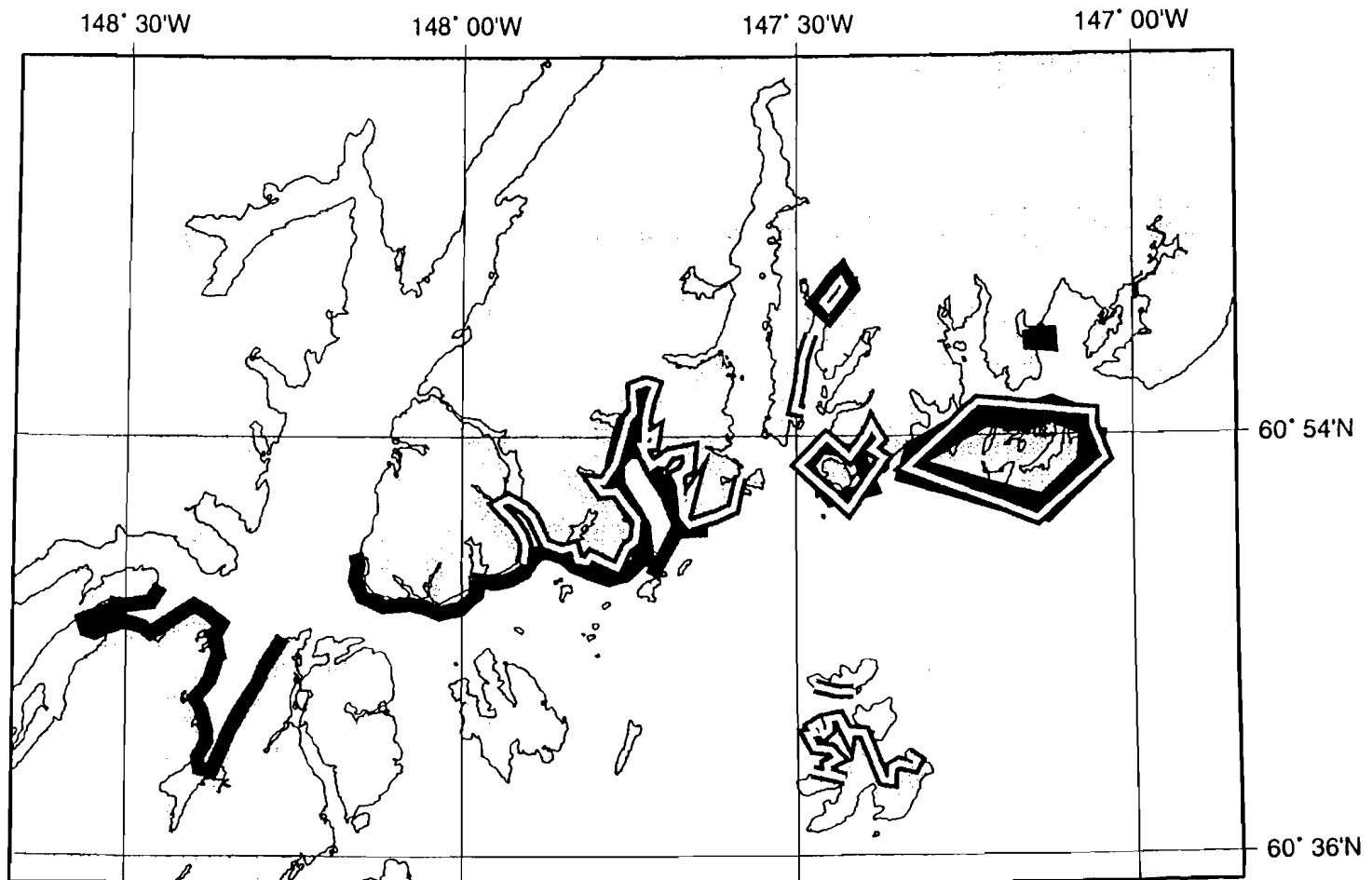
JUVENILE HERRING DISTRIBUTION: SPRING

● 1970s

● 1980s

○ 1990s

PRINCE WILLIAM SOUND



JUVENILE HERRING DISTRIBUTION: SPRING

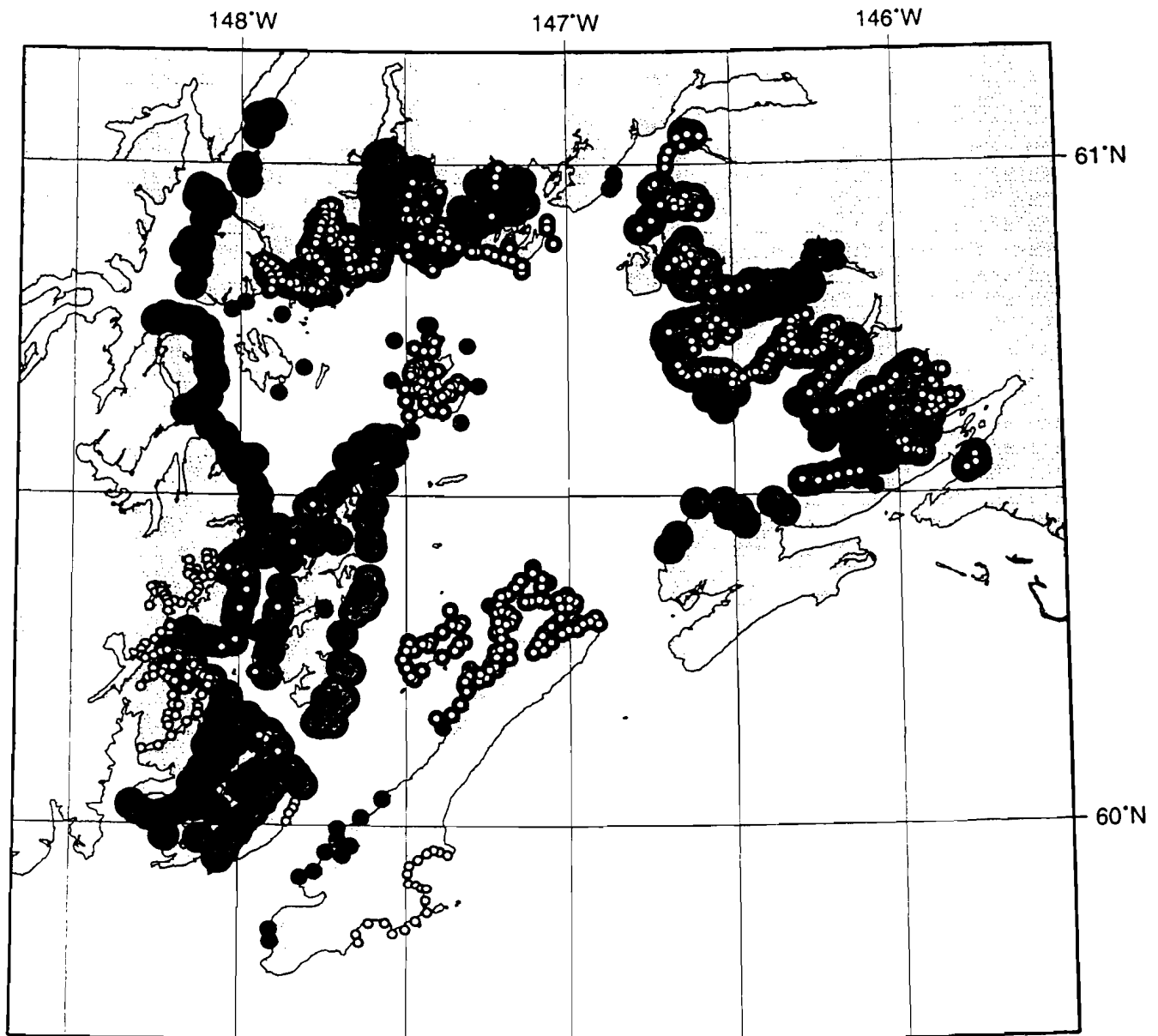
● 1970s

● 1980s

⊗ 1990s

Figure 1C.

PRINCE WILLIAM SOUND



JUVENILE HERRING DISTRIBUTION: SUMMER

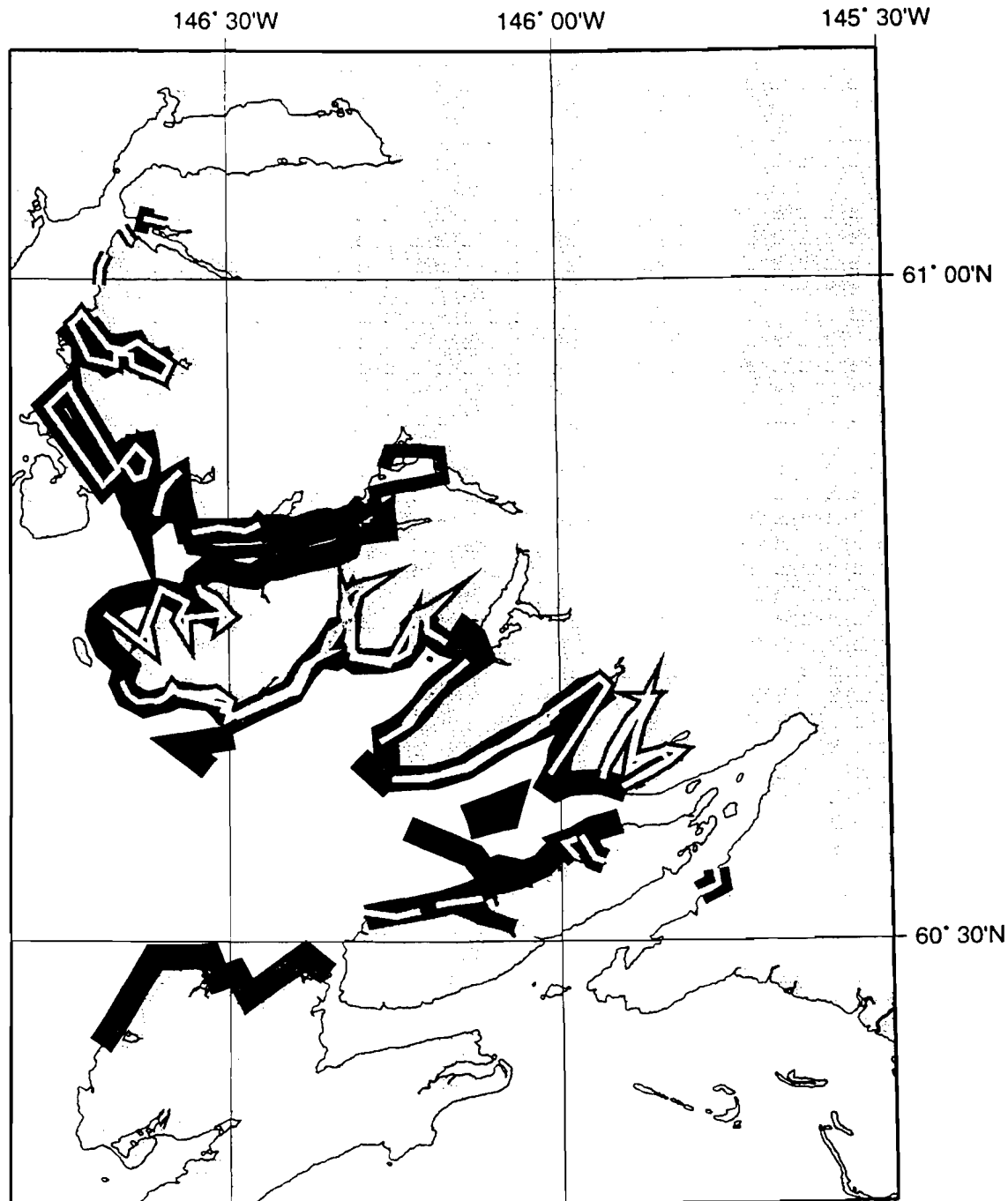
● 1970s
n = 10

● 1980s
n = 15

○ 1990s
n = 10

Figure 2.

PRINCE WILLIAM SOUND



JUVENILE HERRING DISTRIBUTION: SUMMER

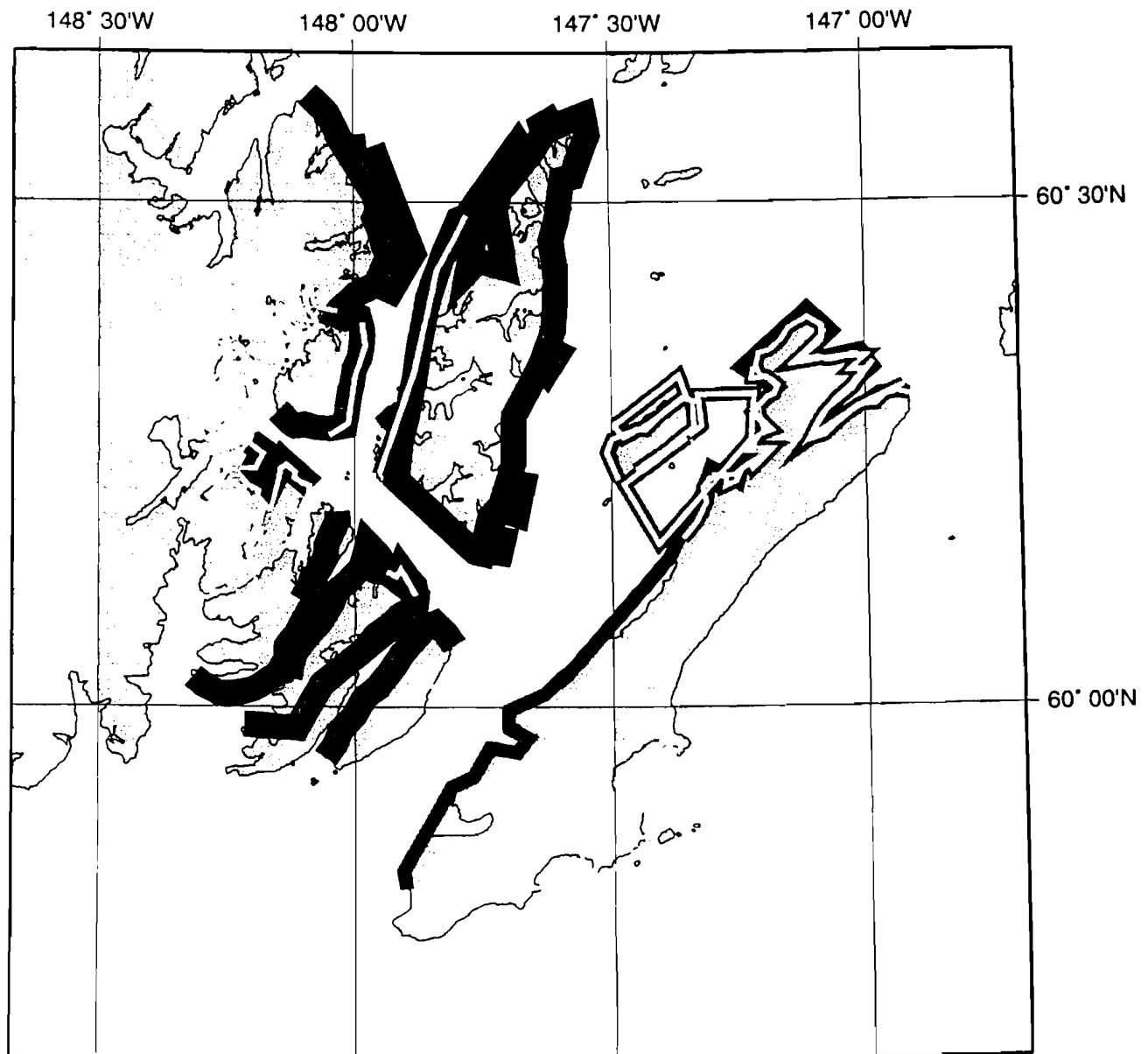
● 1970s

● 1980s

○ 1990s

Figure 2A.

PRINCE WILLIAM SOUND



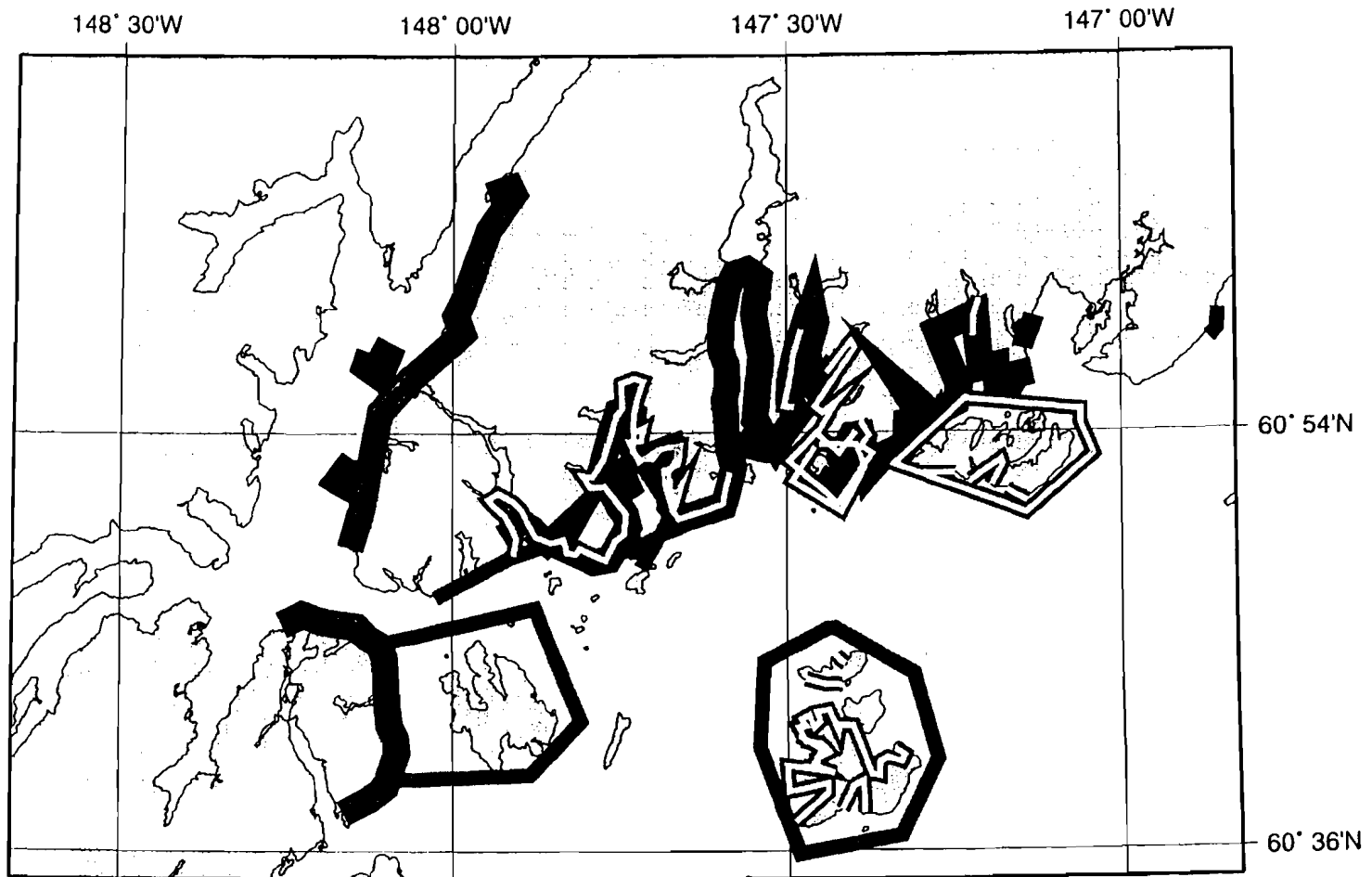
JUVENILE HERRING DISTRIBUTION: SUMMER

● 1970s

● 1980s

○ 1990s

PRINCE WILLIAM SOUND



JUVENILE HERRING DISTRIBUTION: SUMMER

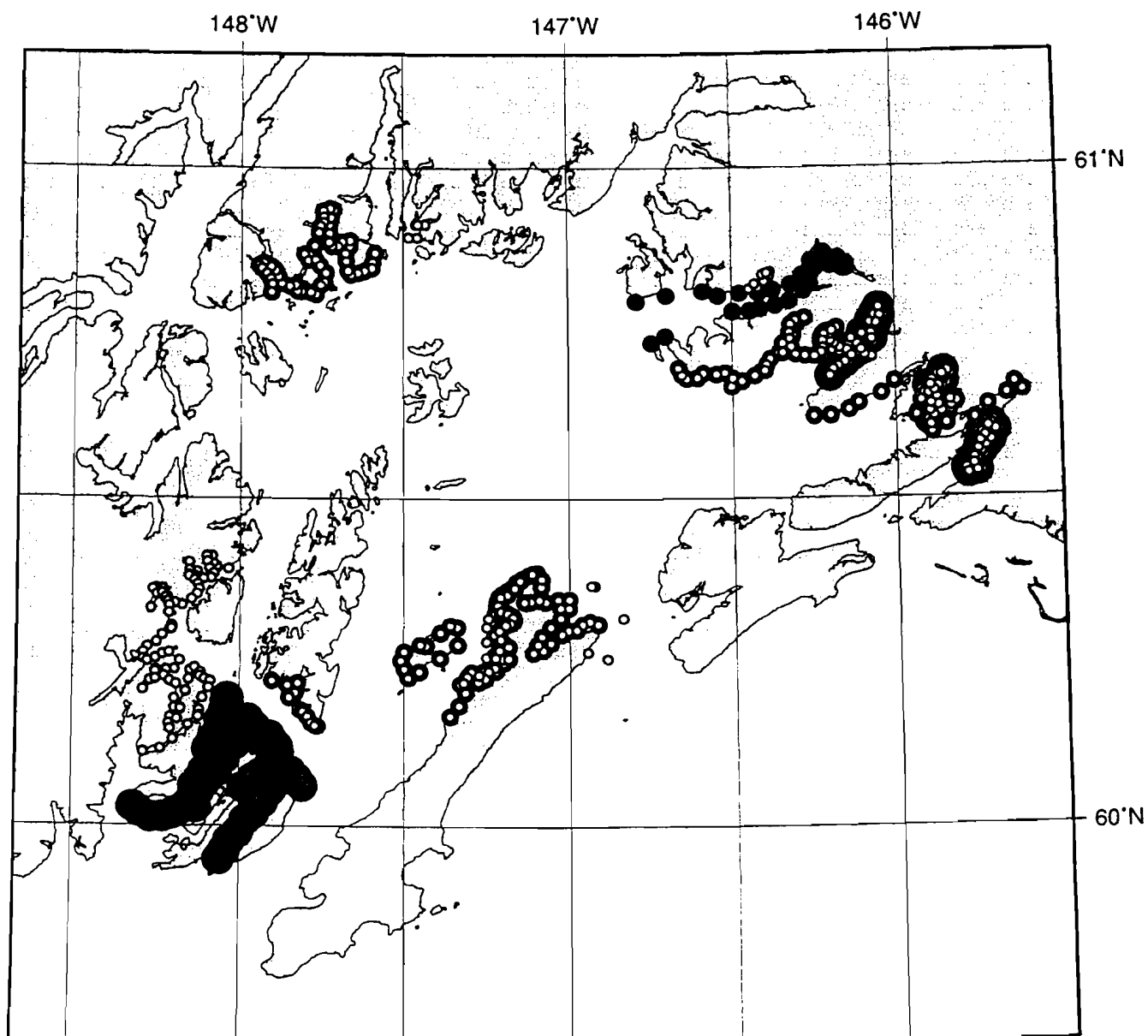
● 1970s

● 1980s

⊗ 1990s

Figure 2C.

PRINCE WILLIAM SOUND



JUVENILE HERRING DISTRIBUTION: AUTUMN

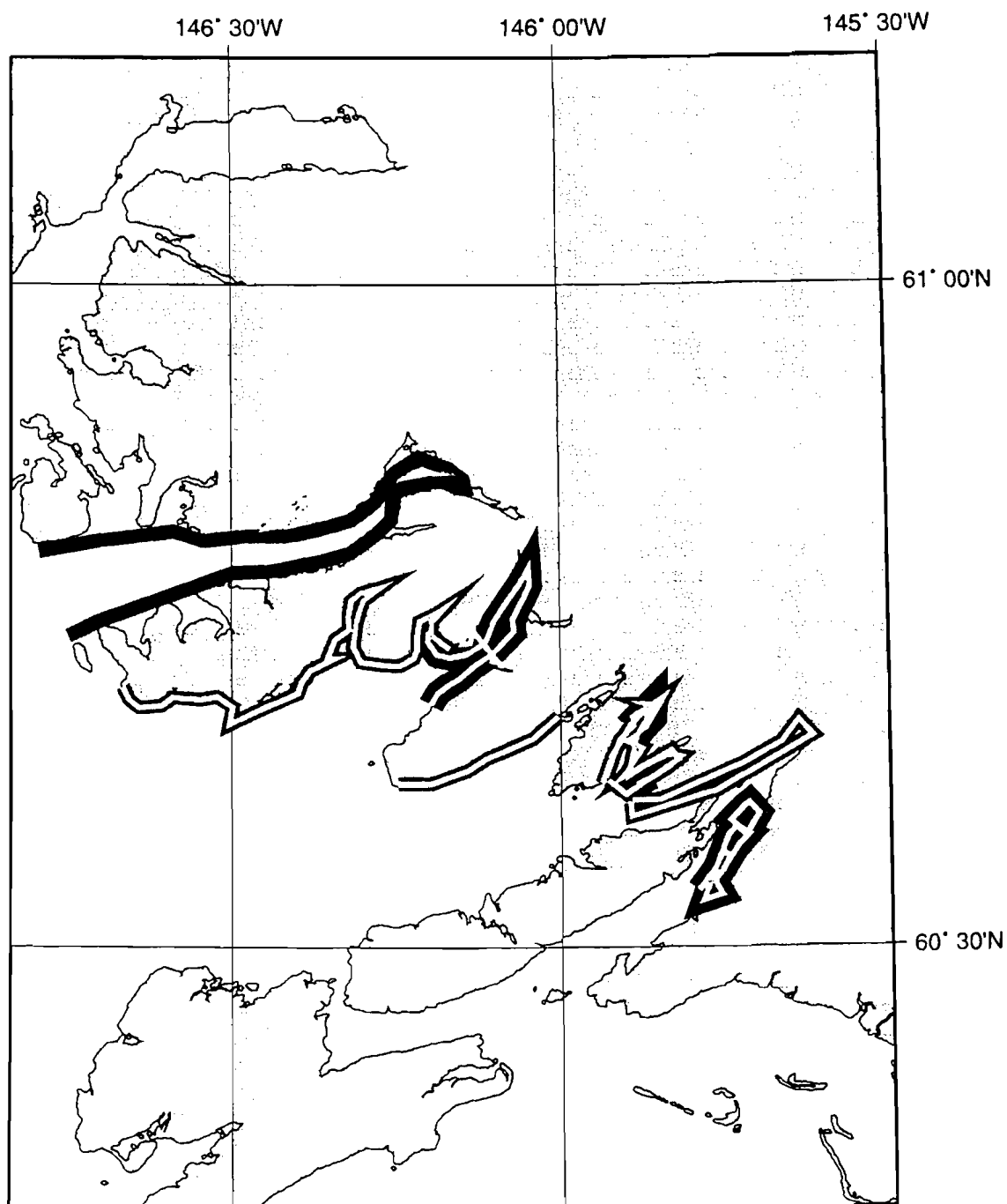
● 1970s
n = 6

● 1980s
n = 9

○ 1990s
n = 8

Figure 3.

PRINCE WILLIAM SOUND



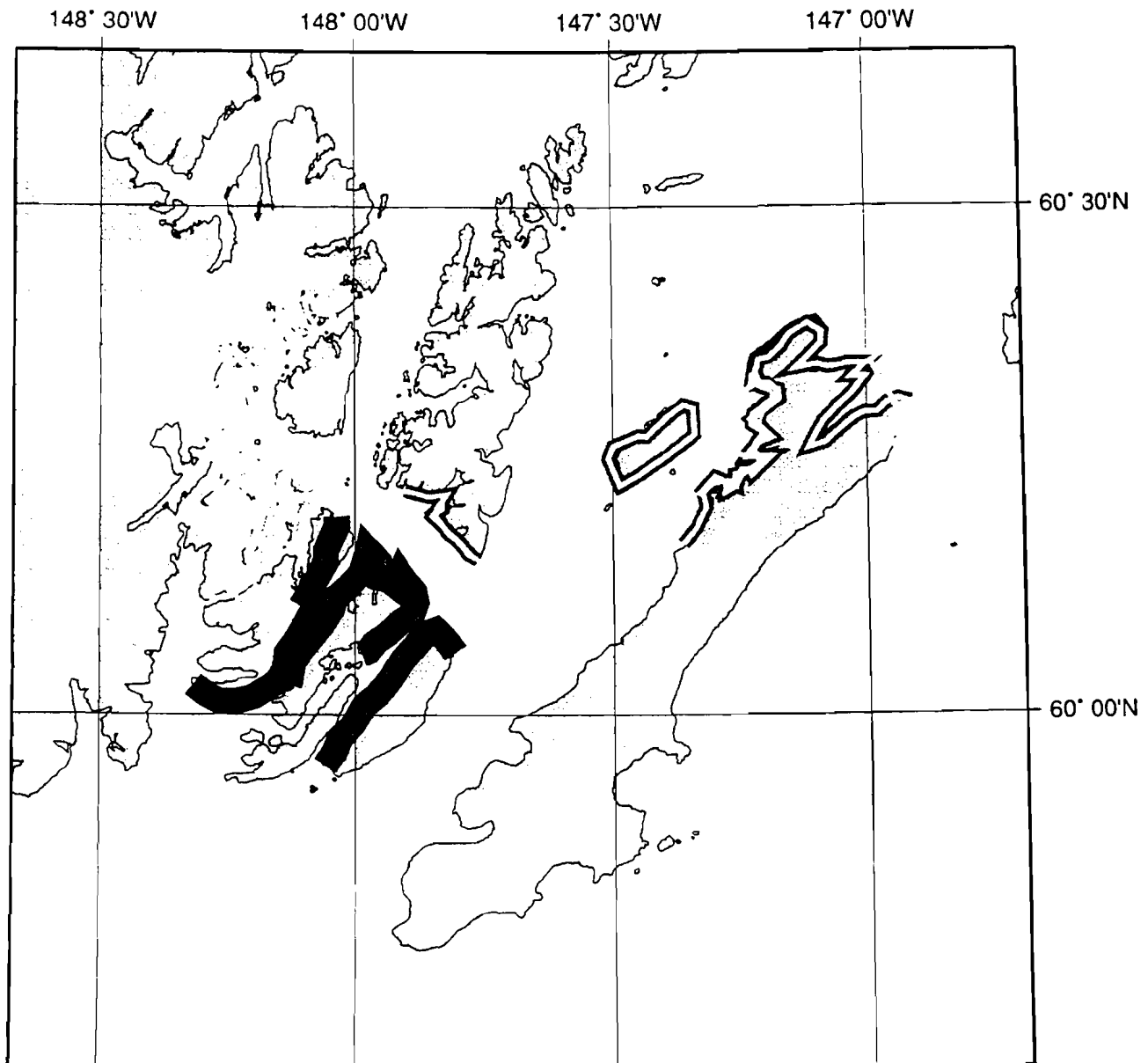
JUVENILE HERRING DISTRIBUTION: AUTUMN

● 1970s

● 1980s

○ 1990s

PRINCE WILLIAM SOUND



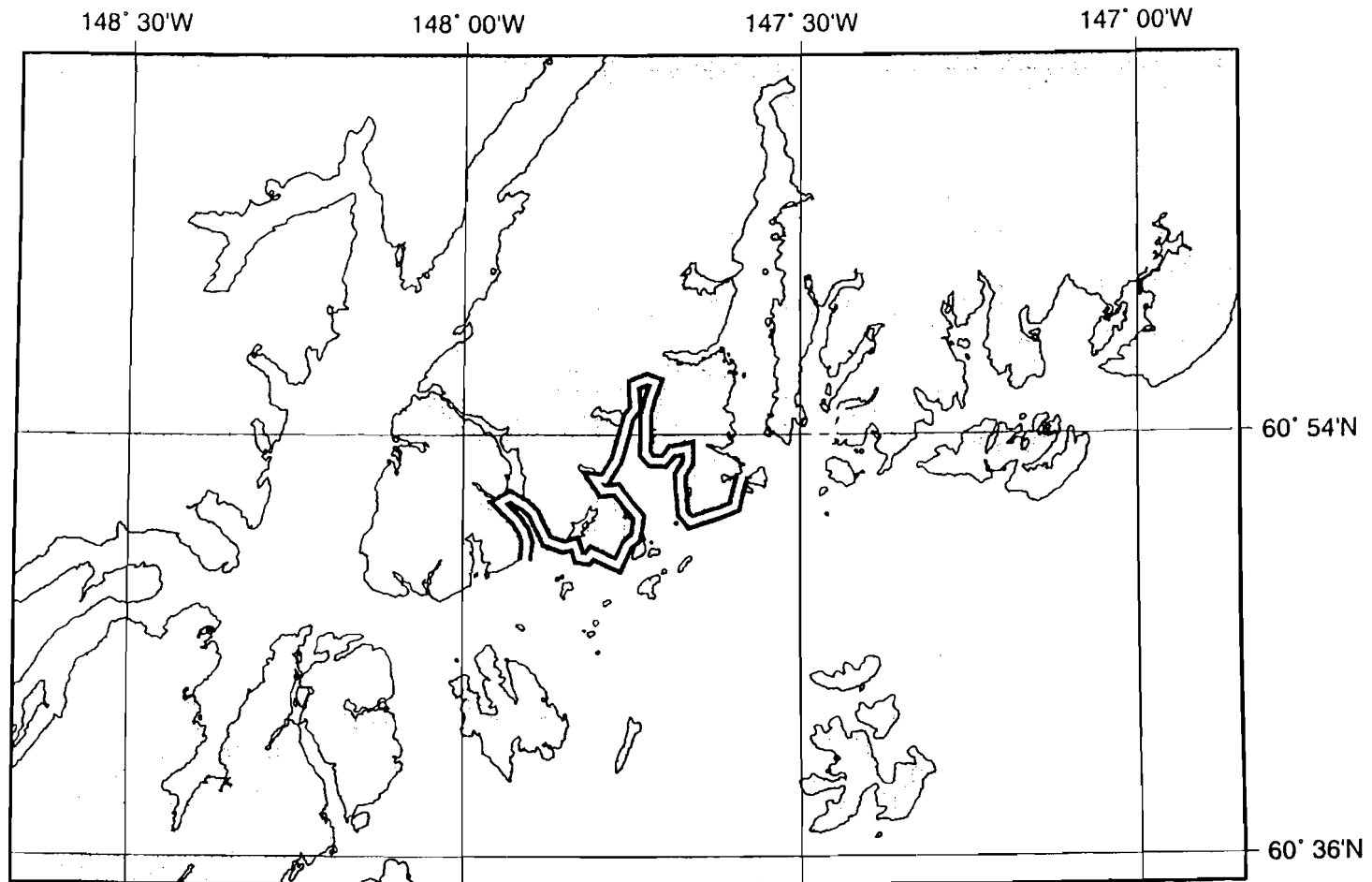
JUVENILE HERRING DISTRIBUTION: AUTUMN

● 1970s

● 1980s

○ 1990s

PRINCE WILLIAM SOUND



JUVENILE HERRING DISTRIBUTION: AUTUMN

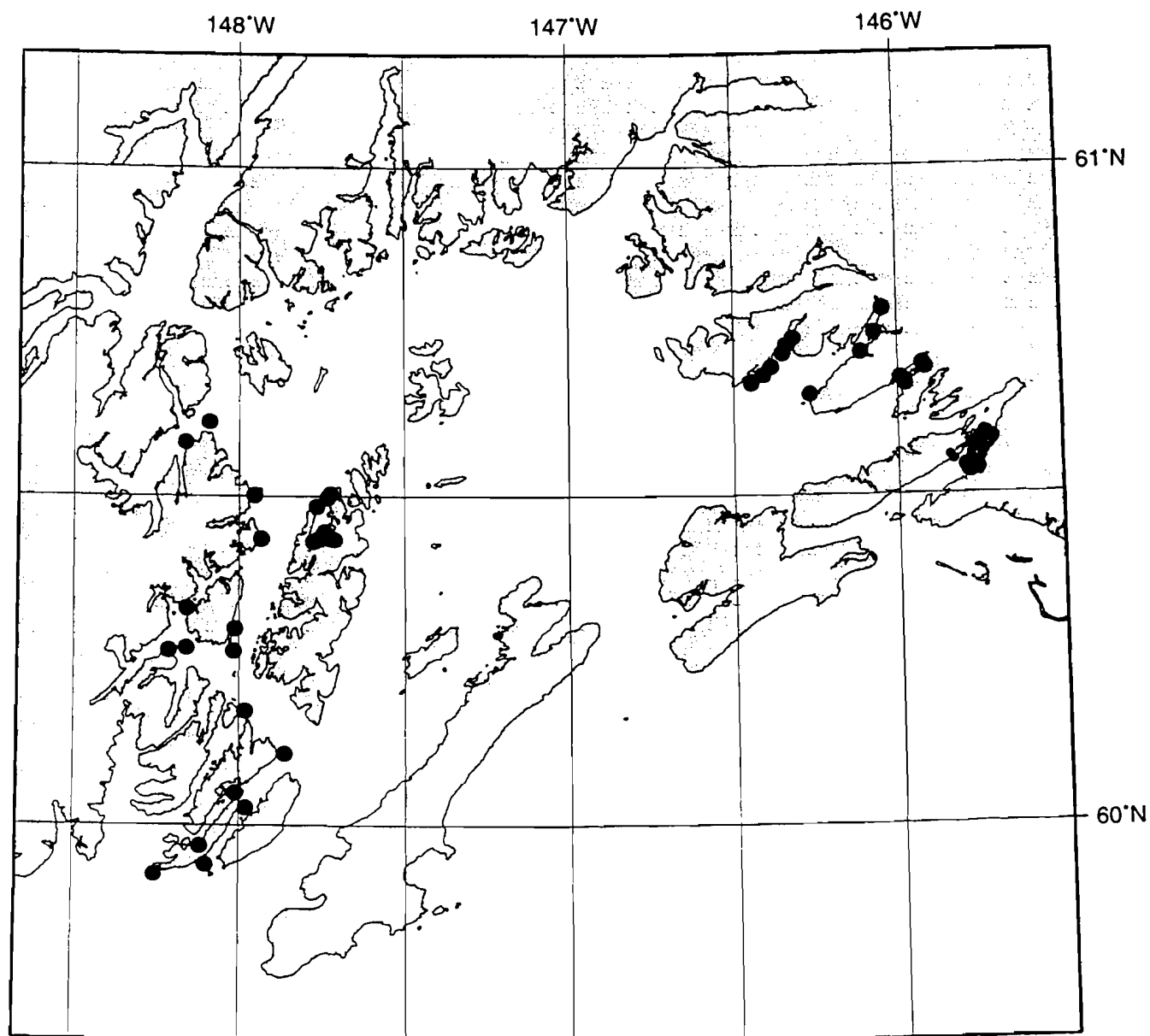
● 1970s

● 1980s

⊙ 1990s

Figure 3C.

PRINCE WILLIAM SOUND



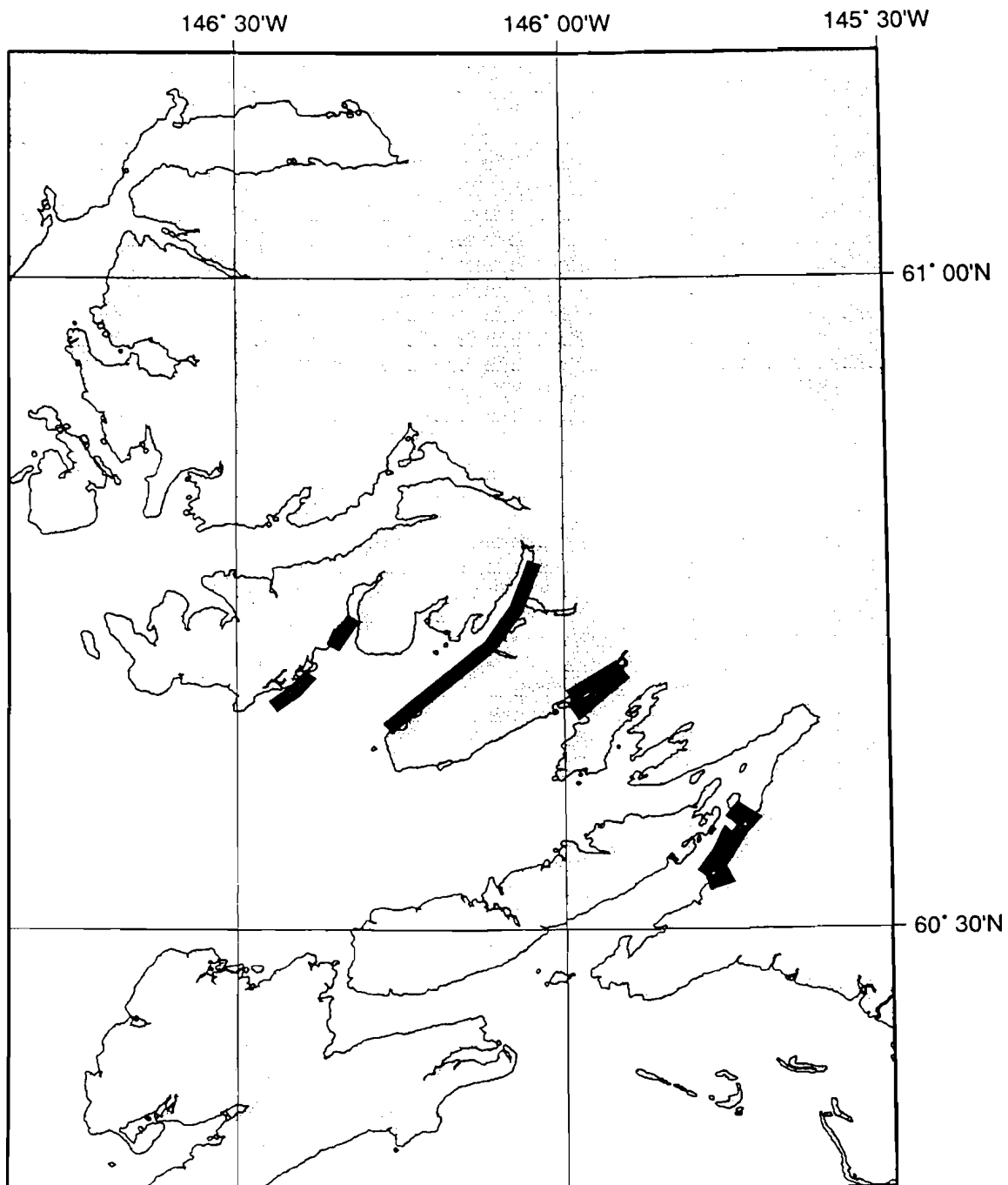
JUVENILE HERRING DISTRIBUTION: WINTER

● 1970s
n = 2

● 1980s
n = 3

Figure 4.

PRINCE WILLIAM SOUND



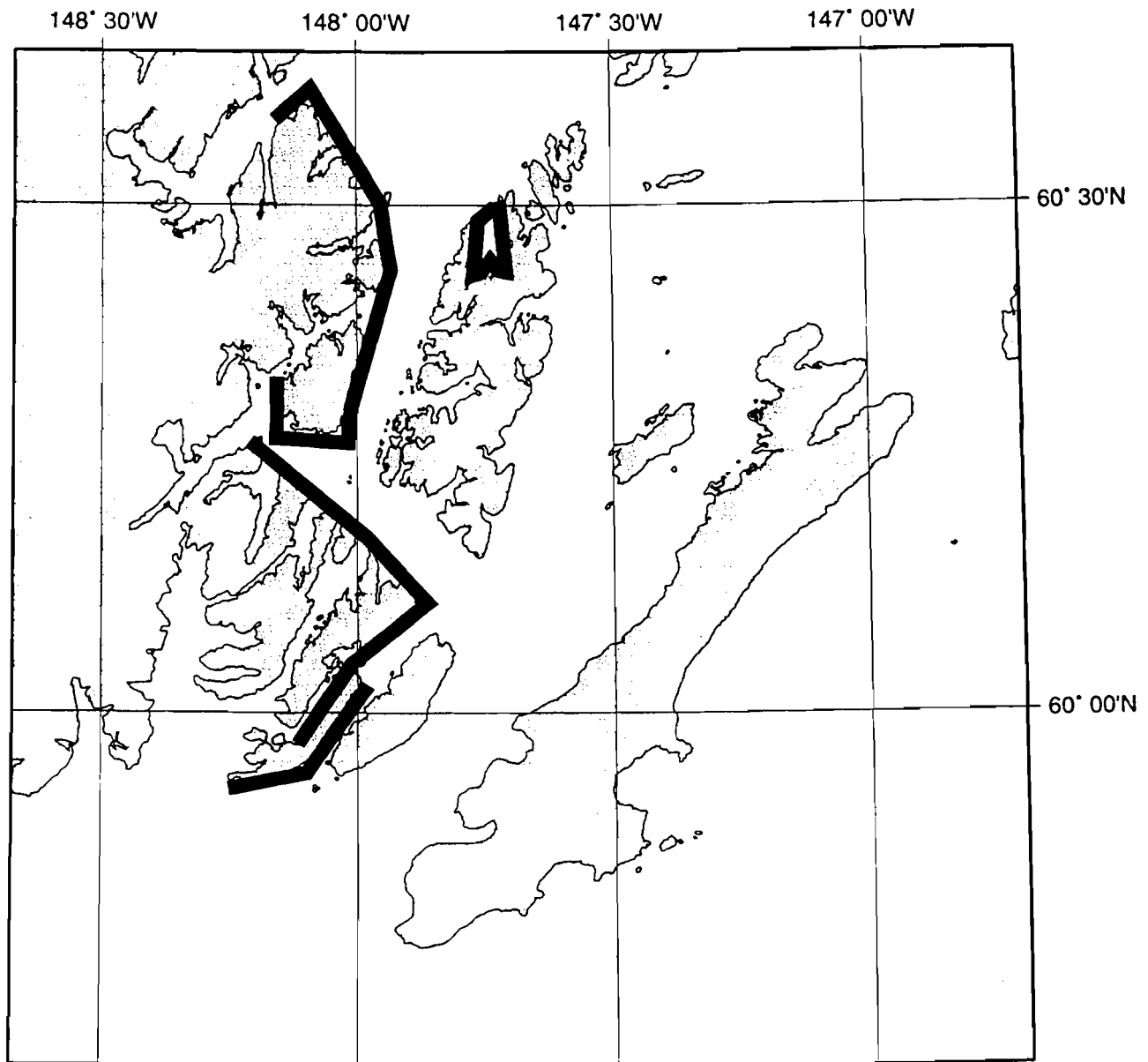
JUVENILE HERRING DISTRIBUTION: WINTER

● 1970s

● 1980s

Figure 4A.

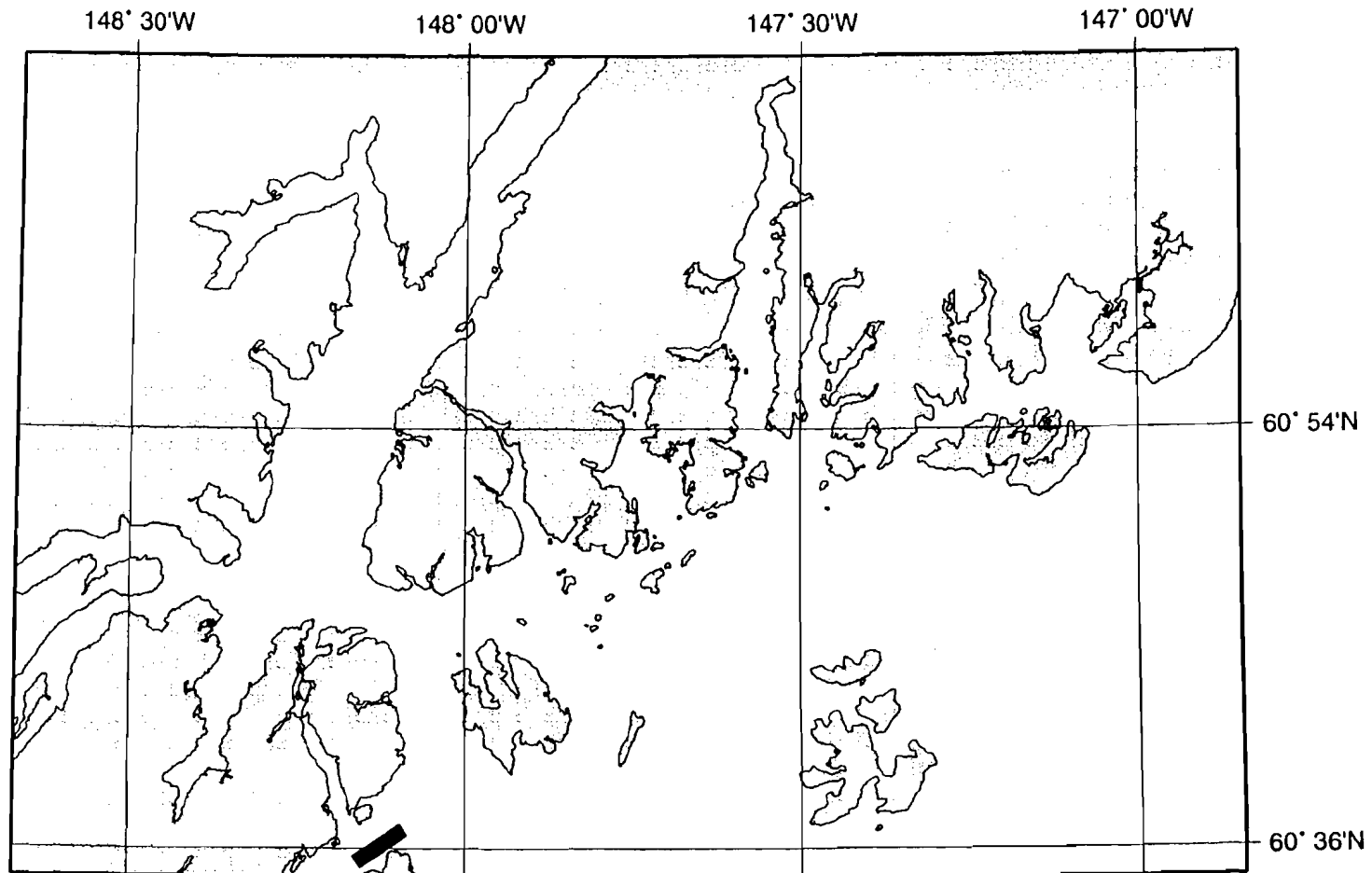
PRINCE WILLIAM SOUND



JUVENILE HERRING DISTRIBUTION: WINTER

● 1970s ● 1980s

PRINCE WILLIAM SOUND

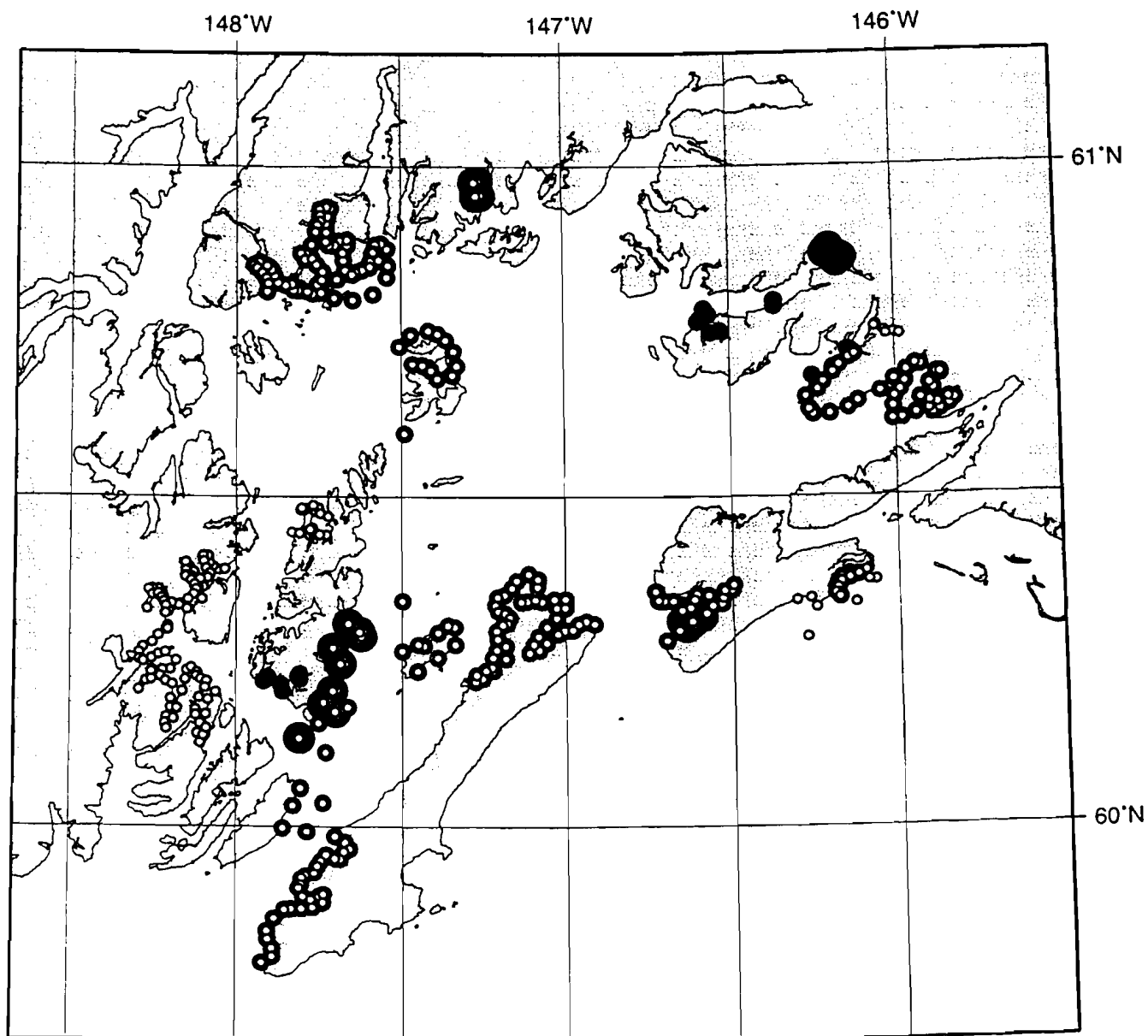


JUVENILE HERRING DISTRIBUTION: WINTER

● 1970s ● 1980s

Figure 4C.

PRINCE WILLIAM SOUND



SMALL FISH, CAPELIN, & SANDLANCE DISTRIBUTION: SUMMER

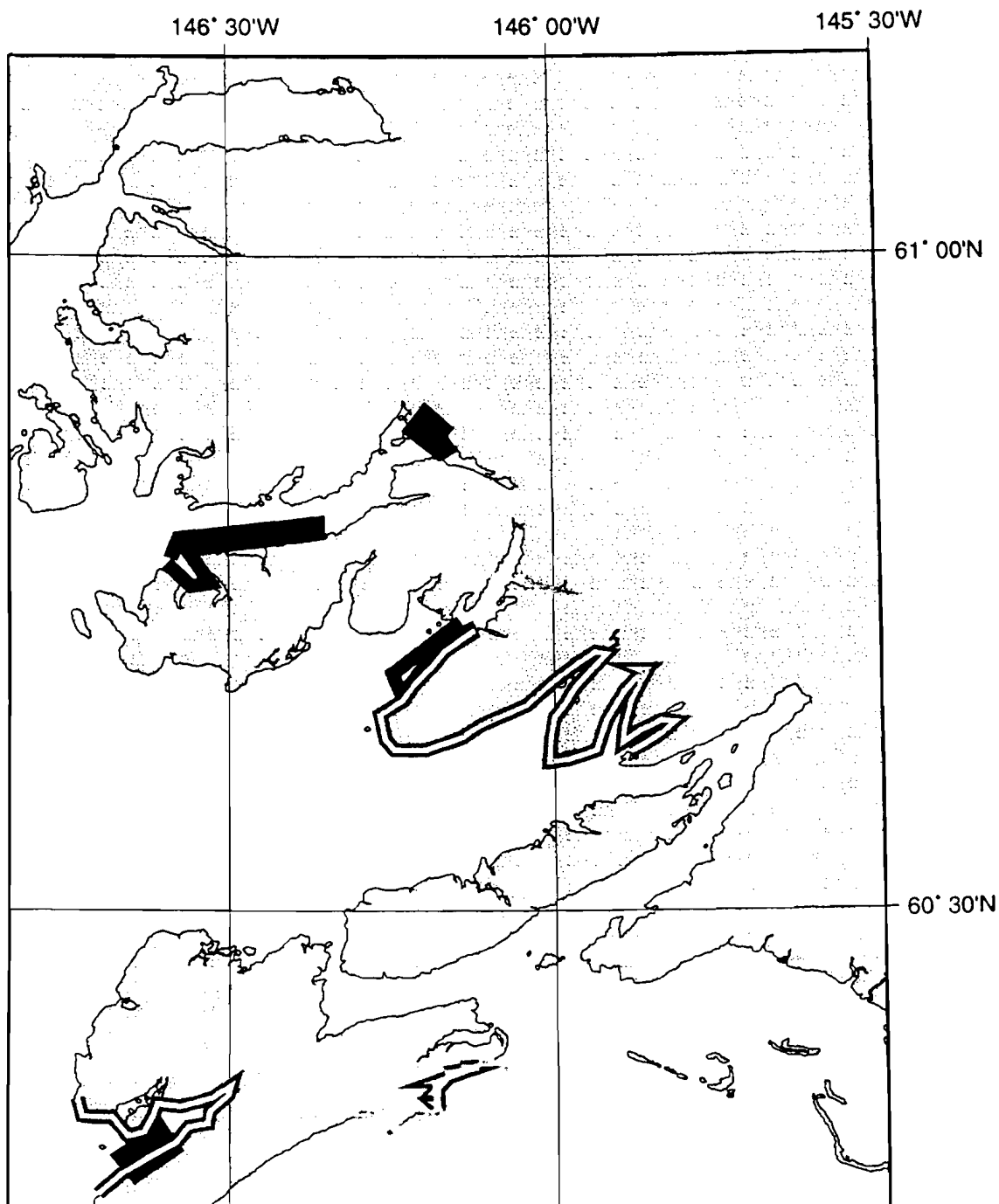
● 1970s
n = 2

● 1980s
n = 7

○ 1990s
n = 7

Figure 5.

PRINCE WILLIAM SOUND



SMALL FISH, CAPELIN, & SANDLANCE DISTRIBUTION: SUMMER

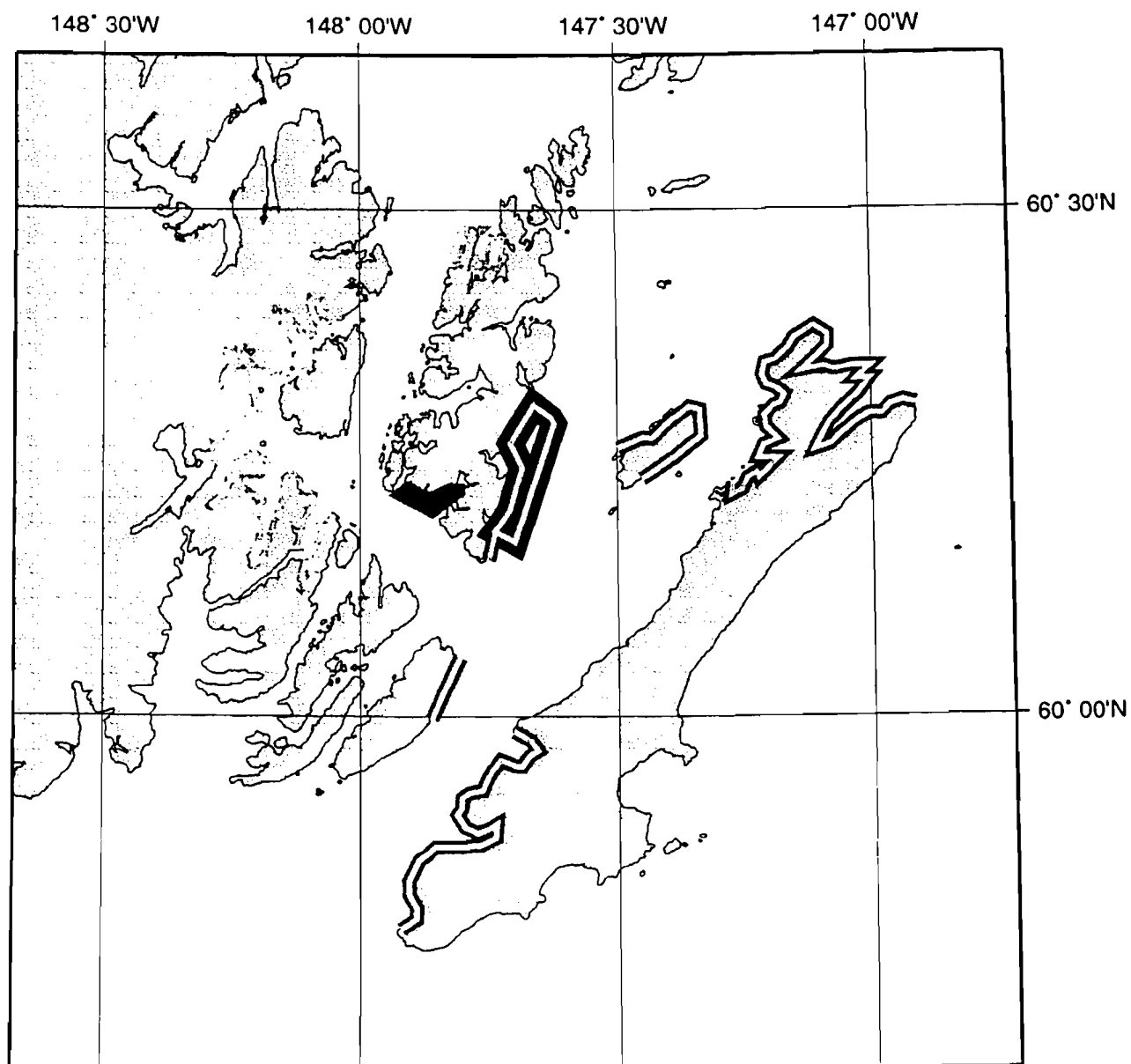
● 1970s

● 1980s

○ 1990s

Figure 5A.

PRINCE WILLIAM SOUND



SMALL FISH, CAPELIN, & SANDLANCE DISTRIBUTION: SUMMER

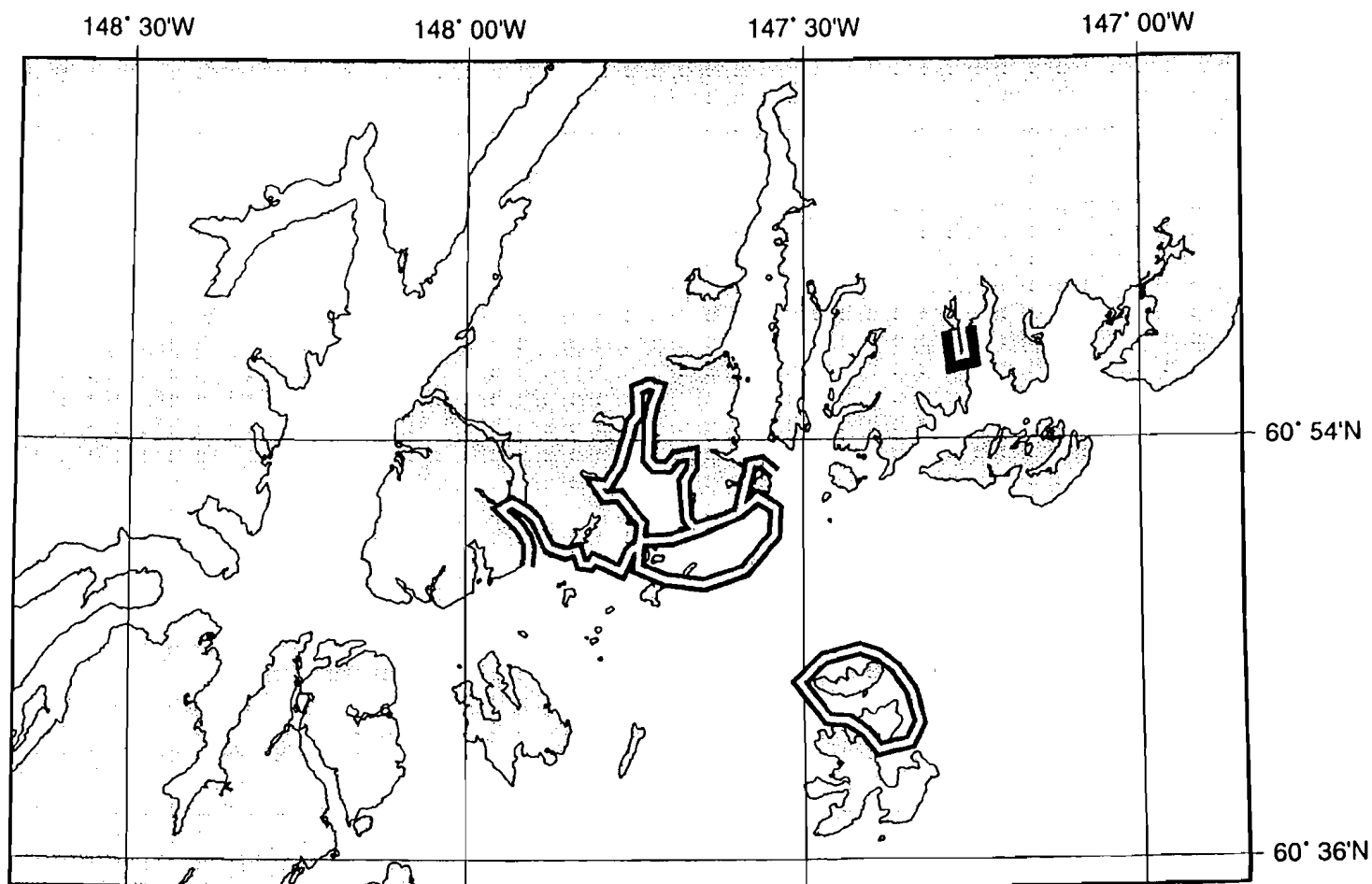
● 1970s

● 1980s

○ 1990s

Figure 5B.

PRINCE WILLIAM SOUND



SMALL FISH, CAPELIN, & SANDLANCE DISTRIBUTION: SUMMER

● **1970s**

● **1980s**

● **1990s**

Figure 5C.

Appendix A: Interview Guide

ID
DATE

BIRTHDATE
COMMUNITY

1. What year did you begin working in the Sound?
2. Please describe what your work was like:

3. Which fisheries were you involved in, in PWS?

- | | | |
|-----------------------|----------------|-------------|
| a) what time of year? | | |
| b) Which years? | | |
| i) salmon seine | _____ to _____ | summer |
| ii) salmon gillnet | _____ to _____ | summer-fall |
| iii) herring pound | _____ to _____ | spring |
| iv) herring seine | _____ to _____ | spring |
| v) herring gillnet | _____ to _____ | spring |
| vi) dive | _____ to _____ | _____ |
| vii) handpick | _____ to _____ | _____ |
| ix) shrimp pot | _____ to _____ | _____ |
| x) bottomfish | _____ to _____ | _____ |
| xi) bait herring | _____ to _____ | _____ |

4. Were you ever a spotter for fisheries

- a). Which fisheries?
- b). Which years?
 - i). Salmon seine _____ to _____
 - ii). Herring pound _____ to _____
 - iii). Herring seine _____ to _____
 - iv). Other _____

5. How did the amount of time you spend in the Sound change since you began working here?

6. What activities take you out in the Sound now?

7. What months are you usually out in the Sound?

8. During those months, how frequently do you go out?

9. SHOW ON THE CHART THE GENERAL AREA OF THE SOUND YOU USE.

10. During what years were you out in the Sound the most?

- a. DRAW CIRCLES AROUND THE PLACES YOU USE MOST INTENSIVELY.
- b. Describe your activities there/ frequency duration

JUVENILE HERRING

11. Are there places you think are particularly important for juvenile herring?

- a) Which places?

- b) Why?

12. Where do you think juvenile herring (age 0-2, about 4 inches long) winter?

13. CIRCLE THE AREAS YOU'VE SEEN JUVENILE HERRING IN ORANGE.

- i) What years did you see them there?
- ii) What season/time of year did you see them?
- iii) Did you identify them? How?

- iv) Describe where you saw them – nearshore/offshore, surface/deep,
- v) Can you recall how much you observed?

14. How often did you see juveniles there: For each observation, mark frequency on the chart or table.

C – CONSISTENTLY – “I’d see them almost everyt ime I went there this time of year.”
O – OCCASIONALLY – “ I’d see them once in a while this time of year.”
R – RARELY – “I remember them showing up there once or twice.”

15. Do you remember seeing concentrations of animals feeding on the herring?

16. Tell me about the changes you’ve seen in abundance of herring in the Sound.

ADULT HERRING - RED

17. Where have you seen schools of adult herring in spring and fall aside from Northern Montague Island, Port Gravina, Port Fidalgo, Tatitlek Narrows, and Green Island?

18. How did you know they were herring?

19. How often have you seen them there?

20. At each place describe where you saw them - nearshore/offshore, surface/deep.

21. What other animals do/did you see with them?

22. Where do you find adult herring in winter?

23. Has the distribution of adult herring changed over the years you’ve been working in the Sound? Tell me about the changes you’ve noticed.

24. Did you fish for herring for home use or gather spawn on kelp this year?

25. Did you notice any signs of disease?

26. Had you ever seen disease in herring before 1993?

OTHER FORAGE FISHES - GREEN

27. Did you ever see or catch other forage fish such as sandlance or capelin while out in the Sound?

- a) Describe what you saw or caught.
- b) Could you identify them? How?
- c) When - year, season?
- d) Where – place, surface, deep

28. Have you seen them there before?

29. How frequently?

30. Have you noticed a change in abundance of these fish?

31. What other animals do you remember commonly associated with these schools of fish?

POLLOCK

32. Describe any changes you’ve noticed in pollock abundance and distribution since you began fishing/working in the Sound.

33. Where, what time of year, which years?

34. How often have you seen them there?

35. How does weather or ocean state on pollock abundance.

36. Did fish ever disappear completely from an area that you fished /hunted/used?

- a). why do you think they disappeared?

Chapter 11

Fish Energetics

Exxon Valdez Oil Spill
Restoration Project Annual Report

SEA Fish Energetics

Restoration Project SEA 320U
Annual Report

This annual report has been prepared for peer review as part of the Exxon Valdez Oil Spill Trustee Council restoration program for the purpose of assessing project progress. Peer review comments have not been addressed in this annual report.

Dr. A. J. Paul
University of Alaska, Seward Marine Center
POB 730, Seward, AK 99664

April 1998

SEA Fish Energetics

Restoration Project SEA 320U Annual Report

Study History: SEA is a hypothesis driven ecosystem study designed to identify the mechanisms that influence herring production in Prince William Sound by investigating their early life stages.

SEA research focuses on the timing and magnitude of energy flowing through the food web. Tracking this flow provides insight into links between primary and secondary production and species interactions. Food and predation are key forces that operate within the context of environmental parameters like temperature and transport. This component of SEA provides information on whole body energy content of key fish species so that interactions within and between species can be quantified, and insight into the feeding conditions on geographical and temporal scales described. The data from 320U supports inquiries into the River-Lake hypothesis, the Over-Winter hypothesis, and the key question "is it food impeding recovery of herring". This project was initiated in April of 1995, thus this report constitutes the third year of a three year field sampling program. During year four 320U findings will be provided to the SEA synthesis project.

Abstract: The Exxon Valdez oil spill may have altered the trophic structure of the plankton feeding fish community by injuring intertidal spawning herring. This project describes the interannual variations in the somatic energy cycle of juvenile *Clupea pallasii*. Collections were (or will be) made in the spring and fall of 1995-98, and summer and fall of 1996 and 1997, and winter 1996-97. This bioenergetic information is needed to determine if food resources are limiting growth of recruits and if the over-winter period is important in regulating recruitment of age 0 herring. The analysis of somatic energy content (SEC) showed that there was large geographical differences in the nutritional status of recruiting herring. This is also true for fish at individual capture sites. Other SEA components are examining the physical oceanographic and prey distribution patterns related to these differences. The energy profile of over-wintering herring showed that the typical recruit was food limited and exhibited nutritional stress during the winters of 1995-96. Few 1996 recruits were captured in the spring of 1997 and at many sites they were in a near death condition. In the fall of 1997 recruits from one bay had high SEC values but at the other two sites they were in poor condition and few of them survived the winter. Acquiring enough energy during the summer and fall feeding season appears to be an important factor in determining survival through their first winter for juvenile herring.

This project measures fall and spring somatic energy content of juvenile pollock (*Theragra chalcogramma*) to compare their nutritional status to that of juvenile herring. Somatic energy content of age 0 walleye pollock was examined in the fall and spring during two years. In the fall

of 34 mm and a mean SEC of 2.7 kJ/g. By 3 August the mean SL increased to 69 mm and SEC averaged 3.4 kJ/g. On 10 October age 0 pollock had an average SL of 81 mm and SEC of 3.6 kJ/g. Based on these mean values growth rates for age 0 pollock in 1996 were 0.4 mm/d. This type of information on seasonal and size specific variations in SEC is critical to understanding the role of pollock in the food web both as predators and prey.

The information gathered by this energetics project is being related to SEA zooplankton surveys, prey selection studies and trophic isotopic studies through the SEA modeling effort. The data also supports the APEX predator-feeding analysis.

Key Words: *Clupea pallasii*, herring, energetics, ovary, somatic energy, *Theragra chalcogramma*, pollock.

Table of Contents

Study History

Abstract

Project Data

Executive Summary

Introduction

Objectives

Methods

Results

Discussion

Conclusions

Literature Cited

Tables

None

Figures

None

Project Data:

The last sampling period for this project will be March of 1998. Samples are frozen fishes that are dried and combusted. The process destroys the sample. Small amounts of tissue from selected fishes are passed on to SEA project 320I (Kline). The data collected is energy content of whole body tissues. Energetic data is stored as SIGMAPLOT, EXCEL, and ASCII files. The data becomes available as the material is published in journals. The custodian is Dr. A. J. Paul, University of Alaska, Seward Marine Center, POB 730, Seward, AK 99664 (Phone 907 224-5261; Fax 224-3392; email ffajp@aurora.uaf.edu).

Executive Summary:

During its third year this project examined somatic energy content of age 0 and 1 herring (spring and late fall) and age 0 pollock (spring and late fall). These parameters are key measures for SEA and other EVOS models which predict levels of fish production and species interactions. The key results for the species under study include:

Herring somatic energy: 1) There is considerable geographical variation in the fall energy content of recruits captured in different areas. 2) From the spring sampling it appears that recruits from the 1994 year class were well nourished and passed the over-winter period in good condition allowing for hope that a reasonable survival of individuals will follow. 3) Most of the 1995 and 1996 year classes were undernourished when entering the winter and survivors were in poor condition the following spring. 4) Few 1996 recruits were captured in the spring of 1997. 5). YOY herring metamorphose in July and so they start this phase of development long after the spring bloom is ended. They then have just a few months to prepare for the poor feeding conditions of winter. Because of this YOY herring are susceptible to being under-nourished for over-wintering.

Age 0 pollock: 1). Pollock metamorphose about a month before the herring and are longer than herring of the same age. 2). Pollock recruits appear to increase in length during the winter at some sites and maintain their nutritional status or improve it unlike herring who lose somatic energy during the winter. The energetic profile for age 0 pollock will aid in the understanding of how they compete with herring recruits.

Introduction:

This project explores the role nutritional status plays in over-winter survival of juvenile herring. In recent history, herring and pollock have been among the most abundant pelagic forage fishes in south central Alaska. After the Exxon Valdez oil spill the herring population of Prince William Sound has been exhibiting reduced abundance and increased prevalence of disease. Age 0 herring store energy during the summer feeding season and either fast or feed at low rates during the winter. If they have insufficient energy stores to maintain normal schooling activities until the spring zooplankton bloom, then high mortalities might occur. Low energy storage might be due to low zooplankton standing stocks or to competition for food resources.

A portion of the effort examined somatic energy in age 0 pollock during the fall and spring, which are trophic analogs with herring, so the nutritional status of these forage species can be compared.

Objectives: This projects objectives follow:

1. Describe the interannual somatic energy content of herring especially age 0 relative to geographical location. This work is in progress.
2. Examine fall and spring energy stores of juvenile herring from several sites in Prince William Sound and describe the role nutritional status plays in over-winter survival. This work is in progress.
3. Describe the spawning energetics of herring. Measure ovarian energy relative to weight, age and spawning site in female herring. This work is completed.
4. Measure fall and spring energy content of adult herring. This work is completed.
5. Measure fall and spring somatic energy content of juvenile pollock and make comparisons of their nutritional status to geographical location and that of juvenile herring. This work is in progress.
6. Relate the analysis of all the above objectives to SEA zooplankton surveys, prey selection studies and trophic isotopic studies through the SEA modeling effort and multi-author journal SEA synthesis papers. This work is in progress.

Methods:

The methods applied to the energy cycles were similar to those used by the investigator in previous bioenergetic studies (Harris *et al.*, 1986; Paul *et al.*, 1993, Smith *et al.*, 1988; Smith *et al.*,

1990; Paul and Willette, 1997). All fish lengths in 320 U were standard length (SL) measured to the nearest mm. All whole fish weights were taken to the nearest 0.1 g. All calorimetric samples were weighed to the 0.0001 g level.

Herring Ovarian Energetics

All this work was completed in 1996 and available in Paul, A. J., J. M. Paul and E. Brown. 1996. Ovarian energy content of Pacific herring from Prince William Sound, Alaska. Alaska Fishery Research Bulletin. 3:103-111.

Somatic Energy of Herring

Juvenile herring were captured with 50m diameter x 4m deep purse seines with 3 mm stretch mesh. At each collection site at least three sets were made to capture specimens. Adult herring were collected with commercial herring purse seines (182m diameter, 22m deep, 3cm mesh). After capture all fish were immediately frozen in seawater aboard ship and kept frozen until processing. Recruiting herring were collected during the fall of 1994 (2 sites), spring of 1995 (6 sites), fall of 1995 (9 sites), spring of 1996 (8 sites), fall of 1996 (4 sites), spring of 1997 (1 of 4 sites surveyed), fall of 1997 (4 sites) and spring of 1998 (4 sites).

In the laboratory the fish were partially thawed, just enough to handle, but not enough so fluids were lost. Scales were removed from selected fish just above or below the lateral line, 3 rows behind the operculum for aging. All fish were measured for standard length (SL) to the nearest mm, then weighed to the nearest 0.1 g. The SEC of the whole individual was determined in terms of kJ/g wet weight. Herring under 150 mm SL were freeze dried whole. Larger fish while still partially frozen were ground, then the ground body made into a paste in a mortar. A 30 g subsample was then freeze dried. After freeze drying, test tissues were placed in a convection oven at 60°C until they reached a constant weight. Individual tissue wet and dry weight values were used to calculate the moisture content of every fish. Dried tissues were ground in a mill and measurements of caloric content made by bomb calorimetry. All calorimetric samples were weighed to the 0.0001 g level with a single sample burned per fish.

Somatic Energy of Age 0 Pollock

Pollock under 115 mm SL were collected at several sites in 1996 and 1997 and frozen in seawater for analysis. Fish were analyzed for standard length, wet weight, and whole body energy content using standard calorimetric methods noted above.

Results:

Somatic Energy of Herring

In herring SEC increases with age, the most profound differences being between the YOY and age 1 fish, and the other age groups. The average fall SEC values for YOY fish and age 1 herring were 5.7 (± 0.6) and 8.0 (± 1.2) kJ/g wet wt respectively. The age 2 and older fish had similar SEC values with mean values ranging from 9.4 to 10.2 kJ/g wet wt. There was considerable range in SEC values between individuals indicating many of them did not eat enough to maximize their energy reserves. In the spring all size classes of herring had markedly less stored energy than those captured in the fall. Like the fall samples, there was also lots of variability in individual SEC values in the spring specimens relative to measures of fish size. The average spring SEC values for all YOY and age 1 fish in their respective age classes were nearly identical at 4.4 (± 0.6) and 4.4 (± 0.6) kJ/g wet wt respectively. The age 2 and older fish

had SEC with mean values ranging from 5.2 to 6.3 kJ/g wet wt with lots of variability.

Changes in SEC of captive age 0 Pacific herring forced to fast during winter was measured and compared to cohorts collected in the field. Somatic energy content of fasting captives declined at a rate of 23 J/g wet wt.d⁻¹ at a mean temperature of 6.6°C. Fish that died during fasts had SEC values ranging from 2.8 to 3.6 kJ/g wet wt. During March 1996 the SEC of field collected age 0 herring averaged 3.8 kJ/g, with ≈40% having SEC ≤ 3.6 kJ/g wet wt. Thus, by March the average recruit had used most of its stored energy. These observations confirmed that in the northern Gulf of Alaska region age 0 herring rely heavily on stored energy to survive their first winter.

The results mentioned in this section were prepared for publication with the following 2 papers accepted:

1). Paul, A. J., J. M. Paul and E. Brown. 1997. Fall and spring somatic energy content for Alaskan Pacific herring (*Clupea pallasii* Valenciennes 1847) relative to age, size and sex. J. Exp. Mar. Biol. Ecol. In press.

2). Paul, A. J. and J. M. Paul. 1997. Comparisons of whole body energy content of fasting age zero Alaskan Pacific herring (*Clupea pallasii*) and cohorts over-wintering in nature. J. Exp. Mar. Biol. Ecol. In press.

Papers in progress deal with changes in SEC during the summer growth period and over the winter of 1996-1997. The final papers will review geographical and interannual variations in SEC of herring recruits for the period of 1994 to 1998.

Somatic Energy of Age 0 Pollock

Pollock samples collected in 1996 and 1997 have been processed. The data provides insight into how recruiting herring and age 0 pollock compete for food resources and their relative success and link to APEX studies of pollock-bird interactions, APEX and SEA fish stomach analysis-isotope studies, and assessments of secondary productivity. A journal paper on seasonal changes in whole body energy content of age 0 walleye pollock and estimated consumption rates is in preparation.

Discussion:

The examination of somatic energy content of age 0 herring, and their competitors age 1 herring and age 0 pollock shows promise for understanding the level of competition between these pelagic analogs. Coupled with SEA models and APEX and SEA stomach analysis these prey competition interactions could be quantified in EVOS synthesis models. The somatic energy measures should identify age 0 herring that have not stored enough energy to survive the winter. The bioenergetic herring over-winter model (Patrick) will help identify poor year classes 3 years in advance of their entry into the fishery. The SEC signatures also are a reflection of zooplankton standing stock.

CONCLUSIONS

Somatic energy measurements are a valuable tool for identifying the transfer of energy through the food web to pelagic fish. They measure subtle differences in individuals that are not observable from length-wet weight measures. Quantifying energy transfers is critical to building

SEA and other EVOS models. Additionally the energetic data set allows for trophic comparisons of pelagic analogs like pollock and herring, and transfer of energy to other animals like APEX birds. Satisfactory progress is being made towards achieving all objectives. No methods problems have occurred. The project should be successfully completed on time.

ACKNOWLEDGEMENTS

Several SEA staff aided in field collections, laboratory analysis and data handling. Youth Area Watch also aided in some fish collections and laboratory work. The Seward Marine Center Laboratory provide all the facilities.

LITERATURE CITED

- Harris, R., T. Nishiyama, and A. J. Paul. 1986. Carbon, nitrogen and caloric content of eggs, larvae, and juveniles of the walleye pollock, *Theragra chalcogramma*. J. Fish. Biol. 29: 87-89.
- Paul, A. J., J. M. Paul, and R. L. Smith. 1993. The seasonal changes in somatic energy content of Gulf of Alaska yellowfin sole *Pleuronectes asper* Pallas 1814. J. Fish Biol. 43: 131-138.
- Paul, A. J., J. M. Paul and E. Brown. 1996. Ovarian energy content of Pacific herring from Prince William Sound, Alaska. Alaska Fishery Research Bulletin. 3:103-111.
- Paul, A. J., J. M. Paul and E. Brown. 1997. Fall and spring somatic energy content for Alaskan Pacific herring (*Clupea pallasii* Valenciennes 1847) relative to age, size and sex. J. Exp. Mar. Biol. Ecol. In press.
- Paul, A. J. and J. M. Paul. Comparisons of whole body energy content of fasting age zero Alaskan Pacific herring (*Clupea pallasii*) and cohorts over-wintering in nature. J. Exp. Mar. Biol. Ecol. In press.
- Paul, A. J. and Mark Willette 1997. Geographical variation in somatic energy content of migrating pink salmon fry from Prince William Sound: a tool to measure nutritional status. In: International symposium on the role of forage fishes in marine ecosystems. Alaska Sea Grant Rpt. 97-01 pp. 707-720.
- Smith, R. L., A. J. Paul, and J. M. Paul. 1988. Aspects of energetics of adult walleye pollock, *Theragra chalcogramma* (Pallas), from Alaska. J. Fish. Biol. 33: 445-454.
- Smith, R. L., J. M. Paul, and A. J. Paul. 1990. Seasonal changes in energy and the energy cost of spawning in Gulf of Alaska Pacific cod. J. Fish. Biol. 36: 307-316.

Chapter 12

Synthesis and Integration

Exxon Valdez Oil Spill
Restoration Project Annual Report

Sound Ecosystem Assessment (SEA): Synthesis and Integration

Restoration Project 97320-Z
Annual Report

This annual report has been prepared for peer review as part of the Exxon Valdez Oil Spill Trustee Council restoration program for the purpose of assessing project progress. Peer review comments have not been addressed in this annual report.

Robert T. Cooney

Institute of Marine Science
University of Alaska Fairbanks
Fairbanks, Alaska 99775-7220

April 1998

Sound Ecosystem Assessment (SEA): Synthesis and Integration

Restoration Project 97320-Z Annual Report

Study History: Project 320-Z was established in FY 96 to assist the SEA lead scientist prepare and distribute single, integrated DPDs and Annual Reports. Funding was also provided to support the many aspects of synthesis and integration within the multi-project program. Conference calls, subgroup meetings and meetings and workshops of all investigators and selected staff and students are examples of synthesis activities supported by project 320-Z. The first annual report for this component of SEA was submitted by the Lead Scientist as part of the SEA 1996 single, integrated annual report in April, 1997. Project 320-Z (re-titled 320-Z1 for FY 99) will close-out in 1999.

Abstract: Support for synthesis and integration activities in FY 97 was used to receive, collate, reproduce, and submit the single, integrated FY 98 DPD and FY 96 Annual Report in April, 1997. Funding also supported participation in the SEA annual meeting, held in conjunction with the 48th Arctic Division AAAS Science Conference, September 24-27, 1997, in Valdez. This meeting developed the titles and suggested authorship for papers comprising the SEA synthesis volume to be written for the journal Fisheries Oceanography in FY 99. SEA web services were used in December, 1996, and January, 1997 to prepare the SEA FY96 public presentation for the EVOS public workshop, and to assist the modeling and herring components of SEA for peer reviews of their activities in January and February, 1997.

Key Words: Synthesis, Integration, SEA, EVOS.

Project Data: Synthesis and integration activities draw upon information generated by all the SEA components. Data sharing and transfer are aided by web and other network tools developed by project 320-J, Information Services and Modeling. SEA supports a web page at the following address: <http://www.pwssc.gen.ak.us/sea/sea.html>.

Citation: Cooney, R.. T. 1998. Sound Ecosystem Assessment (SEA): Synthesis and Integration, Exxon Valdez Oil Spill restoration project annual report (320-Z), Institute of Marine Science, University of Alaska Fairbanks, Fairbanks, Alaska, 99775-7220.

Table of Contents

Executive Summary	4
Objectives	4
Methods	4
Results	4
Discussion	5
Conclusions	5
Acknowledgments	5

Executive Summary

Support for synthesis and integration activities in FY 97 was used to receive, collate, reproduce, and submit the single, integrated FY 98 DPD and FY 96 Annual Report in April, 1997. Funding also supported participation in the SEA annual meeting, held in conjunction with the 48th Arctic Division AAAS Science Conference, September 24-27, 1997, in Valdez. This meeting developed the titles and suggested authorship for papers comprising the SEA synthesis volume to be written for the journal Fisheries Oceanography in FY 99. SEA web services were used in December, 1996, and January, 1997 to prepare the SEA FY96 public presentation for the EVOS public workshop, and to assist the modeling and herring components of SEA for peer reviews of their activities in January and February, 1997.

Objectives

The following general objectives were approved in the FY 97 DPD:

1. Convene meetings of SEA principal investigators and staff as needed for program planning, and the debate and application of SEA results to overall program goals.
2. Use information from all SEA projects to provide the Trustee Council with a single, integrated annual report for work completed in FY 96, and to prepare and submit a single, integrated DPD for continuing studies in FY 98.

Methods

The SEA Lead Scientist (Ted Cooney) works with an executive committee (David Eslinger, Vince Patrick, Kevin Stokesbury for Brenda Norcross, and Mark Willette) to establish agendas for meetings, to review issues arising in SEA, and to make recommendations about program direction and change. Subgroups and others requesting travel approach the Lead Scientist with requests which are then reviewed on the basis of need. Funds are expended until they are exhausted. Each year, the Lead Scientist serves as the focal point for the receipt of hard and electronic copies of budgets for the DPD and manuscripts for the single integrated annual report. The Lead Scientist also provides a synthesis chapter for the annual report - an expanded executive summary of progress requested by the EVOS Chief Scientist, Robert Spies.

Results

The SEA FY 98 single, integrated DPD was submitted for consideration by the Trustee Council on 15 April, 1997. The single, integrated SEA annual report of progress for 1996 was submitted 1 May, 1997. Project 320-Z assisted with travel for investigators to attend the SEA annual meeting in Valdez, September 28, 1997 specifically to review the status of the program and to create titles and authorship for papers proposed for the SEA synthesis volume in FY 99. Some

investigators and staff were also supported to participate in a SEA herring sub-group meeting held during the AAAS science conference in Valdez.

Discussion

The SEA program must respond in a timely manner to formal reviews of progress by EVOS peer reviewers, to proposal and reporting schedules, and to shifts in emphasis responding to streams of information generated by the field and laboratory studies. As the study approaches the termination of its funding and the need for an overall summing up of results, it is imperative that support is available to stimulate communications between all investigators and their respective staffs and students. Without the flexibility of 320-Z funds, it is doubtful that the process of science in a program as complex as SEA could proceed efficiently, or meet its stated goals.

Conclusions

Funding for project 320-Z in FY 97 was the second year that support of this kind was available. There is no question that it fostered a much better climate for synthesis and integration between members and working groups composing the SEA family of projects. In this regard, these were funds well spent.

Acknowledgments

All SEA principal investigators and their staffs and students are gratefully acknowledged for their assistance with report and proposal preparation, and for their dedication to tasks set by SEA to resolve issues concerning ecosystem-dominated production limitations to pink salmon and herring production in Prince William Sound. I am particularly indebted to Maggie Billington in Fairbanks, and to Nancy Bird and Penny Oswalt in Cordova for assistance with budgeting and proposal preparation. Jennifer Allen continues to provide innovative network services that assist communications within SEA. Lastly, I thank Bill Hauser for his skillful hand at program management. Without the continuing contributions from this entire team, SEA would have fallen short long ago of the expectations the stakeholders in the region have for the science.